Errol G. Lewars

Computational Chemistry

Introduction to the Theory and Applications of Molecular and Quantum Mechanics

Third Edition

$$\hat{H}\,\psi = E\,\psi$$

Springer

Computational Chemistry
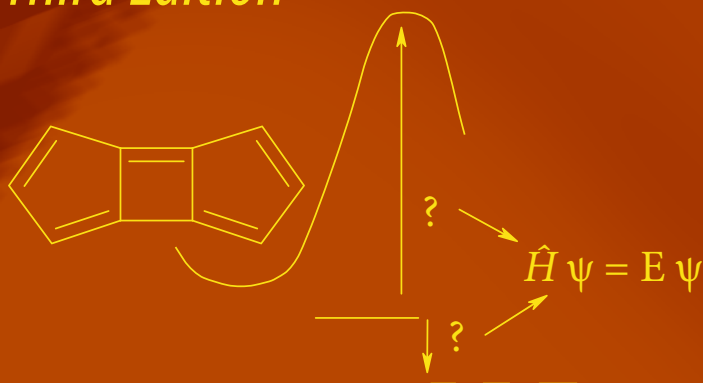
Errol G. Lewars

Computational Chemistry

Introduction to the Theory and Applications
of Molecular and Quantum Mechanics

Third Edition 2016

Errol G. Lewars
Trent University
Peterborough, ON, Canada

To Anne and John,
who know what their contributions were

Preface

Every attempt to employ mathematical methods in the study of chemical questions must be considered profoundly irrational and contrary to the spirit of chemistry. If mathematical analysis should ever hold a prominent place in chemistry-an aberration which is happily almost impossible-it would occasion a rapid and widespread degeneration of that science.
　　Augustus Compte, French philosopher, 1798–1857; in *Philosophie Positive*, 1830.

A dissenting view:

The more progress the physical sciences make, the more they tend to enter the domain of mathematics, which is a kind of center to which they all converge. We may even judge the degree of perfection to which a science has arrived by the facility to which it may be submitted to calculation.
　　Adolphe Quetelet, French astronomer, mathematician, statistician, and sociologist, 1796–1874, writing in 1828.

This third edition differs from the second in these ways:

1. The typographical errors that were found in the first edition have been (I hope) corrected.
2. Sentences and paragraphs have on occasion been altered to clarify an explanation.
3. The biographical footnotes have been updated as necessary.
4. Significant developments since 2010 (the year of the latest references in the second edition), up to the end of 2015, have been added and referenced in the relevant places.

As might be inferred from the word *Introduction*, the purpose of this book, like that of previous editions, is to teach the basics of the core concepts and methods of computational chemistry. This is a textbook, and no attempt has been made to please every reviewer by dealing with esoteric "advanced" topics. Some fundamental concepts are the idea of a potential energy surface, the mechanical picture of a molecule as used in molecular mechanics, and the Schrödinger equation and its elegant taming with matrix methods to give energy levels and molecular orbitals. All the needed matrix algebra is explained before it is used. The fundamental

techniques of computational chemistry are molecular mechanics, ab initio, semi-empirical, and density functional methods. Molecular dynamics and Monte Carlo methods are only mentioned; while these are important, they utilize several fundamental concepts and methods explained here, and if presented at the level of the topics treated here would require a book of their own. I wrote the first edition (2003) because there seemed to be no text quite right for an introductory course in computational chemistry for a fairly general chemical audience, and the second (2011) edition was issued in the same belief; although there are several good books on quantum chemistry and on its disciplinary associate ("handmaiden" might seem somewhat disparaging) computational chemistry, this edition is submitted in the same spirit as the first two. I hope it will be useful to anyone who wants to learn enough about the subject to start reading the literature and to start doing computational chemistry. As implied above, there are excellent books on the field, but evidently none that seeks to familiarize the general student of chemistry with computational chemistry in quite the same sense that standard textbooks of those subjects make organic or physical chemistry accessible. To that end the mathematics has been held on a leash; no attempt is made to prove that molecular orbitals are vectors in Hilbert space, or that a finite-dimensional inner-product space must have an orthonormal basis, and the only sections that the nonspecialist may justifiably view with some trepidation are the (outlined) derivation of the Hartree-Fock and Kohn-Sham equations. These sections should be read, if only to get the flavor of the procedures, but should not stop anyone from getting on with the rest of the book.

Computational chemistry has become a tool used in much the same spirit as infrared or NMR spectroscopy, and to use it sensibly it is no more necessary to be able to write your own programs than the fruitful use of infrared or NMR spectroscopy requires you to be able to build your own spectrometer. I have tried to give enough theory to provide a reasonably good idea of how standard procedures in the programs work. In this regard, the concept of constructing and diagonalizing a Fock matrix is introduced early, and there is little talk of computationally less relevant secular *determinants* (except for historical reasons in connection with the simple Hückel method). Many results of actual computations, some done specifically for this book, are given. Almost all the assertions in these pages are accompanied by literature references, which should make the text useful to researchers who need to track down methods or results, and to anyone who may wish to delve deeper. It would be clearly inappropriate, if not impossible, to exhaustively reference each topic discussed. The choice of references has been oriented toward (besides justifying a particular assertion) reviews, and publications illustrating a topic in a general way, rather than some specialized aspect of it. In this age of the Internet once one is aware of the existence of some subject, it is usually not hard to obtain more information about it. The material should be suitable for senior undergraduates, graduate students, and novice researchers in computational chemistry. A knowledge of the shapes of molecules, covalent and ionic bonds, spectroscopy, and some familiarity with thermodynamics at about the second- or third-year

undergraduate level is assumed. Some readers may wish to review basic concepts from physical and organic chemistry.

The reader, then, should be able to acquire the basic theory of, and a fair idea of the kinds of results to be obtained from, common computational chemistry techniques. You will learn how one can calculate the geometry of (some may quibble and say "a geometry for") a molecule, its IR and UV spectra and its thermodynamic and kinetic stability, and other information needed to make a plausible guess at its chemistry.

Computational chemistry is more accessible than ever. Hardware has become cheaper than it was even a few years ago, and powerful programs once available only for expensive workstations have been adapted to run on inexpensive personal computers. The actual use of a program is best explained by its manuals and by books written for a specific program, and the *directions* for setting up the various computations are not given here. Information on various programs is provided in Chap. 9. Read the book, get some programs, and go out and do computational chemistry. You may make mistakes, but they are unlikely to put you in the same kind of danger that a mistake in a wet lab might.

For the first and second editions, it is a pleasure to acknowledge the help of:

Professor Imre Csizmadia of the University of Toronto, who gave unstintingly of his time and experience;

The knowledgeable people who subscribe to CCL, the computational chemistry list, an exceedingly helpful forum anyone seriously interested in the subject;

My editor for the first edition at Kluwer, Dr Emma Roberts, who was always most helpful and encouraging;

My very helpful editors for the second edition at Springer, Ms Claudia Culierat and Dr Sonia Ojo;

For guidance with the third edition, Ms Karin de Bie at Springer;

Professor Roald Hoffmann of Cornell University, who has insight and knowledge on matters that were at times somewhat arcane;

Dr Andreas Klamt of COSMOlogic GmbH & Co., for sharing his expertise on solvation calculations;

Professor Joel Liebman of the University of Maryland, Baltimore County for stimulating discussions;

Professor Matthew Thompson of Trent University, for stimulating discussions.

For the third edition, it is a pleasure to acknowledge the help of:

Springer Senior Publishing Editor, Chemistry, Dr Sonia Ojo;

Springer Production Editor Books, Ms Karin de Bie;

Professor Robert Stairs of the department of Chemistry, Trent University, for his insight in fruitful discussions;

and finally, since this edition is not fully *de novo*, all those whom I thank, above, for the first and second editions.

No doubt some names have been unjustly and inadvertently omitted, for which I tender my apologies.

Peterborough, ON, Canada   Errol G. Lewars
January 2016

Contents

Chapter 1
An Outline of What Computational Chemistry Is All About

Knowledge is experiment's daughter

Leonardo da Vinci, in *Pensieri*, ca. 1492

Nevertheless:

Abstract You can calculate molecular geometries, rates and equilibria, spectra, and other physical properties with the tools of computational chemistry: molecular mechanics, ab initio, semiempirical and density functional methods, and molecular dynamics. Computational chemistry is widely used in the pharmaceutical industry to explore the interactions of potential drugs with biomolecules, for example by docking a candidate drug into the active site of an enzyme. It is used to investigate the properties of solids (e.g. plastics) in materials science, and to study catalysis in reactions important in the lab and in industry. It does not replace experiment, which remains the final arbiter of truth about Nature.

1.1 What You Can Do with Computational Chemistry

In this chapter we briefly overview the scope and methods of computational chemistry or molecular modelling. One can argue (some might say quibble) over whether there is difference between these two terms [1]. Pursuing this question is probably not a useful activity, and we shall take both terms as denoting a set of techniques for investigating chemical problems on a computer. Matters commonly investigated computationally are:

Molecular geometry: the shapes of molecules–bond lengths, angles and dihedrals.

Energies of molecules and transition states: this tells us which isomer is favored at equilibrium, and (from transition state and reactant energies) how fast a reaction should go.

Chemical reactivity: for example, knowing where the electrons are concentrated (nucleophilic sites) and where they want to go (electrophilic sites) helps us to predict where various kinds of reagents will attack a molecule. A particularly useful application of this is elucidating the likely mode of action of catalysts, which could lead to improved versions.

IR, UV and NMR spectra: these can be calculated, and if the molecule is unknown, someone trying to make it knows what to look for.

The interaction of a substrate with an enzyme: seeing how a molecule fits into the active site of an enzyme is one approach to designing better drugs.

The physical properties of substances: these depend on the properties of individual molecules and on how the molecules interact in the bulk material. For example, the strength and melting point of a polymer (e.g. a plastic) depend on how well the molecules fit together and on how strong the forces between them are. People who investigate things like this work in the field of materials science.

1.2   The Tools of Computational Chemistry

In studying these questions computational chemists have a selection of methods at their disposal. The main tools available belong to five broad classes:

(1) Molecular mechanics is based on a model of a molecule as a collection of balls (atoms) held together by springs (bonds). If we know the normal spring lengths and the angles between them, and how much energy it takes to stretch and bend the springs, we can calculate the energy of a given collection of balls and springs, i.e. of a given molecule; changing the geometry until the lowest energy is found enables us to do a *geometry optimization,* i.e. to calculate a geometry for the molecule.

Molecular mechanics is fast: a fairly large molecule like a steroid (e.g. cholesterol, $C_{27}H_{46}O$) can be optimized in seconds on an ordinary personal computer.

(2) Ab Initio calculations (*ab initio*, Latin: "from the start", i.e. "from first principles") are based on the Schrödinger equation. This is one of the fundamental equations of modern physics and describes, among other things, how the electrons in a molecule behave. The ab initio method solves the Schrödinger equation for a molecule and gives us an energy and a *wavefunction*. The wavefunction is a mathematical function that can be used to calculate the electron distribution (and, in theory at least, anything else about the molecule). From the electron distribution we can tell things like how polar the molecule is, and which parts of it are likely to be attacked by nucleophiles or by electrophiles. The Schrödinger equation cannot be solved exactly for any molecule with more than one (!) electron. Thus approximations are used; the less serious these are, the "higher" the level of the ab initio calculation is said to be. Regardless of its level, an ab initio calculation is based only on basic physical theory (quantum mechanics) and is in this sense "from first principles".

Ab initio calculations are relatively slow: the geometry and IR spectra (= the vibrational frequencies) of propane can be calculated at a high level in a few minutes on a personal computer but a fairly large molecule, like a steroid, could take at least several days for geometry optimization at a reasonably high level. Current personal computers, with four or more GB of RAM and a thousand or more GB of disk space, are serious computational tools and now compete with UNIX machines even for the demanding tasks associated with high-level ab initio calculations. Indeed, one now hears little talk of "workstations", machines that once cost ca. $15 000 or more [2]. For really demanding number crunching, personal access to supercomputers is available through cloud computing, i.e. access to computers at a distant site through the internet [3].

(3) Semiempirical calculations are, like ab initio, based on the Schrödinger equation. However, more approximations are made in solving it, and the very demanding integrals that must be calculated in the ab initio method are not actually evaluated in semiempirical calculations: instead, the program draws on a kind of library of integrals that was compiled by finding the best fit of some calculated entity like geometry or energy (heat of formation) to experimental or, nowadays, high-level theoretical values. This plugging of experimental values into a mathematical procedure to get the best calculated values is called *parameterization* (or *parametrization*). It is the mixing of theory and experiment that makes the method "semiempirical": it is based on the Schrödinger equation, but parameterized with experimental (or high-level theoretical) values (*empirical* means experimental). Of course one hopes that semiempirical calculations will give good answers for molecules for which the program has *not* been parameterized and this is often indeed the case (molecular mechanics, too, is parameterized).

Semiempirical calculations are slower than molecular mechanics but much faster than ab initio calculations. Semiempirical calculations take perhaps roughly 100 times as long as molecular mechanics calculations, and ab initio calculations can take roughly 100–1000 times as long as semiempirical. A semiempirical geometry optimization on a steroid might a minute on a good PC.

(4) Density functional calculations (often called DFT calculations, density functional theory; a functional is a mathematical entity related to a function.) are, like ab initio and semiempirical calculations, based on the Schrödinger equation However, unlike the other two methods, DFT does not calculate a wavefunction, but rather derives the electron distribution (electron *density* function) directly.

Density functional calculations are usually faster than ab initio, but slower than semiempirical. DFT is somewhat new: chemically useful DFT computational chemistry goes back to the 1980s, while "serious" computational chemistry with the ab initio method was being done in the 1970s and with semiempirical approaches in the 1950s.

(5) Molecular Dynamics calculations apply the laws of motion to molecules, which change shape or move under the influence of a *forcefield*. Thus one can simulate the motion of an enzyme as it changes shape on binding to a substrate, or the motion of a swarm of water molecules around a protein molecule. Such biochemically oriented studies rely on molecules moving under he influence of forces calculated by molecular mechanics, and since this is not an electronic structure method, covalent bond-breaking and bond-making (in contrast to conformational changes) cannot be studied with molecular dynamics programs that use this kind of forcefield. For the study of chemical reactions with molecular dynamics a forcefield generated with semiempirical, ab initio, or density functional methods can be used. Do not confuse molecular *dynamics* ("motion") with molecular *mechanics* (a "mechanical" treatment of molecules).

1.3 Putting it All Together

Very large molecules are often studied only with molecular mechanics, because other methods (*quantum mechanical* methods, based on the Schrödinger equation: semiempirical, ab initio and DFT) would take too long. Novel molecules, with unusual structures, are best investigated with ab initio or possibly DFT calculations, since the parameterization inherent in MM or semiempirical methods makes them unreliable for molecules that are very different from those used in the parameterization. DFT is newer than ab initio and semiempirical methods and its limitations and possibilities are less clear than those of the other methods.

Calculations on the structures of large molecules like proteins or DNA are usually done with molecular mechanics. The conformational motions of these large biomolecules can be studied with molecular dynamics utilizing a molecular mechanics forcefield; molecular motions including bond-breaking and -making can be studied with molecular dynamics utilizing semiempirical, ab initio or density functional methods. Key *portions* of a very large molecule, like the active site of an enzyme, can be studied with semiempirical or even ab initio methods. Moderately large molecules like steroids, say, can be studied with semiempirical calculations, or if one is willing to invest the time, with ab initio calculations. Of course molecular mechanics can be used with these too, but note that this technique does not give information on electron distribution, so chemical questions connected with nucleophilic or electrophilic behaviour, say, cannot be addressed by molecular mechanics alone.

The energies of molecules can be calculated by MM, semiempirical, ab initio or DFT. The method chosen depends very much on the particular problem. Reactivity, which depends largely on electron distribution, must usually be studied with a quantum-mechanical method (semiempirical, ab initio or DFT). Spectra are most reliably calculated by high-level ab initio or DFT methods, but useful results can be obtained with semiempirical methods, and some MM programs will calculate fairly good IR spectra (balls attached to springs vibrate!).

Docking a molecule into the active site of an enzyme to see how it fits is an extremely important application of computational chemistry. One could manipulate the substrate with a mouse or a kind of joystick and try to fit it (dock it) into the active site, but automated docking is now standard. This work is usually done with MM, because of the large molecules involved, although selected portions of large biomolecules can be studied by one of the quantum mechanical methods. The results of such docking experiments serve as a guide to designing better drugs, such as molecules that will interact better with the desired enzyme but be ignored by other enzymes.

Computational chemistry is valuable in studying the properties of materials, i.e. in materials science. Semiconductors, superconductors, plastics, ceramics – all these have been investigated with the aid of computational chemistry. A recent ingenious development which could be very potent if it fulfills its promise is a

procedure for discovering materials with computationally specifiable properties [4]. Such studies tend to involve a knowledge of solid-state physics and to be somewhat specialized. On a less utilitarian note, artifacts of artistic value have also been studied with the aid of this science [5].

Computational chemistry is fairly cheap, it is fast compared to experiment, and it is environmentally safe (although the profusion of computers in the last decade has raised concern about the consumption of energy [6] and the disposal of obsolescent machines [7]). It does not replace experiment, which remains the final arbiter of truth about Nature. Furthermore, to *make* something–new drugs, new materials–one has to go into the lab. Also, the caveat is in order that despite the power of computations [8], one should be careful not to so overstep their sphere of validity: in extreme cases you might be, in Pauli's cutting words, "not even wrong" [9]. Nevertheless, computation has become so reliable in some respects that, more and more, scientists in general are employing it before embarking on an experimental project, and the day may come when to obtain a grant for some kinds of experimental work you will have to show to what extent you have computationally explored the feasibility of the proposal.

1.4   The Philosophy of Computational Chemistry

Computational chemistry is the culmination (to date) of the view that chemistry is best understood as the manifestation of the behavior of atoms and molecules, and that these are real entities rather than merely convenient intellectual models [10]. It is a detailed physical and mathematical affirmation of a trend that hitherto found its boldest expression in the structural formulas of organic chemistry [11], and it is the unequivocal negation of the till recently trendy claim [12] that science is a kind of game played with "paradigms" [13].

In computational chemistry we take the view that we are simulating the behaviour of real physical entities, albeit with the aid of intellectual models; and that as our models improve they reflect more accurately the behavior of atoms and molecules in the real world.

1.5   Summary

Computational chemistry allows one to calculate molecular geometries, reactivities, spectra, and other properties. It employs:

Molecular mechanics–based on a ball-and-springs model of molecules
Ab initio methods–based on approximate solutions of the Schrödinger equation
    without appeal to fitting to experiment

Semiempirical methods–based on approximate solutions of the Schrödinger equation with appeal to fitting to experiment (i.e. using parameterization)

Density functional theory (DFT) methods–based on approximate solutions of the Schrödinger equation, bypassing the wavefunction that is a central feature of ab initio and semiempirical methods.

Molecular dynamics methods study molecules in motion.

Ab initio and the faster DFT enable novel molecules of theoretical interest to be studied, provided they are not too big. Semiempirical methods, which are much faster than ab initio or even DFT, can be readily applied to fairly large molecules (e.g. cholesterol, $C_{27}H_{46}O$, and bigger), while molecular mechanics will calculate geometries and energies of very large molecules such as proteins and nucleic acids; however, molecular mechanics does not give information on electronic properties. Computational chemistry is widely used in the pharmaceutical industry to explore the interactions of potential drugs with biomolecules, for example by docking a candidate drug into the active site of an enzyme. It is also used to investigate the properties of solids (e.g. plastics) in materials science.

Easier Questions

1. What does the term *computational chemistry* mean?
2. What kinds of questions can computational chemistry answer?
3. Name the main tools available to the computational chemist. Outline (a few sentences for each) the characteristics of each.
4. Generally speaking, which is the fastest computational chemistry method (tool), and which is the slowest?
5. Why is computational chemistry useful in industry?
6. Basically, what does the Schrödinger equation describe, from the chemist's viewpoint?
7. What is the limit to the kind of molecule for which we can get an exact solution to the Schrödinger equation?
8. What is parameterization?
9. What advantages does computational chemistry have over "wet chemistry"?
10. Why can't computational chemistry replace "wet chemistry"?

Harder Questions

Discuss the following, and justify your conclusions.

1. Was there computational chemistry before electronic computers were available?
2. Can "conventional" physical chemistry, such as the study of kinetics, thermodynamics, spectroscopy and electrochemistry, be regarded as a kind of computational chemistry?

3. The properties of a molecule that are most frequently calculated are geometry, energy (compared to that of other isomers), and spectra. Why is it more of a challenge to calculate "simple" properties like melting point and density?

    Hint: is there a difference between a molecule X and the substance X?

4. Is it surprising that the geometry and energy (compared to that of other isomers) of a molecule can often be accurately calculated by a ball-and-springs model (molecular mechanics)?

5. What kinds of properties might you expect molecular mechanics to be unable to calculate?

6. Should calculations from first principles (ab initio) necessarily be preferred to those which make some use of experimental data (semiempirical)?

7. Both experiments and calculations can give wrong answers. Why then should experiment have the last word?

8. Consider the docking of a potential drug molecule X into the active site of an enzyme: a factor influencing how well X will "hold" is clearly the shape of X; can you think of another factor?

    Hint: molecules consist of nuclei and electrons.

9. In recent years the technique of *combinatorial chemistry* has been used to quickly synthesize a variety of related compounds, which are then tested for pharmacological activity (S. Borman, Chemical & Engineering News: 2001, 27 August, p. 49; 2000, 15 May, p. 53; 1999, 8 March, p. 33). What are the advantages and disadvantages of this method of finding drug candidates, compared with the "rational design" method of studying, with the aid of computational chemistry, how a molecule interacts with an enzyme?

10. Think up some unusual molecule which might be investigated computationally. What is it that makes your molecule unusual?

References

1. For example, summary of a discussion on the Computational Chemistry List (CCL), at www.chem.yorku.ca/profs/renef/whatiscc.html. Accessed 22 Sept 2014
2. Schaefer HF III (2001) The cost-effectiveness of PCs. Theochem 573:129
3. (a) Fox A (2011) Cloud computing-what's in it for me as a scientist? Science 331:406; (b) Mullin R (2009) Chem Eng News. May 25, 10
4. (a) Cerquera TFT et al (2015) J Chem Theory Comput 11:3955; (b) Jacoby M (2015) Chem Eng News, December 30, 8
5. Fantacci S, Amat A (2010) Computational chemistry, art, and our cultural heritage. Acc Chem Res 43:802
6. (a) McKenna P (2006) The waste at the heart of the web. New Sci 192(2582):24; (b) Keipert K, Mitra G, Sunriyal V, Leang SS, Sosokina M (2015) Energy-Efficient Computational Chemistry: Comparison of run times and energy consumption for two kinds of computer architecture (ARM-, i.e. RISC-based and x86) and three families of calculations. J Chem Theory Comput 11:5055
7. Environmental Industry News (2008) Old computer equipment can now be disposed in a way that is safe to both human health and the environment thanks to a new initiative launched

today at a United Nations meeting on hazardous waste that wrapped up in Bali, Indonesia, 4 Nov 2008

8. E.g. Cheng G-J, Zhang X, Chung LW, Xu L, Wu Y-D (2015) J Am Chem Soc 137:1706
9. Peierls R (1960) Pauli's words: the physicist Rudulf Peierls reported that Pauli used these (the German equivalents) in reference to the work of a third party. Biograph Mem Fellows R Soc 5:186; Plata RE, Singleton DA (2015) "Wolfgang Pauli, 1900–1958." The critical paper which invokes them. JACS 137:3811
10. The physical chemist Wilhelm Ostwald (Nobel Prize 1909) was a disciple of the philosopher Ernst Mach. Like Mach, Ostwald attacked the notion of the reality of atoms and molecules ("Nobel laureates in chemistry, 1901–1992", James LK (ed) American Chemical Society and the Chemical Heritage Foundation, Washington, DC, 1993) and it was only the work of Jean Perrin, published in 1913, that finally convinced him, perhaps the last eminent holdout against the atomic theory, that these entities really existed (Perrin showed that the number of tiny particles suspended in water dropped off with height exactly as predicted in 1905 by Einstein, who had derived an equation assuming the existence of atoms). Ostwald's philosophical outlook stands in contrast to that of another outstanding physical chemist, Johannes van der Waals, who staunchly defended the atomic/molecular theory and was outraged by the Machian positivism of people like Ostwald. See Ya Kipnis A, Yavelov BF, Powlinson JS (1996) Van der Waals and molecular science. Oxford University Press, New York. For the opposition to and acceptance of atoms in physics see: Lindley D (2001) Boltzmann's atom. The great debate that launched a revolution in physics. Free Press, New York; and Cercignani C (1998) Ludwig Boltzmann: the man who trusted atoms. Oxford University Press, New York, 1998. Of course, to anyone who knew anything about organic chemistry, the existence of atoms was in little doubt by 1910, since that science had by that time achieved significant success in the field of synthesis, and a rational synthesis is predicated on assembling atoms in a definite way
11. For accounts of the history of the development of structural formulas see Nye MJ (1993) From chemical philosophy to theoretical chemistry. University of California Press; Russell CA (1996) Edward Frankland: chemistry, controversy and conspiracy in Victorian England. Cambridge University Press, Cambridge
12. (a) An assertion of the some adherents of the "postmodernist" school of social studies; see Gross P, Levitt N (1994) The academic left and its quarrels with science. John Hopkins University Press, Baltimore; (b) For an account of the exposure of the intellectual vacuity of some members of this school by physicist Alan Sokal's hoax see Gardner M (1996) Skeptical Inquirer 1996, 20(6):14
13. (a) A trendy word popularized by the late Thomas Kuhn in his book– Kuhn TS (1970) The structure of scientific revolutions. University of Chicago Press, Chicago. For a trenchant comment on Kuhn, see ref. [12b]; (b) For a kinder perspective on Kuhn, see Weinberg S (2001) Facing up. Harvard University Press, Cambridge, MA, chapter 17

Chapter 2
The Concept of the Potential Energy Surface

> *Everything should be made as simple as possible, but not simpler.*
> Attributed to Albert Einstein, but these precise words,
> or the German equivalents, do not appear in his
> collected works (available online).

Abstract The potential energy surface (PES) is a central concept in computational chemistry. A PES is the relationship – mathematical or graphical – between the energy of a molecule (or a collection of molecules) and its geometry. The Born-Oppenheimer approximation says that in a molecule the nuclei are essentially stationary compared to the electrons. This is one of the cornerstones of computational chemistry because it makes the concept of molecular shape (geometry) meaningful, makes possible the concept of a PES, and simplifies the application of the Schrödinger equation to molecules by allowing us to focus on the electronic energy and add in the nuclear repulsion energy later; this third point, very important in practical molecular computations, is elaborated on in Chap. 5. Geometry optimization and the nature of transition states are explained.

2.1 Perspective

We begin a more detailed look at computational chemistry with the potential energy surface (PES) because this is central to the subject. Many important concepts that might appear to be mathematically challenging can be grasped intuitively with the insight provided by the idea of the PES [1].

Consider a diatomic molecule AB. In some ways a molecule behaves like balls (atoms) held together by springs (chemical bonds); in fact, this simple picture is the basis of the important method molecular mechanics, discussed in Chap. 3. If we take a macroscopic balls-and-spring model of our diatomic molecule in its normal geometry (the equilibrium geometry), grasp the "atoms" and distort the model by stretching or compressing the "bonds", we increase the potential energy of the

Fig. 2.1 The potential
energy surface for a
diatomic molecule. The
potential energy increases if
the bond length q is
stretched or compressed
away from its equilibrium
value q_e. The potential
energy at q_e (zero distortion
of the bond length) has been
chosen here as the zero of
energy

energy

0   bond length, q

q_e
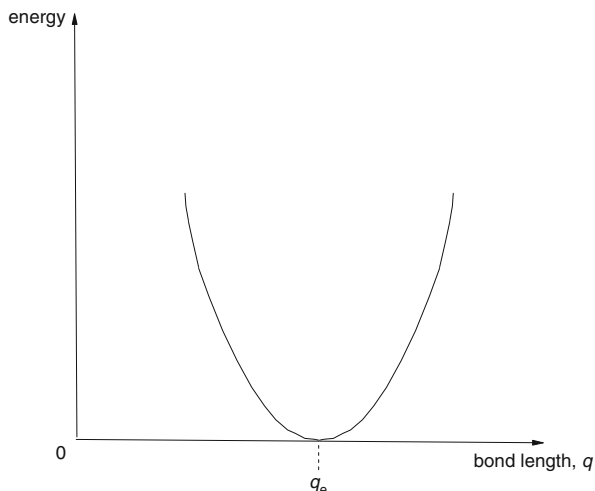
molecular model (Fig. 2.1). The stretched or compressed spring possesses energy, by definition, since we moved a force through a distance to distort it – work was done on the spring. Since the model is motionless while we hold it at the new geometry, this energy is not kinetic and so is by default *potential* ("depending on position"). The graph of potential energy against bond length is an example of a potential energy surface. A line is a one-dimensional "surface"; we will soon see an example of a more familiar two-dimensional surface rather than the line of Fig. 2.1.

Real molecules behave similarly to, but differ from our macroscopic model in two relevant ways:

1. They vibrate incessantly (as we would expect from Heisenberg's uncertainty principle: a stationary molecule would have an exactly defined momentum and position) about the equilibrium bond length, so that they always possess kinetic energy (T) and/or potential energy (V): as the bond length passes through the equilibrium length, $V = 0$, while at the limit of the vibrational amplitude, $T = 0$; at all other positions both T and V are nonzero. The fact that a molecule is never actually stationary with zero kinetic energy (it always has *zero point energy*; ZPE or zero point vibrational energy, ZPVE, Sect. 2.5) is usually shown on potential energy/bond length diagrams by drawing a series of lines above the bottom of the curve (Fig. 2.2) to indicate the possible amounts of vibrational energy the molecule can have (the *vibrational levels* it can occupy). A molecule never sits at the bottom of the curve, but rather occupies one of the vibrational levels, and in a collection of molecules the levels are populated according to their spacing and the temperature [2]. We will usually ignore the vibrational levels and consider molecules to rest on the actual potential energy curves or (see below) surfaces, and:
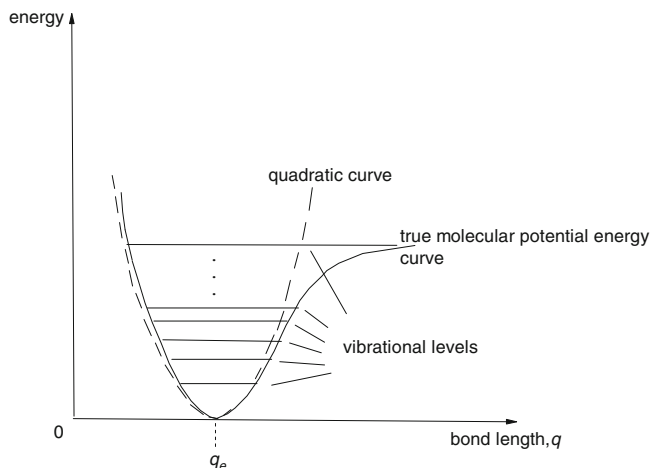
Fig. 2.2 Actual molecules do not sit still at the bottom of the potential energy curve, but instead occupy vibrational levels. Also, only near q_e, the equilibrium bond length, does the quadratic curve approximate the true potential energy curve

2. Near the equilibrium bond length q_e the potential energy/bond length curve for a macroscopic balls-and-spring model or a real molecule is described fairly well by a quadratic equation, that of the simple harmonic oscillator ($E = (\frac{1}{2}) k(q - q_e)^2$, where k is the force constant of the spring). However, the potential energy deviates from the quadratic (q^2) curve as we move away from q_e (Fig. 2.2); that is, the deviations from molecular reality represented by this *anharmonicity* become more important further away from the equilibrium geometry.

Figure 2.1 represents a one-dimensional PES in the two-dimensional graph of E vs. q. A diatomic molecule AB has only one geometric parameter for us to vary, the bond length q_{AB}. Suppose we have a molecule with more than one geometric parameter, for example water: the geometry is defined by two bond lengths and a bond angle. If we reasonably content ourselves with allowing the two bond lengths to be the same, i.e. if we limit ourselves to C_{2v} symmetry (two planes of symmetry and a two-fold symmetry axis; see Sect. 2.6) then the PES for this triatomic molecule is a graph of E vs. two geometric parameters, $q_1 =$ the O–H bond length, and $q_2 =$ the H–O–H bond angle (Fig. 2.3). Figure 2.3 represents a two-dimensional PES (a normal surface is a 2-D object) in the three-dimensional graph; we could make an actual 3-D model of this drawing of a 3-D graph of E vs. q_1 and q_2.

We can go beyond water and consider a triatomic molecule of lower symmetry, such as HOF, hypofluorous acid. This has three geometric parameters, the H–O and O–F lengths and the H–O–F angle. To construct a Cartesian PES graph for HOF analogous to that for H_2O would require us to plot E vs. $q_1 =$ H–O, $q_2 =$ O–F, and $q_3 =$ angle H–O–F. We would need four mutually perpendicular axes (for $E, q_1, q_2,$
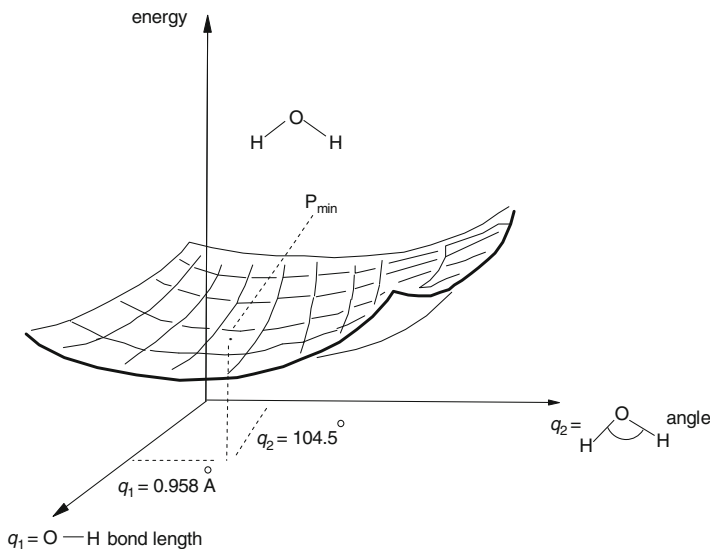
Fig. 2.3 The H_2O potential energy surface. The point P_{min} corresponds to the minimum-energy geometry for the three atoms, i.e. to the equilibrium geometry of the water molecule

Fig. 2.4 To plot energy against three geometric parameters in a Cartesian coordinate system we would need four *mutually perpendicular* axes. Such a coordinate system cannot be actually constructed in our three-dimensional space. However, we can work with such coordinate systems, and the potential energy surfaces in them, mathematically
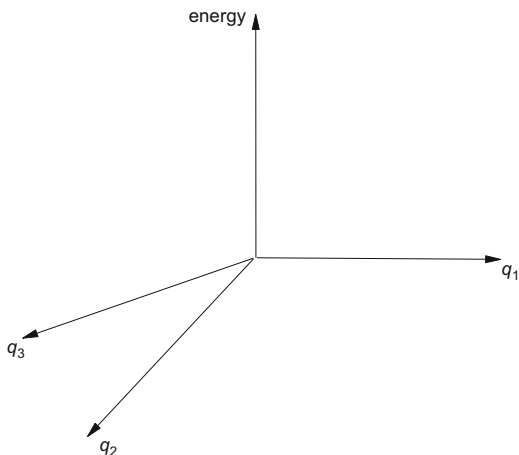
q_3, Fig. 2.4), and since such a four-dimensional graph cannot be constructed in our three-dimensional space we cannot accurately draw it. The HOF PES is a 3-D "surface" of more than two dimensions in 4-D space: it is a hypersurface, and potential energy surfaces are sometimes called potential energy hypersurfaces. Despite the problem of drawing a hypersurface, we can define the *equation $E = f$ (q_1, q_2, q_3)* as the potential energy surface for HOF, where f is the function that describes how E varies with the q's, and treat the hypersurface mathematically. For
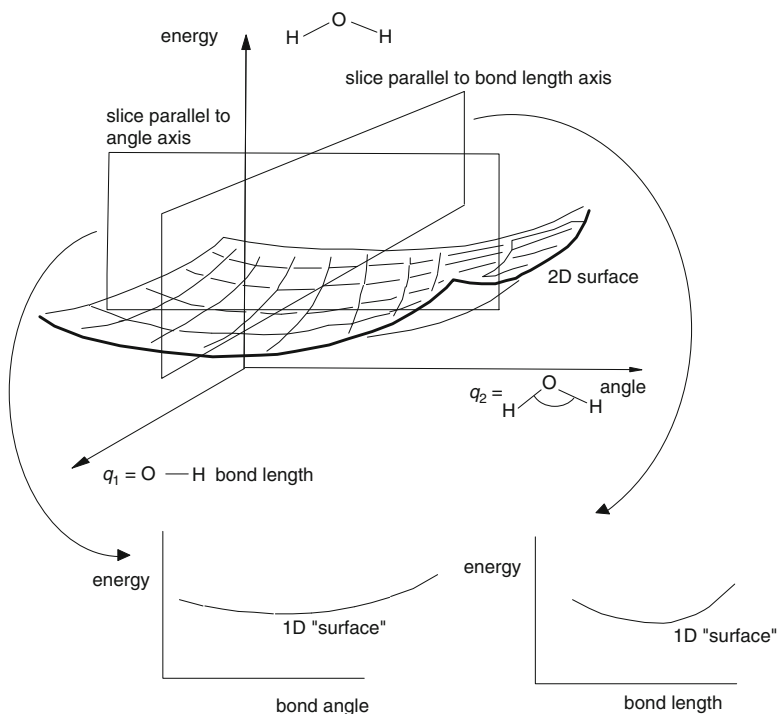
Fig. 2.5 Slices through a 2D potential energy surface give 1D surfaces. A slice that is parallel to neither axis would give a plot of geometry vs. a composite of bond angle and bond length, a kind of average geometry

example, in the AB diatomic molecule PES (a line) of Fig. 2.1 the minimum potential energy geometry is the point at which $dE/dq = 0$. On the H_2O PES (Fig. 2.3) the minimum energy geometry is defined by the point P_m, corresponding to the equilibrium values of q_1 and q_2; at this point $dE/dq_1 = dE/dq_2 = 0$. Although hypersurfaces in general cannot be faithfully rendered pictorially, it is very useful to a computational chemist to develop an intuitive understanding of them. This can be gained with the aid of diagrams like Figs. 2.1 and 2.3, where we content ourselves with a line or a two-dimensional surface, in effect using a slice of a multidimensional diagram. This can be understood by analogy: Fig. 2.5 shows how 2-D slices can be made of the 3-D diagram for water. The slice could be made holding one or the other of the two geometric parameters constant, or it could involve both of them, giving a diagram in which the geometry axis is a composite of more than one geometric parameter. Analogously, we can take a 3-D slice of the hypersurface for HOF (Fig. 2.6) or even a more complex molecule and use an E vs. q_1, q_2 diagram to represent the PES; we could even use a simple 2D diagram, with q representing one, two or all of the geometric parameters. We shall see that these 2D and particularly 3D graphs preserve qualitative and even quantitative features of the mathematically rigorous but unvisualizable $E = f(q_1, q_2, \ldots q_n)$ n-dimensional hypersurface.
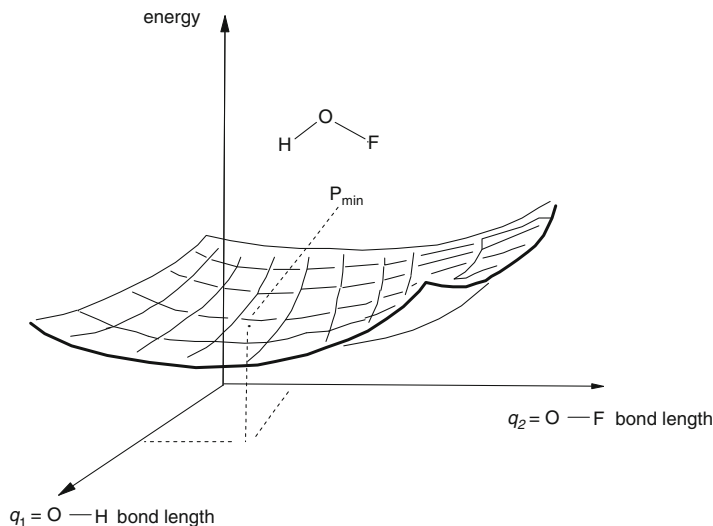
Fig. 2.6 A potential energy surface (PES) for HOF. Here the HOF angle is not shown. This picture could represent one of two possibilities: the angle might be the same (some constant, reasonable value) for every calculated point on the surface; this would be an *unrelaxed or rigid* PES. Alternatively, for each calculated point the geometry might be that for the best angle corresponding to the other two parameters, ie the geometry for each calculated point might be fully optimized (Sect. 2.4); this would be a *relaxed* PES

2.2   Stationary Points

Potential energy surfaces are important because they aid us in visualizing and understanding the relationship between potential energy and molecular geometry, and in understanding how computational chemistry programs locate and character- ize structures of interest. Among the main tasks of computational chemistry are to determine the structure and energy of molecules and of the transition states involved in chemical reactions: our "structures of interest" are molecules and the transition states linking them. Consider the reaction

ozone   transition state   isoozone
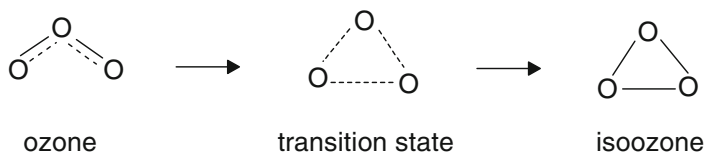
Reaction 1

A priori, it seems reasonable that ozone might have an isomer (call it isoozone) and that the two could interconvert by a transition state as shown in Reaction 1. We can depict this process on a PES. The potential energy E may be plotted against

only two geometric parameters, the bond length and the O–O–O bond angle. We shall (reasonably) assume that the two O–O bonds of ozone are equivalent, and that these bond lengths remain equal throughout the reaction. Figure 2.7 shows the PES for Reaction (2.1), as calculated by the AM1 semiempirical method (Chap. 6; the AM1 method is unsuitable for *quantitative* treatment of this problem, but the potential energy surface shown makes the point), and shows how a 2D slice from this 3D diagram gives the energy/reaction coordinate type of diagram commonly used by chemists. The slice goes along the lowest-energy path connecting ozone, isoozone and the transition state, that is, along the *reaction coordinate*, and the horizontal axis (the reaction coordinate) of the 2D diagram is a composite of O–O bond length and O–O–O angle. In most discussions this horizontal axis is left quantitatively undefined; qualitatively, the reaction coordinate represents the progress of the reaction. The three species of interest, ozone, isoozone, and the transition state linking these two, are called *stationary points*. A stationary point on a PES is a point at which the surface is flat, ie parallel to a horizontal line corresponding to one geometric parameter, or to a plane corresponding to two geometric parameters, or to a hyperplane corresponding to more than two geometric parameters). A marble placed on a stationary point will remain balanced, ie stationary (in principle; for a transition state the balancing would have to be exquisite indeed). At any other point on a potential surface the marble will roll toward a region of lower potential energy.

Mathematically, a stationary point is one at which the first derivative of the potential energy with respect to each geometric parameter is zero:

$$\frac{\partial E}{\partial q_1} = \frac{\partial E}{\partial q_2} = \cdots = 0 \qquad (*2.1)$$

Partial derivatives, $\partial E/\partial q$, are written here rather than dE/dq, to emphasize that each derivative is with respect to just one of the variables q of which E is a function. Stationary points that correspond to actual molecules with a finite lifetime (in contrast to transition states, which exist only for an instant), like ozone or isoozone, are *minima*, or *energy minima*: each occupies the lowest-energy point in its region of the PES, and any small change in the geometry increases the energy, as indicated in Fig. 2.7. Ozone is a *global minimum*, since it is the lowest-energy minimum on the whole PES, while isoozone is a *relative minimum*, a minimum compared only to *nearby* points on the surface. The lowest-energy pathway linking the two minima, the reaction coordinate or *intrinsic reaction coordinate* (IRC; dashed line in Fig. 2.7) is the path that would be followed by a molecule in going from one minimum to another should it acquire just enough energy to overcome the activation barrier, pass through the transition state, and reach the other minimum. Not all reacting molecules follow the IRC exactly: a molecule with sufficient energy can stray outside the IRC to some extent [3].

Inspection of Fig. 2.7 shows that the transition state linking the two minima represents a maximum along the direction of the IRC, but along all other directions
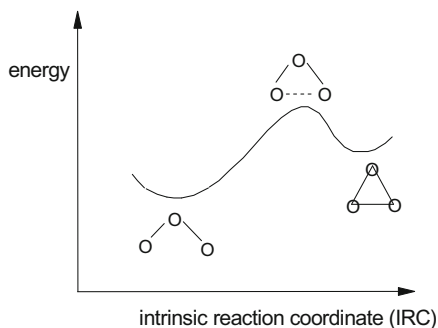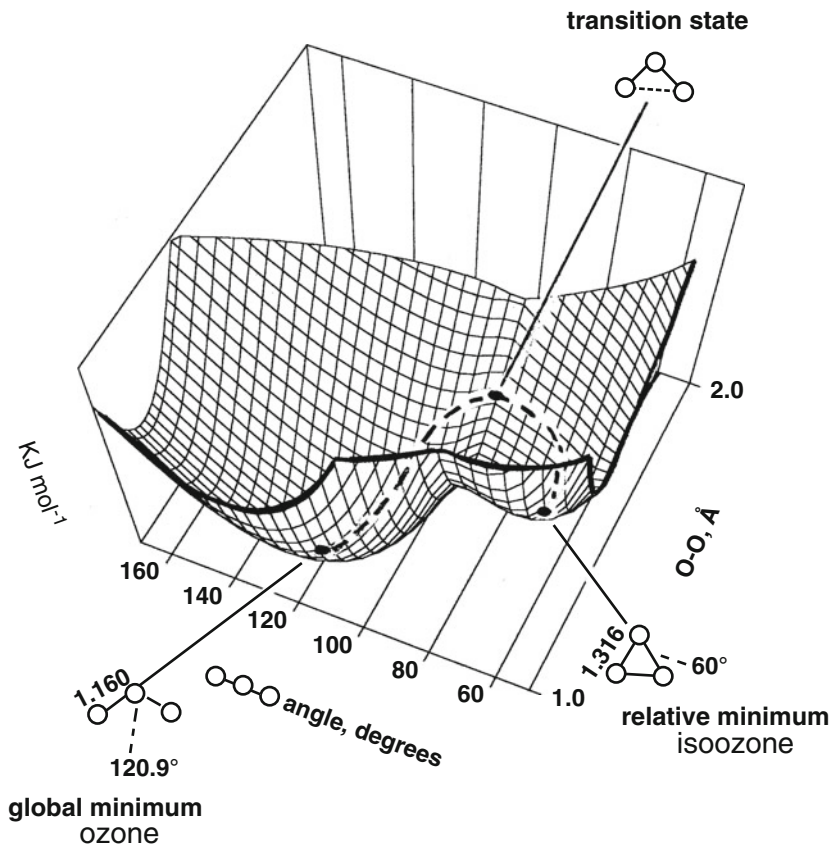
Fig. 2.7 The ozone/isoozone potential energy surface (calculated by the AM1 method; Chap. 6), a 2D surface in a 3D diagram. The *dashed line* on the surface is the reaction coordinate (intrinsic reaction coordinate, IRC). A slice through the reaction coordinate gives a 1D "surface" in a 2D diagram. The diagram is not meant to be quantitatively accurate
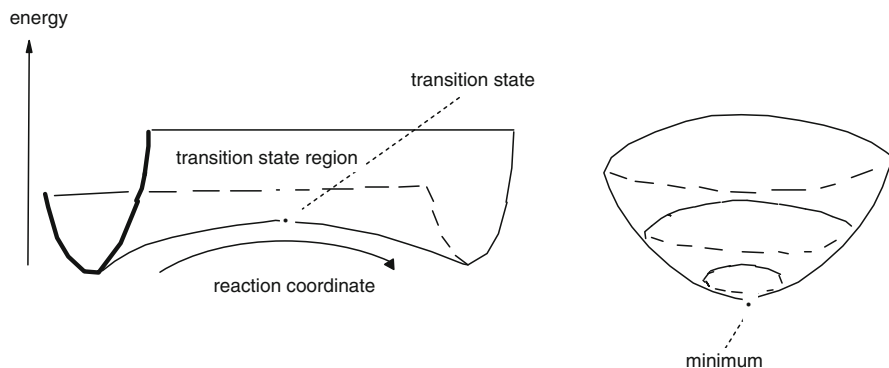
Fig. 2.8 A transition state or saddle point and a minimum. At both the transition state and the minimum $\partial E/\partial q = 0$ for all geometric coordinates q (along all directions). At the transition state $\partial E^2/\partial q^2 < 0$ for $q =$ the reaction coordinate and > 0 for all other q (along all other directions). At a minimum $\partial E^2/\partial q^2 > 0$ for all q (along all directions)

it is a minimum. This is a characteristic of a saddle-shaped surface, and the transition state itself is called a *saddle point* (Fig. 2.8). The saddle point lies at the "center" of the saddle-shaped region and is, like a minimum, a stationary point, since the PES at that point is parallel to the plane defined by the geometry parameter axes: we can see that a marble placed (precisely) there will balance. Mathematically, minima and saddle points differ in that although both are stationary points (they have zero first derivatives; Eq. 2.1), a minimum is a minimum in all directions, but a saddle point is a maximum along the reaction coordinate and a minimum in all other directions (examine Fig. 2.8). Recalling that minima and maxima can be distinguished by their second derivatives, we can write:

For a minimum

$$\frac{\partial^2 E}{\partial q^2} > 0 \qquad (*2.2)$$

for all q.

For a transition state

$$\frac{\partial^2 E}{\partial q^2} > 0 \qquad (*2.3)$$

for all q, *except along the reaction coordinate*, and

$$\frac{\partial^2 E}{\partial q^2} < 0 \qquad (*2.4)$$

along the reaction coordinate.

   The distinction is sometimes made between a *transition state* and a *transition structure* [4]. Strictly speaking, a transition *state* is a thermodynamic concept, a member of an ensemble which is in a kind of equilibrium with the reactants in Eyring's[1] transition-state theory [5]. Since equilibrium constants are determined by free energy differences, the transition state species is logically a free energy maximum along the reaction coordinate, in so far as a single species can be considered representative of the ensemble. This species is also often (but not always [5]) also called an activated complex, a term apparently used more in experimental kinetics. A transition *structure*, in strict usage, is the saddle point (Fig. 2.8) on a theoretically calculated (eg Fig. 2.7) PES. Normally such a surface is drawn (conceptually anyway) through a set of points each of which represents the enthalpy (in this context the potential energy) of a molecular species at a certain geometry; recall that free energy differs from enthalpy by temperature times entropy. The transition structure, the point you "see" when you look at a figure like Fig. 2.7, is thus a saddle point on an enthalpy surface. The energy of each of the calculated points on a PES does not normally include vibrational energy, which by standard calculations is meaningful only for stationary points (Sect. 2.5). In fact, however, any molecular assemblage, stationary or not, has zero point vibrational energy, even at even at 0 K. The usual calculated PES is thus a hypothetical, somewhat physically unrealistic surface in that it neglects vibrational energy, but it should qualitatively, and usually even semiquantitatively, resemble a vibrationally-corrected one since in considering *relative* enthalpies ZPEs commonly at least roughly cancel. In accurate work ZPEs are calculated for stationary points and added to the "frozen-nuclei" energy in an attempt to give improved relative energies; at 0 K these represent enthalpy differences and thus, at this temperature where entropy is zero, free energy differences too. It is also routinely possible to calculate free energies of stationary points at, say, room temperature (Chap. 5, Sect. 5.5.2). This provides theoretically sound energy differences for calculating activation and reaction energies at temperatures above 0 K. For more on energy calculations, (see Chap. 5, Sect. 5.5.2). Many chemists do not routinely distinguish between the terms transition state and transition structure, and in this book the commoner term, transition state, is used. Unless indicated otherwise, it will mean a calculated saddle point species with one imaginary frequency (Sect. 2.5) and "known" (calculated) free energy, normally at standard temperature, 298 K.

   The geometric parameter corresponding to the reaction coordinate is usually a composite of several parameters (bond lengths, angles and dihedrals), although for some reactions one two may predominate. In Fig. 2.7, the reaction coordinate is a composite of the O–O bond length and the O–O–O bond angle.

---

[1] H Eyring, American chemist. Born Colonia Juarárez, Mexico, 1901. Ph.D. University of California, Berkeley, 1927. Professor Princeton, University of Utah. Known for his work on the theory of reaction rates and on potential energy surfaces. Died Salt Lake City, Utah, 1981.
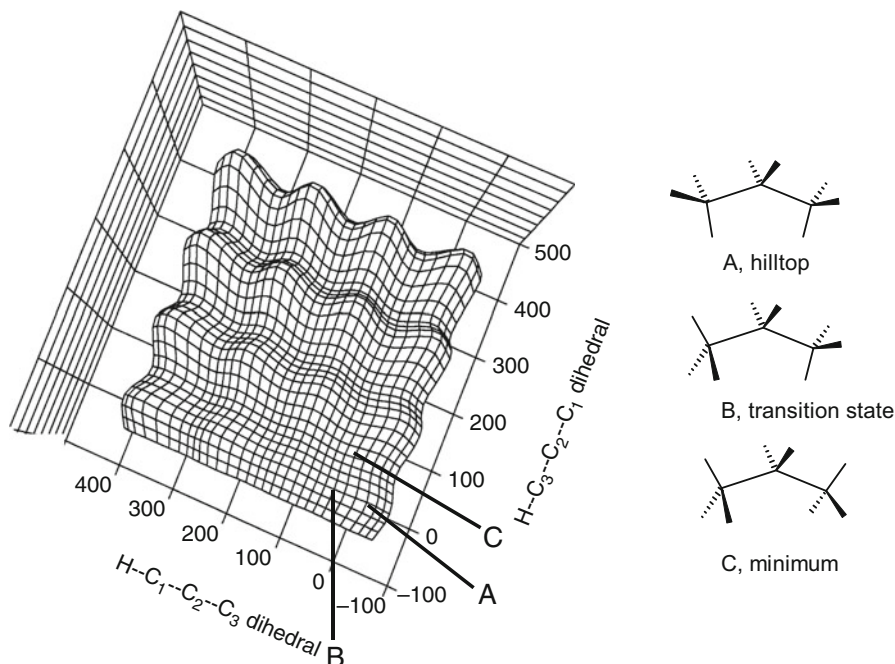
Fig. 2.9 The propane potential energy surface as the two HCCC dihedrals are varied (calculated by the AM1 method, Chap. 6). Bond lengths and angles were not optimized as the dihedrals were varied, so this is not a relaxed PES; however, changes in bond lengths and angles from one propane conformation to another are small, and the relaxed PES should be very similar to this one

A saddle point, the point on a PES where the second derivative of energy with respect to one and only one geometric coordinate (possibly a composite coordinate) is negative, corresponds to a transition state. Some PES's have points where the second derivative of energy with respect to more than one coordinate is negative; these are *higher-order saddle points* or *hilltops*: for example, a *second*-order saddle point is a point on the PES which is a maximum along *two* paths connecting stationary points. The propane PES, Fig. 2.9, provides examples of a minimum, a transition state and a hilltop–a *second*-order saddle point in this case. Figure 2.10 shows the three stationary points in more detail. The "doubly-eclipsed" conformation, A, in which there is eclipsing as viewed along the C1–C2 and the C3–C2 bonds (the dihedral angles are 0° viewed along these bonds) is a second-order saddle point because single bonds do not like to eclipse single bonds and rotation about the C1–C2 and the C3–C2 bonds will remove this eclipsing: there are *two* possible directions along the PES which lead, without a barrier, to lower-energy regions, i.e. changing the H–C1/C2–C3 dihedral and changing the H–C3/C2–C1 dihedral. Changing *one* of these leads to a "singly-eclipsed" conformation (B) with only one offending eclipsing CH_3–CH_2 arrangement, and this is a first-order saddle point, since there is now only *one* direction along the PES which leads to relief of

sawhorse drawings   Newman projections

hiltop

A

total of 6 eclipsing interactions

3 eclipsing interactions
(CH/CC, CH/CH, CH/CH)

3 eclipsing interactions
(CH/CC, CH/CH, CH/CH)

transition state

B

total of 3 eclipsing interactions

no eclipsing interactions

3 eclipsing interactions
(CH/CC, CH/CH, CH/CH)

minimum

C

no eclipsing interactions

no eclipsing interactions

no eclipsing interactions

Fig. 2.10 The stationary points on the propane potential energy surface. Hydrogens at the end of
CH bonds are omitted for clarity

the eclipsing interactions (rotation around C3–C2). This route gives a conformation
C which has no eclipsing interactions and is therefore a minimum. There are no
lower-energy structures on the C_3H_8 PES and so C is the global minimum.

The geometry of propane depends on more than just two dihedral angles, of
course; there are several bond lengths and bond angles and the potential energy

will vary with changes in all of them. Figure 2.9 was calculated by varying in modest steps only the two dihedral angles associated with the H–C–C–H bonds, keeping the other geometrical parameters the same as they are in the all-staggered conformation. If at every point on the dihedral/dihedral grid all the other parameters (bond lengths and angles) had been optimized (adjusted to give the lowest possible energy, for that particular calculational method; Sect. 2.4), the result would have been a *relaxed* PES. In Fig. 2.9 this was not done, but because bond lengths and angles change only slightly with changes in dihedral angles the PES would not be altered much, while the time required for the calculation (for the *potential energy surface scan*) would have been longer. Figure 2.9 is a nonrelaxed or rigid PES, albeit not very different, in this case, from a relaxed one.

Chemistry is essentially the study of the stationary points on potential energy surfaces: in studying more or less stable molecules we focus on minima, and in investigating chemical reactions we study the passage of a molecule from a minimum through a transition state to another minimum. There are four known forces in nature: the gravitational force, the strong and the weak nuclear forces, and the electromagnetic force. Celestial mechanics studies the motion of stars and planets under the influence of the gravitational force and nuclear physics studies the behaviour of subatomic particles subject to the nuclear forces. Chemistry is concerned with aggregates of nuclei and electrons (with molecules) held together by the electromagnetic force, and with the shuffling of nuclei, followed by their obedient retinue of electrons, around a potential energy surface under the influence of this force. A potential energy surface might be called a reactivity surface.

The concept of the chemical potential energy surface apparently originated with R. Marcelin [6]: in a dissertation-long paper (111 pages) which is somehow not well-known he laid the groundwork for transition-state theory 20 years before the much better-known work of Eyring [5, 7]. The importance of Marcelin's work is acknowledged by Rudolph Marcus in his Nobel Prize (1992) speech, where he refers to "…Marcelin's classic 1915 theory which came within one small step of the transition state theory of 1935." The paper was published the year after the death of the author, who was killed in World War I, as shown by the footnote "Tué à l'ennemi en sept 1914". The first potential energy surface was calculated in 1931 by Eyring and Polanyi,[2] using a mixture of experiment and theory [8].

---

[2] Michael Polanyi, Hungarian-British chemist, economist, and philosopher. Born Budapest 1891. Doctor of medicine 1913, Ph.D. University of Budapest, 1917. Researcher Kaiser-Wilhelm Institute, Berlin, 1920–1933. Professor of chemistry, Manchester, 1933–1948; of social studies, Manchester, 1948–1958. Professor Oxford, 1958–176. Best known for book "Personal Knowledge", 1958. Died Northampton, England, 1976.

Our treatment of a PES can be subjected to a more sophisticated examination, by examining changes in the direction and curvature of the reaction path, the reaction path Hamiltonian (RPH) and the united reaction valley approach (URVA) [9]; these can reveal deeper detail about a reaction than one obtains only from the energies of the various species (as in the simple treatment of Sect. 2.4).

The potential energy surface for a chemical reaction has just been presented as a saddle-shaped region holding a transition state which connects wells containing reactant(s) and products(s) (which species we call the reactant and which the product is inconsequential here). This picture is immensely useful, and may well apply to the great majority of reactions. However, for some reactions it is deficient. Carpenter has shown with molecular dynamics that in some cases a reactive intermediate does not tarry in a PES well and then surmount a barrier [10]. Rather it appears to scoot over a plateau-shaped region of the PES, and retaining a memory ("dynamical information") of the atomic motions it acquired when it was formed, diverges along, say, two paths ("bifurcates"). When this happens there are two intermediates with the same crass geometry, but different atomic motions, leading to different products. The details are subtle, and the interested reader is commended to the relevant literature [10]. Such a bifurcating PES has been implicated in the biosynthesis of the natural terpenoid abietic acid [11]. Even a conventional PES, with minima connected by transition states, can exhibit surprises, as in the case of a reaction preferring to go over the higher-rather than the lower-energy transition state (because of quantum-mechanical tunnelling) [12]. Molecular dynamics (above and Chap. 1, Sects. 1.2 and 1.3) is mentioned little more than peripherally in this book, but as indicated it has revealed unexpected features of the traversing of potential energy surfaces by reacting molecules; further, it offers the possibility of providing an intuitive feeling (literally) for the movement of molecules on this surface, by allowing the chemist to experience by interactive feedback the molecular forces experienced by the molecules [13].

2.3   The Born-Oppenheimer Approximation

A potential energy surface is a plot of the energy of a collection of nuclei and electrons against the geometric coordinates of the nuclei—essentially a plot of molecular energy vs. molecular geometry (or it may be regarded as the mathematical equation that gives the energy as a function of the nuclear coordinates). The nature (minimum, saddle point or neither) of each point was discussed in terms of the response of the energy (first and second derivatives) to changes in nuclear coordinates. But if a molecule is a collection of nuclei and electrons why plot energy vs. *nuclear* coordinates—why not against *electron* coordinates? In other words, why are nuclear coordinates the parameters that define molecular geometry? The answer to this question lies in the Born-Oppenheimer approximation.
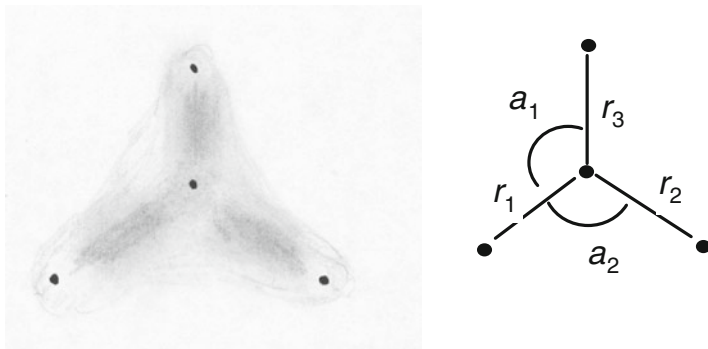
Fig. 2.11 The nuclei in a molecule see a time-averaged electron cloud. The nuclei vibrate about equilibrium points which define the molecular geometry; this geometry can be expressed simply as the nuclear Cartesian coordinates, or alternatively as bond lengths and angles r and a here) and dihedrals, i.e. as internal coordinates. As far as size goes, the experimentally determined van der Waals surface encloses about 98 percent of the electron density of a molecule

Born[3] and Oppenheimer[4] showed in 1927 [14] that to a very good approximation the nuclei in a molecule are stationary with respect to the electrons. This is a qualitative expression of the principle; mathematically, the approximation states that the Schrödinger equation (Chap. 4) for a molecule may be separated into an electronic and a nuclear equation. One consequence of this is that all (!) we have to do to calculate the energy of a molecule is to solve the *electronic* Schrödinger equation and then add the electronic energy to the internuclear repulsion (this latter quantity is trivial to calculate) to get the total internal energy (see Chap. 4, Sect. 4.4.1). A deeper consequence of the Born-Oppenheimer approximation is that a molecule has a shape.

The nuclei see the electrons as a smeared-out cloud of negative charge which binds them in fixed relative positions and which defines the (somewhat fuzzy) surface of the molecule; a standard molecular surface, corresponding to the size as determined experimentally, eg by X-ray diffraction, encloses about 98 % of the electron density [15] (see Fig. 2.11). Because of the rapid motion of the electrons compared to the nuclei the "permanent" geometric parameters of the molecule are the *nuclear* coordinates. The energy (and the other properties) of a molecule is

---

[3] Max Born, German-British physicist. Born in Breslau (now Wroclaw, Poland), 1882, died in Göttingen, 1970. Professor Berlin, Cambridge, Edinburgh. Nobel prize, 1954. One of the founders of quantum mechanics, originator of the probability interpretation of the (square of the) wavefunction (Chap. 4).

[4] J. Robert Oppenheimer, American physicist. Born in New York, 1904, died in Princeton 1967. Professor California Institute of Technology. Fermi award for nuclear research, 1963. Important contributions to nuclear physics. Director of the Manhattan Project 1943–1945. Victimized as a security risk by senator Joseph McCarthy's Un-American Activities Committee in 1954. Central figure of the eponymous PBS TV series (Oppenheimer: Sam Waterston).

The H_3^+ cation: 3 protons, 2 electrons

Definite geometry

No definite geometry
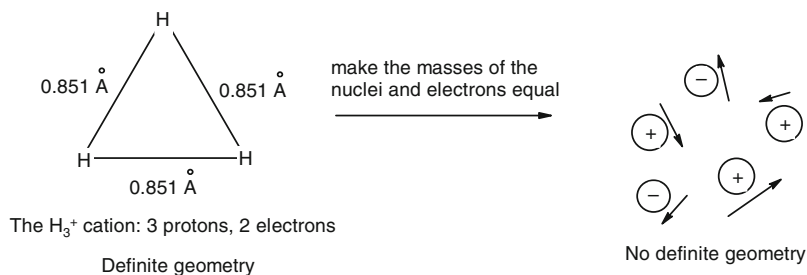
Fig. 2.12 A molecule has a definite shape because unlike the electrons, the nuclei are (relatively) stationary (since they are much more massive). If the masses of the nuclei and the electrons could be made equal, the distinction in lethargy would be lost, and the molecular geometry would dissolve

a *function* of the electron coordinates ($E = \psi$ (*x, y, z* of each electron); Chap. 5, Sect. 5.2), but depends only *parametrically* on the nuclear coordinates, ie for each geometry 1, 2, ... there is a particular energy: $E_1 = \psi_1$ (*x, y, z*...), $E_2 = \psi_2$ (*x, y, z*...); cf. x^n, which is a function of *x* but depends only parametrically on the particular *n*. Actually, the nuclei are not stationary, but execute vibrations of small amplitude about equilibrium positions; it is these equilibrium positions that we mean by the "fixed" nuclear positions. It is only because it is meaningful to speak of (almost) fixed nuclear coordinates that the concepts of molecular geometry or shape and of the PES are valid [16]. The nuclei are much more sluggish than the electrons because they are much more massive (a hydrogen nucleus is about 2000 more massive than an electron).

Consider the molecule H_3^+, made up of three protons and two electrons. Ab initio calculations assign it the geometry shown in (Fig. 2.12). The equilibrium positions of the nuclei (the protons) lie at the corners of an equilateral triangle and H_3^+ has a definite shape. But suppose the protons were replaced by positrons, which have the same mass as electrons. The distinction between nuclei and electrons, which in molecules rests on mass and not on some kind of charge chauvinism, would vanish. We would have a quivering cloud of flitting particles to which a shape could not be assigned on a macroscopic time scale.

A calculated PES, which we might call a Born-Oppenheimer surface, is normally the set of points representing the geometries, and the corresponding energies, of a collection of atomic nuclei; the electrons are taken into account in the calculations as needed to assign charge and multiplicity (multiplicity is connected with the number of unpaired electrons). Each point corresponds to a set of stationary nuclei, and in this sense the surface is somewhat unrealistic (see Sect. 2.5).

Two reservations should be stated about the Born-Oppenheimer approximation: first, it appears that there is actually no rigorous proof of its validity, and second, although it does usually work, there are cases where its use is inappropriate.

Regarding the alleged proof [14], Sutcliffe shows in an amusing (in the opening paragraphs) yet mathematically formidable paper that when the problem is "reformulated in a precise manner and re-examined" the mathematical description of the terms describing the coupling between nuclear and electronic motion is "rather elusive and their theoretical status often problematic." The coupling problem "is, at the moment, without a sensible solution and that is an area where much future work can and must be done" [17]. Nineteen years later, the conclusion seemed the same, although the utility of the potential energy surface concept was conceded:

> The clamped-nuclei Hamiltonian and the associated notion of PES are crucial to the method; on the other hand PES make no appearance in the formally exact description based on spectral projection, so it is hard to claim any fundamental role for Potential Energy Surfaces in the quantum mechanics of molecules. This is not of course, to ignore the important role of PES in approximate calculations and their role in interpreting experimental results. It is simply to place PES properly in relation to quantum theory. [18].

Practising computational chemists have rarely claimed that their calculations are "formally exact", but anyone familiar with the literature knows that on occasion calculations within the Born-Oppenheimer rubric can be highly accurate.

The Born-Oppenheimer approximation is inappropriate in some cases. One is the reaction mentioned above in which the higher-energy transition state was preferred [12]. Another is illustrated by a study of the vibrational levels of ClH_2 (*sic*) and the $Cl + H_2$ reaction; although the results were good with Born-Oppenheimer, they improved about tenfold when this approximation was removed [19]. Another paper on comparing calculations with and without the approximation has a section entitled, "...Corrections to the BO Energy for Molecules Containing up to Three Nuclei", and focusses on H_3^+, hinting at the magnitude of the task of going beyond Born-Oppenheimer for any but the smallest molecules [20]. A study applying non-Born-Oppenheimer calculations (augmented with relativity) to dissociation energies was limited to H_2, HD, D_2, T_2, and HeH^+ [21]. That the approximation would be most approximate for cases where the nuclei are protons or He^{2+} is understandable given that it is these nuclei that most closely resemble the electron in mass. One experiment on $H + H_2$ replaced the H atom with muonium, in which an electron orbits not a proton but rather a positive muon, which is only 206 times heavier than an electron, versus the 1836 proton-electron ratio [22]. This is a remarkable experimental tour de force, but is somewhat removed from standard chemistry.

The possibility of calculating highly accurate potential energy surfaces, and practical approaches to this formidable task, have been examined [23]. Although modern 3D graphics programs render excellent pictures of potential energy surfaces on the screen and on the page (as any observant reader of current chemistry journals will attest), some might wish an actual 3D model; the advent of 3D printing has made possible the translation of digital data beyond the printed page [24].

2.4   Geometry Optimization

The characterization (the "location" or "locating") of a stationary point on a PES, that is, demonstrating that the point in question exists and calculating its geometry and energy, is a *geometry optimization*. The stationary point of interest might be a minimum, a transition state, or, occasionally, a higher-order saddle point. Locating a minimum is often called an energy minimization or simply a minimization, and locating a transition state is often referred to specifically as a transition state optimization. Geometry optimizations are done by starting with an input structure that is believed to resemble (the closer the better) the desired stationary point and submitting this plausible structure to a computer algorithm that systematically changes the geometry until it has found a stationary point. The curvature of the PES at the stationary point, ie the second derivatives of energy with respect to the geometric parameters (Sect. 2.2) may then be determined (Sect. 2.5) to characterize the structure as a minimum or as some kind of saddle point.

Let us consider a problem that arose in connection with an experimental study. Propanone (acetone) was subjected to ionization followed by neutralization of the radical cation, and the products were frozen in an inert matrix and studied by IR spectroscopy [25]. The spectrum of the mixture suggested the presence of the enol isomer of propanone, 1-propen-2-ol:
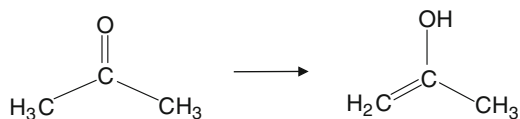
Reaction 2

To confirm (or refute) this the IR spectrum of the enol might be calculated (see Sect. 2.5 and the discussions of the calculation of IR spectra in subsequent chapters). But which conformer should one choose for the calculation? Rotation about the C–O and C–C bonds creates six plausible stationary points (Fig. 2.13), and a PES scan (Fig. 2.14) indicated that there are indeed six such species. Examination of this PES shows that the global minimum is structure **1** and that there is a relative minimum corresponding to structure **3**. Geometry optimization starting from an input structure resembling **1** gave a minimum corresponding to **1**, while optimization starting from a structure resembling **3** gave another, higher-energy minimum, resembling **3**. Transition-state optimizations starting from appropriate structures yielded the transition states **2**, **4** and **5**, and requesting optimization to a "second-order transition state" gave the hilltop **6**, with two imaginary frequencies; these six stationary points were all characterized as minima, transition states or hilltops by second-derivative calculations (Sect. 2.5). Figure 2.15 is a projection onto two dimensions of the surface in Fig. 2.14, with the vertical axis representing the energies of the fully optimized structures of Fig. 2.13; this is a typical representation of a PES, and shows clearly the interrelationships of the various stationary
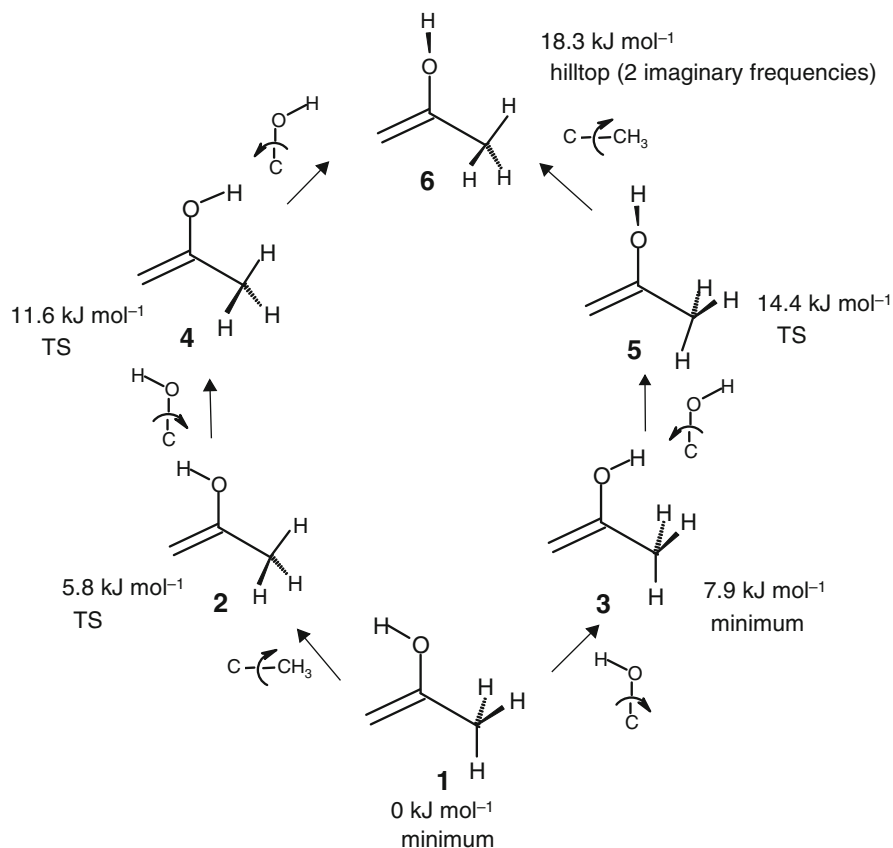
Fig. 2.13 The plausible stationary points on the propenol potential energy surface according to AM1 geometry optimization-frequency calculations (the frequencies show if a stationary point is a minimum, a transition state, or a hilltop). A PES scan (Fig. 2.14) indicated that **1** is the global minimum and **3** is a relative minimum, while **2**, **4** and **5** are transition states and **6** is a hilltop; this is confirmed (at the AM1 level at least) by these calculations. Constructing input structures corresponding to these points on the surface, guided by the dihedral angles, then optimizing, gave the AM1 relative energies for **1–6** (these are room-temperature free energies relative to **1** set as zero).The *arrows* merely show the structural relationships of one-step (rotation about one bond, as indicated) conversion of one species into another, not connectivity on a PES – for example, **2** is not a TS linking **1** and **4**; such reactivity relationships are shown in Figs. 2.14 and 2.15

points. The calculated IR spectrum of **1** (using the ab initio HF/6–31G* method–chapter 5) was in excellent agreement with the observed spectrum of the putative propenol.

This illustrates a general principle: the optimized structure one obtains is that closest in geometry on the PES to the input structure (Fig. 2.16). If we wish to be sure we have found the *global* minimum we must (except for very simple or very rigid molecules) search the potential energy surface. There are algorithms that will do this in an attempt to find the lowest-energy minimum, but there appears to be in
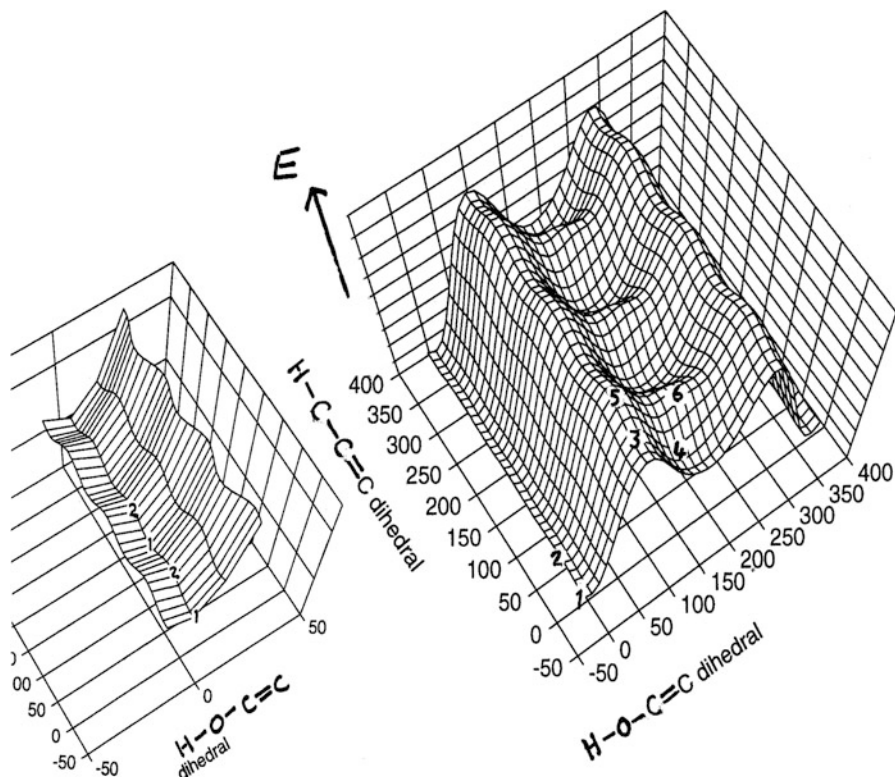
Fig. 2.14 The 1-propen-2-ol potential energy surface (calculated by the AM1 method), the result of a scan in which the H–O–C=C and H–C–C=C dihedral angles were varied. Compare with Figs. 2.13 and 2.15

general no way to *guarantee* that the lowest-energy structure one finds is indeed the global minimum. For concise reviews of this difficult problem see Jensen (six methods) [26] and Levine (nine methods) [27]. These draw attention to the fact that the fairly small, but floppy, unbranched tridecane ($C_{13}H_{28}$) has 59 049 conformers, while for the slightly bigger but more rigid cycloheptadecane ($C_{17}H_{34}$) 20 469 were found. For tridecane a systematic dihedral-stepping search is possible, and 59 049 is presumably the actual number of conformers with the lowest-energy one being the global minimum, but a perfectly systematic search seems to be not feasible for a cyclic molecule (which present special problems) of the size of cycloheptadecane, and, conceivably, the true global minimum eluded this search. Of course we may not be interested in the global minimum; for example, if we wish to study the cyclic isomer of ozone (Sect. 2.2) we will use as input an equilateral triangle structure, probably with bond lengths about those of an O–O single bond.

In the propenol example, the PES scan suggested that to obtain the global minimum we should start with an input structure resembling **1**, but the exact values of the various bond lengths and angles were unknown (the exact values of even the
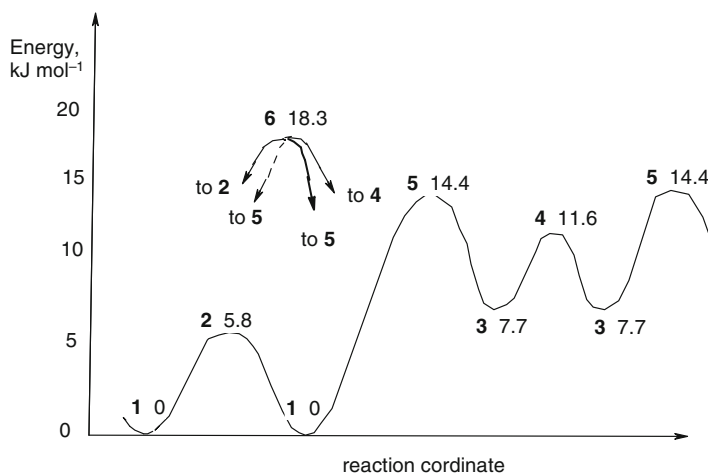
Fig. 2.15 The 1-propen-2-ol potential energy surface, drawn from the result of the geometry optimizations-frequency calculations of Fig. 2.13. The energies are room-temperature free energies relative to **1** set as zero. The reaction coordinate, which is qualitative here, is essentially a composite of the H–O–C=C and H–C–C=C dihedral angles since other geometry parameters, like bond lengths, should change only slightly with conformation. The transition states **2** and **4** are for degenerate reactions, connecting "identical" minima, which could be distinguished by labelling a CH$_3$ hydrogen. The hilltop **6** connects transition states **2** and **4** and the "identical" transition states **5** and **5**
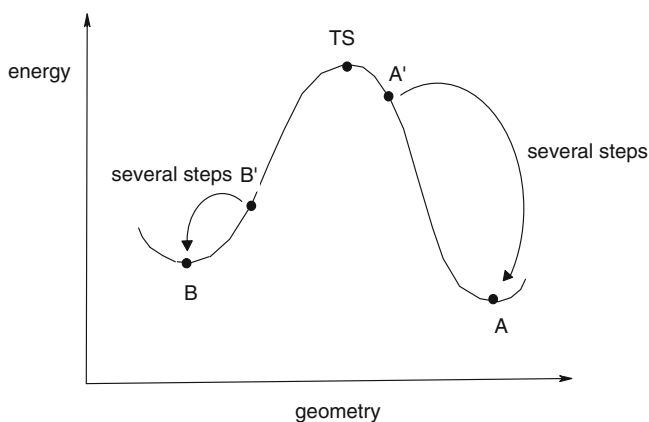
Fig. 2.16 Geometry optimization to a minimum gives the minimum closest to the input structure. The input structure A′ is moved toward the minimum A, and B′ toward B. To locate a transition state a special algorithm is usually used: this moves the initial structure A′ toward the transition state TS. Optimization to each of the stationary points would probably actually require several steps (see Fig. 2.17)
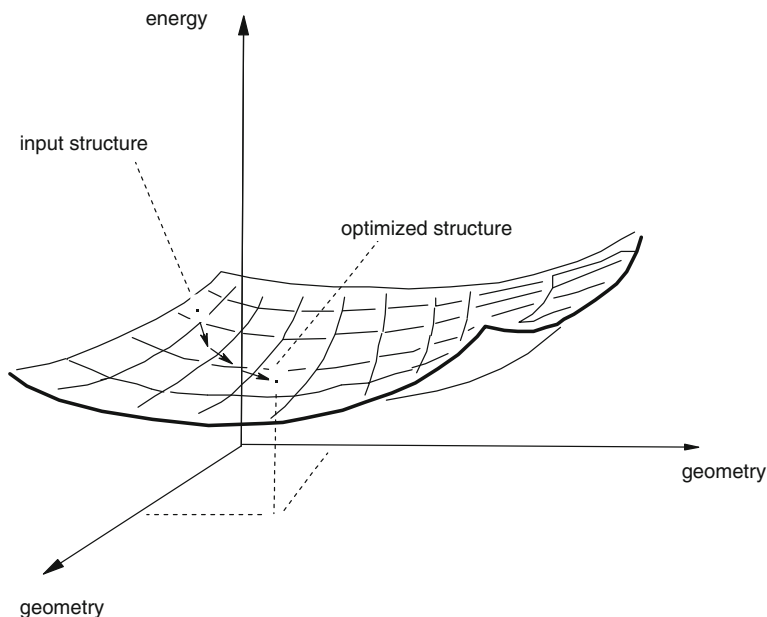
Fig. 2.17 An efficient optimization algorithm knows approximately in which direction to move and how far to step, in an attempt to reach the optimized structure in relatively few (commonly about 5–10) steps

dihedrals was not known with certainty, although general chemical knowledge made H–O–C–C = H–C-C=C = 0° seem plausible). The actual creation of input structures is usually done nowadays with an interactive mouse-driven program, in much the same spirit that one constructs plastic models or draws structures on paper. An older alternative is to specify the geometry by defining the various bond lengths, angles and dihedrals, i.e. by using a so-called Z-matrix (internal coordinates).

To move along the PES from the input structure to the nearest minimum is obviously trivial on the 1-dimensional PES of a diatomic molecule: one simply changes the bond length till that corresponding to the lowest energy is found. On any other surface, efficient geometry optimization requires a sophisticated algorithm. One would like to know in which direction to move, and how far in that direction (Fig. 2.17). It is not possible, in general, to go from the input structure to the proximate minimum in just one step, but modern geometry optimization algorithms commonly reach the minimum in about ten steps, given a reasonable input geometry. The most widely-used algorithms for geometry optimization [28] use the first and second derivatives of the energy with respect to the geometric parameters. To get a feel for how this works, consider the simple case of a 1-dimensional PES, as for a diatomic molecule (Fig. 2.18). The input structure is at the point $P_i(E_i, q_i)$ and the proximate minimum, corresponding to the optimized structure being sought, is at the point $P_o(E_o, q_o)$. Before the optimization has been
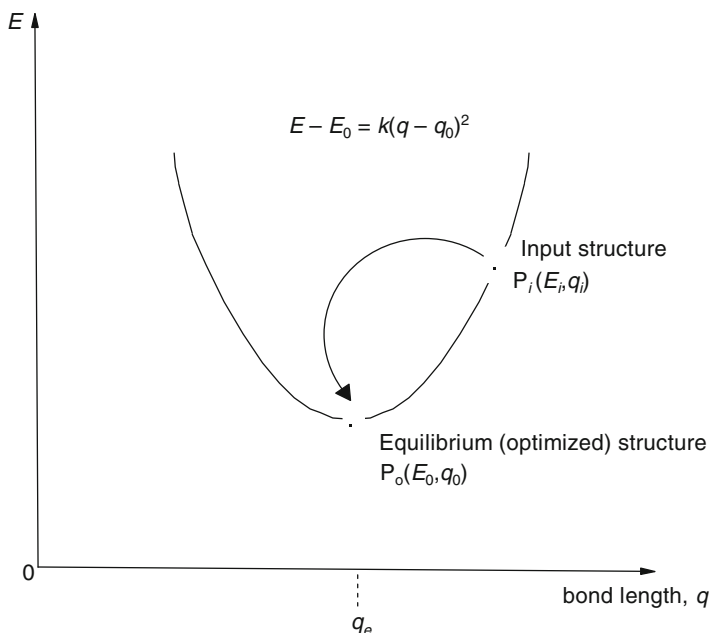
Fig. 2.18 The potential energy of a diatomic molecule near the equilibrium geometry is approximately a quadratic function of the bond length. Given an input structure (i.e. given the bond length q_i), a simple algorithm would enable the bond length of the optimized structure to be found in one step, if the function were strictly quadratic

carried out the values of E_o and q_o are of course unknown. If we assume that near a minimum the potential energy is a quadratic function of q, which is a fairly good approximation, then

$$E - E_o = k(q - q_o)^2 \qquad (2.5)$$

At the input point

$$(dE/dq)_i = 2k(q_i - q_o) \qquad (2.6)$$

At all points

$$d^2E/dq^2 = 2k(= \text{force constant}) \qquad (2.7)$$

From (2.6) and (2.7),

$$(dE/dq)_i = \left(d^2E/dq^2\right)(q_i - q_o) \qquad (2.8)$$

and

$$q_{\rm o} = q_{\rm i} - (dE/dq)_{\rm i}/(d^2E/dq^2) \tag{2.9}$$

Equation 2.9 shows that if we know $(dE/dq)_{\rm i}$, the slope or gradient of the PES at the point of the initial structure, (d^2E/dq^2), the curvature of the PES (which for a quadratic curve $E(q)$ is independent of q) and $q_{\rm i}$, the initial geometry, we can calculate $q_{\rm o}$, the optimized geometry. The second derivative of potential energy with respect to geometric displacement is the force constant for motion along that geometric coordinate; as we will see later, this is an important concept in connection with calculating vibrational spectra.

For multidimensional PES's, i.e. for almost all real cases, far more sophisticated algorithms are used, and several steps are needed since the curvature is not exactly quadratic. The first step results in a new point on the PES that is (probably) closer to the minimum than was the initial structure. This new point then serves as the initial point for a second step toward the minimum, etc. Nevertheless, most modern geometry optimization methods do depend on calculating the first and second derivatives of the energy at the point on the PES corresponding to the input structure. Since the PES is not strictly quadratic, the second derivatives vary from point to point and are updated as the optimization proceeds.

In the illustration of an optimization algorithm using a diatomic molecule, Eq. 2.9 referred to the calculation of first and second derivatives with respect to bond length, which latter is an *internal coordinate* (inside the molecule). Optimizations are actually commonly done using Cartesian coordinates x, y, z. Consider the optimization of a triatomic molecule like water or ozone in a Cartesian coordinate system. Each of the three atoms has an x, y and z coordinate, giving 9 geometric parameters, $q_1, q_2, \ldots, q_9$; the PES would be a 9-dimensional hypersurface on a 10D graph. We need the first and second derivatives of E with respect to each of the 9 q's, and these derivatives are manipulated as matrices. Matrices are discussed in Chap. 4, Sect. 4.3.3; here we need only know that a matrix is a rectangular array of numbers that can be manipulated mathematically, and that they provide a convenient way of handling sets of linear equations. The first-derivative matrix, the gradient matrix, for the input structure can be written as a column matrix

$$\mathbf{g}_{\rm i} = \begin{pmatrix} (\partial \boldsymbol{E}/\partial \boldsymbol{q}_1)_i \\ (\partial \boldsymbol{E}/\partial \boldsymbol{q}_2)_i \\ \vdots \\ (\partial \boldsymbol{E}/\partial \boldsymbol{q}_9)_i \end{pmatrix} \tag{2.10}$$

and the second-derivative matrix, the force constant matrix, is

$$\mathbf{H} = \begin{pmatrix} \partial^2 E/\partial q_1 \partial q_1 & \partial^2 E/\partial q_1 \partial q_2 & \dots & \partial^2 E/\partial q_1 \partial q_9 \\ \partial^2 E/\partial q_2 \partial q_1 & \partial^2 E/\partial q_2 \partial q_2 & \dots & \partial^2 E/\partial q_2 \partial q_9 \\ \vdots & \vdots & \dots & \vdots \\ \partial^2 E/\partial q_9 \partial q_1 & \partial^2 E/\partial q_9 \partial q_2 & \dots & \partial^2 E/\partial q_9 \partial q_9 \end{pmatrix} \quad (2.11)$$

The force constant matrix is called the *Hessian*.[5] The Hessian is particularly important, not only for geometry optimization, but also for the characterization of stationary points as minima, transition states or hilltops, and for the calculation of IR spectra (Sect. 2.5). In the Hessian $\partial^2 E/\partial q_1 q_2 = \partial^2 E/\partial q_2 q_1$, as is true for all well-behaved functions, but this systematic notation is preferable: the first subscript refers to the row and the second to the column. The geometry coordinate matrices for the initial and optimized structures are

$$\mathbf{q_i} = \begin{pmatrix} q_{i1} \\ q_{i2} \\ \vdots \\ q_{i9} \end{pmatrix} \quad (2.12)$$

and

$$\mathbf{q_o} = \begin{pmatrix} q_{o1} \\ q_{o2} \\ \vdots \\ q_{o9} \end{pmatrix} \quad (2.13)$$

The matrix equation for the general case can be shown to be:

$$\mathbf{q_o} = \mathbf{q_i} - \mathbf{H}^{-1}\mathbf{g_i} \quad (2.14)$$

which is analogous to Eq. 2.9 for the optimization of a diatomic molecule, which could be written

$$q_o = q_i - \left(d^2 E/dq^2\right)^{-1}(dE/dq)_i$$

For *n* atoms we have 3*n* Cartesians; $\mathbf{q_o}, \mathbf{q_i}$ and $\mathbf{g_i}$ are $3n \times 1$ column matrices and $\mathbf{H}$ is a 3n × 3n square matrix; multiplication by the inverse of $\mathbf{H}$ rather than division by $\mathbf{H}$ is used because matrix division is not defined. Equation 2.14 shows that for an efficient geometry optimization we need an initial structure (for $\mathbf{q_i}$), initial gradients (for $\mathbf{g_i}$) and second derivatives (for $\mathbf{H}$). With an initial "guess" for the geometry (for example from a model-building program followed by molecular mechanics) as input, gradients can be readily calculated analytically (from the derivatives of the

---

[5] Ludwig Otto Hesse, 1811–1874, German mathematician.

molecular orbital coefficients and the derivatives of certain integrals). An approximate initial Hessian is often calculated from molecular mechanics (Chap. 3). Since the PES is not really exactly quadratic, the first step does not take us all the way to the optimized geometry, corresponding to the matrix $\mathbf{q_o}$. Rather, we arrive at $\mathbf{q_1}$, the first calculated geometry; using this geometry a new gradient matrix and a new Hessian are calculated (the gradients are calculated analytically and the second derivatives are updated using the changes in the gradients–see below). Using $\mathbf{q_1}$ and the new gradient and Hessian matrices a new approximate geometry matrix $\mathbf{q_2}$ is calculated. The process is continued until the geometry and/or the gradients (or with some programs possibly the energy) have ceased to change appreciably.

As the optimization proceeds the Hessian is updated by approximating each second derivative as a ratio of finite increments:

$$\frac{\partial^2 E}{\partial q_i \partial q_j} \approx \frac{\Delta \left(\partial E / \partial q_j \right)}{\Delta q_i} \tag{2.15}$$

i.e. as the change in the gradient divided by the change in geometry, on going from the previous structure to the latest one. Analytic calculation of second derivatives is relatively time-consuming and is not routinely done for each point along the optimization sequence, in contrast to analytic calculation of gradients. A fast lower-level optimization, for a minimum or a transition state, usually provides a good Hessian and geometry for input to a higher-level optimization [29]. Finding a transition state (i.e. optimizing an input structure to a transition state structure) is a more challenging computational problem than finding a minimum, as the characteristics of the PES at the former are more complicated than at a minimum: at the transition state the surface is a maximum in one direction and a minimum in all others, rather than simply a minimum in all directions. Nevertheless, modifications of the minimum-search algorithm enable transitions states to be located, albeit often with less ease than minima. The geometry optimization procedure just outlined is the Newton–Raphson method. Despite the relatively challenging tasks of calculating and inverting the Hessian, it is the probably the default optimization method in most programs. Jensen gives a detailed discussion of the algorithms for geometry optimization [30].

A recent (2015) paper presents a method of calculating geometries which, unlike those just mentioned, does not involve iterative refinement of a "guess" input [31]. In this method geometries were fitted to experimental rotational constants (microwave spectra) with the aid of ab initio vibration-rotation constants. The bond lengths from this are more accurate, except for diatomics, than those from experiment or high-level conventional ab initio geometry optimization. This is understandable since microwave spectra are very sensitive to molecular geometry. Results were reported only for 18 very small molecules, mostly triatomics.

In a recent method of exploring a PES, still under development, an algorithm generates from a reactant possible products and attempts to connect reactant and products in a one-step (elementary) reaction [32]. Products are generated from reactant by specifying the reactant as a *bond electron matrix* (this has no particular connection with the matrices described above for geometry optimization) and allowing a *reaction matrix* to act on this. The bond electron matrix is a square

symmetric matrix with element a_{ij} corresponding to atom i bonded to atom j; the value of the element is the number of covalent bonds between atom i and atom j, or for diagonal elements the number of valence electrons not involved in bonds. So row i specifies atom i, and the sum of the values for this row is the number of valence electrons which belong to that atom; for HOOH numbered 1, 2, 3, 4 row 2 would be 1 4 1 0. The *reaction matrix*, also a square symmetric matrix, is such that when added to the reactant matrix to generate a *product matrix* the total number of electrons is conserved and the product matrix corresponds to an isomeric species. Intermediates are optimized by molecular mechanics (Chap. 3) and appropriate optimization algorithms are invoked to help locate transition states. It may divert the reader to explore the matrix manipulation by which HOOH may generate HO(O)H, where a proton has migrated from one oxygen to the other. The method is said to require no human intervention and to work "fairly well" at discovering new elementary reaction steps. Akin to the electron matrix method in the goal (but not the mathematical details) of automating the exploration of reaction mechanisms is a "heuristics-guided" method [33]. Here electronic structure rules are used to automatically generate intermediates; these are then subjected to geometry optimization by a quantum-mechanical method, and pairs of plausibly related intermediates are automatically selected for a search for a connecting transition state. Searches based on stochastic (probabilistic) methods of locating conformations, rather than on straightforward systematic calculation of the result of torsional changes (as described for simple molecules like propane, Sect. 2.2) can use advanced techniques from computational physics [34]. The methods described in references [31–34] for exploring potential energy surfaces or optimizing geometries are at present (2016) novel, in contrast to the standard approach of optimizing "trial" structures and characterizing them (Sect. 2.5) by Hessian-calculated frequencies.

An incursion into chemistry of what one might have thought was pure, even rarefied, theoretical physics is the connection of reactivity with quantum entanglement. Entanglement is the puzzling connection that persists between particles (photons, electrons, atoms, molecules) that originate from the same event, causing one particle to appear to "know" instantaneously the result of a measurement on the other particle. This is of deep significance for a fundamental question in quantum mechanics, the existence and (if they exist) the nature of hidden variables [35]. Entanglement is relevant to chemical reactivity in at least those cases where a molecule dissociates. In one of the few studies of the relevance of entanglement to chemistry the dissociation of H_2O and of H_3 were studied [36]. The authors compared energy hypersurfaces (standard PESs) and "entanglement hypersurfaces" and concluded that the latter "grasp the chemical capability to transform from one state system to a new one".

2.5 Stationary Points and Normal-Mode Vibrations. Zero Point Energy

Once a stationary point has been found by geometry optimization, it is usually desirable to check whether it is a minimum, a transition state, or a hilltop. This is done by calculating the vibrational frequencies. Such a calculation involves finding
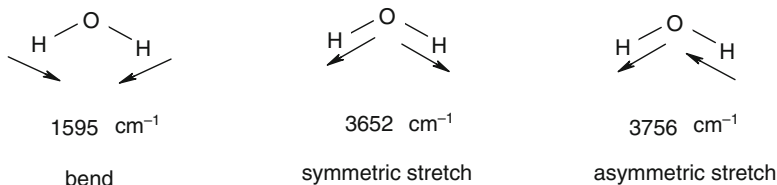
Fig. 2.19 The normal-mode vibrations of water. The *arrows* indicate the directions in which the atoms move; on reaching the maximum amplitude these directions are reversed

the *normal-mode* frequencies; these are the simplest vibrations of the molecule, which, in combination, can be considered to result in the actual, complex vibrations that a real molecule undergoes. In a normal-mode vibration all the atoms move in phase with the same frequency: they all reach their maximum and minimum displacements and their equilibrium positions at the same moment. The other vibrations of the molecule are combinations of these simple vibrations. Essentially, a normal-modes calculation is a calculation of the infrared spectrum, although the experimental spectrum is likely to contain extra bands resulting from interactions among normal-mode vibrations.

A nonlinear molecule with n atoms has $3n - 6$ normal modes: the motion of each atom can be described by 3 vectors, along the x, y, and z axes of a Cartesian coordinate system; after removing the 3 vectors describing the translational motion of the molecule as a whole (the translation of its center of mass) and the 3 vectors describing the rotation of the molecule (around the 3 principal axes needed to describe rotation for a three-dimensional object of general geometry), we are left with $3n - 6$ independent vibrational motions. Arranging these in appropriate combinations gives $3n - 6$ normal modes. A linear molecule has $3n - 5$ normal modes, since we need subtract only three translational and *two* rotational vectors, as rotation about the molecular axis does not produce a recognizable change in the nuclear array. So water has $3n - 6 = 3(3) - 6 = 3$ normal modes, and HCN has $3n - 5 = 3(3) - 5 = 4$ normal modes. For water (Fig. 2.19) mode 1 is a bending mode (the H–O–H angle decreases and increases), mode 2 is a symmetric stretching mode (both O–H bonds stretch and contract simultaneously) and mode 3 is an asymmetric stretching mode (as the O–H_1 bond stretches the O–H_2 bond contracts, and vice versa). At any moment an actual molecule of water will be undergoing a complicated stretching/bending motion, but this motion can be considered to be a combination of the three simple normal-mode motions.

Consider a diatomic molecule A–B; the normal-mode frequency (there is only one for a diatomic, of course) is given by [2]:

$$\widetilde{\nu} = \frac{1}{2\pi c}\left(\frac{k}{\mu}\right)^{1/2} \tag{*2.16}$$

where

$\widetilde{\nu} =$ vibrational "frequency", really wavenumber, in cm^{-1}; from deference to convention we use cm^{-1} although the cm is not an SI unit, and so the other units will also be non-SI;

$\widetilde{\nu}$ signifies the number of wavelengths that will fit into one cm. The symbol ν is the Greek letter nu, which resembles an angular vee; $\widetilde{\nu}$ could be read "nu tilde"; $\overline{\nu}$, "nu bar", has been used less frequently.

$c =$ velocity of light

$k =$ force constant for the vibration

$\mu =$ reduced mass of the molecule $= (m_A m_B)/(m_A + m_B)$;

m_A and m_B are the masses of A and B.

The force constant k of a vibrational mode is a measure of the "stiffness" of the molecule toward that vibrational mode –the harder it is to stretch or bend the molecule in the manner of that mode, the bigger is that force constant (for a diatomic molecule k simply corresponds to the stiffness of the one bond). The fact that the frequency of a vibrational mode is related to the force constant for the mode suggests that it might be possible to calculate the normal-mode frequencies of a molecule, that is, the directions and frequencies of the atomic motions, from its force constant matrix (its Hessian). This is indeed possible: *matrix diagonalization* of the Hessian gives the directional characteristics (which way the atoms are moving), and the force constants themselves, for the vibrations. Matrix diagonalization (Chap. 4, Sect. 4.3.3.) is a process in which a square matrix $\mathbf{A}$ is decomposed into three square matrices, $\mathbf{P}$, $\mathbf{D}$, and $\mathbf{P}^{-1}$: $\mathbf{A} = \mathbf{PDP}^{-1}$. $\mathbf{D}$ is a diagonal matrix: as with $\mathbf{k}$ in Eq. 2.17 all its off-diagonal elements are zero. $\mathbf{P}$ is a premultiplying matrix and $\mathbf{P}^{-1}$ is the inverse of $\mathbf{P}$. When matrix algebra is applied to physical problems, the diagonal row elements of $\mathbf{D}$ are the magnitudes of some physical quantity, and each column of $\mathbf{P}$ is a set of coordinates which give a direction associated with that physical quantity. These ideas are made more concrete in the discussion accompanying Eq. 2.17, which shows the diagonalization of the Hessian matrix for a triatomic molecule, e.g. H_2O.

$$\mathbf{H} = \begin{pmatrix} \partial^2 E/\partial q_1 \partial q_1 & \partial^2 E/\partial q_1 \partial q_2 & \cdots & \partial^2 E/\partial q_1 \partial q_9 \\ \partial^2 E/\partial q_2 \partial q_1 & \partial^2 E/\partial q_2 \partial q_2 & \cdots & \partial^2 E/\partial q_2 \partial q_9 \\ \vdots & \vdots & \cdots & \vdots \\ \partial^2 E/\partial q_9 \partial q_1 & \partial^2 E/\partial q_9 \partial q_2 & \cdots & \partial^2 E/\partial q_9 \partial q_9 \end{pmatrix}$$

$$= \underbrace{\begin{pmatrix} q_{11} & q_{12} & \cdots & q_{19} \\ q_{21} & q_{22} & \cdots & q_{29} \\ \vdots & & & \\ q_{91} & q_{92} & \cdots & q_{99} \end{pmatrix}}_{\mathbf{P}} \underbrace{\begin{pmatrix} k_1 & 0 & \cdots & 0 \\ 0 & k_2 & \cdots & 0 \\ \vdots & & & \\ 0 & 0 & \cdots & k_9 \end{pmatrix}}_{\mathbf{k}} \mathbf{P}^{-1} \qquad (2.17)$$

Equation 2.17 is of the form $\mathbf{A} = \mathbf{PDP}^{-1}$. The 9×9 Hessian for a triatomic molecule (three Cartesian coordinates for each atom) is decomposed by diagonalization into a $\mathbf{P}$ matrix whose columns are "direction vectors" for the vibrations whose force constants are given by the $\mathbf{k}$ matrix. Actually, columns 1, 2 and 3 of $\mathbf{P}$ and the corresponding k_1, k_2 and k_3 of $\mathbf{k}$ refer to *translational* motion of the molecule (motion of the whole molecule from one place to another in space); these three "force constants" are nearly zero. Columns 4, 5 and 6 of $\mathbf{P}$ and the corresponding k_4, k_5 and k_6 of $\mathbf{k}$ refer to *rotational* motion about the three principal axes of rotation, and are also nearly zero. Columns 7, 8 and 9 of $\mathbf{P}$ and the corresponding k_7, k_8 and k_9 of $\mathbf{k}$ are the direction vectors and force constants, respectively, for the normal-mode vibrations: k_7, k_8 and k_9 refer to vibrational modes 1, 2 and 3, while the 7th, 8th, and 9th columns of $\mathbf{P}$ are composed of the x, y and z components of vectors for motion of the three atoms in mode 1 (column 7), mode 2 (column 8), and mode 3 (column 9). "Mass-weighting" the force constants, ie taking into account the effect of the masses of the atoms (cf. Eq. 2.16 for the simple case of a diatomic molecule), gives the vibrational frequencies. The $\mathbf{P}$ matrix is the *eigenvector* matrix and the $\mathbf{k}$ matrix is the *eigenvalue* matrix from diagonalization of the Hessian $\mathbf{H}$. "Eigen" is a German prefix meaning "appropriate, suitable, actual" and is used in this context to denote mathematically appropriate entities for the solution of a matrix equation. Thus the directions of the normal-mode frequencies are the eigenvectors, and their magnitudes are the mass-weighted eigenvalues, of the Hessian.

Vibrational frequencies are calculated to obtain IR spectra, to characterize stationary points, and to obtain zero point energies (below). The calculation of meaningful frequencies is valid only at a stationary point and only using the same method that was used to optimize to that stationary point (for example an ab initio method with a particular correlation level and basis set–see Chap. 5). This is because (1) the use of second derivatives as force constants presupposes that the PES is quadratically curved along each geometric coordinate q (Fig. 2.2) but it is only near a stationary point that this is true, and (2) use of a method other than that used to obtain the stationary point presupposes that the PES's of the two methods are parallel (that they have the same curvature) at the stationary point. Of course, "provisional" force constants at nonstationary points are used in the optimization process, as the Hessian is updated from step to step. Calculated IR frequencies are usually somewhat too high, but (at least for ab initio and density functional calculations) can be brought into reasonable agreement with experiment by multiplying them by an empirically determined factor, commonly about 0.9 [37] (see the discussion of frequencies in Chaps. 5, 6 and 7).

A minimum on the PES has all the normal-mode force constants (all the eigenvalues of the Hessian) positive: for each vibrational mode there is a restoring force, like that of a spring. As the atoms execute the motion, the force pulls and slows them till they move in the opposite direction; each vibration is periodic, over and over. The species corresponding to the minimum sits in a well and vibrates forever (or until it acquires by collisions or absorption of light enough energy to react). For a transition state, however, one of the vibrations, that along the reaction

coordinate, is different: motion of the atoms corresponding to *this* mode takes the transition state toward the product or toward the reactant, without a restoring force. This one "vibration" is not a periodic motion but rather takes the species through the transition state geometry on a one-way journey. Now, the force constant is the first derivative of the gradient or slope (the derivative of the first derivative); examination of Fig. 2.8 shows that along the reaction coordinate the surface slopes downward, so the force constant for this mode is *negative*. A transition state (a first-order saddle point) has one and only one negative normal-mode force constant (one negative eigenvalue of the Hessian). Since a frequency calculation involves taking the square root of a force constant (Eq. 2.16), and the square root of a negative number is an imaginary number, a transition state has one imaginary frequency, corresponding to the reaction coordinate. In general an nth-order saddle point (an nth-order hilltop) has n negative normal-mode force constants and so n imaginary frequencies, corresponding to motion from one stationary point of some kind to another.

A stationary point could of course be characterized just from the number of negative force constants, but the mass-weighting requires much less time than calculating the force constants, and the frequencies themselves are often wanted anyway, for example for comparison with experiment. In practice one usually checks the nature of a stationary point by calculating the frequencies and seeing how many imaginary frequencies are present; a minimum has none, a transition state one, and a hilltop more than one. If one is seeking a particular transition state the criteria to be satisfied are:

1. It should look right. The structure of a transition state should lie somewhere between that of the reactants and the products; for example, the transition state for the unimolecular isomerization of HCN to HNC shows an H bonded to both C and N by an unusually long bond, and the CN bond length is in-between that of HCN and HNC.
2. It must have one and only one imaginary frequency (some programs indicate this as a negative frequency, eg $-1900 \, \text{cm}^{-1}$ instead of the correct $1900i \left(i = \sqrt{(-1)} \right)$.
3. The imaginary frequency must correspond to the reaction coordinate. This is usually clear from animation of the frequency (the motion, stretching, bending, twisting, corresponding to a frequency may be visualized with a variety of programs). For example, the transition state for the unimolecular isomerization of HCN to HNC shows an imaginary frequency which when animated clearly shows the H migrating between the C and the N. Should it not be clear from animation which two species the transition state connects, one may resort to an *intrinsic reaction coordinate* (IRC) calculation [38]. This procedure follows the transition state downhill along the IRC (Sect. 2.2), generating a series of structures along the path to the reactant or product. Usually it is clear where the transition state is going without following it all the way to a stationary point.
4. The energy of the transition state must be higher than that of the two species it connects.

Besides indicating the IR spectrum and providing a check on the nature of stationary points, the calculation of vibrational frequencies also provides the zero point energy (ZPE; most programs will calculate this automatically as part of a frequency job by summing the energies of the normal-mode vibrations). The ZPE is the energy a molecule has even at absolute zero (Fig. 2.2), as a consequence of the fact that even at this temperature it still vibrates [2]. The ZPE of a species is usually not small compared to activation energies or reaction energies, but ZPEs tend to cancel out when these are calculated (by subtraction), since for a given reaction the ZPE of the reactant, transition state and product tend to be roughly the same. However, for accurate work the ZPE should be added to the "total" (electronic + nuclear repulsion) energies of species and the ZPE-corrected energies should then be compared (Fig. 2.20). Like the frequencies, the ZPE is usually corrected by multiplying it by an empirical factor; this is sometimes the same as the frequency correction factor, but slightly different factors have been recommended [37].

The Hessian that results from a geometry optimization was built up in steps from one geometry to the next, approximating second derivatives from the changes in gradients (Eq. 2.15). This Hessian is not accurate enough for the calculation of frequencies and ZPE's. The calculation of an accurate Hessian for a stationary point can be done analytically or numerically. Accurate numerical evaluation approximates the second derivative as in Eq. 2.15, but instead of $\Delta(\partial E/\partial q)$ and Δq being taken from optimization iteration steps, they are obtained by changing the position of each atom of the optimized structure slightly ($\Delta q = \text{about } 0.01\,\text{Å}$) and calculating analytically the change in the gradient at each geometry; subtraction gives $\Delta(\partial E/\partial q)$. This can be done for a change in one direction only for each atom (method of forward differences) or more accurately by going in two directions around the equilibrium position and averaging the gradient change (method of central differences). Analytical calculation of ab initio frequencies is much faster than numerical evaluation, but an analytical algorithm may not be available for a particular method in some program suites, or demands on computer resources may make numerical calculation the only recourse at high ab initio levels (Chap. 5). A method of accurately estimating ZPE which does not involve calculation of second derivatives, but rather draws on tabulated values for atom types has been published recently [39]. This additive, atom-type based (ATB) method requires essentially no time and has been called a "zero-cost estimation" method.

2.6 Symmetry

Symmetry is important in theoretical chemistry (and even more so in theoretical physics), but our interest in it here is bounded by modest considerations: we want to see why symmetry is relevant to setting up a calculation and interpreting the results, and to make sense of terms like C_{2v}, C_s, etc., which are used in various places in this
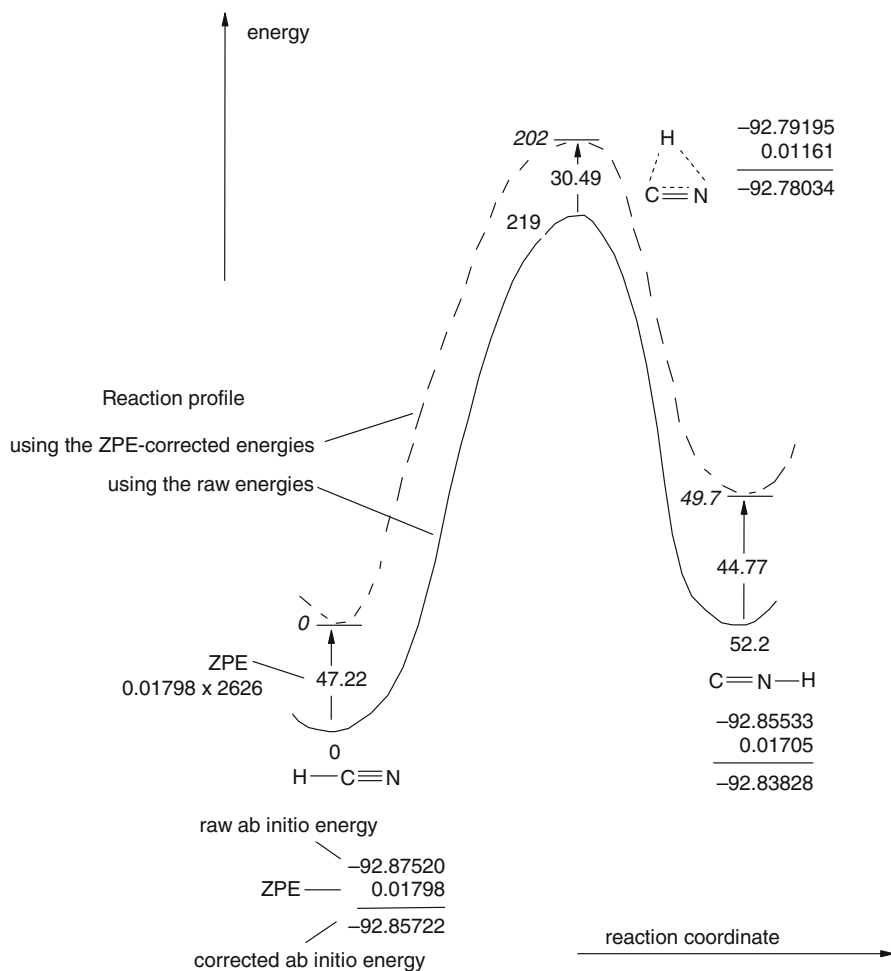
Fig. 2.20 Correcting relative energies for zero-point energy (ZPE). These are ab initio HF/6-31G* (Chap. 5) results for the HCN → HNC reaction. The corrections are most simply made by adding the ZPE to the raw energy (in energy units called hartrees or atomic units), to get the corrected energies. Using corrected or uncorrected energies, relative energies are obtained by setting the energy of one species (usually that of lowest energy) equal to zero. Finally, energy differences in hartrees were multiplied by 2626 to get kJ mol^{-1}. The ZPEs are also shown here in kJ mol^{-1}, just to emphasize that they are not small compared to reaction energies or activation energies, but tend to cancel; for accurate work ZPE-corrected energies should be used

book. Excellent expositions of symmetry are given by, for example, Atkins [40] and Levine [41].

The symmetry of a molecule is most easily described by using one of the standard designations like C_{2v}, C_s. These are called *point groups* (Schoenflies point groups) because when symmetry operations (below) are carried out on a molecule (on any object) with symmetry, at least one point is left unchanged. The

classification is according to the presence of symmetry elements and corresponding symmetry operations. The main symmetry elements are mirror planes (symmetry planes), symmetry axes, and an inversion center; other symmetry elements are the entire object, and an improper rotation axis. The operation corresponding to a mirror plane is reflection in that plane, the operation corresponding to a symmetry axis is rotation about that axis, and the operation corresponding to an inversion center is moving each point in the molecule along a straight line to that center then moving it further, along the line, an equal distance beyond the center. The "entire object" element corresponds to doing nothing (a null operation); in common parlance an object with only this symmetry element would be said to have no symmetry. The improper rotation axis corresponds to rotation followed by a reflection through a plane perpendicular to that rotation axis. We are concerned mainly with the first three symmetry elements. The examples below are shown in Fig. 2.21.

C_1 A molecule with no symmetry elements at all is said to belong to the group C_1 (to have "C_1 symmetry"). The only symmetry operation such a molecule permits is the null operation–this is the only operation that leaves it unmoved. An example is CHBrClF, with a so-called asymmetric atom; in fact, *most* molecules have no symmetry–just think of steroids, alkaloids, proteins, most drugs. Note that a molecule does not need an "asymmetric atom" to have C_1 symmetry: HOOF in the conformation shown is C_1 (has no symmetry).

C_s A molecule with only a mirror plane belongs to the group C_s. Example: HOF. Reflection in this plane leaves the molecule apparently unmoved.

C_2 A molecule with only a C_2 axis belongs to the group C_2. Example: H_2O_2 in the conformation shown. Rotation about this axis through 360° gives the same orientation twice. Similarly C_3, C_4, etc. are possible.

C_{2v} A molecule with two mirror planes whose intersection forms a C_2 axis belongs to the C_{2v} group. Example: H_2O. Similarly NH_3 is C_{3v}, pyramidane is C_{4v}, and HCN is $C_{\infty v}$.

C_i A molecule with only an inversion center (center of symmetry) belongs to the group C_i. Example: *meso*-tartaric acid in the conformation shown. Moving all points in the molecule along a straight line to this center, then continuing on an equal distance leaves the molecule apparently unchanged.

C_{2h} A molecule with a C_2 axis and a mirror plane horizontal to this axis is C_{2h} (a C_{2h} object will also perforce have an inversion center). Example: (*E*)-1,2-difluoroethene. Similarly B(OH)3 is C_{3h}.

D_2 A molecule with a C_2 axis and two more C_2 axes, perpendicular to that axis, has D_2 symmetry. Example: the tetrahydroxycyclobutadiene shown. Similarly, a molecule with a C_3 axis (the *principal axis*) and three other perpendicular C_2 axes is D_3.

D_{2h} A molecule with a C_2 axis and two perpendicular C_2 axes (as for D_2 above), plus a mirror plane is D_{2h}. Examples: ethene, cyclobutadiene. Similarly, a C_3 axis (the principal axis), three perpendicular C_2 axes and a mirror plane horizontal to the
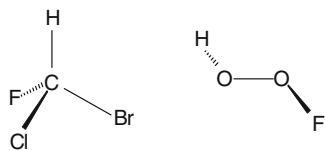
C_1 No symmetry elements
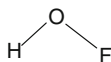
C_s The three atoms lie in a plane
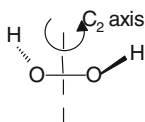
C_2 axis

C_2 Twofold rotation axis
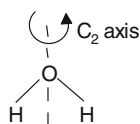
C_2 axis

C_{2v} C_2 axis and two mirror planes passing through this axis, one the molecular plane, the other at right angles to the molecular plane
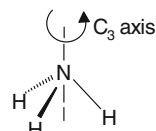
C_3 axis

C_{3v} C_3 axis and three mirror planes
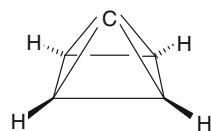
pyramidane

C_{4v}
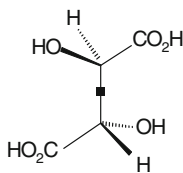
C_i Inversion center (■)
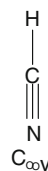
$C_{\infty v}$
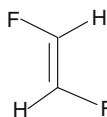
C_{2h} C_2 axis (perpendicular to the molecular plane) and a horizontal mirror plane (the molecular plane)
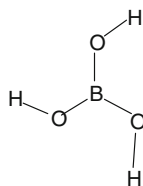
C_{3h} C_3 axis and horizontal mirror plane

Fig. 2.21 Examples of molecules with various symmetry elements (belonging to various point groups)

D_2 A C_2 axis perpendicular to the ring plane, and two C_2 axes perpendicular to that axis

T_d

D_{2h} As for D_2 (above), plus a mirror plane

$C_{\infty h}$

O_h

$\equiv$ $H_2C =\!\!=\!\!= C =\!\!=\!\!= CH_2$

D_{2d} As for D_2 (above), plus two dihedral mirror planes: the two planes that contain the HCH groups bisect the two axes that are shown as dashed lines (the third axis passes through CCC).

buckminsterfullerene, C_{60}
The bonds are of two kinds, with lengths ca. 1.39 and 1.46 Å

Fig. 2.21 (continued)

principal axis confer D_{3h} symmetry, as in the cyclopropenyl cation. Similarly, benzene is D_{6h}, and F_2 is $D_{\infty h}$.

D_{2d} A molecule is D_{2d} if it has a C_2 axis and two perpendicular C_2 axes (as for D_2 above), plus two "dihedral" mirror planes; these are mirror planes that bisect two C_2 axes (in general, that bisect the C_2 axes perpendicular to the principal axis). Example: allene (propadiene). Staggered ethane is D_{3d} (it has D_3 symmetry elements plus three dihedral mirror planes. D_{nd} symmetry can be hard to spot.

Molecules belonging to the *cubic point groups* can, in some sense, be fitted symmetrically inside a cube. The commonest of these are T_d, O_h and I; they will be merely exemplified:

T_d This is tetrahedral symmetry. Example: CH_4,

O_h This might be considered "cubic symmetry". Example: cubane, SF_6.

I Also called icosahedral symmetry. Example: buckminsterfullerene.

Less-common groups are S_4, and the cubic groups T, T_h (dodecahedrane is T_h) and O (see [41]). Atkins [40] and Levine [41] give flow charts which make it relatively simple to assign a molecule to its point group, and Atkins provides pictures of objects of various symmetries which often make it possible to assign a point group without having to examine the molecule for its symmetry elements.

We saw above that most molecules have no symmetry. So why is a knowledge of symmetry important in chemistry? Symmetry considerations are essential in the theory of molecular electronic (UV) spectroscopy and sometimes in analyzing in detail molecular wavefunctions (Chap. 4), but for us the reasons are more pragmatic. A calculation run on a molecule whose input structure has the exact symmetry that the molecule should have will tend to be faster and will yield a "better" (see below) geometry than one run on a structure of lower symmetry, however close this may be to the exact one. Input molecular structures for a calculation are usually created with an interactive graphical program and a computer mouse: atoms are assembled into molecules much as with a model kit, or the molecule might be drawn on the computer screen. If the molecule has symmetry (if it is not C_1) this can be imposed by optimizing the geometry, often with molecular mechanics (Chap. 3). Now consider water: we would of course normally input the H_2O molecule with its exact equilibrium C_{2v} symmetry, but we could also alter the input structure slightly making the symmetry C_s (three atoms must lie in a plane). The C_{2v} structure has two degrees of freedom: a bond length (the two bonds are the same length) and a bond angle. The C_s structure has three degrees of freedom: two bond lengths and a bond angle. The optimization algorithm has more variables to cope with in the case of the lower-symmetry structure. A moderately high-level geometry optimization and frequencies job on $C_{2v}(CH_3)_2O$, dimethyl ether, took 5.7 min, but on the C_s ether 6.8 min (actually, small molecules like water, and low-level calculations, show a levelling effect, taking only seconds and requiring about the same time regardless of symmetry).

What do we mean by a better geometry? Although a successful geometry optimization will give essentially the same geometry from a slightly distorted input structure as from one with the perfect symmetry of the molecule in question, corresponding bond lengths and angles (eg the four C–H bonds and the two HCH angles of ethene) will not be *exactly* the same. This can confuse an analysis of the geometry, and carries over into the calculation of other properties like, say, charges on atoms–corresponding atoms should have exactly the same charges. Thus both esthetic and practical considerations encourage us to aim for the exact symmetry that the molecule should possess. An error still found in the literature is that there is some advantage to optimizing "with no constraints". This may come from the days when the calculation of frequencies was not routine; nowadays, if the optimized structure is not, say, a minimum and such was desired, this can be corrected by altering a geometry coordinate in accordance with the desire of the structure to relax along the direction revealed by an imaginary frequency.

2.7   Summary

The potential energy surface (PES) is a central concept in computational chemistry. A PES is the relationship–mathematical or graphical–between the energy of a molecule (or a collection of molecules) and its geometry.

Stationary points on a PES are points where $\partial E/\partial q = 0$ for all q, where q is a geometric parameter. The stationary points of chemical interest are minima ($\partial^2 E/\partial q_i \partial q_j > 0$ for all q) and transition states or first-order saddle points; $\partial^2 E/\partial q_i \partial q_j < 0$ for one q, along the reaction coordinate (intrinsic reaction coordinate, IRC), and >0 for all other q. Chemistry is the study of PES stationary points and the pathways connecting them.

The Born-Oppenheimer approximation says that in a molecule the nuclei are essentially stationary compared to the electrons. This is one of the cornerstones of computational chemistry because it makes the concept of molecular shape (geometry) meaningful, makes possible the concept of a PES, and simplifies the application of the Schrödinger equation to molecules by allowing us to focus on the electronic energy and add in the nuclear repulsion energy later; this third point, very important in practical molecular computations, is elaborated on in Chap. 5.

Geometry optimization is the process of starting with an input structure "guess" and finding a stationary point on the PES. The stationary point found will normally be the one closest to the input structure, not necessarily the global minimum. A transition state optimization usually requires a special algorithm, since it is more demanding than that required to find a minimum. Modern optimization algorithms use analytic first derivatives and (usually numerical) second derivatives.

It is usually wise to check that a stationary point is the desired species (a minimum or a transition state) by calculating its vibrational spectrum (its normal-mode vibrations). The algorithm for this works by calculating an accurate Hessian (force constant matrix) and diagonalizing it to give a matrix with the "direction vectors" of the normal modes, and a diagonal matrix with the force constants of these modes. A procedure of "mass-weighting" the force constants gives the normal-mode vibrational frequencies. For a minimum all the vibrations are real, while a transition state has one imaginary vibration, corresponding to motion along the reaction coordinate. The criteria for a transition state are appearance, the presence of one imaginary frequency corresponding to the reaction coordinate, and an energy above that of the reactant and the product. Besides serving to characterize the stationary point, calculation of the vibrational frequencies enables one to predict an IR spectrum and provides the zero-point energy. The ZPE is needed for accurate comparisons of the energies of isomeric species. The accurate Hessian required for calculation of frequencies and ZPE's can be obtained either numerically or analytically (faster, but much more demanding of hard drive space).

Easier Questions

1. What is a potential energy surface (give the two viewpoints)?
2. Explain the difference between a relaxed PES and a rigid PES.
3. What is a stationary point? What kinds of stationary points are of interest to chemists, and how do they differ?
4. What is a reaction coordinate?
5. Show with a sketch why it is not correct to say that a transition state is a maximum on a PES.
6. What is the Born-Oppenheimer approximation, and why is it important?
7. Explain, for a reaction A → B, how the potential energy change on a PES is related to the enthalpy change of the reaction. What would be the problem with calculating a free energy/geometry surface?
    Hint: Vibrational frequencies are normally calculated only for stationary points.
8. What is geometry optimization? Why is this process for transition states (often called transition state optimization) more challenging than for minima?
9. What is a Hessian? What uses does it have in computational chemistry?
10. Why is it usually good practice to calculate vibrational frequencies where practical, although this often takes considerably longer than geometry optimization?

Harder Questions

1. The Born-Oppenheimer principle is often said to be a prerequisite for the concept of a potential energy surface. Yet the idea of a potential energy surface (Marcelin, 1915) predates the Born-Oppenheimer principle (1927). Discuss.
2. How high would you have to lift a mole of water for its gravitational potential energy to be equivalent to the energy needed to dissociate it completely into hydroxyl radicals and hydrogen atoms? The strength of the O–H bond is about $400 \, \text{kJ mol}^{-1}$; the gravitational acceleration g at the Earth's surface (and out to hundreds of km) is about $10 \, \text{m s}^{-2}$. What does this indicate about the role of gravity in chemistry?
3. If gravity plays no role in chemistry, why are vibrational frequencies different for, say, C–H and C–D (deuterium is called heavy hydrogen) bonds?
4. We assumed that the two bond lengths of water are equal. *Must* an acyclic molecule AB_2 have equal A–B bond lengths? What about a cyclic molecule AB_2?
5. Why are chemists but rarely interested in finding and characterizing second-order and higher saddle points (hilltops)?
6. What kind(s) of stationary points do you think a second-order saddle point connects?

7. If a species has one calculated frequency very close to 0 cm^{-1} what does that tell you about the (calculated) potential energy surface in that region?

8. The ZPE of many molecules is greater than the energy needed to break a bond; for example, the ZPE of hexane is about 530 kJ mol^{-1}, while the strength of a C–C or a C–H bond is only about 400 kJ mol^{-1}. Why then do such molecules not spontaneously decompose?

9. Only certain parts of a potential energy surface are chemically interesting: some regions are flat and featureless, while yet other parts rise steeply and are thus energetically inaccessible. Explain.

10. Consider two potential energy surfaces for the HCN ⇌ HNC reaction: A, a plot of energy vs. the H–C bond length, and B, a plot of energy vs. the HCN angle. Recalling that HNC is the higher-energy species (Fig. 2.19), sketch qualitatively the diagrams A and B.

References

1. (a) Shaik SS, Schlegel HB, Wolfe S (1992) Theoretical aspects of physical organic chemistry: the SN2 mechanism. Wiley, New York. See particularly Introduction and chapters 1 and 2; (b) Marcus RA (1990) Science 256:1523; (c) For a very abstract and mathematical but interesting treatment, see Mezey PG (1987) Potential energy hypersurfaces. Elsevier, New York; (d) Steinfeld JI, Francisco JS, Hase WL (1999) Chemical kinetics and dynamics, 2nd edn, Prentice Hall, Upper Saddle River
2. Levine IN (2014) Quantum chemistry, 7th edn. Prentice Hall, Upper Saddle River, section 4.3
3. Reference [1a], pp 50–51
4. (a) Houk KN, Li Y, Evanseck JD (1992) Angew Chem Int Ed Engl 31:682; (b) Leach AR (2001) Molecular modeling. Principles and applications. Prentice Hall, Upper Saddle River, p 281
5. Atkins P (1998) Physical chemistry, 6th edn. Freeman, New York, pp 830–844
6. Marcelin R (1915) Annales de Physique 3:152. Potential energy surface: p 158
7. Eyring H (1935) J Chem Phys 3:107
8. Eyring H, Polanyi M (1931) Z Physik Chem B, 12:279
9. Kraka E, Cremer D (2010) Acc Chem Res 43:591
10. (a) Carpenter BK (1992) Acc Chem Res 25:520; (b) Carpenter B (1997) Am Sci 138; (c) Carpenter BK (1998) Angew Chem Int Ed 37:3341; (d) Reyes MB, Carpenter BK (2000) J Am Chem Soc 122:10163; (e) Reyes MB, Lobkovsky EB, Carpenter BK (2002) J Am Chem Soc 124:641; (f) Nummela J, Carpenter BK (2002) J Am Chem Soc 124:8512; (g) Carpenter BK (2003) J Phys Org Chem 16:858; (h) Litovitz AE, Keresztes I, Carpenter BK (2008) J Am Chem Soc 130:12085
11. Siebert MR, Zhang J, Addepalli SV, Tantillo DJ, Hase WL (2011) J Am Chem Soc 133:8335
12. Carpenter BK (2011) Science 332:1269; Schreiner PR, Reisenauer HP, Ley D, Gerbig D, Wu C-H, Allen WD (2011) Science 332:1300
13. Luehr N, Jin AGB, Martínez TJ (2015) J Chem Theory Comput 11:4536
14. Born M, Oppenheimer JR (1927) Ann Physik 84:457
15. (a) Bader RFW, Carroll MT, Cheeseman MT, Chang C (1987) J Am Chem Soc 109: 7968; (b) Kammeyer CW, Whiman DR (1972) J Chem Phys 56:4419
16. (a) For some rarefied but interesting ideas about molecular shape see Mezey PG (1993) Shape in chemistry, VCH, New York; (b) An antimatter molecule lacking definite shape: Surko CM (2007) Nature 449:153; (c) The Cl+H$_2$ reaction: Foreword: Bowman JL (2008) Science

319:40; Garand E, Zhou J, Manolopoulos DE, Alexander MH, Neumark DM (2008) Science 319:72; Erratum 320:612. (d) Baer M (2006) Beyond Born-Haber. Wiley

17. Sutcliffe BT (1993) J Chem Soc Faraday Trans 89:2321
18. Sutcliffe BT, Wooley RG (2012) J Chem Phys 137:22A544, and references therein
19. Garand E, Zhou J, Manolopoulos DE, Alexander MH, Neumark DM (2008) Science 319:72
20. Bubin S, Pavanello M, Tung W-C, Sharkey KL, Adamowicz L (2013) Chem Rev 113:36
21. Stanke M, Adamowitz L (2013) J Phys Chem A 117:10129
22. Fleming DG, Arseneau DJ, Sukhorukov O, Brewer JH, Mielke SL, Schatz GC, Garrett BC, Peterson KA, Truhlar DG (2011) Science 331:448
23. Szidarovszky T, Császár AE (2014) J Phys Chem A 118:6256, and references therein
24. Lolur P, Dawes R (2014) J Chem Educ 91:1181; Blauch DN, Carroll FA (2014) J Chem Educ 91:1254
25. Zhang XK, Parnis JM, Lewars EG, March RE (1997) Can J Chem 75:276
26. Jensen F (2007) Introduction to computational chemistry, 2nd edn. Wiley, West Sussex, section 12.6
27. Levine IN (2014) Quantum chemistry, 7th edn. Prentice Hall, Upper Saddle River, section 15.11
28. See e.g. Cramer C (2004) Essentials of computational chemistry. Wiley, section 2.4.1
29. Hehre WJ (1995) Practical strategies for electronic structure calculations. Wavefunction Inc., Irvine, p 9
30. Jensen F (2007) Introduction to computational chemistry, 2nd edn. Wiley, West Sussex, section 12.2
31. Pawłowski F, Jørgensen P, Olsen J, Hegelund F, Helgaker T, Gauss J, Bak KL, Stanton JF (2015) J Chem Phys 116:6482
32. Suleimanov YV, Green WH (2015) J Chem Theory Comput 11:4248
33. Bergeler M, Simm GN, Proppe J, Reiher M (2015) J Chem Theory Comput 11:5712
34. (a) Dama JF, Hocky GM, Sun R, Voth GA (2015) J Chem Theory Comput 11:5638; (b) Pan L, Zheng Z, Wang T, Merz KM Jr (2015) J Chem Theory Comput 11:5853
35. See e.g. Vedral V (2014) Nat Phys 10:256
36. Molina-Espíritu M, Esquivel RO, López-Rosa S, Dehesa JS (2015) J Chem Theory Comput 11:5144
37. Scott AP, Radom L (1996) J Phys Chem 100:16502
38. Foresman JB, Frisch Æ (1996) Exploring chemistry with electronic structure methods, 2nd edn. Gaussian Inc., Pittsburgh, pp 173–211
39. Cśaszár AG, Furtenbacher T (2015) J Phys Chem A 119:10229
40. Atkins P (1998) Physical chemistry, 6th edn. Freeman, New York, chapter 15
41. Levine IN (2014) Quantum chemistry, 7th edn. Prentice Hall, Upper Saddle River, chapter 12

Chapter 3
Molecular Mechanics

We don't give a damn where the electrons are.
Words to the author, from the president of a well-known
chemical company, emphasizing his firm's position
on basic research.

Abstract Molecular mechanics (MM) rests on a view of molecules as balls held together by springs, ignoring electrons. The potential energy of a molecule can be written as the sum of terms involving (at least) bond, stretching, angle bending, dihedral angles, and nonbonded interactions. Giving these terms explicit mathematical forms constitutes devising a forcefield, and giving actual numbers to the constants in it constitutes parameterizing the forcefield. Calculations on large biomolecules is a very important application of MM, and the pharmaceutical industry designs new drugs with the aid of MM. Organic synthesis now makes use of MM, which enables chemists to estimate which products are likely to be favored in a reaction and to devise realistic routes to a target molecule. In molecular *dynamics* MM is often used to generate the forces acting on molecules and hence to calculate their motions.

3.1 Perspective

Molecular mechanics (MM) [1] is based on a mathematical model of a molecule as a collection of balls (corresponding to the atoms) held together by springs (corresponding to the bonds) (Fig. 3.1). Within the framework of this model, the energy of the molecule changes with geometry because the springs resist being stretched or bent away from some "natural" length or angle, and the balls resist being pushed too closely together. The *mathematical* model is thus conceptually very close to the intuitive feel for molecular energetics that one obtains when manipulating molecular models of plastic or metal: the model resists distortions (it may break!) from the "natural" geometry that corresponds to the bond lengths and angles imposed by the manufacturer, and in the case of space-filling models atoms cannot be forced too closely together. The MM model clearly ignores electrons.
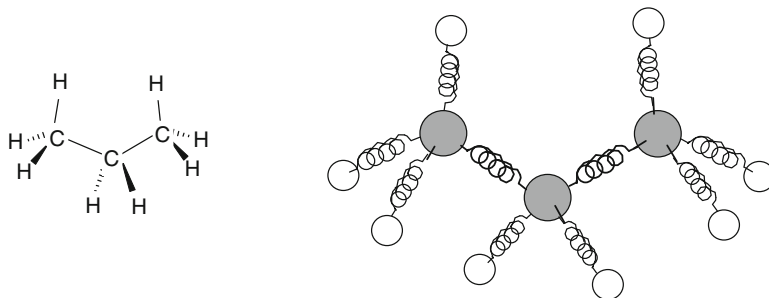
Fig. 3.1 Molecular mechanics (the forcefield method) considers a molecule to be a collection of *balls* (the atoms) held together by *springs* (the bonds)

The principle behind MM is to express the energy of a molecule as a function of its resistance toward bond stretching, bond bending, and atom crowding, and to use this energy equation to find the bond lengths, angles, and dihedrals corresponding to the minimum-energy geometry – or more precisely, to the various possible potential energy surface minima (Chap. 2). In other words, MM uses a conceptually *mechanical* model of a molecule to find its minimum-energy geometry (for flexible molecules, the geometries of the various conformers). The form of the mathematical expression for the energy, and the parameters in it, constitute a *forcefield* (or force field), and molecular mechanics methods are sometimes called forcefield methods. The term arises because the negative of the first derivative of the potential energy of a particle with respect to displacement along some direction is the force on the particle; a "forcefield" $E(x, y, z$ coordinates of atoms) can be differentiated to give the force on each atom.

The method makes no reference to electrons, and so cannot (except by some kind of empirical algorithm) throw light on *electronic* properties like charge distributions or nucleophilic and electrophilic behaviour. Note that MM implicitly uses the Born-Oppenheimer approximation, for only if the nuclei experience what amounts to a static attractive force, whether from electrons or springs, does a molecule have a distinct geometry (Chap. 2, Sect. 2.3).

An important point, which students sometimes have a problem with, is that the concept of a *bond* is central to MM, but not essential – although often useful – in *electronic* structure calculations. In MM a molecule is defined by the atoms and the bonds, which latter are regarded almost literally as springs holding the atoms together. Usually, bonds are placed where the rules for drawing structural formulas require them, and to do a MM calculation you specify with the graphical user input each bond as single, double, etc., since this tells the program how strong a bond to use (Sects. 3.2.1 and 3.2.2). In an electronic structure calculation–ab initio (Chap. 5), semiempirical (Chap. 6), and density functional theory (Chap. 7) – a molecule is defined by the relative positions of its atomic nuclei, the charge, and the "multiplicity" (which follows easily from the number of unpaired electrons). An oxygen nucleus and two protons with the right *x, y, z* coordinates, no charge, and multiplicity one (no unpaired electrons) is a water molecule. There is no mention

of bonds here, although the chemist might wish to somehow extract this useful concept from this picture of nuclei and electrons. This can be done by calculating the electron density and associating a bond with, for example, a path along which electron density is concentrated, but there is no unique definition of a bond in electronic structure theory. It is worth noting, too, that in some computational chemistry graphical interfaces bonds are specified by the user in the input and remain displayed, while in other interfaces they are shown by the program depending on the separation of pairs of atoms. The novice may find it disconcerting to see a specified bond still displayed, as a long line, even when a change in geometry has moved a pair of atoms far apart, or to see a bond vanish when a pair has moved slightly beyond some default distance of the program.

Historically [2], molecular mechanics seems to have begun as an attempt to obtain quantitative information about chemical reactions at a time when the possibility of doing quantitative quantum mechanical (Chap. 4) calculations on anything much bigger than the hydrogen molecule seemed remote. Specifically, the principles of MM, as a potentially general method for studying the variation of the energy of molecular systems with their geometry, were formulated in 1946 by Westheimer[1] and Meyer [3a], and by Hill [3b]. In this same year Dostrovsky, Hughes[2] and Ingold[3] independently applied molecular mechanics concepts to the quantitative analysis of the S_N2 reaction, but they do not seem to have recognized the potentially wide applicability of this approach [3c]. In 1947 Westheimer [3d] published detailed calculations in which MM was used to estimate the activation energy for the racemization of biphenyls.

Among several major contributors to the development of MM have been Schleyer[4] [2b], c and Allinger[5] [1a, d]; one of Allinger's publications on MM [1d] is, according to the Citation Index, one of the most frequently cited chemistry papers. The Allinger group has, since the 1960s, been responsible for the development of the "MM-series" of programs, commencing with MM1 and continuing with MM2 and the currently widely-used MM3, and MM4 [4]. MM programs [5] like Sybil and UFF will handle molecules involving much of the periodic table, albeit with some loss of accuracy that one might expect for trading depth for breadth, and MM is the most widely-used method for computing the geometries and energies of large biological molecules like proteins and nucleic acids (although recently

---

[1] Frank H. Westheimer, born Baltimore, Maryland, 1912. Ph.D. Harvard 1935. Professor University of Chicago, Harvard. Died 2007.

[2] Edward D. Hughes, born Wales, 1906. Ph.D. University of Wales, D.Sc. University of London. Professor, London. Died 1963.

[3] Christopher K. Ingold, born London 1893. D.Sc. London 1921. Professor Leeds, London. Knighted 1958. Died London 1970.

[4] Paul von R. Schleyer, born Cleveland, Ohio, 1930. Ph.D. Harvard 1957. Professor Princeton; institute codirector and professor University of Erlangen-Nürnberg, 1976–1998. Professor University of Georgia. Died 2014.

[5] Norman L. Allinger, born Rochester New York, 1930. Ph.D. University of California at Los Angeles, 1954. Professor Wayne State University, University of Georgia.

semiempirical (Chap. 6) and even ab initio (Chap. 5) methods have begun to be applied to these large molecules. The 2013 Nobel Prize in chemistry was awarded to Martin Karplus, Michael Levitt, and Arieh Warshel for the application of molecular mechanics to large biological molecules [1k].

3.2   The Basic Principles of Molecular Mechanics

3.2.1   Developing a Forcefield

The potential energy of a molecule can be written

$$E = \sum_{bonds} E_{stretch} + \sum_{angles} E_{bend} + \sum_{dihedrals} E_{torsion} + \sum_{pairs} E_{nonbond} \qquad (*3.1)$$

where $E_{stretch}$ etc. are energy contributions from bond stretching, angle bending, torsional motion (rotation) around single bonds, and interactions between atoms or groups which are nonbonded (not directly bonded together). The sums are over all the bonds, all the angles defined by three atoms A–B–C, all the dihedral angles defined by four atoms A–B–C–D, and all pairs of significant nonbonded interactions. The mathematical form of these terms and the parameters in them constitute a particular forcefield. We can make this clear by being more specific; let us consider each of these four terms.

The Bond Stretching Term   The increase in the energy of a spring (remember that we are modelling the molecule as a collection of balls held together by springs) when it is stretched (Fig. 3.2) is approximately proportional to the square of the extension:

$$\Delta E_{stretch} = k_{stretch}\left(l - l_{eq}\right)^2$$

$k_{stretch} = $ the proportionality constant (actually one-half the *force constant* of the spring or bond [6]; but note the warning about identifying MM force constants with the traditional force constant from, say, spectroscopy – see Sect. 3.5, *Weaknesses*); the bigger $k_{stretch}$, the stiffer the bond/spring – the more it resists being stretched.
$l = $ length of the bond when stretched
$l_{eq} = $ reference length of the bond, its "natural" length

If we take the energy corresponding to the reference length l_{eq} as the zero of energy, we can replace $\Delta E_{stretch}$ by $E_{stretch}$:

$$E_{stretch} = k_{stretch}\left(l - l_{eq}\right)^2 \qquad (*3.2)$$
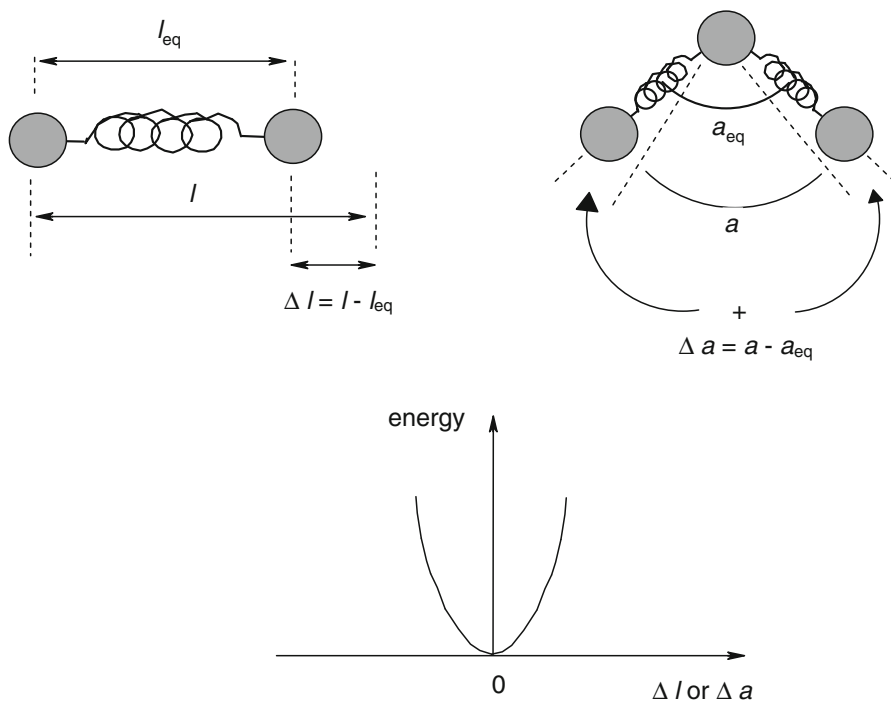
Fig. 3.2 Changes in bond lengths or in bond angles result in changes in the energy of a molecule. Such changes are handled by the $E_{stretch}$ and E_{bend} terms in the molecular mechanics forcefield. The energy is approximately a quadratic function of the change in bond length or angle

The Angle Bending Term The increase in energy of system ball-spring-ball-spring-ball, corresponding to the triatomic unit A–B–C (the increase in "angle energy") is approximately proportional to the square of the increase in the angle (Fig. 3.2); analogously to Eq. (*3.2):

$$E_{bend} = k_{bend}(a - a_{eq})^2 \qquad (*3.3)$$

k_{bend} = a proportionality constant (one-half the angle bending force constant [6]; note the warning about identifying MM force constants with the traditional force constant from, say, spectroscopy – see Sect. 3.3))
a = size of the angle when distorted
a_{eq} = reference size of the angle, its "natural" value

The Torsional Term Consider four atoms sequentially bonded: A–B–C–D (Fig. 3.3). The dihedral angle or torsional angle of the system is the angle between the A–B bond and the C–D bond as viewed along the B–C bond. Conventionally this angle is considered positive if regarded as arising from clockwise rotation (starting with A–B covering or eclipsing C–D) of the back bond (C–D) with respect

dihedral angle = 0°   dihedral angle = 60°
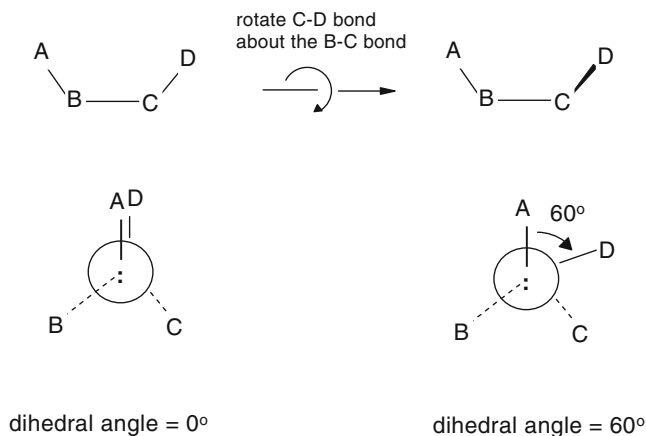
Fig. 3.3 Dihedral angles (torsional angles) affect molecular geometries and energies. The energy is a periodic (cosine or combination of cosine functions) function of the dihedral angle; see e.g. Figs. 3.4 and 3.5
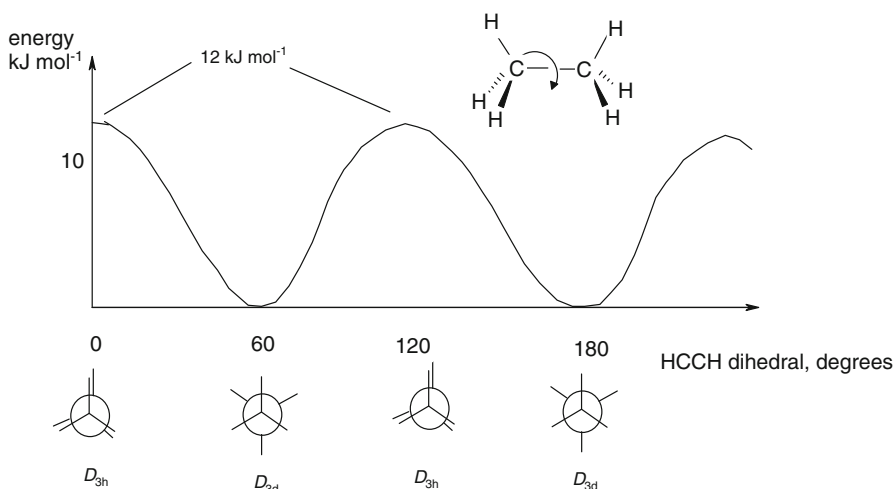
Fig. 3.4 Variation of the energy of ethane with dihedral angle. The *curve* can be represented as a cosine function

to the front bond (A–B). Thus in Fig. 3.3 the dihedral angle A–B–C–D is 60° (it could also be considered as being $-300°$). Since the geometry repeats itself every 360°, the energy varies with the dihedral angle in a sine or cosine pattern, as shown in Fig. 3.4 for the simple case of ethane. For systems A–B–C–D of lower symmetry, like butane (Fig. 3.5), the torsional potential energy curve is more complicated, but a *combination* of sine or cosine functions will reproduce the curve:

$$E_{torsion} = k_0 + \sum_{r=1}^{n} k_r[1 + \cos{(r\theta)}] \qquad (*3.4)$$
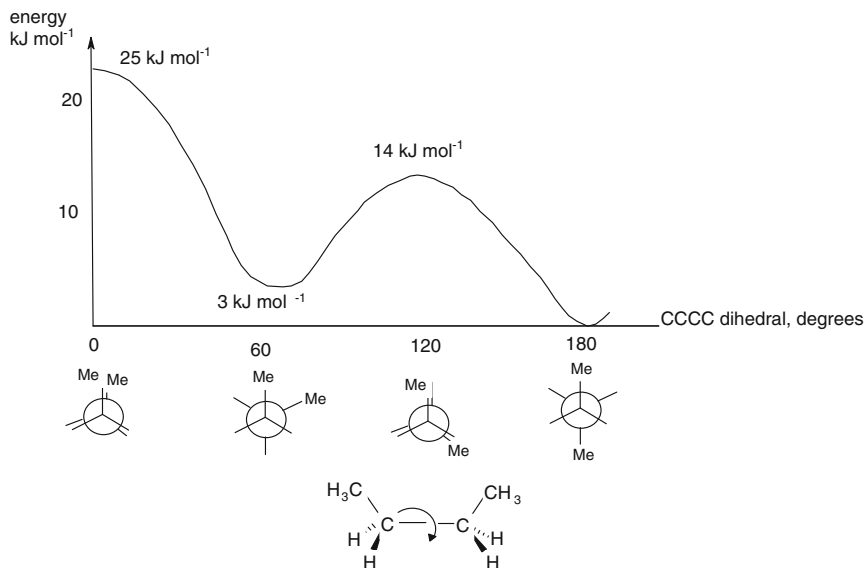
Fig. 3.5   Variation of the energy of butane with dihedral angle. The *curve* can be represented by a sum of cosine functions

The Nonbonded Interactions Term   This represents the change in potential energy with distance apart of atoms A and B that are not directly bonded (as in A–B) and are not bonded to a common atom (as in A–X–B); these atoms, separated by at least two atoms (A–X–Y–B) or even in different molecules, are said to be nonbonded (with respect to each other). Note that the A-B case is accounted for by the bond stretching term E_{stretch}, and the A–X–B term by the angle bending term E_{bend}, but the nonbonded term $E_{nonbond}$ is, for the A–X–Y-B case, superimposed upon the torsional term $E_{torsion}$: we can think of $E_{torsion}$ as representing some factor inherent to resistance to rotation about a (usually single) bond X–Y (MM does not attempt to explain the theoretical, electronic basis of this or any other effect), while for certain atoms attached to X and Y there may also be nonbonded interactions.

The potential energy curve for two nonpolar nonbonded atoms has the general form shown in Fig. 3.6. A simple way to approximate this is by the so-called Lennard-Jones 12–6 potential [7]:

$$E_{nonbond} = k_{nb}\left[\left(\frac{\sigma}{r}\right)^{12} - \left(\frac{\sigma}{r}\right)^{6}\right] \tag{*3.5}$$

r = the distance between the centers of the nonbonded atoms or groups.

The function reproduces the small attractive dip in the curve (represented by the negative term) as the atoms or groups approach one another, then the very steep rise in potential energy (represented by the raising the positive, repulsive term raised to
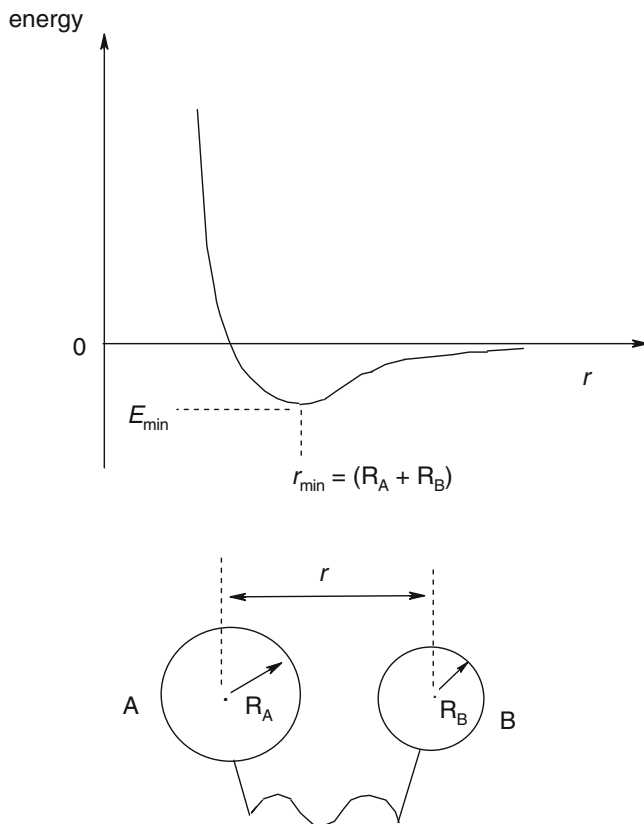
Fig. 3.6 Variation of the energy of a molecule with separation of nonbonded atoms or groups. Atoms/groups A and B may be in the same molecule (as indicated here) or the interaction may be intermolecular. The minimum energy occurs at van der Waals contact. For small nonpolar atoms or groups the minimum energy point represents a drop of a few kJ mol^{-1} ($E_{min} = -1.2$ kJ mol^{-1} for CH_4/CH_4), but short distances can make nonbonded interactions destabilize a molecule by many kJ mol^{-1}

a large power) as they are pushed together closer than their van der Waals radii. Setting $dE/dr = 0$, we find that for the energy minimum in the curve the corresponding value of r is $r_{min} = 2^{1/6}\sigma$,

$$\text{i.e.} \quad \sigma = 2^{-1/6} r_{min} \tag{3.6}$$

If we assume that this minimum corresponds to van der Waals contact of the nonbonded groups, then $r_{min} = (R_A + R_B)$, the sum of the van der Waals radii of the groups A and B. So

$$2^{1/6}\sigma = (R_A + R_B)$$

and so

$$\sigma = 2^{-1/6}(R_A + R_B) = 0.89\,(R_A + R_B) \tag{3.7}$$

Thus σ can be calculated from r_{min} or estimated from the van der Waals radii. Setting $E = 0$, we find that for this point on the curve $r = \sigma$,

$$\text{i.e.} \quad \sigma = r(E = 0) \tag{3.8}$$

If we set $r = r_{min} = 2^{1/6}\sigma$ (from Eq. (3.6)) in Eq. (3.5), we find

$$E(r_{min}) = (-1/4)k_{nb}$$
$$\text{i.e.} \quad k_{nb} = -4E(r_{min}) \tag{3.9}$$

So k_{nb} can be calculated from the depth of the energy minimum.

   In deciding to use equations of the form Eqs. (3.2, 3.3, 3.4 and 3.5) we have decided on a particular MM forcefield. There are many alternative forcefields. For example, we might have chosen to approximate $E_{stretch}$ by the sum of a quadratic and a cubic term:

$$E_{stretch} = k_{stretch}\left(l - l_{eq}\right)^2 + k\left(l - l_{eq}\right)^3$$

This gives a somewhat more accurate representation of the variation of energy with length. Again, we might have represented the nonbonded interaction energy by a more complicated expression than the simple 12–6 potential of Eq. (3.5) (which is by no means the best form for nonbonded repulsions). Such changes would represent changes in the forcefield.

3.2.2   Parameterizing a Forcefield

We can now consider putting actual numbers, $k_{stretch}, l_{eq}, k_{bend}$, etc., into Eqs 3.2, 3.3, 3.4 and 3.5, to give expressions that we can actually use. The process of finding these numbers is called *parameterizing* (or parametrizing) the forcefield. The set of molecules used for parameterization, perhaps hundreds for a good forcefield, is called the *training set*. In the purely illustrative example below we use just ethane, methane and butane.

Parameterizing the Bond Stretching Term   A forcefield can be parameterized by reference to experiment (empirical parameterization) or by getting the numbers from high-level ab initio or density functional calculations, or by a combination of both approaches. For the bond stretching term of Eq. (3.2) we need $k_{stretch}$ and l_{eq}. Experimentally, $k_{stretch}$ could be obtained from IR spectra, as the stretching frequency of a bond depends on the force constant (and the masses of the atoms

Table 3.1 Change in energy as the C–C bond in CH_3–CH_3 is stretched away from its equilibrium length

C–C length, l	$l - l_{eq}$	$(l - l_{eq})^2$	$E_{stretch}$, kJ mol^{-1}
1.538	0	0	0
1.55	0.012	0.00014	0.29
1.56	0.022	0.00048	0.89
1.57	0.032	0.00102	1.86
1.58	0.042	0.00176	3.15
1.59	0.052	0.0027	4.75
1.6	0.062	0.00384	6.67

The calculations are ab initio (STO-3G; Chap. 5). Bond lengths are in Å

involved) [8], and l_{eq} could be derived from X-ray diffraction, electron diffraction, or microwave spectroscopy [9].

Let us find $k_{stretch}$ for the C/C bond of ethane by ab initio (Chap. 5) calculations. Normally high-level ab initio calculations would be used to parameterize a forcefield, but for illustrative purposes we can use the low-level but fast STO-3G method [10]. Eq. (3.2) shows that a plot of $E_{stretch}$ against $(l-l_{eq})^2$ should be linear with a slope of $k_{stretch}$. Table 3.1 and Fig. 3.7 show the variation of the energy of ethane with stretching of the C/C bond, as calculated by the ab initio STO-3G method. The reference bond length has been taken as the STO-3G length:

$$l_{eq}(C - C) = 1.538 \, \text{Å} \tag{3.10}$$

The slope of the graph is

$$k_{stretch}(C - C) = 1735 \, \text{kJ mol}^{-1} \text{Å}^{-2} \tag{3.11}$$

Similarly, the CH bond of methane was stretched using ab initio STO-3G calculations; the results are

$$l_{eq}(C - H) = 1.083 \, \text{Å} \tag{3.12}$$

$$k_{stretch}(C - H) = 1934 \, \text{kJ mol}^{-1} \text{Å}^{-2} \tag{3.13}$$

Parameterizing the Angle Bending Term From Eq. (3.3), a plot of E_{bend} against $(a-a_{eq})^2$ should be linear with a slope of k_{bend}. From STO-3G calculations on bending the H–C–C angle in ethane we get (cf. Table 3.1 and Fig. 3.7)

$$a_{eq}(HCC) = 110.7° \tag{3.14}$$

$$k_{bend}(HCC) = 0.093 \, \text{kJ mol}^{-1} \text{degree}^{-2} \tag{3.15}$$
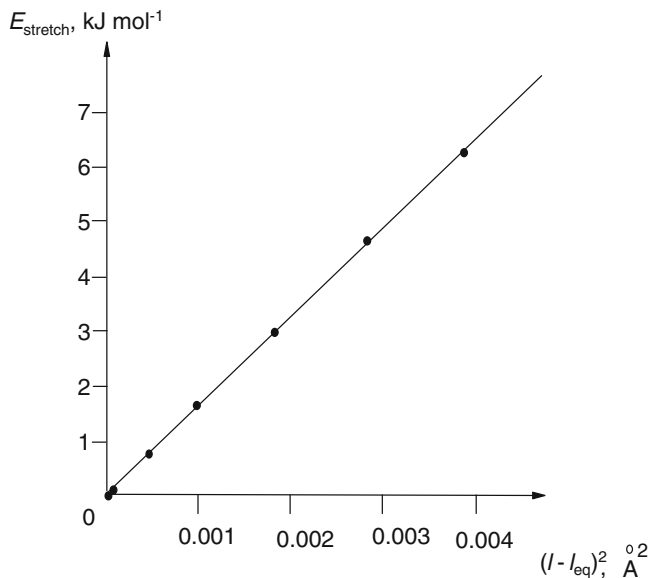
Fig. 3.7 Energy *vs*. the square of the extension of the C–C bond in CH_3–CH_3. The data in Table 3.1 were used

Calculations on staggered butane gave for the C–C–C angle

$$a_{eq}(CCC) = 112.5° \tag{3.16}$$

$$k_{bend}(CCC) = 0.110 \, kJ \, mol^{-1} \, degree^{-2} \tag{3.17}$$

Parameterizing the Torsional Term For the ethane case (Fig. 3.4), the equation for energy as a function of dihedral angle can be deduced fairly simply by adjusting the basic equation $E = \cos\theta$ to give $E = 1/2E_{max}[1 + \cos 3(\theta + 60)]$.

For butane (Fig. 3.5), using Eq. (*3.4) and experimenting with a curve-fitting program shows that a reasonably accurate torsional potential energy function can be created with five parameters, k_0 and k_1–k_4:

$$E_{torsion}(CH_3CH_2 - CH_2CH_3) = k_0 + \sum_{r=1}^{4} k_r[1 + \cos(r\theta)] \tag{3.18}$$

The values of the parameters k_0–k_5 are given in Table 3.2. The calculated curve can be made to match the experimental one as closely as desired by using more terms (Fourier analysis).

Parameterizing the Nonbonded Interactions Term To parameterize Eq. (3.5) we might perform ab initio calculations in which the separation of two atoms or groups in different molecules (to avoid the complication of concomitant changes in bond

Table 3.2 The experimental potential energy values for rotation about the central C−C bond of $CH_3CH_2-CH_2CH_3$ can be approximated by $E_{torsion}(CH_3CH_2 - CH_2CH_3) = k_0 + \sum_{r=1}^{4} k_r[1 + \cos(r\theta)]$ with $k_0 = 20.1$, $k_1 = -4.7$, $k_2 = 1.91$, $k_3 = -7.75$, $k_4 = 0.58$

θ (degrees)	E(calculated)	E(experimental)
0	0.15	0
30	6.7	7
60	14	14
90	8.8	9
120	3.5	3.3
150	15	15
180	25	25

Experimental energy values at 30°, 90°, and 150° were interpolated from those at 0°, 60°, 120°, and 180°; energies are in kJ mol^{-1}

lengths and angles) is varied, and fit Eq. (3.5) to the energy vs. distance results. For nonpolar groups this would require quite high-level calculations (Chap. 5), as van der Waals or dispersion forces are involved. We shall approximate the nonbonded interactions of methyl groups by the interactions of methane molecules, using experimental values of k_{nb} and σ, derived from studies of the viscosity or the compressibility of methane. The two methods give slightly different values [7b], but we can use the values

$$k_{nb} = 4.7 \, kJ \, mol^{-1} \tag{3.19}$$

and

$$\sigma = 3.85 \, \text{Å} \tag{3.20}$$

Summary of the Parameterization of the Forcefield Terms The four terms of Eq. (*3.1) were parameterized to give:

$$E_{stretch}(C - C) = 1735(l - 1.538)^2 \tag{3.21}$$

$$E_{stretch}(C - H) = 1934(l - 1.083)^2 \tag{3.22}$$

$$E_{bend}(HCH) = 0.093(a - 110.7)^2 \tag{3.23}$$

$$E_{bend}(CCC) = 0.110(a - 112.5)^2 \tag{3.24}$$

$$E_{torsion}(CH_3CCCH_3) = k_0 + \sum_{r=1}^{4} k_r[1 + \cos(r\theta)] \tag{3.25}$$

The parameters k of Eq. (3.25) are given in Table 3.2.

$$E_{nonband}(CH_3/CH_3) = 4.7 \left[\left(\frac{3.85}{r} \right)^{12} - \left(\frac{3.85}{r} \right)^{6} \right] \qquad (3.26)$$

Note that this parameterization is only illustrative of the principles involved; any really viable forcefield would actually be much more sophisticated. The kind we have developed here might at the very best give crude estimates of the energies of alkanes. An accurate, practical forcefield would be parameterized as a best fit to many experimental and/or calculational results, and would have different parameters for different kinds of bonds, e.g. C–C for acyclic alkanes, for cyclobutane and for cyclopropane. A forcefield able to handle not only hydrocarbons would obviously need parameters involving elements other than hydrogen and carbon. Practical forcefields also have different parameters for various *atom types*, like sp^3 carbon vs. sp^2 carbon, or amine nitrogen vs. amide nitrogen. In other words, a different value would be used for, say, stretching involving an sp^3/sp^3 C–C bond than for an sp^2/sp^2 C–C bond. This is clearly necessary since the force constant of a bond depends on the hybridization of the atoms involved. Obtaining the force constants for the stretching of an sp^3C/spC^3 and an sp^2C/spC^2 single bond, from examination of the IR spectra of, say, butane and of 1,3-butadiene, is not straightforward, since because these vibrations are coupled with those of C–H bonds, which is "the" appropriate C–C vibration is ambiguous. That the sp^2C/spC^2 C–C bond is significantly stronger and thus presumably significantly stiffer, as expected, is indicated by the fact that its bond energy (the energy needed to break the bond homolytically) is 1.3 times greater, 485 kJ mol^{-1} : 372 kJ mol^{-1}; this is from the values for the central C–C bonds of 1,3-butadiene and of butane [11]. For corresponding atoms, force constants are roughly proportional to bond order (double bonds and triple bonds are about two and three times as stiff, respectively, as the corresponding single bonds). Some forcefields account for the variation of double bond order with conformation (twisting p orbitals out of alignment reduces their overlap) by performing a simple PPP molecular orbital calculation (Chap. 6) to obtain the bond order.

A sophisticated forcefield might also consider all H/H nonbonded interactions explicitly, rather than simply subsuming some into, say, methyl/methyl interactions (combining atoms into groups is the feature of a *united atom* forcefield). Furthermore, nonbonded interactions between groups with charges or partial charges, like $C = O$, need to be accounted for in a field that is not limited to hydrocarbons. These can be handled by the well-known potential energy/electrostatic charge relationship

$$E = k(q_1 q_2 / r)$$

which has also been used to model hydrogen bonding [12]. A dielectric constant can be placed in the denominator to account for attenuation of the electrostatic potential by the medium of the molecule lying between the two groups or atoms. The charges can be assigned to atoms as parameters obtained by electronic structure calculations

on model molecules. Alternatively, electrostatic repulsion can be treated as repulsion between bond dipoles, values of which were assigned by fitting trial dipoles to experimental or calculated dipole moments of small molecules.

Another kind of energy term in good forcefields is one for *out-of-plane bending* around a tricoordinate atom like that in carbonyl compounds. The four atoms of XYC=O are not necessarily in the same plane, but can be made to pay an energy penalty which depends on the deviation of the C=O bond from the XYC plane.

A subtler problem with the naive forcefield developed here is that stretching, bending, torsional, nonbonded etc. terms are not completely independent. For example, the butane torsional potential energy curve (Fig. 3.5) does not apply precisely to all CH_3–C–C–CH_3 systems, because the barrier heights will vary with the length of the central C–C bond, obviously decreasing (other things being equal) as the bond is lengthened, since there will be a decrease in the interactions (whatever causes them) between the CH_3's and H's on one of the carbons of the central C–C and those on the other carbon. This could be accounted for by making the k's of Eq. (3.25) a function of the X−Y length. This would be a stretch-torsion *cross term*. Partitioning the energy of a molecule into stretching, bending, etc. terms is really somewhat formal; for example, the torsional barrier in butane can be considered to be partly due to nonbonded interactions between the methyl groups. It should be realized that there is no one, right functional form for an MM forcefield (see, e.g., [1a, b, c]); accuracy, versatility and speed of computation are the deciding factors in devising a forcefield. Finally, once initial parameters have been obtained in some fashion, as outlined above, the forcefield should be iteratively refined to obtain a parameter set that working together gives the best fit to, say, all geometric parameters (bond length, angle, and torsions), by minimizing the sum of the squares of the deviations from the "correct" (experimental or high-level calculated) values for a training set of molecules.

3.2.3   A Calculation Using our Forcefield

Let us apply the naive forcefield developed here to comparing the energies of two 2,2,3,3-tetramethylbutane ((CH_3)$_3$CC(CH_3)$_3$, i.e. *t*-Bu-Bu-*t*) geometries. We compare the energy of structure **1** (Fig. 3.8) with all the bond lengths and angles at our "natural" or standard values (i.e. at the STO-3G values we took as the reference bond lengths and angles in Sect. 3.2.2) with that of structure **2**, where the central C-C bond has been stretched from 1.538 Å to 1.600 Å, but all other bond lengths, as well as the bond angles and dihedral angles, are unchanged. Fig. 3.8 shows the nonbonded distances we need, which would be calculated by the program from bond lengths, angles and dihedrals. Using Eq. (*3.1):

$$\left(E = \sum_{bonds} E_{stretch} + \sum_{angles} E_{bend} + \sum_{dihedrals} E_{torsion} + \sum_{pairs} E_{nonbond} \right)$$
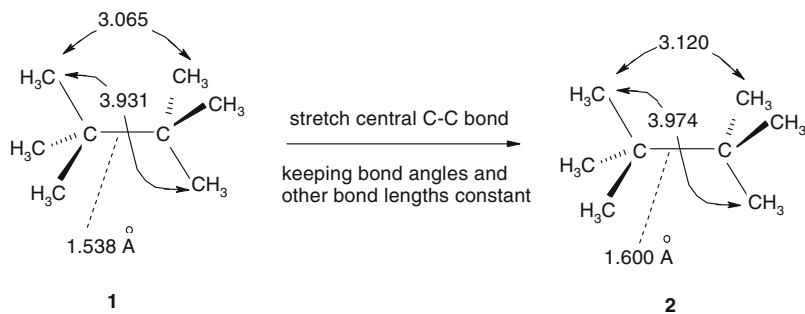
Fig. 3.8 Structures for a simple MM "by hand" calculation on the effect of changing the central C—C length of $(CH_3)_3C–C(CH_3)_3$ from 1.538 Å to 1.600 Å

For Structure **1**

$$\sum_{bonds} E_{stretch}(C - C) = 7 \times 1735(1.538 - 1.538)^2 = 0$$

Bond stretch contribution cf. structure with $l_{eq} = 1.538$

$$\sum_{bonds} E_{stretch}(C - H) = 18 \times 1934(1.083 - 1.083)^2 = 0$$

Bond stretch contribution cf. structure with $l_{eq} = 1.083$

$$\sum_{angles} E_{bend}(HCH) = 18 \times 0.093\,(110.7 - 110.7)^2 = 0$$

Bond bend contribution cf. structure with $a_{eq} = 110.7°$

$$\sum_{angles} E_{bend}(CCC) = 12 \times 0.110\,(112.5 - 112.5)^2 = 0$$

Bond bend contribution cf. structure with $a_{eq} = 112.5°$

$$\sum_{dihedrals} E_{torsion}(CH_3CCCH_3) = 6 \times 3.5 = 21.0$$

Torsional contribution cf. structure with no gauche – butane interactions

Actually, nonbonding interactions are already included in the torsional term (as *gauche*-butane interactions); we might have used an ethane-type torsional function and accounted for CH_3/CH_3 interactions entirely with

$$\sum_{nonbond} E_{nonbond}(anti - CH_3/CH_3) + \sum_{nonbond} E_{nonbond}(gauche - CH_3/CH_3)$$

$$= 3 \times 4.7\left[\left(\frac{3.85}{3.931}\right)^{12} - \left(\frac{3.85}{3.931}\right)^{6}\right] + 6 \times 4.7\left[\left(\frac{3.85}{3.065}\right)^{12} - \left(\frac{3.85}{3.065}\right)^{6}\right]$$

$$= 3 \times (-0.487) + 6 \times (54.05) = -1.463 + 324.3 = 323 \text{ kJ mol}^{-1}$$

nonbonding contribution cf. structure with noninteracting CH_3' s nonbonded terms. However, in comparing calculated *relative* energies the torsional term will cancel out.

$$E_{\text{total}} = E_{\text{stretch}} + E_{\text{bend}} + E_{\text{torsion}} = 0 + 0 + 21.0 + 323 \text{ kJ mol}^{-1} = 344 \text{ kJ mol}^{-1}$$

For Structure **2**

$$\sum_{bonds} E_{stretch}(C - C) = 6 \times 1735(1.538 - 1.538)^2 + 1 \times 1735(1.600 - 1.538)^2$$

$$= 0 + 6.67 = 6.67 \text{ kJ mol}^{-1}$$

Bond stretch contribution cf. structure with $l_{eq} = 1.538$

$$\sum_{bonds} E_{stretch}(C - H) = 18 \times 1934(1.083 - 1.083)^2 = 0$$

Bond stretch contribution cf. structure with $l_{eq} = 1.083$

$$\sum_{angles} E_{bend}(HCH) = 18 \times 0.093(110.7 - 110.7)^2 = 0$$

Bond stretch contribution cf. structure with $a_{eq} = 110.7°$

$$\sum_{angles} E_{bend}(CCC) = 12 \times 0.110(112.5 - 112.5)^2 = 0$$

Bond stretch contribution cf. structure with $a_{eq} = 112.5°$

$$\sum_{dihedrals} E_{torsion}(CH_3CCCH_3) = 6 \times 3.5 = 21.0$$

Torsional contribution cf. structure with no gauche–butane interactions

The stretching and bending terms for structure **2** are the same as for structure **1**, except for the contribution of the central C-C bond; strictly speaking, the torsional term should be smaller, since the opposing $C(CH_3)$ groups have been moved apart.

$$\sum nonbond E_{nonbond}(anti - CH_3/CH_3) + \sum_{nonbond} E_{nonbond}(gauche - CH_3/CH_3)$$

$$= 3 \times 4.7 \left[\left(\frac{3.85}{3.974} \right)^{12} - \left(\frac{3.85}{3.974} \right)^6 \right] + 6 \times 4.7 \left[\left(\frac{3.85}{3.120} \right)^{12} - \left(\frac{3.85}{3.120} \right)^6 \right]$$

$$= 3 \times (-0.673) + 6 \times (41.97) = -2.019 + 251.8$$

$$= 250 \, \text{kJ mol}^{-1}$$

nonbonding contribution cf. structure with noninteracting $CH_3^/$ S

$$E_{\text{total}} = E_{\text{stretch}} + E_{\text{bend}} + E_{\text{torsion}} = 6.67 + 0 + 21.0 + 250 \, \text{kJ mol}^{-1}$$

$$= 277 \, \text{kJ mol}^{-1}$$

So the relative energies are calculated to be

$$E(\text{structure } \mathbf{2}) - E(\text{structure } \mathbf{1}) = 277 - 344 \, \text{kJ mol}^{-1} = -67 \, \text{kJ mol}^{-1}$$

This crude method predicts that stretching the central C/C bond of 2,2,3,3-tetramethylbutane from the approximately normal sp^3–C–sp^3–C length of 1.583 Å (structure 1) to the quite "unnatural" length of 1.600 Å (structure 2) will lower the potential energy by 67 kJ mol^{-1}, and indicates that the drop in energy is due very largely to the relief of nonbonded interactions. A calculation using the accurate forcefield MM3 [13] gave an energy difference of 54 kJ mol^{-1} between a "standard" geometry approximately like structure 1, and a *fully optimized* geometry, which had a central C/C bond length of 1.576 Å. The surprisingly good agreement is largely the result of a fortuitous cancellation of errors, but this does not gainsay the fact that we have used our forcefield to calculate something of chemical interest, namely the relative energy of two molecular geometries. In principle, we could have found the minimum-energy geometry according to this forcefield, i.e. we could have optimized the geometry (Chap. 2). Geometry optimization is in fact the main use of MM. Some people distinguish between a molecular mechanics forcefield, which is an expression like that in Eq. (*3.1) for the energy of a molecule, and a molecular mechanics program, which uses a forcefield along with specific algorithms to calculate, e.g., optimized geometries or vibrational frequencies. Different programs could use the same forcefield but different algorithms, and vice versa.

Geometry optimizations with really viable MM programs are not done piecemeal as was just done here for illustrative purposes. Rather, a systematic algorithm is used, based on the fact that the energy is a known, fairly simple function of the nuclear ("atomic") coordinates and so first and second derivatives of the energy can be calculated analytically and used, with matrices, to iteratively find a potential energy surface minimum. This was explained in Sect. 2.4 and will be only modestly augmented here with regard to molecular mechanics. The MM energy is (cf. Eq. (3.1) etc.):

$$E = f(l, a, \cdots)$$

E is also a *parametric* function (Sect. 2.3) of l_{eq}, a_{eq}, etc., but for a given forcefield these are constants. The variables l, a etc. are *internal* coordinates, since the their values are inherent in the molecule and can be specified without an external frame of reference like Cartesian X, Y, Z axes. Clearly the same geometric information can be conveyed with Cartesian coordinates:

$$E = f(q_1, q_2, q_3 \cdots)$$

where q_1, q_2, q_3 etc. are x, y, z coordinates of atom 1, q_4, q_5, q_6, of atom 2 ("atom" is a more appropriate word than "nucleus" in MM), etc. Bond lengths, angles and dihedrals are simply related to the Cartesians by trigonometry. The Cartesian representation of geometry is preferred for optimization algorithms. The initial geometry matrix (cf. Sect. 2.4) is the column matrix of q_1, q_2, $q_3 \cdots$, and analytical differentiation provides $\partial E / \partial q_1$ and $\partial^2 E / \partial q_1 \partial q_1$ etc. for the gradient and Hessian matrices, so the geometry can be optimized using Eq. (2.14):

$$\mathbf{q}_o = \mathbf{q}_i - \mathbf{H}^{-1}\mathbf{g}_i$$

i.e. a Newton-Raphson algorithm. In fact, because MM is often used to optimize very large molecules, with hundreds or thousands of atoms, the *conjugate gradient* method is sometimes more appropriate in MM, since the time for the inversion of the Hessian rises steeply (as the cube) with the number of atoms, and the conjugate gradient method uses only first derivatives; this and other geometry optimization methods are discussed by Jensen [14]. The Newton-Raphson and conjugate gradient methods are briefly mentioned in comparison by Allinger ([1a], pp. 47 and 310).

The energy calculated by MM, which we have called potential energy, is also sometimes called strain energy, since it is relative to an unobservable standard, by-definition undistorted, *reference structure*. However, the term strain in chemistry has long been used to denote an experimentally observable set of properties connected mostly with distorted angles, and so MM energies are better denoted *steric energies*, steric being perhaps used to acknowledge the dependence of energy on molecular shape in general.

3.3   Examples of the Use of Molecular Mechanics

If we consider the applications of MM from the viewpoint of the goals of those who use it, then the main applications have been:

1. To obtain reasonable input geometries for lengthier (ab initio, semiempirical or density functional) kinds of calculations.
2. To obtain good geometries (and perhaps energies) for small- to medium-sized molecules.

3. To calculate the geometries and energies of very large molecules, usually polymeric biomolecules (proteins and nucleic acids).
4. To generate the potential energy function under which molecules move, for molecular dynamics or Monte Carlo calculations.
5. As a (usually quick) guide to the feasibility of, or likely outcome of, reactions in organic synthesis.

Examples of these five facets of the use of MM will be given.

3.3.1 To Obtain Reasonable Input Geometries for Lengthier (ab Initio, Semiempirical or Density Functional) Kinds of Calculations

The most frequent use of MM is probably to obtain reasonable starting structures for ab initio, semiempirical, or DFT (Chaps. 5, 6 and 7 calculations. Nowadays this is usually done by building the molecule with an interactive builder in a graphical user interface, with which the molecule is assembled by clicking atoms or groups together, much as one does with a "real" model kit. A click of the mouse invokes MM and provides, in most cases, a reasonable geometry. The resulting MM-optimized structure is then subjected to an ab initio, etc. calculation, usually beginning with geometry optimization; one expects this "higher-level" optimization to be faster than if the preliminary MM optimization had not been done.

By far the main use of MM is to find reasonable geometries for "normal" molecules, but it has also been used to investigate transition states. The calculation of transition states involved in *conformational* changes is a fairly straightforward application of MM, since "reactions" like the interconversion of butane or cyclohexane conformers do not involve the deep electronic reorganization that we call bond-making or bond-breaking. The changes in torsional and nonbonded interactions that accompany them are the kinds of processes that MM was designed to model, and so good transition state geometries and energies can be expected for this particular kind of process; transition state *geometries* cannot be (readily) measured, but the MM energies for conformational changes agree well with experiment: indeed, one of the two very first applications of MM [3a, d] was to the rotational barrier in biphenyls (the other was to the S_N2 reaction [3c]). Since MM programs are usually not able to optimize an input geometry toward a saddle point (see below), one normally optimizes to a minimum subject to the symmetry constraint expected for the transition state. Thus for ethane, optimization to a minimum within D_{3h} symmetry (i.e. by constraining the HCCH dihedrals to be 0^0, or by starting with a structure of exactly D_{3h} symmetry) will give the transition state, while optimization with D_{3d} symmetry gives the staggered ground-state conformer (Fig. 3.9). Optimizing an input C_{2v} cyclohexane structure (Fig. 3.10) gives the stationary point nearest this input structure, which is the transition state for interconversion of enantiomeric twist cyclohexane conformers.
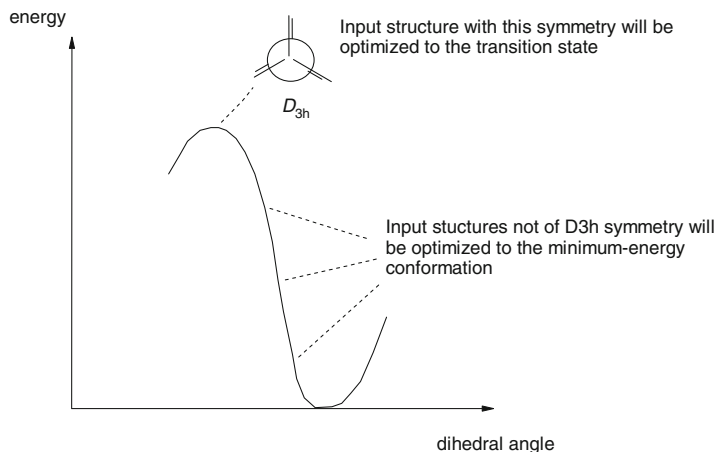
Fig. 3.9 Optimizing ethane within D_{3h} symmetry (i.e. by constraining the HCCH dihedral to be $0°$, or by inputting a structure with exact D_{3h} symmetry)) will give the transition state, while optimization without requiring D_{3d} symmetry gives the ground-state conformer
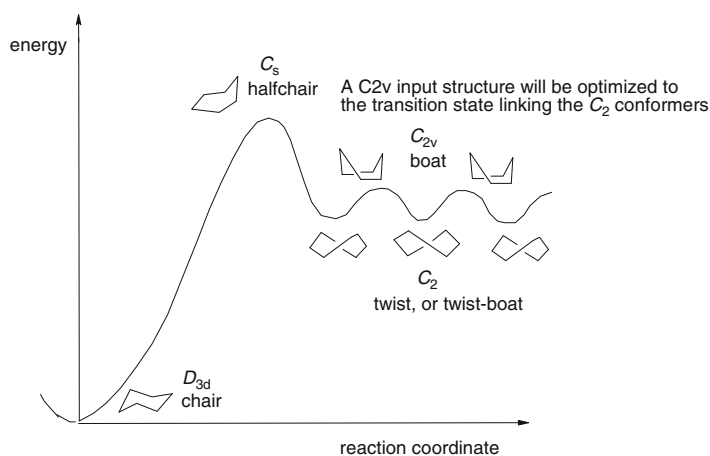
Fig. 3.10 Optimizing cyclohexane within C_{2v} symmetry gives a transition state, not one of the minima

Nevertheless there are several examples of the application of MM to actual chemical reactions, as distinct from conformational changes; the ones mentioned here are taken from the review by Eksterowicz and Houk [15]. The simplest way to apply MM to transition states is to approximate the transition state by a ground-state molecule. This can sometimes give surprisingly good results. The rates of solvolysis of compounds RX to the cation correlated well with the energy difference between the hydrocarbon RH, which approximates RX, and the cation R^+, which approximates the transition state leading to this cation. This is not entirely unexpected, as the Hammond postulate [16] suggests that the transition state should

resemble the cation, a high-energy species. In a similar vein, the activation energy for solvolysis has been approximated as the energy difference between a "methylalkane", with CH_3 corresponding to X in RX, and a ketone, the sp^2 carbon of which corresponds to the incipient cationic carbon of the transition state. MM has been used to study the transition states involved in S_N2 reactions, hydroborations, cycloadditions (mainly the Diels-Alder reaction), the Cope and Claisen rearrangements, hydrogen transfer, esterification, nucleophilic addition to carbonyl groups and electrophilic C/C bonds, radical addition to alkenes, aldol condensations, and various intramolecular reactions [15]. These studies approximate the TS, usually by using a normal molecule or ion as a surrogate, rather than finding a stationary point with one negative force constant.

One may wish a more precise approximation to the transition state geometry than is represented by an intermediate or a compound somewhat resembling the transition state. This can sometimes be achieved by optimizing to a minimum, subject to the constraint that the bonds being made and broken have lengths believed (e.g. from quantum mechanical calculations on simpler systems, or from chemical intuition) to approximate those in the transition state, and perhaps with appropriate angles and dihedrals also constrained. With luck this will take the stretched-bond input structure to a point on the potential energy surface near the saddle point. For example, an approximation to the geometry of the transition state for formation of cyclohexene in the Diels-Alder reaction of butadiene with ethene can be achieved (Fig. 3.11) by essentially building a boat conformation of
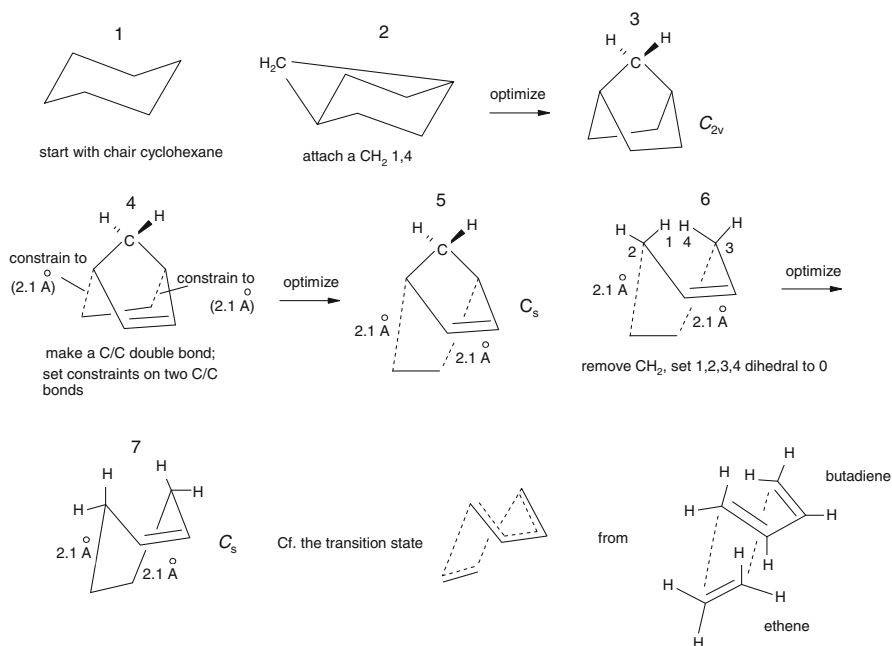
Fig. 3.11 Using molecular mechanics to get the (approximate) transition state for the Diels-Alder reaction of butadiene with ethene. This procedure gives a structure with the desirable C_s, rather than a lower, symmetry

cyclohexene, constraining the two forming C/C bonds to about 2.1 Å, and optimizing, using the CH_2 bridge (later removed) to avoid twisting and to maintain C_s symmetry; optimization with a dihedral constraint removes steric conflict between two hydrogens and gives a reasonable starting structure for, say, an ab initio transition state optimization.

The most sophisticated approach to locating a transition state with MM would be to use an algorithm that optimizes the input structure to a true saddle point, that is to a geometry characterized by a Hessian with one and only one negative eigenvalue (Chap. 2). To do this the MM program would have to be able not only to calculate second derivatives, but should also be parameterized for the partial bonds in transition states. Because this parameterization is lacking in MM forcefields, an approach to transition state location by finding the intersection or seam (the method is called the "SEAM method") of the reactant and product potential energy surfaces has been experimented with [17]. Nevertheless, MM is not much used to find transition states (this is distinct from its routine use in creating approximate input structures for proper transition state optimizations by some other method).

3.3.2 To Obtain (Often Excellent) Geometries

Molecular mechanics can provide excellent geometries for small (roughly C_1 to about C_{10}) and medium-sized (roughly C_{11} to C_{100}) organic molecules. It is by no means limited to organic molecules, as forcefields like SYBYL and UFF [5] have been parameterized for most of the periodic table, but the great majority of MM calculations have been done on organics, perhaps largely because MM was the creation of organic chemists (this is probably because the concept of geometric structure has long been central in organic chemistry). The two salient features of MM calculations on small to medium-sized molecules is that they are *fast* and they *can be* very accurate. Times required for geometry optimization without/with frequencies for unbranched $C_{20}H_{42}$, of C_{2h} symmetry (zigzag conformation), with the Merck Molecular Force Field (MMFF, i. e. MMFF94), the semiempirical AM1 (Chap. 6) and the ab initio HF/3-21G (a lower-level ab initio method, Chap. 5) methods, as implemented in the program SPARTAN [18], on a year 2014 machine, were:

MMFF, input from the molecule builder: optimization effectively 1 s, opt + frequencies effectively 1 s
Starting from the MMFF geometry:
AM1, optimization 1 s, opt + frequencies 52 s
HF/3-21G, optimization 3.0 min, opt + frequencies 9.6 min

Clearly as far as speed goes there is little contest between the methods, and the edge in favor of MM increases sharply with the size of the molecule. In fact, MM was till some years ago the only practical method for calculations on molecules

with more than about 100 heavy atoms (in computational chemistry a heavy atom is any atom heavier than helium). Even MM programs not designed specifically for macromolecules will handle molecules with thousands of atoms on a good personal computer.

MM geometries are usually reasonably good for small to medium-sized molecules [4], [9a], [19]; for the MM3 program (see below) the RMS error in bond lengths for the moderately large cholesteryl acetate was only about 0.007 Å [4a]. "Bond length" is, if unqualified, somewhat imprecise, since different methods of measurement give somewhat different values [4a]; [9a] (Chap. 5, Sect. 5.5.1). MM geometries are routinely used as input structures for quantum-mechanical calculations, but in fact the MM geometry and energy are in some cases as good or better than those from a "higher-level" calculation [20]; see too the discussion in connection with Fig. 3.12 and Tables 3.3 and 3.4. The MM forcefields MM3, OPLS and AMOEBA were better than semiempirical quantum mechanical methods (although these latter are admittedly quite approximate–Chap. 6) for calculating the geometries and binding energies of benzene dimers, species held together by weak "dispersion" forces [21]. The best structures for this were taken as those from the high-level ab initio CCSD(T) method (Chap. 5, Sect. 5.4.3). The benchmark MM programs for small to medium-sized molecules are probably MM3 and MM4. The Merck Molecular Force Field (MMFF) [22] is likely to remain very popular, not least because of its implementation in popular program suites like SPARTAN [18].

Inorganic compounds, particularly organometallics, present special problems for MM because by comparison with organics, on which the vast majority of work in this field has been expended, their bonding tends to be less literally interpretable in a ball-and-springs manner; for example, would the simplest and most widely transferable model of ferrocene (the dicyclopentadienyliron compound) use ten C-Fe bonds or two ring-center to iron bonds? A forcefield called Momec3 has been developed specially for inorganics [23].

3.3.2.1 Some Results for Geometries Calculated by MM

Figure 3.12 compares geometries calculated with the Merck Molecular Force Field (MMFF) with those from a reasonably high-level ab initio calculation $(MP2)FC)/$ 6-31G*; Chap. 5) and from experiment. The MMFF is a popular forcefield, applicable to a wide variety of molecules. Popular prejudice holds that the ab initio method is "higher" than molecular mechanics and so should give superior geometries. The set of 20 molecules in Fig. 3.12 is also used in Chaps. 5, 6, and 7, to illustrate the accuracy of ab initio, semiempirical, and density functional calculations in obtaining molecular geometries. The data in Fig. 3.12 are analyzed in Table 3.3. Table 3.4 compares dihedral angles for eight molecules, which are also used in Chaps. 5, 6, and 7. The experimental data for Fig. 3.12 come from Hehre et al. [24a], and for Table 3.4 from [24a], Harmony et al. [24b], and Huang et al. [24c].
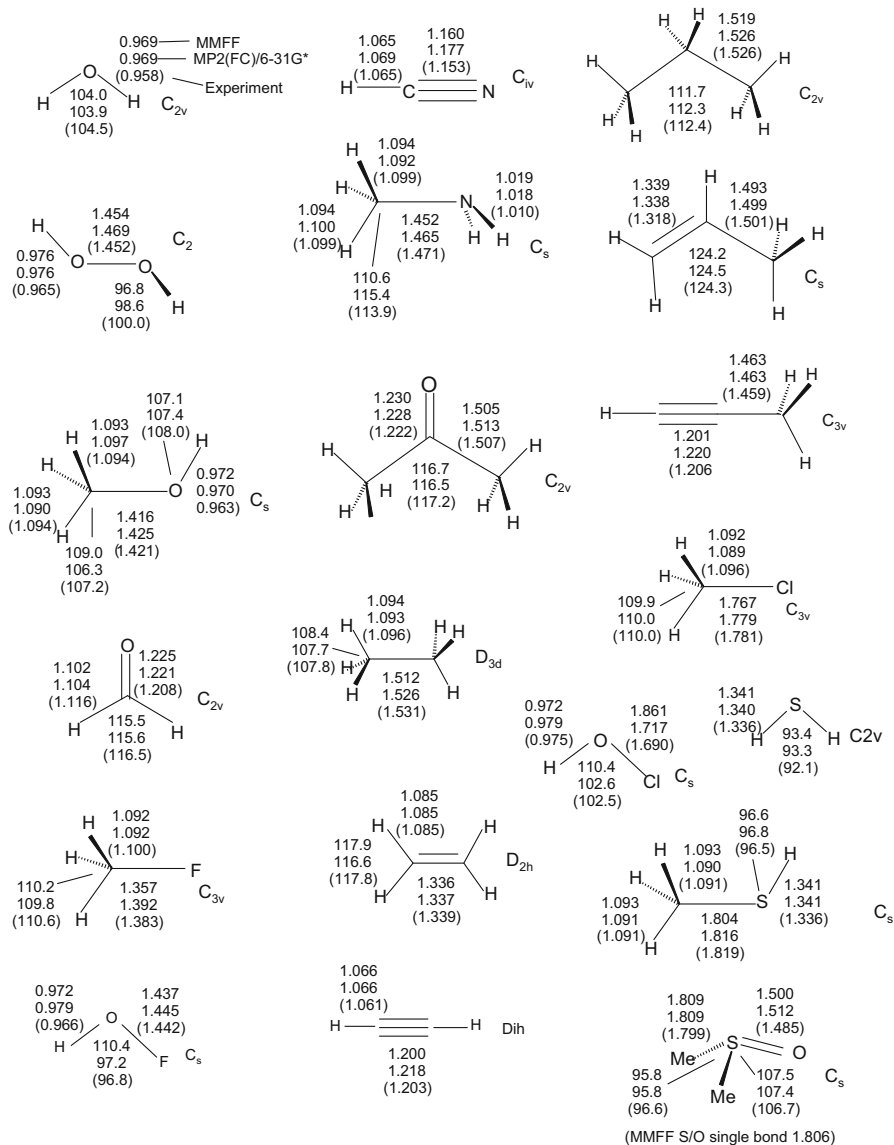
Fig. 3.12 A comparison of some MMFF, MP2(FC)/6-31G* and experimental geometries. Calculations are by the author and experimental geometries are from ref. [23a]. Note that all CH bonds are ca. 1 Å, all other bonds range from ca. 1.2–1.8 Å, and all bond angles (except for linear molecules) are ca. 90–120°

This survey suggests that: For common organic molecules the Merck Molecular Force Field is nearly as good as the ab initio MP2(FC)/6-31G* method for calculating geometries. Both methods give good geometries, but MP2/6-31G* calculations take longer. Admittedly, for these small molecules the difference is

Table 3.3 Error in MMFF molecular mechanics and MP2(FC)/6-31G* bond lengths and angles, from Fig. 3.13

Bond length errors, $r-r_{exp}$, Å			Bond angle errors, $a-a_{exp}$	
C–H	O–H, N–H, S–H	C–C	C–O, N, F, Cl, S	Angles
MeOH	H₂O	Me₂CO	MeOH	H₂O (HOH)
−0.001/−0.004	0.011/0.011	−0.002/0.006	−0.005/0.007	−0.5/−0.6
−0.001/ 0.003				
HCHO	H₂O₂	CH₃CH₃	HCHO	H₂O₂ (HOO)
−0.014/−0.012	0.011/0.011	−0.019/−0.005	0.017/0.013	−3.2/−1.4
MeF	MeOH	CH₂CH₂	MeF	MeOH (HCO)
−0.008/−0.008	0.009/0.007	−0.013/−0.017/−0.002		1.8/−0.9
				(COH)
				−0.9/−0.6
HCN	HOF	HCCH	HCN	HCHO (HCH)
0.000/0.004	0.000/0.004	−0.003/0.015	0.007/0.024	−1.0/−0.9
MeNH₂	MeNH₂	CH₃CH₂CH₃	MeNH₂	MeF (HCH)
−0.005/0.001	0.006/0.013	−0.007/0.000	−0.019/−0.006	−0.4/−0.8
−0.005/−0.007				
CH₃CH₃	MeNH₂	CH₂CHCH₃ −0.008/−0.002	Me₂CO	HOF (HOF)
−0.002/−0.003	0.009/0.008	0.021/0.020	0.008/0.006	13.6/0.4
CH₂CH₂	H₂S	HCCCH₃	MeCl	MeNH₂ (HCN)
0.000/0.000	0.005/0.004	0.004/0.004	−0.014/−0.002	−3.3/1.5
		−0.005/0.014		
CHCH	MeSH		MeSH	Me₂CO (CCC)
0.005/0.005	0.005/0.005		−0.015/−0.003	−0.5/−0.8
MeCl			Me₂SO	CH₃CH₃ (HCH)
−0.004/−0.007			0.010/0.010	0.6/−0.1

(continued)

Table 3.3 (continued)

C–H	Bond length errors, $r-r_{exp}$, Å		Bond angle errors, $a-a_{exp}$	
	O–H, N–H, S–H	C–C	C–O, N, F, Cl, S	Angles
MeSH				CH$_2$CH$_2$ (HCH)
0.002/0.000				0.1/−1.2
0.002/−0.001				
				CH$_3$CH$_2$CH$_3$ (CCC)
				−0.7/−0.1
				CH$_2$CHCH$_3$ (CCC)
				−0.1/0.2
				MeCl (HCH)
				−0.1/0.0
				H$_2$S (HSH)
				1.3/1.2
				MeSH (CSH)
				0.1/0.3
				Me$_2$SO (CSC)
				−0.8/−0.8
				(CSO)
				0.8/0.7
				0.8/0.7
3+, 8−, two 0	7+, 1−, none 0	2+, 7−, none 0	4+, 5−, none 0	7+, 11−, none 0
4+, 7−, two 0	8+, 0−, none 0	5+, 3−, one 0	6+, 3−, none 0	6+, 11−, one 0
mean of 13: 0.004/0.004	mean of 8: 0.007/0.008	mean of 9: 0.009/0.008	mean of 9: 0.011/0.009	mean of 18: 1.7/0.7

Errors are given as MMFF/MP2. In some cases (e.g. MeOH) errors for two bonds are given, on one line and on the line below. A *minus sign* means that the calculated value is less than the experimental. The numbers of positive, negative, and zero deviations from experiment are summarized at the bottom of each column. The averages at the bottom of each column are arithmetic means of the absolute values of the errors

Table 3.4 MMFF, MP2(FC)/6-31G* and experimental dihedral angles (degrees)

Molecule	Dihedral Angles		Errors	
	MMFF	MP2/6-31G*	Exp.	
HOOH	129.4	121.3	119.1[a]	10/2.2
FOOF	90.7	85.8	87.5[b]	3.2/−1.7
FCH$_2$CH$_2$F (FCCF)	72.1	69	73[b]	−1.0/−4
FCH$_2$CH$_2$OH (FCCO)	65.9	60.1	64.0[c]	1.9/−3.9
(HOCC)	53.5	54.1	54.6[c]	−1.1/−0.5
ClCH$_2$CH$_2$OH (ClCCO)	65.7	65.0	63.2[b]	2.5/1.8
(HOCC)	56.8	64.3	58.4[b]	−1.6/5.9
ClCH$_2$CH$_2$F (ClCCF)	69.8	65.9	68[b]	1.8/−2.1
HSSH	84.2	90.4	90.6[a]	−6.4/−0.2
FSSF	82.9	88.9	87.9[b]	−5.0/1.0
				Deviations: 5+, 5−/4+, 6− mean of 10: 3.5/2.3;

Errors are given in the *Errors* column as MMFF/MP2/6-31G*. A *minus sign* means that the calculated value is less than the experimental. The numbers of positive and negative deviations from experiment and the average errors (arithmetic means of the absolute values of the errors) are summarized at the bottom of the *Errors* column. Calculations are by the author; references to experimental measurements are given for each measurement. The AM1 and PM3 dihedrals vary by a fraction of a degree depending on the input dihedral. Some molecules have calculated minima at other dihedrals in addition to those given here, e.g. FCH$_2$CH$_2$F at FCCF 180°
[a][23a], pp.151, 152
[b][23b]
[c][23c]

scarcely consequential: for MM effectively about one second for each of the 20; for MP2(FC)/6 - 31G*, CH$_3$COCH$_3$, 16 s; CH3Cl, 7 s; (CH$_3$)$_2$SO, 33 s, on a vintage 2014 machine. But for larger molecules where MP2 would need hours, MM calculations might still take only seconds. Note, however, that ab initio methods provide information that molecular mechanics cannot, and are far more reliable for molecules outside those of the kind used in the MM training set (Sect. 3.2.2). The worst MMFF bond length deviation from experiment among the 20 molecules is 0.021 Å (the C = C bond of propene; the MP2 deviation is 0.020 Å); most of the other errors are ca. 0.01 Å or less. The worst bond angle error is 13.6°, for HOF, and for HOCl the deviation is 7.9°, the second worst angle error in the set. This suggests a problem for the MMFF with X–O–Halogen angles, but while for CH$_3$OF deviation from the MP2 angle (which is likely to be close to experiment) is MMFF − MP2 = 110.7° − 102.8° = 7.9°, for CH$_3$OCl the deviation is only 112.0° − 109.0° = 3.0°.

MMFF dihedral angles are remarkably good, considering that torsional barriers are believed to arise from subtle quantum mechanical effects. The worst dihedral angle error is 10°, for HOOH, and the second worst, −5.0°, is for the analogous HSSH. The ab initio HF/3-21G (Chap. 5) and semiempirical PM3 (Chap. 6) methods also have trouble with HOOH, predicting a dihedral angle of 180°. For

those dihedrals not involving OO or SS bonds, (an admittedly small selection), the MMFF errors are only ca. $1° − 2°$, cf. ca. $2° − 6°$ for MP2.

3.3.2.2 Geometries of Very Large Molecules, Usually Polymeric Biomolecules (Proteins and Nucleic Acids)

Next to generating geometries and energies of small to medium-sized molecules, the main use of MM is to model polymers, mainly biopolymers (proteins, nucleic acids, polysaccharides). Forcefields have been developed specifically for this; two of the most widely-used of these are CHARMM (Chemistry at HARvard using Molecular Mechanics) [25] (the academic version; the commercial version is CHARMm) and the forcefields in the computational package AMBER (Assisted Model Building with Energy Refinement) [26]. CHARMM was designed to deal with biopolymers, mainly proteins, but has been extended to handle a range of small molecules. AMBER is perhaps the most widely used set of programs for biological polymers, being able to model proteins, nucleic acids, and carbohydrates. Programs like AMBER and CHARMM that model large molecules have been augmented with quantum mechanical methods (semiempirical [27] and even ab initio [28]) to investigate small regions where treatment of electronic processes like transition state formation may be critical. This so-called QM/MM approach utilizes the ability of QM to calculate electronic phenomena and the ability of MM to calculate the geometry of large molecules [1k], [29].

An extremely important aspect of the modelling of biomolecules (which is done largely with MM) is designing pharmacologically active molecules that can fit into active sites (the pharmacophores) of biomolecules and serve as useful drugs. For example, a molecule might be designed to bind to the active site of an enzyme and block the undesired reaction of the enzyme with some other molecule. Pharmaceutical chemists computationally craft a molecule that is sterically and electrostatically complementary to the active site, and try to *dock* the potential drug into the active site. The binding energy of various candidates can be compared and the most promising ones can then be synthesized, as the second step on the long road to a possible new drug. The computationally assisted design of new drugs and the study of the relationship of structure to activity (quantitative structure-activity relationships, QSAR) is one of the most active areas of computational chemistry [30]. Particularly relevant to the investigation of biochemical processes is the combining of quantum mechanics with MM in the QM/MM method mentioned above.

3.3.3 To Obtain (Sometimes Excellent) Relative Energies

As explained in Sect. 3.5, *Weaknesses*, one should not compare the steric energies of molecules of different structural types, like functional group isomers such CH_3CH_2OH and CH_3OCH_3, and even an unbranched 1-alkene cf. an isomeric

internal alkene is suspect, since a monosubstituted and a disubstituted $C = C$ unit are different in a heavily parameterized forcefield. The range of valid energy comparison is greatly extended if the MM program can calculate not merely steric energies, but also enthalpies of formation (heats of formation), ΔH^0_f, the heat energy that must be input to make a mole of the compound from its elements in their standard states: the enthalpies of any two compounds with the same molecular formula can be validly compared since both values are relative to the same number of moles of the elements in their standard states. The MM4 forcefield can calculate accurate enthalpies of formation for hydrocarbons by combining steric energy with appropriate parameterization [31], [1f]. The connection between the steric energy V_{steric} of a molecule and its enthalpy of formation is somewhat involved, since (in essence) one is a kind of strain energy relative to a hypothetical ideal molecule and the other is a kind of difference in bond energies between the molecule and its elements in their standard states. The principle behind the calculation of enthalpies of formation from MM steric energies is shown below.

Consider for conceptual and notational simplicity the specific case of ethane, C_2H_6. The formation reaction equation for ethane from its elements in their standard states is

$$2C(\text{graphite}) + 3H_2 \rightarrow C_2H_6$$
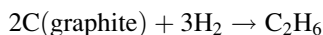
and the change in internal energy for the formation reaction at 0 K is

$$\Delta E^{total} = E^{total}(\text{products}) - E^{total}(\text{reactants}),$$

$$\Delta E^{total} = \left(V_{steric} - \sum BE_{CH} - \sum BE_{CC}\right) - \left(2E^{total}(\text{graphite}) + 3E^{total}(H_2)\right)$$

$$(3.27)$$

Here ΔE^{total} is the change in the total electronic plus internuclear repulsion energy and BE is bond energy. E^{total} (using the notation in this book: Chap. 5, Eq. (5.93)) is conventionally called the electronic energy, although it is really the sum of the electronic energy and the internuclear repulsion energy. We will encounter this in Chap. 5, as the ab initio energy of a molecule. The internal energy of ethane, the product, is here equated to the molecular mechanics steric ("strain" in looser terminology) energy *minus* the energy of the reference structure, whose energy is just the sum of its bond energies; from the definition of bond energy this sets the energy zero here at the energy of the separated atoms. Regarding the reactants, although graphite is polymeric, we consider for energy changes a hypothetical monatomic but standard-state solid graphite, and the other reactant is dihydrogen. The internal energy change of Eq. 3.27 ignores changes in ZPE, which we hope to take into account in parameterization.

All this was at $T = 0$ K because it ignores contributions to internal energy from translational and rotational terms involving RT; we now bring in these terms and go to $T > 0$. We need the gas phase molar change in translational and rotational

internal energies for the formation reaction, ΔE(trans) and ΔE(rot). The usual symbol for internal energy is U, but here I use E for notational concordance with ΔE^{total}, the internal energy change in Eq. (3.26). The gas phase species in the formation equation are dihydrogen and ethane; graphite is a solid. ΔE(trans) is simply the change in the number of gas-phase molecules times $3/2RT = (1-3)$ $(3/2)RT = -3RT$ (since each gas-phase particle regardless of structure has 3 degrees of translational freedom, each corresponding to $(1/2)RT$ of internal energy – see any good book on statistical thermodynamics). ΔE(rot) is $E(\text{rot, C}_2\text{H}_6) - 3E$ $(\text{rot, H}_2) = 1(3)(1/2RT) - 3(2)(1/2)RT = (-3/2)RT$ (since there is one C_2H_6 molecule (or mole), and it has three rotational degrees of freedom, for a factor of $1 \times 3 \times \frac{1}{2}RT$ of internal energy, while there are three H_2 molecules, and as a linear molecule each has 2 rotational degrees of freedom, for a factor of $1 \times 3 \times \frac{1}{2}RT$ of internal energy). The internal energy change due to the translational and rotational energy change is therefore $(-3 - 3/2)RT = (-9/2)RT$. We now go from internal energy to enthalpy, since we want to calculate enthalpy of formation.

The enthalpy change is the internal energy change plus ΔnRT (Chap. 5, Sect. 5.5.2.1.1), where $\Delta n = $ change in the number of gas-phase molecules; here $\Delta n = 1 - 3 = -2$. So at temperature T, usually chosen to be 298 K (298.15 K, "standard ambient temperature") for parameterization (below), the enthalpy change for the formation reaction is (adding to the change in 0 K internal energy the rotational and translational terms $(-9/2)RT$ and the $-2RT$ enthalpy adjustment)

$$\Delta H_{\text{f},T}^\circ = \Delta E^{\text{total}} - (9/2)RT - 2RT = \Delta E^{\text{total}} - (13/2)RT$$

and since (Eq. (3.27))

$$\Delta E^{\text{total}} = \left(V_{\text{steric}} - \sum \text{BE}_{\text{CH}} - \sum \text{BE}_{\text{CC}}\right) - \left(2E^{\text{total}}(\text{graphite}) + 3E^{\text{total}}(\text{H}_2)\right)$$

then

$$\Delta H_{\text{f},T}^\circ = V_{\text{steric}} - \sum \text{BE}_{\text{CH}} - \sum \text{BE}_{\text{CC}} - 2E^{\text{total}}(\text{graphite}) - 3\,E^{\text{total}}(\text{H}_2)$$
$$- (13/2)RT$$

or

$$\Delta H_{\text{f},T}^\circ = V_{\text{steric}} - 6\text{BE}_{\text{CH}} - 1\text{BE}_{\text{CC}} - 2E^{\text{total}}(\text{graphite}) - 3\,E^{\text{total}}(\text{H}_2) - (13/2)RT$$
$$\tag{3.28}$$

for ethane, which has 6 CH bonds and one CC bond.

The problem here is the two E^{total} terms, because MM can't calculate electronic energies. Now, a similar but conceptually more intricate derivation of $\Delta H_{\text{f},T}^\circ$ for a *general* alkane or cycloalkane gives [1f]:

$$\Delta H_{f,T}^{\circ} = V_{\text{steric}}$$
$$- N_{\text{CH}}\left[\text{BE}_{\text{CH}} + (1/4)E^{\text{total}}(\text{graphite}) + (1/2)E^{\text{total}}(\text{H}_2) + (7/4)RT\right]$$
$$- N_{\text{CC}}\left[\text{BE}_{\text{CC}} + (1/2)E^{\text{total}}(\text{graphite})\right] + 4RT$$

$$(3.29)$$

where N_{CH} and N_{CC} are the number of CH and CC bonds. For $N_{\text{CH}} = 6$ and $N_{\text{CC}} = 1$, this reduces to Eq. 3.28, which was derived specifically for ethane. The general Eq. 3.29 solves the problem of the E^{total} terms, because we can write it

$$\Delta H_{f,T}^{\circ} = V_{\text{steric}} + k_{\text{CH}}N_{\text{CH}} + k_{\text{CC}}N_{\text{CC}} + 4RT \qquad (3.30)$$

where

$$k_{\text{CH}} = -\left[\text{BE}_{\text{CH}} + (1/4)E^{\text{total}}(\text{graphite}) + (1/2)E^{\text{total}}(\text{H}_2) + (7/4)RT\right]$$

and

$$k_{\text{CC}} = -\left[\text{BE}_{\text{CC}} + (1/2)E^{\text{total}}(\text{graphite})\right]$$
$$4RT = 9.92 \text{ kJ mol}^{-1} \text{ at } 298\,\text{K}$$

The E^{total} quantities can now be parameterized away by finding the best k_{CH} and k_{CC} that fit MM-calculated enthalpies of formation to those of experimental (or nowadays often high-level ab initio or DFT) enthalpies of formation, for a set of alkanes or cycloalkanes. Parameterization has not only the essential feature of taking care of E^{total} but also the nice features of handling the bond energy terms, and of implicitly accounting for zero point vibrational energy, because E^{total} does not include ZPE. The parameterization is illustrated below. The treatment above has not mentioned the fact that acyclic molecules in particular are usually floppy and so when we measure experimentally an enthalpy of formation, this may be for a Boltzmann distribution mixture of conformers, while a single calculation of V_{steric} is for a particular conformer. So if one conformer does not heavily predominate, or is not, as for a rigid molecule, the sole one, then if the calculated $\Delta H_{f,T}^{\circ}$ is to correspond to what is actually measured, the enthalpy of formation of the conformational mixture must be calculated by weighting $\Delta H_{f,T}^{\circ}$ (calculated) for the individual conformers according to their relative abundance; this could be done automatically as part of the enthalpy of formation calculation by an algorithm which searches V_{steric} conformational space.

The ten compounds in Table 3.5 were used to find the fitting parameters k_{CH} and k_{CC} in Eq. 3.30 and thus obtain a usable equation. These ten compounds each consist of essentially just one conformer, avoiding the conformer mixture problem. In principle the parameterization could be done with a multiple regression analysis computer program, but the k_{CH} and k_{CC} used here were found, in the spirit of Eq. 3.30, by noting ([1f], page 645) that "Typically" these values are ca. -4.5 and $2.5 \text{ kcal mol}^{-1}$, i.e. ca. -19 and 10 kJ mol^{-1}. Using these quantities as starting

Table 3.5 Experimental 298 K enthalpies of formation (kJ mol^{-1}), V_{steric}, N_{CH}, and N_{CC} for ten compounds; data to obtain the parameters k_{CH} and k_{CH} in Eq. (3.30), i.e. to obtain Eq. (3.31)

Compound	Exp $\Delta H_{f,T}°$	V_{steric}	N_{CH}	N_{CC}
Ethane	−84	−19.81	6	1
Propane	−104.7	−20.45	8	2
Isobutane	−134.2	−1.98	10	3
Cyclopentane	−76.4	6.47	10	5
Cyclohexane	−124.6	−14.90	12	6
Methylcyclohexane	−154.8	2.92	14	7
Methylcyclopentane	−106	23.47	12	6
Norbornane	−54.9	82.74	12	7
cis-Decalin	−169.2	34.23	18	11
trans-Decalin	−182.2	26.19	18	11

The experimntal $\Delta H_{f,T}°$ are from the NIST website and V_{steric} was calculated using the Merck Molecular Force Field (MMFF)

points, incremental variations of ca. 0.5 kJ mol^{-1} around these pairs of values gave (within these limitations of parameter space, and using the compounds of Table 3.5) as the best equation of the type (3.30), Eq. (3.31):

$$\Delta H_{f,T}° = V_{steric} - 16N_{CH} + 8N_{CC} + 9.92 \quad 4RT = 9.92 \text{ kJ mol}^{-1} \qquad (3.31)$$

This is our illustrative MM equation for calculating the enthalpies of formation of alkanes and cycloalkanes. It applies to V_{steric} calculated by the Merck Molecular Force Field (MMFF). Now let's check Eq. (3.31) first against the ten compounds used to parameterize it. The results of this are summarized in Table 3.6. The absolute mean deviation of the calculated $\Delta H_{f,T}°$ from the experimental is 13.8 kJ mol^{-1} and the largest deviation is 27.2 kJ mol^{-1}. This doesn't look so bad but, after all, the check is against the training set. As a second check let's try Eq. (3.31) for the first 35 compounds in Allinger's book [1a] in Table 11.1 on page 266. Note that several of these compounds (most of the open-chain alkanes) are mixtures of conformers; in a rigorous treatment the Boltzmann distribution would have to be addressed. The results of this comparison of calculated and experimental values are summarized in Table 3.7. The absolute mean deviation of the calculated $\Delta H_{f,T}°$ from the experimental is 39.7 kJ mol^{-1} and the largest deviation is 214.6 kJ mol^{-1}. Nine of the 35 compounds have an absolute mean deviation |dev| of more than 50 kJ mol^{-1}. All of these have one or more quaternary carbons (a carbon bonded to four other carbons); the only compound with a quaternary carbon for which |dev| < 50 kJ mol^{-1} is 1,1-dimethylcyclopentane, |dev| = 45.5 kJ mol^{-1}. If we accept that this simple parameterization can't handle quaternary carbons and remove the nine offenders and the borderline case, we get Table 3.8, with 25 entries. This has a mean absolute deviation of 17.3 kJ mol^{-1} and a maximum absolute deviation of 43.6 kJ mol^{-1} (nonane). These deviations are way below the spectacular errors seen before removal of the ten cases addressed above, and begin to verge on tolerable accuracy, which is perhaps surprising for such a small training

Table 3.6 Checking Eq. (3.31) with the ten compounds used in the parameterization

Compound	Calc. $\Delta H_{f,T}^{\,\mathrm{o}}$	Exp. $\Delta H_{f,T}^{\,\mathrm{o}}$	|deviation|
Ethane	−97.9	−84	13.9
Propane	−122.5	−104.7	17.8
Isobutane	−128.1	−134.2	6.1
Cyclopentane	−103.6	−76.4	27.2
Cyclohexane	−149	−124.6	24.4
Methylcyclohexane	−155.2	−154.8	0.4
Methylcyclopentane	−110.6	−106	4.6
Norbornane	−43.3	−54.9	11.6
cis-Decalin	−155.9	−169.2	13.3
trans-Decalin	−163.9	−182.2	18.3

Calculated and experimental 298 K enthalpies of formation (kJ mol^{-1}) from $\Delta H_{f,T}^{\,\mathrm{o}} = V_{\mathrm{steric}}$ $-16N_{\mathrm{CH}} + 8N_{\mathrm{CC}} + 9.92$ (Eq. 3.31). Maximum \|deviation\| = 27.2, average \|deviation\| = 13.8 kJ mol^{-1}

Table 3.7 Testing Eq. (3.31) ($\Delta H_{f,T}^{\,\mathrm{o}} = V_{\mathrm{steric}} - 16N_{\mathrm{CH}} + 8N_{\mathrm{CC}} + 9.92$) with the first 35 compounds in [1a], Table 11.1, p. 266 (seven of these 35, marked *, were used in the parameterization list of Tables 3.5 and 3.6). Maximum \|deviation\| = 214.6, average \|deviation\| = 39.7 kJ mol^{-1}

Compound	V_{steric}	N_{CH}	N_{CC}	Calc. $\Delta H_{f,T}^{\,\mathrm{o}}$	Exp. $\Delta H_{f,T}^{\,\mathrm{o}}$	|dev|
Methane	0.11	4	0	−54	−74.9	20.9
Ethane*	−19.8	6	1	−97.9	−84.7	13.2
Propane*	−20.5	8	2	−122.5	−103.3	19.2
Butane	−21.2	10	3	−147.3	−126.1	21.2
Pentane	−22.1	12	4	−128	−146.4	18.4
Hexane	−22.9	14	5	−197	−167.2	29.8
Heptane	−23.8	16	6	−221.8	−187.8	34
Octane	−24.6	18	7	−246.7	−208.4	38.3
Nonane	−25.5	20	8	−271.6	−228	43.6
Isobutane*	−2	10	3	−128.1	−134.5	6.4
Isopentane	1.38	12	4	−148.7	−154.5	5.8
Neopentane	35.57	12	4	−114.5	−168.5	54
2,3-Dimethylbutane	27.75	14	5	−146.3	−177.8	31.5
2,2,3-Trimethylbutane	72.61	16	6	−125.5	−204.8	79.3
2,2-Dimethylpentane	42.3	16	6	−155.8	−205.9	50.1
3,3-Dimethylpentane	52.55	16	6	−145.5	−201.2	55.7
3-Ethylpentane	10	16	6	−188.1	−189.3	1.2
2,4-Dimethylpentane	22.75	16	6	−175.3	−201.7	26.4
2,5-Dimethylhexane	23.48	18	7	−198.6	−222.5	23.9
2,2,3,3-Tetramethylbutane	124.5	18	7	−97.6	−225.6	128
2,2,3,3-Tetramethylpentane	137.2	20	8	−108.9	−237	128.1
di-tert-butylmethane	132.8	20	8	−113.3	−241.8	128.5
Tetraethylmethane	67.51	20	8	−178.6	−232.9	54.3
Tri-tert-butylmethane	363.6	28	12	21.4	−236	214.6

(continued)

Table 3.7 (continued)

Compound	V_{steric}	N_{CH}	N_{CC}	Calc. $\Delta H_{f,T}^{o}$	Exp. $\Delta H_{f,T}^{o}$	|dev|
Cyclopentane[*]	6.47	10	5	−103.6	−78.41	25.2
Cyclohexane[*]	−14.9 0	12	6	−149	−123.1	25.9
Cycloheptane	25	14	7	−133.1	−118.1	15
Cyclooctane	56.82	16	8	−125.3	−124.4	0.9
Cyclononane	74.73	18	9	−131.4	−132.8	1.4
Cyclodecane	84.77	20	10	−145.3	−154.3	9
Cyclododecane	77.14	24	12	−200.9	−228.4	27.5
1,1-Dimethylcyclopentane	65.42	14	7	−92.7	−138.2	45.5
Methylcyclopentane[*]	23.47	12	6	−110.6	−105.7	4.9
Ethylcyclopentane	23.66	14	7	−134.4	−126.8	7.6
Methylcyclohexane[*]	2.92	14	7	−155.2	−154.8	0.4

Table 3.8 The 25 compounds in Table 3.5 without quaternary carbons

Compound	V_{steric}	N_{CH}	N_{CC}	Calc. $\Delta H_{f,T}^{o}$	Exp. $\Delta H_{f,T}^{o}$	|dev|
Methane	0.11	4	0	−54	−74.9	20.9
Ethane[*]	−19.8	6	1	−97.9	−84.7	13.2
Propane[*]	−20.5	8	2	−122.5	−103.3	19.2
Butane	−21.2	10	3	−147.3	−126.1	21.2
Pentane	−22.1	12	4	−128	−146.4	18.4
Hexane	−22.9	14	5	−197	−167.2	29.8
Heptane	−23.8	16	6	−221.8	−187.8	34.0
Octane	−24.6	18	7	−246.7	−208.4	38.3
Nonane	−25.5	20	8	−271.6	−228	43.6
Isobutane[*]	−2.0	10	3	−128.1	−134.5	6.42
Isopentane	1.38	12	4	−148.7	−154.5	5.8
2,3-Dimethylbutane	27.8	14	5	−146.3	−177.8	31.5
3-Ethylpentane	10.0	16	6	−188.1	−189.3	1.2
2,4-Dimethylpentane	22.75	16	6	−175.3	−201.7	26.4
2,5-Dimethylhexane	23.5	18	7	−198.6	−222.5	23.9
Cyclopentane[*]	6.47	10	5	−103.6	−78.41	25.2
Cyclohexane[*]	−14.9	12	6	−149	−123.1	25.9
Cycloheptane	25.0	14	7	−133.1	−118.1	15.0
Cyclooctane	56.8	16	8	−125.3	−124.4	0.9
Cyclononane	74.7	18	9	−131.4	−132.8	1.4
Cyclodecane	84.8	20	10	−145.3	−154.3	9.0
Cyclododecane	77.14	24	12	−200.9	−228.4	27.5
Methylcyclopentane[*]	23.47	12	6	−110.6	−105.7	4.9
Ethylcyclopentane	23.66	14	7	−134.4	−126.8	7.6
Methylcyclohexane[*]	2.92	14	7	−155.2	−154.8	0.4

[*]Compounds with an asterisk were used in the parameterization list of Tables 3.3 and 3.4
With Eq. (3.31), $\Delta H_{f,T}^{o} = V_{steric} - 16 N_{CH} + 8 N_{CC} + 9.92$, the maximum \|deviation\| = 43.6, and average \|deviation\| = 17.3 kJ mol^{-1}
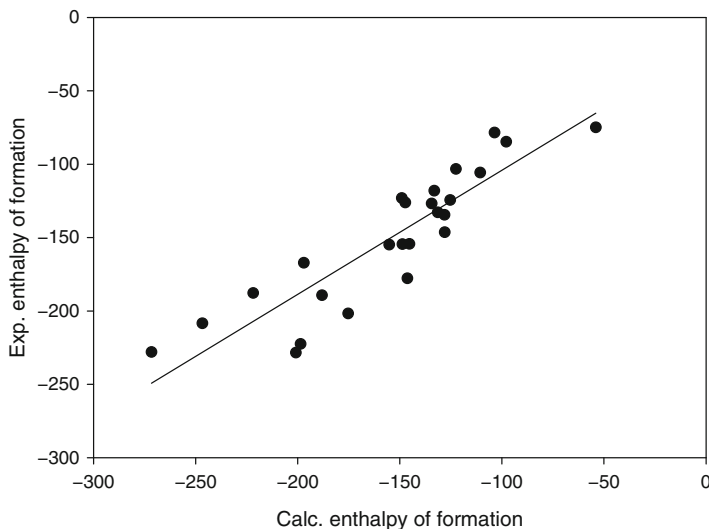
Fig. 3.13 Relationship between experimental enthalpy of formation and that calculated from Eq. (3.31), $\Delta H_{f,T}{}^{\circ} = V_{\text{steric}} - 16N_{\text{CH}} + 8N_{\text{CC}} + 9.92$. The points correspond to the 25 compounds in Table 3.8. Correlation coefficient $r^2 = 0.800$ (the best-fit line, shown, has the equation Exp = 0.846Calc − 19.56)

set. A "real" equation for calculating $\Delta H_{f,T}{}^{\circ}$ from V_{steric} might be based on a far bigger training set. Figure 3.13 shows a plot of the data in Table 3.8. The impression of correlation is obvious, and on a less intuitive note, the correlation coefficient of 0.800, while not spectacular, is as much as might have been expected for a rudimentary parameterization. The errors for quaternary carbon compounds reflect the simple parameterization used here. A more elaborate procedure might have k-parameters not just for the numbers of general CH and CC bonds (the N_{CH} and N_{CC} columns in Table 3.5), but, say, a parameter for the number of CH bonds to methyl groups, another for the number to methylene groups, etc., and analogous distinctions for the number of CC bonds to CH_3, to CH_2, etc. For the MM4 program, for standard hydrocarbons ΔH_f^0 errors are usually less than $4 \, \text{kJ mol}^{-1}$ (less than $1 \, \text{kcal mol}^{-1}$), which is comparable to experimental error [31]; the errors in MM conformational energies are often only about $2 \, \text{kJ mol}^{-1}$ [32].

3.3.4   To Generate the Potential Energy Function Under Which Molecules Move, for Molecular Dynamics or Monte Carlo Calculations

Programs like those in AMBER are used not only for calculating geometries and energies, but also for simulating molecular motion, i.e. for molecular dynamics [33], and for calculating the relative populations of various conformations or

other geometric arrangements (e.g. solvent molecule distribution around a macro-molecule) in Monte Carlo simulations [34]. In molecular dynamics Newton's laws of motion are applied to molecules moving in a molecular mechanics forcefield, although relatively small parts of the system (system: with biological molecules in particular modelling is often done not on an isolated molecule but on a molecule and its environment of solvent and ions) may be simulated with quantum mechanical methods [27, 28]. In Monte Carlo methods random numbers decide how atoms or molecules are moved to generate new conformations or geometric arrangements ("states") which are then accepted or rejected according to some filter. Tens of thousands (or more) of states are generated, and the energy of each is calculated by MM, generating a Boltzmann distribution. Do not confuse molecular *mechanics*, the forcefield approach to calculating molecular structure and properties, with molecular *dynamics*, a set of techniques for following through time the motions, and in some cases the reactions, of molecules.

Molecular dynamics (MD) simulations of actual chemical reactions, in contrast to conformational movements and the shuffling of solvent molecules, cannot be done with MM because, as discussed above in connection with calculating transition states (Sect. 3.3.1), MM cannot handle bond-breaking and -making. Such molecular dynamics simulations are done with electronic structure methods (ab initio, semiempirical and density functional, Chaps. 5, 6, and 7).

3.3.5   As a (Usually Quick) Guide to the Feasibility of, or Likely Outcome of, Reactions in Organic Synthesis

In the past 15 years or so MM has become widely used by synthetic chemists, thanks to the availability of inexpensive computers (personal computers will easily run MM programs) and user-friendly and relatively inexpensive programs [5]. Since MM can calculate the energies and geometries of ground state molecules and (within the strong limitations alluded to above) transition states, it can clearly be of great help in planning syntheses. To see which of two or more putative reaction paths should be favored, one has a choice of three methods: (1) use MM like a hand-held model to examine the substrate molecule for factors like steric hindrance or proximity of reacting groups, or (2) approximate the transition states for alternative reactions using an intermediate or some other plausible proxy (cf. the treatment of solvolysis in the discussion of transition states above), or (3) attempt to calculate the energies of competing transition states (cf. the above discussion of transition state calculations).

The examples given here of the use of MM in synthesis are taken from the review by Lipkowitz and Peterson [35]. In attempts to simulate the metal-binding ability of biological acyclic polyethers, the tricyclic **1** (Fig. 3.14) and a tetracyclic analogue were synthesized, using as a guide the indication from MM that these
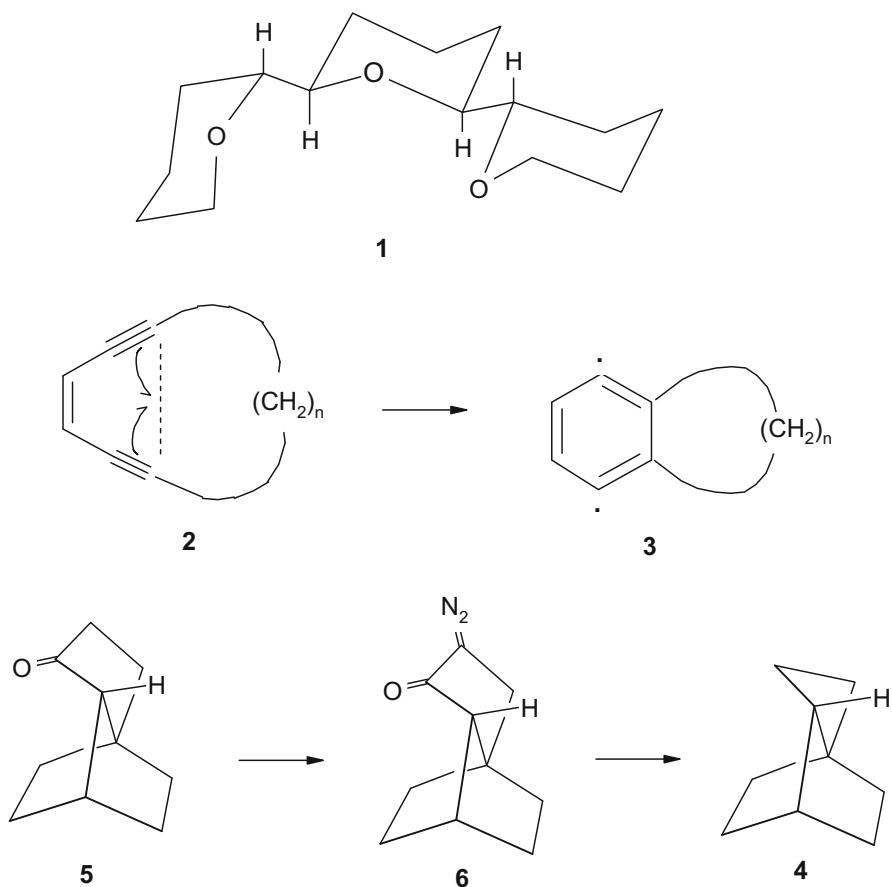
Fig. 3.14 Some molecules (**1**, **2**, **4**) which have been synthesized with the aid of molecular mechanics

molecules resemble the cyclic polyether 18-crown-6, which binds the potassium ion; the acyclic compounds were found to be indeed comparable to the crown ether in metal-binding ability.

Enediynes like **2** (Fig. 3.14) are able to undergo cyclization to a phenyl-type diradical **3**, which *in vivo* can attack DNA; in molecules with an appropriate triggering mecha;nism this forms the basis of promising anticancer activity. The effect of the length of the constraining chain (i.e. of *n* in **2**) on the activation energy was studied by MM, aiding the design of compounds (potential drugs) that were found to be more active against tumors than are naturally-occurring enediyne antibiotics.

To synthesize the very strained tricyclic system of **4** (Fig. 3.14), a photochemical Wolff rearrangement was chosen when MM predicted that the skeleton of **4** should be about $109 \, \text{kJ mol}^{-1}$ less stable than that of the available **5**. Photolysis of the diazoketone **6** gave a high-energy carbene which lay above the carbon skeleton of **4** and so was able to undergo Wolff rearrangement ring contraction to the ketene precursor of **4**.

A remarkable (and apparently still unconfirmed) prediction of MM is the claim that the perhydrofullerene $C_{60}H_{60}$ should be stabler with some hydrogens *inside* the cage [36].

3.4 Frequencies and Vibrational Spectra Calculated by MM

Any method that can calculate the energy of a molecular geometry can in principle calculate vibrational frequencies, since these can be obtained from the second derivatives of energy with respect to molecular geometry (Chap. 2, Sect. 2.5), and the masses of the vibrating atoms. Many commercially available molecular mechanics programs can calculate frequencies. Frequencies are useful (Chap. 2, Sect. 2.5) (1) for characterizing a species as a minimum (no imaginary frequencies) or a transition state or higher-order saddle point (one or more imaginary frequencies), (2) for obtaining zero point vibrational energies to correct frozen-nuclei energies (Chap. 2, Sect. 2.2), and (3) for interpreting or predicting infrared spectra.

1. *Characterizing a species as a minimum or a transition state*. This is not often done with MM, because MM is used mostly to create input structures for other kinds of calculations, and to study known (often biological) molecules. Nevertheless MM can yield information on the curvature of the potential energy surface (see Chap. 2), as calculated by that particular forcefield, anyway, at the point in question. For example, the MMFF-optimized geometries of D_{3d} (staggered) and D_{3h} (eclipsed) ethane (Fig. 3.3) show, respectively, no imaginary frequencies and one imaginary frequency, the latter corresponding to rotation about the C/C bond. Thus the MMFF (correctly) predicts the staggered conformation to be a minimum, and the eclipsed to be a transition state connecting successive minima along the torsional reaction coordinate. Again, calculations on cyclohexane conformations with the MMFF correctly give the boat an imaginary frequency corresponding to a twisting motion leading to the twist conformation, which latter has no imaginary frequencies (Fig. 3.10). Although helpful for characterizing conformations, particularly hydrocarbon conformations, MM is less appropriate for species in which bonds are being formed and broken. For example, the symmetrical (D_{3h}) species in the fluoride/ fluoromethane bimolecular reaction, with equivalent C/F partial bonds, is incorrectly characterized by the MMFF as a minimum rather than a transition state, and the CF bonds are calculated to be 1.298 Å long, cf. the value of ca. 1.8 Å from methods known to be trustworthy for transition states.

2. *Obtaining zero point energies (ZPEs).* ZPEs are essentially the sum of the energies of each normal-mode vibration. They are added to the raw energies (the frozen-nuclei energies, corresponding to the stationary points on a Born-Oppenheimer surface; Chap. 2, Sect. 2.3) in accurate calculations of relative energies using ab initio (Chap. 5) or DFT (Chap. 7) methods. However, the ZPEs used for such corrections are usually obtained from an ab initio or DFT calculation.

3. *Infrared spectra.* The ability to calculate the energies (cm^{-1}) and relative intensities of molecular vibrations amounts to being able to calculate infrared spectra. MM *as such* cannot calculate the *intensities* of vibrational modes, since these involve changes in dipole moments (Chap. 5, Sect. 5.5.3), and dipole moment is related to electron distribution, a concept that lies outside MM. However, approximate intensities can be calculated by assigning dipole moments to bonds or charges to atoms, and such methods have been implemented in MM programs [37]. Figs. 3.15, 3.16, 3.17 and 3.18 compare
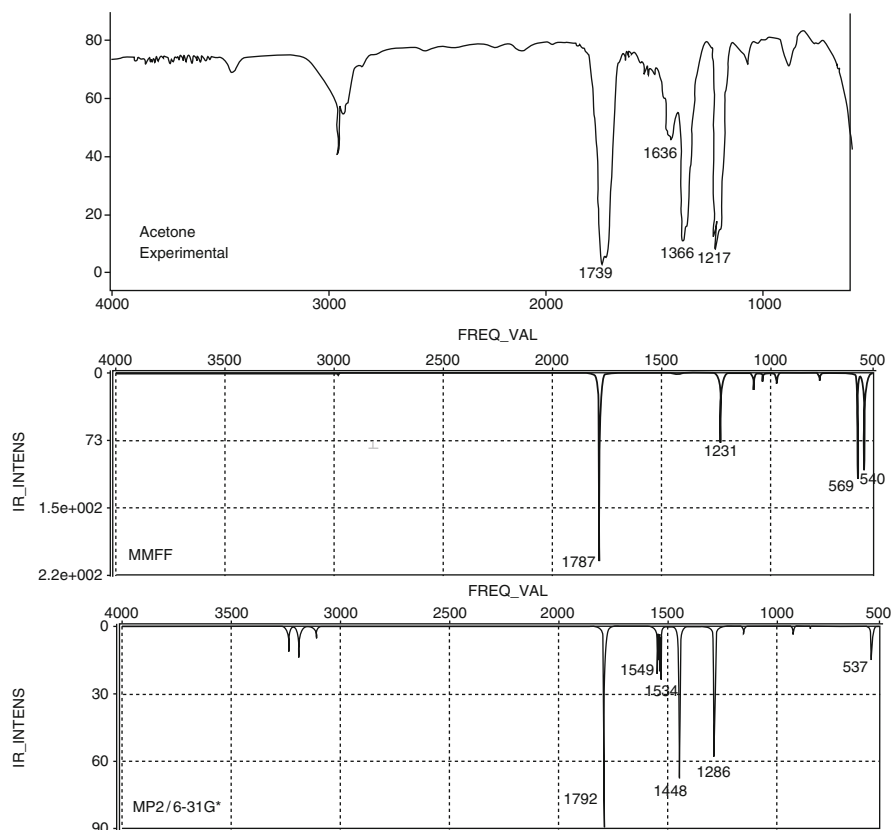
Fig. 3.15 Experimental (gas phase), and MM (MMFF) and ab initio (MP2(FC)/6-31G*) calculated IR spectra of acetone
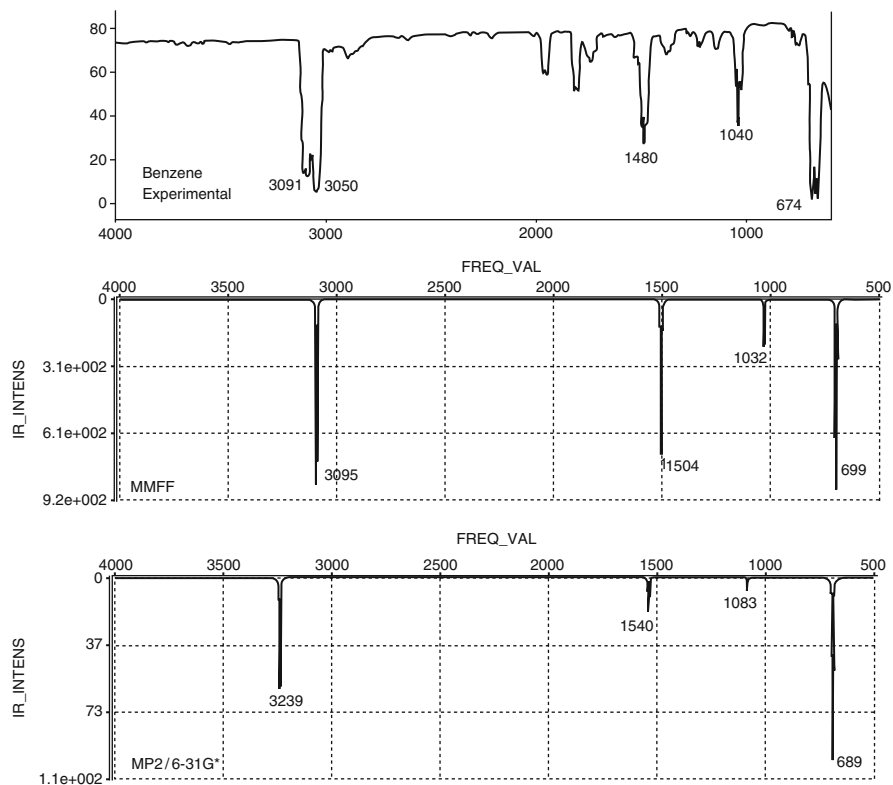
Fig. 3.16 Experimental (gas phase), and MM (MMFF) and ab initio (MP2(FC)/6-31G*) calculated IR spectra of benzene

the experimental IR spectra (taken by the author in the gas phase) of acetone, benzene, dichloromethane and methanol with those calculated with the MMFF program and by the "higher", computationally much more demanding, ab initio MP2(FC)/6 - 31G* method (Chap. 5). In Chaps. 5, 6, and 7, spectra for these four molecules, calculated by ab initio, semiempirical, and density functional methods, respectively, are given. MP2 spectra seem to generally match experiment better than those from MM, but the latter method furnishes a rapid way of obtaining approximate IR spectra. For a series of related compounds, MM might be a reasonable way to quickly investigate trends in frequencies and intensities. Extensive surveys showed that MMFF root-mean-square errors are ca. 60 cm^{-1}, and MM4 errors $25 - 52$ cm^{-1} [5b].
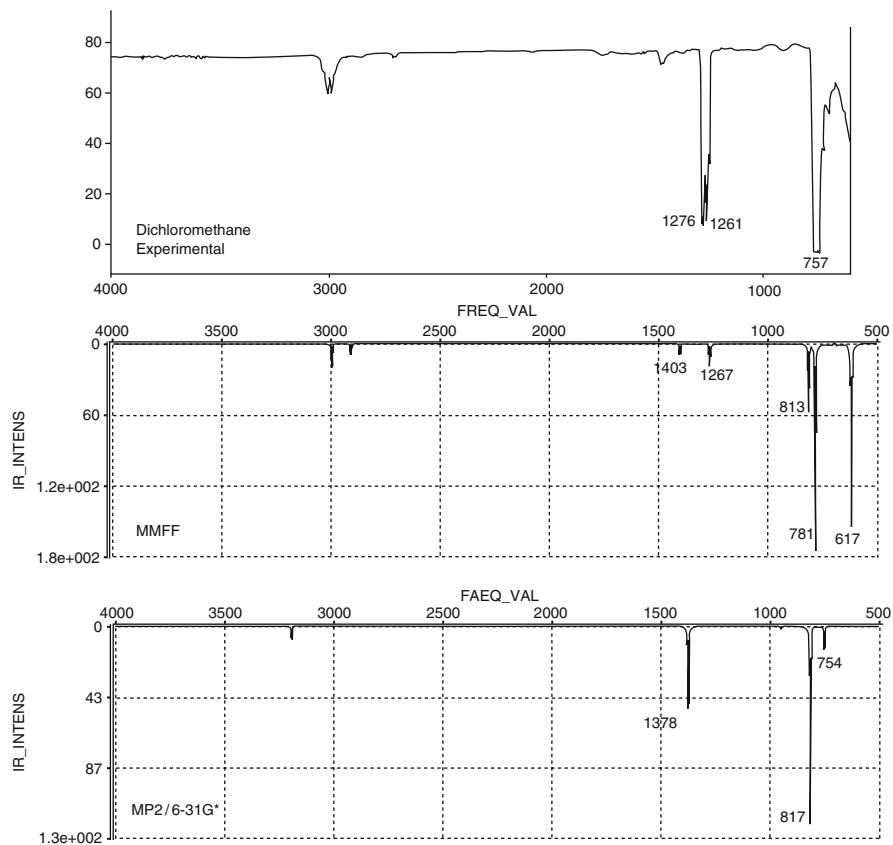
Fig. 3.17 Experimental (gas phase), and MM (MMFF) and ab initio (MP2(FC)/6-31G[*]) calculated IR spectra of dichloromethane

3.5 Strengths and Weaknesses of Molecular Mechanics

3.5.1 Strengths

MM is *fast*, as shown by the times for optimization of $C_{20}H_{42}$ in Sect. 3.3.2. The speed of MM is not always at the expense of accuracy: for the kinds of molecules for which it has been parameterized, it can rival or surpass experiment in the reliability of its results (Sects. 3.3.2 and 3.4). MM is undemanding in its hardware requirements: except perhaps for work on large biopolymers, MM calculations on moderately well-equipped personal computers are quite practical. The characteristics of speed, (frequent) accuracy and modest computer requirements have given MM a place in many modelling program suites.
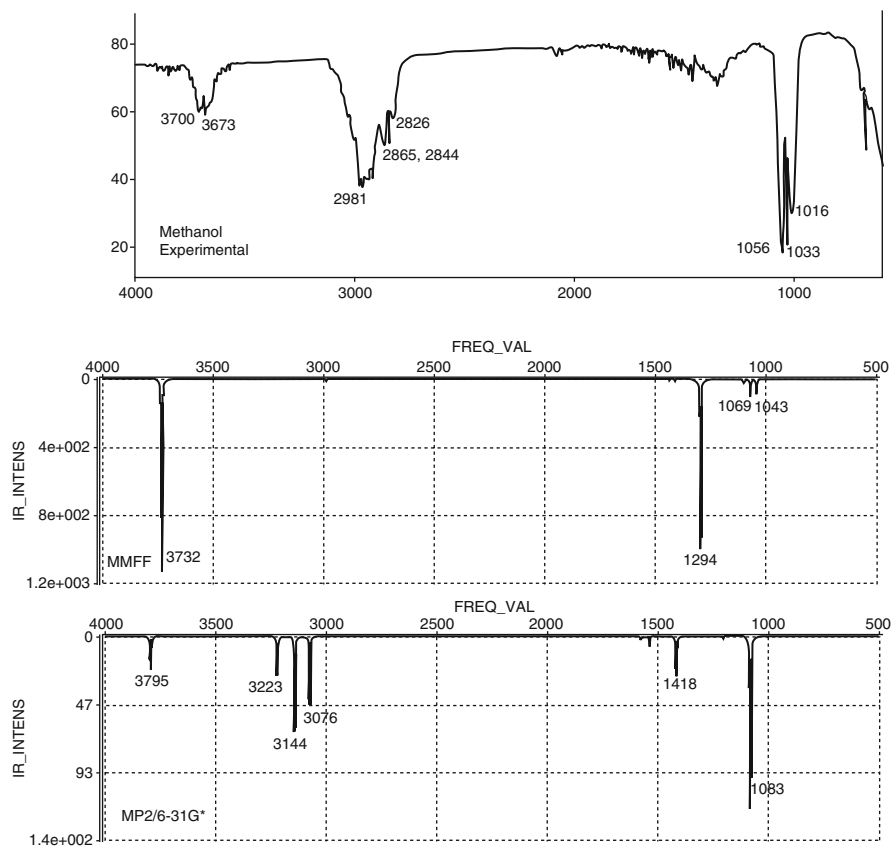
Fig. 3.18 Experimental (gas phase), and MM (MMFF) and ab initio (MP2(FC)/6-31G*) calculated IR spectra of methanol

Because of its speed and the availability of parameters for almost all the elements (Sect. 3.3), MM–even when it does not provide very accurate geometries–can supply reasonably good input structures for semiempirical, ab initio or density functional calculations, and this is one of its main applications. The ability of many MM programs to calculate IR spectra seems to be of somewhat limited application, since although frequency calculation by quantum mechanical methods usually requires considerably more time than geometry optimization, frequencies should be calculated using the same method used for the geometry optimization (Chap. 2, Sect. 2.5).

3.5.2 Weaknesses

The possible pitfalls in using MM are discussed by Lipkowitz [38]. The weaknesses of MM stem from the fact that it ignores electrons. The viewpoint behind MM is to

think of a molecule as a collection of atoms subject to forces and to use any practical mathematical treatment of these forces to express the energy in terms of the geometric parameters. By parameterization MM can "calculate" electronic properties; for example, using assigned atom charges or bond dipoles it can find a dipole moment for a molecule. However, such results are obtained purely by analogy, and their reliability can be negated by unexpected electronic factors to which MM is oblivious. MM cannot provide information about the shapes and energies of molecular orbitals nor about related phenomena such as electronic spectra. Of course, one could perform a quantum mechanical calculation of orbitals, etc., on a geometry obtained by a MM optimization (a so-called single-point calculation, since no quantum mechanical geometry optimization was performed).

Because of the severely empirical nature of MM, interpreting MM parameters in terms of traditional physical concepts is dangerous; for example, the bond-stretching and angle-bending parameters cannot rigorously be identified with spectroscopic force constants [38]; Lipkowitz suggests that the MM proportionality constants (Sect. 3.2.1) be called *potential constants*. Other dangers in using MM are:

1. *Using an inappropriate forcefield*: a field parameterized for one class of compounds is not likely to perform well for other classes.
2. *Transferring parameters form one forcefield to another*. This is usually not valid.
3. *Optimizing to a stationary point that may not really be a minimum* (it could be a "maximum", a transition state), and certainly may not be a *global* minimum (Chap. 2). If there is reason to be concerned that a structure is not a minimum, alter it slightly by bond rotation and reoptimize; a transition state should slide down toward a nearby minimum (e.g. eclipsed ethane altered slightly from the D_{3h} geometry and optimized goes to the staggered conformer (Fig. 3.8).
4. *Being taken in by vendor hype*: MM programs, more so than semiempirical ones and unlike ab initio or DFT programs, are ruled by empirical factors (the form of the forcefield and the parameters used in it), and perhaps some vendors tend not to caution buyers about potential deficiencies.
5. *Ignoring solvent and nearby ions*: for polar molecules using the *in vacuo* structure can lead to quite wrong geometries and energies. This is particularly important for biomolecules. One way to mitigate this problem is to explicitly add solvent molecules or ions to the system, which can considerably increase the time for a calculation. Another might be to subject various plausible *in vacuo*-optimized conformations to single-point (no geometry optimization) calculations that simulate the effect of solvent and take the resulting energies as being more reliable than the *in vacuo* ones. The most practical in-solution calculations, those simulating the solvent as a continuous medium (Chap. 8, Sect. 8.1) can be applied to MM, although ab initio and DFT are the standard, reliable methods here.
6. *Lack of caution about comparing energies calculated with MM*. The method calculates the energy of a molecule relative to a hypothetical strainless idealization of the molecule. Using MM to calculate the relative energy of two isomers by comparing their steric ("strain") energies, the normal MM energies, is dangerous because the two energies are not necessarily relative to the same hypothetical unstrained species (steric energies are not an unambiguous

observable [39]). This is particularly true for functional group isomers, like $(CH_3)_2O/CH_3CH_2OH$ and $CH_3COCH_3/H_2C = C(OH)CH_3$, which have quite different atom types. For isomers consisting of the same kinds of atoms (alkanes cf. alkanes, say), and especially for conformational isomers and *E/Z* isomers (geometric isomers), a good MM forcefield should give steric energies which reasonably represent relative energies. For example, the MMFF gives for CH_3 $COCH_3/H_2C = C(OH)CH_3$ steric energies of $6.9/-6.6 \, kJ \, mol^{-1}$, i.e. relative energies of $0/-13 \, kJ \, mol^{-1}$, but the experimental value is ca. $0/44 \, kJ \, mol^{-1}$, i.e. $H_2C = C(OH)CH_3$ is much the higher-energy molecule. On the other hand, the MMFF yields for *gauche*-butane/*anti*-butane steric energies of $-21.3/-18.0 \, kJ \, mol^{-1}$, i.e. relative energies of $0/3.3 \, kJ \, mol^{-1}$, reasonably close to the experimental value of $0/2.8 \, kJ \, mol^{-1}$. For chair (D_{2d}), twist (D_2), and boat (C_{2v}) cyclohexane, the MMFF steric energies are -14.9, 9.9 and $13.0 \, kJ \, mol^{-1}$, i.e. relative energies of 0, 24.8 and $27.9 \, kJ \, mol^{-1}$, cf. the experimental the estimates of 0, 24 and $29 \, kJ \, mol^{-1}$. As was shown above (Sect. 3.3.3), MM programs can be parameterized to give, not just steric energy, but enthalpies of formation, and the use of these enthalpies makes possible energy comparisons between isomers of even entirely disparate structural kinds.

Although chemists often compare stabilities of isomers using enthalpies, we should remember that equilibria are actually determined by free energies. The lowest-enthalpy isomer is not *necessarily* the one of lowest free energy: a higher-enthalpy molecule may have more vibrational and torsional motion (it may be springier and floppier) and thus possess more entropy and hence have a lower free energy. Free energy has an enthalpy and an entropy component, and to calculate the latter, one needs the vibrational frequencies. Programs that calculate frequencies will usually also provide entropies, and with parameterization for enthalpy (Sect. 3.3.3) this can permit the calculation of free energies. Note that the species of lowest free energy does not necessarily dominate a mixture: one low-energy conformation could be outnumbered by many of higher energy, each demanding its share of the Boltzmann pie.

7. *Assuming that the major conformation determines the product*. In fact, in a mobile equilibrium the product ratio depends on the relative reactivities, not relative amounts, of the conformers (the Curtin-Hammett principle [40]).

8. *Failure to exercise judgement: small energy differences* (say up to $10-20 \, kJ \, mol^{-1}$) mean nothing in many cases. The excellent energy results referred to for the MM4 program in Sect. 3.3.3 can be expected only for families of molecules (usually small to medium-sized) for which a forcefield has been extensively parameterized.

Many of the above dangers can be avoided simply by performing test calculations on systems for which the results are known (experimentally, or "known" from high-level quantum mechanical calculations). Such a reality check can have salutary effects on the reliability of one's results, and not only with reference to molecular mechanics.

3.6   Summary

This chapter explains the basic principles of molecular mechanics (MM), which rests on a view of molecules as balls held together by springs. MM began in the 1940s with attempts to analyze the rates of racemization of biphenyls and S_N2 reactions.

   The potential energy of a molecule can be written as the sum of terms involving bond stretching, angle bending, dihedral angles and nonbonded interactions. Giving these terms explicit mathematical forms constitutes devising a forcefield, and giving actual numbers to the constants in the forcefield constitutes parameterizing the field. An example is given of the devising and parameterization of an MM forcefield.

   MM is used mainly to calculate geometries and energies for small to medium-sized molecules. Such calculations are fast and can be very accurate, provided that the forcefield has been carefully parameterized for the types of molecules under study. Calculations on biomolecules is a very important application of MM; the pharmaceutical industry designs new drugs with the aid of MM: for example, examining how various candidate drugs fit into the active sites of biomolecules (docking) and the related aspect of QSAR are of major importance. MM is of some limited use in calculating the geometries and energies of transition states. Organic synthesis now makes considerable use of MM, which enables chemists to estimate which products are likely to be favored and to devise more realistic routes to a target molecule than was hitherto possible. In molecular dynamics MM is used to generate the forces acting on molecules and hence to calculate their motions, and in Monte Carlo simulations MM is used to calculate the energies of the many randomly generated states.

   MM is fast, it can be accurate, it is undemanding of computer power, and it provides reasonable starting geometries for quantum mechanical calculations. MM ignores electrons, and so can provide parameters like dipole moment only by analogy. One must be cautious about the applicability of MM parameters to the problem at hand. Stationary points from MM, even when they are relative minima, may not be global minima. Ignoring solvent effects can give erroneous results for polar molecules. MM gives so-called steric energies, the difference of which for structurally similar isomers represent enthalpy differences; parameterization to give enthalpies of formation is possible. Strictly speaking, relative amounts of isomers depend on free energy differences. The major conformation (even when correctly identified)y is not necessarily the reactive one.

Easier Questions

  1. What is the basic idea behind molecular mechanics?
  2. What is a forcefield?

3. What are the two basic approaches to parameterizing a forcefield?
4. Why does parameterizing a forcefield for transition states present special problems?
5. What is the main advantage of MM, generally speaking, over the other methods of calculating molecular geometries and relative energies?
6. Why is it not valid in all cases to obtain the relative energies of isomers by comparing their MM steric ("strain") energies?
7. What class of problems cannot be dealt with by MM?
8. Give four applications for MM. Which is the most widely used?
9. MM can calculate the values (cm^{-1}) of vibrational frequencies, but without "outside assistance" it can't calculate their intensities. Explain.
10. Why is it not valid to calculate a geometry by some slower (e.g. ab initio) method, then use that geometry for a fast MM frequency calculation?

Harder Questions

1. One big advantage of molecular mechanics over other methods of calculating geometries and relative energies is speed. Does it seem likely that continued increases in computer speed could make MM obsolete?
2. Do you think it is possible (in practical terms? In principle?) to develop a forcefield that would accurately calculate the geometry of any kind of molecule?
3. What advantages or disadvantages are there to parameterizing a forcefield with the results of "high-level" calculations rather than the results of experiments?
4. Would you dispute the suggestion that no matter how accurate a set of MM results might be, they cannot provide insight into the factors affecting a chemical problem, because the "ball and springs" model is unphysical?
5. Would you agree that hydrogen bonds (e.g. the attraction between two water molecules) might be modelled in MM as weak covalent bonds, as strong van der Waals or dispersion forces, or as electrostatic attractions? Is any one of these three approaches to be preferred in principle?
6. Replacing small groups by "pseudoatoms" in a forcefield (e.g. CH_3 by an "atom" about as big) obviously speeds up calculations. What disadvantages might accompany this simplification?
7. Why might the development of an accurate and versatile forcefield for inorganic molecules be more of a challenge than for organic molecules?
8. What factor(s) might cause an electronic structure calculation (e.g. ab initio or DFT) to give geometries or relative energies very different from those obtained from MM?
9. Compile a list of molecular characteristics/properties that cannot be calculated purely by MM.
10. How many parameters do you think a reasonable forcefield would need to minimize the geometry of 1,2-dichloroethane?

References

1. General references to molecular mechanics: (a) Allinger N (2010) Perhaps the most authoritative, yet delightfully casual and a good read. In: Molecular structure, understanding steric and electronic effects from molecular mechanics. Wiley, Hoboken; (b) Leach AR (1996) Chapter 3. In: Molecular modelling, principles and applications. Addison Wesley Longman, Essex (UK); (c) Rappe AK, Casewit CL (1997) Molecular mechanics across chemistry. University Science Books, Sausalito; (d) Allinger NL (1976) Calculation of molecular structures and energy by force methods. Advances in Physical Organic Chemistry, 13, Gold V, Bethell D(eds), Academic Press, New York; (e) Clark T (1985) A handbook of computational chemistry. Wiley, New York; (f) Levine IN (2014) Quantum chemistry, 7th edn. Prentice Hall, Engelwood Cliffs. section 17.5; (g) Issue No. 7 of Chem. Rev., 1993, 93; (h) Pettersson I, Liljefors T (1996) Reviews in computational chemistry. In: Conformational energies. 9; (I) Landis CR, Root DM, Cleveland T (1995) Reviews in computational chemistry. In: Inorganic and organometallic compounds. 6; (j) Bowen JP, Allinger NL (1991) Reviews in computational chemistry. In: Parameterization. 2; (k)Karplus M (2014) Accounts of early work on molecular mechanics and molecular dynamics, and their application to biological molecules and reactions. Angew Chem, Int Ed Engl 53:9992; Levitt M (2014) Angew Chem, Int Ed Engl 53:10006; Warshel A (2014) Angew Chem, Int Ed Engl 53:10020

2. MM history: (a) References 1; (b) Engler EM, Andose JD, von R Schleyer P (1973) J Am Chem Soc 95:8005 and references therein; (c) Molecular mechanics up to the end of 1967 is reviewed in detail in: Williams JE, Stang PJ, von R Schleyer P (1968) Annu Rev Phys Chem 19:531

3. (a) Westheimer FH, Mayer JE (1946) J Chem Phys 14:733; (b) Hill TL (1946) J Chem Phys 14:465; (c) Dostrovsky I, Hughes ED, Ingold CK (1946) J Chem Soc 173; (d) Westheimer FH (1947) J Chem Phys 15:252

4. (a) Ma B, Lii JH, Chen K, Allinger NL (1997) J Am Chem Soc 119:2570 and references therein; (b) In an MM4 study of amines, agreement with experiment was generally good: Chen KH, Lii JH, Allinger NJ (2007) J Comp Chem 28:2391; (c) Five papers, using MM4, on Alcohols, ethers, carbohydrates, and related compounds, J Comp Chem, 2003, 24; Allinger NL, Chen KH, Lii JH, Durkin KA, 1447; Lii JH, Chen KH, Durkin A, Allinger NL, 1473; Lii JH, Chen KH, Grindley TB, Allinger NL, 1490; Lii JH, Chen KH, Allinger NL, 1504; J Phys Chem A, 2004, 108, Lii JH, Chen KH, Allinger NL, 3006

5. (a) Information on and references to molecular mechanics programs may be found in references 1; (b) For papers on the popular Merck Molecular Force Field and the MM4 forcefield (and information on some others) see the issue of J Comp Chem, (1996) 17

6. The force constant is defined as the proportionality constant in the equation force $= k \times$ extension (of length or angle), so integrating force with respect to extension to get the energy ($=$ force $\times$ extension needed to stretch the bond gives $E = (k / 2)$ (extension)^2, i.e. $k =$ force constant $= 2k_{stretch}$ (or $2k_{bend}$)

7. (a) A brief discussion and some parameters: Atkins PW (1994) Physical chemistry, 5th edn. Freeman New York, p 772–773; it is pointed out here that $e^{-r/\sigma}$ is actually a much better representation of the compressive potential than is r^{-12}; (b) Moore WJ (1972) Physical chemistry, 4th edn. Prentice-Hall, New Jersey p 158 (from Hirschfelder JO, Curtis CF, Bird RB (1954) Molecular theory of gases and liquids. Wiley, New York). Note that our k_{nb} is called 4ε here and must be multiplied by 8.31/1000 to convert it to our units of kJ mol^{-1}

8. Silverstein RM, Webster FX, Kiemle DJ (2005) Infra red spectroscopy. In: Spectrometric identification of organic compounds, Seventhth edn. Wiley, Hoboken, Chapter 2

9. Different methods of structure determination give somewhat different results; this is discussed in reference 4(a) and in: (a) Ma B, Lii JH, Schaefer HF, Allinger NL (1996) J Phys Chem 100:8763 and (b) Domenicano A, Hargittai I (eds) Accurate molecular structures. Oxford Science Publications, New York

10. Handley CM, Popelier PLA (2010) To properly parameterize a molecular mechanics forcefield only high-level ab initio calculations or density functional calculations would actually be used, but this does not affect the principle being demonstrated. The possible use of neural networks, which can learn, to find functional forms for forcefields, has been reviewed. J Phys Chem A 114:3371
11. Blanksby SJ, Ellison GB (2003) Acc Chem Res 36:255, Table 2
12. Reference 1b, p 148–181
13. MM3: Allinger NL, Yuh YH, Lii JH (1989) J Am Chem Soc 111:8551
14. Jensen F (2007) Introduction to computational chemistry, 2nd edn. Wiley, West Sussex, section 12.2
15. Eksterowicz JE, Houk KN (1993) Chem Rev 93:2439
16. E.g. Smith MB, March J (2000) March's advanced organic chemistry. Wiley, New York, p 284–285
17. (a) Jensen F (2007) Introduction to computational chemistry, 2nd edn. Wiley, West Sussex, section 2.9.2; (b) Jensen F, Norby PO (2003) Theor Chem Acc 109:1
18. Spartan is a comprehensive computational chemistry program with molecular mechanics, ab initio, density functional and semiempirical capability, combined with powerful graphical input and output
19. Halgren TA (1996) Comparison of various forcefields for geometry (and vibrational frequencies). J Comp Chem 17:553
20. The Merck forcefield (ref. [22]) often gives geometries that are satisfactory for energy calculations (i.e. for single-point energies) with quantum mechanical methods; this could be very useful for large molecules: Hehre WJ, Yu J, Klunzinger PE (1997) A guide to molecular mechanics and molecular orbital calculations in Spartan. Wavefunction Inc., Irvine, chapter 4
21. Strutyński K, Gomes JANF, Melle-Franco M (2014) J Phys Chem A 118:9561
22. Halgren TA (1996) J Comp Chem 17:490
23. Comba P, Hambley TW, Martin B (2009) Molecular modeling of inorganic compounds, 3rd edn. Wiley, Weinheim
24. (a) Hehre WJ, Radom L, v. R. Schleyer P, Pople JA (1986) Ab initio molecular orbital theory. Wiley, New York, 1986; (b) Harmony MD, W, Laurie V, Kuczkowski RL, Schwenderman RH, Ramsay DA, Lovas FJ, Lafferty WH, Makai AK (1979) Molecular structures of gas-phase polyatomic molecules, determined by spectroscopic methods, J Physical and Chemical Reference data 8:619–721; (c) Huang J, Hedberg K (1989) J Am Chem Soc 111:6909
25. Nicklaus MC (1997) J Comp Chem 18:1056; the difference between CHARMM and CHARMm is explained here
26. (a) http://ambermd.org; (b) Cornell WD, Cieplak P, Bayly CI, Gould IR, Merz KM, Jr., Ferguson DM, Sellmeyer DC, Fox T, Caldwell JW, Kollman PA (1995) J Am Chem Soc 117:5179; (c) Barone V, Capecchi G, Brunel Y, Andries MLD, Subra R (1997) J Comp Chem 18:1720
27. (a) Field MJ, Bash PA, Karplus M (1990) J Comp Chem 11:700; (b) Bash PA, Field MJ, Karplus M (1987) J Am Chem Soc 109:8092
28. Singh UC, Kollman P (1986) J Comp Chem 7:718
29. Acevido O, Jorgenson WL (2010) Acc Chem Res 43:142
30. (a) E.g. reference 1b, chapter 10; (b) Höltje HD, Folkers G (1996) Molecular modelling, applications in medicinal chemistry. VCH, Weinheim, Germany; (c) van de Waterbeemd H, Testa B, Folkers G (eds) (1997) Computer-assisted lead finding and optimization, VCH, Weinheim, Germany
31. Ref. [1a], p 265–284
32. Gundertofte K, Liljefors T, Norby PO, Pettersson I (1996) J Comp Chem 17:429
33. (a) Reference 1b, chapter 6; (b) Karplus M, Putsch GA (1990) Nature 347:631; (c) Brooks III CL, Case DA (1993) Chem Rev 93:2487;(d) Eichinger M, Grubmüller H, Heller H, Tavan P (1993) J Comp Chem 18:1729; (e) Marlow GE, Perkyns JS, Pettitt BM (1993) Chem Rev 93:2503; (f) Aqvist J, Warshel A (1993) Chem Rev 93:2523

34. Reference 1b, chapter 8
35. Lipkowitz KB, Peterson MA (1993) Chem Rev 93:2463
36. (a) Saunders M (1991) Science 253:330; (b) See too Dodziuk H, Lukin O, Nowinski KS (1999) Polish J Chem 73:299
37. Lii J-H, Allinger NL (1992) J Comp Chem 13:1138
38. Lipkowitz KB (1995) J Chem Ed 72:1070
39. (a) Wiberg K (1986) Angew Chem, Int Ed Engl 25:312; (b) Issue No. 5 of Chem Rev, 1989, 89. (c) Inagaki S, Ishitani Y, Kakefu T (1994) J Am Chem Soc 116:5954; (d) Nagase S (1995) Acc Chem Res 28:469; (e) Gronert S, Lee JM (1995) J Org Chem 60:6731; (f) Sella A, Basch H, Hoz S (1996) J Am Chem Soc 118:416; (g) Grime S (1996) J Am Chem Soc 118:1529; (h) Balaji V, Michl J (1988) Pure Appl Chem 60:189; (i) Wiberg KB, Ochterski JW (1997) J Comp Chem 18:108
40. Seeman JI (1983) Chem Rev 83:83

Chapter 4
Introduction to Quantum Mechanics in Computational Chemistry

It is by logic that we prove, but by intuition that we discover.
J.H. Poincaré, ca. 1900.

Abstract A historical view demystifies the subject. The focus is strongly on chemical applications. The use of quantum mechanics (QM) in computational chemistry is shown by explaining the Schrödinger equation and showing how this led to the simple Hückel method, from which the extended Hückel method followed. This sets the stage well for ab initio theory, in Chap. 5.

QM grew out of studies of blackbody radiation and of the photoelectric effect. Besides QM, radioactivity and relativity contributed to the transition from classical to modern physics. The classical Rutherford nuclear atom, the Bohr atom, and the Schrödinger wave-mechanical atom are discussed. Hybridization, wavefunctions, matrices and determinants and other basic concepts are explained. For obtaining eigenvectors and eigenvalues from the secular equations the elegant and simple matrix diagonalization method is explained and used. All the necessary mathematics for this is explained.

4.1 Perspective

Chapter 1 outlined the tools that computational chemists have at their disposal, Chap. 2 set the stage for the application of these tools to the exploration of potential energy surfaces, and Chap 3 introduced one of these tools, molecular mechanics. In this chapter you will be introduced to *quantum mechanics*, and to *quantum chemistry*, the application of quantum mechanics to chemistry. Molecular mechanics is severely empirical and insofar as it makes appeals to theory it uses largely principles from basic *classical* physics, physics before *modern* physics; it treats a molecule as a collection of balls and springs, with refinements for such deviations as interatomic repulsions and attractions. One of the cornerstones of modern physics is quantum mechanics, and ab initio (Chap. 5), semiempirical (Chap. 6), and density functional (Chap. 7) methods, on which most of the remainder of this book focusses, belong to quantum chemistry. This chapter is designed to ease the way to an understanding of the role of quantum mechanics in computational

chemistry. The word *quantum* comes from Latin (*quantus*, "how much?", plural *quanta*) and was first used in our sense by Max Planck in 1900, as an adjective and noun, to denote the constrained *quantities* or amounts in which in which energy can be emitted or absorbed. The term *quantum mechanics* was apparently first used by Born (of the Born-Oppenheimer approximation, Chap. 2, Sect. 2.3) in 1924, as a contrast to classical mechanics. Techniques for tackling the quantum mechanics of atoms and molecules not as patches to classical physics (Bohr, 1913; Sommerfeld, 1915), but rather head-on, were presented in 1925 (Heisenberg, matrix mechanics) and 1926 (Schrödinger, a wave equation).

"Mechanics" as used in physics is traditionally the study of the behavior of bodies under the action of forces like, e.g., gravity (celestial mechanics). Molecules are made of nuclei and electrons, and quantum chemistry deals, fundamentally, with the motion of electrons under the influence of the electromagnetic force exerted by nuclear charges and other electrons. An understanding of the behavior of electrons in atoms and molecules, and thus of the structures and reactions of chemical entities, rests on quantum mechanics and in particular on that adornment of quantum chemistry, the Schrödinger equation. For that reason we will consider in outline the development of quantum mechanics leading up to the Schrödinger equation, and then the birth of quantum chemistry with (at least as far as molecules of reasonable size goes) the application of the Schrödinger equation to chemistry by Hückel. This *simple Hückel method* is currently disdained by some theoreticians, but its discussion here is justified by the fact that (1) it continues to be useful in research and (2) it "is immensely useful as a model, today...Because it is the model which preserves the ultimate physics, that of nodes in wave functions. It is the model which throws away absolutely everything except the last bit, the only thing that if thrown away would leave nothing. So it provides fundamental understanding."[1] A discussion of a generalization of the simple Hückel method, the extended Hückel method, sets the stage for Chap. 5. The historical approach used here, although perforce somewhat superficial, may help to ameliorate the apparent arbitrariness of certain features of quantum chemistry [1, 2]. An excellent introduction to quantum chemistry is the text by Levine [3].

Our survey of the factors that led to modern physics and quantum chemistry will follow the sequence:

1. The origins of quantum theory: blackbody radiation and the photoelectric effect.
2. Radioactivity (brief)
3. Relativity (very brief)
4. The nuclear atom
5. The Bohr atom
6. The wave mechanical atom and the Schrödinger equation

---

[1] Personal communication from Professor Roald Hoffmann, 2002 February 13. See too Sect. 4.4.1, footnote).

4.2   The Development of Quantum Mechanics. The Schrödinger Equation

4.2.1   The Origins of Quantum Theory: Blackbody Radiation and the Photoelectric Effect

Three discoveries mark the transition from classical to modern physics: quantum theory, radioactivity, and relativity (Fig. 4.1). Quantum theory had its origin in the study of blackbody radiation and the photoelectric effect.

4.2.1.1   Blackbody Radiation

A black body (blackbody) in physics is one that is a perfect absorber of radiation: it absorbs all the radiation falling on it, without reflecting any. More relevant for us, the radiation emitted by a hot black body depends, as far as the distribution of energy with wavelength goes, only on the temperature, not on the material the body is made of, and is thus amenable to relatively simple analysis. The sun is approximately a black body (in terms of its radiation-temperature characteristics; a hot black body need not be literally black). In the lab a good source of blackbody radiation is a furnace with blackened insides and a small aperture for the radiation to escape. In the second half of the nineteenth century the distribution of energy with respect to wavelength that characterizes blackbody radiation was studied, in research that is associated mainly with Lummer and Pringsheim [1]. They plotted the flux ΔF (in modern SI units, J s^{-1}m^{-2}, energy emitted per second per unit area, power output per unit area) per wavelength increment $\Delta\lambda$ versus the wavelength λ for a black body, for various temperatures (Fig. 4.2): $\Delta F/\Delta\lambda$ vs. λ. The result is a histogram or bar graph in which the area of each rectangle is $(\Delta F/\Delta\lambda)\Delta\lambda = \Delta F$ and represents the flux in the wavelength range covered by that $\Delta\lambda$; $\Delta F/\Delta\lambda$ can be called the flux density for that particular wavelength range $\Delta\lambda$. The total area of all
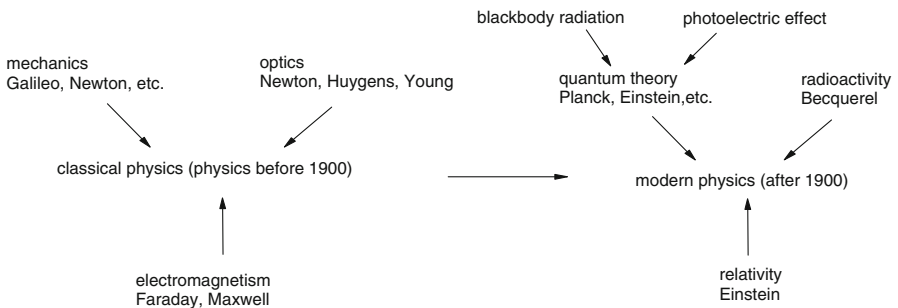
Fig. 4.1 The discoveries marking the transition from classical to modern to physics. Although radioactivity was discovered in 1896, its understanding had to wait for relativity and quantum theory
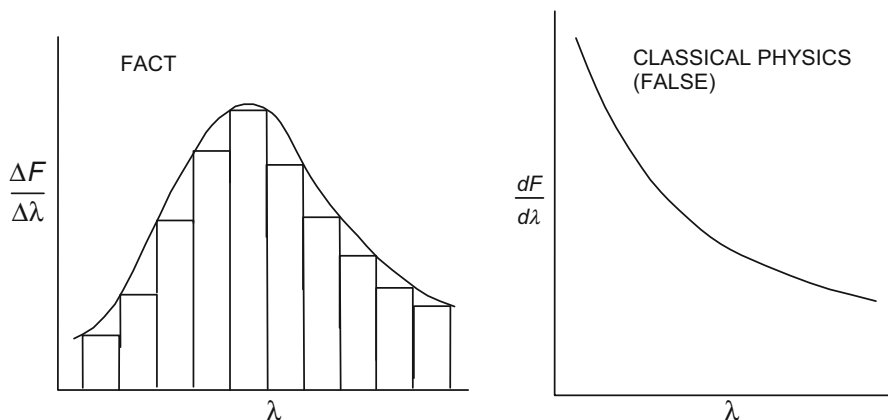
Fig. 4.2 In the limit the bar graph becomes a curve, the graph of $f(\lambda)$ vs. λ, where $f(\lambda) = \lim\limits_{\Delta\lambda \to 0} \frac{\Delta F}{\Delta\lambda} = \frac{dF}{d\lambda}$, essentially intensity of radiation vs. wavelength. Planck's efforts to find the function $f(\lambda)$ led to the quantum theory

the rectangles is the total flux emitted over its whole wavelength range by the black body. As $\Delta\lambda$ approaches zero (note that for the nonmonochromatic radiation from a black body the flux *at* a particular wavelength is essentially zero) the histogram approaches being a smooth curve, the ratio of finite increments approximates a derivative, and we can ask: what is the function (Fig. 4.2) $dF/d\lambda = f(\lambda)$? In the answer to this question lay the beginnings of quantum theory.

Late nineteenth century physics, classical physics at its zenith, predicted that the flux density from a black body should rise without limit as the wavelength decreases. This is because classical physics held that radiation of a particular frequency was emitted by oscillators (atoms or whatever) vibrating with that frequency, and that the average energy of an oscillator was independent of its frequency; since the number of possible frequencies increases without limit, the flux density (energy per second per unit area per wavelength interval) from the black body should rise without limit toward higher frequencies or shorter wavelengths, into the ultraviolet, and so the total flux (energy per second per unit area) should be infinite. This is clearly absurd and was recognized as being absurd; in fact, it was called "the ultraviolet catastrophe" [1]. To understand the nature of blackbody radiation and to escape the ultraviolet catastrophe, physicists in the 1890s tried to find the function (Fig. 4.2) $f(\lambda)$.

Without breaking with classical physics, Wien had found a theoretical equation that fit the Lummer-Pringsheim curve at relatively short wavelengths, and Rayleigh and Jeans one that fit at relatively long wavelengths. Max Planck[2] adopted a different approach: he found, in 1900, a purely empirical equation $dF/d\lambda = f(\lambda)$

---

[2] Max Planck, born Kiel, Germany, 1858. Ph.D. Berlin 1879. Professor, Kiel, Berlin. Nobel prize in physics for quantum theory of blackbody radiation 1918. Died Göttingen, 1947.

that fit the facts, and then tried to interpret the equation theoretically. To do this he had to make two assumptions:

(1) the total energy possessed by the oscillators in the frequency range $v + dv$ (v is the Greek letter *nu*, commonly used for frequency, not to be confused with v, vee, commonly used for velocity) is proportional to the frequency:

$$E_{tot}(v + dv) \propto v \qquad (4.1)$$

and (2), the emission or absorption of radiation of frequency v by the collection of oscillators is caused by jumps between energy levels, with loss or gain of a quantity of energy kv:

$$\Delta E = kv \qquad (4.2)$$

The constant k, now recognized as a fundamental constant of nature, 6.626×10^{-34} J.s particle^{-1}, is called Planck's constant, and is denoted by h, so Eq. (4.2) becomes

$$\Delta E = hv \qquad (*4.3)$$

Why the letter h? Evidently because h is sometimes used in mathematics to denote infinitesimals and Planck intended to let this quantity go to zero (this was suggested to the author by the late Professor Philip Morrison of MIT). In the event, it turned out to be small but finite. Apparently the letter was first used to denote the new constant in a talk given by Planck at a session (*Sitzung*) of the German Physical Society in Berlin, on 14 December 1900 [4]. The interpretation of Eq. (4.3), a fundamental equation of quantum theory, as meaning that the energy represented by radiation of frequency v is absorbed and emitted in *quantized* amounts hv (definite, constrained amounts; jerkily rather than smoothly) was, ironically, apparently never fully accepted by Planck [5]. It does not belittle his achievement to suggest that his discovery of the discontinuity of energy transfer was almost accidental. Planck's constant is a measure of the graininess of our universe: because it is so small processes involving energy changes often seem to take place smoothly, but on an ultramicroscopic scale the graininess is there [6]. The constant h is the hallmark of quantum expressions, and its finite value distinguishes our universe from a nonquantum one.

4.2.1.2   The Photoelectric Effect

An apparently quite separate (but in science no two phenomena are really ever completely unrelated) phenomenon that led to Eq. (4.3), which is to say to quantum theory, is the photoelectric effect: the ejection of electrons from a metal surface
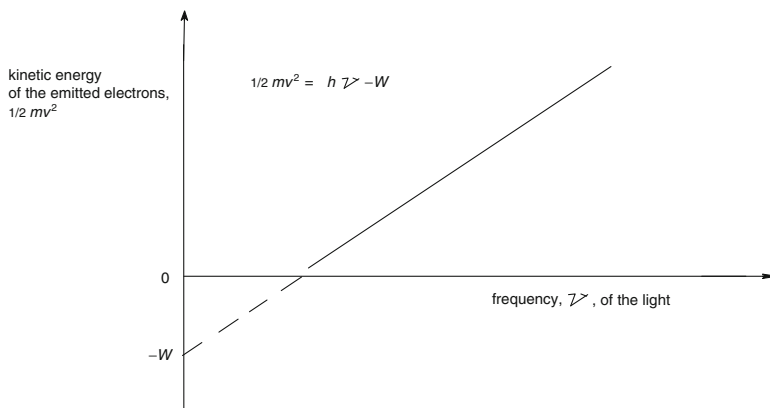
Fig. 4.3 The photoelectric effect. Einstein explained the effect by extending to light Planck's idea of the absorption and emission of energy in discrete amounts: he postulated that light itself consisted of discrete particles

exposed to light. The first inkling of this phenomenon was due to Hertz,[3] who in 1888 noticed that the potential needed to elicit a spark across two electrodes decreased when ultraviolet light shone on the negative electrode. Beginning in 1902, the photoelectric effect was first studied systematically by Lenard,[4] who showed that the phenomenon observed by Hertz was due to electron emission.

Facts (Fig. 4.3) that classical physics could not explain were the existence of a threshold frequency for electron ejection, that the kinetic energy of the electrons is linearly related to the frequency of the light, and the fact that the electron flux (electrons per unit area per second) is proportional to the intensity of the light. Classical physics predicted that the electron flux should be proportional to the light frequency, decreasing with a decrease in frequency, but without sharply falling to zero below a certain frequency, and that the kinetic energy of the electrons should be proportional to the intensity of the light, not the frequency.

These facts were explained by Einstein[5] in 1905 in a way that now appears very simple, but in fact relies on concepts that were at the time revolutionary. Einstein went beyond Planck and postulated that not only was the *process* of absorption and

---

[3] Heinrich Hertz, born Hamburg, Germany, 1857. Ph.D. Berlin, 1880. Professor, Karlsruhe, Bonn. Discoverer of radio waves. Died Bonn, 1894.

[4] Philipp Lenard, German physicist, born Pozsony, Austria-Hungary (now Bratislava, Slovakia), 1862. Ph.D. Heidelberg 1886. Professor, Heidelberg. Nobel prize in physics 1905, for work on cathode rays. Lenard supported the Nazis and rejected Einstein's theory of relativity. Died Messelhausen, Germany, 1947.

[5] Albert Einstein, German-Swiss-American physicist. Born Ulm, Germany, 1879. Ph.D. Zürich 1905. Professor Zürich, Prague, Berlin; Institute for Advanced Studies, Princeton, New Jersey. Nobel Prize in physics 1921 for theory of the photoelectric effect. Best known for the special (1905) and general (1915) theories of relativity. Died Princeton, 1955.

emission of light quantized, but that light itself was quantized, consisting in effect of particles of energy

$$E_{\text{particle}} = h\nu \tag{4.4}$$

$\nu = $ frequency of the light

These particles became known as *photons* (the word was coined by Gilbert Lewis, ca. 1923, but his photon was not the particle of modern physics). If the energy of the photon before it removes an electron from the metal is equal to the energy required to tear the electron free of the metal, plus the kinetic energy of the free electron, then

$$h\nu = W + \tfrac{1}{2}m_{\text{e}}v^2 \tag{4.5}$$

$W = $ work function of the metal, energy needed to remove an electron (with no energy left over)
$m_{\text{e}} = $ mass of an electron
$v = $ velocity of electron ejected by the photon
$\tfrac{1}{2}m_{\text{e}}v^2 = $ kinetic energy of the free electron

Rearranging Eq. (4.5):

$$\tfrac{1}{2}m_{\text{e}}v^2 = h\nu - W \tag{4.6}$$

Thus a plot of the kinetic energies of the electrons $(\tfrac{1}{2}m_{\text{e}}v^2)$ vs. the frequency ν of the light should be a straight line of positive slope (h; this is another way to find Planck's constant) intersecting the horizontal axis at a positive value, as experiment indeed showed (Fig. 4.3).

Planck's explanation of the blackbody radiation curves (1900 [4]) and Einstein's explanation of the facts of the photoelectric effect (1905 [7]) indicated that the flow of energy in physical processes did not take place continuously, as had been believed, but rather jerkily, in discrete jumps, quantum by quantum. The contributions of Planck and Einstein were the signal developments marking the birth of quantum theory and the transition from classical to modern physics.

4.2.2 Radioactivity

Brief mention of radioactivity is in order because it, along with quantum mechanics and relativity, transformed classical into modern physics. Radioactivity was discovered by Becquerel in 1896. However, an understanding of how materials like uranium and radium could emit, over the years, a million times more energy than would be permitted by chemical reactions, had to await Einstein's special theory of

relativity (Sect. 4.2.3), which showed that a tiny, unnoticeable decrease in mass represented the release of a large amount of energy.

4.2.3 Relativity

Relativity is relevant to computational chemistry because it must often be explicitly taken into account in accurate calculations involving atoms heavier than about chlorine or bromine (see below), and because the Schrödinger equation, the fundamental equation of quantum chemistry, is an approximation to a relativistic equation, the Dirac[6] equation.

Relativity was discovered by Einstein in 1905, when he formulated the special theory of relativity, which deals with nonaccelerated motion in the absence of significant gravitational fields (general relativity, published by Einstein in 1915, is concerned with accelerated motion and gravitation). Special relativity predicted a relationship between mass and energy, the famous $E = mc^2$ equation and, of more direct relevance to computational chemistry, showed that the mass of a particle increases with its velocity, dramatically so near the velocity of light. In heavier elements the inner electrons are moving at a significant fraction of the speed of light, and the relativistic increase in their masses affects the chemistry of these elements (actually, some physicists do not like to think in terms of separate rest mass and relativistic mass, but that is a controversy that need not concern us here). In computational chemistry relativistic effects on electrons are usually accounted for by what are called effective core potentials or pseudopotentials (Chap. 5, Sect. 5.3.3).

4.2.4 The Nuclear Atom

The "nuclear atom" is the picture of the atom as a positive nucleus surrounded by negative electrons. Although the idea of atoms in speculative philosophy goes back to at least the time of Democritus,[7] the atom as the basis of a scientifically credible theory emerges only in nineteenth century, with the rationalization by Dalton[8] in

---

[6] Paul Adrien Maurice Dirac, born Bristol, England, 1902. Ph.D. Cambridge, 1926. Professor, Cambridge, Dublin Institute for Advanced Studies, University of Miami, Florida State University. Nobel prize in physics 1933 (shared with Schrödinger). Known for his mathematical elegance, for connecting relativity with quantum theory, and for predicting the existence of the positron. Died Tallahassee, Florida, 1984.

[7] Democritus, Greek philosopher, born Abdera, Thrace (the eastern Balkans) ca. 460 B.C. Died ca. 370 B.C.

[8] John Dalton, born Eaglesfield, England, 1766. Considered the founder of quantitative chemical atomic theory: law of definite proportions, pioneered determination of atomic weights. Cofounder of British Association for the Advancement of Science. Died Manchester, England, 1844.

1808 of the law of definite proportions. Nevertheless, atoms were regarded by many scientists of the positivist school of Ernst Mach as being at best a convenient hypothesis, despite the success of the atomistic Maxwell-Boltzmann[9] kinetic theory of gases and it was not until 1908, when Perrin's[10] experiments confirmed Einstein's atomistic analysis of Brownian motion that the reality of atoms was at last accepted by such eminent holdouts as Boltzmann's opponent Ostwald[11].

The atom has an internal structure; it is thus not "atomic" in the Greek sense and is more than the mere restless particle of kinetic theories of gases or of Brownian motion. This was shown by two lines of work: the study of the passage of electricity through gases and the behavior of certain solutions. The study of the passage of electricity through gases at low pressure was a very active field of research in the nineteenth century and only a few of the pioneers in what we can now see as the incipient field of subatomic physics will be mentioned here. The observation by Plücker in 1858 of a fluorescent glow near the cathode on the glass walls of a current-carrying evacuated tube was one of the first inklings that particles might be elicited from atoms. That these were indeed particles rather than electromagnetic rays (in the language of classical physics) was indicated by Crookes in the 1870s, by showing that they could be deflected by a magnet. Goldstein showed in 1886 the presence of particles of opposite charge to those emitted from the cathode, and christened the latter "cathode rays". That the cathode rays were negative particles was proved by Perrin in 1895, when he showed that they imparted this charge to an object on which they fell. Further evidence of the negative particle nature of cathode rays came at around the same time from Thomson[12], who showed (1897) that they are deflected in the expected direction by an electric field. Thomson also measured their mass-to-charge ratio and from the smallest possible value of charge in electrochemistry calculated the mass of these particles to be about 1/1837 of the mass of a hydrogen atom. Lorentz later applied the name "electron" to the particle, adopting a term that had been appropriated from the Greek by Stoney for a unit of electric current ($\varepsilon\lambda\varepsilon\kappa\tau\rho o\nu$: amber, which acquires a charge when rubbed). Thomson has been called the discoverer of the electron.

---

[9] Ludwig Boltzmann, born Vienna 1844. Ph.D. Vienna. Professor Graz, Vienna. Developed the kinetic theory of gases independently of Maxwell (viz., Boltzmann constant's, k). Firm supporter of the atomic theory in opposition to Mach and Ostwald, helped develop concept of entropy (S). Died Duino, Austria (now in Italy), 1906 (suicide incurred by depression). Inscribed on gravestone: S = k log W.

[10] Jean Perrin, born Lille, France, 1870. Ph.D. École Normal Supérieure, Paris. Professor University of Paris. Nobel prize in physics 1923. Died New York, 1942.

[11] Wilhelm Friedrich Ostwald, German chemist, born Riga, Latvia, 1853. Ph.D. Dorpat, Estonia. Professor Riga, Leipzig. A founder of physical chemistry, opponent of the atomic theory till convinced by the work of Einstein and Perrin. Nobel prize in chemistry 1909. Died near Leipzig, 1932.

[12] Sir Joseph John Thomson, born near Manchester, 1856. Professor, Cambridge. Nobel prize in physics 1906. Knighted 1908. Died Cambridge, 1940.

It was perhaps Thomson who first suggested a specific structure for the atom in terms of subatomic particles. His "plum pudding" model (ca. 1900), which placed electrons in a sea of positive charge, like raisins in a pudding, accorded with the then-known facts in evidently permitting electrons to be removed under the influence of an electric potential. The modern picture of the atom as a positive nucleus with extranuclear electrons was proposed by Rutherford[13] in 1911. It arose from experiments in which alpha particles from a radioactive sample were shot through very thin gold foil. Most of the time the particles passed through, but occasionally one bounced back, indicating that the foil was mostly empty space, but that present were particles which were small and, compared to the mass of the electron (which was much too light to stop an alpha particle), massive. From these experiments emerged our picture of the atom as consisting of a small, relatively massive positive nucleus surrounded by electrons: the nuclear atom. Rutherford gave the name *proton* (from Greek $\pi\rho\omega\tau o\zeta$, primary or first) to the least massive of these nuclei (the hydrogen nucleus).

There is another thread to the development of the concept of the atom as a composite of subatomic particles. The enhanced effect of electrolytes (solutes that provide electrically conducting solutions) on boiling and freezing points and on the osmotic pressure of solutions led Arrhenius[14] in 1884 to propose that these substances exist in water as atoms or groups of atoms with an electric charge. Thus sodium chloride in solution would not, as was generally held, exist as NaCl molecules but rather as a positive sodium "atom" and a negative chlorine "atom"; the presence of two particles instead of the expected one accounted for the enhanced effects. The ability of atoms to lose or gain charge hinted at the existence of some kind of subatomic structure, and although the theory was not warmly received (Arrhenius was almost failed on his Ph.D. exam), the confirmation by Thomson (ca. 1900) that the atom contains electrons made acceptable the concept of charged atoms with chemical properties quite different from those of the neutral ones. Arrhenius was awarded the Nobel prize for his (albeit significantly modified) Ph.D. work.

4.2.5 The Bohr Atom

The nuclear atom as formulated by Rutherford faced a serious problem: the electrons orbit the nucleus like planets orbiting the Sun. An object engaged in circular (or elliptical) motion experiences an acceleration because its direction is

---

[13] Ernest Rutherford (Baron Rutherford), born near Nelson New Zealand, 1871. Studied at Cambridge under J. J. Thomson. Professor McGill University (Montreal), Manchester, and Cambridge. Nobel prize in chemistry 1908 for work on radioactivity, alpha particles, and atomic structure. Knighted 1914. Died London, 1937.

[14] Svante Arrhenius, born near Uppsala, Sweden, 1859. Ph.D. University of Stockholm. Nobel prize in chemistry 1903. Professor Stockholm. Died Stockholm 1927.

changing and thus its velocity, which unlike speed is a vector, is also changing. An electron in circular motion about a nucleus would experience an acceleration toward the nucleus, and since from Maxwell's equations of electromagnetism an accelerated electric charge radiates away energy, the electron should lose energy by spiralling in toward the nucleus, ending up there, with no kinetic and potential energy; calculations show this should happen in a fraction of a second [8].

A way out of this dilemma was suggested by Bohr[15] in 1913 [9, 10]. He retained the classical picture of electrons orbiting the nucleus in accord with Newton's laws, but subject to the constraint that the angular momentum of an electron must be an integral multiple of $h/2\pi$:

$$mvr = n(h/2\pi), \quad n = 1, 2, 3, \ldots \tag{4.7}$$

$m =$ electron mass
$v =$ electron velocity
$r =$ radius of electron orbit
$h =$ Planck's constant

Equation (4.7) is the Bohr postulate, that electrons can defy Maxwell's laws provided they occupy an orbit whose angular momentum (i.e. an orbit of appropriate radius) satisfies Eq. (4.7). The Bohr postulate is not based on a whim, as most textbooks imply, but rather follows from: (1) the Planck equation Eq. (4.3), $\Delta E = h\nu$ and (2) starting with an orbit of large radius such that the motion is essentially linear and classical physics does not force the electron to radiate since no acceleration is involved, then extrapolating to small-radius orbits. The fading of quantum-mechanical equations into their classical analogues as macroscopic conditions are approached, the reverse of the reasoning just described, is called the *correspondence principle* [11].

Using the postulate of Eq. (4.7) and classical physics, Bohr derived an equation for the energy of an orbiting electron in a one-electron atom (a hydrogenlike atom, H or He$^+$, etc.) in terms of the charge on the nucleus and some constants of nature. Starting with the total energy of the electron as the sum of its kinetic and potential energies:

$$E_t = \frac{1}{2}mv^2 - \frac{Ze^2}{4\pi\epsilon_0 r} \tag{4.8}$$

$Z =$ nuclear charge (1 for H, 2 for He, etc.)
$e =$ electron charge
$\epsilon_0 =$ permitivity of the vacuum

---

[15] Niels Bohr, born Copenhagen, 1885. Ph.D. University of Copenhagen. Professor, University of Copenhagen. Nobel prize in physics 1922. Founder of the "Copenhagen school" interpretation of quantum theory. Died Copenhagen, 1962.

Using force = mass × acceleration:

$$\frac{Ze^2}{4\pi\epsilon_0 r^2} = \frac{mv^2}{r} \tag{4.9}$$

i.e.

$$\frac{Ze^2}{4\pi\epsilon_0 r} = mv^2 \tag{4.10}$$

So from Eq. (4.8)

$$E_t = \frac{1}{2}mv^2 - mv^2 = -\frac{1}{2}mv^2 \tag{4.11}$$

From Eqs. (4.7) and (4.10):

$$v = \frac{Ze^2}{2\epsilon_0 nh} \tag{4.12}$$

So from Eqs. (4.11) and (4.12):

$$E_t = -\frac{Z^2 e^4 m}{8\epsilon_0^2 n^2 h^2} \tag{4.13}$$

Equation (4.13) expresses the total (kinetic plus potential) energy of the electron of a hydrogenlike atom in terms of four fundamental quantities of our universe: electron charge, electron mass, the permittivity of empty space, and Planck's constant. From Eq. (4.13) the energy change involved in emission or absorption of light by a hydrogenlike atom is simply

$$\Delta E = E_{t2} - E_{t1} = \frac{mZ^2 e^4}{8\epsilon_0^2 h^2}\left(\frac{1}{n_1^2} - \frac{1}{n_2^2}\right) \tag{4.14}$$

where ΔE is the energy of a state characterized by *quantum number n_2*, minus the energy of a state characterized by quantum number n_1. Note that from Eq. (4.13) the total energy increases (becomes less negative) as n increases ($= 1, 2, 3, \cdots$), so higher-energy states are associated with higher quantum numbers n and $\Delta E > 0$ corresponds to absorption of energy and $\Delta E < 0$ to emission of energy. The Planck relation between the amount of radiant energy absorbed or emitted and its frequency ($\Delta E = hv$, Eq. (4.3)), Eq. (4.14) enables one to calculate the frequencies of spectroscopic absorption and emission lines for hydrogenlike atoms. The agreement with experiment is excellent, and the same is true too for the calculated ionization energies of hydrogenlike atoms (ΔE for $n_2 = \infty$ in Eq. (4.14)).

4.2.6   The Wave Mechanical Atom and the Schrödinger Equation

The Bohr approach works well for hydrogenlike atoms, atoms with one electron: hydrogen, singly-ionized helium, doubly-ionized lithium, etc. However, it showed several deficiencies for all other atoms. The problems with the Bohr model for these cases were:

1. There were lines in the spectra corresponding to transitions other than simply between two n values (cf. Eq. (4.14)). This was rationalized by Sommerfeld in 1915, by the hypothesis of elliptical rather than circular orbits, which essentially introduced a new quantum number k, a measure of the eccentricity of the elliptical orbit. Electrons could have the same n but different k's, increasing the variety of possible electronic transitions; k is related to what we now call the azimuthal quantum number, l; $l = k - 1$.
2. There were lines in the spectra of the alkali metals that were not accounted for by the quantum numbers n and k. In 1925 Goudsmit and Uhlenbeck showed that these could be explained by assuming that the electron spins on an axis; the magnetic field generated by this spin around an axis could reinforce or oppose the field generated by the orbital motion of the electron around the nucleus. Thus for each n and k there are two closely-spaced "magnetic levels", making possible new, closely-spaced spectral lines. The spin quantum number, $m_s = +1/2$ or $-1/2$, was introduced to account for spin.
3. There were new lines in atomic spectra in the presence of an *external* magnetic field (not to be confused with the fields generated by the electron itself) This Zeeman effect (1896) was accounted for by the hypothesis that the electron orbital plane can take up only a limited number of orientations, each with a different energy, with respect to the external field. Each orientation was associated with a magnetic quantum number m_m (often designated m) $= -l, -(l-1), \ldots, (l-1), l$. Thus in an external magnetic field the numbers n, k (later l) and m_s are insufficient to describe the energy of an electron and new transitions, invoking m_m, are possible.

The only quantum number that flows naturally from the Bohr approach is the principal quantum number, n; the azimuthal quantum number l (a modified k), the spin quantum number m_s and the magnetic quantum number m_m are all ad hoc, improvised to meet an experimental reality. Why should electrons move in elliptical orbits that depend on the principal quantum number n? Why should electrons spin, with only two values for this spin? Why should the orbital plane of the electron take up with respect to an external magnetic field only certain orientations, which depend on the azimuthal quantum number? All four quantum numbers should follow naturally from a satisfying theory of the behaviour of electrons in atoms.

The limitations of the Bohr theory arise because it does not reflect a fundamental facet of nature, namely the fact that particles possess wave properties. These limitations were transcended by the *wave mechanics* of Schrödinger[16], when he devised his famous equation in 1926 [12, 13]. Actually, the year before the Schrödinger equation was published, Heisenberg[17] published his matrix mechanics approach to calculating atomic (and in principle molecular) properties. The matrix approach is at bottom equivalent to Schrödinger's use of differential equations, but the latter has appealed to chemists more because, like physicists of the time, they were unfamiliar with matrices (Sect. 4.3.3), and because the wave approach lends itself to a physical picture of atoms and molecules while manipulating matrices perhaps tends to resemble numerology. Matrix mechanics and wave mechanics are usually said to mark the birth of quantum *mechanics* (1925, 1926), as distinct from the more purely conceptual quantum theory (1900). We can think of quantum mechanics as the rules and equations used to calculate the properties of molecules, atoms, and subatomic particles.

Wave mechanics grew from the work of de Broglie[18], who in 1923 was led to this "wave-particle duality" by his ability to deduce the Wien blackbody equation (Sect. 4.2.1) by treating light as a collection of particles ("light quanta") analogous to an ideal gas [14]. This suggested to de Broglie that light (traditionally considered a wave motion) and the atoms of an ideal gas were actually not fundamentally different. He derived a relationship between the wavelength of a particle and its momentum, by using the time-dilation principle of special relativity, and also from an analogy between optics and mechanics. The reasoning below, while perhaps less profound than de Broglie's, may be more accessible. From the special theory of relativity, the relation between the energy of a photon and its mass is

$$E_\mathrm{p} = mc^2 \qquad (*4.15)$$

where c is the velocity of light. From the Planck Eq. (4.3) for the emission and absorption of radiation, the energy E_p of a photon may be equated with the energy change ΔE of an oscillator, and we may write

$$E_\mathrm{p} = h\nu \qquad (*4.16)$$

From Eqs. (4.15) and (4.16)

---

[16] Erwin Schrödinger, born Vienna, 1887. Ph.D. University of Vienna. Professor Stuttgart, Berlin, Graz (Austria), School for Advanced Studies Dublin, Vienna. Nobel prize in physics 1933 (shared with Dirac). Died Vienna, 1961.

[17] Werner Heisenberg, born Würzburg, Germany, 1901. Ph.D. Munich, 1923. Professor, Leipzig University, Max Planck Institute. Nobel Prize 1932 for his famous uncertainty principle of 1927. Director of the German atomic bomb/reactor project 1939–1945. Held various scientific administrative positions in postwar (Western) Germany 1945–1970. Died Munich 1976.

[18] Louis de Broglie, born Dieppe, 1892. Ph.D. University of Paris. Professor Sorbonne, Institut Henri Poincaré (Paris). Nobel prize in physics 1929. Died Paris, 1987.

$$mc^2 = hv \tag{4.17}$$

Since $v = c/\lambda$, Eq. (4.17) can be written

$$mc = h/\lambda \tag{4.18}$$

and because the product of mass and velocity is momentum, Eq. (4.18) can be written

$$p_{\mathrm{p}} = h/\lambda \tag{4.19}$$

relating the momentum of a photon (in its particle aspect) to its wavelength (in its wave aspect). If Eq. (4.19) can be generalized to any particle, then we have

$$p = h/\lambda \tag{*4.20}$$

relating the momentum of a particle to its wavelength; this is the de Broglie equation.

   If a particle has wave properties it should be describable by somehow combining the de Broglie equation and a classical wave equation. A highly developed nineteenth century mathematical theory of waves was at Schrödinger's disposal, and the union of a classical wave equation with Eq. (4.20) was one of the ways that he derived his wave equation. Actually, it is sometimes said that the Schrödinger equation cannot actually be *derived*, but is rather a postulate of quantum mechanics that can only be justified by the fact that it works [15]; this fine philosophical point will not be pursued here. Of his three approaches [15], Schrödinger's simplest is outlined here. A standing wave (one with fixed ends like a vibrating string or a sound wave in a flute) whose amplitude varies with time and with the distance from the ends is described by

$$\frac{d^2 f(x)}{dx^2} = -\frac{4\pi^2}{\lambda^2} f(x) \tag{4.21}$$

$f(x) =$ amplitude of the wave
$x =$ distance from some chosen origin
$\lambda =$ wavelength

From Eq. (4.20):

$$\lambda = h/mv \tag{4.22}$$

$\lambda =$ wavelength of particle of mass m and velocity v

Identifying the wave with a particle and substituting for λ from (4.22) into (4.21):

$$\frac{d^2f(x)}{dx^2} = -\frac{4\pi^2 m^2 v^2}{h^2} f(x) \qquad (4.23)$$

Since the total energy of the particle is the sum of its kinetic and potential energies:

$$E_{kin} = E - E_{pot} = E - V \qquad (4.24)$$

E = total energy of the particle
V = potential energy (the usual symbol)

$$\frac{1}{2} mv^2 = E - V \qquad (4.25)$$

i.e.

Substituting Eq. (4.25) for mv^2 into Eq. (4.23):

$$\frac{d^2f(x)}{dx^2} = -\frac{8\pi^2 m}{h^2}(E - V)f(x) \qquad (4.26)$$

$f(x)$ = amplitude of the particle/wave at a distance x from some chosen origin
m = mass of the particle
E = total energy (kinetic + potential) of the particle
V = potential energy of the particle (possibly a function of x)

This is the Schrödinger equation for one-dimensional motion along the spatial coordinate x. It is usually written

$$\frac{d^2\psi}{dx^2} + \frac{8\pi^2 m}{h^2}(E - V)\psi = 0 \qquad (4.27)$$

ψ = amplitude of the particle/wave at a distance x from some chosen origin

The one-dimensional Schrödinger equation is easily elevated to three-dimensional status by replacing the one-dimensional operator d^2/dx^2 by its three-dimensional analogue

$$\frac{\partial^2}{\partial x^2} + \frac{\partial^2}{\partial y^2} + \frac{\partial^2}{\partial z^2} = \nabla^2 \qquad (4.28)$$

∇^2 is the Laplacian operator "del squared." Replacing d^2/dx^2 by ∇^2, Eq. (4.27) becomes

$$\nabla^2\psi + \frac{8\pi^2 m}{h^2}(E - V)\psi = 0 \qquad (*4.29)$$

This is a common way of writing the Schrödinger equation; it relates the amplitude ψ of the particle/wave to the mass m of the particle, its total energy E and its potential energy V. The equation is frequently written by introducing $\hbar$ (h-bar), the reduced Planck constant or the Dirac constant, $= h/2\pi$; the reader can verify that this effects a minor notational simplification.

The meaning of ψ itself is, we might venture to say, unknown [2] but the currently popular interpretation of ψ^2, due to Born (Chap. 2, Sect. 2.3) and Pauli[19] is that it is proportional to the probability of finding the particle near a point $P(x, y, z)$ (recall that ψ is a function of x, y, z):

$$Prob(dx,\ dy,\ dz) = \psi^2 dxdydz \qquad (*4.30)$$

$$Prob(V) = \int_V \psi^2 dxdydz \qquad (4.31)$$

The probability of finding the particle in an infinitesimal cube of sides dx, dy, dz is $\psi^2 dxdydz$, and the probability of finding the particle somewhere in a volume V is the integral over that volume of ψ^2 with respect to dx, dy, dz (a triple integral); ψ^2 is thus a *probability density function*, with units of probability per unit volume. Born's interpretation was in terms of the probability of a particular state, Pauli's the chemist's usual view, that of a particular location.

The Schrödinger equation overcame the limitations of the Bohr approach (see the beginning of Sect. 4.2.6): the quantum numbers follow naturally from it (actually the spin quantum number m_s requires a relativistic form of the Schrödinger equation, the Dirac equation, and electron "spin" is apparently not really due to the particle spinning like a top). The Schrödinger equation can be solved in an exact analytical way only for one-electron chemical systems like the hydrogen atom, the helium monocation and the hydrogen molecule ion, but the mathematical approach is complicated and of no great relevance to the application of this equation to the study of serious molecules. However a brief account of the results for hydrogenlike atoms is in order.

The standard approach to solving the Schrödinger equation for *hydrogenlike atoms* involves transforming it from Cartesian (x, y, z) to polar coordinates (r, θ, ϕ), since these accord more naturally with the spherical symmetry of the system. This makes it possible to separate the equation into three simpler equations, $f(r) = 0$, $f(\theta) = 0$, and $f(\phi) = 0$. Solution of the $f(r)$ equation gives rise to the n quantum number, solution of the $f(\theta)$ equation to the l quantum number, and solution of the $f(\phi)$ equation to the m_m (often simply called m) quantum number.

---

[19] Wolfgang Pauli, born Vienna, 1900. Ph.D. Munich 1921. Professor Hamburg, Zurich, Princeton, Zurich. Best known for the Pauli exclusion principle. Nobel Prize 1945. Died Zurich 1958.

For each specific $n = n'$, $l = l'$ and $m_{\mathrm{m}} = m_{\mathrm{m}}{}'$ there is a mathematical function obtained by combining the appropriate $f(r)$, $f(\theta)$ and $f(\phi)$:

$$\psi\left(r,\ \theta,\ \phi,\ n',\ l',\ m_{\mathrm{m}}{}'\right) = f(r)f(\theta)f(\phi) \tag{4.32}$$

The function $\psi(r, \theta, \phi)$ (clearly ψ could also be expressed in Cartesians), depends *functionally* on r, θ, ϕ and *parametrically* on n, l and m_{m}: for each particular set $(n', l', m_{\mathrm{m}}')$ of these numbers there is a particular function with the spatial coordinates variables r, θ, ϕ (or x, y, z). A function like $k\sin x$ is a function of x and depends only parametrically on k. This ψ function is an *orbital* ("quasi-orbit"; the term was invented by Mulliken, Sect. 4.3.4), and you are doubtless familiar with plots of its variation with the spatial coordinates. Plots of the variation of ψ^2 with spatial coordinates indicate variation of the electron density (recall the Born interpretation of the wavefunction) in space due to an electron with quantum numbers n', l' and m_{m}'. We can think of an orbital as a region of space occupied by an electron with a particular set of quantum numbers, or as a mathematical function ψ describing the energy and the shape of the spatial domain of an electron. For an atom or molecule with more than one electron, the assignment of electrons to orbitals is an (albeit very useful) *approximation*, since orbitals follow from solution of the Schrödinger equation for a hydrogen atom.

The Schrödinger equation that we have been talking about is actually the *time-independent* (and nonrelativistic) Schrödinger equation: the variables in the equation are spatial coordinates, or spatial and spin coordinates (Chap. 5, Sect. 5.2.3.1) when electron spin is taken into account. The time-independent equation is the one most widely-used in computational chemistry, but the more general *time-dependent Schrödinger equation*, which we shall not examine, is important in certain applications, like some treatments of the interaction of a molecule with light, since light (radiation) is composed of time-varying electric and magnetic fields. The time-dependent density functional theory method of calculating UV spectra (Chap. 7) is based on the time-dependent Schrödinger equation.

The (reluctant) recognition of the *de facto* discontinuous absorption and emission of radiation by Planck, the quantum mechanics of the Bohr atom, based on a semi-classical modification of Newtonian mechanics, and Sommerfeld's attempts to extend this by attaching refinements such as elliptical orbits, constitute the *old quantum theory* (1900–1925). Its application to atoms and molecules is characterized by attempts to modify classical dynamics with limitations imposed by the quantum of action h; this is clearly seen in the work on atoms by Bohr and by Sommerfeld. The physically austere (almost numerological?) matrix formalism of Heisenberg (1925), and the more visual but mathematically equivalent application to atoms by Schrödinger (1926) of the wave-mechanical postulate of de Broglie (1923), constitute the beginning of modern quantum mechanics, sometimes called the *new quantum theory*. Some regard quantum *mechanics* as having arisen in the development of quantum theory when physicists ceased appending the concept of quantum jumps to classical motion as had been done by, for example, Bohr and Sommerfeld.

4.3   The Application of the Schrödinger Equation to Chemistry by Hückel

4.3.1   Introduction

The quantum mechanical methods described in this book are all molecular orbital (MO) methods, or oriented toward the molecular orbital approach: ab initio and semiempirical methods use the MO method, and density functional methods are oriented toward the MO approach. There is another approach to applying the Schrödinger equation to chemistry, namely the valence bond method. Basically the MO method allows atomic orbitals to interact to create the molecular orbitals of a molecule, and does not focus on individual bonds as shown in conventional structural formulas. As is the case with the wavefunction, the question of the physical significance of molecular orbitals, to what extent they are mathematical conveniences or potentially observable, is unsettled [2(i)]. The term "the orbital approximation" implies that they are "only" a mathematical convenience for handling the overall molecular wavefunction. The VB method, on the other hand, takes the molecule, mathematically, as a sum (a linear combination) of structures each of which corresponds to a structural formula with a certain pairing of electrons [16]. The MO method explains in a relatively simple way several phenomena that can be understood only with difficulty using the VB method, like the triplet nature of dioxygen or the fact that benzene is aromatic but cyclobutadiene is not [17]. The MO approach also lends itself well to computational algorithms. With the application of computers to quantum chemistry the MO method almost eclipsed the VB, but the latter has in recent years made a limited comeback [18].

The first application of quantitative quantum theory to chemical species significantly more complex than the hydrogen atom was the work of Hückel[20] on unsaturated organic compounds, in 1930–1937 [19]. This approach, in its simplest form, focuses on the p electrons of double bonds, aromatic rings and heteroatoms. Although Hückel did not initially explicitly consider orbital hybridization (the concept is usually credited to Pauling[21], 1931 [20]), the method as it became widely applied [21] confines itself to planar arrays of sp^2-hybridized atoms, usually carbon atoms, and evaluates the consequences of the interactions among the p electrons (Fig. 4.4). Actually, the simple Hückel method has been occasionally applied to nonplanar systems [22]. Because of the importance of the hybridization concept in the simple Hückel method a brief discussion of this is warranted.

---

[20] Erich Hückel, born Berlin, 1896. Ph.D. Göttingen. Professor, Marburg. Died Marburg, 1980.

[21] Linus Pauling, born Portland, Oregon, 1901. Ph.D. Caltech. Professor, Caltech. Known for work in quantum chemistry and biochemistry, campaign for nuclear disarmament, and controversial views on vitamin C. Nobel prize for chemistry 1954, for peace 1963. Died near Big Sur, California, 1994.
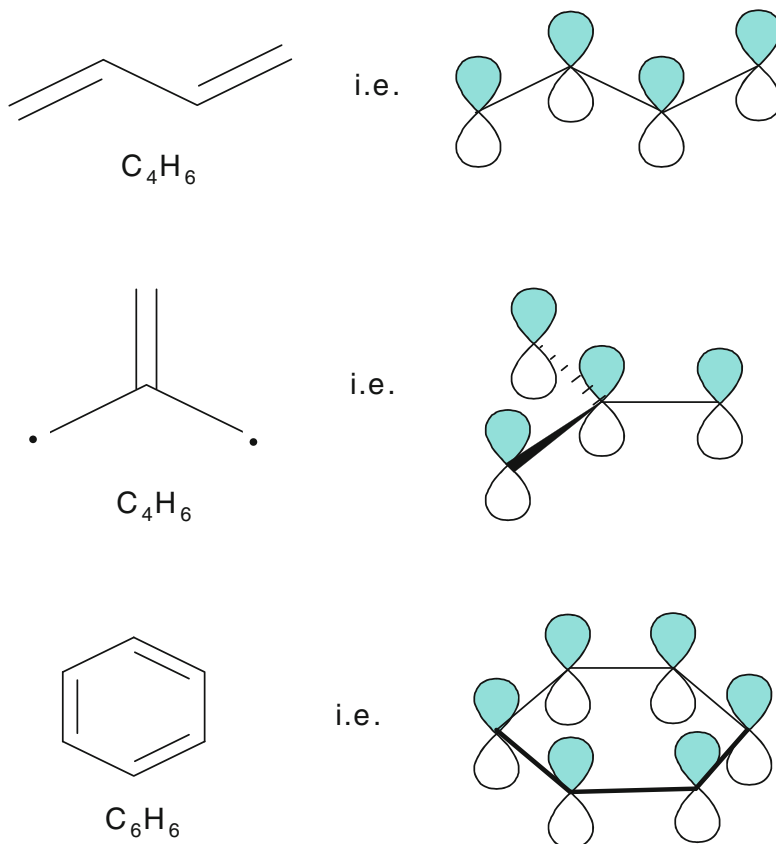
Fig. 4.4 The simple Hückel method is used mainly for planar arrays of π systems

4.3.2 Hybridization

Hybridization is the mixing of orbitals on an atom to produce new, "hybridized" (in the spirit of the biological use of the term), atomic orbitals. This is done mathematically but can be appreciated pictorially (Fig. 4.5). One way to justify the procedure theoretically is to recognize that atomic orbitals are vectors in the generalized mathematical sense of being elements of a vector space [23] (if not in the restricted sense of the physicist as physical entities with magnitude and direction); it is therefore permissible to take linear combinations of these vectors to produce new members of the vector space. A good, brief introduction to hybridization in is given by Streitwieser [24].
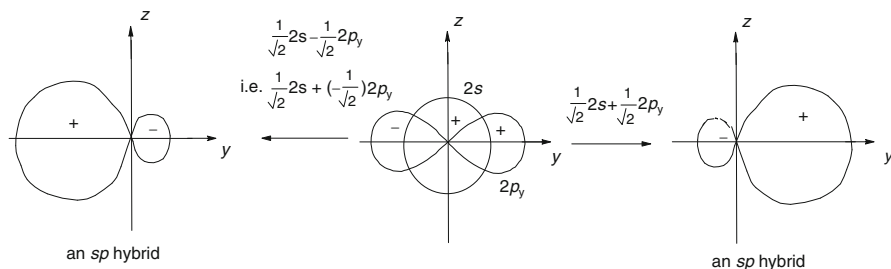
Fig. 4.5 Hybridization is forming new atomic orbitals, on an atom, by mathematically mixing (combining) "original" atomic orbitals on that atom. Mixing two orbitals gives two hybrid orbitals, and in general n AOs give n hybrid AOs. Orbitals are mathematical functions and so can be added and subtracted as shown above

In a familiar example, a $2s$ orbital can be mixed with three $2p$ orbitals to give four hybrid orbitals; this can be done in an infinite number of ways, such as (from now on ϕ will be used for atomic orbitals and ψ for molecular orbitals):

$$
\begin{aligned}
\phi_1 &= \frac{1}{2}(s + p_x + p_y + p_z) \\
\phi_2 &= \frac{1}{2}(s + p_x + p_y - p_z) \\
\phi_3 &= \frac{1}{2}(s + p_x - p_y - p_z) \\
\phi_4 &= \frac{1}{2}(s + p_x - p_y + p_z)
\end{aligned}
\tag{4.33}
$$

or

$$
\begin{aligned}
\phi_a &= \frac{1}{2}\left(s + p_x + 2^{1/2}p_z\right) \\
\phi_b &= \frac{1}{2}\left(s + p_x - 2^{1/2}p_z\right) \\
\phi_c &= \frac{1}{2}\left(s - p_x + 2^{1/2}p_y\right) \\
\phi_d &= \frac{1}{2}\left(s - p_x - 2^{1/2}p_y\right)
\end{aligned}
\tag{4.34}
$$

Both the set (4.33) and the set (4.34) consist of four sp^3 orbitals, since the electron density contributions from the component s and p orbitals to the hybrid is, in each case (considering the *squares* of the coefficients; recall the Born interpretation of the square of a wavefunction, Sect. 4.2.6) in the ratio 1:3, i.e. 1/4:3(1/4) and 1/4: (1/4 + 2/4), and in each set we have used a total of one s orbital, and one each of the p_x, p_y and p_z orbitals. An sp^3 orbital is said to have 25 % s character (and 75 % p character), from the ratio of the squares of the atomic orbital coefficients, 1/4:3/4. "Character" here is most easily interpreted as diffuseness of electron density: an electron in an sp^2 orbital, with 33 % s character, spends more time close to the
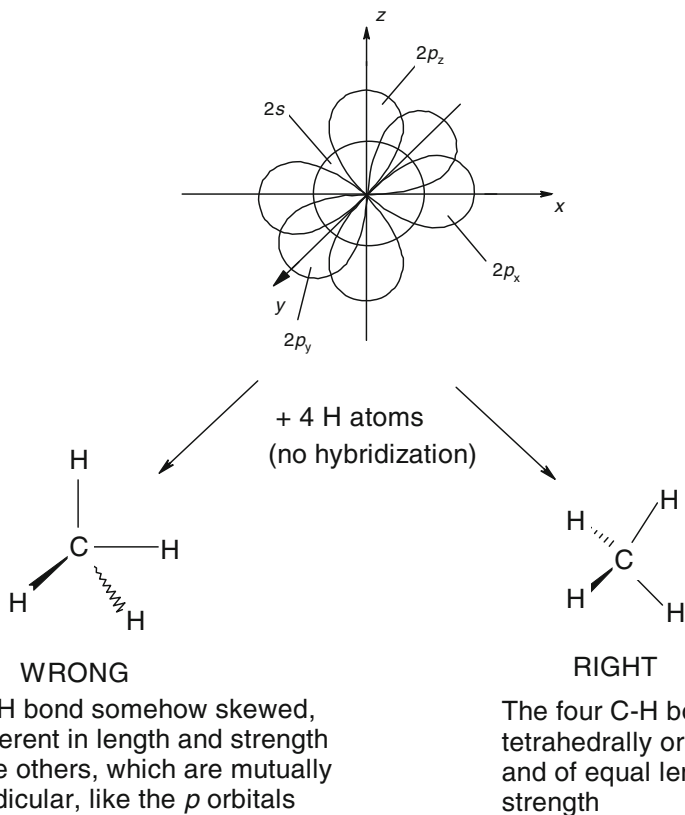
Fig. 4.6 Hybridization is not needed to explain bonding, e.g. the tetrahedral geometry of methane

nucleus than one in an sp^3 orbital, following the order of "tightness" of s and p atomic orbitals of the same quantum number. This has consequences for the acidity and NMR signal of an attached hydrogen.

Hybridization is purely a mathematical procedure, originally invented to reconcile the quantum mechanical picture of electron density in s, p, etc. orbitals with traditional views of directed valence. For example, it is sometimes said that in the absence of hybridization combining a carbon atom with four unpaired electrons with four hydrogen atoms would give a methane molecule with three equivalent, mutually perpendicular bonds and a fourth, different, bond (Fig. 4.6). Actually, this is incorrect: the $2s$ and three $2p$ orbitals of an unhybridized carbon along with the four 1 s orbitals of four hydrogen atoms provide, without invoking hybridization, a tetrahedrally symmetrical valence electron distribution that leads to tetrahedral methane with four equivalent bonds (Fig. 4.6). In fact, it has been said "It is sometimes convenient to combine aos [atomic orbitals] to form hybrid orbitals that have well defined directional character and then to form mos [molecular orbitals] by combining these hybrid orbitals. This recombination of aos to form

hybrids is *never* necessary ..." [25]. Interestingly, the MOs accommodating the four highest-energy electron pairs of methane (the eight valence electrons) are *not* equivalent in *energy* (not *degenerate*). This is an experimental fact that can be shown by photoelectron spectroscopy [26]. Instead of four orbitals of the same energy we have three degenerate orbitals and one lower in energy (and of course the almost undisturbed $1s$ core orbital of carbon). This surprising arrangement is a consequence of the fact that symmetry requires one combination (i.e. one MO) of carbon and hydrogen orbitals (essentially a weighted sum of the C2s and the four H1s orbitals) to be unique and the other three AO combinations (the other three MOs) to be degenerate (they involve the C2p and the H1s orbitals) [26, 27]. It must be emphasized that although the methane valence orbitals are *energetically* different, the electron and nuclear distribution *is* tetrahedrally symmetrical–the molecule indeed has T_d (Chap. 2, Sect. 2.6) symmetry. The four MOs formed directly from AOs are the *canonical* MOs. They are *delocalized* (spread out over the molecule), and do not correspond to the familiar four bonding Csp^3/H1s MOs,, each of which is localized between the carbon nucleus and a hydrogen nucleus. However, the canonical MOs can be mathematically manipulated to give the familiar localized MOs (Chap. 5, Sect. 5.2.3.1). Truhlar addresses the matter of hybridization, delocalized and localized orbitals, and the photoelectron results, in a short exposition (which might be clearer after reading Chap. 5, Sects. 5.2.3.1 and 5.4.3) [28].

Another example illustrates a situation somewhat similar to that we saw with methane, and what was until not so long ago a serious controversy: the best way to represent the carbon/carbon double bond [29]. The currently popular way to conceptualize the C $=$ C bond has it resulting from the union of two sp^2-hybridized carbon atoms (Fig. 4.7); the sp^2 orbitals on each carbon overlap end-on forming a σ bond and the p orbitals on each carbon overlap sideways forming a π bond. Note that the usual depiction of a carbon p orbital is unrealistically spindle-shaped, necessitating depicting overlap with connecting lines as in Fig. 4.7. Figure 4.8 shows a picture in better accord with the calculated electron density in the p orbital, i.e. corresponding to the square of the wavefunction. The leftover sp^2 orbitals can be used to bond to, say, hydrogen atoms (Fig. 4.7). From this viewpoint the double bond is thus composed of a σ bond and a π bond. However, this is not the only way to represent the C $=$ C bond. One can, for example, mathematically construct a carbon atom with two sp^2 orbitals and two sp^5 orbitals; the union of two such carbons gives a double bond formed from two sp^5/sp^5 bonds (Fig. 4.9; this shows why bonds that do not overlap end-on are called bent bonds; the more jocular "banana bonds" has also been used), rather than from a σ bond and a π bond. Which is right? They are only different ways of viewing the same thing: the electron density in the C $=$ C bond decreases smoothly from the central C/C axis in both models (Fig. 4.10), and the experimental ^{13}C/H NMR coupling constant for the C-H bond would, in both models, be predicted to correspond to 33 % s character in the orbital used by carbon to bond to hydrogen [30]. The ability of the hybridization concept to correlate and rationalize acidities of hydrocarbons in terms of the s character of the carbon orbital in a C-H bond [30] is an example of the usefulness of this idea. Most of the systems studied by the simple Hückel method are essentially flat, as expected for sp^2 arrays, and many properties of these molecules
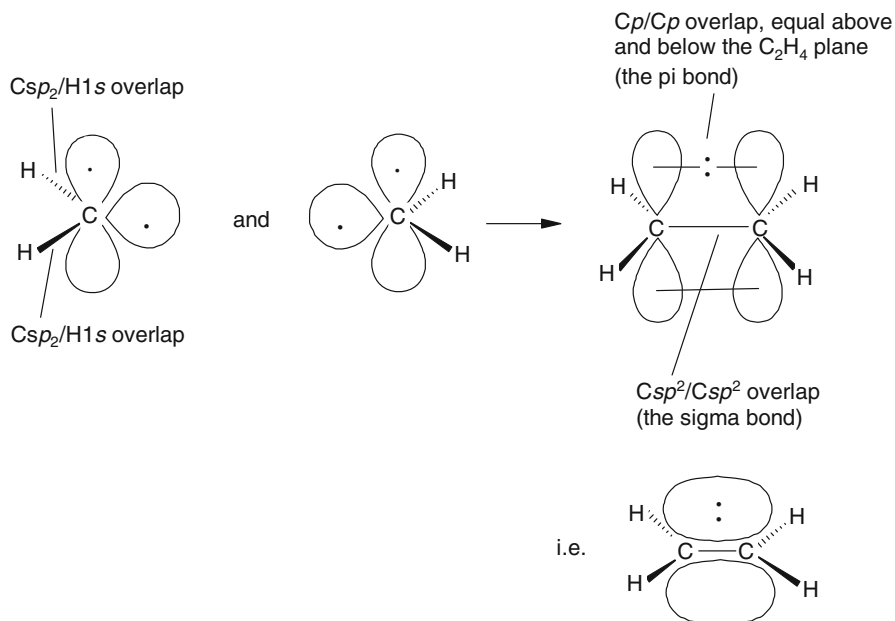
Fig. 4.7 The currently popular view of the C/C double bond: an sp^2/sp^2 σ bond and a p/p π bond. Compare this with Figs. 4.8 and 4.9
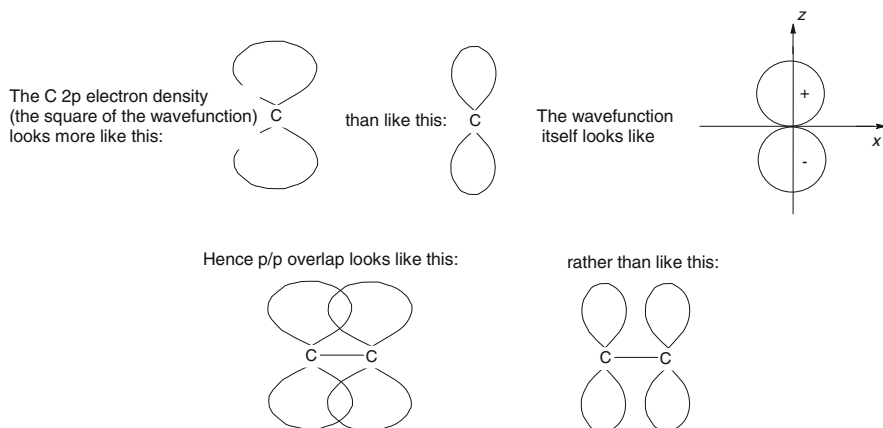
Fig. 4.8 The electron density is represented by the *square* of the mathematical function we call the orbital. A carbon $2p$ orbital is actually more buxom than its conventional representation, and two $2p$ orbitals overlap better than the usual picture, e.g. Fig. 4.7, suggests

can be at least qualitatively understood by considering the in-plane σ electrons of overlapping sp^2 orbitals to simply represent a framework that holds the perpendicular p orbitals, in which we are interested, in an orientation allowing neighboring p orbitals to overlap.
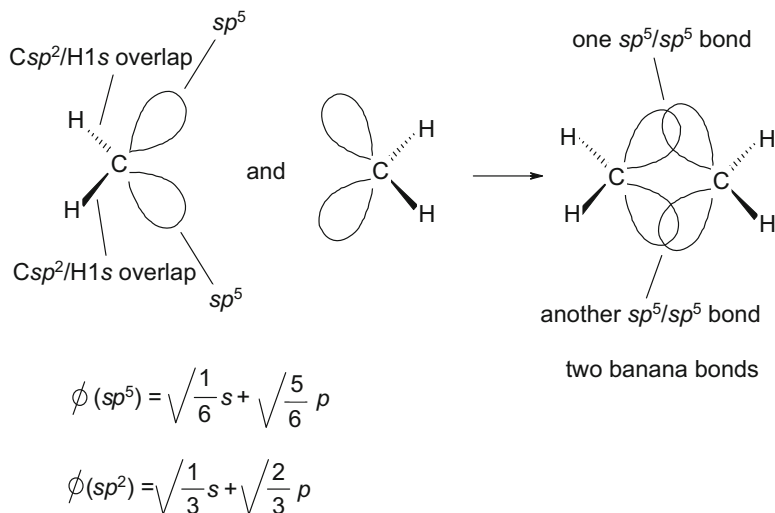
Fig. 4.9   The C/C double bond can be built from two sp^5 orbitals. The result is the same as using a σ bond and a π bond (Fig. 4.7): see Fig. 4.10

Before moving on to Hückel theory we take a look at matrices, since matrix algebra is the simplest and most elegant way to handle the linear equations that arise when MO theory is applied to chemistry.

4.3.3   Matrices and Determinants

Matrix algebra was invented by Cayley[22] as a systematic way of dealing with systems of linear equations. The single equation in one unknown

$$ax = b$$

has the solution $x = a^{-1}b$

Consider next the system of two equations in two unknowns

1. $a_{11}x + a_{12}y = c_1$
2. $a_{21}x + a_{22}y = c_2$

---

[22] Arthur Cayley, lawyer and mathematician, born Richmond, England, 1821. Graduated Cambridge. Professor, Cambridge. After Euler and Gauss, history's most prolific author of mathematical papers. Died Cambridge, 1895.
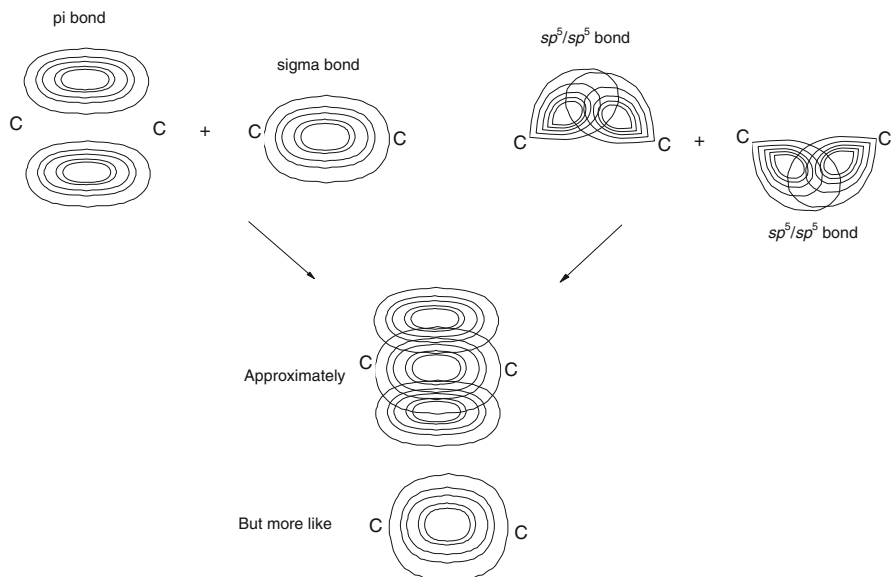
Fig. 4.10 The model of a C/C double bond as a σ/π bond is at bottom really equivalent to the $sp^5/sp^5 + sp^5/sp^5$ model: both result in the same electron distribution, which is the physically significant thing. There are no gaps in electron density between the carbons: as the contribution to density from the σ bond (or one of the sp^5/sp^5 bonds) falls off, the contribution from the π bond (or the other sp^5/sp^5 bond) increases. The electron density falls off smoothly with distance from the C/C axis. For some purposes one of the models, σ/π or bent (banana) bonds, may be more useful

The subscripts of the unknowns coefficients a indicate row 1, column 1, row 1, column 2, etc. We'll see that using matrices the solutions (the values of x and y) can be expressed in a way analogous to that for the equation $ax = b$.

A matrix is a rectangular array of "elements" (numbers, derivatives, etc.) that obeys certain rules of addition, subtraction, and multiplication. Curved or angular brackets are used to denote a matrix:

$$\begin{pmatrix} 1 & 2 \\ 7 & 2 \end{pmatrix} \qquad \begin{pmatrix} 5 \\ 2 \\ 0 \end{pmatrix} \qquad (0\ \ 0\ \ 7\ \ 4)$$

$$2 \times 2\,\text{matrix} \quad 3 \times 1\,\text{matrix} \quad 1 \times 4\,\text{matrix}$$

or:

$$\begin{bmatrix} 1 & 2 \\ 7 & 2 \end{bmatrix} \qquad\qquad \begin{bmatrix} 5 \\ 2 \\ 0 \end{bmatrix} \qquad\qquad [0\ \ 0\ \ 7\ \ 4]$$

Do not confuse matrices with determinants (below), which are written with straight lines, e.g.

$$\begin{vmatrix} 1 & 2 \\ 7 & 3 \end{vmatrix}$$

is a determinant, not a matrix. This determinant represents the number $1 \times 3 - 2 \times 7 = 3 - 14 = -11$. In contrast to a determinant, a matrix is not a number, but rather a vector in some cases, or an operator, although some would consider matrices to be generalizations of numbers, with e.g. the 1×1 matrix $(3) = 3$. An operator *acts on* a function (or a vector) to give a new function, e.g. d/dx acts on (differentiates) $f(x)$ to give $f'(x)$:

$$\frac{d}{dx}f(x) = \frac{df(x)}{dx} = f'(x)$$

and the square root operator acts on y^2 to give y. When we have done matrix multiplication you will see that a matrix can act on a vector and rotate it through an angle to give a new vector.

Let's look at matrix addition, subtraction, multiplication by scalars, and matrix multiplication (multiplication of a matrix by a matrix).

4.3.3.1   Addition and Subtraction

Matrices of the same size (2×2 and 2×2, 3×1 and 3×1, etc.) can be added just by adding corresponding elements:

$$\begin{pmatrix} 2 & 1 \\ 7 & 4 \end{pmatrix} + \begin{pmatrix} 1 & 3 \\ 5 & 6 \end{pmatrix} = \begin{pmatrix} 2+1 & 1+3 \\ 7+5 & 4+6 \end{pmatrix} = \begin{pmatrix} 3 & 4 \\ 12 & 10 \end{pmatrix}$$

$$\begin{pmatrix} 7 \\ 0 \\ 3 \end{pmatrix} + \begin{pmatrix} 4 \\ 4 \\ 1 \end{pmatrix} = \begin{pmatrix} 7+4 \\ 0+4 \\ 3+1 \end{pmatrix} = \begin{pmatrix} 11 \\ 4 \\ 4 \end{pmatrix}$$

Subtraction is similar:

$$\begin{pmatrix} 2 & 1 \\ 7 & 4 \end{pmatrix} - \begin{pmatrix} 1 & 3 \\ 5 & 6 \end{pmatrix} = \begin{pmatrix} 2-1 & 1-3 \\ 7-5 & 4-6 \end{pmatrix} = \begin{pmatrix} 1 & -2 \\ 2 & -2 \end{pmatrix}$$

4.3.3.2   Multiplication by a Scalar

A scalar is an ordinary number (in contrast to a vector or an operator), e.g. 1, 2, $\sqrt{2}$, 1.714, π, etc. To multiply a matrix by a scalar we just multiply every element by the number:

$$2\begin{pmatrix} 2 & 1 \\ 7 & 4 \end{pmatrix} = \begin{pmatrix} 2 \times 2 & 2 \times 1 \\ 2 \times 7 & 2 \times 4 \end{pmatrix} = \begin{pmatrix} 4 & 2 \\ 14 & 8 \end{pmatrix}$$

4.3.3.3 Matrix Multiplication

We could define matrix multiplication to be analogous to addition: simply multiplying corresponding elements. After all, in mathematics any rules are permitted, as long as they do not lead to contradictions. However, as we shall see in a moment, for matrices to be useful in dealing with simultaneous equations we must adopt a slightly more complex multiplication rule. The easiest way to understand matrix multiplication is to first define series multiplication. If

$$\text{series } a = S_a = a_1\ a_2\ a_3\ \ldots, \text{ and series } b = S_b = b_1\ b_2\ b_3\ \ldots$$

then we define the series product as

$$S_a\ S_b = a_1 b_1 + a_2 b_2 + a_3 b_3 + \ldots$$

So for example, if $S_a = 5\ 2\ 1$ and $S_b = 3\ 6\ 2$

then $S_a\ S_b = 5(3) + 2(6) + 1(2) = 15 + 12 + 2 = 29$

Now it's easy to understand matrix multiplication: if $\mathbf{AB}=\mathbf{C}$, where $\mathbf{A}$, $\mathbf{B}$, and $\mathbf{C}$ are matrices, then element i,j of the product matrix $\mathbf{C}$ is the series product of row i of $\mathbf{A}$ and column j of $\mathbf{B}$. For example

$$\mathbf{AB} = \begin{pmatrix} 1 & 3 \\ 7 & 2 \end{pmatrix}\begin{pmatrix} 2 & 4 \\ 5 & 6 \end{pmatrix} = \begin{pmatrix} 1(2) + 3(5) & 1(4) + 3(6) \\ 7(2) + 2(5) & 7(4) + 2(6) \end{pmatrix} = \begin{pmatrix} 17 & 22 \\ 24 & 40 \end{pmatrix}$$

(With practice, you can multiply simple matrices in your head). Note that matrix multiplication is not *commutative*: $\mathbf{AB}$ is not *necessarily* $\mathbf{BA}$, e.g.

$$\mathbf{BA} = \begin{pmatrix} 2 & 4 \\ 5 & 6 \end{pmatrix}\begin{pmatrix} 1 & 3 \\ 7 & 2 \end{pmatrix} = \begin{pmatrix} 2(1) + 4(7) & 2(3) + 4(2) \\ 5(1) + 6(7) & 5(3) + 6(2) \end{pmatrix} = \begin{pmatrix} 30 & 14 \\ 47 & 27 \end{pmatrix}$$

(two matrices are identical if and only if their corresponding elements are the same). Note that two matrices may be multiplied together only if the number of columns of the first equals the number of rows of the second. Thus we can multiply $\mathbf{A}(2 \times 2)\mathbf{B}(2 \times 2)$, $\mathbf{A}(2 \times 2)\mathbf{B}(2 \times 3)$, $\mathbf{A}(3 \times 1)\mathbf{B}(1 \times 3)$, and so on. A useful mnemonic is $(a \times b)(b \times c) = (a \times c)$, meaning, for example that $\mathbf{A}(2 \times 1)$ times $\mathbf{B}(1 \times 2)$ gives $\mathbf{C}(2 \times 2)$:

$$\begin{pmatrix} 5 \\ 2 \end{pmatrix}(0\ 3) = \begin{pmatrix} 5(0) & 5(3) \\ 2(0) & 2(3) \end{pmatrix} = \begin{pmatrix} 0 & 15 \\ 0 & 6 \end{pmatrix}$$

It is helpful to know beforehand the size i.e. (2×2), (3×3), whatever, of the matrix you will get on multiplication.

To get an idea of why matrices are useful in dealing with systems of linear equations, let's go back to our system of equations

(1) $\qquad\qquad\qquad a_{11}x + a_{12}y = c_1$
(2) $\qquad\qquad\qquad a_{21}x + a_{22}y = c_2$

Provided certain conditions are met this can be solved for x and y, e.g. by solving (1) for x in terms of y then substituting for x in (2) etc. Now consider the equations from the matrix viewpoint. Since

$$\mathbf{AB} = \begin{pmatrix} a_{11} & a_{12} \\ a_{21} & a_{22} \end{pmatrix}\begin{pmatrix} x \\ y \end{pmatrix} = \begin{pmatrix} a_{11}x + a_{12}y \\ a_{21}x + a_{22}y \end{pmatrix}$$

clearly $\mathbf{AB}$ corresponds to the lefthand side of the system, and the system can be written

$$\mathbf{AB} = \mathbf{C} \qquad \text{where } \mathbf{C} = \begin{pmatrix} c_1 \\ c_2 \end{pmatrix}$$

$\mathbf{A}$ is the coefficients matrix, $\mathbf{B}$ is the unknowns matrix, and $\mathbf{C}$ is the constants matrix. Now, if we can find a matrix $\mathbf{A}^{-1}$ such that $\mathbf{A}^{-1}\mathbf{AB} = \mathbf{B}$ (analogous to the numbers $a^{-1}ab = b$) then

$$\mathbf{A}^{-1}\mathbf{AB} = \mathbf{A}^{-1}\mathbf{C} \qquad i.e.\ \mathbf{B} = \mathbf{A}^{-1}\mathbf{C}$$

Thus the unknowns matrix is simply the inverse of the coefficients matrix times the constants matrix. Note that we multiplied by $\mathbf{A}^{-1}$ on the left ($\mathbf{A}^{-1}\mathbf{AB} = \mathbf{A}^{-1}\mathbf{C}$), which is not the same as multiplying on the right, which would give $\mathbf{ABA}^{-1} = \mathbf{C}$ $\mathbf{A}^{-1}$; this is not necessarily the same as $\mathbf{B}$.

To see that a matrix can act as an operator consider the vector from the origin to the point $P(3,4)$. This can be written as a column matrix, and multiplying it by the rotation matrix shown transforms it (rotates it) into another matrix:
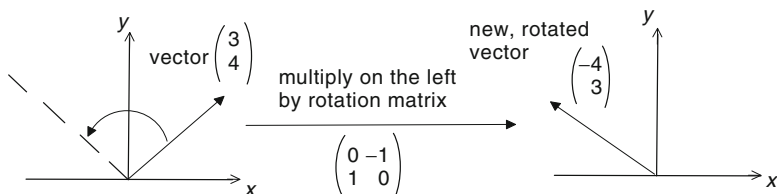
4.3.3.4   Some Important Kinds of Matrices

These matrices are particularly important in computational chemistry:

1. the zero matrix (the null matrix)
2. diagonal matrices
3. the unit matrix (the identity matrix)
4. the inverse of another matrix
5. symmetric matrices
6. the transpose of another matrix
7. orthogonal matrices

1. The zero matrix or null matrix, **0**, is any matrix with all its elements zero. Examples:

$$\begin{pmatrix} 0 & 0 \\ 0 & 0 \end{pmatrix} \qquad \begin{pmatrix} 0 & 0 & 0 \\ 0 & 0 & 0 \end{pmatrix} \qquad (0\ 0\ 0\ 0)$$

   Clearly, multiplication by the zero matrix (when the $(a \times b)(b \times c)$ mnemonic permits multiplication) gives a zero matrix.
2. A diagonal matrix is a *square* matrix that has all its off-diagonal elements zero; the (principal) diagonal runs from the upper left to the lower right. Examples:

$$\begin{pmatrix} 2 & 0 \\ 0 & 4 \end{pmatrix} \qquad \begin{pmatrix} 3 & 0 & 0 \\ 0 & 6 & 0 \\ 0 & 0 & 1 \end{pmatrix} \qquad \begin{pmatrix} 0 & 0 & 0 \\ 0 & 0 & 0 \\ 0 & 0 & 0 \end{pmatrix}$$

3. the unit matrix or identity matrix **1** or **I** is a diagonal matrix whose diagonal elements are all unity. Examples:

$$(1) \qquad \begin{pmatrix} 1 & 0 \\ 0 & 1 \end{pmatrix} \qquad \begin{pmatrix} 1 & 0 & 0 \\ 0 & 1 & 0 \\ 0 & 0 & 1 \end{pmatrix}$$

   Since diagonal matrices are square, unit matrices must be square (but zero matrices can be any size). Clearly, multiplication (when permitted) by the unit matrix leaves the other matrix unchanged: **1A**=**A1**=**A**
4. The inverse $\mathbf{A}^{-1}$ of another matrix **A** is the matrix that, multiplied **A**, on the left or right, gives the unit matrix: $\mathbf{A}^{-1}\mathbf{A} = \mathbf{A}\mathbf{A}^{-1} = \mathbf{1}$. Examples:

$$\text{If } \mathbf{A} = \begin{pmatrix} 1 & 2 \\ 3 & 4 \end{pmatrix} \text{ then } \mathbf{A}^{-1} = \begin{pmatrix} -2 & 1 \\ 3/2 & -1/2 \end{pmatrix}$$

   Check it out.

5. A symmetric matrix is a square matrix for which $a_{ij} = a_{ji}$ for each element. Examples:

$$\begin{pmatrix} 1 & 4 \\ 4 & 3 \end{pmatrix} \quad a_{12} = a_{21} = 4 \qquad \begin{pmatrix} 2 & 7 & 1 \\ 7 & 3 & 5 \\ 1 & 5 & 4 \end{pmatrix} \quad a_{12} = a_{21} = 7, \; etc.$$

Note that a symmetric matrix is unchanged by rotation about its principal diagonal. The complex-number analogue of a symmetric matrix is a *Hermitian matrix* (after the mathematician Charles Hermite); this has $a_{ij} = a_{ji}{}^*$, e.g. if element (2,3) $= a + bi$, then element (3,2) $= a - bi$, the complex conjugate of element (2,3); $i = \sqrt{-1}$. Since all the matrices we will use are *real* rather than complex, attention has been focussed on real matrices here.

6. The transpose ($\mathbf{A}^T$ or $\tilde{A}$) of a matrix $\mathbf{A}$ is made by exchanging rows and columns. Examples:

$$\text{If } \mathbf{A} = \begin{pmatrix} 2 & 3 \\ 4 & 7 \end{pmatrix} \quad \text{then } \mathbf{A}^T = \begin{pmatrix} 2 & 4 \\ 3 & 7 \end{pmatrix}$$

$$\text{If } \mathbf{A} = \begin{pmatrix} 2 & 1 & 6 \\ 1 & 7 & 2 \end{pmatrix} \quad \text{then } \mathbf{A}^T = \begin{pmatrix} 2 & 1 \\ 1 & 7 \\ 6 & 2 \end{pmatrix}$$

Note that the transpose arises from twisting the matrix around to interchange rows and columns. Clearly the transpose of a symmetric matrix $\mathbf{A}$ is the same matrix $\mathbf{A}$. For complex-number matrices, the analogue of the transpose is the *conjugate transpose* $\mathbf{A}^\dagger$; to get this form $\mathbf{A}^*$, the complex conjugate of $\mathbf{A}$, by converting each complex number element $a + bi$ in $\mathbf{A}$ to its complex conjugate $a - bi$, then switch the rows and columns of $\mathbf{A}^*$ to get $(\mathbf{A}^*)^T = \mathbf{A}^\dagger$. Physicists call $\mathbf{A}^\dagger$ the *adjoint* of $\mathbf{A}$, but mathematicians use adjoint to mean something else.

7. An orthogonal matrix is a square matrix whose inverse is its transpose: if $\mathbf{A}^{-1} = \mathbf{A}^T$ then $\mathbf{A}$ is orthogonal. Examples:

$$\mathbf{A}_1 = \begin{pmatrix} 1/\sqrt{2} & -1/\sqrt{2} \\ 1/\sqrt{2} & 1/\sqrt{2} \end{pmatrix} \qquad \mathbf{A}_2 = \begin{pmatrix} 1/\sqrt{6} & -1/\sqrt{2} & -1/\sqrt{3} \\ 2/\sqrt{6} & 0 & 1/\sqrt{3} \\ 1/\sqrt{6} & 1/\sqrt{2} & -1/\sqrt{3} \end{pmatrix}$$

We saw that for the inverse of a matrix $\mathbf{A}^{-1}\mathbf{A} = \mathbf{A}\mathbf{A}^{-1} = \mathbf{1}$, so for an orthogonal matrix $\mathbf{A}^T\mathbf{A} = \mathbf{A}\mathbf{A}^T = \mathbf{1}$, since here the transpose is the inverse. Check this out for the matrices shown. The complex analogue of an orthogonal matrix is a *unitary matrix*; its inverse is its conjugate transpose.

The columns of an orthonormal matrix are orthonormal vectors. This means that if we let each column represent a vector, then these vectors are mutually orthogonal and each one is normalized. Two or more vectors are orthogonal if they are

mutually perpendicular (i.e. at right angles), and a vector is normalized if it is of unit length. Consider the matrix A_1 above. If column 1 represents the vector v_1 and column 2 the vector v_2, then we can picture these vectors like this (the long side of a right triangle is of unit length if the squares of the other sides sum to 1):

$$v_1 = \begin{pmatrix} \dfrac{1}{\sqrt{2}} \\ \dfrac{1}{\sqrt{2}} \end{pmatrix}$$

$$v_2 = \begin{pmatrix} -\dfrac{1}{\sqrt{2}} \\ \dfrac{1}{\sqrt{2}} \end{pmatrix}$$
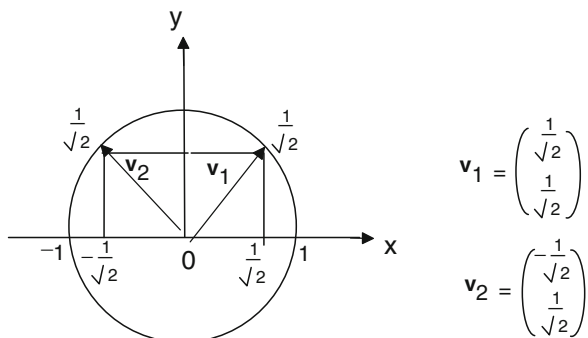
The two vectors are orthogonal: from the diagram the angle between them is clearly 90° since the angle each makes with, say, the x-axis is 45°. Alternatively, the angle can be calculated from vector algebra: the dot product (scalar product) is

$$v_1 \cdot v_2 = |v_1||v_2| \cos \theta$$

where |v| ("mod v") is the absolute value of the vector, i.e. its length:

$$|v| = \left(v_x^2 + v_y^2 \right)^{1/2} \quad \left(\text{or } \left(v_x^2 + v_y^2 + v_z^2 \right)^{1/2} \text{for a 3D vector} \right).$$

Each vector is normalized, i.e. $|v_1| = |v_2|(\frac{1}{2} + \frac{1}{2})^{1/2} = 1$.

The dot product is also

$$v_1 \cdot v_2 = v_{1x} v_{2x} + v_{1y} v_{2y} \text{ (with an obvious extension to 3D space)}$$

i.e.

$$\cos \theta = \left(v_{1x} v_{2x} + v_{1y} v_{2y} \right) / |v_1||v_2|$$
$$= \left[(1/\sqrt{2})(-1/\sqrt{2}) + (1/\sqrt{2})(1/\sqrt{2}) \right] / (1)(1) = 0$$

and so

$$\theta = 90°$$

Likewise, the three columns of the matrix A_2 above represent three mutually perpendicular, normalized vectors in 3D space. A better name for an orthogonal matrix would be an orthonormal matrix. Orthogonal matrices are important in computational chemistry because molecular orbitals can be regarded as orthonormal vectors in a generalized n-dimensional space (Hilbert space, after the mathematician David Hilbert). We extract information about molecular orbitals from matrices with the aid of *matrix diagonalization*.

4.3.3.5   Matrix Diagonalization

Modern computer programs use matrix diagonalization to calculate the energies (*eigenvalues*) of molecular orbitals and the sets of coefficients (*eigenvectors*) that help define their size and shape. We met these terms, and matrix diagonalization, briefly in Chap. 2, Sect. 2.5; "eigen" means suitable or appropriate, and we want solutions of the Schrödinger equation that are appropriate to our particular problem. If a matrix $\mathbf{A}$ can be written $\mathbf{A} = \mathbf{PDP}^{-1}$, where $\mathbf{D}$ is a diagonal matrix (you could call $\mathbf{P}$ and $\mathbf{P}^{-1}$ pre- and postmultiplying matrices), then we say that $\mathbf{A}$ is *diagonalizable* (can be diagonalized). The process of finding $\mathbf{P}$ and $\mathbf{D}$ (getting $\mathbf{P}^{-1}$ from $\mathbf{P}$ is simple for the matrices of computational chemistry–see below) is *matrix diagonalization*. For example

$$\mathbf{A} = \begin{pmatrix} 4 & -2 \\ 1 & 1 \end{pmatrix} \quad \text{then} \quad \mathbf{P} = \begin{pmatrix} 1 & 2 \\ 1 & 1 \end{pmatrix}, \quad \mathbf{D} = \begin{pmatrix} 2 & 0 \\ 0 & 3 \end{pmatrix}, \quad \text{and} \quad \mathbf{P}^{-1} = \begin{pmatrix} -1 & 2 \\ 1 & -1 \end{pmatrix}$$

Check it out. Linear algebra texts describe an analytical procedure using determinants, but computational chemistry employs a numerical iterative procedure called Jacobi matrix diagonalization, or some related method, in which the off-diagonal elements are made to approach zero stepwise.

Now, it can be proved that if and only if $\mathbf{A}$ is a symmetric matrix (or more generally, if we are using complex numbers, a Hermitian matrix–see symmetric matrices, above), then $\mathbf{P}$ is orthogonal (or more generally, unitary–see orthogonal matrices, above) and so the inverse $\mathbf{P}^{-1}$ of the premultiplying matrix $\mathbf{P}$ is simply the transpose of $\mathbf{P}$, $\mathbf{P}^{\mathrm{T}}$ (or more generally, what computational chemists call the *conjugate transpose* $\mathbf{A}^{\dagger}$ –see transpose, above). Thus

$$\text{If } \mathbf{A} = \begin{pmatrix} 0 & 1 \\ 1 & 0 \end{pmatrix} \text{ then}$$

$$\mathbf{P} = \begin{pmatrix} 0.707 & 0.707 \\ 0.707 & -0.707 \end{pmatrix}, \quad \mathbf{D} = \begin{pmatrix} 1 & 0 \\ 0 & -1 \end{pmatrix}, \quad \mathbf{P}^{-1} = \begin{pmatrix} 0.707 & 0.707 \\ 0.707 & -0.707 \end{pmatrix}$$

(In this simple example the transpose of $\mathbf{P}$ happens to be identical with $\mathbf{P}$). In the spirit of numerical methods 0.707 is used instead of $1/\sqrt{2}$. A matrix like $\mathbf{A}$ above, for which the premultiplying matrix $\mathbf{P}$ is orthogonal (and so for which $\mathbf{P}^{-1} = \mathbf{P}^{\mathrm{T}}$) is said to be *orthogonally diagonalizable*. The matrices we will use to get molecular orbital eigenvalues and eigenvectors are orthogonally diagonalizable. A matrix is orthogonally diagonalizable if and only if it is symmetric; this has been described as "one of the most amazing theorems in linear algebra" (see S. Roman, "An Introduction to Linear Algebra with Applications", Harcourt Brace, 1988, p. 408) because the concept of orthogonal diagonalizability is not simple, but that of a symmetric matrix is very simple.

4.3.3.6 Determinants

A determinant is a *square* array of elements that is a shorthand way of writing a sum of products; if the elements are numbers, then the determinant is a number. Examples:

$$\begin{vmatrix} a_{11} & a_{12} \\ a_{21} & a_{22} \end{vmatrix} = a_{11}a_{22} - a_{12}a_{21}, \quad \begin{vmatrix} 5 & 2 \\ 4 & 3 \end{vmatrix} = 5(3) - 2(4) = 7$$

As shown here, a 2×2 determinant can be expanded to show the sum it represents by "cross multiplication". A higher-order determinant can be expanded by reducing it to smaller determinants until we reach 2×2 determinants; this is done like this:

$$\begin{vmatrix} 2 & 1 & 3 & 0 \\ 1 & 7 & 3 & 5 \\ 3 & 4 & 6 & 1 \\ 1 & 8 & 2 & -2 \end{vmatrix} = 2\begin{vmatrix} 7 & 3 & 5 \\ 4 & 6 & 1 \\ 8 & 2 & -2 \end{vmatrix} - 1\begin{vmatrix} 1 & 3 & 5 \\ 3 & 6 & 1 \\ 1 & 2 & -2 \end{vmatrix} + 3\begin{vmatrix} 1 & 7 & 5 \\ 3 & 4 & 1 \\ 1 & 8 & -2 \end{vmatrix}$$

$$- 0\begin{vmatrix} 1 & 7 & 3 \\ 3 & 4 & 6 \\ 1 & 8 & 2 \end{vmatrix}$$

Here we started with element (1,1) and moved across the first row. The first of the above four terms is 2 times the determinant formed by striking out the row and column in which 2 lies, the second term is *minus* 1 times the determinant formed by striking out the row and column in which 1 lies, the third term is *plus* 3 times the determinant formed by striking out the row and column in which 3 lies, and the fourth term is *minus* 0 times the determinant formed by striking out the row and column in which 0 lies; thus starting with the element of row 1, column 1, we move along the row and multiply by $+1, -1, +1, -1$. It is also possible to start at, say element (2,1), the number 1, and move across the second row $(-, +, -, +)$, or to start at element (1,2) and go down the column $(-, +, -, +)$, etc. One would likely choose to work along a row or column with the most zeroes. The $(n-1) \times (n-1)$ determinants formed in expanding an $n \times n$ determinant are called *minors*, and a minor with its appropriate + or − sign is a *cofactor*. Expansion of determinants using minors/cofactors is called Lagrange expansion (Joseph Louis Lagrange, 1773). There are also other approaches to expanding determinants, such as manipulating them to make all the elements but one of a row or column zero; see any text on matrices and determinants. The third-order determinants in the example above can be reduced to second-order ones and so the fourth-order determinant can be evaluated as a single number. Obviously every determinant has a corresponding square matrix and every square matrix has a corresponding determinant, but a determinant is not a matrix; it is a *function* of a matrix, a rule that tells us how to take the set of numbers in a matrix and get a new number. Approaches to the study of determinants were made by Seki in Japan and Leibnitz in Europe, both in 1683.

The word "determinant" was first used in our sense by Cauchy (1812), who also wrote the first definitive treatment of the topic.

4.3.3.7   Some Properties of Determinants

These are stated in terms of rows, but also hold for columns; D is "the determinant".

1. If each element of a row is zero, D is zero (obvious from Lagrange expansion).
2. Multiplying each element of a row by k multiplies D by k (obvious from Lagrange expansion).
3. Switching two rows changes the sign of D (since this changes the sign of each term in the expansion).
4. If two rows are the same D is zero. (follows from 3, since if $n = -n$, n must be zero.
5. If the elements of one row are a multiple of those of another, D is zero (follows from 2 to 4).
6. Multiplying a row by k and adding it (adding corresponding elements) to another row leaves D unchanged (in the Laplace expansion the terms with k cancel).
7. A determinant A can be written as the sum of two determinants B and C which differ only in row i in accordance with this rule: if row i of A is $b_{i1} + c_{i1}\, b_{i2} + c_{i2}$ ... then row i of B is $b_{i1} + b_{i2}$ ... and row i of C is $c_{i1} + c_{i2}$ ... An example makes this clear; with row i = row 3:

$$\begin{vmatrix} 1 & 3 & 6 \\ 5 & 4 & 2 \\ 8 & 11 & 9 \end{vmatrix} = \begin{vmatrix} 1 & 3 & 6 \\ 5 & 4 & 2 \\ 5+3 & 7+4 & 4+5 \end{vmatrix} = \begin{vmatrix} 1 & 3 & 6 \\ 5 & 4 & 2 \\ 5 & 7 & 4 \end{vmatrix} + \begin{vmatrix} 1 & 3 & 6 \\ 5 & 4 & 2 \\ 3 & 4 & 5 \end{vmatrix}$$

4.3.4   The Simple Hückel Method–Theory

The derivation of the Hückel method (SHM, or simple Hückel theory, SHT; also called Hückel molecular orbital method, HMO method) given here is not rigorous and has been strongly criticized [31]; nevertheless it has the advantage of showing how with simple arguments one can use the Schrödinger equation to develop, more by a plausibility argument than a proof, a method that gives useful results and which can be extended to more powerful methods with the retention of many useful concepts from the simple approach.

The Schrödinger equation (Sect. 4.2.6, Eq. (4.29))

$$\nabla^2 \psi + \frac{8\pi^2 m}{h^2}(E - V)\psi = 0$$

can after very simple algebraic manipulation be rewritten

$$\left(-\frac{h^2}{8\pi^2 m}\nabla^2 + V\right)\psi = E\psi \tag{4.35}$$

This can be abbreviated to the seductively simple-looking form

$$\hat{H}\psi = E\psi \tag{*4.36}$$

where

$$\hat{H} = \left(-\frac{h^2}{8\pi^2 m}\nabla^2 + V\right) \tag{*4.37}$$

The symbol $\hat{H}$ ("H hat" or "H peak") is an *operator* (Sect. 4.3.3): it specifies that an operation is to be performed on ψ, and Eq. (4.36) says that the result of the operation will be E multiplied by ψ. The operation to be performed on ψ (i.e. ψ (x,y,z)) is "differentiate it twice with respect to x, to y and to z, add the partial derivatives, and multiply the sum by $-h^2/8\pi^2 m$; then add this result to V times ψ" (now you can see why symbols replaced words in mathematical discourse). The notation $\hat{H}\psi$ means $\hat{H}$ *of* ψ, not $\hat{H}$ *times* ψ.

Equation (4.36) says that an operator ($\hat{H}$) acting on a function (ψ) equals a constant (E) times the function ("H hat of psi equals E psi"). Such an equation

$$\hat{O}f = kf, \quad \hat{O} = \text{operator} \tag{4.38}$$

is called an *eigenvalue equation*. The functions f and constants k that satisfy Eq. (4.38) are eigenfunctions and eigenvalues, respectively, of the operator $\hat{O}$. The operator $\hat{H}$ is called the Hamiltonian operator, or simply the Hamiltonian. The term is named after the mathematician Sir William Rowan Hamilton, who formulated Newton's equations of motion in a manner analogous to the quantum mechanical Eq. (4.36). Eigenvalue equations are very important in quantum mechanics, and we shall again meet eigenfunctions and eigenvalues.

The eigenvalue formulation of the Schrödinger equation is the starting point for our derivation of the Hückel method. We will apply Eq. (4.36) to molecules, so in this context $\hat{H}$ and ψ are the molecular Hamiltonian and wavefunction, respectively.

From $\hat{H}\psi = E\psi$
We get

$$\psi\hat{H}\psi = E\psi^2 \tag{4.39}$$

Note that this is not the same as $\hat{H}\psi^2 = E\psi^2$, just as $xdf(x)/dx$, say, is not the same as $dxf(x)/dx$. Integrating and rearranging we get

$$E = \frac{\displaystyle\int \psi\hat{H}\psi dv}{\displaystyle\int \psi^2 dv} \tag{4.40}$$

The integration variable dv indicates integration with respect to spatial coordinates $(x, y, z$ in a Cartesian coordinate system), and integration over all of space is

implied, since that is the domain of an electron in a molecule, and thus the domain of the variables of the function ψ. One might wonder why not simply use $E = \hat{H}\psi/\psi$; the problems with this function are that it goes to infinity as ψ approaches zero, and it is not well-behaved with regard to finding a minimum by differentiation.

Next we approximate the molecular wavefunction ψ as a linear combination of atomic orbitals (LCAO). The molecular orbital (MO) concept as a tool in interpreting electronic spectra was formalized by Mulliken[23] starting in 1932 and building on earlier (1926) work by Hund[24] [32] (recall that Mulliken coined the word orbital). The postulate behind the LCAO approach is that an MO can be "synthesized" by combining simpler functions, now called *basis functions*; these functions comprise a *basis set*. This way of calculating MOs is based on suggestions of Pauling (1928) [33] and Lennard-Jones[25] (1929) [34]. Perhaps the most important early applications of the LCAO method were the simple Hückel method (1931) [19], in which p AOs orbitals are combined to give πAOs (probably the first time that the MOs of relatively big molecules were represented as a weighted sum of AOs with optimized coefficients), and the treatment of all the lower electronic states of the hydrogen molecule by Coulson[26] and Fischer (1949) [35]. The basis functions are usually located on the atoms of the molecule, and may or may not (see the discussion of basis functions in Chap. 5, Sect. 5.3) be conventional atomic orbitals. So strictly speaking we use in general a linear combination of *basis functions* rather than atomic orbitals, but the term LCAO is still popular. The wavefunction can in principle be approximated as accurately as desired by using enough suitable basis functions. In this simplified derivation of the Hückel method we at first consider a molecule with just two atoms, with each atom contributing one basis function to the MO. Combining basis functions on different atoms to give MOs spread over the molecule is somewhat analogous to combining atomic orbitals on the same atom to give hybrid atomic orbitals (Sect. 4.3.2) [27]. The combination of n basis functions always gives n MOs, as indicated in Fig. 4.11, and we expect two MOs for the two-atomic-orbital diatomic molecule we are using here.

---

[23] Robert Mulliken, born Newburyport, Massachusetts, 1896. Ph.D. University of Chicago. Professor New York University, University of Chicago, Florida State University. Nobel prize in chemistry 1966, for the MO method. Died Arlington, Virginia, 1986.

[24] Friedrich Hund, born Karlsruhe, Germany, 1896. Ph.D. Marburg, 1925, Professor Rostock, Leipzig, Jena, Frankfurt, Göttingen. Died Göttingen, 1997.

[25] John Edward Lennard-Jones, born Leigh, Lancaster, England, 1894. Ph.D. Cambridge, 1924. Professor Bristol. Best known for the Lennard-Jones potential function for nonbonded atoms. Died Stoke-on-Trent, England, 1954.

[26] Charles A. Coulson, born Worcestershire, England, 1910. Ph.D. Cambridge, 1935. Professor of theoretical physics, King's College, London; professor of mathematics, Oxford; professor of theoretical chemistry, Oxford. Best known for his book "Valence" (the 1st Ed., 1952). Died Oxford, 1974.
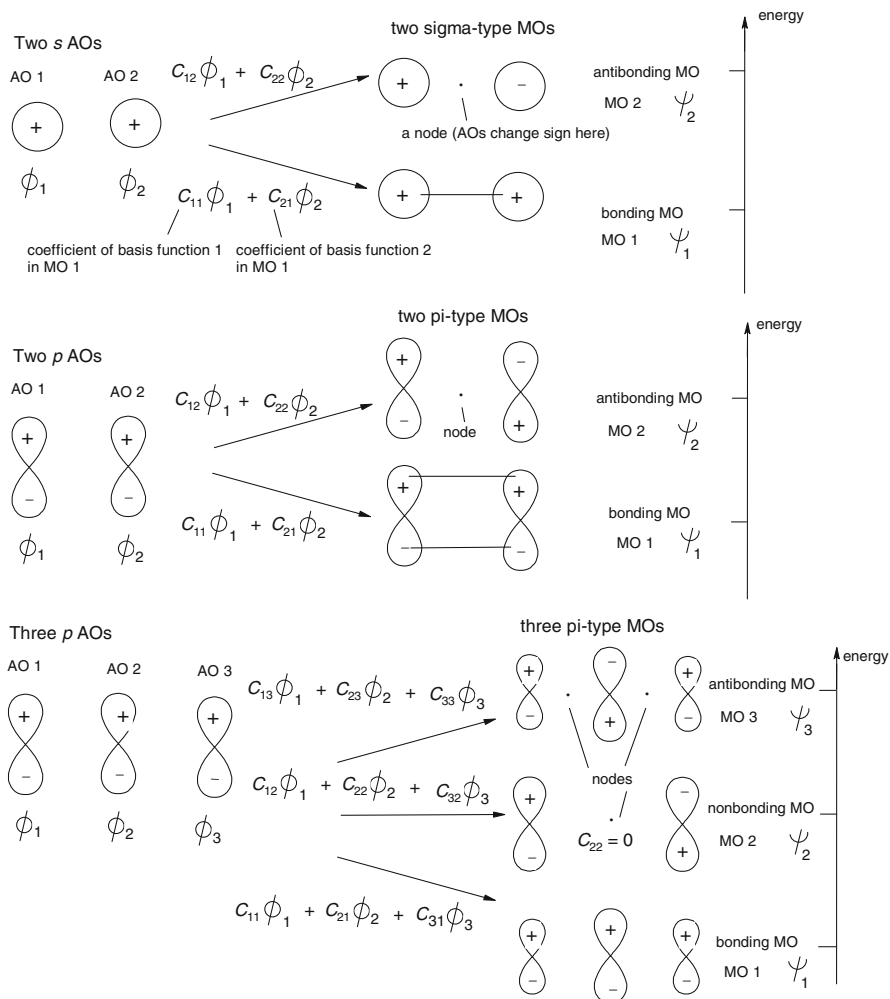
Fig. 4.11 Linear combination of n atomic orbitals (or, more generally, basis functions) gives n MOs. The coefficients c are weighting factors that determine the magnitude and the sign of the contribution from each basis function. The functions contributing to the MO change sign at a node (actually a *nodal plane*) and the energy of the MOs increases with the number of nodes

Using the LCAO approximation

$$\psi = c_1\phi_1 + c_2\phi_2 \qquad (4.41)$$

where ϕ_1 and ϕ_2 are basis functions on atoms 1 and 2, and c_1 and c_2 are weighting coefficients to be adjusted to get the best ψ, and substituting into Eq. (4.40) we get

$$E = \frac{\int (c_1\phi_1 + c_2\phi_2)\hat{H} \, (c_1\phi_1 + c_2\phi_2)dv}{\int (c_1\phi_1 + c_2\phi_2)^2 dv} \tag{4.42}$$

If we multiply out the terms in Eq. (4.42) we get

$$E = \frac{c_1^2 H_{11} + 2c_1 c_2 H_{12} + c_2^2 H_{22}}{c_1^2 S_{11} + 2c_1 c_2 S_{12} + c_2^2 S_{22}} \tag{4.43}$$

where

$$
\begin{aligned}
&\int \phi_1 \hat{H} \, \phi_1 dv = H_{11} \\
&\int \phi_1 \hat{H} \, \phi_2 dv = H_{12} = \int \phi_2 \hat{H} \, \phi_1 dv = H_{21} \\
&\int \phi_2 \hat{H} \, \phi_2 dv = H_{22} \\
&\int \phi_1^2 dv = S_{11} \\
&\int \phi_1 \phi_2 dv = S_{12} = \int \phi_2 \phi_1 dv = S_{21} \\
&\int \phi_2^2 dv = S_{22}
\end{aligned}
\tag{4.44}
$$

Note that in Eqs. (4.43) and (4.44) the H_{ij} are not operators hence are not given hats; they are *integrals* involving $\hat{H}$ and basis functions ϕ.

For any particular molecular geometry (i.e. nuclear configuration: Chap. 2, Sect. 2.3, the Born-Oppenheimer approximation) the energy of the ground electronic state is the minimum energy possible for that particular nuclear arrangement and the collection of electrons that goes with it. Our objective now is to minimize the energy with respect to the basis set coefficients. We want to find the c's corresponding to the minimum on an energy vs. c's potential energy surface. To do this we follow a standard calculus procedure: set $\partial E/\partial c_1$ equal to zero, explore the consequences, then repeat for $\partial E/\partial c_2$. In theory, setting the first derivatives equal to zero guarantees only that we will find in "MO space" (an abstract space defined by an energy axis and two or more coefficient axes) a stationary point (cf. Chap. 2, Sect. 2.2), but examining the second derivatives shows that the procedure gives an energy minimum if all or most of the electrons are in bonding MOs, which is the case for most real molecules [36]. Write Eq. (4.43) as

$$E\big(c_1^2 S_{11} + 2c_1 c_2 S_{12} + c_2^2 S_{22}\big) = c_1^2 H_{11} + 2c_1 c_2 H_{12} + c_2^2 H_{22} \tag{4.45}$$

and differentiate with respect to c_1:

$$\left(\frac{\partial E}{\partial c}\right)\big(c_1^2 S_{11} + 2c_1 c_2 S_{12} + c_2^2 S_{22}\big) + E(2c_1 S_{11} + 2c_2 S_{12}) = 2c_1 H_{11} + 2c_2 H_{12}$$

Set $\partial E/\partial c_1 = 0$

$$E(2c_1 S_{11} + 2c_2 S_{12}) = 2c_1 H_{11} + 2c_2 H_{12}$$

This can be written

$$(H_{11} - ES_{11})c_1 + (H_{12} - ES_{12})c_2 = 0 \qquad (4.46)$$

The analogous procedure, beginning with Eq. (4.45) and differentiating with respect to c_2 leads to

$$(H_{12} - ES_{12})c_1 + (H_{22} - ES_{22})c_2 = 0 \qquad (4.47)$$

Equation (4.47) can be written as Eq. (4.48):

$$(H_{21} - ES_{21})c_1 + (H_{22} - ES_{22})c_2 = 0 \qquad (4.48)$$

since as shown in Eq. (4.44) $H_{12} = H_{21}$ and $S_{12} = S_{21}$, and the form used in Eq. (4.48) is preferable because it makes it easy to remember the pattern for the two-basis function system examined here and for the generalization (see below) to n basis functions. Equations (4.46) and (4.48) form a system of simultaneous linear equations:

$$
\begin{aligned}
(H_{11} - ES_{11})c_1 + (H_{12} - ES_{12})c_2 = 0 \\
(H_{21} - ES_{21})c_1 + (H_{22} - ES_{22})c_2 = 0
\end{aligned}
\qquad (4.49)
$$

The pattern is that the subscripts correspond to the row and column in which they lie; this is literally true for the matrices and determinants we will consider later, but even for the system of Eq. (4.49) we note that in the first equation ("row 1"), the coefficient of c_1 has the subscripts 11 (row 1, column 1) and the coefficient of c_2 has the subscripts 12 (row 1, column 2), while in the second equation ("row 2") the coefficient of c_1 has the subscripts 21 (row 2, column 1) and the coefficient of c_2 has the subscripts 22 (row 2, column 2).

The system of Eq. (4.49) are called *secular equations*, because of a supposed resemblance to certain equations in astronomy that treat the long-term motion of the planets; from the Latin *saeculum*, a long period of time (not to be confused with secular meaning worldly as opposed to religious, which is from the Latin *secularis*, worldly, temporal). From the secular equations we can find the basis function coefficients c_1 and c_2, and thus the MOs ψ, since the c's and the basis functions ϕ make up the MOs (Eq. (4.41)). The simplest, most elegant and most powerful way to get the coefficients and energies of the MOs from the secular equations is to use matrix algebra (Sect. 4.3.3). The following exposition may seem a little involved, but it must be emphasized that in practice the matrix method is implemented automatically on a computer, to which it is highly suited.

The secular Eq. (4.49) are equivalent to the single matrix equation

$$\begin{pmatrix} H_{11} - ES_{11} & H_{12} - ES_{12} \\ H_{21} - ES_{21} & H_{22} - ES_{22} \end{pmatrix} \begin{pmatrix} c_1 \\ c_2 \end{pmatrix} = \begin{pmatrix} 0 \\ 0 \end{pmatrix} \tag{4.50}$$

Since the *H-ES* matrix is an *H* matrix minus an *ES* matrix, and since the *ES* matrix is the product of an *S* matrix and the scalar *E*, Eq. (4.50) can be written:

$$\left[\begin{pmatrix} H_{11} & H_{12} \\ H_{21} & H_{22} \end{pmatrix} - \begin{pmatrix} S_{11} & S_{12} \\ S_{21} & S_{22} \end{pmatrix} E \right] \begin{pmatrix} c_1 \\ c_2 \end{pmatrix} = \begin{pmatrix} 0 \\ 0 \end{pmatrix} \tag{4.51}$$

which can be more concisely rendered as

$$[\mathbf{H} - \mathbf{S}E]\mathbf{c} = \mathbf{0} \tag{4.52}$$

and Eq. (4.52) can be written

$$\mathbf{Hc} = \mathbf{S}E\mathbf{c} \tag{4.53}$$

H and **S** are square matrices and **c** and **0** are column matrices (Eq. (4.51)), and *E* is a scalar (an ordinary number). We have been developing these equations for a system of two basis functions, so there should be two MOs, each with its own energy and its own pair of *c*'s (Fig. 4.11). We need two energy values and four *c*'s: we want to be able to calculate c_{11} and c_{12} of ψ_1 (MO$_1$, energy level 1) and c_{12} and c_{22} of ψ_2 (MO$_2$, energy level 2); in keeping with common practice the energies of the MOs are designated ε_1 and ε_2. Equation (4.53) can be extended (our simple derivation shortchanges us here) [31] to encompass the four *c*'s and two ε's; the result we want is

$$\mathbf{HC} = \mathbf{SC}\boldsymbol{\varepsilon} \tag{*4.54}$$

The much more elaborate and rigorous derivation in Chap. 5 leads naturally to this. We now have only square matrices; in Eq. (4.53) **c** was a column matrix and *E* was not a matrix, but rather a scalar–an ordinary number. The four matrices are:

$$\mathbf{H} = \begin{pmatrix} H_{11} & H_{12} \\ H_{21} & H_{22} \end{pmatrix}$$
$$\mathbf{C} = \begin{pmatrix} c_{11} & c_{12} \\ c_{21} & c_{22} \end{pmatrix}$$
$$\mathbf{S} = \begin{pmatrix} S_{11} & S_{12} \\ S_{21} & S_{22} \end{pmatrix} \tag{*4.55}$$
$$\boldsymbol{\varepsilon} = \begin{pmatrix} \varepsilon_1 & 0 \\ 0 & \varepsilon_2 \end{pmatrix}$$

The **H** matrix is an energy-elements matrix, the *Fock*[27] *matrix*, whose elements are integrals H_{ij} (Eq. (4.44)). Fock actually developed an elaborate mathematically explicit form of the matrix elements for *ab initio* calculations; we will meet "real" Fock matrices in Chap. 5. For now, we just note that in the simple (and extended) Hückel methods as an *ad hoc* prescription, at most two electrons, paired, are allowed in each MO. Each H_{ij} represents some kind of energy term, since $\hat{H}$ is an energy operator (Sect. 4.3.3). The meaning of the H_{ij}'s is discussed later in this section.

The **C** matrix is the *coefficients matrix*, whose elements are the weighting factors c_{ij} that determine to what extent each basis function ϕ (roughly, each atomic orbital on an atom) contributes to each MO ψ. Thus c_{11} is the coefficient of ϕ_1 in ψ_1, c_{21} the coefficient of ϕ_2 in ψ_1, etc., with the first subscript indicating the basis function and the second subscript the MO (Fig. 4.11). In each column of **C** the c's belong to the same MO.

The **S** matrix is the *overlap matrix*, whose elements are *overlap integrals S_{ij}* which are a measure of how well pairs of basis functions (roughly, atomic orbitals) overlap. Perfect overlap, between identical functions on the same atom, corresponds to $S_{ij} = 1$, while zero overlap, between different functions on the same atom or well-separated functions on different atoms, corresponds to $S_{ij} = 0$.

The diagonal $\boldsymbol{\varepsilon}$ matrix is an energy-levels matrix, whose diagonal elements are MO energy levels ψ_i, corresponding to the MOs ε_i. Each ε_i is ideally the negative of the energy needed to remove an electron from that orbital, i.e. the negative of the ionization energy for that orbital. Thus it is ideally the energy of an electron attracted to the nuclei and repelled by the other electrons, relative to the energy of that electron and the corresponding ionized molecule, infinitely separated from one another. This is seen by the fact that photoelectron spectra correlate well with the energies of the occupied orbitals, in more elaborate (ab initio) calculations [26]. In simple Hückel calculations, however, the quantitative correlation is largely lost.

Now suppose that the basis functions ϕ had these properties (the H and S integrals, involving ϕ, are defined in Eq. (4.44)):

$$\begin{aligned} S_{11} &= 1 \\ S_{12} &= S_{21} = 0 \\ S_{22} &= 1 \end{aligned} \tag{4.56}$$

More succinctly, suppose that

$$S_{ij} = \delta_{ij} \tag{4.57}$$

---

[27] Vladimer Fock, born St. Petersburg, 1898. Ph.D. Petrograd University, 1934. Professor Leningrad University, also worked at various institutes in Moscow. Worked on quantum mechanics and relativity, e.g. the Klein-Fock equation for particles with spin in an electromagnetic field. Died Leningrad, 1974.

a twisted allyl species

* = +,   ·or –
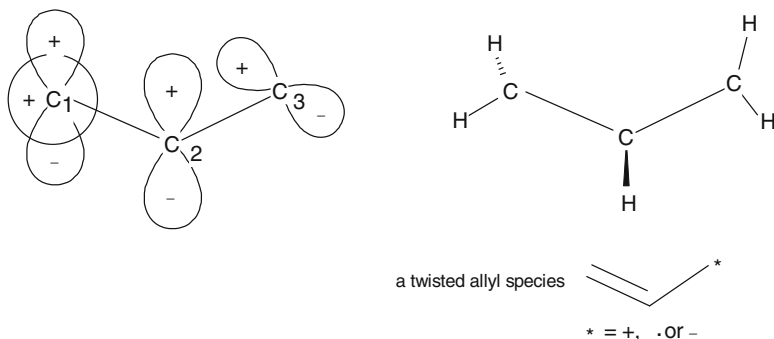
Fig. 4.12 We cannot simply choose a set of orthonormal basis functions, because in a typical molecule many pairs of basis functions will not be orthogonal, i.e will not have zero overlap. In the allyl species shown, the $2s$ and the $2p$ functions (i.e. AOs) on C_1 are orthogonal (the + part of the p orbital cancels the – part in overlap with the s orbital; in general AOs on the same atom are orthogonal), and the $2p$ functions on C_2 and C_3 are also orthogonal, if their axes are at right angles. However, the $C_1(2s)/C_2(2p)$ and the $C_1(2p)/C_2(2p)$ pairs are not orthogonal

where δ_{ij} is the Kronecker delta (Leopold Kronecker, German mathematician, ca. 1860) which has the property of being 1 or 0 depending on whether i and j are the same or different. Then the **S** matrix (Eq. (4.55)) would be

$$\mathbf{S} = \begin{pmatrix} 1 & 0 \\ 0 & 1 \end{pmatrix} \tag{4.58}$$

Since this is a unit matrix Eq. (4.54) would become

$$\mathbf{HC} = \mathbf{C\varepsilon} \tag{4.59}$$

and by multiplying on the right by the inverse of **C** we get

$$\mathbf{H} = \mathbf{C\varepsilon C^{-1}} \tag{*4.60}$$

So from the definition of matrix diagonalization, diagonalization of the **H** matrix will give the **C** and the **ε** matrices, i.e. it will give the coefficients c and the MO energies ε (Eq. (4.55)), if $S_{ij} = \delta_{ij}$ (Eq. (4.57)). This is a big if, and in fact it is not true. $S_{ij} = \delta_{ij}$ would mean that the basis functions are both orthogonal and normalized, i.e. orthonormal. *Orthogonal* atomic (or molecular) orbitals or functions ϕ have zero net overlap (Fig. 4.12), corresponding to $\int \phi_i \phi_j dv = 0$. A *normalized* orbital or function ϕ has the property $\int \phi\phi dv = 1$. We can indeed use a set of normalized basis functions: a suitable normalization constant k applied to an unnormalized basis function ϕ' will ensure normalization $(\phi = k\phi')$. However, we cannot simply choose a set of *orthogonal* atom-centered basis functions, because orthogonality implies zero

overlap between the two functions in question, and in a molecule the overlap between pairs of basis functions will depend on the geometry of the molecule (Fig. 4.12). (However, as we will see later, the basis functions can be manipulated mathematically to give *combinations* of the original functions which *are* orthonormal).

The assumption of basis function orthonormality is a drastic approximation, but it greatly simplifies the Hückel method, and in the present context it enables us to reduce Eq. (4.54) to Eq. (4.59), and thus to obtain the coefficients and energy levels by diagonalizing the Fock matrix without further ado. Later we will see that in the absence of the orthogonality assumption the set of basis functions can be mathematically transformed so that a *modified* Fock matrix can be diagonalized; in the simple Hückel method we are spared this transformation. In the matrix approach to the Hückel method, then, we must diagonalize the Fock matrix **H**; to do this we have to assign numbers to the matrix elements H_{ij}, so that the computer algorithm will have something to work with. This brings us to other simplifying assumptions of the SHM, concerning the H_{ij}.

In the SHM the energy integrals H_{ij} are approximated as just three quantities (the units are of energy per "amount", e.g., kJ mol^{-1}):

α, the *coulomb integral*

$$\int \phi_i \hat{H} \phi_i dv = H_{ii} = \alpha \quad \text{i.e basis functions on the same atom,} \qquad (*4.61a)$$

β, the *bond integral* or *resonance integral*

$$\int \phi_i \hat{H} \phi_j dv = H_{ij} = \int \phi_j \hat{H} \phi_i dv = H_{ij} = \beta \qquad (*4.61b)$$

for basis functions on adjacent atoms,
and finally

$$\int \phi_i \hat{H} \phi_j dv = H_{ij} = \int \phi_j \hat{H} \phi_i dv = H_{ji} = 0 \qquad (*4.61c)$$

for basis functions neither on the same or on adjacent atoms.

To give these approximations some physical significance, we must realize that in quantum mechanical calculations the zero of energy is normally taken as corresponding to infinite separation of the particles of a system. In the simplest view, α, the coulomb integral, is the energy of the molecule relative to a zero of energy taken as the electron and basis function (i.e. AO; in the simple Hückel method, ϕ is usually a carbon p AO) at infinite separation. Since the energy of the system actually *decreases* as the electron falls from infinity into the orbital, α is negative (Fig. 4.13). The negative of α, in this view, is the ionization energy (a positive quantity) of the orbital (the ionization energy of the orbital is defined as the energy needed to remove an electron from the orbital to an infinite distance away).

The quantity β, the bond integral or resonance integral is, in the simplest view, the energy of an electron in the overlap region (roughly, a two-center MO) of
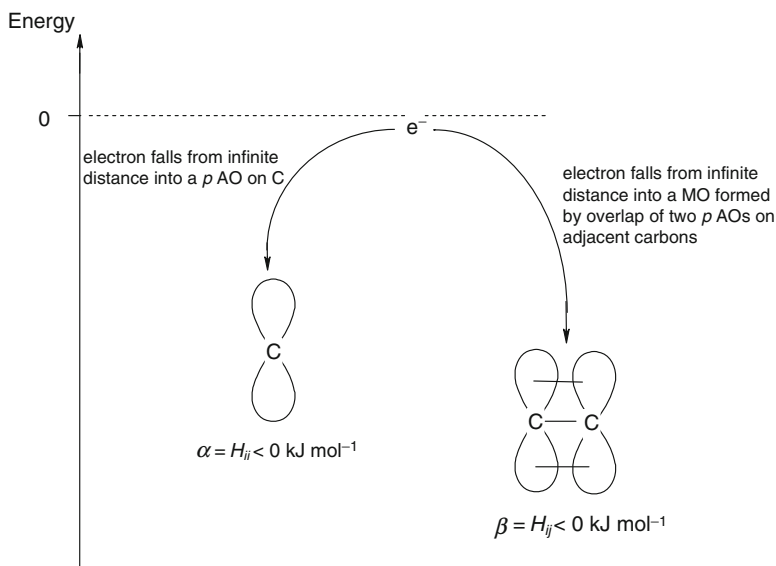
Fig. 4.13 The coulomb integral α is most simply (but not too accurately) viewed as the energy of an electron in a carbon $2p$ orbital, relative to its energy an infinite distance away. The bond integral (resonance integral) β is most simply (but not too accurately) viewed as the energy of an electron in an MO formed by adjacent $2p$ orbitals, relative to its energy an infinite distance away

adjacent p orbitals relative to a zero of energy taken as the electron and two-center MO at infinite separation. Like α, β is a negative energy quantity. A rough, naive estimate of the value of β would be the average of the ionization energies (a positive quantity) of the two adjacent AOs, multiplied by some fraction to allow for the fact that the two orbitals do not coincide but are actually separated. These views of α and β are oversimplifications [31].

We derived the 2×2 matrices of Eq. (4.55) starting with a two-orbital system. These results can be generalized to n orbitals:

$$\mathbf{H} = \begin{pmatrix} H_{11} & H_{12} & \cdots & H_{1n} \\ H_{21} & H_{22} & \cdots & H_{2n} \\ \vdots & \vdots & \cdots & \vdots \\ H_{n1} & H_{n2} & \cdots & H_{nn} \end{pmatrix} \qquad (4.62)$$

The H elements of Eq. (4.62) become α, β, or 0 according to the rules of Eq. (4.61). This will be clear from the examples in Fig. 4.14.

The computer algorithms for matrix diagonalization use some version of the Jacobi rotation method [37], which proceeds by successive numerical approximations (mathematics textbooks describe a diagonalization method based on expanding the determinant corresponding to the matrix; this is not used in computational chemistry). Therefore, to diagonalize our Fock matrices we need numbers in place of α and β. In methods more advanced than the SHM, like the extended

a

b

* = + or · or −

c
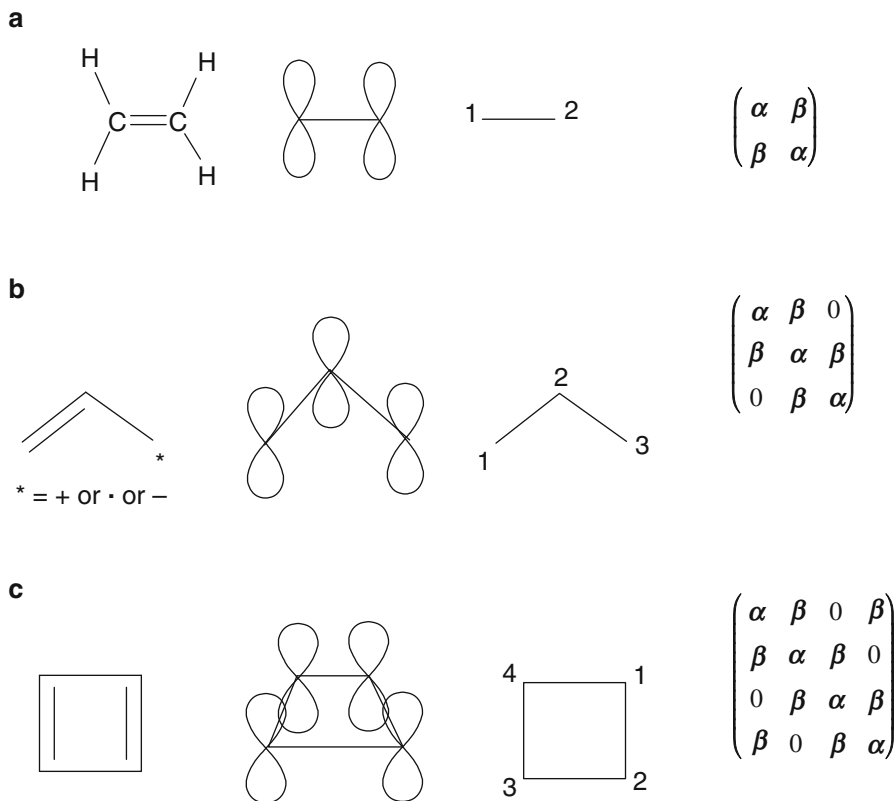
Fig. 4.14 Some conjugated molecules, their p orbital arrays, simplified representations of the molecules, and their simple Hückel Fock matrices. Same-atom interactions are α adjacent-atom interactions are β, and all other interactions are 0. To diagonalize the matrices, we use $\alpha = 0$ and $\beta = -1$

Hückel method (EHM), other semiempirical methods, and ab initio methods, the H_{ij} integrals are calculated to give numerical (in energy units) values. In the SHM we simply use energy values in $|\beta|$ units relative to α (recall that β is a negative quantity: Fig. 4.13). The matrix of Fig. 4.14a then becomes

$$\mathbf{H} = \begin{pmatrix} \alpha & \beta \\ \beta & \alpha \end{pmatrix} = \begin{pmatrix} 0 & -1 \\ -1 & 0 \end{pmatrix} \tag{4.63}$$

An electron in an MO represented by a 1,2-type interaction is lower in energy than one in a p orbital (1,1-type interaction) by one $|\beta|$ energy unit. Similarly, the **H** matrix of Fig. 4.14b becomes

$$\mathbf{H} = \begin{pmatrix} 0 & -1 & 0 \\ -1 & 0 & -1 \\ 0 & -1 & 0 \end{pmatrix} \tag{4.64}$$

and the **H** matrix of Fig. 4.14c becomes

$$\mathbf{H} = \begin{pmatrix} 0 & -1 & 0 & -1 \\ -1 & 0 & -1 & 0 \\ 0 & -1 & 0 & -1 \\ -1 & 0 & -1 & 0 \end{pmatrix} \tag{4.65}$$

The $\mathbf{H}$ matrices can be written down simply by setting all i,i-type interactions equal to 0, and all i,j-type interactions equal to -1 where i and j refer to atoms that are bonded together, and equal to 0 when i and j refer to atoms that are not bonded together.

Diagonalization of the two-basis-function matrix of Eq. (4.63) gives

$$\mathbf{H} = \begin{pmatrix} 0 & -1 \\ -1 & 0 \end{pmatrix} = \underbrace{\begin{pmatrix} 0.707 & 0.707 \\ 0.707 & -0.707 \end{pmatrix}}_{\mathbf{C}} \underbrace{\begin{pmatrix} -1 & 0 \\ 0 & 1 \end{pmatrix}}_{\boldsymbol{\varepsilon}} \underbrace{\begin{pmatrix} 0.707 & 0.707 \\ 0.707 & -0.707 \end{pmatrix}}_{\mathbf{C}^{-1}} \tag{4.66}$$

Comparing Eq. (4.66) with Eq. (4.60), we see that we have obtained the matrices we want: the coefficients matrix $\mathbf{C}$ and the MO energy levels matrix ε. The columns of $\mathbf{C}$ are eigenvectors, and the diagonal elements of $\boldsymbol{\varepsilon}$ are eigenvalues; cf. Eq. (4.38) and the associated discussion of eigenfunctions and eigenvalues. The result of Eq. (4.66) is readily checked by actually multiplying the matrices (multiplication here is aided by knowing that an analytical rather than numerical diagonalization shows that ± 0.707 are approximations to $1/\sqrt{2}$). Note that $\mathbf{C}\mathbf{C}^{-1} = \mathbf{1}$, and that $\mathbf{C}^{-1}$ is the transpose of $\mathbf{C}$. The first eigenvector of $\mathbf{C}$, the left-hand column, corresponds to the first eigenvalue of $\boldsymbol{\varepsilon}$, the top left element; the second eigenvector corresponds to the second eigenvalue; in Eqs. (4.67) the "equivalent to hat" symbol means "corresponds to". The individual eigenvectors, $\mathbf{v}_1$ and $\mathbf{v}_2$, are column matrices:

$$\underbrace{\begin{pmatrix} 0.707 \\ 0.707 \end{pmatrix}}_{\mathbf{v}_1} \hat{=} -1 \qquad \text{and} \qquad \underbrace{\begin{pmatrix} 0.707 \\ -0.707 \end{pmatrix}}_{\mathbf{v}_2} \hat{=} 1 \tag{4.67}$$

Figure 4.15 shows a common way of depicting the results for this two-orbital calculation. Since the coefficients are weighting factors for the contributions of the basis functions to the MOs (Fig. 4.11 and associated discussion), the c's of eigenvector $\mathbf{v}_1$ combine with the basis functions to give MO_1 (ψ_1) and the c's of eigenvector $\mathbf{v}_2$ combine with these same basis functions to give MO_2 (ψ_2). MOs below α are bonding and MOs above α are antibonding. The ε matrix translates into an energy level diagram with ψ_1 of energy $\alpha + \beta$ and ψ_2 of energy $\alpha - \beta$, i.e. the MOs lie one $|\beta|$ unit below and one $|\beta|$ above the nonbonding α level. Since β, like α, is negative, the $\alpha + \beta$ and $\alpha - \beta$ levels are of lower and higher energy, respectively, than the nonbonding α level.

Fig. 4.15 The π molecular orbitals and π energy levels for a two-p-orbital system in the simple Hückel method. The MOs are composed of the basis functions (two p AOs) and the eigenvectors, while the energies of the MOs follow from the eigenvalues (Eq. (4.66)). The paired arrows represent a pair of electrons of opposite spin (in the electronic ground state of the neutral ethene molecule ψ_1 is occupied and ψ_2 is empty)

Diagonalization of the three-basis function matrix of Eq. (4.64) gives

$$
\begin{pmatrix} 0 & -1 & 0 \\ -1 & 0 & -1 \\ 0 & -1 & 0 \end{pmatrix} =
$$

$$
\underbrace{\begin{pmatrix} 0.500 & 0.707 & 0.500 \\ 0.707 & 0 & -0.707 \\ 0.500 & -0.707 & 0.500 \end{pmatrix}}_{\substack{\mathbf{v}_1 \quad \mathbf{v}_2 \quad \mathbf{v}_3 \\ \mathbf{C}}}
\underbrace{\begin{pmatrix} -1.414 & 0 & 0 \\ 0 & 0 & 0 \\ 0 & 0 & 1.414 \end{pmatrix}}_{\substack{\varepsilon_1, \quad 0, \quad 0 \\ 0, \quad \varepsilon_2, \quad 0 \\ 0, \quad 0, \quad \varepsilon_3 \\ \boldsymbol{\varepsilon}}}
\underbrace{\begin{pmatrix} 0.500 & 0.707 & 0.500 \\ 0.707 & 0 & -0.707 \\ 0.500 & -0.707 & 0.500 \end{pmatrix}}_{\mathbf{C}^{-1}}
$$

$$(4.68)$$

The energy levels and MOs corresponding to these results are shown in Fig. 4.16.

energy

$\psi_3 = 0.500\ \phi_1 - 0.707\ \phi_2 + 500\ \phi_3$

$\varepsilon = 1.414$ antibonding MO

$\alpha - \beta$

α

$\psi_2 = 0.700\ \phi_1 + 0.000\ \phi_2 - 0.700\ \phi_3$

$\varepsilon = 0$ nonbonding MO

$\alpha + \beta$

$\psi_1 = 0.500\ \phi_1 + 0.707\ \phi_2 + 0.500\ \phi_3$

$\varepsilon = -1.414$ bonding MO
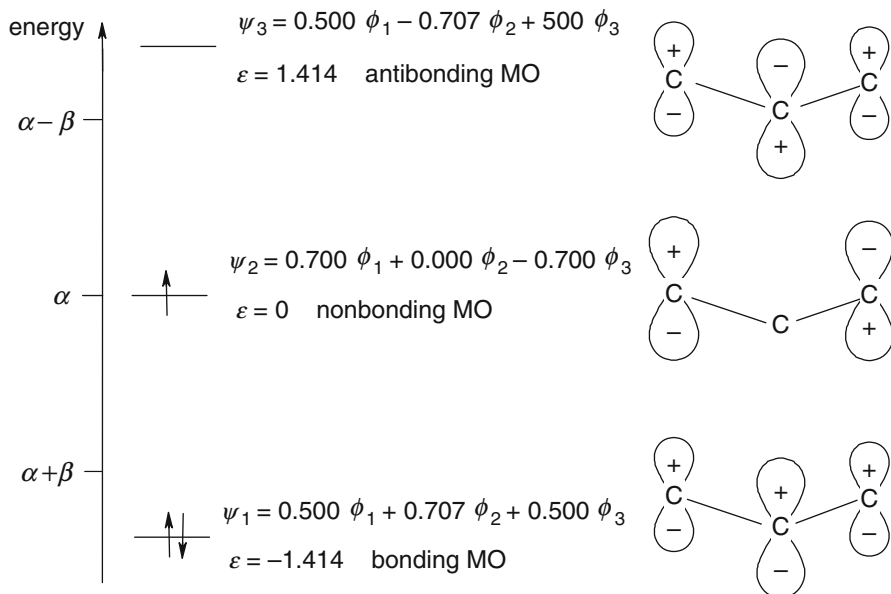
Fig. 4.16 The π molecular orbitals and π energy levels for an acyclic three-p-orbital system in the simple Hückel method. The MOs are composed of the basis functions (three p AOs) and the eigenvectors (the c's), while the energies of the MOs follow from the eigenvalues (Eq. (4.68)). In the drawings of the MOs, the relative sizes of the AOs in each MO suggest the relative contribution of each AO to that MO. This diagram is for the propenyl radical. The *paired arrows* represent a pair of electrons of opposite spin, in the fully-occupied lowest MO, ψ_1, and the single arrow represents an unpaired electron in the nonbonding MO, ψ_2; the highest π MO, ψ_3, is empty in the radical

Diagonalization of the four-basis-function matrix of Eq. (4.65) gives

$$
\begin{pmatrix}
0 & -1 & 0 & -1 \\
-1 & 0 & -1 & 0 \\
0 & -1 & 0 & -1 \\
-1 & 0 & -1 & 0
\end{pmatrix} =
$$

$$
\begin{pmatrix}
0.500 & 0.500 & 0.500 & 0.500 \\
0.500 & -0.500 & 0.500 & -0.500 \\
0.500 & -0.500 & -0.500 & 0.500 \\
0.500 & 0.500 & -0.500 & -0.500
\end{pmatrix}
\begin{pmatrix}
-2 & 0 & 0 & 0 \\
0 & 0 & 0 & 0 \\
0 & 0 & 0 & 0 \\
0 & 0 & 0 & 2
\end{pmatrix}
\begin{pmatrix}
0.500 & 0.500 & 0.500 & 0.500 \\
0.500 & -0.500 & -0.500 & 0.500 \\
0.500 & 0.500 & -0.500 & -0.500 \\
0.500 & -0.500 & 0.500 & -0.500
\end{pmatrix}
$$

$$
\begin{matrix}
& & \varepsilon_1 & 0 & 0 & 0 \\
& & 0 & \varepsilon_2 & 0 & 0 \\
\mathbf{v}_1 \quad \mathbf{v}_2 \quad \mathbf{v}_3 \quad \mathbf{v}_4 & & 0 & 0 & \varepsilon_3 & 0 \\
& & 0 & 0 & 0 & \varepsilon_4
\end{matrix}
$$

$$\mathbf{C} \qquad\qquad\qquad \boldsymbol{\varepsilon} \qquad\qquad\qquad \mathbf{C}^{-1}$$

(4.69)

energy

$\psi_4 = 0.500\ \phi_1 - 0.500\ \phi_2 + 0.500\ \phi_3 - 0.500\ \phi_4$

$\alpha - 2\beta$ ——— $\varepsilon = 2$ antibonding MO

$\alpha - \beta$

$\psi_3 = 0.500\ \phi_1 + 0.500\ \phi_2 - 0.500\ \phi_3 - 0.500\ \phi_4$

α nonbonding MOs

$\varepsilon = 0$ $\varepsilon = 0$

$\psi_2 = 0.500\ \phi_1 - 0.500\ \phi_2 - 0.500\ \phi_3 + 0.500\ \phi_4$

$\alpha + \beta$

$\psi_1 = 0.500\ \phi_1 + 0.500\ \phi_2 + 0.500\ \phi_3 + 0.500\ \phi_4$

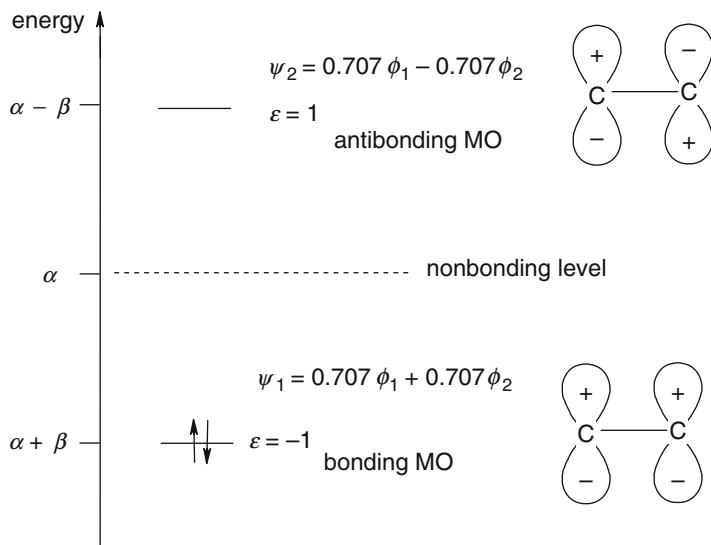$\alpha + 2\beta$ $\varepsilon = -2$ bonding MO
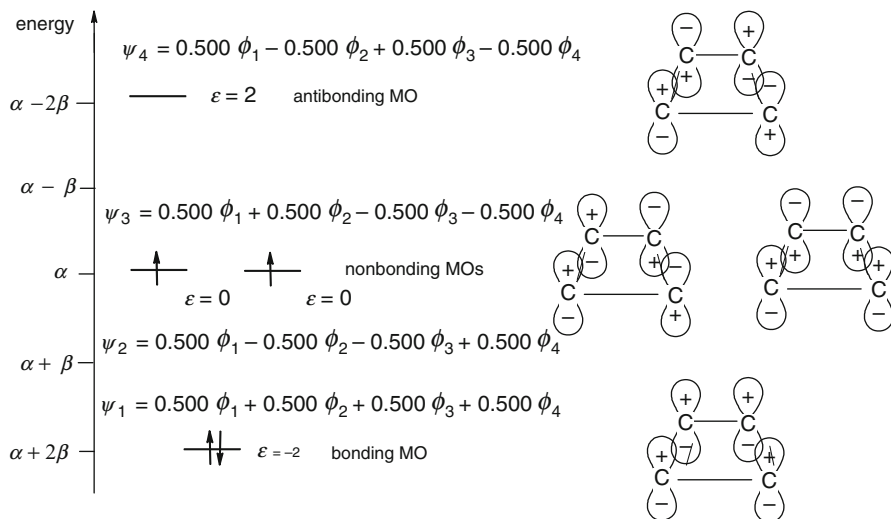
Fig. 4.17 The π molecular orbitals and π energy levels for a cyclic four-p-orbital system in the simple Hückel method. The MOs are composed of the basis functions (four p AOs) and the eigenvectors, while the energies of the MOs follow from the eigenvalues (Eq. (4.69)). This particular diagram is for the square cyclobutadiene molecule. The paired arrows represent a pair of electrons of opposite spin, in the fully-occupied lowest MO, ψ_1, and the single arrows represents unpaired electrons of the same spin, one in each of the two nonbonding MOs, ψ_2 and ψ_3; the highest π MO, ψ_4, is empty in the neutral molecule

The energy levels and MOs from these results are shown in Fig. 4.17. Note that all these matrix diagonalizations yield orthonormal eigenvectors: $\mathbf{v}_i \cdot \mathbf{v}_i = 1$ and $\mathbf{v}_i \cdot \mathbf{v}_j = 0$, as required the fact that the Fock matrices are symmetric (see the discussion of matrix diagonalization in Sect. 4.3.3).

4.3.5   The Simple Hückel Method–Applications

Applications of the SHM are discussed in great detail in several books [21]; here we will deal only with those applications which are needed to appreciate the utility of the method and to smooth the way for the discussion of certain topics (like bond orders and atomic charges) in later chapters. We will discuss: the nodal properties of the MOs; stability as indicated by energy levels and aromaticity (the $4n + 2$ rule); resonance energies; and bond orders and atomic charges.

4.3.5.1   The Nodal Properties of the MOs

A node of an MO is a plane at which, as we proceed along the sequence of basis functions, the sign of the wavefunction changes (Figs. 4.15, 4.16 and 4.17). For a

given molecule, the number of nodes in the π orbitals increases with the energy. In the two-orbital system (Fig. 4.15), ψ_1 has zero nodes and ψ_2 has one node. In the three-orbital system (Fig. 4.16), ψ_1, ψ_2 and ψ_3 have zero, one and two nodes, respectively. In the cyclic four-orbital system (Fig. 4.17), ψ_1 has zero nodes, ψ_2 and ψ_3, which are degenerate (of the same energy) each have one node (one nodal plane), and ψ_4 has two nodes. We can take a node as lying midway between the sign-change atoms. In a given molecule, the energy of the MOs increases with the number of nodes. The nodal properties of the SHM π orbitals form the basis of one of the simplest ways of understanding the predictions of the Woodward-Hoffmann orbital symmetry rules [38]. For example, the thermal conrotatory and disrotatory ring closure/opening of polyenes can be rationalized very simply in terms of the symmetry of the highest occupied π MO of the open-chain species. That the highest π MO should dominate the course of this kind of reaction is indicated by more detailed considerations (including extended Hückel calculations) [38]. Figure 4.18 shows the situation for the ring closure of a 1,3-butadiene to a cyclobutene. The phase $(+\text{or}-)$ of the π HOMO (ψ_2) at the end carbons (the atoms that bond) is opposite on each face, because this orbital has one node in the middle of the C_4 chain. You can see this by sketching the MO as the four AOs contributing to it, or even–remembering the node–drawing just the end AOs. For the electrons in ψ_2 to bond, the end groups must rotate in the same sense (*conrotation*) to bring orbital lobes of the same phase together. Remember that plus and minus phase has nothing to do with electric charge, but is a consequence of the wave nature of electrons (Sect. 4.2.6): two electron waves can reinforce one another and form a bonding pair if they are "vibrating in phase"; an out-of-phase interaction represents an antibonding situation. Rotation in opposite senses (*disrotation*) would bring opposite-phase lobes together, an antibonding situation. The mechanism of the reverse reaction is simply the forward mechanism in reverse, so the fact that the thermodynamically favored process is the *ring-opening* of a cyclobutene simply means that the cyclobutene shown would open to the butadiene shown on heating. Photochemical processes can also be accommodated by the Woodward-Hoffmann orbital symmetry rules if we realize that absorption of a photon creates an electronically excited molecule in which the previous lowest unoccupied MO (LUMO) is now the HOMO. For more about orbital symmetry and chemical reactions see e.g. the book by Woodward and Hoffmann [38].

4.3.5.2   Stability as Indicated by Energy Levels, and Aromaticity

The MO energy levels obtained from an SHM calculation must be filled with electrons according to the species under consideration. For example, the neutral ethene molecule has two π electrons, so the diagrams of Fig. 4.19a (cf. 4.15) with one, two and three π electrons, would refer to the cation, the neutral and the anion. We might expect the neutral, with its bonding π orbital ψ_1 full and its antibonding π orbital ψ_2 empty, to be resistant to oxidation (which would require removing
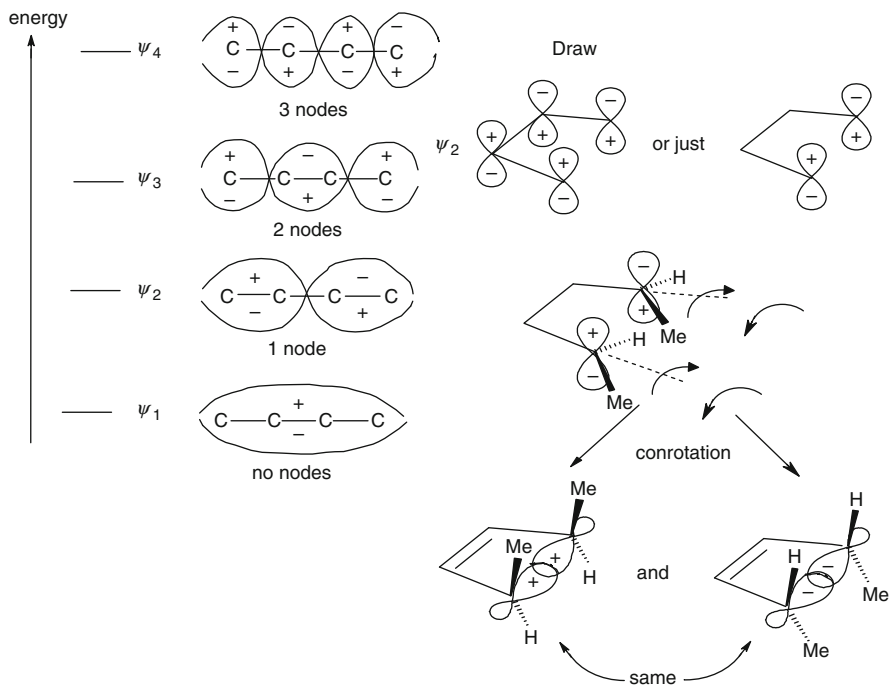
Fig. 4.18 The stereochemistry of many reactions is easily predicted from the symmetry of molecular orbitals, usually the highest occupied π MO (π HOMO). In the ring closure of 1,3-butadiene to cyclobutene the phase (+ or −) of the HOMO (ψ_2) at the end carbons (the atoms that bond) is such that closure must occur in a conrotatory sense, giving a definite stereochemical outcome. In the example above there is only one product. The *reverse* process is actually thermodynamically favored, and the *cis* dimethyl cyclobutene opens to the *cis*, *trans* diene. No attempt is made here to show quantitatively the positions of the energy levels or to size the AOs according to their contributions to the MOs

electronic charge from the low-energy ψ_1) and to reduction (which would require adding electronic charge to the high-energy ψ_2).

The propenyl (allyl) system has two, three or four π electrons, depending on whether we are considering the cation, radical or anion (Fig. 4.19b; cf. Fig. 4.16). The cation might be expected to be resistant to oxidation, which requires removing an electron from a low-lying π orbital (ψ_1) and to be moderately readily reduced, as this involves adding an electron to the nonbonding π orbital ψ_2, a process that should not be strongly favorable or unfavorable. The radical should be easier to oxidize than the cation, for this requires removing an electron from a nonbonding, rather than a lower-lying bonding, orbital, and the ease of reduction of the radical
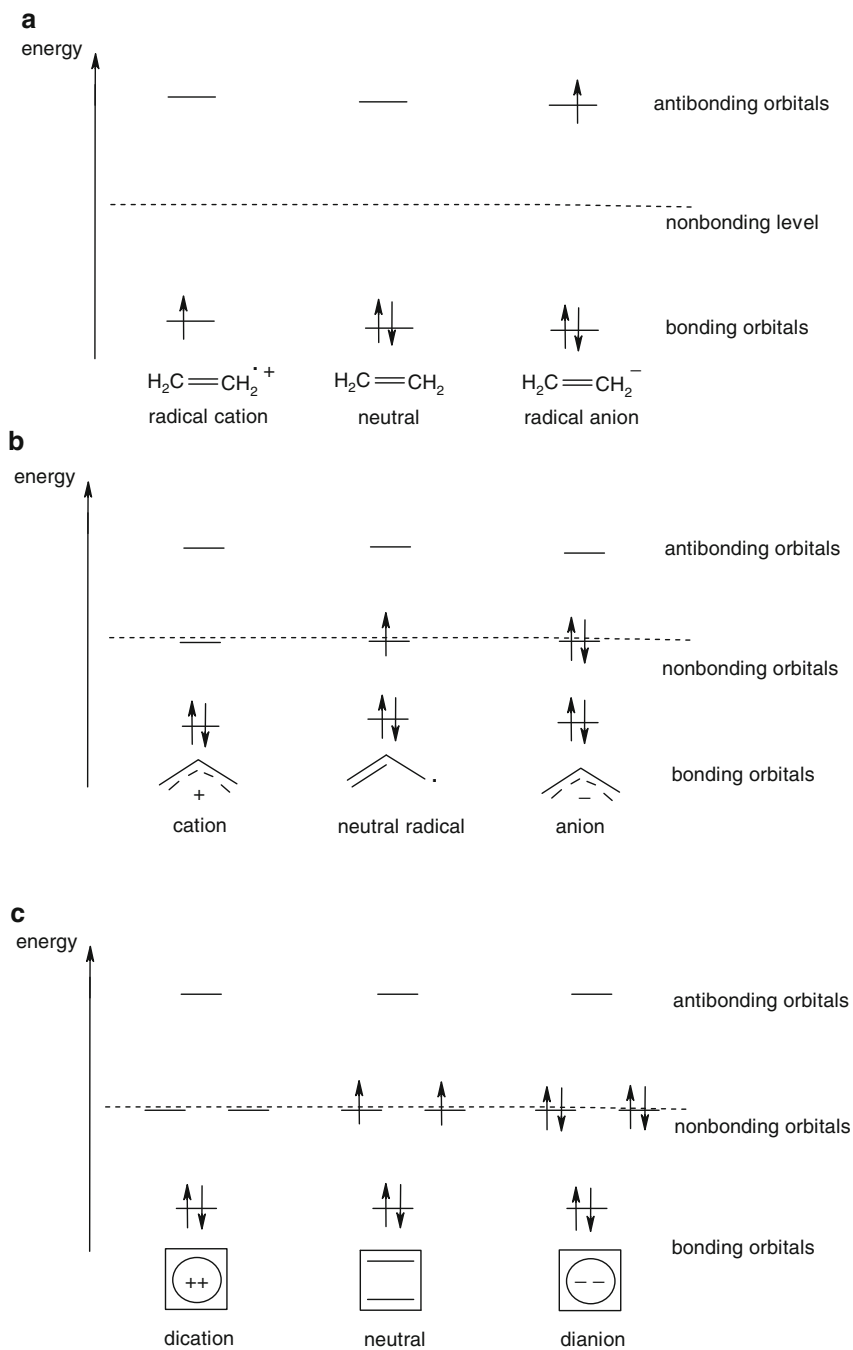
Fig. 4.19 Filling π MOs with electrons
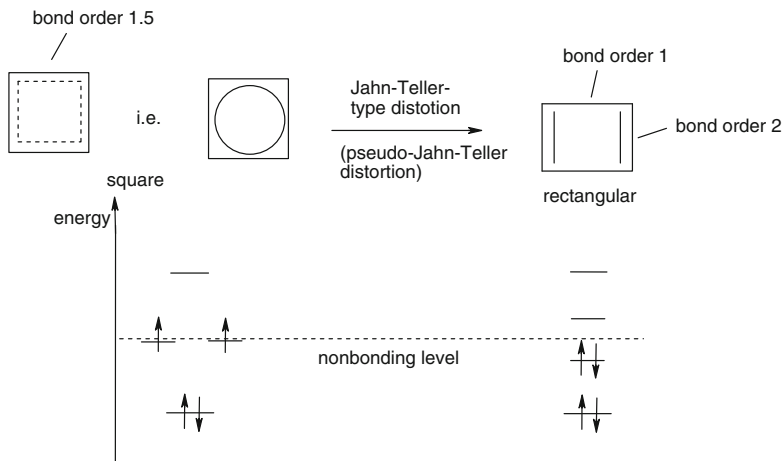
Fig. 4.20 Cyclic systems with degenerate energy levels tend to undergo a geometric distortion to remove the degeneracy, a consequence of the Jahn-Teller theorem

should be roughly comparable to that of the cation, as both can accommodate an electron in a nonbonding orbital. The anion should be oxidized with an ease comparable to that of the radical (removal of an electron from the nonbonding ψ_2), but be harder to reduce (addition of an electron to the antibonding ψ_3).

The cyclobutadiene system (Fig. 4.19c; cf. Fig. 4.17) can be envisaged with, amongst others, two (the dication), four (the neutral molecule) and six π (the dianion) electrons. The predictions one might make for these the behavior of these three species toward redox reactions are comparable to those just outlined for the propenyl cation, radical and anion, respectively (note the occupancy of bonding, nonbonding and antibonding orbitals). The neutral cyclobutadiene molecule is, however, predicted by the SHM to have an unusual electronic arrangement for a diene: in filling the π orbitals, from the lowest-energy one up, one puts electrons of the same spin into the degenerate ψ_2 and ψ_3 in accordance with Hund's rule of maximum multiplicity. Thus the SHM predicts that cyclobutadiene will be a diradical, with two unpaired electrons of like spin. Actually, more advanced calculations [39] indicate, and experiment confirms, that cyclobutadiene is a singlet molecule with two single and two double C/C bonds. A square cyclobutadiene diradical with four 1.5 C/C bonds would distort to a rectangular, closed-shell (i.e. no unpaired electrons) molecule with two single and two double bonds (Fig. 4.20). This could have been predicted by augmenting the SHM result with a knowledge of the phenomenon known as the Jahn-Teller effect [40]: cyclic systems (and certain others) with an odd number of electrons in degenerate (equal-energy) MOs will distort to remove the degeneracy.

What general pattern of molecular orbitals emerges from the SHM? Acyclic π systems (ethene, the propenyl system, 1,3-butadiene, etc.), have MOs distributed singly and evenly on each side of the nonbonding level; the odd-AO systems also have one nonbonding MO (Fig. 4.21). Cyclic π systems (the cyclopropenyl system,
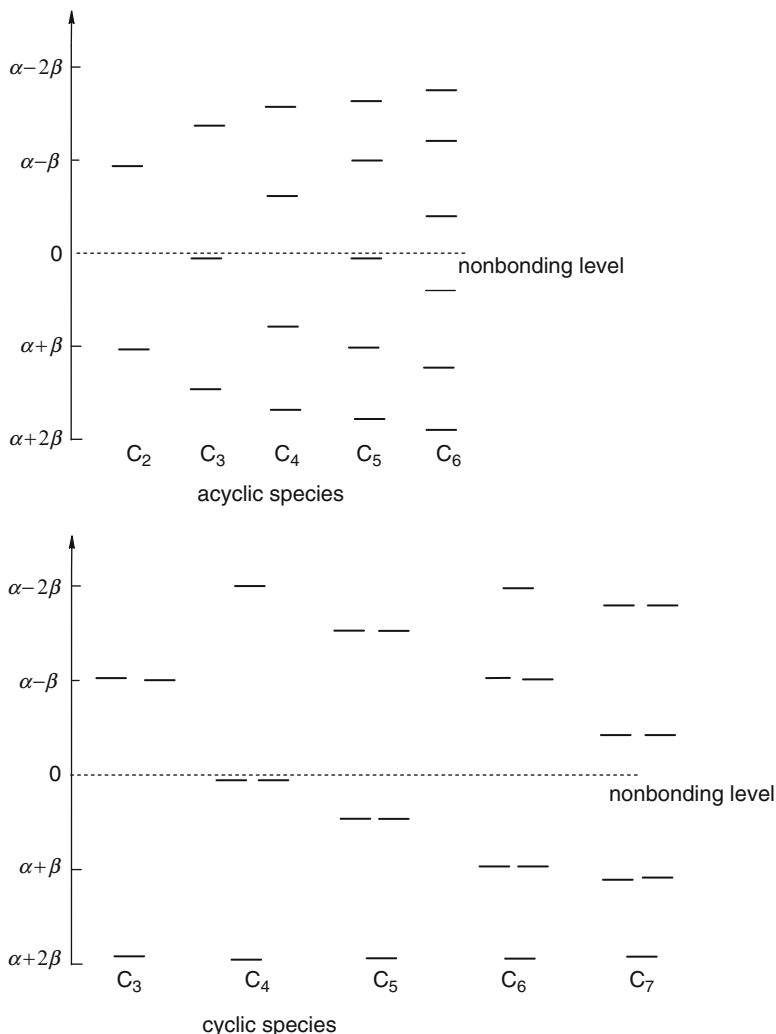
Fig. 4.21 The MO pattern for acyclic and cyclic π systems, as predicted by the simple Hückel method

cyclobutadiene, the cyclopentadienyl system, benzene, etc.) have a lowest MO and pairs of degenerate MOs, ending with one highest or a pair of highest MOs, depending on whether the number of MOs is even or odd. The total number of MOs is always equal to the number of basis functions, which in the SHM is, for organic polyenes, the number of p orbitals (Fig. 4.21). The pattern for monocyclic systems can be predicted qualitatively simply by sketching the polygon, with one vertex down, inside a circle (Fig. 4.22). If the circle is of radius $2 |\beta|$ the energies can
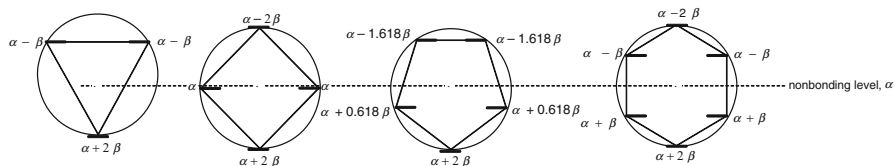
Fig. 4.22 A useful mnemonic for getting the simple Hückel method pattern for cyclic π systems. Setting the radius of the circle at $2|\beta|$, the energy separations from the nonbonding level can even be calculated by trigonometry
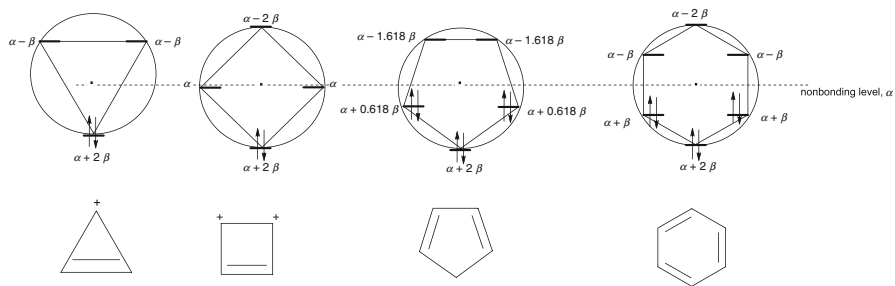
Fig. 4.23 Hückel's rule says that cyclic π systems with $4n+2$ π electrons ($n = 0, 1, 2, \ldots$; $4n+2 = 2, 6, 10, \ldots$) should be especially stable, since they have all bonding levels full and all antibonding levels empty. The special stability is usually equated with aromaticity. Shown here are the cyclopropenyl cation, the cyclobutadiene dication, the cyclopentadienyl anion, and benzene; *formal* structures are given for these species-the actual molecules do not have single and double bonds, but rather electron delocalization makes all C/C bonds the same

even be calculated by trigonometry [41]. It follows from this pattern that cyclic species (not necessarily neutral) with 2, 6, 10, ... π electrons have filled δ MOs and might be expected to show particular stability, analogously to the filled AOs of the unreactive noble gases (Fig. 4.23). The archetype of such molecules is, of course, benzene, and the stability is associated with the general collection of properties called aromaticity [17]. These results, which were first perceived by Hückel [19] (series of papers 1931–1937), are summarized in a rule called the $4n + 2$ rule or Hückel's rule, although the $4n + 2$ formulation was evidently actually due to Doering and Knox (1954) [42]. This says that cyclic arrays of sp^2-hybridized atoms with $4n + 2$ π electrons are characteristic of aromatic molecules; the canonical aromatic molecule benzene with six π electrons corresponds to $n = 1$. For neutral molecules with formally fully conjugated perimeters this amounts to saying that those with an odd number of C/C double bonds are aromatic and those with an even number are antiaromatic (see *resonance energies*, below).

Hückel's rule has been abundantly verified [17] notwithstanding the fact that the SHM, when applied without regard to considerations like the Jahn-Teller effect (see above) incorrectly predicts $4n$ species like cyclobutadiene to be triplet diradicals. The Hückel rule also applies to ions; for example, the cyclopropenyl with system two π electrons, the cyclopropenyl cation, corresponds to $n = 0$, and is strongly

aromatic. Other aromatic species are the cyclopentadienyl anion (six π electrons, $n = 1$; Hückel predicted the enhanced acidity of cyclopentadiene) and the cycloheptatrienyl cation. Only reasonably planar species can be expected to provide the AO overlap need for cyclic electron delocalization and aromaticity, and care is needed in applying the rule. Electron delocalization and aromaticity within the SHM have fairly recently been revisited [43].

4.3.5.3   Resonance Energies

The SHM permits the calculation of a kind of stabilizing energy, or, more logically stated, an energy that reflects the stability in some sense of molecules. This energy is calculated by comparing the total electronic energy of the molecule in question with that of a reference compound, as shown below for the propenyl systems, cyclobutadiene, and the cyclobutadiene dication.

The propenyl cation, Fig. 4.19b; cf. Fig. 4.16. If we take the total π electronic energy of a molecule to be simply the number of electrons in a π MO times the energy level of the orbital, summed over occupied orbitals (a gross approximation, as it ignores interelectronic repulsion), then for the propenyl cation

$$E_\pi(\text{prop. cation}) = 2(\alpha + 1.414\beta) = 2\alpha + 2.828\beta$$

We want to compare this energy with that of two electrons in a normal molecule with no special features (the propenyl cation has the special feature of an empty p orbital adjacent to the formal C/C double bond), and we can choose neutral ethene for our reference energy (Fig. 4.15)

$$E_\pi(\text{reference}) = 2(\alpha + \beta) = 2\alpha + 2\beta$$

The stabilization energy is then

$$E(\text{stab, cation}) = E_\pi(\text{prop. cation}) - E_\pi(\text{reference})$$
$$= (2\alpha + 2.828\beta) - (2\alpha + 2\beta) = 0.828\beta$$

Since β is negative, the π-electronic energy of the propenyl cation is calculated to be below that of ethene: providing an extra, empty p orbital for the electron pair causes the energy to drop. Actually, resonance energy is usually presented as a positive quantity, e.g. "100 kJ mol^{-1}". We can interpret this as 100 k mol^{-1} below a reference system. To avoid a negative quantity in SHM calculations like these, we could use $|\beta|$ instead of β.

The propenyl radical, Fig. 4.16. The total δ electronic energy by the SHM is

$$E_\pi(\text{prop. radical}) = 2(\alpha + 1.414\beta) + \alpha = 3\alpha + 2.828\beta$$

For the reference energy we can use one ethene molecule and one nonbonding p electron (like the electron in a methyl radical):

$$E_\pi(\text{reference}) = (2\alpha + 2\beta) + \alpha = 3\alpha + 2\beta$$

The stabilization energy is then

$$
\begin{aligned}
E(\text{stab, radical}) \;&=\; E_\pi(\text{prop. radical}) \;-\; E_\pi(\text{reference}) \\
&=\; (3\alpha \,+\, 2.828\beta) \,-\, (3\alpha \,+\, 2\beta) \,=\, 0.828\beta
\end{aligned}
$$

The propenyl anion. An analogous calculation (cf. Fig. 4.16, with four electrons for the anion) gives

$$
\begin{aligned}
E(\text{stab anion}) \;&=\; E_\pi(\text{prop. anion}) \;-\; E_\pi(\text{reference}) \\
&=\; (4\alpha \,+\, 2.828\beta) \,-\, (4\alpha \,+\, 2\beta) \,=\, 0.828\beta
\end{aligned}
$$

Thus the SHM predicts that all three propenyl species will be lower in energy than if the π electrons were localized in the formal double bond and (for the radical and anion) in one p orbital. Because this lower energy is associated with the ability of the electrons to spread or be delocalized over the whole π system, what we have called $E(\text{stab})$ is often denoted as the delocalization energy, and designated E_D. Note that E_R (or E_D) is always some multiple of β (or is zero). Since electron delocalization can be indicated by the familiar resonance symbolism the Hückel delocalization energy is often equated with resonance energy, and designated E_R. The accord between calculated delocalization and the ability to draw resonance structures is not perfect, as indicated by the next example.

Cyclobutadiene (Fig. 4.17). The total π electronic energy is

$$E_\pi(\text{cyclobutadiene}) \;=\; 2(\alpha \,+\, 2\beta) \,+\, 2\alpha \,=\, 4\alpha \,+\, 4\beta$$

Using two ethene molecules as our reference system:

$$E_\pi(\text{reference}) \;=\; 2\alpha \,+\, 2\beta$$

and so for $E(\text{stab})$ ($= E_D$ or E_R) we get

$$
\begin{aligned}
E(\text{stab, cyclobutadiene}) \;&=\; E_\pi(\text{cyclobutadiene}) \;-\; E_\pi(\text{reference}) \\
&=\; (4\alpha \,+\, 4\beta) \,-\, (4\alpha \,+\, 4\beta) \,=\, 0
\end{aligned}
$$

Cyclobutadiene is predicted by this calculation to have no resonance energy, although we can readily draw two "resonance structures" apparently exactly analogous to the Kekulé structures of benzene. The SHM predicts a resonance energy of 2β for benzene. Equating $2|\beta|$ with the commonly-quoted resonance energy of 150 kJ mol^{-1} (36 kcal mol^{-1}) for benzene gives a value of 75 kJ mol^{-1} for $|\beta|$, but this should be taken with more than a grain of salt, for outside a closely related series of

molecules, β has little or no quantitative meaning [44]. However, in contrast to the failure of simple resonance theory in predicting aromatic stabilization (and other chemical phenomena) [45], the SHM is quite successful.

The cyclobutadiene dication (cf. Fig. 4.17). The total π electronic energy is

$$E_\pi(\text{dication}) \ = \ 2(\alpha + 2\beta) \ = \ 2\alpha + 4\beta$$

Using one ethene molecule as the reference:

$$E_\pi(\text{reference}) \ = \ 2\alpha + 2\beta$$

and so

$$\begin{aligned} E(\text{stab, dication}) &= E_\pi(\text{dication}) - E_\pi(\text{reference}) \\ &= (2\alpha + 4\beta) - (2\alpha + 2\beta) \ = \ 2\beta \end{aligned}$$

Thus the stabilization energy calculation agrees with the deduction from the disposition of filled MOs (i.e. with the $4n + 2$ rule) that the cyclobutadiene dication should be stabilized by electron delocalization, which is in some agreement with experiment [46].

More sophisticated calculations indicate that cyclic $4n$ systems like cyclobutadiene (where planar; cyclooctatetraene, for example, is buckled and is simply an ordinary polyene) are actually *destabilized* by π electronic effects: their resonance energy is not just zero, as predicted by the SHM, but less than zero. Such systems are *antiaromatic* [17, 46]. This dramatic contrast between $4n$ and $4n + 2$ cyclic polyenes can actually be captured by the SHM if as the reference molecule for calculating the stabilization energy one uses not, as above, isolated ethene double bonds and nonbonding electrons, but instead an acyclic conceptual precursor. Thus we can compare cyclobutadiene with 1,3-butadiene, and the stabilization energy is the energy gained when the chain is closed (in reality two H atoms would have to be removed) to make cyclobutadiene. Do not confuse this possibly only hypothetical process with the known reaction, a quite different cyclization, the isomerization of 1,3-butadiene to cyclobutene, discussed above in connection with conrotatory and disrotatory precesses. For this hypothetical process:

$$\begin{aligned} E(\text{stab, cyclobutadiene}) &= E_\pi(\text{cyclobutadiene}) - E_\pi(\text{reference}) \\ &= E_\pi(\text{cyclobutadiene}) - E_\pi(\text{butadiene}) \\ &= (4\alpha + 4\beta) - (4\alpha + 4.472\beta) \ = \ \text{-}0.472\beta, \end{aligned}$$

rather than zero as above.

Since β is itself a negative energy quantity the stabilization energy of cyclobutadiene is predicted within the convention used here to be positive, or more conventionally the resonance energy is $-0.472\,|\beta|$, negative. It is destabilized (of higher energy) compared to 1,3-butadiene.

Similarly, comparing benzene with 1,3,5-hexatriene:

$$
\begin{aligned}
E(\text{stab, benzene}) &= E_\pi(\text{benzene}) - E_\pi(\text{reference}) \\
&= E_\pi(\text{benzene}) - E_\pi(\text{hexatriene}) \\
&= (6\alpha + 8\beta) - (6\alpha + 6.988\beta) = 1.012\beta
\end{aligned}
$$

Here the stabilization energy is negative, more conventionally the resonance energy is $1.012|\beta|$, positive. It is stabilized (of lower energy) compared to hexatriene. Using as the reference for resonance energy an acyclic conjugated molecule seems intuitively to be a more reasonable choice than isolated double bonds and nonbonding electrons, because it focusses on the effect on the π-electron energy of converting an acyclic π-system into one differing only by cyclic conjugation.

4.3.5.4 Bond Orders

The meaning of this term is easy to grasp in a qualitative, intuitive way: an ideal single bond has a bond order of one, and ideal double and triple bonds have bond orders of two and three, respectively. Invoking Lewis electron-dot structures, one might say that the order of a bond is the number of electron pairs being shared between the two bonded atoms. However, calculated quantum mechanical bond orders should be more widely applicable than those from the Lewis picture, because electron pairs are not localized between atoms in a clean pairwise manner; thus a weak bond, like a hydrogen bond or a long single bond, might be expected to have a bond order of less than one. However, there is no unique definition of bond order in computational chemistry, because there seems to be no single, correct method to assign electrons to particular atoms or pairs of atoms [47]. Various quantum mechanical definitions of bond order can be devised [48], based on basis-set coefficients. Intuitively, these coefficients for a pair of atoms should be relevant to calculating a bond order, since the bigger the contribution two atoms make to the wavefunction (whose square is a measure of the electron density; Sect. 4.2.6), the bigger should be the electron density between them. In the SHM the order of a bond between two atoms A_i and B_j is defined as

$$
B_{i,j} = 1 + \sum_{all\ occ} nc_ic_j \tag{4.70}
$$

Here the 1 denotes the single bond of the ubiquitous spectator σ bond framework, which is taken as always contributing a σ bond order of unity. The other term is the π bond order; its value is obtained by summing over all the occupied MOs the number of electrons n in each of these MOs times the product of the c's of the two atoms A, B for each MO. This is illustrated in these examples:

Ethene The occupied orbital is ψ_1, which has 2 electrons), and the coefficients of c_1 and c_2 for this orbital are 0.707, 0.707 (Eq. (4.67)). Thus

$$B_{i,j} = 1 + \sum_{all\ occ} nc_i c_j \quad = 1 + 2(0.707)0.707 = 1 + 1.000 = 2.000$$

which is reasonable for a double bond. The order of the σ bond is 1 and that of the π bond is 1.

The ethene radical anion The occupied orbitals are ψ_1, which has 2 electrons, and ψ_2, which has 1 electron; the coefficients of c_1 and c_2 for ψ_1 are 0.707, 0.707 and for ψ_2, 0.707, -0.707 (Eq. (4.66)). Thus

$$B_{i,j} = 1 + \sum_{all\ occ} nc_i c_j \quad = 1 + 2(0.707)0.707 + 1(0.707)(-0.707)$$
$$= 1 + 1\ -\ 0.500 = 1.500$$

The π bond order of 0.500 (1.500 $-\ \sigma$ bond order) accords with two electrons in the bonding MO and one electron in the antibonding orbital.

4.3.5.5   Atomic Charges

In an intuitive way, the charge on an atom might be thought to be a measure of the extent to which the atom repels or attracts a charged probe near it, and to be measurable from the energy it takes to bring a probe charge from infinity up to near the atom. However, this would tell us the charge at a point *outside* the atom, for example a point on the van der Waals surface of the molecule, and the repulsive or attractive forces on the probe charge would be due to the molecule as a whole. Although atomic charges are generally considered to be experimentally unmeasurable, chemists find the concept very useful (thus calculated charges are used to parameterize molecular mechanics force fields–Chap. 3), and much effort has gone into designing various definitions of atomic charge [48, 49]. Intuitively, the charge on an atom should be related to the basis set coefficients of the atom, since the more the atom contributes to a multicenter wavefunction (one with contributions from basis functions on several atoms), the more it might be expected to lose electronic charge by delocalization into the rest of the molecule (cf. the discussion of bond order above). In the SHM the charge on an atom A_i is defined as (cf. Eq. (4.70))

$$q_i = 1 - \sum_{all\ occ} nc_i^2 \tag{4.71}$$

The summation term is the *charge density*, and is a measure of the electronic charge on the molecule due to the π electrons. For example, having no π electrons (an empty p orbital, formally a cationic carbon) would mean a π electron charge density of zero; subtracting this from unity gives a charge on the atom of $+1$. Again,
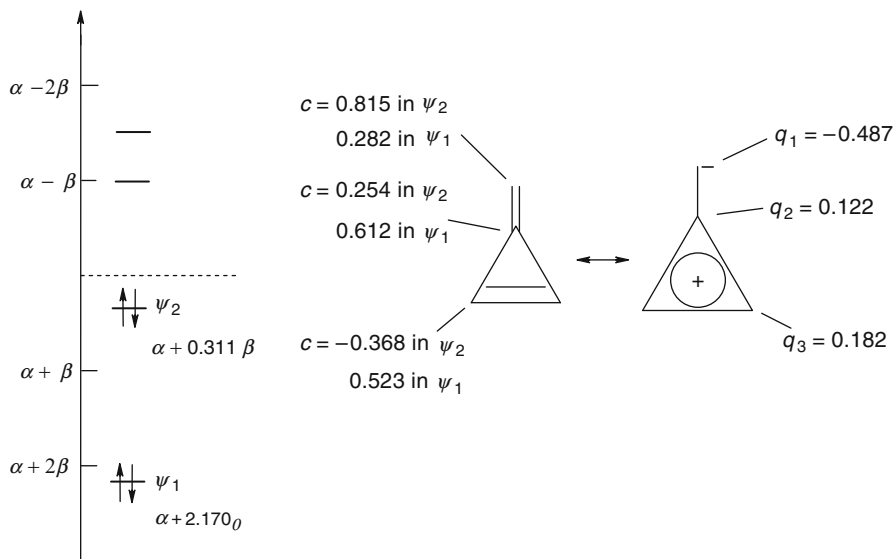
Fig. 4.24 The SHM charges on the atoms of a molecule can be calculated from the number of electrons in each occupied MO and the coefficients of these MOs. The predicted dipolar nature of methylenecyclopropene has been ascribed to a cyclopropenyl-cation-like resonance contributor

having two π electrons in a p orbital would mean a π electron charge density of 2 on the atom; subtracting this from unity gives a charge on the atom of -1 (a filled p orbital, formally an anionic carbon). The application of Eq. (4.72) will be illustrated using methylenecyclopropene (Fig. 4.24).

4.3.5.6   Methylenecyclopropene

$$q_1 = 1 - \sum_{all\ occ} nc_1^2 \quad = 1 - \left[2(0.282)^2 + 2(0.815)^2\right] = 1 - 1.487 = -0.487$$

$$q_2 = 1 - \sum_{all\ occ} nc_2^2 \quad = 1 - \left[2(0.612)^2 + 2(0.254)^2\right] = 1 - 0.878 = 0.122$$

$$q_3 = q_4 = 1 - \sum_{all\ occ} nc_3^2 \quad = 1 - \left[2(0.523)^2 + 2(-0.368)^2\right] = 1 - 0.817$$

$$= 0.182$$

The results of this charge calculation are summarized in Fig. 4.24; the negative charge on the exocyclic carbon and the positive charges on the ring carbons are in accord with the resonance picture (Fig. 4.24), which invokes a contribution from the aromatic cyclopropenyl cation [50]. Note that the charges sum to (essentially) zero, as they must for a neutral molecule (the hydrogens, which actually also carry

charges, have been excluded from consideration here). A HF/$6-31G^*$ calculation (Chap. 5) places a total charge (carbon plus hydrogen) – albeit defined in a different way – of -0.430 on the CH_2 group and $+0.430$ on the ring, and about 0.24 on each hydrogen, compared with -0.487 and $+0.487$ for the exocyclic carbon and the ring carbons in the SHM calculation.

There are many other applications of the SHM [21c, e] including recent and perhaps unexpected ones such as correlation with UV solvent shifts [51] and even physicochemical properties [52].

4.3.6   Strengths and Weaknesses of the Simple Hückel Method

4.3.6.1   Strengths

The SHM has been extensively used to correlate, rationalize, and predict many chemical phenomena, having been applied with surprising success to dipole moments, esr spectra, bond lengths, redox potentials, ionization energies, UV and IR spectra, aromaticity, acidity/basicity, and reactivity, and specialized books on the SHM should be consulted for details [21]. The method will give probably give some insight into any phenomenon that involves predominantly the π electron systems of conjugated molecules. The SHM may have been underrated [53] and reports of its death are probably exaggerated. However, it is not used very much in research nowadays, partly because more sophisticated π electron approaches like the PPP method (Chap. 6, Sect. 6.2.2) are available, but mainly because of the great success of all-valence-electron semiempirical methods (Chap. 6), and the increasing applicability to quite large molecules of sophisticated all-electron ab initio (Chap. 5) and density functional (Chap. 7) methods, thanks to improvements in algorithms and to phenomenal increases in computer speed.

4.3.6.2   Weaknesses

The defects of the SHM arise from the fact that it treats only π electrons, and these only very approximately. The basic Hückel method described here has been augmented in an attempt to handle non- π substituents, e.g. alkyl groups, halogen groups, etc., and heteroatoms instead of carbon. This has been done by treating the substituents as π centers and embodying empirically altered values of α and β, so that in the Fock matrix values other than -1 and 0 appear. However, the values of these modified parameters that have been employed vary considerably [54], which tends to diminish one's confidence in their reliability.

The approximations in the SHM are its peremptory treatment of the overlap integrals S (Sect. 4.3.4, discussion in connection with Eq. (4.55)), its drastic truncation of the possible values of the Fock matrix elements into just α, β and

0 (Sect. 4.3.4, discussion in connection with Eq. (4.61)), its complete neglect of electron spin, and its glossing over (although not exactly ignoring) interelectronic repulsion by incorporating this into the α and β parameters. In some more detail:

The overlap integrals S are divided into just two classes:

$$\int \phi_i \phi_j dv \quad = S_{ij} = 1 \text{ or } 0$$

depending on whether the orbitals on the atoms i and j are on the same or different atoms. This approximation, as explained earlier, reduces the matrix form of the secular equations to standard eigenvalue form $\mathbf{HC} = \mathbf{C\varepsilon}$ (Eq. (4.59)), so that the Fock matrix can (after giving its elements numerical values) be diagonalized without further ado (the ado is explained in Sect. 4.4.1, in connection with the extended Hückel method). In the older determinant, as opposed to matrix, treatment (Sect. 4.3.7), the approximation greatly simplifies the determinants. In fact, however, the overlap integral between adjacent carbon p orbitals is ca. 0.24 [55].

Setting the Fock matrix elements equal to just α, β and 0: Setting

$$\int \phi_i \hat{H} \phi_j dv \quad = H_{ij} = \alpha, \ \beta \text{ or } 0$$

depending on whether the orbitals on the atoms i and j are on the same, adjacent or further-removed atoms is an approximation, because all the H_{ii} terms are not the same, and all the adjacent-atom H_{jj} terms are not the same either; these energies depend on the environment of the atom in the molecule. For example, atoms in the middle of a conjugated chain should have somewhat different H_{ii} and H_{jj} parameters than ones at the end of the chain. Of course, the approximation simplifies the Fock matrix (or the determinant in the old determinant method, Sect. 4.3.7).

The neglect of electron spin and the deficient treatment of interelectronic repulsion is obvious. In the usual derivation (Sect. 4.3.4): in Eq. (4.40) the integration is carried out with respect to only spatial coordinates (ignoring spin coordinates; contrast ab initio theory, Chap. 5, Sect. 5.2), and in calculating π energies (Sect. 4.3.5, *Resonance energies* subsection) we simply took the sum of the number of electrons in each occupied MO times the energy level of the MO. However, the energy of an MO is the energy of an electron in the MO moving in the force field of the nuclei *and* all the other electrons (as pointed out in Sect. 4.3.4, in explaining the matrices of Eq. (4.55)). If we calculate the total electronic energy by simply summing MO energies times occupancy numbers, we are assuming, wrongly, that the electron energies are independent of one another, i.e. that the electrons do not interact. An energy calculated in this way is said to be a sum of one-electron energies. The resonance energies calculated by the SHM can thus be only very rough, unless the errors tend to cancel in the subtraction step, which probably occurs to some extent (this is presumably why the method of Hess and Schaad for calculating resonance energies works so well [53]). The neglect of electron repulsion and spin in the usual derivation of the SHM is discussed in reference [31a].

4.3.7   The Determinant Method of Calculating the Hückel c's and Energy Levels

An older method of obtaining the coefficients and energy levels from the secular equations (Eq. (4.49)) utilizes determinants rather than matrices. The method is much more cumbersome than the matrix diagonalization approach of Sect. 4.3.4, but in the absence of cheap, readily-available, easy-to-use computers (matrix diagonalization is easily handled by a personal computer) its erstwhile employment may be forgiven; it could be done with paper, pencil and patience. It is outlined here because traditional presentations of the SHM [21] use it.

Consider again the secular Eq. (4.49):

$$(H_{11} - ES_{11})c_1 + (H_{12} - ES_{12})c_2 = 0$$
$$(H_{21} - ES_{21})c_1 + (H_{22} - ES_{22})c_2 = 0$$

By considering the requirements for nonzero values of c_1 and c_2 we can find how to calculate the c's and the molecular orbital energies (since the coefficients are weighting factors that determine how much each basis function contributes to the MO, zero c's would mean no contributions from the basis functions and hence no MOs; that would not be much of a molecule). Consider the system of linear equations

$$A_{11}x_1 + A_{12}x_2 = b_1$$
$$A_{21}x_1 + A_{22}x_2 = b_2$$

Using determinants:

$$x_1 = \frac{\begin{vmatrix} b_1 & A_{12} \\ b_2 & A_{22} \end{vmatrix}}{D}$$

$$x_2 = \frac{\begin{vmatrix} A_{11} & b_1 \\ A_{21} & b_2 \end{vmatrix}}{D}$$

$$D = \begin{vmatrix} A_{11} & A_{12} \\ A_{21} & A_{22} \end{vmatrix}$$

where D is the *determinant of the system*. This is Cramer's rule– see any book on linear algebra.

If $b_1 = b_2 = 0$ (the situation in the secular equations), then in the equations for x_1 and x_2 the numerator is zero, and so $x_1 = 0/D$ and $x_2 = 0/D$. The only way that x_1 and x_2 (corresponding to our basis function coefficients) can be nonzero in this case is that the determinant of the system be zero, i.e.

$$D = 0$$

for then $x_1 = 0/0$ and $x_2 = 0/0$, and $0/0$ can have any finite value; mathematicians call it indeterminate. This is easy to see (the argument is more persuasive than mathematically rigorous):

Let

$$\frac{0}{0} = a$$

then

$$a \times 0 = 0$$

which is true for any finite value of a.

So for the secular equations the requirement that the c's be nonzero is that the determinant of the system be zero:

$$D = \begin{vmatrix} H_{11} - ES_{11} & H_{12} - ES_{12} \\ H_{21} - ES_{21} & H_{22} - ES_{22} \end{vmatrix} = 0 \qquad (4.72)$$

Equation (4.74) can be generalized to n basis functions (cf. the matrix of Eq. (4.62)):

$$\begin{vmatrix} H_{11} - ES_{11} & H_{12} - ES_{12} & \dots & H_1n - ES_{1n} \\ H_{21} - ES_{21} & H_{22} - ES_{22} & \dots & H_2n - ES_{2n} \\ \vdots & \vdots & \dots & \vdots \\ H_{n1} - ES_{n1} & H_{n2} - ES_{n2} & \dots & H_{nn} - ES_{nn} \end{vmatrix} = 0 \qquad (4.73)$$

If we invoke the SHM simplification of orthogonality of the S integrals (pp. 37–39), then $S_{ii} = 1$ and $S_{ij} = 0$ and Eq. (4.75) becomes

$$\begin{vmatrix} H_{11} - E & H_{12} & \dots & H_{1n} \\ H_{21} & H_{22} - E & \dots & H_{2n} \\ \vdots & \vdots & \dots & \vdots \\ H_{n1} & H_{n2} & \dots & H_{nn} - E \end{vmatrix} = 0 \qquad (4.74)$$

Substituting α, β and 0 for the appropriate H's (p. 39) we get

$$\begin{vmatrix} \alpha - E & \beta & \dots & 0 \\ \beta & \alpha - E & \dots & 0 \\ \vdots & \vdots & \dots & \vdots \\ 0 & 0 & \dots & \alpha - E \end{vmatrix} = 0 \qquad (4.75)$$

The diagonal terms will always be α - E, but the placement of β and 0 will depend on which i, j terms are adjacent and which are further-removed, which depends on the numbering system chosen (see below). Since multiplying or dividing a determinant by a number is equivalent to multiplying or dividing the elements of one row or

column by that number (Sect. 4.3.3), multiplying both sides of Eq. (4.76) by $1/\beta n$ times, i.e. by $(1/\beta)^n$ gives

$$
\begin{vmatrix}
(\alpha\text{-}E)/\beta & 1 & \ldots & 0 \\
1 & (\alpha\text{-}E)/\beta & \ldots & 0 \\
\vdots & \vdots & \ldots & \vdots \\
0 & 0 & \ldots & (\alpha\text{-}E)/\beta
\end{vmatrix} = 0
\tag{4.76}
$$

Finally, if we define $(\alpha\text{-}E)/\beta = x$, we get

$$
\begin{vmatrix}
x & 1 & \ldots & 0 \\
1 & x & \ldots & 0 \\
\vdots & \vdots & \ldots & \vdots \\
0 & 0 & \ldots & x
\end{vmatrix} = 0
\tag{4.77}
$$

The diagonal terms are always x but the off-diagonal terms, 1 for adjacent and 0 for nonadjacent orbital pairs, depend on the numbering (which does not affect the results: Fig. 4.25). Any specific determinant of the type in Eq. (4.77) can be expanded into a polynomial of order n (where the determinant is of order $n \times n$), making Eq. (4.78) yield polynomial equation:

$$
x^n + a_1 x^{n-1} + a_2 x^{n-2} + \cdots a_n = 0
\tag{4.78}
$$

The polynomial can be solved for x and then the energy levels can be found from $(\alpha - E)/\beta = x$, i.e. from

$$
E = \alpha - \beta x
\tag{4.79}
$$

The coefficients can then be calculated from the energy levels by substituting the E's into one of the secular equations, finding the ratio of the c's, and normalizing to get the actual c's. An example will indicate how the determinant method can be implemented.

Consider the propenyl system. In the secular determinant the i,i-type interactions will be represented by x, adjacent i,j-type interactions by 1, and non-adjacent i,j-type interactions by 0. For the determinantal equation we can write (Fig. 4.25)

$$
\begin{vmatrix}
x & 1 & 0 \\
1 & x & 1 \\
0 & 1 & x
\end{vmatrix} = 0
\tag{4.80}
$$

(compare this with the Fock matrix for the propenyl system). Solving this equation (see Sect. 4.3.3):

$$
\begin{vmatrix} x & 1 & 1 \\ 1 & x & 1 \\ 1 & 1 & x \end{vmatrix} = x^3 - 3x + 2
$$

$$
\begin{vmatrix} x & 1 & 0 \\ 1 & x & 1 \\ 0 & 1 & x \end{vmatrix} = x^3 - 2x
$$

$$
\begin{vmatrix} x & 1 & 1 \\ 1 & x & 0 \\ 1 & 0 & x \end{vmatrix} = x^3 - 2x
$$

Fig. 4.25 The determinants corresponding to different numbering patterns can seem to differ, but on expansion they give the same polynomial

$$
\begin{vmatrix} x & 1 & 0 \\ 1 & x & 1 \\ 0 & 1 & x \end{vmatrix} = x \begin{vmatrix} x & 1 \\ 1 & x \end{vmatrix} - 1 \begin{vmatrix} 1 & 1 \\ 0 & x \end{vmatrix} + 1 \begin{vmatrix} 1 & x \\ 0 & 1 \end{vmatrix}
\tag{4.81}
$$
$$
= x(x^2 - 1) - (x - 0) + 0 \; = x^3 - x - x = x^3 - 2x = 0
$$

This cubic can be factored (but in general polynomial equations require for practical solution numerical approximation methods):

$$
x(x^2 - 2) = 0 \text{ so } x = 0 \text{ and } x^2 - 2 = 0 \text{ or } x = \pm\sqrt{2}
$$

From $(\alpha - E)/\beta = x$, $E = \alpha - x\beta$ and

$$
x = 0 \text{ leads to } E = \alpha
$$
$$
x = +\sqrt{2} \text{ leads to } E = \alpha - \sqrt{2}\beta
$$
$$
x = -\sqrt{2} \text{ leads to } E = \alpha + \sqrt{2}\beta
$$

So we get the same energy levels as from matrix diagonalization ($(\sqrt{2} = 1.414)$).

   To find the coefficients we substitute the energy levels into the secular equations; for the propenyl system these are, projecting from the secular equations for a two-orbital system, Eq. (4.49):

$$(H_{11} - ES_{11})c_1 + (H_{12} - ES_{12})c_2 + (H_{13} - ES_{13})c_3 = 0$$
$$(H_{21} - ES_{21})c_1 + (H_{22} - ES_{22})c_2 + (H_{23} - ES_{23})c_3 = 0 \qquad (4.82)$$
$$(H_{31} - ES_{31})c_1 + (H_{32} - ES_{32})c_2 + (H_{33} - ES_{33})c_3 = 0$$

These can be simplified (Eqs. (4.57), (4.61) to

$$(\alpha - E)c_1 + \beta c_2 + 0c_3 = 0$$
$$\beta c_1 + (\alpha - E)c_2 + \beta c_3 = 0 \qquad (4.83)$$
$$0c_1 + \beta c_2 + (\alpha - E)c_3 = 0$$

For the energy level $E = \alpha + \sqrt{2}\beta$ (MO level 1, ψ_1), substituting into the first secular equation we get

$$-\sqrt{2}\beta c_{11} + \beta c_{21} = 0, \quad \text{so} \quad c_{21}/c_{11} = \sqrt{2}$$

(Recall the c_{ij} notation; c_{11} is the coefficient for atom 1 in ψ_1, c_{21} is the coefficient for atom 2 in ψ_1, etc.). Substituting $E + \alpha + \sqrt{2}\beta$ into the second secular equation we get

$$\beta c_{11} + \beta c_{31} = 0, \quad \text{so} \quad c_{11}/c_{31}$$

We now have the relative values of the c's:

$$c_{11}/c_{11} = 1, \; c_{21}/c_{11} = \sqrt{2}, c_{31}/c_{11} = 1 \qquad (4.84)$$

To find the actual values of the c's, we utilize the fact that the MO (we are talking at present about MO level 1, ψ_1) must be normalized:

$$\int \psi_1^2 dv = 1 \qquad (4.85)$$

Now, from the LCAO method

$$\psi_1 = c_{11}\phi_1 + c_{21}\phi_2 + c_{31}\phi_3 \qquad (4.86)$$

Therefore

$$\psi_1^2 = c_{11}^2\phi_1^2 + c_{21}^2\phi_2^2 + c_{31}^2\phi_3^2 + 2c_{11}c_{21}\phi_1\phi_2 + 2c_{11}c_{31}\phi_1\phi_3 + 2c_{21}c_{31}\phi_2\phi_3$$
$$(4.87)$$

So from Eq. (4.87), and recalling that in the SHM we pretend that the basis functions ϕ are orthonormal, i.e. that $S_{ij} = \delta_{ij}$, we get

$$\int \psi_1^2 dv = c_{11}^2 + c_{21}^2 + c_{31}^2 = 1 \tag{4.88}$$

Using the ratios of the c's from Eq. (4.84):

$$\frac{c_{11}^2}{c_{11}^2} + \frac{c_{21}^2}{c_{11}^2} + \frac{c_{31}^2}{c_{11}^2} = \frac{1}{c_{11}^2}$$

i.e.

$$1^2 + \left(\sqrt{2}\right)^2 + 1^2 = \frac{1}{c_{11}^2}$$

and so

$$c_{11} = \frac{1}{2}$$

and

$$c_{21} = \left(\sqrt{2}\right)c_{11} = \frac{1}{\sqrt{2}}$$

and

$$c_{31} = c_{11} = \frac{1}{2}$$

By substituting into the secular Eq. (4.83) the E values for ψ_2 and ψ_3 we could find the ratios of the c's for ψ_2 and ψ_3 and with the aid of the orthonormalization equation analogous to Eq. (4.89) we could get the actual values of c_{12}, c_{22}, c_{32} and c_{13}, c_{23}, and c_{33}.

Large determinants that would give higher-order polynomial equations can be reduced to a series of smaller determinants by group theory, if the molecule has symmetry (in addition to a symmetry plane of course). Thus the 4×4 butadiene determinant can be reduced to two 2×2 determinants and the 10×10 determinant for naphthalene can be reduced to two 2×2 and two 3×3 determinants.

Although the determinant method was streamlined (see particularly [21d], compared to matrix diagonalization it is conceptually and algorithmically clumsy, and has been replaced by matrix diagonalization implemented in a computer program. In fact, free online programs now allow one to do SHM calculations without writing out either matrices or determinants, just by sketching the molecule on a computer screen [56].

4.4 The Extended Hückel Method

4.4.1 Theory

In the *simple* Hückel method, as in all modern molecular orbital methods, a Fock matrix is diagonalized to give coefficients (which with the basis set give the wavefunctions of the molecular orbitals) and energy levels (i.e. molecular orbital energies). The SHM and the extended Hückel method (EHM, extended Hückel theory, EHT) differ in how the elements of the Fock matrix are obtained and how the overlap matrix is treated. The EHM was popularized and widely applied by Hoffmann[28] [57], although earlier work using the approach had been done by Wolfsberg and Helmholz [58]. We now compare point by point the SHM and the EHM.

4.4.1.1 Simple Hückel Method

1. *Basis set is limited to p orbitals*. Each element of the Fock matrix **H** is an integral that represents an interaction between two orbitals. The orbitals are in almost all cases a set of *p* orbitals (usually carbon 2*p*) supplied by an sp^2 framework, with the *p* orbital axes parallel to one another and perpendicular to the plane of the framework. In other words, the set of basis orbitals – the *basis set* – is limited (in the great majority of cases) to p_z orbitals (taking the framework plane, i.e. the molecular plane, to be the *xy* plane).
2. *Orbital interaction energies are limited to α, β and* 0. The Fock matrix orbital interactions are limited to α, β and 0, depending on whether the H_{ij} interaction is, respectively *i,i*, adjacent, or further-removed. The value of β does not vary smoothly with the separation of the orbitals, although logically it should decrease continuously to zero as the separation increases.
3. *Fock matrix elements are not actually calculated*. The Fock matrix elements are not any definite physical quantities, but rather energy levels relative to α in units of $|\beta|$, making them 0 or -1. The Fock matrix depends only on connectivity, not on geometry (except for unusual cases where one performs a SHM calculation on a nonplanar molecule, when an H_{ij} element might depend on the cosine of the atomic orbital p_i/p_j axes). One can try to estimate α and β, but the SHM does not define them quantitatively.
4. *Overlap integrals are limited to* 1 *or* 0. We pretend that the overlap matrix **S** is a unit matrix, by setting $S_{ij} = \delta_{ij}$. This enables us to simplify $\mathbf{HC} = \mathbf{SC}\boldsymbol{\varepsilon}$

---

[28] Roald Hoffmann, born Zloczow, Poland, 1937. Ph.D. Harvard, 1962, Professor, Cornell. Nobel prize 1981(shared with Kenichi Fukui; Chap. 7, Sect. 7.3.5) for work with organic chemist Robert B. Woodward, showing how the symmetry of molecular orbitals influences the course of chemical reactions (the Woodward Hoffmann rules or the conservation of orbital symmetry). Main exponent of the extended Hückel method. He has written poetry, and several popular books on chemistry.

(Eq. (4.54)) to the standard eigenvalue form $\mathbf{HC} = \mathbf{C\varepsilon}$ (Eq. (4.59)) and so $\mathbf{H} = \mathbf{C\varepsilon C}^{-1}$, which is the same as saying that the SHM Fock matrix is directly diagonalized to give the c's and ε's.

Now compare these four points with the corresponding features of the EHM:

4.4.1.2   Extended Hückel Method

1. *All valence s and p orbitals are used in the basis set.* As in the SHM each element of the Fock matrix is an integral representing an interaction between two orbitals; however, in the EHM the basis set is not just a set of $2p_z$ orbitals but rather the set of valence-shell orbitals of each atom in the molecule (the derivation we saw of the secular equations says nothing about what kinds of orbitals we are considering). Thus each hydrogen atom contributes a $1s$ orbital to the basis set and each carbon atom a $2s$ and three $2p$ orbitals. Lithium and beryllium, although they have no $2p$ electrons, are assigned a $2s$ and three $2p$ orbitals (experience shows that this works better than omitting these basis functions) so the atoms from lithium to fluorine each contribute a $2s$ and three $2p$ orbitals. A basis set like this, which uses the normal valence orbitals of atoms, is called a *minimal valence basis set*.
2. *Orbital interaction energies are calculated and vary smoothly with geometry.* The EHM Fock matrix orbital interactions H_{ij} are calculated in a way that depends on the distance apart of the orbitals, so their values vary smoothly with orbital separation with the help of the overlap integrals, see below.
3. *Fock matrix elements are actually calculated.* The EHM Fock matrix elements are calculated from well-defined physical quantities (ionization energies) with the aid of well-defined mathematical functions (overlap integrals), and so are closely related to ionization energies and have definite quantitative values.
4. *Overlap integrals are actually calculated.* We do not in effect ignore the overlap matrix, i.e. we do not set it equal to a unit matrix. Instead, the elements of the overlap matrix are calculated, with each S_{ij} integral depending on the distance apart of the atoms i and j, which has the important consequence that the S values depend on the geometry of the molecule. Because the S values play a role in the calculation of the Fock matrix integrals (see below) these vary smoothly with geometry and the energy levels depend on molecular geometry. Since $\mathbf{S}$ is not taken as a unit matrix, we cannot go directly from $\mathbf{HC} = \mathbf{SC\varepsilon}$ to $\mathbf{HC} = \mathbf{C\varepsilon}$ and thus we cannot simply diagonalize the EHM Fock to get the c's and ε's.

These four points are elaborated on below.

1) *Use of a minimal valence basis set* in the EHM is more realistic than treating just the $2p_z$ orbitals, since all the valence electrons in a molecule are likely to be involved in determining its properties. Further, the SHM is largely limited to π systems, i.e. to alkenes and aromatics and derivatives of these with attached π electron groups, but the EHM, in contrast, can in principle be applied to any molecule. The use
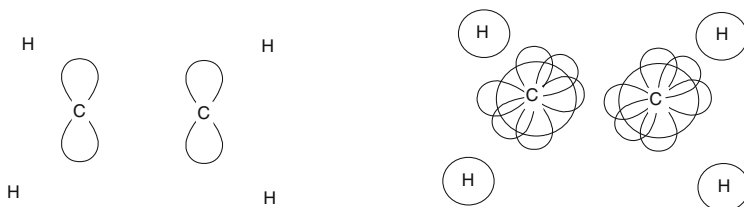
The simple Hückel method basis set for ethene.
Each carbon has one $2p$ basis function.
C_2H_4 has two basis functions

The extended Hückel method basis set for ethene.
Each carbon has one $2s$ and three $2p$ basis functions.
Each H has one $1s$ basis function.
C_2H_4 has 12 basis functions.

Fig. 4.26 The simple Hückel method normally uses only one basis function per "heavy atom": only one $2p$ orbital on each carbon, oxygen, nitrogen, etc., ignoring the hydrogens. The extended Hückel method uses for each carbon, oxygen, nitrogen, etc., a $2s$ and three $2p$ orbitals, and for each hydrogen a $1s$ orbital. This is called a minimal valence basis set

of a minimal valence basis set makes the Fock matrix much larger than in the "corresponding" SHM calculation. For example in an SHM calculation on ethene, only two orbitals are used, the $2p_z$ on C_1 and the $2p_z$ on C_2, and the SHM Fock matrix is (using the compact Dirac notation $\langle \phi_i | \hat{H} | \phi_j \rangle = \int \phi_i \hat{H} \phi_j dv$)

$$
\begin{aligned}
H(SHM) &= \begin{pmatrix} \langle C_1(2p_z)|\hat{H}|C_1(2p_z)\rangle & \langle C_1(2p_z)|\hat{H}|C_2(2p_z)\rangle \\ \langle C_2(2p_z)|\hat{H}|C_1(2p_z)\rangle & \langle C_2(2p_z)|\hat{H}|C_2(2p_z)\rangle \end{pmatrix} \\
&= \begin{pmatrix} 0 & -1 \\ -1 & 0 \end{pmatrix} 2 \times 2 \text{ matrix}
\end{aligned}
\tag{4.89}
$$

To write down the EHM Fock matrix, let us label the valence orbitals like this:

$$
\begin{array}{ccccc}
H_1(1s)\,\phi_1 & C_1(2s)\,\phi_5 & C_1(2p_x)\,\phi_7 & C_1(2p_y)\,\phi_9 & C_1(2p_z)\,\phi_{11} \\
H_2(1s)\,\phi_2 & C_2(2s)\,\phi_6 & C_2(2p_x)\,\phi_8 & C_2(2p_y)\,\phi_{10} & C_2(2pz)\,\phi_{12} \\
& & H_3(1s)\,\phi_3 & & \\
& & H_4(1s)\,\phi_4 & &
\end{array}
$$

The size of the Fock matrix (12×12) is equal to the number of basis functions (12):

$$
H(EHM) = \begin{pmatrix} \langle \phi_1|\hat{H}|\phi_1\rangle & \langle \phi_1|\hat{H}|\phi_2\rangle & \cdots & \langle \phi_1|\hat{H}|\phi_{12}\rangle \\ \langle \phi_2|\hat{H}|\phi_1\rangle & \langle \phi_2|\hat{H}|\phi_2\rangle & \cdots & \langle \phi_2|\hat{H}|\phi_{12}\rangle \\ \vdots & \vdots & \cdots & \vdots \\ \langle \phi_{12}|\hat{H}|\phi_1\rangle & \langle \phi_{12}|\hat{H}|\phi_2\rangle & \cdots & \langle \phi_{12}|\hat{H}|\phi_{12}\rangle \end{pmatrix}
\tag{4.90}
$$
$$
12 \times 12 \text{ matrix}
$$

The SHM and EHM basis sets are shown in Fig. 4.26.

2) *The EHM Fock matrix interactions i,j do not have just two values (α or β) as in the SHM, but are functions of the orbitals (the basis functions) ϕ_i and ϕ_j and of the separation of these orbitals,* as explained in (3) below.

3) *The EHM matrix elements* $\langle\phi_i|\hat{H}|\phi_j\rangle$ *and* $\langle\phi_i|\hat{H}|\phi_j\rangle$ *are calculated* (rather than set equal to 0 or -1), although the calculation is a simple one using overlap integrals and experimental ionization energies; in ab initio calculations (Chap. 5) and more advanced semiempirical calculations (Chap. 6), the actual mathematical form of the operator $\hat{H}$ is taken into account. Here the *i,i*-type interactions are taken as being proportional to the negative of the ionization energy [59] of the orbital ϕ_i and the *i,j*-type interactions as being proportional to the overlap integral between ϕ_i and ϕ_j and the negative of the average of the ionization energies I_i and I_j of ϕ_i and ϕ_j (the negative of the orbital ionization energy is the energy of an electron in the orbital, compared to the zero of energy of the electron and the ionized species infinitely separated and at rest):

$$\langle\phi_i|\hat{H}|\phi_i\rangle = -I_i \qquad (4.91)$$

$$\langle\phi_i|\hat{H}|\phi_j\rangle = -\frac{1}{2}KS_{ij}(I_i+I_j) \qquad (4.92)$$

A proportionality constant K of about 2 seems to work best.

For H(1 s), C(2 s) and C(2p), experiment shows

$$I(\text{H(1s)}) = 13.6 \text{ eV}, \quad I(\text{C(2s)}) = 20.8 \text{ eV}, \quad I(\text{C(2s)}) = 11.3 \text{ eV} \qquad (4.93)$$

The overlap integrals are calculated using Slater-type (Chap. 5, Sect. 5.3.2) functions for the basis functions, e.g.

$$\phi(1s) = \left(\frac{\zeta_1^3}{\pi}\right)^{\frac{1}{2}} \exp(-\zeta_1|\mathbf{r} - \mathbf{R}_{1s}|) \qquad (4.94)$$

$$\phi(2s) = \left(\frac{\zeta_2^5}{96\pi}\right)^{\frac{1}{2}} |\mathbf{r} - \mathbf{R}_{2s}| \exp\left(\frac{-\zeta_2|\mathbf{r} - \mathbf{R}_{2s}|}{2}\right) \qquad (4.95)$$

where the parameters ζ depend on the particular atom (H, C, etc.) and orbital (1 s, 2 s, etc). The variable $\mathbf{r} - \mathbf{R}$ is the distance of the electron from the atomic nucleus on which the function is centered; $\mathbf{r}$ is the vector from the origin of the Cartesian coordinate system to the electron, a variable, and $\mathbf{R}$ is the vector from the origin to the nucleus on which the basis function is centered, a structural parameter:

$$|\mathbf{r} - \mathbf{R}_A| = \left[(x - x_A)^2 + (y - y_A)^2 + (z - z_A)^2\right]^{\frac{1}{2}} \qquad (4.96)$$

where (x_A, y_A, z_A) are the coordinates of the nucleus bearing the Slater function. The Slater function is thus a function of three variables x,y,z and depends

parametrically on the location (x_A, y_A, z_A) of the nucleus A on which it is centered. The Fock matrix elements are thus calculated with the aid of overlap integrals whose values depend the location of the basis functions; this means that the molecular orbitals and their energies will depend on the actual *geometry* used in the input, whereas in a simple Hückel calculation, the MOs and their energies depend only on the *connectivity* of the molecule).

4) *The overlap matrix* **S** in the EHM is not simply treated as a unit matrix, in effect ignoring it, for the purpose of diagonalizing the Fock matrix. Rather, the overlap integrals are actually evaluated, not only to help calculate the Fock elements, but also to reduce the equation **HC=SCε** to the standard eigenvalue form **HC=Cε**. This is done in the following way. Suppose the original set of basis functions $\{\phi_i\}$ could be transformed by some process into an *orthonormal* set $\{\phi_i'\}$ (since atom-centered basis functions can't be orthogonal, as explained in Sect. 4.3.4, the new set must be delocalized over several centers and is a linear combination of the atom-centered set) such that with a new set of coefficients c' we have LCAO molecular orbitals with the same energy levels as before, i.e.

$$S_{ij}' = \int \phi_i' \phi_j' dv = \delta_{ij} \tag{4.97}$$

where δ_{ij} is the Kronecker delta (Eq. 4.57). The result of the process referred to above is

$$\mathbf{HC} = \mathbf{SC\varepsilon} \xrightarrow{\textbf{Process}} \mathbf{H'C'} = \mathbf{S'C'\varepsilon} \tag{4.98}$$

($\boldsymbol{\varepsilon}$, not $\boldsymbol{\varepsilon}'$, as the energy will not depend on algebraic manipulation of a fundamentally fixed, given set of basis functions) where the matrices **H**, **C**, **S** and $\boldsymbol{\varepsilon}$ were defined in Sect. 4.3.4 (Eq. (4.55)) and **H'** and **S'** are analogous to **H** and **S** with ϕ' in place of ϕ; **C'** is the matrix of coefficients c' that satisfies the equation with the energy levels ε (the elements of $\boldsymbol{\varepsilon}$) being the same as in the original equation **HC=SCε**. Since from Eq. (4.97) $\mathbf{S'} = 1$, the unit matrix (Sect. 4.3.3), Eq. (4.98) simplifies to

$$\mathbf{HC} = \mathbf{SC\varepsilon} \xrightarrow{\textbf{Process}} \mathbf{H'C'} = \mathbf{C'\varepsilon} \tag{*4.99}$$

The *Process* that effects the transformation is called *orthogonalization*, since the result is to create an orthogonal basis set. The favored orthogonalization procedure in computational chemistry, which I will now illustrate, is Löwdin orthogonalization (after the quantum chemist Per-Olov Löwdin; also called symmetric othogonalization) [60].

Define a matrix **C'** such that

$$\mathbf{C}' = \mathbf{S}^{1/2}\mathbf{C} \qquad \text{i.e.} \quad \mathbf{C} = \mathbf{S}^{-1/2}\mathbf{C}' \tag{4.100}$$

(By multiplying on the left by $\mathbf{S}^{-1/2}$ and noting that $\mathbf{S}^{-1/2}\mathbf{S}^{1/2} = \mathbf{S}^0 = \mathbf{1}$).
Substituting (4.100) into $\mathbf{HC} = \mathbf{SC}\varepsilon$ and multiplying on the left by $\mathbf{S}^{-1/2}$ we get

$$\mathbf{S}^{-1/2}\mathbf{H}\mathbf{S}^{-1/2}\mathbf{C}' = \mathbf{S}^{-1/2}\mathbf{S}\mathbf{S}^{-1/2}\mathbf{C}'\varepsilon \tag{4.101}$$

Let

$$\mathbf{S}^{-1/2}\mathbf{H}\mathbf{S}^{-1/2} = \mathbf{H}' \tag{4.102}$$

and note that $\mathbf{S}^{-1/2}\mathbf{S}\mathbf{S}^{-1/2} = \mathbf{S}^{1/2}\mathbf{S}^{-1/2} = \mathbf{1}$ Then we have from (4.101) and
(4.102)

$$\mathbf{H}'\mathbf{C}' = \mathbf{1}\mathbf{C}'\varepsilon$$

i.e

$$\mathbf{H}'\mathbf{C}' = \mathbf{C}'\varepsilon \tag{4.103}$$

Thus the orthogonalizing *Process* of (4.99) (or rather one possible orthogonaliza-
tion process, Löwdin orthogonalization) is the use of an *orthogonalizing matrix*
$\mathbf{S}^{-1/2}$ to transform $\mathbf{H}$ by pre- and postmultiplication (Eq. 4.102) into $\mathbf{H}'$. $\mathbf{H}'$ satisfies
the standard eigenvalue equation (Eq. 4.103), so

$$\mathbf{H}' = \mathbf{C}'\varepsilon\mathbf{C}'^{-1} \tag{4.104}$$

In other words, using $\mathbf{S}^{-1/2}$ we transform the original Fock matrix $\mathbf{H}$, which is not
directly diagonalizable to eigenvector and eigenvalue matrices $\mathbf{C}$ and ε, into a
related matrix $\mathbf{H}'$ which *is* diagonalizable to eigenvector and eigenvalue matrices
$\mathbf{C}'$ and ε. The matrix $\mathbf{C}'$ is then transformed to the desired $\mathbf{C}$ by multiplying by
$\mathbf{S}^{-1/2}$ (Eq. 4.100). So without using the drastic $\mathbf{S} = \mathbf{1}$ approximation we can use
matrix diagonalization to get the coefficients and energy levels from the Fock
matrix.

The orthogonalizing matrix $\mathbf{S}^{-1/2}$ is calculated from $\mathbf{S}$: the integrals S are
calculated and assembled into $\mathbf{S}$, which is then diagonalized:

$$\mathbf{S} = \mathbf{P}\mathbf{D}\mathbf{P}^{-1} \tag{4.105}$$

Now it can be shown that any function of a matrix $\mathbf{A}$ can be obtained by taking the
same function of its corresponding diagonal alter ego and pre- and postmultiplying
by the diagonalizing matrix $\mathbf{P}$ and its inverse $\mathbf{P}^{-1}$:

$$f(\mathbf{A}) \;=\; \mathbf{P}f(\mathbf{D})\mathbf{P}^{-1} \tag{4.106}$$

and diagonal matrices have the nice property that $f(\mathbf{D})$ is the diagonal matrix whose diagonal element $i, j \;=\; f$ (element i,j of $\mathbf{D}$). So the inverse square root of $\mathbf{D}$ is the matrix whose elements are the inverse square roots of the corresponding elements of $\mathbf{D}$. Therefore

$$\mathbf{S}^{-1/2} \;=\; \mathbf{P}\mathbf{D}^{-1/2}\mathbf{P}^{-1} \tag{4.107}$$

and to find $\mathbf{D}^{-1/2}$ we (or rather the computer) simply take the inverse square root of the diagonal (i.e. the nonzero) elements of $\mathbf{D}$. To summarize: $\mathbf{S}$ is diagonalized to give $\mathbf{P}$, $\mathbf{P}^{-1}$ and $\mathbf{D}$, $\mathbf{D}$ is used to calculate $\mathbf{D}^{-1/2}$, then the orthogonalizing matrix $\mathbf{S}^{-1/2}$ is calculated (Eq. (4.107)) from $\mathbf{P}$, $\mathbf{D}^{-1/2}$ and $\mathbf{P}^{-1}$. The orthogonalizing matrix is then used to convert $\mathbf{H}$ to $\mathbf{H}'$, which can be diagonalized to give the eigenvalues and the eigenvectors (Sect. 4.4.2). All this will be clearer after you read the review of the procedure and, especially, the example worked out for the protonated helium molecule.

4.4.1.3   Review of the EHM Procedure

The EHM procedure for calculating eigenvectors and eigenvalues, i.e. coefficients (or in effect molecular orbitals – the c's along with the basis functions comprise the MOs) and energy levels, bears several important resemblances to that used in more advanced methods (Chaps. 5 and 6) and so is worth reviewing.

1. An input structure (a molecular geometry) must be specified and submitted to calculation. The geometry can be specified in Cartesian coordinates (probably the usual way nowadays) or as bond lengths, angles and dihedrals (internal coordinates), depending on the program. In practice a virtual molecule would likely be created with an interactive model-building program (usually by clicking together groups and atoms) which would then supply the EHM program with the coordinates.
2. The EHM program calculates the overlap integrals S and assembles the overlap matrix $\mathbf{S}$.
3. The program calculates the Fock matrix elements $H_{ij} = \langle \phi_i | \hat{H} | \phi_j \rangle$ (Eqs. (4.91, 4.92)) using stored values of ionization energies I, the overlap integrals S, and the proportionality constant K of that particular program. The matrix elements are assembled into the Fock matrix $\mathbf{H}$.
4. The overlap matrix is diagonalized to give $\mathbf{P}$, $\mathbf{D}$ and $\mathbf{P}^{-1}$ (Eq. (4.105)) and $\mathbf{D}^{-1/2}$ is then calculated by finding the inverse square roots of the diagonal elements of $\mathbf{D}$. The orthogonalizing matrix $\mathbf{S}^{-1/2}$ is then calculated from $\mathbf{P}$, $\mathbf{D}^{-1/2}$ and $\mathbf{P}^{-1}$ (Eq. 4.107).

5. The Fock matrix $\mathbf{H}$ in the atom-centered nonorthogonal basis $\{\phi\}$ is transformed into the matrix $\mathbf{H}'$ in the delocalized, linear combination orthogonal basis $\{\phi'\}$ by pre- and postmultiplying $\mathbf{H}$ by the orthogonalizing matrix $\mathbf{S}^{-1/2}$ (Eq. (4.102)).

6. $\mathbf{H}'$ is diagonalized to give $\mathbf{C}'\boldsymbol{\varepsilon}$ and $\mathbf{C}'^{-1}$ (Eq. (4.104)). We now have the energy levels ε (the diagonal elements of the $\boldsymbol{\varepsilon}$ matrix).

7. $\mathbf{C}'$ must be transformed to give the coefficients c of the original, atom-centered set of basis functions $\{\phi\}$ in the MOs (i.e. to convert the elements c' to c). To get the c's in the MOs $\psi_j = c_{1j}\phi_1 + c_{2j}\phi_2 + \cdots$, we transform $\mathbf{C}'$ to $\mathbf{C}$ by premultiplying by $\mathbf{S}^{-1/2}$ (Eq. (4.100)).

4.4.1.4   Molecular Energy and Geometry Optimization in the Extended Hückel Method

Steps (1)–(7) take an input geometry and calculate its energy levels (the elements of $\boldsymbol{\varepsilon}$) and their MOs or wavefunctions (the ψ's; from the c's, the elements of $\mathbf{C}$, and the basis functions ϕ). Now, clearly any method in which the energy of a molecule depends on its geometry can in principle be used to find minima and transition states (see Chap. 2). This brings us to the matter of how the EHM calculates the energy of a molecule. The energy of a molecule, that is, the energy of a particular nuclear configuration on the potential energy surface, is the sum of the electronic energies and the internuclear repulsions ($E_{\text{electronic}} + V_{\text{NN}}$). Actually, this is the energy on a Born-Oppenheimer surface, ignoring zero point energy (Chap. 2).

   In comparing the energies of isomers, or of two geometries of the same molecule, one should, strictly, compare $E_{\text{total}} = E_{\text{electronic}} + V_{\text{NN}}$. The electronic energy is the sum of kinetic energy and potential energy (electron-electron repulsion and electron-nucleus attraction) terms. The internuclear repulsion, due to all pairs of interacting nuclei and trivial to calculate, is usually represented by V, a symbol for potential energy. The EHM ignores V_{NN}. Furthermore, the method calculates electronic energy simply as the sum of one-electron energies (Sect. 4.3.5 *Weaknesses*), ignoring electron-electron repulsion. Hoffmann's tentative justification [57a] for ignoring internuclear repulsion and using a simple sum of one-electron energies was that when the *relative* energies of isomers are calculated, by subtracting two values of E_{total}, the electron repulsion and nuclear repulsion terms approximately cancel, i.e. that changes in energy that accompany changes in geometry are due mainly to alterations of the MO energy levels. Actually, it seems that the (quite limited) success of the EHM in predicting molecular geometry is due to the fact that E_{total} is approximately *proportional* to the sum of the occupied MO energies; thus although the EHM energy difference is not equal to the difference in total energies, it is (or tends to be) approximately proportional to this difference [61]. In any case, the real strength of the EHM lies in the ability of this fast and widely applicable method to assist chemical intuition, if *provided with* a reasonable molecular geometry.

4.4.2 *An Illustration of the EHM: The Protonated Helium Molecule*

Protonation of a helium atom gives He-H$^+$, the helium hydride cation, the simplest heteronuclear molecule [62]. Conceptually, of course, this can also be formed by the union of a helium dication and a hydride ion, or a helium cation and a hydrogen atom:

$$\text{He: } + \text{ H}^+ \quad \rightarrow \quad \text{He:H}^+$$
$$\text{or } \text{ He}^{2+} + \text{ :H}^- \rightarrow \text{He:H}^+$$
$$\text{or } \text{ He}^{+\bullet} + {}^\bullet\text{H} \rightarrow \text{He:H}^+$$
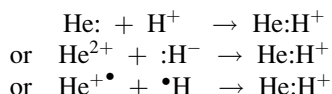
Its lower symmetry makes this molecule better than H_2 for illustrating molecular quantum mechanical calculations (most molecules have little or no symmetry). Following the prescription in points (1)–(7):

(1) *Input structure*

We choose a plausible bond length: 0.800 Å (the H–H bond length is 0.742 Å and the H-X bond length is ca. 1.0 Å, where X is a "first-row" element (in quantum chemistry, first-row means Li to F, not H and He). The Cartesian coordinates could be written H$_1$ (0,0,0), He$_2$ (0,0, 0.800).

(2) *Overlap integrals and overlap matrix*

The minimal valence basis set here consists of the hydrogen 1s orbital (ϕ_1) and the helium 1s orbital (ϕ_2). The needed integrals are $S_{11} = S_{22}$ and $S_{12} = S_{21}$, where $S_{ij} = \int \overline{\phi}_i \phi_j dv$. The Slater functions for ϕ_1 and ϕ_2 are [63]

$$\phi_1(\text{H}1s) = \left(\frac{\zeta_H^3}{\pi}\right)^{1/2} e^{-\zeta_H|\mathbf{r}-\mathbf{R}_H|} \tag{4.108}$$

and

$$\phi_2(\text{He}1s) = \left(\frac{\zeta_{He}^3}{\pi}\right)^{1/2} e^{-\zeta_H|\mathbf{r}-\mathbf{R}_{He}|} \tag{4.109}$$

Reasonable values [62] are $\zeta_H = 1.24$ Bohr^{-1} and $\zeta_{He} = 2.0925$ Bohr^{-1}, if r is in atomic units, a.u. (see Chap. 5, Sect. 5.2.2); 1 a.u. $= 0.5292$ Å. The overlap integrals are

$S_{11} = S_{22} = 1$ (as must be the case if ϕ_1 and ϕ_2 are normalized) and $S_{12} = S_{21} = 0.435$ (for all well-behaved functions $\int f_1 f_2 dq = \int f_2 f_1 dq$).

The overlap matrix is thus

$$\mathbf{S} = \begin{pmatrix} 1 & 0.435 \\ 0.435 & 1 \end{pmatrix} \tag{4.110}$$

(3) *Fock matrix*

We need the matrix elements $H_{11} = H_{22}$ and $H_{12} = H_{21}$, where the integrals $H_{ij} = <\phi_i|\hat{H}|\phi_j>$ are not actually calculated from first principles but rather are estimated with the aid of overlap integrals and orbital ionization energies:

$$\langle\phi_i|\hat{H}|\phi_i\rangle = -I_i$$

$$\langle\phi_i|\hat{H}|\phi_j\rangle = -\frac{1}{2}KS_{ij}(I_i+I_j)$$

Using simply the ionization energies (cf. [59], and *harder questions*, (9)):

$$I(\text{H}) = I_1 = 13.6\,\text{eV},\ I(\text{He}) = I_2 = 24.6\,\text{eV}$$

Hoffmann used in his initial calculations [57a] $K = 1.75$.
So

$$H_{11} = -13.6\,\text{eV}$$
$$H_{12} = H_{21} = -\tfrac{1}{2}(1.75)(0.435)(13.6 + 24.6) = -14.5$$
$$H_{22} = -24.6$$

And the Fock matrix is

$$H = \begin{pmatrix} -13.6 & -14.5 \\ -14.5 & -24.6 \end{pmatrix} \tag{4.111}$$

(4) *Orthogonalizing matrix*

As explained above, we (a) diagonalize $\mathbf{S}$, (b) calculate $\mathbf{D}^{-1/2}$, then (c) calculate the orthogonalizing matrix $\mathbf{S}^{-1/2}$:

(a) diagonalize $\mathbf{S}$

$$\mathbf{S} = \begin{pmatrix} 1 & 0.435 \\ 0.435 & 1 \end{pmatrix} = \underbrace{\begin{pmatrix} 0.707 & 0.707 \\ 0.707 & -0.707 \end{pmatrix}}_{\mathbf{P}} \underbrace{\begin{pmatrix} 1.435 & 0 \\ 0 & 0.565 \end{pmatrix}}_{\mathbf{D}} \underbrace{\begin{pmatrix} 0.707 & 0.707 \\ 0.707 & -0.707 \end{pmatrix}}_{\mathbf{P}^{-1}}$$

$$\tag{4.112}$$

(b) calculate $\mathbf{D}^{-1/2}$

$$\mathbf{D}^{-1/2} = \begin{pmatrix} 1.435^{-1/2} & 0 \\ 0 & 0.565^{-1/2} \end{pmatrix} = \begin{pmatrix} 0.835 & 0 \\ 0 & 1.330 \end{pmatrix} \tag{4.113}$$

(c) calculate the orthogonalizing matrix $\mathbf{S}^{-1/2}$

$$\mathbf{S}^{-1/2} = \underbrace{\begin{pmatrix} 0.707 & 0.707 \\ 0.707 & -0.707 \end{pmatrix}}_{\mathbf{P}} \underbrace{\begin{pmatrix} 0.835 & 0 \\ 0 & 1.330 \end{pmatrix}}_{\mathbf{D}^{-1/2}} \underbrace{\begin{pmatrix} 0.707 & 0.707 \\ 0.707 & -0.707 \end{pmatrix}}_{\mathbf{P}^{-1}} = \begin{pmatrix} 1.083 & -0.248 \\ -0.248 & 1.083 \end{pmatrix}$$

$$\tag{4.114}$$

(5) *Transformation of the original Fock matrix* **H** *to* **H**′Using Eq. (4.102):

$$\mathbf{H}' = \underbrace{\begin{pmatrix} 1.083 & -0.248 \\ -0.248 & 1.083 \end{pmatrix}}_{\mathbf{S}^{-1/2}} \underbrace{\begin{pmatrix} -13.6 & -14.5 \\ -14.5 & -24.6 \end{pmatrix}}_{\mathbf{H}} \underbrace{\begin{pmatrix} 1.083 & -0.248 \\ -0.248 & 1.083 \end{pmatrix}}_{\mathbf{S}^{-1/2}} = \begin{pmatrix} -9.67 & -7.65 \\ -7.68 & -21.74 \end{pmatrix}$$

(4.115)

(6) *Diagonalization of* **H**′

From Eq. (4.104) $\left(\mathbf{H}' = \mathbf{C}' \boldsymbol{\varepsilon} \mathbf{C}'^{-1}\right)$, diagonalization of **H**′ gives an eigenvector matrix **C**′ and the eigenvalue matrix ε; the columns of **C**′ are the coefficients of the transformed, orthonormal basis functions:

$$\mathbf{H}' = \begin{pmatrix} -9.67 & -7.65 \\ -7.68 & -21.74 \end{pmatrix} = \underbrace{\begin{pmatrix} 0.436 & 0.899 \\ 0.900 & -0.437 \end{pmatrix}}_{\mathbf{C}'} \underbrace{\begin{pmatrix} -25.5 & 0 \\ 0 & -5.95 \end{pmatrix}}_{\boldsymbol{\varepsilon}} \underbrace{\begin{pmatrix} 0.436 & 0.900 \\ 0.899 & -0.437 \end{pmatrix}}_{\mathbf{C}'^{-1}}$$

(4.116)

We now have the energy levels (−25.5 eV and −5.95 eV), but the eigenvectors of **C**′ must be transformed to give us the coefficients of the original, nonorthogonal basis functions.

(7) *Transformation of* **C**′ *to* **C**

Using Eq. (4.102), p. 81 ($\mathbf{C} = \mathbf{S}^{-1/2}\mathbf{C}'$):

$$\mathbf{C} = \underbrace{\begin{pmatrix} 1.083 & -0.248 \\ -0.248 & 1.083 \end{pmatrix}}_{\mathbf{S}^{-1/2}} \underbrace{\begin{pmatrix} 0.436 & 0.839 \\ 0.900 & -0.437 \end{pmatrix}}_{\mathbf{C}'} = \underbrace{\begin{pmatrix} 0.249 & 1.082 \\ 0.867 & -0.696 \end{pmatrix}}_{\begin{matrix} c_{11} & c_{12} \\ c_{21} & c_{22} \end{matrix}}$$

(4.117)

Note that unlike the case in the SHM, the sum of the squares of the c's for an MO does not equal 1, since overlap integrals S_{ij} for basis functions on different atoms are not set equal to 0; in other words, the basis functions are not assumed to be orthogonal, and the overlap matrix is not a unit matrix. Thus for ψ_1 (recall that ϕ_1 is for H and ϕ_2 for He):

$$\psi_1 = c_{11}\phi_1 + c_{21}\phi_2, \text{ so}$$
$$\int \psi_1^2 dv = \int \left(c_{11}^2\phi_1^2 + 2c_{11}c_{21}\phi_1\phi_2 + c_{21}^2\phi_2^2\right)dv = 1$$

since the probability of finding an electron in ψ_1 somewhere in space is 1. The basis functions ϕ are normalized, so

$$c_{11}^2 + 2c_{11}c_{21}S_{12} + c_{21}^2 = 1, \quad i.e.$$
$$c_{11}^2 + c_{21}^2 = 1 - 2c_{11}c_{21}S_{12}$$

not = 1 as in the simple Hückel method.

4.4.3   The Extended Hückel Method–Applications

The EHM was initially applied to the geometries (including conformations) and relative energies of hydrocarbons [57a], but the calculation of these two basic chemical parameters is now much better handled by molecular mechanics (Chap. 3) and semiempirical methods like AM1 and PM3 (Chap. 6) and by ab initio (Chap. 5) and DFT (Chap. 7) methods. The main use of the EHM nowadays is to study large, extended systems [64] like polymers, solids and surfaces. Indeed, of four papers by Hoffmann and coworkers in the *J. Am. Chem. Soc.* in 1995, using the EHM, three applied it to such polymeric systems [65]. The ability of the method to illuminate problems in solid-state science makes it useful to physicists. Even when not applied to polymeric systems, the EHM is frequently used to study large, heavy-metal-containing molecules [66] that might not be very amenable to more elaborate approaches.

4.4.4   Strengths and Weaknesses of the Extended Hückel Method

4.4.4.1   Strengths

One advantage of the EHM over ab initio methods (Chap. 5), more elaborate semiempirical methods (Chap. 6), and density functional theory (DFT) methods (Chap. 7), is that the EHM can be applied to very large systems, and can treat almost any element since the only element-specific parameter needed is an ionization energy (valence-state ionization energy is preferred [59]), which is usually available. In contrast, more elaborate semiempirical methods have not been parameterized for many elements (although recent parameterizations of PM3 and MNDO for transition metals make these much more generally useful than hitherto–Chap. 6, Sect. 6.2.6.7). For ab initio and DFT methods, basis functions may not be available for basis sets and elements of interest, and besides, ab initio and even DFT methods are hundreds or thousands of times slower than the EHM and thus limited to much smaller systems. The applicability of the EHM to large systems and a wide variety of elements is one reason why it has been extensively applied to polymeric and solid-state structures. The EHM is faster than more elaborate semiempirical methods because calculation of the Fock matrix elements is so simple and because this matrix needs to be diagonalized only *once* to yield the eigenvalues and eigenvectors; in contrast, semiempirical methods like AM1 and PM3 (Chap. 6), as well as ab initio and DFT calculations, require repeated matrix diagonalization because the Fock matrix must be iteratively refined in the SCF (self-consistent-field) procedure (Chap. 5, Sect. 5.2.3.6).

The spartan reliance of the EHM on empirical parameters helps to make it relatively easy (in the right hands) to interpret its results, which depend, in the last analysis, only on geometry (which affects overlap integrals) and ionization

energies. With a strong dose of chemical intuition this has enabled the method to yield powerful insights, such as counterintuitive orbital mixing [67], and the very powerful Woodward-Hoffmann rules [38].

The applicability to large systems, including polymers and solids, containing almost any kind of atom, and the relative transparency of the physical basis of the results, are the main advantages of the EHM.

Surprisingly for such a conceptually simple method, the EHM has a theoretically-based advantage over otherwise more elaborate semiempirical methods like AM1 and PM3, in that it treats orbital overlap properly: those other methods use the "neglect of differential overlap" or NDO approximation (Chap. 6, Sect. 6.2), meaning that they take $S_{ij} = \delta_{ij}$, as in the simple Hückel method . This can lead to superior results from the EHM [68].

The EHM is a very valuable teaching tool because it follows straightforwardly from the simple Hückel method yet uses overlap integrals and matrix orthogonalization in the same fashion as the mathematically more elaborate ab initio method.

Finally, the EHM, albeit more elaborately parameterized than in its original incarnation, has been claimed to offer some promise as a serious competitor to the very useful and popular semiempirical AM1 method (Chap. 6, Sect. 6.2.6.4) for calculating molecular geometries [69]; however, this variation on the EHM does not seem to have become a recognized, generally available method.

4.4.4.2 Weaknesses

The weaknesses of the standard EHM probably arise at least in part from the fact that it does not (contrast the ab initio method, Chap. 5) take into account electron spin or electron-electron repulsion, ignores the fact that molecular geometry is partly determined by internuclear repulsion, and makes no attempt to overcome these defects by parameterization (a variation with careful parameterization has been claimed to give good geometries [69]).

The standard EHM gives, by and large, poor geometries and relative energies. Although it predicts a C-H bond length of ca. 1.0 Å, it yields C/C bond lengths of 1.92 Å, 1.47 Å and 0.85 Å for ethane, ethene and ethyne, respectively, cf. the actual values of 1.53 Å, 1.33 Å and 1.21 Å, and although the favored conformation of an alkane is usually correctly identified, the energy barriers and differences are generally at best in only modest agreement with experiment. Because of this inability to reliably calculate geometries, EHM calculations are usually not used for geometry optimizations, but rather utilize experimental or otherwise-calculated geometries as inputs.

4.5 Summary

This chapter introduces the application of quantum mechanics (QM) to computational chemistry by outlining the development of QM up to the Schrödinger equation and then showing how this equation led to the simple Hückel method, from which the extended Hückel method followed.

QM teaches, basically, that energy is *quantized*: absorbed and emitted in discrete packets (*quanta*) of magnitude hv, where h is Planck's constant and v (Greek *nu*) is the frequency associated with the energy. QM grew out of studies of blackbody radiation and of the photoelectric effect. Besides QM, radioactivity and relativity contributed to the transition from classical to modern physics. The classical Rutherford nuclear atom suffered from the deficiency that Maxwell's electromagnetic theory demanded that its orbiting electrons radiate away energy and swiftly fall into the nucleus. This problem was countered by Bohr's quantum atom, in which an electron could orbit stably if its angular momentum was an integral multiple of $h/2\pi$. However, the Bohr model contained several ad hoc fixes and worked only for the hydrogen atom. The deficiencies of the Bohr atom were surmounted by Schrödinger's wave mechanical atom; this was based on a combination of classical wave theory and the de Broglie postulate that any particle is associated with a wavelength $\lambda = h/p$, where p is the momentum. The quantum numbers, except spin, follow naturally from the wave mechanical treatment and the model does not break down for atoms beyond hydrogen.

Hückel was the first to apply QM to species significantly more complex than the hydrogen atom. The Hückel approach is treated nowadays within the framework of the concept of hybridization: the π electrons in p orbitals are taken into account and the σ electrons in an sp^2 framework are ignored. Hybridization is a purely mathematical convenience, a procedure in which atomic (or molecular) orbitals are combined to give new orbitals; it is analogous to the combination of simple vectors to give new vectors (an orbital is actually a kind of vector).

The simple Hückel method (SHM; simple Hückel theory, SHT; Hückel molecular orbital method, HMO method) starts with the Schrödinger equation in the form $\hat{H}\psi = E\psi$ where $\hat{H}$ is a Hamiltonian operator, ψ is a MO wavefunction and E is the energy of the system (atom or molecule). By expressing ψ as a linear combination of atomic orbitals (LCAO) and minimizing E with respect to the LCAO coefficients one obtains a set of simultaneous equations, the secular equations. These are equivalent to a single matrix equation, $\mathbf{HC} = \mathbf{SC\varepsilon}$; $\mathbf{H}$ is an energy matrix, the Fock matrix, $\mathbf{C}$ is the matrix of the LCAO coefficients, $\mathbf{S}$ is the overlap matrix and ε is a diagonal matrix whose nonzero, i.e. diagonal, elements are the MO energy levels. The columns of $\mathbf{C}$ are called eigenvectors and the diagonal elements of ε are called eigenvalues. By the drastic approximation $\mathbf{S} = \mathbf{1}$ ($\mathbf{1}$ is the unit matrix), the matrix equation becomes $\mathbf{HC} = \mathbf{C\varepsilon}$, i.e. $\mathbf{H} = \mathbf{C\varepsilon}\,\mathbf{C}^{-1}$ which is the same as saying that diagonalization of $\mathbf{H}$ gives $\mathbf{C}$ and ε, i.e gives the MO coefficients in the LCAO, and the MO energies. To get numbers for $\mathbf{H}$ the SHM reduces all the Fock matrix elements to α (the coulomb integral, for AOs on the same atom) and β (the bond

integral or resonance integral, for AOs not on the same atom; for nonadjacent atoms β is set $= 0$), and to get actual numbers for the Fock elements, α and β are defined as energies relative to α, in units of $|\beta|$; this makes the Fock matrix consist of just 0's and -1's, where the 0's represent same-atom interactions and nonadjacent-atom interactions, and the -1's represent adjacent-atom interactions. The use of just two Fock elements is a big approximation. The SHM Fock matrix is easily written down just by looking at the way the atoms in the molecule are connected.

Applications of the SHM include predicting:

The nodal properties of the MOs, very useful in applying the Woodward-Hoffmann rules.

The stability of a molecule based on its filled and empty MOs, and its delocalization energy or resonance energy, based on a comparison of its total π-energy with that of a reference system. The pattern of filled and empty MOs led to Hückel's rule (the $4n + 2$ rule) which says that planar molecules with completely conjugated p orbitals containing $4n + 2$ electrons should be aromatic.

Bond orders and atom charges, which are calculated from the AO coefficients of the occupied MOs (in the SHM LCAO treatment, p AOs are basis functions that make up the MOs).

The strengths of the SHM lie in the qualitative insights it gives into the effect of molecular structure on π orbitals. Its main triumph in this regard was its spectacularly successful prediction of the requirements for aromaticity (the Hückel $4n + 2$ rule).

The weaknesses of the SHM arise from the fact that it treats only π electrons (limiting its applicability largely to planar sp^2 arrays), its all-or-nothing treatment of overlap integrals, the use of just two values for the Fock integrals, and its neglect of electron spin and interelectronic repulsion. Because of these approximations it is not used for geometry optimizations and its quantitative predictions are sometimes viewed with suspicion. For obtaining eigenvectors and eigenvalues from the secular equations an older and inelegant alternative to matrix diagonalization is the use of determinants.

The extended Hückel method (EHM; extended Hückel theory, EHT) follows from the SHM by using a basis set that consists not just of p orbitals, but rather of all the valence AOs (a minimal valence basis set), by calculating (albeit very empirically) the Fock matrix integrals, and by explicitly calculating the overlap matrix $\mathbf{S}$ (whose elements are also used in calculating the Fock integrals). Because $\mathbf{S}$ is not taken as a unit matrix, the equation $\mathbf{HC} = \mathbf{SC\varepsilon}$ must be transformed to one without $\mathbf{S}$ before matrix diagonalization can be applied. This is done by a matrix multiplication process called orthogonalization, involving $\mathbf{S}^{-1/2}$, which converts the original Fock matrix $\mathbf{H}$, based on nonorthogonal atom-centered basis functions, into a Fock matrix $\mathbf{H}'$, based on orthogonal linear combinations of the original basis functions. With these new basis functions, $\mathbf{H}'\mathbf{C}' = \mathbf{C}'\mathbf{\varepsilon}$, i.e $\mathbf{H}' = \mathbf{C}'\mathbf{\varepsilon}\,\mathbf{C}'^{-1}$, so that diagonalization of $\mathbf{H}'$ gives the eigenvectors (of the new basis functions, which are transformed back to those corresponding to the original set: $\mathbf{C}' \rightarrow \mathbf{C}$) and eigenvalues of $\mathbf{H}$.

Because the overlap integrals needed by the EHM depend on molecular geometry, the method can in principle be used for geometry optimization, although the results are generally poor, so more reliable geometries are used as input. Applications of the EHM involve largely the study of big molecules and polymeric systems, often containing heavy metals.

The strengths of the EHM derive from its simplicity: it is very fast and so can be applied to large systems; the only empirical parameters needed are (valence-state) ionization energies, which are available for a wide range of elements; the results of calculations lend themselves to intuitive interpretation since they depend only on geometry and ionization energies, and on occasion the proper treatment of overlap integrals even gives better results than those from more elaborate semiempirical methods. The fact that the EHM is conceptually simple yet incorporates several features of more sophisticated methods enables it to serve as an excellent introduction to higher-level quantum mechanical computational methods.

The weaknesses of the EHM are due largely to its neglect of electron spin and electron-electron repulsion and the fact that it bases the energy of a molecule simply on the sum of the one-electron energies of the occupied orbitals, which ignores electron-electron repulsion and internuclear repulsion; this is at least partly the reason it usually gives poor geometries.

Easier Questions

1. What do you understand by the term *quantum mechanics*?
2. Outline the experimental results that led to quantum mechanics.
3. What approximations are used in the simple Hückel method?
4. How could the SHM Fock matrix for 1,3-butadiene be modified in an attempt to recognize explicitly the fact that the molecule has, formally anyway, two double bonds and one single bond?
5. What are the most important kinds of results that can be obtained from Hückel calculations?
6. Write down the simple Hückel Fock matrices (in each case using α, β and 0, and 0, -1 and 0) for: (1) the pentadienyl radical (2) the cyclopentadienyl radical (3) trimethylenemethane, $C(CH_2)_3$ (4) trimethylenecyclopropane (5) 3-methylene-1,4-pentadiene.
7. The SHM predicts the propenyl cation, radical and anion to have the same resonance energy (stabilization energy). Actually, we expect the resonance energy to decrease as we add π electrons; why should this be the case?
8. What molecular feature cannot be obtained at all from the simple Hückel method? Why?
9. List the differences between the underlying theory of the simple Hückel method and the extended Hückel method.
10. A 400×400 matrix is easily diagonalized. How many carbons would an alkane have for its EHM Fock matrix to be 400×400 (or just under this size)? How many carbons would a (fully) conjugated polyene have if its SHM Fock matrix were 400×400?

Harder Questions

1. Do you think it is reasonable to describe the Schrödinger equation as a postulate of quantum mechanics? What is a postulate?
2. What is the probability of finding a particle *at* a point?
3. Suppose we tried to simplify the simple Hückel method even further, by ignoring *all* interactions i, j; $i \neq j$ (ignoring adjacent instead interactions of setting them $= \beta$). What effect would this have on energy levels? Can you see the answer without looking at a matrix or determinant?
4. How might the i,j-type interactions in the simple Hückel Fock matrix be made to assume values other than just -1 and 0?
5. What is the result of using as a reference system for calculating the resonance energy of cyclobutadiene, not two ethene molecules, but 1,3-butadiene? What does this have to do with antiaromaticity? Is there any way to decide if one reference system is better than another?
6. What is the problem with unambiguously defining the charge on an atom in a molecule?
7. It was claimed that the extended Hückel method can be parameterized to give good geometries. Do you think this might be possible for the simple Hückel method? Why or why not?
8. Give a reference to a journal paper that used the SHM, and one that used the EHM, since the year 2000. For each paper quote the sentence in the abstract or the paper that states that the SHM was used..
9. The ionization energies usually used to parameterize the EHM are not ordinary atomic ionization energies, but rather *valence-state atomic orbital ionization energies* (VSAO ionization energies, valence state ionization energies). What does the term "valence state" mean here? Should the VSAO ionization energies of the orbitals of an atom depend somewhat on the hybridization of the atom? In what way?
10. Which should require more empirical parameters: a molecular mechanics force field (Chap. 3) or an extended Hückel method program? Explain.

References

1. For general accounts of the development of quantum theory see: Mehra J, Rechenberg H (1982) The historical development of quantum theory. Springer, New York; Kuhn TS (1978) Black-body theory and the quantum discontinuity 1894–1912. Oxford University Press, Oxford: (b) An excellent historical and scientific exposition, at a somewhat advanced level: Longair MS (1983) Theoretical concepts in physics. Cambridge University Press, Cambridge, chapters 8–12
2. A great deal has been written speculating on the meaning of quantum theory, some of it serious science, some philosophy, some mysticism. Some leading references are: (a) Whitaker A (1996) Einstein, Bohr and the quantum dilemma. Cambridge University Press; (b) Stenger VJ (1995) The unconscious quantum. Prometheus, Amherst; (c) Yam P (1997) Scientific

American, June 1997, p. 124; (d) Albert DZ (1994) Scientific American, May 1994, p. 58; (e) Albert DZ (1992) Quantum mechanics and experience. Harvard University Press, Cambridge, MA; (f) Bohm D, Hiley HB (1992) The undivided universe. Routledge, New York; (g) Baggott J (1974) The meaning of quantum theory. Oxford University Press, New York; (h) Jammer M (1974) The philosophy of quantum mechanics. Wiley, New York; (i) Particularly on the reality of orbitals: Mulder P (2011) Hyle 17(1):24

3. Levine N (2014), Quantum chemistry, 7th edn, Prentice Hall, Engelwood Cliffs

4. Sitzung der Deutschen Physikalischen Gesellschaft, 14 December 1900, Verhandlung 2, p. 237. This presentation and one of October leading up to it (Verhandlung 2, p. 202) were combined in: Planck M (1901) Annalen Phys 4(4):553

5. (a) Klein MJ (1966) Physics Today 19:23; (b) For a detailed account of Planck's role in and attitude to the birth of quantum theory see Brown BR (2015) Planck: Driven by Vision, Broken by War. Oxford University Press, and references therein; particularly chapter 10

6. For a good and amusing account of quantum strangeness (and relativity effects) and how things might be if Planck's constant had a considerably different value, see Gamow G, Stannard R (1999) The new world of Mr Tompkins. Cambridge University Press, Cambridge. This is based on the classics by George Gamow, "Mr Tompkins in Wonderland" (1940) and Mr Tompkins Explores the Atom (1944), which were united in "Mr Tompkins in Paperback" (Cambridge University Press, Cambridge, 1965)

7. Einstein A (1905) Actually, the measurements were very difficult to do accurately, and the Einstein linear relationship may have been more a prediction than an explanation of established facts. Ann Phys 17:132

8. (a) For an elementary treatment of Maxwell's equations and the loss of energy by an accelerated electric charge, see Adair RK (1969) Concepts in physics. Academic Press, New York, chapter 21; (b) For a brief historical introduction to Maxwell's equations see Longair MS (1983) Theoretical concepts in physics. Cambridge University Press, Cambridge, chapter 3. For a rigorous treatment of the loss of energy by an accelerated electric charge see Longair, chapter 9

9. Bohr N (1913) Philos Mag 26:1

10. E.g. Thornton ST, Rex A (1993) Modern physics for scientists and engineers. Saunders, Orlando, pp 155–164

11. See e.g. ref. [2a], *loc. cit*

12. Schrödinger E (1926) This first Schrödinger equation paper, a nonrelativistic treatment of the hydrogen atom, has been described as "one of the greatest achievements of twentieth-century physics" Ann Phys 79, 361 (ref. [13], p. 205)

13. Moore W (1989) Schrödinger. Life and thought. Cambridge University Press, Cambridge

14. de Broglie L (1924) "Recherche sur la Theorie des Quanta", thesis presented to the faculty of sciences of the University of Paris

15. Ref. [13], chapter 6

16. E.g. ref. [3], pp. 410–419 and pp. 604–613

17. Minkin VI, Glukhovtsev MN, Ya B (1994) Simkin, "aromaticity and antiaromaticity: electronic and structural aspects". Wiley, New York

18. (a) Generalized valence bond method: Friesner RA, Murphy RB, Beachy MD, Ringnalda MN, Pollard WT, Dunietz BD, Cao Y (1999) J Phys Chem A 103:1913, and refs. therein; (b) Hamilton JG, Palke WE (1993) J Am Chem Soc 115:4159

19. (a) The pioneering benzene paper: Hückel E, Physik Z (1931) 70: 204; (b) Other papers by Hückel, on the double bond and on unsaturated molecules, are listed in his autobiography, "Ein Gelehrtenleben. Ernst und Satire", Verlag Chemie, Weinheim, 1975, pp 178–179; (c) Kutzelnigg W (2007) Historical review: essay, "What I like about Hückel theory". J Comput Chem 28:25; (d) A Google search reveals a considerable amount of biographical information about Hückel

20. Pauling L (1960) The nature of the chemical bond, 3rd edn. Cornell University Press, Ithaca, pp 111–126

21. (a) A compact but quite thorough treatment of the simple Hückel method see ref. [3], pp 629–649; (b) A good, brief introduction to the simple Hückel method is: Roberts JD (1962) Notes on molecular orbital calculations. Benjamin, New York; (c) A detailed treatment: Streitwieser A (1961) Molecular orbital theory for organic chemists. Wiley, New York; (d) The simple Hückel method and its atomic orbital and molecular orbital background are treated in considerable depth in Zimmerman HE (1975) Quantum mechanics for organic chemists. Academic Press, New York; (e) Perhaps the definitive presentation of the simple Hückel method is Heilbronner E, Bock H (1968) Das HMO Modell und seine Anwendung, vol 1. Verlag Chemie, Weinheim (basics and implementation); vol 2, (examples and solutions), 1970; vol. 3 (tables of experimental and calculated quantities), 1970. An English translation of vol. 1 is available: "The HMO model and its application. Basics and manipulation", Verlag Chemie, 1976

22. E.g. ref. [21b], pp 87–90; ref. [21c], pp 380–391 and references therein; ref. [21d], chapter 4

23. See any introductory book on linear algebra

24. ref. [21c], chapter 1

25. Simons J, Nichols J (1997) Quantum mechanics in chemistry. Oxford University Press, New York, p 133

26. See e.g. Carey FA, Sundberg RJ (1990) Advanced organic chemistry. Part A", 3rd edn. Plenum, New York, pp 30–34

27. Jean Y, Volatron F (1993) An introduction to molecular orbitals. Oxford University Press, New York, pp 143–144

28. Truhlar DG (2012) J Chem Educ 89:573

29. (a) Schultz PA, Messmer RP (1993) J Am Chem Soc 115:10925; (b) Karadakov PB, Gerratt J, Cooper DL, Raimondi M (1993) J Am Chem Soc 115:6863

30. (a) Lowry TH, Richardson KS (1981) Mechanism and theory in organic chemistry. Harper and Row, New York, pp 26–270; (b) Streitwieser A, Caldwell RA, Ziegler GR (1969) J Am Chem Soc 91:5081, and references therein

31. (a) Dewar MJS (1969) The molecular orbital theory of organic chemistry. McGraw-Hill, New York, pp 92–98. As Dewar points out, this derivation is not really satisfactory. He gives a more rigorous approach which is a simplified version of the derivation of the Hartree-Fock equations in chapter 5, section *5.2.3*. The rigorous approach (Chapter 5) starts with the total molecular wavefunction expressed as a determinant, writes the energy in terms of this wavefunction and the Hamiltonian and finds the condition for minimum energy subject to the molecular orbitals being orthonormal (cf. orthogonal matrices, section *4.3.3*). The procedure is explained in considerable detail in chapter 5, section *5.2.3*); (b) An interpretation of α and β which gives for simple diatomics semiquantitative accuracy for bond lengths and accurate bond energies: Magnasco V (2002) Chem Phys Lett 363:544

32. (a) For a short review of the state of MO theory in its early days see Mulliken RS (1935) J Chem Phys 3:375; (b) A personal account of the development of MO theory: Mulliken RS (1989) Life of a scientist: an autobiographical account of the development of molecular orbital theory with an introductory memoir by Friedrich Hund. Springer, New York; (c) For an account of the "tension" between the MO approach of Mulliken and the valence bond approach of Pauling see Simões A, Gavroglu K (1997) Conceptual perspectives in quantum chemistry. In: Calais J-L, Kryachko E (eds) Kluwer Academic Publishers, London

33. Pauling L (1928) Chem Rev 5:173

34. Lennard-Jones JE (1929) Trans Faraday Soc 25:668

35. Coulson CA, Fischer I (1949) Philos Mag 40:386

36. Ref. [21d], pp. 52–53

37. See e.g. Rogers DW (1990) Computational chemistry using the PC. VCH, New York, pp 92–94

38. Woodward RB, Hoffmann R (1970) The conservation of orbital symmetry. Verlag Chemie, Weinheim

39. (a) For a nice review of the cyclobutadiene problem see Carpenter BK (1988) Advances in molecular modelling. JAI Press, Greenwich; (b) Calculations on the degenerate interconversion of the rectangular geometries: Santo-García JC, Pérez-Jiménez AJ, Moscardó F (2000) Chem Phys Lett 317:245

40. (a) Strictly speaking, cyclobutadiene exhibits a pseudo-Jahn-Teller effect: Kohn DW, Chen P (1993) J Am Chem Soc 115:2844; (b) For "A beautiful example of the Jahn-Teller effect" (MnF_3) see Hargittai M (1997) J Am Chem Soc 119:9042; (c) Review: Miller TA (1994) Angew Chem Int Ed 33:962

41. Frost AA, Musulin B (1953) J Chem Phys 21:572

42. Doering WE, Knox LH (1954) J Am Chem Soc 76:3203

43. Matito E, Feixas F, Solà M (2007) J Mol Struct (Theochem) 811:3

44. Dewar MJS (1969) The molecular orbital theory of organic chemistry. McGraw-Hill, New York, pp 95–98

45. Dewar MJS (1969) The molecular orbital theory of organic chemistry. McGraw-Hill, New York, pp 236–241

46. (a) Ref. [17], pp 157–161; (b) Krogh-Jespersen K, von P, Schleyer R, Pople JA, Cremer D (1978) J Am Chem Soc 100:4301; (c) The cyclobutadiene dianion, another potentially aromatic system, has recently been prepared: Ishii K, Kobayashi N, Matsuo T, Tanaka M, Sekiguchi A (2001) J Am Chem Soc 123:5356

47. Zilberg S, Haas Y (1998) J Phys Chem A 102:10843–10851

48. The most rigorous approach to assigning electron density to atoms and bonds within molecules is probably the atoms-in molecules (AIM) method of Bader and coworkers: Bader RFW (1990) Atoms in molecules. Clarendon Press, Oxford

49. Various approaches to defining bond order and atom charges are discussed in Jensen F (1999) Introduction to computational chemistry. Wiley, New York, chapter 9

50. Ref. [17], pp 177–180

51. Heintz H, Suter UW, Leontidas E (2001) J Am Chem Soc 123:11229

52. Estrada E (2003) J Phys Chem A 107:7482

53. For leading references see: (a) Hess BA, Schaad LJ (1974) J Chem Educ 51:640, and (b) Hess BA, Schaad LJ (1980) Pure Appl Chem 52:1471

54. See e.g. ref. [21c], chapters 4 and 5

55. See e.g. ref. [21c], pp. 13, 16.

56. Try Google and "simple Huckel program; examples are www.chem.ucalgary.ca/SHMO/ and www.hulis.free.fr/

57. (a) Hoffmann R (1963) J Chem Phys 39:1397; (b) Hoffmann (1964) J Chem Phys 40:2474; (c) Hoffmann R (1964) J Chem Phys 40:2480; (d) Hoffmann R (1964) J Chem Phys 40:2745; (e) Hoffmann R (1966) Tetrahedron 22:521' (f) Hoffmann R (1966) Tetrahedron 22:539; (g) Hay PJ, Thibeault JC, Hoffmann R (1975) J Am Chem Soc 97:4884

58. Wolfsberg M, Helmholz L (1952) J Chem Phys 20:837

59. Actually, *valence state* ionization energies are generally used: (a) Hinze J, Jaffe HH (1962) J Am Chem Soc 84:540 (especially pp 541–545), and references therein. (b) Pritchard HO, Skinner HA (1955) Chem Rev 55:745 (especially pp 754–755); (c) Stockis A, Hoffmann R (1980) J Am Chem Soc 102:2952. For hydrogen and helium which use their *s*-orbitals to bond, here we simply take the ordinary ionization energy as the valence state value

60. Löwdin PO (1950) J Chem Phys 18:365

61. Pilar FL (1990) Elementary quantum chemistry. McGraw-Hill, New York, pp 493–494

62. Szabo A, Ostlund NS (1989) Modern quantum chemistry. McGraw-Hill, pp 168–179. This describes an ab initio (chapter 5) calculation on HeH^+, but gives information relevant to our EHM calculation

63. Roothaan CCJ (1951) J Chem Phys 19:1445

64. Hoffmann R (1988) Solids and surfaces: a chemist's view of bonding in extended structures. VCH Publishers

65. (a) A polymeric rhenium compound: Genin HS, Lawler KA, Hoffmann R, Hermann WA, Fischer RW, Scherer W (1995) J Am Chem Soc 117:3244' (b) Chemisorption of ethyne on silicon, Liu Q, Hoffmann R (1995) J Am Chem Soc 117:4082; (c) A carbon/sulfur polymer, Genin H, Hoffmann R (1995) J Am Chem Soc 117:12328

66. (a) $IrH_2(SC_5H_5N)_2(PH_3)_2$: Liu Q, Hoffmann R (1995) J Am Chem Soc 117:10108; (b) [Ni$(SH)_2]_6$: Alemany P, Hoffmann R (1993) J Am Chem Soc 115:8290; Mn clusters: Proserpio DM, Hoffmann R, Dismukes GC (1992) J Am Chem Soc 114:4374

67. Ammeter JH, Bürgi H-B, Thibeault JC, Hoffmann R (1978) J Am Chem Soc 100:3686

68. Superior results from EHM compared to MINDO/3 and MNDO, for nonplanarity of certain C/C double bonds: Spanget-Larsen J, Gleiter R (1983) Tetrahedron 39:3345

69. An EHM that was said to give good geometries: Dixon SL, Jurs PC (1994) J Comput Chem 15:733. This method does not seem to have become widely used

Chapter 5
Ab initio Calculations

"I could have done it in a much more complicated way", said the Red Queen, immensely proud.
Attributed, probably apocryphally, to Lewis Carroll

Abstract Ab initio calculations rest on solving the Schrödinger equation; the nature of the necessary approximations determines the level of the calculation. In the simplest approach, the Hartree-Fock method, the total molecular wavefunction Ψ is approximated as a Slater determinant composed of occupied spin orbitals. To use these in practical calculations the spatial orbitals are approximated as a linear combination (a weighted sum) of basis functions. Electron correlation methods are also discussed. The main uses of the ab initio method are calculating molecular geometries, energies, vibrational frequencies, spectra, ionization energies and electron affinities, and properties like dipole moments which are connected with electron distribution. These calculations find theoretical and practical applications, since, for example, enzyme-substrate interactions depend on shapes and charge distributions, reaction equilibria and rates depend on energy differences, and spectroscopy plays an important role in identifying and understanding novel molecules. The visualization of calculated phenomena can be very important in interpreting results.

5.1 Perspective

Chapter 4 showed how quantum mechanics was first applied to molecules of real chemical interest (*pace* chemical physics) by Erich Hückel, and how the extension of the simple Hückel method by Hoffmann gave a technique of considerable usefulness and generality, the extended Hückel method. The simple and the extended Hückel methods (SHM and EHM) are both based on the Schrödinger equation, and this makes them quantum mechanical methods. Both depend on

reference to experimental quantities (i.e. on parameterization against experiment) to give actual values of calculated parameters: the SHM gives energy levels in terms of a parameter β which we could try to assign a value by comparison with experiment (actually the results of SHM calculations are usually left in terms of β), while the EHM needs experimental valence ionization energies to calculate the Fock matrix elements. The need for parameterization against experiment makes the SHM and the EHM *semiempirical* ("semiexperimental") theories. In this chapter we deal with a quantum mechanical approach that does not rely on calibration against measured chemical parameters and is therefore called *ab initio* [1, 2] meaning "from the first", from first principles. It is true that ab initio calculations give results in terms of fundamental physical constants – Planck's constant, the speed of light, the charge of the electron – that must be measured to obtain their actual numerical values, but a chemical theory could hardly be expected to calculate the fundamental physical parameters of our universe; for that we might be content to defer to cosmology.

5.2   The Basic Principles of the Ab initio Method

5.2.1   Preliminaries

In Chap. 4 we saw that wavefunctions and energy levels could be obtained by diagonalizing a Fock matrix: the equation

$$\mathbf{H} = \mathbf{C}\boldsymbol{\varepsilon}\mathbf{C}^{-1} \tag{*5.1}$$

is just another way of saying that diagonalization of $\mathbf{H}$ gives the coefficients or eigenvectors (the columns of $\mathbf{C}$ that, combined with the basis functions, yield the wavefunctions of the molecular orbitals) and the energy levels or eigenvalues (the diagonal elements of ε). Eq. (5.1) followed from

$$\mathbf{HC} = \mathbf{SC}\boldsymbol{\varepsilon} \tag{*5.2}$$

which gives Eq. (5.1) when $\mathbf{S}$ is approximated as a unit matrix (simple Hückel method, Chap. 4 Sect. 4.3.4) or when the original Fock matrix is transformed into $\mathbf{H}$ (into $\mathbf{H}'$ in the notation of Chap. 4, Sect. 4.4.1) using an orthogonalizing matrix calculated from $\mathbf{S}$ (extended Hückel method, Chap. 4 Sect. 4.4.1). To do a simple or an extended Hückel calculation the algorithm assembles the Fock matrix $\mathbf{H}$ and diagonalizes it. This is also how an ab initio calculation is done; the essential difference compared to the Hückel methods lies in the *evaluation of the matrix elements*.

In the simple Hückel method the Fock matrix elements H_{ij} are not calculated, but are instead set equal to 0 or -1 according to simple rules based on atomic connectivity (Chap. 4, Sect. 4.3.4); in the extended Hückel method the H_{ij} are

calculated from the relative positions (through S_{ij}) of the orbitals or basis functions and the ionization energies of these orbitals (Chap. 4, Sect. 4.4.1); in neither case is H_{ij} calculated from first principles. Chapter 4, Sect. 4.3.4, Eqs. (4.44) imply that H_{ij} is:

$$H_{ij} = \int \phi_i \hat{H} \phi_j dv \qquad (*5.3)$$

In ab initio calculations H_{ij} is calculated from Eq. (5.3) by actually performing the integration using explicit mathematical expressions for the basis functions ϕ_i and ϕ_j and the Hamiltonian operator $\hat{H}$; of course the integration is done by a computer following a detailed algorithm. How this algorithm works will now be outlined.

5.2.2   The Hartree SCF Method

The simplest kind of ab initio calculation is a Hartree-Fock (HF) calculation. Modern molecular HF calculations grew out of calculations first performed on atoms by Hartree[1] in 1928 [3]. The problem that Hartree addressed arises from the fact that for any atom (or molecule) with more than *one* electron an exact analytic solution of the Schrödinger equation (Chap. 4, Sect. 4.3.2) is not possible, because of the electron-electron repulsion term(s). Thus for the helium atom the Schrödinger equation (cf. Chap. 4, Sect. 4.3.3, Eqs. (4.36) and (4.37)) is, in SI units

$$\left[-\frac{h^2}{8\pi^2 m}(\nabla_1^2 + \nabla_2^2) - \frac{Ze^2}{4\pi\varepsilon_0 r_1} - \frac{Ze^2}{4\pi\varepsilon_0 r_2} + \frac{e^2}{4\pi\varepsilon_0 r_{12}} \right] \psi = E\psi \qquad (5.4)$$

Here m is the mass (kg) of the electron, e is the charge (Coulombs, positive) of the proton (= minus the charge on the electron), the variables r_1, r_2, and r_{12} are the distances (meters) of electrons 1 and 2 from the nucleus, and from each other, $Z = 2$ is the number of protons in the nucleus, and ε_0 is something called the permitivity of empty space; the factor $4\pi\varepsilon_0$ is needed to make SI units consistent. The force (newtons) between charges q_1 and q_2 separated by r is $q_1 q_2 / 4\pi\varepsilon_0 r^2$, so the potential energy (joules) of the system is $q_1 q_2 / 4\pi\varepsilon_0 r$ (energy is force × distance).

Hamiltonians can be written much more simply by using *atomic units*. Let's take Planck's constant, the electron mass, the proton charge, and the permitivity of space as the building blocks of a system of units in which $h/2\pi$, m, e, and $4\pi\varepsilon_0$ are numerically equal to 1 (i.e. $h = 2\pi$, $m = 1$, $e = 1$, and $\varepsilon_0 = 1/4\pi$; the numerical values of physical constants are always dependent on our system of units). These

---

[1]Douglas Hartree, born Cambridge, England, 1897. Ph.D. Cambridge, 1926. Professor applied mathematics, theoretical physics, Manchester, Cambridge. Died Cambridge, 1958.

$(h/2\pi$, m, e, and $4\pi\varepsilon_0)$ are the units of angular momentum, mass, charge, and permitivity in the system of atomic units. In this system Eq. (5.4) becomes

$$\left(-\frac{1}{2}\nabla_1^2 - \frac{1}{2}\nabla_2^2 - \frac{Z}{r_1} - \frac{Z}{r_2} + \frac{1}{r_{12}}\right)\psi = E\psi \tag{5.5}$$

Using atomic units simplifies writing quantum-mechanical expressions, and also means that the numerical (in these units) results of calculations are independent of the currently accepted values of physical constants in terms of kg, Coulombs, meters, and seconds (of course, when we convert from atomic to SI units we must use accepted SI values of m, e, etc.). The atomic units of energy and length are particularly important to us. We can get the atomic unit of a quantity by combining $h/2\pi$, m, e, and $4\pi\varepsilon_0$ to give the ab expression with the required dimensions. The atomic units of length and energy, the bohr and the hartree, turn out to be:

Length 1 bohr $=$ a$_0 = 4\pi\varepsilon_0(h/2\pi)^2/me^2 = \varepsilon_0 h^2/\pi me^2 = 0.05292\,\text{nm} = 0.5929\,\text{Å}$
Energy 1 hartee $=$ E$_h$ (or h) $= e^2/4\pi\varepsilon_0 a_0$; 1 hartree/particle $= 2625.5\,\text{kJ mol}^{-1}$

The bohr is the radius of a hydrogen atom in the Bohr model (Chap. 4, Sect. 4.2.5), or the most probable distance of the electron from the nucleus in the fuzzier Schrödinger picture (Chap. 4, Sect. 4.2.5). The hartree is the energy needed to move a stationary electron one bohr distant from a proton away to infinity. The energy of a hydrogen atom, relative to infinite proton/electron separation as zero, is $-\frac{1}{2}$ hartree: the potential energy is -1 h and the kinetic energy (always positive) is $+\frac{1}{2}$ h. Note that atomic units derived by starting with the old Gaussian system (cm, grams, statcoulombs) differ by a $4\pi\varepsilon_0$ factor from the SI-derived ones.

The helium atom Hamiltonian

$$\hat{H} = -\frac{1}{2}\nabla_1^2 - \frac{1}{2}\nabla_2^2 - \frac{Z}{r_1} - \frac{Z}{r_2} + \frac{1}{r_{12}} \tag{*5.6}$$

consists of five terms, signifying (Fig. 5.1) from left to right: the kinetic energy of electron 1, the kinetic energy of electron 2, the potential energy of the attraction of the nucleus (charge $Z = 2$) for electron 1, the potential energy of the attraction of the nucleus for electron 2, and the potential energy of the repulsion between electron 1 and electron 2. This is not the *exact* Hamiltonian, for it neglects effects due to relativity and to magnetic interactions such as spin-orbit coupling [4]; these effects are rarely important in calculations involving lighter atoms, say those in the first two or three full rows of the periodic table (up to about chlorine or bromine). Relativistic quantum chemical calculations will be briefly discussed later. The wavefunction ψ is the "total", overall wavefunction of the atom and can be approximated, as we will see later for molecular HF calculations, as a combination of wavefunctions for various energy levels. The problem with solving Eq. (5.5) exactly arises from the $1/r_{12}$ term. This makes it impossible to separate the
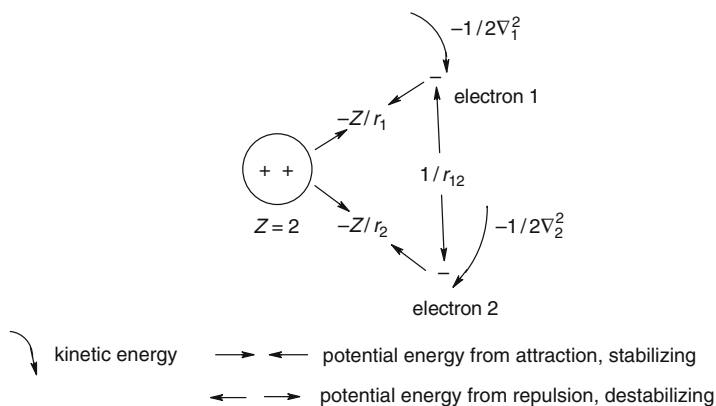
Fig. 5.1 The terms in the helium atom Hamiltonian, $\hat{H} = -\frac{1}{2}\nabla_1^2 - \frac{1}{2}\nabla_2^2 - \frac{Z}{r_1} - \frac{Z}{r_2} + \frac{1}{r_{12}}$

Schrödinger equation for helium into two one-electron equations which, like the hydrogen atom equation, could be solved exactly (for treatments of the hydrogen and helium atoms see the appropriate sections of references 1). This problem arises in any system with three or more interacting moving objects, whether subatomic particles or planets. In fact the *many-body problem* is an old one even in classical mechanics, going back to eighteenth century studies in celestial mechanics [5]. The three-particle hydrogen molecule ion, HH$^{\cdot+}$, with two heavy particles and one light one, can be solved"exactly" – but only within the Born-Oppenheimer approximation [6]. The impossibility of an analytic solution to polyelectronic atoms and molecules prompted Hartree's approach to calculating wavefunctions and energy levels for atoms.

Hartree's method was to write a plausible approximate polyelectronic wavefunction (a "guess") for an atom as the product of one-electron wavefunctions:

$$\psi_0 = \psi_0(1)\psi_0(2)\psi_0(3)\cdots\psi_0(n) \tag{5.7}$$

This function is called a Hartree product. Here ψ_0 is a function of the coordinates of all the electrons in the atom, $\psi_0(1)$ is a function of the coordinates of electron 1, $\psi_0(2)$ is a function of the coordinates of electron 2, etc.; the one-electron functions $\psi_0(1)$, $\psi_0(2)$, etc. are called atomic orbitals (molecular orbitals if we were dealing with a molecule). The initial guess, ψ_0, is our zeroth approximation to the true total wavefunction ψ, zeroth because we have not yet started to refine it with the Hartree process; it is based on the zeroth approximations $\psi_0(1)$, $\psi_0(2)$, etc. To apply the Hartree process we first solve for electron one a *one-electron* Schrödinger equation in which the electron-electron repulsion comes from electron one and an average, smeared-out electrostatic field calculated from $\psi_0(2)$, $\psi_0(3)$, ..., $\psi_0(n)$, due to all the *other* electrons. The only moving particle in this equation is

electron one. Solving this equation gives $\psi_1(1)$, an improved version of $\psi_0(1)$. We next solve for electron 2 a one-electron Schrödinger equation with electron two moving in an average field due to the electrons of $\psi_1(1)$, $\psi_0(3)$, ..., $\psi_0(n)$, continuing to electron n moving in a field due to $\psi_1(1)$, $\psi_1(2)$, ..., $\psi_1(n-1)$. This completes the first cycle of calculations and gives

$$\Psi_1 = \psi_1(1)\psi_1(2)\psi_1(3)\cdots\psi_1(n) \tag{5.8}$$

Repetition of the cycle gives

$$\Psi_2 = \psi_2(1)\psi_2(2)\psi_2(3)\cdots\psi_2(n) \tag{5.9}$$

The process is continued for k cycles till we have a wavefunction Ψ_k and/or an energy calculated from Ψ_k that are essentially the same (according to some reasonable criterion) as the wavefunction and/or energy from the previous cycle. This happens when the functions $\psi(1)$, $\psi(2)$, ..., $\psi(n)$ are changing so little from one cycle to the next that the smeared-out electrostatic field used for the electron-electron potential has (essentially) ceased to change. At this stage the field of cycle k is essentially the same as that of cycle $k-1$, i.e. it is "consistent with" this previous field, and so the Hartree procedure is called the *self-consistent-field-procedure*, which is usually abbreviated as the *SCF* procedure.

There are two problems with the Hartree product of Eq. (5.7). Electrons have a property called spin, among the consequences of which is that not more than two electrons can occupy one atomic or molecular orbital (this is one statement of the Pauli exclusion principle (Chap. 4, Sect. 4.2.6). In the Hartree approach we acknowledge this only in an *ad hoc* way, simply by not placing more than two electrons in any of the component orbitals ψ that make up our (approximate) total wavefunction ψ. The second problem comes from the fact that electrons are indistinguishable. If we have a wavefunction of the coordinates of two or more indistinguishable particles, then switching the positions of two of the particles, i.e. exchanging their coordinates, must either leave the function unchanged or change its sign. This is because all physical manifestations of the wavefunction must be unchanged on switching indistinguishable particles, and these manifestations depend only on its *square* (more strictly on the square of its absolute value, i.e. on $|\psi|^2$, to allow for the fact that ψ may be a complex, as distinct from a real, function). This should be clear from the equations below for a two-particle function:

$$\text{if} \qquad \psi_a = f(x_1, y_1, z_1; x_2, y_2, z_2)$$

$$\text{and} \qquad \psi_b = f(x_2, y_2, z_2; x_1, y_1, z_1)$$

$$\text{then} \qquad \left|\psi_a\right|^2 = \left|\psi_b\right|^2$$

$$\text{if and only if} \qquad \psi_b = \psi_a \text{ or } \psi_b = -\psi_a$$

If switching the coordinates of two of the particles leaves the function unchanged, it is said to be symmetric with respect to particle exchange, while if the function changes sign it is said to be antisymmetric with respect to particle exchange. Comparing the predictions of theory with the results of experiment shows [7] that electronic wavefunctions are actually antisymmetric with respect to exchange (such particles are called fermions, after the physicist Enrico Fermi; particles like photons whose wavefunctions are exchange-symmetric are called bosons, after the physicist S. Bose). Any rigorous attempt to approximate the wavefunction ψ should use an antisymmetric function of the coordinates of the electrons $1, 2, \cdots n$, but the Hartree product is symmetric rather than antisymmetric; for example, if we approximate a helium atom wavefunction as the product of two hydrogen atom $1s$ orbitals, then if $\psi_a = 1s(x_1, y_1, z_1)\, 1s(x_2, y_2, z_2)$ and $\psi_b = 1s(x_2, y_2, z_2)\, 1s(x_1, y_1, z_1)$, then $\psi_a = \psi_b$.

These defects of the Hartree SCF method were corrected by Pauling (1928) [8a], Slater (1929) [8b] and Fock (1930) [8c]. Pauling (Chap. 4, footnote 21) and Slater showed that as a first approximation at least a wavefunction can be written as a determinant of spin orbitals (Sect. 5.2.3.1). Although Slater's publication appeared in the year after Pauling's, this determinant is called a Slater[2] determinant, perhaps because physicists paid little attention to publications by chemists. Fock (Chap. 4, footnote 27), in a long, mathematically elaborate paper [8c], developed the explicit form of the Fock operator (Sect. 5.2.3.4), the operator which acts on the wavefunction to create atomic or molecular energy levels in the Hartree-Fock equations. Slater, in the year following his presentation of the determinant formulation of the wavefunction, made an admittedly tenuous suggestion [8d] for extending the Hartree method to molecules, but its brevity and the lack of any explicit equations justifies limiting the name of the method to Hartree-Fock.

5.2.3   The Hartree-Fock Equations

5.2.3.1   Slater Determinants

The Hartree wavefunction (above) is a product of one-electron functions called orbitals, or, more precisely, *spatial* orbitals: these are functions of the usual space

---

[2]John Slater, born Oak Park Illinois, 1900. Ph.D. Harvard, 1923. Professor of physics, Harvard, 1924–1930; MIT 1930–1966; University of Florida at Gainesville, 1966–1976. Author of 14 textbooks, contributed to solid-state physics and quantum chemistry, developed X-alpha method (early density functional theory method). Died Sanibel Island, Florida, 1976.

coordinates *x,y,z*. The Slater wavefunction is composed, not just of spatial orbitals, but of *spin orbitals*. A spin orbital ψ(spin) is the product of a spatial orbital and a spin function, α or β: The spin orbitals corresponding to a given spatial orbital are

$$\psi(\text{spin}\,\alpha) = \psi(\text{spatial})\alpha = \psi(x, y, z)\alpha$$

and
$$\psi(\text{spin}\,\beta) = \psi(\text{spatial})\beta = \psi(x, y, z)\beta$$

As the function ψ(spatial) has as its variables the coordinates *x,y,z*, so the spin functions α and β have as *their* variables a spin coordinate, sometimes denoted ξ (Greek letter *kzi* or *zi*) or ω (Greek *omega*). We know that a wavefunction ψ fits in with an operator and eigenvalues, say the energy operator and energy eigenvalues, according to the equation $\hat{H}\psi = E\psi$. Analogously, the spin functions α and β are associated with the spin operator $\hat{S}_z$ according to $\hat{S}_z\alpha = \frac{1}{2}(h/2\pi)\alpha$ and $\hat{S}_z\beta = -\frac{1}{2}(h/2\pi)\beta$. Unlike most other functions, then, α and β each have only one eigenvalue, $\frac{1}{2}(h/2\pi)$ and $-\frac{1}{2}(h/2\pi)$, respectively. A spin function has the peculiar property that it is zero unless $\xi = \frac{1}{2}$ (α spin function) or $\xi = -\frac{1}{2}$ (β spin function). A function that is zero everywhere except at one value of its variable, where it spikes sharply, is a *delta function* (invented by Dirac–footnote Chap. 4, Sect. 4.2.3). Since the spin function ψ (spin α or β) describing an electron exists only when the spin variable $\xi = \pm 1/2$, these two values can be considered the allowed values of the spin quantum number m_s mentioned in Chap. 4, Sect. 4.2.6. Sometimes an electron with spin quantum number 1/2 ("an electron with spin 1/2") is called an α electron, and said to have *up* spin, and an electron with spin $-1/2$ is called a β electron, and said to have *down* spin. Up and down electrons are often denoted by arrows $\uparrow$ and $\downarrow$, respectively. A nice, brief treatment of the delta function and of the mathematical treatment of the spin functions is given by Levine [9].

The Slater wavefunction differs from the Hartree function not only in being composed of spin orbitals rather than just spatial orbitals, but also in the fact that it is not a simple product of one-electron functions, but rather a *determinant* (Chap. 4, Sect. 4.3.3) whose elements are these functions. To construct a Slater wavefunction (Slater determinant) for a closed-shell species (the only kind we consider in any detail here), we use each of the occupied spatial orbitals to make two spin orbitals, by multiplying the spatial orbital by α and, separately, by β. The spin orbitals are then filled with the available electrons. An example should make the procedure clear (Fig. 5.2). Suppose we wish to write a Slater determinant for a four-electron closed-shell system. We need two spatial molecular orbitals, since each can hold a maximum of two electrons; each spatial orbital ψ(spatial) is used to make two spin orbitals, ψ(spatial)α and ψ(spatial)β (alternatively, each spatial orbital could be thought of as a composite of two spin orbitals, which we are separating and using to build the determinant). Along the first (top) row of a determinant we write successively the first α spin orbital, the first β spin orbital, the second α spin orbital, and the second β spin orbital, using up our occupied spatial (and thus spin) orbitals. Electron one is then assigned to all four spin orbitals of the first row–in a sense it is allowed to roam among these four spin orbitals [10]. The second row of the
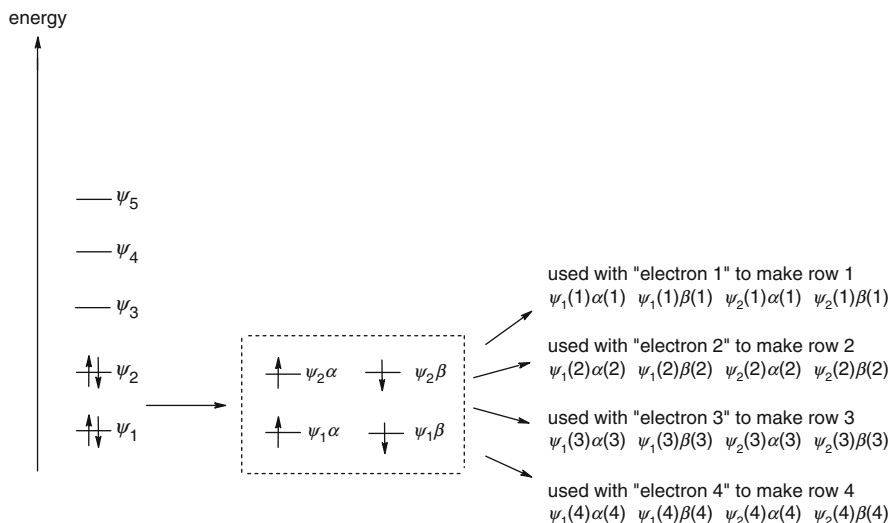
energy

used with "electron 1" to make row 1
$\psi_1(1)\alpha(1)$ $\psi_1(1)\beta(1)$ $\psi_2(1)\alpha(1)$ $\psi_2(1)\beta(1)$

used with "electron 2" to make row 2
$\psi_1(2)\alpha(2)$ $\psi_1(2)\beta(2)$ $\psi_2(2)\alpha(2)$ $\psi_2(2)\beta(2)$

used with "electron 3" to make row 3
$\psi_1(3)\alpha(3)$ $\psi_1(3)\beta(3)$ $\psi_2(3)\alpha(3)$ $\psi_2(3)\beta(3)$

used with "electron 4" to make row 4
$\psi_1(4)\alpha(4)$ $\psi_1(4)\beta(4)$ $\psi_2(4)\alpha(4)$ $\psi_2(4)\beta(4)$

Fig. 5.2 A Slater determinant is made from spin orbitals derived from the occupied spatial molecular orbitals and two spin functions, α and β

determinant is the same as the first, except that it refers to electron two rather than electron one; likewise the third and fourth rows refer to electrons three and four, respectively. The result is the determinant of Eq. (5.10).

$$\Psi = \frac{1}{\sqrt{4!}} \begin{vmatrix} \psi_1(1)\alpha(1) & \psi_1(1)\beta(1) & \psi_2(1)\alpha(1) & \psi_2(1)\beta(1) \\ \psi_1(2)\alpha(2) & \psi_1(2)\beta(2) & \psi_2(2)\alpha(2) & \psi_2(2)\beta(2) \\ \psi_1(3)\alpha(3) & \psi_1(3)\beta(3) & \psi_2(3)\alpha(3) & \psi_2(3)\beta(3) \\ \psi_1(4)\alpha(4) & \psi_1(4)\beta(4) & \psi_2(4)\alpha(4) & \psi_2(4)\beta(4) \end{vmatrix} \qquad (*5.10)$$

The $1/\sqrt{(4!)}$ factor ensures that the wavefunction is normalized, i.e. that $|\psi|^2$ integrated over all space $= 1$. This *Slater determinant* ensures that there are no more than two electrons in each spatial orbital, since for each spatial orbital there are only two one-electron spin functions, and it ensures that ψ is antisymmetric since switching two electrons amounts to exchanging two rows of the determinant, and this changes its sign (Chap. 4, Sect. 4.3.3). Note that instead of assigning the electrons successively to row 1, row 2, etc., we could have placed them in column 1, column 2, etc.: ψ' of Eq. (5.11) $= \psi$ of Eq. (5.10). Some authors use the row format for the electrons, others the column format:

$$\Psi' = \frac{1}{\sqrt{4!}} \begin{vmatrix} \psi_1(1)\alpha(1) & \psi_1(2)\alpha(2) & \psi_1(3)\alpha(3) & \psi_1(4)\alpha(4) \\ \psi_1(1)\beta(1) & \psi_1(2)\beta(2) & \psi_1(3)\beta(3) & \psi_1(4)\beta(4) \\ \psi_2(1)\alpha(1) & \psi_2(2)\alpha(2) & \psi_2(3)\alpha(3) & \psi_2(4)\alpha(4) \\ \psi_2(1)\beta(1) & \psi_2(2)\beta(2) & \psi_2(3)\beta(3) & \psi_2(4)\beta(4) \end{vmatrix} \quad (5.11)$$

Slater determinants enforce the Pauli exclusion principle, which forbids any two electrons in a system to have all quantum numbers the same. This is readily seen for an atom: if the three quantum numbers n, l and m_{m} of $\psi(x, y, z)$ (Chap. 4, Sect. 4.2.6) and the spin quantum number m_{s} of α or β were all the same for any electron, two rows (or columns, in the alternative formulation) would be identical and the determinant, hence the wavefunction, would vanish (Chap. 4, Sect. 4.3.3).

For $2n$ electrons (we are limiting ourselves for now to *even*-electron species, as the theory for these is simpler) the general form of a Slater determinant is clearly the $2n \times 2n$ determinant

$$\Psi_{2n} = \frac{1}{\sqrt{(2n)!}}$$

$$\times \begin{vmatrix} \psi_1(1)\alpha(1) & \psi_1(1)\beta(1) & \psi_2(1)\alpha(1) & \psi_2(1)\beta(1) & \cdots & \psi_n(1)\beta(1) \\ \psi_1(2)\alpha(2) & \psi_1(2)\beta(2) & \psi_2(2)\alpha(2) & \psi_2(2)\beta(2) & \cdots & \psi_n(2)\beta(2) \\ \vdots & \vdots & \vdots & \vdots & & \\ \psi_1(2n)\alpha(2n) & \psi_1(2n)\beta(2n) & \psi_2(2n)\alpha(2n) & \psi_2(2n)\beta(2n) & \cdots & \psi_n(2n)\beta(2\mathrm{n}) \end{vmatrix}$$

$$(5.12)$$

The Slater determinant for the total wavefunction ψ of a $2n$-electron atom or molecule is a $2n \times 2n$ determinant with $2n$ rows due to the $2n$ electrons and $2n$ columns due to the $2n$ spin orbitals (you can interchange the row/column format); since these are closed-shell species, the number of spatial orbitals ψ is half the number of electrons. We use the n occupied spatial orbitals (the $2n$ occupied spin orbitals) to make the determinant. Antisymmetry can also be imposed on the wavefunction, less transparently, with an *antisymmetrization operator* [11].

The determinant (= total molecular wavefunction ψ) just described will lead to (remainder of Sect. 5.2) n occupied, and a number of unoccupied, component spatial molecular orbitals ψ. These orbitals ψ from the straightforward Slater determinant are called *canonical* (in mathematics the word means "in simplest or standard form") molecular orbitals. Since each occupied spatial ψ can be thought of as a region of space which accommodates a pair of electrons, we might expect that when the shapes of these orbitals are displayed ("visualized"; Sect. 5.5.4) each one would look like a bond or a lone pair. However, this is often not the case; for example, we do not find that one of the canonical MOs of water connects the O with one H, and another canonical MO connects the O with another H. Instead most of these MOs are spread over much of a molecule–delocalized (lone pairs, unlike conventional bonds, do tend to stand out). However, it is possible to combine the canonical MOs to get localized MOs which look like our conventional bonds and lone pairs. This is done by using the columns (or rows) of the Slater ψ to create

a ψ with modified columns (or rows): if a column/row of a determinant is multiplied by k and added to another column/row, the determinant is unchanged (Chap. 4, Sect. 4.3.3). We see that if this is applied to the Slater determinant, we will get a "new" determinant corresponding to exactly the same total wavefunction, i.e. to the same molecule, but built up from different component occupied MOs ψ. The new ψ and the new ψ's are no less or more correct than the previous ones, but by appropriate manipulation of the columns/rows the ψ's can be made to correspond to our ideas of bonds and lone pairs. These localized MOs are sometimes useful.

5.2.3.2 Calculating the Atomic or Molecular Energy

The next step in deriving the Hartree-Fock equations is to express the energy of the molecule or atom in terms of the total wavefunction ψ; the energy will then be minimized with respect to each of the component molecular (or atomic; an atom is a special case of a molecule) spin orbitals $\psi\alpha$ and $\psi\beta$ (cf. the minimization of energy with respect to basis function coefficients in Chap. 4, Sect. 4.3.4). The derivation of these equations involves considerable algebraic manipulation, which is at times hard to follow without actually writing out the intermediate expressions. The procedure has been summarized by Pople and Beveridge [12a] and Pople and Nesbet [12b], and a less condensed account is given by Lowe [13].

It follows from the Schrödinger equation that the energy of a system is given by

$$E = \frac{\int \psi^* \hat{H} \psi d\tau}{\int \psi^* \psi d\tau} \tag{5.13}$$

This is similar to Eq. (4.40) in Chap. 4, but here the total wavefunction ψ has been specified, and allowance has been made for the possibility of ψ being a complex function by utilizing its complex conjugate ψ^*; this ensures that E, the energy of the atom or molecule, will be real. If ψ is complex then $\psi^2 d\tau$ will not be a real number, while $\psi^* \psi d\tau = |\psi|^2 d\tau$ will, as must be the case for a probability. Integration is with respect to three spatial coordinates and one spin coordinate, for each electron. This is symbolized by $d\tau$ (τ = Greek *tau*), which means *dxdydzdξ*, so for a $2n$-electron system these integrals are actually $4 \times 2n$-fold, each electron having its set of four coordinates. Working with the usual normalized wavefunctions makes the denominator unity, and Eq. (5.13) can then be written

$$E = \int \psi^* \hat{H} \psi \, d\tau$$

or using the more compact Dirac notation for integrals (Chap. 4, Sect. 4.4.1)

$$E = \langle \psi | \hat{H} | \psi \rangle \tag{5.14}$$

In Eq. (5.14) it is understood that the first ψ is really ψ^*, and that the integration variables are the space and spin coordinates. The vertical bars are only to visually separate the operator from the two functions, supposedly for clarity.

We next substitute into Eq. (5.14) the Slater determinant for ψ (and ψ^*) and the explicit expression for the Hamiltonian. A simple extension of the helium Hamiltonian of Eq. (5.5) to a molecule with $2n$ electrons and μ atomic nuclei (the μth nucleus has charge Z_μ) gives

$$\hat{H} = \sum_{i=1}^{2n} -\frac{1}{2}\nabla_i^2 - \sum_{\text{all }\mu, i}\frac{Z_\mu}{r_{\mu i}} + \sum_{\text{all }ij}\frac{1}{r_{ij}} \tag{5.15}$$

Just like the helium Hamiltonian, the molecular Hamiltonian $\hat{H}$ in Eq. (5.15) is composed (from left to right) of electron kinetic energy terms, nucleus-electron attraction potential energy terms, and electron-electron repulsion potential energy terms (cf. Fig. 5.1). This is actually the *electronic* Hamiltonian, since nucleus-nucleus repulsion potential energy terms have been omitted; from the Born-Oppenheimer approximation (Chap. 2, Sect. 2.3) these can simply be added to the electronic energy after this has been calculated, giving the total molecular energy for a molecule with "frozen nuclei" (calculation of the vibrational energy, the zero-point energy, is discussed later). Calculation of the internuclear potential energy is trivial:

$$V_{NN} = \sum_{\text{all }\mu, v}\frac{Z_\mu Z_v}{r_{\mu v}} \tag{5.16}$$

Substituting into Eq. (5.14) the Slater determinant and the molecular Hamiltonian gives, after much algebraic manipulation

$$E = 2\sum_{i=1}^{n}H_{ii} + \sum_{i=1}^{n}\sum_{j=1}^{n}\left(2J_{ij} - K_{ij}\right) \tag{5.17}$$

for the electronic energy of a $2n$-electron molecule (the sums are over the n occupied spatial orbitals ψ). The terms in Eq. (5.17) have these meanings:

$$H_{ii} = \int \psi_i^*(1)\hat{H}^{\,\text{core}}(1)\psi_i(1)dv \tag{5.18}$$

where

$$\hat{H}^{\,\text{core}}(1) = -\frac{1}{2}\nabla_1^2 - \sum_{\text{all }\mu}\frac{Z_\mu}{r_{\mu 1}} \tag{5.19}$$

The operator $\hat{H}^{\,\text{core}}$ is so called because it leads to H_{ii}, the electronic energy of a single electron moving simply under the attraction of a nuclear "core", with all the

other electrons stripped away; H_{ii} is the electronic energy of, for example, H, He$^+$, H$_2^+$, or CH$_4^{9+}$ (of course, it is different for these various species) . Note that $\hat{H}^{core}$ (1) represents the kinetic energy of electron 1 plus the potential energy of attraction of that electron to each of the nuclei μ; the 1 in parentheses in these equations is just a label showing that the same electron is being considered in ψ_i^*, ψ_i and $\hat{H}^{core}$ (we could have used, say, 2 instead). The integration in Eq. (5.18) is respect to spatial coordinates only, ($dv = dxdydz$, not $d\tau$) because spin coordinates have been "integrated out": on integration, i.e. on summation over the discrete spin variable, these give 0 or 1 [12, 14]. We are left with the three spatial coordinates as integration variables (x,y,z) for each electron and so the integral is sixfold:

$$J_{ij} = \int \psi_i^*(1)\psi_i(1)\left(\frac{1}{r_{12}}\right)\psi_j^*(2)\psi_j(2)dv_1dv_2 \tag{5.20}$$

J is called a Coulomb integral; it represents the electrostatic (i.e. Coulombic) repulsion between an electron in ψ_i and one in ψ_j (ψ_{ii} for repulsion between electrons in the same spatial orbital). This may be clearer if one considers the integral as a sum of potential energy terms involving repulsion between infinitesimal volume elements dv (Fig. 5.3). The 1 and 2 are just labels showing we are considering two electrons. The integrals J and K allow each electron to experience the *average electrostatic repulsion of a charge cloud due to all the other electrons*. This pretence that electron-electron repulsion occurs between an electron and a charge cloud rather than between all possible pairs of electrons as point particles is *the major deficiency of the Hartree-Fock method* and transcending this approximation is the reason for the development of the post-Hartree-Fock methods discussed
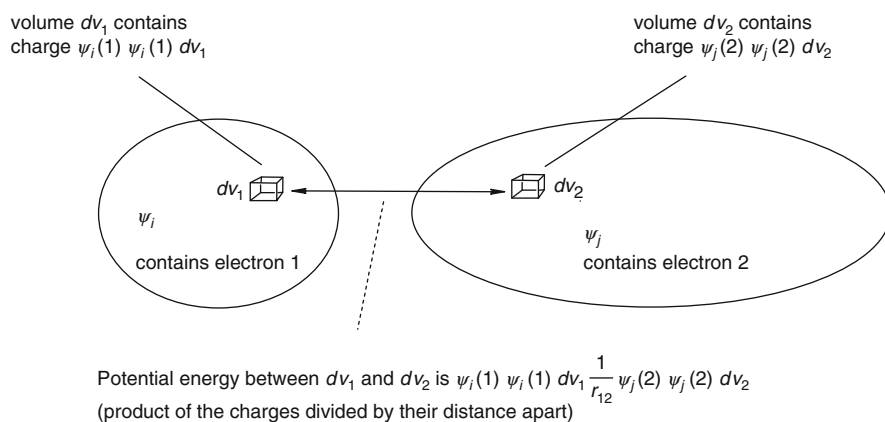
volume dv_1 contains
charge $\psi_i(1)\,\psi_i(1)\,dv_1$

volume dv_2 contains
charge $\psi_j(2)\,\psi_j(2)\,dv_2$

dv_1 ψ_i contains electron 1

dv_2 ψ_j contains electron 2

Potential energy between dv_1 and dv_2 is $\psi_i(1)\,\psi_i(1)\,dv_1\dfrac{1}{r_{12}}\psi_j(2)\,\psi_j(2)\,dv_2$
(product of the charges divided by their distance apart)

Fig. 5.3 The coulomb integral (J integral) represents the electrostatic repulsion between two charge clouds, due to electron 1 in orbital ψ_i and electron 2 in orbital ψ_j (for an electron pair in the same spatial orbital, the charge clouds can be taken as due to different spin orbitals).
$$J_{ij} = \int \psi_i^*(1)\psi_i(1)\left(\frac{1}{r_{12}}\right)\psi_j^*(2)\psi_j(2)dv_1dv_2$$

later. Since J represents potential energy corresponding to a destabilizing electrostatic repulsion, it is positive. As for H_{ii} in Eq. (5.18), the integration is with respect to spatial coordinates because the spin coordinates have been integrated out. There are six integration variables, x,y,z for electron 1 (dv_1) and x,y,z for electron 2 (dv_2), and so the integral is sixfold. Note that the ab initio Coulomb integral J is not the same as what we called a Coulomb integral in simple Hückel theory; that was $\alpha = \int \phi_i \hat{H} \phi_i dv$ (Chap. 4, Eq. (4.61)) and represents at least very crudely the energy of an electron in the p orbital ϕ_i (Chap. 4, Sect. 4.3.4). The ab initio Coulomb integral can also be written

$$J_{ij} = \int \psi_i^*(1)\psi_j^*(2)\left(\frac{1}{r_{12}}\right)\psi_i(1)\psi_j(2)dv_1 dv_2 \qquad (5.21)$$

but unlike (20) this does not notationally emphasize the repulsion (invoked by the $1/r_{12}$ operator) between electron 1 and electron 2, on the left and right, respectively, of $1/r_{12}$ in Eq. (5.20).

$$K_{ij} = \int \psi_i^*(1)\psi_j^*(2)\left(\frac{1}{r_{12}}\right)\psi_i(2)\psi_j(1)dv_1 dv_2 \qquad (5.22)$$

K is called an exchange integral; mathematically, it arises from Slater determinant expansion terms that differ only in exchange of electrons. Note that the terms on either side of $1/r_{12}$ differ by exchange of electrons. It is often said to have no simple physical interpretation, and even to represent an "exchange force", but looking at Eq. (5.17), we see we can regard K as a kind of correction to J, reducing the effect of J (both J and K are positive, with K smaller), i.e. reducing the electrostatic potential energy due to the mutual ψ_i, ψ_j charge cloud repulsion referred to above in connection with J and K. This reduction in repulsion arises because as particles with an antisymmetric wavefunction, two electrons can't occupy the same spin orbital (roughly, can't be at the same point at the same time), and can occupy the same spatial orbital only if they have opposite spins. Thus two electrons *of the same spin* avoid each other more assiduously than expected only from the Coulombic repulsion that is taken into account by J. We could consider the summed $2J - K$ terms of Eq. (5.17) to be the true Coulombic repulsion, corrected for electron spin, i.e. corrected for the Pauli exclusion principle effect. The J and K interactions are shown in Fig. 5.4 for a four-electron molecule, the smallest closed-shell system in which K integrals arise. A detailed exposition of the significance of the Hartree-Fock integrals is given by Dewar [15]. The extra tendency of same-spin electrons to avoid one another is sometimes called "Pauli repulsion", and is said to be what prevents all material objects (like molecules) from interpenetrating; this term is convenient but can be misleading, because there is no special force associated with the effect: the only forces known to science are the electromagnetic, gravitational, weak nuclear and strong nuclear. Note that outside the nucleus the only significant forces in atoms and molecules are electrostatic
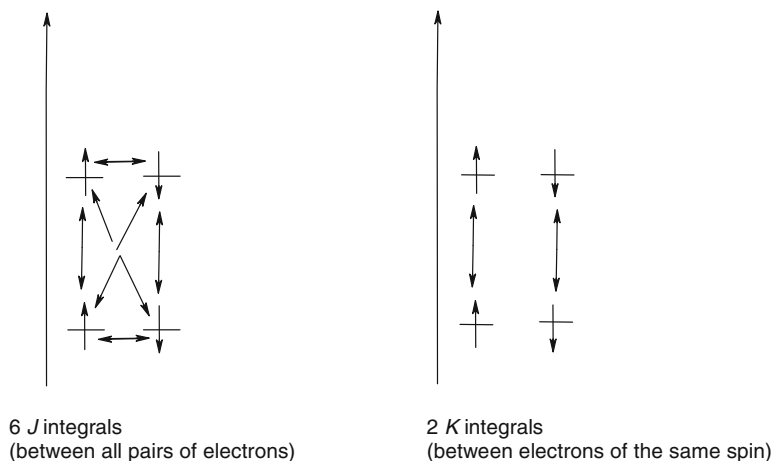
6 *J* integrals
(between all pairs of electrons)

2 *K* integrals
(between electrons of the same spin)

Fig. 5.4 The *J* integrals represent interactions between all pairs of electrons; the *K* integrals represent interactions between only electrons of the same spin

i.e. electromagnetic); there are no weird "quantum-mechanical forces" in chemistry [16] (in nuclear chemistry the well-defined weak and strong forces may come into play). Chemical reactions involve the shuffling of atomic nuclei under the influence of the electromagnetic force.

5.2.3.3 The Variation Theorem (Variation Principle)

The energy calculated from Eq. (5.14) is the *expectation value* of the energy operator $\hat{H}$, i.e. the expectation value of the Hamiltonian operator. In quantum mechanics an integral of a wavefunction "over" an operator, like $\langle \psi | \hat{H} | \psi \rangle$ in Eq. (5.14), is the *expectation value* of that operator. The expectation value is the value (strictly, the quantum-mechanical average value) of the physical quantity represented by the operator. Every "observable", i.e. every measurable property of a system, is thought to have a quantum mechanical operator from which the property could be calculated, at least in principle, by integrating the wavefunction over the operator. The expectation value of the energy operator $\hat{H}$ (for which a better symbol might have been $\hat{E}$) is the energy E of the molecule or atom. Of course this energy will be the exact, true energy of the molecule only if the wavefunction Ψ and the Hamiltonian $\hat{H}$ are exact. The variation theorem states that *the energy calculated from* Eq. (5.14) *must be greater than or equal to the true ground-state energy of the molecule*. The theorem [17] (it can be stated more rigorously, specifying that $\hat{H}$ must be time-independent and Ψ must be normalized and well-behaved) assures us that any ground state (we examine electronic ground states much more frequently than we do excited states) energy we calculate

"variationally", i.e. using Eq. (5.14), must be greater than or equal to the true energy of the molecule. This is useful because it tells us that a test for the quality of a wavefunction is the value of the energy calculated from it variationally: the lower the better. We can try to improve our wavefunction, checking the variational energy against that from previous functions. In practice, any molecular wavefunction we insert into Eq. (5.14) is always only an approximation to the true wavefunction and so the variationally calculated molecular energy will always be greater than the true energy. The Hartree-Fock energy is variational, but as we will see, not all quantum chemical energies are. The Hartree-Fock energy levels off at a value above the true energy as the Hartree-Fock wavefunction, based on a Slater determinant, is improved; this is discussed in Sect. 5.5, in connection with post-Hartree-Fock methods.

5.2.3.4   Minimizing the Energy; The Hartree-Fock Equations

The Hartree-Fock equations are obtained from Eq. (5.17) by minimizing the energy with respect to the atomic or molecular orbitals ψ. The minimization is carried out with the constraint that these orbitals ψ comprising Ψ in Eq. (5.14) remain orthogonal, for any two eigenvectors of the energy operator corresponding to different eigenvalues (energy levels) are orthogonal (see the discussion of Hermitian operators in any standard book on quantum mechanics), and we also choose to make the ψ normalized, thus making their overlap matrix $\mathbf{S}$ simply orthonormal. Minimizing a function subject to constraints can be done using the method of undetermined Lagrangian multipliers [18]. For orthonormality the overlap integrals S of $\mathbf{S}$ must be constants ($= \delta_{ij}$, i.e. 0 or 1) and at the minimum the energy is constant ($= E_{\min}$). Thus at $E_{\min}$ any linear combination of E and S_{ij} is constant:

$$E + \sum_{i=1}^{n} \sum_{j=1}^{n} l_{ij} S_{ij} = constant \tag{5.23}$$

where l_{ij} are the Lagrangian multipliers; we don't know what they are, physically, yet (after all, they are "undetermined"). Differentiating with respect to the ψ's of the S's:

$$dE + d \sum_{i=1}^{n} \sum_{j=1}^{n} l_{ij} S_{ij} = 0 \tag{5.24}$$

Substituting the expression for E from Eq. (5.17) into Eq. (5.24) we get

$$2 \sum_{i=1}^{n} dH_{ii} + \sum_{i=1}^{n} \sum_{j=1}^{n} \left(2 dJ_{ij} - dK_{ij} \right) + \sum_{i=1}^{n} \sum_{j=1}^{n} l_{ij} dS_{ij} = 0 \tag{5.25}$$

Note that this procedure of minimizing the energy with respect to the *molecular orbitals* ψ is somewhat analogous to the minimization of energy with respect to the *atomic orbital coefficients c* in the less rigorous procedure which gave the Hückel secular equations in Chap. 4, Sect. 4.3.4. It is also somewhat similar to finding a relative minimum on a PES (Chap. 2, Sect. 2.4), but with energy in that case being varied with respect to geometry rather than parameters of MOs. Since the procedure starts with Eq. (5.14) and varies the MO's to find the minimum value of E, it is called the *variation method*; the variation theorem/principle (Sect. 5.2.3.3) assures us that the energy we calculate from the results will be greater than or equal to the true energy.

From the definitions of H_{ii}, J_{ij}, K_{ij} and S_{ij} we get

$$dH_{ii} = \int d\psi_i^*(1)\hat{H}^{\text{core}}(1)\psi_i(1)dv_1 + \int \psi_i^*(1)\hat{H}^{\text{core}}(1)d\psi_i(1)dv_1 \qquad (5.26)$$

$$dJ_{ij} = \int d\psi_i^*(1)\hat{J}_j(1)\psi_i(1)dv_1 + \int d\psi_j^*(1)\hat{J}_i(1)\psi_j(1)dv_1 + complex\ \ conjugate \qquad (5.27)$$

$$dK_{ij} = \int d\psi_i^*(1)\hat{K}_j(1)\psi_i(1)dv_1 + \int d\psi_j^*(1)\hat{K}_i(1)\psi_j(1)dv_1 + complex\ \ conjugate \qquad (5.28)$$

where

$$\hat{J}_i(1) = \int \psi_i^*(2)\left(\frac{1}{r_{12}}\right)\psi_i(2)dv_2 \qquad (5.29)$$

and

$$\hat{K}_i(1)\psi_j(1) = \psi_i(1)\int \psi_i^*(2)\left(\frac{1}{r_{12}}\right)\psi_j(2)dv_2 \qquad (5.30)$$

and similarly for $\hat{J}_j$ and $\hat{K}_j$.

$$dS_{ij} = \int d\psi_i^*(1)\psi_j(1)dv_1 + \psi_i^*(1)d\psi_j(1)v_1 \qquad (5.31)$$

Using for dH, dJ, dK and dS the expressions in Eqs. (5.26), (5.27), (5.28) and (5.31), Eq. (5.25) becomes

$$2\sum_{i=1}^{n}\int d\psi_i^*(1)\left[\hat{H}^{\text{core}}(1)\psi_i(1) + \sum_{j=1}^{n}(2\hat{J}_j(1) - \hat{K}_j(1))\psi_i(1) + \frac{1}{2}\sum_{j=1}^{n}l_{ij}\psi_j(1)\right]dv$$
$$+ \text{complex conjugate} = 0$$

$$(5.32)$$

Since the MOs can be varied independently, and the expression on the left side is zero, both parts of Eq. (5.32) (the part shown and the complex conjugate) equal zero. It can be shown that a consequence of

$$2\sum_{i=1}^{n} \int d\psi_i^*(1) \left[\hat{H}^{core}(1)\psi_i(1) + \sum_{j=1}^{n} \left(2\hat{J}_j(1) - \hat{K}_j(1)\right)\psi_i(1) + \frac{1}{2}\sum_{j=1}^{n} l_{ij}\psi_j(1) \right] dv = 0$$

(5.33)

is that

$$\hat{H}^{core}(1)\psi_i(1) + \sum_{j=1}^{n} \left(2\hat{J}_j(1) - \hat{K}_j(1)\right)\psi_i(1) + \frac{1}{2}\sum_{j=1}^{n} l_{ij}\psi_j(1)dv = 0$$

i.e.

$$\left[\hat{H}^{core}(1) + \sum_{j=1}^{n} \left(2\hat{J}_j(1) - \hat{K}_j(1)\right)\right]\psi_i(1) = -\frac{1}{2}\sum_{j=1}^{n} l_{ij}\psi_j(1)$$

(5.34)

Eq. (5.34) can be written

$$\hat{F}\psi_i(1) = -\frac{1}{2}\sum_{j=1}^{n} l_{ij}\psi_j(1)$$

(5.35)

where $\hat{F}$ is the *Fock operator* :

$$\hat{F} = \hat{H}^{core}(1) + \sum_{j=1}^{n} \left(2\hat{J}_j(1) - \hat{K}_j(1)\right)$$

(5.36)

We want an eigenvalue equation because (cf. Sect. 4.3.4) we hope to be able to use the matrix form of a series of such equations to invoke matrix diagonalization to get eigenvalues and eigenvectors. Eq. (5.35) is not quite an eigenvalue equation, because it is not of the form Operation on function $= k \times$ function, but rather Operation on function $=$ sum of ($k \times$ functions). However, by transforming the molecular orbitals ψ to a new set the equation can be put in eigenvalue form (with a caveat, as we shall see). Eq. (5.35) represents a system of equations

$$\hat{F}\psi_1(1) = -\frac{1}{2}[l_{11}\psi_1(1) + l_{12}\psi_2(1) + l_{13}\psi_3(1) + \cdots + l_{1n}\psi_n(1)] \quad i = 1$$

$$\hat{F}\psi_2(1) = -\frac{1}{2}[l_{21}\psi_1(1) + l_{22}\psi_2(1) + l_{23}\psi_3(1) + \cdots + l_{2n}\psi_n(1)] \quad i = 2 \quad (5.37)$$

$$\vdots$$

$$\hat{F}\psi_n(1) = -\frac{1}{2}[l_{n1}\psi_1(1) + l_{n2}\psi_2(1) + l_{n3}\psi_3(1) + \cdots + l_{nn}\psi_n(1)] \quad i = n$$

There are n spatial orbitals ψ since we are considering a system of $2n$ electrons and each orbital holds two electrons. The 1 in parentheses on each orbital emphasizes that each of these n equations is a *one*-electron equation, dealing with the same electron (we could have used a 2 or a 3, etc.), i.e. the Fock operator (Eq 5.36)) is a one-electron operator, unlike the general electronic Hamiltonian operator of Eq. (5.15), which is a multi-electron operator (a $2n$ electron operator for our specific case). The Fock operator acts on a total of n spatial orbitals, the $\psi_1, \psi_2, \ldots, \psi_n$ in Eqs. (5.35).

The series of Eqs. (5.37) can be written as the single matrix equation (cf. Chap. 4, Eq. (4.50))

$$\hat{F}\begin{pmatrix} \psi_1(1) \\ \psi_2(1) \\ \psi_3(1) \\ \vdots \\ \psi_n(1) \end{pmatrix} = -\frac{1}{2}\begin{pmatrix} l_{11} & l_{12} & l_{13} & \cdots & l_{1n} \\ l_{21} & l_{22} & l_{23} & \cdots & l_{2n} \\ \vdots & \vdots & \cdots & & \vdots \\ l_{n1} & l_{n2} & l_{n3} & \cdots & l_{nn} \end{pmatrix}\begin{pmatrix} \psi_1(1) \\ \psi_2(1) \\ \psi_3(1) \\ \vdots \\ \psi_n(1) \end{pmatrix} \tag{5.38}$$

i.e.

$$\hat{F}\boldsymbol{\psi} = -\frac{1}{2}\mathbf{L}\boldsymbol{\psi} \tag{5.39}$$

In Eqs. (5.37), each equation will be of the form $\hat{F}\psi_i = k\psi_i$, which is what we want, if all the $l_{ij} = 0$ except for $i = j$ (for example, in the first equation $\hat{F}\psi_1(1) = -(1/2)l_{11}\psi_1(1)$ if the only nonzero l is l_{11}). This will be the case if in Eq 5.39) $\mathbf{L}$ is a diagonal matrix. It can be shown that $\mathbf{L}$ is diagonalizable (Chap. 4, Sect. 4.3.3), i.e. there exist matrices $\mathbf{P}$, $\mathbf{P}^{-1}$ and a diagonal matrix $\mathbf{L}'$ such that

$$\mathbf{L} = \mathbf{P}\mathbf{L}'\mathbf{P}^{-1} \tag{5.40}$$

Substituting $\mathbf{L}$ from Eq. (5.40) into Eq. (5.39):

$$\hat{F}\boldsymbol{\psi} = -\frac{1}{2}\mathbf{P}\mathbf{L}'\mathbf{P}^{-1}\boldsymbol{\psi} \tag{5.41}$$

Multiplying on the left by $\mathbf{P}^{-1}$ and on the right by $\mathbf{P}$ we get

$$\hat{F}\mathbf{P}^{-1}\boldsymbol{\psi}\mathbf{P} = -\frac{1}{2}\left(\mathbf{P}^{-1}\mathbf{P}\right)\mathbf{L}'\left(\mathbf{P}^{-1}\boldsymbol{\psi}\mathbf{P}\right)$$

which, since $\mathbf{P}^{-1}\mathbf{P} = \mathbf{1}$ can be written

$$\hat{F}\boldsymbol{\psi}' = -\frac{1}{2}\mathbf{L}'\boldsymbol{\psi}' \tag{5.42}$$

where

$$\boldsymbol{\psi}' = \mathbf{P}^{-1}\boldsymbol{\psi}\mathbf{P} \tag{5.43}$$

We may as well remove the -1/2 factor by incorporating it into $\mathbf{L}'$, and we can omit the prime from Ψ (had we been prescient we could have *started* the derivation using primes then written $\Psi = \mathbf{P}^{-1}\boldsymbol{\psi}'\mathbf{P}$ for Eq. (5.43)). Equation (5.42) then becomes (notationally anticipating the soon-to-be-apparent fact that the diagonal matrix is an energy-level matrix)

$$\hat{F}\boldsymbol{\psi} = \boldsymbol{\varepsilon}\,\boldsymbol{\psi} \tag{5.44}$$

where

$$\boldsymbol{\varepsilon} = \begin{pmatrix} (-1/2)l_{11} & 0 & 0 & \dots & 0 \\ 0 & (-1/2)l_{22} & 0 & \dots & 0 \\ \vdots & \vdots & & \dots & \vdots \\ 0 & 0 & 0 & \dots & (-1/2)l_{nn} \end{pmatrix} \tag{5.45}$$

Equation (5.44) is the compact form of (cf. Eq. (5.38)). Thus

$$\hat{F}\begin{pmatrix} \psi_1(1) \\ \psi_2(1) \\ \psi_3(1) \\ \vdots \\ \psi_n(1) \end{pmatrix} = \begin{pmatrix} \varepsilon_1 & 0 & 0 & \dots & 0 \\ 0 & \varepsilon_2 & 0 & \dots & 0 \\ \vdots & \vdots & & \dots & \vdots \\ 0 & 0 & 0 & \dots & \varepsilon_n \end{pmatrix}\begin{pmatrix} \psi_1(1) \\ \psi_2(1) \\ \psi_3(1) \\ \vdots \\ \psi_n(1) \end{pmatrix} \tag{5.46}$$

where the superfluous double subscripts on the ε's have been replaced by single ones. Eqs. (5.44/5.46) are the matrix form of the system of equations

$$\begin{aligned}
\hat{F}\psi_1(1) &= \varepsilon_1\psi_1(1) \\
\hat{F}\psi_2(1) &= \varepsilon_2\psi_2(1) \\
\hat{F}\psi_3(1) &= \varepsilon_3\psi_3(1) \\
&\vdots \\
\hat{F}\psi_n(1) &= \varepsilon_n\psi_n(1)
\end{aligned} \tag{*5.47}$$

These Eqs. (5.47) are the Hartree-Fock equations; the matrix form is Eq. (5.44) or Eq. (5.46). By analogy with the Schrödinger equation $\hat{H}\psi = E\psi$, we see that they show that the Fock operator acting on a one-electron wavefunction (an atomic or molecular orbital) generates an energy value times the wavefunction. Thus the Lagrangian multipliers l_{ii} turned out to be (with the $-1/2$ factor) the energy values associated with the orbitals ψ_i. Unlike the Schrödinger equation the Hartree-Fock equations are not quite eigenvalue equations (although they are closer to this ideal than is Eq. (5.35)), because here in $\hat{F}\psi_i = k\psi_i$ the Fock operator $\hat{F}$ is itself dependent on ψ_i; in a true eigenvalue equation the operator can be written down without reference to the function on which it acts. The significance of the Hartree-Fock equations is discussed in the next section.

5.2.3.5 The Meaning of the Hartree-Fock Equations

The Hartree-Fock Eqs. (5.47) (in matrix form Eqs. (5.44) and (5.46)) are *pseudoeigenvalue* equations asserting that the Fock operator $\hat{F}$ acts on a wavefunction ψ_i to generate an energy value ε_i, times ψ_i. *Pseudo*eigenvalue because, as stated above, in a true eigenvalue equation the operator is not dependent on the function on which it acts; in the Hartree-Fock equations $\hat{F}$ depends on ψ because (Eq. (5.36)) the operator contains $\hat{J}$ and $\hat{K}$, which in turn depend (Eqs. (5.29) and (5.30)) on ψ. Each of the equations in the set (5.47) is for a single electron ("electron one" is indicated, but any ordinal number could be used), so the Hartree-Fock operator $\hat{F}$ is a one-electron operator, and each spatial molecular orbital ψ_i is a one-electron function (of the coordinates of the electron). Two electrons can be placed in a spatial orbital because the *full* description of each of these electrons requires a *spin function α or β* (Sect. 5.2.3.1) and each electron "moves in" a different spin orbital. The result is that the two electrons in the spatial orbital ψ do not have all four quantum numbers the same (for an atomic $1s$ orbital, for example, one electron has quantum numbers $n = 1$, $l = 0$, $m = 0$ and $s = 1/2$, while the other has $n = 1$, $l = 0$, $m = 0$ and $s = -1/2$), and so the Pauli exclusion principle is not violated.

The *functions ψ* are the spatial molecular (or atomic) orbitals or wavefunctions that (along with the spin functions) make up the overall or total molecular (or atomic) wavefunction ψ, which can be written as a Slater determinant (Eq. (5.12)). Concerning the *energies ε_i*, from the fact that

$$\varepsilon_i = \int \psi_i \hat{F} \psi_i dv \tag{5.48}$$

(this follows simply from multiplying both sides of a Hartree-Fock equation by ψ_i and integrating, noting that ψ_i is normalized) and the definition of $\hat{F}$ (Eq. (5.36)) we get

$$\varepsilon_i = \int \psi_i(1) \hat{H}^{\text{core}}(1) \psi_i(1) dv + \sum_{j=1}^{n} \left(2J_{ij}(1) - K_{ij}(1) \right) \tag{5.49}$$

i.e.

$$\varepsilon_i = H_{ii}^{\text{core}} + \sum_{j=1}^{n} \left(2J_{ij}(1) - K_{ij}(1) \right) \tag{5.50}$$

(the *operators $\hat{J}$ and $\hat{K}$* in Eq. (5.36) have been transformed by integration into the *integrals J and K* in Eq 5.49)). Eq. (5.50) shows that ε_i is the energy of an electron in ψ_i subject to interaction with all the other electrons in the molecule: H_{ii}^{core} (Eq (5.18)) is the integral giving the energy of the electron due only to its motion

(kinetic energy) and to the attraction of the nuclear core (electron-nucleus potential energy), while the sum of J and K terms represents the exchange-corrected (via K) Coulombic repulsion (through J) energy resulting from the interaction of the electron with all the other electrons in the molecule or atom [19].

In principle the Eqs. (5.47) allow us to calculate the molecular orbitals (MO's) ψ and the energy levels ε. We could start with "guesses" (possibly obtained by intuition or analogy) of the MO's (the zeroth approximation to the MOs) and use these to construct the operator $\hat{F}$ (Eq. (5.36), then allow $\hat{F}$ to operate on the guesses to yield energy levels (the first approximation to the ε_i) and new, improved functions (the first calculated approximations to the ψ_i). Using the improved functions in $\hat{F}$ and operating on these gives the second approximations to the ψ_i and ε_i, and the process is continued until ψ_i and ε_i no longer change (within preset limits), which occurs when the smeared-out electrostatic field represented in Eq. (5.17) by $\sum\sum (2J - K)$ (cf. Fig. 5.3) ceases to change appreciably–is consistent from one iteration cycle to the next, i.e. is self-consistent. How do we know that iterations *improve* psi and epsilon? This is usually, but not invariably, the case [20]; in practice "initial guess" solutions to the Hartree-Fock equations usually converge fairly smoothly to give the best wavefunction and orbital energies (and thus total energy) that can be obtained by the HF method from the particular kind of guess wavefunction (e.g. basis set; Sect. 5.2.3.6.5).

To expand a bit on Dewar's cautious endorsement of the SCF procedure [20] ("SCF calculations are by no means foolproof; ...Usually one finds a reasonably rapid convergence to the required solution"): occasionally a wavefunction is obtained that is not the best one available from the chosen basis set. This phenomenon is called *wavefunction instability*. To see how this could happen note that the SCF method is an optimization procedure somewhat analogous to geometry optimization (Chap. 2, Sect. 2.4). In geometry optimization we seek a relative minimum or a transition state on a hypersurface in a mathematical energy versus nuclear coordinates space defined by $E = f$ (nuclear coordinates); in wavefunction optimization we seek a global minimum on a hypersurface in an energy versus basis function coefficients space defined by $E = f$ (basis function coefficients). The wavefunction found may correspond to a point on the hypersurface that is not even a minimum, but rather a saddle point. Even if it is the global minimum, if we are using a restricted Hartree-Fock (RHF) wavefunction rather than an unrestricted (UHF) one (end of Sect. 5.2.3.6.5), there are cases in which a lower energy will be obtained by switching to a UHF function. The RHF function is then said to show external or triplet instability. If within the type of wavefunction we are using (RHF or UHF) a better function can be found by moving to another point on the hypersurface, away from a saddle point or a higher-energy minimum, the wavefunction is said to show internal instability. There are algorithms that will test for wavefunction instability and alter coefficients to obtain the best wavefunction from the chosen basis set. Seeger and Pople pioneered the mathematical analysis of and some cures for wavefunction instability [21], and in more chemical language Dahareng and Dive have examined about 80 molecules for the

phenomenon and offer some generalizations [22]. Instability can occur also with post-Hartree-Fock (correlated) (Sect. 5.4) wavefunctions [23]. Chemists do not routinely test for wavefunction stability, and indeed it is rarely a problem except for unusual molecules, e.g. p-benzyne [24]. However, when investigating exotic (as judged by the experienced chemist) molecules, it is good practice to carry out this check.

The Hartree-Fock SCF method is, of course, in exactly the same iterative spirit as the procedure described in Sect. 5.2.2 using the Hartree product as our total or overall wavefunction Ψ. The main difference between the two methods is that the Hartree-Fock method represents Ψ as a Slater determinant of component spin MOs rather than as a simple product of spatial MOs, and a consequence of this is that the calculation of the average Coulombic field in the Hartree method involves only the Coulomb integral J, but in the Hartree-Fock modification we need the Coulomb integral J *and* the exchange integral K, which arises from Slater determinant terms that differ in exchange of electrons. Because K acts as a kind of "Pauli correction" to the classical electrostatic repulsion, reminding the electrons that two of them of the same spin cannot occupy the same spatial orbital, electron-electron repulsion is less in the Hartree-Fock method than if a simple Hartree product were used. Of course K does not arise in calculations involving no electrons of like spin, as in H_2 or (Chap. 4, Sect. 4.4.2; also Sect. 5.2.3.6.5) HHe^+, which have only two, paired-spin, electrons. At the end of the iterative procedure we have the MO's ψ_i and their corresponding energy levels ε_i, and the total wavefunction Ψ, the Slater determinant of the ψ_i's. The ε_i can be used to calculate the total electronic energy of the molecule, and the MO's ψ_i are useful heuristic approximations to the electron distribution, while the total wavefunction Ψ can in principle be used to calculate anything about the molecule, as the expectation value of some operator. Applications of the energy levels and the MO's are given in Sect. 5.4.

5.2.3.6   Basis Functions and The Roothaan-Hall Equations

5.2.3.6.1   Deriving the Roothaan-Hall Equations

As they stand, the Hartree-Fock Eqs. (5.44), (5.46) or (5.47) are not very useful for molecular calculations, mainly because (1) they do not prescribe a mathematically viable procedure getting the initial guesses for the MO wavefunctions ψ_i, which we need to initiate the iterative process (Sect. 5.2.3.5), and (2) the wavefunctions may be so complicated that they contribute nothing to a qualitative understanding of the electron distribution.

For calculations on *atoms*, which obviously have much simpler orbitals than molecules, we could use for the ψ's atomic orbital wavefunctions based on the solution of the Schrödinger equation for the hydrogen atom (taking into account the increase of atomic number and the screening effect of inner electrons on outer ones. This yields the atomic wavefunctions, which in pre-computer days, anyway, were recorded as tables of ψ at various distances from the nucleus [25]. This is not a

suitable approach for molecules because among molecules there is no prototype species occupying a place analogous to that of the hydrogen atom in the hierarchy of atoms, and as indicated above it does not readily lend itself to an interpretation of how molecular properties arise from the nature of the constituent atoms.

In 1951 Roothaan and Hall independently pointed out [26] that these problems can be solved by representing MO's as linear combinations of basis functions (just as in the simple Hückel method, in Chap. 4, the π MO's are constructed from atomic p orbitals). Roothaan's paper was more general and more detailed than Hall's, which was oriented to semiempirical calculations and alkanes, and the method is sometimes called the Roothaan method. For a basis-function expansion of MO's we write

$$
\begin{aligned}
\psi_1 &= c_{11}\phi_1 + c_{21}\phi_2 + c_{31}\phi_3 + \cdots + c_{m1}\phi_m \\
\psi_2 &= c_{12}\phi_1 + c_{22}\phi_2 + c_{32}\phi_3 + \cdots + c_{m2}\phi_m \\
\psi_3 &= c_{13}\phi_1 + c_{23}\phi_2 + c_{33}\phi_3 + \cdots + c_{m3}\phi_m \\
&\vdots \\
\psi_m &= c_{1m}\phi_1 + c_{2m}\phi_2 + c_{3m}\phi_3 + \cdots + c_{mm}\phi_m
\end{aligned}
\qquad (*5.51)
$$

In devising a more compact notation for this set of equations it is very helpful, particularly when we come to the matrix treatment in Sect. 5.2.3.6.3, to use different subscripts to denote the MO's ψ and the basis functions ϕ. Conventionally, Roman letters have been used for the ψ's and Greek letters for the ϕ's, or $i, j, k, l, \ldots$ for the ψ's and $r, s, t, u, \ldots$ for the ϕ's. The latter convention will be adopted here, and we can write the Eqs. (5.51) as

$$
\psi_i = \sum_{s=1}^{m} c_{si}\,\phi_s \qquad i = 1, 2, 3, \ldots, m \ (m \text{ MOs}) \tag{5.52}
$$

with labels: m basis functions; sth basis function; ith MO; c of the sth basis function of ith MO.

We are expanding each MO ψ in terms of m basis functions. The basis functions are usually (but not necessarily) located on atoms, i.e. for the function $\phi(x, y, z)$, where x, y, z are the coordinates of the electron being treated by this one-electron function, the distance of the electron from the nucleus is:

$$
r = \left[(x - x_0)^2 + (y - y_0)^2 + (z - z_0)^2 \right]^{1/2} \tag{5.53}
$$

where x_0, y_0, z_0 are the coordinates of the atomic nucleus in the coordinate system used to define the geometry of the molecule. Because each basis function may usually be regarded (at least vaguely) as some kind of atomic orbital, this linear combination of basis functions approach is commonly called a linear combination of atomic orbitals (LCAO) representation of the MO's, as in the simple and

extended Hückel methods (Chap. 4, Sects. 4.3.4 and 4.4.1). The set of basis functions used for a particular calculation is called the *basis set*.

We need at least enough spatial MO's ψ to accommodate all the electrons in the molecule, i.e. we need at least n ψ's for the $2n$ electrons (recall that we are dealing with closed-shell molecules). This is ensured because even the smallest basis sets used in ab initio calculations have for each atom at least one basis function corresponding to each orbital conventionally used to describe the chemistry of the atom, and the number of basis functions ϕ is equal to the number of (spatial) MOs ψ (Chap. 4, Sect. 4.3.4; this is analogous to two AOs generating two MOs). An example will make this clear: for an ab initio calculation on CH_4, the smallest basis set would specify for C:

$$\phi(C,\ 1s),\ \ \phi(C,\ 2s),\ \ \phi(C,\ 2p_x),\ \ \phi(C,\ 2p_y),\ \ \phi(C,\ 2p_z)$$

and for each H:

$$\phi(H,\ 1s)$$

These nine basis functions ϕ (5 on C and $4 \times 1 = 4$ on H) create nine spatial MO's ψ, which could hold 18 electrons; for the 10 electrons of CH_4 we need only 5 spatial MO's. There is no *upper* limit to the size of a basis set: there are commonly many more basis functions, and hence MO's, than are needed to hold all the electrons, so that there are usually many unoccupied ("virtual") MO's. In other words, the number of basis functions m in the expansions (5.52) can be much bigger than the number n of pairs of electrons in the molecule, although only the n occupied spatial orbitals are used to construct the Slater determinant which represents the HF wavefunction (Sect. 5.2.3.1). This point, and basis sets, are discussed further in Sect. 5.3.

To continue with the Roothaan-Hall approach, we substitute the expansion (5.52) for the ψ's into the Hartree-Fock Eqs. (5.47), getting (we will work with m, not n, HF equations since there is one such equation for each MO, and our m basis functions will generate m MO's):

$$\sum_{s=1}^{m} c_{s1} \hat{F} \phi_{sj} = \varepsilon_1 \sum_{sj=1}^{m} c_{s1} \phi_s$$

$$\sum_{s=1}^{m} c_{s2} \hat{F} \phi_s = \varepsilon_2 \sum_{s=1}^{m} c_{s2} \phi_s \qquad (5.54)$$

$$\vdots$$

$$\sum_{s=1}^{m} c_{sm} \hat{F} \phi_s = \varepsilon_m \sum_{s=1}^{m} c_{sm} \hat{F} \phi_s$$

($\hat{F}$ perates on the functions ϕ, not on the c's, which have no variables x, y, z). Multiplying each of these m equations by $\phi_1, \phi_2, \ldots, \phi_m$, (or ϕ_1^* etc. if the ϕ's are complex functions, as is occasionally the case) and integrating transforms the Fock operators into Fock integrals, and we get m sets of equations (one for each of the basis functions ϕ).

Basis function ϕ_1 gives

$$
\sum_{s=1}^{m} c_{s1}F_{1s} = \varepsilon_1 \sum_{s=1}^{m} c_{s1}S_{1s}
$$
$$
\sum_{sj=1}^{m} c_{s2}F_{1s} = \varepsilon_2 \sum_{s=1}^{m} c_{s2}S_{1s}
$$
$$
\vdots
$$
$$
\sum_{s=1}^{m} c_{sm}F_{1s} = \varepsilon_m \sum_{s=1}^{m} c_{sm}S_{1s}
$$

(5.54-1)

where

$$
F_{rs} = \int \phi_r \hat{F} \phi_s dv \ \text{ and } \ S_{rs} = \int \phi_r \phi_s dv
$$

(5.55)

Basis function ϕ_2 gives

$$
\sum_{s=1}^{m} c_{s1}F_{2s} = \varepsilon_1 \sum_{s=1}^{m} c_{s1}S_{2s}
$$
$$
\sum_{s=1}^{m} c_{s2}F_{2s} = \varepsilon_2 \sum_{s=1}^{m} c_{s2}S_{2s}
$$
$$
\vdots
$$
$$
\sum_{s=1}^{m} c_{sm}F_{2s} = \varepsilon_m \sum_{s=1}^{m} c_{sm}S_{2s}
$$

(5.54-2)

Finally, basis function ϕ_m gives

$$
\sum_{s=1}^{m} c_{s1}F_{ms} = \varepsilon_1 \sum_{s=1}^{m} c_{s1}S_{ms}
$$
$$
\sum_{s=1}^{m} c_{s2}F_{ms} = \varepsilon_2 \sum_{s=1}^{m} c_{s2}S_{ms}
$$
$$
\vdots
$$
$$
\sum_{s=1}^{m} c_{sm}F_{ms} = \varepsilon_m \sum_{s=1}^{m} c_{sm}S_{ms}
$$

(5.54-m)

In the m sets of Eqs. (5.54) each set itself contains m equations (the subscript of ε, for example, runs from 1 to m), for a total of $m \times m$ equations. These equations are the Roothaan-Hall version of the Hartree-Fock equations; they were obtained by substituting for the MO's ψ in the HF equations a linear combination of basis functions (ϕ's weighted by c's). The Roothaan-Hall equations are usually written more compactly, as

$$\sum_{s=1}^{m} F_{rs}c_{si} = \sum_{s=1}^{m} S_{rs}c_{si}\varepsilon_i \quad r = 1, 2, 3, \ldots, m,$$
$$(\text{for each } i = 1, 2, 3, \ldots, m) \tag{5.56}$$

We have $m \times m$ equations because each of the m spatial MO's ψ we used (recall that there is one HF equation for each ψ, Eqs. (5.47)) is expanded with m basis functions. The Roothaan-Hall equations connect the basis functions ϕ (contained in the integrals F and S, Eqs. (5.55)), the coefficients c, and the MO energy levels ε. Given a basis set $\{\phi_s, s = 1, 2, 3, \ldots, m\}$ they can be used to calculate the c's, and thus the MOs ψ (Eq. (5.52)) and the MO energy levels ε. The overall electron distribution in the molecule can be calculated from the total wavefunction Ψ, which can be written as a Slater determinant of the "component" spatial wavefunctions ψ (by including spin functions), and in principle anyway, any property of a molecule can be calculated from Ψ. The component wavefunctions ψ and their energy levels ε are extremely useful, as chemists rely heavily on concepts like the shape and energies of, for example, the HOMO and LUMO of a molecule (MO concepts are reviewed in Chap. 4). The energy levels enable (with a correction term) the total energy of a molecule to be calculated, and so the energies of molecules can be compared and reaction energies and activation energies can be calculated. The Roothaan-Hall equations, then, are a cornerstone of modern ab initio calculations, and the procedure for solving them is outlined next. These ideas are summarized pictorially in Fig. 5.5.
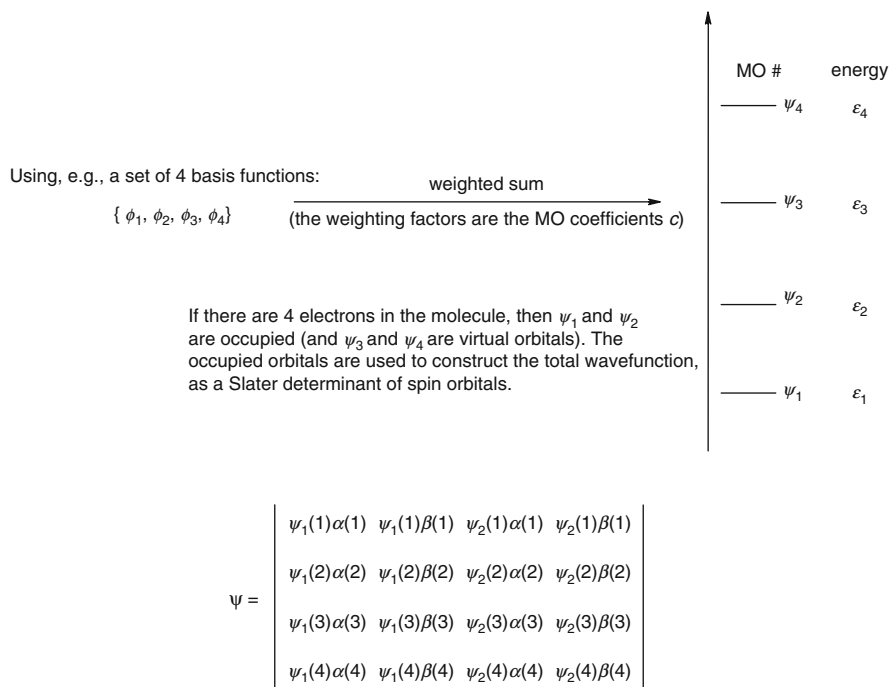
Fig. 5.5 Pictorial representation of basis functions, MO's, total wavefunction, and energy levels

The fact that the Roothaan-Hall equations Eqs. (5.56) are really a total of $m \times m$ equations suggests that they might be expressible as a single matrix equation, since the single matrix equation $\mathbf{AB} = \mathbf{0}$, where $\mathbf{A}$ and $\mathbf{B}$ are $m \times m$ matrices, represents $m \times m$ "simple" equations, one for each element of the product matrix $\mathbf{AB}$ (work it out for two 2×2 matrices). A single matrix equation would be easier to work with than m^2 equations and might allow us to invoke matrix diagonalization as in the case of the simple and extended Hückel methods (Chap. 4, Sects. 4.3.4 and 4.4.1). To subsume the sets of Eqs. (5.54), i.e. Eqs. (5.56), into one matrix equation, we might (eschewing a rigorous deductive approach) suspect that the matrix form is the fairly obvious possibility

$$\mathbf{FC} = \mathbf{SC\varepsilon} \tag{*5.57}$$

Here $\mathbf{F}$, $\mathbf{C}$ and $\mathbf{S}$ would have to be $m \times m$ matrices, since there are m^2 F's, c's and S's, and $\mathbf{\varepsilon}$ would be an $m \times m$ diagonal matrix with the nonzero elements $\varepsilon_1, \varepsilon_2, \ldots, \varepsilon_m$, since $\mathbf{\varepsilon}$ must contain only m elements, but has to be $m \times m$ to make the right hand side matrix product the same size as that on the left.

This is easily checked: the left hand side of Eq. (5.57) is

$$\mathbf{FC} = \begin{pmatrix} F_{11} & F_{12} & F_{13} & \cdots & F_{1m} \\ F_{21} & F_{22} & F_{23} & \cdots & F_{2m} \\ \vdots & \vdots & \ldots & & \vdots \\ F_{m1} & F_{m2} & F_{m3} & \cdots & F_{mm} \end{pmatrix} \begin{pmatrix} c_{11} & c_{12} & c_{13} & \cdots & c_{1m} \\ c_{21} & c_{22} & c_{23} & \cdots & c_{2m} \\ \vdots & \vdots & \ldots & & \vdots \\ c_{m1} & c_{m2} & c_{m3} & \cdots & c_{mm} \end{pmatrix}$$

$$= \begin{pmatrix} F_{11}c_{11} + F_{12}c_{21} + F_{13}c_{31} & \cdots & F_{11}c_{12} + F_{12}c_{22} + F_{13}c_{32} & \cdots & \cdots \\ F_{21}c_{11} + F_{22}c_{21} + F_{23}c_{31} & \cdots & F_{21}c_{12} + F_{22}c_{22} + F_{23}c_{33} & \cdots & \cdots \\ & & \vdots & & \end{pmatrix}$$

$$\tag{5.58}$$

The right hand side of Eq. (5.57) is

$$\mathbf{SC\varepsilon} = \begin{pmatrix} S_{11} & S_{12} & \cdots & S_{1m} \\ S_{21} & S_{22} & \cdots & S_{2m} \\ \vdots & \vdots & \ldots & \vdots \\ S_{m1} & S_{m2} & \cdots & S_{mm} \end{pmatrix} \begin{pmatrix} c_{11} & c_{12} & \cdots & c_{1m} \\ c_{21} & c_{22} & \cdots & c_{2m} \\ \vdots & \vdots & \ldots & \vdots \\ c_{m1} & c_{m2} & \cdots & c_{mm} \end{pmatrix} \begin{pmatrix} \varepsilon_{11} & 0 & \cdots & 0 \\ 0 & \varepsilon_{22} & \cdots & 0 \\ \vdots & \vdots & \ldots & \vdots \\ 0 & 0 & \cdots & \varepsilon_{mm} \end{pmatrix}$$

$$= \begin{pmatrix} \varepsilon_1(S_{11}c_{11} + S_{12}c_{21} + S_{13}c_{31}\cdots) & \varepsilon_2(S_{11}c_{12} + S_{12}c_{22} + S_{13}c_{32}\cdots) & \cdots \\ \varepsilon_1(S_{21}c_{11} + S_{22}c_{21} + S_{23}c_{31}\cdots) & \varepsilon_2(S_{21}c_{12} + S_{22}c_{22} + S_{23}c_{33}\cdots) & \cdots \\ & \vdots & \end{pmatrix} \mathbf{\varepsilon}$$

$$= \begin{pmatrix} S_{11}c_{11} + S_{12}c_{21} + S_{13}c_{31} & \cdots & S_{11}c_{12} + S_{12}c_{22} + S_{13}c_{32} & \cdots & \cdots \\ S_{21}c_{11} + S_{22}c_{21} + S_{23}c_{31} & \cdots & S_{21}c_{12} + S_{22}c_{22} + S_{23}c_{33} & \cdots & \vdots \\ & & \vdots & & \end{pmatrix}$$

$$\tag{5.59}$$

Now compare $\mathbf{FC}$ (5.58) and $\mathbf{SC\varepsilon}$ (5.59). Comparing element a_{11} of $\mathbf{FC}$ (multiplied out to give a single matrix as shown in (5.58)) with element a_{11} of $\mathbf{SC\varepsilon}$ (multiplied out to give a single matrix as shown in (5.59)) we see that if $\mathbf{FC} = \mathbf{SC\varepsilon}$, i.e. if (5.57) is true, then

$$F_{11}c_{11} + F_{12}c_{21} + F_{13}c_{31} + \cdots = \varepsilon(S_{11}c_{11} + S_{12}c_{21} + S_{13}c_{31} + \cdots)$$

i.e.

$$\sum_{s=1}^{m} c_{si}F_{rs} = \varepsilon \sum_{s=1}^{m} c_{si}S_{rs} \tag{5.60}$$

But this is the first equation of the set (5.54-1). Continuing in this way we see that matching each element of the multiplied-out matrix **FC** (5.58) with the corresponding element of the multiplied-out matrix **SCε** gives one of the equations of the set (5.54), i.e. of the set (5.56). This can be so only if **FC = SCε**, so this matrix equation is indeed equivalent to the set of Eqs. (5.54-1 to 5.54-*m*).

Now we have **FC = SCε** (5.57), the matrix form of the Roothaan-Hall equations. These equations are sometimes called the Hartree-Fock-Roothaan equations, and, often, the Roothaan equations, as Roothaan's exposition was the more detailed and addresses itself more clearly to a general treatment of molecules. Before showing how they are used to do ab initio calculations, a brief review of how we got these equations is in order.

Summary of the Derivation of the Roothaan-Hall Equations

1. The total wavefunction Ψ of an atom or molecule was expressed as a Slater determinant of spin MO's ψ(spatial)α and ψ(spatial)β, Eq. (5.12).
2. From the Schrödinger equation we got an expression for the electronic energy of the atom or molecule, $E = \langle \Psi | \hat{H} | \Psi \rangle$, Eq. (5.14).
3. Substituting the Slater determinant for the total molecular wavefunction Ψ and inserting the explicit form of the Hamiltonian operator $\hat{H}$ into (5.14) gave the energy in terms of the spatial MO's ψ, (Eq. (5.17):

$$E = 2\sum_{i=1}^{n} H_{ii} + \sum_{i=1}^{n}\sum_{j=1}^{n} \left(2J_{ij} - K_{ij}\right)$$

4. Minimizing E in (5.17) with respect to the ψ's (to find the best ψ's) gave the Hartree-Fock equations $\hat{F}\psi = \varepsilon\psi$ (5.44).
5. Substituting into the Hartree-Fock equations $\hat{F}\psi = \varepsilon\psi$ (5.44) the Roothaan-Hall linear combination of basis functions (LCAO) expansions $\psi_i = \sum c_{si}\phi_s$ (5.52) for the MO's ψ gave the Roothaan-Hall equations (Eqs. (5.56)), which can be written compactly as **FC = SCε** (Eqs. (5.57)).

5.2.3.6.2 Using the Roothaan-Hall Equations to Do Ab initio Calculations–The SCF Procedure

The Roothaan-Hall matrix equations **FC = SCε** (Eqs. (5.57)) (**F**, **C**, **S** and **ε** are defined in connection with Eqs. (5.58) and (5.59); the matrix elements F and S,

defined by Eq. (5.55), are of the same matrix form as Eq. (4.54), $\mathbf{HC} = \mathbf{SC\varepsilon}$, in the simple Hückel method (Chap. 4, Sect. 4.3.4) and the extended Hückel (Chap. 4, Sect. 4.4.1) method. Here, however, we have seen (in outline) how the equation may be rigorously derived. Also, unlike the case in the Hückel methods the Fock matrix elements are rigorously defined theoretically: from Eqs. (5.55)

$$F_{rs} = \int \phi_r \hat{F} \phi_s dv \qquad (5.61 = 4.54)$$

and Eq. (5.36)

$$\hat{F} = \hat{H}^{\text{core}}(1) + \sum_{j=1}^{n} \left(2\hat{J}_j(1) - \hat{K}_j(1) \right) \qquad (5.62 = 5.36)$$

it follows that

$$F_{rs} = \int \phi_r \left[\hat{H}^{\text{core}}(1) + \sum_{j=1}^{n} \left(2\hat{J}_j(1) - \hat{K}_j(1) \right) \right] \phi_s dv \qquad (5.63)$$

where

$$\hat{H}^{\text{core}}(1) = -\frac{1}{2} \nabla_1^2 - \sum_{\text{all } \mu} \frac{Z_\mu}{r_{\mu 1}} \qquad (5.64 = 5.19)$$

$$\hat{J}_j(1) = \int \psi_j^*(2) \left(\frac{1}{r_{12}} \right) \psi_j(2) dv_2 \qquad (5.65 = 5.29)$$

and

$$\hat{K}_i(1)\psi_j(1) = \psi_i(1) \int \psi_i^*(2) \left(\frac{1}{r_{12}} \right) \psi_j(2) dv_2 \qquad (5.66 = 5.30)$$

To use the Roothaan-Hall equations we want them in standard eigenvalue-like form so that we can diagonalize the Fock matrix $\mathbf{F}$ of Eq. (5.57) to get the coefficients c and the energy levels ε, just as we did in connection with the extended Hückel method (Chap. 4, Sect. 4.4.1). The procedure for diagonalizing $\mathbf{F}$ and extracting the c's and ε's and is exactly the same as that explained for the extended Hückel method (although here the cycle is iterative, i.e. repetitive, see below):

1. The overlap matrix $\mathbf{S}$ is calculated and used to calculate an orthogonalizing matrix $\mathbf{S}^{-1/2}$, as in Eqs. (4.105, 4.106, 4.107):

$$\mathbf{S} \rightarrow \mathbf{D} \rightarrow \mathbf{S}^{-1/2} \qquad (5.67)$$

2. $\mathbf{S}^{-1/2}$ is used to convert $\mathbf{F}$ to $\mathbf{F}'$ (cf. (4.104)):

$$\mathbf{F}' = \mathbf{S}^{-1/2}\mathbf{F}\mathbf{S}^{-1/2} \tag{5.68}$$

The transformed Fock matrix $\mathbf{F}'$ satisfies

$$\mathbf{F}' = \mathbf{C}'\boldsymbol{\varepsilon}\mathbf{C}'^{-1} \tag{5.69}$$

(*cf.* Eq. (4.104)). The overlap matrix $\mathbf{S}$ is readily calculated, so if $\mathbf{F}$ can be calculated it can be transformed to $\mathbf{F}'$, which can be diagonalized to give $\mathbf{C}'$ and $\boldsymbol{\varepsilon}$, which latter yields the MO energy levels ε_i.

3. Transformation of $\mathbf{C}'$ to $\mathbf{C}$ (Eq. (4.102)) gives the coefficients c_{si} in the expansion of the MO's ψ in terms of basis functions ϕ:

$$\mathbf{C} = \mathbf{S}^{-1/2}\mathbf{C}' \tag{5.70}$$

Equations (5.63, 5.64, 5.65 and 5.66) show that to calculate $\mathbf{F}$, i.e. each of the matrix elements F, we need the wavefunctions ψ_i, because $\hat{J}$ hat and $\hat{K}$ hat, the Coulomb and exchange operators (Eqs. (5.65) and (5.66)), are defined in terms of the ψ's. It looks like we are faced with a dilemma: the point of calculating $\mathbf{F}$ is to get (besides the ε's) the ψ's (the c's with the chosen basis set $\{\phi\}$ make up the ψ's), but to get $\mathbf{F}$ we need the ψ's. The way out of this is to start with a set of approximate c's, e.g. from an extended Hückel calculation (there are several other possibilities), which needs no c's to begin with because the extended Hückel "Fock" matrix elements are calculated from experimental ionization energies (Chap. 4, Sect. 4.4.1). These c's, the *initial guess*, are used with the basis functions ϕ to in effect (Sect. 5.2.3.6.5) calculate initial MO wavefunctions ψ, which are used to calculate the $\mathbf{F}$ elements F_{rs}. Transformation of $\mathbf{F}$ to $\mathbf{F}'$ and diagonalization gives a "first- cycle" set of ε's and (after transformation of $\mathbf{C}'$ to $\mathbf{C}$) a first-cycle set of c's. These c's are used to calculate new F_{rs}, i.e. a new $\mathbf{F}$, and this gives a second-cycle set of ε's and c's. The process is continued until things–the ε's, the c's (as the density matrix–Sect. 5.2.3.6.4), the energy, or, more usually, some combination of these – stop changing within certain pre-defined limits, i.e. until the cycles have essentially converged on the limiting ε's and c's. Typically, about ten cycles are needed to achieve convergence. It is because the operator $\hat{F}$ depends on the functions ϕ on which it acts, making an iterative approach necessary, that the Roothaan-Hall equations, like the Hartree-Fock equations, are called *pseudo*eigenvalue (see Sect. 5.2.3.5).

Now, in the Hartree-Fock method (the Roothaan-Hall equations represent one implementation of the Hartree-Fock method) each electron moves in an *average field* due to all the other electrons (see the discussion in connection with Fig. 5.3, Sect. 5.2.3.2). As the c's are refined the MO wavefunctions improve and so this average field that each electron feels improves (since J and K, although not explicitly calculated (Sect. 5.2.3.2) improve with the ψ's). When the c's no longer

change the field represented by this last set of c's is (practically) the same as that of the previous cycle, i.e. the two fields are "consistent" with one another, i.e. "self-consistent". This Roothaan-Hall-Hartree-Fock iterative process (initial guess, first **F**, first-cycle c's, second **F**, second-cycle c's, third **F**, etc.) is therefore a *self-consistent-field- procedure* or *SCF procedure*, like the Hartree procedure of Sect. 5.2.2. The terms "Hartree-Fock calculations/method" and "SCF calculations/method" are in practice synonymous. *The key point to the iterative nature of the SCF procedure* is that to get the c's (for the MO's Ψ) and the MO ε's we diagonalize a Fock matrix **F**, but to calculate **F** we need an initial guess for the c's and we then improve the c's by repeatedly recalculating and diagonalizing **F**. The procedure is summarized in Fig. 5.6. Note that in the simple and extended Hückel methods we do not need the c's to calculate **F**, and there is no iterative refinement of the c's, so these are not SCF methods (other semiempirical procedures, however (Chap. 6) do use the SCF approach). A corollary of the SCF procedure is that the

Step 1

Specify geometry, charge and electronic state,
e.g. CH_4 cartesian coordinates, charge = 0, singlet
or CH_4 cartesian coordinates, charge = 0, triplet, etc.

Choose a basis set.

Start the calculation.

1 Define molecule

Step 2

Program calculates integrals: kinetic energy, potential energy, and overlap integrals.

2 calculate integrals

Step 3

Program calculates orthogonalizing matrix using overlap matrix (composed of overlap integrals).

3 calculate othogonalizing matrix

Step 4

Program calculates initial Fock matrix using kinetic energy and potential energy integrals and an initial guess of basis set coefficients (initial guess from, e.g., an extended Hückel calculation; the guess c's usually have to be "projected" to the ab initio basis, which is almost always bigger than that used for the guess calculation).

4 calculate initial Fock matrix

Step 5

Program uses orthogonalizing matrix to transform Fock matrix to one based on an orthonormal set of functions derived from the original atom-centered basis functions.

5 transform Fock matrix

Step 6

Program diagonalizes Fock matrix to get c's (based on the orthonormal, derived basis set) and energy levels.

6 diagonalize Fock matrix

Step 7

Program transforms the c's to a set based on the original, atom-centered basis functions.

7 transform c's

Step 8

Program compares c's (and/or energy, or other parameters) with the previous set; if the match is *not* close enough, another SCF cycle, steps 4--8, is done, using as input for step 4 the latest c's. If the match *is* close enough, the iterations stop.

8 compare parameters with previous ones

Fig. 5.6 Summary of the steps in the Hartree-Fock-Roothaan-Hall SCF procedure

molecular orbitals ψ to be filled are chosen *before* calculation of these orbitals. This is clear from the fact that the MO coefficients of the filled orbitals are used to construct the elements of the density matrix (Sect. 5.2.3.6.4). In contrast, in the simple and extended Hückel methods the MOs are calculated with the aid of a coefficients-free prescription and simply filled according to the electronic state desired (from the bottom up for the ground state).

5.2.3.6.3   Using The Roothaan-Hall Equations to Do Ab initio Calculations– The Equations in Terms of The c's and ϕ's of The LCAO Expansion

The key process in the HF ab initio calculation of energies and wavefunctions is calculation of the Fock matrix, i.e. of the matrix elements F_{rs} (Sect. 5.2.3.6.2). Eq. (5.63) expresses these in terms of the basis functions φ and the operators $\hat{H}^{\text{core}}, \hat{J}$ and $\hat{K}$, but the $\hat{J}$ and $\hat{K}$ operators (Eqs. (5.28) and (5.31)) are themselves functions of the MO's ψ and therefore of the c's and the basis functions ϕ. Obviously the F_{rs} can be written explicitly in terms of the c's and ϕ's; such a formulation enables the Fock matrix to be efficiently calculated from the coefficients and the basis functions without *explicitly* evaluating the operators $\hat{J}$ and $\hat{K}$ after each iteration. This formulation of the Fock matrix will now be explained.

To see more clearly what is required, write Eq. (5.63) as

$$F_{rs} = \left\langle \phi_r(1)\big|\hat{H}^{\text{core}}(1)\big|\phi_s(1)\right\rangle + \sum_{j=1}^{n}\left[2\left\langle\phi_r(1)\big|\hat{J}_j(1)\phi_s(1)\right\rangle - \left\langle\phi_r(1)\big|\hat{K}_j(1)\big|\phi_s(1)\right\rangle\right]$$

$$(5.71)$$

using the compact Dirac notation. The operator $\hat{H}^{\text{core}}(1)$ involves only the Laplacian differentiation operator, atomic numbers and electron coordinates, so we do not have to consider substituting the Roothaan-Hall c's and ϕ's into $\hat{H}^{\text{core}}$. The operators $\hat{J}$ and $\hat{K}$, however, invoke the integrals $\left\langle\phi_r(1)\big|\hat{J}(1)\phi_s(1)\right\rangle$ and $\left\langle\phi_r(1)\big|\hat{K}(1)\phi_s(1)\right\rangle$. We now examine these two integrals.

The first integral, from Eq. (5.65) is

$$\hat{J}_j(1)\phi_s(1) = \phi_s(1)\int\frac{\psi_j^*(2)\psi_j(2)}{r_{12}}dv_2$$

Substituting for $\psi_j^*(2)$ the basis function expansion $\sum c_{tj}^*\phi_t^*(2)$ and for $\psi_j(2)$ the expansion $\sum c_{uj}\phi_u(2)$ (cf. Eq. (5.52)):

$$\hat{J}_j(1)\phi_s(1) = \phi_s(1)\sum_{t=1}^{m}\sum_{u=1}^{m}c_{tj}^*c_{uj}\int\frac{\phi_t^*(2)\phi_u(2)}{r_{12}}dv_2$$

where the double sum arises because we multiply the ψ^* sum by the ψ sum. To get the desired expression for $\langle \phi_r(1)|\hat{J}(1)\phi_s(1)\rangle$ we multiply this by $\phi_r^*(1)$ and integrate with respect to the coordinates of electron 1, getting:

$$\langle \phi_r(1)|\hat{J}_j(1)\phi_s(1)\rangle = \sum_{t=1}^{m}\sum_{u=1}^{m} c_{tj}^* c_{uj} \int \int \frac{\phi_r^*(1)\phi_s(1)\phi_t^*(2)\phi_u(2)}{r_{12}} dv_1 d$$

Note that this is really a sixfold integral, since there are three variables (x_1, y_1, z_1) for electron 1, and three (x_2, y_2, z_2) for electron 2, represented by dv_1 and dv_2 respectively. This equation can be written more compactly as

$$\langle \phi_r(1)|\hat{J}_j(1)\phi_s(1)\rangle = \sum_{t=1}^{m}\sum_{u=1}^{m} c_{tj}^* c_{uj} (rs|tu) \tag{5.72}$$

The notation

$$(rs|tu) = \int \int \frac{\phi_r^*(1)\phi_s(1)\phi_t^*(2)\phi_u(2)}{r_{12}} dv_1 dv_2 \tag{5.73}$$

is a common shorthand for this kind of integral, which is called a *two-electron repulsion integral* (or two-electron integral, or electron repulsion integral: the physical significance of these is outlined in Fig. 5.10 and the discussion immediately following Eq. (5.110)). This parentheses notation should not be confused with the Dirac bra-ket notation, $\langle|$ (a bra) and $|\rangle$ a ket:
by definition

$$\langle f|g\rangle = \int f^*(q)g(q)dq \tag{5.74}$$

so

$$\langle rs|tu\rangle = \int (\phi_r(1)\phi_s(1))^* \phi_t(1)\phi_u(1)dv_1 \tag{5.75}$$

Several notations have been used for the integrals of Eq. (5.73) and for other integrals; make sure to ascertain which symbolism a particular author is using.

The second integral, from Eq. (5.66), is

$$\hat{K}_j(1)\phi_s(1) = \psi_j(1) \int \frac{\psi_j^*(2)\phi_s(2)}{r_{12}} dv_2$$

Substituting for $\psi_j(1)$ the basis function expansion $\sum c_{uj}\phi_u(1)$ and for $\psi_j^*(2)$ the expansion $\sum c_{tj}^*\phi_t^*(2)$ (cf. Eq. (5.52)):

$$\hat{K}_j(1)\phi_s(1) = \phi_u(1)\sum_{t=1}^{m}\sum_{u=1}^{m}c_{tj}^{*}c_{uj}\int\frac{\phi_t^{*}(2)\phi_s(2)}{r_{12}}\,dv_2$$

To get the desired expression for $\langle\phi_r(1)|\hat{K}(1)\phi_s(1)\rangle$ we multiply this by $\phi_r^{*}(1)$ and integrate with respect to the coordinates of electron 1:

$$\langle\phi_r(1)|\hat{K}_j(1)\phi_s(1)\rangle = \sum_{t=1}^{m}\sum_{u=1}^{m}c_{tj}^{*}c_{uj}\iint\frac{\phi_r^{*}(1)\phi_u(1)\phi_t^{*}(2)\phi_s(2)}{r_{12}}\,dv_1dv$$

which can be written more compactly as

$$\langle\phi_r(1)|\hat{K}_j(1)\phi_s(1)\rangle = \sum_{t=1}^{m}\sum_{u=1}^{m}c_{tj}^{*}c_{uj}\left(ru|ts\right) \tag{5.76}$$

where of course (cf. (5.73))

$$\left(ru|ts\right) = \iint\frac{\phi_r^{*}(1)\phi_u(1)\phi_t^{*}(2)\phi_s(2)}{r_{12}}\,dv_1dv_2 \tag{5.77}$$

Substituting Eqs. (5.72) and (5.76) for $\langle\phi_r(1)|\hat{J}(1)\phi_s(1)\rangle$ and $\langle\phi_r(1)|\hat{K}(1)\phi_s(1)\rangle$ into Eq. (5.71) for F_{rs} we get

$$F_{rs} = \left\langle\phi_r(1)|\hat{H}^{\text{core}}(1)|\phi_s(1)\right\rangle + \sum_{j=1}^{n}\left[2\sum_{t=1}^{m}\sum_{u=1}^{m}c_{tj}^{*}c_{uj}\left(rs|tu\right) - \sum_{t=1}^{m}\sum_{u=1}^{m}c_{tj}^{*}c_{uj}\left(ru|ts\right)\right]$$

i.e.

$$F_{rs} = H_{rs}^{\text{core}}(1) + \sum_{t=1}^{m}\sum_{u=1}^{m}\sum_{j=1}^{n}c_{tj}^{*}c_{uj}\left[2\left(rs|tu\right) - \left(ru|ts\right)\right] \tag{5.78}$$

where the integral of the operator $\hat{H}^{\text{core}}$ over the basis functions has been written

$$H_{rs}^{core}(1) = \left\langle\phi_r(1)|\hat{H}^{\text{core}}(1)|\phi_s(1)\right\rangle \tag{5.79}$$

with $\hat{H}^{\text{core}}$ defined by Eq. (5.64).

Equation (5.78), with its ancillary definitions Eqs. (5.73), (5.77) and (5.79), is what we wanted: the Fock matrix elements in terms of the basis functions ϕ and their weighting coefficients c, for a closed-shell molecule; m is the number of basis functions and n is the number of electrons. We can use Eq. (5.78) to calculate MO's and energy levels (Sects. 5.2.3.6.4 and 5.2.3.6.5). Given a basis set and molecular geometry (the integrals depend on molecular geometry, as will be illustrated) and

starting with an initial guess at the c's, one (or rather the computer algorithm) calculates the matrix elements F_{rs}, and assembles them into the Fock matrix $\mathbf{F}$, etc. (Fig. 5.6). Let us now examine certain details connected with Eq. (5.78) and this procedure.

5.2.3.6.4   Using The Roothaan-Hall Equations to Do Ab initio Calculations–Some Details

Equation (5.78) is normally modified by subsuming the c's into P_{tu}, the elements of the density matrix $\mathbf{P}$:

$$\mathbf{P} \begin{pmatrix} P_{11} & P_{12} & P_{13} & \cdots & P_{1m} \\ P_{21} & P_{22} & P_{23} & \cdots & P_{2m} \\ \vdots & \vdots & \cdots & & \vdots \\ P_{m1} & P_{m2} & P_{m3} & \cdots & P_{mm} \end{pmatrix} \tag{5.80}$$

where the density matrix elements are

$$P_{tu} = 2\sum_{j=1}^{n} c_{tj}^{*}c_{uj} \quad t = 1, 2, \quad \ldots, \quad m \quad \text{and} \quad u = 1, 2, \ldots, m \tag{*5.81}$$

(sometimes P is defined as $\sum c^{*}c$). From Eq. (5.78) and Eq. (5.81):

$$F_{rs} = H_{rs}^{\text{core}}(1) + \sum_{t=1}^{m} \sum_{u=1}^{m} P_{tu}\left[(rs|tu) - \frac{1}{2}(ru|ts)\right] \tag{*5.82}$$

Equation (5.82), a slight modification of Eq. (5.78), is the key equation in calculating the ab initio Fock matrix. Each density matrix element P_{tu} represents the coefficients c for a particular pair of basis functions ϕ_t and ϕ_u, summed over all the occupied MO's $\psi_i (i = 1, 2, \ldots, n)$. We use the density matrix here just as a convenient way to express the Fock matrix elements, and to formulate the calculation of properties arising from electron distribution (Sect. 5.5.4), although there is far more to the density matrix concept [27]. Equation (5.82) enables the MO wavefunctions ψ (which are linear combinations of the c's and ϕ's) and their energy levels ε to be calculated by iterative diagonalization of the Fock matrix.

Equation (5.17) $(E = 2\sum H + \sum\sum(2J - K))$ gives one expression for the molecular electronic energy E. If we wish to calculate E from the energy levels, we must note that in the HF method E is not simply twice the sum of the energies of the n occupied energy levels, i.e. it is not the sum of the one-electron energies (as we take it to be in the simple and extended Hückel methods). This is because the MO energy level value ε represents the energy of one electron *subject to interaction with all the other electrons*. The energy of an electron is thus its kinetic energy plus

its electron-nuclear attractive potential energy (H^{core}), plus, courtesy of the J and K integrals (Sect. 5.2.3.5 and Eqs. (5.48), (5.49) and (5.50 = 5.83)), the potential energy from repulsion of all the other electrons:

$$\varepsilon_i = H_{ii}^{\text{core}} + \sum_{j=1}^{n} \left(2J_{ij}(1) - K_{ij}(1)\right) \qquad (5.83 = 5.50)$$

If we add the energies of electron 1 and electron 2, say, we are adding, besides the kinetic energies of these electrons, the repulsion energy of electron 1 on electron 2, 3, 4, ..., and the repulsion energy of electron 2 on electron 1, 3, 4, ... – in other words, we are counting each repulsion twice. The simple sum thus represents properly the total kinetic and electron-nuclear attraction potential energy, but overcounts the electron-electron repulsion potential energy (recall that we are working with $2n$ electrons and thus n filled MOs):

$$E(\text{overestimated}) = 2\sum_{i=1}^{n} \varepsilon_i \qquad (5.84)$$

Note that we cannot just take half of this simple sum, because only the electron-electron energy terms, not all the terms, have been doubly-counted. The solution is to subtract from $2\sum \varepsilon$ the superfluous repulsion energy; from our discussion of Eq. (5.50) in Sect. 5.2.3.5 we saw that the sum $\sum (2J - K)$ over n represents the repulsion energy of one electron interacting with all the other electrons, so to remove the superfluous interactions we subtract $\sum\sum (2J - K)$, the sum over n of the repulsion energy sum, to get [15]

$$E_{\text{HF}} = 2\sum_{i=1}^{n} \varepsilon_j - \sum_{i=1}^{n}\sum_{j=1}^{n} \left(2J_{ij}(1) - K_{ij}(1)\right) \qquad (5.85)$$

E_{HF} is the Hartree-Fock electronic energy: the sum of one-electron energies corrected (within the average-field HF approximation) for electron-electron repulsion. We can get rid of the integrals J and K over MO's ψ and obtain an equation for E_{HF} in terms of c's and ϕ's. From (5.83),

$$\sum_{i=1}^{n}\sum_{j=1}^{n} \left(2J_{ij}(1) - K_{ij}(1)\right) = \sum_{i=1}^{n} \varepsilon_i - \sum_{i=1}^{n} H_{ii}^{\text{core}}$$

and from this and (5.85) we get

$$E_{\text{HF}} = \sum_{i=1}^{n} \varepsilon_i + \sum_{i=1}^{n} H_{ii}^{\text{core}} \qquad (5.86)$$

From the definition of H_{ii}^{core} in Eqs. (5.49) and (5.50), i.e. from

$$H_{ii}^{\text{core}} = \left\langle \psi_i(1)\big|\hat{H}^{\text{core}}\big|\psi_i \right\rangle \tag{5.87}$$

and the LCAO exapansion (5.52)

$$\psi_i = \sum_{s=1}^{m} c_{si}\phi_s \tag{5.88 = 5.52}$$

we get from Eq. (5.86)

$$E_{\text{HF}} = \sum_{i=1}^{n} \varepsilon_i + \sum_{r=1}^{m}\sum_{s=1}^{m}\sum_{i=1}^{n} c_{ri}^* c_{si} H_{rs}^{\text{core}} \tag{5.89}$$

Using Eq. (5.81), Eq. (5.89) can be written in terms of the density matrix elements P:

$$E_{\text{HF}} = \sum_{i=1}^{n} \varepsilon_i + \frac{1}{2}\sum_{r=1}^{m}\sum_{s=1}^{m} P_{rs} H_{rs}^{\text{core}} \tag{5.90}$$

This is the key equation for calculating the HF electronic energy of a molecule. It can be used when self-consistency has been reached, or after each SCF cycle employing the ε's and c's yielded by that particular iteration, and H_{rs}^{core}, which latter does not change from iteration to iteration, since it is composed only of the fixed basis functions and an operator which does not contain ε's or c's: from Eqs. (5.64 = 5.19) and (5.79)

$$H_{rs}^{\text{core}} = \left\langle \phi_r \big| \frac{1}{2}\nabla_i^2 - \sum_{\text{all }\mu} \frac{Z_\mu}{r_{\mu i}} \big| \phi_s \right\rangle \tag{5.91}$$

H_{rs}^{core} does not change because the SCF procedure refines the electron-electron repulsion (till the field each electron feels is "consistent" with the previous one), but H_{rs}^{core} in contrast represents only the contribution to the kinetic energy plus the potential energy represented by electron-nucleus attraction of the electron density associated with each pair of basis functions ϕ_r and ϕ_s.

Equation (5.90) gives the HF electronic energy of the molecule or atom–the energy of the electrons due to their motion (their kinetic energy) plus their energy due to electron-nucleus attraction and (within the HF approximation) to electron-electron repulsion (their potential energy). The *total* energy of the molecule, however, involves not just the electrons but also the nuclei, which contribute potential energy due to internuclear repulsion, and kinetic energy due to nuclear motion. This motion persists even at 0 K, because the molecule vibrates even at this

temperature; this unavoidable vibrational energy is called the *zero point vibrational energy* or *zero point energy* (ZPVE or ZPE; Chap. 2, Sect. 2.5, Fig. 2.20 and associated discussion). Calculation of the internuclear repulsion energy is trivial, as this is just the sum of all pairs of Coulombic repulsions between

$$V_{NN} = \sum_{\text{all } \mu, v} \frac{Z_\mu Z_v}{r_{uv}} \qquad (5.92 = 5.16)$$

Calculation of the ZPE is more involved; the standard method requires calculating the harmonic frequencies (i.e. the normal-mode vibrations of Chap. 2, Sect. 2.5) and summing the energies of each mode [28a] (all this is done by standard programs, which print out the ZPE after the frequencies). Adding the HF electronic energy and the internuclear repulsion gives what we might call $E_{\text{HF}}^{\text{total}}$, the total "frozen-nuclei" (no ZPE) energy:

$$E_{\text{HF}}^{\text{total}} = E_{\text{HF}} + V_{NN} = \sum_{i=1}^{n} \varepsilon_i + \frac{1}{2} \sum_{r=1}^{m} \sum_{s=1}^{m} P_{rs} H_{rs}^{\text{core}} + V_{NN} \qquad (5.93)$$

from (5.90) to (5.92). $E_{\text{HF}}^{\text{total}}$, the energy usually displayed at the end of a Hartree-Fock calculation is, in ordinary parlance, "the Hartree-Fock energy". Some program printouts state or imply that this is the HF electronic energy, but strictly speaking it is electronic plus internuclear energy.

An aggregate of such energies, plotted against various geometries, represents an HF Born-Oppenheimer PES (Chap. 2, Sect. 2.3). The zero of energy for the Schrödinger equation for an atom or molecule is normally taken as the energy of the electrons and nuclei at rest at infinite separation. The Hartree-Fock energy (any ab initio energy, in fact) of a species in thus relative to the energy of the electrons and nuclei at rest at infinite separation, i.e. it is the negative of the minimum energy required to break up the molecule or atom and separate the electrons and nuclei to infinity. We are normally interested in *relative* energies, *differences* in "absolute" ab initio energies of chemical species. Ab initio energies are discussed in Sect. 5.5.2.

In a geometry optimization (Chap. 2, Sect. 2.4) a series of single-point calculations (calculations at a single point on the potential energy surface, i.e. at a single geometry) is done, each of which requires the calculation of $E_{\text{HF}}^{\text{total}}$, and the geometry is changed systematically until a stationary point is reached (one where the potential energy surface is flat; *ideally* $E_{\text{HF}}^{\text{total}}$ should fall monotonically in the case of optimization to a minimum). The ZPE calculation, which is valid only for a stationary point on the potential energy surface (Chap. 2, Sect. 2.5; discussion in connection with Fig. 2.19), can be used to correct $E_{\text{HF}}^{\text{total}}$ of the optimized structure for vibrational energy; adding the ZPE gives the total internal energy of the molecule at 0 K, which we could call $E_{\text{0K}}^{\text{total}}$:

$$E_{\text{0K}}^{\text{total}} = E_{\text{HF}}^{\text{total}} + \text{ZPE} \qquad (*5.94)$$

The relative energies of isomers may be calculated by comparing $E_{\text{HF}}^{\text{total}}$, but for accurate work the ZPE should be taken into account, even though the required frequency calculations usually take significantly longer than the geometry optimization–see Sect. 5.3.3, Table 5.3). Fortunately, it is valid to correct $E_{\text{HF}}^{\text{total}}$ with a ZPE from a lower-level optimization-plus-frequency job (not a lower-level frequency job on the higher-level geometry). Figure 2.19 in Chap. 2, Sect. 2.5 compares energies for the species in the isomerization of HNC to HCN. The relative energies with/without the ZPE correction for HCN, transition state, and HNC are 0/0, 202/219, and 49.7/52.2 kJ mol^{-1}. The ZPEs of isomers tend to be roughly equal and so to cancel when relative energies are calculated (less so where transition states are involved), but, as implied above, in accurate work it is standard to compare the ZPE-corrected energies $E_{\text{0K}}^{\text{total}}$. A method of accurately estimating ZPE which does not involve the sometimes-lengthy calculation of second derivatives (Chap. 2, Sect. 2.5), but rather draws on tabulated values for atom types has been published [28b]. This additive, atom-type based (ATB) method requires essentially no time and has been called a "zero-cost estimation" method.

5.2.3.6.5   Using The Roothaan-Hall Equations to Do Ab initio Calculations– An Example

The application of the Hartree-Fock method to an actual calculation will now be illustrated in detail with protonated helium, $H-He^+$, the simplest closed-shell heteronuclear molecule. This species was also used to illustrate the details of the extended Hückel method (EHM) in Chap. 4, Sect. 4.3.2. In this simple example all the steps were done with a pocket calculator, except for the evaluation of the integrals (this was done with the ab initio program Gaussian 92 [29]) and the matrix multiplication and diagonalization steps (done with the program Mathcad [30]).

Step 1 Specifying the geometry, basis set and MO orbital occupancy

We start by specifying a geometry and a basis set. We will use same geometry as with the EHM, 0.800 Å, i.e. 1.5117 a.u. (bohr). In ab initio calculations on molecules, the basis functions are almost always *Gaussian functions* (basis functions are discussed in Sect. 5.3). Gaussian functions differ from the Slater functions we used in the EHM in Chap. 4 in that the exponent involves the *square* of the distance of the electron from the point (usually an atomic nucleus) on which the function is centered:

An s-type Slater function

$$\phi = a\exp(-br) \tag{5.95}$$

An *s*-type Gaussian function

$$\phi = a\exp\left(-br^2\right) \tag{5.96}$$

In ab initio calculations the mathematically more tractable Gaussians are used to approximate the physically more realistic Slater functions (see Sect. 5.3). We use here the simplest possible Gaussian basis set: a $1s$ atomic orbital on each of the two atoms, each $1s$ orbital being approximated by one Gaussian function. This is called an STO-1G basis set, meaning Slater-type orbitals-one Gaussian, because we are approximating a Slater-type $1s$ orbital with a Gaussian function. The best STO-1G approximations to the hydrogen and helium $1s$ orbitals in a molecular environment [31] are

$$\phi(H) = \phi_1 = 0.3696 \exp\left(-0.4166|\mathbf{r} - \mathbf{R}_1|^2\right) \tag{5.97}$$

$$\phi(He) = \phi_2 = 0.5881 \exp\left(-0.7739|\mathbf{r} - \mathbf{R}_2|^2\right) \tag{5.98}$$

where $|\mathbf{r} - \mathbf{R}_i|$ is the distance of the electron in ϕ_i (ϕ is a one-electron function) from nucleus i on which ϕ_i is centered (Fig. 5.7). The larger constant in the helium exponent as compared to that of hydrogen (0.7739 vs. 0.4166) reflects the intuitively reasonable fact that since an electron in ϕ_2 is bound more tightly to its doubly-charged nucleus than is an electron in ϕ_1 is to its singly-charged nucleus, electron density around the helium nucleus falls off more quickly with distance than does that around the hydrogen nucleus (Fig. 5.8).
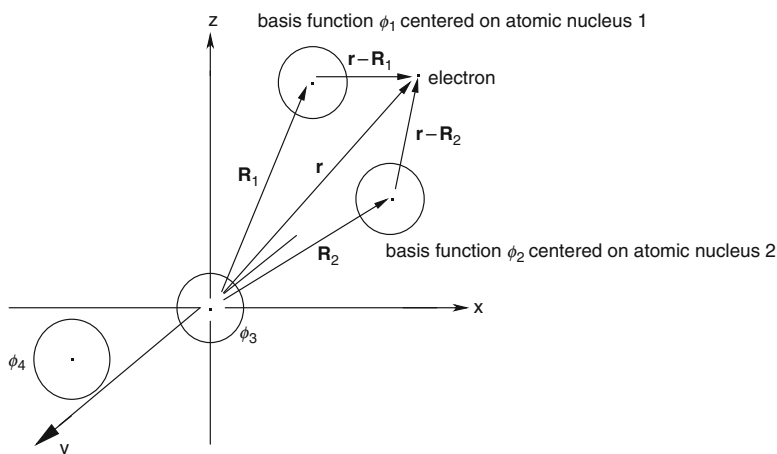
Fig. 5.7 A four-atom molecule in a coordinate system. Only one of possibly many electrons is shown. The basis functions ϕ are one-electron functions, usually centered on atomic nuclei. $\mathbf{R}_1$, $\mathbf{R}_2$, etc., are vectors representing the x, y, z coordinates (conveniently as 3×1 column matrices; Chap. 4, Sect. 4.3.3) of the nuclei ("of the atoms"), and $\mathbf{r}$ is a vector representing the x, y, z coordinates of an electron. The distances of the electron from the centers of the various basis functions are the absolute values of the various vector differences: $|\mathbf{r} - \mathbf{R}_1|$, $|\mathbf{r} - \mathbf{R}_2|$, etc. For a particular molecular geometry, $\mathbf{R}_1$, $\mathbf{R}_2$, etc. are fixed and enter the functions ϕ_1, ϕ_2, etc., only parametrically, i.e. to denote where the ϕ's are centered; $\mathbf{r}$ is the variable in these functions, which are thus $\phi(x, y, z)$. Several basis functions may be centered on each nucleus

$\phi(x, y, z) = \phi(|\mathbf{r} - \mathbf{R}|)$

$|\mathbf{r} - \mathbf{R}|$	$\phi(H) = 0.3696\exp(-0.4166|\mathbf{r} - \mathbf{R}_1|)$	$\phi(He) = 0.5881\exp(-0.7739|\mathbf{r} - \mathbf{R}_2|)$
0	0.370	0.588
0.5	0.333	0.485
1.0	0.244	0.271
2.0	0.070	0.027
3.0	0.009	0.0006
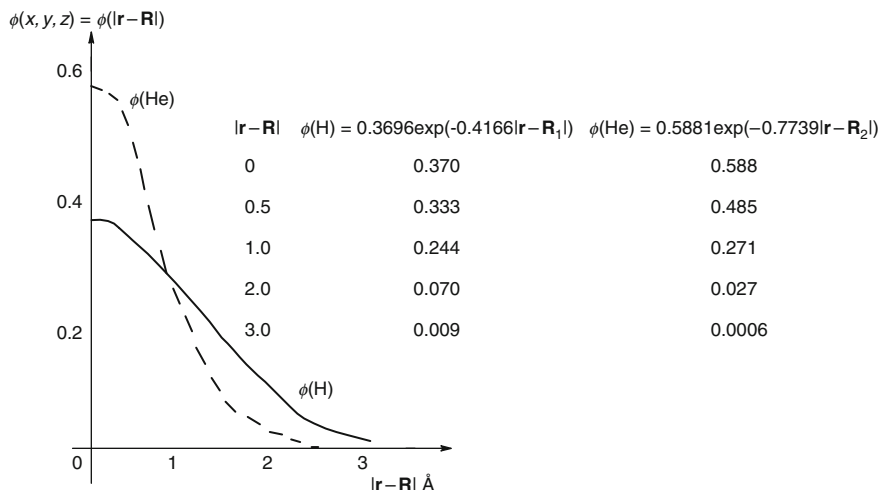
Fig. 5.8 Electron density around the helium nucleus falls off more quickly than electron density around the lower-charge hydrogen nucleus

We have a geometry and a basis set, and wish to do an SCF calculation on HHe$^+$ with both electrons in the lowest MO, ψ_1, i.e. on the *singlet* ground state. In general, SCF calculations proceed from specification of geometry, basis set, charge and multiplicity. The multiplicity is a way of specifying the number of unpaired electrons:

$$\text{Multiplicity} = S = 2s + 1 \qquad (5.99)$$

where $S = $ total number of unpaired electron spins (each electron has a spin of $\pm\frac{1}{2}$), taking each unpaired spin as $+\frac{1}{2}$. Figure 5.9 shows some examples of the specification of charge and multiplicity. By default an SCF calculation is performed on the *ground state* of specified multiplicity, i.e. the MO's are filled from ψ_1 up to give the lowest-energy state of that multiplicity.

Step 2 Calculating the integrals

Having specified a Hartree-Fock calculation on singlet HHe$^+$, with H–He $=$ 0.800 Å (1.5117 bohr), using an STO-1G basis set, the most straightforward way to proceed is to now calculate all the integrals, and the orthogonalizing matrix $\mathbf{S}^{-1/2}$ that will be used to transform the Fock matrix $\mathbf{F}$ to $\mathbf{F}'$ and to convert the transformed coefficient matrix $\mathbf{C}'$ to $\mathbf{C}$ (Eqs. (5.67), (5.68), (5.69), and (5.70)). The integrals are those required for H^{core}, the one-electron part of the elements F_{rs} of $\mathbf{F}$, and the two-electron repulsion integrals $(rs|tu)$, $(ru|ts)$ (Eq. (5.82)), as well as the overlap integrals, which are needed to calculate the overlap matrix $\mathbf{S}$ and thus the orthogonalizing matrix $\mathbf{S}^{-1/2}$ (Eq. (5.67)).

eV (1 eV particle^{-1} = 96.5 kJ mol^{-1})

	H_2O	H_2O	H_2O
	neutral, singlet	neutral, triplet	radical cation, doublet
			i.e. $H_2O^{\cdot+}$
	0 unpaired electrons,	2 unpaired electrons,	1 unpaired electron,
	S = 0	S = 1/2 + 1/2 = 1	S = 1/2
	multiplicity = 2S + 1 = 1	multiplicity = 2S + 1 = 3	multiplicity = 2S + 1 = 2
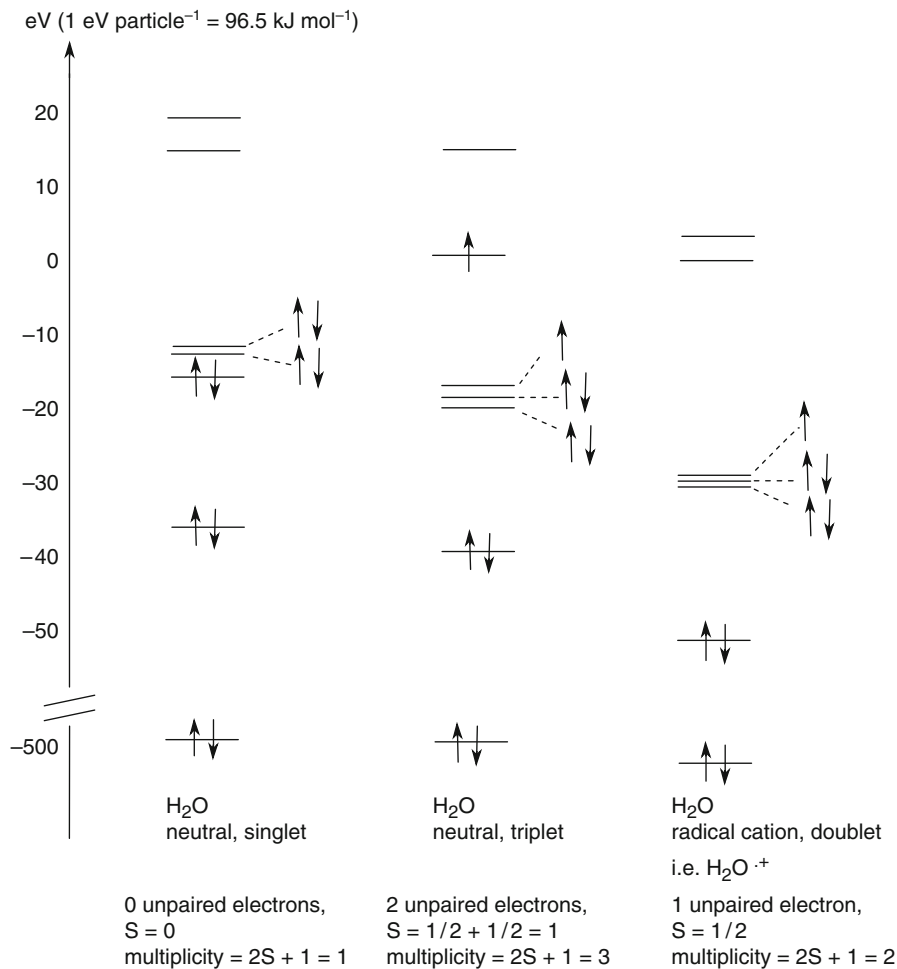
Fig. 5.9 Some examples of the results of specification of charge and multiplicity. The calculations used the STO-3G basis set (Sect. 5.3) which has seven basis functions, and so creates seven MOs. All calculations were at the HF/STO-3G geometry of the neutral singlet

Efficient methods have been developed for calculating these integrals [32] and their values will simply be given later. For our calculation the elements F_{rs} of the Fock matrix (Eq. (5.82)) are conveniently written

$$F_{rs} = H_{rs}^{\text{core}}(1) + \sum_{t=1}^{m}\sum_{u=1}^{m} P_{tu}\left[(rs|tu) - \frac{1}{2}(ru|ts)\right]$$

$$= T_{rs} + V_{rs}(\text{H}) + V_{rs}(\text{He}) + G_{rs}$$

(5.100)

Here $H^{\text{core}}(1)$ has been dissected into a kinetic energy integral T and two potential energy integrals, $V(\text{H})$ and $V(\text{He})$. From the definition of the operator

$\hat{H}^{\mathrm{core}}$ (Eq. (5.64)) and the Roothaan-Hall expression for the integral H^{core} (Eq. (5.79)) we see that (the (1) emphasizes that these integrals involve the coordinates of only one electron):

$$T_{rs}(1) = \int \phi_r \left(-\frac{1}{2} \nabla_1^2 \right) \phi_s dv$$

$$= \int \phi_r \left[-\frac{1}{2} \left(\frac{\partial^2}{\partial x^2} + \frac{\partial^2}{\partial y^2} + \frac{\partial^2}{\partial z^2} \right) \right] \phi_s dv \tag{5.101}$$

$$V_{rs}(\mathrm{H}, 1) = \int \phi_r \left(\frac{Z_\mathrm{H}}{r_\mathrm{H1}} \right) \phi_s dv \tag{5.102}$$

and

$$V_{rs}(\mathrm{He}, 1) = \int \phi_r \left(\frac{Z_\mathrm{He}}{r_\mathrm{He1}} \right) \phi_s dv \tag{5.103}$$

In Eq. (5.102) the variable is the distance of the electron ("electron 1"–see the discussion in connection with Eqs. (5.18) and (5.19)) from the hydrogen nucleus, and in Eq. (5.103) the variable is the distance of the electron from the helium nucleus; Z_H and Z_He are 1 and 2, respectively.

From Eq. (5.100) the two-electron contribution to each Fock matrix element is

$$G_{rs} = \sum_{t=1}^{m} \sum_{u=1}^{m} P_{tu} \left[(rs|ts) - \frac{1}{2}(ru|ts) \right] \tag{5.104}$$

Each element G_{rs} is calculated from a density matrix element P_{tu} (Eqs. (5.80) and (5.81)) and two two-electron integrals $(rs|tu)$ and $(ru|ts)$ (Eqs. (5.73) and (5.77)).

The required 1-electron integrals for calculating the Fock matrix $\mathbf{F}$ are

$$\begin{array}{lll} T_{11} = 0.6249 & T_{12} = T_{21} = 0.2395 & T_{22} = 1.1609 \\ V_{11}(\mathrm{H}) = -1.0300 & V_{12}(\mathrm{H}) = V_{21}(\mathrm{H}) = -0.4445 & V_{22}(\mathrm{H}) = -0.6563 \\ V_{11}(\mathrm{He}) = -1.2555 & V_{12}(\mathrm{He}) = V_{21}(\mathrm{He}) = -1.1110 & V_{22}(\mathrm{He}) = -2.8076 \end{array} \tag{5.105}$$

To see which two-electron integrals are needed we evaluate the summation in Eq. (5.104) for each of the matrix elements (G_{11}, G_{12}, G_{21}, G_{22}):

$$G_{11} = \sum_{t=1}^{2} \sum_{u=1}^{2} P_{tu} \left[(11|tu) - \frac{1}{2}(1u|t1) \right]$$

$$\text{i.e } G_{11} = \sum_{t=1}^{2} \left[P_{t1}\left[(11|t1) - \frac{1}{2}(11|t1)\right] + P_{t2}\left[(11|t2) - \frac{1}{2}(12|t1)\right] \right]$$

$$= P_{11}\left[(11|11) - \frac{1}{2}(11|11)\right] + P_{12}\left[(11|12) - \frac{1}{2}(12|11)\right] \qquad (5.106)$$

$$+ P_{21}\left[(11|21) - \frac{1}{2}(11|21)\right] + P_{22}\left[(11|22) - \frac{1}{2}(12|21)\right]$$

$$G_{12} = G_{21} = \sum_{t=1}^{2}\sum_{u=1}^{2} P_{tu}\left[(12|tu) - \frac{1}{2}(1u|t2)\right]$$

$$\text{i.e } G_{12} = G_{21} = \sum_{t=1}^{2}\left[P_{t1}\left[(12|t1) - \frac{1}{2}(11|t2)\right] + P_{t2}\left[(12|t2) - \frac{1}{2}(12|t2)\right]\right]$$

$$= P_{11}\left[(12|11) - \frac{1}{2}(11|12)\right] + P_{12}\left[(12|12) - \frac{1}{2}(12|12)\right]$$

$$+ P_{21}\left[(12|21) - \frac{1}{2}(11|22)\right] + P_{22}\left[(12|22) - \frac{1}{2}(12|22)\right]$$

$$(5.107)$$

$$G_{22} = \sum_{t=1}^{2}\sum_{u=1}^{2} P_{tu}\left[(22|tu) - \frac{1}{2}(2u|t2)\right]$$

$$\text{i.e. } G_{22} = \sum_{t=1}^{2}\left[P_{t1}\left[(22|t1) - \frac{1}{2}(21|t2)\right] + P\left[(22|t2) - \frac{1}{2}(22|t2)\right]\right]$$

$$= P_{11}\left[(22|11) - \frac{1}{2}(21|12)\right] + P_{12}\left[(22|12) - \frac{1}{2}(22|12)\right] \qquad (5.108)$$

$$+ P_{21}\left[(22|21) - \frac{1}{2}(21|22)\right] + P_{22}\left[(22|22) - \frac{1}{2}(22|22)\right]$$

Each element of the electron repulsion matrix **G** has eight 2-electron repulsion integrals, and of these 32 there appear to be 14 different ones:

from G_{11} : $(11|11)$, $(11|12)$, $12|11)$, $(11|21)$, $(11|22)$, $(12|21)$
new with $G_{12} = G_{21}$: $(12|12)$, $(12|22)$
new with G_{22} : $(22|11)$, $(21|12)$, $(22|12)$, $(22|21)$, $(21|22)$, $(22|22)$

However, examination of Eq. (5.73) shows that many of these are the same. It is easy to see that if the basis functions are real (as is almost always the case) then

$$(rs|tu) = (rs|ut) = (sr|tu) = (sr|ut) = (tu|rs) = (tu|sr)$$
$$= (ut|rs) = (ut|sr) \qquad (5.109)$$

Taking this into account, there are only six unique 2-electron repulsion integrals, whose values are:

$$
\begin{aligned}
(11|11) &= 0.7283 & (21|21) &= 0.2192 \\
(21|11) &= 0.3418 & (22|21) &= 0.4368 \\
(22|11) &= 0.5850 & (22|22) &= 0.9927
\end{aligned}
\tag{5.110}
$$

The integrals $(11|11)$ and $(22|22)$ represent repulsion between two electrons both in the same orbital (ϕ_1 or ϕ_2, respectively), while $(22|11)$ represents repulsion between an electron in ϕ_2 and one in ϕ_1; $(21|11)$ could be regarded as representing the repulsion between an electron associated with ϕ_2 and ϕ_1 and one confined to ϕ_1, and analogously for $(22|21)$, while $(21|21)$ can be thought of as the repulsion between two electrons both of which are associated with ϕ_2 and ϕ_1 (Fig. 5.10). Note that in the T and V terms of the Fock matrix elements, the operator in the integrals is $-(1/2)\nabla^2$ and Z_H/r_{H1} or Z_{He}/r_{He1}, while in the G terms it is $1/r_{12}$ (Eqs. (5.101), (5.102), (5.103), and (5.73)).

The overlap integrals are

$$
S_{11} = 1.0000 \quad S_{12} = S_{21} = 0.5017 \quad S_{22} = 1.0000
\tag{5.111}
$$

and the overlap matrix is

$$
\mathbf{S} = \begin{pmatrix} 1.0000 & 0.5017 \\ 0.5017 & 1.0000 \end{pmatrix}
\tag{5.112}
$$

ϕ_1 superposed right on ϕ_1
(11|11)

ϕ_2 ϕ_1
(22|11)

ϕ_2 ϕ_1
(21|11)

ϕ_2 ϕ_1
(21|21)
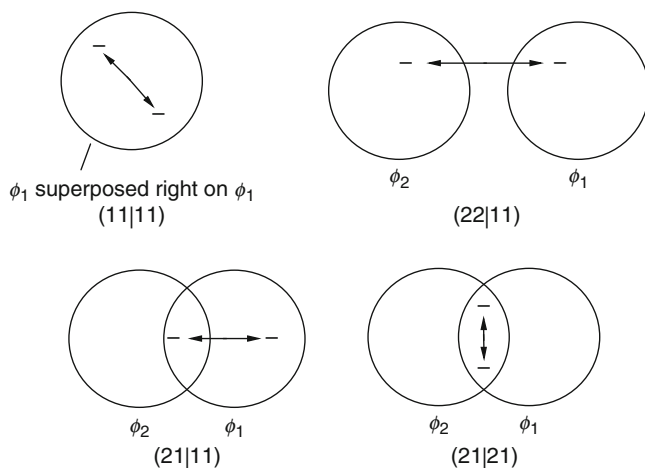
Fig. 5.10 Schematic depictions of the physical meaning of some two-electron repulsion integrals (Sect. 5.2.3.6.5). Each basis function ϕ is normally centered on an atomic nucleus. The integrals shown here are one-center and two-center two-electron repulsion integrals–they are centered on one and on two atomic nuclei, respectively. For molecules with three nuclei three-center integrals arise, and for molecules with four or more nuclei, four-center integrals arise

Step 3 Calculating the orthogonalizing matrix

Calculating the orthogonalizing matrix $S^{-1/2}$ (see Eqs. (5.67), (5.68), and (5.69) and the discussion referred to in Chap. 4):Diagonalizing **S**:

$$\mathbf{S} = \underbrace{\begin{pmatrix} 0.7071 & 0.7071 \\ 0.7071 & -0.7071 \end{pmatrix}}_{\mathbf{P}} \underbrace{\begin{pmatrix} 1.5017 & 0.0000 \\ 0.0000 & -0.4983 \end{pmatrix}}_{\mathbf{D}} \underbrace{\begin{pmatrix} 0.7071 & 0.7071 \\ 0.7071 & -0.7071 \end{pmatrix}}_{\mathbf{P}^{-1}}$$

$$(5.113)$$

Calculating $\mathbf{D}^{-1/2}$:

$$\mathbf{D}^{-1/2} = \begin{pmatrix} 1.5017^{-1/2} & 0.0000 \\ 0.0000 & 0.4983^{-1/2} \end{pmatrix} = \begin{pmatrix} 1.8160 & 0.0000 \\ 0.0000 & 1.4166 \end{pmatrix} \qquad (5.114)$$

Calculating $\mathbf{S}^{-1/2}$:

$$\mathbf{S}^{-1/2} = \mathbf{P}\mathbf{D}^{-1/2}\mathbf{P}^{-1} = \begin{pmatrix} 1.1163 & -0.3003 \\ -0.3003 & 1.1163 \end{pmatrix} \qquad (5.115)$$

Step 4 Calculating the Fock matrix

(a) The 1-electron matrices

From Eq. (5.100)

$$\mathbf{F} = \mathbf{T} + \mathbf{V}(\mathrm{H}) + \mathbf{V}(\mathrm{He}) + \mathbf{G} = \mathbf{H}^{\mathrm{core}} + \mathbf{G} \qquad (5.116)$$

The 1-electron matrices $\mathbf{T}$, $\mathbf{V}(\mathrm{H})$ and $\mathbf{V}(\mathrm{He})$ (i.e. $\mathbf{H}^{\mathrm{core}}$) follow immediately from the 1-electron integrals. The kinetic energy matrix is

$$\mathbf{T}\begin{pmatrix} T_{11} & T_{12} \\ T_{21} & T_{22} \end{pmatrix} = \begin{pmatrix} 0.6249 & 0.2395 \\ 0.2395 & 1.1609 \end{pmatrix} \qquad (5.117)$$

T_{11} is smaller than T_{22}, as the kinetic energy of an electron in ϕ_1 ($\phi(\mathrm{H})$) is smaller than that of an electron in ϕ_2 ($\phi(\mathrm{He})$); this is expected since the larger charge on the helium nucleus results in a larger kinetic energy for an electron in its $1s$ orbital than for an electron in the hydrogen $1s$ orbital–classically speaking, the electron must move faster to stay in orbit around the stronger-pulling He nucleus. T_{12} can be regarded as the kinetic energy of an electron in the H($1s$)-He($1s$) overlap region.

The hydrogen potential energy matrix is

$$\mathbf{V}(\mathrm{H}) = \begin{pmatrix} V_{11}(\mathrm{H}) & V_{12}(\mathrm{H}) \\ V_{21}(\mathrm{H}) & V_{22}(\mathrm{H}) \end{pmatrix} = \begin{pmatrix} -1.0300 & -0.4445 \\ -0.4445 & -0.6563 \end{pmatrix} \qquad (5.118)$$

All the $V(H)$ values represent the attraction of an electron to the hydrogen nucleus. $V_{11}(H)$ is the potential energy due to attraction of an electron in ϕ_1 to the hydrogen nucleus, and $V_{22}(H)$ is the potential energy due to attraction of an electron in ϕ_2 to the hydrogen nucleus. As expected, an electron in ϕ_1 ($\phi(H)$) is attracted to the H nucleus more strongly (the potential energy is more negative) than is an electron in ϕ_2 ($\phi(He)$). $V_{12}(H)$ can be regarded as the potential energy of attraction to the hydrogen nucleus of an electron in the H$(1\,s)$–He$(1\,s)$ overlap region.

The helium potential energy matrix is

$$\mathbf{V}(\text{He}) = \begin{pmatrix} V_{11}(\text{He}) & V_{12}(\text{He}) \\ V_{21}(\text{He}) & V_{22}(\text{He}) \end{pmatrix} = \begin{pmatrix} -1.2555 & -1.1110 \\ -1.1110 & -2.8076 \end{pmatrix} \qquad (5.119)$$

All the $V(He)$ values represent the attraction of an electron to the helium nucleus. $V_{11}(He)$, the potential energy of attraction of an electron in $\phi(H)$ to the helium nucleus, is of course less negative than the potential energy of attraction of an electron in $\phi(He)$ to this same nucleus. $V_{12}(He)$ can be taken as the potential energy of attraction to the helium nucleus of an electron in the H$(1\,s)$-He$(1\,s)$ overlap region. An electron in $\phi(He)$ is attracted to the helium nucleus more strongly than an electron in $\phi(H)$ is attracted to the hydrogen nucleus (-2.8076 in $\mathbf{V}(He)$ *cf.* -1.0300 in $\mathbf{V}(H)$), due to the greater nuclear charge of helium.

The total 1-electron energy matrix, $\mathbf{H}^{core}$, is

$$\mathbf{H}^{core} = \mathbf{T} + \mathbf{V}(H) + \mathbf{V}(He) = \begin{pmatrix} -1.6606 & -1.3160 \\ -1.3160 & -2.3030 \end{pmatrix} \qquad (5.120)$$

This matrix represents the 1-electron energy (the energy the electron would have if interelectronic repulsion did not exist) of an electron in H$-$He$^+$, at the specified geometry, for this STO-1G basis set. The (1,1), (2,2) and (1,2) terms represent, ignoring electron-electron repulsion, the energy of an electron in ϕ_1, ϕ_2, and the $\phi_1-\phi_2$ overlap region, respectively; the values are the net result of the various kinetic energy and potential energy terms discussed above.

(b) The 2-electron matrix

The 2-electron matrix $\mathbf{G}$, the electron repulsion matrix (Eq. (5.111)), is calculated from the 2-electron integrals and the density matrix elements (Eq. (5.104)). This is intuitively plausible since each 2-electron integral describes one interelectronic repulsion in terms of basis functions(Fig. 5.10) while each density matrix element represents (see Sect. 5.2.3.6.4) the electron density *on* (the diagonal elements of $\mathbf{P}$ in Eq. (5.80)) or *between* (the off-diagonal elements of $\mathbf{P}$) basis functions. To calculate the matrix elements G_{rs} (Eqs. (5.106), (5.107) and (5.108)) we need the appropriate integrals (Eqs. 5.110) and density matrix elements. These latter are calculated from

$$P_{tu} = 2\sum_{j=1}^{n} c_{tj}^* c_{uj} \quad t = 1, 2, \cdots, m \text{ and } u = 1, 2, \cdots, m \qquad (5.121 = 5.81)$$

Each P_{rs} involves the sum over the occupied MO's ($j = 1$–n; we are dealing with a closed-shell ground-state molecule with $2n$ electrons) of the products of the coefficients of the basis functions ϕ_r and ϕ_s. As pointed out in Sect. 5.2.3.6.2 the Hartree-Fock procedure is usually started with an "initial guess" at the coefficients. We can use as our guess the extended Hückel coefficients we obtained for HeH⁺, with this same geometry (Chap. 4, Sect. 4.4.2); we need the c's only for the *occupied* MO's:

$$c_{11} = 0.249, \qquad c_{21} = 0.867 \tag{5.122}$$

(Usually we need more c's than the small basis set of an extended Hückel or other semiempirical calculation supplies; a *projected* semiempirical wavefunction is then used, with the missing c's extrapolated from the available ones). Using these c's and Eq. (5.121) we calculate the initial-guess P's for Eqs. (5.106), (5.107), and (5.108); since there is only one occupied MO ($n = 1$ in Eq 5.121) the summation has only one term:

$$
\begin{aligned}
P_{11} &= 2c_{11}c_{11} = 2(0.249)0.249 = 0.1240 \\
P_{12} &= 2c_{11}c_{21} = 2(0.249)0.867 = 0.4318 \\
P_{22} &= 2c_{21}c_{21} = 2(0.867)0.867 = 1.5034
\end{aligned}
\tag{5.123}
$$

G may now be calculated. From Eqs. (5.106), (5.107), and (5.108), using the above values of P and the integrals of Eq. (5.110), and recalling that integrals like $(11|12)$ and $(21|11)$ are equal (Eq. (5.109) we get:

$$
\begin{aligned}
G_{11} = P_{11}&\left[(11|11) - \frac{1}{2}(11|11)\right] + P_{12}\left[(11|12) - \frac{1}{2}(12|11)\right] \\
+P_{21}&\left[(11|21) - \frac{1}{2}(11|21)\right] + P_{22}\left[(11|22) - \frac{1}{2}(12|21)\right] \\
= 0.1240&(0.3642) + 0.4318(0.1709) \\
+0.4318&(0.1709) + 1.5034(0.4754) = 0.9075
\end{aligned}
\tag{5.124}
$$

$$
\begin{aligned}
G_{12} = G_{21} = P_{11}&\left[(12|11) - \frac{1}{2}(11|12)\right] + P_{12}\left[(12|12) - \frac{1}{2}(12|12)\right] \\
+P_{21}&\left[(12|21) - \frac{1}{2}(11|22)\right] + P_{22}\left[(12|22) - \frac{1}{2}(12|22)\right] \\
= 0.1240&(0.1709) + 0.4318(0.1096) \\
+0.4318&(0.0733) + 1.5034(0.2184) = 0.3652
\end{aligned}
\tag{5.125}
$$

$$
\begin{aligned}
G_{22} = P_{11}&\left[(22|11) - \frac{1}{2}(21|12)\right] + P_{12}\left[(22|12) - \frac{1}{2}(22|12)\right] \\
+P_{21}&\left[(22|21) - \frac{1}{2}(21|22)\right] + P_{22}\left[(22|22) - \frac{1}{2}(22|22)\right] \\
= 0.1240&(0.4754) + 0.4318(0.2184) \\
+0.4318&(0.2184) + 1.5034(0.4964) = 0.9938
\end{aligned}
\tag{5.126}
$$

From the G values based on the initial guess c's the initial-guess electron repulsion matrix is

$$\mathbf{G}_0 = \begin{pmatrix} 0.9075 & 0.3652 \\ 0.3652 & 0.9938 \end{pmatrix} \tag{5.127}$$

The initial-guess Fock matrix is (Eqs. (5.116), (5.120) and (5.126))

$$\begin{aligned}
\mathbf{F}_0 &= \mathbf{T} + \mathbf{V}(\mathrm{H}) + \mathbf{V}(\mathrm{He}) + \mathbf{G}_0 = \mathbf{H}^{\mathrm{core}} + \mathbf{G}_0 \\
&= \begin{pmatrix} -1.6606 & -1.3160 \\ -1.3160 & -2.3030 \end{pmatrix} + \begin{pmatrix} 0.9095 & 0.3652 \\ 0.3652 & 0.9938 \end{pmatrix} = \begin{pmatrix} -0.7511 & -0.9508 \\ -0.9508 & -1.3092 \end{pmatrix}
\end{aligned} \tag{5.128}$$

The zero subscripts in Eqs. (5.127) and (5.128) emphasize that the initial-guess c's, with no iterative refinement, were used to calculate $\mathbf{G}$; in the subsequent iterations of the SCF procedure $\mathbf{H}^{\mathrm{core}}$ will remain constant while $\mathbf{G}$ will be refined as the c's, and thus the P's, change from SCF cycle to cycle. The change in the electron repulsion matrix $\mathbf{G}$ corresponds to that in the molecular wavefunction as the c's change (recall the LCAO expansion); it is the wavefunction (squared) which represents the time-averaged electron distribution and thus the electron/charge cloud repulsion.

Step 5 Transforming $\mathbf{F}$ to $\mathbf{F}'$, the Fock matrix that satisfies $\mathbf{F}' = \mathbf{C}' \boldsymbol{\varepsilon} \, \mathbf{C}'^{-1}$

As in Chap. 4, Sect. 4.4.2, we use the orthogonalizing matrix $\mathbf{S}^{-1/2}$ (*of Step 3*) to transform $\mathbf{F}$ to a matrix $\mathbf{F}'$ which when diagonalized gives the energy levels $\boldsymbol{\varepsilon}$ and a coefficient matrix $\mathbf{C}'$ which is subsequently transformed to the matrix $\mathbf{C}$ of the desired c's (see Sect. 5.2.3.6.2):

$$\begin{aligned}
\mathbf{F}'_0 &= \underbrace{\begin{pmatrix} 1.1163 & -0.3003 \\ -0.3003 & 1.1163 \end{pmatrix}}_{\mathbf{S}^{-1/2}} \underbrace{\begin{pmatrix} -0.7511 & -0.9508 \\ -0.9508 & 1.3092 \end{pmatrix}}_{\mathbf{F}_0} \underbrace{\begin{pmatrix} 1.1163 & -0.3003 \\ -0.3003 & 1.1163 \end{pmatrix}}_{\mathbf{S}^{-1/2}} \\
&= \underbrace{\begin{pmatrix} -0.4166 & -0.5799 \\ -0.5799 & -1.0617 \end{pmatrix}}_{\mathbf{F}'_0}
\end{aligned} \tag{5.129}$$

Step 6 Diagonalizing $\mathbf{F}'$ to obtain the energy level matrix $\boldsymbol{\varepsilon}$ and a coefficient matrix $\mathbf{C}'$

$$\mathbf{F}'_0 = \underbrace{\begin{pmatrix} 0.5069 & 0.8620 \\ 0.8620 & -0.5069 \end{pmatrix}}_{\mathbf{C}'_1} \underbrace{\begin{pmatrix} -1.4027 & 0.0000 \\ 0.0000 & -0.0756 \end{pmatrix}}_{\boldsymbol{\varepsilon}_1} \underbrace{\begin{pmatrix} 0.5069 & 0.8620 \\ 0.8620 & -0.5069 \end{pmatrix}}_{\mathbf{C}'^{-1}_1} \tag{5.130}$$

The energy levels (the eigenvalues of $\mathbf{F}'_0$) from this first SCF cycle are -1.4027 h and -0.0756 h (h = hartrees, the unit of energy in atomic units), corresponding to the occupied MO ψ_1 and the unoccupied MO ψ_2. The MO coefficients (the eigenvectors of $\mathbf{F}'_0$) of ψ_1 and ψ_2, *for the transformed, orthonormal basis functions*, are, from $\mathbf{C}'_1$ (here $\mathbf{C}'_1$ and its inverse, $\mathbf{C}'_1{}^{-1}$ are the same):

$$\mathbf{v}'_1 = \begin{pmatrix} 0.5069 \\ 0.8620 \end{pmatrix} \quad \text{and} \quad \mathbf{v}'_2 = \begin{pmatrix} 0.8620 \\ -0.5069 \end{pmatrix} \tag{5.131}$$

$\mathbf{v}'_1$ is the first column of $\mathbf{C}'_1$ and $\mathbf{v}_2'$ is the second column of $\mathbf{C}'_1$. These coefficients are the weighting factors that with the transformed, orthonormal basis functions give the MO's:

$$\psi_1 = 0.5069\phi'_1 + 0.8620\phi'_2 \quad \text{and} \quad \psi_2 = 0.8620\,\phi'_1 - 0.5069\phi'_2 \tag{5.132}$$

where ϕ'_1 and ϕ'_2 are linear combinations of our *original* basis functions ϕ_1 and ϕ_2. The original basis functions ϕ were centered on atomic nuclei and were normalized but not orthogonal, while the transformed basis functions ϕ' are delocalized over the molecule and are orthonormal (Chap. 4, Sect. 4.4.2)). Note that the sum of the squares of the coefficients of ϕ'_1 and ϕ'_2 is unity, as must be the case if the basis functions are orthonormal. In the next step $\mathbf{C}'_1$ is transformed to obtain the coefficients of the original basis functions ϕ in the MO's. We want the MOs in terms of the original, atom-centered basis functions (roughly, atomic orbitals–Sect. 5.3) because such MOs are easier to interpret.

Step 7 Transforming $\mathbf{C}'$ to $\mathbf{C}$, the coefficient matrix of the original, nonorthogonal basis functions

As in Chap. 4, Sect. 4.4.2, we use the orthogonalizing matrix $\mathbf{S}^{-1/2}$ to transform $\mathbf{C}'$ to $\mathbf{C}$:

$$\mathbf{C}_1 = \underbrace{\begin{pmatrix} 1.1163 & -0.3003 \\ -0.3003 & 1.1163 \end{pmatrix}}_{\mathbf{S}^{-1/2}} \underbrace{\begin{pmatrix} 0.5069 & 0.8620 \\ 0.8620 & -0.5069 \end{pmatrix}}_{\mathbf{C}'_1} = \underbrace{\begin{pmatrix} 0.3070 & 1.1145 \\ 0.8100 & -0.8247 \end{pmatrix}}_{\mathbf{C}_1}$$
$$\tag{5.133}$$

This completes the first SCF cycle. We now have the first set of MO energy levels and basis function coefficients:

From Eq. (5.130):

$$\varepsilon_1 = -1.4027 \quad \text{and} \quad \varepsilon_2 = -0.0756 \tag{5.134}$$

From Eq. (5.133) (cf. Eq. (5.132)):

$$\psi_1 = 0.3070\,\phi_1 + 0.8100\,\phi_2 \quad \text{and} \quad \psi_2 = 1.1145\phi_1 - 0.8247\phi_2 \qquad (5.135)$$

Note that the sum of the squares of the coefficients of ϕ_1 and ϕ_2 is not unity, since these atom-centered functions are not orthogonal (contrast the simple Hückel method, Chap. 4, Sect. 4.3.4)).

Step 8 Comparing the density matrix from the latest c's with the previous density matrix to see if the SCF procedure has converged

The density matrix elements based on the c's of $\mathbf{C}_1$ (Eq. (5.133) can be compared with those (Eq. (5.123)) based on the initial guess:

$$\begin{aligned}
P_{11} &= 2c_{11}c_{11} = 2(0.3070)0.3070 = 0.1885 \\
P_{12} &= 2c_{11}c_{21} = 2(0.3070)0.8100 = 0.4973 \qquad (5.136) \\
P_{22} &= 2c_{21}c_{21} = 2(0.8100)0.8100 = 1.3122
\end{aligned}$$

Suppose our convergence criterion was that the elements of $\mathbf{P}$ must agree with those of the previous $\mathbf{P}$ matrix to within 1 part in 1000. Comparing Eq. (5.136) with Eq. (5.123) we see that this has not been achieved: even the smallest change is $|(1.312 - 1.503)/1.503| = 0.127$, far above the required 0.001. Therefore another SCF cycle is needed.

Step 9 Beginning the second SCF cycle: using the c's of $\mathbf{C}_1$ to calculate a new Fock matrix $\mathbf{F}_1$ (*cf. Step 4*, (b))

The first Fock matrix $\mathbf{F}_0$ used c's from our initial guess (*Step 4*, (b)). An improved $\mathbf{F}$ may now be calculated using the c's from the first SCF cycle. Calculating $\mathbf{G}_1$ as we did in *Step 4*, (b) for $\mathbf{G}_0$, but using the new P's:

$$\begin{aligned}
G_{11} =\ &P_{11}\left[(11|11) - \frac{1}{2}(11|11)\right] + P_{12}\left[(11|12) - \frac{1}{2}(12|11)\right] \\
&+P_{21}\left[(11|21) - \frac{1}{2}(11|21)\right] + P_{22}\left[(11|22) - \frac{1}{2}(12|21)\right] \qquad (5.137) \\
=\ &0.1885(0.3642) + 0.4973(0.1709) \\
&+0.4973(0.1709) + 1.3122(0.4754) = 0.8624
\end{aligned}$$

$$\begin{aligned}
G_{12} = G_{21} =\ &P_{11}\left[(12|11) - \frac{1}{2}(11|12)\right] + P_{12}\left[(12|12) - \frac{1}{2}(12|12)\right] \\
&+P_{21}\left[(12|21) - \frac{1}{2}(11|22)\right] + P_{22}\left[(12|22) - \frac{1}{2}(12|22)\right] \qquad (5.138) \\
=\ &0.1885(0.1709) + 0.4973(0.1096) \\
&+0.4973(-0.0733) + 1.3122(0.2184) = 0.3369
\end{aligned}$$

$$G_{22} = P_{11}\left[(22|11) - \frac{1}{2}(21|12)\right] + P_{12}\left[(22|12) - \frac{1}{2}(22|12)\right]$$

$$+ P_{21}\left[(22|21) - \frac{1}{2}(21|22)\right] + P_{22}\left[(22|22) - \frac{1}{2}(22|22)\right] \quad (5.139)$$

$$= 0.1885(0.4754) + 0.4973(0.2184)$$

$$+ 0.4973(0.2184) + 1.3122(0.4964) = 0.9582$$

From the G values based on the first-cycle c's the electron repulsion matrix is

$$\mathbf{G}_1 = \begin{pmatrix} 0.8624 & 0.3369 \\ 0.3369 & 0.9582 \end{pmatrix} \quad (5.140)$$

and the Fock matrix from this is

$$\mathbf{F}_1 = \mathbf{H}^{\text{core}} + \mathbf{G}_1 = \begin{pmatrix} -1.6606 & -1.3160 \\ -1.3160 & -2.3030 \end{pmatrix} + \begin{pmatrix} 0.8624 & 0.3369 \\ 0.3369 & 0.9582 \end{pmatrix}$$

$$= \begin{pmatrix} -0.7982 & -0.9791 \\ -0.9791 & -1.3448 \end{pmatrix} \quad (5.141)$$

Step 10 Transforming $\mathbf{F}_1$ to $\mathbf{F}_1'$ (cf. Step 5)

$$\mathbf{F}_1' = \underbrace{\begin{pmatrix} 1.1163 & -0.3003 \\ -0.3003 & 1.1163 \end{pmatrix}}_{\mathbf{S}^{-1/2}} \underbrace{\begin{pmatrix} -0.7982 & -0.9791 \\ -0.9791 & 1.3448 \end{pmatrix}}_{\mathbf{F}_1} \underbrace{\begin{pmatrix} 1.1163 & -0.3003 \\ -0.3003 & 1.1163 \end{pmatrix}}_{\mathbf{S}^{-1/2}}$$

$$= \underbrace{\begin{pmatrix} -0.4595 & -0.5900 \\ -0.5900 & -1.0913 \end{pmatrix}}_{\mathbf{F}_1'}$$

$$(5.142)$$

Step 11 Diagonalizing $\mathbf{F}_1'$ to obtain the energy levels ε and a coefficient matrix $\mathbf{C}'$ (*cf. Step 6*)

$$\mathbf{F}_1' = \underbrace{\begin{pmatrix} 0.5138 & 0.8579 \\ 0.8579 & -0.5138 \end{pmatrix}}_{\mathbf{C}_2'} \underbrace{\begin{pmatrix} -1.4447 & 0.0000 \\ 0.0000 & -0.1062 \end{pmatrix}}_{\varepsilon_2} \underbrace{\begin{pmatrix} 0.5138 & 0.8579 \\ 0.8579 & -0.5138 \end{pmatrix}}_{\mathbf{C}_2'^{-1}}$$

$$(5.143)$$

The energy levels from this second SCF cycle are -1.4447 h and -0.1062 h. To get the MO coefficients corresponding to these MO energy levels in terms of the original basis functions ϕ_1 and ϕ_2 we now transform $\mathbf{C}_2'$ to $\mathbf{C}_2$.

Step 12 Transforming $\mathbf{C}_2'$ to $\mathbf{C}_2$ (*cf. Step 7*)

$$\mathbf{C}_2 = \underbrace{\begin{pmatrix} 1.1163 & -0.3003 \\ -0.3003 & 1.1163 \end{pmatrix}}_{\mathbf{S}^{-1/2}} \underbrace{\begin{pmatrix} 0.5138 & 0.8579 \\ 0.8579 & -0.5138 \end{pmatrix}}_{\mathbf{C}_2'} \underbrace{\begin{pmatrix} 0.3159 & 1.1120 \\ 0.8034 & -0.8319 \end{pmatrix}}_{\mathbf{C}_2}$$

$$\tag{5.144}$$

This completes the second SCF cycle. We now have the MO energy levels and basis function coefficients:

From Eq. (5.143):

$$\varepsilon_1 = -1.4447 \quad \text{and} \quad \varepsilon_2 = -0.1062 \tag{5.145}$$

From Eq. (5.144):

$$\psi_1 = 0.3159\,\phi_1 + 0.8034\phi_2 \quad \text{and} \quad \psi_2 = 1.1120\phi_1 - 0.8319\phi_2 \tag{5.146}$$

Step 13 Comparing the density matrix from the latest c's with the previous density matrix to see if the SCF procedure has converged

The density matrix elements based on the c's of $\mathbf{C}_2$ are

$$\begin{aligned} P_{11} &= 2c_{11}c_{11} = 2(0.3159)0.3159 = 0.1996 \\ P_{12} &= 2c_{11}c_{21} = 2(0.3159)0.8034 = 0.5076 \\ P_{22} &= 2c_{21}c_{21} = 2(0.8034)0.8034 = 1.2909 \end{aligned} \tag{5.147}$$

Comparing Eqs. (5.147) with Eqs. (5.136) we see that convergence to within our 1-part- in-1000 criterion has not occurred: the largest change in the density matrix is $|(0.1996 - 0.1885)/0.1885| = 0.059$, which is above 0.001, so the SCF procedure is repeated.

Three more SCF cycles were carried out; the results of the "zeroth cycle" (the initial guess) and the five cycles are summarized in Table 5.1. Only with the fifth cycle has convergence been achieved, i.e. have the changes in all the density matrix elements fallen below 1 part in 1000 (the largest change is in P_{11}, $|(0.2020 - 0.2019)/0.2019 = 0.0005 < 0.001$). In actual practice, a convergence criterion of from about 1 part in 10^4 to 1 in 10^8 is used, depending on the program and the particular kind of calculation. The coefficients and the density matrix elements change smoothly, although the energy levels and $E_{\mathrm{HF}}^{\mathrm{total}}$ show some oscillation. To reduce the number of steps needed to achieve convergence, programs sometimes extrapolate the density matrix, i.e. estimate the final P values and use these estimates to initiate the final few SCF cycles.

Often the main result from a Hartree-Fock (i.e. an SCF) calculation is the energy of the molecule (the calculation of energy may be subsumed into a geometry

Table 5.1 Results of initial guess and SCF cycles on HHe + at bond length 0.800 Å using the STO-1G basis set. Energies (ε_1, ε_2, and E_{HF}^{total}) are in hartrees

	Initial guess (zeroth cycle)	1st cycle	2nd cycle	3rd cycle	4th cycle	5th cycle
ε_1, ε_2,	–	−1.4027, −0.0756	−1.4447, −0.1062	−1.4466, −0.1054	−1.4473, −0.1056	−1.4470, −0.1051
c_{11}, c_{21}	0.249, 0.867	0.3070, 0.8100	0.3159, 0.8034	0.3175, 0.8022	0.3177, 0.8021	0.3178, 0.8020
c_{12}, c_{22}	–	1.1145, −0.8247	1.1120, −0.8319	1.1115, −0.8323	1.1115, −0.8325	1.1114, −0.8325
P_{11}	0.1240	0.1885	0.1996	0.2010	0.2019	0.2020
P_{12}	0.4318	0.4973	0.5076	0.5094	0.5097	0.5097
P_{22}	1.5034	1.3122	1.2909	1.2870	1.2867	1.2864
E_{HF}^{total}	–	−2.3992	−2.4419	−2.4428	−2.4443	−2.4438

optimization, which is the task of finding the minimum-energy geometry). The STO-1G energy of HHe$^+$ with an internuclear distance of 0.800 Å may be calculated from our results:

the electronic energy is

$$E_{HF} = \sum_{i=1}^{n} \varepsilon_i + \frac{1}{2} \sum_{r=1}^{m} \sum_{s=1}^{m} P_{rs} H_{rs}^{core} \qquad (5.147 = 5.90)$$

the internuclear repulsion energy is

$$V_{NN} = \sum_{\text{all } \mu, v} \frac{Z_\mu Z_v}{r_{\mu v}} \qquad (5.148 = 5.92)$$

and the total internal energy of the molecule at 0 K (except for zero point energy—Sect. 5.2.3.6.4) is

$$E_{HF}^{total} = E_{HF} + V_{NN} = \sum_{i=1}^{n} \varepsilon_i + \frac{1}{2} \sum_{r=1}^{m} \sum_{s=1}^{m} P_{rs} H_{rs}^{core} + V_{NN} \qquad (5.149 = 5.93)$$

E_{HF}^{total}, which is what is normally meant by the Hartree-Fock energy, is printed by the program at the end of a single-point calculation or a geometry optimization, or by some programs at the end of each step of a geometry optimization.

Using the energy levels and density matrix elements from the first cycle (Table 5.1), with the H^{core} elements from Eq. (5.120), Eq. (5.147) gives for the purely electronic energy

$$
\begin{aligned}
E_{\mathrm{HF}} &= \varepsilon_1 + \frac{1}{2}\sum_{r=1}^{2}\sum_{s=1}^{2}P_{rs}H_{rs}^{\mathrm{core}} \\
&= \varepsilon_1 + \frac{1}{2}\sum_{r=1}^{2}\left[P_{r1}H_{r1}^{\mathrm{core}} + P_{r2}H_{r2}^{\mathrm{core}}\right] \\
&= \varepsilon_1 + \frac{1}{2}\left[P_{11}H_{11}^{\mathrm{core}} + P_{12}H_{12}^{\mathrm{core}} + P_{21}H_{21}^{\mathrm{core}} + P_{22}H_{22}^{\mathrm{core}}\right. \\
&= -1.4027\,\mathrm{h} + \frac{1}{2}\left[0.1885(-1.6606) + 0.4973(-1.3160)\right. \\
&\quad \left. + 0.4973(-1.3160) + 1.3122(-2.3030)\right]\mathrm{h} \\
&= -3.7222\,\mathrm{h}
\end{aligned}
\tag{5.150}
$$

From Eq. (5.148) the internuclear repulsion energy is (0.800 Å $= 1.5117$ bohr)

$$
\begin{aligned}
V_{NN} &= \frac{Z_{\mathrm{H}}Z_{\mathrm{He}}}{r_{\mathrm{HHe}}} \\
&= \frac{1(2)}{1.5117}\ \mathrm{h} = 1.3230\,\mathrm{h}
\end{aligned}
\tag{5.151}
$$

and from Eq. (5.149) the total Hartree-Fock energy is

$$
E_{\mathrm{HF}}^{\mathrm{total}} = E_{\mathrm{HF}} + V_{NN} = -3.7222\ \mathrm{h}\ +\ 1.3230\ \mathrm{h}\ = -2.3992\ \mathrm{h}
\tag{5.152}
$$

The Hartree-Fock energies for the five SCF cycles are given in Table 5.1.

Instead of starting with eigenvectors from a non-SCF method like the extended Hückel method, as was done in this illustrative procedure, an SCF calculation is occasionally initiated by taking $\mathbf{H}^{\mathrm{core}}$ as the Fock matrix, that is, by initially ignoring electron-electron repulsion, setting equal to zero the second term in Eq. (5.82), or G in Eq. (5.100), whereupon F_{rs} becomes H_{rs}^{core}. This is usually a poor initial guess, but is occasionally useful. You are urged to work your way through several SCF cycles starting with this Fock matrix; this tedious calculation will help you to appreciate the power and utility of modern electronic computers and may enhance your respect for those who pioneered complex numerical calculations when the only arithmetical aids were mathematical tables and mechanical calculators (mechanical calculators were machines with rotating wheels, operated by hand-power or electricity. There were also, in astronomy at least, armies of women arithmeticians called computers–the original meaning of the word).

If we calculate the electronic energy simply as twice the sum of the energies of the occupied MO orbitals, as with the simple and extended Hückel methods, we get a much higher value than from the correct procedure (Eq. (5.147)); with a 0.800 Å bond length and the converged results this naive electronic energy is $2(-1.4470)$ h $= -2.8940$ h, while the correct electronic energy (not given in Table 5.1–the HF energies there are electronic plus internuclear repulsion) is
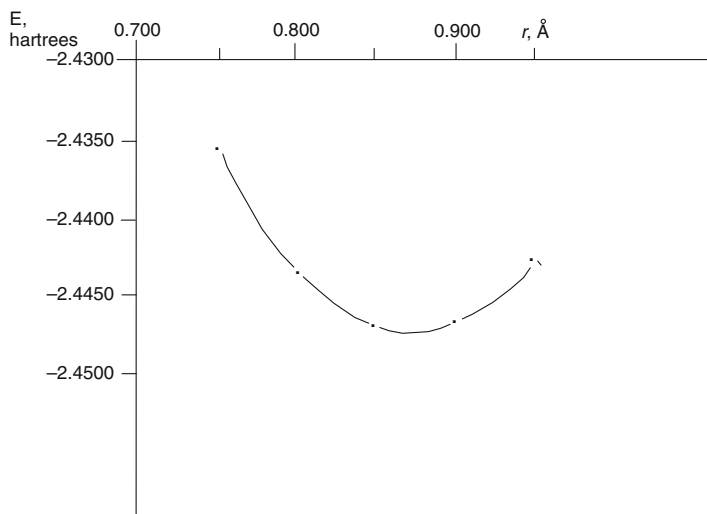
Fig. 5.11 STO-1G energy vs. bond length r for $H-He^+$. The calculation for $r = 0.800$ Å was done largely "by hand" (see Sect. 5.2.3.6.5); the others were done with the program Gaussian 92 [29]

-3.7668 h, i.e. 30 % lower when we correct for the fact that simply double-summing the MO energies counts electron repulsion terms twice (Sect. 5.2.3.6.4).

A geometry optimization for HHe^+ can be done by calculating the Hartree-Fock energy (electronic plus internuclear) at different bond lengths to get the minimum-energy geometry. The results are shown in Fig. 5.11; the optimized bond length for the STO-1G basis set is ca. 0.86 Å. Note that it is customary to report ab initio energies in hartrees to 5 or 6 decimal places (and bond lengths in Å to 3 decimals); the truncated values used here are appropriate for these illustrative calculations.

Summary of the steps in a single-point Hartree-Fock (SCF) calculation using the Roothaan-Hall LCAO expansion of the MO's

1. Specify a geometry, basis set, and orbital occupancy (this latter is done by specifying the charge and multiplicity, with an electronic ground state being the default).
2. Calculate the integrals: T_{rs}, V_{rs} for each nucleus, and the 2-electron integrals $(ru|ts)$ etc. needed for G_{rs}, as well as the overlap integrals S_{rs} for the orthogonalizing matrix derived from **S** (see step 3). Note: in the *direct SCF* method (Sect. 5.3) the 2-electron integrals are calculated as needed, rather than all at once.
3. Calculate the orthogonalizing matrix $\mathbf{S}^{-1/2}$

   (a) diagonalize **S**: $\mathbf{S} = \mathbf{PDP}^{-1}$ $\mathbf{S} = \mathbf{PDP}^{-1}$
   (b) Calculate $\mathbf{D}^{-1/2}$ (take the $-1/2$ power of the elements of **D**)
   (c) Calculate $\mathbf{S}^{-1/2} = \mathbf{PD}^{-1/2}\mathbf{P}^{-1}$

4. Calculate the Fock matrix **F**

   (a) Calculate the 1-electron matrix $\mathbf{H}^{\text{core}} = \mathbf{T} + \mathbf{V}_1 + \mathbf{V}_2 + \cdots$ using the T and V integrals from step 2.
   (b) The 2-electron matrix (the electron repulsion matrix) **G**:

   Use an initial guess of the coefficients of the occupied MO's to calculate initial-guess density matrix elements:

   $$P_{tu} = 2\sum_{j=1}^{n} c_{tj}^* c_{uj} \quad t = 1, 2, \cdots, m \text{ and } u = 1, 2, \cdots, m$$

   Use the density matrix elements and the 2-electron integrals to calculate **G**:

   $$G_{rs} = \sum_{t=1}^{m} \sum_{u=1}^{m} P_{tu}\left[(rs|tu) - \tfrac{1}{2}(ru|ts)\right]$$

   The Fock matrix is $\mathbf{F} = \mathbf{H}^{\text{core}} + \mathbf{G}$

5. Transform **F** to **F'**, the Fock matrix that satisfies $\mathbf{F}' = \mathbf{C}'\boldsymbol{\varepsilon}\,\mathbf{C}'^{-1}$

   $$\mathbf{F}' = \mathbf{S}^{-1/2}\mathbf{F}\mathbf{S}^{-1/2}$$

6. Diagonalize **F'** to get energy levels and a **C'** matrix

   $$\mathbf{F}' = \mathbf{C}'\boldsymbol{\varepsilon}\,\mathbf{C}'^{-1}$$

7. Transform **C'** to **C**, the coefficient matrix of the original basis functions

   $$\mathbf{C} = \mathbf{S}^{-1/2}\mathbf{C}'$$

8. Compare the density matrix elements calculated from the **C** of the previous step with those of the step before that one (and/or use other criteria, e.g. the molecular energy); if convergence has not been achieved go back to step 4 and calculate a new Fock matrix using the P's from the latest c's. If convergence has been achieved, stop.

It should be realized modern ab initio programs do not rigidly follow the basic SCF procedure described in this section. To speed up calculation they employ a variety of tricks. Among these are: the use of symmetry to avoid duplicate calculation of identical integrals; testing two-electron integrals quickly to see if they are small enough to be neglected (as is the case for functions on distant nuclei; this decreases the time of a calculation from an n^4 dependence on the number of basis function to about an $n^{2.3}$ dependence); recalculating integrals to avoid the bottleneck of hard-drive access (direct SCF, Sect. 5.3.2); representing the MOs as a set of gridpoints in space, in addition to a basis set expansion, which eliminates the need

to explicitly calculate two-electron integrals (this *pseudospectral method* speeds up ab initio calculations by a factor of perhaps three or four); for very large systems, calculating the Coulomb interaction between distant regions as the repulsion between points at the centers of the regions (*fast multipole method*). Methods of speeding up calculations are explained, with references to the literature, by Levine [33].

The method of calculating wavefunctions and energies that has been described in this chapter applies to *closed-shell*, *ground-state* molecules. The Slater determinant we started with (Eq. (5.12)) applies to molecules in which the electrons are fed pairwise into the MO's, starting with the lowest-energy MO; this is in contrast to free radicals, which have one or more unpaired electrons, or to electronically excited molecules, in which an electron has been promoted to a higher-level MO (e.g. Fig. 5.9, neutral triplet). The Hartree-Fock method outlined here is based on closed-shell Slater determinants and is called the *restricted Hartree-Fock* method or RHF method; "restricted" means that the electrons of α spin are forced to occupy (restricted to) the same spatial orbitals as those of β spin: inspection of Eq. (5.12) shows that we do not have a set of α *spatial* orbitals and a set of β *spatial* orbitals. The same spatial orbital, ψ_1 for example, is used to create an alpha and a beta spin orbital. If unqualified, a Hartree-Fock (i.e. an SCF) calculation means an RHF calculation.

The commonest way to treat free radicals is with the *unrestricted Hartree-Fock* method or UHF method [12b]. In this method, we employ separate spatial orbitals for the α and the β electrons, giving two sets of MO's, one for α and one for β electrons. There are thus basis function coefficients to be optimized separately for the α-accommodating and for the β-accommodating spatial orbitals, and we have α- and β-Fock matrices . That these spatial orbitals are not identical is apparent from the fact that the "lone" (unpaired) electron of a free radical is expected to interact differently with α- than with β-electrons, since electrons of the same spin have an extra aversion to one another due to "Pauli repulsion". The UHF method is "unrestricted" because the alternative of putting α- and β-electrons in the same spatial orbitals would force (restrict) them to trace out the same spatial regions despite their different interactions with the unpaired electron(s). Less commonly, free radicals are treated by the *restricted open-shell Hartree-Fock* or ROHF method, in which electrons occupy MO's in pairs as in the RHF method, except for the necessarily unpaired electron(s).

Both the UHF and ROHF methods have their advantages and problems. UHF calculations mirror reasonably well spin densities from electron spin resonance and so are useful in analyzing electron distribution in open-shell species. A ROHF, in contrast, cannot reflect properly the interaction of paired-up electrons with an unpaired electron, because the paired electrons are in mutually restricted spatial orbitals. The main problem with UHF is that it does not give a true wavefunction of the system, but rather one that may be significantly contaminated with contributions from wavefunctions of higher multiplicity; for example, a simple free monoradical, properly a doublet, may have contributions from a quartet, sextet, and so on. The extent of this contamination can be judged from inspection of the expectation

values (the eigenvalues if the wavefunction is uncontaminated by higher spin states) $< S^2 >$ of the spin-squared operator S^2. This is automatically evaluated for a calculation on a radical, and if the deviation from the expectation value seems unreasonable, the geometry and energy may be unacceptable. For a mono-, a di-, and a triradical, the total spin is respectively 1/2, 1, and 3/2 and the multiplicity (Eq. 5.99) is $2S + 1$ is 2 (doublet), 3 (triplet), and 4 (quartet). The theoretical expectation values $< S^2 >$ are, from the eigenvalue expression $S(S + 1)$ (reference 1a, p 266), 0.7500, 2.0000, and 3.7500. Most algorithms apply an "annihilation operator" which attempts to remove higher-spin contamination, and print $< S^2 >$ before and after annihilation. Here is a comparison of $< S^2 >$ from UHF and ROHF for the monoradicals **A** and **B**, the diradical **C**, and the triradical **D**, below:

A	**B**	**C**	**D**
	C_6H_5	C_6H_{10}	$C_6H_9CH_2$
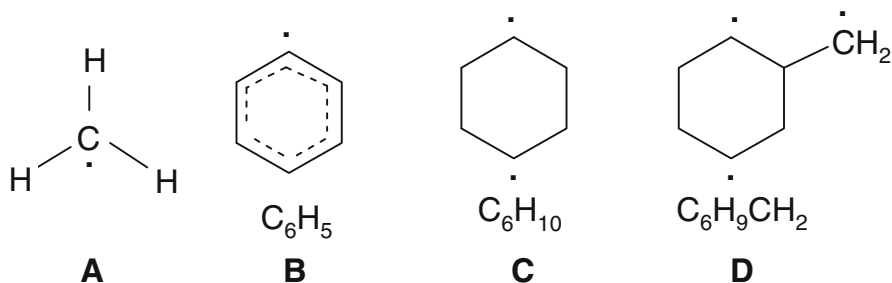
A   UHF before/after annihilation 0.7625/0.7501; theory 0.7500
       ROHF before/after annihilation 0.7500/0.7500; theory 0.7500
B   UHF before/after annihilation 1.4330/1.1781; theory 0.7500
       ROHF before/after annihilation 0.7500/0.7500; theory 0.7500
C   UHF before/after annihilation 2.0237/2.0004; theory 2.0000
       ROHF before/after annihilation 2.0000/2.0000; theory 2.0000
D   UHF before/after annihilation 3.7880/3.7507; theory 3.7500
       ROHF before/after annihilation 3.7500/3.7500; theory 3.7500

We see that with UHF, for **A**, **C** and **D** contamination is small and annihilation brings the expectation value $< S^2 >$ still closer to theoretical. Contamination is bad for **B**, and annihilation helps little; properties from this wavefunction are of questionable validity. The ROHF wavefunctions are uncontaminated. An advantage of ROHF over UHF is that when the latter gives a strongly spin-contaminated result, the ROHF geometry is likely to be more reliable.

Excited states, and those unusual molecules with electrons of opposite spin singly occupying different spatial MO's (open-shell singlets) cannot be properly treated with a single-determinant wavefunction. They must be handled with approaches beyond the Hartree-Fock level, such as configuration interaction (Sect. 5.4). The theoretical treatment of open-shell species is discussed in references [1] and [10], and [1k] and [11], in particular, compare the performance of the UHF and ROHF methods.

5.3 Basis Sets

5.3.1 Introduction

We encountered basis sets in the simple Hückel and extended Hückel methods (Sects. 4.4.1.1 and 4.4.1.2). A basis set is a set of mathematical functions (basis functions), linear combinations of which yield molecular orbitals, as shown in Eqs. (5.51) and (5.52). The functions are usually, but not invariably, centered on atomic nuclei (Fig. 5.7). Approximating molecular orbitals as linear combinations of basis functions is usually called the LCAO or linear combination of atomic orbitals approach, although the functions are not necessarily conventional atomic orbitals: they can be any set of mathematical functions that are convenient to manipulate and which in linear combination give useful representations of MO's. With this reservation, LCAO is a useful acronym. Physically, several (usually) basis functions describe the electron distribution around an atom and combining atomic basis functions yields the electron distribution in the molecule as a whole. Basis functions not centered on atoms (occasionally used) can be considered to lie on "ghost atoms"; see basis set superposition error, Sect. 5.4.3.3.

The simplest basis sets are those used in the simple Hückel and the extended Hückel methods (SHM and EHM, Chap. 4). As applied to conjugated organic compounds (its usual domain), the simple Hückel basis set consists of just p atomic orbitals (or "geometrically p-type" atomic orbitals, like a lone-pair orbital which can be considered not to interact with the σ framework). The extended Hückel basis set consists of only the atomic *valence* orbitals. In the SHM we don't worry about the mathematical form of the basis functions, reducing the interactions between them to 0 or -1 in the SHM Fock matrix (e.g. Eqs. 4.62 and 4.64). In the EHM the valence atomic orbitals are represented as Slater functions (Sect. 4.4.1.2).

5.3.2 Gaussian Functions; Basis Set Preliminaries; Direct SCF

The electron distribution around an atom can be represented in several ways. Hydrogenlike functions based on solutions of the Schrödinger equation for the hydrogen atom, polynomial functions with adjustable parameters, Slater functions (Eq. (5.95)), and Gaussian functions (Eq. (5.96)) have all been used [34]. Of these, Slater and Gaussian functions are mathematically the simplest, and it is these that are currently used as the basis functions in molecular calculations. Slater functions are used in semiempirical calculations, like the extended Hückel method (Chap. 4, Sect. 4.4) and other semiempirical methods (Chap. 6). Modern molecular ab initio programs employ Gaussian functions.

Slater functions are good approximations to atomic wavefunctions and would be the natural choice for ab initio basis functions, were it not for the fact that the evaluation of certain 2-electron integrals requires excessive computer time if Slater

functions are used. The 2-electron integrals (Sects. 5.2.3.6.3 and 5.2.3.6.5) of the
G matrix (Eq. (5.100)) involve four functions, which may be on from one to four
centers (normally atomic nuclei). Those 2-electron integrals with three or four
different functions $((rs|tt)$, $(rs|rt)$ and $(rs|tu))$ and three or four nuclei (three-
center or four-center integrals) are extremely difficult to calculate with Slater
functions, but are readily evaluated with Gaussian basis functions. The reason is
that the product of two Gaussians on two centers is a Gaussian on a third center.
Consider an s-type Gaussian centered on nucleus A and one on nucleus B; we are
considering *real* functions, which is what basis functions normally are:

$$g_A = a_A e^{-\alpha_A |\mathbf{r}-\mathbf{r_A}|^2}, \quad g_B = a_B e^{-\alpha_B |\mathbf{r}-\mathbf{r_B}|^2} \tag{5.153}$$

where

$$
\begin{aligned}
|\mathbf{r}-\mathbf{r_A}|^2 &= (x-x_A)^2 + (y-y_A)^2 + (z-z_A)^2 \\
|\mathbf{r}-\mathbf{r_B}|^2 &= (x-x_B)^2 + (y-y_B)^2 + (z-z_B)^2
\end{aligned} \tag{5.154}
$$

and

with the nuclear and electron positions in Cartesian coordinates (if these were not s-type
functions, the preexponential factor would contain one or more cartesian variables to
give the function – the "orbital"– nonspherical shape). It is not hard to show that

$$g_A g_B = a_c e^{-\alpha_C |\mathbf{r}-\mathbf{r}_C|^2} = g_C \tag{5.155}$$

The product of g_A and g_B is the Gaussian g_C, centered at $\mathbf{r}_C$. Now consider the
general electron-repulsion integral

$$(rs|tu) = \iint \frac{\phi_r^*(1)\phi_s(1)\phi_t^*(2)\phi_u(2)}{r_{12}} dv_1 dv_2 \tag{5.156 = 5.73}$$

If each basis function ϕ were a single, real Gaussian, then from Eq. (5.155) this
would reduce to

$$(v/w) = \iint \frac{\phi_v(1)\phi_w(2)}{r_{12}} dv_1 dv_2 \tag{5.157}$$

i.e. three- and four-center two-electron integrals with four basis functions would
immediately simplify to tractable two-center integrals with two functions. Actually,
things are a little more complicated. A single Gaussian is a poor approximation to
the nearly ideal description of an atomic wavefunction that a Slater function pro-
vides. Figure 5.12 shows that a Gaussian (designated STO-1G) is rounded near
$r=0$ while a Slater function has a cusp there (zero slope *vs.* a finite slope at $r=0$);
the Gaussian also decays somewhat faster than the Slater function at large r. The
solution to the problem of this poor functional behaviour is to use several Gaussians
to approximate a Slater function. In Fig. 5.12 a single Gaussian and a linear
combination of three Gaussians have been used to approximate the Slater function
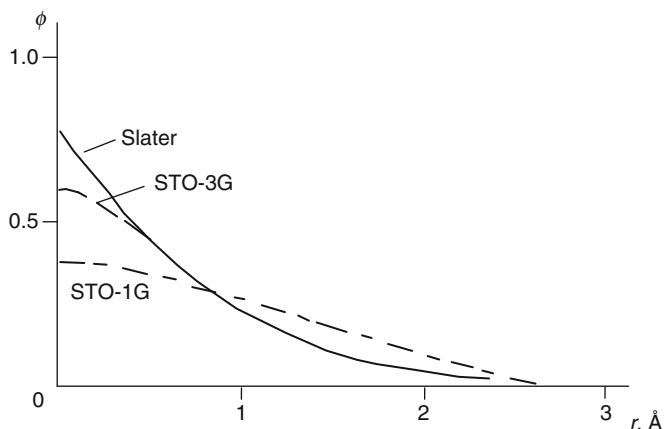
$$\phi \, (\text{Slater}) = \left(\frac{\zeta^3}{\pi}\right)^{1/2} e^{-\zeta r} = 0.7790 e^{-1.24r}$$

$$\phi \, (\text{STO}-1\text{G}) = \left(\frac{2\alpha}{\pi}\right)^{3/4} e^{-\alpha r^2} = 0.3696 e^{-0.4166 r^2}$$

$$\phi \, (\text{STO}-3\text{G}) = 0.4446 \left(\frac{2\alpha}{\pi}\right)^{3/4} e^{-\alpha r^2} + 0.5353 \left(\frac{2\alpha}{\pi}\right)^{3/4} e^{-\alpha r^2} + 0.1543 \left(\frac{2\alpha}{\pi}\right)^{3/4} e^{-\alpha r^2}$$

$$= 0.0835 \, e^{-0.1689 r^2} + 0.2678 \, e^{-0.6239 r^2} + 0.2769 \, e^{-3.4253 r^2}$$

Fig. 5.12 Comparison of Slater, STO-1G and STO-3G functions for hydrogen. The Slater function shown is the most appropriate one for hydrogen *in a molecular environment*, and the Gaussians are the best 1-G and 3-G fits to this Slater function. Slater and Gaussian functions are usually characterized by parameters designated ζ (zeta) and α, respectively, as shown [31]

shown; the nomenclature STO-1G and STO-3G mean "Slater-type orbital (approximated by) one Gaussian" and "Slater-type orbital (approximated by) three Gaussians", respectively. The Slater function shown is one suitable for a hydrogen atom in a molecule ($\zeta = 1.24$ [31]) and the Gaussians are the best fit to this Slater function. STO-1G functions were used in our illustrative Hartree-Fock calculation on HHe$^+$ (Sect. 5.2.3.6.5), and the STO-3G function is the smallest basis function used in standard ab initio calculations by commercial programs. Three Gaussians are a good speed vs. accuracy compromise between two and four or more [31].

The STO-3G basis function in Fig. 5.12 is a *contracted Gaussian* consisting of three *primitive Gaussians* each of which has a *contraction coefficient* (0.4446, 0.5353 and 0.1543). Typically, an ab initio basis function consists of a set of primitive Gaussians bundled together with a set of contraction coefficients. Now consider the 2-electron integral $(rs|tu)$ (Eq. (5.156)). Suppose each basis function is an STO-3G contracted Gaussian, i.e.

$$\phi_r = d_{1r} g_{1r} + d_{2r} g_{2r} + d_{3r} g_{3r} \tag{5.158}$$

and analogously for ϕ_s, ϕ_t, and ϕ_u. Then it is easy to see that

$$(rs|tu) = \iint d_{1r}d_{1s}g_{1r1s}\frac{1}{r_{12}}d_{1t}d_{1u}g_{1t1u}dv_1dv_2$$
$$+ \iint d_{1r}d_{1s}g_{1r1s}\frac{1}{r_{12}}d_{1t}d_{2u}g_{1t2u}dv_1dv_2 + \cdots \qquad (5.159)$$
$$+ \iint d_{3r}d_{3s}g_{3r3s}\frac{1}{r_{12}}d_{3t}d_{3u}g_{3t3u}dv_1d$$

where $g_{1r1s} = g_{1r} \times g_{1s}$ and so on. Thus with contracted Gaussians as basis functions, each two-electron integral becomes a sum of easily calculated two-center two-electron integrals. Gaussian integrals can be evaluated so much faster than Slater integrals that the use of contracted Gaussians instead of Slater functions speeds up the calculation of the integrals enormously, despite the larger number of integrals. Discussions of the number of integrals in an ab initio calculation usually refer to those at the contracted Gaussian level, rather than the greater number engendered by the use of primitive Gaussians; thus the program Gaussian 92 [29] says that both an STO-1G and an STO-3G calculation on water use the same number (144) of 2-electron integrals, although the latter clearly involves more "primitive integrals." The fruitful suggestion to use Gaussians in molecular calculations came from Boys (1950 [35]); it played a major role in making ab initio calculations practical, and this is epitomized in the names of the Gaussian series of programs, which are primarily devoted to ab initio and DFT (Chap. 7) and are among the most widely-used quantum mechanics -oriented computational chemistry programs [36].

Fast calculation of integrals is particularly important for the 2-electron integrals, as their number increases rapidly with the size of the molecule and the basis set (basis sets are discussed in Sect. 5.3.3). Consider a calculation on water with an STO-1G basis set (and bear in mind that the smallest basis set normally used in ab initio calculations is the STO-3G set). In a standard ab initio calculation we use at least one basis function for each core orbital and each valence-shell orbital. Thus the oxygen requires five basis functions, for the $1s$, $2s$, $2p_x$, $2p_y$ and $2p_z$ orbitals; we can designate these functions $\phi_1, \phi_2, \ldots \phi_5$, and denote the 1s hydrogen functions, one for each H, ϕ_6 and ϕ_7. In computational chemistry atoms beyond hydrogen and helium in the periodic table are called "heavy atoms", and the computational "first row" is lithium–neon. With experience, the number of heavy atoms in a molecule gives a quick indication of about how many basis functions will be invoked by a specified basis set. Following the procedure for HHe$^+$ in Eq. (5.106):

$$G_{11} = \sum_{t=1}^{7}\sum_{u=1}^{7} P_{tu}\left[(11|tu) - \frac{1}{2}(1u|t1)\right]$$

Now u runs from 1 to 7 and t from 1 to 7, so G_{11} will consist of 49 terms, each containing two 2-electron integrals for a G_{11} total of 98 integrals. The Fock matrix for seven basis functions is a 7×7 matrix with 49 elements, G_{11}, G_{12},... G_{17}, ...G_{77}, so apparently there are $49 \times 98 = 4802$ 2-electron integrals. Actually,

Table 5.2 Molecular size, number of basis functions, and number of 2-electron integrals

		Basis functions		2-Electron integrals			
		STO-3G	3–21G$^{(*)}$	from $m^4/8$	from G92^a	from $m^4/8$	from G92
HHe+	$C_{\infty v}$	2	4	2	6	32	55
H_2O	C_{2v}	7	13	300	144	3570	1314
H_2O_2	C_{2h}	12	22	2592	738	29,282	7713
H_2O_2	C_1^*	12	22	2592	2774	29,282	28,791
H_2O_3	C_{2v}	17	31	10,440	3421	115,440	31,475
H_2O_3	C_1	17	31	10,440	11,046	115,440	107,869

^{a}The coordinates of one of the atoms was altered slightly to get this unnatural symmetry

many of these are duplicates ($G_{ij} = G_{ji}$, so an $n \times n$ Fock matrix has only about $n^2/2$ *different* elements), differ from other integrals only in sign, or are very small, and the number of unique nonvanishing 2-electron integrals is 119 (calculated with Gaussian 92 [29]). For an STO-1G calculation on hydrogen peroxide (12 basis functions), there are ca. 700 unique nonvanishing 2-electron integrals (cf. a naive theoretical maximum of 41,472). The usual formula for estimating the maximum number of unique 2-electron integrals for a set of m real basis functions derives from the fact that there are four basis functions in each integral and $(rs|tu)$ is eightfold degenerate (Eq. (5.109)); this approximates the maximum number of these integrals as

$$N_{max} = m^4/8 \tag{5.160}$$

In the above calculations the symmetry of water (C_{2v}) and hydrogen peroxide (C_{2h}) plays an important role in reducing the number of integrals which must really be calculated, and modern ab initio programs recognize and utilize symmetry where it can be used (most molecules lack symmetry, but the small molecules of particular theoretical interest usually possess it), and are also able to recognize and avoid calculating integrals below a threshold size. Nevertheless the rapid rise in the number of 2-electron integrals with molecular and basis set size portends problems for ab initio calculations. An ab initio calculation on aspirin, a fairly small ($C_9H_8O_4$, 13 heavy atoms) molecule of practical interest, using the 3–21G basis set (Sect. 5.3.3), which is the smallest that is usually used, requires 133 basis functions, which from Eq. (5.160) could invoke up to 39 million ($133^4/8$) 2-electron integrals. Clearly, a modest ab initio calculation could require tens of millions of integrals. Information on molecular size, symmetry, basis sets and number of integrals is summarized in Table 5.2 (the 3–21G basis set is explained in Sect. 5.3.3). Note that for those molecules with no symmetry (C_1), the number of 2-electron integrals calculated from Eq. (5.160) is about the same as that actually calculated by Gaussian 92.

There are two problems with so many 2-electron integrals: the time needed to calculate them, and where to store them. Solutions to the first problem are, as explained, to use Gaussian functions, to utilize symmetry where possible, and to

ignore those integrals that a preliminary check reveals are "vanishing". The other problem can be dealt with by storing the integrals in the RAM (the random access memory, i.e. the electronic memory), storing the integrals on the hard drive, or not storing them at all, but rather calculating them as they are required. Calculating all the integrals at the outset and storing them somewhere is called *conventional scf*, being the earlier-used procedure. The latter procedure of calculating only those 2-electron integrals needed at the moment, and recalculating them again when necessary, is called *direct scf* (presumably using "direct" in the sense of "just now" or "at the moment"). Calculating all the 2-electron the integrals and storing them in the RAM is the fastest approach, since it requires them to be calculated only once, and accessing information from the electronic memory is fast. However, RAM cannot yet store as many integrals as the hard drive. A (currently) modest memory of 4 GB can store all the integrals generated by perhaps about 2000 basis functions (up to about 100 million); beyond this the computer essentially grinds to a halt. The capacity of the hard drive is typically considerably greater than that of the RAM (say, 1000 GB for a moderately respectable hard drive, and storing all the 2-electron integrals on the hard drive is often a viable option, but suffers from the disadvantage that the time taken to read data from a mechanical device into the RAM, where it can be used by the cpu, is much greater (perhaps a millisecond or so compared to a nanosecond) than the time needed to access the information were it stored in a purely electronic device like the RAM (which is the only alternative to direct scf in, for example, Spartan [37]). For these reasons, ab initio calculations with many basis functions (beyond some hundreds, depending on the size of the RAM) nowadays use direct scf, despite the need to recalculate integrals [38]. These considerations will change with improvements in hardware, and the availability of very large electronic memories may make storage of all the 2-electron integrals in RAM the only choice for ab initio calculations.

5.3.3   Types of Basis Sets and Their Uses

We have met the STO-1G (Sects. 5.2.3.6.5 and 5.3.2) and STO-3G (Sect. 5.3.2) basis sets. We saw that a single Gaussian gives a poor representation of a Slater function, but that this approximation can be improved by using a linear combination of Gaussians (Fig. 5.12). In this section the basis sets commonly used in ab initio calculations are described and their domains of utility are outlined. Note that the STO-1G basis, although it was useful for our illustrative purposes, is not used in research calculations (Fig. 5.12 shows how poorly it approximates a Slater function). We will consider the STO-3G, 3–21G, 6–31G*, and 6–311G* basis sets, which, with variations obtained by adding polarization (*) and diffuse (+) functions, are the most widely-used; other sets will be briefly mentioned. Information on some basis sets is summarized in Fig. 5.13. Good discussions of currently popular basis sets are given in, e.g., references 1a, 1e and 1i; the compilations by Hehre et al. [1g, 39] are extensive and critically evaluated.

a, STO-3G

₁H 1*s* 1 function		₂He 1*s* 1 function
	₃Li–₁₀Ne 1*s* 2*s* 2*p* 2*p* 2*p* 5 functions	
	₁₁Na–₁₈Ar 1*s* 2*s* 2*p* 2*p* 2*p* 3*s* 3*p* 3*p* 3*p* 9 functions	
₁₉K–₂₀Ca 1*s* 2*s* 2*p* 2*p* 2*p* 3*s* 3*p* 3*p* 3*p* 4*s* 4*p* 4*p* 4*p* 13 functions	₂₁Sc–₃₀Zn 1*s* 2*s* 2*p* 2*p* 2*p* 3*s* 3*p* 3*p* 3*p* 4*s* 4*p* 4*p* 4*p* 3*d* 3*d* 3*d* 3*d* 3*d* 18 functions	₃₁Ga–₃₆Kr 1*s* 2*s* 2*p* 2*p* 2*p* 3*s* 3*p* 3*p* 3*p* 4*s* 4*p* 4*p* 4*p* 3*d* 3*d* 3*d* 3*d* 3*d* 18 functions
₃₇Rb–₃₈Sr 1*s* 2*s* 2*p* 2*p* 2*p* 3*s* 3*p* 3*p* 3*p* 4*s* 4*p* 4*p* 4*p* 5*s* 5*p* 5*p* 5*p* 3*d* 3*d* 3*d* 3*d* 3*d* 22 functions	₃₉Y–₄₈Cd 1*s* 2*s* 2*p* 2*p* 2*p* 3*s* 3*p* 3*p* 3*p* 4*s* 4*p* 4*p* 4*p* 5*s* 5*p* 5*p* 5*p* 3*d* 3*d* 3*d* 3*d* 3*d* 4*d* 4*d* 4*d* 4*d* 4*d* 27 functions	₄₉In–₅₄Xe 1*s* 2*s* 2*p* 2*p* 2*p* 3*s* 3*p* 3*p* 3*p* 4*s* 4*p* 4*p* 4*p* 5*s* 5*p* 5*p* 5*p* 3*d* 3*d* 3*d* 3*d* 3*d* 4*d* 4*d* 4*d* 4*d* 4*d* 27 functions

Fig. 5.13 (**a**) The STO-3G basis set (**b**) The 3–21G basis set (**c**) The 3–21G[(*)] basis set (**d**) The 6–31G[*] basis set

The basis sets described here in most detail are those developed by Pople[3] and coworkers [40], which are probably the most popular now, but all general-purpose (those not used just on small molecules or on atoms) basis sets utilize some sort of contracted Gaussian functions to simulate Slater orbitals. A brief discussion of basis sets and references to many, including the widely-used Dunning correlation-consistent (below) and Huzinaga sets, is given by Simons and Nichols [41]. There is no one procedure for developing a basis set. One method is to optimize *Slater* functions for atoms or small molecules, i.e. to find the values of ζ that give the lowest energy for these, and then to use a least-squares procedure to fit contracted Gaussians to the optimized Slater functions [42]. Whatever the details

---

[3]John Pople, born in Burnham-on-Sea, Somerset, England, 1925. Ph.D. (Mathematics) Cambridge, 1951. Professor, Carnegie-Mellon University, 1960–1986, Northwestern University (Evanston, Illinois) 1986–2004. Nobel Prize in chemistry 1998 (with Walter Kohn, chapter 5, section *7.1*). Died Chicago, 2004.

b, 3-21G

$_1$H $1s'$ $1s''$ 2 functions		$_2$He $1s'$ $1s''$ 2 functions
	$_3$Li–$_{10}$Ne $1s$ $2s'$ $2p'$ $2p'$ $2p'$ $2s''$ $2p''$ $2p''$ $2p''$ 9 functions	
	$_{11}$Na–$_{18}$Ar $1s$ $2s$ $2p$ $2p$ $2p$ $3s'$ $3p'$ $3p'$ $3p'$ $3s''$ $3p''$ $3p''$ $3p''$ 13 functions	
$_{19}$K–$_{20}$Ca $1s$ $2s$ $2p$ $2p$ $2p$ $3s$ $3p$ $3p$ $3p$ $4s'$ $4p'$ $4p'$ $4p'$ $4s''$ $4p''$ $4p''$ $4p''$ 17 functions	$_{21}$Sc–$_{30}$Zn $1s$ $2s$ $2p$ $2p$ $2p$ $3s$ $3p$ $3p$ $3p$ $4s'$ $4p'$ $4p'$ $4p'$ $4s''$ $4p''$ $4p''$ $4p''$ $3d'$ $3d'$ $3d'$ $3d'$ $3d'$ $3d'$ $3d''$ $3d''$ $3d''$ $3d''$ $3d''$ $3d''$ 29 functions	$_{31}$Ga–$_{36}$Kr $1s$ $2s$ $2p$ $2p$ $2p$ $3s$ $3p$ $3p$ $3p$ $4s'$ $4p'$ $4p'$ $4p'$ $4s''$ $4p''$ $4p''$ $4p''$ $3d$ $3d$ $3d$ $3d$ $3d$ $3d$ 23 functions
$_{37}$Rb–$_{38}$Sr $1s$ $2s$ $2p$ $2p$ $2p$ $3s$ $3p$ $3p$ $3p$ $4s$ $4p$ $4p$ $4p$ $5s'$ $5p'$ $5p'$ $5p'$ $5s''$ $5p''$ $5p''$ $5p''$ $3d$ $3d$ $3d$ $3d$ $3d$ $3d$ 27 functions	$_{39}$Y–$_{48}$Cd $1s$ $2s$ $2p$ $2p$ $2p$ $3s$ $3p$ $3p$ $3p$ $4s$ $4p$ $4p$ $4p$ $5s'$ $5p'$ $5p'$ $5p'$ $5s''$ $5p''$ $5p''$ $5p''$ $3d$ $3d$ $3d$ $3d$ $3d$ $3d$ $4d'$ $4d'$ $4d'$ $4d'$ $4d'$ $4d'$ $4d''$ $4d''$ $4d''$ $4d''$ $4d''$ $4d''$ 39 functions	$_{49}$In–$_{54}$Xe $1s$ $2s$ $2p$ $2p$ $2p$ $3s$ $3p$ $3p$ $3p$ $4s$ $4p$ $4p$ $4p$ $5s'$ $5p'$ $5p'$ $5p'$ $5s''$ $5p''$ $5p''$ $5p''$ $3d$ $3d$ $3d$ $3d$ $3d$ $3d$ $4d$ $4d$ $4d$ $4d$ $4d$ $4d$ 33 functions

Fig. 5.13 (continued)

of their genesis, ab initio basis sets are constructed by some kind of mathematical minimization procedure, and not by fitting them to reproduce experimental atomic or molecular properties: they are not semiempirical.

5.3.3.1 STO-3G

This is called a *minimal basis set*, although some atoms actually have more basis functions (which for this basis can be equated with atomic orbitals) than are needed to accommodate all their electrons. For the earlier part of the periodic table (hydrogen to argon) each atom has one basis function corresponding to its usual atomic orbital description, with the proviso that the orbitals used by the later atoms of a row are available to all those of the row. A hydrogen or helium atom has a $1s$ basis function. Each "first-row" atom (lithium to neon) has a $1s$, a $2s$, and a $2p_x$, $2p_y$ and $2p_z$ function, giving 5 basis functions for each of these atoms: although lithium

c, 3-21G$^{(*)}$

266 $_1$H 1s′ 1s′′ 2 functions		$_2$He 1s′ 1s′′ 2 functions
	$_3$Li–$_{10}$Ne 1s 2s′ 2p′ 2p′ 2p′ 2s′′ 2p′′ 2p′′ 2p′′ 9 functions	
	$_{11}$Na–$_{18}$Ar 1s 2s 2p 2p 2p 3s′ 3p′ 3p′ 3p′ 3s′′ 3p′′ 3p′′ 3p′′ 3d 3d 3d 3d 3d 19 functions	
$_{19}$K–$_{20}$Ca 1s 2s 2p 2p 2p 3s 3p 3p 3p 4s′ 4p′ 4p′ 4p′ 4s′′ 4p′′ 4p′′ 4p′′ 3d 3d 3d 3d 3d 3d 23 functions	$_{21}$Sc–$_{30}$Zn 1s 2s 2p 2p 2p 3s 3p 3p 3p 4s′ 4p′ 4p′ 4p′ 4s′′ 4p′′ 4p′′ 4p′′ 3d′ 3d′ 3d′ 3d′ 3d′ 3d′′ 3d′′ 3d′′ 3d′′ 3d′′ 29 functions	$_{31}$Ga–$_{36}$Kr 1s 2s 2p 2p 2p 3s 3p 3p 3p 4s′ 4p′ 4p′ 4p′ 4s′′ 4p′′ 4p′′ 4p′′ 3d′ 3d′ 3d′ 3d′ 3d′ 3d′ 3d′ 3d′ 3d′ 3d′ 3d′ 3d′ 29 functions
$_{37}$Rb–$_{38}$Sr 1s 2s 2p 2p 2p 3s 3p 3p 3p 4s 4p 4p 4p 5s′ 5p′ 5p′ 5p′ 5s′′ 5p′′ 5p′′ 5p′′ 3d 3d 3d 3d 3d 3d 4d 4d 4d 4d 4d 4d 33 functions	$_{39}$Y–$_{48}$Cd 1s 2s 2p 2p 2p 3s 3p 3p 3p 4s 4p 4p 4p 5s′ 5p′ 5p′ 5p′ 5s′′ 5p′′ 5p′′ 5p′′ 3d 3d 3d 3d 3d 3d 4d′ 4d′ 4d′ 4d′ 4d′ 4d′ 4d′′ 4d′′ 4d′′ 4d′′ 4d′′ 4d′′ 39 functions	$_{49}$In–$_{54}$Xe 1s 2s 2p 2p 2p 3s 3p 3p 3p 4s 4p 4p 4p 5s′ 5p′ 5p′ 5p′ 5s′′ 5p′′ 5p′′ 5p′′ 3d 3d 3d 3d 3d 4d′ 4d′ 4d′ 4d′ 4d′ 4d′ 4d′′ 4d′′ 4d′′ 4d′′ 4d′′ 4d′′ 39 functions

d, 6-31G*

$_1$H 1s′ 1s′′ 2 functions		$_2$He 1s′ 1s′′ 2 functions
	$_3$Li–$_{10}$Ne 1s 2s′ 2p′ 2p′ 2p′ 2s′′ 2p′′ 2p′′ 2p′′ 3d 3d 3d 3d 3d 3d 15 functions	
	$_{11}$Na–$_{18}$Ar 1s 2s 2p 2p 2p 3s′ 3p′ 3p′ 3p′ 3s′′ 3p′′ 3p′′ 3p′′ 3d 3d 3d 3d 3d 3d 19 functions	

Fig. 5.13 (continued)

and beryllium are often not thought of as using p orbitals, all the atoms of this row are given the same basis, because this has been found to work better than a literally minimum basis set. Second-row atoms (sodium to argon) have a $1s$ and a $2s$, as well as three $2p$ functions, plus a $3s$ and three $3p$ functions, giving 9 basis functions. In the third row, potassium and calcium, as expected, have the 9 functions of the previous row, plus a $4s$ and three $4p$ functions, for a total of 13 basis functions. Starting with the next element, scandium, five $3d$ orbitals are added, so that scandium to krypton have $13 + 5 = 18$ basis functions. The STO-3G basis is summarized in Fig. 5.13(a).

The STO-3G basis introduces us to the concept of *contraction shells* in constructing contracted Gaussians from primitive Gaussians (Sect. 5.3.2). The Gaussians of a contraction shell share common exponents. Carbon, for example, has one s shell and one sp shell. This means that the $2s$ and $2p$ Gaussians (belonging to the $2sp$ shell) share common α exponents (which differ from those of the $1s$ function). Consider the contracted Gaussians

$$\phi(2s) = d_{1s}e^{-\alpha_{1s}\mathbf{r}} + d_{2s}e^{-\alpha_{2s}\mathbf{r}} + d_{3s}e^{-\alpha_{3s}\mathbf{r}}$$
$$\phi(2p_x) = d_{1p}xe^{-\alpha_{1p}\mathbf{r}} + d_{2p}xe^{-\alpha_{2p}\mathbf{r}} + d_{3p}xe^{-\alpha_{3p}\mathbf{r}}$$
$$\phi(2p_z) = d_{1p}ze^{-\alpha_{1p}\mathbf{r}} + d_{2p}ze^{-\alpha_{2p}\mathbf{r}} + d_{3p}ze^{-\alpha_{3p}\mathbf{r}}$$
$$\phi(2p_y) = d_{1p}ye^{-\alpha_{1p}\mathbf{r}} + d_{2p}ye^{-\alpha_{2p}\mathbf{r}} + d_{3p}ye^{-\alpha_{3s}\mathbf{r}}$$

The usual practice is to set $\alpha_{1s} = \alpha_{1p}$, $\alpha_{2s} = \alpha_{2p}$, and $\alpha_{3s} = \alpha_{3p}$. Using common α's for the s and p primitives reduces the number of distinct integrals that must be calculated. An STO-3G calculation on CH_4, for example, involves nine basis functions (five for C and one for each H) in six shells: for C one s (i.e. a $1s$) shell, and one sp (i.e. a $2s$ plus $2p$) shell, and for each H one s (i.e. a $1s$) shell. The current view is that the STO-3G basis is not very good, and it would normally be considered unacceptable for research. Nevertheless, one hesitates to endorse Dewar and Storch's assertion that "it must be considered obsolete" [43]. We do not know how many publications report work which began with preliminary and unreported but valuable investigations using this basis. Its advantages are speed (it is probably the smallest basis set that would even be considered for an ab initio calculation) and the ease with which the molecular orbitals can be dissected into atomic orbital contributions. The STO-3G basis is roughly twice as fast (Table 5.3) as the next larger commonly used one, the 3–21G. Sophisticated semiempirical methods (Chap. 6) are perhaps more likely to be used nowadays in preliminary investigations, and to obtain reasonable starting structures for ab initio optimizations, but for systems significantly different from those for which the semiempirical methods were parameterized one might prefer to use the STO-3G basis. As for examining atomic contributions to bonding, interpreting bonding in terms of hybrid orbitals and the contribution of particular atoms to MO's is simpler when each atom has just one conventional orbital, rather than split orbitals (as in the basis sets to be discussed). Thus an analysis of the electronic structure of three- and four-membered rings used the STO-3G basis explicitly for this reason [44], as did an interpretation of the bonding in the unusual molecule pyramidane [45].

Table 5.3 Effect of basis set and symmetry on times for single-point, geometry optimization and geometry optimization + frequencies calculations on acetone, $(CH_3)_2CO$

Basis set	Single point		Geometry optimization		Geometry optimization + frequencies	
	Time, seconds		Time, seconds		Time, seconds	
	C_{2v}	C_1	C_{2v}	C_1	C_{2v}	C_1
STO-3G	0.2 (0.2)	0.3 (0.2)	1 (2)	2 (7)	2 (13)	3 (59)
$3–21G^{(*)}$	0.5 (0.3)	0.6 (0.5)	2 (2)	3 (5)	3 (20)	8 (75)
$6–31G^{*}$	1.4 (2)	2 (3)	9 (15)	22 (54)	15 (172)	30 (586)

The starting geometry for the ab initio jobs was a molecular mechanics (MMFF) one. The C_{2v} geometry is that with two C–H/C=O eclipsed arrangements (the global minimum). The C_1 symmetry starting geometry was obtained by rotating one C–C bond very slightly (by 1°) in the C_{2v} precursor molecular mechanics structure (after MM optimization). These calculations were done with a 2006 version of Spartan [37] on a quadcore 2.66 GHz personal computer with 4.0 GB of RAM, vintage 2007. For times of ca. one second, time differences are scarcely meaningful. Numbers in parentheses were for calculations done in ca. 2001
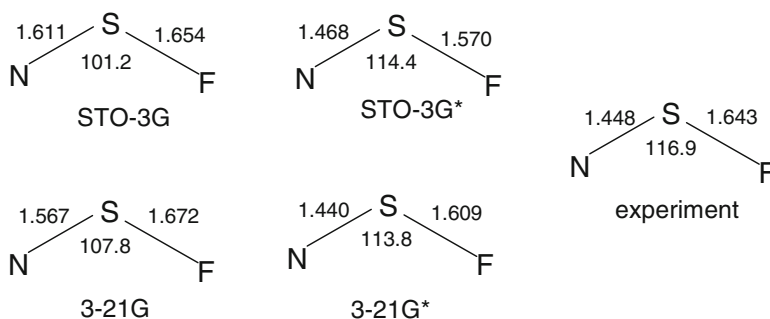
Fig. 5.14 Some STO-3G, STO-3G*, 3–21G and 3–21G* geometries

The shortcomings (and virtues) of the STO-3G basis are extensively documented throughout Ref. [1g]. Basically, the drawbacks are that by comparison with the 3–21G basis, which is not excessively more demanding of time, it gives significantly less accurate geometries and energies (this was the reason for the call to abandon this basis [43]). Actually, even for second-row atoms (Na–Ar), where the defects of such a small basis set should be, and are, most apparent, the STO-3G basis supplemented with five d or *polarization* functions (the STO-3G* basis; polarization functions are discussed below) can give results comparable to those of the 3–21G basis set. Thus for the S–O bond length of Me_2SO we get (Å): STO-3G, 1.820; STO-3G*, 1.480; 3–21G, 1.678; $3–21G^{(*)}$, 1.490; exp., 1.485, and for NSF [46] the geometries shown in Fig. 5.14. Nevertheless, the STO-3G* basis is not in the normally-used repertoire.

5.3.3.2 3–21G and 3–21G* Split Valence and Double-Zeta Basis Sets

First consider what we could denote as the "simple" 3–21G basis set. This splits each valence orbital into two parts, an inner shell and an outer shell. The basis function of the inner shell is represented by two Gaussians, and that of the outer shell by one Gaussian (hence the "21"); the core orbitals are each represented by one basis function, each composed of three Gaussians (hence the "3"). Thus H and He have a 1s orbital (the only valence orbital for these atoms) split into $1s'$ (1s inner) and $1s''$ (1s outer), for a total of 2 basis functions. Carbon has a 1s function represented by three Gaussians, an inner 2s, $2p_x$, $2p_y$ and $2p_z$ ($2s'$, $2p_x'$, $2p_y'$ $2p_z'$) function, each composed of two Gaussians, and an outer 2s, $2p_x$, $2p_y$ and $2p_z$ ($2s''$, $2p_x''$, $2p_y''$, $2p_z''$) function, each composed of one Gaussian, making 9 basis functions. The terms inner and outer derive from the fact that the Gaussian of the outer shell has a smaller α than the Gaussians of the inner shell, and so the former function falls off more slowly, i.e. it is more diffuse and effectively spreads out further, into the outer regions of the molecule. The purpose of splitting the valence shell is to give the SCF algorithm more flexibility in adjusting the contributions of the basis functions to the molecular orbitals, thus achieving a more realistic simulated electron distribution. Consider carbene, CH_2 (Fig. 5.15). We can denote the basis functions $\phi_1 - \phi_{13}$:

C1s: ϕ_1
C2s$'$, $2p_x'$, $2p_y'$, $2p_z'$: ϕ_2, ϕ_3, ϕ_4, ϕ_5 (inner valence shell)
C2s$''$, $2p_x''$, $2p_y''$, $2p_z''$: ϕ_6, ϕ_7, ϕ_8, ϕ_9 (outer valence shell)
H$_1$1s$'$: ϕ_{10} (inner shell)
H$_1$1s$''$: ϕ_{11} (outer shell)
H$_2$1s$'$: ϕ_{12} (inner shell)
H$_2$1s$''$: ϕ_{13} (outer shell)

Thirteen basis functions ("atomic orbitals") give thirteen LCAO MO's:

$$\psi_1 = c_{11}\phi_1 + c_{21}\phi_2 + \cdots + c_{13,1}\phi_{13}$$
$$\psi_1 = c_{12}\phi_1 + c_{22}\phi_2 + \cdots + c_{13,2}\phi_{13}$$
$$\vdots$$
$$\psi_{13} = c_{1,13}\phi_1 + c_{2,13}\phi_2 + \cdots + c_{13,13}\phi_{13}$$

Fig. 5.15 Carbene, with
3–21G basis functions

C, 9 basis functions

H, 2 basis functions   H, 2 basis functions

13 basis functions
8 electrons
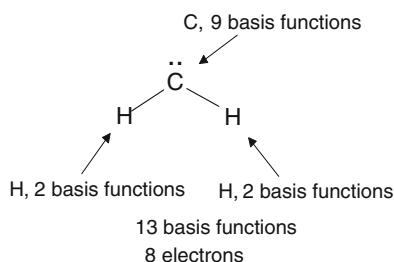
Note that since there are thirteen MO's but only eight electrons to be accommodated, only the first four MO's ($\psi_1-\psi_4$) are occupied (recall that we are talking about closed-shell molecules in the ground electronic state). The nine empty MO's are called *unoccupied* or *virtual molecular orbitals*. We shall see that virtual MO's are important in certain kinds of calculations. Now, in the course of the SCF process the coefficients of the various inner-shell and outer-shell basis functions can be varied independently to find the best wavefunctions ψ (those corresponding to the lowest energy). As the iterations proceed some outer-shell functions, say, could be given greater (or lesser) emphasis, independently of any inner-shell functions, allowing a finer-tuning of the electron distribution and a lower energy, than would be possible with unsplit basis functions.

A still more malleable basis set would be one with *all* the basis functions, not just those of the valence AO's but the core ones too, split; this is called a *double zeta* (double ζ) basis set (perhaps from the days before Gaussians, with $\exp(-\alpha r^2)$, had almost completely displaced Slater functions with $\exp(-\zeta \mathbf{r})$ for molecular calculations). Double zeta basis sets are much less widely used than *split valence* sets, since the former are computationally more demanding and for many purposes only the contributions of the "chemically active" valence functions to the MO's need to be fine-tuned, and "double zeta" is sometimes used to refer to split valence basis sets.

Returning to the 3–21G basis: here lithium to neon have a 1s function and inner and outer 2s, $2p_x$, $2p_y$ and $2p_z$ (2s', 2s'', ..., $2p_z$") functions, for a total of 9 basis functions. These inhabit three contraction shells (see the STO-3G discussion): a 1s, an *sp* inner and an *sp* outer contraction shell. Sodium to argon have a 1s, a 2s and three 2p functions, and an inner and outer shell of 3s and 3p functions, for a total of $1 + 4 + 8$ basis functions. These are in four shells: a 1s, an *sp* (2s, 2p), an *sp* inner and an *sp* outer (3s and 3p inner, 3s and 3p outer). Potassium and calcium have a 1s, a 2s and three 2p, and a 3s and three 3p functions, plus inner and outer 4s and 4p functions, for a total of $1 + 4 + 4 + 8 = 17$ basis functions. The 3–21G basis set is summarized in Fig. 5.13b.

For molecules with atoms beyond the first row (beyond neon), this "simple" 3–21G basis set tends to give poor geometries. This problem is largely overcome for second-row elements (sodium to argon) by supplementing this basis with *d* functions, called *polarization functions*. The term arises from the fact that *d* functions permit the electron distribution to be polarized (displaced along a particular direction), as shown in Fig. 5.16. Polarization functions enable the SCF process to establish a more anisotropic electron distribution (where this is appropriate) than would otherwise be possible (cf. the use of split valence basis sets to permit more flexibility in adjusting the inner and outer regions of electron density). The 3–21G basis set augmented where appropriate (beyond neon) with six *d* functions is in some computational programs designated 3–21G$^{(*)}$, where the asterisk indicates polarization functions (*d* in this case) and the parentheses emphasize that these extra (compared to the "simple" 3–21G basis) functions are present only beyond the first row. For H to Ne, the 3–21G and the 3–21G* basis sets are identical. The simple 3–21G basis, *without* the possibility of invoking polarization
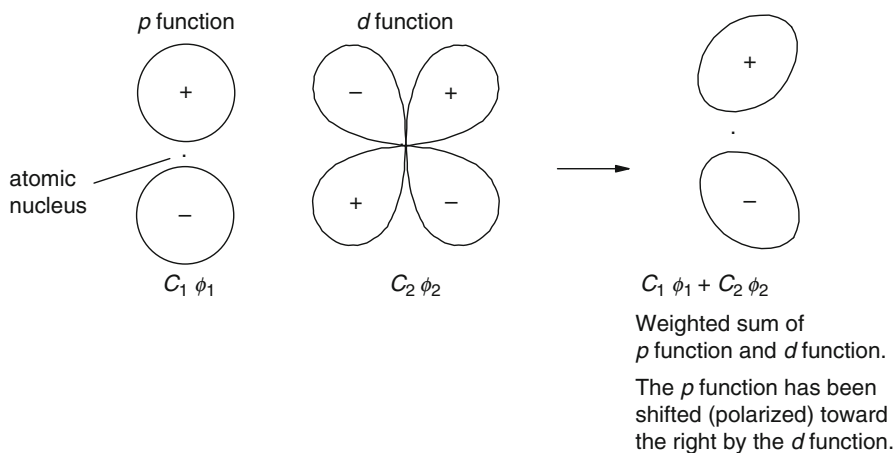
Fig. 5.16 One basis function can be used to shift another in a given direction (to polarize it). In minimizing the energy, the program adjusts the relative contributions of the two functions to shift the electron density where it is needed to get the minimum energy. *p* Functions are also commonly used to polarize the *s* functions on hydrogen atoms, but the main use of polarization functions is the utilization of *d* functions on "heavy" atoms (atoms other than H and He)

functions, is probably obsolete, and when we see "3–21G" we can usually take it to mean, really, the 3–21G$^{(*)}$ basis summarized in Fig. 5.13c; for precision, the 3–21G$^{(*)}$ designation will be preferred here from now on. *p*-Polarization functions can also be added not only to heavy atoms (recall that in computational chemistry atoms beyond hydrogen and helium in the periodic table are called heavy atoms), but to hydrogen and helium also (below).

   Examples of geometries calculated with the simple and augmented 3–21G basis sets are shown in Fig. 5.14. The 3–21G$^{(*)}$ gives remarkably good geometries for such a small set, and it is used for the geometry optimization step of some high-accuracy energy methods (Sect. 5.5.2). Since it is roughly five times as fast (Table 5.3) as the next bigger widely-used basis, the 6–31G* (below) and is much less demanding of computer power, the 3–21G$^{(*)}$ basis set has been used as a kind of workhorse for relatively big molecules; see for example a study using it for geometry optimization investigations of pericyclic reactions [47]. As long ago as 1988 the somewhat similar but now obsolete 4–21G basis was used, with the 3–21G$^{(*)}$ basis specifically on sulfur, for geometry optimization of a protein (crambin) with 46 amino acid residues and 642 atoms. This represented 3597 basis functions, and the job took 260 days [48]. It seems likely that now it would be shorter by a factor of at least about 20, on an inexpensive desktop machine. Nevertheless, the 6–31G* and even bigger basis sets seem to have largely displaced the 3–21G$^{(*)}$. More recently novel approaches, such as dividing a large molecule into fragments, have been explored [49]. The general problem of optimizing large molecules has been reviewed [50]. Even where geometry optimizations with larger bases are practical, a survey of the problem with the 3–21G$^{(*)}$ basis is sometimes useful (it is HF/3–21G$^{(*)}$ *geometries* rather than *relative energies* which are

reasonable; consistently getting good relative energies is a more challenging problem–see Sect. 5.5.2).

5.3.3.3 6–31G*

This is a split valence basis set with polarization functions (these terms were explained in connection with the 3–21G$^{(*)}$ basis set, above). The valence shell of each atom is split into an inner part composed of three Gaussians and an outer part composed of one Gaussian (hence "31"), while the core orbitals are each represented by one basis function, each composed of six Gaussians ("6"). The polarization functions (*) are present on "heavy atoms"–those beyond helium. Thus H and He have a $1s$ orbital represented by an inner $1s$' and an outer $1s$' basis function, making two basis functions. Carbon has a $1s$ function represented by six Gaussians, an inner $2s$, $2p_x$, $2p_y$ and $2p_z$ ($2s$', $2p_x$', $2p_y$' $2p_z$') function, each composed of three Gaussians, and an outer $2s$, $2p_x$, $2p_y$ and $2p_z$ ($2s$'', $2p_x$'', $2p_y$'' $2p_z$'') function, each composed of one Gaussian, and six (not five) $3d$ functions, making a total of 15 basis functions. A 6–31G* calculation on CH_2 uses $15 + 2 + 2 = 19$ basis functions, and generates 19 MO's. In the closed-shell species the eight electrons occupy four of these MO's, so there are 15 unoccupied or virtual MO's; compare this with a 3–21G$^{(*)}$ calculation on CH_2 (above) where there are a total of 13 MO's with nine of them virtual. The 6–31G* basis, also often called 6–31G(d), is summarized in Fig. 5.13d.

The 6–31G* is perhaps the most popular basis at present. It gives good geometries and, often, reasonable relative energies (Sect. 5.5.2); however, there seems to be little evidence that it is, *in general*, much better than the 3–21G$^{(*)}$ basis for geometry optimizations. Since it is about five times as slow (Table 5.3) as the 3–21G$^{(*)}$ basis, the general preference for the 6–31G* for geometry optimizations may be due to its better relative energies (Sect. 5.5.2). The 3–21G$^{(*)}$ basis *does* have certain geometry deficiencies compared to the 6–31G*, particularly its tendency to overzealously flatten nitrogen atoms (the N of aniline is wrongly predicted to be planar), and this, along with inferior relative energies and less consistency, may be responsible for its being moribund in favor of the 6–31G* basis set [51]. The virtues of the 3–21G$^{(*)}$ and 6–31G* basis sets for geometry optimizations are discussed further in Sect. 5.5.1. Note that the geometries and energies referred to here are those from Hartree-Fock-level calculations. Post-Hartree-Fock (Sect. 5.4) calculations, which can give significantly better geometries and much better relative energies (Sects. 5.5.1 and 5.5.2), are considered to require a basis set of at least the 6–31G* size for meaningful results.

The 6–31G* basis adds polarization functions only to so-called heavy atoms (those beyond helium). Sometimes it is helpful to have polarization functions on the hydrogens as well; a 6–31G* basis with three $2p$ functions on each H and He atom (in addition to their $1s$' and $1s$'' functions) is called the 6–31G** (or 6–31(d,p)) basis. The 6–31G* and 6–31G** bases are the same except that in the 6–31G** each H and He has five, rather than two, functions. The 6–31G** basis probably offers

little advantage over the 6–31G* unless the hydrogens are engaged in some special activity like hydrogen bonding or bridging [52]. In high-level calculations on hydrogen bonding or on boron hydrides, for example, polarization functions are placed on hydrogen. For calculations on and references to the hydrogen bonded water dimer, see Sect. 5.4.3.

5.3.3.4   Diffuse Functions

Core electrons or electrons engaged in bonding are relatively tightly bound to the molecular nuclear framework. Lone-pair electrons or electrons in a (previously) virtual orbital, are relatively loosely held, and are on the average at a larger distance from the nuclei than core or bonding electrons. These "expanded" electron clouds are found in molecules with heteroatoms, in anions, and in electronically excited molecules. To simulate well the behaviour of such species *diffuse functions* are used. These are Gaussian functions with small values of α; this causes $\exp(-\alpha \mathbf{r}^2)$ to fall off very slowly with the distance $\mathbf{r}$ from the nucleus, so that by giving enough weight to the coefficients of diffuse functions the SCF process can generate significant electron density at relatively large distances from the nucleus. Typically a basis set with diffuse functions has one such function, composed of a single Gaussian, for each valence atomic orbital of the "heavy atoms". The $3\text{–}21+\text{G}$ basis set for carbon ($= 3\text{–}21+\text{G}^{(*)}$ for this element) is

1s
2s' 2p' 2p' 2p'
2s'' 2p'' 2p'' 2p''
2s+, 2p+, 2p+, 2p+
13 basis functions
and the $6\text{–}31+\text{G}^*$ basis for carbon is
1s
2s' 2p' 2p' 2p'
2s'' 2p'' 2p'' 2p''
3d 3d 3d 3d 3d 3d
2s+, 2p+, 2p+, 2p+
19 basis functions

Sometimes diffuse functions are added to hydrogen and helium as well as to the heavy atoms; such a basis set is indicated by ++. The 3–21++G and 6–31++G basis for hydrogen and helium is

1s
1s'
1s+
3 basis functions

A 3–21++G calculation on CH_2 would use $13+3+3=19$ basis functions, a 6–31++G* calculation $19+3+3=25$ basis functions, and a 6–31++G** calculation $19+6+6=31$ basis functions.

There is some disagreement over when diffuse functions should be used. Certainly most workers employ them routinely in studying anions and excited states, but not ordinary lone pair molecules (molecules with heteroatoms, like ethers and amines). A reasonable recommendation is to study with and without diffuse functions species representative of the problem at hand, for which experimental results are known, and see if these functions help. A paper by Warner [52] gives useful references and a good account of the efficacy of diffuse functions in treating certain molecules with heteroatoms. He settles on the 6–31+G*, i.e. 6–31+G(d), basis.

5.3.3.5   Large Basis Sets

The 3–21G$^{(*)}$ is a small basis set and the 6–31G* and 6–31G** are moderate-size basis sets. Of those we have discussed, only the 6–31G* and 6–31G** with diffuse functions (6–31+G*, 6–31++G*, 6–31+G** and 6–31++G**) might be considered *fairly* large. A large basis set might have a doubly-split or even triply-split valence shell with d, p and f, and maybe even g, functions on at least the heavy atoms. An example of a large (but not very large) basis set is the 6–311G** (i.e. 6–311(d,p)) set. This is a split valence set with each valence orbital split into three shells, composed of three, one and one Gaussian, while the core orbitals are represented by one basis function composed of six Gaussians; each heavy atom also has five (not six in this case) $3d$ functions and each hydrogen and helium has three $2p$ functions. The 6–31G** basis for carbon is then

1s
2s' 2p' 2p' 2p'
2s'' 2p'' 2p'' 2p''
2s''' 2p''' 2p''' 2p'''
3d 3d 3d 3d 3d
18 basis functions
and for hydrogen
1s'
1s''
1s'''
2p 2p 2p
6 basis functions

Unequivocally large basis sets would be triply-split valence shell sets with d and f functions on heavy atoms and p functions on hydrogen. At the smaller end of such sets is the 6–311G(df,p) basis, with five $3d$'s and seven $4f$'s on each heavy atom and three $2p$'s on each hydrogen and helium. For carbon this is

1*s*
2*s'* 2*p'* 2*p'* 2*p'*
2*s''* 2*p''* 2*p''* 2*p''*
2*s'''* 2*p'''* 2*p'''* 2*p'''*
3*d* 3*d* 3*d* 3*d* 3*d*
4*f* 4*f* 4*f* 4*f* 4*f* 4*f* 4*f*
25 basis functions
and for hydrogen
1*s'*
1*s''*
1*s'''*
2*p* 2*p* 2*p*
6 basis functions

A more impressive example of a large basis set would be 6–311G(3df,3pd). This has for each heavy atom three sets of five *d* functions and one set of seven *f* functions, and for each hydrogen and helium three sets of three *p* functions and one set of five *d* functions, i.e. for carbon

1*s*
2*s'* 2*p'*2*p'* 2*p'*
2*s''* 2*p''* 2*p''* 2*p''*
2*s'''* 2*p'''* 2*p'''* 2*p'''*
3*d* 3*d* 3*d* 3*d* 3*d*
3*d* 3*d* 3*d* 3*d* 3*d*
3*d* 3*d* 3*d* 3*d* 3*d*
4*f* 4*f* 4*f* 4*f* 4*f* 4*f* 4*f*
35 basis functions
and for hydrogen
1*s'*
1*s''*
1*s'''*
2*p* 2*p* 2*p*
2*p* 2*p* 2*p*
2*p* 2*p* 2*p*
3*d* 3*d* 3*d* 3*d* 3*d*
17 basis functions

Note that all these large basis sets can be made still bigger by adding diffuse functions to heavy atoms (+) or to heavy atoms and hydrogen/helium (++). The number of basis functions on CH_2 using some small, medium and large bases is summarized $C + H + H$):

STO–3G $5 + 1 + 1 = 7$ functions

3 − 21G (= 3 − 21G$^{(*)}$ here) $9 + 2 + 2 = 13$ functions

$$6-31G* \ (6-31G(d)) \qquad 15+2+2 = 19 \text{ functions}$$

$$6-31G** \ (6-31G(d,p)) \qquad 15+5+5 = 25 \text{ functions}$$

$$6-311G** \ (6-311G(d,p)) \quad 18+6+6 = 30 \text{ functions}$$

$$6-311G(df,p) \qquad 25+6+6 = 37 \text{ functions}$$

$$6-311G(3df,3pd) \qquad 35+17+17 = 69 \text{ functions}$$

$$6-311++G \ (3df,3pd) \qquad 39+18+18 = 75 \text{ functions}$$

Large basis sets are used mainly for post-Hartree-Fock level (Sect. 5.4) calculations, where the use of a basis smaller than the 6–31G* seems to be essentially pointless. At the Hartree-Fock level the smallest basis normally used is the 6–31G* or 6–31G** (augmented if appropriate by diffuse functions), and post- HF geometry optimizations are frequently done using the 6–31G* or 6–31G** basis too. Use of the larger bases (6–311G** and up) tends to be confined to *single-point* calculations on structures optimized with a smaller basis set (e.g. Sect. 5.4.2). These are not firm rules: the high-accuracy CBS (complete basis set) methods (Sect. 5.5.2.3.2) use as part of their procedure single-point HF (rather than post-HF) level calculations with very large basis sets, and geometry optimizations with large basis sets were performed at both HF and post-HF levels in studies of the theoretically and experimentally challenging oxirene system [53].

5.3.3.6 Correlation-Consistent Basis Sets

All the previously explicitly designated basis sets, from STO-3G through 6–311++G (3df,3pd) (in *Large basis sets*), are Pople (from the group of John Pople; see above) basis sets. Another class of popular basis sets was developed by the research group of T. H. Dunning, Jr. [54]. These are specially designed for post-Hartree Fock calculations (Sect. 5.4), methods in which electron correlation is better taken into account than at the Hartree Fock level. Because they are intended, ideally, to give with such calculations improved results in step with (correlated with) their increasing size, they are called correlation-consistent (cc) basis sets. Ideally, they systematically improve results with increasing basis set size, and permit extrapolation to the infinite basis set limit. The cc-sets are designated cc-pVXZ, where p stands for polarization functions, V for valence, X for the number of shells the valence functions are split into, and Z for zeta (cf. *Split valence and double-zeta basis sets*, above). Thus we have cc-pVDZ (cc polarized valence doubly-split zeta), cc-pVTZ (cc polarized valence triply-split zeta), cc-pVQZ (cc polarized valence quadruply-split zeta), and cc-pV5Z (cc polarized valence fivefold-split zeta). These basis sets can be augmented with diffuse and extra

polarization functions, giving aug-cc-pVXZ sets. The number of basis functions on CH_2 using some Dunning sets (cf. the data on Pople sets, above) is $C + H + H$:

cc-pVDZ $14 + 5 + 5 = 24$ functions
cc-pVTZ $30 + 14 + 14 = 58$ functions
cc-pVQZ $55 + 30 + 30 = 115$ functions
cc-pV5Z $91 + 55 + 55 = 201$ functions

We see that only the cc-pVDZ is (roughly) comparable in size to the 6–31G* $(15 + 2 + 2 = 19$ functions); the other cc sets are much bigger. Correlation-consistent basis sets sometimes [55] but do not necessarily [56] give results superior to those with Pople sets that require about the same computational time.

Ideally an ab initio calculation would use an infinite basis set (and perfect electron correlation). In attempts to simulate an infinite basis, techniques for extrapolation to this limit have been devised; as hinted above, the preferred basis sets in this iterative procedure are correlation-consistent. Clearly, basis set limit calculations can in principle be applied to any correlation level, for example Hartree-Fock (conventionally considered uncorrelated, Sect. 5.4.1), MP2 (Sect. 5.4.2), or coupled-cluster (Sect. 5.4.3), but efforts in this area have evidently been applied mainly to MP2 and coupled-cluster; see e.g. R12 and F12 methods [57]. The most widely-used methods incorporating extrapolation to the basis set limit are automated multistep procedures that we might designate Gx, CBSx, and Wx (Sect. 5.5.2.3.2).

5.3.3.7 Effective Core Potentials (Pseudopotentials)

At about the third row (potassium to krypton) of the periodic table, the large number (19 or more) of electrons in each atom begins to have a significant slowing effect on conventional ab initio calculations, because of the many two-electron repulsion integrals they engender. The usual way of avoiding this problem is to add to the Fock operator a one-electron operator that takes into account in a collective way the effect of the core electrons on the valence electrons, which latter are still considered explicitly. This "average core effect" operator is called an effective core potential (ECP) or a pseudopotential. With a set of valence orbital basis functions optimized for use with it, it simulates the effect on the valence electrons of the atomic nuclei plus the core electrons. A distinction is sometimes made between an ECP and a pseudopotential, the latter term being used to mean any approach limited to the valence electrons, while ECP is sometimes used to designate a simplified pseudopotential corresponding to a function with fewer orbital nodes than the "correct" functions. However, the terms are usually used interchangeably to designate a nuclei-plus-core electrons potential used with a set of valence functions, and that is what is meant here. The use of an ECP stands in contrast to using *all-electron basis sets* like the Pople or Dunning sets discussed above.

So far we have discussed *nonrelativistic* ab initio methods: they ignore those consequences of Einstein's special theory of relativity that are relevant to chemistry

(Chap. 4, Sect. 4.2.3 [58](a)). These consequences arise from the dependence of mass on velocity [58](b). This dependence causes the masses of the inner electrons of heavy atoms to be significantly greater than the electron rest mass; since the Hamiltonian operator in the Schrödinger equation contains the electron mass (Eqs. (5.36) and (5.37)), this change of mass should be taken into account. Relativistic effects in heavy-atom molecules affect geometries, energies, and other properties [59]. Relativity is accounted for in the relativistic form of the Schrödinger equation, the Dirac equation (interestingly, Dirac thought his equation would not be relevant to chemistry [60]). This equation is not commonly used explicitly in molecular calculations, but is instead used to develop [61] *relativistic effective core potentials* (relativistic pseudopotentials). Relativistic effects can begin to become significant for about third-row elements, i.e. the first transition metals. For molecules with these atoms ECPs begin to be useful for speeding up calculations, so it makes sense to take these effects into account in developing these potential operators and their basis functions, and indeed ECPs are generally relativistic. Such ECPs can give accurate results for molecules with third-row and beyond atoms by simulating the electronic relativistic mass increase. Examples are calculations on reactions with transition metals [62a] and on platinum compounds [62b]. Weigend and Ahlrichs have published an extensively-tested collection of basis sets for all elements, except lanthanides, from hydrogen to radon [63].

Calculations on "very-heavy-atom" molecules, particularly transition metal molecules, rely heavily on the use of pseudopotentials, although all-electron basis sets sometimes give good results with quite heavy atoms [64]. A concise description of pseudopotential theory [33] and relativistic effects in molecules [65], with several references, is given by Levine. Reviews oriented toward transition metal molecules [66a,b,c] and the lanthanides [66d] have appeared, as well as detailed reviews of the more "technical" aspects of the theory [67]. After all this concerning ECPs and ab initio calculations, one should nevertheless note that the currently favored method for computations on transition metal compounds is density functional theory, DFT (Chap. 7), rather than ab initio, albeit also with ECP use favored for heavy atoms; for example the ECP calculations of [62a,b] were done with DFT. The dominant position of DFT here could change as faster computers make very high-level ab initio methods more practical.

5.3.3.8   Which Basis Set Should I Use?

Scores, perhaps hundreds of basis sets have been developed, and new ones appear yearly, if not monthly. There is something to be said for having a variety of tools in our armamentarium, but one tends to be not entirely unsympathetic to the description, more than two decades ago, of this situation as a "chaotic proliferation" [68]. There are books of practical advice [1, 69] which help to provide a feel for the appropriateness of various basis sets. By reading the research literature one learns what approaches, including which basis sets, are being applied to a various problems, especially those related to the one's research. This said, one should avoid

simply assuming that the basis used in published work was the most appropriate one: it is possible that it was either too small or unnecessarily big. Hehre has shown [39] that in many cases the use of very large bases is pointless; on the other hand some problems yield, if at all, only to very large basis sets (see below). A Goldilocks-like basis can rarely (except for calculations of a cursory or routine nature) be correctly simply picked; rather, one homes in on an it, by experimenting and comparing results with experimental facts as far as possible. Where egregious deviations from experiment are found at theoretical levels that experience suggests should be reliable, one may be justified in questioning the "facts". Bachrach places "the first chink in the armor of the inherent superiority of experiment over computation" in 1970 [70].

A rational approach in many cases might be to survey the territory first with a semiempirical method (Chap. 6) or with the STO-3G basis and to use one of these to create input structures and input Hessians (Chap. 2, Sect. 2.4) for higher-level calculations) then to move on to the 3–21G$^{(*)}$ or the 6–31G* basis for a better exploration of the problem. For a novel system for which there is no previous work to serve as a guide one should move up to larger basis sets and to post-Hartree-Fock methods (Sect. 5.4), climbing the latter of sophistication until reasonable convergence of at least *qualitative* results has been obtained. It is possible for results to become *worse* with increasing basis set size [71, 72], because of fortuitous cancellation of errors at a lower level. This kind of thing is discussed, albeit with the focus not directly on basis functions, in several papers with the very apposite words "...the right answer for the right reason" [73]. To achieve this happy coincidence of experiment and reality, quite high theoretical levels may be necessary. A somewhat bizarre phenomenon is that at post Hartree-Fock levels, at least, some fairly large basis sets predict nonplanar geometries for benzene and similar aromatic hydrocarbons! [74]. Janoschek has given an excellent survey indicating the reliability of ab initio calculations and the level at which one might need to work to obtain trustworthy results by [75]. After this short litany of warnings, let the reader be reassured that good geometries, reasonably reliable relative energies, and useful reactivity parameters, based e.g. on orbital shapes and energies, can often obtained routinely by standard methods which were chosen by comparing their predictions with the experimental facts for a set of related compounds. Examples of such results are given later in this chapter.

Oxirene (oxacyclopropene) provides a canonical example of a molecule which even at the highest current levels of theory has declined to reveal its basic secret: whether it can exist ("Oxirene: to Be or Not to Be?" [53b]). Very large basis sets and advanced post-Hartree-Fock methods suggest it is a true minimum on the potential energy surface, but its disconcerting tendency to display an imaginary (Chap. 2, Sect. 2.5) calculated ring-opening vibrational mode at some of the highest levels used leaves the judicious chemist with no choice but to reserve judgement on its being. The nature of a series of *substituted* oxirenes, studied likewise at high levels, appears to be clearer [53a].

Another system that has yielded results which are dependent on the level of theory used, but which unlike the oxirene problem provides a textbook example of a
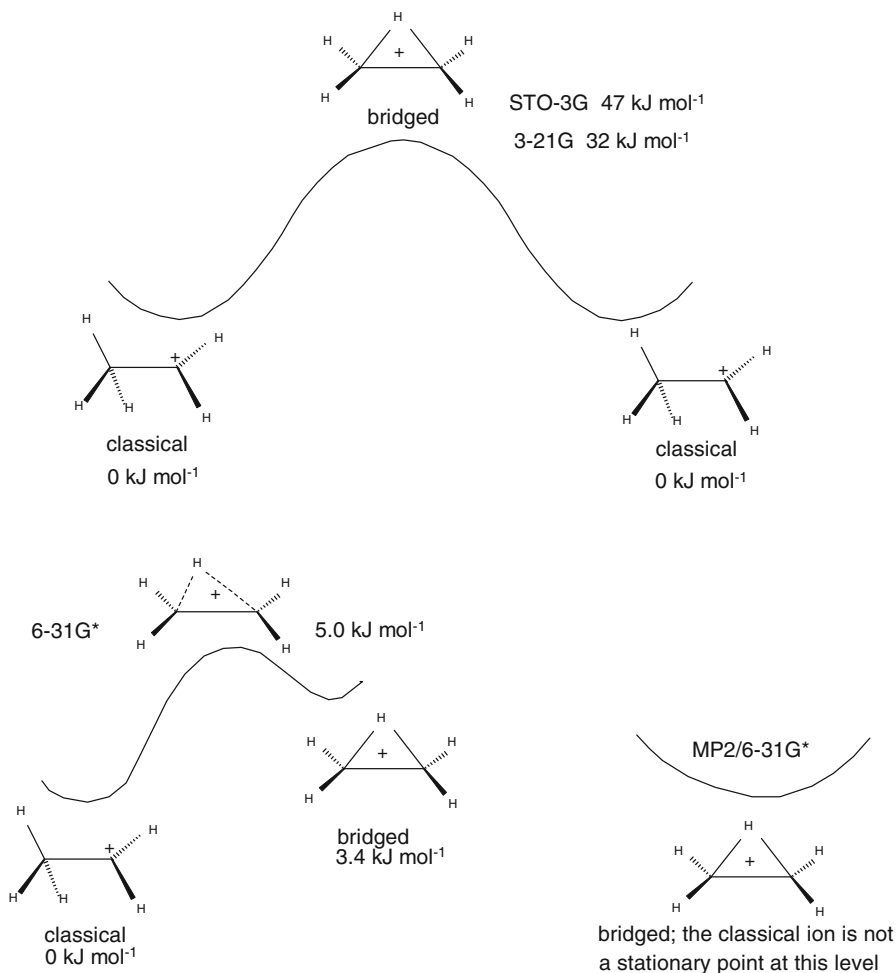
Fig. 5.17 The ethyl cation problem at various levels. At the three Hartree-Fock levels the classical cation is a minimum, but at the post-Hartree-Fock (MP2/6–31G*) level only the symmetrical bridged ion is a minimum. The HF/6–31G* results are calculations by the author (ZPE ignored), the other three levels are taken from Ref. [75]

smooth gradation in the nature of the answers obtained, is the ethyl cation (Fig. 5.17). At the Hartree-Fock STO-3G and 3–21G$^{(*)}$ levels the classical structure is a minimum and the bridged nonclassical structure is a transition state, but with the 6–31G* basis the bridged ion has become a minimum and the classical one, although the global minimum, is not securely ensconced as such, being only 3.4 kJ mol^{-1} lower than the bridged ion. At the post-Hartree-Fock (Sect. 5.4) MP2 level with the 6–31G* basis the bridged ion is a minimum and the classical one has lost the dignity of being even a stationary point. The ethyl cation and several other systems have been reviewed [75].

In summary, in many cases [39] the 3–21G (i.e. 3–21G$^{(*)}$ or 6–31G* basis sets, or for that matter even the much faster molecular mechanics (Chap. 3) or semiempirical (Chap. 6) methods, are entirely satisfactory, but there *are* problems that require quite high levels of attack.

5.4   Post-Hartree-Fock Calculations: Electron Correlation

5.4.1   *Electron Correlation*

Electron correlation is the phenomenon of the motion of pairs of electrons in atoms or molecules being connected ("correlated") [76]. The purpose of *post-Hartree-Fock calculations* (correlated calculations) is to treat such correlated motion better than does the Hartree-Fock method. In the Hartree-Fock treatment, electron-electron repulsion is handled by having each electron move in a smeared-out, average electrostatic field due to all the other electrons (Fig. 5.3), and the probability that an electron will have a particular set of spatial coordinates at some moment is independent of the coordinates of the other electrons at that moment. In reality, however, each electron at any moment moves under the influence of the repulsion, not of an average electron cloud, but rather of *individual* electrons (actually current physics regards electrons as point particles–with wave properties of course). The consequence of this is that the motion of an electron in a real atom or molecule is more complicated than that for an electron moving in a smeared-out field [77] and the electrons are thus better able to avoid one another. Because of this enhanced (compared to the Hartree-Fock treatment) standoffishness, electron-electron repulsion is really smaller than predicted by a Hartree-Fock calculation, i.e. the electronic energy is in reality lower (more negative). If you walk through a crowd, regarding it as a smeared-out collection of people, you will experience collisions that could be avoided by looking at individual motions and correlating yours accordingly. The Hartree-Fock method overestimates electron-electron repulsion and so gives higher electronic energies than the correct ones, even with the biggest basis sets, because it does not treat electron correlation properly.

Hartree-Fock calculations are sometimes said to ignore, or at least to neglect, electron correlation. Actually, the Hartree-Fock method allows for *some* electron correlation: according to our current understanding, two electrons of the same spin can't be in the same place at the same time. This is reflected in the Hartree-Fock formulation of the wavefunction as a determinant (Sect. 5.2.3.1). Because their spatial and spin coordinates of the two electrons would then be the same, the Slater determinant representing the total molecular wavefunction would vanish, since a determinant is zero if two rows or columns are the same (Chap. 4, Sect. 4.3.3). This is just a consequence of the antisymmetry of the wavefunction: switching rows or columns of a determinant changes its sign; if two rows/columns are the same then

$D_1 = D_2$ and $D_1 = -D_2$, so $D_1 = D_2 = 0$. If the wavefunction were to vanish so would the electron density, which can be calculated from the wavefunction; this seems physically unreasonable. This is one way of looking at the Pauli exclusion principle. The probability of finding an electron in a small region centered on a point defined by a triplet of spatial coordinates can in principle be calculated from the wavefunction. Now, since the probability is zero that at any moment two electrons of like spin are at the *same* point in space, and since the wavefunction is continuous, the probability of finding them at a given separation should decrease smoothly with that separation. This means that *even if electrons were uncharged*, with no electrostatic repulsion between them, around each electron there would still be a region increasingly (the closer we approach the electron) unfriendly to other electrons of the same spin. This quantum mechanically engendered "Pauli exclusion zone" around an electron is called a *Fermi hole*, after Enrico Fermi; it applies to fermions (Sect. 5.2.2) in general. Besides the quantum mechanical Fermi hole, each electron is surrounded by a region unfriendly to all other electrons, regardless of spin, because of the classical electrostatic (Coulomb) repulsion *between point particles* (= electrons). For electrons of opposite spin, to which the Fermi hole effect does not apply, this electrostatic exclusion zone is called a Coulomb hole (of course, electrons of the same spin also repel one another electrostatically). Since the HF method does not treat the electrons as discrete point particles it largely ignores the existence of the Coulomb hole, allowing electrons to get too close on the average. This is the main source of the overestimation of electron-electron repulsion in the HF method. Post-HF calculations attempt to allow electrons, even of different spin, to avoid one another better than in the HF approximation.

Hartree-Fock calculations give an electronic energy (and thus a total internal energy, Sect. 5.2.3.6.4) that is too high (the variation theorem, Sect. 5.2.3.3, assures us that the Hartree-Fock energy will never be too *low*). This is partly because of the overestimation of electronic repulsion and partly because of the fact that in any real calculation the basis set is not perfect. For sensibly-developed basis sets, as the basis set size increases the Hartree-Fock energy gets smaller, i.e. more negative. The limiting energy that would be given by an infinitely large basis set is called the *Hartree-Fock limit* (i.e. the energy in the Hartree-Fock limit). Table 5.4 and Fig. 5.18 show the results of some Hartree-Fock and post-Hartree-Fock calculations on the hydrogen molecule; the limiting energies are close to the accepted ones [78]. Errors in energy, or in any other molecular feature, that can be ascribed to using a finite basis set are said to be caused by *basis set truncation*. Basis set truncation does not always cause serious errors; for example, the small HF/3–21G$^{(*)}$ basis often gives good geometries (Sect. 5.3.3). Where necessary, the truncation problem can be minimized by using a large (provided the size of the molecule makes this practical), appropriate basis set.

A measure of the extent to which any particular ab initio calculation does not deal perfectly with electron correlation is the *correlation energy*. In a canonical exposition [79] Löwdin defined correlation energy thus: "The correlation energy for a certain state with respect to a specified Hamiltonian is the difference between the exact eigenvalue of the Hamiltonian and its expectation value in the Hartree-Fock

Table 5.4 Dependence of the calculated energy of H_2 on basis set and on correlation level

Basis	Correlated energy			
	No. basis functions	HF energy	Method	Energy
3–21G$^{(*)}$	4	−1.12292	–	–
6–31G*	10	−1.13127	MP2	−1.15761
6–311++G**	14	−1.13248	MP2	−1.16029
6–311++G(3df,3pd)	36	−1.13303	MP2	−1.16493
6–311++G(3df,3p2d)	46	−1.13307	MP2	−1.16543
6–311++G(3df,3p2d)	46	−1.13307	MP4	−1.17226
6–311++G(3df,3p2d)	46	−1.13307	full Cl	−1.17288

cf. Fig. 5.18

All calculations are single-point, without ZPE correction, on H_2 at the experimental bond length of 0.742 Å, using G94W [199]; energies are in hartrees. The accepted Hartree-Fock (E_{HF}^{total}; Eq. (5.149)) and correlated limiting energies are about −1.1336 and −1.1744 h, respectively [78], cf. −1.13307 and −1.17288 h here)
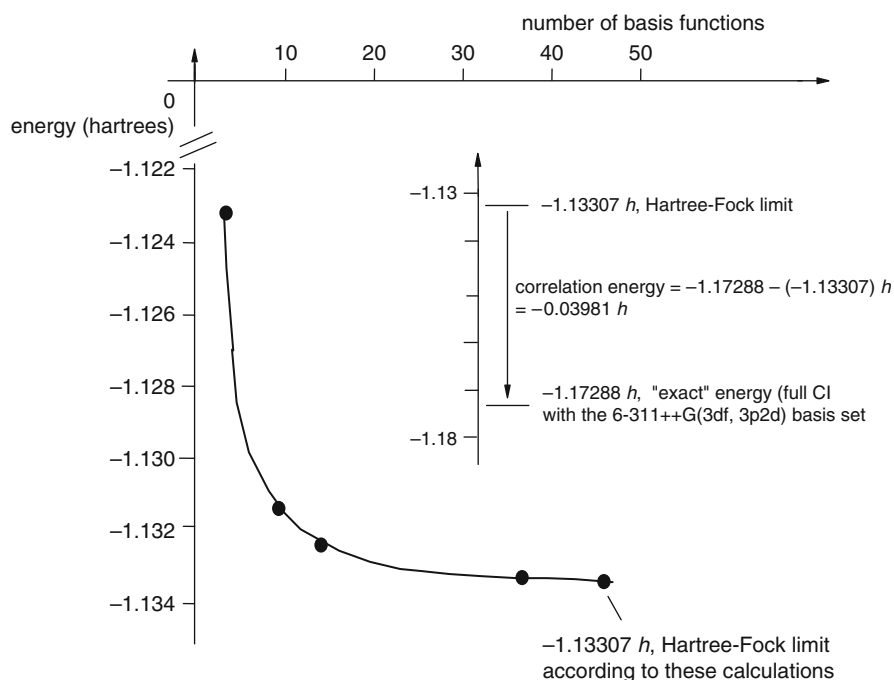
Fig. 5.18 (based on Table 5.4). The Hartree-Fock limit and correlation energy for H_2. From the values calculated here, the HF limit, the exact energy (see text) and the correlation energy are −1.13307, −1.17288 and −0.03981 hartrees (see inset); the accepted values [78] are about −1.1336, −1.17439 and −0.04079

approximation for the state under consideration." This is usually taken to be the energy from a nonrelativistic but otherwise perfect quantum mechanical procedure, minus the energy calculated by the Hartree-Fock method with the same nonrelativistic Hamiltonian and a huge ("infinite") basis set:

$$E_{\text{correl}} = E(\text{exact}) - E(\text{HF limit})$$
using the same Hamiltonian for both terms

From this definition the correlation energy is negative, since $E(\text{exact})$ (a nonrelativistic energy here) is more negative than $E(\text{HF limit})$. The Hamiltonians of Sect. 5.2.2, Eqs. (5.4), (5.5), (5.6) and associated discussion exclude relativistic effects, which are significant only for heavy atoms. Unless qualified the term correlation energy means nonrelativistic correlation energy. The correlation energy is essentially the energy that the Hartree-Fock procedure fails to account for. *If* relativistic effects (and other, usually small, effects like spin-orbit coupling) are negligible then E_{correl} is the difference between the experimental value (of the energy required to dissociate the molecule or atom into infinitely separated nuclei and electrons) and the limiting Hartree-Fock energy.

A distinction is sometimes made between dynamic (or dynamical), and nondynamic or static correlation energy. Dynamic correlation energy is the energy a Hartree-Fock calculation does not account for because it fails to keep the electrons sufficiently far apart; this is the usual meaning of "correlation energy". Static correlation energy is the energy a calculation (Hartree-Fock or otherwise) may not account for because it uses a single determinant, or starts from a single determinant (is based on a single-determinant reference–Sect. 5.4.3); this problem arises with singlet diradicals, for example, where a closed-shell description of the electronic structure is qualitatively wrong. This is because there are (two, usually) highest-energy orbitals (frontier orbitals) of equal or nearly equal energy and the Hartree-Fock method cannot unambiguously decide which of these should receive an electron pair and which should be empty–which should be the HOMO and which the LUMO. A singlet diradical actually has two essentially half-filled orbitals. The term correlation energy is applied to the unaccounted-for energy in such cases perhaps because as with dynamic correlation energy the problem can be at least partly overcome by expressing the wavefunction with more than one determinant. Dynamic correlation energy can be calculated ("recovered") by the Møller-Plesset method or by multideterminant configuration interaction methods (Sects. 5.4.2 and 5.4.3) and static correlation energy can likewise be recovered by basing the wavefunction on more than one determinant, as in a multiconfigurational method like a complete active space SCF (CASSCF, Sect. 5.4.3) calculation.

Although Hartree-Fock calculations are satisfactory for many purposes (Sect. 5.5) there are cases where a better treatment of electron correlation is needed. This is particularly true for the calculation of relative energies, although geometries and other some other properties can benefit from post-Hartree-Fock calculations Sect. 5.4). As an illustration of a shortcoming of Hartree-Fock

Table 5.5 The C–C bond energy of ethane calculated by the Hartree-Fock and MP2 methods

	Energy		
Method/basis	$CH_3\cdot$	CH_3CH_3	$E(2CH_3\cdot -CH_3CH_3)$
HF/6–31G*	−39.55899	−79.22876	0.09451
	0.02829	0.07285	248
	−39.53070	−79.15591	
HF/6–311++G(3df,3p2d)	−39.57712	−79.25882	0.08831
	0.02829	0.07285	232
	−39.54883	−79.18597	
MP2/6–31G*	−39.66875	−79.49474	0.14097
	0.02829	0.07285	370
	−39.64046	−79.42189	
MP2/6–311++G**	−39.70866	−79.57167	0.13808
	0.02829	0.07285	363
	−39.68037	−79.49882	

The radical $CH_3\cdot$ and the closed-shell CH_3CH_3 were calculated by unrestricted and restricted methods, respectively: UHF and UMP2, vs. RHF and RMP2–see concluding part of Sect. 5.2.3.6.5); the HF method largely ignores electron correlation, while MP2 recovers about 85 % of the electron correlation. The set of three numbers for each species are respectively, in hartrees, the uncorrected ab initio energy, the corrected (0.9135 factor, see text) HF/6–31G* ZPE, and the corrected ab initio energy (uncorrected energy + ZPE). Calculated (by subtraction) bond energies are in hartrees and kJ mol^{-1} (2626 × hartrees). The experimental C–C energy of ethane has been reported at 377 kJ mol^{-1} [81]. Each species was optimized at the level shown (i.e. none of these are single-point calculations)

calculations consider an attempt to find the C/C single bond dissociation energy of ethane by comparing the energy of ethane with that of two methyl radicals:

$$H_3C - CH_3 + E_{diss} \rightarrow H_3C \cdot CH_3$$
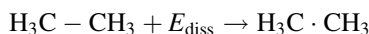
Let us simply subtract the energy of two methyl radicals from that of an ethane molecule, and compare with experiment the results of Hartree-Fock calculations and (anticipating Sect. 5.4.2) the post-Hartree-Fock (i.e. correlated) MP2 method. In Table 5.5 the energies shown for $CH_3\cdot$ and CH_3CH_3 are successively the "uncorrected" ab initio energies (the energy displayed at the end of any calculation; this is the electronic energy + the internuclear repulsion), the ZPE, and the "corrected" energy (uncorrected energy + ZPE); see Sect. 5.2.3.6.4. The ZPEs used here are from HF/6–31G* optimization/frequency jobs; these are fairly fast and give reasonable ZPEs. The ZPEs were all calculated by multiplying by an empirical correction factor of 0.9135. This brings them into better agreement with experiment [80a] (recently a *quadratic* correction to frequencies has been recommended [80b], rather than the popular linear correction normally used for ZPEs and frequencies). Although *frequencies* must be calculated with the same method (HF, MP2, etc.) and basis set as were used for the geometry optimization, *ZPEs* from a particular method/basis may legitimately be used to correct energies
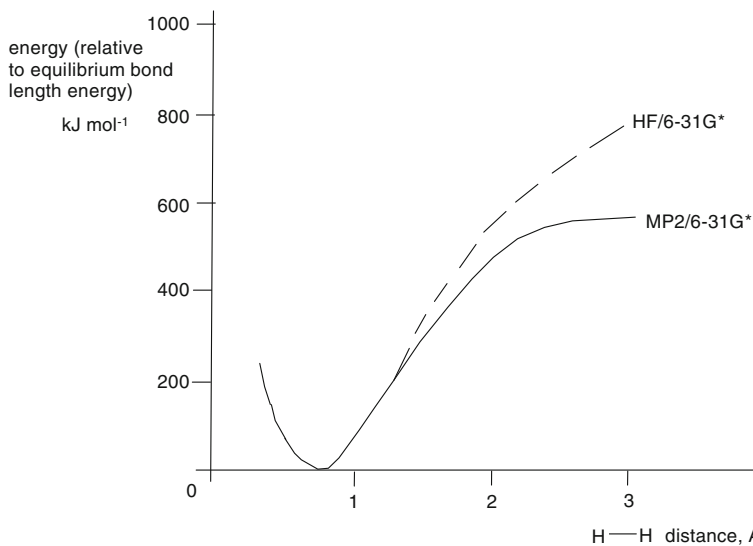
Fig. 5.19 Dissociation curves (change in energy as the bond is stretched) for H_2, from HF/6–31G* and MP2/6–31G* calculations. The equilibrium bond lengths are reasonable (HF/6–31G*, 0.730; MP2/6–31G*, 0.737 (cf. experimental, 0.742), but only the MP2 curve approximates the actual dissociation behavior of the molecule

obtained with another method/basis. The only calculations that give reasonable agreement with the experimental ethane C–C dissociation energy (reported at 377 kJ mol^{-1} [81]) are the correlated (MP2) ones, 370 and 363 kJ mol^{-1} with different basis sets; because of error in the experimental value the two MP2 results may be equally good. The Hartree-Fock values (248 and 232 kJ mol^{-1}) are very poor, even (especially!) when the very large 6–311++G (3df,3p2d) basis is used. Accurate calculation of reaction energies is now usually done with one of the multistep methods like G4 or a CBS method (Sect. 5.5.2.3.2).

This inability of Hartree-Fock calculations to model correctly homolytic bond dissociation is commonly illustrated by curves of the change in energy as a bond is stretched, e.g. Fig. 5.19. The phenomenon is discussed in detail in numerous expositions of electron correlation [82]. Suffice it to say here that representing the wavefunction as one determinant (or a few), as is done in Hartree-Fock theory, does not permit correct homolytic dissociation to two radicals because while the reactant (e.g. H_2) is a closed-shell species that can (usually) be represented well by one determinant made up of paired electrons in the occupied MOs, the products are two radicals, each with an unpaired electron. Ways of obtaining satisfactory energies, with and without the use of electron correlation methods, for processes involving homolytic cleavage, are discussed further in Sect. 5.5.2.

There are basically three approaches to dealing with electron correlation: explicit use of the interelectronic distances as variables in the Schrödinger equation, treatment of the real molecule as a perturbed Hartree-Fock system, and explicit

inclusion in the wavefunction of electronic configurations other than the ground-state one. Using interelectronic distances explicitly can quickly become mathematically intractable but recent methods offer accurate energies and near-linear scaling with quite large systems. For example an "explicitly correlated pair natural orbital local second-order Møller-Plesset perturbation theory (PNO-LMP2-F12)" method calculates an energy with up to 10,000 basis functions on a small cluster in an hour [83]. The other two methods, below, are general and very important: the perturbation approach is used in the very popular Møller-Plesset[4] methods, and the use of higher electronic configurations in the wavefunction forms the basis of configuration interaction, which in various forms is employed in some of the most advanced ab initio methods currently used for dealing with electron correlation. A powerful method that is becoming increasingly popular and incorporates mathematical features of the perturbation and higher-electronic-state methods, the coupled-cluster approach, is also described.

5.4.2 The Møller-Plesset Approach to Electron Correlation

The Møller-Plesset (MP) treatment of electron correlation [84] is based on perturbation theory, a very general approach used in physics to treat complex systems [85]; this particular approach was described by Møller and Plesset in 1934 [86] and developed into a practical molecular computational method by Binkley and Pople [87] in 1975. The basic idea behind perturbation theory is that if we know how to treat a simple (often idealized) system then a more complex (and often more realistic) version of this system, if it is not too different, can be treated mathematically as an altered (perturbed) version of the simple one. Møller-Plesset calculations are denoted as MP, MPPT (Møller-Plesset perturbation theory) or MBPT (many-body perturbation theory) calculations. The derivation of the Møller-Plesset method [88] is somewhat involved, and only the flavor of the approach will be given here. There is a hierarchy of MP energy levels: MP0, MP1 (these first two designations are not actually used), MP2, etc. . . ., which successively account more thoroughly for interelectronic repulsion.

"MP0" would use the electronic energy obtained by simply summing the Hartree-Fock one-electron energies (Sect. 5.2.3.6.4, Eq. (5.84)). This ignores interelectronic repulsion except for refusing to allow more than two electrons in the same spatial MO. "MP1" corresponds to MP0 corrected with the Coulomb and exchange integrals J and K (Eqs. (5.85) and (5.90)), i.e. MP1 is just the Hartree-Fock energy. As we have seen (Sects. 5.2.3.2, 5.2.3.6.2), this handles interelectronic repulsion in an average way. We could write $E_{MP1} = E_{HF}^{total} = E_{MP0} + E^{(1)}$, where E_{MP0} is the sum of one-electron energies and internuclear repulsions and $E^{(1)}$ is the J, K correction (corresponding respectively to the two terms in Eqs. (5.85) and (5.90)), regarding

---

[4]Møller-Plesset: the Danish-Norwegian letter ø is pronounced like French *eu* or German *ö*.

the second term as a kind of perturbational correction to the sum of one-electron energies.

MP2 is the first MP level to go beyond the HF treatment: it is the first "real" Møller-Plesset level. The MP2 energy is the HF energy plus a correction term (a perturbational adjustment) that represents a lowering of energy brought about by allowing the electrons to avoid one another better than in the HF treatment:

$$E_{MP2} = E_{HF}^{total} + E^{(2)} \tag{5.161}$$

The HF term includes internuclear repulsions, and the perturbation correction $E^{(2)}$ is a purely electronic term. $E^{(2)}$ is a sum of terms each of which models the promotion of pairs of electrons. So-called *double excitations* from occupied to formally unoccupied MOs (virtual MOs) are required by Brillouin's theorem [89], which says, essentially, that a wavefunction based on the HF determinant D_1 plus a determinant corresponding to exciting just one electron from D_1 cannot improve the energy.

Let's do an MP2 energy calculation on HHe$^+$, the molecule for which a Hartree-Fock (i.e. an SCF) calculation was shown in detail in Sect. 5.2.3.6.5. As we did for the HF calculation, we will take the internuclear distance as 0.800 Å and use the STO-1G basis set; we can then use for our MP2 calculation these HF results that we obtained in Sect. 5.2.3.6.5:

The MO coefficients:

For the occupied MO $\psi_1, c_{11} = 0.3178, c_{21} = 0.8020$
    Recall that these are respectively the coefficient of basis function 1, ϕ_1, in MO1 and the coefficient of basis function 2, ϕ_2, in MO1. In this simple case there is one function on each atom: ϕ_1 and ϕ_2 on atoms 1 and 2 (H and He).
For the unoccupied (virtual) MO $\psi_2, c_{12} = 1.1114, c_{22} = -0.8325$

The 2-electron repulsion integrals:

$$(11|11) = 0.7283 \qquad (21|21) = 0.2192$$

$$(21|11) = 0.3418 \qquad (22|21) = 0.4368$$

$$(22|11) = 0.5850 \qquad (22|22) = 0.9927$$

The energy levels:

Occupied MO, $\varepsilon_1 = -1.4470$, virtual MO, $\varepsilon_2 = -0.1051$
The HF energy: $E_{HF}^{total} = -2.4438$

The MP2 energy correction for a closed-shell two-electron/two-MO system is [90]:

$$E^{(2)} = \frac{\left[\iint \psi_1(1)\psi(2)\left(\frac{1}{r_{12}}\right)\psi_2(1)\psi(2)dv_1dv_2\right]^2}{2(\varepsilon_1 - \varepsilon_2)} \tag{5.162}$$

Applying this formula "by hand" is straightforward, although the arithmetic is tedious. Nevertheless it is worth doing (as was true for the *Hartree-Fock* calculation in Sect. 5.2.3.6.5) in order to appreciate how much arithmetical work is involved in even this simplest molecular MP2 job. Consider the integral in the numerator of Eq. (5.162); substituting for ψ_1 and ψ_2:

$$\iint \psi_1(1)\psi_1(2)\left(\frac{1}{r_{12}}\right)\psi_2(1)\psi_2(2)dv_1dv_2$$
$$= \iint \left[\left(c_{11}\phi_1(1) + c_{21}\phi_2(1)\right)\left(c_{11}\phi_1(2) + c_{21}\phi_2(2)\right)\left(\frac{1}{r_{12}}\right)\right.$$
$$\left. \times \left(c_{12}\phi_1(1) + c_{22}\phi_2(1)\right)\left(c_{12}\phi_1(2)\right)\right]$$

Multiplying out the integrand gives a total of 16 terms (from 4 terms to the left of $1/r_{12}$ and 4 terms to the right), and leads to a sum of 16 integrals:

$$\iint \psi_1(1)\psi_1(2)\left(\frac{1}{r_{12}}\right)\psi_2(1)\psi_2(2)dv_1dv_2$$
$$= c_{11}^2 c_{12}^2 \int \phi_1(1)\phi_1(2)\left(\frac{1}{r_{12}}\right)\phi_1(1)\phi_1(2)dv_1dv_2 + \cdots + c_{21}^2 c_{22}^2 \int \phi_2(1)\phi_2(2)\left(\frac{1}{r_{12}}\right)$$
$$= c_{11}^2 c_{12}^2 (11|11) + \cdots + c_{21}^2 c_{22}^2 (22|22),$$

recalling the notational degeneracy in the two-electron integrals (Sect. 5.2.3.6.5, "*Step 2* Calculating the integrals"). Substituting the values of the coefficients and the 2-electron integrals:

$$\iint \psi_1(1)\psi_1(2)\left(\frac{1}{r_{12}}\right)\psi_2(1)\psi_2(2)dv_1dv_2$$
$$= 0.12475(0.7283) + \cdots + 0.44577(0.9927)h = 0.12932\,h$$

So from Eq. (5.162)

$$E^{(2)} = \frac{0.12932^2}{2(\varepsilon_1 - \varepsilon_2)}h = \frac{0.12932^2}{2(-1.4470 + 0.1051)}h = -0.00623\,h$$

The MP2 energy is the Hartree-Fock energy plus the MP2 correction (Eq. (5.162)):

$$E_{\text{MP2}} = E_{\text{HF}}^{\text{total}} + E^{(2)} = -2.4438\,\text{h} - 0.00623\,\text{h} = -2.4500\,\text{h}$$

This energy, which includes internuclear repulsion, since $E_{\text{HF}}^{\text{total}}$ includes this (Eq. (5.93)), is the MP2 energy normally printed out at the end of the calculation. To get an intuitive feel for the physical significance of the calculation just performed look again at Eq. (5.162), which applies to any two-electron/two-basis function species. The equation shows that the absolute value (the correction is negative since ε_1 is smaller than ε_2 – the occupied MO has a lower energy than the virtual one) of the correlation correction increases, i.e. the energy decreases, with the magnitude of the integral (which is positive). This integral represents the decrease in energy arising from allowing an electron pair in the occupied MO (ψ_1) to spill over into the virtual MO (ψ_2):

$\psi_1(1)$ represents electron 1 in ψ_1 and $\psi_1(2)$ represents electron 2 in ψ_1.
$\psi_2(1)$ represents electron 1 in ψ_2 and $\psi_2(2)$ represents electron 2 in ψ_2.

The operator $1/r_{12}$ brings in Coulombic interaction: the Coulombic repulsion energy between infinitesimal volume elements $\psi_1(1)\psi_1(2)dv_1$ and $\psi_2(1)\psi_2(2)dv_2$ separated by a distance r_{12} is $(\psi_1(1)\psi_1(2)dv_1)\,(\psi_2(1)\psi_2(2)dv_2)/r_{12}$, and the integral is simply the sum over all such volume elements (cf. the discussion in connection with Fig. 5.3 and the average-field integrals J and K in Sect. 5.2.3.2). Physically, the decrease in energy makes sense: allowing the electrons to be partly in the formally unoccupied virtual MO rather than confining them strictly to the formally occupied MO enables them to avoid one another better than in the HF treatment, which is based on a Slater determinant consisting only of occupied MOs (Sect. 5.2.3.1). *The essence of the Møller-Plesset method* (MP2, MP3, etc.) is that the correction term handles electron correlation by promoting electrons from occupied to unoccupied (virtual) MOs, giving electrons, in some sense, more room to move and thus making it easier for them to avoid one another; the decreased interelectronic repulsion results in a lower electronic energy. The contribution of the "ψ_1/ψ_2 interaction" to $E^{(2)}$ decreases as the occupied/virtual MO gap $\varepsilon_1 - \varepsilon_2$, increases, since this is in the denominator . Physically, this makes sense: the bigger the gap between the occupied and higher-energy virtual MO, the harder it is to promote electrons from the one into the other, so the less can such promotion contribute to electronic stabilization. So in the expression for $E^{(2)}$ (Eq. 5.162), the numerator represents the promotion of electrons from the occupied to the virtual orbital, and the denominator represents a check on how hard it is to do this.

As we just saw, MP2 calculations utilize the Hartree-Fock MOs (their coefficients c and energies ε). The HF method gives the best *occupied* MOs obtainable from a given basis set and a one-determinant total wavefunction $\boldsymbol{\psi}$, but it does not optimize the *virtual* orbitals (after all, in the HF procedure we start with a determinant consisting of only the *occupied* MOs–Sects. 5.2.3.1, 5.2.3.2, 5.2.3.3 and 5.2.3.4). To get a reasonable description of the virtual orbitals and to obtain a reasonable number of them into which to promote electrons, we need a basis set that is not too small. The use of the STO-1G basis in the above example was purely illustrative; the smallest basis set generally considered acceptable for correlated calculations is the 6–31G*, and in fact this is perhaps the one most frequently used

for MP2 calculations. The 6–311G** basis set is also widely used for MP2 and MP4 calculations. Both bases can of course be augmented (Sect. 5.3.3) with diffuse functions. MP2 calculations increase rapidly in complexity with the number of electrons and orbitals, involving as they do a *sum of terms* (rather than just one term as in HHe+), each representing the promotion of an electron pair from an occupied to a virtual orbital; thus an MP2 calculation on CH_2 with the 6–31G* basis involves 8 electrons and 19 MOs (4 occupied and 15 virtual MOs).

In MP2 calculations doubly excited states (doubly excited configurations) interact with the ground state (the integral in Eq. (5.162) involves ψ_1 with electrons 1 and 2, and ψ_2 with electrons 1 and 2). In MP3 calculations doubly excited states interact with one another (there are integrals involving two virtual orbitals). In MP4 calculations singly, doubly, triply and quadruply excited states are involved. MP5 and higher expressions have been developed, but MP2 and MP4 are by far the most popular Møller-Plesset levels (also called MBPT(2) and MBPT(4)–many-body perturbation theory). MP2 calculations, which are much slower than Hartree-Fock, can be speeded up somewhat by specifying MP2(fc), MP2 frozen-core, in contrast to MP2(full); frozen-core means that the core (non-valence electrons) are "frozen", i.e. not promoted into virtual orbitals, in contrast to full MP2 which takes all the electrons into account in summing the contributions of excited states to the lowering of energy. Most programs, e.g. Gaussian, Spartan) perform MP2(fc) by default when MP2 is specified, and "MP2" usually means frozen-core. When seen in this book referring to a specific calculation rather than a general method, it may be taken as shorthand for MP2(fc). MP4 calculations are sometimes done omitting the triply excited terms (MP4SDQ) but the most accurate (and slowest) implementation is MP4SDTQ (singles, doubles, triples, quadruples).

Calculated properties like geometries and relative energies tend to be better (to be closer to the true ones) when done with correlated methods (Sects. 5.5.1, 5.5.2, 5.5.3 and 5.5.4). To save time, energies are sometimes calculated with a correlated method on a Hartree-Fock geometry, rather than carrying out the geometry optimization at the correlated level. This is called a *single-point* calculation (it is performed at a single point on the HF potential energy surface, without changing the geometry). A single-point MP2(fc) calculation using the 6–311G** basis, on a structure that was optimized with the Hartree-Fock method and the 6–31G* basis, is designated as MP2(fc)/6–311G**//HF/6–31G*. A HF/6–31G* (say) geometry optimization, without a subsequent single-point calculation, is sometimes designated HF/6–31G*//HF/6–31G*, and an MP2 optimization MP2/6–31G*//MP2/6–31G*. The correlation treatment (HF, MP2, MP4, …) is often called the *method*, and the basis set (STO-3G, 3–21G$^{(*)}$, 6–31G*, …) the *level*, but we will often find it convenient to let *level* denote the combined procedure of method and basis set, referring, say, to an MP2/6–31G* calculation as being at a higher level than an HF/6–31* one. Actually, thanks to increases in computer speed, nowadays single-point calculations are frequently done not with correlation on a Hartree-Fock geometry, but with higher correlation on a lower-level correlated geometry.

Figure 5.20 shows the rationale behind the use of single-point calculations for obtaining relative energies. In the diagram a single-point MP2 calculation on a stationary point at the HF geometry gives the same energy as would be obtained by
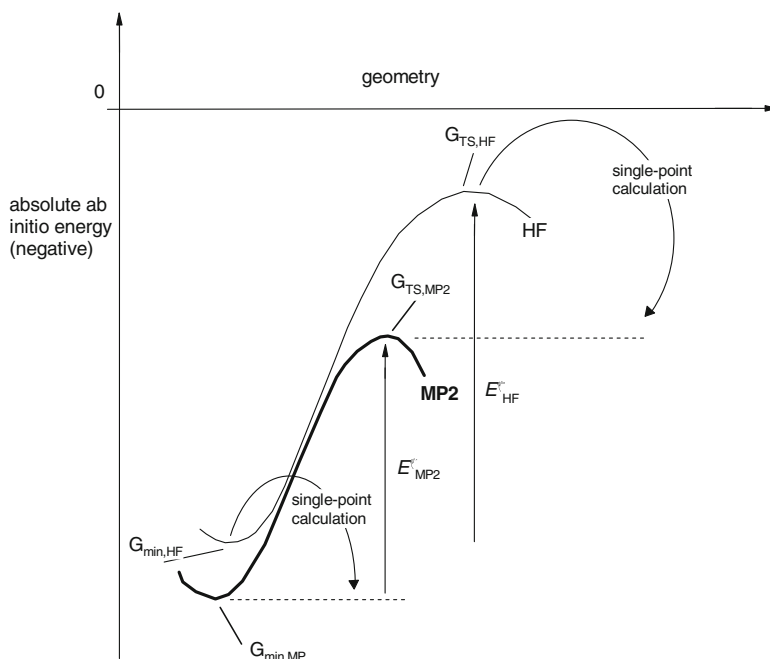
Fig. 5.20 Hartree-Fock and MP2 (or other correlated) potential energy surfaces. "Absolute" (as distinct from relative) ab initio energies are negative, and correlated energies are lower (more negative) than Hartree-Fock energies. The geometries of the minima and the transition states are designated G_{min} and G_{TS}. Activation energies are denoted by $E^{\ddagger}$. HF activation energies are, as shown, usually bigger than MP2. In this diagram a single-point MP2 calculation on a stationary point at the HF geometry gives the same energy as would be obtained by optimizing the species at the MP2 level; this is often true, but single-point MP2 relative energies would be similar to optimized-MP2 relative energies even if it were not so, provided the incremental energy change were about the same for the two species being compared (e.g. reactant and TS for an activation energy, reactant and product for a reaction energy)

optimizing the species at the MP2 level, which is often true (it would be exactly true if the MP2 and HF geometries were identical). For example, the single-point and optimized energies of butanone are -231.68593 h and -231.68818 h, a difference of 0.00225 h (2.3 mh) or 6 kJ mol^{-1}, not large bearing in mind that special high-accuracy calculations (Sect. 5.5.2.2) are needed to reliably get relative energies to within, say, 10 kJ mol^{-1}. Single-point calculations would also give *relative* energies similar to those from the use of optimized correlated geometries if the incremental deviations from the optimized-geometry energies were about the same for the two species being compared (e.g. reactant and TS for an activation energy, reactant and product for a reaction energy).

The method can occasionally give not just quantitatively, but qualitatively wrong results. The HF and correlated surfaces may have different curvatures: for example a minimum on one surface may be a transition state or may not exist (may

not be a stationary point) on another. Thus difluorodiazomethane is a minimum at the HF level but not at the MP2: it dissociates at this level [91]. Nevertheless, because HF optimizations followed by single-point correlated (MP2 or higher-level) energy calculations are much faster ("cheaper") than correlated optimizations, and do usually give improved relative energies, the method is widely used for large molecules. Figure 5.21 compares some MP2 single-point, MP2-optimized, and HF energies; the biggest MP2 single-point/MP2 optimized difference is 6.9 kJ mol^{-1} (HCN reaction energy). The limited salient experimental information on these reactions is given in [92]. Because of the sketchy and uncertain nature of the experimental values, relative enthalpies from CBS-APNO (Sect. 5.5.2.3.2, *Comparison of high-accuracy multistep methods*; see too Chap. 7, Sect. 7.3.2.2.) calculations are given in Fig. 5.21. These are considered to be excellent surrogates for, and likely superior to, any available experimental values. The other relative energies in Fig. 5.21 are 0 K enthalpy differences (with raw energy corrected for ZPE), for uniformity and simplicity, but usually experimental barriers are given as Arrhenius activation energies E_a, which are simply related to enthalpies of activation $\Delta H^{\ddagger}$ (Eq. (5.175)), and the extent of a reaction is quantified as an equilibrium constant which is related (Eq. (5.183)) to a Gibbs free energy difference ΔG_{react} (Sect. 5.5.2.1). Free energies of activation $\Delta G^{\ddagger}$ can be used to calculate rate constants (Sect. 5.5.2.3.4) and enthalpies of reaction ΔH_{react} are often used (not theoretically rigorously) as an indication of the extent and even the ease of a reaction. To give a feel for the quantitative difference in the values of the relative 0 K energies and these five other energy quantities, the calculated values are given below for the four reactions of Fig. 5.21. The 0 K energies are ZPE-corrected MP2/6–31G* energies relative to that of the reactant, and the other energies are at 291 K (standard room temperature) and are also from MP2/6–31G* calculations and employ standard ideal-gas statistical thermodynamics algorithms; energy units are kJ mol^{-1}.

Ethenol to Ethanal

Transition state 0 K relative E $= 233$ Product 0 K relative E $= -71.7$

$$E_a = \Delta H^{\ddagger} + RT = \Delta H^{\ddagger} + 2.48 = 234.3$$

$\Delta H^{\ddagger} = 231.8$
$\Delta G_{\text{react}} = -73.1$
$\Delta G^{\ddagger} = 233.1$
$\Delta H_{\text{react}} = -70.9$
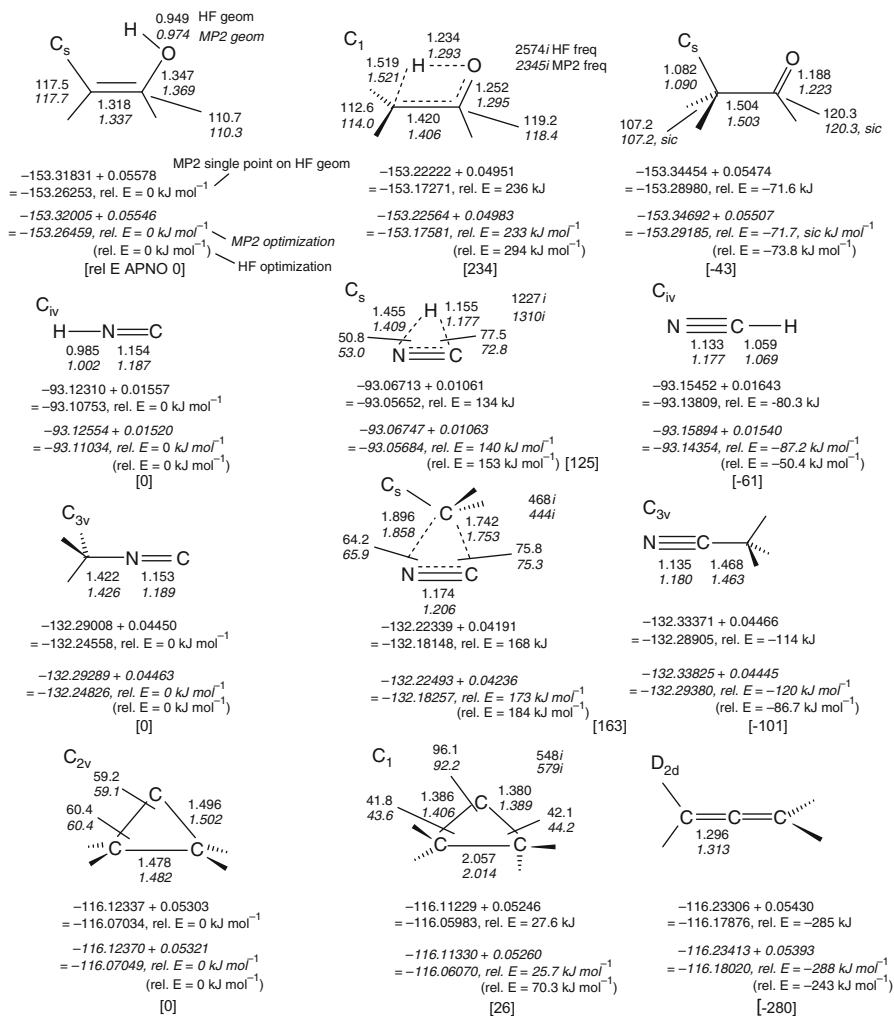
Fig. 5.21 Calculated geometries and energies for four reactions (most H's are omitted, for clarity). One purpose of the Fig. is to compare the single-point energies with energies from optimization at a higher level. Geometries are HF/6–31G* and MP2/6–31G*. Energies are MP2/6–31G*//HF/6–31G* (i.e. single-point) with HF ZPE, MP2/6–31G*//MP2//6–31G* with MP2/6–31G* ZPE, and (only relative energies shown, in parentheses) HF/6–31G*//HF/6–31G* with HF ZPE. Ab initio E (hartrees) + ZPE (hartrees) = corrected ab initio E; relative E (strictly speaking, 0 K enthalpy differences): E differences are hartrees × 2626 = kJ mol^{-1}). The ZPEs shown are the ab initio ZPEs multiplied by 0.9135 (HF) or 0.967 (MP2) [80]. The relative energies in brackets (0, 234, −43; 0, 125, −61; 0, 163, −101; 0, 26, −280) are CBS-APNO energies (see text) and are expected to be excellent surrogates for the skimpy and sometimes uncertain experimental values [92]

HNC to HCN
Transition state 0 K relative E $= 140$ Product 0 K relative E $= -87.2$

$$E_a = \Delta H^{\ddagger} + RT = \Delta H^{\ddagger} + 2.48 = 142.7$$

$\Delta H^{\ddagger} = 140.2$
$\Delta G_{react} = -86.9$
$\Delta G^{\ddagger} = 136.1$
$\Delta H_{react} = -87.8$

CH$_3$NC to CH$_3$CN
Transition state 0 K relative E $= 173$ Product 0 K relative E $= -120$

$$E_a = \Delta H^{\ddagger} + RT = \Delta H^{\ddagger} + 2.48 = 174.0$$

$\Delta H^{\ddagger} = 171.5$
$\Delta G_{react} = -119.3$
$\Delta G^{\ddagger} = 169.2$
$\Delta H_{react} = -120.0$

Cyclopropylidene to Allene
Transition state 0 K relative E $= 25.7$ Product 0 K relative E $= -288$

$$E_a = \Delta H^{\ddagger} + RT = \Delta H^{\ddagger} + 2.48 = 27.8$$

$\Delta H^{\ddagger} = 25.3$
$\Delta G_{react} = -285.1$
$\Delta G^{\ddagger} = 23.9$
$\Delta H_{react} = -285.9$

For these reactions the 0 K activation enthalpy and the room temperature activation enthalpies and free energies are almost the same, and so are the 0 K reaction enthalpy and the room temperature reaction enthalpies and free energies. This is presumably so because these are unimolecular reactions, in which the relative translational velocities of reacting molecules are not a factor.

The HF method tends to overestimate the barriers, making unstable molecules seem stabler than they really are. Geometries are discussed further in Sect. 5.5.1. Approximate versions of the MP2 method that speed up the process with little loss of accuracy are available in some program suites: LMP2, localized MP2, and RI-MP2, resolution of identity MP2. LMP2 starts with a Slater determinant which has been altered so that its MOs are localized, corresponding to our ideas of bonds and lone pairs (Sect. 5.2.3.1), and permits only excitations into spatially nearby virtual orbitals [93]. RI-MP2 [94a,b,c] approximates four-center integrals

(Sect. 5.3.1) by three-center ones. Other variations on MP2 which may not be widely available are MP2[V] [94d], which is said to provide essentially the same results using smaller basis sets, and MP2.5 [94e] which strikes a balance between overestimating (MP2) an underestimating (MP3) noncovalent interactions and thus improves results for thermochemistry and kinetics.

5.4.3 The Configuration Interaction Approach to Electron Correlation. The Coupled Cluster Method

The configuration interaction (CI) treatment of electron correlation [82, 95] is based on the simple idea that one can improve on the HF wavefunction, and hence energy, by adding on to the HF wavefunction terms that represent promotion of electrons from occupied to virtual MOs. The HF term and the additional terms each represent a particular electronic configuration, and the actual wavefunction and electronic structure of the system can be conceptualized as the result of the interaction of these configurations. This electron promotion, which makes it easier for electrons to avoid one another, is as we saw (Sect. 5.4.2) also the physical idea behind the Møller-Plesset method; the MP and CI methods differ in their mathematical approaches.

HF theory (Sects. 5.2.3.1, 5.2.3.2, 5.2.3.3, 5.2.3.4, 5.2.3.5, and 5.2.3.6) starts with a total wavefunction or total MO Ψ which is a Slater determinant made of "component" wavefunctions or MOs ψ. In Sect. 5.2.3.1 we approached HF theory by considering the Slater determinant for a four-electron system:

$$\Psi = \frac{1}{\sqrt{4!}} \begin{vmatrix} \psi_1(1)\alpha(1) & \psi_1(1)\beta(1) & \psi_2(1)\alpha(1) & \psi_2(1)\beta(1) \\ \psi_1(2)\alpha(2) & \psi_1(2)\beta(2) & \psi_2(2)\alpha(2) & \psi_2(2)\beta(2) \\ \psi_1(3)\alpha(3) & \psi_1(3)\beta(3) & \psi_2(3)\alpha(3) & \psi_2(3)\beta(3) \\ \psi_1(4)\alpha(4) & \psi_1(4)\beta(4) & \psi_2(4)\alpha(4) & \psi_2(4)\beta(4) \end{vmatrix} \qquad (5.163 = 5.10)$$

To construct the HF determinant we used only occupied MOs: four electrons require only two spatial "component" MOs, ψ_1 and ψ_2, and for each of these there are two spin orbitals, created by multiplying ψ by one of the spin functions α or β; the resulting four spin orbitals ($\psi_1\alpha, \psi_1\beta, \psi_2\alpha, \psi_2\beta$) are used four times, once with each electron. The determinant Ψ, the HF wavefunction, thus consists of the four lowest-energy spin orbitals; it is the simplest representation of the total wavefunction that is antisymmetric and satisfies the Pauli exclusion principle (Sect. 5.2.2), but as we shall see it is not a complete representation of the total wavefunction.

In the Roothaan-Hall implementation of ab initio theory each "*component*" ψ is composed of a set of basis functions (5.2.3.6):

$$\psi_i = \sum_{s=1}^{m} c_{si}\phi_s \quad i = 1, 2, 3, \cdots, m \text{ (component MOs)} \qquad (5.164 = 5.52)$$

Now note that there is no definite limit to how many basis functions $\phi_1, \phi_2, \ldots$ can be used for our four-electron calculation; although only two spatial ψ's, ψ_1 and ψ_2, (i.e. four *spin* orbitals) are *required* to accommodate the four electrons of this ψ, the total number of ψ's can be greater. Thus for the hypothetical H–H–H–H an STO-3G basis gives four ψ's, a 3–21G basis gives 8, and a 6–31G** basis gives 20 (Sect. 5.3.3). The idea behind CI is that a better total wavefunction, and from this a better energy, results if the electrons are confined not just to the four spin orbitals $\psi_1\alpha, \psi_1\beta, \psi_2\alpha, \psi_2\beta$, but are allowed to roam over all, or at least some, of the virtual spin orbitals $\psi_3\alpha, \psi_3\beta, \psi_4\alpha, \ldots, \psi_m\beta$. To permit this we could write Ψ as a linear combination of determinants

$$\Psi = c_1D_1 + c_2D_2 + c_3D_3 + \cdots + c_iD_i \tag{5.165}$$

where D_1 is the HF determinant of Eq. (5.163) and D_2, D_3, etc. correspond to the promotion of electrons into virtual orbitals, e.g. we might have

$$D_i = \frac{1}{\sqrt{4!}} \begin{vmatrix} \psi_1(1)\alpha(1) & \psi_1(1)\beta(1) & \psi_3(1)\alpha(1) & \psi_2(1)\beta(1) \\ \psi_1(2)\alpha(2) & \psi_1(2)\beta(2) & \psi_3(2)\alpha(2) & \psi_2(2)\beta(2) \\ \psi_1(3)\alpha(3) & \psi_1(3)\beta(3) & \psi_3(3)\alpha(3) & \psi_2(3)\beta(3) \\ \psi_1(4)\alpha(4) & \psi_1(4)\beta(4) & \psi_3(4)\alpha(4) & \psi_2(4)\beta(4) \end{vmatrix} \tag{5.166}$$

D_i was obtained from D_1 by promoting an electron from spin orbital $\psi_2\alpha$ to the spin orbital $\psi_3\alpha$. Another possibility is

$$D_j = \frac{1}{\sqrt{4!}} \begin{vmatrix} \psi_1(1)\alpha(1) & \psi_1(1)\beta(1) & \psi_3(1)\alpha(1) & \psi_3(1)\beta(1) \\ \psi_1(2)\alpha(2) & \psi_1(2)\beta(2) & \psi_3(2)\alpha(2) & \psi_3(2)\beta(2) \\ \psi_1(3)\alpha(3) & \psi_1(3)\beta(3) & \psi_3(3)\alpha(3) & \psi_3(3)\beta(3) \\ \psi_1(4)\alpha(4) & \psi_1(4)\beta(4) & \psi_3(4)\alpha(4) & \psi_3(4)\beta(4) \end{vmatrix} \tag{5.167}$$

Here two electrons have been promoted, from the spin orbitals $\psi_2\alpha$ and $\psi_2\beta$ to $\psi_3\alpha$ and $\psi_3\beta$. D_i and D_j represent promotion into virtual orbitals of one and two electrons, respectively, starting with the HF electronic configuration (Fig. 5.22).

Equation (5.165) is analogous to Eq. (5.164): in (5.164) "component" MOs ψ are expanded in terms of basis functions ϕ, and in (5.165) a total MO Ψ is expanded in terms of determinants, each of which represents a particular electronic configuration. We know that the m basis functions of Eq. (5.164) generate m component MOs ψ (Sect. 5.2.3.6.1), so the i determinants of Eq. (5.165) must generate i total wavefunctions Ψ, and Eq. (5.165) should really be written

$$\begin{aligned} \Psi_1 &= c_{11}D_1 + c_{21}D_2 + c_{31}D_3 + \cdots + c_{i1}D_i \\ \Psi_2 &= c_{12}D_1 + c_{22}D_2 + c_{32}D_3 + \cdots + c_{i2}D_i \\ &\vdots \\ \Psi_i &= c_{1i}D_1 + c_{2i}D_2 + c_{3i}D_3 + \cdots + c_{ii}D_i \end{aligned} \tag{5.168}$$
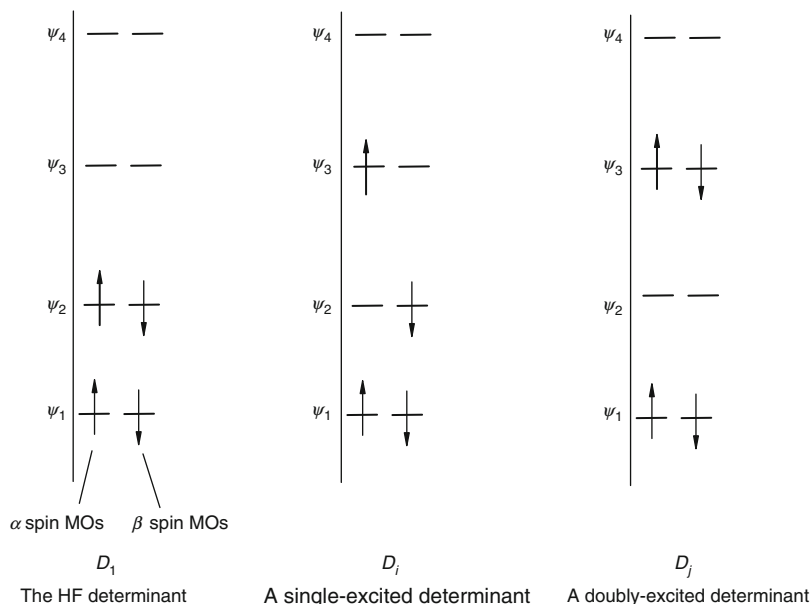
Fig. 5.22 Configuration interaction (CI): promotion of electrons from the occupied MOs (corresponding to the Hartree-Fock determinant) gives determinants corresponding to excited states. A weighted sum of determinants $D_1, D_2, \ldots, D_i, \ldots$, corresponds to a molecule in which the electrons partly populate virtual MOs and are not strictly confined to the lowest-energy MOs, thus giving them a better chance to avoid one another and decreasing electron-electron repulsion. The method generates a series of wavefunctions and energies; the lowest-energy wavefunction and energy corresponds to the ground electronic state, the others to excited states

i.e. (cf. Eq. (5.164))

$$\Psi_i = \sum_{s=1}^{i} c_{si} D_s \quad i = 1, 2, 3, \cdots, i \,(\text{total MOs}) \tag{5.169}$$

What is the physical meaning of all these total wavefunctions Ψ? In order of correspondence to increasing energy (the expectation value of the integral of a wavefunction over a Hamiltonian operator) Ψ_1 is the wavefunction for the ground electronic state and Ψ_2, Ψ_3 etc. represent the wavefunctions of excited electronic states.

The single-determinant HF wavefunction of Eq. (5.163) (or the general single-determinant wavefunction of Eq. (5.12)) is merely an approximation to the Ψ_1 of Eqs. (5.168). Each determinant D (or possibly a linear combination of a few determinants for an open-shell species [96]), represents an idealized (in the sense of contributing to the *real* electron distribution) configuration, called a *configuration state function* (or configuration function), CSF. A CSF is a linear combination of determinants for equivalent states, states which differ only by whether an α or a β

electron was promoted. In many cases one determinant suffices for the Hartree-Fock wavefunction, and then this determinant is the CSF. The CI wavefunctions of Eqs. (5.168) or Eqs. (5.169), then, are linear combinations of CSFs. No single CSF *fully* represents any particular electronic state. Each wavefunction Ψ_i is the total wavefunction of one of the possible electronic states of the molecule, and the weighting factors c in its expansion determine to what extent particular CSF's (idealized electronic states) contribute to any Ψ_i. For Ψ_1, representing the ground electronic state, we expect the HF determinant D_1 to make the largest contribution to the wavefunction.

If every possible idealized electronic state of the system, i.e. every possible determinant D, were included in the expansions of Eqs. (5.168), then the wavefunctions Ψ would be *full CI* wavefunctions. Full CI calculations are possible only for very small molecules, because the promotion of electrons into virtual orbitals can generate a huge number of states unless we have only a few electrons and orbitals. Consider for example a full CI calculation on a very small system, H–H–H–H with the 6–31G* basis set. We have eight basis functions and four electrons, giving eight spatial MOs and 16 spin MOs, of which the lowest four are occupied. There are two α electrons to be promoted into 6 virtual α spin MOs, i.e. to be distributed among 8 α spin MOs, and likewise for the β electrons and β spin orbitals. This can be done in $[8!/(8-2!)2!]^2 = 784$ ways. The number of configuration state functions is about half this number of determinants (since some CSFs are composed of a few determinants). CI calculations with more than five billion (*sic*) CSFs have been performed on ethyne, C_2H_2 [97]; rightly called benchmark calculations, such computational tours de force are, although of limited direct application, important for evaluating the efficacy, by comparison, of other methods.

The simplest implementation of CI is analogous to the Roothaan-Hall implementation of the HF method: Eq. (5.168) lead to a CI matrix, as the HF equations (Eq. (5.164)) lead to a HF matrix (Fock matrix; Sect. 5.2.3.6). Do not confuse a matrix with a determinant (Chap. 4, 4.3.3)! We saw that the Fock matrix $\mathbf{F}$ can be calculated from the c's and ϕ's of Eq. (5.164) (starting with a "guess" of the c's), and that $\mathbf{F}$ (after transformation to an orthogonalized matrix $\mathbf{F}'$ and diagonalization) gives eigenvalues ε and eigenvectors c, i.e. $\mathbf{F}$ leads to the energy levels and the wavefunctions ($c\phi$) of the component MOs ψ; all this was shown in detail in Sect. 5.2.3.6.5. Similarly, a CI matrix can be calculated in which the determinants D play the role that the basis functions ϕ play in the Fock matrix, since the D's in Eq. (5.168) correspond mathematically to the ϕ's in Eq. (5.164)). The D's are composed of spin orbitals $\psi\alpha$ and $\psi\beta$, and the spin factors can be integrated out, reducing the elements of the CI matrix to expressions involving the basis functions and the coefficients of the spatial component MOs ψ. The CI matrix can thus be calculated from the MOs resulting from an HF calculation. Orthogonalization and diagonalization of the CI matrix gives the energies and the wavefunctions of the ground state Ψ_1 and, from i determinants, $i-1$ excited states. A full CI matrix would give the energies and wavefunctions of the ground state and all the excited states obtainable from the basis set being used. Full CI with an infinitely large basis set would give the exact energies of all the electronic states; more realistically, full CI with a large basis set gives good energies for the ground and many excited states.

Full CI is out of the question for any but small molecules, and the expansion of Eq. (5.169) must usually be limited by including only the most important terms. Which terms can be neglected depends partly on the purpose of the calculation. For example, in calculating the ground state energy quadruply excited states are, unexpectedly, much more important than triply and singly excited ones, but the latter are usually included too because they affect the electron distribution of the ground state, and in calculating excited state energies single excitations are important. A CI calculation in which all the D's involve only single excitations is called CIS (CI singles); such a calculation yields the energies and wavefunctions of excited states and often gives a reasonable account of electronic spectra. Another common kind of CI calculation is CI singles and doubles (CISD, which actually indirectly includes triply and quadruply excited states). Various mathematical devices have been developed to make CI calculations recover a good deal of the correlation energy despite the necessity of (judicious) truncation of the CI expansion. Probably the currently most widely-used implementations of CI are *multiconfigurational SCF* (MCSCF) and its variant *complete active space SCF* (CASSCF), and the *coupled-cluster* (CC) method.

The CI strict analogue of the iterative refinement of the coefficients that we saw in HF calculations (Sect. 5.2.3.6.5) would refine just the weighting factors of the determinants (the c's of Eqs. (5.168)), but in the MCSCF version of CI the spatial MOs *within* the determinants are also optimized (by optimizing the c's of the LCAO expansion, Eq. (5.164)). A widely-used version of the MCSCF method is the CASSCF method, in which one carefully chooses the orbitals to be used in forming the various CI determinants. These *active orbitals*, which constitute the *active space*, are the MOs that one considers to be most important for the process under study. Thus for a Diels-Alder reaction, the two π and two π* MOs of the diene and the π and π* MO of the alkene (the dienophile) would be a reasonable minimum as candidates for the active space of the reactants [98a]; the six electrons in these MOs would be the *active electrons*, and with the 6–31G* basis this would be a (specifying electrons, MOs) CASSCF (6,6)/6–31G* calculation. CASSCF calculations are used to study chemical reactions and to calculate electronic spectra. They require judgement in the proper choice of the active space and are not essentially automatic algorithms like other methods [98b]. Approaches that make possible the use of active spaces much bigger than those in conventional CASSCF are being explored [99].

An extension of the MCSCF method is multireference CI (MRCI), in which the determinants (the CSFs) from an MCSCF calculation are used to generate still more determinants, by promoting electrons in them into virtual orbitals (multireference, since the final wavefunction "refers back" to several, not just one, determinant). A "fast, robust and versatile code for accurate multireference computations", BALOO, is said to be much faster than conventional codes for multireference calculations [100].

Just as HF geometries can be subjected to MPn (commonly MP2) single-point calculations to account for dynamic correlation and obtain better relative energies, geometries from CASSCF calculations, which are commonly used to take static

correlation into account, can be subjected to (usually single-point) perturbational calculations to account for *dynamic* correlation. The most reliable and widely-used of these "post-CAS") methods is the CASPT2N (complete active space perturbational treatment second order, a kind of analogue of MP2) [101].

The *coupled cluster* (CC) method is related to both the perturbation (Sect. 5.4.2) and the CI approaches (Sect. 5.4.3). Like perturbation theory, CC theory is connected to the linked cluster theorem (linked diagram theorem) [102], which proves that MP calculations are size-consistent (see below). Like standard CI it expresses the correlated wavefunction as a sum of the HF ground state determinant and determinants representing the promotion of electrons from this into virtual MOs. As with the Møller-Plesset equations, the derivation of the CC equations is complicated. The basic idea is to express the correlated wavefunction Ψ as a sum of determinants by allowing a series of operators $\hat{T}_1, \hat{T}_2, \cdots$, to act on the HF wavefunction:

$$\Psi = \left(1 + \hat{T} + \frac{\hat{T}^2}{2!} + \frac{\hat{T}^3}{3!} + \cdots \right) \Psi_{HF} = e^{\hat{T}} \Psi_{HF} \qquad (5.170)$$

where $\hat{T} = \hat{T}_1 + \hat{T}_2 + \cdots$. The operators $\hat{T}_1, \hat{T}_2, \cdots$ are *excitation operators* and have the effect of promoting one, two, etc., respectively, electrons into virtual spin orbitals. Depending on how many terms are actually included in the summation for $\hat{T}$, one obtains the *coupled cluster doubles* (CCD), *coupled cluster singles and doubles* (CCSD) or *coupled cluster singles, doubles and triples* (CCSDT) method:

$$\hat{T}_{CCD} = e^{\hat{T}_2} \Psi_{HF}$$
$$\hat{T}_{CCSD} = e^{\left(\hat{T}_1 + \hat{T}_2 \right)} \Psi_{HF}$$
$$\hat{T}_{CCSDT} = e^{\left(\hat{T}_1 + \hat{T}_2, \hat{T}_3 \right)} \Psi_{HF}$$

CCSDT calculations are very demanding except for very small systems, and a compromise often used is CCSD(T) (note the parentheses), coupled cluster singles and doubles with approximate triples (or perturbative triples). The *quadratic configuration interaction* method, QCI, is very similar to the CC method. QCISD(T) (quadratic CI singles, doubles, with approximate triples) has been largely replaced by the CCSD(T) method, which is usually only moderately slower than QCISD(T), and is more reliable [103]. CCSD(T) calculations are, generally speaking, the current benchmark for practical molecular calculations on molecules of up to moderate size.

Like MP methods, CI and CC methods require reasonably large basis sets for good results. The smallest basis used with these methods is the 6–31G*, but where practical the 6–311G** basis, developed especially for post-HF calculations, might be preferable (see Table 5.6). The energies by themselves mean little: it is energy *differences*, corresponding to a chemical (or conformational) change that counts.

Table 5.6 Energies and times for some calculations on acetone involving electron correlation; a HF job is shown for comparison

Method/basis	Input geometry	Energy	Time, sec.
HF/6–31G* opt + freq	AM1	−191.962236	19
MP2/6–31G* opt + freq	AM1	−192.523905	41
MP2/6–311G** opt + freq	AM1	−192.647954	142
CCSD(T)/6–31G* single point	MP2/6–311G**	−192.577986	21
CCSD(T)/6–311G** single point	MP2/6–311G**	−192.707241	58

The calculations were done with the G09 program suite on a computer with a 64-bit 3.40 GHz Intel Core 2 Duo Quad CPU, 16 GB RAM, and 1.8 TB diskspace, running under Windows 7. They reflect the times for these methods on a well-equipped personal computer as of ca. mid-2013. Energies here are those immediately following the optimization (or single point calculation), before the frequency calculation, i.e. without ZPE, but times are for optimization + frequency where frequencies were requested. A lower absolute energy does not guarantee that a method/basis will give a more accurate activation or reaction energy, as these latter two are energy *differences*, not absolute energies. MP2 was the usual MP2(fc). Methods are given in order of the increasing thoroughness with which they might be expected to treat electron correlation. Note that none of the correlation methods is variational: they can give an energy lower than the true energy

Higher-correlated single-point calculations on MP2 geometries tend to give more reliable relative energies than do MP2 single-point calculations on HF geometries (Sect. 5.4.2, in connection with Figs. 5.20 and 5.21). There is some limited evidence that *when a correlation method is already being used*, one tends to get improved geometries if the next step is to use a bigger basis set rather than to go to a yet higher correlation level [104]. Figure 5.21 shows the results of HF and MP2 methods applied to chemical reactions. The limitations and advantages of numerous such methods are shown in a practical way in the Gaussian 94 workbook by Foresman and Frisch [1e]. Energies and times for a Hartree-Fock level and some correlated calculations are given in Table 5.6.

A big advance in coupled-cluster implementation is the domain-based local pair natural orbital coupled cluster method with single, double and perturbative triple excitations (DLPNO-CCSD(T)), which is based on local pair natural orbital (LPNO), localized, rather than canonical, Slater determinants (Sect. 5.2.3.1) [105a]. This approach is largely associated with the group of Neese. It is said to give energies nearly as good (within 1 kJ mol^{-1} with the Tight setting) as those from conventional CCSD(T) at a "cost" (i.e. time) "Many orders of magnitude" less, and scales nearly linearly with system size. This paper [105a] showed that DLPNO-CCSD(T) was more accurate than any of the DFT functionals (Chap. 7) tested against it and concluded that "coupled cluster energies can indeed be obtained at near DFT cost". Anticipating Chap. 7, we note that modern DFT is, broadly speaking, more accurate than Hartree-Fock and roughly as fast, but that unlike HF it lacks a satisfying theoretical transparency. In contrast, conventional CCSD(T) is very accurate but much slower than DFT. So DLPNO-CCSD(T) promises the theoretical rigor of ab initio with the speed of DFT. These methods are available in the program ORCA (ORCA is cited in Chap. 9). DLPNO-CCSD(T)

made possible a CC-level calculation (albeit single point) on the protein crambin, with 644 atoms, 6187 basis functions [105b]. Another recent modification of conventional CCSD(T) based on local orbitals is the divide-expand-consolidate model, DEC-CCSD(T), which does not seem to offer increased speed but does scale linearly [105c].

5.4.3.1   Size-Consistency

Two factors that should be mentioned in connection with post-HF calculations are the questions of whether a method is *size-consistent* and whether it is *variational*. A method is size-consistent if it gives the energy of a collection of n widely-separated atoms or molecules as being n times the energy of one of them. For example, the HF method gives the energy of two water molecules 20 Å apart (considered as a single system, i.e. a "supermolecule") as being twice the energy of one water molecule. The example below gives the result of HF/3–21G$^{(*)}$ geometry optimizations on a water molecule, and on two water molecules at increasing distances (with the two-H_2O supermolecule the O/H internuclear distance r was held constant at 10, 15. . .Å while all the other geometric parameters were optimized):
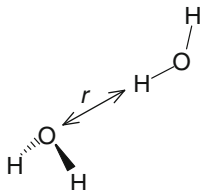
Energy of $H_2O = -75.58596$
$2 \times$ Energy or $H_2O = -151.17192$
Energy of $(H_2O)_2 = -151.17206$, at $r = 10$ Å
Energy of $(H_2O)_2 = -151.17196$, at $r = 15$ Å
Energy of $(H_2O)_2 = -151.17194$, at $r = 20$ Å
Energy of $(H_2O)_2 = -151.17193$, at $r = 25$ Å
Energy of $(H_2O)_2 = -151.17193$, at $r = 30$ Å

   As the two water molecules are separated any stabilizing intermolecular interactions tend to zero and the energy rises, levelling off at 20–25 Å to twice the energy of one water molecule. With the HF method we find that for any number n of molecules M, at large separation the energy of a "noninteracting supermolecule" $(M)_n$ equals n times the energy of one M. The HF method is thus size-consistent. We might say that a size-consistent method is one that scales with the number of species in a way that makes sense.
   Now, it is hard to see why, *physically*, the energy of n identical molecules so widely-separated that they cannot affect one another should *not* be n times the

energy of one molecule. Any *mathematical* method that does not mimic this physical behaviour would seem to have a conceptual flaw, and in fact lack of size-consistency also places limits on the utility of the computational method. For instance, in trying to study the hydrogen-bonded water dimer we would not be able to equate the decrease in energy (compared to twice the energy of one molecule) with stabilization due to hydrogen bonding, and it is unclear how we could computationally turn off hydrogen bonding and evaluate the size-consistency error separately (actually, there is a separate problem, basis set superposition error–see below–with species like the water dimer, but this source of error can be dealt with). It might seem that any computational method must be size-consistent (why shouldn't the energy of a large-separation $(M)_n$ come out at n times that of M?). However, it is not hard to show that CI is not size-consistent unless Eqs. (5.168) include all possible determinants, i.e. unless it is *full* CI. Consider a CISD calculation with a very large ("infinite") basis set on two helium atoms which are separated by a large ("infinite"; say ca. 20 Å) distance, and are therefore non-interacting. Note that although helium atoms do not form covalent He_2 molecules, at short distances they *do* interact to form van der Waals molecules. The wavefunction for this four-electron system will contain, besides the HF determinant, only determinants with single and double excitations (because we are using CI *SD*). Lacking the triple and quadruple excitations which are possible in principle for a four-electron system, it is not a full CI calculation, and so it will not yield the exact, full-CI energy of our noninteracting He-He system, which logically must be twice the full-CI energy one helium atom; instead it will yield a higher energy. Now, a CISD calculation with an infinite basis set on a *single* He atom *will* give the exact wavefunction, and thus the exact energy of the atom (because only single and double promotions are possible for a two-electron system, this is a full CI calculation). Thus in this CISD calculation, the energy of the infinitely-separated He–He system is not, as it "should" be, twice the energy of a single He atom. This conclusion holds for any CI calculation which does not confer full "upward mobility" on all the electrons.

5.4.3.2   Variational Behavior

The other factor to be discussed in connection with post-HF calculations is whether a particular method is *variational*. A method is variational (see the variation theorem, Sect. 5.2.3.3) if any energy calculated from it is not less than the true energy of the electronic state and system in question, i.e. if the calculated energy is an *upper bound* to the true energy. Using a variational method, as the basis set size is increased we get lower and lower energies, levelling off above the true energy (or at the true energy in the unlikely case that our method treats perfectly electron correlation, relativistic effects, and any other minor effects). Figure 5.18 shows that the calculated energy of H_2 using the HF method approaches a limit (-1.133 h) with increasingly large basis sets. The calculated energy can be lowered by using a

correlated method and an adequate basis: full CI with the very big 6–311++G (3df,3p2d) basis gives -1.17288 h, only 4.0 kJ mol^{-1} (small compared with the H–H bond energy of 435 kJ mol^{-1}) above the accepted exact energy of -1.17439 h (Fig. 5.18). Variational behavior is helpful because it serves as a guide to the quality of our wavefunction–the lower the energy the better the function.

If we can't have both, it is more important for a method to be size-consistent than variational. Of the methods we have seen in this book:

Hartree-Fock is size-consistent and variational.

MP (MP2, MP3, MP4, etc.) is size-consistent but not variational.

Full CI, including its full MCSCF and MRCI variants, are size-consistent and variational.

Straightforward truncated CI (CIS, CISD, etc.) is not size-consistent but is variational.

CASSCF, a kind of truncated CI, can be size-consistent: if the active space is chosen properly so that the MOs correspond throughout the process being examined. CASSCF is not variational.

CC (e.g. CCSD, CCSD(T), CCSDT) and its QCI variants (e.g. QCISD, QCISD(T), QCISDT) are size-consistent but not variational.

We could use one of the size-consistent methods to compare the energies of, say, water and the water dimer, but only with HF or full CI can we be *sure* that the calculated energy is an upper bound to the exact energy, i.e. that the exact energy is really lower than the calculated (only a very high correlation level and big basis set are likely to give essentially the *exact* energy; see Sect. 5.5.2). There is however another thing to consider in connection the energy of water compared to its dimer, and similar problems: basis set superposition error, below.

5.4.3.3 Basis Set Superposition Error, BSSE

This is not associated with a particular method, like HF or CI, but rather is a basis set problem. Consider what happens when we compare the energy of the hydrogen-bonded water dimer with that of two noninteracting water molecules. Here is the result of an MP2(fc)/6–31G* calculation; both structures were geometry-optimized, and the energies are corrected for ZPE:

Energy of H2O $= -76.27547$ h
$2 \times$ Energy of $H_2O = -152.55094$ h
Energy of H_2O dimer $= -152.55658$ h
$(2 \times$ Energy of $H_2O) - ($Energy of H_2O dimer$)$
$= -152.55094 - (-152.55658)$ h $= 0.00564$ h $= 14.8$ kJ mol^{-1}

The straightforward conclusion is that at the MP2(fc)/6–31G* level the dimer is stabler than two noninteracting water molecules by 14.8 kJ mol^{-1}. If there are no other significant intermolecular forces, then we might say the H-bond energy in the water dimer [106] is 14.8 kJ mol^{-1} (that it takes this energy to break the bond–to

separate the dimer into noninteracting water molecules). Unfortunately there is a problem with using this simple subtraction approach to compare the energy of a weak molecular association AB with the energy of A plus the energy of B. If we do this we are assuming that if there were no interactions at all between A and B at the geometry of the AB species, then the AB energy would be that of isolated A plus that of isolated B. The problem is that when we do a calculation on the AB species (say the dimer $HOH\cdots OH_2$), in this "supermolecule" the basis functions ("atomic orbitals") of B are available to A so A in AB has a bigger basis set than does isolated A; likewise B has a bigger basis than isolated B. In AB each of the two components can borrow basis functions from the other. The error arises from "imposing" (superimposing) B's basis set upon A and vice versa, hence the name basis set superposition error. Because of BSSE the separated species A and B are not being fairly compared with AB, which has an unfair basis set advantage. We should use for the energies of separated A and of B lower, "better" values than we get in the absence of the borrowed functions available in the weak complex. Accounting for BSSE will thus give a smaller energy drop on AB formation. Treated properly, the value for the hydrogen bond energy (or van der Waals' energy, or dipole-dipole attraction energy, or whatever weak interaction is being studied) will be less than if BSSE were ignored.

There are two ways to deal with BSSE. One is to say, as we implied above, that we should really compare the energy of AB with that of A with the extra basis functions provided by B, plus the energy of B with the extra basis functions provided by A. This method of correcting the energies of A and B with extra functions is called the *counterpoise method* [107], presumably because it balances (counterpoises) functions in A and B against functions in AB. In the counterpoise method the calculations on the components A and B of AB are done with *ghost orbitals*, which are basis functions ("atomic orbitals") not accompanied by atoms (spirits without bodies, one might say): one specifies for A, at the positions that *would* be occupied by the various atoms of B in AB, atoms of zero atomic number bearing the same basis functions as the real atoms of B. This way there is no effect of atomic nuclei or extra electrons on A, just the availability of B's basis functions. Likewise one uses ghost orbitals of A on B. A detailed description of the use of ghost orbitals in Gaussian 82 was given by Clark [107a] (the actual implementation of BSSE in Gaussian has changed since then). The counterpoise correction is rarely applied to anything other than *weakly-bound* dimers, like hydrogen-bonded and van der Waals species: strangely, the correction *worsens* calculated atomization energies (e.g. covalent $AB \rightarrow A + B$), and it is has been said to be not uniquely defined for species of more than two components [107b]; however, see calculations on a ternary complex, ethene-water-ethene [107c]. A review of criticisms and a defence of the counterpoise method is given in [107d], and the controversy continues with fairly recent rejection of the validity of the method from a study of Be_2 [107e]. Until the situation is clearer one might best report results for weakly-bound dimers with and without the counterpoise correction, and, where possible, from the use of very large basis sets (below).

The second way one might handle BSSE is to swamp it with basis functions. If each fragment A and B is endowed with a very big basis set, then extra functions from the other fragment won't alter the energy much–the energy will already be near the asymptotic limit. So if one simply carries out a calculation on A, B and AB with a sufficiently big basis, the straightforward procedure of subtracting the energy of AB from that of A + B should give a stabilization energy essentially free of BSSE. Nevertheless, the counterpoise method is the standard way of overcoming BSSE. The best *experimental* estimate of the binding enthalpy of the water dimer was said to be -13.4 kJ mol^{-1} (-3.2 ± 0.5 kcal mol^{-1}) [106c]; this is the enthalpy, at room-temperature, 298 K, of the dimer minus twice the enthalpy of the monomer. Here are four calculated values of this binding enthalpy, *without* the BSSE correction; hartrees are converted to kJ mol^{-1} by multiplying by 2626:

CBS-Q, a high-accuracy multistep method with correlation energy correction and large basis sets (Sect. 5.5.2.3.2)

$$-152.67093 - (-152.66546) = -0.00547 = -14.4 \text{ kJ},$$
$$\text{MP2/6} - 311 + +\text{G(3df, 3pd)}$$
$$-152.60355 - (-152.59780) = -0.00575 = -15.1 \text{ kJ},$$
$$\text{MP2/6} - 31\text{G}^*$$
$$-152.35198 - (-152.34318) = -0.00880 = -23.1 \text{ kJ},$$
$$\text{HF/6} - 311 + +\text{G(3df, 3pd)}$$
$$-152.06881 - (-152.06510) = -0.00371 = -9.74 \text{ kJ},$$
$$\text{HF/6} - 31\text{G}^*$$
$$-151.97417 - (-151.96798) = -0.00619 = -16.3 \text{ kJ}$$

The correlation-correction/large basis CBS-Q calculation gives a binding enthalpy -14.4 kJ mol^{-1} not too far from the experimental -13.4 kJ mol^{-1} and the MP2 method with the very big MP2/6–311++G(3df,3pd) basis gives a slightly worse deviation, while with MP2 and a smaller basis the binding value is still worse. This is in accord with the above assertion that accounting for BSSE will give a smaller energy drop than without it, i.e. that non-counterpoise calculations give the bigger energy drop. However one should add "other things being equal": with the Hartree-Fock method, the smaller basis (6–31G*) actually gives a *smaller* enthalpy drop (9.74 kJ mol^{-1}) than the ca. 13 kJ mol^{-1} decrease expected from a good counterpoise calculation (and the binding enthalpy is, coincidentally, slightly better estimated than with HF/6–311++G(3df,3pd)). Presumably the somewhat erratic results at the HF level are due to neglect of dynamic correlation (Sect. 5.4.1).

The water dimer has been examined in detail with the accent on density functional (Chap. 7) methods [108a], and with ab initio as well as DFT in counterpoise calculations on it [108b]. Using large basis sets and high correlation levels to get high-quality *atomization energies* (which are of course not of a weak interaction type, and which the counterpoise correction is said to worsen [107b]) is explained

in the book by Foresman and Frisch [1e]. BSSE may also be significant *intramolecularly*; for attempts to treat this and weak interactions in general (dispersion forces) within density functional theory see Chap. 7, Sect. 7.2.3.4.8. Less effort seems to have been expended on grappling with dispersion by ab initio, rather than by DFT, methods. Conrad and Gordon describe a method with an empirical DFT dispersion correction to $\pi - \pi$ interactions at the Hartree-Fock level [109a], and in a somewhat similar vein Goldey et al. supplemented MP2 with DFT and parameters from high-level ab initio databases of noncovalent interactions [109b]. Accurate purely ab initio (no empirical or DFT assistance) calculation of noncovalent interaction energies (which includes dispersion) requires high-level correlation methods, which nowadays means some form of coupled-cluster calculations, and may only now be becoming practical for other than very small molecules. See for example Řezáč et al., including e.g. benzene-trifluoroiodomethane [109c]; for very elaborate calculations on the hydrogen fluoride dimer, see Řezáč and Hobza [109d]. At the other end of the computational effort scale, some molecular mechanics forcefields were better than semiempirical methods (Chap. 6; albeit not ab initio) in reproducing dispersion in the benzene dimer [109e]. Energy calculations are discussed further in Sect. 5.5.2.

5.5 Applications of The Ab initio Method

An extremely useful book by Hehre [39] discusses critically the merits of various computational levels (ab initio and others) for calculating molecular properties, and contains a wealth of information, admonitory and tabular, on this general subject.

5.5.1 Geometries

It is probably the case that the two parameters most frequently sought from ab initio calculations (and most semiempirical and DFT calculations too) are geometries and (Sect. 5.5.2) energies, although this is not to say that other quantities, like vibrational frequencies (Sect. 5.5.3) and parameters arising from electron distribution (Sect. 5.5.4) are unimportant. Molecular geometries are important: they can reveal subtle effects of theoretical importance, and in designing new materials and, particularly, new drugs [110] the shapes of the candidates for particular roles should be known with reasonable accuracy–for example, docking a putative drug into the active site of an enzyme requires that we know the shape of the drug and the active site. While the creation of new pharmaceuticals or materials can be realized with the aid of molecular mechanics (Chap. 3) or semiempirical methods (Chap. 6), the increasingly facile application of ab initio techniques to large molecules makes it likely that this method will play a more important role in such utilitarian pursuits. Novel molecules of theoretical interest can be studied reliably only by ab initio

methods, or possibly by density functional theory (Chap. 7), which is closer in theoretical tenor to the ab initio, rather than semiempirical, approach. The theory behind geometry optimizations was outlined in Chap. 2, Sect. 2.4, and some mention has been made of the suitableness of different basis sets and correlation methods for optimizations. Extensive discussions of the virtues and shortcomings of various ab initio levels for calculating geometries can be found in references [1e], [1g] and [39].

Molecular geometries or structures refer to the bond lengths, bond angles, and dihedral angles that are defined by two, three and four, respectively, *atomic nuclei*. In speaking of the distance, say, between two "atoms" we really mean the *internuclear* distance, unless we are considering nonbonded interactions, when we might also wish to examine the separation of the van der Waals surfaces. In comparing calculated and experimental structures we must remember that calculated geometries correspond to a fictional frozen-nuclei molecule, one with no zero-point energy (Sect. 5.2.3.6.4), while experimental geometries are averaged over the amplitudes of the various vibrations [111a]. Furthermore, different methods measure somewhat different things. The most widely-used experimental methods for finding geometric parameters are X-ray diffraction, electron diffraction and microwave spectroscopy. X-ray diffraction determines geometries in a crystal lattice, where they may be somewhat different from in the gas phase to which ab initio reactions usually apply (although structures and energies can be calculated taking solvent effects into account; see Refs. [1a, e, f, i, k, l]. X-ray diffraction depends on the scattering of photons by the electrons around nuclei, while electron diffraction depends on the scattering of electrons by the nuclei, and microwave spectroscopy measures rotational energy levels, which depend on nuclear positions. Neutron diffraction, which is less used than these three methods, depends on scattering by atomic nuclei.

The main differences are between X-ray diffraction (which probes nuclear positions via electron location) on the one hand and electron diffraction, microwave spectroscopy and neutron diffraction (which probe nuclear positions more directly), on the other hand. The differences result from (1) the fact that X-ray diffraction measures distances between *mean* nuclear positions, while the other methods measure essentially *average* distances, and (2) from errors in internuclear distances caused by the nonisotropic (uneven) electron distribution around atoms. The mean vs. average distinction is illustrated here:
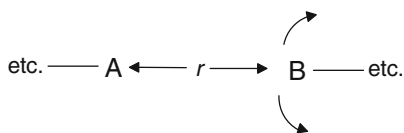
Suppose that nucleus A is fixed and nucleus B is vibrating in an arc as indicated. The distance between the mean positions is r (shown), but on the average B is further away than r.

Differences resulting from nonisotropic electron distribution are significant only for H=X bond lengths: X-rays see electrons rather than nuclei, and the simplest inference of a nuclear position is to place it at the center of a sphere whose surface is defined by the electron density around it. However, since a hydrogen atom has only one electron, for a bonded hydrogen there is relatively little electron density left over from covalent sharing to blanket the nucleus, and so the proton, unlike other nuclei, is *not* essentially at the center of an approximate sphere defined by its surrounding electron density:

H———X

actual position of proton

position inferred from supposing it to be at center of sphere defined by electron density around proton i.e. X-ray-inferred position

X nucleus
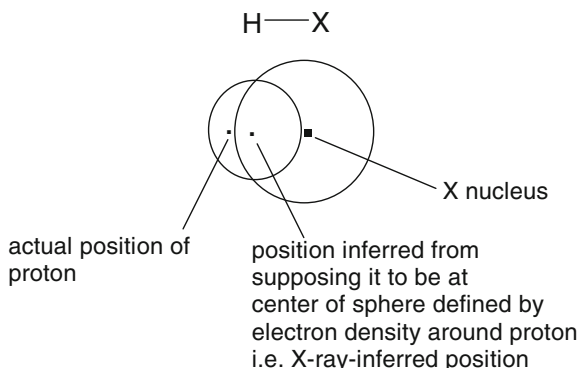
Clearly, the X-ray-inferred H–X distance will be less than the actual internuclear distance measured by electron diffraction, neutron diffraction, or microwave spectroscopy, methods which see nuclei rather than electrons. These and other sources of error that can arise in experimental bond length measurements (like bond length, bond angles and dihedral angles will obviously also depend on nuclear positions) are detailed by Burkert and Allinger [111b], who mention nine (!) kinds of internuclear distance r, and a comprehensive reference to the techniques of structure determination may be found in the book edited by Domenicano and Hargittai [112]. Despite all these problems with defining and measuring molecular geometry we will adopt the position that it is meaningful to speak of experimental geometries to within 0.01 Å or better for bond lengths, and to within 0.5° for bond angles and dihedrals [113].

Let's briefly compare HF/3–21G$^{(*)}$, HF/6–31G* and MP2/6–31G* geometries. Figure 5.23 gives bond lengths and angles calculated at these three levels and experimental bond lengths and angles, for 20 molecules. The geometries shown in Fig. 5.23 are analyzed in Table 5.7, and Table 5.8 provides information on dihedral angles in eight molecules. There should be little difference between MP2 (full) geometries and the MP2(fc) geometries used here. This (admittedly limited) survey suggests that:

HF/3–21G$^{(*)}$ geometries are almost as good as HF/6–31G* geometries.
MP2/6–31G* geometries are on the whole slightly but significantly better than HF/6–31G* geometries, although individual MP2 parameters are *sometimes* a bit worse.

Fig. 5.23 A comparison of some HF/3–21G$^{(*)}$, HF/6–31G* and MP2(fc)/6–31G* geometries. Calculations are by the author and experimental geometries are from Ref. [1g]. Note that all CH bonds are ca. 1 Å, all other bonds range from ca. 1.2–1.8 Å, and all bond angles (except for linear molecules) are ca. 90–120°

HF/3–21G$^{(*)}$ and HF/6–31G* C–H bond lengths are consistently slightly (ca. 0.01–0.03 and ca. 0.01 Å, respectively) shorter than experimental, while MP2/6–31G* C-H bond lengths are not systematically over- or underestimated.

HF/6–31G* O-H bonds are consistently slightly (ca. 0.01 Å) shorter than experimental, while MP2/6–31G* O-H bond lengths are consistently slightly (ca. 0.01 Å) longer. HF/3–21G$^{(*)}$ O-H bond lengths are not consistently over- or underestimated.

Table 5.7 Errors in HF/3–21G$^{(*)}$, HF/6–31G*, and MP2(fc)/6–31G* bond lengths and angles, from Fig. 5.23

C–H	O–H, N–H, S–H	C–C	C–O, N, F, Cl, S	Angles
MeOH −0.015/−0.013/−0.004 −0.009/−0.006/0.003	H$_2$O 0.009/−0.010/0.011	Me$_2$CO 0.008/0.007/0.006	MeOH 0.020/−0.021/0.004	H$_2$O (HOH) 3.2/1.0/−0.6
HCHO −0.033/−0.024/−0.012	H$_2$O$_2$ 0.005/−0.016/0.011	CH$_3$CH$_3$ 0.011/−0.010/−0.003	HCHO −0.001/−0.024/0.013	H$_2$O$_2$ (HOO) −0.5/2.1/−1.4
MeF −0.021/−0.018/−0.008	MeOH 0.003/−0.017/0.007	CH$_2$CH$_2$ −0.024/−0.022/−0.002	MeF 0.021/−0.018/0.008	MeOH (HCO) −0.9/0.0/−0.9 (COH) 2.3/1.4/−0.6
HCN −0.015/−0.006/0.004	HOF 0.010/−0.014/0.013	HCCH −0.015/−0.017/0.015	HCN −0.016/−0.020/0.024	HCHO (HCH) −1.6/−0.8/−0.9
MeNH$_2$ −0.009/−0.008/0.001 −0.016/−0.015/−0.007	MeNH$_2$ −0.007/−0.008/0.008	CH$_3$CH$_2$CH$_3$ 0.015/0.002/0.000	MeNH$_2$ 0.000/−0.018/−0.006	MeF (HCH) −1.1/−0.7/−0.8
CH$_3$CH$_3$ −0.012/−0.010/−0.003	HOCl −0.002/−0.024/0.004	CH$_2$CHCH$_3$ 0.009/0.001/−0.002 −0.002/0.000/0.020	Me$_2$CO −0.011/−0.030/0.006	HOF (HOF) 2.2/3.0/0.4
CH$_2$CH$_2$ −0.011/−0.009/0.000	H$_2$S −0.009/−0.010/0.004	HCCCH$_3$ 0.007/0.009/0.004 −0.018/−0.019/0.014	MeCl 0.025/0.004/−0.002	MeNH$_2$ (HCN) 0.9/0.9/1.5
CHCH −0.010/−0.004/0.005	MeSH −0.009/−0.009/0.005		MeSH 0.003/−0.001/−0.003	Me$_2$CO (CCC) −2.2/−0.6/−0.7
MeCl −0.020/−0.018/−0.007			Me$_2$SO −0.008/−0.003/0.010	CH$_3$CH$_3$ (HCH) 0.3/−0.1/−0.1
MeSH −0.010/−0.009/0.000 −0.011/−0.010/−0.001				CH$_2$CH$_2$ (HCH) −1.6/−1.4/−1.2

(continued)

Table 5.7 (continued)

C–H	O–H, N–H, S–H	C–C	C–O, N, F, Cl, S	Angles
				CH₃CH₂CH₃ (CCC) -0.8/0.4/-0.1
				CH₂CHCH₃ (CCC) 0.4/0.9/0.2
				MeCl (HCH) 0.8/0.5/0.0
				H₂S (HSH) 2.1/2.3/1.2
				MeSH (CSH) 1.1/1.4/0.3
				Me2SO (CSC) 0.0/1.1/-0.8 (CSO) 1.1/0.0/1.7
0+, 13-, none 0	4+, 4-, none 0	5+, 4-, none 0	4+, 4-, one 0	10+, 7-, one 0
0+, 13-, none 0	0+, 8-, none 0	4+, 4-, one 0	1+, 8-, none 0	11+, 5-, two 0
4+, 7-, two 0	8+, 0-, none 0	5+, 3-, one 0	6+, 3-, none 0	6+, 11-, one 0
Mean of 13: 0.015/0.012/0.004	Mean of 8: 0.007/0.014/0.008	Mean of 9: 0.012/0.010/0.007	Mean of 9: 0.012/0.015,0.009	Mean of 18: 1.3/1.0/0.7

Errors are given as HF/3–21G$^{(*)}$/HF/6–31G*/MP2/6–31G*. In some cases (e.g. MeOH) errors for two bonds are given, on one line and on the line below. A minus sign means that the calculated value is less than the experimental. The numbers of positive, negative, and zero deviations from experiment are summarized at the bottom of each column. The averages at the bottom of each column are arithmetic means of the absolute values of the errors

Table 5.8 HF/3–21G$^{(*)}$, HF/6–31G* and MP2(fc)/6–31G* dihedral angles (degrees)

Molecule	Dihedral angles				
	HF/3–21G$^{(*)}$	HF/6–31G*	MP2/6–31G*	Experiment	Errors
HOOH	180.0	116.0	121.3	119.1[a]	61(sic)/−3.1/2.2
FOOF	84.1	84.1	85.8	87.5[b]	−3.4/−3.4/−1.7
FCH$_2$CH$_2$F (FCCF)	74.9	69.4	69.0	73[b]	1.9/−4/−4
FCH$_2$CH$_2$OH (FCCO)	58.4	61.3	60.1	64.0[c]	−5.6/−2.7/−3.9
(HOCC)	52.7	57.8	54.1	54.6[c]	−1.9/2.5/−0.5
ClCH$_2$CH$_2$OH (ClCCO)	65.8	65.7	65.0	63.2[b]	2.6/2.5/1.8
(HOCC)	66.0	67.0	64.3	58.4[b]	7.6/8.6/5.9
ClCH$_2$CH$_2$F (ClCCF)	65.9	67.0	65.9	68[b]	−2.1/−1/−2.1
HSSH	89.8	89.8	90.4	90.6[a]	−0.8/−0.8/−0.2
FSSF	89.4	88.7	88.9	87.9[b]	1.5/0.8/1.0
					Deviations: 5+, 5−/4+, 6−/4+, 6− mean of 10: 8.8/2.9/ 2.3.*

Omitting the largest error for each of the three methods (61/8.6/8.9/ for HF/3–21G$^{(*)}$/HF/6–31G*/ MP2(fc)/6–31G*, respectively, the mean of 9 errors for each method is 3.0/2.3/1.9

Errors are given in the *Errors* column as HF/3–21G$^{(*)}$/HF/6–31G*/MP2/6–31G* A minus sign means that the calculated value is less than the experimental. The numbers of positive and negative deviations from experiment and the average errors (arithmetic means of the absolute values of the errors) are summarized at the bottom of the *Errors* column. Calculations are by the author; references to experimental measurements are given for each measurement. Some molecules have calculated minima at other dihedrals in addition to those given here, e.g. FCH$_2$CH$_2$F at 180°. Errors are presented: HF/3–21G$^{(*)}$/HF/6–31G*/MP2/6–31G*

[a]Reference [1g], pp.151, 152

[b]M. D. Harmony, V. W. Laurie, R. L. Kuczkowski, R. H. Schwenderman, D. A. Ramsay, F. J. Lovas, W. H. Lafferty, A. G. Makai, "Molecular Structures of Gas-Phase Polyatomic Molecules Determined by Spectroscopic Methods", J. Physical and Chemical Reference Data, **1979**, *8*, 619–721

[c]J. Huang and K. Hedberg, J. Am. Chem. Soc., **1989**, *111*, 6909

None of the three levels consistently over- or underestimates C–C bond lengths.
HF/6–31G* C − X(X = O, N, Cl, S) bond lengths tend to be underestimated slightly (ca. 0.015 Å) while MP2/6–31G* C–X bond lengths may tend to be slightly (ca. 0.01 Å) overestimated. HF/3–21G$^{(*)}$ C–X bond lengths are not consistently over- or underestimated.
HF/6–31G* bond angles may tend to be slightly larger (ca. 1°) than experimental, while MP2/6–31G* angles may tend to be slightly (0.7°) smaller.

HF/3–21G$^{(*)}$ bond angles are not consistently over- or underestimated. Dihedrals do not seem to be consistently over-or underestimated by any of the

three levels. The HF/3–21G$^{(*)}$ level breaks down completely for HOOH, where a dihedral angle of 180°, far from the experimental 119.1°, is calculated; omitting this error of 61° and the ClCH$_2$CH$_2$OH HOCC dihedral error of 7.6° lowers the HF/3–21G$^{(*)}$ error from 8.8 to 2.5°. The experimental value of 58.4° for the ClCH$_2$CH$_2$OH HOCC dihedral is suspect because of its anomalously large deviation from all three calculated results, and because it is among those dihedrals which are said to be suspect or having a large or unknown error (designated X in Harmony et al.–see reference in Table 5.8). The error for the HOOH dihedral is represents a clear failure of the HF/3–21G$^{(*)}$ level and is an example of a case which provides an argument for using the 6–31G* rather than the 3–21G$^{(*)}$ basis, although the latter is much faster and often of comparable accuracy (of course with correlated methods like MP2 a smaller basis than 6–31G* should not be used, as pointed out in Sect. 5.4). The errors in calculated dihedral angles are ca. 2–3° for HF/6–31G*, and ca. 2° for MP2/6–31G*: omitting the ClCH$_2$CH$_2$OH HOCC dihedral errors of 8.6° and 5.9° from the sample lowers the HF error from 2.9° to 2.3° and the MP2 error from 2.3 to 1.9.

   The accuracy of ab initio geometries is astonishing, in view of the approximations present: the 3–21G$^{(*)}$ basis set is small (it is in fact used little nowadays) and the 6–31G* is only moderately large, and so these probably cannot approximate closely the true wavefunction; the HF method does not account properly for electron correlation, and the MP2 method is only the simplest approach to handling electron correlation; the Hamiltonian in both the HF and the MP2 methods used here neglects relativity and spin-orbit coupling. Yet with all these approximations the largest error (Table 5.7) in bond lengths is only 0.033 Å (HF/3–21G$^{(*)}$ level for HCHO) and the largest error in bond angles is only 3.2° (HF/3–21G$^{(*)}$ level for H$_2$O). The largest error in dihedral angles (Table 5.8), omitting the 3–21G$^{(*)}$ result for H$_2$O$_2$, is 8.6° (HF/6–31G* for ClCH$_2$CH$_2$OH HOCC), but as stated above the reported experimental dihedral of 58.4° is suspect.

   From Fig. 5.23 and Table 5.7, the mean error in 39(13 + 8 + 9 + 9) bond lengths is 0.01−0.015 Å at the HF/3–21G$^{(*)}$ and MP/6–31G* levels, and ca. 0.05−0.008 Å at the MP2/6–31G* level. The mean error in 18 bond angles is only 1.3° and 1.0° at the HF/3–21G$^{(*)}$ and HF/6–31G* levels, respectively, and 0.7° at the MP2(fc)/6–31G* level. From Table 5.8 the mean dihedral angle error at the HF/3–21G$^{(*)}$ level for 9 dihedrals (omitting the questionable ClCH$_2$CH$_2$OH dihedral) is 3.0°; the mean of 8 dihedral errors (omitting the ClCH$_2$CH$_2$OH and the HOOH errors) is 2.5°. For the other two levels the mean of 10 dihedral angles (including the questionable ClCH$_2$CH$_2$OH dihedral) is 2.9° (HF/6–31G*) and 2.3° (MP2/6–31G*). If we agree that errors in calculated bond lengths, angles and dihedrals of up to 0.02 Å, 3° and 4° respectively correspond to fairly good structures, then *all* the HF/3–21G$^{(*)}$, HF/6–31G* and MP2/6–31G* geometries, with the exception of the HF/3–21G$^{(*)}$ HOOH dihedral, which is simply wrong, and the possible exception of the HOCC dihedral of ClCH$_2$CH$_2$OH, are fairly good. We should, however, bear in mind that, as with the HF/3–21G$^{(*)}$ HOOH dihedral, there is the possibility of an occasional unwelcome surprise. Interestingly, HF/3–21G$^{(*)}$ geometries are, for some series of

compounds, somewhat better than MP2/6–31G* ones. For example, the RMS errors in geometry for the series H_2, CH, NH, OH, HF, CN, N_2, H_2O, HCN, CH_3, and CH_4 using UHF/3–21$^{(*)}$, MP2/6–31G*, and MP2/6–31G† (a modified basis used in CBS calculations–Sect. 5.5.3.2.2) are 0.012 Å, 0.016 Å and 0.015 Å, respectively [113].

The calculations summarized in Tables 5.7 and 5.8 are in reasonable accord with conclusions based on information available ca. 1985 and given by Hehre, Radom, Schleyer and Pople [114]: HF/6–31G* parameters for A-H, A/B single and A/B multiple bonds are usually accurate to 0.01, 0.03 and 0.02 Å, respectively, bond angles to ca. 2° and dihedral angles to ca. 3°, with HF/3–21G$^{(*)}$ values being not quite as good. MP2 bond lengths appear to be somewhat better, and bond angles are usually accurate to ca. 1°, and dihedral angles to ca. 2°. These conclusions from Hehre et al. hold for molecules composed of first-row elements (Li to F) and hydrogen; for elements beyond the first row larger errors not uncommon.

The main advantage of MP2/6–31G* optimizations over HF/3–21G$^{(*)}$ or HF/6–31G* ones is not that the geometries are *much* better, but rather that for a stationary point, MP2 optimizations followed by frequency calculations are more likely to give the correct curvature of the potential energy surface (Chap. 2) for the species than are HF optimizations/frequencies. In other words, the correlated calculation tells us more reliably whether the species is a relative minimum or merely a transition state (or even a higher-order saddle point; see Chap. 2). Thus difluorodiazomethane [91] and several oxirenes [53] are (apparently correctly) predicted by MP2 calculations not to be PES relative minima, while HF calculations indicate them to be minima. The interesting hexaazabenzene ("benzene-N_6") is predicted to be a minimum at the HF/6–31G* level, but a hilltop with two imaginary frequencies at the MP2/6–31G* level [115]. For transition states, in contrast to ground states, we don't have experimental geometries, but correlation effects can certainly be important for their *energies* (Sect. 5.5.2), which can be experimentally probed by kinetics, and MP2/6–31G* geometries for transition states are probably significantly better in general than HF/6–31G* ones.

Suppose we want something better than "fairly good" structures? Experienced workers in computational chemistry have said [116]

> When we speak of "accurate" geometries, we generally refer to bond lengths that are within about 0.01–0.02 Å of experiment and bond and dihedral angles that are within about 1–2° of the experimentally-measured value (with the lower end of both ranges being more desirable).

Even by these somewhat exacting criteria, MP2/6–31G* and even HF/6–31G* calculations are not, in the cases studied here, far wanting; the worst deviations from experimental values seem to be for dihedral angles, and these may be the least reliable experimentally. However, since some larger deviations from experiment are seen in our sample, it must be conceded that HF/6–31G* and even MP2/6–31G* calculations cannot be *relied* on to provide "accurate" (sometimes called high-quality) geometries. Furthermore, there are some molecules that are particularly recalcitrant to accurate calculation of geometry (and sometimes other characteristics); two notorious examples are FOOF (dioxygen difluoride) and ozone (these

have been described as "pathological" [117]). Here are the HF/6–31G*, MP(fc)/6–31G* and experimental [118] geometries:

F-O-O-F dihedral

84.1
85.8
(87.5)
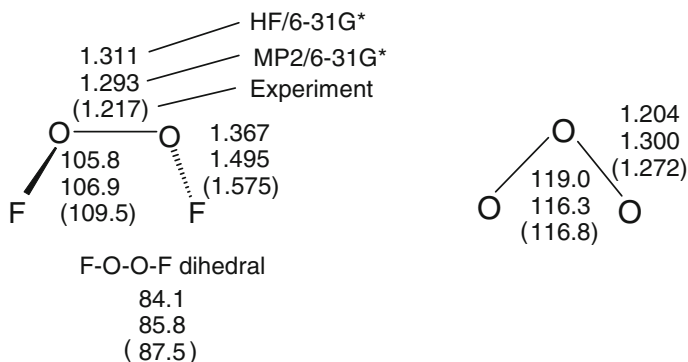
The errors (calculated – experimental) in the calculated geometries are (HF/6–31G*/MP2/6–31G*):

FOOF: FO length   −0.208/−0.080 Å
       OO length   0.094/0.076 Å
       FOO angle   −3.7°/−2.6°
       FOOF dihedral   −3.4°/−1.7°
O_3:   OO length   −0.068/−0.028 Å
       OOO angle   −2.2/−0.5

These calculated geometries do not satisfy even our "fairly good" criterion (errors in calculated bond lengths, angles and dihedrals of up to 0.02 Å, 3° and 4° respectively) and are well short of being "accurate" (bond lengths about 0.01−0.02 Å, bond and dihedral angles about 1 − 2°); the bond lengths are particularly bad. Using the HF method and the 6–311++G** basis (for FOOF, 88 vs. 60 basis functions; for O_3, 66 vs. 45 basis functions) we get for calculated geometries (errors) using (HF/3–311++G**):

FOOF: FO length   1.353 Å (−0.222)
       OO length   1.300(0.083) Å
       FOO angle   106.5°(−3.0)
       FOOF dihedral   85.3°(−2.2)
O_3:   OO length   1.194 Å (−0.078)
       OOO angle   119.4°(2.6)

Thus with a much larger basis than 6–31G*, but still using the Hartree-Fock method, the FOOF geometry is about the same and the O_3 geometry has become even worse than at the HF/6–31G* level !

In a 2001 paper FOOF was called "the unsolved problem" of structure prediction, and a really good structure was obtained only by DFT with the aid of a somewhat contrived procedure [119]. How has the situation changed since then?

Here are the best results for FOOF from two 2007 studies [120, 121] of that and other small O/F molecules:

CCSD(T)/aug-cc-pVDZ [118]

G96PW91/D95(3df) [119]

Experiment

1.209
1.211
(1.217)

1.628
1.579
(1.575)

O —— O

109.2
111.0
(109.5)

F   F

OOOF dihedral:
88.7
88.8
(87.5)
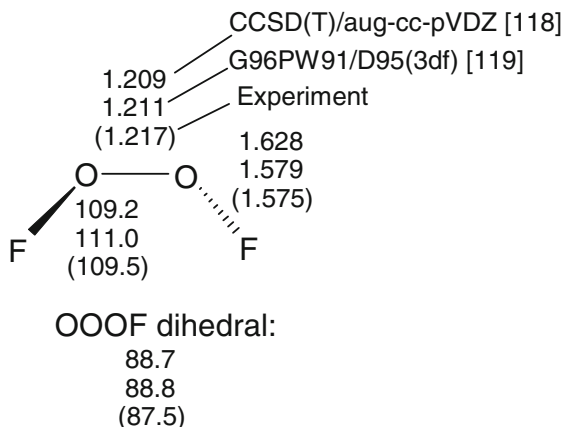
The errors in the CCSD(T) (their DFT results were quite similar) [120] and the G96PW91 (a DFT method) [121] calculations are:

FO length	0.053 [120]/0.004 Å [121]
OO length	-0.008 [120]/ -0.006 Å [121]
FOO angle	-0.3 [120]/-1.5 [121]
FOOF dihedral	-0.2 [120]/1.3° [121]

Here the only problematic parameter is the CCSD(T) FO bond length: the CCSD(T) error was 0.053 Å, still a bit outside our imposed $0.01 - 0.02$ Å error limits. The DFT geometry is fully high-quality.

Ozone is an easier target than FOOF for a high-quality geometry. Some results for this molecule are [122]:

CCSD(T)/aug-cc-pVTZ

BPW91)/aug-cc-pVTZ

Experiment

1.276
1.277
(1.272)

O

117.1
118.2
(116.8)

O   O
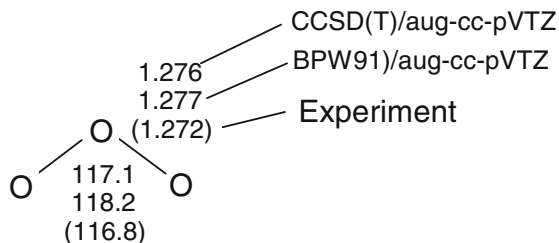
The errors in the CCSD(T) and BPW91 (a DFT method) calculations easily fall within our limits:

OO length	0.004 (CCSD(T)/0.005 ÅS (BPW91)
OOO angle	0.3° (CCSD(T))/1.4° (BPW91)

Other coupled-cluster calculations [123] and CASPT2 [124] gave similar results.

The problem with ozone probably arises at least partly from the fact that this molecule has singlet diradical character: it is approximately a species in which two electrons, although having opposite spin, are not paired in the same orbital [125]:
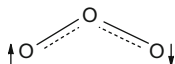
The Hartree-Fock method works best with normal closed-shell molecules, because it uses a single Slater determinant, but ozone has open-shell diradical character: it is, or at least resembles, a species with two half-filled orbitals, one with a single α electron and the other with a single β electron. Correlated methods, which go beyond the HF method by including in the wavefunction determinants corresponding to states in which electrons have been promoted ("excited") into virtual orbitals, handle molecules like ozone better, but can still give problems if we demand highly accurate geometries (or energies). For some techniques for handling molecules like this see Foresman and Frisch [118] and Chap. 8, Sect. 8.2.

The cause of the problems with FOOF are harder to explain, but fluorine is known to be a somewhat troublesome element [126], although some fluoro organics apparently give good geometries at moderate computational levels [127].

If we do not insist of purely ab initio calculations, there is a possible route to very accurate geometries which, however, has so far been reported only for a few, very small, molecules. This is based on fitting geometries to experimental rotational constants (Chap. 2, Sect. 2.4).

5.5.2   Energies

5.5.2.1   Energies: Preamble

We used the concept of energy in Chaps. 2 (potential energy surfaces), 3 (molecular mechanics energies), and 4 (molecular orbital energy levels from simple and extended Hückel calculations). We saw that all these energies were *relative to something*: that of a species on a potential energy surface (PES) can be taken as being relative to the energy of the global minimum, the MM energy is relative to that of some hypothetical unstrained isomer, and the energy of a molecular orbital is, with qualifications, the energy of an electron in it compared to the energy of the electron infinitely distant from the orbital, at rest. Before considering the ab initio calculation of energy, it is worthwhile to look briefly further into the meaning of "energy", because this entity manifests itself in several ways and in favorable cases all of them can be calculated by ab initio methods. We will take cognisance of seven kinds of energy: potential, kinetic, internal, "heat energy" or enthalpy, Gibbs free energy, Helmholtz free energy, and Arrhenius activation energy. The reader may wonder why we need so many kinds of energy (we could add even more, like electrical energy and nuclear energy). The answer is, partly because in different

situations energy appears in different guises, and partly because although some kinds are really composites of others with thermodynamic concepts like temperature and entropy (thus the Gibbs free energy is enthalpy minus the product of temperature and entropy), it is neater to have one word and symbol for the composite. I present the seven kinds of energy in the approximate order in which some build conceptually on others. Five are of considerable importance in chemistry: potential energy, internal energy, enthalpy, Gibbs free energy, and, in experimental studies of reaction rates, Arrhenius activation energy. In this short preliminary to the calculation of energies, we consider the subject from the viewpoint of molecular chemistry, rather than that of classical thermodynamics, which, albeit elegant, knows nothing of atoms and molecules. The connection between the two stances is made in the subject of statistical mechanics. Besides the many standard texts on these subjects, one may recommend Atkin's graceful, compact, and masterful book on the four laws of thermodynamics [128]. We can safely ignore here relativity theory, which requires conservation of "mass-energy".

1. *Potential energy* is the work obtainable from a body that "temporarily" resists a restoring force, so that if the body is allowed to submit to the force it will do work. We use here Newton's concept of a force: something that acting on a body produces an acceleration. An example is a stone at the edge of a cliff, temporarily resisting the gravitational force; a kick submits it to gravity and it will gain kinetic energy, which *could* be converted into useful work by a machine (replace the stone by water and you get hydroelectric power). In chemistry the relevant potential energy is the energy of a molecule on a Born-Oppenheimer surface (a potential energy surface, Chap. 2). In this more abstract situation, a molecule not at the global minimum resists the electromagnetic force–chemistry's only force – that could eventually (delayed by kinetic barriers) pull it downhill to that minimum. In this process energy is released as heat or light. On the usual Born-Oppenheimer surfaces, which include simple two-dimensional potential energy curves such as plots of energy against torsional (dihedral) angle, as well as hypersurfaces, the energy at various points can be taken as being relative to the global minimum. The units of this energy could be from molecular mechanics or some kind of quantum mechanical (ab initio, semiempirical, density functional) calculation. In any case, since vibrational calculations are meaningful only at stationary points, the surface usually excludes ZPE and thermal contributions to energy, and is a hypothetical 0 K energy surface, corresponding at least roughly to the electronic energy plus internuclear repulsion, cf. Eq. (5.94), but with the ZPE term excluded and the E term obtained from any quantum mechanical method or from a molecular mechanics surrogate of one by virtue of parameterization. Although we may not explicitly consider potential energy here, electronic energy is partly, and internuclear repulsion wholly, this kind of energy.

   Symbol: potential energy on a Born-Oppenheimer surface (i.e. in a PES diagram) is denoted in Chap. 2 by E. Other common designations are V (origin obscure) and PE, and sometimes U, but this latter is best reserved for internal energy.

   Equation: potential energy is the integral over the relevant distance of the force, itself usually a function of distance.

2. *Kinetic energy* (translational energy) is the energy of motion, and is taken into account for the motion of a molecule as a whole by a term $(3/2)RT$, $(1/2)RT$ for each degree of freedom of motion; R is the ideal gas constant and T the temperature. Part of the electronic energy of a molecule is the electronic kinetic energy.
   Symbol: kinetic energy is denoted by KE or by T (origin obscure), although this could occasionally be confused with temperature.
   Equation: in classical physics kinetic energy is the $(1/2)mv^2$. The electronic kinetic energy of a molecule can be calculated from the Schrödinger equation as explained in Sect. 5.2.

3. The internal energy of a molecule is the energy due to its electronic kinetic and potential energy, its internuclear potential energy and nuclear ZPE, its rotational energy, and its translational motion (this does not include the "external" translational motion imposed on the molecule by moving the vessel containing a collection of molecules). Changes in internal energy are usually largely changes in bond energies, arising from changes in electronic energy.
   Symbol: internal energy is denoted by U (occasionally E), possibly because in the alphabet U lies close to other thermodynamic quantities: Q (heat), R (the gas constant), S (entropy), T (temperature), V (volume) and W (work), and U was not yet (ca. 1860) taken. According to the English translation [129]a *The Mechanical Theory of Heat* of Clausius's *Die Mechanische Wärmetheorie*, [129]b. the symbol was introduced by simply saying "... U denotes an arbitrary function of v and t" but the German edition attributes the symbol to Zeuner, 1860, although Clausius with considerable circumspection denotes his U as meaning the sum of kinetic and potential energy, the latter being however called by him without etymological explanation *Ergal*, a Greek word meaning work; "potentielle Energie" was deemed somewhat too long.
   Equation: for a molecule we can write for the internal energy at T Kelvins (cf. Eq. (5.94)):

$$U_T = E_{0K}^{\text{total}} = E^{\text{total}} + E_{vr} + \frac{3}{2}RT \qquad (*5.171)$$

where E^{total} is the electronic energy + internuclear repulsion, not necessarily at the Hartree-Fock level, E_{vr} is the total vibrational and rotational energy, and $(3/2)RT$ is the translational energy, $(1/2)RT$ for each translational degree of freedom. Internal rotations tend to be regarded as low-energy vibrations, although more realistic treatments are possible [130]. Rotation of the molecule as a whole, and population of upper vibrational levels, is taken into account in calculating by statistical mechanics the thermal contribution to the energy at temperatures above 0 K [130]. Upper electronic levels are usually scarcely significantly populated at "chemically accessible" temperatures. R, the gas constant, is 8.314×10^{-3} kJ K^{-1} mol^{-1} and at 298 K, $RT = 2.478$ kJ mol^{-1} and $(3/2)RT$ is 3.717 kJ mol^{-1}. Thus the internal energy of the proton at 298 K, with no electronic, vibrational or rotational energy, is $(3/2)RT$ [131]. Both E^{total}

and ZPE are often readily calculated quantum mechanically. Differences in U at 0 K (where there is no translational term) take into account the electronic energy and the ZPE and are the simplest realistic measure of molecular energy differences like reaction energies and activation energies, although differences of just E^{total} (no ZPE) provide a *rough* measure of these quantities (Chap. 2, Sect. 2.5).

4. Enthalpy is the "heat content" of a system. This term is not very precise, for as Atkins points out [128] heat is not a thing, but rather a process, the transfer of energy because of a difference of temperature (or accompanied by a difference of temperature in the case of phase transition enthalpies). Nevertheless "amount of heat" is a useful shorthand for amount of energy transferred because of a temperature difference. The enthalpy change is the amount of heat released or absorbed when a reaction occurs at constant pressure. The standard conditions are 298 K and 101.3 kPa (1 atmosphere). The enthalpy of formation, or heat of formation, of a substance is a useful quantity (Sect. 5.5.2.3.3). Like Gibbs free energies of formation, these have been widely tabulated. These enable the heat evolved or absorbed in reactions (reaction enthalpies) to be calculated by simply taking the enthalpy difference of the products and reactants. These enthalpy changes refer, strictly, to changes at constant pressure, although the difference compared to constant volume is usually less than 1% [128]. Reaction enthalpies can also be calculated from the change in bond energies in a reaction, but this is quite approximate since bond energies are not fully transferable, but vary somewhat from molecule to molecule and can even differ from one, say C-H, bond to another C-H bond even in the same molecule. Enthalpies of formation can be accurately calculated with the aid of quantum mechanical methods if the molecule is not too big (Sect. 5.5.2.3.3). The enthalpy change of a reaction is often taken as measure of its thermodynamic feasibility, and often, tacitly, as an indication of its kinetic ease, but the rigorous criteria for these are really the Gibbs free energies (below) of reaction and activation.

Symbol: enthalpy is denoted by H: the word comes (H. Kammerlingh-Onnes, 1909) from the Greek *thalpos*, heat, or *enthalpos*, internal heat. Denoting it by H was suggested by H. W. Porter in 1922, because the symbol H is a letter in the Roman alphabet and also the capital Greek initial letter *eta* (H or η) of *enthalpos* ($\eta\nu\theta\alpha\lambda\pi o\zeta$) [132].

Equation: the "energy" (internal energy) of an atom or molecule at a temperature T can be converted to its enthalpy by adding RT, since $H = U + PV$ and $PV = RT$, on a molar basis, assuming ideal gas behavior. Thus

$$H = \text{interal energy} + RT \qquad (*5.172)$$

$= $ internal energy $+ 2.478$ kJ mol^{-1} at 298 K. The enthalpy of the proton at 298 K (cf. its internal energy, above) is $(3/2)RT + RT = 6.195$ kJ mol^{-1} [131].

5. Gibbs free energy is the work obtainable from a system at a constant temperature and pressure. Unless specified otherwise, in chemistry we may take "free

energy" to mean Gibbs free energy. A free energy change is an enthalpy change adjusted by a temperature-weighted entropy change:

$$\Delta G = \Delta H - T\Delta S \qquad (*5.173)$$

The $T\Delta S$ term is often a minor contributor to ΔG at room temperature or below, but will dominate at sufficiently high temperatures. If the entropy change is positive (increased freedom of motion), this tends to make the free energy change favorable (negative). Entropy can also be viewed in terms of dispersal of energy (Sect. 5.5.2.2). A change in free energy is the best indicator of the ease, as measured by rate, or the extent, as measured by completeness, of a chemical reaction. Rate and completeness are quantified by the rate constant and the equilibrium constant, which can be calculated, respectively, from the free energy of activation and the free energy of reaction. These two energy differences (transition state energy minus reactants energy, and products energy minus reactants energy) can often be calculated quantum-mechanically fairly readily. Free energies of formation have been tabulated and the values can be used to calculate free energies of reaction and thus equilibrium constants. Such tables should be better for such purposes than enthalpy tables, but actually are less widely used. This is probably because free energy tends to be harder to measure than enthalpy, and could not be calculated accurately until fairly recently, largely because of the problem of calculating accurate vibrational frequencies. Free energy changes can be obtained from experiment when equilibrium constants (Eq. (5.183)) can be accurately measured, and enthalpies can usually be obtained from combustion measurements.

Symbol: Gibbs free energy is denoted eponymously by G, after Josiah Willard Gibbs, ca. 1873, who single-handedly created much of chemical thermodynamics. In the older literature F was sometimes used.

Equation: since $G = H - TS$, the free energy of a molecule can be calculated from its enthalpy (above) and entropy at temperature T; the entropy is calculated by standard statistical mechanics methods [130a].

6. Helmholtz free energy (or Helmholtz energy) is the work obtainable from a system at a constant temperature and volume. It is much less used in chemistry than Gibbs free energy, because most chemical reactions occur at constant pressure, not constant volume. However, Helmholtz free energy is relevant to reactions with rapid pressure changes (explosions).

Symbol: Helmholtz free energy is denoted in chemistry by A (German *Arbeit*, work), in physics by F, free energy.

Equation: $A = U - TS$, where U = internal energy, T = Temperature, S = entropy.

7. Arrhenius activation energy is the energy term in an empirical equation that shows the dependence of the rate constant on temperature (experiments of J. H. van't Hoff, 1884, interpreted by S. Arrhenius, 1889):

$$k = Ae^{-Ea/RT} \qquad (*5.174)$$

The preexponential factor is tied to the probability of some favorable situation like a propitious collision and involves entropy, while the exponential term reflects the energy barrier for the reaction. A and E_a are usually approximately constant over the limited range of laboratory interest. The modified version of Eyring, Polanyi and Evans (the "Eyring equation") lends itself directly to the theoretical calculation of rate constants: $k = k_B T/h \exp(-\Delta G^{\ddagger}/RT)$, where k_B is Boltzmann's constant, h is Planck's constant, and $\Delta G^{\ddagger}$ is the free energy of activation. High-level calculation of rate constants is best done with a specialized program like, e.g., Polyrate [133] for unimolecular reactions, using RRKM (Rice-Ramsperger-Kassel-Marcus) theory [134].

Symbol: E_a.

Equation: the activation energy calculated as the transition state enthalpy minus the reactant enthalpy, $\Delta H^{\ddagger}$ (or $E^{\ddagger}$), is related to the Arrhenius activation energy for a gas-phase unimolecular reaction by [135]

$$E_a = \Delta H^{\ddagger} + RT = \Delta H^{\ddagger} + 2.48 \text{ kJ mol}^{-1} \qquad (*5.175)$$

at room temperature (298.15 K).

A nice mnemonic for the relationships among various forms of energy is [136]:

ie.
U − TS = A
U + PV = H
H − TS = G
A + PV = G
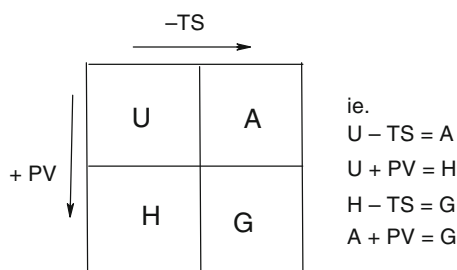
5.5.2.2 Energies: Preliminaries

Along with geometries (Sect. 5.5.1), the molecular features most frequently sought from ab initio calculations are probably energies. An ab initio calculation gives an energy quantity that represents the energy of the molecule (or atom) relative to its constituent electrons and nuclei at rest at infinite separation; this separated state is taken as the zero of energy. The ab initio energy of a species is thus the negative of the energy needed to dissociate it completely, to infinite separation, into the electrons and nuclei, with no kinetic energy left over, or the negative of the energy given out when the electrons and nuclei "fall together" from rest at infinite separation to form the species. This was pointed out for Hartree-Fock energies (Sect. 5.2.3.6.4, in connection with Eq. (5.93)), and the infinite-separation reference point also holds for correlated ab initio energies. By ab initio energy, then, we normally mean the purely electronic energy (the kinetic and potential energy

of the electrons, whether calculated by the Hartree-Fock or by a correlation method) plus the internuclear repulsion (cf. Eq. (5.93)):

Ab initio energy (Hartree-Fock):

$$E_{\text{HF}}^{\text{total}} = E_{\text{HF}} + V_{NN} \qquad\qquad (*5.176)$$

Ab initio energy (a correlated method):

$$E_{\text{correl}}^{\text{total}} = E_{\text{correl}} + V_{NN} \qquad\qquad (*5.177)$$

If the ab initio energy has been corrected by adding the zero-point energy (cf. Eq. (5.94)), giving the total internal energy at 0 K, this should be pointed out: ab initio energy, corrected for ZPE:

$$E_{0K}^{\text{total}} = E^{\text{total}} + \text{ZPE} \qquad\qquad (*5.178)$$

As has been pointed out, the ZPE-corrected ab initio energy is preferred over the uncorrected for calculating relative energies. At the end of a calculation E^{total} (HF or correlated) is given; if we wish to include ZPE and so get E_{0K}^{total} a frequency calculation is necessary. The format in which these quantities appear at the end of a calculation depends on the program.

What we really want is rarely these "absolute" ab initio energies, because chemistry deals with *relative* energies; *all* energies are relative to something of course, but in this context it is useful to restrict the term to the energy difference between reactants and products or between reactants and transition states (the energy difference between isomers is a special case reactants/products). We are thus interested in the reaction energy (product energy minus reactant energy) and what we might call the activation energy (transition state energy minus reactant energy; note however–see below and Eq. (5.175)–that above 0 K the well-known Arrhenius activation energy is not exactly simply the difference in calculated energies of transition state and reactants).

Figure 5.24 shows what Coulson meant when he said that calculating the relative stabilities of isomers by subtracting absolute energies is like finding the weight of the captain by weighing the ship with and without him [137]. The absolute ab initio energies of the two isomers shown are each about 407,700 kJ mol^{-1}, and the difference in their energies is only about 9 kJ mol^{-1}, which is 1 part in 45,000, and these figures are quite typical. If we conservatively assign a captain a weight of 100 kg, the analogy corresponds to a small ship weighing 4,500,000 kg or about 5000 tonnes. Yet the astonishing thing is that modern ab initio calculations can, as we shall see, accurately and reliably predict relative energies. Comprehensive accounts of energy calculations by ab initio and other methods are given by Irikura and Frurip [138] and by Cramer [139].
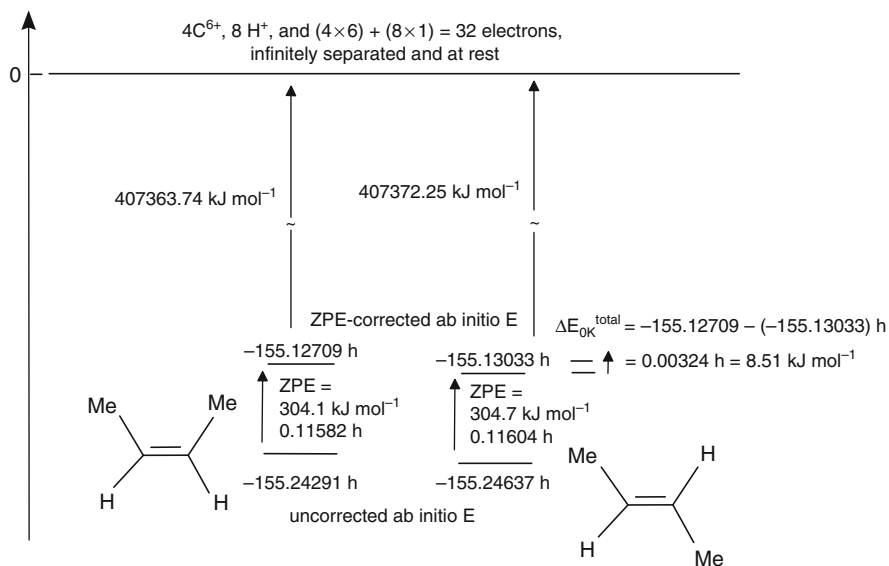
Fig. 5.24 Absolute and relative ab initio energies, with and without ZPE correction. These are from HF/3–21G$^{(*)}$ calculations. The calculated reaction energy for the (*E*) to (*Z*) (*cis* to *trans*) isomerization is −8.51 kJ mol^{-1}

Reaction energies belong to the realm of thermodynamics, and activation energies to that of kinetics: the energy difference between the products and the reactants ("difference" is defined here as product energy minus reactant energy) governs the extent to which a reaction has progressed at equilibrium, i.e. to the equilibrium constant, and the energy difference between the transition state and the reactants (transition state energy minus reactant energy) governs (partially; see Sect. 5.5.2.3.4) the rate of the reaction, i.e. the rate constant (Fig. 5.25). The term "energy" in chemistry usually means potential energy (often denoted by *E*), enthalpy *H*, or Gibbs free energy, *G*. The potential energy on a computed Born-Oppenheimer surface (the usual "potential energy surface"; Chap. 2, Sect. 2.3) represents 0 K enthalpy differences without ZPE. Enthalpy differences, ΔH, and free energy differences, ΔG, are related through the temperature-weighted entropy difference:

$$\Delta G = \Delta H - T\Delta S \qquad (*5.179 = 5.173)$$

More detailed discussions of enthalpy, free energy, and entropy are given in books on thermodynamics, and the relationships between these quantities and processes at the molecular level are explained in books on statistical mechanics [140]; general discussions of these topics are given in physical chemistry texts.

To get an intuitive feel for ΔH we can regard it as essentially a measure of the strengths of the bonds in the products or the transition state, compared to the strengths of the bonds in the reactants [141]:
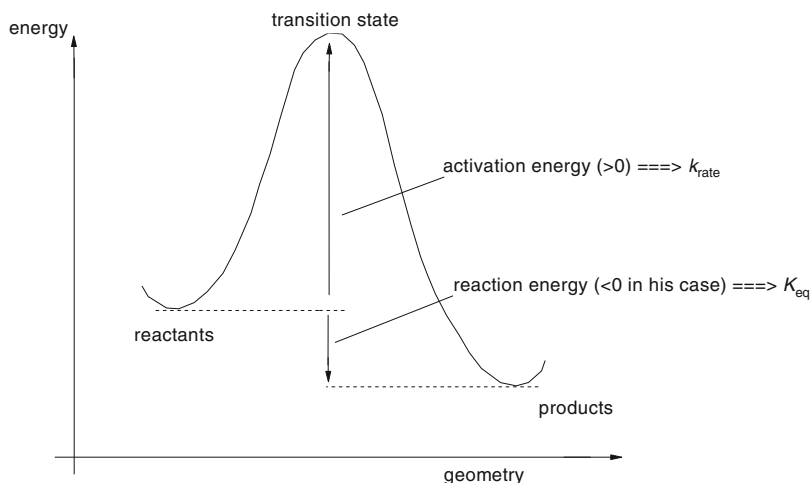
Fig. 5.25 The reaction energy, the energy difference of products and reactants, determines the extent of a reaction, i.e. its equilibrium constant. The activation energy (the simple ab initio energy difference shown here is not exactly the conventional Arrhenius activation energy), the energy difference of transition state and reactants, partially determines the rate of a reaction, i.e. its rate constant. Unfortunately, "energy" is ambiguous, since chemists use the terms potential energy, enthalpy (heat energy), and free energy: see Sect. 5.5.2.1

$$\Delta H = H(\text{pdts}/\text{TS}) - H(\text{reactants})$$
$$\simeq \Sigma \text{ bond energies (reactants)} - \Sigma \text{ bond energies(pdts/TS)} \qquad (*5.180)$$

(pdt or TS depending on whether we are considering reaction enthalpy or activation enthalpy; we can ignore bonds that are neither broken nor made). Thus an exothermic process, which from the definition has $\Delta H < 0$, has stronger bonds in the products than in the reactants; in some sense the bonds lose heat energy, becoming tighter and stabler. The bond energy tables given in most organic chemistry textbooks can be used to calculate rough values of ΔH (reaction), and *accurate* reaction enthalpies can sometimes be obtained from the more sophisticated use of bond energies and similar quantities [142]. To see an application of simple bond energy tables [143], consider the keto/enol reaction:

Using Eq. (5.180):
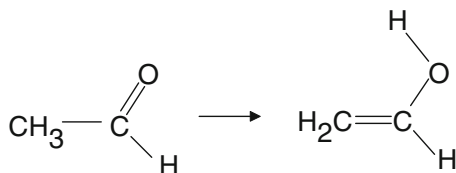
$$\Delta H = \simeq \Sigma \text{ bond energies(reactants)} - \Sigma \text{ bond energies(pdfs/TS)}$$
$$= (4C - H + C - C + C = O) - (3C - H + C = C + C - O + O - H)$$
$$= (4 \times 414 + 347 + 749) - (3 \times 414 + 611 + 360 + 464) \text{ kJ mol}^{-1}$$
$$= 2752 - 2677 \text{ kJ mol}^{-1} = 75 \text{ kJ mol}^{-1}$$

The ethanal to ethenol (acetaldehyde to vinyl alcohol) reaction is predicted to be endothermic by 75 kJ mol^{-1}, i.e. neglecting entropy the enol is predicted to lie 75 kJ mol^{-1} above the aldehyde. Because these are only average bond energies, the apparently remarkable agreement with the ab initio calculations in Fig. 5.21 (71.6 kJ mol^{-1}; the connection between ΔH from calculations like this and ΔE from ab initio calculations is discussed below) must be regarded as a coincidence. In any case, the correct (experimental) free energy value is ca. 36 kJ mol^{-1} [92]. Crude bond energy calculations like this can be expected to be in error by 50 or more kJ mol^{-1}. More accurate bond energy calculations can be done [142] using bond energies that refer to very specific structural environments; for example, a C–H bond on a primary sp^3 carbon that is in turn attached to another sp^3 carbon.

For a reaction taking place at 0 K the enthalpy change is simply the internal energy change at 0 K:

$$\Delta H(0K) = \Delta E_{0K}^{\text{total}} \tag{5.181}$$

Note that although the calculation of E_{0K}^{total} values to get $\Delta E_{0K}^{\text{total}}$ demands frequency jobs, which are relatively time-consuming ("expensive"), accurate relative energy differences do require this, and we will regard the ZPE-uncorrected ab initio energy difference ΔE^{total}, the difference in electronic energy + internuclear repulsion, as only an approximation to $\Delta E_{0K}^{\text{total}}$ (see Eq. (5.94) and Chap. 2, Fig. 2.20). At temperatures other than 0 K, ΔH is $\Delta E_{0K}^{\text{total}}$ plus the increases in translational, rotational, vibrational and electronic energies on going from 0 K to the higher temperature T, plus the work done by the system in effecting a pressure or volume change:

$$\Delta H(T) = \Delta E_{0K}^{\text{total}} + \Delta E_{\text{trans}} + \Delta E_{\text{rot}} + \Delta E_{\text{vib}} + \Delta E_{\text{el}} + \Delta(PV) \tag{5.182}$$

One frequently chooses the standard temperature of 298.15 K, about room temperature. From 0 K to room temperature the increase in electronic energy is negligible and the increase in vibrational energy is small.

The entropy difference ΔS for a process is a measure of the disorder of the products or the transition state, compared to the disorder of the reactants:

$$\Delta S = S(\text{pdts/TS}) - S(\text{reactants})$$
$$= \text{disorder(pdts/TS)} - \text{disorder(reactants)}$$

(pdt or TS depending on whether we are considering reaction entropy or activation entropy). Entropy is a sophisticated concept, and explaining it in terms of disorder

has been strongly criticized [144], but in the author's opinion this viewpoint works quite well used pictorially at the molecular level and is more useful in interpreting reactions than is the counterview of dispersal of energy. Suffice it to say that a disordered system is more probable than an ordered one, and the entropy of a system is proportional to the logarithm of its probability [145]. Intuitively, we see that $\Delta S > 0$ for a process in which the product or the transition state is less symmetrical or has more freedom of motion than the reactants–is less ordered. For example, ring-opening reactions, since they relieve constraints on intramolecular motion, should be accompanied by an increase in entropy. Note that an increase in entropy favors a process: it increases a rate constant (activation entropy) or an equilibrium constant (reaction entropy), while an increase in *enthalpy* disfavors a process.

Details on the calculation of entropies are given by Ochterski [130a] and in the book by Hehre, Radom, Schleyer and Pople, who also tabulate the errors in calculated entropy for small molecules composed of elements from H to F [146]. Errors in calculated entropies at 300 K are 1.7, 1.3 and 0.8 J mol^{-1} K^{-1} (0.4, 0.3 and 0.2 cal mol^{-1} K^{-1}) at 300 K, for frequency calculations at the HF/3–21G$^{(*)}$, HF/6–31G* and MP2/6–31G* levels, respectively. From Eq. (5.173) this corresponds to an error in free energy at 300 K of about 0.5 kJ mol^{-1}. This is much smaller than the enthalpy error of ca. 10 kJ mol^{-1} which can be routinely reliably obtained with practical high-accuracy methods (see below) and shows that in current ab initio work errors in free energies can be expected to come mainly from the enthalpy. Many programs, e.g. Gaussian and Spartan, automatically calculate the correction terms to be added to ΔE_{0K}^{total} in Eq. (5.182) at the end of a frequency calculation, and print out the 298.15 K enthalpy or the correction to the 0 K enthalpy. Reaction entropies are needed to calculate free energies of reaction (from Eq. (5.179)), from which equilibrium constants [147] can be calculated:

$$\Delta G_{react} = -RT \text{ In } K_{eq} \qquad (*5.183)$$

Where several species are in equilibrium, the ratios are proportional to their Boltzmann exponential factors. For example, if the relative free energies G of A, B and C are 0, 5.0 and 20.0 kJ mol^{-1} (here G for species A has been set to zero and B and C lie 5.0 and 20.0 kJ mol^{-1} higher) then

$$[A] : [B] : [C] = \exp(-0/RT) : \exp(-5.0/RT) : \exp(-20.0/RT);$$

at room temperature $RT = 2.48$ kJ mol^{-1} and so at this temperature

$$[A] : [B] : [C] = 1 : 0.133 : 0.000315 = 3175 : 422 : 1$$

Activation entropies are useful because they can give information on the structure of a transition state (as stated above, a more confined transition state is signalled by a negative, unfavorable, activation entropy), but the ab initio calculation of *rate* constants [148] from activation free energies is not as straightforward as

is the calculation of *equilibrium* constants from reaction free energies. The crudest way to calculate a rate constant is to use the Arrhenius equation [140, 149]

$$k = Ae^{-E_a/RT} \qquad (*5.184 = 5.174)$$

and to simply approximate the preexponential factor A by that known for a similar reaction (a typical value for unimolecular reactions is $10^{12} - 10^{15}$ [150])and to approximate E_a by ΔE_{0K}^{total} (Eq. (5.181) and discussion). Theoretically more satisfying is to represent E_a by $\Delta H^{\ddagger} + RT$, using the temperature in question, in accordance with

$$E_a = \Delta H^{\ddagger} + RT \qquad (*5.185 = 5.175)$$

for a gas-phase unimolecular reaction, and by

$$E_a = \Delta H^{\ddagger} + 2RT \qquad (5.186)$$

for a gas phase bimolecular reaction [151]. The main problem with this is that the preexponential A varies by a large factor even for, say, reactions which are formally unimolecular [150]:

$CH_3NC \rightarrow CH_3CN$	3.98×10^{13}
cyclopropane $\rightarrow$ propene	1.58×10^{15}
$C_2H_6 \rightarrow 2\ CH_3$	2.51×10^{17}

so that this method of guessing A by analogy could give a value that was out by a factor of 10^4 unless one was judicious (or lucky) enough to choose a good model reaction. The *exponential* factor is prone to smaller errors, since calculating $\Delta H^{\ddagger}$ to within 10 kJ mol^{-1} or better is now feasible, and an error of this size corresponds to an error factor in $\exp(-\Delta E_a)$ of $\exp(-10/2.48) = 57$ (at $T = 298$ K). This may seem to be itself very big, but an easy method of reliably calculating rate constants to within a factor of even just 100 might be useful for estimating the stability of unknown substances. In fact, a simple and very useful rule is that the threshold barrier for the stability of a compound at room temperature is about 100 kJ mol^{-1}; allow a latitude of about 20 kJ mol^{-1} [152]. This rule has been used frequently in the computational search for stable nitrogen allotropes [153a], and was used to conclude that the novel aromatic molecule bowtiene (a tricyclodecapentaene) should be stable at room temperature [153b].

Note that for unimolecular processes the halflife, an intuitively more meaningful quantity than the rate constant, is simply

$$t_{1/2} = \frac{\ln 2}{k_r} = \frac{0.693}{k_r}$$

i.e. the halflife of a unimolecular reaction is approximately the reciprocal of its rate constant.

5.5.2.3   Energies: Calculating Quantities Relevant to Thermodynamics and to Kinetics

5.5.2.3.1   Thermodynamics; "Direct" Methods; Isodesmic Reactions

Here we are concerned with the relative energies of species other than transition states. Such molecules are sometimes called "stable species", even if they are not at all stable in the usual sense, to distinguish them from transition states, which exist only for an instant on the way from reactants to products. A "stable species", in contrast, sits in a potential energy well and survives at least a few molecular vibrations ($>$ ca. 10^{-13} s). The very useful book by Hehre [39] contains a wealth of information on computational and experimental results concerning thermodynamic quantities.

The ab initio reaction energy that is most commonly calculated is simply the difference in ZPE-corrected energies, ΔE_{0K}^{total}, which is the reaction enthalpy change at 0 K (Eq. (5.181)). This provides an easily-obtained indication of whether a reaction is likely to be exothermic or endothermic, or of the relative stabilities of isomers. Table 5.9 illustrates this procedure. The results are only semiquantitatively correct, and the HF/6–31G* method is not necessarily much better here than the HF/3–21G$^{(*)}$ for such "direct" (simple subtraction) energies. In fact, it has been

Table 5.9 Reaction energies and relative energies of isomers (HF/3–21G$^{(*)}$ and *HF*/6–31G*)

Reactants, E, h	Reactants, E, h	Reaction energy, or relative energy of isomers	
		Calculated, h/ kJ mol^{-1}	Exp, kJ mol^{-1}
$H_2 + Cl_2$ $-1.11234 + (-914.75715)$ $= -915.86949$ $-1.11625 + (-918.91145)$ $= -920.02770$	2HCl $2(-457.97423)$ $= -915.94846$ $2(-460.05272)$ $= -920.10544$	$-915.94846 - (-915.86949)$ $= -0.07897/-207$ $-920.10544 - (-920.02770)$ $= -0.07774/-204$	-185
$2H_2 + O_2$ 2 $(-1.11234) + (-148.76540)$ $= -150.99008$ $2(-1.11625)$ $+(-149.61336)$ $= -151.84586$	2H$_2$O $2(-75.56419)$ $= -151.12838$ $2(-75.98778)$ $= -151.97556$	$-151.12838 - (-150.99008)$ $= -0.13830/-363$ $-151.97556 - (-151.84586)$ $= -0.12970/-341$	-484
trans-2-butene -155.13032 -155.99472	*cis*-2-butene -155.12768 -155.99196	$-155.12768 - (-155.13032)$ $= 0.00264/6.93$ $-155.99196 - (-155.99472)$ $= 0.00276/7.2$	4.6
HCN -92.33570 -92.85721	HNC -92.32215 -92.83828	$-92.32215 - (-92.33570)$ $= 0.01355/35.6$ $-92.83828 - (-92.85721)$ $= 0.01893/49.7$	60.7

The energies in hartrees are ab initio energies including ZPE. The calculations on O$_2$ are UHF, on triplet O$_2$. Calculations are by the author, experimental energies are from reference [39], Tables 2.13 and 2.14

documented by extensive calculations that such HF/3–21G and HF/6–31G* energy differences generally give only a rough indication of energy changes. Much better results are obtained from MP2/6–31G* calculations on MP2/6–31G*, HF/3–21G or even semiempirical AM1 geometries (the latter two are single-point energies), and it is well worth consulting the book by Hehre for details [154]. We shall see in Sect. 5.5.2.3.2 that it *is* possible to obtain good relative energies "directly".

To get from relatively low-level calculations the best energy changes, one can utilize *isodesmic reactions* (Greek: "same bond", i.e. similar bonding on both sides of the equation). These are reactions in which the number of each kind of bond is conserved. For example

$$NH_3 + CH_3NH_3^+ \rightarrow NH_4^+ + CH_3NH_2 \qquad (5.187)$$

and

$$CH_2F_2 + CH_4 \rightarrow CH_3F + CH_3F \qquad (5.188)$$

are isodesmic reactions; the first one conserves six N–H, three C–H, and one C–N bond and the second conserves six C–H and two C–F bonds. The reaction

$$H_3C - CH_3 + H_2 \rightarrow 2CH_4 \qquad (5.189)$$

is, strictly speaking, not isodesmic, since although it has the same number of bonds, even the same number of single bonds (eight), on both sides, there are six C–H, one C–C, and one H–H bonds on one side and eight C–H bonds on the other. Note that an isodesmic reaction does not have to be *experimentally* realizable: it is an artifice to obtain a reasonably accurate energy difference by ensuring that as far as possible errors due to limitations of basis sets and treatment of electron correlation cancel. This will happen to the extent that particular errors are associated with particular structural features; electron correlation effects are thought to be especially important in calculating energy differences, and such effects tend to cancel when the number of electron pairs of each kind is conserved. The concept and the name appear first in a 1970 paper by Hehre et al., where the method was introduced to calculate enthalpy changes for complete hydrogenation of molecules using the small basis sets then available [155], and the approach was applied to many kinds of reaction in the classic book by Hehre, Pople, Radom and Schleyer [1g]. The purpose of such reactions is to calculate stabilization or destabilization energies that can be ascribed to factors like aromaticity [156], strain [157], or replacement of one group by another, say H by F [158]. In attempts to focus on these factors and exclude the beside-the-point effect of different bond strengths, a hierarchy of increasingly finicky reactions grew up, and the nomenclature for isodesmic-type reactions spun out of control. One encounters the terms homodesmotic, hyperhomodesmotic, semihomodesmotic, quasihomodesmotic, homomolecular homodesmotic, isogeitonic, and isoplesiotic, to cite some. To "expose the wide-spread confusion over such classes of equations" and bring order and rigor to what

might well be called a chaotic proliferation (to borrow a term [68]), Wheeler, Houk, Schleyer and Allen extensively reviewed the subject and made recommendations [159]. Here we can sidestep technicalities and the menagerie of terms and simply call this general class of reactions isodesmic. We shall look at examples of two applications of isodesmic reactions, namely, calculation of: *strain energy*, and of *aromatic stabilization energy* ASA, which measures stabilization by aromaticity or destabilization by its opposite, antiaromaticity. We can take the ASA as being the time-honored resonance energy, RE.

Strain Energy   Molecular strain is a concept nicely grasped by trying to build with rigid plastic components a model of a molecule with small angles, like cyclopropane, and noting that the bonds break. This old concept of angle strain [160a] has been expanded to encompass torsional and steric strain [160b]. We will consider two examples of angle strain, that in cyclopropane and that in norbornane. We (conceptually) open cyclopropane to propane by using two Hs from two ethanes and join the resulting ethyl groups to make butane; we use ethane rather than methane to effect cleavage because with ethane we break a bond between secondary carbons and make a bond, in butane, joining secondary carbons, but with methane we would make a bond, in ethane, joining primary carbons. Following Khoury et al. [157] we use B3LYP/6–31G* (a DFT method, Chap. 7) energies/geometries without ZPE; this energy is shown under each species:
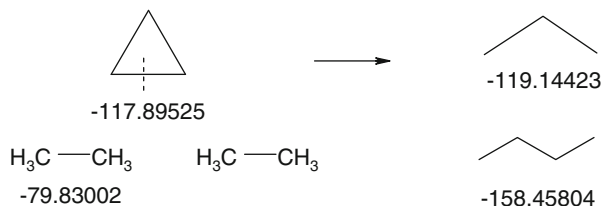
Release of strain must correspond to an exothermic process and by convention we take strain energy as being positive (where not zero), so the strain energy is the energy of the reactants minus that of the products:

$$\text{SE(cyclopropane)} = [-117.89525 + 2(-79.83002)] - [-119.14423 - 158.45804]$$
$$= -277.55529 + 277.60227 = 0.04698 = 123 \text{ kJ mol}^{-1}$$

We've converted atomic units (hartrees) to kJ mol^{-1} by multiplying by 2626. Khoury et al. report a value of 121 kJ mol^{-1} (29.0 kcal mol^{-1}), similar to the experimental (115 kJ mol^{-1}) and to other calculated values, which they cite. A concept called protobranching leads to a substantially lower strain energy for cyclopropane than the accepted value of ca. 120 kJ mol^{-1}; this has been challenged (Fishtik) and rebutted (Schleyer, McKee) [161].

A slightly more involved example is the strain of norbornane, bicyclo[2.2.1] heptane. We can open this to heptane (two steps are hinted at here for clarity);

molecules like butane and heptane are used in the all-transoid, lowest-energy conformations:
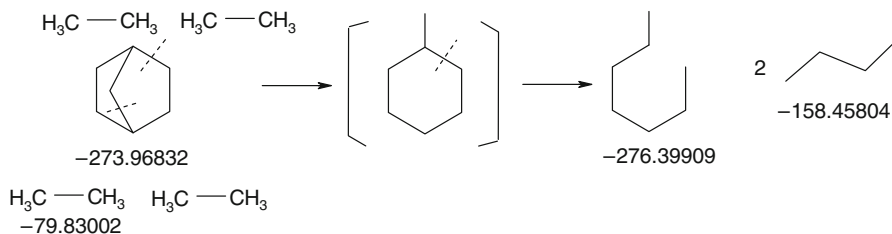
$$SE(\text{norbornane}) = [-273.96832 + 4(-79.83002)]$$
$$- [-276.39909 \ + \ 2(-158.45804)]$$
$$= -593.28840 + 593.31517 = 0.02677 = 70.3 \text{ kJ mol}^{-1}$$

Khoury et al. report a value of 69.5 kJ mol^{-1} (16.6 kcal mol^{-1}), tolerably close to the experimental value (60.2 kJ mol^{-1}), which they cite.

The two calculations shown here are simplified versions of the slightly more involved methods of Khoury et al. [157], which attempt to make the bonds in the reactants and the products more alike than in the very straightforward manner used here; for example, the two C-C bonds in norbornane that we break are between a secondary and a tertiary carbon, but the two C–C bonds we make to form two butanes are between a secondary and a secondary carbon. Instead of using ethane and ethane and making butane, we might have used ethane and propane and made a bond between a secondary and a tertiary carbon in 2-methylbutane. This gives a strain energy of 64.7 kJ mol^{-1}, closer to the experimental one.

In comparing the strain in two hydrocarbon molecules, it is probably fairer to compare the strain per C–C bond, because other things being equal, in a bigger molecule the strain is more dispersed. Thus cubane, with six cyclobutane rings and twelve C–C bonds, has a strain energy of 622 kJ mol^{-1} [162], while cyclobutane, with only one ring and four C–C bonds, has a strain energy of 110.0 kJ mol^{-1} [157]. With the raw numbers, cubane is 5.7 times as strained as cyclobutane. On a per-C–C-bond basis however, the strain energy of cubane and cyclobutane are $622/12 = 52$ kJ mol^{-1} and $110.0/4 = 27.5$ kJ mol^{-1}; using *these* numbers, cubane is effectively only about twice as strained as cyclobutane. The role of strain in connection with kinetic and thermodynamic stability has been discussed for polyprismanes and superstrained C$_5$ molecules [163]. Calculations of the kind we have done here are approximations to 0 K enthalpy changes (because ZPE and thermal energy increases on going above 0 K are ignored). The importance of an appropriate choice for the reference molecules has been emphasized with calculations on substituted cyclohexanes, where instead of acyclic references, a series of lesser-substituted cyclohexanes was referred to, to obtain realistic ring-strain energies; this semi-homodesmotic method was said to properly cancel intramolecular interactions [164]. Previous isodesmic-type (homodesmotic) calculations had given unrealistic and erratic results, like the strain energy of $c-C_6Cl_{12}$ ranging from 431 to -163 kJ mol^{-1}.

Aromatic Stabilization Energy, ASE We skirt the enormous literature on the meaning and detection of aromaticity [165] and assert that a good measure of the phenomenon is the aromatic stabilization energy, the energy rise when an aromatic ring is opened isodesmically [166]. This gives consistent results in an incrementally varying series of compounds [167]. Let's apply this approach to benzene using the same kind of equation as we did for cyclopropane and for norbornane, above, continuing with B3LY/6–31G* energies/geometries. We should think in terms of the numbers of sp^2–sp^2 C-C bonds and sp^2 C-H bonds, rather than view benzene as having three double and three single C-C bonds, although we will use the useful Kekulé structure. Here we have 8 sp^2–sp^2 C–C bonds and 14 sp^2 C–H bonds on each side; we break an sp^2–sp^2 C–C bond and make an sp^2–sp^2 C–C bond, effecting this by breaking and making and making two sp^2 C–H bonds:
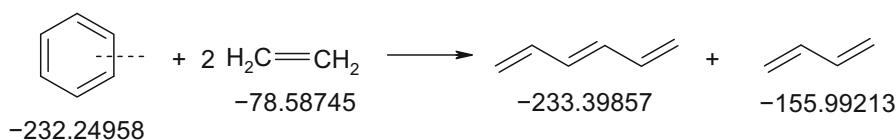
Loss of aromaticity must correspond to an endothermic process (since aromaticity is stabilizing) and we take the ASE as being positive for an aromatic compound, so this quantity is the energy of the products minus that of the reactants. If the molecule being opened were strained, that would have to be taken into account, for example by an extrapolation method [168] or by balancing the strain on both sides of the equation, as in the oxirene calculation below. The ASE is calculated here thus:

$$ASE = [-233.39857 - 155.99213] - [-232.24958 + 2(-78.58745)]$$
$$= -398.39070 + 389.42448 = 0.03378 = 89 \text{ kJ mol}^{-1}$$

There is no single correct isodesmic reaction for studying a phenomenon; another reasonable, although conceptually less straightforward, reaction for obtaining an ASE for benzene is:
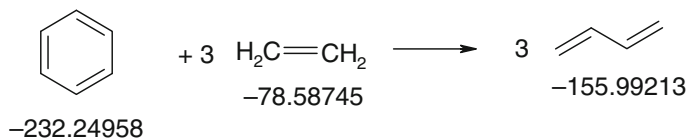
This too satisfies our isodesmic criterion, because on both sides of the equation we have nine sp^2–sp^2 C–C bonds and 18 sp^2 C–H bonds. This equation gives:

$$ASE = [3(-155.99213)] - [-232.24958 + 3(-78.58745)]$$
$$= -467.97639 + 468.01193 = 0.03554 = 93 \text{ kJ mol}^{-1}$$

Isodesmic reactions have also been applied to heteroatom analogues of benzene [167, 169]. Like our strain energy calculations, these energy changes are approximations to 0 K enthalpy changes (we ignored ZPE and thermal energy increases on

going above 0 K). Isodesmic reactions and other aspects of the energetics of benzene, cyclobutadiene and related compounds have been reviewed by Slayden and Liebman [170]. Schleyer and Puhlhofer discuss various isodesmic schemes and recommend for calculating resonance energies (which we take here as being aromatic stabilization energies) isomerization methyl/methylene reactions like [171]:
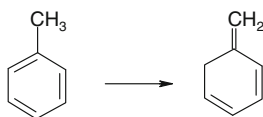
They consider the resonance energy of benzene from reasonable isodesmic reactions to be ca. 125 kJ mol^{-1}. Mo has reviewed the various ways of assigning resonance energy to benzene and studied the problem with the valence bond method [172].

Now we turn from benzene to another formally cyclically delocalized molecule, oxirene or oxacyclopropene [173]. Is oxirene stabilized or destabilized by its π-electron system? We can answer this question using an isodesmic equation, with B3LYP/6–31G* energies/geometries as usual. Here we try to cancel out the strain in oxirene by having on each side of the equation about the same amount of ring strain (on each side two sp^2 C–O bonds, etc.):

$$-152.46609 \qquad -194.03545 \qquad -116.61905 \qquad -229.93969$$
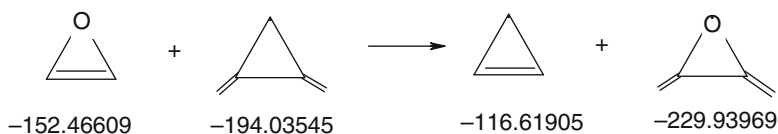
$$\begin{aligned} ASE &= [-116.61905 - 229.93969] - [152.46609 - 194.03545] \\ &= -346.55874 + 346.50154 = -0.05720 = -150 \text{ kJ mol}^{-1} \end{aligned}$$

We calculated the ASE as product energies minus reactant energies, as we did for benzene, and it came out negative, which means that the aromatic "stabilization" energy here is really destabilizing: oxirene is antiaromatic [174].

One has to be careful with balancing bonds in isodesmic reactions. Consider this equation:

$$-232.24958 \qquad -235.87949 \qquad -234.64832$$
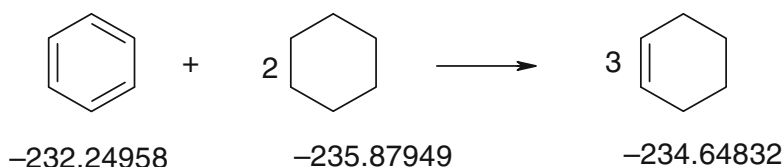
$$\begin{aligned} \text{Here ASE} &= [3(-234.64832] - [-232.24958 + 2(-235.87949)] \\ &= -703.94496 + 704.00856 = 0.06360 = 167 \text{ kJ mol}^{-1} \end{aligned}$$

This seems unreasonably big: above, we got 89 and 93 kJ mol^{-1} for the benzene ASA. Yet the equation seems at first sight reasonable: on each side 3 C=C, 15 C–C, and 30 C–H bonds. But actually the numbers of each kind of bond differ at the hybridization level; for example, the reactants have six sp^2–sp^2 C-C bonds but the products have only three of these. Overall, we are converting stronger bonds into weaker ones, and part of the rise in energy is due to this, rather than to loss of aromatic stabilization, inflating the supposed ASE. Another example of an ill-chosen isodesmic-type reaction is illustrated by Slayden and Liebman, where benzene seems to have an ASE of 270 kJ mol^{-1} (!) [170]:

$$C_6H_6 + 6CH_4 \rightarrow 3H_2C = CH_2 + 3H_3C - CH_3$$
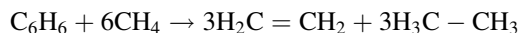
(Our B3LYP/6–31G* energy/geometry method gives 286 kJ mol^{-1}). This shows the need to choose isodesmic-type reactions judiciously, and helps to explain the profusion of methods and terms [159]. The only "perfect" isodesmic reaction would be an identity reaction, which would be useless.

5.5.2.3.2 Thermodynamics; High-Accuracy Calculations

As the previous discussion suggests (Sect. 5.5.2.3.1), the calculation of good relative energies is much more challenging than the calculation of good geometries. Nevertheless, it is now possible to reliably calculate energy differences to within about ±10 kJ mol^{-1}. An energy difference with an error of ±10 kJ mol^{-1} is said to be within *chemical accuracy*. The term seems to have been first used in connection with computational chemistry in 1984 by Moskowitz and Schmidt ("Can Monte Carlo Methods Achieve Chemical Accuracy?") [175] and was popularized by Pople (biographical footnote Sect. 5.3.3) in connection with the G1 and G2 (see below) methods. Around the time these pioneering high-accuracy methods were being developed, the term appeared in the title of a review by Bauschlicher and Langhoff [176]. An accuracy of about 2 kcal mol^{-1} (8.4 kJ mol^{-1}, rounded here to 10 kJ mol^{-1}) was set by Pople and coworkers in 1989 for the G1 method [177] as a realistic and chemically useful goal, perhaps because this is small compared to typical bond energies (roughly 400 kJ mol^{-1}), and comparable or superior to typical experimental errors. The ab initio energies and methods needed for results of chemical accuracy are called *high-accuracy* (or multistep, or multilevel, or high-accuracy multistep) energies and methods. These seem to have raised the bar, for in their application to thermochemistry the term "chemical accuracy" has been said to mean ca. 4 kJ mol^{-1} (1 kcal mol^{-1}) – see below.

As one might expect, high-accuracy energy methods are based on high- level correlational methods and big basis sets. However, because the straightforward application of such computational levels would require unreasonable times (be very "expensive" in the language of pre-personal computer days), the calculations are broken up into several steps, each of which provides an energy value; summing these gives a final energy close to that which would be obtained from the more unwieldy one-step calculation. There are two classes of widely-used high-accuracy

energy methods: the *Gaussian methods*, which originated in the Pople group and derive their names from being first available as keywords in the Gaussian series of computational chemistry suites [178], and the *complete basis set methods*, which come from Petersson's group.

The Gaussian Methods

The key to these methods is the use of high correlation levels and big basis sets. This series began in 1989 with (note: by G1 to G4 here is meant methods, not versions of the Gaussian suite of programs) Gaussian 1, G1 [177], continued with G2 (1991) [179] and G3 (1998) [180], and saw the publication (2007) of G4 [181]. G1 and G2 are obsolete. The most popular Gaussian high-accuracy methods at present are probably G4 and G3 and their faster but nearly as accurate variants, G4(MP2) [182] and G3(MP2) [183]. Continued use of G3 and G3(MP2) (rather G4 and G4(MP2)) may be justified by the desire to compare some current work with the body of results accumulated with these somewhat older methods).

For G3 the average absolute deviation from experiment is 1.13 kcal mol^{-1} (4.7 kJ mol^{-1}) and for G3(MP2) 1.2–1.3 kcal mol^{-1} (5.0–5.4 kJ mol^{-1}), and G3 (MP2) seems to be 7–8 times as fast as G3 [183]. Curtiss et al. give the details of the G4 [181] method and compare it with G3 and to some extent G1 and G2. They report that "...the average absolute deviation from experiment shows significant improvement from 1.13 kcal/mol [4.7 kJ mol^{-1}] (G3 theory) to 0.83 kcal/mol [3.5 kJ mol^{-1}] (G4 theory)". G4 is about 2–3 times as slow as G3. To speed up the G4 method, its MP4 steps were replaced with MP2 and MP3 (Sect. 5.4.2) giving G4(MP2) and G4(MP3) [182]. These have respectively average absolute deviations from experiment of 1.04 kcal/mol [4.35 kJ mol^{-1}] and 1.03 kcal/mol [4.3 kJ mol^{-1}]. The G4(MP2) method appears overall to be the better of the two; it is 2–3 times as fast as G3 and although about twice as slow as G3(MP2) (see below), Curtiss et al. say [182] "Overall, the G4(MP2) method provides an accurate and economical method for thermodynamic predictions". It has an overall accuracy for the G3/05 test set of molecules that is significantly better than G3(MP2) theory (1.04 vs 1.39 kcal/mol) [4.35 vs 5.8 kJ mol^{-1}] and even better than G3 theory (1.04 vs 1.13 kcal/mol) [4.35 vs 4.7 kJ mol^{-1}]. G4(MP2) was said to perform "reasonably well" for the thermochemistry of transition metals, species that present special problems for computational chemistry [184]. G4(MP2) and G3(MP2) can handle molecules with up to about 16 heavy atoms. See Table 5.10.

Because the G4(MP2) method [182] is far faster and almost as accurate (see below) as the G4 [181], the steps in the G4(MP2) will be summarized here. A G4(MP2) calculation, invoked in Gaussian 09 simply with the keyword G4MP2, reports seven steps:

1.   A density functional (Chap. 7) B3LYP/6–31G(2df,p) geometry optimization. All subsequent calculations are on this geometry.
      geometry optimization, to get a structure for a frequency calculation
2.   A B3LYP/6–31G(2df,p) frequency calculation on the optimized geometry to get the ZPE (which is then scaled by 0.9854). Subsequent calculations are for high-level estimates of electron correlation.

3.   An energy calculation, CCSD(T)/6–31G*. This is followed by three
            energy corrections, in steps 4, 5 and 6:
4.   An MP2 energy calculation with a special large basis set..
5 and 6.   Two HF calculations with modified aug-cc-pVTZ and aug-cc-pVQZ basis
            sets, to extrapolate to the basis set limit (for applying the correlation
            corrections to this).
7.   Finally, a high level correction (HLC) with six empirical parameters is
            added to minimize any remaining insufficiencies in the electron correla-
            tion treatment.

These seven steps are used to assemble a molecular energy as the sum of various
energy differences and a final empirical energy increment (the "higher level
correction") based on the number of paired and unpaired electrons. The G4(MP2)
energy is essentially a kind of CCSD(T)/6–31G* energy performed on a B3LYP/
6–31G(2df,p) geometry, with a B3LYP/6–31G(2df,p) scaled-ZPE and an empirical
energy correction, but such a *direct* calculation would be slower than breaking it
into the steps used here.

   One way G4(MP2) saves time is by replacing an MP3 and an MP4 calculation
with an MP2 one. A key improvement in G4/G4(MP2) over G3/G3(MP2) is the
replacement of the quadratic CI correlation method by the coupled cluster method
(Sect. 5.4.3); this particular change did not alter the accuracy for the test set of
molecules, but it presumably improves the reliability, as ". . .the QCISD(T) method
has rather dramatic failures, which does not occur with the CCSD(T) method"
[181]. See too Hrusak et al. for a comparison of quadratic CI and coupled-cluster
[103]. In the G3(MP2) method, the main change from G3 is that MP2 calculations
replace MP4 ones [183].

   Because of the empirical energy corrections in the Gaussian multistep methods,
they are not fully ab initio, but rather somewhat semiempirical, except when these
corrections cancel out. This cancelling happens, for example, in calculating proton
affinities as the energy difference of the protonated and unprotonated species,
where the spin-orbit corrections and the number of α- and β-spin electrons are the
same on both sides of the equation. We shall take G4(MP2) as the Gaussian method
of choice, with a good compromise between accuracy and speed, but we will also
refer to G3(MP2) calculations, because of their competitive speed and accuracy and
their widespread legacy. These Gaussian methods, and others not mentioned here,
as well as the CBS methods (below) are reviewed (2012) by Peterson, Feller and
Dixon, with the accent on thermochemistry, structures and frequencies; these
authors recognize ca. 4 kJ mol^{-1} (1 kJ mol^{-1}) as accepted chemical accuracy in
thermochemistry [185]. Here is a comparison of Gaussian methods and a CBS
method, using 1,4-benzoquinone (*p*-benzoquinone, $O=C_6H_4=O$) and showing
times (done on a 2013 vintage computer) and, as an indication of accuracy,
enthalpies of formation calculated by the atomization method (Sect. 5.5.2.3.3);
note that the G4 calculation took nine times as long (160/18) as the G4(MP2), and
both gave almost the same enthalpy of formation:

Enthalpy of formation, kJ mol^{-1} and times, minutes/relative times

G4	−117.5	160/21
G4(MP2)	−118.5	18/2.4
G3	−118.6	24/3.2
G3(MP2)	−120.0	7.5/1
CBS-QB3	−115.9	16/2.1

The accepted literature enthalpy of formation is −122.6 ± 3.8 kJ mol^{-1} [186]. The first four calculated values accommodate the experimental value to within 1 kJ mol^{-1}, however the CBS-QB3 value is 3 kJ mol^{-1} above the higher estimated error. But one should not generalize from a sample of one compound.

The CBS Methods

The key to these methods is the extrapolation of the basis set to an infinite limit (to completion). There are three basic CBS methods: CBS-4 (for fourth-order extrapolation), CBS-Q (for quadratic CI) and CBS-APNO (for asymptotic pair natural orbitals, referring to extrapolation to the basis set limit), in order of increasing accuracy (and increasing computer time) [113]. These methods are available with keywords in the Gaussian 94 and later Gaussian programs, where the preferred versions of CBS-4 and CBS-Q are specified by the keywords CBS-4M [187a] and CBS-QB3 [187b] (M for minimum population localization, B3 for use of the B3LYP density functional). CBS-4M can handle molecules with up to about 19 heavy atoms and its has its "largest errors in the neutral heats of formation . . . for ClF3 (13.6 kcal/mol), O3 (12.6 kcal/mol), and C_2Cl_4 (11.0 kcal/mol)" but "these errors are systematic and their effect may be greatly reduced by the use of isodesmic bond additivity corrections." [187a]. More typical CBS-4M errors are (mean absolute deviation from experiment) 3.26 kcal mol^{-1} (13.6 kJ mol^{-1}) [187a]. There is a modification of CBS-4M designed to decrease the accumulation of errors with increasing molecular size [188]. CBS-QB3 can handle molecules with up to about 13 heavy atoms and has a mean absolute deviation from experiment of 1.10 kcal mol^{-1} (4.6 kJ mol^{-1}) [187b]. CBS-APNO can handle molecules with up to about 7 heavy atoms and has a mean absolute deviation from experiment of 0.53 kcal mol^{-1} (2.2 kJ mol^{-1}) [113]. See Table 5.10.

Complete basis set methods [113] involve essentially seven or eight steps:

1. A geometry optimization (at the HF/3–21G$^{(*)}$ or MP2/6–31G* level, depending on the particular CBS method).
2. A ZPE calculation at the optimization level.
3. An HF single-point calculation with a very big basis set (6–311 + G(3d2f,2df,p) or 6–311 + G(3d2f,2df,2p), depending on the particular CBS method).
4. An MP2 single-point calculation (basis depending on the particular CBS method).
5. Something called a *pair natural orbital extrapolation* to estimate the error due to using a finite basis set.
6. An MP4 single-point calculation.

7. For some CBS methods, a QCISD(T) single-point calculation.
8. One or more empirical corrections.

Note, as with Gaussian methods, the semiempirical aspect of CBS methods.

Comparison of High-Accuracy Multistep Methods

We will concentrate on Gaussian-type and CBS methods, because these have been the most widely-used and have thus accumulated an archive of results, are the most accessible, and because several versions of them are available. However, there are other high-accuracy multistep methods, such as the Weizmann procedures of Martin and de Oliveira, W1 and W2 [189], and of Boese et al., W3 and W4 [190a] and the faster modifications of these like W2X and W3X-L of Chan and Radom [190b], which like the CBS methods are based on basis set extrapolation. W1 and W2 have a mean absolute deviation for relative energies of about 1 kJ mol^{-1} (not 1 kcal mol^{-1}), and incorporate relativistic effects, and W2 has no empirical parameters, unlike the Gaussian and CBS methods. W3 and W4 methods have similar errors to W1 and W2, and the authors speculate on the reasons for the obstinate "0.1 kcal/mol barrier". Some of these Weizmann methods (W1, W2X, W1X-1, W1X-2), can be used for molecules with up to 10 or 12 heavy atoms. See the review of high-accuracy multistep methods by Peterson et al. [185]. Note: the lead author of this review is Professor K. A. Peterson of Washington State University; the CBS methods come primarily from the research group of Professor G. A. Petersson (different spelling) of Wesleyan University; both researchers are active in computational quantum thermochemistry.

Of the Gaussian-type and CBS methods, for high accuracy on very small molecules CBS-APNO is the appropriate choice, and for "large" molecules the choice falls on CBS-4M with the acceptance of the possibility of moderately large errors. For intermediate size molecules the best choice is probably between G4(MP2) and CBS-QB3. Recall that G4(MP2) is much faster than G4, with little loss of accuracy in most cases. Within these confines, the question will then be whether to use G4(MP2) or CBS-QB3. Which one, if either, has the edge can be found only by comparing calculations with experiment for the properties and the kinds of molecules of interest. Here are a few examples of studies using these methods. Pokon et al. compared CBS-QB3, CBS-APNO, and G3 (this latter being presumably similar to G3(MP2) and a bit less accurate than G4(MP2) for such calculations) for the enthalpies and free energies of gas-phase deprotonation reactions and found that "The combination of high accuracy and relatively low computational cost makes the CBS-QB3 method the best choice of the three" (all three gave a mean absolute deviation from experiment of about 1 kcal mol^{-1}, i.e. about 4 kJ mol^{-1}) [191]. Bond compared G2, G2(MP2), G3, G3(MP2), G3(B3), G3(MP2B3), CBS-QB3, and DFT for the calculation of enthalpies and free energies of formation of nearly 300 organic compounds and found G3 to be best with G3 (MP2) a little worse; CBS-QB3 was also accurate but more limited in the size of

molecules it could handle [192]. The mean absolute deviations for those three methods using an isodesmic reaction (see Sect. 5.5.2.3.3) were (kJ mol^{-1}):

	Enthalpy	Free energy
G3	3.1	3.7
G3(MP2)	3.2	4.1
CBS-QB3	4.5	5.6

Other work by Bond also showed little difference between enthalpies of formation by isodesmic-type reactions from the G3 and the G3(MP2) methods [193]. Ess and Houk found CBS-QB3 to be satisfactory for the activation enthalpies of pericyclic reactions [194], which is noteworthy because the high-accuracy methods we are discussing were designed to give good results for thermodynamics, not kinetics; the problem here lies in the parameterization, particularly for paired and unpaired spins, the number of which might alter along a reaction coordinate [195]. However, CBS-QB3 has been explicitly stated to be suitable for activation energies [187b]. An indication of the speed and size capacities of G4(MP2), G3(MP2) and CBS-4M, CBS-QB3, and CBS-APNO is given in Table 5.10.

5.5.2.3.3   Thermodynamics; Calculating Enthalpies of Formation

A discussion of enthalpy and other flavors of energy was given in Sect. 5.5.2.3.1. The enthalpy of formation (heat of formation; enthalpy is a better word than heat here since it is more precisely defined in this context: see Sect. 5.5.2.3.1) of a compound is an important thermodynamic quantity, because a table of enthalpies of

Table 5.10 Comparison of speed and ability to handle molecular size for five popular high-accuracy multistep methods: G4(MP2), G3(MP2), CBS-4M, CBS-QB3, and CBS-APNO

Time, minutes or hours						
Molecule	N(heavy)[a]	G4(MP2)	G3(MP2)	CBS-4M	CBS-QB3	CBS-APNO
CH3COO$^-$	4	5.5 m	1.1 m	0.9 m	2.2 m	22 m
CH2FCOO$^-$	5	8.9 m	2.0 m	0.9 m	4.2 m	45 m
CHF2COO$^-$	6	12 m	4.8 m	1.1 m	7.0 m	3.4 h
CF3COO$^-$	7	18 m	5.7 m	1.6 m	15 m	2.9 h
C2F5COO$^-$	10	80 m	37 m	5.4 m	89 m	failed
C3F7COO$^-$	13	4.3 h	7.1 h	5.8 m	6.9 h	failed
C4F9COO$^-$	16	13.2 h	25.1 h	26 m	failed	failed
C5F11COO$^-$	19	failed	failed	55 m	failed	failed
C6F13COO$^-$	22	failed	failed	failed	failed	failed

The calculations were done with the G09 program suite on a computer with a 64-bit 3.40 GHz Intel Core 2 Duo Quad CPU, 16 GB RAM, and 1.8 TB diskspace, running under Windows 7. They reflect the times and size limitations of these methods on a well-equipped personal computer as of ca. mid-2013. The use of anions here is adventitious, stemming from another project. Input geometries were Merck Molecular Force Field, Cs symmetry, zigzag carbon chain
[a]N(heavy) is the number of heavy (non-hydrogen) atoms

formation of a limited number of compounds enables one to calculate the enthalpies of reaction (heats of reaction) of a great many processes, that is, how exothermic or endothermic these reactions are. The enthalpy of formation of a compound at a specified temperature T is defined [196] as the standard enthalpy of reaction (standard heat of reaction) for formation of the compound at T from its elements in their standard states (their reference states). By the standard state of an element we mean the thermodynamically stablest state at 10^5 Pa (standard pressure, about normal atmospheric pressure), at the specified temperature. The exception is phosphorus, for which the standard state is white phosphorus; although red phosphorus is stabler under normal conditions, these allotropes are apparently somewhat ill-defined. The specified temperature is usually 298.15 K ("room temperature"). The enthalpy of formation of a compound at a specified temperature is thus the amount of heat energy (enthalpy) that must be put into the reaction at that temperature to make the compound from its elements in their normal (room temperature and atmospheric pressure) states; it is the "heat content" or enthalpy of the compound compared to that of the elements. For example, at 298 K the enthalpy of formation of CH_4 is -74 kJ mol^{-1}, and the enthalpy of formation of CF_4 is -933 kJ mol^{-1} [197]. To make a mole of CH_4 from solid graphite (carbon in its standard state at 298 K) and hydrogen gas (dihydrogen) requires -74 kJ, i.e. 74.9 kJ are given out – the reaction is mildly exothermic. To make a mole of CF_4 from solid graphite and fluorine gas requires -933 kJ, i.e. 933 kJ are given out–the reaction is strongly exothermic. In some sense CF_4 is thermodynamically much stabler with respect to its elements than is CH_4 with respect to its elements, in their standard states. Note that the standard enthalpy of formation of an *element* is zero, since the reaction in question is the formation of the element from the element, in the same state (no reaction). Enthalpy of formation is denoted $\Delta H_f^\ominus$ and enthalpy of formation at, say, 298 K by $\Delta H_{f298}^\ominus$, "delta H sub f standard at 298 K". The delta indicates that this is a difference (enthalpy of the compound minus enthalpy of the elements) and the superscript denotes "standard".

There are extensive tabulations of experimentally-determined heats of formation, mostly at 298 K. One way to determine $\Delta H_{f298}^\ominus$ is from heats of combustion: burning the compound and measuring calorimetrically the heat evolved enables one to calculate the enthalpy of formation (for a C, H, O compound, anyway). $\Delta H_{f298}^\ominus$ can also be obtained by ab initio calculations. This is valuable because (1) it is far easier and cheaper than doing a thermochemical experiment, (2) many compounds have not had their enthalpies of formation measured and tabulated, and (3) highly reactive compounds, or valuable compounds available only in very small quantity, cannot be subjected to the required experimental protocol, e.g. combustion. Let's see how enthalpies of formation can be calculated.

Atomization Method

By far the most frequent temperature quoted for the enthalpy of formation of a compound is the standard "room temperature", 298.15 K. Suppose we want to calculate the enthalpy of formation of methanol. We will now see a detailed

calculation of the enthalpy of formation, first at 0 K($\Delta H_{f0}^{\ominus}$) and then the adjustment of this to 298 K. After this instructive calculation, a much shorter calculation giving $\Delta H_{f298}^{\ominus}$ directly is shown.

Figure 5.26 shows the principle behind what has been called the "atomization" method [198]. Methanol is (conceptually) atomized at 0 K into carbon, hydrogen and oxygen atoms, in their ground electronic states. The elements in their normal, unatomized states are also used to make these atoms, and to make methanol. The enthalpy of formation of methanol at 0 K follows from equating the energy (the enthalpy, to be precise) needed to generate the atoms (in their ground electronic states) from the elements via methanol ($\Delta H_{f0}^{\ominus}(CH_3OH) + \Delta H_{a0}^{\ominus}(CH_3OH)$) to that needed to make them *directly* from the elements in their normal states:

$$\Delta H_{f0}^{\ominus}(CH_3OH) + \Delta H_{a0}^{\ominus}(CH_3OH) = \Delta H_{f0}^{\ominus}\left(C(^3P) + 4H(^2S) + O(^3S)\right)$$

i.e.

$$\Delta H_{f0}^{\ominus}(CH_3OH) = \Delta H_{f0}^{\ominus}\left(C(^3P) + 4H(^2S) + O(^3S)\right) - \Delta H_{f0}^{\ominus}(CH_3OH) \quad (5.190)$$

$\Delta H_{a0}^{\ominus}(CH_3OH)$ is the 0 K ab initio atomization enthalpy of methanol, the enthalpy difference between the atoms and methanol. There are a couple points to note about this conceptual scheme. We are converting into carbon atoms graphite, a polymeric material, so strictly speaking Fig. 5.26 should show $n\,C(graphite) \rightarrow n\,C(^3P)$, where n is a number large enough to represent the *substance* graphite rather than just an atom. All the species in the figure will then be increased in number by a factor of n, but division by this common factor will still give us Eq. (190). Another point is that although hydrogen and oxygen are solids at 0 K, we are considering isolated molecules being atomized.
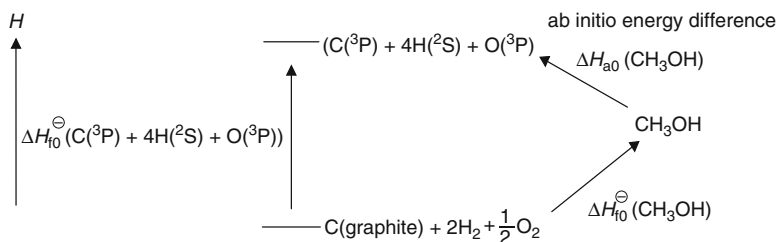
Fig. 5.26 The principle behind the ab initio calculation of heat of formation (enthalpy of formation) by the atomization method. Methanol is (conceptually) atomized at 0 K into carbon, hydrogen and oxygen atoms; the elements in their standard states are also used to make these atoms, and to make methanol. The heat of formation of methanol at 0 K, $\Delta H_{f'0}^{\ominus}(CH_3OH)$, follows from equating the energy needed to generate the atoms via methanol ($\Delta H_{f'0}^{\ominus}(CH_3OH) + \Delta H_{a0}^{\ominus}(CH_3OH)$) to that needed to make them directly from the elements in their standard states. The diagram is not meant to imply that methanol *necessarily* lies above its elements in enthalpy

To calculate $\Delta H_{f0}^{\ominus}(CH_3OH)$ we need the 0 K enthalpy of formation of C, H and O atoms, i.e. the atomization enthalpies of graphite, molecular hydrogen, and molecular oxygen, and the 0 K atomization enthalpy of methanol. The atomization enthalpies of hydrogen and oxygen can be calculated ab initio, but not reliably accurately that of graphite, which is a very big "molecule". For consistency we will use experimental values of all three elemental atomization enthalpies, as recommended [198]. From Eq. (5.191), the 0 K atomization enthalpy of methanol is simply the ab initio enthalpies of its constituent atoms minus the ZPE-corrected ab initio enthalpy of methanol:

$$\Delta H_{a0}^{\ominus}(CH_3OH) = \Delta E_{0K}^{total}\left(C\left(^3P\right) + 4H\left(^2S\right) + O\left(^3S\right)\right) - \Delta E_{0K}^{total}(CH_3OH)$$

$$(5.191)$$

Experimental values of 0 K atomization enthalpies $\Delta H_{f0}^{\ominus}C(^3P)$, $\Delta H_{f0}^{\ominus}H(^2S)$, and $\Delta H_{f0}^{\ominus}O(^3S)$ (as well as $\Delta H_{f0}^{\ominus}$ for other atoms, and references to more extensive tabulations) are given in [198]; in kJ mol^{-1}:

C	711.2
H	216.035
O	246.8

To calculate $\Delta H^{\ominus}_{a0}(CH_3OH)c$ we need (Eq. (191)) ΔE_{0K}^{total} for C, H and O atoms in the electronic states shown and for methanol. Instead of the G2 method that was employed by Nicolaides et al. [198] and was used here (from the Gaussian 94 program suite [199]) in earlier editions of this book, we now use the G4(MP2) method in Gaussian 09 [178]. We get these values (hartrees) for the G4(MP2) 0 K enthalpies of the atoms and the molecule:

C	−37.79420
H	−0.50209
O	−75.00248
CH$_3$OH	−115.57107

The methanol value of −115.57107 h could be called the "absolute" 0 K enthalpy of methanol, the enthalpy relative to that of the dissociated nuclei and electrons (cf. the zero-energy reference point of an ab initio energy, explained following Eq. (5.93)); this is shown at the end of any Gaussian-suite geometry optimization/frequency calculation (although only for very high-accuracy calculations is the value suitable for accurate atomization enthalpy determinations). This absolute enthalpy will be used in the calculation of the enthalpy of formation.

From Eq. (191) the calculated atomization energy of methanol at 0 K is:

$$\Delta H_{a0}^{\ominus}(CH_3OH) = -37.79420 + 4(-0.50209) - 75.00248 - (-115.57107) \text{ h}$$
$$= -114.80504 + 115.57107 \text{ h} = 0.76603 \times 2625.5 \text{ kJ mol}^{-1}$$
$$= 2011.2 \text{ kJ mol}^{-1}$$

From Eq. (190) the 0 K enthalpy of formation of methanol is:

$$\Delta H_{f'0}^{\ominus}(CH_3OH) = 711.2 + 4(216.035) + 246.8 - 2011.21 \text{ kJ mol}^{-1}$$
$$= 1822.1 - 2011.2 \text{ kJ mol}^{-1} = -189.1 \text{ kJ mol}^{-1}$$

Reference [198] gives the 0 K G2 value by the atomization method as -195.7 kJ mol^{-1} and the experimental value (from two sources) as -190.7 or -189.8 kJ mol^{-1}, in essentially perfect agreement with the G4(MP2) value calculated here. Any inaccuracy in the calculated atomization energy will show up correspondingly in the enthalpy of formation, and only a good high-accuracy method can reliably mitigate this error.

To adjust the 0 K enthalpy of formation to that at 298.15 K we add the increase in enthalpy of methanol on going from 0 K to 298 K and subtract the corresponding increases for the elements in their standard states. The value for methanol is the difference of two G4(MP2) quantities (298 K and 0 K) provided in the thermochemical summary at the end of the G4(MP2) calculation as implemented in Gaussian 09. Increase in enthalpy of methanol on going from 0 K to 298 K:

$$\Delta\Delta H^{\ominus}(CH_3OH) = G4(MP2) \text{ Enthalpy (i.e. at 298 K)} - G4(MP2)(0 \text{ K})$$
$$= -115.56679 - (-115.57107) \text{ h}$$
$$= 0.00428 \times 2625.5 \text{ kJ mol}^{-1}$$
$$= 11.24 \text{ kJ mol}^{-1}$$

G4(MP2) (0 K) is the G4(MP2) value for what we have called ΔE_{0K}^{total}.

The experimental enthalpy increases for the elements are given in [198]; in kJ mol^{-1}:

$\Delta\Delta H^{\ominus}$ element

C(graphite)	1.050
H_2	8.468
O_2	8.680

From these and $\Delta\Delta H_f^{\ominus}(CH_3OH)$, the 298 K enthalpy of methanol is calculated to be (we add the increase in enthalpy of methanol on going from 0 K to 298 K and subtract the corresponding increases for the elements in their standard states):

$$\Delta H_{f298}^{\ominus}(CH_3OH) = \Delta H_{f0}^{\ominus}(CH_3OH) + \Delta\Delta H^{\ominus}(CH_3OH)$$
$$- \left(\Delta\Delta H^{\ominus}(C) + 2\Delta\Delta H^{\ominus}(H_2) + \frac{1}{2}\Delta\Delta H^{\ominus}(O_2)\right)$$
$$= -189.1 + 11.24 - \left(1.050 + 2(8.468) + \frac{1}{2}(8.680)\right) kJ\,mol^{-1}$$
$$= -189.1 + 11.2 - 22.3)\,kJ\,mol^{-1} = -189.1 - 11.1\,kJ\,mol^{-1}$$
$$= -200.2\,kJ\,mol^{-1}$$

$$(5.192)$$

The accepted 298 K experimental value [200] is -205 ± 10 kJ mol^{-1}. The calculated value is well within the estimated experimental error.

Note that if $\Delta H_{f0}^{\ominus}$ is not wanted, which it usually is not, $\Delta H_{f298}^{\ominus}$ can be calculated directly, since from Eqs. (5.190) and (5.192) the 0 K ab initio energy of the compound is subtracted out and it follows that

$$\Delta H_{f298}^{\ominus}(CH_3OH) = [\Delta H_{f0}^{\ominus}(C) + 4\Delta H_{f0}^{\ominus}(H) + (\Delta H_{f0}^{\ominus}(O))]$$
$$- \left[\Delta E_{0K}^{total} + 4\Delta E_{0K}^{total}(H) + \Delta E_{0K}^{total}(O)\right] + G4MP2\,Enthalpy(CH_3OH)$$
$$- \left[\Delta\Delta H^{\ominus}(C) + 2\Delta\Delta H^{\ominus}(H_2) + \frac{1}{2}\Delta\Delta H^{\ominus}(O_2)\right]$$
$$= [(711.2 + 4(216.035) + 246.8)]kJ\,mol^{-1}$$
$$- [(-37.79420 + 4(-0.50209) - 75.00248)]h + (-115.56679)\,h$$
$$- \left[1.050 + 2(8.468) + \frac{1}{2}(8.680)\right]kJ\,mol^{-1}$$
$$= 1822.1\,kJ\,mol^{-1}[-114.80504]h - 115.56679h - 22.33\,kJ\,mol^{-1}$$
$$= 1822.1\,kJ\,mol^{-1} - 0.76175 \times 2625.5\,kJ\,mol^{-1} - 22.33\,kJ\,mol^{-1}$$
$$= 1822.1 - 2000.0 - 22.33\,kJ\,mol^{-1} = -200.2\,kJ\,mol^{-1}$$

$$(5.193)$$

as obtained more circuitously above (Eq. (5.192)). This straightforward direct calculation of 298 K enthalpies of formation can be implemented on a spreadsheet.

Formation Method

An alternative to the atomization method is what has been called the "formation" method, which is illustrated for methanol in Fig. 5.27. This method utilizes a kind of "pseudo enthalpy of formation", $\Delta H_{f0}'(pseudo)$, of the compound from atomic carbon and molecular hydrogen and oxygen (the conventional enthalpy of formation is relative to graphite and molecular hydrogen and oxygen). From Fig. 5.27

$$\Delta H_{f0}^{\ominus}(CH_3OH) = \Delta H_{f0}^{\ominus}(C(^3P)) + \Delta H_{f0}(pseudo) \qquad (5.194)$$

where the experimental value of $\Delta H_{f0}^{\ominus}(^3C)$ is used, and
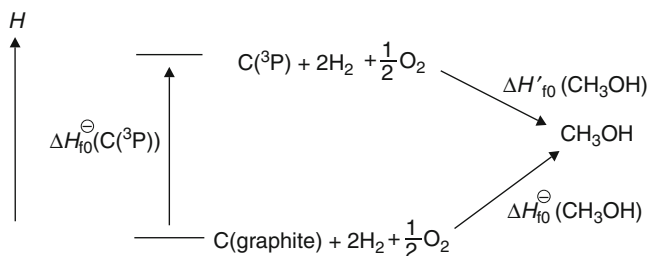
Fig. 5.27 The principle behind the ab initio calculation of heat of formation (enthalpy of formation) by the formation method. Methanol is (conceptually) formed from atomic carbon and molecular hydrogen and oxygen; the enthalpy input for this resembles that for the heat of formation of methanol (hence the name) except that atomic carbon rather than graphite is used. Graphite is converted to atomic carbon, and the elements in their normal states are also used to make methanol. The heat of formation of methanol at 0 K follows from equating this quantity to the heat of atomization of graphite plus the energy needed to make methanol from atomic carbon and molecular hydrogen and oxygen. The diagram is not meant to imply that methanol *necessarily* lies above its elements in enthalpy

$$\Delta H_{f0}^{\ominus}(\text{pseudo}) = \Delta E_{0K}^{\text{total}}(\text{CH}_3\text{OH}) - \Delta E_{0K}^{\text{total}}\left(\text{C}(^3\text{P})\right) + 2\text{H}_2 + \frac{1}{2}\text{O}_2) \quad (5.195)$$

A calculation of the 0 K enthalpy of formation of methanol using G4(MP2) gives (711.2 kJ mol^{-1} is the experimental 0 K atomization enthalpy of graphite; dioxygen here is of course triplet, the ground state):

$$
\begin{aligned}
\Delta H^{\ominus}{}_{f0}(\text{CH}_3\text{OH}) &= 711.2\,\text{kJ mol}^{-1} + \Delta H_{f0}'(\text{pseudo}) \\
&= 711.2\,\text{kJ mol}^{-1} + [-115.57107] \\
&\quad -(-37.79420 + 2(-1.17040) + \frac{1}{2}(-150.19099)\,\text{h} \\
&= 711.2\,\text{kJ mol}^{-1} + [-115.57107 + 115.23050]\,\text{h} \\
&= 711.2\,\text{kJ mol}^{-1} - 0.34058\,\text{h} \\
&= 711.2 - 0.34058 \times 2625.5\,\text{kJ mol}^{-1} \\
&= 711.2 - 894.2\,\text{kJ mol}^{-1} = -183.1\,\text{kJ mol}^{-1}.
\end{aligned}
$$

Like the atomization calculation in the previous method, the pseudo enthalpy of formation requires a good high-accuracy method. The 0 K value calculated in [198] by this procedure using the G2 method was -191.3 kJ mol^{-1}; the G4(MP2) value calculated above by the atomization method was -189.1 kJ mol^{-1}. The atomization method was said [198] to "perform somewhat better, especially for organic molecules" (the methods in that paper were all Gaussian type, G2 and G2 variants). Here the atomization method G4(MP2) 0 K enthalpy of formation (-189.1 kJ mol^{-1}, above) is indeed better than the formation method value, the experimental value being -190.7 or -189.8 kJ mol^{-1} [198].
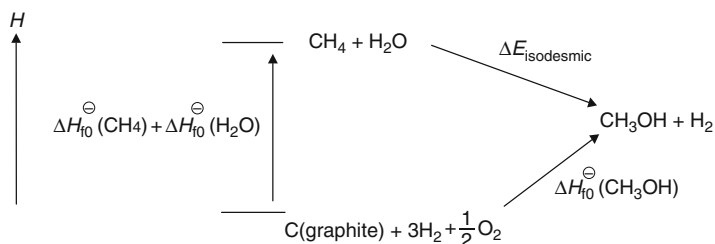
Fig. 5.28 The principle behind the ab initio calculation of heat of formation (enthalpy of formation) using an isodesmic reaction. Methanol and hydrogen are (conceptually) made from methane and water (other isodesmic reactions could be used); the 0 K enthalpy input for this is the ab initio energy difference between the products and reactants. Graphite, hydrogen and oxygen are converted into methane and water and into methanol and hydrogen, with input of the appropriate heats of formation. The heat of formation of methanol at 0 K follows from equating the heat of formation of methanol with the sum of the energy inputs for the other two processes. The diagram is not meant to imply that methanol *necessarily* lies above its elements in enthalpy

Isodesmic Reaction Method

Finally, heats of reaction can be calculated by ab initio methods with the aid of isodesmic reactions (Sect. 5.5.2.3.1), as indicated in Fig. 5.28; see reference 39 in [198]. Actually, the scheme in Fig. 5.28 is not strictly isodesmic – for example, only on one side of the "isodesmic" equation is there an H-H bond. From this scheme

$$\Delta H^{\ominus}_{f0}(CH_3OH) = \Delta H^{\ominus}_{f0}(CH_4) + \Delta H^{\ominus}_{f0}(H_2O) + \Delta E_{isodesmic} \qquad (5.196)$$

where

$$\Delta E_{isodesmic} = \Delta E^{total}_{0K}(CH_3OH + H_2) - \Delta E^{total}_{0K}(CH_4 + H_2O)$$

Using G4(MP2) values :

$$\Delta E_{isodesmic} = (-115.57107 - 1.17040) - (-40.42767 - 76.35585)\,h$$
$$= -116.74147 + 116.78352\,h = 0.04205\,h$$

With this and the experimental 0 K heats of formation of CH_4 and H_2O [198]:

$$\Delta H^{\ominus}_{f0}(CH_3OH) = -66.8 - 238.92 + 0.04205 \times 2625.5\,kJ\,mol^{-1}$$
$$= -195.3\,kJ\,mol^{-1}.$$

So the isodesmic value is ca. 6 kJ mol^{-1} lower, and the formation value ca. 6 kJ mol^{-1} higher, than the value from atomization (atomization, formation, isodesmic: -189.1, -183.1, -195.3 kJ mol^{-1}; the experimental value is -190.7 or -189.8 kJ mol^{-1} [198]).

Of the three approaches to calculating heats of formation (atomization, formation and isodesmic), the atomization was recommended over the formation,

although the isodesmic approach was said, within G2-type methods, to "In certain special cases, e.g. specific large hydrocarbons...perform better": reference 39 in [198]. One might expect the isodesmic method with carefully-chosen reactions to be at least as accurate as the other two, because of the ability of isodesmic processes to compensate for basis set and correlation deficiencies (Sect. 5.5.2.3.1). In principle isodesmic calculations do not demand high-accuracy methods for reasonably good energy differences. Indeed, for the calculation of free energies of formation, which is methodically related to enthalpies of formation but includes entropies, Bond found in his study of nearly 300 organic compounds that a kind of isodesmic reaction method gave considerably smaller errors than did the atomization method: with G3(MP2), 4.1 vs. 17.3 kJ mol^{-1}, with CBS-QB3, 5.6 vs. 13.1 kJ mol^{-1} [192]. In a related paper, these studies were said to be the "first comprehensive review of computational methodologies used to compute free energies" [193]. The atomization approach to enthalpies and free energies of formation is conceptually the most straightforward, but requires a good high-accuracy method (CBS-APNO would be very suitable were it not for its size limitations) because dissociating a molecule into its atoms makes drastic demands on the accurate treatment of correlation energy. A nice feature of the atomization method is that, unlike the use of isodesmic reactions, it is a *model chemistry*; a term apparently first used by Pople to denote a sharply-defined procedure that does not require choosing among various possibilities (like different isodesmic schemes) and which will thus not vary from one worker to another [[201]. For a collection of various approaches to calculating heats of formation see [202]. The conclusion from all this is that when the size of the molecules makes it practical, to calculate enthalpies of formation ab initio the atomization approach with the best applicable high-accuracy multistep method should probably be used, not omitting where possible a reality check against experimental values.

Note that these three calculations of enthalpy of formation are not *purely* ab initio (quite apart in from the empirical correction terms in the multistep high-accuracy methods), since they required experimental values of either the enthalpy of atomization of graphite (atomization and formation methods) or the enthalpy of formation of some molecules like methane and water (formation method). Also, adjustment from 0 K to 298 K uses experimental values for the elements. The inclusion of experimental values makes the calculation of enthalpy of formation with the aid of ab initio methods a somewhat *semiempirical* procedure (do not confuse the term as used here with semiempirical programs like AM1, discussed in Chap. 6). Augmentation with experimental data is still needed for accurate calculations when an ab initio calculation would involve an extended, solid substance like graphite (see the discussion in connection with the atomization method); other examples are phosphorus and sulfur. For estimation of solid-state enthalpies see [203]; there has been work on the ab initio calculation of enthalpies of sublimation, which is relevant to the enthalpy change in going from the solid to isolated atoms [204].

Let us briefly compare the atomization calculation of the 298 K enthalpies of formation of 1,4- and 1,2-benzoquinone by the G4(MP2) and the CBS-QB3

methods. These calculations summarize the procedure of going directly to the 298 K enthalpies of formation (i.e. without calculating first the 0 K value).

1,4-Benzoquinone (p-benzoquinone), $C_6H_4O_2$, using G4(MP2)

$\Delta H_{f0}^{\ominus}(C, {}^3P)$	$711.2\,\mathrm{kJ\,mol^{-1}}$	experimental 0 K atomization E
$\Delta H_{f0}^{\ominus}(H, {}^2S)$	$216.035\,\mathrm{kJ\,mol^{-1}}$	experimental 0 K atomization E
$\Delta H_{f0}^{\ominus}(O, {}^3P)$	$246.8\,\mathrm{kJ\,mol^{-1}}$	experimental 0 K atomization E
$\Delta E_{0K}^{total}(C, {}^3P)$	$-37.79420\,\mathrm{h}$	G4(MP2) enthalpy at 0 K
$\Delta E_{0K}^{total}(H, {}^2S)$	$-0.50209\,\mathrm{h}$	G4(MP2) enthalpy at 0 K
$\Delta E_{0K}^{total}(O, {}^2P)$	$-75.00248\,\mathrm{h}$	G4(MP2) enthalpy at 0 K
$H_{298K}(1,4-BQ)$	$-380.95376\,\mathrm{h}$	G4(MP2) enthalpy at 298.15 K
$\Delta\Delta H^{\ominus}(C, graphite)$	$1.050\,\mathrm{kJ\,mol^{-1}}$	experimental enthalpy increase, 0 K to 298 K
$\Delta\Delta H^{\ominus}(H_2)$	$8.468\,\mathrm{kJ\,mol^{-1}}$	experimental enthalpy increase, 0 K to 298 K
$\Delta\Delta H^{\ominus}(O_2)$	$8.680\,\mathrm{kJ\,mol^{-1}}$	experimental enthalpy increase, 0 K to 298 K

$$\Delta H_{f298}^{\ominus}(1,4-BQ,\ G4(MP2))$$
$$= [6(711.2) + 4(216.035) + 2(246.8)]\,\mathrm{kJ\,mol^{-1}}$$
$$\quad - [6(-37.79420) + 4(-0.50209) + 2(-75.00248)] + (-380.95376)\,\mathrm{h}$$
$$\quad - (6(1.050) + 2(8.468) + (8.680)\,\mathrm{kJ\,mol^{-1}}$$
$$= 5624.9\,\mathrm{kJ\,mol^{-1}} - [-378.77852\,\mathrm{h}] - 380.95376\,\mathrm{h} - 31.92\,\mathrm{kJ\,mol^{-1}}$$
$$= 5593.0\,\mathrm{kJ\,mol^{-1}} - [-378.77852\,\mathrm{h}] - 380.95376\,\mathrm{h}$$
$$= 2.13026\ \mathrm{h} - [-378.77852\,\mathrm{h}] - 380.95376\,\mathrm{h}$$
$$= 380.90878\ \mathrm{h} - 380.95376\ \mathrm{h} = 0.04498\ \mathrm{h},$$
$$\text{i.e. } 2625.5 \times -0.04498\ \mathrm{kJ\,mol^{-1}} = -118.1\ \mathrm{kJ\,mol^{-1}}$$

The best experimental value for the enthalpy of formation of 1,4-benzoquinone appears to be -122.6 ± 3.8 kJ mol^{-1} (-29.3 ± 0.9 kcal mol^{-1}) [186], although an overlapping value of -115.9 ± 12.6 kJ mol^{-1} has been reported [205].

1,4-Benzoquinone, using CBS-QB3

$\Delta H_{f0}^{\ominus}(C, {}^3P)$	$711.2\,\mathrm{kJ\,mol^{-1}}$	experimental 0 K atomization E
$\Delta H_{f0}^{\ominus}(H, {}^2S)$	$216.035\,\mathrm{kJ\,mol^{-1}}$	experimental 0 K atomization E
$\Delta H_{f0}^{\ominus}(O, {}^3P)$	$246.8\,\mathrm{kJ\,mol^{-1}}$	experimental 0 K atomization E
$\Delta E_{0K}^{total}(C, {}^3P)$	$-37.785377\,\mathrm{h}$	CBS-QB3 enthalpy at 0 K
$\Delta E_{0K}^{total}(H, {}^2S)$	$-0.499818\,\mathrm{h}$	CBS-QB3 enthalpy at 0 K
$\Delta E_{0K}^{total}(O, {}^2P)$	$-74.987629\,\mathrm{h}$	CBS-QB3 enthalpy at 0 K
$H_{298K}(1,4-BQ)$	$-380.861093\,\mathrm{h}$	CBS-QB3 enthalpy at 298.15 K
$\Delta\Delta H^{\ominus}(C, graphite)$	$1.050\,\mathrm{kJ\,mol^{-1}}$	experimental enthalpy increase, 0 K to 298 K
$\Delta\Delta H^{\ominus}(H_2)$	$8.468\,\mathrm{kJ\,mol^{-1}}$	experimental enthalpy increase, 0 K to 298 K
$\Delta\Delta H^{\ominus}(O_2)$	$8.680\,\mathrm{kJ\,mol^{-1}}$	experimental enthalpy increase, 0 K to 298 K

$$\Delta H^{\ominus}_{f298}(1,4-BQ, CBS-QB3)$$
$$= [6(711.2) + 4(216.035) + 2(246.8)] \text{ kJ mol}^{-1}$$
$$\quad - [6(-37.785377) + 4(-0.499818) + 2(-74.987629)]$$
$$\quad + (-380.861093) \text{ h} - (6(1.050) + 2(8.468) + (8.680) \text{ kJ mol}^{-1}$$
$$= 5624.9 \text{ kJ mol}^{-1} - [-378.68679 \text{ h}] - 380.861093 \text{ h} - 31.92 \text{ kJ mol}^{-1}$$
$$= 5624.9 \text{ kJ mol}^{-1} - 2.17430 \times 2625.5 \text{ kJ mol}^{-1} - 31.92 \text{ kJ mol}^{-1}$$
$$= 5624.9 - 5708.62 - 31.92 \text{ kJ mol}^{-1} = -115.6 \text{ kJ mol}^{-1}$$

The best experimental value for the enthalpy of formation of 1,4-benzoquinone appears to be -122.6 ± 3.8 kJ mol^{-1} (-29.3 ± 0.9 kcal mol^{-1}) [186], although an overlapping value of -115.9 ± 12.6 kJ mol^{-1} has been reported [205].

It follows from this method that to calculate the 298 K enthalpy of formation of any other $C_6H_4O_2$ compound, e.g. 1,2-benzoquinone (*o*-benzoquinone), we now need only the value for 1,4-benzoquinone and the "absolute" molecular enthalpies of the two compounds, since these are isomers:

Using the G4(MP2) value for 1,4-benzoquinone, the G4(MP2) 298 K enthalpy of formation of 1,2-benzoquinone is $\Delta H^{\ominus}_{f'298}(1,2\text{-BQ, G4(MP2)}) = \Delta H^{\ominus}_{f'298}(1,4-BQ) + [\text{enthalpy } 1,2-BQ - \text{enthalpy } 1,4\text{-BQ}]$

$$= -118.1 + [-380.94160 - (-380.95376)] \times 2625.5 \text{ kJ mol}^{-1}$$
$$= -118.1 + 0.01216 \times 2625.5 \text{ kJ mol}^{-1} = -118.1 + 31.9 \text{ kJ mol}^{-1} = -86.2 \text{ kJ mol}^{-1}$$

For the CBS-QB3 value $\Delta H^{\ominus}_{f'298}(1,2-BQ, CBS-QB3) = \Delta H^{\ominus}_{f'298}(\text{enthalpy of formation } 1,4-BQ) + [\text{enthalpy } 1,2-BQ - \text{enthalpy } 1,4-BQ]$

$$= -115.6 + [-380.848379 - (-380.861093)] \times 2625.5 \text{ kJ mol}^{-1}$$
$$= -115.6 + 33.38 \text{ kJ mol}^{-1} = -81.9 \text{ kJ mol}^{-1}$$

The best experimental value for the enthalpy of formation of 1,2-benzoquinone appears to be -87.9 ± 13.0 kJ mol^{-1} [205].

Both G4(MP2) and CBS-QB3 give reasonably satisfactory enthalpies of formation for these quinones by the atomization method.

Considerable attention has been given here to heats (enthalpies) of formation, because there are extensive tabulations of these, e.g. [206] and papers on their calculation appear often in the literature, e.g. [202]. However, we should remember that equilibria [147] are dependent not just on enthalpy differences, but also on the often-ignored entropy changes, as reflected in free energy differences, and so the calculation of entropies is also important [192, 193, 207].

5.5.2.3.4   Kinetics; Calculating Reaction Rates

Ab initio kinetics calculations are far more challenging than thermodynamics calculations. In other words, the calculation of rate constants is much more involved than that of equilibrium constants or quantities like reaction enthalpy, reaction free energy, and enthalpy of formation, which are related to equilibrium constants. Why is this so? After all, both rates and equilibria are related to the energy difference between two species: the rate constant to that between the reactant and transition state (TS), and the equilibrium constant to that between the reactant and product (Fig. 5.25). Furthermore, the energies of transition states, like those of reactants and products, can be calculated. The reason for the difference is partly because the energies of transition states are harder to calculate to high accuracy than are those of relative minima ("stable species"). Another problem is that the rate does not depend strictly on the TS/reactant free energy difference (which can often, at sufficiently high levels, be accurately calculated).

To understand the problem consider a unimolecular reaction (here B is a transition state)

$$A \rightarrow B$$

Figure 5.29 shows the potential energy surface for two reactions of this type, $A_1 \rightarrow B_1$ and $A_2 \rightarrow B_2$. The reactions have identical calculated free energies of activation. By calculated, we mean here using some computational chemistry method (e.g. ab initio) and locating a stationary point with no imaginary frequencies, corresponding to A, and an appropriate stationary point with one imaginary
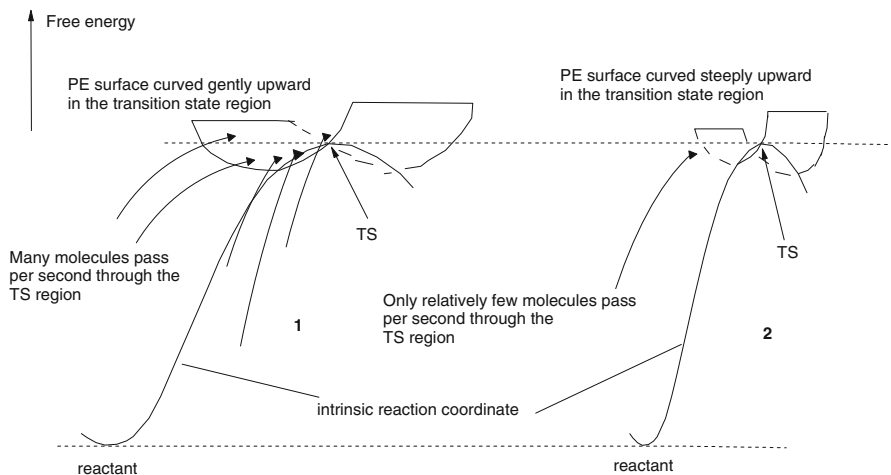
Fig. 5.29 Possible potential energy surfaces for two reactions with the same calculated free energy of activation. Reaction 1 is nevertheless faster than reaction 2 because its transition state region is flatter. As a result, in a given time more molecules can stray from the intrinsic reaction coordinate and pass through the transition state region to the product

frequency, etc. (Chap. 2, Sect. 2.5), corresponding to B. The "traditional" calculated rate constant then follows from a standard expression involving from the energy difference between the TS and reactant (our calculated free energy of activation) and the partition functions of the two species. However, in the TS region the PES for the first process is flatter than for the second process–the saddle-shaped portion of the surface is less steeply-curved for reaction 1 than for reaction 2. If all reacting A molecules followed *exactly* the intrinsic reaction coordinate (IRC; Chap. 2, Sect. 2.2; the minimum-energy path, MEP) and passed through the calculated TS species, then we might expect the two reactions to proceed at exactly the same rate, since all A_1 and A_2 molecules would have to surmount identical barriers. However, the IRC is only an idealization [208], and molecules passing through the TS region toward the product frequently stray from this path. Clearly for the reaction $A_1 \rightarrow B_1$ at any finite temperature more molecules (reflected in a Boltzmann distribution) will have the extra energy needed to traverse the higher-energy regions of this flatter saddle, away from the exact TS point, than in the case of $A_2 \rightarrow B_2$; if the saddle were curved infinitely steeply, *no* molecules could stray outside the reaction path. Thus reaction 1 must be faster than reaction 2, although they have identical computed free energies of activation; the rate constant for reaction 1 must be bigger than that for reaction 2. The difficulty of obtaining good rate constants from accurate calculations on just two PES points, the reactant and the TS, is mitigated by the fact that the vibrational frequencies of the TS sample the curvature of the saddle region both along the reaction path (this curvature is represented by the imaginary frequency) and at "right angles" to the reaction path (represented by the other frequencies). High frequencies correspond to steep curvature. So when we use the TS frequencies in the partition function equation for the rate constant we are, in a sense, exploring regions of the PES saddle other than just the stationary point. The role of the curvature of the PES in affecting reaction rates is nicely alluded to by Cramer, who also shows the place of partition functions in rate equations [209].

Another way to calculate rates is by *molecular dynamics* [210]. Molecular dynamics calculations use the equations of classical physics to simulate the motion of a molecule under the influence of forces; in general the required force fields can be computed by ab initio methods or, for large systems, semiempirical methods (Chap. 6) or molecular mechanics (Chap. 3). For investigating chemical reactions, which involve breaking and making bonds, a quantum-mechanical method, not molecular mechanics, must be used. In a molecular dynamics simulation of the reaction $A \rightarrow B$, molecules of A are "shaken" out of their potential well, and some pass through the saddle region. A shaken mechanical model with a molded surface and ball-bearing molecules would represent an analogue of the computer simulation. At a given temperature, the rate of passage of molecules (or ball bearings) through the saddle region will depend on the height of this region *and* on its curvature. The shape of the hypersurface is a function of atomic coordinates

$$E = f(q_1, q_2, \ldots)$$

The hypersurface can be found by fitting to a finite number of calculated points, or it can be calculated "on the fly". The function E can in favorable cases be used to calculate reliable rate constants. The situation can be complicated by quantum mechanical tunnelling [211], which, particularly where light atoms like hydrogen move, can speed up a reaction by orders of magnitude compared to classical predictions. Furthermore, since 1992 [212] it has been shown by molecular dynamics that the traditional concept of a potential energy surface with a straightforward intrinsic reaction coordinate (minimum energy path) may in some cases be inadequate and even incorrect. Briefly, reacting molecules sometimes move on to a plateau region or a "bifurcated" region of the surface and then head toward products in directions determined by their internal motions; the details can be "quite complex" [213]. Such surfaces are probably exceptional and the traditional picture of Chap. 2 seems likely to be applicable in most cases. Here we will merely attempt to apply some fundamentals of rate theory to unimolecular reactions to illustrate how straightforward calculations can provide useful information about the stability of molecules. For rigorous calculations of rate constants one best utilizes a specialized program, for example Polyrate ([133], based on RRKM theory [134]). There are many discussions of the theory of reaction rates, in various degrees of detail [148, 214]. A particularly rigorous application of RRKM code to alkene ozonolysis is by Oliveira and Bauerfeldt [214d]. In this section we limit ourselves to gas-phase unimolecular reactions [215] and examine the results of some calculations. We will use the simplified Eyring (Chap. 2, Sect. 2.2) equation, and make no claims to very high accuracy

$$k_r = \frac{k_B T}{h} e^{-\Delta G^{\ddagger}/RT} \qquad (*5.197)$$

where k_r = unimolecular rate constant (units = s^{-1})

k_B = Boltzmann constant, 1.381×10^{-23} J K^{-1}

T = temperature, K

h = Planck's constant, 6.626×10^{-34} J s

$\Delta G^{\ddagger}$ = the transition-state-reactant free energy difference (in some calculations we will try the ZPE-corrected 0 K energy difference, ΔE_{0K}^{total}, which is the 0 K enthalpy difference)

R = gas constant, 8.314 J K^{-1} mol^{-1}

For $T = 298$ K ("room temperature"), $(k_B T)/h = 6.22 \times 10^{12}$ s^{-1} and $RT = 2.478$ kJ mol^{-1}

With these values Eq. (5.197) becomes

$$k_r = 6.22 \times 10^{12} e^{-\Delta G^{\ddagger}/2.478} \qquad (5.198)$$
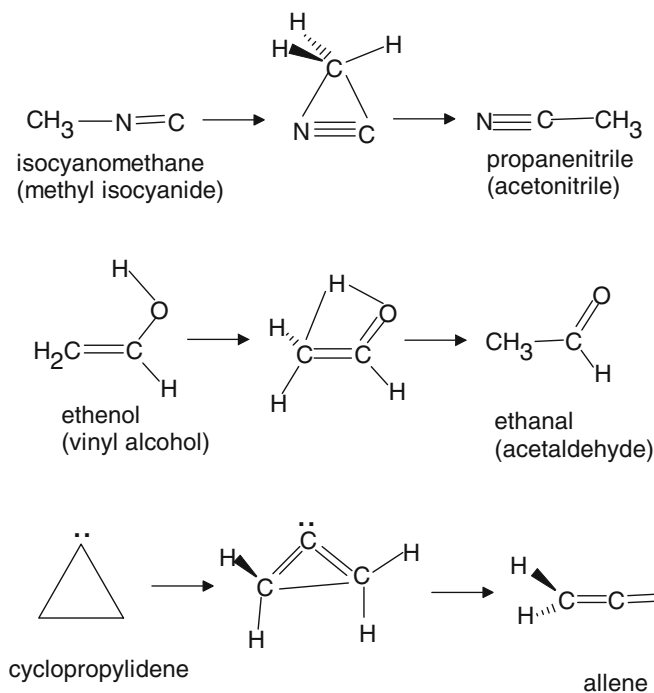
Fig. 5.30 Reactions used to illustrate the calculation of rate constants and half lives with Eq. (5.198) (cf. Fig. 5.21)

Equation (5.198) was used to calculate rate constants for the three unimolecular reactions in Fig. 5.30 (cf. Fig. 5.21). Reactants, products and transition state structures were created with Spartan [37, 216] at the AM1 (a kind of semiempirical method; Chap. 6) level. Transition states were calculated with Spartan's transition state routine starting from a guess based on the reactant and product structures and the experience that bonds being broken or made in a transition state tend to be roughly 50 percent longer than in a reactant or product. The AM1 structures were used as inputs for MP2/6–31G* (Sect. 5.4.2), B3LYP/6–31G* (a kind of DFT calculation; Chap. 7), G3(MP2), G4(MP2) and CBS-QB3 calculations (Sect. 5.5.2.3.2) with Gaussian 09 [178]. A few remarks are appropriate on the choice of these five computational levels. First, a correlated electron method (Sect. 5.4) is almost mandatory for a reasonably accurate reaction rate. MP2 and B3LYP (or instead of this latter some other density functional method) are probably the most popular methods for routine calculations at correlated levels. Both are often used with bigger basis sets than 6–31G*, while G3(MP2), G4(MP2) and CBS-QB3 are, where applicable (Sect. 5.5.2. 3.2), reasonable choices for high-accuracy multistep calculations. The Hartree-Fock level does not, as a rule, give reasonably accurate reaction barriers [217], although the rule is not quite unbreakable; for example, simple HF/6–31G* calculations give fairly good tor-sional barriers for hindered methylbenzenes [218]. Hartree-Fock *relative* barriers in

a series of related reactions can be useful [219]. Note that the high-accuracy Gaussian and CBS methods were developed for thermodynamics, not kinetics. Nevertheless, they have been applied to the calculation of reaction barriers, and CBS-QB3 in particular has been implied to be suitable for this purpose [187b]. However, this and other standard Gaussian and CBS high-accuracy methods were unsatisfactory for the reaction of ozone with ethyne and ethene, and CBS-QB3 was singled out for special cautioning; the reaction did yield to a kind of extrapolation method, the "reference focal point approach" [220]. Ozone is, of course, a problem molecule (Sect. 5.5.1), and CBS-QB3 worked well for other cycloadditions [194].

The results of the calculations are summarized in Table 5.11 (calculated from the data in Table 5.12). For each of the five computational levels, the free energy of

Table 5.11 Calculated (298 K) rate constants k_r (s^{-1}) and halflives $t_{1/2}$ (s) from $k_r = (k_B T/h)e^{\Delta G/RT}$ /$k_r = (6.22 \times 10^{12})e^{-\Delta G\ddagger/2.478}$ (Eqs. (5.197/5.198)) and $t_{1/2} = \ln2/k_r = 0.693/k_r$, using free energies of activation $\Delta G^\ddagger$ (kJ mol^{-1}) from five methods. The calculation of the free energies of activation are given in Table 5.12

Reaction	MP2/6–31G*	B3LYP/6–31G*	G3(MP2)	G4(MP2)	CBS-QB3
CH$_3$NC → CH$_3$CN	k_r 1.50×10^{-17}	k_r 3.63×10^{-16}	k_r 1.17×10^{-15}	k_r 1.82×10^{-15}	k_r 4.26×10^{-16}
	$t_{1/2}$ 4.6×10^{16}	$t_{1/2}$ 1.9×10^{15}	$t_{1/2}$ 5.9×10^{14}	$t_{1/2}$ 8.5×10^{14}	$t_{1/2}$ 1.6×10^{15}
	$\Delta G^\ddagger$ 169.2	$\Delta G^\ddagger$ 161.1	$\Delta G^\ddagger$ 158.2	$\Delta G^\ddagger$ 157.1	$\Delta G^\ddagger$ 160.7
CH$_2$ = CHOH → CH$_3$CHO	k_r 8.72×10^{-29}	k_r 3.17×10^{-27}	k_r 7.15×10^{-30}	k_r 1.11×10^{-29}	k_r 6.33×10^{-30}
	$t_{1/2}$ 7.95×10^{27}	$t_{1/2}$ 2.2×10^{26}	$t_{1/2}$ 9.7×10^{28}	$t_{1/2}$ 6.2×10^{28}	$t_{1/2}$ 1.1×10^{29}
	$\Delta G^\ddagger$ 233.1	$\Delta G^\ddagger$ 224.2	$\Delta G^\ddagger$ 239.3	$\Delta G^\ddagger$ 238.2	$\Delta G^\ddagger$ 239.6
cyclopropylidene → allene	k_r 4.03×10^{8}	k_r 4.19×10^{8}	k_r 4.36×10^{9}	k_r 6.28×10^{8}	k_r 4.19×10^{8}
	$t_{1/2}$ 2.5×10^{-9}	$t_{1/2}$ 2.4×10^{-9}	$t_{1/2}$ 1.6×10^{-10}	$t_{1/2}$ 1.0×10^{-9}	$t_{1/2}$ 2.4×10^{-9}
	$\Delta G^\ddagger$ 23.9	$\Delta G^\ddagger$ 23.8	$\Delta G^\ddagger$ 18.0	$\Delta G^\ddagger$ 22.8	$\Delta G^\ddagger$ 23.8

Table 5.12 Free energies of reactant and transition state (hartrees) and free energy of activation $\Delta G^\ddagger$ (hartrees/kJ mol^{-1}) by five methods; hartrees were converted to kJ mol^{-1} by multiplying by 2626

Reaction	MP2/6–31G*	B3LYP/6–31G*	G3(MP2)	G4(MP2)	CBS-QB3
CH$_3$NC → CH$_3$CN	−132.26990	−132.69425	−132.53125	−132.55043	−132.51216
	−132.20547	−132.63289	−132.47102	−132.49063	−132.45098
	$\Delta G^\ddagger$ 0.06443/ 169.2	$\Delta G^\ddagger$ 0.06136/ 161.1	$\Delta G^\ddagger$ 0.06023/ 158.2	$\Delta G^\ddagger$ 0.05980/ 157.1	$\Delta G^\ddagger$ 0.06118/ 160.7
CH$_2$ = CHOH → CH$_3$CHO	−153.28714	−153.77339	−153.60839	−153.63152	−153.59006
	−153.19837	−153.68802	−153.51725	−153.54081	−153.49883
	$\Delta G^\ddagger$ 0.08877/ 233.1	$\Delta G^\ddagger$ 0.08537/ 224.2	$\Delta G^\ddagger$ 0.09114/ 239.3	$\Delta G^\ddagger$ 0.09071/ 238.2	$\Delta G^\ddagger$ 0.09123/ 239.6
cyclopropylidene → allene	−116.09212	−116.51746	−116.35895	−116.37680	−116.33697
	−116.08301	−116.50839	−116.35211	−116.36813	−116.32789
	$\Delta G^\ddagger$ 0.00911/ 23.9	$\Delta G^\ddagger$ 0.00907/ 23.8	$\Delta G^\ddagger$ 0.00684/ 18.0	$\Delta G^\ddagger$ 0.00867/ 22.8	$\Delta G^\ddagger$ 0.00908/ 23.8

The rate constants and halflives calculated from these values are given in Table 5.11

activation was used to calculate a rate constant and halflife for each of the three reactions, using Eq. (5.197/5.198). Table 5.12 reveals the usefulness of this simple way of calculating unimolecular reaction rates. All five methods yield for each reaction *approximately* the same activation free energy: for $CH_3NC \rightarrow CH_3CN$, ca. 160 kJ mol^{-1}, for $CH_2=CHOH \rightarrow CH_3CHO$, ca. 238 kJ mol^{-1}, and for cyclopropylidene $\rightarrow$ allene, ca. 20 kJ mol^{-1}. For the three high-accuracy methods, the calculated activation free energies are particularly similar, all within 6 kJ mol^{-1}. The qualitative, and even semiquantitative, predictions for the kinetic stability of each compound are the same for all five methods (Table 5.11): for CH_3NC, a halflife of ca. $10^{15} - 10^{16}$ s, for $CH_2=CHOH$ a halflife of ca. $10^{26} - 10^{29}$ s, and for cyclopropylidene, a halflife of ca. $10^{-10} - 10^{-9}$ s. Note however, that using Eq. (5.198), a change in activation free energy of 5 kJ mol^{-1} can alter a rate constant or halflife by a factor of about 10:

$$\Delta G^{\ddagger} = 100\,kJ\,mol^{-1}, \quad k_r = 1.9 \times 10^{-5}s^{-1}, \quad t_{1/2} = 4 \times 10^4\,s$$
$$\Delta G^{\ddagger} = 105\,kJ\,mol^{-1}, \quad k_r = 2.5 \times 10^{-6}s^{-1}, \quad t_{1/2} = 3 \times 10^5\,s$$
$$\Delta G^{\ddagger} = 110\,kJ\,mol^{-1}, \quad k_r = 3.3 \times 10^{-7}s^{-1}, \quad t_{1/2} = 3 \times 10^6\,s$$

Comparing our calculations with the experimental facts:

$$CH_3NC \rightarrow CH_3NC\,Reaction$$

The experimental Arrhenius activation energy and rate constant for the gas phase isomerization of methyl isocyanide have been reported; at the lowest pressure used, $E_a = 36.27$ kcal mol^{-1}, i.e. 151.8 kJ mol^{-1}, and log A = 10.46, i.e. $A = 2.88 \times 10^{10}s^{-1}$ [221]. We want to compare our calculated activation free energy with an experimental value, so we must calculate $\Delta G^{\ddagger}$ from E_a and A. From the Arrhenius equation Eq. (5.174) and the Eyring equation Eq. (5.197) it follows that

$$\Delta G^{\ddagger} = -RT\ln(A/k_BT/h) + E_a \qquad (5.199)$$

Using the values of the constants given above for Eq. (5.197), we find

$$\Delta G^{\ddagger} = -2.478\ln(A/(6.22 \times 10^{12}) + E_a \qquad (5.200)$$

with energies in kJ mol^{-1} as usual. Using this equation and E_a and A from [221], the experimentally-derived $\Delta G^{\ddagger}$ is 165.1 kJ mol^{-1}. This is in good agreement with the calculated values of $157 - 169$ kJ mol^{-1} in Table 5.12.

$$CH_2 = CHOH \rightarrow CH_3CHO\,Reaction$$
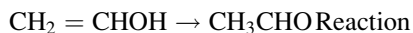
The reported halflife of ethenol (vinyl alcohol) in the gas phase at room temperature is ca. 30 minutes [222], far shorter than our calculated $10^{28} - 10^{29}$ s.

However, the 30 minute halflife is very likely that for a protonation/deprotonation isomerization catalyzed by the walls of the vessel, rather than for the concerted hydrogen migration (Fig. 5.30) considered here. Indeed, the related *ethynol* has been detected in planetary atmospheres and interstellar space [223], showing that that molecule, in isolation, is long-lived. Even under the more confined conditions of the lab, ethenol can be studied in the gas phase [222, 224] and in solution [225]. All five computational methods predict very long halflives for the uncatalyzed reaction.

<div align="center">Cyclopropylidene → allene Reaction</div>

Cyclopropylidene has apparently never been isolated [226], so its halflife is likely to be short even well below room temperature. Employing a variety of methods, Bettinger et al. obtained a barrier for its rearrangement to allene of about 4 kcal mol^{-1}, i. e ca. 17 kJ mol^{-1} [227], close to our values of $18-24$ kJ mol^{-1}. Our calculations predict room temperature halflives for cyclopropylidene of about 10^{-9} to 10^{-10} s. Attempts to generate cyclopropylidene at 77 K gave allene [226]. We can calculate the halflife at 77 K, instructing Gaussian 03 to use this temperature for thermochemistry. Using CBS-QB3, the resulting $\Delta G^{\ddagger}$ is 25.1 kJ mol^{-1} (very little change from the 298 K value of 23.8 kJ mol^{-1}), and with this and $T = 77$ K, Eq. (5.197) gives $k_r = 1.49 \times 10^{-5}$ and a halflife of 4.7×10^5 s, ca. 13 h. Cyclopropylidene ought to be observable at 77 K.

From Eq. (5.197) and the fact that for a unimolecular reaction $t_{1/2} = \ln 2/k_r$ it follows that

$$\log t_{1/2} = \log\left[(\ln 2)\frac{h}{k_{\mathrm B}T}\right] + \frac{\Delta G^{\ddagger}}{RT} \cdot \log e \qquad (5.201)$$

At 298 K (about room temperature) this becomes

$$\log t_{1/2} = 0.175\Delta G^{\ddagger} - 13.0 \qquad (5.202)$$

where $\Delta G^{\ddagger}$ is in kJ mol^{-1}. Eq. (5.201) shows that for $\Delta G^{\ddagger} = 0$ kJ mol^{-1}, $t_{1/2}$ is $10^{-12}-10^{-13}$ s; this is as expected, since the period of a molecular vibration is about $10^{-13}-10^{-14}$ s and with no barrier a species should survive for only about one vibrational motion (the one along the reaction coordinate, corresponding to the imaginary frequency) as it passes through the saddle region (e.g. Fig. 5.29). Figure 5.31, a graph of Eq. (5.202), can be used to estimate halflives at room temperature from the free energy of activation, for unimolecular isomerizations. This regards $\Delta G^{\ddagger}$ as only a weak function of T, as seems to be the case–see the above calculation for cyclopropylidene at 77 K. We see that the threshold value of $\Delta G^{\ddagger}$ for observability at room temperature for a species that decays by a unimolecular process is predicted to be about $80-90$ kJ mol^{-1}($t_{1/2} = 10$ s $-$ 9 min), with quite a strong dependence on $\Delta G^{\ddagger}$. Experience gives a similar result: the
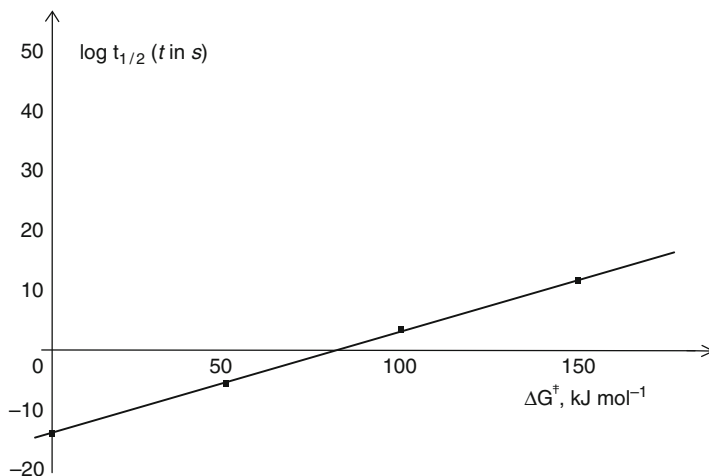
Fig. 5.31 Graph of $\log t_{1/2} = 0.175\Delta G^{\ddagger} - 13.0$. If this equation for the halflife of a unimolecular reaction were strictly true, then the threshold value of $\Delta G^{\ddagger}$ for ready observability at room temperature would be about 85 kJ mol^{-1}, corresponding to $t_{1/2} = 75$ s. Actually, a rough rule of thumb is that the threshold barrier for observability at room temperature is about 100 kJ mol^{-1}

threshold barrier for observing or isolating a compound at room temperature is about 100 kJ mol^{-1} [152, 153].

So far as Eq. (5.197) can deliver them, loosely "quantitatively accurate" reaction rates, say to within a factor of two, require activation energies accurate to within about 2 kJ mol^{-1}. Nevertheless, the equation does provide a simple way of obtaining serviceably good rate constants. The (admittedly small) selection of reactions here shows no bias toward low or high calculated barriers for any of the four methods, and for a particular kind of reaction it is advisable to choose a method based on a comparison of methods with experimental results where this information is available.

5.5.2.3.5 Energies: Concluding Remarks

Foresman and Frisch [228], in a chapter with very useful data and recommendations regarding accuracy, show large mean absolute deviations (MAD) and unreservedly enormous maximum errors for Hartree-Fock calculations and even for MP2 calculations with reasonably big basis sets; for example:

HF/6$-$31 + G**	MAD, 195 kJ mol^{-1} (46.7 kcal mol^{-1})
	Max. Error, 753 kJ mol^{-1} (179.9 kcal mol^{-1})
MP2/6$-$311 + G(2d, 9)	MAD, 37 kJ mol^{-1} (8.9 kcal mol^{-1})
	Max. Error, 164 kJ mol^{-1} (39.2 kcal mol^{-1})

How can this be reconciled with the results shown in this chapter and the modest levels endorsed by Hehre [39]? As hinted in reference [228] ("Don't Panic!" p. 146, and "Don't be overly alarmed, p. 149), the large errors reported are a composite including some "tough cases" [229] like atomization energies (Sect. 5.4.1). A good feel for the accuracy of various levels of calculation will emerge from examining the extensive data in Hehre's book [39], not losing sight of the fact that there *are* cases, like accurate atomization energies, that yield only to high-accuracy methods.

For relief and reassurance, Table 5.13 compares with experiment the relative energies of some isomers calculated at the modest levels HF/6–31G* and MP2/6–31G*; for a reality check, we also see values from G3(MP2) and G4 (MP2) and experiment (experiment: fulvene/benzene, [230]/[231]; cyclopropane/propene, [232]/[232]; dimethyl ether/ethanol, [233]/[234]; methylcyclopentane/cyclohexane, [231]/[235]). The calculated energy differences chosen for this illustration are enthalpy differences, because differences in experimental enthalpies of formation yield these, and enthalpies of formation represent the most extensive compilations of experimental energy quantities relevant to our purpose. All the levels predict the correct stability orders. Even the HF/6–31G* level is not wildly inaccurate, being out by at most about $10 - 20$ kJ mol^{-1}, for fulvene/benzene and dimethyl ether/ethanol. MP2/6–31G* is similar or even in one case a bit worse (cyclopropane/propene, about 11 kJ mol^{-1} smaller than the HF/6–31G* value). The G3(MP2) and G3(MP2) methods give essentially the same results and agree with experiment to within 5 kJ mol^{-1}, except for the apparent 10 kJ mol^{-1} discrepancy for fulvene/benzene, which could be due to experimental error (footnote in the table) for fulvene [230], a reactive, sensitive compound difficult to purify.
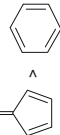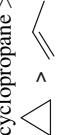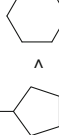
Of course the values shown here are *differences* in heats of formation, and may benefit from cancellation of errors in calculated 298 K enthalpies. However, it is enthalpy differences that are of primary interest to chemists.

5.5.3 Frequencies and Vibrational (IR) Spectra

The calculation of normal-mode frequencies (Chap. 2, Sect. 2.5) is important because:

1. The number of imaginary frequencies of a molecular species tells us the curvature of the potential energy surface at that particular stationary point: whether an optimized structure (i.e. a stationary point-species) is a minimum, a transition state (a first-order saddle point), or a higher-order saddle point. Note that frequency calculations are normally valid only for stationary points; this rule is knowingly violated occasionally, e.g. when technically invalid but useful force constants or frequencies are calculated as aids to an algorithmic process like geometry optimization (Chap. 2, Sect. 2.4) or following an IRC (Chap. 2, Sects. 2.2, 2.5, 2.6). Routinely checking optimized structures with a frequency calculation is a good idea. Frequency calculations can take much longer than

Table 5.13 Enthalpy differences (kJ mol⁻¹) of some isomers, calculated at two modest ab initio levels, and at the G3(MP2) and G4(MP2) levels, and from experiment

Isomer pair	HF/6–31G*	MP2/6–31G*	G3(MP2)	G4(MP2)	Experiment
fulvene > benzene	150.0 (−230.53328 > −230.59042 Δ = 0.05714)	151.4 (−231.29393 > −231.35158 Δ = 0.05765)	132.1 (−231.77396 > −231.82428 Δ = 0.05032)	130.1 (−231.80516 > −231.85470 Δ = 0.04954)	141.5[a] (224–82.5) [229/230]
cyclopropane > propene	36.0 (−116.96743 > −116.98113 Δ = 0.01370)	22.3 (−117.36047 > −117.36895 Δ = 0.00848)	38.4 (−117.65305 > −117.66768 Δ = 0.01463)	35.7 (−117.66989 > −117.68349 Δ = 0.01360)	33.1 (53.1–20.1) [231/231]
dimethyl ether > ethanol Me^{O}Me > CH₃CH₂OH	29.4 (−153.97345 > −153.98465 Δ = 0.01120)	35.8 (−154.41606 > −154.42971 Δ = 0.01365)	50.4 (−154.76644 > −154.78565 Δ = 0.01921)	50.2 (−154.79044 > −154.80955 Δ = 0.01911)	50.7 (−184.1 − (−234.8)) [232/233]
methylcyclopentane > cyclohexane	19.5 (−234.01184 > −234.01925 Δ = 0.00741)	16.7 (−234.80454 > −234.81090 Δ = 0.00636)	17.3 (−235.38913 > −235.39570 Δ = 0.00657)	16.8 (−235.42107 > −235.42748 Δ = 0.00641)	18.6 (−106.0 − (−124.6)) [230/234]

Calculated enthalpies are 298 K gas-phase values, thus the differences are differences in standard enthalpies of formation, i.e. $\Delta \Delta H^{\ominus}_{f298}$. The higher-energy molecule is shown first, e.g. fulvene lies above benzene in energy. For each of the four calculated levels the enthalpies of the two molecules are given in parentheses, and their differences (Δ), in hartrees; hartrees were converted to kJ mol⁻¹ by multiplying by 2626. For each of the experimental difference values, the two enthalpies of formation are shown in parentheses, and the literature references in brackets

[a] If the heat of formation of fulvene is really 214 kJ mol⁻¹ [229], then the enthalpy difference is 214–82.5 = 131.5, essentially the same as the G3(MP2) and G4(MP2) values

optimizations, and for very big molecules and extended systems like crystals methods for calculating frequencies on only a part of the system have been developed [236].

2. The frequencies must be calculated to get the zero point energy of the molecule. This is needed for accurate energy comparisons (Chap. 2, Sect. 2.5).

3. The normal-mode vibrational frequencies of a molecule correspond, with qualifications, to the bands seen in the infrared (IR) spectrum of the substance. Discrepancies may arise from overtone and combination bands in the experimental IR, and from problems in accurate calculation of relative intensities (less so from problems in calculation of frequency positions). Thus the IR spectrum of a substance that has never been made can be calculated to serve as a guide for the experimentalist. Unidentified IR bands observed in an experiment can sometimes be assigned to a particular substance on the basis of the calculated spectrum of a suspect; if the spectra of the usual suspects are not available from experiment (they might be extremely reactive, transient species), we can calculate them.

The characterization of stationary points by the number of imaginary frequencies was discussed in Chap. 2, and zero-point energies in Chap. 2 and earlier sections of this chapter. Here we will examine the utility of ab initio calculations for the prediction of IR spectra [237]. It is important to remember that frequencies should be calculated at the same level (e.g. HF/3–21G$^{(*)}$, MP2/6–31G*,...) as was used for the geometry optimization (Chap. 2, Sect. 2.4). This is because accurate calculation of the curvature of the PES at a stationary point requires that the second derivatives $\partial^2 E / \partial q_i \partial q_j$ be found at the same level as was used to create the surface on which the point sits.

5.5.3.1 Positions (Frequencies) of IR Bands

In Chap. 2, Sect. 2.5, we saw that diagonalization of the force constant matrix gives an eigenvector matrix whose elements are the "direction vectors" of the normal-mode vibrations, and an eigenvalue matrix whose elements are the force constants of these vibrations. "Mass-weighting" the force constants gives the wavenumbers ("frequencies") of the normal-mode vibrations, and their motions can be identified by using the direction vectors to animate the vibrations. So we can calculate the wavenumbers of IR bands and associate each band with some particular vibrational mode (the *details* of the calculation of vibrational frequencies/wavenumbers is actually quite complex [130b]). The wavenumbers ("frequencies") from ab initio calculations are larger than the experimental ones, i.e. the frequencies are too high. There are two reasons why this might be so: the principle of equating second derivatives of energy (with respect to geometry changes) with force constants might be at fault, or the basis set and/or correlation level might be deficient.

The principle of equating a second derivative with a stretching or bending force constant is not exactly correct. A second derivative $\partial^2 E / \partial q^2$ would be strictly equal
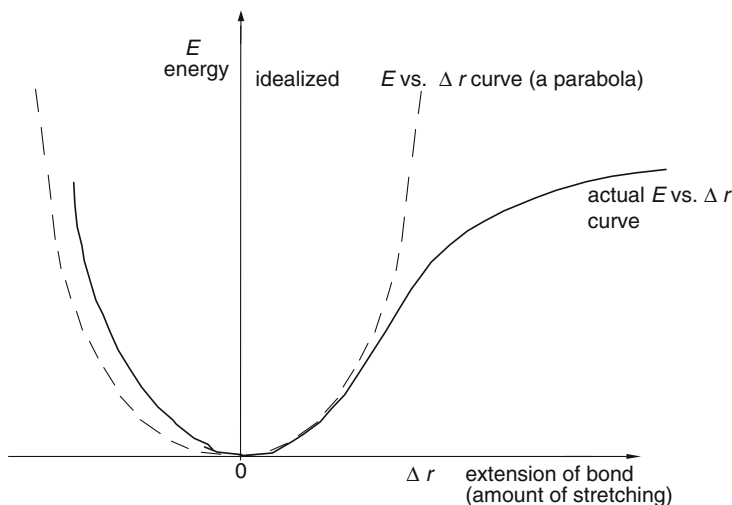
Fig. 5.32 The actual curve for potential energy vs. stretch for a bond is not really a parabola, i.e. not really $E = (\Delta r)^2$, but near the equilibrium bond length ($\Delta r = 0$) the parabola fits the actual curve fairly well

to a force constant only if the energy were a quadratic function of the geometry, i.e. if a graph of E vs. q were a parabola. However vibrational curves are not exactly parabolas (Fig. 5.32). For a parabolic E/q relationship, and considering a diatomic molecule for simplicity, we would have:

$$E = \frac{k}{2}\left(q - q_{eq}\right)^2 \tag{5.203}$$

where q_{eq} is the equilibrium geometry. Here k is by definition the force constant, the second derivative of E, i.e. $\partial^2 E/\partial q^2 = k$. For a real molecule, however, the E/q relationship is more complicated, being a power series in q^2, q^3, etc., terms, and there is not just one constant. Eq. (5.203) holds for what is called *simple harmonic motion*, and the coefficients of the higher-power terms in the more accurate equation are called *anharmonicity corrections*. Assuming that bond vibrations are simple harmonic is the *harmonic approximation*.

For small molecules it is possible to calculate from the experimental IR spectrum the simple harmonic force constant k and the anharmonicity corrections. Using k, *theoretical harmonic frequencies* can be calculated [238]. These correspond to a parabolic E/q relationship (Fig 5.32), i.e. to a steeper curve than the real one, and thus to stiffer bonds. Stiffer bonds need more energy to stretch them (or bend them, for bending force constants), and thus absorb higher-frequency infrared light. These theoretical harmonic frequencies are not real-world frequencies, but rather the frequencies that would be observed if bonds were simple harmonic oscillators. Such theoretical harmonic frequencies, derived from experimental IR spectra, are

higher than the *observed* "raw" experimental frequencies, and are closer to ab initio frequencies than are the observed frequencies [239]. Since both theoretically calculated (e.g. by ab initio methods) frequencies and experimentally-derived theoretical harmonic frequencies are based on a parabolic E/q relationship, it is sometimes considered better to compare calculated frequencies with theoretical experimentally-derived harmonic frequencies rather than with observed frequencies [240]. Because both ab initio- and experimentally-derived harmonic frequencies rest on second derivatives, we might expect ab initio frequencies to converge not toward the *observed* experimental, but rather toward the theoretical experiment-derived harmonic frequencies, as correlation level/basis set are increased. This is indeed the case, as has been shown by calculations on water with high correlation levels (CCSD(T); Sect. 5.4.3) and large basis sets (polarization functions and triply- or quadruply- split valence shells (Sect. 5.3.3). The *observed* water frequencies are 3756, 3657, and 1595 cm^{-1}. For these three fundamental frequencies, the deviations fell from 269, 282, and 127 cm^{-1} at the Hartree-Fock level to only 9, 13 and 10 cm^{-1} higher than the theoretical experiment-derived harmonic values of 3943, 3832 and 1649 cm^{-1} [241]. Such harmonic frequencies are typically about 5 % higher, and ab initio calculated frequencies about 5–10 % higher, than observed frequencies. From the foregoing discussion it appears that the fundamental reason ab initio frequencies are too high is because of the harmonic approximation: equating of $\partial^2 E/\partial q^2$ with a force constant. There is no theoretical reason why high-level calculations should converge toward the *observed* frequencies; this statement applies to frequencies calculated, as is almost always the case, by the harmonic approximation (above). Frequencies (theoretical experiment-derived harmonic values) accurate to within about 1 % were obtained for a set of small molecules using high correlation levels and medium-size basis sets [242].

Fortunately for us, we often wish only to calculate IR spectra that resemble, or would resemble, experimental spectra, and for this there is a simple expedient. Calculated and observed frequencies differ by a fairly constant factor, and ab initio (and other theoretically-calculated) frequencies can be brought into reasonable agreement with experiment by multiplying them by a correction factor. An extensive comparison by Scott and Radom of calculated and experimental frequencies [80a] has provided empirical correction factors for frequencies calculated by a variety of methods. A few of the correction factors from this compilation are:

HF/3−21G$^{(*)}$	0.9085
HF/6−31G*	0.8953
HF/6−311G(df, p)	0.9054
MP2(fc)/6−31G*	0.9434
MP2(fc)/6−311G**	0.9496

The correction factors at the HF level with the three basis sets are similar, 0.90–0.91; the factors at the MP2 level are significantly closer to 1, but Scott and

Radom say that "MP2/6–31(d) does not appear to offer a significant improvement in performance over HF/6–31G(d) and occasionally shows large errors", and "The most cost-effective procedures found in this study for predicting vibrational frequencies are HF/6–31(d) and [certain density functional methods]". Separate correction factors for zero-point vibrational energies were also given, and although it was hitherto common practice to use the same correction factor for frequencies and for ZPEs, the use of separate factors may now be standard. Better agreement with experiment can be obtained by using empirical correction factors for specific kinds of vibrations (Scott and Radom give separate factors for low-frequency vibrations, as opposed to the relatively high-frequency ones to which the factors listed above refer), but this is rarely done. A recent paper recommends correction of ab initio frequencies, and to a lesser extent DFT (Chap. 7) ones using quadratic, rather than linear, increments [80b].

5.5.3.2 Intensities of IR bands

The bands in an IR spectrum have not just *positions* ("frequencies", denoted by various wavenumbers), but also *intensities*. IR intensities present considerably more difficulties in their measurement and theoretical calculation than do frequencies, and actually experimental intensities are not routinely quantified, but are commonly merely described as weak, medium, or strong. To calculate an IR spectrum for visual comparison with experiment it is desirable to compute both wavenumbers and intensities. The intensity of a vibration is determined by the change in dipole moment accompanying the vibration. If a vibrational mode leads to no change in dipole moment, the mode will, theoretically, not result in absorption of an IR photon, because the oscillating electric fields of the radiation and the vibrational mode will be unable to couple. Such a vibrational mode is said to be *IR-inactive*, i.e. it should cause no observable band in the IR spectrum. Stretching vibrations that, because of symmetry, are not accompanied by a change in dipole moment, are expected to be IR-inactive. These occur mainly in homonuclear molecules like O_2 and N_2, and in linear molecules; thus the C/C triple bond stretch in symmetrical akynes, and the symmetric OCO stretch in carbon dioxide, do not engender bands in the IR spectrum. For Raman spectroscopy, in which one measures the scattered rather than the transmitted IR light, the requirement for observing a vibrational mode is that the vibration occur with a change in polarizability. Raman spectra are routinely calculable (e.g. by the Gaussian programs [36]; the IR and Raman *frequencies*, but not intensities, are the same) along with IR spectra. The complementarity of IR and Raman spectra can be useful in studying the symmetry of molecules. A band which should be IR-inactive or at least very weak can sometimes be seen because of coupling with other vibrational modes; thus the triple-bond stretch of 1,2-benzyne (o-benzyne, dehydrobenzene, C_6H_4) has been observed [243], although it apparently should be accompanied by

only a very small change in dipole moment. Bands like this are expected to be, at best, weak.

As might be expected from the foregoing discussion, the intensity of an IR normal mode can be calculated from the change in the dipole moment with the change in geometry accompanying the vibration. The intensity is proportional to the square of the change in dipole moment with respect to geometry (to displacements along the directions of the normal coordinates):

$$I = \text{constant} \times \left(\frac{d\mu}{dq}\right)^2 \tag{5.204}$$

This can be used to calculate the relative intensities of IR bands; the calculation of absolute intensities, which are very rarely measured, requires calculation of the proportionality constant. The calculation of dipole moments is discussed in the next section. One way to calculate the derivative is to approximate it as a ratio of finite increments (d becomes Δ) and calculate the change in dipole moment with a small change in geometry; there are also analytical methods for calculating the derivative [244]. A book has been written on the subject of vibrational intensities [245]. It has been reported that at the HF-level calculated IR-band intensities often differ from experiment by a factor of over 100% but at the MP2 level are typically within 30% of experiment [246]. Nevertheless, Scott and Radom, surprisingly, in their paper on corrections to frequencies and ZPEs (above) recommend HF/6–21G* over MP2/6–31G* [80a]. Schaefer and coworkers achieved "Quantitative accord" between theory and experiment for the absolute IR intensities of six very small molecules using QCISD, CCSD, and CCSD(T) (Sect. 5.4.3) with Dunning's aug-cc-pVTZ (Sect. 5.3.1) basis sets [247], but these levels may be currently too high for routine optimization and frequencies on even small to medium (say about 10 heavy atoms) molecules. With continued growth in computer power this situation will change. It should be possible to increase the accuracy of predicted spectra empirically by performing calculations on a series of known compounds and fitting the experimental to the calculated wavenumbers, and perhaps intensities, to obtain empirical corrections tailored specifically to the functional group of interest. Such painstaking work would be unusual. A few IR spectra calculated at routinely very practical levels are compared with experiment (taken in the gas phase by the author) in Figs. 5.33, 5.34, 5.35, and 5.36. This sample, although limited, gives an idea of the kind of similarity one can expect between experimental and ab initio IR spectra. A detailed resemblance cannot be expected, but the general features of a spectrum are reproduced. Probably the main utility of calculated ab initio IR spectra is in predicting the IR spectra of unknown molecules, as an aid to their synthesis, and the levels shown here are evidently adequate for this.
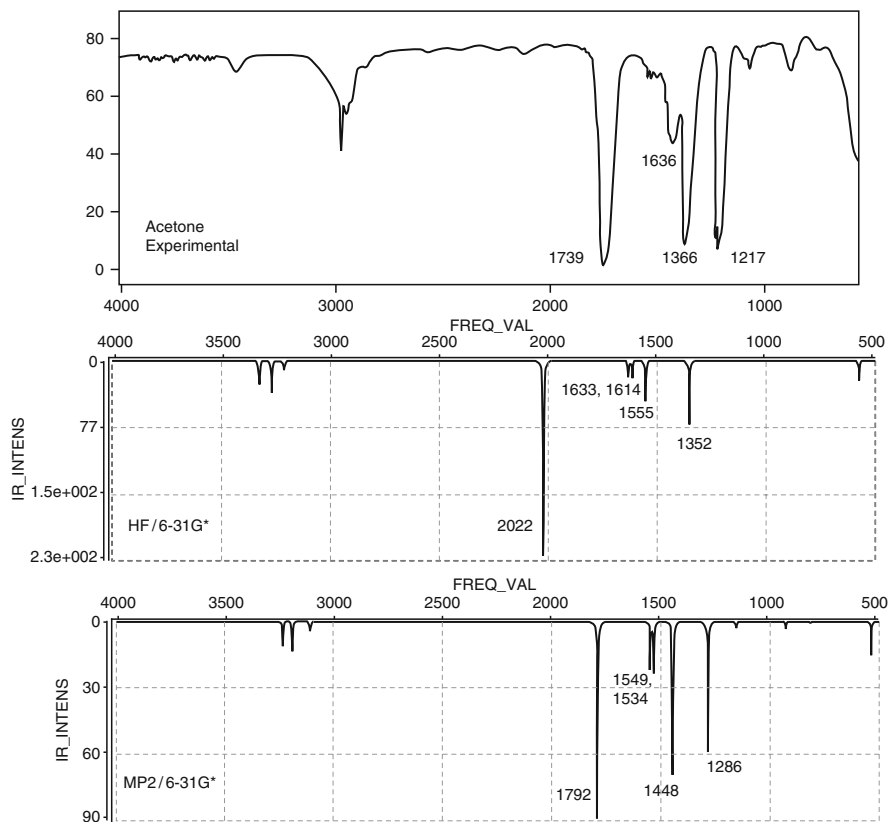
Fig. 5.33 Experimental (gas phase), HF/6–31G* and MP2(fc)/6–31G* calculated IR spectra of acetone

5.5.4   Properties Arising from Electron Distribution: Dipole Moments, Charges, Bond Orders, Electrostatic Potentials, Atoms-in-Molecules

We have seen three applications of ab initio calculations: finding the shapes (geometries), the relative energies, and the frequencies of stationary points (usually minima and transition states) on a potential energy surface:

1. The *shape* of a molecular species can provide clues to the existence of theoretical principles (why is it that benzene has six equal-length CC bonds, but cyclobutadiene has two "short" and two "long" bonds [248]?), or act as a guide to designing useful molecules (docking a candidate drug snugly into the active site of an enzyme requires a knowledge of the shapes of the drug and of the active site [110]). Although shape is one of the fundamental characteristics of a molecule, it is amusing and yet thought-provoking that the question has been
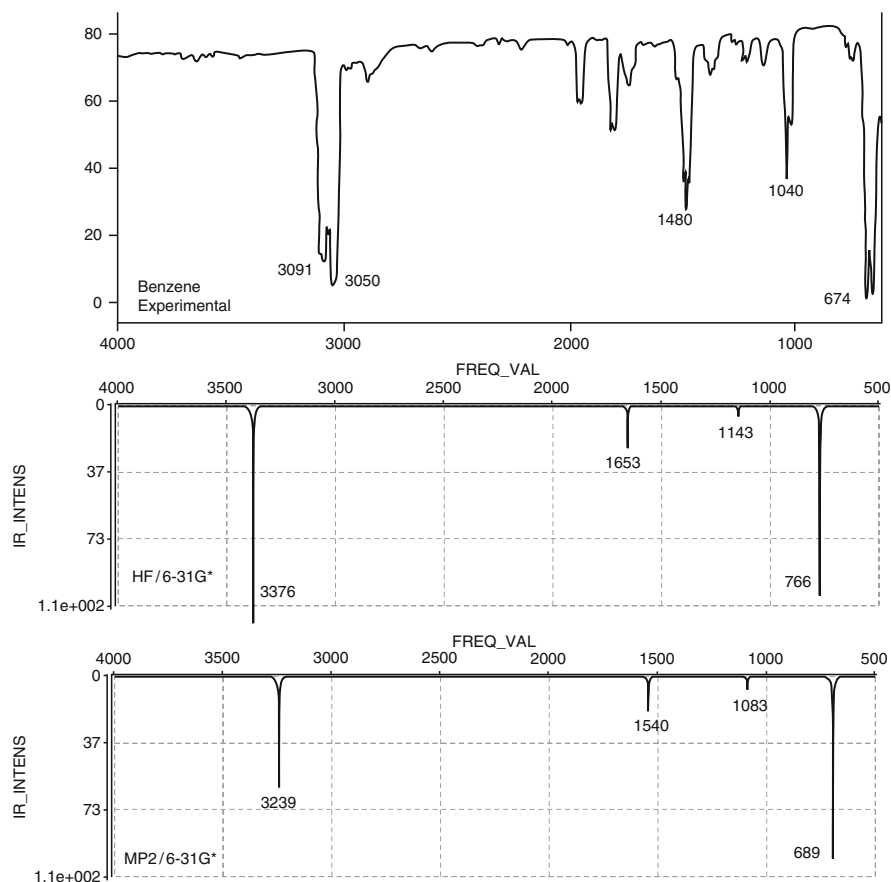
Fig. 5.34 Experimental (gas phase), HF/6–31G* and MP2(fc)/6–31G* calculated IR spectra of benzene

asked whether this is really a necessary property [249]! The basic problem here seems to be that according to quantum mechanics, for any observable property of a system there is a corresponding operator, which in principle allows the property (its expectation value, strictly speaking) to be calculated using the wavefunction (Sect. 5.2.3.3); however, there is no shape operator. Trindle has worked on reconciling this quantum mechanical conundrum with reality [250a]. Molecular shape has been treated at book length by Mezey [250b].

2. The *energy* of a molecular species relative to the energies of other species on a potential energy surface is fundamental to a knowledge of its kinetic and thermodynamic behaviour, and this can be important in attempts to synthesize it.

3. The *vibrational frequencies* of a molecule provide information about the electronic nature of its bonds, and prediction of the spectra represented by these frequencies may be useful to experimentalists.
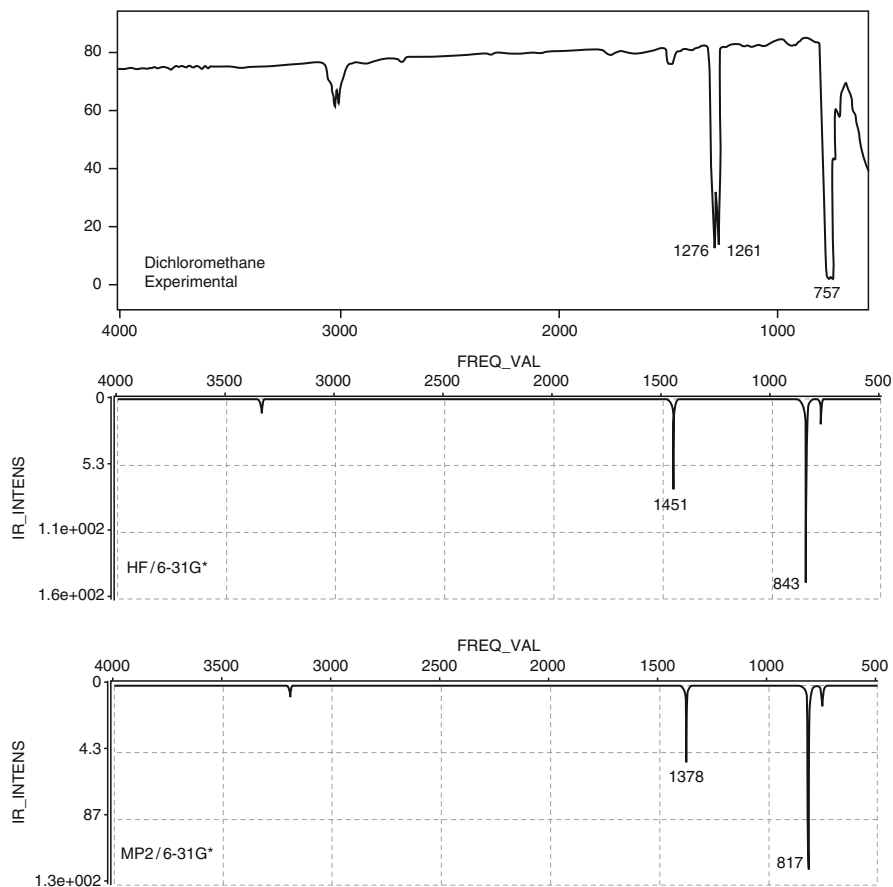
Fig. 5.35 Experimental (gas phase), HF/6–31G* and MP2(fc)/6–31G* calculated IR spectra of dichloromethane

A fourth important characteristic of a molecule is the *distribution of electron density* in it. Calculation of the electron density distribution enables one to predict the dipole moment, the charge distribution, the bond orders, and the shapes of various molecular orbitals.

5.5.4.1 Dipole Moments

The dipole moment [251] of a system of two charges Q and $-Q$ separated by a distance r is, by definition, the vector $\mathbf{Qr}$; the direction of the vector is officially from $-Q$ toward $+Q$, but chemists usually assign a molecular or bond dipole (see below) the direction from the positive end of the bond or molecule to the
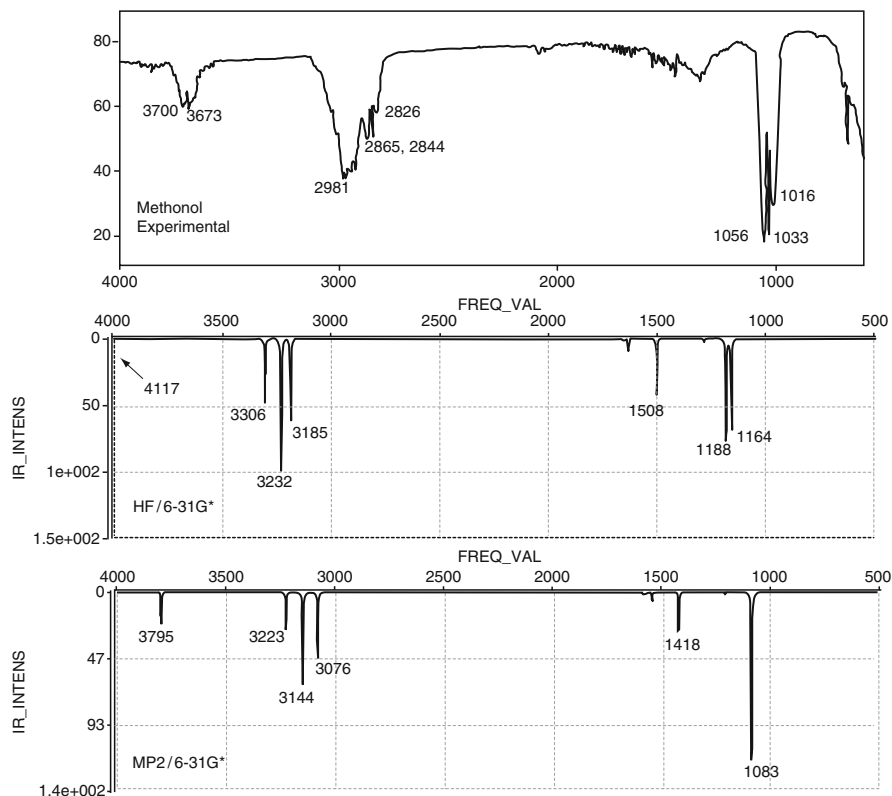
Fig. 5.36 Experimental (gas phase), HF/6–31G* and MP2(fc)/6–31G* calculated IR spectra of methanol

negative (Fig. 5.37a). The dipole moment of a collection of charges $Q_1, Q_2, \ldots, Q_n$, with corresponding position vectors $\mathbf{r}_1, \mathbf{r}_2, \ldots, \mathbf{r}_n$ (Fig. 5.37b) is

$$\boldsymbol{\mu} = \sum_1^n Q_i \mathbf{r}_i \tag{5.205}$$

and the so the dipole moment of a molecule is seen to arise from the charges and positions of its component electrons and nuclei. For a neutral molecule the dipole moment is an unambiguous experimental observable [252] (unlike some other quantities based on electron distribution), and comparison of calculated and experimental dipole moments is in principle sound methodology. The dipole moment is the simplest quantitative measure of the evenness or unevenness of electron distribution in a molecule. It is often convenient to think of the molecular dipole moment in a more pictorial form than that presented by Eq. (5.205), namely as the vector sum of bond moments (Fig. 5.37c). Two points should be noted: we are discussing an *average* dipole moment, because electron and nuclear motions will cause the

a

b

(vector sum of products of charges and distance vectors)

c

μ = vector sum of μ_1 and μ_2
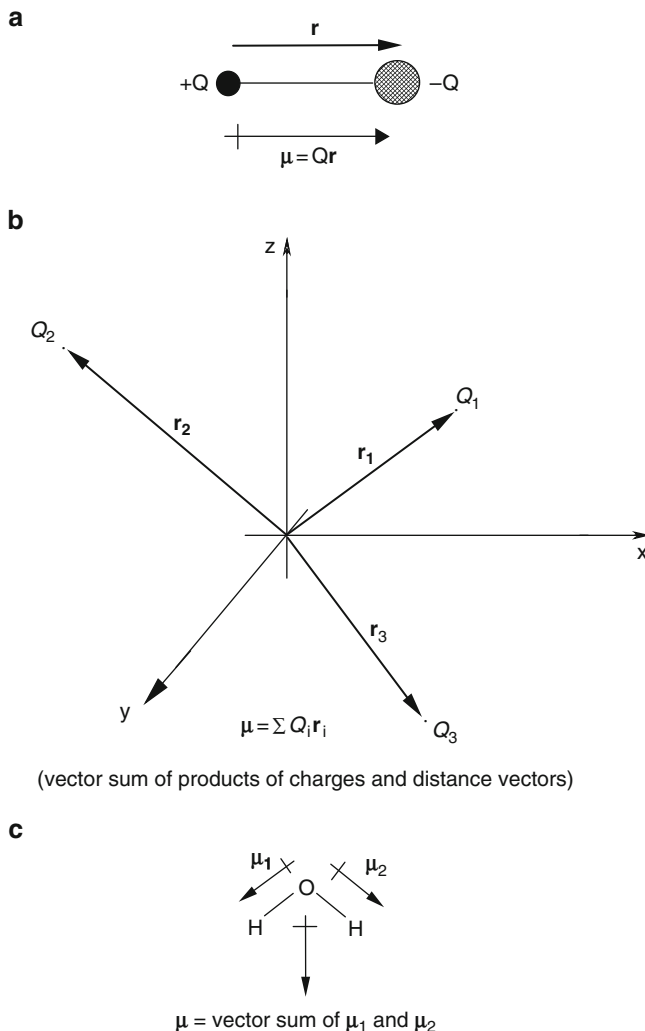
Fig. 5.37 (**a**) Chemists usually consider the dipole moment of a diatomic molecule, the vector $Q\mathbf{r}$, to be directed from the positive to the negative atom. (**b**) The dipole moment of a collection of charges, such as a molecule, arises from the magnitudes of the charges, and their locations (i.e. distances and directions from the origin. (**c**) The dipole moment of a molecule can be thought of as the vector sum of bond moments

dipole moment to fluctuate, so that even a spherical atom can have (very) temporary nonzero dipole moments. Another point is that we usually consider the dipole moments of *neutral* molecules only, not of ions, because the dipole moment of a charged species is not unique, but depends on the choice of the point in the coordinate system from which the position vectors are measured.

Let us look at the calculation of the dipole moment within the Hartree-Fock approximation. The quantum mechanical analogue of Eq. (5.205) for the electrons in a molecule is

$$\boldsymbol{\mu} = \left\langle \psi \middle| \sum_{j=1}^{2n} e\mathbf{r}_j \middle| \psi \right\rangle \tag{5.206}$$

Here the summation of charges times position vectors is replaced by the integral over the total wavefunction Ψ (the square of the wavefunction is a measure of charge) of the dipole moment operator (the summation over all electrons of the product of an electronic charge and the position vectors of the electrons). To perform an ab initio calculation of the dipole moment of a molecule we want an expression for the moment in terms of the basis functions ϕ, their coefficients c, and the geometry (for a molecule of specified charge and multiplicity these are the only "variables" in an ab initio calculation). The Hartree-Fock total wavefunction ψ is composed of those component orbitals ψ which are occupied, assembled into a Slater determinant (Sect. 5.2.3.1), and the ψ's are composed of basis functions and their coefficients (Sect. 5.3). Eq. (5.201), with the inclusion of the contribution of the nuclei to the dipole moment, leads to the dipole moment in Debyes as (Ref. [1g], p. 41)

$$\boldsymbol{\mu} = -2.5416 \left[\sum_A^N Z_A \mathbf{R}_A - \sum_r^m \sum_s^m P_{rs} \langle \phi_r | \mathbf{r} | \phi_s \rangle \right] \tag{5.207}$$

Here the first term refers to the nuclear charges and position vectors and the second term (the double summation) refers to the electrons. $P_{rs} =$ the density matrix elements (Sects. 5.2.3.6.4 and 5.2.3.6.5), cf.:

$$P_{tu} = 2 \sum_{j=1}^n c_{tj}^* c_{uj} \tag{5.208 = 5.81}$$

The P summation is over the occupied orbitals ($j = 1, 2, \ldots, n$; we are considering for simplicity closed-shell systems, so there are $2n$ electrons) and the double summation in Eq. (5.207) is over the m basis functions. The operator $\mathbf{r}$ is the electronic position vector.

How good are ab initio dipole moments? Hehre's extensive survey of practical ab initio methods [39] indicates that fairly good results are given by HF/6–31G*//HF/6–31G* (dipole moment from a HF/6–31G* calculation on a HF/6–31G* geometry) calculations, and that MP2/6–31G*//MP2/6–31G* calculations are usually not much better. Some calculated and experimental dipole moments are compared in Table 5.14. These results, which are quite typical, indicate that calculated values tend to be about 0.0–0.5 D higher than experimental, with a mean deviation of about 0.3 D; negative deviations are rare.

Table 5.14 Some calculated dipole moments compared to experimental ones

	Computational level				
	HF/3–21G$^{(*)}$// HF/3–21G$^{(*)}$	HF/6–31G*// HF/3–21G$^{(*)}$	HF/6–31G*// HF/6–31G*	MP2(fc)/6–31G*// MP2(fc)/6–31G*	exp.
CH_3NH_2	1.44	1.3	1.53	1.6	1.3
H_2O	2.39	2.18	2.2	2.24	1.9
HCN	3.04	3.2	3.21	3.26	3
CH_3OH	2.12	1.95	1.87	1.95	1.7
Me_2O	1.85	1.64	1.48	1.6	1.3
H_2CO	2.66	2.79	2.67	2.84	2.3
CH_3F	2.34	2.18	1.99	2.11	1.9
CH_3Cl	2.31	2.32	2.25	2.21	1.9
Me_2SO	4.27	4.55	4.5	4.63	4
CH_3CCH	0.71	0.64	0.64	0.66	0.8
Deviations	9+, 1–	8+, 2–	9+, 1–	9+, 1–	
Mean:	0.33	0.31	0.26	0.34	

Dipole moments are in Debyes; the computational levels are arranged, from left to right, in what is conventionally considered lowest to highest. Calculations are by the author; experimental values are taken from reference [1g], pages 326, 329, 332, 335. For each level is given the number of positive and negative deviations and the arithmetic mean of the absolute values of the deviations

HF/3–21G$^{(*)}$//HF/3–21G$^{(*)}$ (a low ab initio level unlikely to be used nowadays) calculations may show the largest deviations. Single-point HF/3–21G$^{(*)}$ calculations on HF/6–31G* geometries appear to give results about as good as (or better than? Note CH_3NH_2, and Ref. [39], pp. 76, 77) those from MP2(fc)/6–31G*//MP2 (fc)/6–31G* calculations. As is the case for other properties, 3–21G$^{(*)}$ calculations of dipole moments on molecules with atoms beyond neon require polarization functions for reasonable results (the 3–21G$^{(*)}$ basis; Ref. [39], pp. 23–30). The 3–21G$^{(*)}$ calculations in Table 5.14 show a mean deviation 0.33; the HF/6–31G* calculations are only slightly better (mean deviation 0.26) and the MP2/6–31G* calculations appear to be, if anything, slightly worse (mean error 0.34). If high-accuracy calculated dipole moments (0.1 D or better) are needed, high-level correlation and large basis sets must be used; such calculations may be needed to reproduce the magnitude and even the direction of small dipole moments [253], such as in carbon monoxide, a notoriously fickle case [254].

5.5.4.2 Charges and Bond Orders

Chemists make extensive use of the idea that the atoms in a molecule can be assigned electrical *charges*. Thus in a water molecule each hydrogen atom is considered to have an equal, positive, charge, and the oxygen atom to have a negative charge, equal in magnitude to the sum of the hydrogen charges. This concept is clearly related to the dipole moment: in a diatomic (for simplicity) molecule one expects the negative end of the dipole vector to point toward the

a

Where does atom A end and B begin?

b
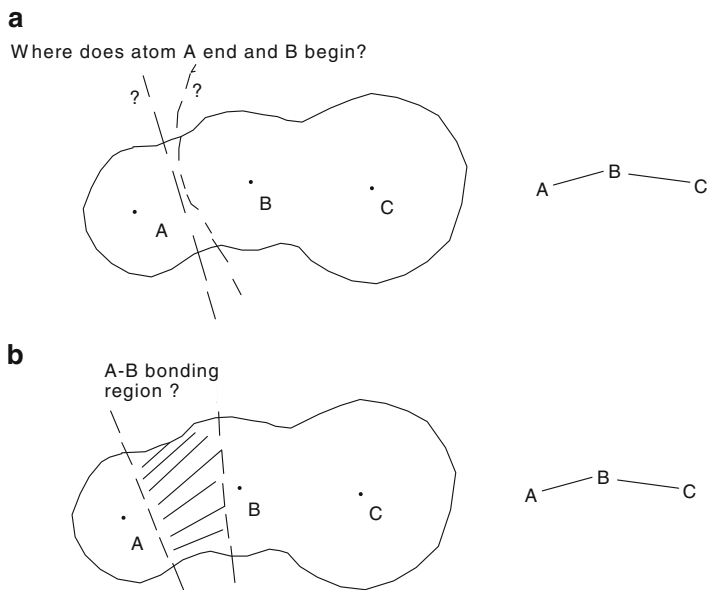
A-B bonding region ?

Fig. 5.38 (**a**) In a molecule where does one atom end and another begin? How is the dividing surface to be drawn? (**b**) How is the bonding region between two nuclei to be defined?

atom assigned the negative charge. However, there are two problems with the concept: first, the charge on an atom in a molecule, unlike the dipole moment of a molecule, cannot be (readily [255]) measured. Second, there is no unique, correct theoretical method for calculating the charge on an atom in a molecule (devotees of atoms-in-molecules (AIM) theory, to be discussed, may dispute this).

Both the measurement and calculational problems arise from the difficulty of defining what we mean by "an atom in a molecule". Consider the hydrogen chloride molecule. As we move from the hydrogen *nucleus* to the chlorine *nucleus*, where does the hydrogen atom end and the chlorine atom begin? If we had a scheme for partitioning the molecule into atoms (Fig. 5.38a), the charge on each atom could be defined as the net electric charge within the space of the atom, i.e. the algebraic sum of the electronic and the nuclear charges. The electronic charge in the defined space could be found by integrating the electron density (which can be calculated from the wavefunction–see *Atoms-in-molecules*, below) over that region of space.

Bond order is a term with conceptual difficulties related to those associated with atom charges. The simplest electronic interpretation of a bond is that it is a pair of electrons shared between two nuclei, somehow [256] holding them together. From this criterion and Lewis structures the C/C bond order in ethane is 1, in ethene 2, and in ethyne 3, in accordance with the classical assignment of a single, a double, and a triple bond, respectively. However, if a bond is a manifestation of the electron density between two nuclei, then the bond order need not be an integer; thus the $C=C$ bond in $H_2C=CH–CHO$, might be expected to have a lower bond order than

the C=C in $H_2C=CH–CH_3$, because the C=O group might drain electron density away toward the electronegative oxygen. However, an attempt to calculate bond order from electron density runs into the problem that in a polyatomic molecule, at any rate, it is not clear how to define precisely the region "between" two atomic nuclei (Fig. 5.38b).

Assigning atom charges and bond orders involves, respectively, calculating the number of electrons "belonging to" an atom or shared "between" two atoms, i.e. the "population" of electrons on or between atoms; hence such calculations are said to involve *population analysis*. Earlier schemes for population analysis bypassed the problem of defining the space occupied by atoms in molecules, and the space occupied by bonding electrons, by partitioning electron density in a somewhat arbitrary way. The earliest such schemes were utilized in the simple Hückel or similar methods [257], and related these quantities to the basis functions (which in these methods are essentially valence, or even just p, atomic orbitals; see Chap. 4, Sect. 4.3.4). The simplest scheme used in ab initio calculations is *Mulliken population analysis* [258].

Mulliken population analysis is in the general spirit of the scheme used in the simple Hückel method, but allows for several basis functions on an atom and does not require the overlap matrix to be a unit matrix. In ab initio theory each molecular orbital has a wavefunction ψ (Sect. 5.2.3.6.1):

$$
\begin{aligned}
\psi_1 &= c_{11}\phi_1 + c_{21}\phi_2 + c_{31}\phi_3 + \ \ldots \ + c_{m1}\phi_m \\
\psi_2 &= c_{12}\phi_1 + c_{22}\phi_2 + c_{32}\phi_3 + \ \ldots \ + c_{m2}\phi_m \\
\psi_3 &= c_{13}\phi_1 + c_{23}\phi_2 + c_{33}\phi_3 + \ \ldots \ + c_{m3}\phi_m \\
&\vdots \\
\psi_m &= c_{1m}\phi_1 + c_{2m}\phi_1 + c_{3m}\phi_3 + \ \ldots \ + c_{mm}\phi_m
\end{aligned}
\tag{5.209 = 5.51}
$$

Here the chosen basis set $\{\phi_1, \phi_2, \ldots \phi_m\}$ engenders MOs $\psi_1, \psi_2, \ldots, \psi_m$. Several basis functions can reside on each atom, so c_{si} is the coefficient of basis function s in MO i (not, as in simple Hückel theory, the sole coefficient of atom s in MO i). For any MO ψ_i, squaring and integrating over all space gives

$$
\int |\psi_i|^2 dv = 1 = c_{1i}c_{1i}S_{11} + c_{2i}c_{2i}S_{22} + \cdots \\
+ 2c_{1i}c_{2i}S_{12} + 2c_{1i}c_{3i}S_{13} + 2c_{2i}c_{3i}S_{23} + \cdots
\tag{5.210}
$$

The integral equals one because the probability that the electron is *somewhere* in the MO (which, strictly, extends over all space) is one; the S_{ij} (both ϕ's the same) overlap integrals are also unity, since the basis functions are normalized (cf. Chap. 4, Sect. 4.4.2).

In the Mulliken scheme each electron in ψ_i is taken to contribute a "fraction of an electron" $c_{1i}c_{1i}S_{11} = c^2{}_{1i}$ to basis function ϕ_1 and a fraction of an electron $2c_{1i}c_{2i}S_{12}$ (see Eq. (5.210)) to the $\phi_1\phi_2$ overlap region, and in general to contribute a fraction of an electron c^2_{ri} to the basis function (loosely, the atomic orbital) ϕ_r on an atom, and a fraction of an electron $2c_{ri}c_{si}S_{rs}$ to the ϕ_r/ϕ_s interatomic overlap

a

MO ψ_i, formed from basis functions ϕ_1 and ϕ_2

ϕ_r ϕ_r ϕ_s
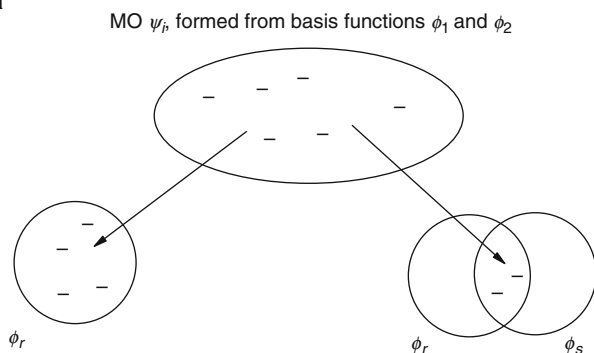
In the MUlliken scheme (Eqs (5.211) and (5.212)):

Each electron in $\mathrm{MO}\psi_i$ contributes a fraction of an electron c_{ri}^2 to $\varPhi_r$ and $2c_{ri}c_{si}S_{rs}$ to the $\varPhi_r / \varPhi_s$ overlap region. If there are n_i electrons in ψ_i , then the MO contributes to the electron population of basis function $\varPhi_r$ $n_{r1} = n_i c_{ri}^2$ electrons, and to the electron population of the $\varPhi_r / \varPhi_s$ overlap region $n_{r/s,i} = n_i(2\,c_{ri}c_{si}S_{rs})$ electrons.

b

ϕ_r ϕ_{s1} ϕ_r ϕ_{s2}

n_r $n_{r/s1}$ $n_{r/s2}$
(population due solely to ϕ_r)
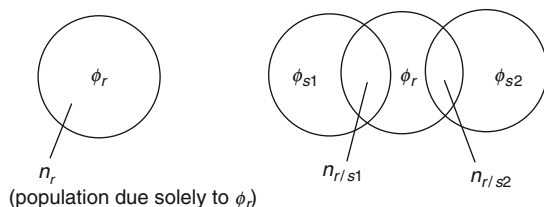
In the Mulliken scheme (Eq (5.215)):

The gross electron population in $\varPhi_r$ is n_r (due solely to $\varPhi_r$), plus half the sum of all the overlap populations: $N_r = n_r + 1/2\,n_{r/s1} + 1/2\,n_{r/s2}$.

Fig. 5.39 The Mulliken scheme for partitioning electron density

space; see Fig. 5.39a. This seems reasonable since (1), the terms sum to one (the "fractions" of the electron must add to one), and (2) it seems reasonable to partition out the contribution of electrons to basis functions and to overlap regions from the "electron density sum" in Eq. (5.210). Now if there are n_i electrons in MO ψ_i, then the contributions of ψ_i to the electron population of basis function ϕ_r and of the overlap region between ϕ_r and ϕ_s are

$$n_{r,i} = n_i c_{ri}^2 \tag{5.211}$$

and

$$n_{r/s,i} = n_i(2c_{ri}c_{si}S_{rs}) \tag{5.212}$$

The total contributions from all the MOs to the electron population in ϕ_r and in the overlap region between ϕ_r and ϕ_s are

$$n_r = \sum_i n_{r,i} = \sum_i n_i c_{ri}^2 \tag{5.213}$$

and

$$n_{r/s} = \sum_i n_{r/s,i} = \sum_i n_i(2c_{ri}c_{si}S_{rs}) \tag{5.214}$$

The sums are over the occupied MOs, since $n_i = 0$ for the virtual MOs. The number n_r is the *Mulliken net population* in the basis function ϕ_r, and the number $n_{r/s}$ is the *Mulliken overlap population* for the pair of basis functions ϕ_r and ϕ_s. The net population summed over all r plus the overlap population summed over all r/s pairs equals the total number of electrons in the molecule.

The quantities n_r and n_s are used to calculate atom charges and bond orders. The *Mulliken gross population in the basis function ϕ_r* is defined as the Mulliken net population n_r (Eq. (5.211)) plus one half of all those Mulliken overlap populations $n_{r/s}$ (Eq. (5.212)) which involve ϕ_r (of course for some ϕ_s, $n_{r/s}$ may be negligible; e.g. for well-separated atoms S_{rs} is very small):

$$N_r = n_r + \frac{1}{2}\sum_{s \neq r} n_{r/s} \tag{5.215}$$

The gross population N_r is an attempt to represent the *total* electron population in the basis function ϕ_r; this is considered here to be the net population n_r, the population that all the occupied MOs contribute to ϕ_r through the representation of ϕ_r in each ψ_i by its coefficient c_{ri} (Eq. (5.213), plus one-half of the all the populations in the overlap regions involving ϕ_r (Fig. 5.39b). Assigning to ϕ_r one-half, rather than some other fraction, of the electron population in an overlap region with ϕ_s is said to be arbitrary. Of course it is not arbitrary, in the sense that Mulliken thought about it carefully and decided that one-half was at least as good as any other fraction. One might imagine a more elaborate partitioning in which the fraction depends on the electronegativity difference between the atoms on which ϕ_r and ϕ_s reside, with the more electronegative atom getting the larger share of the electron population. To get the charge on an atom A we calculate the *gross atomic population for A*:

$$N_A = \sum_{r \in A} N_r \tag{5.216}$$

This is the sum over all the basis functions ϕ_r on atom A (r $\in$ A qualifying the summation means "r belonging to A") of the gross populations in each ϕ_r (Eq. (5.215)); it involves all the basis functions on A and all the overlap regions these functions have with other basis functions ϕ_s. We can regard N_A as the total electron population on atom A (within the limits of the Mulliken treatment). The *Mulliken charge* on atom A, the *net charge* on A, is then simply the algebraic sum of the charges due to the electrons and the nucleus:

$$q_A = Z_A - N_A \qquad (5.217)$$

The *Mulliken bond order* for the bond between atoms A and B is the total population for the A/B overlap region:

$$b_{AB} = \sum_{r,\,s \in A,\,B} n_{r/s} \qquad (5.218)$$

The overlap population for basis functions ϕ_r and ϕ_s (Eq. (5.214)) is summed over all the overlaps between basis functions on atoms A and B.

Since the formulas for calculating Mulliken charges and bond orders (Eqs. (5.211), (5.212), (5.213), (5.214), (5.215), (5.216), (5.217), and (5.218)) involve summing basis function coefficients and overlap integrals, it is not too surprising that they can be expressed neatly in terms of the density matrix (Sect. 5.2.3.6.4) **P** and the overlap matrix **S** (Chap. 4, Sect. 4.3.3). The elements of the density matrix **P** are (cf. Eqs. (5.208 = 5.81))

$$P_{rs} = 2 \sum_{i=1}^{n} c_{ri} c_{si} \qquad (5.219)$$

The matrix element P_{rs} is summed over all filled MOs (from ψ_1 to ψ_n for the ground electronic state of a $2n$-electron closed-shell molecule); an example of the calculation of **P** was given in Sect. 5.2.3.6.5. The elements of the overlap matrix **S** are simply the overlap integrals:

$$S_{rs} = \int \phi_r \phi_s dv \qquad (5.220)$$

From Eq. (5.219) it follows that the matrix (**PS**) obtained by multiplying corresponding elements of **P** and **S**,

$$(PS) = \begin{pmatrix} (PS)_{11} & (PS)_{12} & (PS)_{13} & \cdots & (PS)_{1m} \\ (PS)_{21} & (PS)_{22} & (PS)_{23} & \cdots & (PS)_{2m} \\ \vdots & \vdots & \cdots & \vdots & \\ (PS)_{m1} & (PS)_{m2} & (PS)_{m3} & \cdots & (PS)_{mm} \end{pmatrix} \qquad (5.221)$$

has elements

$$(PS)_{rs} = P_{rs}S_{rs} = 2\sum_{i=1}^{n} c_{ri}c_{si}S_{rs} \qquad (5.222)$$

Note that $(\mathbf{PS})$ is *not* the matrix $\mathbf{PS}$ obtained by matrix multiplication of $\mathbf{P}$ and $\mathbf{S}$; each element of *that* matrix would result from series multiplication: a row of $\mathbf{P}$ times a column of $\mathbf{S}$ (Chap. 4, Sect. 4.3.3).

The diagonal elements of $(\mathbf{PS})$ are

$$(PS)_{rr} = P_{rr}S_{rr} = 2\sum_{i=1}^{n} c_{ri}^2 \qquad (5.223)$$

Compare this with Eq. (5.213): for a ground-state closed-shell molecule there are two electrons in each occupied MO and Eq. (5.213) can be written

$$n_r = 2\sum_{i=1}^{n} c_{ri}^2 \qquad (5.224)$$

i.e.

$$n_r = (PS)_{rr} \qquad (5.225)$$

The off-diagonal elements of $(\mathbf{PS})$ are given by Eq. (5.222), $r \neq s$. Compare this with Eq. (5.214): for a ground-state closed-shell molecule there are 2 electrons in each occupied MO and Eq. (5.214) can be written

$$n_{r/s} = 2\sum_{i=1}^{n} \left(2c_{ri}c_{si}S_{rs}\right) \qquad (5.226)$$

i.e.

$$n_{r/s} = 2(PS)_{rs} \qquad (5.227)$$

Thus the matrix $(\mathbf{PS})$ can be written

$$(\mathbf{PS}) = \begin{pmatrix} n_1 & \frac{1}{2}n_{1/2} & \frac{1}{2}n_{1/3} & \cdots & \frac{1}{2}n_{1/m} \\ \frac{1}{2}n_{2/2} & n_2 & \frac{1}{2}n_{3/3} & \cdots & \frac{1}{2}n_{2/m} \\ \vdots & \vdots & \cdots & & \vdots \\ \frac{1}{2}n_{m/1} & \frac{1}{2}n_{m/2} & \frac{1}{2}n_{m/3} & \cdots & n_m \end{pmatrix} \qquad (5.228)$$

The matrix $(\mathbf{PS})$ (or sometimes $2(\mathbf{PS})$) is called a *population matrix*.

5.5.4.3   An Example of Population Analysis: $\mathbf{H - He^+}$

As a simple illustration of the calculation of atom charges and bond orders, consider $H-He^+$. From our ab initio Hartree-Fock calculations on this molecule (Sect. 5.2.3.6.5) we have

$$\mathbf{P} = \begin{pmatrix} 0.2020 & 0.5097 \\ 0.5079 & 1.2864 \end{pmatrix} \quad \text{and} \quad \mathbf{S} = \begin{pmatrix} 1.0000 & 0.5017 \\ 0.5017 & 1.0000 \end{pmatrix} \tag{5.229}$$

$$\text{Therefore} \quad (\mathbf{PS}) = \begin{pmatrix} 0.2020 & 0.2557 \\ 0.2557 & 1.2864 \end{pmatrix} \tag{5.230}$$

From Eq. (5.228), (**PS**) gives us

$$\begin{aligned} n_1 &= 0.2020 \\ n_2 &= 1.2864 \\ n_{1/2} &= n_{2/1} = 2(0.2557) = 0.5114 \end{aligned}$$

Charge on H, q_H For this we need N_H, the sum of all the N_r on H (Eqs. (5.216) and (5.215)). There is only one basis function on H, ϕ_1, so there is only one relevant N_r for H, and for ϕ_1 there is only one overlap, with ϕ_2, so the summation involves only one term, $n_{1/2}$. Using Eq. (5.215):

$$N_r = N_1 = n_r + \frac{1}{2}\sum_{s \neq r} n_{r/s} = n_1 + \frac{1}{2}\left(n_{1/2}\right) = 0.2020 + \frac{1}{2}(0.5114) = 0.4577$$

The sum of all the N_r on H has only one term, N_1, since there is only one basis function on H. Using Eq. (5.216):

$$N_A = N_H = \sum_{r \in H} N_r = N_1 = 0.4577$$

The charge on H, q_H, is the algebraic sum of the gross electronic population and the nuclear charge: (Eq. (5.217)):

$$q_A = q_H = Z_H - N_H = 1 - 0.4577 = 0.5423$$

Charge on He, q_{He} For this we need N_{He}, the sum of all the N_r on He (Eq. (5.216). There is only one basis function on He, ϕ_2, so there is only one relevant N_r for He, and for ϕ_2 there is only one overlap, with ϕ_1, so the summation involves only one term, $n_{2/1}(=n_{2/1})$:

$$N_r = N_2 = n_r + \frac{1}{2}\sum_{s \neq r} n_{r/s} = n_2 + \frac{1}{2}\left(n_{2/1}\right) = 1.2864 + \frac{1}{2}(0.5114) = 1.5421$$

The sum of all the N_r on He has only one term, N_2, since there is only one basis function on He:

$$N_A = N_{He} = \sum_{r \in He} N_r = N_2 = 1.5421$$

The charge on He, q_{He}, is the algebraic sum of the gross electronic population and the nuclear charge:

$$q_A = q_{He} = Z_{He} - N_{He} = 2 - 1.5421 = 0.4579$$

The charges sum to $0.5423 + 0.4579 = 1.000$, the total charge on the molecule. The less positive charge on helium is in accord with the fact that electronegativity increases from left to right along a row of the periodic table. Charges for HHe^+ from bigger basis sets and other methods likewise give helium the smaller charge, but make the distribution much more uneven, with ca. 0.8 on H and 0.2 on He.

H-He bond order For this we use Eq. (5.218); $n_{r/s}$ is summed for all overlaps between basis functions on atoms A and B. There is only one such overlap, that between ϕ_1 and ϕ_2, so

$$b_{AB} = b_{HHe} = \sum_{r, s \in A, B} n_{r/s} = n_{1/2} = 2(0.2557) = 0.5114$$

Note that the elements of the population matrix (**PS**) sum to the number of electrons in the molecule: $0.2020 + 1.2864 + 0.2557 + 0.2557 = 2.000$. This is expected, since the diagonal elements are the number of electrons in the "atomic space" of the basis functions, and the off-diagonal elements are the number of electrons in the overlap space of the basis functions. Bond orders for HHe^+ from bigger basis sets and other methods are similar, in the range 0.4–0.5. The higher charge on hydrogen and the low bond order are consistent with a very low basicity or proton affinity for a helium atom: G4 calculations on the equilibrium

$$HHe^+ + H_2O \leftrightarrows He + H_3O^+$$
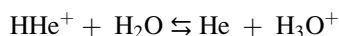
place the products (as written) 503 kJ mol^{-1} lower in free energy than the reactants, corresponding to an equilibrium constant of ca. 10^{88} in favor of the protonation of water.

The Mulliken approach to population analysis has problems; for example, it sometimes assigns more than two electrons, and sometimes a negative number of electrons, to an orbital. It is also fairly basis-set dependent (Hehre, Radom, Schleyer and Pople compare Mulliken charges for a variety of molecules using the STO-3G, 3–21G$^{(*)}$ and 6–31G* basis sets: Ref. [1g], pp. 337–339). Partitioning half of the electrons "arbitrarily" in the overlap region is not as serious as one might have thought, because in a series of calculations a meaningful trend can emerge, even if a charge or bond order taken in isolation is of dubious quantitative significance.

No doubt Mulliken never intended his population analysis numbers to be of stand-alone quantitative significance – see the comments on this in Chap. 6, Sect. 6.3.4.2. Other approaches to manipulating basis function coefficients for partitioning electrons among orbitals and thus calculating charges and bond orders are those of Mayer [259] and Löwdin [260] and the natural population analysis (NPA) of Weinhold [261]. One point of interest in the Mayer method is that it seems to be the only one that assigns the hydrogen molecule ion, $H_2^{\bullet+}$, with one electron, the intuitively sensible bond order of 0.5, rather than 0.25 [262]. Mayer bond orders appear to have been used particularly in inorganic chemistry [263]. The most popular method of population analysis now is probably Weinhold's NPA, and the favored atom charges are evidently those from NPA, and electrostatic potential charges (next section). The methods of Mulliken, Löwdin and Weinhold are explained and compared in more detail by Cramer [264], and those of Mulliken, Löwdin and Mayer by Leach [265]. Atom charges have been calculated from IR stretching intensities, and show generally good agreement with those from methods based on electrostatic potential [266].

A fairly recent (2013), rather elaborate procedure for resolving the electron distribution in molecules into orbitals that seem chemically more intuitively sensible than the delocalized canonical molecular orbitals (end of Sect. 5.2.3.1) is based on the idea of "quasi-atomic" orbitals. These minimal-basis localized orbitals resemble the orbitals of isolated atoms and "reveal the atomic structure and the bonding pattern of a molecule" [267a]. This work rests largely on a series of papers by Ruedenberg and coworkers, beginning with a conceptually deep and mathematically very elaborate exploration of how a wavefunction might be analyzed to exhibit chemically useful information [267b]. Quasi-atomic orbitals have been used to analyze the electron distribution in urea [267c] and the dissociation of dioxetane, $C_2H_4O_2$, into formaldehyde [267d]. For some purposes one may be satisfied with interpreting electron distribution with the aid of the simpler methods in this section: dipole moment, atom charges, bond orders, electrostatic potential, and even atoms-in-molecules.

5.5.4.4 Electrostatic Potential

The *electrostatic potential* (ESP) is a measure of charge distribution that also provides other useful information [268]. The electrostatic potential at a point P in a molecule is defined as the amount of energy (work) needed to bring a unit point positive "probe charge" (e.g. a proton) from infinity to P. It can be thought of as a measure of how positive or negative the molecule is at P: a positive value at the point means that the net effect experienced by the probe charge as it was brought from infinity was repulsion, while a negative value means that the probe charge was attracted to P, i.e. energy was *released* as it fell from infinity to P. The ESP at a point is the net result of the effect of the positive nuclei and the negative electrons. The calculation of the effect of the nuclei is trivial, following directly from the fact

that the potential due to a point charge Z at a distance r away from the unit charge is, at point P:

$$V(P) = \int_r^{\infty} \frac{Z \times 1}{r^2} dr = \frac{Z}{r} \tag{5.231}$$

Thus the ESP created by the nuclei is

$$V(P)_{\text{nuc}} = \sum_A \frac{Z_A}{|\mathbf{r}_P - \mathbf{r}_A|} \tag{5.232}$$

where $|\mathbf{r}_p - \mathbf{r}_A|$ is the distance from nucleus A to the point P, i.e. the absolute value of the difference of two vectors. To obtain the expression for the ESP due to the electrons, we can modify Eq. (5.232) by replacing the summation over the nuclei by an integral over infinitesimal volume elements of the electron density or charge density $\rho(\mathbf{r})$ (see Sect. 5.5.4.5, *Atoms-in-molecules*). We get for the total ESP at P

$$V(P)_{\text{tot}} = V(P)_{\text{nuc}} + V(P)_{\text{el}} = \sum_A \frac{Z_A}{|\mathbf{r}_P - \mathbf{r}_A|} - \int \frac{\rho(\mathbf{r})}{|\mathbf{r}_P - \mathbf{r}|} d\mathbf{r} \tag{5.233}$$

The ESP at many points on the surface of the molecule can be calculated (Sect. 5.5.6) and a set of atom charges then calculated to fit (by a least-squares procedure) the ESP values, and also to sum to the net charge on the molecule (the use of visualization of the ESP is discussed in Sect. 5.5.6). Values of Mulliken and Löwdin bond orders, and Mulliken, natural and ESP atom charges, are compared in Table 5.15, for hydrogen fluoride. We see that the Mulliken charges vary considerably, but apart from the STO-3G values, the electrostatic charges vary very little,

Table 5.15 Comparing Mulliken, electrostatic potential and natural charges, and Mulliken and Löwdin bond orders, at various levels, for hydrogen fluoride

level	charge on H (= − charge on F)			bond order	
	Mulliken	electrostatic	natural	Mulliken	Löwdin
HF/STO-3G	0.19	0.28	0.23	0.96	0.98
HF/3–21G$^{(*)}$	0.45	0.49	0.5	0.78	0.93
HF/6–31G*	0.52	0.45	0.56	0.72	0.82
HF/6–31G**	0.39	0.45	0.56	0.86	1.07
HF/6–311G**	0.32	0.46	0.54	0.95	1.32
6–31 + G*	0.57	0.48	0.58	0.64	0.75
6–311++G**	0.3	0.47	0.55	0.98	1.27
MP2/6–31G*	0.52	0.45	0.56	0.72	0.81

The geometry used in each case corresponds to the method/basis set for that charge or bond order, but any reasonable geometry should give essentially the same results. There are no experimental data!

and the natural charges little, with the level of calculation. Bond orders, however, are more sensitive to the level of calculation. The utility of charges and bond orders lies not in their absolute values, but rather in the fact that a comparison of, say, Löwdin charges or bond orders, calculated at the same level for a *series* of molecules, can provide insights into a trend. For example, one might argue that the electron-withdrawing power of a series of groups A, B, etc. could be compared by comparing the C/C bond orders in A–$CH=CH_2$, B–$CH=CH_2$, etc. Bond orders have been used to judge whether a species is free or really covalently bonded, and have been proposed as an index of progress along a reaction coordinate [269].

5.5.4.5   Atoms-In-Molecules (AIM)

A method of population analysis that may be less arbitrary than any of those mentioned so far is based on the theory of atoms in molecules, designated AIM, or the quantum theory of atoms in molecules, QTAIM. This was developed by Bader[5] and coworkers, and is based on the mathematical partitioning of molecules into regions which correspond to atoms. The concept may have developed from Berlin's ca. 1950 work on partitioning molecules into "binding" and "antibinding" regions [270a], cited by Bader in a 1964 paper on electron distribution [270b]. The first specific assertion that atoms in molecules in a sense retain their identities rather than dissolving into a molecular pool of nuclei and electrons seems to have been made even before the use of the terms encapsulated in the AIM or QTAIM acronyms: in a 1973 paper by Bader and Beddall the question "are there atoms in molecules?" was posed and answered in the affirmative [271]. An early review (1975) proposed "a return to....'the atoms in molecules' approach to chemistry" ("return" in the sense of focussing on atoms rather than on bonds, which latter had risen to supremacy with MO theory) and summarized the essential concepts of AIM theory [272]. Bader reviewed the subject a decade later [273], and summarized it a few years after that in his comprehensive 1990 book [274] and in a 1991 review [275]. Popelier updated the subject in his 1999 book [276] and in the 2007 book edited by Matta and Boyd, the ideas of Bader's "classic 1990 treatise" are again updated [277]. Bader simplified the derivation of the theory in seven pages optimistically titled "Everyman's Derivation of the Theory of Atoms in Molecules" which he hoped would aid "its general acceptance by experimental chemists" [278]. We now examine the theory and some applications.

The AIM approach rests on analyzing the variation from place to place in a molecule of the electron density function (electron probability function, charge density function, charge density), ρ. This is a function $\rho(x, y, z)$ which gives the variation of the total electron density from point to point in the molecule: $\rho(x, y, z) \, dxdydz = \rho(x, y, z)dv$ is the probability of finding an electron in the infinitesimal

---

volume dv centered on the point (x, y, z) (the probability of finding *more than one* electron in dv is insignificant). This probability is the same as the charge in dv if we take the charge on an electron as our unit of charge, hence the name charge density for the electron density function ρ. Since ρdv has the "units" of probability, a pure number, the function ρ logically has the units volume^{-1}. However, the probability we deal with here is the same as the number (or fraction) of electrons in dv, which is the charge in dv in electronic units, so the units of ρ can be taken more physically concretely as electrons volume^{-1} or charge volume^{-1}. In atomic units this is electrons bohr^{-3}. The electron density function can be calculated from the wavefunction. It is not, as one might have thought, simply $|\psi|^2$, where ψ is the multielectron wavefunction of space and spin coordinates (Sect. 5.2.3.1). *This* latter is the probability function for finding in the region of (x, y, z) electron 1 with a specified spin, electron 2 with a specified spin, etc., at points (x, y, z). The function ρ is the number of electrons in the molecule times the sum over all their spins of the integral of the square of the molecular wavefunction integrated over the coordinates of all but one of the electrons [279]. We can write it in the condensed notation

$$\rho(x, y, z) = n \sum_{\text{all spins}} \int_2^n \psi^2 d\mathbf{r}_2 \dots d\mathbf{r}_n \qquad (5.234)$$

where $\mathbf{r}$ is vector notation for the coordinates of electrons. If we think of the electrons as being smeared out in a fog around the molecule, then the variation of ρ from point to point corresponds to the varying density of the fog, and $\rho(x, y, z)$ centered on a point $P(x, y, z)$ corresponds to the amount of fog in the volume element $dxdydz = dv$. Alternatively, in a scatterplot of electron density (charge density) in a molecule, the variation of ρ with position can be indicated by varying the volume density of the points. The electron density function ρ is the "density" in density functional theory, DFT (Chap. 7). Let us look at some properties of ρ that are relevant to AIM, the theory of atoms in molecules.

Consider first the electron density function ρ around an atom. As we approach the nucleus this rises toward a maximum, or the *negative* of the electron density, $-\rho$, falls toward a minimum (Fig. 5.40). Viewing the electron distribution in terms of $-\rho$ rather than ρ is useful because it more easily enables us to discern analogies between the variation of ρ in a molecule (a ρ vs. location-in-molecule graph), and a potential energy surface (PES, an energy vs. geometry graph), with which we are familiar from Chap. 2. Examine the distribution of $-\rho$ in a homonuclear diatomic molecule X_2 (Fig. 5.41). This shows a plot of $-\rho$ vs. two of the three Cartesian coordinates needed to assign positions to all the points in the molecule. The graph retains the internuclear axis (by convention the z-axis) and one other axis, say y; the molecule is symmetrical with respect to reflection in the yz plane. The negative of the electron density, $-\rho$, dips toward a minimum at the atomic nuclei (ρ goes toward a maximum), analogously to the occurrence of a minimum on a PES. The analogy is not perfect, because the nuclei do not correspond to true stationary points: the point is a *cusp*, where $\partial\rho/\partial q$ is discontinuous rather than zero (unlike $\partial E/\partial q$ for a stationary point on a PES; q is a geometric parameter) [280]. This is not the death knell for our analogy, because there is always a function "similar" –
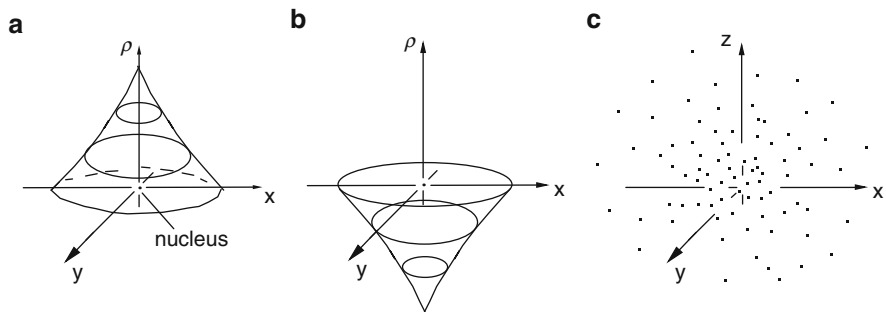
Fig. 5.40 The distribution of electron density (charge density) ρ for an atom; the nucleus is at the origin of the coordinate system. (**a**) Variation of ρ with distance from the nucleus. Moving away from the nucleus ρ decreases from its maximum value and fades asymptotically toward zero. (**b**) Variation of $-\rho$ with distance from the nucleus; $-\rho$ becomes less negative and approaches zero as we move away from the nucleus. The $-\rho$ picture is useful for molecules (Fig. 5.41) because it makes clearer analogies with a potential energy surface. (**c**) A "4-D" picture (ρ vs. x, y, z) of the variation of ρ in an atom: the density of the dots (number of dots per unit volume) indicates qualitatively electron density ρ in various regions
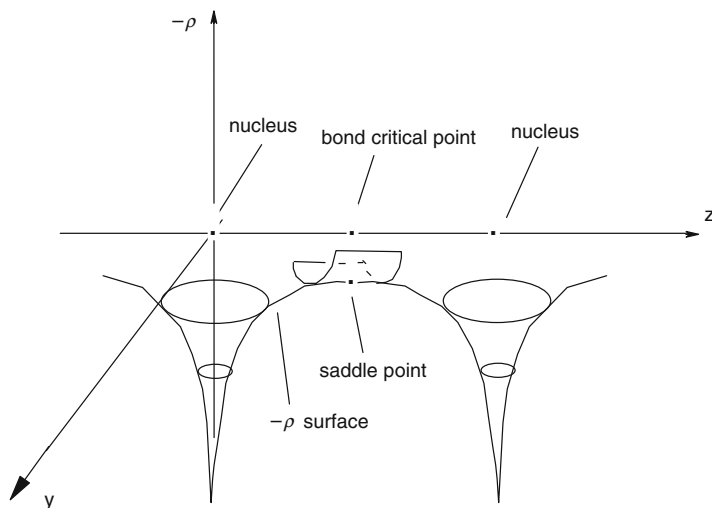
Fig. 5.41 The distribution of the electron density (charge density) ρ for a homonuclear diatomic molecule X_2. One nucleus lies at the origin, the other along the positive z-axis (the z-axis is commonly used as the molecular axis). The xz plane represents a slice through the molecule along the z-axis. The $-\rho = f(x, z)$ surface is analogous to a potential energy surface $E = f$ (nuclear coordinates), and has minima at the nuclei (maximum value of ρ) and a saddle point, corresponding to a bond critical point, along the z axis (midway between the two nuclei since the molecule is homonuclear)

technically, *homeomorphic* – to $\rho(x, y, z)$ for which the nuclear positions are stationary points [280]. With the caveat that strictly speaking the derivatives apply to the homeomorphic function, we can write:

$$\frac{\partial(-\rho)}{\partial z} = 0, \quad \frac{\partial(-\rho)}{\partial y} = 0, \quad \frac{\partial(-\rho)}{\partial x} = 0 \qquad (5.235)$$

and

$$\frac{\partial^2(-\rho)}{\partial z^2} > 0, \quad \frac{\partial^2(-\rho)}{\partial y^2} > 0, \quad \frac{\partial^2(-\rho)}{\partial x^2} > 0 \qquad (5.236)$$

Moving along the internuclear line we find a point in a saddle-shaped region, analogous to a transition state, where the surface again has zero slope (all first derivatives zero), and is negatively curved along the z-axis but positively curved in all other directions (Fig. 5.41), i.e.

$$\frac{\partial^2(-\rho)}{\partial z^2} < 0, \quad \frac{\partial^2(-\rho)}{\partial y^2} > 0, \quad \frac{\partial^2(-\rho)}{\partial x^2} > 0 \qquad (5.237)$$

This transition-state-like point is called a *bond critical point*. All points at which the first derivatives are zero (caveat above) are critical points, so the nuclei are also critical points. Analogously to the energy/geometry Hessian of a potential energy surface, an electron density function critical point (a relative maximum or minimum or saddle point) can be characterized in terms of its second derivatives by diagonalizing the ρ/q Hessian ($q = x$, y, or z) to get the number of positive and negative eigenvalues:

$$\rho/q \text{ Hessian} = \begin{pmatrix} \partial^2\rho/\partial x^2 & \partial^2\rho/\partial xy & \partial^2\rho/\partial xz \\ \partial^2\rho/\partial yx & \partial^2\rho/\partial y^2 & \partial^2\rho/\partial yz \\ \partial^2\rho/\partial zx & \partial^2\rho/\partial zy & \partial^2\rho/\partial z^2 \end{pmatrix} \qquad (5.238)$$

For the ρ/q surface of Fig. 5.41 the number of positive and negative eigenvalues for a nuclear critical point are 3 and 0, and for a bond critical point, 2 and 1. Thus for the ρ/q surface to which the Hessian of Eq. (5.238) refers (the mirror image of the $-\rho/q$ surface), the number of positive and negative eigenvalues is, respectively, 0 and 3 (for a nucleus), and 1 and 2 (for a bond critical point). The behavior of the second derivative of ρ, the Laplacian of ρ, $\left(\partial^2/\partial x^2 + \partial^2/\partial y^2 + \partial^2/\partial z^2\right)\rho = \nabla^2\rho$, is a key concept in AIM theory.

The minimum-$(-\rho)$ path (maximum ρ path) from one X nucleus to the other is the *bond path*; with certain qualifications this can be regarded as a bond. It is analogous to the minimum-energy path connecting a reactant and its products, i.e. to the intrinsic reaction coordinate. Such a bond is not necessarily a straight
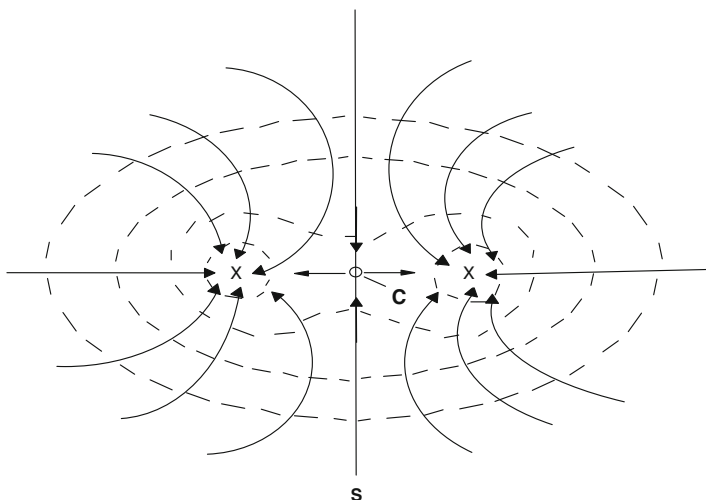
Fig. 5.42 Contour lines for ρ, the electron density distribution, in a homonuclear diatomic molecule X_2. The *lines* originating at infinity and terminating at the nuclei and at the bond critical point **C** are trajectories of the gradient vector field (the *lines* of steepest increase in ρ; two trajectories also *originate* at **C**). The *line* **S** represents the dividing surface between the two atoms (the *line* is where the plane of the paper cuts this surface). **S** passes through the bond critical point and is not crossed by any trajectories

line: in strained molecules it may be curved (bent bonds). The bond passes through the bond critical point, which for a homonuclear diatomic molecule X_2 is the midpoint between of the internuclear line. Now consider Fig. 5.42, which shows in the X_2 molecule another characteristic of the electron density function. The contour lines represent electron density, which rises as we approach a nucleus and falls off as we go to and beyond the van der Waals surface. If it is true that the molecule can be divided into atoms, then for X_2 the dividing surface S (represented as vertical lines in Fig. 5.42) must lie midway between the nuclei, with the internuclear line being normal to S and meeting S at the bond critical point. The electron density defines a *gradient vector field*, the totality of the *trajectories* each of which results from starting at infinity and moving along the path of steepest increase in ρ. Figure 5.42 shows that only two of the trajectories (of those in the plane of the paper) that originate at infinity do not end at the nuclei; these end at the bond critical point. These two trajectories define the intersection of S with the plane of the paper. None of the trajectories cross S, which is thus called a *zero-flux* surface (the gradient vector field is analogous to an electric field whose "flux lines" point along the direction of attraction of a positive charge toward a central negative charge). Because X_2 is homonuclear, the zero-flux surface S is a plane. For a molecule with different nuclei, the zero-flux surfaces are curved, convex in one direction, concave in the other (Fig. 5.43). The space within a molecule bounded by one (for a diatomic molecule) or more zero-flux surfaces is an *atomic basin*. Away from the nuclei toward the outside of the molecule the basin extends outward to
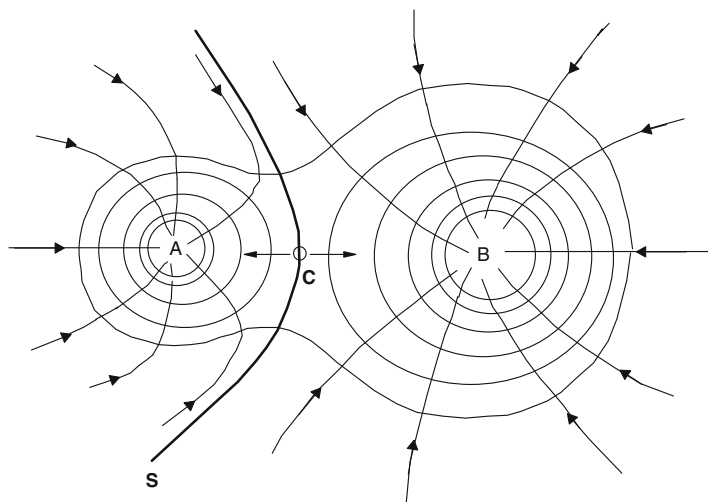
Fig. 5.43 Heteronuclear (as well as homonuclear; cf. Fig. 5.42) molecules can be partitioned into atoms. **S** represents a slice through the zero-flux surface that defines the atoms A and B in a molecule AB. The lines with arrows are the trajectories of the gradient vector field. **S** passes through the bond critical point **C** and is not crossed by any trajectory lines

infinity, becoming shallower as the electron density fades toward zero. The nucleus and the electron density in an atomic basin constitute an atom in a molecule. Even for molecules other than homonuclear diatomics, atoms are still defined by atomic basins partitioned off by unique zero-flux surfaces, as illustrated in Fig. 5.43.

In the AIM method, the charge on an atom is calculated by integrating the electron density function $\rho(x, y, z)$ over the volume of its atomic basin. The charge is the algebraic sum of the electronic charge and the nuclear charge (i.e. the atomic number of the nucleus minus the number of electrons, which could be fractional, in the basin). An AIM bond order can be defined in terms of the electron density ρ_b at the bond critical point, and the bond order b_{AB} for two particular atoms A and B is then defined by an empirical equation obtained by fitting ρ_b to a few accepted A–B bond orders [281]. For example, for nitrogen/nitrogen bonds a linear equation $b_{AB} = a_{NN}\rho_b + b_{NN}$ correlates b_{AB} and ρ_b for, say, $H_2N–NH_2$, $HN{=}NH$ and $N{\equiv}N$; from this equation bond orders can be assigned to other nitrogen/nitrogen bonds from their ρ_b values. AIM bond orders seem surprisingly empirical in contrast to the general spirit of the theory, but this may be because of the need to connect the rigorous mathematical nature of the continuous electron density function with the discrete (1, 2, 3, . . .) concept of bond order.

The main application of AIM has been to investigate whether, in questionable cases, there really is a bond between certain atoms. Fairly recent (2006–2009) examples of this are studies of: the differences between results from AIM and from other methods of population analysis [282], hydrogen bonding to π-donors [283], hydrogen bonding to σ-donors [284], and secondary interactions (i.e. weak bonding) in Diels-Alder reactions [285]. Other recent applications are studies of strain

energies in small rings [286] and of electron distribution in protonated nitriles [287].

AIM theory and applications, and the inextricable question of the virtues and defects of the wavefunction versus the electron density, have engendered an entertaining series of polemics. Frenking censured Gillespie and Popelier for being enamored with electron density and slighting wavefunctions [288], eliciting a spirited reply from those authors [289] and then a defence of his review by Frenking [290]. Bader jumped into the fray with a rather spirited appeal to fundamental physics, defending what he took to be Schrödinger's prescient view that the wavefunction should be regarded as a mathematical abstraction en route to the electron density [291] (a more sedate defence of AIM calculation of atom charges rebutted criticisms of charges as being not observable or not unique [292]). A return to polemics was seen when Kovacs et al. [293] allegedly used "wrong physics" [294] in interpreting the Laplacian of the electron density. This educed a rebuke of (in a certain context at least) "orthodox understanding of physics" and an assertion that "*Chemical research begins where the physics of Richard Bader ends.*" [295]. Another, almost anticlimactic, thread sprung from an AIM analysis by Bader and coworkers that inferred bonding between *ortho*-hydrogens in planar biphenyl [296]. This was criticised by Poater et al. [297], defended by Bader [298], and again criticised by Poater et al. with an interesting reference to the apparent (according to AIM) bonding of helium trapped in an adamantane cage [299].

There are many technical terms, qualifications, and fine points which could not be gone into here. The reader will gather that the correct use of the AIM method can be tricky, and one is urged to consult review papers and books for more details, and to proceed with caution, especially if one is sensitive to criticism.

5.5.5 *Miscellaneous Properties–UV and NMR Spectra, Ionization Energies, and Electron Affinities*

A few other properties that can be calculated by ab initio methods are briefly treated here.

5.5.5.1 **UV Spectra**

Ultraviolet spectra result from the promotion of an electron in an occupied MO of a ground electronic state molecule into a virtual MO, thus forming an electronically excited state [300] (excited state-to-excited state spectra are not much studied by experimentalists). Calculation of UV spectra with reasonable accuracy requires some method of dealing with excited states. Simply equating energy differences between ground and excited states with $h\nu$ does not give satisfactory results for the

Table 5.16 Calculated and experimental UV spectra of methylenecyclopropene, using the RCIS/6–3+G* method on the HF/6–31G* geometry

Calculated		Experimental	
wavelength (nm)	Relative intensity	wavelength (nm)	Relative intensity
222	15	309	13
209	7	242	0.6
196	0	206	100
193	9		
193	100		

The procedure and the experimental values are given in reference [1e], Chap. 9

absorption frequency/wavelength, because the energy of a virtual orbital, unlike that of an occupied one, is not a good measure of its energy (of the energy needed to remove an electron from it; this is dealt with in connection with ionization energies and electron affinities) and because this method ignores the energy difference between a singlet and a triplet state.

Electronic spectra of modest accuracy can be calculated by the configuration interaction CIS method (Sect. 5.4.3) [301]. Compare, for example, the UV spectra of methylenecyclopropene calculated by the CIS/6–31+G* method (diffuse functions appear to be desirable in treating excited states, as the electron cloud is relatively extended) with the experimental spectrum, in Table 5.16. The geometry used is not critical; here HF/6–31G* was employed, but the AM1 geometry (a semiempirical method, Chap. 6, far faster than ab initio) gave essentially the same UV. The agreement in wavelength is not particularly good for the longest-wavelength band, although this result can be made more palatable by noting that both calculation and experiment agree reasonably well on relative intensities, if we take the two calculated bands not observed to correspond to the strong band seen at 206 nm. The CIS approach to excited states has been said [302] to be analogous to the Hartree-Fock approach to ground states in that both give at least qualitatively useful results. Better results are sometimes obtained by semiempirical methods like ZINDO (Chap. 6) or density functional methods like TDDFT (Chap. 7).

5.5.5.2 NMR Spectra

NMR spectra result from the transition of an atomic nucleus in a magnetic field from a low-energy to a high-energy state [236]. There are two aspects to the quantum-mechanical calculation of NMR spectra [303]: calculation of shielding (chemical shifts) and calculation of splitting (coupling constants). Most of the computational work on NMR spectra has focussed on calculating the shielding (magnetic field strength needed for the transition relative to that needed for some reference) of a nucleus. This requires calculation of the magnetic shielding of the nuclei of the molecule of interest, and of the reference nuclei, usually those of tetramethylsilane, TMS. The chemical shift of (e.g.) the ^{13}C or ^1H nucleus is then its

(absolute) shielding value minus that of the TMS ^{13}C or ^1H nucleus. The theory behind the calculation of shielding and splitting has been reviewed [303]. NMR chemical shifts can be calculated with remarkable accuracy even at the Hartree-Fock level [304], and good results were obtained for ^{13}C, ^{15}N, and ^{17}O nuclei even using HF/6–31G*, although density functional calculations gave smaller errors [305]. More advanced calculations, considering electron correlation and even relativity, and biochemical applications (the binding of ^{129}Xe to proteins), have been reviewed [306]. Highly accurate "near quantitative agreement with experimental gas-phase values..." were achieved by highly correlated (CCSD and CCSD (T)) methods with big basis sets on methanol [307]. Such elaborate calculations on a very small molecule are valuable as theoretical benchmarks rather than practical methods, and near the other extreme, a study of (possibly pharmacologically relevant?) chloropyrimidines in solution tackled the "accuracy vs. time dilemma" and compared ab initio and density functional ^{13}C and ^1H chemical shifts with results from database programs [308]. The latter method of obtaining shift values relies on comparing the locations of the various nuclei in one's molecule with the locations and experimental shifts of nuclei in a large library of molecules. With a judicious comparison algorithm, good results can be obtained (references in [308]). One conclusion of this study was that "Unlike ^{13}C chemical shifts, high correlated levels of theory and large basis sets are equally very important for the accurate prediction of proton chemical shieldings." Nevertheless, if high accuracy is not demanded, then as stated above [304, 305] useful results can be obtained at modest levels. This is clearly shown in Fig. 5.44; particularly interesting is the nice replication of the remarkable shielding effect of the benzene ring in [7] paracyclophane [309]. In this connection, the calculation of NMR spectra has become an important tool in probing aromaticity [156] and antiaromaticity [174], using the NICS (nucleus-independent chemical shift) test [310].

NMR splitting (obtaining coupling constants) is harder to calculate than shielding (chemical shifts), because it requires "calculation of the response of the wave function with respect to the full set of nuclear magnetic moments" and "is a much more expensive undertaking than the evaluation of all the shielding constants." [303]. The subject has been treated in a review which concurs that "Accurate calculation of spin-spin coupling constants is a difficult task" [311].

5.5.5.3   Ionization Energies and Electron Affinities

Ionization energies (the term is preferred to the older one, ionization potentials) and electron affinities are related in that both involve transfer of an electron between a molecular orbital and infinity: in one case (IE) we have removal of an electron from an occupied orbital and in the other (EA) addition of an electron to a virtual (or a half-occupied) orbital. The IE for an orbital (or an atom or molecule) is defined as the energy needed to remove an electron from the entity to infinite separation, while the EA of an orbital (or an atom or molecule) can be defined as the energy released when the it accepts an electron from infinity [312]. Molecules often don't have
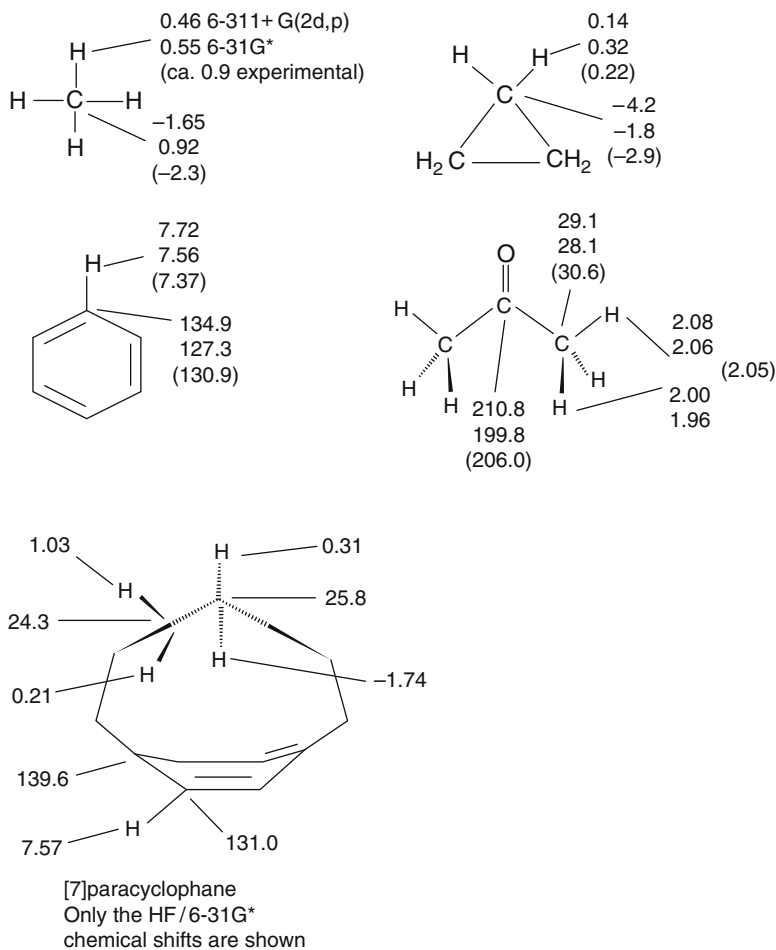
Fig. 5.44 Calculated and experimental ^{1}H and ^{13}C NMR spectra: chemical shifts relative to TMS H and C, respectively. The calculations were done on the B3LYP/6–31G* geometry (B3LYP is a density functional method; Chap. 7) at the HF/6–311+G(2d,p) and HF/6–31G* levels using the default NMR method (GIAO) implemented in Gaussian 94W [199]. The experimental values are from Ref. [236], except for the values for [7]paracyclophane [309]. The larger basis set *may* be somewhat more accurate (note acetone CO ^{13}C), but takes longer. Compare with Chap. 7, Fig. 7.9

a "real" electron affinity, frequently ejecting an added electron spontaneously. The term IE when applied to a molecule means the *minimum* energy needed to remove an electron to infinity, i.e. to form the radical (for an originally closed-shell molecule) cation. The IE of a "stable" species, i.e. any molecule or atom that can exist (a relative minimum on the potential energy surface), is always positive. The EA of a molecule as defined above is positive if the accepted electron is bound, i.e. if it is not spontaneously ejected; if the new electron is ejected in microseconds or less (is unbound), the molecule has a negative EA (is a "resonance state"–this has

nothing to do with the term resonance as in a resonance hybrid). These quantities are commonly given in eV, electron volts; $1 \text{ eV} = 96.485 \text{ kJ mol}^{-1} = 0.03675$ hartrees, 1 hartree $= 27.212$ eV. A typical IE for an organic molecule is 8–9 eV (e.g. benzene 9.24 eV), which is ca. 800 kJ mol^{-1} or about twice the energy of a typical covalent bond. For a positive EA a reasonable value might be ca. 2 eV (1,4-benzoquinone, 1.9 eV).

IEs and EAs may be *vertical* or *adiabatic*: the energy difference between the precursor molecule M_1 and the species M_2 formed by removing or adding an electron gives the vertical value if M_2 is at the same geometry as M_1, while the adiabatic value is obtained if M_2 has its own actual, relaxed, equilibrium geometry. Since the equilibrium geometry of M_2 is clearly of lower energy than the unrelaxed geometry corresponding to M_1, vertical IEs are larger than adiabatic, relaxed, IEs, and vertical EAs are smaller than adiabatic EAs. *Experimental* IEs and EAs may be vertical or adiabatic, depending on how fast the ionization process is; see the discussion by Gross [313]. Compilations of IEs and EAs sometimes do not state explicitly whether their listed values are adiabatic or vertical; a welcome exception is the book by Levin and Lias [314]. Many IEs and EAs are available on the worldwide web, e.g. [206a], and a good brief discussion of these, including various measurement techniques, is to be found in the compilation by Lias et al. [206b]. The review by Rienstra-Kiracofe et al. lists many EAs [312b]. The vertical values ought to be of more interest to chemists, since these represent a more inherent property of the molecule (see Koopmans' theorem below) than the adiabatic, the latter being the energy difference between a neutral and a cation *after* its geometric reorganization. The initial cation may even rearrange to a species with quite a different structure.

Ionization energies and electron affinities can be calculated simply as the energy difference between the neutral and the ion. Approximate IEs can be obtained by applying Koopmans' (not Koopman's) theorem [315], which says that the energy required to remove an electron from an orbital is the negative of the orbital energy. Thus the IE of a molecule is approximately the negative of the energy of its HOMO (the principle does not work as well for ionization of electrons more tightly bound than those in the HOMO). This makes it simple to obtain approximate IEs for comparison with photoelectron spectroscopy [316] results. Unfortunately, the principle does not work well for EAs: the EA of a molecule is not reasonably well approximated as the negative of the LUMO energy. In fact, ab initio calculations normally give virtual MOs (vacant MOs) positive energies, implying that molecules will not accept electrons to form anions (i.e. that they have negative EAs), which is sometimes false. Koopmans' theorem works because of a cancellation of errors in the IE case (which actually leads to modest overestimation of the IE) but not for EAs. Errors arise from approximate treatment of electron correlation, and from the fact that when an electron is removed from or added to a molecule electronic relaxation (not to be confused with geometry relaxation) occurs. A further problem for EAs is that the procedure for minimizing the energies of MOs (Sect. 5.2.3.4) gives, within the limits of the HF procedure and the basis set, the best *occupied*, but not the best virtual, MOs.

Table 5.17 Some ionization energies (eV). The basis set is 6–31G*; the calculations are based on the data in Table 5.18

	IE from ΔE		IE from Koopmans' theorem		Exp.
	HF	MP2(fc)	HF	MP2(fc)	
CH$_3$OH adiabatic	9.38	10.57	–	–	10.9
CH$_3$OH vertical	9.66	10.79	12.06	12.12	10.95
CH$_3$SH adiabatic	8.34	8.97	–	–	9.44
CH$_3$SH vertical	8.38	9.03	9.69	9.69 *(sic)*	–
CH$_3$COCH$_3$ adiabatic	8.19	9.63	–	–	9.71, 9.74
CH$_3$COCH$_3$ vertical	8.37	9.78	11.07	11.19	9.5, 9.72

The experimental values are from Ref. [314], except for CH$_3$SH [317]

Some calculated and experimental [314, 317] IEs are given in Table 5.17, based on the raw data in Table 5.18. Because of the problem of assigning a meaningful ZPE to a non-stationary state structure like the unrelaxed cation at the neutral geometry (Chap. 2, Sect. 2.5), the cation and neutral energies used for the vertical IEs do not include ZPE. The calculations (experimental data are sparse) indicate vertical IEs to be indeed slightly (about 0.2 eV) higher than adiabatic. The HF/6–31G*ΔE values underestimate the IE by about $1 - 1.5$eV while MP2(fc)/6–31G*ΔE values underestimate it by only about $0.1 - 0.4$ eV (others have reported them to be generally too low by 0.3–0.7 eV [318]). The Koopmans' theorem ($-$HOMO) energies for both the HF and MP2 level calculations are about $1 - 1.5$ eV too high. Electron affinities (which seem to be generally of less interest than ionization energies) can be calculated as the energy difference between the neutral molecule and its anion. High-accuracy adiabatic IEs and EAs can be calculated by multistep high-accuracy methods (Sect. 5.5.2.3.2); the convenient procedures implemented for these methods in the Gaussian programs do not allow calculation of vertical values since the geometry of the ion will be automatically optimized. Better-calculated IEs than those from the ab initio methods in Tables 5.17 and 5.18, and good EAs, can be obtained with density functional methods (Chap. 7).

The subject of electron affinity leads to a closer look at the concept of the lowest unoccupied molecular orbital (LUMO) than has so far been considered. Although this idea is used even in elementary presentations of molecular electronic theory, it is not easy to attach a simple, precise meaning to it, even apart from the question of the reality of the orbitals used to construct the overall molecular wavefunction from basis functions in the "orbital approximation" (Sect. 5.2.3). From a practical, operational viewpoint the highest occupied molecular orbital (HOMO) is a reasonable approximation to the experimentally measurable ionization energy. In contrast, the LUMO as calculated by all standard methods is not a reasonable quantitative approximation to anything. Further, while the HOMO can be qualitatively envisaged as a region of space occupied by one or two electrons of definite energy, the LUMO is only a region potentially available to an electron. Schmidt et al. even refer to the traditional LUMO as "hypothetical" in contrast to "the much more concrete

Table 5.18 The raw data for Table 5.17: energies, ZPEs and HOMO values, for calculating ionization energies

	HF/6–31G*	MP2(fc)/6–31G*
CH_3OH	−115.03542	−115.34514
	0.05055	0.05086
	−114.98487	−115.29528
$CH_3OH^{.+}$ cation geom.	−114.68722	−114.95358
	0.04723	0.04665
	−114.63999	−114.90693
$CH_3OH^{.+}$ neutral geom.	−114.6804	−114.94849
CH_3OH, HOMO	−0.44328	−0.44526
CH_3SH	−437.70032	−437.95267
	0.04534	0.04621
	−437.65498	−437.90646
$CH_3SH^{.+}$ cation geom.	−437.39316	−437.62211
	0.04468	0.04526
	−437.34848	−437.57685
$CH_3SH^{.+}$ neutral geom.	−437.39227	−437.62089
CH_3SH, HOMO	−0.35596	−0.35627
CH_3COCH_3	−191.96224	−192.52391
	0.08214	0.08309
	−191.88010	−192.44082
$CH_3COCH_3^{.+}$ cation geom.	−191.65994	−192.16837
	0.08071	0.08128
	−191.57923	−192.08709
$CH_3COCH_3^{.+}$ neutral geom.	−191.65451	−192.16448
CH_3COCH_3, HOMO	−0.40692	−0.41119

The numbers are hartrees, and represent (other than the HOMO energies): for the neutrals and the cations at the cation geometry, uncorrected ab initio energy, ZPE, and corrected ab initio energy. The ZPEs shown have been multiplied [80] by 0.9135 (HF) or 0.9670 (MP2(fc)). For the cations at the neutral geometry, ZPE was not used and is not shown. Adiabatic IE $= E$(cation) $- E$(neutral), both corrected for ZPE. Vertical IE $= E$(cation) $- E$(neutral), both without ZPE. Hartrees were converted to eV in Table 5.17 by multiplying by 27.2116

highest occupied molecular orbital", and assert that the "poor connection between the LUMO concept and the lowest empty canonical orbital" although well recognized by theoretical chemists, is less well understood in the wider chemical community [319a]. These observations were the impetus for these workers to devise *valence virtual orbitals* (VVOs), which they present as "an unambiguous ab initio quantification of the LUMO concept" [319a]. VVOs are said to have sensible energies and realistic shapes, to be nearly independent of the basis set, and to provide excellent starting orbitals for multireference computations. The procedure involves constructing from the "large sea" of canonical virtual orbitals (Sect. 5.2.3.1) a set of unoccupied molecular orbitals with the characteristics specified for VVOs. In density functional theory (Chap. 7) in contrast to ab initio

wavefunction methods, van Meer et al. reported that the Kohn-Sham orbitals for hypothetical noninteracting electrons, calculated in a certain way, can show characteristics similar to those just mentioned for VVOs [319]b].

Another case of orbital ambiguity is the assignment of occupied orbitals as bonding or antibonding, which may not be obvious in complex molecules. Robinson and Alexandrova showed that the bonding nature of orbitals is revealed by their energetic response to compression (or stretching) [320]. They tested the effect on the eigenvalues of orbitals of compressing or expanding the molecule, preserving symmetry. Squeezing atoms together tends to lower the energy of a bonding orbital, and stretching the interatomic distance tends to raise the energy; electrons in antibonding orbitals show the opposite effect. This is intuitively reasonable, as the effect (bonding or antibonding) of the electrons in the orbital on the relevant atoms should be more pronounced, the less separated the atoms are.

5.5.6 *Visualization*

Modern computer graphics have given visualization, the pictorial presentation of the results of calculations, a very important place in science. Not only in chemistry, but in physics, aerodynamics, meteorology, and even mathematics, the remarkable ability of the human mind to process visual information is being utilized [321]. Gone are the days when it was *de rigeur* to pore over tables of numbers to comprehend the factors at work in a system, whether it be a galaxy, a supersonic airliner, a thunderstorm, or a novel mathematical entity. We will briefly examine below the role of computer graphics in computational chemistry, limiting ourselves to molecular vibrations, van der Waals surfaces, charge distribution, and molecular orbitals.

With due respect to the tremendous power of *virtual* models on a computer screen or within virtual reality glasses [322], I feel it worthwhile to add, with a small apology (for this is a book on computational chemistry) that *real* molecular models which you can hold and examine still have a place in chemistry. Professor Roald Hoffmann has cautioned against slavish adherence to computer graphics and commended traditional molecular models, saying there is no substitute to "running one's hands" over a molecular model and experiencing the "visual-tactile link [that is] so important for establishing three-dimensionality in our minds....What I believe is that the two generations of chemists who have seen molecules only on a screen are missing something in their three-dimensional perception. The visual-tactile link is so strong, and so direct – when we handle a model of a molecule in our hands as we struggle to draw down on paper, in some primitive visual code its structure, the molecule's three-dimensionality forever enters our mind. As long as we are alive we will see it and feel it".[6] Hoffmann and Laszlo point out that for most chemists

---

[6]R. Hoffmann, personal communication, 2009 August 12.

"the real, physical handling of models" imprints better the "full glory" of a three-dimensional structure than do the (possibly somewhat problematically) direct results of, say, X-ray crystallography [323].

5.5.6.1   Molecular Vibrations

Animation of normal-mode frequencies usually readily enables one to ascribe a band in the calculated vibrational (i.e. IR) spectrum to a particular molecular motion (a stretching, bending, or torsional mode, involving particular atoms). It sometimes requires a little ingenuity to *describe* clearly the motion involved, but animation is far superior to trying to discern the motion by the presumably now obsolete method of examining printed direction vectors (Chap. 2, Sect. 2.5; these show the extent of motion in the x, y, and z directions). Useful, however, are the direction vectors that some programs, GaussView [324] for example, can attach as arrows to a picture of the molecule, catching the vibration in the act so to speak.

Animating vibrations is useful not only for predicting or interpreting an IR spectrum; it can be extremely valuable in probing a potential energy surface. Suppose we wish to locate computationally the intermediate through which the chair conformers of cyclohexane interconvert $1 \rightleftarrows 1'$, Fig. 5.45). This reaction, although degenerate, can be studied by NMR spectroscopy [325]. One might surmise that the intermediate is the boat conformation **2**, but a geometry
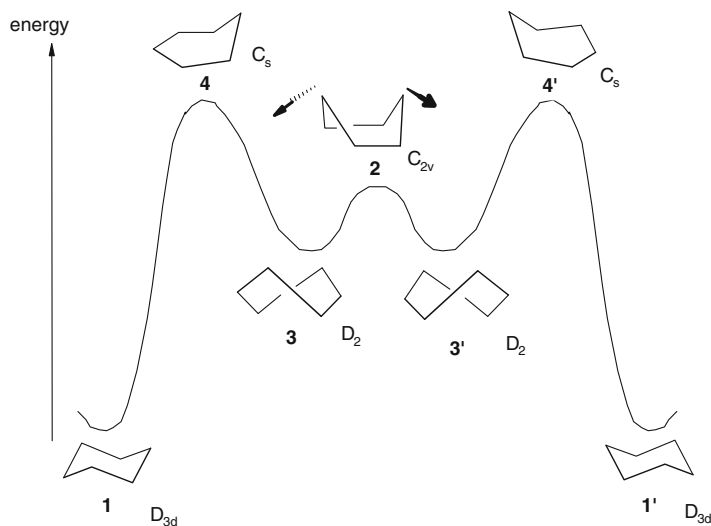
Fig. 5.45 One might have guessed that the chair cyclohexane conformations **1** and **1'** are connected by a boat-shaped intermediate **2**. However, this C_{2v} structure shows an imaginary frequency: it is a transition state which wants to twist toward **3** (*arrows*) or **3'** (*arrows* in opposite directions, not shown), which are the actual intermediates (no imaginary frequencies) between **1** and **1'**. The chair conformation reaches the twist via a half-chair **4**

optimization and frequencies calculation on this C_{2V} structure (note that in a quantum mechanical calculation, whether ab initio or otherwise, the input symmetry is normally preserved) followed by animation of the vibrations, shows otherwise. There is one imaginary vibration (Chap. 2, Sect. 2.5), and this transition state wants to escape from its saddle point by twisting to a D_2 structure **3**, called the twist or twist-boat, which latter is the true intermediate. The enantiomeric twist structures **3** and **3**′ go to **1** and **1**′, respectively, over a high-energy form **4** (or **4**′) called the half-chair. A geometry optimization starting with a D_2 structure leads to the desired relative minimum. Similarly, if one obtains a second-order saddle point (one kind of hilltop), animation of the two imaginary frequencies often indicates what the species seeks to do to escape from the hilltop to a become a first-order saddle point (a transition state) or a minimum, and it is often possible to obtain the desired transition state or minimum by altering the shape of the input structure so that it has the symmetry and approximates the shape of the desired structure.

In this connection another example (E. Lewars, unpublished) is provided by cyclopropylamine (Fig. 5.46). At the B3LYP/6–31G* level (a density functional
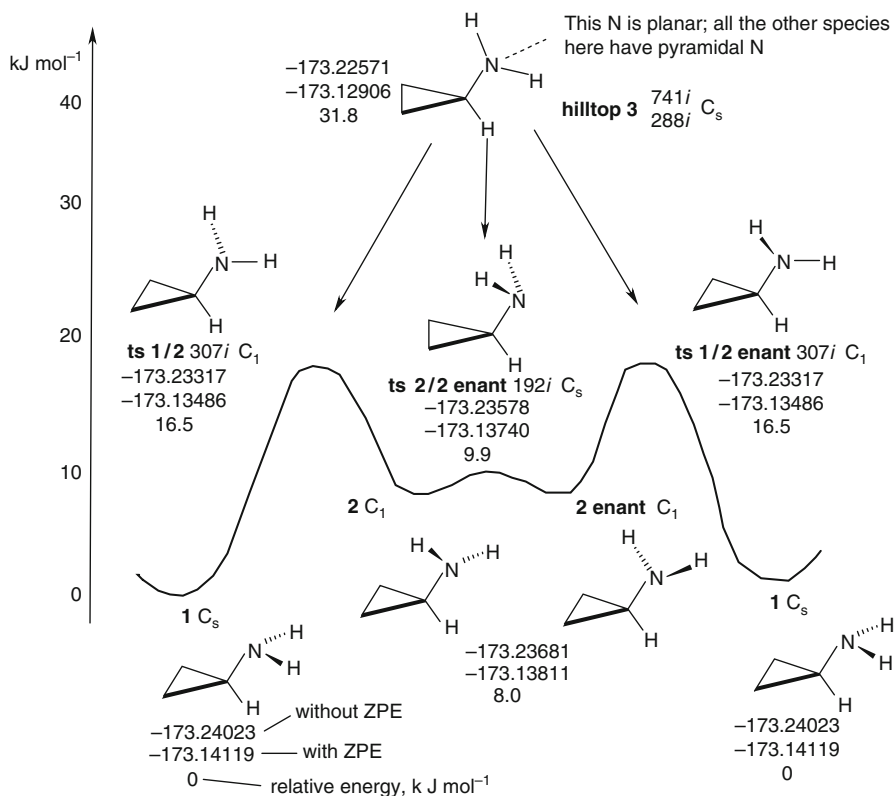
Fig. 5.46 Cyclopropylamine conformations at the B3LYP/6–31G* level. Structure **3** is a hilltop whose two imaginary frequencies indicate that it wants to undergo nitrogen pyramidalization and rotation about the C–N bond to form the transition states (nomenclature: **ts** 1/2 connects **1** and **2**, etc.) and, eventually, the minima. Each C_1 species has an enantiomer of the same energy

method, Chap. 7), apart from enantiomers five stationary points were found: two minima, two transition states, and one hilltop. The structure **3** is a hilltop whose two imaginary frequencies indicate that it wants to undergo nitrogen pyramidalization and rotation about the C-N bond to form other conformations. Removing the stricture of a planar nitrogen without further disturbing the structure, and optimizing, yields the relative minimum **2**. Rotating the planar N around the C-N bond to the alternative C_s structure and optimizing gives the global minimum **1**. The transition states were found by allowing the transition state algorithm to operate on input structures lying structurally between the two relevant minima. The experimental gas-phase structure of cyclopropylamine, from electron diffraction, corresponds to **1** [326].

5.5.6.2   Electrostatic Potential

Electrostatic potential (ESP), the net electrostatic potential energy (roughly, the charge) due to nuclei and electrons was mentioned in Sect. 5.5.4 in connection with calculation of atom charges. The ESP can be displayed (visualized) by (a) showing it with contour lines on a slice through the molecule, by (b) displaying it as a surface itself, or by (c) color-coding it onto the van der Waals surface; the three possibilities are shown for the water molecule in Fig. 5.47. Color-coding (mapping) the ESP onto the surface of the molecule enables one to see how an approaching reagent would perceive the charge distribution. Showing the ESP as a surface residing in the region of space where the net charge is negative gives a very useful picture of those parts of a molecule where the electrostatic effect of the electrons wins out over that of the nuclei; this is a particularly good way of seeing the presence of lone pairs, as Fig. 5.48, also, makes clear. Note that in Fig. 5.47a and b (slice, and depicting the ESP itself as a surface) the lone pairs do not stick out like rabbit ears [327]. This is because as electron density which can be ascribed to one orbital falls off, that due to
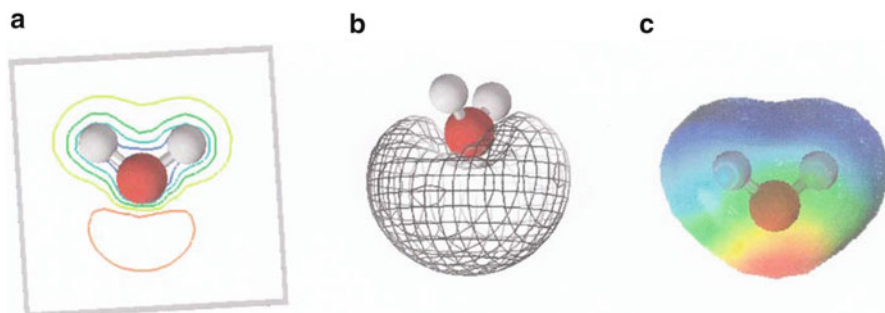
Fig. 5.47 Distribution of net charge in the water molecule (electrostatic charge, calculated with AM1–Chap. 6). Negative to positive: *red* to *blue* R O Y G B). (**a**) Slice through the plane of the molecule; the *contour lines* show the decrease in net negative charge. (**b**) Charge in space; this corresponds essentially to the lone pairs. (**c**) Charge mapped on the van der Waals surface
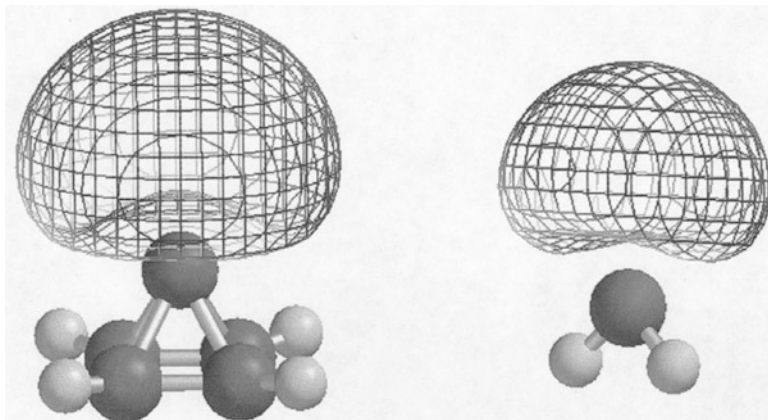
Fig. 5.48 The hydrocarbon pyramidane, C_5H_4, evidently (pyramidane has not been synthesized) has a lone pair of electrons on its pyramidal carbon atom, like carbene (methylene), CH_2. While the lone pair on CH_2 is no surprise (draw the Lewis structure for the singlet), a cycloalkane with an unshared electron pair is remarkable

another increases: there is no "electron hole" between the two lone pairs (for the same reason the electron density cross section through a σ-π double bond is elliptical and through a σ-π-π triple bond circular; see Chap. 4, Sect. 4.3.2). Showing the ESP as a surface made clear that the remarkable cycloalkane pyramidane [45] has a lone pair, like the carbene CH_2 (Fig. 5.48). Depicting the ESP by contour lines on a slice through the molecule reveals its internal structure, but sometimes more relevant to reactivity is the picture seen by mapping it onto the van der Waals surface, because this is the picture presented to the outside molecular world. Examining the ESP interactions between a molecule and the active site of an enzyme can be important in drug design [110]. Various applications of the ESP are discussed by Politzer and Murray [328] and Brinck [267a]. The ESP at any point on the van der Waals surface can be assigned a quantitative value, namely the energy needed to move a charge (say, a proton) from infinity to that point, and some programs will calculate the ESP at any point on the surface on which one clicks with the mouse.

5.5.6.3 Molecular Orbitals

Visualization of molecular orbitals shows the location of those regions where the highest-energy electrons are concentrated (the highest occupied MO, the HOMO), and those regions which offer the lowest-energy accommodation to any donated electrons (the lowest unoccupied MO, the LUMO). Electrophiles should bond to the atom where the HOMO is "strongest" (where the electron density due to the highest-energy electron pair is greatest) and nucleophiles to the atom where the LUMO is strongest, at least as seen on the van der Waals surface by an approaching
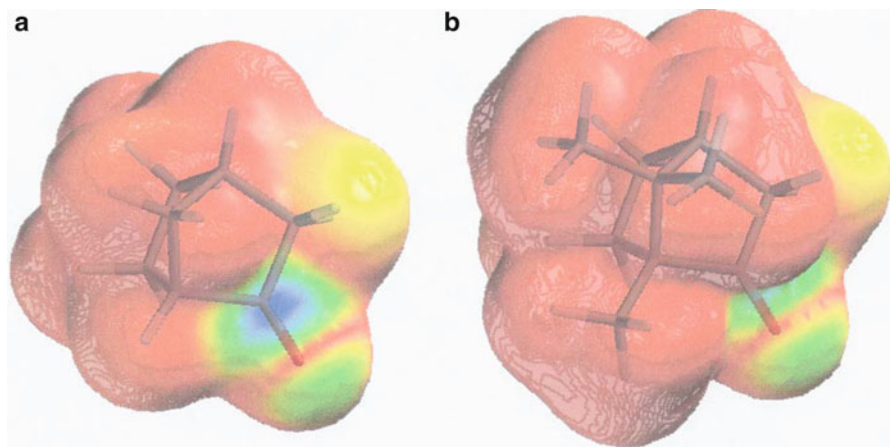
Fig. 5.49 (**a**) Norcamphor, with the LUMO mapped onto the van der Waals surface. The LUMO as seen on the surface is most prominent at the carbonyl carbon, on the "*top*" of the molecule (the *exo* face), as shown by the *blue* area. Viewed from the bottom of the molecule (not shown here), the LUMO still lies at the C=O carbon, but is less prominent (the *blue* is less intense). We can thus predict that nucleophiles will attack the C=O carbon, from the *exo* direction. (**b**) Camphor (norcamphor with three methyl groups): the carbonyl carbon is shielded from *exo* attack by a methyl group, so for steric reasons nucleophiles tend to attack this carbon from the *endo* direction, despite *exo* attack being electronically favored

reagent. The information provided by inspection of the HOMO and LUMO (the frontier orbitals) is thus somewhat akin to that given by visualizing the ESP (electrophiles should tend to go to regions of negative ESP, nucleophiles to regions of positive ESP). Figure 5.49 shows the LUMOs of the ketones norcamphor and camphor, mapped onto their van der Waals surfaces. For norcamphor (Fig. 5.49a), the prominence of its LUMO at the carbonyl carbon as seen from the "top" or *exo* face (the face with the CH_2 bridge) rather than the bottom (*endo*) face, suggests that nucleophiles should attack from the *exo* direction. In accord with this, hydride donors, for example, approach from the *exo* face to give mainly the *endo* alcohol. For camphor (Fig. 5.49b), where the bridge is $CH(CH_3)_2$ instead of CH_2, the *exo* face is shielded by a CH_3 group which sterically thwarts the electronically preferred attack from this direction, and so nucleophiles tend to approach rather the *endo* face (a fact which could be nicely depicted by visualizing *simultaneously* the LUMO and the van der Waals surface) [329].

Figure 5.50 shows three related molecules, the 7-methyl substituted (the visual orbital progression explained here is not quite as smooth for the unsubstituted molecules) derivatives of the 7-norbornyl cation (a), the neutral alkene norbornene (b), and the 7-norbornenyl cation (c) (the *Chemical Abstracts* names are, respectively, the bicyclo[2.2.1]hept-7-yl cation, bicyclo[2.2.1]hept-2-ene, and the bicyclo [2.2.1]hept-2-ene-7-yl cation). For each species an orbital is shown as a 3D region of space, rather than mapping it onto a surface as was done in Fig. 5.49. In (a) we see the LUMO, which is as expected essentially an empty p atomic orbital on C7,
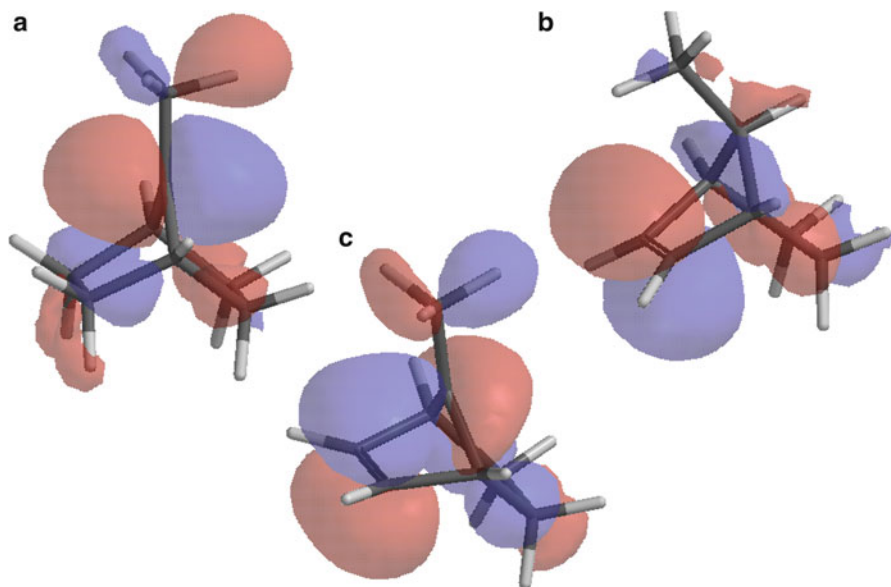
Fig. 5.50 Visualization supports the view that the 7-methyl-7-norbornenyl cation is delocalized: (**a**) In the 7-methyl-7-norbornyl cation (no double bond) the LUMO is largely an empty p atomic orbital on C7; (**b**) In the neutral alkene norbornene the HOMO is largely the filled CC Π molecular orbital; (**c**) In the 7-methyl-7-norbornenyl cation the HOMO is essentially the merged HOMO of (b) and LUMO of (a), indicating donation of electron density from the CC double bond into the "previously" empty orbital on C7

and in (b) the HOMO, which is, as expected, largely the π molecular orbital of the double bond. The interesting conclusion from (c) is that in this ion the HOMO of the double bond has donated electron density into the vacant orbital on C7 forming a 3-center, 2-electron bond. Two π electrons may be cyclically delocalized, making the cation a bishomo (meaning expansion by two carbons) analogue of the aromatic cyclopropenyl cation [330]. This delocalized bishomocyclopropenyl structure for 7-norbornenyl cations has been controversial, but is supported by NMR studies [331].

5.5.6.4 Visualization–Closing Remarks

Other molecular properties and phenomena that can benefit from the aid of visualization are the distribution of unpaired electron spin in radicals and the changes in orbitals and charge distribution as a reaction progresses. These and many other visualization exercises are described in publications by Wavefunction, Inc., e.g. [332].

5.6   Strengths and Weaknesses of Ab initio Calculations

5.6.1   Strengths

Ab initio calculations are based on a fundamental physical equation, the Schrödinger equation, without empirical adjustments. This makes them esthetically satisfying, and ensures (if the Schrödinger equation is true) that they will give correct answers *provided the approximations needed to obtain numerical results (to solve the Schrödinger equation) are not too severe for the problem at hand*. The level of theory needed for a reliable answer to a particular problem must be found by experience – comparison with experiment for related cases–so in this sense current ab initio calculations are not fully *a priori* [2, 43]. A few "ab initio methods" do not even fully eschew empirical parameters: the Gaussian and the CBS series of methods have empirical factors which, unless they cancel (as in proton affinity calculations, Sect. 5.5.2.3.2) make these methods somewhat semiempirical. A consequence of the (usual) absence of empirical parameters is that ab initio calculations can be performed for any kind of molecular species, including transition states and even non-stationary points, rather than only species for which empirical parameters are available (see Chap. 6). These characteristics of reliability (with the reservations alluded to) and generality are the strengths of ab initio calculations.

5.6.2   Weaknesses

Compared to other methods (molecular mechanics, semiempirical calculations, density functional calculations–Chaps. 3, 6 and 7, respectively) ab initio calculations are slow, and they are relatively demanding of computer resources (memory and disk space, depending on the program and the particular calculation). These disadvantages, which increase with the level of the calculation, have been very largely overcome by tremendous increases in computer power, accompanied by impressive decreases in price. In 1959 Coulson doubted the possibility (he also questioned the desirability, but in this regard visualization has been of enormous help) of "accurate" calculations on molecules with more than 20 electrons [333a], but about 30 years later (1992 cf. 1959) computer speed had increased by a factor of 100,000, and ab initio calculations on molecules with 100 electrons (about 15 heavy atoms) were common [333b]. Not too wide of the mark would be the estimate that in ca. 2015, less than 60 years after Coulson's cheerfully fatalistic assessment and about 6 years after the 2009 reassessment of computer power in reference [333b], computers had again increased in speed by a factor of two or three. This assessment refers to inexpensive desktop machines, "personal (in a non-proprietary sense) computers". The popularity of computer gaming has made available cheap graphical processing units (GPUs), and these have been applied to computational chemistry: a recent paper describes a calculation on a silicon nanoparticle, $Si_{72}H_{64}$, by a

modification of CASSCF called complete active space configuration interaction, CASCI [334]. This used a 6–31G** basis and a 16-active-electron/16-active-orbital space with more than 100,000,000 configurations, taking only 39 minutes. GPUs are said to be comparable in power to a small cluster, at a cost of hundreds to a few thousand dollars. The increase in power of expensive institutional machines has of course been even more impressive.

More efficient algorithms (software) have accompanied the increase in hardware speed. Augmenting the fast but electronically oblivious method of molecular mechanics is the treatment of a small part of a large molecule by quantum mechanics (Chap. 3, Sect. 3.3.3), i.e. by ab initio, or by semiempirical (Chap. 6), or density functional (Chap. 7) calculations, in the so-called QM/MM method [335]. Recently, full QM treatments of large molecules have been accomplished by dividing the molecule into more manageable parts, in so-called fragment QM methods [336]. It appears that continued increases in computer power and algorithm efficiencies will, for the foreseeable future, steadily overcome those weaknesses of the ab initio approach that remain.

5.7 Summary

Ab initio calculations rest on solving the Schrödinger equation; the nature of the necessary approximations determine the level of the calculation. In the simplest approach, the Hartree-Fock method, the total molecular wavefunction Ψ is approximated as a Slater determinant composed of occupied spin orbitals (each spin orbital is a product of a conventional spatial orbital ψ and a spin function). Writing the molecular energy as the expectation value of the wavefunction ($E = \langle \Psi | \hat{H} | \Psi \rangle$) i.e. invoking the Schrödinger equation, then differentiating E with respect to the spin orbitals that compose the wavefunction (= the Slater determinant), we get the HF equations. To use these in practical calculations the spatial orbitals are approximated as a linear combination (a weighted sum) of basis functions. These are usually identified with atomic orbitals, but can be any mathematical functions that give a reasonable wavefunction, i.e. a wavefunction which gives reasonable answers when we do the calculations. The main defect of the HF method is that it does not treat electron correlation properly: each electron is considered to move in an electrostatic field represented by the average positions of the other electrons, whereas actually electrons avoid each other better than this model predicts, since any electron A really sees any other electron B as a moving particle and the two mutually adjust (correlate) their motions to minimize their interaction energy. Electron correlation is treated better in post-HF methods, such as the Møller-Plesset (MP), configuration interaction (CI), and coupled cluster (CC) methods. These methods lower electron-electron interaction energy by allowing the electrons to reside not just in conventionally occupied MOs (the n lowest MOs for a $2n$-electron species), but also in formally unoccupied MOs (virtual MOs).

The main uses of the ab initio method are calculating molecular geometries, energies, vibrational frequencies, spectra (IR, UV, NMR), ionization energies and electron affinities, and properties like dipole moments which are directly connected with electron distribution. These calculations find theoretical and practical applications, since, for example, enzyme-substrate interactions depend on shapes and charge distributions, reaction equilibria and rates depend on energy differences, and spectroscopy plays an important role in identifying and understanding novel molecules. The visualization of calculated phenomena, such as molecular vibrations, charge distributions, and molecular orbitals, can be very important in interpreting the results of calculations.

Easier Questions

1. In the term *Hartree-Fock*, what, essentially, were the contributions of each of these two people?
2. What is a spin orbital? A spatial orbital?
3. At which step in the derivation of the Hartree-Fock energy does the assumption that each electron sees an "average electron cloud" appear?
4. For a closed-shell molecule the number of occupied molecular orbitals is half the number of electrons, but there is no limit to the number of virtual orbitals. Explain.
5. In the simple Hückel method, c_{si} denotes the basis function coefficient for the contribution of atom number s (in whatever numbering scheme we choose) to MO number i. In the ab initio method, c_{si} still refers to MO number i, but the s does not necessarily denote atom number s. Explain.
6. The derivation of the Roothaan-hall equations involves some key concepts: Slater determinant, Schrödinger equation, explicit Hamiltonian operator, energy minimization, and LCAO. Using these, summarize the steps leading to the Roothaan-Hall equations $\mathbf{FC} = \mathbf{Sc\varepsilon}$.
7. What are the similarities and the differences between the basis set of the extended Hückel method and the ab initio STO-3G basis set?
8. In the simple and extended Hückel methods, the molecular orbitals are calculated and then filled from the bottom up with the available electrons. However, in ab initio calculations the occupancy of the orbitals is taken into account as they are being calculated. Explain.
   Hint: look at the expression for the Fock matrix elements in terms of the density matrix.
9. Isodesmic reactions have been used to investigate aromatic stabilization, but there is not a unique isodesmic reaction for each problem. Write two isodesmic reactions for the ring-opening of benzene, both of which have on each side of the equation the same number of each kind of bond. Have you any reason to prefer one of the equations to the other?

10. List the strengths and weaknesses of ab initio calculations compared to molecular mechanics and extended Hückel calculations. State the molecular features that can be calculated by each method.

Harder Questions

1. Does the term *ab initio* imply that such calculations are "exact"? In what sense might ab initio calculations be said to be semiempirical–or at least not fully *a priori*?
2. Can the Schrödinger equation be solved *exactly* for a species with two protons and one electron? Why or why not?
3. The input for an ab initio calculation (or a semiempirical calculation of the type discussed in Chap. 6, or a DFT calculation–Chap. 7) on a molecule is usually just the cartesian coordinates of the atoms (plus the charge and multiplicity). So how does the program know where the bonds are, i.e. what the structural formula of the molecule is?
4. Why is it that (in the usual treatment) the calculation of the internuclear repulsion energy term is easy, in contrast to the electronic energy term?
5. In an ab initio calculation on H_2 or HHe^+, one kind of interelectronic interaction does not arise; what is it, and why?
6. Why are basis functions not necessarily the same as atomic orbitals?
7. One desirable feature of a basis set is that it should be "balanced." How might a basis set be unbalanced?
8. In a Hartree-Fock calculation, you can always get a lower energy (a "better" energy, in the sense that it is closer to the true energy) for a molecule by using a bigger basis set, as long as the HF limit has not been reached. Yet a bigger basis set does not *necessarily* give better geometries and better relative (i.e. activation and reaction) energies. Why is this so?
9. Why is size-consistency in an ab initio method considered more important than variational behavior (MP2 is size-consistent but not variational)?
10. A common alternative to writing a Hartree-Fock wavefunction as an explicit Slater determinant is to express it using a *permutation operator* $\hat{P}$ which permutes (switches) electrons around in MOs. Examine the Slater determinant for a two-electron closed-shell molecule, then try to rewrite the wavefunction using $\hat{P}$.

References

1. General discussions of and references to ab initio calculations are found in: (a) Levine IN (2014) Quantum chemistry, 7th edn. Prentice Hall, Engelwood Cliffs; (b) Lowe JP (1993) "Quantum chemistry", 2nd edn. Academic Press, New York; (c) Pilar FL (1990) Elementary quantum chemistry", 2nd edn. McGraw-Hill, New York; (d) An advanced book: Szabo A,

Ostlund NS (1989) "Modern quantum chemistry". McGraw-Hill, New York; (e) Foresman JB, Frisch Æ (1996) "Exploring chemistry with electronic structure methods". Gaussian Inc., Pittsburgh; (f) Leach AI (2001) "Molecular modelling, 2nd edn". Prentice Hall, Essex, England; (g) A useful reference is still: Hehre WJ, Radom L, Schleyer PVR, Pople JA (1986) "Ab initio molecular orbital theory". Wiley, New York; (h) An evaluation of the state and future of quantum chemical calculations, with the emphasis on ab initio methods: Head-Gordon M (1996). J Phys Chem 100, 13213; (i) Jensen F (2007) Introduction to computational chemistry, 2nd edn. Wiley, Hoboken, New Jersey; (j) Dewar MJS (1969) The molecular orbital theory of organic chemistry. McGraw-Hill, New York. This book contains many trenchant comments by one of the major contributors to computational chemistry; begins with basic quantum mechanics and ab initio theory, although it later stresses semiempirical theory. (k) Young D (2001) Computational chemistry. A practical guide for applying techniques to real world problems. Wiley, New York; (l) Cramer CJ (2004) "Essentials of computational chemistry", 2nd edn. Wiley, Chichester

2. Regarding the first use of the term in chemistry: Dewar casts aspersions on this (Dewar MJS (1992) "A semiempirical life", profiles, pathways and dreams series. In: Seeman JI (ed). American Chemical Society, Washington, D.C., p. 129) by saying that in the paper in which it evidently first appeared (Parr RG, Craig DP, Ross IG (1950). J Chem Phys 18 1561 it merely meant that the collaboration of Parr on the one hand with Craig and Ross on the other had been carried through from the start in Parr's lab. However, the PCR paper states "The computations, which are heavy, were carried through independently *ab initio* by RGP on the one hand, and DPC and IGR on the other." In this author's view this means either that both groups did the calculations independently from the beginning, or it is conceivably a nod to the complexity of evaluating complicated integrals without semiempirical assistance in those pre-computer days, and may then indeed be taken as being consonant with the current meaning of the term. Rudenberg states (Rudenberg K, Schwarz WHE (2013) Chapter 1 in "Pioneers of quantum chemistry", ACS Symposium Series 1122, Eds. E. T. Strom, A. K. Wilson, American Chemical Society, Washington, DC, p. 36) that he recalled the use of *ab initio* by Mulliken in a lecture at the University of Chicago sometime in 1953–1955. The first appearance in print in its unambiguous modern sense seems to be Chen TC (1955). J Chemical Physics 23 2200, where it is explicitly contrasted with the term semiempirical.

3. Hartree DR (1928) Proc Cambridge Philos Soc 24:89

4. (a) The relativistic one-electron Schrödinger equation is called the Dirac equation. It can be used with the Hartree-Fock approach to do Dirac-Fock (Dirac-Hartree-Fock) calculations; see Levine IN (2014) Quantum chemistry, 7th edn. Prentice Hall, Engelwood Cliffs, section 16.11; (b) For a brief discussion of spin-orbit interaction see Levine IN (2014) Quantum chemistry, 7th edn. Prentice Hall, Engelwood Cliffs, section 11.6

5. The many-body problem in chemistry has been reviewed: Tew DP, Klopper W, Helgaker T (2007). J Comp Chem 28 1307

6. Levine IN (2014) Quantum chemistry, 7th edn. Prentice Hall, Engelwood Cliffs, sections 13.4, 13.5 , pp 425–426

7. Lowe JP (1993) Quantum chemistry, 2nd edn. Academic, New York, pp 129–131

8. (a) Pauling L (1928). Chem Rev 5 173; see p. 208 of this paper. (b) Slater JC (1929). Phys Rev 34 1293; the simple-seeming representation of a wavefunction as a spin orbital determinant made it much easier for physicists to deal with electron spin than by group theory, with which many were, ca. 1930, unfamiliar. In his biography ("Solid-state and molecular theory: a scientific biography", Wiley-Interscience, New York, 1975), Slater, while acknowledging Pauling's 1928 paper, says this was his most popular publication, since it was responsible for slaying the *Gruppenpest* (German for group theory plague). (c) Fock V, Physik Z (1930). 61 126; (d) Slater JC (1930). Phys Rev 35 210. In his biography ((b) above, p. 79) Slater says "I had planned to work out these additional terms [with electron exchange], but did not have the opportunity on account of other things I was working on, and in the meantime Fock..."

independently suggested the method and worked out the details." This "Note on Hartree's method" occupies ca. one page; Fock's paper extends over 23 pages, replete with equations.

9. Levine IN (2014) Quantum chemistry, 7th edn. Prentice Hall, Engelwood Cliffs, sections 7.7 and 10.1

10. Although it is sometimes convenient to speak of electrons as belonging to a particular atomic or molecular orbital, and although they sometimes behave as if they were localized, no electron is really confined to a single orbital, and in a sense all the electrons in a molecule are delocalized; Dewar MJS (1969) The molecular orbital theory of organic chemistry. McGraw-Hill, New York, pp. 139–143

11. Pilar FL (1990) Elementary quantum chemistry, 2nd edn. McGraw-Hill, New York, pp 200–204

12. (a) Pople JA, Beveridge DL (1970) Approximate molecular orbital theory. McGraw-Hill, New York, chapters 1 and 2; (b) The first clear, explicit presentation of the UHF procedure: Pople JA, Nesbet RK (1954). J Chem Phys 22 571

13. Lowe JP (1993) Quantum chemistry", 2nd edn. Academic Press, New York, Appendix 7

14. Levine IN (2014) Quantum chemistry, 7th edn. Prentice Hall, Engelwood Cliffs, pp 267–268

15. Dewar MJS (1969) The molecular orbital theory of organic chemistry. McGraw-Hill, New York, chapter 2

16. Levine IN (2014) Quantum chemistry, 7th edn. Prentice Hall, Engelwood Cliffs, p 430

17. Levine IN (2014) Quantum chemistry, 7th edn. Prentice Hall, Engelwood Cliffs, pp 197–198

18. (a) See e.g. Perrin CL (1970) Mathematics for chemists. Wiley-Interscience, New York, pp. 39--41; (a) A caveat on the use of Lagrangian multipliers: Goedecke GH (1966). Am J Phys 34 571

19. Lowe JP (1993) Quantum chemistry, 2nd edn. Academic, New York, pp 354–355

20. Dewar MJS (1969) The molecular orbital theory of organic chemistry. McGraw-Hill, New York, p 35

21. Seeger R, Pople JA (1977) J Chem Phys 66:3045

22. Dahareng D, Dive G (2000) J Comp Chem 21:483

23. Crawford TD, Stanton JF, Allen WD, Schaefer HF (1997) J Chem Phys 107:10626

24. Crawford TD, Kraka E, Stanton JF, Cremer D (2001) J Chem Phys 114(10638)

25. Levine IN (2014) Quantum chemistry, 7th edn. Prentice Hall, Engelwood Cliffs, p 293

26. Roothaan CCJ (1951). Rev Mod Phys 23 69; G. G. Hall, Proc. Roy. Soc. (London), *A205*, 541.

27. Pilar FL (1990) Elementary quantum chemistry, 2nd edn. McGraw-Hill, New York, pp 288–299

28. (a) Frequencies and zero point energies are discussed in [1g], section 6.3. Some quantum chemists are moving beyond this standard treatment in which electron and nuclear motion are regarded as being uncoupled: Császár AG, Fábri C, Szidarovszky T, Mátyus E, Furtenbacher T, Czakó G (2012). Phys Chem Chem Phys 14 1085. They consider this as characterizing "The fourth age of quantum chemistry", the first three ages being those seeing increasingly sophisticated treatment of (nuclear-uncoupled) electron motion. So far the fourth (electron-nuclear motion coupled) age seems limited to very small molecules. (b) Cśaszár AG, Furtenbacher T (2015). J Phys Chem A 119(10229)

29. GAUSSIAN 92, Revision F.4: Frisch MJ, Trucks GW, Head-Gordon M, Gill PMW, Wong MW, Foresman JB, Johnson BG, Schlegel HB, Robb MA, Repogle ES, Gomperts R, Andres JL, Raghavachari K, Binkley JS, Gonzales C, Martin RL, Fox DJ, Defrees DJ, Baker J, Stewart JJP, Pople JA (1992). Gaussian, Inc., Pittsburgh

30. See e.g. Porter GJ, Hill DR (1966) Interactive linear algebra: a laboratory course using mathcad. Springer Verlag, New York

31. Szabo A, Ostlund NS (1989) "Modern quantum chemistry". McGraw-Hill, New York, Sect. 3.5.1.

32. Szabo A, Ostlund NS (1989) "Modern quantum chemistry". McGraw-Hill, New York, Appendix A

33. Levine IN (2014) Quantum chemistry, 7th edn. Prentice Hall, Engelwood Cliffs, section 15.16

34. 34 See references 1a–i.

35. Boys SF (1950). Proc. Roy. Soc. (London), *A200*, 542.

36. Gaussian is available for several operating systems; see Gaussian, Inc., http://www.gaussian.com, 340 Quinnipiac St., Bldg. 40, Wallingford, CT 06492, USA. As of late 2014, the latest "full" version (as distinct from more frequent revisions) of the Gaussian suite of programs was Gaussian 09. A graphical interface designed specifically for Gaussian is GaussView, also available from Gaussian, Inc.

37. Spartan is an integrated molecular mechanics, ab initio and semiempirical program with an excellent input/output graphical interface, available for several operating systems: see Wavefunction Inc., http://www.wavefun.com, 18401 Von Karman, Suite 370, Irvine CA 92715, USA. As of late 2014, the latest version of Spartan was Spartan '14, available in several versions.

38. Foresman JB, Frisch Æ (1996) Exploring chemistry with electronic structure methods. Gaussian Inc., Pittsburgh, pp 32–33

39. Hehre WJ (1995) Practical strategies for electronic structure calculations. Wavefunction, Inc., Irvine

40. Hehre WJ, Radom L, Schleyer PVR, Pople JA (1986) Ab initio molecular orbital theory. Wiley, New York, pp 65–88

41. Simons J, Nichols J (1997) Quantum mechanics in chemistry. Oxford University Press, New York, pp 412–417

42. Levine IN (2014) Quantum chemistry, 7th edn. Prentice Hall, Engelwood Cliffs, section 15.4

43. Dewar MJS, Storch DM (1984). 107 3898

44. Inagaki S, Ishitani Y, Kakefu T (1994). J Am Chem Soc 116 5954

45. (a) Lewars E (1998). J Mol Struct (Theochem) 423 173; (b) Lewars E (2000). J. Mol. Struct. (Theochem) 507 165; (c) Kenny JP, Krueger KM, Rienstra-Kiracofe JC, Schaefer HF (2001). J. Phys. Chem. A 105 7745

46. The experimental geometries of Me_2SO and NSF are taken from [1g], Table 6.14.

47. Wiest O, Montiel DC, Houk KN (1997). J. Phys. Chem. A 101 8378, and references therein

48. Van Alsenoy C, Yu C-H, Peeters A, Martin JML, Schäfer L (1998) J Phys Chem A 102:2246

49. See e.g. (a) Hua W, Fang T, Li W, Yu JG, Li S (2008). J. Phys. Chem. A 112 10864; (b) Exner TE, Myers PG (2003). J. Comp. Chem. 24 1980

50. (a) Whole issue of Chem. Rev.: 2015, 115 12; (b) Clary DC (2006) Science. 314 265

51. Basis sets without polarization functions evidently make lone-pair atoms like tricoordinate N and tricoordinate O^+ too flat: Pye CC, Xidos JS, Poirer RA, Burnell DJ (1997). J Phys Chem A 101 3371. Other problems with the 6–31G** basis are that cation-metal distances tend to be too short (e.g. Rudolph W, Brooker MH, Pye CC (1995). J. Phys. Chem. 99 3793) and that adsorption energies of organics on aluminosilicates are overestimated, and charge separation is exaggerated (private communication ca. 2000 from G. Sastre, Instituto de Technologica Quimica, Universidad Polytechnica de Valencia). Nevertheless, the 3–21G$^{(*)}$ basis apparently usually gives good geometries (section 5.5.1).

52. Warner PM (1996) J Org Chem 61:7192

53. (a) Fowler JE, Galbraith JM, Vacek G, Schaefer HF (1994). J. Am. Chem. Soc. 116 9311; (b) Vacek G, Galbraith JM, Yamaguchi Y, Schaefer HF, Nobes RH, Scott AP, Radom L (1994). J. Phys. Chem. 98 8660

54. DeYonker NJ, Peterson KA, Wilson AK (2007). J Phys Chem A 111 11383, and references therein. This whole issue (number 44) of J Phys Chem A is a tribute to Dunning, and includes a short autobiography.

55. See e.g. Mebel AM, Kislov VV (2005). J Phys Chem A 109 6993

56. See e.g. Wiberg KB (2004). J Comp Chem 25 1342

57. See e.g. (a) Höfener S, Klopper W (2010). Mol. Phys. 108 1783; (b) Peterson KA, Kesharwani MJK, Martin JML (2015). Mol. Phys. 113 1551; (c) Friedrich J (2015). J

Chem Theory and Computation 11 3596; (d) The designations R12 and F12 come from R, distance, later replaced by better functions (F?) of the "electrons 1, 2" distance; for some leading references see T. Shiozaki, JunQ,1 [Journal of Unsolved Questions], 2010, Issue 1-A,1-4, and references therein.

58. (a) The special theory of relativity (the one germane to chemistry, since gravity is irrelevant to our science) and its chemical consequences are nicely reviewed in Balasubramanian K (1997) "Relativistic effects in chemistry", Parts A and B. Wiley, New York; (b) For a tirade against the conventional way of viewing the effect of velocity on mass see L. Okum, Physics Today, 1989, June, 30.

59. See e.g. Jacoby M (1998). Chem Eng News, 23 March, 48

60. Dirac PAM (1929) [relativity is]. . .of no importance in the consideration of atomic and molecular structure, and ordinary chemical reactions. . .. Proc R Soc A123:714

61. Krauss M, Stevens WJ (1984). Annu. Rev. Phys. Chem. 35 357; Szasz L (1985) Pseudopotential theory of atoms and molecules. Wiley, New York; (b) Pisani L, Clementi E (1994) Relativistic Dirac-Fock calculations on closed-shell molecules. J Comput Chem 15 466

62. (a) Figg T, Webb JR, Cundari TR, Gunnoe TB (2012). J Am Chem Soc 134 2332; (b) Rabilloud F, Harb M, Ndome H, Archirel P (2010). J Phys Chem A 114 6451

63. Weigend F, Ahlrichs R (2005) Phys Chem Chem Phys 7:3297

64. Sosa C, Andzelm J, Elkin BC, Wimmer E, Dobbs KD, Dixon DA (1992) J Phys Chem 96 6630

65. Levine IN (2014) Quantum chemistry, 7th edn. Prentice Hall, Engelwood Cliffs, section 16.11

66. (a) A good source of information on various kinds of calculations on transition metal compounds is McCleverty JA, Meyer TJ (eds) (2004) "Comprehensive coordination chemistry. II". Elsevier, Amsterdam; (b) A detailed review: Frenking G, Antes I, Böhme M, Dapprich S, Ehlers AW, Jonas V, Neuhaus A, Otto M, Stegmann R, Veldkamp A, Vyboishchikov S (1996) chapter 2 in Reviews in computational chemistry, vol 8. In: Lipkowitz KB, Boyd DB (eds) VCH, New York; (c) The main points of reference [51a] are presented in G. Frenking, U. Pidun, J Chem Soc, Dalton Trans., 1997, 1653. (d) Cundari TR, Sommerer SO, Tippett L (1995). J Chem Phys 103, 7058.

67. J. Comp. Chem., 2002, 23 8 (special issue on relativity in chemistry)

68. Dewar MJS (1992) "A semiempirical life", profiles, pathways and dreams series. Seeman JI, Series Editor, American Chemical Society, Washington, D.C., p. 185

69. (a) Hehre WJ, Huang WW, Klunzinger PE, Deppmeier BJ, Driessen AJ (1997) "A spartan tutorial". Wavefunction Inc., Irvine; (b) Hehre WJ, Yu J, Klunzinger PE (1997) "A guide to molecular mechanics and molecular orbital calculations in spartan". Wavefunction Inc., Irvine; (c) Hehre WJ, Shusterman AJ, Huang WW (1996) A laboratory book of computational organic chemistry". Wavefunction Inc., Irvine

70. Bachrach SM (2014) Computational organic chemistry, 2nd edn. Wiley-Interscience, San Antonio, p 298

71. At the HF level calculated rotation barriers of methyltoluenes become less accurate with very big bases: del Rio A, Boucekkine A, Meinnel J (2003). J. Comp. Chem. 24, 2093.

72. At correlated levels bigger bases did not always give better results for metal hydrides; the authors say this "refutes the dogma" that bigger basis sets are necessarily better: Klein RA, Zottola MA (2006). Chem. Phys. Lett. 419, 254

73. (a) Bartlett RJ, Schweigert IV, Lotrich VF (2006). J Mol Struct (Theochem) 771 1; (b) Lotrich VF, Bartlett RJ, Grabowski I (2005). Chem Phys Lett 405 43; (c) Wilson AK (2004) Abstracts, 60th Southwest Regional meeting of the American Chemical Society, Fort Worth, TX, united States, September 29-October 4 (2004). (d) Yau AD, Perera SA, Bartlett RJ (2002). Mol. Phys. 100 835

74. Moran D, Simmonett AC, Leach III FE, Allen WD, Schleyer PVR, Schaefer III HF (2006). J. Am. Chem. Soc. 128, 9342.

75. Janoschek R (1995) Chemie in unserer Zeit 29:122
76. (a) Raghavachari K, Anderson JB (1996). J. Phys. Chem. 100, 12960; (b) A historical review: P-O Löwdin (1995). Int. J. Quantum Chem. 55 77; (c) Fermi and Coulomb holes and correlation: [1c], pp. 296–297.
77. Pilar FL (1990) Elementary quantum chemistry, 2nd edn. McGraw-Hill, New York, p 286
78. For example: Hurley AC (1976) "Introduction to the electron theory of small molecules". Academic Press, New York, pp 286–288, or Ermler WC, Kern CW (1974). J. Chem. Phys. 61, pp 3860
79. Löwdin P-O (1959) Adv Chem Phys 2:207
80. (a) Scott AP, Radom L (1996). J. Phys. Chem. 100,pp 16502; (b) Sibaev M, Crittenden DL (2015). J. Phys. Chem. A 119, pp 13107
81. Blanksby SJ, Ellison GB (2003). Acc. Chem. Res. 36 255; Chart 1
82. See e.g. Levine IN (2014) Quantum chemistry, 7th edn. Prentice Hall, Engelwood Cliffs, chapter 16
83. Ma Q, Werner H-J (2015) J Chem Theory Comput 11:1564–5291
84. Brief introductions to the MP treatment of atoms and molecules: (a) Levine IN (2014) Quantum chemistry, 7th edn. Prentice Hall, Engelwood Cliffs, section 16.3; (b) Lowe JP (1993) "Quantum chemistry", 2nd edn. Academic Press, New York, section 11-13; (c) Leach AR (2001) "Molecular modelling, 2nd edn". Prentice Hall, Essex, England, section 3.3.2
85. Levine IN (2014) Quantum chemistry, 7th edn. Prentice Hall, Engelwood Cliffs, chapter 9
86. Møller C, Plesset MS (1934) Phys Rev 46:618
87. Binkley JS, Pople JA (1975) Int J Quantum Chem 9:229
88. Cramer CJ (2004) "Essentials of computational chemistry", 2nd edn. Wiley, Chichester section 7.4
89. Lowe JP (1993) Quantum chemistry, 2nd edn. Academic, New York, pp 367–368
90. Szabo A, Ostlund NS (1989) "Modern quantum chemistry". McGraw-Hill, New York, p 353; Leach AR (2001) "Molecular modelling, 2nd edn". Prentice Hall, Essex, England, p 115
91. Boldyrev A, Schleyer PVR, Higgins D, Thomson C, Kramarenko SS (1992) Fluoro- and difluorodiazomethanes are minima by HF calculations, but difluorodiazomethane does not exist (it dissociates) with the MP2 method. J. Comput. Chem. 9, 1066
92. $H_2C = CHOH$ *reaction* The only quantitative experimental information on the barrier for this reaction seems to be: S. Saito, Chem Phys Lett, 1976, *42*, 399, halflife in the gas phase in a Pyrex flask at room temperature ca. 30 minutes. From this one calculates (section 5.5.2.3.4, Eq. (5.202)) a free energy of activation of 93 kJ mol^{-1}. Since isomerization may be catalyzed by the walls of the flask, the purely concerted reaction may have a much higher barrier. This paper also shows by microwave spectroscopy that ethenol has the O-H bond *syn* to the C = C. The most reliable measurement of the ethenol/ethanal equilibrium constant, by flash photolysis, is 5.89×10^{-7} in water at room temperature (Chiang Y, Hojatti M, Keeffe JR, Kresge AK, Schepp NP, Wirz J (1987). J. Am. Chem. Soc. 109, 4000). This gives a free energy of equilibrium of 36 kJ mol^{-1} (ethanal 36 kJ mol^{-1} below ethenol). *HNC reaction* The barrier for rearrangement of HNC to HCN has apparently never been actually measured. The equilibrium constant in the gas phase at room temperature was calculated (Maki AG, Sams RL (1981). J Chem Phys 75, 4178) at 3.7×10^{-8} from actual measurements at higher temperatures; this gives a free energy of equilibrium of 42 kJ mol^{-1} (HCN 42 kJ mol^{-1} below HNC). According to high-level ab initio calculations supplemented with experimental data (Active Thermochemical Tables) HCN lies 62.35 ± 0.36 kJ mol^{-1} (converting the reported spectroscopic cm^{-1} energy units to kJ mol^{-1}) below HNC; this is "a recommended value…based on all currently available knowledge": Nguyen TL, Baraban JH, Ruscic B, Stanton JF (2015). J. Phys. Chem. A 119, 10929. *CH$_3$NC reaction* The reported experimental activation energy is 161 kJ mol^{-1} (Wang D, Qian X (1996). J. Peng, Chem. Phys. Lett., 258 149; Bowman JM, Gazy B, Bentley JA, Lee TJ, Dateo CE (1993). J Chem Phys, 99 308; Rabinovitch BS, Gilderson PW (1965). J. Am. Chem. Soc. 87 158; Schneider FW,

Rabinovitch BS (1962). J. Am. Chem. Soc. 84, 4215). The energy difference between CH$_3$NC and CH$_3$CN has apparently never been actually measured. *Cyclopropylidene reaction* Neither the barrier nor the equilibrium constant for the cyclopropylidene/allene reaction have been measured. The only direct experimental information of these species come from the failure to observe cyclopropylidene at 77 K (Chapman OL (1974) Pure and applied chemistry 40 511). This and other experiments (references in Bettinger HF, Schleyer PVR, Schreiner PR, Schaefer HF (1997). J. Org. Chem. 62, 9267 and in Bettinger HF, Schreiner PR, Schleyer PVR, Schaefer HF (1996). J. Phys. Chem. 100, 16147) show that the carbene is much higher in energy than allene and rearranges very rapidly to the latter. Bettinger et al., 1997 (above) calculate the barrier to be 21 kJ mol^{-1} (5 kcal mol^{-1}).

93. (a) Saebø S, Pulay P (1987). J Chem Phys 86, 914; (b) Pulay P (1983). Chem. Phys. Lett. 100 151

94. (a) Vahtras O, Almlöf J, Feyereisen MW, Pulay P (1993). Chem Phys Lett 213:514; (b) Feyereisen M, Fitzgerald G, Komornicki A (1993). Chem. Phys. Lett. 208:359; (c) The virtues of RI-MP2 are extolled in: Jurečka P, Nachtigall P, Hobza P (2001). Chem Phys, 3, 4578; (d) Deng J, Gilbert ATB, Gill PMW (2015). J. Chem. Theory Comput. 11: 1639–1644; (e) Soydaş E, Bozkaya U (2015). J. Chem. Theory Comput. 11: 1564–1573

95. (a) An excellent brief introduction to CI is given in Levine IN (2014) Quantum chemistry, 7th edn. Prentice Hall, Engelwood Cliffs section 16.2; (b) A comprehensive review of the development of CI: Shavitt, Mol. Phys.(1998), 94 3; (c) See also Lowe JP (1993) "Quantum chemistry", 2nd edn. Academic Press, New York, pp 363–369; Pilar FL (1990) Elementary quantum chemistry", 2nd edn. McGraw-Hill, New York, pp 388–393; Szabo A, Ostlund NS (1989) "Modern quantum chemistry". McGraw-Hill, New York, chapter 4; Hehre WJ, Radom L, Schleyer PVR, Pople JA (1986). "Ab initio molecular orbital theory". Wiley, New York, pp 29–38.

96. Levine IN (2014) Quantum chemistry, 7th edn. Prentice Hall, Engelwood Cliffs, p. 299, section 16.2

97. Ben-Amor N, Evangelisti S, Maynau D, Rossi EPS (1998) Chem Phys Lett 288:348

98. (a) Woodward RB, Hoffmann R (1970) "The conservation of orbital Symmetry". Academic Press, New York, chapter 6; (b) Foresman JB, Frisch Æ (1996) "Exploring chemistry with electronic structure methods". Gaussian Inc., Pittsburgh, pp. 228–236 shows how to do CASSCF calculations. For CASSCF calculations on the Diels-Alder reaction, see Li Y, Houk KN (1993). J. Am. Chem. Soc. 115, 7478

99. E.g. (a) Vogiatzis KD, Manni GL, Stoneburner SJ, Ma D, Gagliardi L (2015) Systematic expansion of active spaces beyond the CASSCF limit: a GASSCF/SplitGAS benchmark study, J. Chem. Theory Comput. 11, 3010; (b) Thomas RE, Sun Q, Alavi A, Booth GH (2015) Stochastic multiconfigurational self-consistent field theory, J. Chem. Theory Comput. 11, 5316

100. Cacelli I, Ferretti A, Prampolini G, Barone V (2015) J Chem Theory Comput 11:2024

101. (a) Karlstrom G, Lindh L, Malmqvist PA, Roos BO, Ryde, Veryazov V, Widmark PO, Cossi M, Schimmelpfennig B, Neogrady P, Seijo L (2003). Comput. Mater. Sci. 28, 222; (b) Anderssson K, Malmqvist PA, Roos BO (1992). J. Chem Phys. 96, 1218

102. Szabo A, Ostlund NS (1989) Modern quantum chemistry. McGraw-Hill, New York, chapter 6

103. Hrusak J, Ten-no S, Iwata S (1997).A paper boldly titled "Quadratic CI versus coupled-cluster theory. . ." J Chem Phys 106, 7185

104. Alberts IL, Handy NC (1988) J Chem Phys 89:2107

105. (a) Liakos DG, Neese F (2015). J Chem Theory Comput. 11, 4054, and references therein; (b) Riplinger C, Sandhoefer B, Hansen A, Neese F (2013). J Chem Phys 139, 134101; (c) Eriksen JJ, Baudin P, Ettenhuber P, Kristensen K, Kjærgaard T, Jørgensen P (2015). J Chem Theory Comput 11, 2984

106. The water dimer has been extensively studied, theoretically and experimentally: (a) Schuetz M, Brdarski S, Widmark PO, Lindh R, Karlström R (1997). J Chem Phys

107, 4597; these report an interaction energy of -20.7 kJ mol^{-1} (-4.94 kcal mol^{-1}), and give a method of implementing the counterpoise correction with modest basis sets; (b) Halkier A, Koch H, Jorgensen P, Christiansen O, Nielsen MB, Halgaker T (1997). Theor Chem Acc 97, 150; these report an interaction energy of -20.9 kJ mol^{-1} (-5.0 kcal mol^{-1}).; (c) Feyereisen MW, Feller D, Dixon DA (1996). J Phys Chem 100, 2993; these workers "best estimate" of binding electronic energy is -20.9 kJ mol^{-1} (-5.0 kcal mol^{-1}).; (d) Gordon MS, Jensen JH (1996) A general review of the hydrogen bond, Acc Chem Res 29, 536

107. For discussions of BSSE and the counterpoise method see: (a) Clark T (1985) "A handbook of computational chemistry". Wiley, New York, pp. 289–301; (b) J. M. Martin in (1998) "Computational thermochemistry".In: Irikura KK, Frurip DJ(eds) American Chemical Society, Washington, D.C., p. 223; (c) Thompson MGK, Lewars EG, Parnis JM (2005). J. Phys. Chem. A 109, 9499; (d) van Duijneveldt FB, van Duijneveldt-van de Rijdt JGCM, van Lenthe JH (1994). Chem. Rev. 94, 1873; (e) Mentel LM, Baerends EJ (2014). J. Chem. Theory Comput. 10, 252. (f) References [106] give leading references to BSSE and [106(a)] describes a method for bringing the counterpoise correction closer to the basis set limit. (g) Halasz GJ, Vibok A, Mayer I (1999) Methods designed to be free of BSSE. J. Comput. Chem. 20, 274

108. (a) Xu X, Goddard WA (2004). J. Phys. Chem. A 108, 2313; (b) Garza J, Ramírez JZ, Vargas R (2005). J. Phys. Chem. A 109, 643

109. (a) Conrad JA, Gordon MS (2015). J. Phys. Chem. A, 119, 5377; (b) Goldey MB, Belzunces B, Head-Gordon M (2015). J. Chem. Theory Comput. 11, 4159; (c) Řezáč J, Riley KE, Hobza P (2012). J. Chem. Theory Comput., 8, 4285; (d) Řezáč J, Hobza P (2014). J. Chem. Theory Comput., 10, 3066; (e) Strutyński K, Gomes JA, Melle-Franco M (2014). J. Phys. Chem. A, 118, 9561

110. (a) Boyd DB (2007) chapter 7 in Reviews in computational chemistry. In: Lipkowitz KB, Cundari TR (eds), vol 23. Wiley, Hoboken; (b) Mannhold R, Kubinyi H, Folkers G (eds) (2005) "Chemoinformatics in drug discovery". VCH, New York; (c) Höltje HD, Folkers G (1997) "Molecular modelling". VCH, New York; (d) Tropsha A, Bowen JP (1997) chapter 17 in "Using computers in chemistry and chemical education".In: Zielinski TJ, Swift ML (eds). American Chemical Society, Washington D.C.; (e) Balbes LM, Mascarella SW, Boyd DB (1994) chapter 7 in Reviews in computational chemistry. In:Lipkowitz KB, Boyd DB (eds) vol 5. VCH, New York; (f) Vinter JL, Gardner M (1994) "Molecular modelling and drug design". Macmillan, London

111. (a) See e.g. Bartlett RJ, Stanton JF (1994) chapter 2 in "Reviews in computational chemistry". In: Lipkowitz KB, Boyd DB (eds) vol 5. VCH, New York, p 106; (b) Burkert U, Allinger NL (1982) "Molecular mechanics". ACS Monograph 177, American Chemical Society, Washington, D.C., pp. 6–10; See also Ma B, Lii JH, Schaefer HF, Allinger NL (1996) J. Phys. Chem. 100, 8763; Ma M, Lii JH, Chen K, Allinger NL (1997) J. Am. Chem. Soc., 119, 2570

112. (a) Domenicano A, Hargittai I (eds) (1992) "Accurate molecular structures". Oxford University Press, New York; (b) V. G. S. Box (2002) A "wake-up call". Chem. & Eng. News, Feb. 18, 6

113. Petersson GA (1998) in chapter 13, "Computational thermochemistry". In: Irikura KK, Frurip DJ (eds) American Chemical Society, Washington, D.C.

114. Hehre WJ, Radom L, Schleyer PVR, Pople JA (1986) "Ab initio molecular orbital theory". Wiley, New York, pp. 133–226; note the summary on p. 226.

115. (a) Engelke EGR (1992). J. Phys. Chem., 96, 10789 (HF/4–31G, HF/4–31G*, MP2/6–31G*). (b) For references to various calculations see: Lewars E (2008) "Modeling marvels". Springer, Amsterdam, pp. 151–155

116. Foresman JB, Frisch Æ (1996) Exploring chemistry with electronic structure methods. Gaussian Inc., Pittsburgh, p 118

117. Reference [1e], p. 118 (ozone) and p. 128 (FOOF).

118. Foresman JB, Frisch Æ (1996) "Exploring chemistry with electronic structure methods". Gaussian Inc., Pittsburgh, p 36; other calculations on ozone are on pp 118, 137, and 159.
119. Kraka E, He Y (2001) J Phys Chem A 105:3269
120. Maciel GS, Bitencourt ACP, Ragni M, Aquilanti V (2007) J Phys Chem A 111:12604
121. Ju XH, Wang ZY, Yan XF, Xiao HM (2007) J Mol Struct (Theochem) 804:95
122. Grein F (2009) J Chem Phys 130:124118
123. Denis PA (2004) Chem Phys Lett 395:12
124. Ljubić I, Sabljić A (2004) Chem Phys Lett 385:214
125. Pakiari AH, Nazari F (2003). J. Mol. Struct. (Theochem), 640, 109, and references therein.
126. For thermochemical calculations, at least, fluoroorganics present special problems, e.g. Bond D (2007). J. Org. Chem., 72, 7313, and references therein; note p. 7322: "Difficulties in obtaining consistent and accurate data are found even with the simplest of the organofluoro compounds, fluoromethane."
127. Good DA, Francisco JS (1998) Fluoro ethers. J Phys Chem A 102:1854
128. Atkins P (2007) Four laws that drive the universe. Oxford University Press, Oxford
129. (a) Clausius R (1867) "The mechanical theory of heat". English translation, Editor, T. Hirst; John Van Voorst, London; (b) "Die Mechanische Wärmetheorie", R. Clausius, Zweite Auflage, Druck und Verlag von Friedrich Vieweg und Sohn, 1876; see pp 21 and 33–34. Available online from e.g. https://archive.org/details/diemechanischew01claugoog.
130. (a) Ochterski JW (2000) Details of statistical mechanics calculations utilizing vibrational frequencies. "Thermochemistry in Gaussian" www.gaussian.com/g_whitepap/thermo.htm; (b) Ochterski JW (2000) Details of the calculations of vibrational frequencies in Gaussian. "Thermochemistry in Gaussian" http://www.gaussian.com/g_whitepap/vib.htm.
131. von Nagy-Felsobuki EI (1990) J Phys Chem 94:8041
132. Howard IK (2002) J Chem Educ, 79, 697
133. Polyrate, http://lqtc.fcien.edu.uy/cursos/Ct2/polydoc80.pdf.
134. (a) See e.g. Deng WQ, Han KL, Zhan JP, He GZ (1988). Chem. Phys. 288, 33; (b) Hase WL Computer simulations of bimolecular reactions . Science, 266, 998; (c) Lourderaj U, Hase WL (2009) Non-RRKM unimolecular reactions. J. Phys. Chem. A, 113, 2236
135. Cramer CJ (2004) Essentials of computational chemistry, 2nd edn. Wiley, Chichester, p 528
136. Schroeder DV (2000) An introduction to thermal physics. Addison Wesley, New York
137. Coulson CA (1961) Valence, 2nd edn. Oxford University Press, London, p 91
138. Irikura KK, Frurip DJ (eds) "Computational thermochemistry". American Chemical Society, Washington, D.C.
139. Cramer CJ (2004) "Essentials of computational chemistry", 2nd edn. Wiley, Chichester, chapters 10 and 15.
140. (a) McGlashan ML (1979) "Chemical thermodynamics". Academic Press, London; (b) Nash LK (1968) "Elements of statistical thermodynamics". Addison-Wesley, Reading, MA; (c) Irikura KK (1998) A good, brief introduction to statistical thermodynamics is given by Irikura KK, in Frurip DJ (eds) "Computational thermochemistry". American Chemical Society, Washington, D.C., Appendix B.
141. Treptow RS (1995) J Chem Educ 72:497
142. See K. K. Irikura and D. J. Frurip, chapter 1, S. W. Benson and N. Cohen, chapter 2, and M. R. Zachariah and C. F. Melius, chapter 9, in "Computational Thermochemistry", K. K. Irikura and D. J. Frurip, Eds., American Chemical Society, Washington, D.C., 1998
143. These bond energies were taken from Fox MA, Whitesell JK (1994) "Organic Chemistry". Jones and Bartlett, Boston, p. 72
144. Although in the author's opinion it works well in chemistry, the disorder concept can lead to misunderstanding: a discussion of such popular misconceptions of entropy is given by F. L. Lambert, J. Chem. Educ., 1999, 76, 1385. Related discussions can be invoked on the web with the words "Lambert entropy".
145. For good accounts of the history and meaning of the concept of entropy, see (a), (b): (a) von Baeyer HC (1998) "Maxwell's Demon. Why warmth disperses and time passes". Random

House, New York; (b) Greenstein G (1998) "Portraits of Discovery. Profiles in Scientific Genius", chapter 2 ("Ludwig Boltzmann and the second law of thermodynamics"). Wiley, New York

146. Hehre WJ, Radom L, Schleyer PVR, Pople JA (1986) "Ab initio molecular orbital theory". Wiley, New York, section 6.3.9

147. Bohr F, Henon E (1998) A sophisticated study of the calculation of gas-phase equilibrium constants. J. Phys. Chem. A, 102, 4857

148. A very comprehensive treatment of rate constants, from theoretical and experimental viewpoints, is given in J. I. Steinfeld, J. S. Francisco, W. L. Hase, "Chemical Kinetics and Dynamics", Prentice Hall, New Jersey, 1999.

149. For the Arrhenius equation and problems associated with calculations involving rate constants and transition states see Durant JL in Irikura KK, Frurip DJ (1998) in "Computational thermochemistry". In: Irikura KK, Frurip DJ (eds). American Chemical Society, Washington, D.C., chapter 14

150. E.g., Atkins PW (1998) "Physical chemistry", 6th edn. Freeman, New York. p. 949

151. "Chemical kinetics and dynamics". Prentice Hall, New Jersey, 1999, p 302.

152. Some barriers/room temperature halflives for unimolecular reactions: (a) Benin V, Kaszynski P, Radziszki JG (2002) Decomposition of pentazole and its conjugate base: 75 kJ mol^{-1}/10 minutes and 106 kJ mol^{-1}/2 days, respectively. J. Org. Chem. 67, 1354; (b) Ahsen SV, Garciá P, Willner H, Paci MB, Argüello G (2003) Decomposition of CF_3CO) $OOO(COCF_3)$: 86.5 kJ mol^{-1}/1 minute. Chem. Eur. J. 9, 5135; (c) Lu J, Ho DM, Vogelaar NJ, Kraml CM, Pascal RA, Jr., (2004) Racemization of a twisted pentacene: 100 kJ mol^{-1}/ 6–9 h:. J. Am. Chem. Soc. 126, 11168

153. (a) Lewars E (2008) "Modeling marvels: computational anticipation of novel molecules". Springer, Netherlands, chapter 10; (b) Lewars E (2014) Can. J. Chem., 92, 378

154. Practical strategies for electronic structure calculations. Wavefunction, Inc., Irvine, 1995, chapter 2

155. Hehre WJ, Ditchfield R, Radom L, Pople JA (1970) J Am Chem Soc 92:4796

156. (a) Cyranski MW (2005) Chem. Rev., 105, 3773; (b) Suresh CH, Koga N (1965) J. Org. Chem. 67, 1965

157. Khoury PR, Goddard JD, Tam W (2004) Tetrahedron 60:8103

158. Wiberg KB, Marwuez M (1998) J Am Chem Soc 120:2932

159. Wheeler SE, Houk KN, Schleyer PVR, Allen WD (2009) J Am Chem Soc 131:2547

160. (a) Baeyer A, Ber.(1885), 18, 2269; (b) Smith MB, March J (2001) March's advanced organic chemistry. Wiley, New York, pp. 180–191

161. (a) Fishtik I (2010) J. Phys. Chem. A, 114, 3731; (b) Schleyer PVR, McKee WC (2010) J. Phys. Chem. A, 114, 3737

162. Kybett BD, Carroll S, Natalis P, Bonnell DW, Margrave JL, Franklin JL (1966) J Am Chem Soc 88:626

163. Lewars E (2008) Modeling marvels: computational anticipation of novel molecules. Springer, Netherlands, chapters 12 and 13

164. De Lio AM, Durfey BL, Gilbert TM (2015) J Org Chem 80:10234

165. (a) Whole issue devoted to reviews of aromaticity (2005). Chem Rev., 105; (b) Whole issue devoted to reviews of aromaticity (2001). Chem Rev., 101

166. (a) Schleyer PVR, Jiao H, GoldfussB (1995) Angew. Chem. Int. Ed. Engl., 34, 337; (b) George P, Trachtman M, Brett AM, Bock CW (1977) J. Chem. Soc. Perkin Trans 2, 1036; (c) Hehre WJ, McIver RT, Pople JA, Schleyer PVR (1974). J. Am. Chem. Soc., 96, 7162; (d) Radom L (1974) Chem. Commun., 403

167. Fabian J, Lewars E (2004) Can J Chem 82:50

168. (a) Golas E, Lewars E, Liebman J (2009) J. Phys. Chem. A, accepted June 2009; (b) Delamere C, Jakins C, Lewars E (2001) Can. J. Chem., 79, 1492

169. Fink WH, Richards JC (1991) J Am Chem Soc 113:3393

170. Slayden SW, Liebman JF (2001) Chem Rev 101:1541

171. Schleyer PVR, Puhlhofer F (2002) Org. Lett., 4, 2873
172. Mo Y (2009) J Phys Chem A 113:5163
173. Lewars E (2008) Modeling marvels: computational anticipation of novel molecules. Springer, Netherlands, chapter 3
174. (a) Wiberg KB (2001) Chem Rev., 101, 1317; (b) de Meijere A, Haag R, Schüngel FM, Kozhushkov SI, Emme I (1999) Pure Appl. Chem., 71, 253
175. Moskowitz JW, Schmidt KE, NATO ASI Series, Series C: Mathematical and Physical Sciences (1984), 125(Monte Carlo Methods Quantum Probl.), 59–70.
176. Bauschlicher CW, Langhoff SR (1991) Science 254:394
177. G1: Pople JA, Head-Gordon M, Fox DJ, Raghavachari K, Curtiss LA (1989). J. Chem. Phys., 90, 5622
178. The first in the series was Gaussian 70 and the latest (as of mid- 2016) is Gaussian 09. Gaussian Inc., 340 Quinnipiac St Bldg 40, Wallingford, CT 06492 USA. Info@gaussian.com
179. G2: Curtiss LA, Raghavachari K, Trucks GW, Pople JA (1991). J. Chem. Phys. 94, 7221
180. G3: Curtiss LA, Raghavachari K, Redfern PC, Rassolov V, Pople JA (1998) J. Chem. Phys., 109, 7764
181. G4: Curtiss LA, Redfern PC, Raghavachari K (2007) J. Chem. Phys., 126, 084108
182. Curtiss LA, Redfern PC, Raghavachari K (2007) J Chem Phys 127:124105
183. G3(MP2): Curtiss LA, Redfern PC, Raghavachari K, Rassolov V, Pople JA (1999) J. Chem. Phys., 110, 4703
184. Mayhall NJ, Raghavachari K, Redfern PC, Curtiss LA (2009) J Phys Chem A 113:5170
185. Peterson KA, Feller D, Dixon DA (2012) Theor Chem Acc 131:1079
186. Reference 7 in Fatthi A, Kass SR, Liebman JF, Matos MAR, Miranda MS, Morais VMF (2005) J. Am. Chem. Soc., 127, 6116
187. (a) Petersson GA, Montgomery JA, Jr., Frisch MJ, Ochterski JW (2000) J. Chem. Phys., 112, 6532; (b) Montgomery JA, Jr., Frisch MJ, Ochterski JW, Petersson GA (1999) J. Chem. Phys., 110, 2822
188. (a) Benassi R, Taddei F (2000) J. Comput. Chem., 21, 1405; (b) Benassi R (2001) Theor. Chem. Acc., 106, 259
189. Martin JML, de Oliveira G (1999) J Chem Phys 111:1843
190. (a) Boese AD, Oren M, Atasoylu O, Martin JML, Kállay M, Gauss J (2004) J. Chem. Phys., 120, 4129; (b) Chan B, Radom L (2015) J. Chem. Theory Comput., 11, 2109
191. Pokon EK, Liptak MD, Feldgus S, Shields GC (2001) J Phys Chem A 105:10483
192. Bond D (2007) J Org Chem 72:5555
193. Bond D (2007) J Org Chem 72:7313
194. Ess DH, Houk KN (2005) J Phys Chem A 109:9542
195. For this and other caveats regarding the multistep methods see Cramer CJ (2004) Essentials of computational chemistry, 2nd edn. Wiley, Chichester, pp. 241–244
196. E.g. Atkins PW (1998) Physical chemistry, 6th edn. Freeman, New York, p. 70
197. M. W. Chase, Jr, J. Phys. Chem. Ref. Data, Monograph 9, 1998, 1-1951. NIST-JANAF Thermochemical Tables, Fourth Edition
198. Nicolaides A, Rauk A, Glukhovtsev MN, Radom L (1996) J Phys Chem 100:17460
199. Gaussian 94 for Windows (G94W): Gaussian 94, Revision E.1, Frisch MJ, Trucks GW, Schlegel HB, Gill PMW, Johnson BG, Robb MA, Cheeseman JR, Keith T, Petersson GA, Montgomery JA, Raghavachari K, Al-Laham MA, Zakrzewski VG, Ortiz JV, Foresman JB, Cioslowski J, Stefanov BB, Nanayakkara A, Challacombe M, Peng CY, Ayala PY, Chen W, Wong MW, Andres JL, Replogle ES, Gomperts R, Martin RL, Fox DJ, Binkley JS, Defrees DJ, Baker J, Stewart JP, Head-Gordon M, Gonzalez C, Pople JA (1995) Gaussian, Inc., Pittsburgh PA, G94 and G98 are available for both UNIX workstations and PCs
200. Afeefy HY, Liebman JF, Stein SE (2009) Neutral thermochemical data. In: Linstrom PJ, Mallard WG (eds) NIST Chemistry WebBook, NIST Standard Reference Database Number 69, , National Institute of Standards and Technology, Gaithersburg MD, 20899, http://webbook.nist.gov, (retrieved July 15, 2009).

201. Pople JA (1970) Acc Chem Res 3:217
202. (a) Irikura KK, Frurip DJ (1998) Worked examples, with various fine points. In: Irikura KK, Frurip DJ (eds) Computational Thermochemistry. American Chemical Society, Washington, D.C., Appendix C; (b) Rodrigues CF, Bohme DK, Hopkinson AC (1996) Heats of formation of neutral and cationic chloromethanes. J Phys Chem, 100, 2942; (c) Turecek F, Cramer CJ (1995) Heats of formation, entropies and enthalpies of neutral and cationic enols. J Am Chem Soc, 117, 12243; (d) D. DeTar F (1995) Heats of formation by ab initio and molecular mechanics. J Org Chem, 60, 7125; (e) Glukhovtsev MN, Laiter S, Pross A (1995) Heats of formation and antiaromaticity in strained molecules. J Phys Chem, 99, 6828; (f) Schmitz LR, Chen YR (1994) Heats of formation of organic molecules with the aid of ab initio and group equivalent methods. J Comp Chem, 15, 1437; (f) Li Z, Rogers DW, McLafferty FJ, Mandziuk M, Podosenin AV (1999) Isodesmic reactions in ab initio calculation of enthalpy of formation of cyclic C_6 hydrocarbons and benzene isomers. J Phys Chem A, 103, 426; (g) Cheung YS, Wong CK, Li WK (1998) Isodesmic reactions in ab initio calculation of enthalpy of formation of benzene isomers. Mol Struct (Theochem), 454, 17
203. Abou-Rachid H, Song Y, Hu A, Dudiy S, Zybin SV, Goddard WA III (2008) J Phys Chem A 112:11914
204. Ringer AL, Sherrill CD (2008) Chem Eur J 14:2442
205. Fatthi A, Kass SR, Liebman JF, Matos MAR, Miranda MS, Morais VMF (2005) J Am Chem Soc, 127, 6116, Table 5
206. (a) http://webbook.nist.gov. (b) Lias SG, Bartmess JE, Holmes JFL, Levin RD, Mallard WG (1988) J Phys Chem Ref Data, 17, Suppl. 1., American Chemical Society and American Institute of Physics, 1988; (c) Pedley JB (1994) Thermochemical data and structures of organic compounds. Thermodynamics Research Center, College Station, Texas
207. 207 DeL. F. DeTar (1998) J. Phys. Chem. A, 102, 5128
208. Shaik SS, Schlegel HB, Wolfe S (1992) Theoretical aspects of physical organic chemistry. The SN2 mechanism. Wiley, New York, pp 50–51
209. Cramer CJ (2004) Essentials of computational chemistry, 2nd edn. Wiley, Chichester, sections 15.2 and 15.3
210. (a) Zhang JZH (1999) Theory and applications of quantum molecular dynamics. World Scientific, Singapore, New Jersey, London and Hong Kong; (b) Thompson DL (ed) Modern methods for multidimensional dynamics in chemistry. World Scientific, Singapore, New Jersey, London and Hong Kong; (c) Rapaport DC (1995) The art of molecular dynamics simulation. Cambridge University Press, New York; (d) Devoted to big biomolecules like proteins and nucleic acids: Schlick T (2002) Molecular modeling and simulation. An interdisciplinary guide. Springer, New York
211. (a) Levine IN (2014) Quantum chemistry, 7th edn. Prentice Hall, Engelwood Cliffs, section 2.5, p 591; (b) Reference [148], section 12.3. (c) Bell RP (1980) The tunnel effect in chemistry. Chapman and Hall, London
212. Carpenter BK (1992) Acc Chem Res 25:520
213. (a) Litovitz AE, Keresztes I, Carpenter BK (2008) J Am Chem Soc, 130, 12085, and references therein; (b) Carpenter BK (1997) American Scientist, March-April, 138
214. (a) Shaik SS, Schlegel HB, Wolfe S (1992) Theoretical aspects of physical organic chemistry. The SN2 mechanism. Wiley, New York, p. 84–88; (b) Kinetics of halocarbons reactions: R. J. Berry, M. Schwartz, P. Marshall in [138], chapter 18. (c) The ab initio calculation of rate constants is given in some detail in these two references: Smith DM, Nicolaides A, Golding BT, Radom L (1998) J AmChem Soc, 120, 10223; Heuts JPA, Gilbert RG, Radom L (1995) Macromolecules, 28, 8771; reference [1l], pp. 471–489, 492–497. (d) R. C. de M. Oliveira, Bauerfeldt GF (2015) J Phys Chem A, 119, 2802
215. Steinfeld JI, Francisco JS, Hase WL (1999) Chemical kinetics and dynamics. Prentice Hall, New Jersey, chapter 11
216. Spartan '04. Wavefunction Inc., http://www.wavefun.com, 18401 Von Karman, Suite 370, Irvine CA 92715, USA.

217. Hehre WJ (1995) Practical strategies for electronic structure calculations. Wavefunction, Inc., Irvine, pp 148–150
218. del Rio A, Boucekkine A, Meinnel J (2003) J Comp Chem 24:2093
219. Wiest O, Montiel DC, Houk KN (1997) J Phys Chem A 101:8378
220. Wheeler SE, Ess DH, Houk KN (2008) J Phys Chem A 112:1798
221. Schneider FW, Rabinivitch BS (1962) J Am Chem Soc 84:4215
222. Saito S (1978) Pure Appl Chem 50:1239
223. Defrees DJ, McLean AD (1982) J Chem Phys 86:2835
224. (a) Rodler M, Bauder A (1984) J Am Chem Soc, 106, 4025; (b) Rodler M, Blom CE, Bauder A (1984) J Am Chem Soc, 106, 4029
225. Capon B, Guo B-Z, Kwok FC, Siddhanta AK, Zucco C (1988) Acc Chem Res 21:135
226. Chapman OL (1974) Pure Appl Chem 40:511
227. Bettinger HF, Schreiner PR, Schleyer PVR, Schaefer HF III (1996) J Phys Chem 100:16147
228. Foresman JB, Frisch Æ (1996) Exploring chemistry with electronic structure methods. Gaussian Inc., Pittsburgh, chapter 7
229. Foresman JB, personal communication, October 1998.
230. Lories X, Vandooren J, Peeters D (2008) Chem Phys Lett, 452, 29, and references therein. The authors point out that "no theoretical calculation seems to reproduce that value", and from high-level ab initio calculations suggest a value of 214.1 kJ mol^{-1} (51.17 kcal mol^{-1}).
231. Good WD, Smith NK (1969) J Chem Eng Data 14:102
232. Pedley JB, Naylor RD, Kirby SP (1986) Thermochemical data of organic compounds, 2nd edn. Chapman and Hall, London
233. Pilcher G, Pell AS, Coleman DJ (1964) Trans Faraday Soc 60:499
234. 234 L. V. Gurvich, I. V. Vetts, C. B. Alcock, "Thermodynamic Properties of Individual Substances", Fourth Edition, Hemisphere Publishing Corp., New York, 1991, vol. 2.
235. Spitzer R, Huffmann HM (1947) J Am Chem Soc 69:211
236. Ghysels A, Van Neck D, Van Speybroeck V, Verstraelen T, Waroquier M (2007) J Chem Phys, 126, 224102, and references therein
237. For introductions to the theory and interpretation of mass, infrared, and NMR spectra, see Silverstein RM, Webster FX, Kiemle DJ (2005) Spectrometric identification of organic compounds, 7th edn. Wiley, Hoboken NJ
238. Huber KP, Herzberg G (1979) Molecular spectra and molecular structure, IV. Constants of diatomic molecules. Van Nostrand Reinhold, New York
239. Hehre WJ, Radom L, Schleyer PVR, Pople JA (1986) Ab initio molecular orbital theory. Wiley, New York, pp 234–235
240. E.g. "...it is unfair to compare frequencies calculated within the harmonic approximation with experimentally observed frequencies...": A. St-Amant, chapter 2, p. 235 in Reviews in Computational Chemistry, Volume 7, K. B. Lipkowitz and D. B. Boyd, Eds., VCH, New York, 1996.
241. Jensen F (2007) Introduction to computational chemistry, 2nd edn. Wiley, Hoboken, pp 358–360
242. Thomas JR, DeLeeuw BJ, Vacek G, Crawford TD, Yamaguchi Y, Schaefer HF (1993) J Chem Phys 99:403
243. Radziszewski JG, Hess BA, Jr., Zahradnik R (1992) A tour-de-force mainly experimental study of the IR spectrum of 1,2-benzine. J Am Chem Soc, 114, 52
244. (a) Komornicki A, Jaffe RL (1979) J Chem Phys, 71, 2150; (b) Yamaguchi Y, Frisch M, Gaw J, Schaefer HF,Binkley JS (1986) J Chem Phys, 84, 2262; (c) Frisch M, Yamaguchi Y, Schaefer HF,, Binkley JS (1986) J Chem Phys, 84, 531; (d) Amos RD (1984) Chem Phys Lett, 108 185; (e) Gready JE, Bacskay GB,, Hush NS (1978) J Chem Phys, 90, 467
245. Galabov BS, Dudev T (1996) Vibrational intensities. Elsevier Science, Amsterdam
246. Magers DH, Salter EA, Bartlett RJ, Salter C, Hess Ba, Jr., Schaad LJ (1988) J Am Chem Soc, 110, 3435 (comments on intensities on p. 3439)
247. Galabov B, Yamaguchi Y, Remington RB, Schaefer HF (2002) J Phys Chem A 106:819

248. For a good review of the cyclobutadiene problem, see Carpenter BK (1988). In: Liotta D (ed) Advances in Molecular Modelling. JAI Press Inc., Greenwich, Connecticut

249. (a) Amann A (1992) South African J Chem, 45, 29; (b) Wooley G (1988) New Scientist, 120, 53; (c) Wooley G (1978) J Am Chem Soc, 100, 1073

250. (a) Trindle C (1980) Israel J Chem, 19, 47; (b) Mezey PG (1993) Shape in chemistry: an introduction to molecular shape and topology. VCH, New York

251. (a) Theoretical calculation of dipole moments: reference [1a], section 14.2; (b) Measurement and application of dipole moments: Exner O (1975) Dipole moments in organic chemistry. Georg Thieme Publishers, Stuttgart

252. McClellan AL (1963) Tables of experimental dipole moments, vol. 1. W. H. Freeman, San Francisco, CA; vol. 2. Rahara Enterprises, El Cerrita, CA, 1974.

253. Bartlett RJ, Stanton JF (1994). In: Lipkowitz KB, Boyd DB (eds) Reviews in computational chemistry, vol 5. VCH, New York, p 152

254. (a) Huzinaga S, Miyoshi E, Sekiya M (1993) J Comp Chem, 14, 1440; (b) Ernzerhof M, Marian CM, Peyerimhoff SD (1993) Chem Phys Lett, 204, 59

255. Carefully defined atom charges are, it has been said, "in principle subject to experimental realization": Cramer CJ (2004) Essentials of computational chemistry, 2nd edn. Wiley, Chichester, p 309

256. The reason why an electron pair forms a covalent bond has perhaps not been fully settled. See (a) Levine IN (2014) Quantum chemistry, 7th edn. Prentice Hall, Engelwood Cliffs, p 362–363, and top of p 364; (b) Backsay GB, Reimers JR, Nordholm S (1997) J Chem Ed, 74, 1494

257. E.g. (a) Wheland GW, Pauling L (1935) Electron density on an atom. J Am Chem Soc, 57, 2086; (b) Coulson CA (1939) Pi-bond order. Proc Roy Soc, A169, 413

258. (a) Mulliken RS (1955) J Chem Phys., 23, 1833; (b) Mulliken RS (1962) J Chem Phys, 36, 3428; (c) Reference [1a], section 15.6.

259. Mayer I (1983) Chem Phys Lett 97:270

260. Löwdin P-O (1970) Adv Quantum Chem 5:185

261. Reed AE, Curtiss LA, Weinhold F (1988) Chem Rev 88:899

262. Mayer I (1995) email to the Computational Chemistry List (CCL), 1995 March 30.

263. Some examples: (a) Bridgeman A, Cavigliasso G, Ireland LR, Rothery J (2001) General survey. J Chem Soc, Dalton Trans, 2095;(b) Fowe EP, Therrien B, Suss-Fink G, Daul C (2008) Ruthenium complexes. Inorg Chem, 47, 42; (c) Mayer I, Revesz M (1983) Simple sulfur compounds. Inorganica Chimica Acta, 77, L205

264. Cramer CJ (2004) Essentials of computational chemistry, 2nd edn. Wiley, Chichester, pp 312–315

265. Leach AR (2001) Molecular modelling, 2nd edn. Prentice Hall, Essex, pp 79–83

266. Milani A, Castiglioni C (2010) J Phys Chem A 114:624

267. (a) West AC, Schmidt MW, Gordon MS, Ruedenberg K (2013) J Chem Phys, 139, 234107; (b) Ruedenberg K (1962) Rev Mod Phys, 34, 326; (c) West AC, Schmidt MW, Gordon MS, Ruedenberg K (2015) J Phys Chem A, 119, 10368; (d) West AC, Schmidt MW, Gordon MS, Ruedenberg K (2015) J Phys Chem A, 119, 10376

268. (a) Brinck T (1998). In: Parkanyi C (ed) Theoretical organic chemistry. Elsevier, New York; (b) Marynick DS (1997) J Comp Chem, 18, 955

269. (a) Schleyer PVR, Buzek P, Müller T, Apeloig Y, Siehl HU (1993) Use of bond orders in deciding if a covalent bond is present. Angew Chem int Ed Engl, 32, 1471; (b) Lendvay G (1994) Use of bond order in estimating progress along a reaction coordinate. J Phys Chem, 98, 6098

270. (a) Berlin T (1951) J Chem Phys, 19, 208; (b) Bader RWF (1964) J Am Chem Soc, 86, 5070

271. Bader RWF, Beddall PM (1973) J Am Chem Soc 95:305

272. Bader RWF (1975) Acc Chem Res 8:34

273. Bader RWF (1985) Acc Chem Res 18:9

274. Bader RFW (1990) Atoms in molecules. Oxford University Press, Oxford

275. Bader RWF (1991) Chem Rev 91:893
276. Popelier PLA (1999) Atoms in molecules: an introduction. Pearson Education, UK
277. Matta CF, Boyd RJ (eds) (2007) The quantum theory of atoms in molecules: from solid state to DNA and drug design. Wiley-VCH, Weinheim
278. Bader RFW (2007) J Phys Chem A 111:7966
279. Reference [1a], section 14.1.
280. Reference [274], p. 40.
281. Reference [274], p. 75.
282. Jacobsen H (2009) J Comp Chem 30:1093
283. Grabowski SJ (2007) J Phys Chem A 111:13537
284. (a) Grabowski SL, Sokalski WA, Leszczynski J (2006) Chem Phys Lett, 432, 33; (b) Grabowski SL (2007) J Phys Chem A, 111, 13537
285. Werstiuk NH, Sokol W (2008) Can J Chem 86:737
286. Vila A, Mosquera RA (2006) J Phys Chem A 110:11752
287. Lopez JL, Grana AM, Mosquera RA (2009) J Phys Chem A 113:2652
288. Long review of "Chemical Bonding and Molecular Geometry from Lewis to Electron Densities", R. J. Gillespie, P. L. A. Popelier, Oxford University press, New York, 2001: G. Frenking, Angew. Chem. Int. Ed. Engl., 2003, 42, 143.
289. Gillespie RJ, Popelier PLA (2003) Angew Chem Int Ed Engl 42:3331
290. Frenking G (2003) Angew Chem Int Ed Engl 42:3335
291. Bader RFW (2003) Int J Quantum Chem 94:173
292. Bader RFW, Matta CF (2004) J Phys Chem A 108:8385
293. Kovacs A, Esterhuysen C, Frenking G (2005) Chem Eur J 11:1813
294. Bader RFW (2006) Chem Eur J 12:7769
295. Frenking G, Esterhuysen C, Kovacs A (2006) Chem Eur J 12:7773
296. Matta CF, Hernández-Trujillo J, Tang T-H, Bader RFW (2003) Chem Eur J 9:1940
297. Poater J, Solà M, Bickelhaupt M (2006) Chem Eur J 12:2889
298. Bader RFW (2006) Chem Eur J 12:2896
299. Poater J, Solà M, Bickelhaupt M (2006) Chem Eur J 12:2902
300. An old classic that is still useful: Jaffé HH, Orchin M, Theory and applications of ultraviolet spectroscopy. Wiley, New York
301. Foresman JB, Frisch Æ (1996) Exploring chemistry with electronic structure methods. Gaussian Inc., Pittsburgh, pp 213–227
302. Foresman JB, Frisch Æ (1996) Exploring chemistry with electronic structure methods. Gaussian Inc., Pittsburgh, p 213
303. Helgaker T, Jaszuński M, Ruud K (1999) Chem Rev 99:293
304. Foresman JB, Frisch Æ (1996) Exploring chemistry with electronic structure methods. Gaussian Inc., Pittsburgh, pp 53–54 and 104–105
305. Cheeseman JR, Trucks GW, Keith TA, Frisch MJ (1996) J Chem Phys 104:5497
306. Casabianca LB, de Dios AC (2008) J Chem Phys 128:052201
307. Auer AA (2009) Chem Phys Lett 467:230
308. Pérez MP, Peakman TM, Alex A, Higginson PD, Mitchell JC, Snowden MJ, Inaki I (2006) J Org Chem 71:3103
309. Wolf AD, Kane VV, Levin RH, Jones M (1973) J Am Chem Soc 95:1680
310. (a) Schleyer PVR, Maerker C, Dransfeld A, Jiao H, Van Eikema Hommes NJR (1996) J Am Chem Soc 118, 6317; (b) West R, Buffy J, Haaf M, Müller T, Gehrhus B, Lappert MF, Apeloig Y (1998) J Am Chem Soc, 120, 1639; (c) Chen Z, Wannere CS, Corminboef C, Puchta R, Schleyer PVR (2005) Chem Rev 105, 3842; (d) Morao I, Cossio FP (1999) J Org Chem, 64, 1868; (e) Stanger A (2010) Useful "NICS curves". J Prog Chem 75, 2281; (f) Stanger A (2013) Connection of NICS with stabilization energy. J Org Chem, 78, 12374; (g) Torres JJ, Islas R, Osorio E, Harrison JG, Tiznado W, Merino G Complicated, cautionary work. J Phys Chem A, 117, 5529
311. Antušek A, Kędziera D, Jackowski K, Jaszuński M, Makulski W (2008) Chem Phys 352:320

312. (a) Lowe JP (1993) Quantum chemistry, 2nd edn. Academic Press, New York, pp 276–277, 288, 372–373; (b) Rienstra-Kiracofe JC, Tschumper GS, Schaefer III HF, Nandi S, Ellison GB (2002) General review of EA. Chem Rev, 102, 231
313. Gross JH (2004) Mass spectrometry. Springer, New York, pp. 16–20
314. Levin RD, Lias SG (1982) Ionization potential and appearance potential measurements, 1971–1981. National Bureau of Standards, Washington, DC
315. (a) Maksić ZB, Vianello R (2002) How good is Koopmans' approximation?. J Phys Chem A, 106, 6515; (b) See e.g. reference [1b], pp. 361–363; reference [1c], pp. 278–280; reference [1d], pp. 127–128; reference [1g], pp. 24, 116. (c) Angeli C (1998) A novel look at Koopmans' theorem. J Chem Ed, 75, 1494; (c) Koopmans T (1934) Physica, 1, 104
316. Smith MB, March J (2001) March's advanced organic chemistry, 5th edn. Wiley, New York, pp 10–12
317. Curtiss LA, Nobes RH, Pople JA, Radom I (1992) J Chem Phys 97:6766
318. Lyons JE, Rasmussen DR, McGrath MP, Nobes RH, Radom L (1994) Angew Chem Int Ed Engl 33:1667
319. (a) Schmidt MW, Hull EA, Windus TL (2015) J Phys Chem A, 119, 10408; (b) van Meer R, Gritsenko OV, Baerends EJ (2014) DFT with close-to-exact Kohn-Sham orbitals give virtual-occupied energy gaps very close to excitation energies, good values for ionization energies and Rydberg transitions, and realistic shapes of virtual orbitals. J Chem Theory Comput, 10, 4432
320. Robinson PJ, Alexandrova N (2015) J Phys Chem A 119:12862
321. (a) Habraken CL (1996) "...Chemistry, the most visual of sciences...". J Science Educ And Philosophy, 5, 193; (b) Bower JE (ed) (1995) Data visualization in molecular science: tools for insight and innovation. Addison-Wesley, Reading, MA; (c) Pickover C, Tewksbury S (1994) Frontiers of scientific visualization. Wiley; (d) Johnson G (2001) Colors are truly brilliant in trek up mount metaphor. New York Times, 2001, 25 December.
322. Ihlenfeldt W-D (1997) J Mol Model 3:386
323. Hoffmann R, Laszlo P (1991) Angew Chem Int Ed Engl 30:1
324. GaussView: Gaussian Inc., Carnegie Office Park, Bldg. 6, Pittsburgh 15106, USA.
325. Eliel EL, Wilen SH (1994) Stereochemistry of carbon compounds. Wiley, New York, pp. 502–507 and 686–690
326. Iijima T, Kondou T, Takenaka T (1998) J Mol Struct 445:23
327. The term is not just whimsy on the author's part: certain stereoelectronic phenomena arising from the presence of lone pairs on heteroatoms in a 1,3-relationship were once called the "rabbit-ear effect", and a photograph of the eponymous creature even appeared on the cover of the Swedish journal Kemisk Tidskrift. History of the term, photograph: Eliel EL (1990) From cologne to Chapel Hill. American Chemical Society, Washington, DC, pp. 62–64
328. Politzer P, Murray JS (1996).In: Lipkowitz KB, Boyd DB (eds) chapter 7 in Reviews in Computational Chemistry, vol 2. VCH, New York
329. Hehre WJ, Shusterman AJ, Huang WW (1996) A laboratory book of computational organic chemistry. Wavefunction Inc., Irvine, pp 141–142
330. (a) Laube T (1989) J Am Chem Soc, 111, 9224; (b) Kirmse W, Rainer S, Streu J (1984) J Am Chem Soc, 106, 24654; (c) Houriet R, Schwarz H, Zummack W, Andrade JG, Schleyer PVR (1981) Nouveau J de Chimie, 5, 505; (d) Olah GA, Prakash GKS, Rawdah TN, Whittaker D, Rees JC (1979) J Am Chem Soc, 101, 3935; (e) Sorenson TS (1976) A polemic against the formation of a bishomocyclopropenyl cation in a certain case: Chem Commun, 45.
331. Olah GA, Liang G (1975) J Am Chem Soc, 97, 6803, and references therein
332. Hehre WJ, Shusterman AJ, Nelson JE (1998) The molecular modelling workbook of organic chemistry. Wavefunction Inc., Irvine
333. (a) Bolcer JD, Hermann RB (1996) Coulson's remarks.In: Lipkowitz KB, Boyd DB (eds) chapter 1 in Reviews in Computational Chemistry, vol 5. VCH, New York, p. 12; see too further remarks, quoted on p. 13; (b) The increase in computer speed is also dramatically shown in data provided in *Gaussian News*, 1993, *4*, 1. The approximate times for a

single-point HF/6–31G** calculation on 1,3,5-triamino-2,4,6-trinitrobenzene (300 basis functions) are reported as: ca. 1967, on a CDC 1604, 200 years (estimated); ca. 1992, on a 486 DX personal computer, 20 hours. This is a speed factor of 90,000 in 25 years. The price factor for the machines may not be as dramatic, but suffice it to say that the CDC 1604 was not considered a personal computer. In mid-2009, on a well-endowed personal computer (ca. $4000) these results were obtained for single-point HF/6–31G** calculations on 1,3,5-triamino-2,4,6-trinitrobenzene: starting from a C3 geometry, 23 seconds; starting from a C1 geometry, 42 seconds. The increase in speed represented by 42 seconds in 2009 is, cf. 200 years in 1967, a factor of about 10^8 in 42 years; cf. 20 hours in 1992, a factor of about 1700 in 17 years.

334. Fales BS, Levine BG (2015) J Chem Theory Comput 11:4708
335. Acevido O, Jorgenson WL (2010) Acc Chem Res 43:142
336. Fragment QM methods: "Beyond QM/MM" issue: Acc Chem Res, 2014, *47*(9)

Chapter 6
Semiempirical Calculations

> Current "ab initio" methods were limited to very inaccurate
> calculations for very small molecules.
> M.J.S. Dewar, *A Semiempirical Life, 1992*

Abstract Semiempirical quantum mechanical calculations are based on the Schrödinger equation. This chapter deals with SCF semiempirical methods, in which repeated (in contrast to the simple and extended Hückel methods) diagonalization of a Fock matrix refines the wavefunction and molecular energy. These calculations are much faster than ab initio ones, mainly because the number of integrals to be dealt with is greatly reduced by ignoring some and approximating others with the help of experimental quantities, or with values from high-level ab initio or DFT calculations. In order of increasing sophistication, these SCF semiempirical methods have been developed: PPP (Pariser-Parr-Pople), CNDO (complete neglect of differential overlap), INDO (intermediate neglect of differential overlap), and NDDO (neglect of diatomic differential overlap). Today the most popular SCF semiempirical methods are variations of NDDO: AM1 (Austin model 1, from Austin, Texas) and its offshoot PM3 (parametric method 3), which are carefully parameterized to reproduce experimental quantities, mainly heats of formation. Fairly recent extensions of AM1 (RM1, Recife model 1, from Recife, Brazil) and PM3 (PM6, PM7) seem to represent substantial improvements and may become the standard semiempirical methods.

6.1 Perspective

We have already seen examples of semiempirical methods, in Chap. 4: the simple Hückel method (SHM, Erich Hückel, ca. 1931) and the extended Hückel method (EHM, Roald Hoffmann, 1963). These are semiempirical ("semi-experimental") because they combine physical theory with experiment. Both methods start with the Schrödinger equation (theory) and derive from this a set of secular equations which may be solved for energy levels and molecular orbital coefficients (most efficiently by diagonalizing a Fock matrix; see Chap. 4). However, the SHM gives energy

levels in units of a parameter (β) that can be translated into actual quantities only by comparing SHM results with experiment, and the EHM uses experimental ionization energies to translate the Fock matrix elements into actual energy quantities. Semiempirical calculations stand in contrast to purely empirical methods, like molecular mechanics (Chap. 3), and theoretical methods, like ab initio calculations (Chap. 5). Molecular mechanics starts with a model of a molecule as balls and springs, a model that works and whose justification lies in this fact. The ab initio method, like the Hückel methods, starts with the Schrödinger equation but strictly ab initio calculations do not appeal to experiment, beyond invoking, when actual quantities are needed, experimental values for Planck's constant, the charge on the electron and proton, and the masses of the electron and atomic nuclei. These fundamental physical constants could be calculated only by some deep theory of the origin and nature of our universe [1].

The Hückel methods were discussed in Chap. 4 rather than here because extensive application of those methods came before widespread use of ab initio methods, and because the simple Hückel, extended Hückel and ab initio methods form a conceptual progression in which the first two methods aid understanding of the third in this hierarchy of complexity. The semiempirical methods treated in this chapter are logically regarded as simplifications of the ab initio method, since they use the SCF procedure (Chap. 5) to refine the Fock matrix, but do not evaluate these matrix elements *ab initio*. The SHM was developed (1931) outside the realm of SCF theory (which was invented for atoms: Hartree, 1928 [2]), as the first application of the Schrödinger equation to molecules of reasonable size, and the EHM is a straightforward extension of this. In contrast, the methods of this chapter began as *a conscious attempt to provide practical alternatives to the ab initio approach*, the application of which to molecules of reasonable size understandably seemed hopeless in the infancy of electronic computers. The PPP method, one of the first SCF semiempirical methods, was published in 1953, just when the first electronic computers began to be available to chemists [3]. Semiempirical calculations are much less demanding of computer power than ab initio ones, because parameterization and approximations drastically reduce the number of integrals which must be calculated. The pessimism with which the ab initio approach was viewed is clear in the words of several pioneers of quantum chemistry:

C. A. Coulson, 1959: "I see little chance–and even less desirability–of dealing in this accurate manner with systems containing more than 20 electrons. . ." [4]

M. J. S. Dewar,[1] 1969: "How then shall we proceed? The answer lies in abandoning attempts to carry out rigorous a priori calculations." [5].

Neither Coulson nor Dewar could have foreseen the enormous increase in computer power that was to come over the next few decades. What Coulson

---

[1]Michael J. S. Dewar, born Ahmednagar, India, 1918. Ph.D. Oxford, 1942. Professor of chemistry at Universities of London, Chicago, Texas at Austin, and University of Florida. Died Florida, 1997.

meant by "even less desirability" was perhaps that the computed results would be too complex to interpret; one factor which has obviated this problem is the visual display of information (Chap. 5, Sect. 5.5.6, Chap. 6, Sect. 6.3.6). The development of improved algorithms and far faster computers has altered the situation almost out of recognition; for example, an energy calculation on a moderate-size molecule (1,3,5-triamino-2,4,6-trinitrobenzene) was faster in mid-2009 by these factors: compared to 17 years before, 1700; compared to 25 years before, 90,000; compared to 42 years before, 10^8 [6]. Why, then, are semiempirical calculations still used? Because they are still about 100–1000 times faster than ab initio (Chap. 5) or density functional (Chap. 7) methods. The increase in computer speed means that we can now routinely examine by ab initio methods moderately large molecules – up to, say, steroids, with about 30 heavy atoms (non-hydrogen atoms), and by semiempirical methods huge molecules, even proteins and nucleic acids.

In the following presentation of the development of semiempirical methods, the general approach and the distinction between the various methods is perhaps best appreciated by understanding the concepts in words, rather than attempting to memorize admittedly somewhat formidable-looking equations (unless you plan to develop a new semiempirical method).

6.2   The Basic Principles of SCF Semiempirical Methods

6.2.1   Preliminaries

The semiempirical methods we saw in Chap. 4 simply construct a Fock matrix and diagonalize it once to get MO energy levels and MOs (i.e. the coefficients of the basis functions that make up the MOs). The simple Hückel method Fock matrix elements are just relative energies, 0 and -1 (in $|\beta|$ units, relative to the nonbonding level α), and the extended Hückel method Fock matrix elements are calculated from ionization energies. In both the simple and extended Hückel methods a single matrix diagonalization gives the energy levels and MO coefficients. This chapter is concerned with semiempirical methods that are closer to the ab initio method in that the SCF procedure (Chap. 5, Sect. 5.2.3.6, particularly Sects. 5.2.3.6.4 and 5.2.3.6.5) is used to refine the energy levels and MO coefficients: basis set coefficients from a "guess" are improved by repeated matrix diagonalization. As in ab initio calculations each Fock matrix element is calculated from a core integral H_{rs}^{core}, density matrix elements P_{tu}, and electron repulsion integrals $(rs|tu)$, $(ru|ts)$:

$$F_{rs} = H_{rs}^{\text{core}}(1) + \sum_{t=1}^{m} \sum_{u=1}^{m} P_{tu}\left[(rs|tu) - \frac{1}{2}(ru|ts)\right] \qquad (6.1 = 5.82)$$

As stated above, the following discussion applies to semiempirical methods that, like ab initio, use the SCF procedure and so pay some service to Eq. (6.1).

To initiate the process we need an *initial guess* of the coefficients, to calculate the density matrix values P_{tu}. The guess can come from a simple Hückel calculation (for a π electron theory like the PPP method) or from an extended Hückel calculation (for an all-valence-electron theory, like CNDO and its descendants). The Fock matrix of F_{rs} elements is diagonalized repeatedly to refine energy levels and coefficients.

The semiempirical methods we consider here diverge from ab initio calculations through the use of several approximations. The basic ideas were discussed in detail by Dewar (ca. 1969) well before the currently popular AM1 (1985) and its variants appeared [7]. An excellent yet compact survey of the principles behind all the major semiempirical methods is given by Levine [8], and semiempirical methods have also been reviewed (ca. 1996) by Thiel [9]. A detailed exposition of the basic (pre-1970) theory behind these methods can be found in the book by Pople and Beveridge [10]. Clark has written (ca. 2000) a very thoughtful review going beyond purely technical details, of the "philosophy" of the semiempirical approach, its strengths and weaknesses, its past and future [11]. The divergence from the ab initio method lies in (1) treating only valence or π electrons, i.e. in the meaning of the "core", (2) the mathematical functions used to expand the MOs (the nature of the basis set functions), (3) how the core and two-electron repulsion integrals are evaluated, and (4) the treatment of the overlap matrix.

Expanding on points (1)–(4):

1. *Treating only valence or π electrons, i.e. the meaning of the "core"*. In an ab initio calculation H_{rs}^{core} is the kinetic energy of an electron moving in the force-field of the atomic nuclei, plus the potential energy of attraction of the electron to these atomic nuclei: the electron is moving under the influence of a positive core composed of atomic nuclei. Semiempirical calculations handle at most valence electrons (the PPP method handles only π electrons), so each element of the core becomes an atomic nucleus *plus its core electrons* (for the PPP method, a nucleus with the core electrons plus all σ valence electrons). Instead of a cloud of all the electrons moving in a framework of nuclei, we have a cloud of *valence* electrons (for the PPP method, π electrons) moving in a framework of atomic cores (atomic core = nuclei + all electrons not being used in the calculation). The SCF semi-empirical energy is calculated in a manner analogous to that of an ab initio calculation of the Hartree-Fock energy (cf. Eq. (5.149)), but n in Eq. (6.2) is not half the total number of electrons, but rather half the number of valence electrons (half the number of π electrons for a PPP calculation), i.e. n is the number of MOs formed from the those electrons being included in the basis set. E_{SE} is the valence electronic (π electronic for the PPP method) energy, rather than the total electronic energy, and V_{CC} is the core–core repulsion, rather than the nucleus–nucleus repulsion:

$$E_{\text{SE}}^{\text{total}} = E_{\text{SE}} + V_{\text{CC}} = \sum_{i=1}^{n} \varepsilon_i + \frac{1}{2} \sum_{r=1}^{m} \sum_{s=1}^{m} P_{rs} H_{rs}^{\text{core}} + V_{\text{CC}} \qquad (6.2)$$

Treating the core electrons in effect as part of the atomic nuclei means that we need basis functions only for the valence electrons. With a minimal basis set

(Chap. 5, Sect. 5.3.3) an ab initio calculation on ethene, C_2H_4, needs five basis functions ($1\,s$, $2\,s$, $2p_x$, $2p_y$, $2p_z$) for each carbon and one basis function ($1\,s$) for each hydrogen, a total of 14 basis functions, while a semiempirical calculation needs four functions for each carbon and one for each hydrogen, for a total of 12; for cholesterol, $C_{27}H_{46}O$, the numbers of basis functions are 186 and 158 for ab initio and semiempirical, respectively. For both molecules the semiempirical calculation needs about 85 % as many basis functions as the ab initio calculation. The semiempirical basis set advantage is small compared to a minimal basis set ab initio calculation, a kind not much used nowadays, but it is large compared to ab initio calculations with split valence and split valence plus polarization (Chap. 5, Sect. 5.3.3) basis sets. For ethene, comparing a 6 - 31G * ab initio calculation with a minimal basis semiempirical calculation, the numbers of basis functions are 38 and 12, for cholesterol, 522 and 158; the semiempirical calculation needs only about 30 % as many basis functions for both molecules. Semiempirical calculations use only a minimal basis set and hope to compensate for this by parameterization of the two-electron integrals (below).

2. *The basis set functions*. In semiempirical methods the basis functions correspond to atomic orbitals (valence AOs or $p - \pi$ AOs), while in ab initio calculations this is strictly true only for a minimal basis set, since an ab initio calculation can use many more basis functions than there are conventional AOs. Almost all the SCF-type semiempirical methods we are considering in this chapter use Slater basis functions, rather than approximating Slater functions as sums of Gaussian functions (Chap. 5, Sect. 5.3.2). Recall that the only reason ab initio calculations use Gaussian, rather than the more accurate Slater, functions, is because calculation of the electron repulsion integrals is far faster with Gaussian functions (Chap. 5, Sect. 5.3.2). In semiempirical calculations these integrals have been parameterized into the calculation (see below). Mathematical forms of the basis functions ϕ are still needed, to calculate overlap integrals $\langle\phi_r|\phi_s\rangle$, for although these methods treat the overlap matrix as a unit matrix, some overlap integrals are evaluated rather than simply being taken as 0 or 1. Approximate MO theory has some apparent logical contradictions [7]. The calculated overlap integrals are used to help calculate core integrals and electron-repulsion integrals. As in ab initio calculations linear combinations of the basis functions are used to construct MOs, which in turn are multiplied by spin functions and used to represent the total molecular wavefunction as a Slater determinant (Chap. 5, Sect. 5.2.3.1).

3. *The integrals*. The core integrals and the two-electron repulsion integrals (electron-repulsion integrals), Eq. (6.1), are not calculated from first principles (i.e. not from an explicit Hamiltonian and basis functions, as illustrated in Chap. 5, Sect. 5.2.3.6.5), but rather many integrals are taken as zero, and those that *are* used are evaluated in an empirical way from the kinds of atoms involved and their distances apart. Recall that calculation of the two-electron integrals, particularly the three- and four-center ones (those involving three or four different atoms) takes up most of the time in an ab initio calculation. The

integrals to be ignored (set equal to zero) are determined from the extent to which *differential overlap* is neglected. The differential overlap dS is the differential of the overlap integral (e.g. Sect. 4.3.3) S:

$$S = \int \phi_r(1)\phi_s(1)dv_1 \qquad (*6.3)$$

$$dS = \phi_r(1)\phi_s(1)dv_1 \qquad (*6.4)$$

Semiempirical methods differ amongst themselves in, amongst other ways, the criteria for setting $dS = 0$, i.e. for applying *zero differential overlap*, ZDO.

4. *The overlap matrix.* SCF-type semiempirical methods take the overlap matrix as a unit matrix, $\mathbf{S} = \mathbf{1}$, so $\mathbf{S}$ vanishes from the Roothaan-Hall equations $\mathbf{FC} = \mathbf{SC\varepsilon}$ without the necessity of using an orthogonalizing matrix to transform these equations into standard eigenvalue form $\mathbf{FC} = \mathbf{C\varepsilon}$ so that the Fock matrix can be diagonalized to give the MO coefficients and energy levels (Chap. 4, Sect. 4.4.1.2; Chap. 5, Sect. 5.2.3.6.5). A partial exception is the OMx methods (Sect. 6.2.5.9), where orthogonalization is applied to some integrals.

We begin our examination of specific SCF-type semiempirical methods with the simplest, the Pariser-Parr-Pople method.

6.2.2   *The Pariser-Parr-Pople (PPP) method*

The first semiempirical SCF-type method to gain widespread use was the Pariser-Parr-Pople method (1953) [12, 13]. Like the simple Hückel method, PPP calculations are limited to π electrons, with the other electrons forming a σ framework to hold the atomic p orbitals in place. The Fock matrix elements are calculated from Eq. (6.1); for a PPP calculation H_{rs}^{core} represents the nuclei plus all non-π-system electrons, P_{tu} is calculated from the coefficients of those p AOs contributing to the π system, and the two-electron repulsion integrals refer to electrons in the π system. The one-center core integrals H_{rs}^{core} are estimated empirically from the ionization energy of a *2p* AO and (see below) the two-electron integral $(rr|ss)$. The two-center core integrals H_{rs}^{core} are calculated from

$$H_{rs}^{core} = k\langle\phi_r(1)|\phi_s(1)\rangle \qquad r \neq s \qquad (6.5 = 5.82)$$

where k is an empirical parameter chosen to give the best agreement with experiment of the wavelength of UV absorption bands, and the overlap integral $\langle\phi_r|\phi_s\rangle$ is calculated from the basis functions, with the proviso that if ϕ_r and ϕ_s are on atoms that are not connected then the integral is taken as zero.

The two-electron integrals are evaluated by applying the ZDO approximation (above) to all different orbitals r and s:

$$dS = \phi_r(1)\phi_s(1)dv_1 = 0 \quad \text{for } r \neq s \qquad (6.6)$$

From Eq. (6.6) and the definition of the two-electron integral

$$(rs|tu) = \int \int \frac{\phi_r^*(1)\phi_s(1)\phi_t^*(2)\phi_u(2)}{r_{12}}dv_1dv_2 \qquad (6.7 = 5.73)$$

it follows that (1) for $r \neq s$, $(rs|tu) = 0$, and (2) for $r = s$ and $t = u$, $(rs|tu) = (rr|tt)$. Both cases are taken into account by writing

$$(rs|tu) = \delta_{rs}\delta_{tu}(rr|tt) \qquad (6.8)$$

where the δ_s are Kronecker deltas ($= 1$ if the subscripts are the same, zero otherwise). Thus the four-center (i.e. $(rs|tu)$) and three-center (i.e. $(rr|tu)$) two-electron integrals are ignored, but not the two-center (i.e. $(rr|tt)$) and one-center (i.e. $(rr|rr)$) two-electron integrals. The one-center integrals $(rr|rr)$ are taken as the difference between the valence-state ionization energy and the electron affinity of the atom bearing ϕ_r (these valence-state parameters refer to a hypothetical isolated atom in the same hybridization state as in the molecule, and can be found spectroscopically; Chap. 4, Sect. 4.4.4.1). The two-center integrals $(rr|tt)$ are estimated from $(rr|rr)$ and $(tt|tt)$ and the distance between the ϕ_r and ϕ_t atoms.

Although the overlap integrals $\langle f_r|f_s \rangle$ are actually calculated for the evaluation of H_{rs}^{core} (Eq. (6.5), the overlap matrix is taken as a unit matrix as far as the matrix Roothaan-Hall equations $\mathbf{FC} = \mathbf{SC}\boldsymbol{\varepsilon}$ go; thus $\mathbf{FC} = \mathbf{C}\boldsymbol{\varepsilon}$ or $\mathbf{F} = \mathbf{C}\boldsymbol{\varepsilon}\mathbf{C}^{-1}$ and the Fock matrix is diagonalized, without transforming it with an orthogonalizing matrix (but see the OMx methods, Sect. 6.2.5.9), to give the MO coefficients and energy levels. That the overlap matrix is a unit matrix is a corollary of the ZDO approximation of Eq. (6.6), from which it follows that the off-diagonal matrix elements are zero; the diagonal elements are of course unity if normalized AO basis functions are used. PPP energies are π electron electronic energies E_{SE}, or electronic energies plus core-core repulsions, E_{SE}^{total}, if V_{CC} is added (Eq. (6.2)).

The PPP method has been used to calculate the UV spectra of conjugated compounds, especially dyes [14], a task it performs fairly well. The accuracy of these calculations can be improved by incorporating electron correlation (Chap. 5, Sect. 5.4), using the configuration interaction (CI) method. The calculations were usually done at a fixed geometry, although an empirical bond length-bond order relation permits optimization of bond length. The classical PPP method is not much used now, having evolved into other neglect of differential overlap (NDO) methods, especially those parameterized for spectra, like INDO/S and the very successful ZINDO/S (below). We now look at a hierarchy NDO methods that, unlike the PPP approach, are not limited to planar arrays of p-orbitals, but instead permit calculations on molecules of general geometry. In order of increasing sophistication these are complete neglect of differential overlap CNDO), intermediate neglect of differential overlap (INDO), and neglect of diatomic differential overlap (NDDO).

6.2.3 The Complete Neglect of Differential Overlap (CNDO) Method

The first semiempirical SCF-type method to go beyond just π electrons was the complete neglect of differential overlap method (ca. 1966) [15]. This was a general-geometry method, since it is not limited to planar π systems (molecules with conjugated π electron systems, like benzene, are usually planar). Like the other early general-geometry method, the extended Hückel method, which appeared in 1963 (Chap. 4, Sect. 4.4), CNDO calculations use a minimal valence basis set of Slater-type orbitals, using just the valence electrons and the conventional atomic orbitals of each atom. The Fock matrix elements are calculated from Eq. (6.1); for a CNDO calculation H_{rs}^{core} represents the nuclei plus all core electrons, P_{tu} is calculated from the coefficients of the valence AOs, and the two-electron repulsion integrals refer to valence electrons. The CNDO to PPP relationship is analogous to the extended Hückel to the simple Hückel one, a main difference between the two duos being that CNDO/PPP are SCF-type methods, unlike EH/SH.

There are two versions of CNDO, CNDO/1 and an improved version, CNDO/2. First look at CNDO/1. Consider the core integrals $H_{r_A r_A}^{\text{core}}$, where both orbitals are the same (i.e. the same orbital occurs twice in the integral $\langle\phi_r(1)|\hat{H}_{rr}^{\text{core}}|\phi_r(1)\rangle$) and are on the same atom A. Recall the example of an ab initio calculation on HHe$^+$ (Chap. 5, Sect. 5.2.3.6.5). Consider, say, element (1,1) of that $\mathbf{H}^{\text{core}}$ matrix. From Eq. 5.116:

$$\begin{aligned}
H_{11}^{\text{core}} &= \langle\phi_1(1)|\hat{T}|\phi_1(1)\rangle + \langle\phi_1(1)|\hat{V}_H|\phi_1(1)\rangle + \langle\phi_1(1)|\hat{V}_{\text{He}}|\phi_1(1)\rangle \\
&= \langle\phi_1(1)|\hat{T} + \hat{V}_H|\phi_1(1)\rangle + \langle\phi_1(1)|\hat{V}_{\text{He}}|\phi_1(1)\rangle
\end{aligned} \tag{6.9}$$

Equation (6.9) can be generalized to a matrix element (r,r) and a molecule with atoms A, B, etc. . . ., giving

$$\begin{aligned}
H_{r_A r_A}^{\text{core}} &= \langle\phi_{r_A}(1)|\hat{T} + \hat{V}_A|\phi_{r_A}(1)\rangle + \langle\phi_{r_A}(1)|\hat{V}_B|\phi_{r_A}(1)\rangle \\
&\quad + \langle\phi_{r_A}(1)|\hat{V}_C|\phi_{r_A}(1)\rangle + \cdots \\
&= U_{rr} + \sum_{B \neq A}\langle\phi_{r_A}(1)|\hat{V}_B|\phi_{r_A}(1)\rangle = U_{rr} + V_{AB}
\end{aligned} \tag{6.10}$$

where ϕ_{r_A} is a basis function on atom A. The U_{rr} term in Eq. (6.10) is regarded as the energy of an electron in the AO on A corresponding to the function ϕ_{r_A}, and is taken as the negative of the valence-state ionization energy of such an electron. The integrals in the V_{AB} term are simply calculated as the potential energy of a valence s orbital in the electrostatic field of the core of atom A, B, etc., e.g.

$$\langle\phi_{r_A}(1)|\hat{V}_B|\phi_{r_A}(1)\rangle = \left\langle S_A(1)\left|\frac{C_B}{r_{1B}}\right|S_A(1)\right\rangle \tag{6.11}$$

where C_B is the charge on the core of atom B, i.e. the atomic number minus the number of core (non-valence) electrons, and the variable r_{1B} is the distance of the $2s$ electron from the center of the core (from the atomic nucleus). The core integrals

with different orbitals ϕ_r and ϕ_s, on the same atom (A = B; one-center integrals) or on different atoms are taken as being proportional to the overlap integral of the relevant orbitals:

$$H_{rAsB}^{core} = \beta_{AB} \langle \phi_r(1)|\phi_s(1) \rangle \qquad r \neq s \qquad (6.12)$$

The overlap integral here is calculated from the basis functions, although (as for the PPP method, above) the overlap matrix is simply taken as a unit matrix as far as the matrix Roothaan-Hall equations are concerned. The proportionality constant β_{AB} is taken as the arithmetic mean of parameters for atoms A and B, these parameters being those that give the best fit of CNDO MO coefficients to those of minimal-basis-set ab initio calculations. Since different AOs on the same atom are orthogonal, when A = B these integrals are zero. Note that calculating β_{AB} from a best-fit to minimal-basis-set ab initio calculations means that CNDO parameterization is not purely empirical, but rather to some extent attempts to match (low-level) ab initio results. This is a weakness of CNDO and a *potential* weakness of its successors INDO and NDDO (below). As repeatedly emphasized by Dewar, this deficiency was avoided in his methods (Sect. 6.2.5.1) by consistently parameterizing to match *experiment*.

As with the PPP method, the two-electron repulsion integrals are evaluated by applying the ZDO approximation to all different orbitals r and s (Eq. (6.6)). Thus the two-electron integrals reduce to $(rs|tu) = \delta_{rs}\delta_{tu}(rr|tt)$ (Eq. (6.8), i.e. only one- and two-center two-electron integrals are considered. All one-center integrals on the same atom A are given the same value, γ_{AA}, and all two-center integrals between atoms A and B are given the same value, γ_{AB}. These integrals are calculated from valence s Slater functions on A and B.

CNDO/2 differs from CNDO/1 in two modifications to the H_{rArA}^{core} matrix elements (Eq. (7.0)): (1) to account better for both ionization energy and electron affinity, U_{rr} is evaluated not just from ionization energy but as a kind of average of ionization energy and electron affinity, and (2) the integrals in the V_{AB} term are calculated from the two-electron integrals γ_{AB}, as $V_{AB} = -C_B\gamma_{AB}$. This latter evaluation amounts to neglecting so-called *penetration integrals*; these integrals make nonbonded atoms attract one another, and cause bond lengths to be too short and bond energies to be too large [15–18]. CNDO energies are valence electron electronic energies E_{SE}, or electronic energies plus core-core repulsions, E_{SE}^{total}, if V_{CC} is added (Eq. (6.2)). CNDO is now obsolete, having served its purpose as a precursor to the more effective general-geometry methods INDO and NDDO (below).

6.2.4 The Intermediate Neglect of Differential Overlap (INDO) Method

INDO [19] goes beyond CNDO by curtailing the application of the ZDO approximation. Instead of applying it to all different ($r \neq s$) atomic orbitals in the two-electron integrals (Eq. (6.6)), as in the PPP and CNDO methods, in INDO

ZDO is not applied to those one-center two-electron integrals, $(rs|tu)$, with ϕ_r, ϕ_s, ϕ_t, and ϕ_u all on the same atom; obviously, these repulsion integrals should be the most important. Although more accurate than CNDO, INDO is nowadays used mostly only for calculating UV spectra, in specially parameterized versions called INDO/S and ZINDO/S (S denoting spectra), which give good UV-spectral predictions for a variety of compounds [20].

6.2.5   The Neglect of Diatomic Differential Overlap (NDDO) Methods

NDDO [21] goes beyond INDO in that the ZDO approximation (Sect. 6.2.1, point (3)) is not applied to orbitals on the same atom, i.e. ZDO is used only for atomic orbitals on different atoms. NDDO is the basis of the currently popular semiempirical methods developed by M. J. S. Dewar and by coworkers who took up the torch: MNDO, AM1 and PM3 (as well as SAM1, PM5, PM6 and PM7). NDDO methods are the gold standard in general-purpose semiempirical methods, and the rest of this chapter concentrates on them.

6.2.5.1   NDDO-Based Methods from the Dewar Group: MNDO, AM1, PM3 and SAM1, and Related Methods–Preliminaries

SCF-type (see Sect. 6.1) semiempirical theories are based to a large extent on the approximate molecular orbital theory (see the book of this title [10]) developed by Pople and coworkers. The Pople school, however, went on to concentrate on the development of ab initio methods, and indeed it is for his contributions to these, which are largely encapsulated in the Gaussian series of programs [22], that Pople was awarded the 1998 Nobel Prize in chemistry [23] (shared with Walter Kohn, a pioneer in density functional theory; see Chap. 7). In contrast, Dewar pursued the semiempirical approach almost exclusively [24], taking to heart his stricture "The answer lies in abandoning attempts to carry out rigorous a priori calculations" (quoted in Perspective near the start of this chapter). He continued till the end of his career to stoutly maintain that at least as far as molecules of real chemical interest go his semiempirical methods were superior to ab initio ones ("There is clearly little point in using a procedure that requires thousands of times more computing time than ours do if it is no better than ours, let alone one that is inferior.") [25]. The rivalry between the Dewar school and the adherents of the ab initio approach began relatively early in the development of Dewar methods (see e.g. [26–28]), intensified to actual polemic [29], and is passionately described from an unabashedly partisan viewpoint in Dewar's autobiography [24]. The ab initio *vs.* Dewar semiempirical controversy was largely rooted in a difference of viewpoints and in a focus by Dewar on the inability of ab initio calculations to give reasonably accurate absolute molecular energies (an absolute molecular energy is the energy needed to dissociate a molecule into its nuclei and electrons, infinitely separated

and at rest; for this discussion it may be taken as the atomization energy). In the absence of error cancellation, errors in absolute energies lead to errors in activation and reaction energies, and the errors in absolute energies were, ca. 1970, commonly in the region of a 1000 kJ mol^{-1}. Cancellation (actually not as untrustworthy as Dewar thought–Chap. 5, Sect. 5.5.2.1) could not, he held, be relied on to provide chemically useful relative energies (reaction and activation energies), say with errors of no more than a few tens of kilojoules per mole. The exchange with Halgren, Kleir and Lipscomb nicely illustrates the viewpoint difference [28]: one side held that even when inaccurate, ab initio calculations can teach us something fundamental, while semiempirical calculations, no matter how good, do not contribute to fundamental theory. Dewar focussed on the study of reactions of "real" chemical interest. Toward the end of his career as an active chemist, he coauthored a review of pericyclic reactions such as the Cope and Diels-Alder processes, defending the results of AM1 (below) studies [30]. The divergence of these conclusions from those of other workers engendered a rebuke from Houk and Li, [31]. Interestingly, most of the high-accuracy multistep "ab initio" methods that in recent years have achieved chemical accuracy (Chap. 5, Sect. 5.5.2.3.2), considered to be about 10 kJ mol^{-1} or better, employ some empirical parameters (an exception is W2), a fact that would have amused Dewar.

   In contrast to the viewpoint of the ab initio school, Dewar regarded the semiempirical method not merely as an approximation to ab initio calculations, but rather as an approach that, carefully parameterized, could give results far superior to those from ab initio calculations, at least for the foreseeable future: "The situation [ca. 1992] could be changed only by a huge increase in the speed of computers, larger than anything likely to be attained before the end of the century, or by the development of some fundamentally better ab initio approach." [32]. The conscious decision to strive for experimental accuracy rather than merely to reproduce low-level ab initio results (note the remarks in connection with Eq. (6.12)) was clearly stated several times [27, 29, 33] in the course of the development of these semiempirical methods: "We set out to parametrize [semiempirical methods] in an entirely different manner, to reproduce the results of experiment rather than those of dubious *ab initio* calculations." [33]. Of the several experimental parameters that the Dewar methods are designed to reproduce, probably the two most important are geometry and heat of formation. As with ab initio calculations, optimized geometries are found by an algorithm which uses first and second derivatives of energy with respect to geometric parameters to locate stationary points (Chap. 2, Sect. 2.4). The method of finding heats of formation is described below.

6.2.5.2   Enthalpies of Formation (Heats of Formation) from Semiempirical Electronic Energies

As with ab initio calculations, SCF-type semiempirical calculations *initially* find electronic energies E_{SE}, using Eq. (6.2), but the energy finally reported is commonly the enthalpy of formation. For this the procedure encoded in the methods is the following [34]. Inclusion of the core-core repulsion V_{CC}, which is necessary for geometry optimization, gives the total semiempirical energy E_{SE}^{total}, which could be

expressed in atomic units (hartrees), as in an ab initio calculation (e.g. Chap. 5, Sect. 5.2.3.6.4). This energy E_{SE}^{total}, the total internal energy of the molecule except for zero point vibrational energy, is used to calculate the heat of formation (enthalpy of formation) of the molecule. Fig. 6.1 will help to make it clear how this is done. The quantities in Fig. 6.1 are

1. $\Delta H_{f298}^{\ominus}(M)$, the 298 K heat of formation of the molecule M, i.e. the heat energy needed to make M from its elements. This is the quantity we want.

2. The atomization energy of M, which is the energy of the atoms minus the energy of M. The energy of the atoms is $F \sum E_{SE}(A_i)$; the conversion factor F converts $E_{SE}(A_i)$, the energy per atom in hartrees, into the same units, kJ mol^{-1} or kcal mol^{-1}, as is used for the experimental heats of formation of the atoms; F is 2625.5 kJ mol^{-1} per hartree atom^{-1} (or molecule^{-1}). The energy of the molecule M is $F\, E_{SE}^{total}$ (M), the optimized geometry being used. The same semiempirical method is used to calculate atomic and molecular energies, both of which are negative quantities, the energy of the species relative to electrons and one or more atomic cores infinitely separated. $E_{SE}(A_i)$ is purely electronic, since an atom has no core-core repulsion (i.e. it has no atoms to separate), while the molecular energy E_{SE}^{total} (M) includes core-core repulsion.

3. $\sum \Delta H_{f298}^{\ominus}(A_i)$ the sum, over all the atoms A of M, of the experimental 298 K heats of formation of these atoms.

Equating the two paths from the elements in their standard states at 298 K to atoms we get

$$\Delta H_{f298}^{\ominus}(M) = \sum \Delta H_{f298}^{\ominus}(A_i) - F \sum E_{SE}(A_i) + FE_{SE}^{total}(M) \tag{6.13}$$
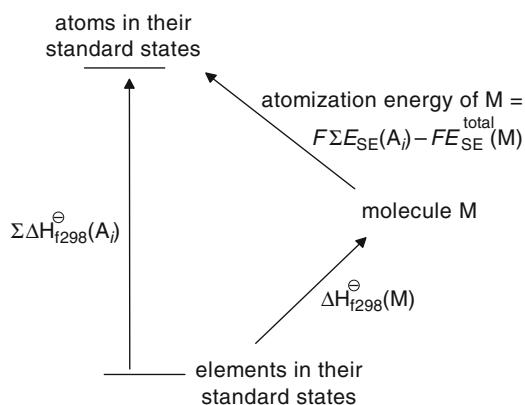
Fig. 6.1 The principle behind the semiempirical calculation of heat of formation (enthalpy of formation). The molecule is (conceptually) atomized at 298 K; the elements in their standard states are also used to make these atoms, and to make the molecule M. The heat of formation of M at 298 K follows (with some approximations) from equating the energy needed to generate the atoms via M to that needed to make them directly from the elements

Thus the desired quantity, the heat of formation of the molecule, can be calculated from the experimental heats of formation of the atoms and the semiempirical energies of the atoms and the molecule. The calculation using Eq. (6.13) is automatically done by the program using stored values for atomic heats of formation and semiempirical atomic energies, and the "freshly calculated" calculated molecular energy, and one may never see E_{SE}^{total} (M). These calculations are for the gas phase, and if one wants the heat of formation of a liquid or a solid, then the experimental heat of vaporization or sublimation must be taken into account. Note that this procedure is conceptually almost the same as the atomization method for ab initio calculation of heats of formation (Chap. 5, Sect. 5.5.2.3.3). However, the purpose here is to obtain the heat of formation at room temperature (298 K) from the molecular "total semiempirical energy", the electronic energy plus core-core repulsion; in the ab initio atomization method the 0 K heat of formation is calculated with the aid of the molecular energy including ZPE (the 0 K heat of formation can be corrected to 298 K – see Sect. 5.5.2.3.3). The semiempirical procedure for enthalpy of formation involves some approximations. The ZPE of the molecule is not used (so a frequency calculation is not needed for this), and the increase in thermal energy from 0 to 298 K is not calculated. The good news is that $E_{SE}^{total}(M)$ is parameterized (below) to reproduce $\Delta H_{f298}^{\ominus}(M)$; to the extent that this parameterization succeeds the neglect of ZPE and of the 0–298 K increase in thermal energy are overcome, and electron correlation is also implicitly taken into account. The key to obtaining reasonably accurate heats of formation from these methods is thus their parameterization to give the values of $E_{SE}^{total}(A_i)$ and E_{SE}^{total} (M) used in Eq. (6.13). This parameterization, which is designed to also give reasonable geometries, dipole moments and ionization energies, is discussed below.

6.2.5.3   MINDO

The first (1967) of the Dewar-type methods was PNDDO [35], partial NDDO), but because further development of the NDDO approach turned out to be "unexpectedly formidable" [33], Dewar's group temporarily turned to INDO, creating MINDO/1 [36] (modified INDO, model 1). The third version of this method, MINDO/3, was said [33] "[to have] so far survived every test without serious failure", and it became the first widely-used Dewar-type method. Keeping their promise to return to NDDO the group soon came up with MNDO, modified NDDO, the first of their NDDO methods. MINDO/3 was made essentially obsolete by MNDO, except perhaps for the study of carbocations (Clark has summarized the strengths and weaknesses of MINDO/3, and the early work on MNDO [37]). MNDO (and MNDOC and MNDO/d, C and d for correlation and *d*-orbitals) and its descendants, the very popular AM1 and PM3, are discussed below. Briefly mentioned are modifications of AM1 and PM3 and successors to PM3, up to PM7.

6.2.5.4   MNDO

MNDO [37], a modified NDDO (Sect. 6.2.5) method, was reported in 1977 [38]. MNDO is conveniently explained by reference to CNDO (Sect. 6.2.3). MNDO is a general geometry method with a minimal valence basis set of Slater-type orbitals. The Fock matrix elements are calculated using Eq. (6.1=5.82). We discuss the core and two-electron integrals in the same order as for CNDO.

The core integrals $H_{r\text{A}r\text{A}}^{\text{core}}$, with the same orbital ϕ_r twice on the same atom A are calculated using Eq. (6.10). Unlike the case in CNDO, where U_{rr} is found from ionization energies (CNDO/1) or ionization energies and electron affinities (CNDO/2), in MNDO U_{rr} is one of the parameters to be adjusted. The integrals in the summation term V_{AB} are evaluated similarly to the CNDO/2 method from a two-electron integral (see below) involving $\phi_{r\text{A}}$ and the valence s orbital on atom B:

$$\langle \phi_{r\text{A}}(1)|\hat{V}_{\text{B}}|\phi_{r\text{A}}(1)\rangle = -C_{\text{B}}(\phi_r\phi_r|s_{\text{B}}s_{\text{B}}) \tag{6.14}$$

The core integrals $H_{r\text{A}s\text{A}}^{\text{core}}$ with different orbitals ϕ_r and ϕ_s, on the same atom A are not simply taken as being proportional to the overlap integral, as in CNDO (Eq. (6.12)), but rather are also (like the case of both orbitals on the same atom) evaluated from Eq. (6.10), which in this case becomes

$$\begin{aligned}
H_{r\text{A}s\text{A}}^{\text{core}} &= \langle \phi_{r\text{A}}(1)|\hat{T} + \hat{V}_{\text{A}}|\phi_{s\text{A}}(1)\rangle + \langle \phi_{r\text{A}}(1)|\hat{V}_{\text{B}}|\phi_{s\text{A}}(1)\rangle \\
&\quad + \langle \phi_{r\text{A}}(1)|\hat{V}_{\text{C}}|\phi_{s\text{A}}(1)\rangle + \cdots \\
&= U_{rs} + \sum_{\text{B}\neq\text{A}} \langle \phi_{r\text{A}}(1)|\hat{V}_{\text{B}}|\phi_{s\text{A}}(1)\rangle
\end{aligned} \tag{6.15}$$

The first term is zero from symmetry [39]. Each integral of the summation term is again evaluated, as in CNDO/2, from a two-electron integral:

$$\langle \phi_{r\text{A}}(1)|\hat{V}_{\text{B}}|\phi_{s\text{A}}(1)\rangle = -C_{\text{B}}(\phi_{r\text{A}}\phi_{s\text{A}}|s_{\text{B}}s_{\text{B}}) \tag{6.16}$$

The core integrals $H_{r\text{A}s\text{B}}^{\text{core}}$ with different orbitals ϕ_r and ϕ_s, on different atoms A and B are taken, as in CNDO (cf. Eq. (6.12)), to be proportional to the overlap integral between ϕ_r and ϕ_s, where again the proportionality constant is the arithmetic mean of parameters for atoms A and B:

$$H_{r\text{A}s E}^{\text{core}} = \frac{1}{2}(\beta_{r\text{A}} + \beta_{s\text{B}})\langle \phi_r(1)|\phi_s(1)\rangle \qquad r \neq s \tag{6.17}$$

The overlap integral is calculated from the basis functions although the overlap matrix is taken as a unit matrix as far as the Roothaan-Hall equations go (Sect. 6.2.2). These core integrals are sometimes called core resonance integrals.

The two-electron integrals are evaluated applying ZDO (Sect. 6.2.1) within the framework of the NDDO approximation (Sect. 6.2.5). As with the PPP (Sect. 6.2.2) and CNDO (Sect. 6.2.3) methods, this makes all two-electron integrals become $(rs|tu) = \delta_{rs}\delta_{tu}(rr|tt)$, i.e only one- and two-center two-electron integrals are non-zero. The one-center integrals are evaluated from valence-state ionization energies. The two-center integrals are evaluated from the one-center integrals and the separation of the nuclei by an involved procedure in which the integrals are expanded as sums of multipole-multipole interactions [38a, 40] that make the two-center integrals show correct limiting behavior at zero and infinite separation.

As in CNDO, in MNDO the penetration integrals are neglected (Sect. 6.2.3, CNDO/2). A consequence of this is that the core-core repulsions (V_{CC} in Eq. (6.2)) cannot be realistically calculated simply as the sum of pairs of classical electrostatic interactions between point charges centered on the nuclei. Instead, Dewar and coworkers chose [38a] the expression

$$V_{CC} = \sum_{B>A}\sum_{A} [C_A C_B (s_A s_B | s_B s_B) + f(R_{AB})] \tag{6.18}$$

where C_A and C_B are the core charges of atoms A and B and s_A and s_B are the valence s orbitals on A and B (the two-electron integral in Eq. (6.18) is actually approximately proportional to $1/R_{AB}$, so there is some connection with the simple electrostatic model). The $f(R_{AB})$ term is a correction increment to make the result come out better; it depends on the core charges and the valence s functions on A and B, their separation R, and empirical parameters α_A and α_B:

$$f(R_{AB}) = C_A C_B (s_A s_A | s_B s_B)\left(e^{-\alpha_A R_{AB}} + e^{-\alpha_B R_{AB}}\right) \tag{6.19}$$

The above mathematical treatment constitutes the creation of the *form* of the semiempirical equations. To actually use these equations, they must be parameterized somehow (as stressed above, Dewar used experimental data). This is analogous to the situation in molecular mechanics (Chap. 3), where a force field, defined by the form of the functions used (e.g. a quadratic function of the amount by which a bond is stretched, for the bond-stretch energy term) is constructed, and must then be parameterized by inserting specific quantities for the parameters (e.g. values for the stretching force constants of various bonds). For each kind of atom A (a maximum of) six parameters is needed:

1. the kinetic-energy-containing term U_{rr} of Eq. (6.10) (as explained above, this CNDO equation is also used in MNDO to evaluate H_{rArA}^{core} where ϕ_{rA} is a valence s AO.
2. the term U_{rr} of Eq. (6.10) where ϕ_{rA} is a valence p AO.
3. the parameter ζ in the exponent of the Slater function (e.g Sect. 5.3.2, Fig. 5.12) for the various valence AOs (MNDO uses the same ζ for the s and p AOs).

4. the parameter β (Eq. (6.17)) for a valence s AO.
5. the parameter β for a valence p AO.
6. the parameter α in the correction increment ($f(R_{AB})$, (Eq. (6.19))) to the core-core repulsion (Eq. (6.18)).

Some atoms have five parameters because for them MNDO takes β to be the same for s and p orbitals, and hydrogen has four parameters because MNDO does not assign it p orbitals.

We want the parameters that will give the best results, for a wide range of molecules. What we mean by "results" depends on the molecular characteristics of most interest to us. MNDO (and its siblings AM1 and PM3, below) was parameterized [38a] to reproduce heat of formation, geometry, dipole moment, and the first vertical ionization energy (from Koopmans' theorem; Chap. 5, Sect. 5.5.5.3). To parameterize MNDO a training set of molecules (a "molecular basis set" is Dewar's term – no connection with a basis set of functions used to construct molecular orbitals) of small, common molecules (e.g. methane, benzene, dinitrogen, water, methanol; 34 molecules were used for the C, H, O, N set) was chosen and the six parameters above (U_{rr} etc.) were adjusted in an attempt to give the best values of the four molecular characteristics (heat of formation, geometry, dipole moment, ionization energy). Specifically, the objective was to minimize Y, the sum of the weighted squares of the deviations from experiment of the four molecular characteristics:

$$Y = \sum_{i=1}^{N} W_i \big[Y_i(\text{calc}) - Y_i(\text{exp}) \big]^2 \qquad (16.20)$$

N is the number of molecules in the training set, and W_i is a weighting factor chosen to determine the relative importance of each characteristic Y_i. The actual process of assigning values to the parameters is formally analogous to the problem of geometry optimization (Chap. 2, Sect. 2.4). In geometry optimization we want the set of atomic coordinates that correspond to a minimum (sometimes to a transition state) on a potential energy hypersurface. In parameterizing a semiempirical method we want the set of parameters that correspond to the minimum overall calculated deviation of the chosen characteristics from their experimental values–the parameters that give the minimum Y, above. Details of the parameterization process for MNDO have been given by Dewar [38a] and by Stewart [41].

The results of MNDO calculations on 138 compounds limited to the elements C, H, O, N were reported by Dewar and Thiel [38b]. The absolute mean errors were: in heat of formation, 26 kJ mol^{-1} for all 138 compounds; in geometry, 0.014 Å for bond lengths for 228 bonds, 2° for angles at C for acyclics (less for cyclic molecules); in dipole moment, 0.30 D for 57 compounds; in ionization energy, 0.48 eV for 51 compounds. To put the errors in perspective, typical values of these quantities are, respectively, roughly -600 to 600 kJ mol^{-1}, 1.0–1.5 Å, 0–3 D, and 10–15 eV. Although MNDO can reproduce these and other properties of a wide variety of molecules [37, 42], it is little-used nowadays, having been largely superseded by AM1 and, perhaps to a somewhat lesser extent, PM3 (below).

Variations on the basic MNDO are MNDO/d and MNDOC, both developed by the research group of Thiel. MNDO/d has d functions added to the minimal-basis valence s and p functions, in an attempt to solve one of the most persistent problems of semiempirical methods, that of obtaining good results for compounds traditionally believed to utilize d orbitals, including "hypervalent" compounds [43]. Although the term hypervalent is not unambiguous, *hypercoordinate* being perhaps preferable, and the role of d orbitals here is controversial [44], parameterization with d functions is a pragmatic approach to finding a semiempirical method that works. MNDO/d was applied to "normal" molecules and, more to the point, compounds of metals like magnesium, zinc, cadmium and mercury, and some hypercoordinate molecules. MNDO/d was said to give "significant improvements over established semiempirical methods, especially for hypervalent compounds'" [43a]. The particularly difficult task of parameterizing MNDO for transition metal compounds does not appear to have been ever satisfactorily solved. The application of MNDO and related methods to such compounds has been reviewed [45].

MNDOC denotes MNDO with configuration interaction (CI; Chap. 5, Sect. 5.4.3) [46]. This may seem odd, since MNDO (and the related AM1 and PM3, ..., PM6) are parameterized to match experiment, and should therefore "automatically" include electron correlation (Chap. 5, Sect. 5.4.1), which configuration interaction is designed to handle. However, the parameterization uses compounds (ground-electronic state species), not transition states and excited states, and electron correlation changes on going from a ground state to a transition or excited state. In a transition state this is because of a loosening of bonds, akin to the effect discussed in connection with homolytic bond cleavage (Chap. 5, Sect. 5.4.1), and in an excited state there is of course a dramatic altering of the electron arrangement. A perfect parameterization based on compounds would therefore give perfect properties, such as heats of formation and geometries, for ground-state molecules only. Specific inclusion of CI in MNDO is designed to improve the modeling of transition states and excited states, and MNDOC was said, compared to MNDO, to be "superior for [transition states]" [46b] and to warrant "cautious applications...to photochemical problems" [46c]. In other studies involving transition states, MNDOC was said to outperform MNDO and compare reasonably well with ab initio calculations [47]. Augmenting an experimental study in which matrix-isolated dimethyloxirene was said to be have been observed, Bachmann et al. performed MNDOC calculations to estimate the barriers for the ring-opening of some oxirenes to the oxo carbenes ("ketocarbenes") [48]:
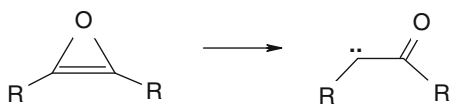
They obtained these barriers (kJ mol^{-1}/kcal mol^{-1}): oxirene (R = H, 24/5.8); dimethyloxirene (R = CH_3, 31/7.3); di-*t*-butyloxirene (R = $t - C_4H_9$, 56/13.5); cyclohexyne oxide (R, R = $CH_2CH_2CH_2CH_2$, 0/0); benzyne oxide (R, R = CHCHCHCH, 67/16). The ordering of energies may well be correct, but MNDOC seems to

considerably exaggerate the barriers (assuming high-level ab initio calculations are correct here!). High-level calculations are available for oxirene and dimethyloxirene. For oxirene, these gave a barrier of merely $1 - 4\,\mathrm{kJ\,mol^{-1}}$ [49] and $3\,\mathrm{kJ\ mol^{-1}}$ [50]; in this later case the carbene is not a stationary point and the barrier is for direct rearrangement of oxirene to ketene ($H_2C=C=O$) with hydrogen migration. For dimethyloxirene there do not appear to be high-level results for the actual barrier, but based on a not-fully-optimized transition state a barrier of about $11\,\mathrm{kJ\ mol^{-1}}$ was estimated [50], and a "periodic scan" (R=H, BH_2, CH_3, NH_2, OH, F) by Fowler et al. showed only dimethyloxirene to be clearly stabilized by the substituents [51]. The oxirene problem has been reviewed [52]; it is one that does not yield readily to even high-level probing (see particularly [53]), and thus constitutes a quite rigorous test for a semiempirical method. Curiously, more than two decades after its development, it was said that MNDOC "has not yet been compared to other NDDO methods to the degree necessary to evaluate whether the formalism lives up to [its] potential" [54]. This may be because MNDOC (and MNDO/d) were not widely available, unlike MNDO, AM1 and PM3, which have long been included in popular "multimethod" (molecular mechanics, semiempirical, ab initio and DFT) program suites like Gaussian [55] and Spartan [56]. MNDOC and MNDO/d are included in the AMPAC [57], and MNDO/d in the very widely-used MOPAC [58] two specifically semiempirical suites.

6.2.5.5 AM1

AM1 (Austin method 1, developed at the University of Texas at Austin [59]) was introduced by Dewar, Zoebisch, Healy and Stewart in 1985 [60]. AM1 is an improved version of MNDO in which the main change is that the core-core repulsions (Eq. (6.18)) were modified to overcome the tendency of MNDO to overestimate repulsions between atoms separated by about their van der Waals distances (the other change is that the parameter ζ in the exponent of the Slater function – see parameter 3 in the list of the six parameters above – need not be the same for s and p AOs on the same atom). The core-core repulsions were modified by introducing attractive and repulsive Gaussian functions centered at internuclear points [61], and the method was then re-parameterized. The great difficulties experienced in the parameterization of AM1 and its predecessors are emphasized by Dewar and coworkers in many places, e.g.: "All our work has therefore been based on a very laborious purely empirical technique…" for the MINDO methods [33]; parameterization is a "purely empirical affair" and "needs infinite patience and enormous amounts of computer time" for AM1 [60]. In his autobiography Dewar says [62] "This success [of these methods] is no accident and it has not been obtained easily" and summarizes the problems with parameterizing these methods: (1) the parametric functions are of unknown form, (2) the choice of molecules for the training set affects the parameters to some extent, (3) the parameters are not unique, there is no way to tell if the set of values found is the best one, and there is

no systematic way to find alternative sets, (4) deciding if a set of parameters is acceptable is a matter of judgment. Dewar et al. chose to call their modified MNDO method AM1, rather than MNDO/2, because they felt that their methods were being confused (presumably because of the "INDO" and "NDO" components of the appellations) with "grossly inaccurate" [60] ZDO SCF semiempirical methods like CNDO and INDO.

Dewar et al. reported [60] that AM1 calculations on compounds containing nitrogen and/or oxygen gave an absolute mean error in heats of formation of 25 kJ mol^{-1} for 80 compounds, "generally satisfactory" agreement with experiment for the geometries of 138 molecules, absolute mean error in dipole moment of 0.26 D for 46 compounds, and absolute mean error in ionization energy of 0.40 eV for 29 compounds. These results are slightly better than those for MNDO, but the real advantages of AM1 over MNDO were said [60] to lie in its better treatment of crowded molecules, four-membered rings, activation energies, and hydrogen bonding. Nevertheless, misrepresentations of hydrogen bonding remain a problem with AM1 [63]. AM1 and PM3 (below) are probably still the most widely-used semiempirical methods, and are available in practically all commercial program suites which have not made a point of being strictly devoted to some other method(s) than semiempirical ones.

A fairly recent reparameterization of AM1, called RM1 (for Recife, a city in Brazil where three of the four authors work; by analogy with Austin method 1) is said to be better than AM1 and PM3 and to be "at least very competitive" with PM5 (PM3, PM5 and PM6: see below) [64]. RM1 keeps "the mathematical structure and qualities of AM1, while significantly improving its quantitative accuracy with the help of today's computers and also of the more advanced techniques available for nonlinear optimization." RM1 can be implemented in AM1 software without changing the code, other than altering the parameters. For 1736 species considered in the parameterization some average errors were:

Heat of formation ($\text{kJ mol}^{-1}/\text{kcal mol}^{-1}$):
AM1 47/11.15, PM3 33/7.98, PM5 25/6.03, RM1 24/5.77

Bond length (Å):
AM1 0.036, PM3 0.029, PM5 0.037, RM1 0.027

Bond angle (degrees):
AM1 5.88, PM3 6.98, PM5 9.83, RM1 6.82

The impetus behind RM1 was to make calculations on big biomolecules more accurate. RM1 is available in Spartan '06 [56] and later versions and in AMPAC 9.0 [57] and MOPAC2009 [58] and later versions of these.

Another variation of AM1 is AM1/d. This is similar in structure to MNDO/d; d functions appear to have been first introduced into AM1 to parameterize it for molybdenum [65], and other parameterizations seem to have been done on an as-needed basis, e.g. for magnesium [66] and for phosphoryl transfer reactions [67]. AM1/d was available in an early version of MOPAC [58], WinMOPAC v.2.0 (reported in a study of the reaction of ethene with oxygen atoms on a silver surface) [68], and in MOPAC2000 [58] but it is unclear if any current commercial program

suite carries it. AM1/d was modified and parameterized for P, S and Cl to give a variant called AM1 * [69].

6.2.5.6   PM3 and Extensions (PM3(tm), PM5, PM6 and PM7)

PM3, parametric method 3, is a variation of AM1 differing mainly in how the parameterization is done. There were no explicit PM1 and PM2 because the developer (below) considered the first two viable parameterized methods of this type to be MNDO and AM1. When PM3 was first published [41], those two parameterizations of MNDO-type methods had been carried out, and PM3 was at first called MNDO-PM3, meaning MNDO parametric method 3. Three papers [41, 70, 71] define the PM3 method. The Dewar school's approach to parameterization was a painstaking one (see e.g. Sect. 6.2.5.5, "infinite patience"), making liberal use of chemical intuition. The developer of PM3, J. J. P. Stewart, employed a faster, more algorithmic approach, "several orders of magnitude faster than those previously employed." [41]. Although it is based on AM1, PM3 did not enjoy Dewar's blessing. The reasons for this appear to be at least twofold: (1) Dewar felt (on the basis of very early results [72]) that PM3 represented at best an only marginal improvement over AM1, and that a new semiempirical method should make previous ones essentially obsolete, as MNDO made MINDO/3 obsolete, and AM1 largely replaced MNDO. Stewart defended his approach [73] with the rejoinder, *inter alia*, that if PM3 was only a marginal improvement over AM1, then AM1 was only a marginal improvement over MNDO. (2) Dewar objected strongly to any proliferation of computational chemistry methods, whether it be in the realm of ab initio basis sets [74] or of semiempirical methods [72, 74].

For compounds containing H, C, N, O, F, Cl, Br, and I, Holder *et al.* reported [75] that PM3 calculations gave an absolute mean error in heat of formation of 22 kJ mol^{-1} for 408 compounds (cf. 27 kJ mol^{-1} for AM1), and Dewar *et al.* reported an absolute mean error in bond lengths of 0.022 Å for 344 bonds (cf. 0.027 for AM1), 2.8° for 146 angles (cf. 2.3° for AM1) [76], and 0.40 D for 196 compounds (cf. 0.35 D for AM1) [76].

PM3(tm) is a version (1996, 1997) parameterized with d orbitals for geometries, but not for heats of formation, dipole moments, or ionization energies, for transition metals [77]. It was evaluated ca. 2000 by Bosque and Maseras [78], who also briefly mentioned 11 earlier (1996–1999) publications testing this method. The consensus seems to be that the method tends to be good for geometries but not for energies, and that "its reliability has to be proved on a case by case basis" [78]. There have since been many published tests of PM3/tm, a few of which are given in reference [79].

The designation PM4 is said to have been reserved for "a separate, collaborative parameterization effort" [80], and the results of this do not appear to have been published. PM5 was an improvement of PM3 that appeared in MOPAC2002 [58]. An idea of the accuracy of PM5 compared to MNDO, AM1, and PM3 is given by this information on errors in the MOPAC2002 manual [81] (I converted kcal mol^{-1} to kJ mol^{-1}):

	MNDO	AM1	PM3	PM5
Heat of formation	77	50	42	$25 \, \text{kJ mol}^{-1}$
Bond length	0.066	0.053	0.065	$0.051 \, \text{Å}$
Bond angle	6.298	5.467	5.708	$5.413°$

In mid 2009 the latest version of the PMx series was PM6, which Stewart described in detail in a long paper [82]; in this paper, which also gives a brief history of NDDO methods, it was explicitly said that PM4 and PM5 were "unpublished", presumably meaning that the details of their parameterization had not been revealed. PM6 is available in Gaussian 09 [55], Spartan'14, AMPAC 10 [57], and MOPAC 12 (MOPAC2012) [58]. It appears to be a significant improvement over PM3 and AM1 and will likely be the standard general-purpose semiempirical method for some years, except in those program suites which retain PM3 and AM1 without introducing a later PM version. A brief summary of the performance of PM6, from the MOPAC2009 brochure [83] (much more detail is given in [82], mainly for the parameterization for heats of formation) indicates that this method:

1. Was parameterized with data from over 9000 compounds; experimental *and* ab initio data were used, so unlike earlier NDDO methods (MNDO, AM1, PM3; ca. 1975–1990) the parameterization is not purely empirical). Only about 500 compounds were used for PM3.
2. Gives better heats of formation (from tests on 1373 compounds) than those from B3LYP/6‑31G* (a DFT method), PM3, HF/6‑31G*, and AM1: the average unsigned errors for PM6 and those four methods were 20.0 (PM6), 21.7, 26.2, 30.8, and $41.9 \, \text{kJ mol}^{-1}$. Using a version of NDDO specially parameterized just for heats of formation and somewhat more accurate for this purpose than PM6 (average unsigned errors 16.1 vs. $20.0 \, \text{kJ mol}^{-1}$), several errors were identified in a survey of ca. 1300 compounds in the NIST Chemistry WebBook database [84].
3. Treats hydrogen bonds better than PM3 and AM1.
4. Is parameterized for all main group and transition elements.

Some other information on the accuracy of PM6 is available from the MOPAC2009 manual [85]:

	PM6	PM3	AM1
Bond length	0.091	0.104	$0.130 \, \text{Å}$
Bond angle	7.86	8.50	$8.77°$
Dipole moment	0.85	0.72	0.67 Debye
Ionization energy	0.50	0.68	0.63 eV

As of the beginning of 2015 the latest version of the PMx series is PM7, which was presented in 2012 in MOPAC 12 (http://openmopac.net/MOPAC2012brochure.pdf); its salient features are outlined in that website. Details of PM7 are soberly given in a 2013 paper [86] which focusses on comparing it with PM6; it seems to be a modest improvement.

PM3 and MNDO have been modified by further parameterizing their core-core repulsion functions with another parameterized function, called the pairwise distance directed Gaussian function (PDDG function), giving PDDG/PM3 and PDDG/MNDO, with the aim of improving the calculated heats of formation without causing significant changes in geometries, ionization energies and dipole moments [87]. The parameterization for C, H, N, O compounds gave a reduction in mean absolute errors for heats of formation of from 18.4 to 13.4 kJ mol^{-1} for PDDG/PM3 cf. PM3 and from 35.1 to 21.8 kJ mol^{-1} for PDDG/MNDO cf. MNDO [87a]. Parameterization for halogen-containing compounds gave significant heats of formation improvement over reparameterized (with the same training set) PM3 and MNDO, called PM3′ and MNDO′, and considerable improvement over PM3, MNDO and AM1 [87b]. Among the semiempirical methods investigated, PDDG/PM3 gave the best agreement with ab initio G2 and CCSD(T) calculations of activation energy for S_N2 reactions of methyl halides with halogen anions [87b]. PDDG parameterization was extended to compounds with S, Si and P. For 1480 neutrals, ions and complexes with H, C, N, O, F, Si, P, S, Cl, Br, and I the mean absolute errors in heats of formation were (kJ mol^{-1}) 27.2 (PDDG/PM3), 36.4 (PM3), 43.1 (MNDO/d), 45.2 (AM1), and 82.8 (MNDO) [87c].

6.2.5.7   SAM1 and SCC-DFTB

SAM1 (semi ab initio method number 1) was the last semiempirical method to be reported (1993, [76]) by Dewar's group. SAM1 is essentially a modification of AM1 in which the two-electron integrals are calculated ab initio using contracted Gaussians (an STO-3G basis set) as in standard ab initio calculations (Chap. 5, Sect. 5.3.2). This is in contrast to AM1, where the two-center two-electron integrals are calculated from the one-center two-electron integrals, which are estimated spectroscopically. As Holder and Evleth point out in a brief but lucid outline of the basis of AM1 and SAM1 [88], a key distinguishing feature of each semi-empirical method is how it calculates the two-electron repulsion integrals. Since the NDDO approximation discards all the three- and four-center two-electron integrals, the number of two-electron integrals to be calculated is greatly reduced. This, and the limitation to valence electrons, makes SAM1 only about twice as slow as AM1 [88].

One of the main reasons for developing SAM1 was to improve the treatment of hydrogen bonding (this was also a primary reason for developing AM1 from MNDO; evidently success there was only limited [63]). SAM1 is indeed an improvement over AM1 in this respect, and "appears to be the first semiempirical parameterization to handle a wide variety of [hydrogen bonded] systems correctly."; in fact, it was said that "The results from SAM1 for virtually every system has improved over AM1 and PM3, fulfilling the criteria for SAM1 to be a reasonable successor to AM1 and PM3 for general purpose semiempirical calculations" [88]. An extensive list of experimental heats of formation compared with those

calculated by SAM1, AM1 and PM3 has been published [75]. Actually, despite its apparent generally significant superiority over AM1, there have been relatively few publications using SAM1. This is probably because the program is at present available only in the commercial semiempirical package AMPAC [57], and because the latest "PMX", the fully semiempirical PM6, appears to be so powerful. That the parameterization of SAM1 has not been fully disclosed in the open literature may also play a role–researchers are perhaps uncomfortable about using a set of black box techniques.

The melding of semiempirical methods with some ab initio computation seen in SAM1 has an analogue in the intrusion of density functional theory (DFT, Chap. 7) into the semiempirical sphere: the self-consistent-charge density functional tight-binding (SCC-DFTB) method of Elstner [89]. In SAM1 ab initio calculations are used only to calculate the two-electron integrals; in SCC-DFTB, in keeping with the ethos of DFT, the wavefunction has been replaced by the electron density function. The semiempirical methods mentioned previously were *wavefunction* methods: the simple and extended Hückel (Chap. 4), and the SCF semiempirical methods of this chapter, all use a wavefunction created by diagonalizing a Fock matrix to give the coefficients of chosen basis functions; these weighted basis functions in linear combination are molecular orbital wavefunctions which arrayed in one or more Slater determinants comprise the total atomic or molecular wavefunction (Chaps 4 and 5). In contrast, density function theory is based on the electron density function, a conceptually simple function of the variation of electron density with position in space. Although DFT does not demand a wavefunction, current practical DFT methods use a wavefunction of hypothetical noninteracting electrons to calculate the electron density function, which is then transformed into a molecular energy with aid of a mathematical recipe called a functional (Chap. 7). Tight-binding refers to a variation of the LCAO method that was developed for treating extended solids in solid-state physics; for a detailed review see Goringe et al. [90]. The SCC-DFTB method is an application to molecules of a method that was used (ca. 2000) in the physics of solids and clusters. It is derived from standard DFT "by neglect, approximation, and parametrization of interaction integrals" [89]. The impetus behind its development was the study of large biomolecules, and its speed is said to be comparable to that of other semiempirical methods.

6.2.5.8   Polarized Molecular Orbital Model, PMO; Dispersion Effects

This is a fairly recent NDDO method, initially (2011) used for only H, O molecules but now extended to include also at least C, N, S [91a]. The PMO2 version is said to be "especially accurate for polarizabilities, atomization energies, proton transfer energies, noncovalent complexation energies, and chemical reaction barrier heights, and to have good across-the-board accuracy for a range of other properties, including dipole moments, partial atomic charges, and molecular geometries" [91b]. The PMO method includes an optional explicit empirical dispersion term; explicit recognition of dispersion is a feature lacking in most semiempirical

programs (it has been introduced into AM1 and PM3, giving AM1-D and PM3-D, see references in [91b]). Some molecular mechanics forcefields were found to be more accurate than semiempirical methods for dispersion in the case of the benzene dimer [91c]. For references to dispersion in ab initio and in DFT, see Chap. 5, Sect. 5.4.3.3, at end of discussion of BSSE, and Chap. 7, Sect. 7.2.3.4.8. As of mid-2015 the use of the PMO semiempirical method may have been confined to the Truhlar group.

6.2.5.9   OMx, Orthogonalization Method x (x = 1, 2, 3)

These NDDO methods are variations of MNDO in which orthogonalization has been applied, not straightforwardly to the whole Fock matrix as in the extended Hückel method and ab initio methods (Chap. 4, Sect. 4.4.1; Chap. 5, Sect. 5.2.3.6.2), but instead in a more involved way, only to certain integrals of the Fock matrix; the way these "orthogonalization corrections" are applied distinguishes among OM1, OM2, and OM3 [92a]. Also, unlike MNDO and most other semiempirical SCF methods, the OMx methods use Gaussian rather than Slater orbitals. Although the OMx methods are not new, going back to 1993–2003 [92a], there seems to have been more recently (ca. 2011) a renewed interest in testing their accuracy: an extensive benchmarking study found them, especially OM2 and OM3, to significantly outperform AM1, PM6, and SCC-DFTB. OM2 and OM3 compared well with DFT (Chap. 7) [92b]. As of 2014 these methods appear to have been parameterized only for H, C, N, O, F.

6.2.5.9.1   General Comments on NDDO Methods

The general-purpose (not limited to π-electrons) methods presented in this Sect. (6.2.5) are all variations on the theme of Dewar's first reasonably successful NDDO method, MINDO/3 (SCC-DFTB, above, as a DFT rather than a wave-function method, lies outside this group). MINDO/3 was made obsolete by MNDO and MNDO was largely replaced by AM1, which today competes with PM3 (and PM6 and PM7). The variants of Dewar-type methods in use today, to a greater or lesser extent, are MNDO, MNDO/d, MNDOC, AM1, RM1, PM3, PM6, PM7, PDDG/PM3, and SAM1. Here is the availability of general-purpose semiempirical methods in four widely-used program suites, as of December 2015:

AMPAC 10   MNDO/3, MNDO, MNDO/d, MNDOC, AM1, RM1, PM3, PM6, SAM1

    See Semichem, Inc.

Gaussian 09   Extended Hückel, CNDO/2, INDO, ZINDO, MINDO/3, MNDO, AM1, PM3, PM3MM (optional molecular mechanics amide correction), PM6, PDDG/PM3, DFTB (original Elstner et al.), DFTBA (modified DFTB).

See Gaussian, Inc.

MOPAC 12   MNDO, AM1, RM1, PM3, PM6, PM7, PM7-TS (for transition states), MOZYME. J. J. P. Stewart informed the author[2] "MNDOD is included in MOPAC2012, and in all earlier versions after MNDOD was published" under the keyword MNDOD, and now (2015 November 19) MNDO/d; "MNDOC was never in any copy of MOPAC. This was my choice. MNDOC is theoretically a more correct formulation than any of the other NDDO methods, in that it included correlation, via C.I.. However in practice it was much slower and offered no significant advantage. For this reason, I decided not to put it in MOPAC".

See Stewart Computational Chemistry – MOPAC Home page.

Spartan '14   MNDO, MNDO/d, AM1, RM1, PM3, PM6

See Wavefunction, Inc.

If this seems, ironically, like a chaotic proliferation, the charge Dewar levelled against what he saw as the wild growth of ab initio basis sets (Chap. 5, Sect. 5.3.3, Which basis Set Should I Use?) the situation is somewhat ameliorated by the fact that the currently very widely used methods are possibly only AM1, PM3, PM6 and PM7 (this does not mean that for some purposes others may not be better).

6.3   Applications of Semiempirical Methods

A good, brief overview of the performance of AM1, PM3, and related semiempirical methods as of ca. 2014 is given by Levine [93]. Hehre has compiled a very useful book comparing AM1 with molecular mechanics (Chap. 3), ab initio (Chap. 5) and DFT (Chap. 7) "practical strategies" for calculating geometries and other properties [94], and an extensive collection of AM1 and PM3 geometries is to be found in Stewart's second PM3 paper [70].

6.3.1   Geometries

Many of the general remarks on molecular geometries in Chap. 5, Sect. 5.5.1, preceding the discussion of results of specifically ab initio calculations, apply also to semiempirical calculations. Geometry optimizations of large biomolecules like proteins and nucleic acids, which a few years ago were limited to molecular

---

[2]J. J. P. Stewart, personal communication, 2015 November 19.

mechanics, can now be done routinely [95a] with semiempirical methods on inexpensive personal computers with the program MOZYME (a program in the suite of semiempirical programs MOPAC), which uses localized orbitals to solve the SCF equations [95b]. Localized orbitals speed up the Roothaan-Hall SCF process (Chap. 5, Sect. 5.2.3.6.2) because with these more compact (compared to the dispersed canonical orbitals; Chap. 5, Sect. 5.2.3.1) fewer long-range basis function interactions need be considered. Clearly, this saving in "outreach" is especially important in a very big molecule.

Let's compare AM1, PM3, and MP2(fc)/6-31G* (Chap. 5, Sect. 5.4.2) and experimental geometries; the MP2(fc)/6-31G* method is a reasonably high-level ab initio method that is routinely used. Fig. 6.2 gives bond lengths and angles calculated by these three methods and experimental [96] bond lengths and angles, for the same 20 molecules as in Chap. 5, Fig. 5.23. The geometries shown in Fig. 6.2 are analyzed in Table 6.1, and Table 6.2 provides information on dihedral angles for the same eight molecules as in Chap. 5, Table 5.8. Fig. 6.2 corresponds to Fig. 5.23, Table 6.1 to Table 5.7, and Table 6.2 to Table 5.8.

This survey suggests that: AM1 and PM3 give quite good geometries (although dihedral angles, below, sometimes show quite significant errors): bond lengths are mostly within 0.02 Å of experimental (although the AM1 C–S bonds are about 0.06 Å too short), and angles are usually within 3° of experimental (the worst case is the AM1 HOF angle, which is 7.1° too big).

Of AM1 and PM3, neither has a clear advantage over the other in predicting geometry, although PM3 C–H and C–X (X=O, N, F, Cl, S) bond lengths appear to be more accurate than AM1. MP2 geometries are considerably better than AM1 and PM3, but HF/3-21G$^{(*)}$ and HF/6-31G* (basis sets: Chap. 5, Sect. 5.3.3) geometries (Chap. 5, Fig. 5.23 and Table 5.7) are only moderately better.

AM1 and PM3 C-H bond lengths are almost always (AM1) or tend to be (PM3) longer than experimental, by ca. 0.004–0.025 (AM1) or ca. 0.002 Å (PM3). AM1 O–H bonds tend to be slightly longer (up to 0.016 Å) and PM3 O–H bonds to be somewhat shorter (up to 0.028 Å) than experimental.

Both AM1 and PM3 consistently underestimate C–C bond lengths (by about 0.02 Å).

C–X (X=O, N, F, Cl, S) bond lengths appear to be consistently neither over- nor underestimated by AM1, while PM3 tends to underestimate them; as stated above, the PM3 lengths seem to be the more accurate (mean errors 0.013 Å vs. 0.028 Å for AM1). Both AM1 and PM3 give quite good bond angles (largest error ca. 4°, except for HOF for which the AM1 error is 7.1°).

AM1 tends to overestimate dihedrals (10 + , 0−), while PM3 may do so to a lesser extent (7 + , 3−). PM3 breaks down for HOOH (calculated 180°, experimental 119.1°, and does poorly for FCH$_2$CH$_2$F (calculated 57°, experimental 73°). Omitting the case of HOOH, the mean dihedral angle errors for AM1 and PM3 are 5° and 4.5°.; however, the variation here is from 1° to 11° for AM1 and from −1° to −16° for PM3 (although not wildly out of line with the AM1, PM3 or MP2 calculations, the reported experimental ClCH$_2$CH$_2$OH HOCC dihedral of 58.4° is suspect; see Chap. 5, Sect. 5.5.1).
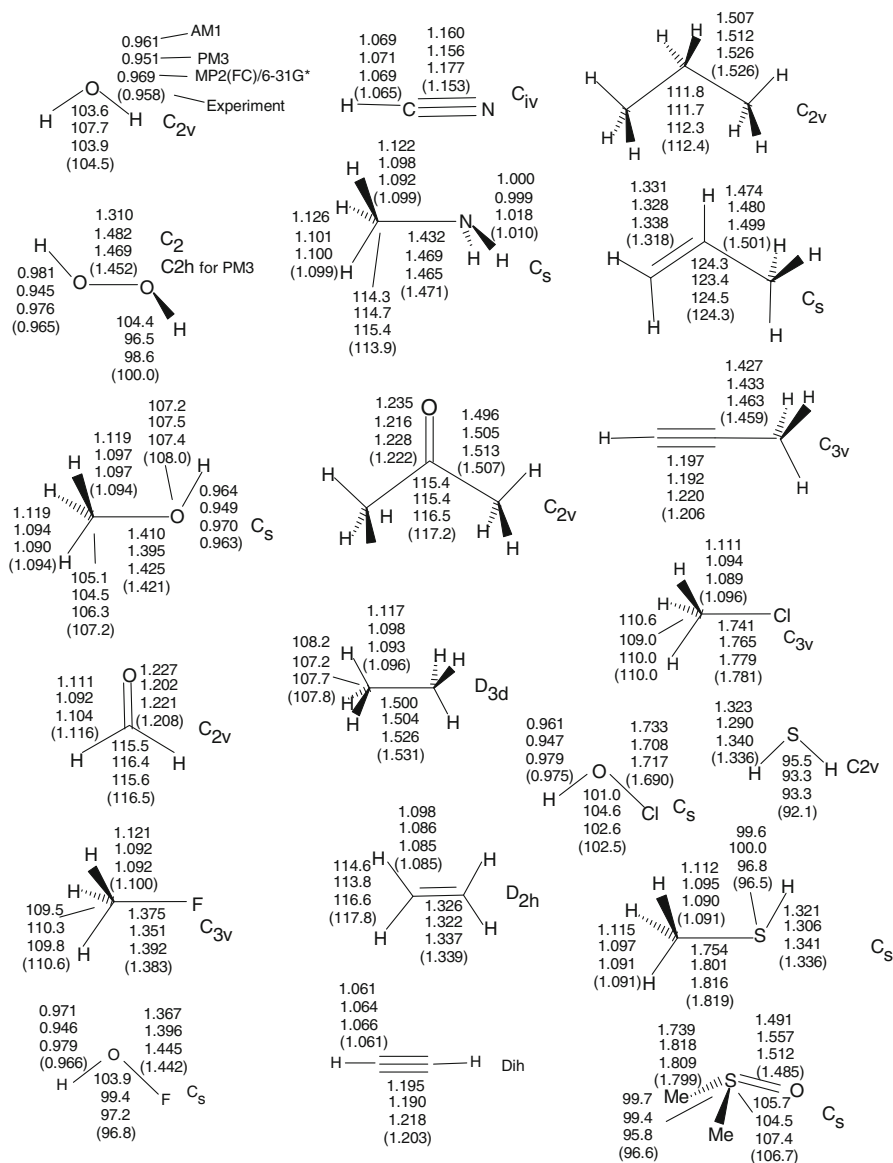
Fig. 6.2 A comparison of some AM1, PM3, MP2(fc)/6–31G* and experimental geometries. Calculations are by the author and experimental geometries are from reference [96]. Note that all CH bonds are ca. 1 Å, all other bonds range from ca. 1.2–1.8 Å, and all bond angles (except for linear molecules) are ca. 90°–120°

The accuracy of AM1 and PM3 then, is quite good for bond lengths and angles, but fairly approximate for dihedrals. The largest error (Table 6.1) in bond lengths is 0.065 Å (AM1 for MeSH) and in bond angles 7.1° (AM1 for HOF). The largest

Table 6.1 Errors in AM1, PM3, and MP2(fc)/6-31G* bond lengths and angles, from Fig. 6.2

Bond length errors, $r-r_{exp}$, Å				Bond angle errors, $a-a_{exp}$, degrees
C–H	O–H, N–H, S–H	C–C	C–O, N, F, Cl, S	
MeOH 0.025/0.000/−0.004 0.025/0.003/ 0.003	H₂O 0.003/−0.007/0.011	Me₂CO −0.011/−0.002/0.006	MeOH 0.001/−0.014/0.007	H₂O (HOH) −0.9/3.2/−0.6
HCHO −0.005/−0.024/−0.012	H₂O₂ 0.016/−0.020/0.011	CH₃CH₃ −0.031/−0.027/−0.005	HCHO 0.019/−0.006/0.013	H₂O₂ (HOO) 4.4/−3.5/−1.4
MeF 0.021/−0.008/−0.008	MeOH 0.001/−0.014/0.007	CH₂CH₂ −0.013/−0.017/−0.002	MeF −0.008/−0.032/0.009	MeOH (HCO) −2.2/−2.7/−0.9 (COH) −0.2/−0.5/−0.6
HCN 0.004/0.006/0.004	HOF 0.005/−0.020/0.013	HCCH −0.008/−0.013/0.015	HCN 0.007/0.003/0.024	HCHO (HCH) −1.0/−0.1/−0.9
MeNH₂ 0.021/0.002/0.001 0.023/−0.001/−0.007	MeNH₂ −0.010/−0.011/0.008	CH₃CH₂CH₃ −0.019/−0.014/0.000	MeNH₂ −0.039/−0.002/−0.006	MeF (HCH) −1.1/−0.3/−0.8
CH₃CH₃ 0.021/0.002/−0.003	HOCl −0.014/−0.028/0.004	CH₂CHCH₃ −0.027/−0.021/−0.002 0.013/0.010/0.020	Me₂CO 0.013/−0.006/0.006	HOF (HOF) 7.1/2.6/0.4
CH₂CH₂ 0.013/0.001/0.000	H₂S −0.013/−0.046/0.004	HCCCH₃ −0.032/−0.026/0.004 −0.009/−0.014/0.014	MeCl −0.040/−0.016/−0.002	MeNH₂ (HCN) 0.4/0.8/1.5
CHCH 0.000/0.003/0.005	MeSH −0.015/−0.030/0.005		MeSH −0.065/−0.018/−0.003	Me₂CO (CCC) −1.8/−1.8/−0.8
MeCl 0.015/−0.002/−0.007			Me₂SO −0.060/0.019/0.010	CH₃CH₃ (HCH) 0.4/−0.6/−0.1
MeSH 0.024/0.006/0.000				CH₂CH₂ (HCH) −3.2/−4.0/−1.2

0.021/0.004/−0.001				CH₃CH₂CH₃ (CCC)
				−0.6/−0.7/−0.1
				CH₂CHCH₃ (CCC)
				0.0/−0.9/0.2
				MeCl (HCH)
				0.6/−1.0/0.0
				H₂S (HSH)
				3.4/1.2/1.2
				MeSH (CSH)
				3.1/3.5/0.3
				Me2SO (CSC)
				3.1/2.8/−0.8 (CSO)
				−1.0/−2.2/0.7
12+, 1−, none 0	4+, 4−, none 0	1+/ 8−, none 0	4+, 5−, none 0	8+, 9−, one 0
8+, 4−, one 0	0+, 8−, none 0	1+, 8−, none 0	2+, 7−, none 0	6+, 12−, none 0
4+, 7−, two 0	8+, 0−, none 0	5+, 3−, one 0	6+, 3−, none 0	6+, 11−, one 0
Mean of 13: 0.017/0.005/ 0.004	Mean of 8: 0.010/0.022/ 0.008	Mean of 9: 0.018/0.016/ 0.008	Mean of 9: 0.028/0.013/ 0.009	Mean of 18: 1.9/1.8/0.7

Errors are given as AM1/PM3/MP2. In some cases (e.g. MeOH) errors for two bonds are given, on one line and on the line below. A minus sign means that the calculated value is less than the experimental. The numbers of positive, negative, and zero deviations from experiment are summarized at the bottom of each column. The averages at the bottom of each column are arithmetic means of the absolute values of the errors

Table 6.2 AM1, PM3, MP2(fc)/6-31G* and experimental dihedral angles (degrees)

Molecule	Dihedral Angles				
	AM1	PM3	MP2/6-31G*	Exp.	Errors
HOOH	128	180	121.3	119.1[a]	9/61(*sic*)/2.2
FOOF	89	90	85.8	87.5[b]	1.5/2.5/−1.7
FCH$_2$CH$_2$F (FCCF)	81	57	69	73[b]	8/−16/−4
FCH$_2$CH$_2$OH (FCCO)	65	66	60.1	64.0[c]	1/2/−3.9
(HOCC)	58	62	54.1	54.6[c]	3/7/−0.5
ClCH$_2$CH$_2$OH (ClCCO)	74	65	65.0	63.2[b]	11/2/1.8
(HOCC)	62	59	64.3	58.4[b]	4/1/5.9
ClCH$_2$CH$_2$F (ClCCF)	79	61	65.9	68[b]	11/−7/−2.1
HSSH	99	93	90.4	90.6[a]	8/2/−0.2
FSSF	89	87	88.9	87.9[b]	1/−1/1.0
					Deviations: 10+, 0−/7+, 3−/4+, 6− mean of 10: 6/10/2.3; mean of 9, omitting 9/61/2.2 errors: 5/4.5/1.9

Errors are given in the *Errors* column as AM1/PM3/MP2/6-31G*. A minus sign means that the calculated value is less than the experimental. The numbers of positive and negative deviations from experiment and the average errors (arithmetic means of the absolute values of the errors) are summarized at the bottom of the *Errors* column. Calculations are by the author; references to experimental measurements are given for each measurement. The AM1 and PM3 dihedrals vary by a fraction of a degree depending on the input dihedral. Some molecules have calculated minima at other dihedrals in addition to those given here, e.g. FCH$_2$CH$_2$F at FCCF 180°

[a] W. J. Hehre, L. Radom, p. v. R. Schleyer, J. A. Pople, "Ab initio molecular orbital theory", Wiley, New York, 1986, pp 151, 152

[b] M. D. Harmony, V. W. Laurie, R. L. Kuczkowski, R. H. Schwenderman, D. A. Ramsay, F. J. Lovas, W. H. Lafferty, A. G. Makai, "Molecular structures of gas-phase polyatomic molecules determined by spectroscopic methods", J. Physical and Chemical Reference Data, 1979, *8*, 619–721

[c] J. Huang and K. Hedberg, J. Am. Chem. Soc., 1989, *111*, 6909

error in dihedrals (Table 6.2), omitting the PM3 result for HOOH, is 16° (PM3 for FCH$_2$CH$_2$F).

From Fig. 6.2 and Table 6.1, the mean error in 39 (13 + 8 + 9 + 9) bond lengths is ca. 0.01 − 0.03 Å for the AM1 and PM3 methods, with PM3 being somewhat better except for O-H and O-S. The mean error in 18 bond angles is ca. 2° for both AM1 and PM3. From Table 6.2, the mean dihedral angle error for 9 dihedrals for AM1 and PM3 (omitting the case of HOOH, where PM3 simply fails) is ca. 5°; if we include HOOH, the mean errors for AM1 and PM3 are 6° and 10°, respectively.

Schröder and Thiel have compared MNDO (Sect. 6.2.5.4) and MNDOC (Sect. 6.2.5.4) with ab initio calculations for the study of the geometries and energies of 47 transition states [47]. AM1 and PM3 calculations should give somewhat better results than MNDO for these systems, since these two methods are essentially improved versions of MNDO. The general impression is that the

semiempirical and ab initio transition states are qualitatively similar in most cases, with MNDOC geometries being sometimes a bit better. The semiempirical and ab initio geometries were in most cases fairly similar, so that as far as geometry goes one would draw the same qualitative conclusions.

Semiempirical and ab initio geometries are compared further in Fig. 6.3, which presents results for four reactions, the same as for the ab initio calculations summarized in Fig. 5.21. As expected from the results of Fig. 6.2, the semiempirical
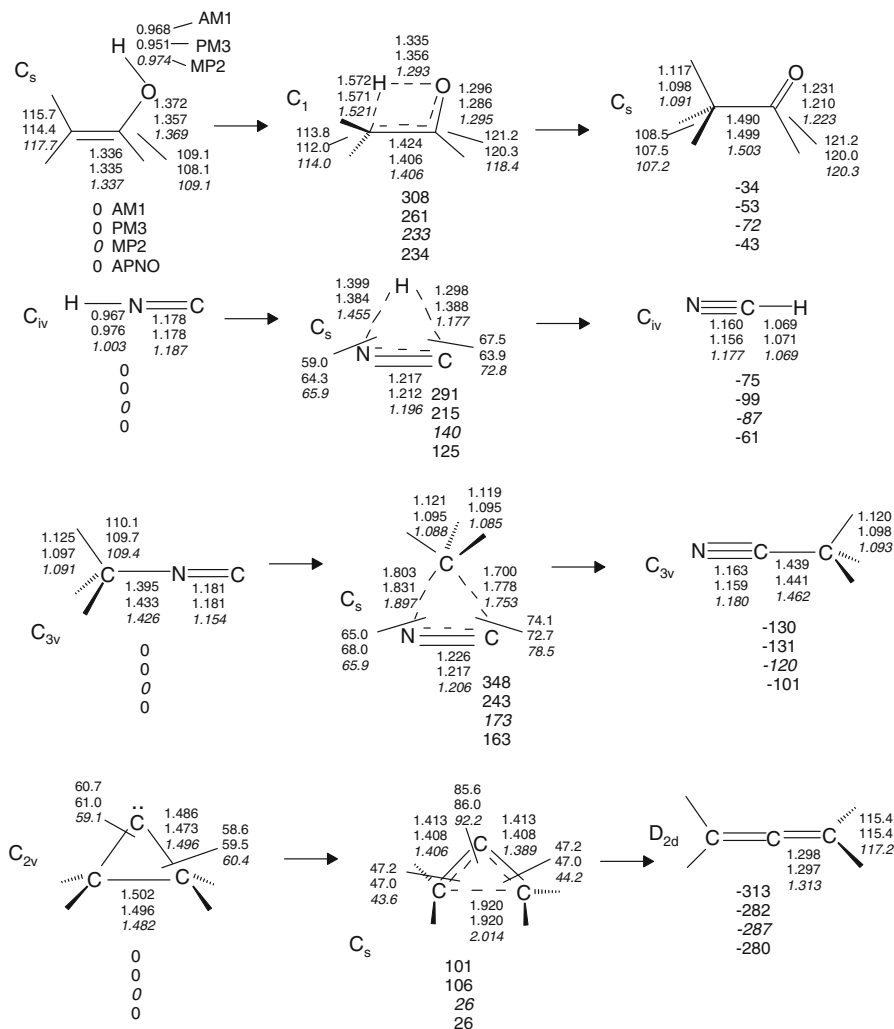
Fig. 6.3 Geometries (Å, degrees) and relative energies (kJ mol⁻¹) for four reactions, the same as for the ab initio calculations of Chap. 5, Fig. 5.21; most Hs are omitted, for clarity. In Fig. 5.21, raw energies in hartrees and ZPEs are given. The APNO enthalpies (see text) are considered to be good surrogates for the somewhat skimpy and approximate experimental values [97]

geometries of the reactants and products (energy minima) are quite good, taking the MP2/6-31G* results as our standard. The semiempirical transition state geometries, however, also seem to be surprisingly good: with only small differences between the AM1 and PM3 results, in all four cases the semiempirical transition states resemble the ab initio ones so closely that qualitative conclusions based on geometry would be the same whether drawn from the AM1 or PM3, or from the MP2/6-31G* calculations. The largest bond length error (if we accept the MP2 geometries as accurate) is about 0.09 Å (for the CH_3NC transition state, 1.897–1.803), and the largest angle error is 9° (for the HNC transition state, $72.8° − 63.9°$; most of the angle errors are less than 3°).

These results, together with those of Schröder and Thiel [47], indicate that semiempirical geometries are usually quite good, even for transition states. Exceptions might be expected for hypervalent compounds, and for unusual structures like the C_2H_5 cation; for the latter AM1 and PM3 predict the classical CH_3CH_2 structure, but MP2/6-31G* calculations predict this species to have a hydrogen-bridged structure (Chap. 5, Fig. 5.17). Semiempirical energies are considered in Sect. 6.3.2.

6.3.2   Energies

6.3.2.1   Energies: Preliminaries

As with ab initio (Chap. 5) and molecular mechanics (Chap. 4) calculations, the molecular parameters usually sought from semiempirical calculations are geometries (preceding section) and relative energies. As explained (Sect. 6.2.5.2), SCF-type semiempirical methods, AM1 and PM3 and their variations (and the DFT-type SCC-DFTB), give standard (room temperature, 298 K) enthalpies (heats) of formation. It is enthalpies that are meant in this chapter in reference to semiempirical energies, enthalpies of formation, reaction or activation, depending on the context. This is in distinct contrast to ab initio calculations, which give (the negative of) the energy for total dissociation of the molecule into nuclei and electrons, starting from a hypothetical zero-vibrational energy state or from the 0 K state with ZPE included (Chap. 5, Sect. 5.5.2.2). Ab initio methods *can* be made to provide heats of formation, by slightly roundabout methods (Chap. 5, Sect. 5.5.2.3.3). Semiempirical energies are addressed in Figs. 6.3 and 6.4, and Tables 6.3, 6.4 and 6.5. Table 6.3 compares with experiment calculated enthalpies of formation for the 20 compounds used to test geometries in Fig. 6.2; although the accuracy of semiempirical methods for energies has been tested for much larger sample sizes (Sect. 6.3.2.2), this table and the errors summarized there nevertheless convey the flavor of the accuracy that may be expected from these five methods.

Figure 6.3, which was discussed above in connection with geometries, also gives the relative energies for the reaction profiles (reactant, transition state, product) of four reactions, for AM1, PM3, ab initio MP2/6-31G*, and from experiment [97].

Relative E, kJ

transition
states

400 —

AM1 348
RM1 320

300 —
— AM1 308   PM6 304   PM6 292
— exp 282   AM1 291
— PM3 261   RM1 287
— RM1 243   PDDG 252
— MP2 233   PM3 243
            PDDG 228   PM3 215
PM6 219   PDDG 206
                                                                              ___PM6 138
                                                          MP2 173   ___PDDG 114
                              MP2 140   exp 161   — PM3 106
200 —   exp 129   — AM1 101
                                                                                RM1 95
      H   C:
        O   reaction
100 —   N=C
                    reaction   H—N=C   C   C
                               reaction   reaction   — MP2 26
                                                                              ⁓ exp 13-20
0 —
          PM6 −21
          AM1 −34, RM1 −35   RM1 −50 PM6 −56
          PDDG −39   exp −58   −101 RM1
          exp −42   PDDG −69   exp −98
          PM3 −53   AM1 −75   −104 PM6
MP2 −72   −112 PDDG
−100 —   PM3 −99   MP2 −87   MP2 −120
                                                  AM1 −130
                                                  PM3 −131

−200 —
                                                              PDDG −239
                                                                      PM6 −249
                                              PM3 −282
                                              RM1 −285
−300 —   MP2 −287   exp −293

                              products   AM1 −314

−400 —

Fig. 6.4 Relative energies (kJ mol^{-1}) for the four reactions of Fig. 6.3. Compared to the reactants (the four species shown), the transition state energies are all positive and the product energies all negative

The relative energies in Fig. 6.4 are based on the data in Table 6.4, which also gives the semiempirical "raw data" (enthalpies of formation); Table 6.4 and Fig. 6.4 augment the AM1 and PM3 values of Fig. 6.3 with those from RM1, PDDG/PM3, and PM6. The APNO energies of Fig. 6.3 and Table 6.4 are relative enthalpies from the very high-accuracy CBS-APNO method (Chap. 5, Sect. 5.5.2.3.2, *Comparison of high-accuracy multistep methods*) and should serve as good surrogates for the

Table 6.3 Enthalpies of formation (kJ mol^{-1}) of the 20 compounds in Fig. 6.2, from the five semiempirical methods used to study reaction profiles (Table 6.4)

Compound	AM1	RM1	PM3	PDDG	PM6	Exp.
H_2O	−248	−242	−224	−221	−227	−241.8
HOOH	−148	−155	−171	−171	−100	−136.1
HOF	−94.5	−78.2	−122	−121	−72.6	−98.3
HOCl	−91.0	−87.6	−144	−70.7	−74.4	−74.5
H_2S	5.0	8.7	−3.8	4.9	−7.1	−20.6
CH_3SH	−18.2	−24.8	−23.1	−22.0	−14.1	−22.8
Me_2SO	−165	−173	−162	−163	−137	−150.5
CH_3F	−255	−221	−225	−220	−224	−234.3
CH_3Cl	−79.3	−78.9	−61.4	−70.2	−63.0	−83.7
CH_3OH	−239	−210	−217	−205	−202	−205.
HCHO	−132	−124	−154	−126	−86.5	−115.9
Me_2CO	−206	−221	−223	−234	−228	−218.5
HCN	130	128	138	112	139	135.1
Me_2NH_2	−30.9	−17.7	−21.7	−30.1	−10.1	−23.5
CH_3CH_3	−72.9	−73.3	−75.9	−78.9	−66.1	−84.
$CH_3CH_2CH_3$	−102	−94.6	−98.8	−101	−87.6	−104.7
H_2CCH_2	68.9	61.7	69.6	60.9	65.9	52.5
$CH_3CH=CH_2$	27.5	32.7	26.8	19.4	23.8	20.4
HCCH	229	194	212	199	238	226.7
CH_3CCH	182	159	168	172	190	185.4

Experimental values are from the NIST website; when errors were given these were < 2 kJ mol^{-1}, except for CH3OH ($\pm 10.$ kJ mol^{-1})

Average absolute error/maximum error (molecule), kJ mol^{-1}: AM1 10.9/33.6 (CH$_3$OH); RM1 10.6/32.4 (HCCH); PM3 16.8/38.5 (HCHO); PDDG 12.7/35.2 (HOOH); PM6 13.5/35.9 (HOOH)

sketchy experimental information for these four reactions [97]. See too Chap. 7, Sect. 7.3.2.2. The reaction profiles in Table 6.4 are perhaps better apprehended in the visual presentation of Fig. 6.4. Table 6.5 shows enthalpy values for two "elemental" reactions ($H_2 + Cl_2$ and $H_2 + O_2$) for AM1, RM1, PM3, PDDG/ PM3, and PM6, and provides reaction enthalpies and semiempirical enthalpies of formation for H_2, Cl_2 and O_2 (which by definition should be zero, but here are not).

6.3.2.2 Energies: Calculating Quantities Relevant to Thermodynamics and Kinetics

What do Table 6.4 (an elaboration with more semiempirical methods of the energies in Fig. 6.3) and Fig. 6.4, a visual presentation of the reaction energies of Table 6.4, indicate? Literature results for much larger test samples than these four reactions are presented below for several methods. Consider first the enthalpies of formation in Table 6.4 (from which are obtained the *relative* enthalpies of reactant, transition state and product in Fig. 6.4). For each of the four reactions

Table 6.4 Enthalpies of formation (kJ mol^{-1}) for reactant, transition state and product for each of the four reactions in Fig. 6.3, using AM1, RM1 (a modified AM1), PM3, PDDG/PM3 (a modified PM3), and PM6

Method	Reaction	Species			Relative Enthalpy		
		Reactant	TS	Product			
AM1	Ethenol to ethanal	−140.3	167.9	−173.9	0	308	−34
	HNC to HCN	204.3	495.6	129.7	0	291	−75
	CH$_3$NC to CH$_3$CN	210.8	558.4	80.7	0	348	−130
	Cyclopropylidene to allene	506.5	607.5	193.0	0	101	−314
RM1	Ethenol to ethanal	−136.4	106.6	−171.6	0	243	−35
	HNC to HCN	177.6	464.2	127.7	0	287	−50
	CH$_3$NC to CH$_3$CN	192.1	512.2	91.0	0	320	−101
	Cyclopropylidene to allene	469.7	565.1	184.5	0	95	−285
PM3	Ethenol to ethanal	−132.1	128.5	184.9	0	261	−53
	HNC to HCN	236.8	452.2	137.9	0	215	−99
	CH$_3$NC to CH$_3$CN	228.8	471.4	97.4	0	243	−131
	Cyclopropylidene to allene	479.2	584.8	196.9	0	106	−282
PDDG/PM3	Ethenol to ethanal	−143.0	84.9	−182.3	0	228	−39
	HNC to HCN	180.9	386.4	112.2	0	206	−69
	CH$_3$NC to CH$_3$CN	197.0	449.1	85.2	0	252	−112
	Cyclopropylidene to allene	435.2	549.4	196.4	0	114	−239
PM6	Ethenol to ethanal	−138.6	80.4	−159.6	0	219	−21
	HNC to HCN	194.8	498.9	139.1	0	304	−56
	CH$_3$NC to CH$_3$CN	190.2	482.0	85.9	0	292	−104
	Cyclopropylidene to allene	406.5	544.5	157.5	0	138	−249

The relative enthalpies from CBS-APNO (see text), which should be good surrogates for experiment, are: ethenol to ethanal, 0 : 234 : −43; HNC to HCN, 0 : 125 : −61; CH$_3$NC to CH$_3$CN, 0 : 163 : −101; cyclopropylidene to allene, 0 : 26 : −280

Table 6.5 Enthalpies of formation and reaction (kJ mol^{-1}) for two reactions using AM1, RM1 (a modified AM1), PM3, PDDG/PM3 (a modified PM3), and PM6

Method	Reaction	
	H$_2$ + Cl$_2$ → 2HCl $\Delta H^{\ominus}_{f'}$(exp) = −185	H$_2$ + O$_2$ → 2H$_2$O $\Delta H^{\ominus}_{f'}$(exp) = −484
AM1	−21.7 −59.3 → 2(−103) $\Delta H^{\ominus}_{f'}$(calc) = 2(−103) −(−81.0) = −125	2(−21.7) −116 → 2(−248) $\Delta H^{\ominus}_{f'}$(calc) = 2(−248) −(−159) = −337
RM1	−8.0 −30.5 → 2(−100) $\Delta H^{\ominus}_{f'}$(calc) = 2 (−100) −(−38.5) = −162	2(−8.0) −89.7 → 2(−242) $\Delta H^{\ominus}_{f'}$(calc) = 2(−242) −(−106) = −378
PM3	−56.0 −48.4 → 2(−85.6) $\Delta H^{\ominus}_{f'}$(calc) = 2(−85.6) −(−104) = −67.2	2(−56.0) −17.5 → 2(−224) $\Delta H^{\ominus}_{f'}$(calc) = 2(−224) −(−130) = −318
PDDG/ PM3	−93.0 −40.9 → 2(−117) $\Delta H^{\ominus}_{f'}$(calc) = 2(−117) −(−134) = −100	2(−93.0) −27.5 → 2(−221) $\Delta H^{\ominus}_{f'}$(calc) = 2(−221) −(−214) = −228
PM6	−108 −1.7 → 2(−134) $\Delta H^{\ominus}_{f'}$(calc) = 2 (−134) −(−110) = −158	2(−108) −72.9 → 2(−227) $\Delta H^{\ominus}_{f'}$(calc) = 2(−227) −(−289) = −165

The enthalpy of reaction is the enthalpy of formation of the products minus the sum of the enthalpies of formation of the reactants. Note that the semiempirical methods use enthalpies of formation of the elements in their standard states (H$_2$, Cl$_2$, O$_2$) which are well-removed from the theoretical values of zero. Experimental reaction enthalpies (inferred): NIST website; the enthalpies of formation reported for HCl and H$_2$O are −92.31 and −241.826 kJ mol^{-1}, respectively

we can summarize the ranges of enthalpies of formation thus R = reactant, TS = transition state, P = product; kJ mol^{-1}):

Ethenol reaction:
R -143 — -132, -138 ± 6; TS 80 — 168, 124 ± 44; P -185 — -160, -173 ± 13

HNC reaction:
R 178 — 237, 208 ± 30; TS 386 — 488, 443 ± 57; P 112 — 138, -125 ± 13

CH$_3$NC reaction:
R 190 — 229, 210 ± 20; TS 449 — 558, 504 ± 55; P 81 — 97, -89 ± 8

Cyclopropylidene reaction:
R 407 — 507, 457 ± 50; TS 545 — 608, 577 ± 32; P 158 — 197, -178 ± 20

   This shows for each species of each reaction the range (across the five semiempirical methods) of calculated enthalpies of formation and the mean (average) value. Here plus/minus accommodates the maximum and minimum values, rather than indicating the possible error in the value. Thus for the ethenol isomerization the lowest (most negative) heat of formation for the reactant is -143 kJ mol^{-1} (PDDG/PM3) and the highest is -132 kJ mol^{-1} (PM3), and this range is accommodated by the mean value -138 ± 6 kJ mol^{-1}. As might be expected for species more difficult to pin down computationally than "stable" molecules (than relative minima on the potential energy surface), the transition states show the biggest variation around the average value, 44, 57, 55, 32 kJ mol^{-1}; the variations for the reactants are 6, 30, 20, 50 and for the products 13, 13, 8, 20 kJ mol^{-1}. These are not wild variations and indicate that none of the methods is so superior as to render others obsolete.

   What about the range of semiempirical enthalpies for the *reaction profiles*, the *relative* energies rather than absolute ones, of reactants, transition states, and products, from Table 6.4 and Fig. 6.4? Again, the spread is bigger for enthalpies involving transition states (for barriers, i.e. activation enthalpies) than for reaction enthalpies (product enthalpy minus reactant enthalpy). In kJ mol^{-1}:

Ethenol reaction, barriers 219–308, 264 ± 45; reaction enthalpies -53 to -21, -37 ± 16.
HNC reaction, barriers 206–304, 255 ± 49; reaction enthalpies -99 to -50, -75 ± 25.
CH3NC reaction, barriers 243–348, 296 ± 53; reaction enthalpies -131 to -101, -116 ± 15.
Cyclopropylidene reaction, barriers 95–138, 117 ± 22; reaction enthalpies -314 to -239, -277 ± 38.

   The variations of the barriers for the four reactions are 45, 49, 53, 22 and for the overall reactions 16, 25, 15, 38 kJ mol^{-1}; only the cyclopropylidene isomerization

shows a smaller spread for the barrier than for the overall reaction. Again, these are not wild variations among different methods for barriers whose calculated absolute values are in the area of about, respectively, 260, 260, 300, and 120 kJ mol^{-1}, and for overall reactions in the range -40, -75, -120, and -300 kJ mol^{-1}.

We have seen that the five semiempirical methods being discussed do not differ wildly for the four reactions being examined here. How *accurate* are these methods? The very limited size of this survey (only four reactions) does not warrant a detailed numerical evaluation of the results, but a few points may be noted. Fig. 6.4 shows that for the HNC, CH$_3$NC and cyclopropylidene isomerizations the semiempirical methods overestimate the barriers compared to experiment [97] and MP2/6‑31G* (by roughly 100 kJ mol^{-1}), which is in accord with the literature (below). For the ethenol reaction only AM1 overestimates the reported barrier (MP2 underestimates it). The reaction enthalpies are mostly underestimated (not negative enough) for the ethenol and cyclopropylidene reactions, and overestimated (too negative) for the HNC and CH$_3$NC cases. The MP2 reaction enthalpy is lower than the experimental, by ca. $20 - 30$ kJ mol^{-1}, except for the cyclopropylidene reaction, where the values are close, -287 and -293 kJ mol^{-1}. None of the five semiempirical methods is statistically consistently closer to the experimental barrier or reaction enthalpy than any other. None of the semiempirical methods matches MP2 consistently for the barriers, while MP2 is within 50 kJ mol^{-1} of experiment for all these barriers (within 49 for the ethenol isomerization). The semiempirical reaction enthalpies are all within ca. 40 kJ mol^{-1} (within 41 for the HNC isomerization), not far from the MP2 accuracy, for which the largest absolute error is 30 kJ mol^{-1} (ethenol case).

Table 6.5 shows enthalpy values and reaction enthalpies for $H_2 + Cl_2 \rightarrow 2HCl$ and $H_2 + O_2 \rightarrow 2H_2O$ for our five semiempirical methods. This shows that semiempirical enthalpies of formation for elements need be nowhere near the theoretical (by definition) value of zero. For H_2 the PM6 value is -108 kJ mol^{-1}, for Cl_2 the AM1 value is -59 kJ mol^{-1}, and for O_2 the AM1 value is -116 kJ mol^{-1}. Other calculations confirm this perhaps unexpected discrepancy: for F_2, Br_2, and I_2 the AM1/PM3 heats of formation are $-94/-90.8$, $-22.1/+20.6$, $+83.0/+86.8$ kJ mol^{-1}; for N_2, $+46.7/+73.5$ kJ mol^{-1}. Evidently parameterizing a semiempirical method for acceptable enthalpies of formation for compounds requires sacrificing the by-definition enthalpies of formation for elements in their standard states. The calculated enthalpies of the compounds (HCl and H_2O), in contrast to the case of the elements (H_2, Cl_2 and O_2), are more reasonable: for HCl the mean absolute error (from AM1, 103–92, etc.) is 18 kJ mol^{-1}, and for H_2O (from AM1, 248–242, etc.) 12 kJ mol^{-1}; the maximum absolute errors for the two compounds are 42 (PM6) and 21 kJ mol^{-1} (PDDG/PM3). As expected from poor elemental enthalpies of formation but more tolerable product enthalpies of formation, the calculated reaction enthalpies are poor: for the HCl reaction the mean absolute error (from AM1 185–125, etc.) is 63 kJ mol^{-1}, and for the H_2O reaction (from AM1 484–337, etc.) 199 kJ mol^{-1}; the maximum absolute errors for the two reactions are 118 and

319kJ mol^{-1}. Of course if one simply uses the by-definition zero values for the elements, the calculated reaction enthalpies follow from only the calculated enthalpies of formation of the compounds. From the stoichiometry of the reactions these will be e.g. for the AM1 method $2(-103) \text{kJ mol}^{-1} = -206$ cf. experimental $2(-92.31) = -185 \text{kJ mol}^{-1}$ for formation of HCl, and $2(-248) = -496$ cf. experimental $2(-241.826) = -484 \text{kJ mol}^{-1}$ for formation of H_2O. Here the maximum absolute errors in calculated reaction enthalpies are 83kJ mol^{-1} (for the HCl reaction using PM6, -268 cf. -185) and 42kJ mol^{-1} (for the H_2O reaction using PDDG/PM3, -442 cf. -484), twice the compound formation enthalpies, as required arithmetically.

The accuracy of semiempirical methods for enthalpies of formation and for reactions (barriers and enthalpy of reaction) has been tested for very large sample sizes. An extensive compilation of AM1 and PM3 heats of formation (which corrects errors in earlier values) [70] gave for 657 normal-valent compounds these average errors for the absolute deviations (AM1/PM3, kJ mol^{-1}): 53/33; for 106 hypervalent compounds 348 (*sic*)/57. These results are not as bad as they may at first seem if we note that (1) the heats of formation of organic compounds are commonly in the region of $\pm 400 - 800 \text{kJ mol}^{-1}$, (2) often we are interested in trends, which are more likely to be qualitatively right than actual numbers are to be quantitatively accurate, and (3) usually chemists are concerned with energy *differences*, i.e. *relative* energies (below). AM1 heats of formation for hypervalent compounds (above and reference [47]) appear to be distinctly inferior to those from PM3. Thiel has compared MNDO, AM1, PM3, and MNDO/d heats of formation with those from some ab initio and DFT methods [98]. The results (ca. 1998) are somewhat dated, as more accurate ab initio (e.g. G3- and G4-type; Chap. 5, Sect. 5.5.2.3.2), DFT (Chap. 7) and semiempirical (RM1, PM6) methods (above) are now available. However, it remains true that multistep high-accuracy ab initio methods are the most accurate ways to calculate heats of formation. These give an error of about $3 - 5 \text{kJ mol}^{-1}$ compared with about 20kJ mol^{-1} for RM1 and PM6. Nevertheless, the fact that semiempirical calculations are faster than ab initio by factor of the order of about 1000 can be decisive when dealing with big molecules or with a large collection of molecules. As mentioned. Such a survey uncovered several errors in reported experimental heats of formation [84].

The discussion of enthalpy, free energy, and reaction and activation energies in Sect. 5.5.2.1 applies to semiempirical calculations too. Now let's retrace some of the calculations of Chap. 5, using AM1 and PM3 rather than ab initio methods. We are usually interested in *relative* energies. A simple ab initio energy difference (for isomers, or isomeric systems like reactants cf. products), preferably including the zero point energies, represents a 0 K energy difference, i.e. a 0 K enthalpy difference (entropy being zero at 0 K), whereas an energy difference from a standard SCF semiempirical method like AM1, PM3 or PM6 represents a room temperature enthalpy difference. Thus even if the ab initio and semiempirical

calculations both had negligible errors, they would not be expected to give exactly the same relative energy, unless the 0–298 K enthalpy change on both sides of the equation cancelled. A typical change in heat of formation is shown by methanol; the (ab initio calculated) heats of formation of methanol at 0 K and 298 K are -195.9 and $-207.0 \, \text{kJ mol}^{-1}$, respectively (Chap. 5, Sect. 5.5.2.3.3). This change of $11 \, \text{kJ mol}^{-1}$ is fairly small compared to the errors in semiempirical and many ab initio calculations, so discrepancies between energy changes calculated by the two approaches must be due to factors other than the 0–298 K enthalpy change. The errors in heats of formation cannot be counted on to consistently cancel when we subtract to obtain relative energies, and because of average errors in individual heats of formation of ca. $20 \, \text{kJ mol}^{-1}$ (above) for some of the best current methods, RM1 and PM6, errors of about $40 \, \text{kJ mol}^{-1}$ should not be surprising, although much smaller errors are often obtained. Consider the relative energies of (Z)- and (E)-2-butene (Chap. 5, Fig. 5.24). The HF/3-21G$^{(*)}$ energy difference, corrected for ZPE (although in this case the ZPE is practically the same for both isomers) is $(Z) - (E) = -155.12709 \quad - \quad (-155.13033) \quad \text{h} = 0.00324 \quad \text{h} = 8.5 \, \text{kJ mol}^{-1}$. AM1 calculations (ZPE is not considered here, since as explained in Sect. 6.2.5.2, this is taken into account in the parameterization) give $(Z) - (E) = -9.24 - (-14.01) \, \text{kJ mol}^{-1} = 4.8 \, \text{kJ mol}^{-1}$. The experimental heats of formation (298 K, gas phase) are $(Z) = -29.7 \, \text{kJ mol}^{-1}$, $(E) = -47.7 \, \text{kJ mol}^{-1}$, i.e. $(Z) - (E) = 18.0 \, \text{kJ mol}^{-1}$ [99b].

The comparison by Schröder and Thiel [47a] (Sect. 6.3.1) of semiempirical (MNDO and MNDOC) and ab initio geometries and energies concluded that the semiempirical methods usually overestimate barriers (activation energies). Of 21 activation energies (Table IV in ref. [47a], entries I, K, W omitted), MNDO overestimated (compared with "best" correlated ab initio calculations) 19 and underestimated 2; the overestimates ranged from $8 - 201 \, \text{kJ mol}^{-1}$ and the underestimates were 46 and $13 \, \text{kJ mol}^{-1}$. MNDOC overestimated 16 and underestimated 5; the overestimates ranged from $2 - 109 \, \text{kJ mol}^{-1}$ and the underestimates from $4 - 63 \, \text{kJ mol}^{-1}$. Thus for calculating activation energies MNDOC is significantly better than MNDO, and it is probably better than AM1 for this purpose, since, like MNDO but unlike MNDOC, AM1 is parameterized to take into account electron correlation for ground states, but not transition states. For these 21 reactions, restricted Hartree-Fock calculations overestimated 18 activation energies and underestimated 3; the overestimates of energies ranged from $3 - 105 \, \text{kJ mol}^{-1}$ and the underestimates from $13 - 28 \, \text{kJ mol}^{-1}$. The mean absolute deviations from the "best" correlated ab initio calculations for the 21 reactions were: MNDO, $92 \, \text{kJ mol}^{-1}$; MNDOC, $38 \, \text{kJ mol}^{-1}$; RHF, $50 \, \text{kJ mol}^{-1}$. Evidently MNDOC is somewhat better than RHF (uncorrelated) calculations for activation energies. Correlated-level ab initio calculations, however, appear to be superior to MNDOC; in particular, MNDOC predicts substantial barriers for isomerization of carbenes by hydrogen migration. Other work showed that AM1 greatly overestimates the barrier for decomposition or rearrangement of some highly reactive species [100]. Despite the lack of quantitative accuracy, semiempirical methods

have been used fairly frequently to study transition states in biochemical reactions, where large molecules are involved [101].

From all this information then, we can conclude that semiempirical heats of formation and reaction energies (reactant cf. product) tend to be semiquantitatively reliable. Activation energies (reactant cf. transition state) are often considerably overestimated by all these methods except MNDOC, which actually gives results somewhat better than those from RHF calculations, at least in many cases. An extensive comparison of AM1 with ab initio and density functional methods for calculating geometries and relative energies is given in Hehre's book [94]. Consistently good calculated reaction energies and especially activation energies require correlated ab initio methods (Chap. 5, Sects 5.4.2, 5.4.3) or DFT methods (Chap. 7). However, semiempirical methods are well suited for a preliminary exploration of a potential energy surface, and are usually good for creating input structures for refinement by ab initio or DFT. It is interesting that these methods, which were parameterized mainly to give good energies (heats of formation) actually commonly provide fairly good geometries but energies of only modest quality.

6.3.3   Frequencies and Vibrational Spectra

The general remarks and the theory concerning frequencies in Chap. 5, Sect. 5.5.3, apply to semiempirical frequencies too, but the zero-point energies associated with a frequency calculation are usually not needed, since the semiempirical energy is normally not adjusted by adding the ZPE (Sect. 6.2.5.2). As with ab initio calculations, semiempirical frequencies are used to characterize a species as a minimum or a transition state (or a higher-order saddle point), and to get an idea of what the IR spectrum looks like. As with ab initio frequencies too, in semiempirical methods the wavenumbers ("frequencies") of vibrations are calculated from a mass-weighted second-derivative matrix (a Hessian) and intensities are calculated from the changes in dipole moment accompanying the vibrations. Like their ab initio counterparts, semiempirical frequencies are higher than the experimental ones; presumably this is at least partly due to the harmonic approximation, as was discussed in Chap. 5, Sect. 5.5.3.

Correction factors improve the fit between semiempirically calculated and experimentally measured spectra, but the agreement does not become as good as does the fit of corrected ab initio to experimental spectra. This is because deviations from experiment are less systematic for semiempirical than for ab initio methods (a characteristic that has been noted for errors in semiempirical energies [102]). For AM1 calculations, correction factors of 0.9235 [103] and 0.9532 [104], and for PM3, factors of 0.9451 [103] and 0.9761 [104], have been recommended. A factor of 0.86 has been recommended for SAM1 for non-H stretches [105]. However, the variation of the correction factor with the *kind* of frequency is bigger for semiempirical than for ab initio calculations; for example, for correcting carbonyl stretching frequencies, examination of a few molecules indicated (author's work) that (at least for C, H, O compounds) correction factors of 0.83 (AM1) and 0.86 (PM3) give a much better fit to experiment.

The calculated intensities of semiempirical vibrations seem likely to be in general more approximate than those for ab initio vibrations [106], which latter are typically within 30 % of the experimental intensity at the MP2 level [107]. This is somewhat surprising, since semiempirical (AM1 and PM3 and later derivatives) dipole moments, from the vibrational changes of which intensities are calculated, are fairly accurate (Sect. 6.3.4.1). Note however that unlike the case with UV spectra, IR intensities are rarely actually measured; rather, one usually simply visually classifies a band as strong, medium, etc., by visual comparison with the strongest band in the spectrum. There do not seem to have been any published surveys comparing, for a variety of compounds, the intensities of IR bands calculated by modern NDDO methods with those from experiment, but an idea of the reliability of semiempirical frequencies and intensities is given by the IR spectra in Figs. 6.5, 6.6, 6.7, and 6.8, which compare experimental spectra (taken by the author in the gas phase) with AM1 and ab initio
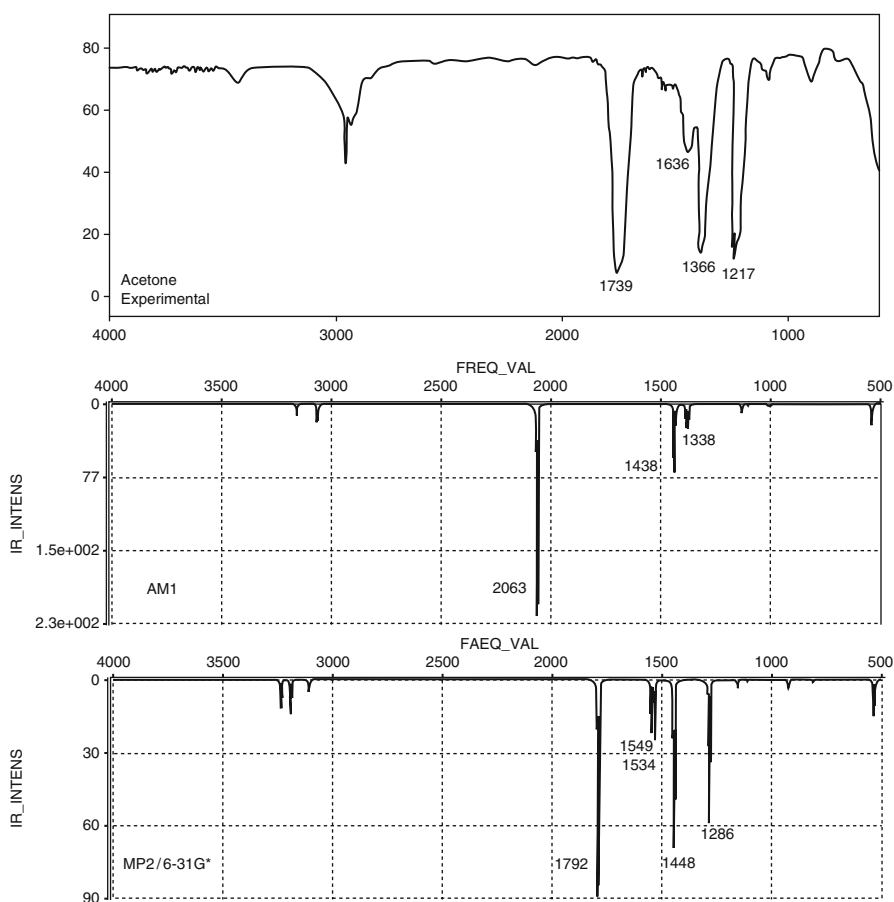
Fig. 6.5 Experimental (gas phase), AM1 and ab initio (MP2(fc)/6-31G*) calculated IR spectra of acetone
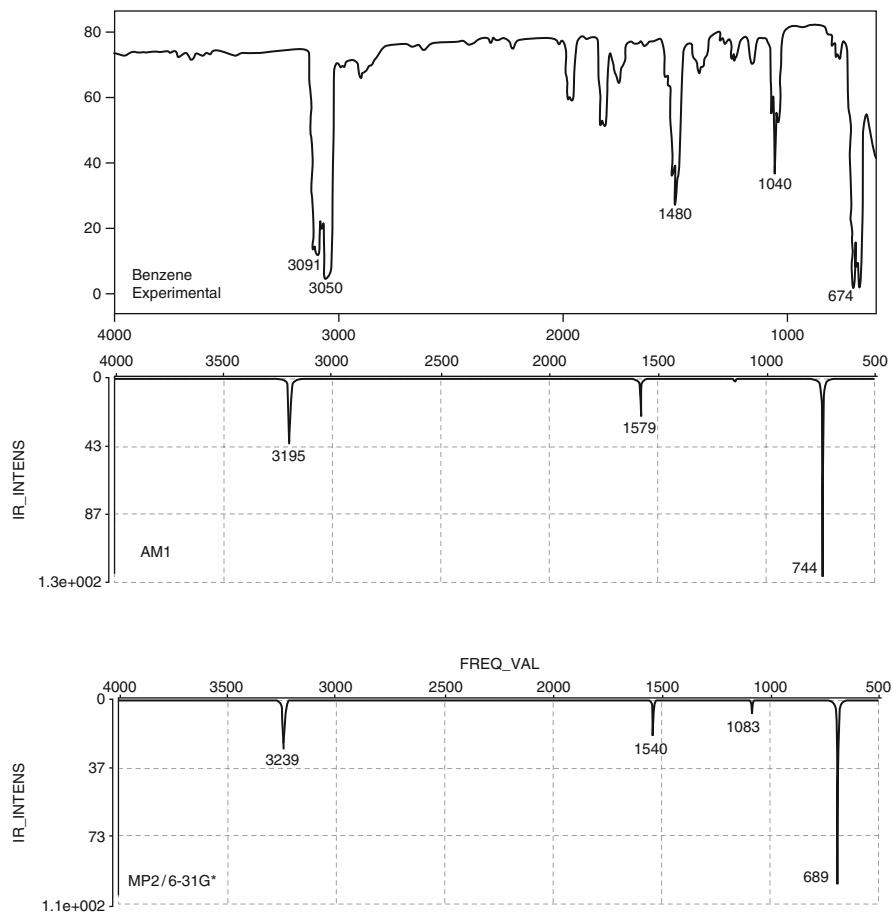
Fig. 6.6 Experimental (gas phase), AM1 and ab initio (MP2(fc)/6-31G*) calculated IR spectra of benzene

(MP2/6-31G*) spectra, for the same four compounds (acetone, benzene, dichloromethane, methanol) shown in Chap. 5, Figs. 5.33, 5.34, 5.35 and 5.36. The experimental and MP2 spectra are the ones used in Chap. 5, Figs. 5.33, 5.34, 5.35 and 5.36. For acetone and methanol (Figs. 6.5 and 6.8) the MP2 spectra match the experimental distinctly better than do the AM1; and other work [106] indicates that MP2 IR spectra resemble the experimental spectra more closely than do AM1 spectra.

All the normal (in the technical sense) modes are formally (some may be very weak or even of zero intensity) present in the results of a semiempirical frequency calculation, as is the case for an ab initio or DFT calculation, and animation of these
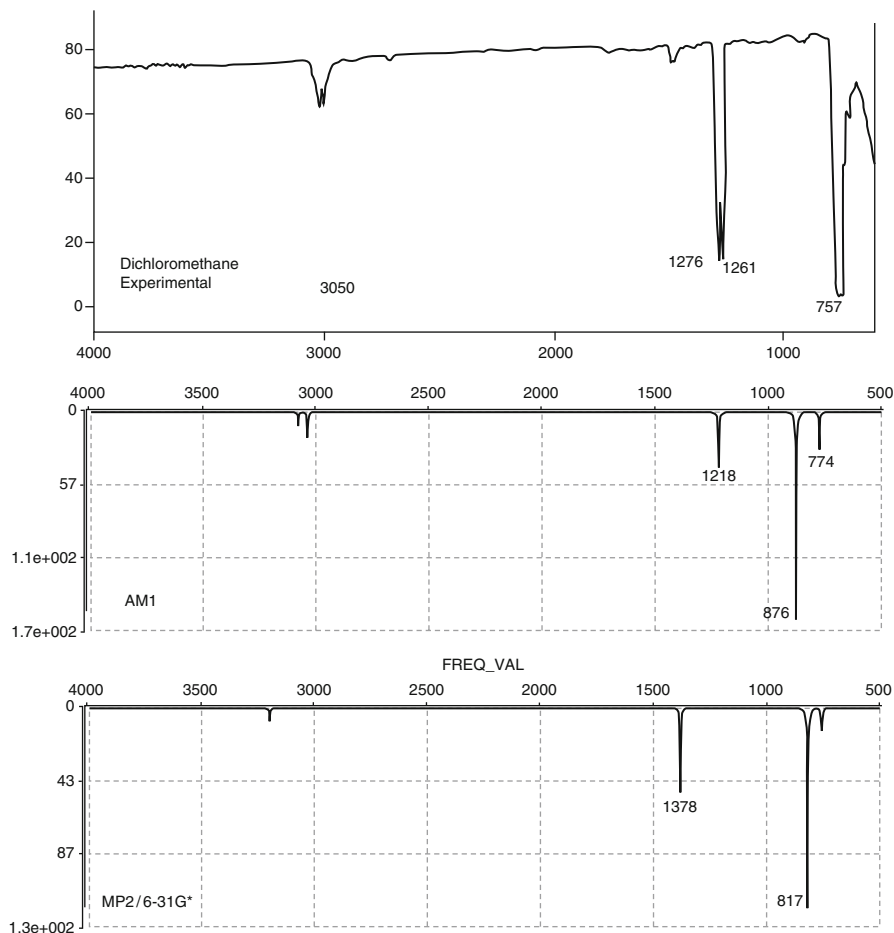
Fig. 6.7 Experimental (gas phase), AM1 and ab initio (MP2(fc)/6-31G*) calculated IR spectra of dichloromethane

will usually give, approximately, the frequencies of these modes. A very extensive compilation of experimental, MNDO and AM1 frequencies has been given by Healy and Holder, who conclude that the AM1 error of 10 % can be reduced to 6 % by an empirical correction, and that entropies and heat capacities are accurately calculated from the frequencies [108]. In this regard, Coolidge *et al*. conclude–surprisingly, in view of our results for the four molecules in Figs. 6.5, 6.6, 6.7, and 6.8 – from a study of 61 molecules that (apart from problems with ring- and heavy atom-stretch for AM1 and S-H, P-H and O-H stretch for PM3) "both AM1 and PM3 should provide results that are close to experimental gas phase spectra" [109].
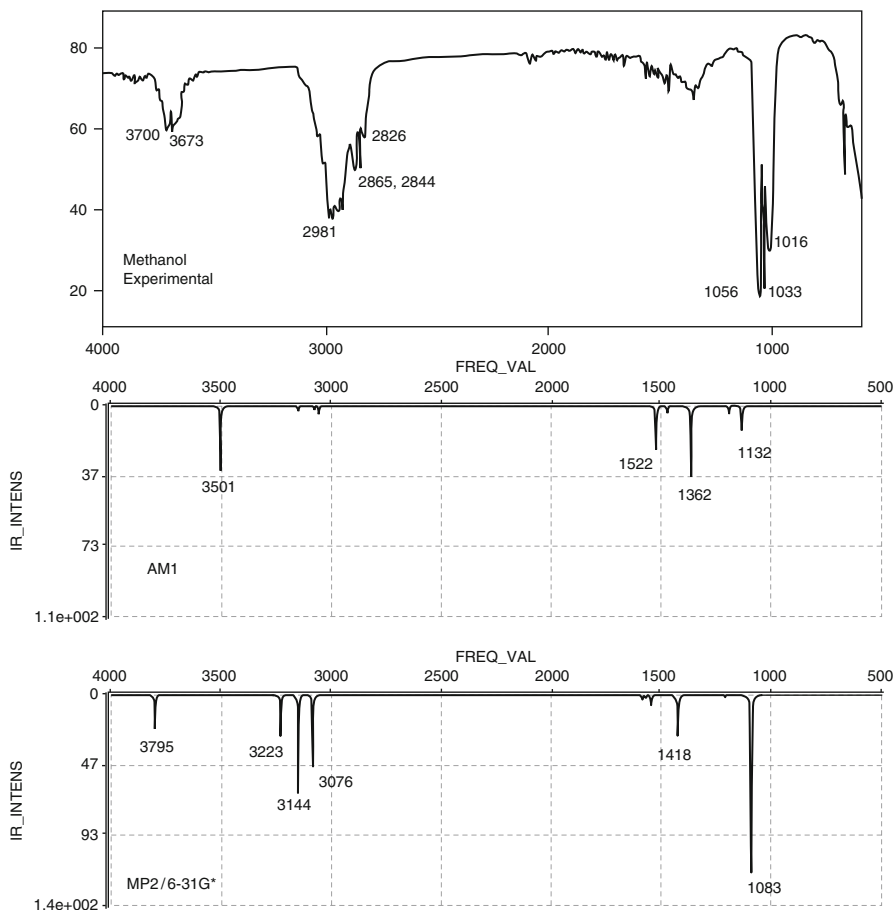
Fig. 6.8 Experimental (gas phase), AM1 and ab initio (MP2(fc)/6-31G*) calculated IR spectra of methanol

6.3.4 Properties Arising from Electron Distribution: Dipole Moments, Charges, Bond Orders

The discussion in Chap. 5, Sect. 5.5.4 on dipole moments, charges and bond orders applies in a general way to the calculation of these quantities by semiempirical methods too. Electrostatic potentials, whether visualized as regions of space or mapped onto van der Waals surfaces, are usually qualitatively the same for AM1 and PM3 as for ab initio methods. Atoms-in-molecules calculations are not viable for semiempirical methods, because the core orbitals, lacking in these methods, are important for AIM calculations.

6.3.4.1 Dipole Moments

Hehre's extensive survey of practical computational methods reports the results of ab initio and DFT single point dipole moment (μ) calculations on AM1 geometries [110]. There does not appear to be much advantage to calculating HF/6-31G* dipole moments on HF/6-31G* geometries (HF/6-31G*//HF/6-31G* calculations) rather than on the much more quickly- obtained AM1 geometries (HF/6-31G*// AM1 calculations). Indeed, even the relatively time-consuming MP2/6-31G*// MP2/6-31G* calculations seem to offer little advantage over fast HF/6-31G*// AM1 calculations as far as dipole moments are concerned (Tables 2.19 and 2.21 in ref. [94]). This is consistent with our finding that AM1 geometries are usually quite good (Sect. 6.3.1). Table 6.6 compares calculated with experimental [94, 111] dipole moments for ten molecules, using these methods: AM1 (using the AM1 method to calculate μ for the AM1 geometry, AM1//AM1), HF/6-31*//AM1, PM3 (PM3//PM3), HF/6-31G*//PM3, and MP2/6-31G* (MP2/6-31G*//MP2/6-31G*). For this set of molecules, the smallest deviation from experiment, as judged by the arithmetic mean of the absolute deviations from the experimental values, is shown by the AM1 calculation (0.21 Debyes), and the largest deviation is shown by the "highest" method, MP2/6-31G* (0.34 D). The other three methods give essentially the same errors (0.27–0.29 D). It is of course possible that AM1 gives the best results (for this set on molecules, at least) because errors in geometry and errors in the calculation of the electron distribution cancel. A study of 196 C, H, N, O, F, Cl, Br, I molecules gave these mean absolute errors: AM1, 0.35 D; PM3, 0.40 D; SAM1, 0.32 D [76]. Another study with 125 H, C, N, O, F, Al, Si, P, S, Cl, Br, I

Table 6.6 Some calculated dipole moments compared to experimental ones. Dipole moments are in Debyes

	Computational method					
	AM1	HF/6-31G* //AM1	PM3	HF/6-31G* //PM3	MP2/6-31G*	exp
CH_3NH_2	1.5	1.42	1.4	1.54	1.6	1.3
H_2O	1.86	2.25	1.74	2.16	2.24	1.9
HCN	2.36	3.24	2.7	3.24	3.26	3
CH_3OH	1.62	1.9	1.49	1.88	1.95	1.7
Me_2O	1.43	1.54	1.25	1.51	1.6	1.3
H_2CO	2.32	2.87	2.16	2.76	2.84	2.3
CH_3F	1.62	2	1.44	1.91	2.11	1.9
CH_3Cl	1.51	2.07	1.38	2.14	2.21	1.9
Me_2SO	3.95	4.56	4.49	4.83	4.63	4
CH_3CCH	0.4	0.58	0.36	0.6	0.66	0.8
Deviations	4 +, 6− mean 0.21	9+, 1− mean 0.29	2+, 8− mean 0.27	9+, 1− mean 0.29	9+, 1− mean 0.34	

Calculations are by the author; experimental values are taken from [94] and [111]. For each method is given the number of positive and negative deviations from experiment and the arithmetic mean of the absolute values of the deviations

molecules gave mean absolute errors of: AM1, 0.35 D and PM3, 0.38 D [70]. So with these larger samples the AM1 errors were somewhat bigger. Nevertheless, all these results taken together do indicate that unless one is prepared to use a slower approach, e.g. large basis sets with density functional (Chap. 7) methods (errors of ca. 0.1 D [112]; this paper also gives some results for ab initio calculations), AM1 dipole moments using AM1 geometries may be as good a way as any to calculate this quantity. This applies, of course, only to conventional molecules; molecules of exotic structure and "hypervalent" molecules (Sects 6.3.1, 6.3.2.1) tend to defy accurate semiempirical predictions.

6.3.4.2 Charges and Bond Orders

The conceptual and mathematical bases of these concepts were outlined in Chap. 5, Sect. 5.5.4, in the discussion of population analysis. We saw that unlike, say, frequencies and dipole moments, there are problems with regarding charges and bond orders as experimental observables (carefully defined atom charges can, it is said be measured [113]), and with settling on a single, right way to calculate them. Some would argue that the atoms-in-molecules theory does provide such a unique ansatz. Nevertheless, we saw that there are several prescriptions for calculating charges and bond orders, and as with ab initio calculations, semiempirical charges and bond orders can be defined in various ways. The concepts are nevertheless useful, and for charges and bond orders the methods of Mayer, Löwdin or Weinhold are often now preferred. One might almost wonder what all the fuss is about: evidently Mulliken never intended his population analysis method to be taken quantitatively, but rather to be a guide to trends: his friend and colleague Roothaan is reported to have said (in a close paraphrase by P. S. Bagus) that "Robert didn't believe populations had quantitative value. He meant them to be a guide to the chemistry and the bonding." [114].

Figure 6.9 shows charges and bond orders calculated for an enolate (the conjugate base of ethenol or vinyl alcohol) and for a protonated enone system (protonated propenal). Consider first Mulliken charges and bond orders of the enolate (Fig. 6.9a). The AM1 and PM3 charges, which are essentially the same, are a bit surprising in that the carbon which shares charge with the oxygen in the alternative resonance structure is given a bigger charge than the oxygen; intuitively, one expects most of the negative charge to be on the more electronegative atom, oxygen; this "defect" of AM1 and PM3 has been noted by Anh *et al.* [115]. The HF/3-21G$^{(*)}$ method gives the oxygen the bigger charge (-0.80 vs. -0.67). The two semiempirical and the HF methods all give C/C and C/O bond orders of about 1.5; this, and the rough equality of O and C charges, suggests approximately equal contributions from the O-anion and C-anion resonance structures.

The Mulliken charges of the protonated enone system (Fig. 6.9b) make the oxygen negative, which may seem surprising. However, this is normal for protonated oxygen and nitrogen (though not protonated sulfur and phosphorus): the hetero

a

−0.60 AM1
−0.65 PM3
−0.80 HF/3-21G

O⁻

1.48 AM1
1.47 PM3
1.49 HF/3-21G

1.51
1.50
1.42

−0.66
−0.72
−0.67

All Mulliken

b

−0.11 AM1
−0.08 PM3
−0.63 HF/3-21G

H

O⁺

1.45 AM1
1.47 PM3
1.18 HF/3-21G

1.69   1.19
1.71   1.18
1.59   1.15

0.30
0.42
0.45

0.09
0.23
−0.25

All Mulliken

c

−0.76 AM1, ESP
−0.80 PM3, ESP
−0.82 HF/3-21G, ESP

O⁻

1.48 AM1, Mulliken
1.47 PM3, Mulliken
1.69 HF/3-21G, Lowdin

1.51
1.50
1.61

−0.92
−0.94
−1.13

d

−0.37 AM1, ESP
−0.35 PM3, ESP
−0.63 HF/3-21G, ESP

H

O⁺

1.45 AM1, Mulliken
1.47 PM3, Mulliken
1.55 HF/3-21G, Löwdin

1.69   1.19
1.71   1.18
1.76   1.29

0.67
0.76
0.76

0.17
0.26
−0.03

Fig. 6.9 Atom charges and bond orders calculated using the AM1, PM3 and HF/3-21G$^{(*)}$ methods. In (**a**) and (**b**) the charges and bond orders are all from the Mulliken approach. In (**c**) and (**d**) the charges are all electrostatic potential charges, and the bond orders are Mulliken for AM1 and PM3, and Löwdin for HF/3-21G (Löwdin bond orders were not available for AM1 and PM3 from the Spartan program used). Note that charges and bond orders involving hydrogens have been omitted

atom in H_3O^+ and in NH_4^+ is calculated to be negative (i.e. the positive charge is on the hydrogens) and the hetero atom is also negative in $H_2C=OH^+$ and $H_2C=NH_2^+$. On the oxygen and the carbon furthest from the oxygen (C_3) the HF/3-21G$^{(*)}$ charges differ considerably from the semiempirical ones: the HF calculations make the O much more negative, and make C_3 negative, suggesting that they place more positive charge on the hydrogens than do the semiempirical calculations (in all cases the charge on C_2 is 0.3–0.5). The three methods do not differ as greatly in their bond orders (that bond orders are less fickle than charges has been noticed before [116]), although the HF method makes the formal C/O double bond essentially a single bond (bond order 1.18).

Finally, electrostatic potential (ESP) charges and, for the HF/3-21G$^{(*)}$ calculations, Löwdin bond orders, are shown (Fig. 6.9c, d). For the enolate, all three methods make the ESP charge on carbon more negative than that on oxygen, but the bond orders are not greatly altered. For the protonated enone system, AM1 and PM3 suggest more polarization of electrons toward the O in the C/O bond than is shown by the Mulliken charges, but while the HF ESP charge on this carbon is greater than the Mulliken (0.76 vs. 0.45), the charge on oxygen is unchanged. The Hartree-Fock Löwdin bond orders for all three bonds of the CCO framework (1.55, 1.29, 1.76) are all somewhat bigger than the Mulliken bond orders (1.18, 1.15, 1.59).

These results suggest that charges are more dependent than are bond orders on the method used to calculate them, and that charges are also harder to interpret than are bond orders. As with ab initio charges and bond orders, the semiempirically calculated parameters may be useful in revealing trends in a series of compounds or changes as a reaction proceeds. For example, ab initio bond order changes along a reaction coordinate have been shown to be useful [117], but presumably semiempirically calculated bond orders would also yield similar information, at least if the species being studied were not too exotic. Clearly, one must use the same semiempirical method (e.g. AM1) and the same procedure (e.g. the Mulliken procedure) in studying a series.

6.3.5   Miscellaneous Properties–UV Spectra, Ionization Energies, and Electron Affinities

All the properties that can be calculated by ab initio methods can in principle also be calculated semiempirically, bearing in mind that the more the molecule of interest differs from the training set used to parameterize the semiempirical program, the less reliable the results will be. For example, a program parameterized to predict the UV spectra of aromatic hydrocarbons may not give good predictions for the UV spectra of heterocyclic compounds. NMR spectra are usually calculated with ab initio (Chap. 5, Sect. 5.5.5.2) or density functional (Chap. 7) methods. UV spectra, and ionization energies (ionization potentials) and electron affinities will be discussed here.

6.3.5.1   UV Spectra

As pointed out in Sect. 5.5.5, although ultraviolet spectra result from the promotion of electrons from occupied to unoccupied orbitals, UV spectra cannot be calculated with reasonable accuracy simply from the HOMO/LUMO gap of the ground electronic state, since the UV bands represent energy differences between the ground and *excited* states. Furthermore the HOMO/LUMO gap does not account

Table 6.7 Calculated and experimental [118] UV spectra of methylenecyclopropene

Calculated					
ZINDO/S//AM1		RCIS/6-31+G*// HF/6-31G*		Experimental	
Wavelength (nm)	Relative intensity	Wavelength (nm)	Relative intensity	Wavelength (nm)	Relative intensity
288	12	222	15	309	13
224	0.2	209	7	242	0.6
213	100	196	0	206	100
204	1	193	9		
		193	100		

The semiempirical calculations were done with ZINDO/S in G94W; the ab initio results are from Chap. 5, Table 5.16. The ab initio method shown was explained in Chap. 5

for the presence of the *several* bands often found in UV spectra, and gives no indication of the intensity of a band. In wavefunction theory, accurate prediction of UV spectra requires calculation of the energies of excited states. Semiempirical UV spectra are usually calculated with programs specifically parameterized for this purpose, such as INDO and ZINDO (intermediate neglect of differential overlap and Zerner's INDO), sometimes denoted INDO/S and ZINDO/S, S = spectra (Sect. 6.2.4) [20]. INDO and ZINDO, which appears to have largely superseded INDO, are included in the primarily ab initio and DFT package Gaussian [55]. Table 6.7 compares the UV spectrum of methylenecyclopropene calculated by ZINDO/S on the AM1 geometry with the ab initio-calculated RCIS (Chap. 5, Table 5.16) and the experimental spectra [118] (calculations with Gaussian 03 [55]). The ZINDO/S spectrum resembles the experimental spectrum considerably better than does the ab initio one (the experimental 242 nm, and particularly the 309 nm band, are matched better than by the ab initio calculation). The times for the calculations on a vintage ca. 2002 computer were 0.5 and 1 min (ZINDO/S and RCIS). Parameterized methods like ZINDO/S are probably the only way to calculate reasonably accurate UV spectra for large molecules.

6.3.5.2 Ionization Energies and Electron Affinities

The concepts of IE and EA were discussed in Chap. 5, Sect. 5.5.5.3. In Table 6.8 the results of some semiempirical calculations are compared with ab initio and experimental values [119, 120], for the molecules of Chap. 5, Table 5.17. This admittedly very small sample suggests that semiempirical IEs calculated as energy differences might be comparable to ab initio values. Koopmans' theorem (the IE for an electron is approximately the negative of the energy of its molecular orbital; applying this to the HOMO gives the IE of the molecule) values are consistently bigger than those from energy differences using the same method (by 0.1–0.8 eV). No consistent advantage for any of the six methods is evident here, but a large sample would

Table 6.8 Some ionization energies (eV)

	ΔE			Koopmans'			
	AM1	PM3	ab in.	AM1	PM3	ab in.	experiment
CH_3OH	10.5	10.7	10.6	11.1	11.1	12.1	10.9
CH_3SH	8.7	9	9	8.9	9.2	9.7	9.4
CH_3COCH_3	9.9	10.1	9.6	10.7	10.8	11.2	9.7

The ΔE values (cation energy minus neutral energy) correspond to adiabatic, and the Koopmans' theorem values to vertical IEs. The ab initio energies are MP2(fc)/6-31G* (Table 5.17). Experimental values are adiabatic, from [119] (CH_3OH and CH_3COCH_3) and [120] (CH_3SH)

likely show the most accurate of these methods to be the energy difference using MP2(fc)/6-31G* (see Table 5.17 and accompanying discussion).

Calculations by Stewart on 256 molecules (of which 201 were organic), using Koopmans' theorem, gave mean absolute IE errors of 0.61 eV for AM1 and 0.57 eV for PM3; 60 of the AM1 errors (23 %) and 88 of the PM3 (34 %) were negative (smaller than the experimental values) [70]. Particularly large errors (2.0–2.9 eV) were reported for nine molecules: 1-pentene, 2-methyl-1-butene, acetylacetone, alanine (AM1), SO_3 (AM1), CF_3Cl (AM1), 1,2-dibromotetrafluoroethane, H_2SiF (PM3), and PF_3 (AM1). For some of these it may be the *experimental* results that are at fault; for example, there seems to be no reason why 2-methyl-1-butene and 2-methyl-2-butene should have such different IEs, and in the opposite order to those calculated: experimental, 7.4 and 8.7 eV; calculated, 9.7 and 9.3 (AM1), 9.85 and 9.4 (PM3) eV, respectively. Ab initio HF/3-21G$^{(*)}$ energy-difference calculations by the author give IEs in line with the AM1, rather than the claimed experimental, results: 2-methyl-1-butene, 9.4 eV; 2-methyl-2-butene, 9.1 eV. Calculations by the author on the first 50 of these 256 molecules (of these 50 all but H_2 and H_2O are organic) gave these mean absolute IE errors: AM1, 0.46 (12 negative); PM3, 0.58 (5 negative); ab initio HF/3-21G$^{(*)}$, 0.71 (11 negative). So for the set of 256 mostly organic molecules AM1 and PM3 gave essentially the same accuracy, and for the set of 50 molecules AM1 was slightly better than PM3 and the ab initio method was slightly worse than the semiempirical ones. The HF/3-21G$^{(*)}$ level is the lowest ab initio one routinely used (or at least reported) nowadays, and is less popular now than HF/6-31G*. Ionization energies and electron affinities comparable in accuracy to those from experiment can be obtained by high-accuracy ab initio calculations (Chap. 5, Sects 5.5.2.3.2 and 5.5.5) and by DFT (Chap. 7), using the energy difference of the two species involved.

Dewar and Rzepa found that the MNDO (Sect. 6.2.5.3) electron affinities of 26 molecules with delocalized HOMOs (mostly radicals and conjugated organic molecules) had an absolute mean error of 0.43 eV; for ten molecules with the HOMO localized on one atom, the error was 1.40 eV [121]. The errors from AM1 or PM3 should be less than for these MNDO calculations.

6.3.6   *Visualization*

Many molecular features that have been calculated semiempirically can be visualized, in a manner analogous to the case of ab initio calculations (Chap. 5, Sect. 5.5.6). Clearly, one wishes to be able to view the molecule, rotate it, and query it for geometric parameters. Semiempirically calculated vibrations, electrostatic potentials, and molecular orbitals also provide useful information when visualized, and little need be added beyond that already discussed for the visualization of ab initio results. AM1 and PM3 surfaces (van der Waals surfaces, electrostatic potentials, orbitals) are usually very similar in appearance to those calculated by ab initio methods, but exceptions occasionally occur. An example is the case of HCC^-, the conjugate base of ethyne (acetylene), Fig. 6.10. AM1 predicts that there is one HOMO and that it is of σ symmetry (symmetric about the molecular axis), but an HF/3-21G$^{(*)}$ calculation predicts that there are two HOMOs of equal energy at right angles, each of π symmetry (having a nodal plane containing the molecular axis; one of these π-HOMOs is shown in Fig. 6.10). The HF/3-21G orbital pattern persists at the HF/6-31G* and MP2/6-31G* levels. Different orbital patterns at different calculational levels is not the rule, but is understandable since near-lying MOs may have their energetic priorities reversed on going to a different level.
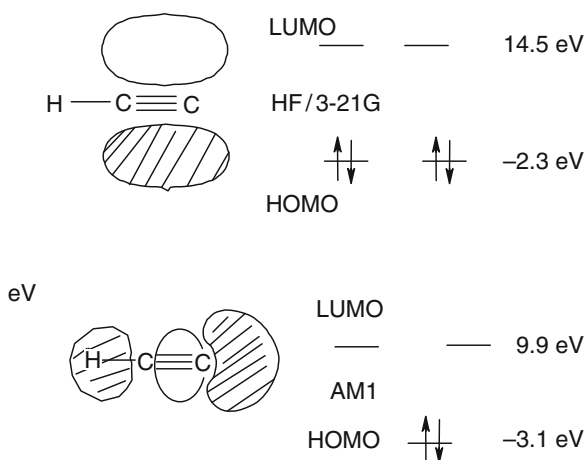
Fig. 6.10   The HOMO of the ethyne conjugate base, calculated by AM1 and by HF/3-21G$^{(*)}$. AM1 predicts the HOMO to be unique and of σ symmetry (symmetrical about the molecular axis), but HF/3-21G$^{(*)}$ predicts degenerate HOMO levels (the other is rotated 90° about the molecular axis) of π symmetry (with nodal planes containing the molecular axis) Only one of the degenerate 3-21G HOMOs is shown here. The orbitals were calculated and visualized with Spartan [56]. From your knowledge of the anion as a reagent in synthesis, which result do you think is more likely to be the correct one?

6.3.7 Some General Remarks

AM1 and PM3 have become extremely useful not only because they allow quantum mechanical calculations to be done on molecules which are still too big for ab initio or DFT (Chap. 7) methods, but also as adjuncts to these latter methods, since they often allow a relatively rapid survey of a problem, such as an exploration of a potential energy surface: one can locate minima and transition states, then use the semiempirical structures as inputs for initial geometries, wavefunctions and Hessians (Chap. 5, Sect. 2.4) in a higher-level geometry optimization, size permitting. If geometry optimizations are not feasible, single-point calculations on AM1 or PM3 geometries, which are usually reasonably good, will likely give improved relative energies. The time is well past when semiempirical calculations were regarded by many as "worthless" [122], or, at best, a poor substitute for ab initio calculations. In fact, in his thoughtful review Tim Clark, a major worker in the field of developing semiempirical methods has described "The NDDO-approximation [as] one of the most successful and least appreciated in modern theoretical chemistry" [11]. Recall that modern general-purpose semiempirical methods are based on NDDO (Sect. 6.2.5). In his book which focusses on ab initio and density functional methods, Bachrach implies that faster computers and more efficient algorithms will make semiempirical methods less important [123]; a more extreme view was recently expressed by the president of a major computational chemistry software company, who told this author that he thought semiempirical methods would soon be replaced by DFT; and a rather dismissive rejection of the general enterprise of employing the semiempirical approach in science came from the mathematician John von Neumann " [124]: "With four parameters I can cover an elephant, and with five I can make him wiggle his trunk." Elephants aside, Clark rejects the opinion of "pundits [who] predict the demise" of modern semiempirical methods. He makes the interesting point that Dewar (Sect. 6.2.5.1 and [24]) may have made a mistake in "trying to match" the ab initio methods of the time "on its own ground", namely achieving good geometries and energies for small molecules, instead of concentrating on the forte of semiempirical methods, large molecules. This review [11] is commended to the reader. A caveat is in order regarding the application of semiempirical methods to large biomolecules: the most popular program suites for studying proteins and nucleic acids, AMBER [125] and CHARMM/CHARMm [125], use molecular mechanics (MM, Chap. 3). One seems justified in being sceptical [e.g. [126]] of the appropriateness of semiempirical methods for geometry optimization of such biomolecules, since the relevant MM forcefields have been very carefully parameterized for them and are much faster. A useful procedure would be to optimize the molecule with MM, then perform a single-point (unchanged geometry) semiempirical calculation to obtain a wavefunction, from which electronic properties like charges can be calculated.

The philosophical divide we saw in, for example, the exchange between Dewar and Halgren, Kleir and Lipscomb (Sect. 6.2.5.1), persists. One gets the impression that certain journals are reluctant to publish purely theoretical semiempirical

papers; ironically, these journals have no such reservations against density functional theory (Chap. 7), despite its significant semiempirical characteristics [11]. Where the emphasis is on getting practical results for commercial applications, rather than on esthetic purity, semiempirical and molecular mechanics methods rule. In the fields of cheminformatics (chemoinformatics, chemical informatics) [127], and quantitative structure-activity relationships, QSAR [128], thousands of drug candidates (usually "small" molecules) can be geometry-optimized and screened for potential pharmacological activity in 1 day [11]. In this connection, since ca. 2012 machine-learning methods have been applied to improving the parameterization of semiempirical programs, which can greatly reduce average and maximum energy errors for sets of compounds, and is said to hold "promise for fast and reasonably accurate high-throughput screening of materials and molecules." [129]

6.4 Strengths and Weaknesses of Semiempirical Methods

These remarks refer to NDDO methods like AM1 and PM3.

6.4.1 Strengths

Semiempirical calculations are very fast compared to ab initio and even to DFT (Chap. 7), and this speed is often obtained with at most a tolerable loss of accuracy. Semiempirical geometries of normal molecules are entirely adequate for many purposes, and even transition state geometries are often adequate. Reaction and activation energies, although not accurate (except by chance cancellation of heat of formation errors), will probably expose any marked trends in a series. Surprisingly, although they were parameterized using normal, stable molecules, AM1 and PM3 usually give fairly realistic geometries and useful relative energies for cations, radicals, anions, strained molecules, and even transition states.

6.4.2 Weaknesses

A major weakness of semiempirical methods is that they must be assumed to be unreliable outside molecules of the kind used for their training set (the set of molecules used to parameterize them), until shown otherwise by comparison of their predictions with experiment or with high-level ab initio (or probably DFT) calculations. Although, as Dewar and Storch pointed out [130], the reliability of ab initio calculations, too, should be checked against experiment, the situation is somewhat different for these latter, at least at the higher levels; studies of exotic

species, in particular, are certainly more trustworthy when done ab initio than semiempirically (see Chap. 8). Semiempirical heats of formation are subject to errors of tens of kJ mol^{-1}, and thus heats (enthalpies) of reaction and activation could be in error by scores of kJ mol^{-1}. AM1 and PM3 underestimate steric repulsions, overestimate basicity and underestimate nucleophilicity, and can give unreasonable charges and structures; PM3 has been reported to tend to give more reliable structures, and AM1 better energies [115]. Neither AM1 nor PM3 are generally reliable in modelling hydrogen bonds [131, 132], and the reclusive SAM1 appears to be the semiempirical method of choice here [88], although PM6 (Sect. 6.2.5.6) has been said [82, 83] to represent an improvement in the treatment of hydrogen bonds.

In general, the accuracy of semiempirical methods, particularly in energetics, falls short of that of current routine ab initio methods (this may not have been the case when AM1 was developed, in 1985 [130]). Parameters may not be available for the elements in the molecules one is interested in, and obtaining new parameters is something rarely done by people not actively engaged in developing new methods. Semiempirical errors are less systematic than ab initio, and thus harder to correct for. Clark has soberly warned that "All parameterized techniques can interpolate and none can extrapolate consistently and well", thus we can expect on occasion "a catastrophic failure"; but semiempirical methods "will do what they are designed to do." [11].

6.5 Summary

Semiempirical quantum mechanical calculations are based on the Schrödinger equation. This chapter deals with SCF semiempirical methods, in which repeated diagonalization of the Fock matrix refines the wavefunction and the molecular energy. The simple and extended Hückel methods, in contrast, need only one matrix diagonalization because their Fock matrix elements are not calculated using a wavefunction guess (Chap. 4). The methods of this chapter are much faster than ab initio ones, mainly because the number of integrals to be dealt with is greatly reduced by ignoring some and approximating others with the help of experimental ("empirical") quantities, and, nowadays, results from high-level ab initio or DFT calculations. In order of increasing sophistication, these SCF semiempirical procedures have been developed: PPP (Pariser-Parr-Pople), CNDO (complete neglect of differential overlap), INDO (intermediate neglect of differential overlap), and NDDO (neglect of diatomic differential overlap). The PPP method is limited to π electrons, while CNDO, INDO and NDDO use all the valence electrons. All four use the ZDO (zero differential overlap) approximation, which sets the differential of the overlap integral equal to zero; this greatly reduces the number of integrals to be calculated. Traditionally, these methods were parameterized mostly using experimental quantities (usually ionization energies and electron affinities), but also (PPP and CNDO) making some use of minimal-basis-set (i.e. low-level) ab initio calculations. Of

these original methods, only versions of INDO parameterized to reproduce experimental UV spectra (INDO/S and its variant ZINDO/S) are much used nowadays. Today the most popular SCF semiempirical methods are AM1 (Austin method 1) and PM3 (parametric method 3), which are NDDO-based, carefully parameterized to reproduce experimental quantities (primarily heats of formation). AM1 and PM3 perform similarly and usually give quite good geometries, but less satisfactory heats of formation and relative energies. A modification of AM1 called SAM1 (semi-ab initio method 1), relatively little-used, is said to be an improvement over AM1. AM1 and SAM1 represent work by the group of M. J. S. Dewar. PM3 is a version of AM1, by J. J. P. Stewart, differing mainly in a more automatic approach to parameterization. Recent extensions of AM1 (RM1) and PM3 (PM6. PM7) seem to represent significant improvements and are likely to be the standard general-purpose semiempirical methods in the near future.

Easier Questions

1. Outline the similarities and differences between the extended Hückel method on the one hand and methods like AM1 and PM3 on the other. What advantages does the EHM have over more accurate semiempirical methods?
2. Outline the similarities and differences between molecular mechanics, ab initio, and semiempirical methods.
3. Both the simple Hückel and the PPP methods are π electron methods, but PPP is more complex. Itemize the added features of PPP.
4. What is the main advantage of an all-valence-electron method like, say, CNDO over a purely π electron method like PPP?
5. Explain the terms ZDO, CNDO, INDO, and NDDO, showing why the latter three represent a progressive conceptual improvement.
6. How does an AM1 or PM3 "total electron wavefunction" Ψ differ from the Ψ of an ab initio calculation?
7. Ab initio energies are "total dissociation" energies (dissociation to electrons and atomic nuclei) and AM1 and PM3 energies are standard heats of formation. Is one of these kinds of energy more useful? Why or why not?
8. For certain kinds of molecules molecular mechanics can give better geometries and relative energies than can even sophisticated semiempirical methods. What kinds of properties can the latter calculate that MM cannot?
9. Why do transition metal compounds present special difficulties for AM1 and PM3?
10. Although both AM1 and PM3 normally give good molecular geometries, they are not too successful in dealing with geometries involving hydrogen bonds. Suggest reasons for this deficiency.

Harder Questions

1. Why are even very carefully-parameterized semiempirical methods like AM1 and PM3 not as accurate and reliable as high-level (e.g. MP2, CI, coupled-cluster) ab initio calculations?

2. Molecular mechanics is essentially empirical, while methods like PPP, CNDO, and AM1/PM3 are semiempirical. What are the analogies in PPP etc. to MM procedures of developing and parameterizing a forcefield? Why are PPP etc. only *semi*empirical?

3. What do you think are the advantages and disadvantages of parameterizing semiempirical methods with data from ab initio calculations rather than from experiment? Could a SE method parameterized using ab initio calculations logically be called semi*empirical*?

4. There is a kind of contradiction in the Dewar-type methods (AM1, etc.) in that overlap integrals are calculated and used to help evaluate the Fock matrix elements, yet the overlap matrix is taken as a unit matrix as far as diagonalization of the Fock matrix goes. Discuss.

5. What would be the advantages and disadvantages of using the general MNDO/AM1 parameterization procedure, but employing a minimal basis set instead of a minimal valence basis set?

6. In SCF semiempirical methods major approximations lie in the calculation of the H_{rs}^{core}, $(rs|tu)$, and $(ru|ts)$ integrals of the Fock matrix elements F_{rs} (Eq. (6.1=5.82)). Suggest an alternative approach to approximating one of these integrals.

7. Read the exchange between Dewar on the one hand and Halgren, Kleir and Lipscomb on the other [27]. Do you agree that semiempirical methods, even when they give good results "inevitably obscure the physical bases for success (however striking) and failure alike, thereby limiting the prospects for learning why the results are as they are." Explain your answer.

8. It has been said of semiempirical methods: "They will never outlive their usefulness for correlating properties across a series of molecules...I really doubt their predictive value for a one-off calculation on a small molecule on the grounds that whatever one is seeking to predict has probably already been included in with the parameters." (A. Hinchliffe, "Ab Initio Determination of Molecular Properties", Adam Hilger, Bristol, 1987, p. x). Do you agree with this? Why or why not? Compare the above quotation with ref. [24], pp 133–136.

9. For a set of common organic molecules Merck Molecular Force field geometries are nearly as good as MP2(fc)/6–31G* geometries (Chap. 3, Sect. 3.4). For such molecules single-point MP2(fc)/6–31G* calculations (Chap. 5, Sect. 5.4.2), which are quite fast, on the MMFF geometries, should give energy differences comparable to those from MP2(fc)/6–31G*//MP2(fc)/6–31G* calculations. Example: $CH_2 = CHOH/CH_3CHO$, ΔE (MP2 opt, including ZPE) $= 71.6 \, kJ \, mol^{-1}$, total time 1064 s.; ΔE (MP2 single point on MMFF

geometries) $= 70.7\,\mathrm{kJ\,mol^{-1}}$, total time $= 48$ s. (G98 on a Pentium 3). What role does this leave for semiempirical calculations?

10. Semiempirical methods are untrustworthy for "exotic" molecules of theoretical interest. Give an example of such a molecule and explain why it can be considered exotic. Why can't semiempirical methods be trusted for molecules like yours? For what other kinds of molecules might these methods fail to give good results?

References

1. (a) Weinberg S (1992) Dreams of a final theory: the search for the fundamental laws of nature. Pantheon Books, New York; (b) Watson A (2000) Measuring the physical constants. Science 287:1391
2. Hartree DR (1928) Proc Cambridge Phil Soc 24:89, 111, 426
3. Bolcer JD, Hermann RB (1994) Chapter 1: The history of the development of computational chemistry (in the United States). In: Lipkowitz KB, Boyd DB (eds) Reviews in computational chemistry, vol 8. VCH, New York
4. Ref. 3, p 12
5. Dewar MJS (1969) The molecular orbital theory of organic chemistry. McGraw-Hill, New York, p 73
6. This book, Chapter 5, reference [333]
7. Dewar MJS (1969) The molecular orbital theory of organic chemistry. McGraw-Hill, New York, chapter 3
8. Levine IN (2014) Quantum chemistry, 7th edn. Prentice Hall, Engelwood Cliffs, sections 17.1–17.4
9. Thiel W (1996) In: Prigogine I, Rice SA (eds) Adv Chem Phys XCIII Wiley, New York
10. Pople JA, Beveridge DL (1970) Approximate molecular orbital theory. McGraw-Hill, New York
11. Clark T (2000) J Mol Struct (Theochem) 530:1
12. Pariser R, Parr RG (1953) J Chem Phys 21:466, 767
13. Pople JA (1953) Trans Faraday Soc 49:1475
14. (a) Chemie in unserer Zeit (1993) 12:21–31; (b) Griffiths J (1986) Chemistry in Britain. 22:997–1000
15. Pople JA, Segal GA (1966) J Chem Phys 44:3289, and refs. therein
16. Coffey P (1974) Int J Quantum Chem 8:263
17. Ref. 7, pp 90–91
18. Ref. 10, p 76
19. (a) Pople JA, Beveridge DL, Dobosh PA (1967) J Chem Phys 47:2026; (b) Dixon RN (1967) Mol Phys 12:83
20. INDO/S: Kotzian M, Rösch N, Zerner MC (1992) Theor Chim Acta 81:201. (b) ZINDO is a version of INDO/S with some modifications, plus the ability to handle transition metals. The Z comes from the name of the late Professor Michael C. Zerner, whose group developed the suite of (mostly semiempirical) programs called ZINDO, which includes ZINDO/S. ZINDO is available from, e.g., Molecular Simulations Inc., San Diego, CA., and CAChe Scientific, Beaverton, OR, and Gaussian
21. Pople JA, Santry DP, Segal GA (1965) J Chem Phys 43:S 129; Pople JA, Segal GA (1965) J Chem Phys 43:S 136; Pople JA, Segal GA (1966) J Chem Phys 44:3289
22. Boyd DB (1995) Chapter 5. In: Lipkowitz B, Boyd DB (eds) Reviews in computational chemistry. vol 6. VCH, New York

23. (a) Wilson E (1998) Chemical & engineering news. 19:12; (b) Malakoff D (1998) Science 282:610; (c) Nobel lecture. Angew Chem Int. Ed, (1999) 38:1895
24. Dewar MJS (1992) A semiempirical life. American Chemical Society, Washington, DC
25. Ref. 24, p 131
26. Dewar MSJ (1975) J Am Chem Soc 97:6591. In response to criticisms of MINDO/3 by Pople (Pople JA (1975) J Am Chem Soc 97:5306) and Hehre (Hehre WJ (1975) J Am Chem Soc 97:5308)
27. Dewar MJS (1975) Science 187:1037
28. Halgren TA, Kleier DA, Lipscomb WN (1975) Science 190:591; response: Dewar MJS (1975) Science 190:591
29. Dewar MJS (1983) J Mol Struct 100:41
30. Dewar MJS, Jie C (1992) Acc Chem Res 25:537
31. Li Y, Houk KN (1993) J Am Chem Soc 115:7478
32. Ref. 24, p 125
33. Bingham RC, Dewar MJS, Lo DH (1975) J Am Chem Soc 97:1285
34. Levine IN (2014) Quantum chemistry, 7th edn. Prentice Hall, Engelwood Cliffs, pp 626–627
35. Dewar MJS, Klopman G (1967) J Am Chem Soc 89:3089
36. Baird NC, Dewar MJS (1969) J Chem Phys 50:1262
37. Clark T (1985) A handbook of computational chemistry. Wiley, New York, chapter 4
38. (a) First appearance of MNDO: Dewar MJS, Thiel W (1977) J Am Chem Soc 99:4899; (b) Results of MNDO calculations on molecules with H, C, N, O: Dewar MJS, Thiel W (1977) J Am Chem Soc 99:4907; (c) Results for molecules with B; Dewar MJS, McKee ML (1977) J Am Chem Soc 99:5231
39. Offenhartz PO'D (1970) Atomic and molecular orbital theory. McGraw-Hill, New York, p 325, (these matrix elements are zero because the AO functions belong to different symmetry species, while the operator (kinetic plus potential energy) is spherically symmetric
40. Dewar MJS, Thiel W (1977) Theor Chim Acta 46:89
41. Stewart JJP (1989) J Comp Chem 10:209
42. Thiel W (1988) Tetrahedron 44:7393
43. (a) Thiel W, Voityuk AA (1996) J Phys Chem 100:616; (b) Thiel W (1996) Adv Chem Phys 93:703; in particular, pp 722–725
44. Lewars E (2008) Modeling marvels. Springer, Amsterdam; chapter 4
45. Gorelsky SI (2004) In McCleverty JA, Meyer TJ (eds) Comprehensive coordination chemistry, II. 2:467
46. (a) Thiel W (1981) J Am Chem Soc 103:1413; (b) Thiel W (1981) J Am Chem Soc 103:1420. (c) Schweig A, Thiel W (1981) J Am Chem Soc 103:1425
47. (a) Schröder S, Thiel W (1985) J Am Chem Soc 107:4422; (b) Schröder S, Thiel W (1986) J Am Chem Soc 108:7985; (c) Schröder S, Thiel W (1986) J Mol Struct (Theochem) 138:141
48. Bachmann C, Huessian TY, Debû F, Monnier M, Pourcin J, Aycard J-P, Bodot H (1990) J Am Chem Soc 112:7488
49. Scott AP, Nobes RH, Schaefer HF, Radom L (1994) J Am Chem Soc 116:10159
50. Delamere C, Jakins C, Lewars E (2002) Can J Chem 80:94
51. Fowler JE, Galbraith JM, Vacek G, Schaefer HF (1994) J Am Chem Soc 116:9311
52. (a) Lewars L (2008) Modeling marvels. Springer, Amsterdam; chapter 3; (b) Lewars E (1983) Chem Rev 83:519
53. (a) Vacek G, Galbraith JM, Yamaguchi Y, Schaefer HF, Nobes RH, Scott AP, Radom L (1994) J Phys Chem 98:8660; (b) Vacek G, Colegrove BT, Schaefer HF (1991) Chem Phys Lett 177:468
54. Cramer J (2004) Essentials of computational chemistry, 2nd edn. Wiley, Chichester, p 145
55. Gaussian is available for several operating systems; see Gaussian, Inc., http://www.gaussian.com, 340 Quinnipiac St., Bldg. 40, Wallingford, CT 06492, USA. As of 2015, the latest "full" version (as distinct from more frequent revisions) of the Gaussian suite of programs was Gaussian 09. The name arises from the fact that ab initio basis sets use Gaussian functions

56. Spartan is an integrated molecular mechanics, ab initio and semiempirical program with an input/output graphical interface. It is available for several operating systems; see Wavefunction Inc., http://www.wavefun.com, 18401 Von Karman, Suite 370, Irvine CA 92715, USA. As of 2015, the latest version of Spartan was Spartan'14. The name arises from the adjective spartan, in the sense of simple, unpretentious

57. AMPAC is a semiempirical suite of programs. It can be leased from Semichem, Inc., http://www.semichem.com/default.php, 12456 W, 62nd Terrace, Suite D, Shawnee, KS 66216, USA. As of 2015, the latest version of AMPAC was AMPAC 10. The name means Austin method package; cf. AM1

58. MOPAC is a semiempirical suite of programs. It can be obtained from http://www.cacheresearch.com/mopac.html, CAChe Research, CAChe Research LLC, 13690 SW Otter Lane, Beaverton, OR 97008, USA. As of 2015, the latest version of MOPAC was MOPAC 12. The name means Molecular Orbital Package, but is said to have been inspired by this geographical oddity: "The original program was written in Austin, Texas. One of the roads in Austin is unusual in that the Missouri-Pacific railway runs down the middle of the road. Since this railway was called the MO-PAC, when names for the program were being considered, MOPAC was an obvious contender". See http://openmopac.net/manual/index_troubleshooting.html

59. For Dewar's very personal reminiscences of Austin see ref. 24, pp 111–120

60. Dewar MJS, Zoebisch EG, Healy EF, Stewart JJP (1985) J Am Chem Soc 107:3902

61. Levine IN (2014) Quantum chemistry, 7th edn. Prentice Hall, Engelwood Cliffs, p 630

62. Reference [24], pp 134, 135

63. Dannenberg JJ, Evleth EM (1992) Int J Quantum Chem 44:869

64. Rocha GB, Freire RO, Simas AM, Stewart JJP (2006) J Comp Chem 27:1101

65. Voityuk AA, Roesch N (2000) J Phys Chem A 104:4089

66. Imhof P, Noe F, Fischer S, Smith JC (2006) J Chem Theory Comput 2:1050

67. Nam K, Cui Q, Gao J, York DM (2007) J Chem Theory Comput 3:486

68. Jomoto J, Lin J, Nakajima T (2002) J Mol Struct (Theochem) 577:143

69. Winget P, Horn AHC, Selçuki C, Bodo M, Clark T (2003) J Mol Model 9:408

70. Stewart JJP (1989) J Comp Chem 10:221

71. Stewart JJP (1991) J Comp Chem 12:320

72. Dewar MJS, Healy EF, Holder AJ, Yuan Y-C (1990) J Comp Chem 11:541

73. Stewart JJP (1990) J Comp Chem 11:543

74. Ref. 24, p 185

75. Holder AJ, Dennington RD, Jie C (1994) Tetrahedron 50:627

76. Dewar MJS, Jie C, Yu J (1993) Tetrahedron 49:5003

77. (a) Hehre WJ, Yu J, Adei E (1996) Abstracts of papers of the ACS 212, COMP 092; (b) Hehre WJ, Yu J, Klunziger PE (1997) A guide to molecular mechanics and molecular orbital calculations in spartan. Wavefunction Inc., Irvine, CA

78. Bosque R, Maseras F (2000) J Comp Chem 21:562

79. (a) Cobalt and nickel: Zakharian TY, Coon SR (2001) Computers and chemistry (Oxford) 25:135; (b) Transition metal complexes of C_{60} and C_{70}: Jemmis ED, Sharma PF (2001) J Molec Graphics and Model 19:256; (c) Spin state of transition metal complexes: Ball DM, Buda C, Gillespie AM, White DP, Cundari TR (2002) Inorg Chem 41:152; (d) Technetium: Buda C, Burt SK, Cundari TR, Shenkin PS (2002) Inorg Chem 41:2060; (e) Molybdenum and vanadium: Nemykin VN, Basu P (2003) Inorg Chem 42:4046; (f) review of semiempirical methods for transition metals: Gorelski SI (2004) In: McCleverty JA, Meyer TJ Comprehensive coordination chemistry II. 2:467; (g) Comparison of PM3/tm with CATIVIC, a new parameterized method: Martinez R, Brito F, Araujo ML, Ruette F, Sierraalta A (2004) Int J Quantum Chem 97:854; (h) De novo prediction of ground states: Buda C, Cundari TR (2004) J Mol Struct (Theochem) 686:137; (i) De novo prediction of ground states: Buda C, Flores A, Cundari TR (2005) J Coord Chem 58:575; (j) Chromium derivatives of sucrose: Parada J, Ibarra C, Gillitt ND, Bunton CA (2005) Polyhedron 24:1002

80. Cramer CJ (2004) Essentials of computational chemistry, 2nd edn. Wiley, Chichester, p 155
81. http://www.cache.fujitsu.com/mopac/Mopac2002manual/node650.html
82. Stewart JJP (2007) J Mol Model 13:1173
83. http://openmopac.net/MOPAC2009brochure.pdf
84. Stewart JJP (2004) J Phys Chem Ref Data 33:713
85. From "Accuracy", in MOPAC2009 manual: http://openmopac.net/manual/accuracy.html
86. Stewart JJP (2013) J Mol Model 19:1
87. (a) Repasky MP, Chandrasekhar J, Jorgensen WL (2002) J Comp Chem 23:1601; (b) Tubert-Brohman I, Guimarães CRW, Repasky MP, Jorgensen WL (2004) J Comp Chem 25:138; (c) Tubert-Brohman I, Guimarães CRW, Jorgensen WL (2005) J Chem Theory Comput 1:817
88. Holder AJ, Evleth EM (1994) Chapter 7. In Smith DA (ed) Modelling the hydrogen Bond. American Chemical Society, Washington, DC
89. Elstner M (2006) Theor Chem Acc 116:316, and references therein
90. Goringe CM, Bowler DR, Hernández E (1997) Rep Prog Phys 60:1447
91. (a) Version PMO2a, the study of aerosol clusters of H_2SO_4, Me_2NH, NH_3: L. Fiedler, H. Leverentz R, Nachimuthu S, Friedrich J, Truhlar DG (2014) J Chem Theory Comput 10:3129; (b) Theory of PMO2: Isegawa M, Fiedler L, Leverentz HR, Wang Y, Nachimuthu S, Gao J, Truhlar DJ (2013) J Chem Theory Comput 9:33; (c) Strutyński K, Gomes JANF, Melle-Franco M (2014) J Phys Chem A 118:9561
92. (a) Thiel W (2014) *WIREs Comput Mol Sci* 4:145. doi: 10.1002/wcms.1161, and references therein; (b) Korth M, Thiel W (2011) J Chem Theory Comput 7:2929
93. Levine IN (2014) Quantum chemistry, 7th edn. Prentice Hall, Engelwood Cliffs, pp 626–634
94. Hehre WJ (1995) Practical strategies for electronic structure calculations. Wavefunction, Inc, Irvine
95. (a) Stewart JJP (1997) J Mol Struct (Theochem) 410:195. (b) Stewart JJP (1996) Int J Quantum Chem 58:133
96. Hehre WJ, Radom L, Schleyer PVR, Pople JA (1986) Ab initio molecular orbital theory. Wiley, New York; section 6.2
97. *$H_2C=CHOH$ reaction* The only quantitative experimental information on the barrier for this reaction seems to be: Saito S (1976) Chem Phys Lett 42:399, halflife in the gas phase in a Pyrex flask at room temperature ca. 30 minutes. From this one calculates (section 5.5.2.2d, Eq (5.202)) a free energy of activation of 93 kJ mol^{-1}. Since isomerization may be catalyzed by the walls of the flask, the purely concerted reaction may have a much higher barrier. This paper also shows by microwave spectroscopy that ethenol has the O-H bond *syn* to the C=C. The most reliable measurement of the ethenol/ethanal equilibrium constant, by flash photolysis, is $5.89 \times 10{-}7$ in water at room temperature (Chiang Y, Hojatti M, Keeffe JR, Kresge AK, Schepp NP, Wirz J (1987) J Am Chem Soc 109:4000). This gives a free energy of equilibrium of 36 kJ mol^{-1} (ethanal 36 kJ mol^{-1} below ethenol). *HNC reaction* The barrier for rearrangement of HNC to HCN has apparently never been actually measured. The equilibrium constant in the gas phase at room temperature was calculated (Maki AG, Sams RL (1981) J Chem Phys 75:4178) at 3.7×10^{-8}, from actual measurements at higher temperatures; this gives a free energy of equilibrium of 42 kJ mol^{-1} (HCN 42 kJ mol^{-1} below HNC). According to high-level ab initio calculations supplemented with experimental data (Active Thermochemical Tables) HCN lies 62.35 ± 0.36 kJ mol^{-1} (converting the reported spectroscopic cm^{-1} energy units to kJ mol^{-1}) below HNC; this is "a recommended value...based on all currently available knowledge": Nguyen TL, Baraban JH, Ruscic B, Stanton JF (2015) J Phys Chem 119:10929. *CH_3NC reaction* The reported experimental activation energy is 161 kJ mol^{-1} (Wang D, Qian X, Peng J (1996) Chem Phys Lett 258:149; Bowman JM, Gazy B, Bentley JA, Lee TJ, Dateo DE (1993) J Chem Phys 99:308; Rabinovitch BS. Gilderson PW (1965) J Am Chem Soc 87:158; Schneider FW, Rabinovitch BS (1962) J Am Chem Soc 84:4215). The energy difference between CH_3NC and CH_3NC has apparently never been actually measured. *Cyclopropylidene reaction* Neither the barrier nor the equilibrium constant for the cyclopropylidene/allene reaction have been measured. The only

direct experimental information of these species come from the failure to observe cyclopropylidene at 77 K (Chapman OL (1974) Pure and applied chemistry 40:511). This and other experiments (references in Bettinger HF, Schleyer PVR, Schreiner PR, Schaefer HF (1997) J Org Chem 62:9267 and in Bettinger HF, Schreiner PR, Schleyer PVR, Schaefer HF (1996) J Phys Chem 100:16147) show that the carbene is much higher in energy than allene and rearranges very rapidly to the latter. Bettinger et al., 1997 (above) calculate the barrier to be 21 kJ mol^{-1} (5 kcal mol^{-1})

98. Thiel W (1998) Chapter 8. In: Irikura KK, Frurip DJ (eds) Computational thermochemistry. American Chemical Society, Washington, DC

99. (a) Bond D (2007) J Org Chem 72:5555; (b) Pedley JB (1994) Thermochemical data and structures of organic compounds. Thermodynamics Research Center, College Station, Texas.

100. (a) CO_2/N_2 copolymers: Bylykbashi J, Lewars E (1999) J Mol Struct (Theochem) 469:77; (b) Oxirenes: Lewars E (2000) Can J Chem, 78:297–306

101. Some examples are (a) Activation enthalpies of cytochrome-P450-mediated hydrogen abstractions; comparison of PM3, SAM1, and AM1 with a DFT method: Mayeno AN, Robinson JL, Yang RSH, Reisfeld B (2009) J Chem Inf Model 49:1692. (b) Pyruvate to lactate transformation catalyzed by L-lactate dehydrogenase, attempt to improve accuracy of semiempirical descriptors (AM1/MM): Ferrer S, Ruiz-Pernia JJ, Tunon I, Moliner V, Garcia-Viloca M, Gonzalez-Lafont A, Lluch JM (2005) J Chem Theory Comput 1:750. (c) Mechanism of tyrosine phosphorylation catalyzed by the insulin receptor tyrosine kinase (PM3): Pichierri F, Matsuo Y (2003) J Mol Struct (Theochem) 622:257. (d) A novel type of irreversible inhibitor for carboxypeptidase A (PM3): Chung SJ, Chung S, Lee HS, Kim E-J, Oh KS, Choi HS, Kim KS, Kim JJ, Hahn JH, Kim DH (2001) J Org Chem 66:6462

102. Reference [98], p 157

103. Information supplied by Dr. R. Johnson of the National Institutes of Standards and Technology, USA (NIST): best fits to about 1100 vibrations of about 70 closed-shell molecules. An extensive collection of scaling factors is available on the NIST website (http://srdata.nist.gov/cccbdb/)

104. Scott AP, Radom L (1996) J Phys Chem,.Phys Chem 100:16502

105. Holder AJ, Dennington II RD (1997) J Mol Struct (Theochem) 401:207

106. AM1, MP2(fc)/6–31G*, and experimental IR spectra were compared for 18 of the 20 compounds in Fig. 6.2 (suitable IRs were not found for HOCl and CH_3SH) and for these 10: cyclopentane, cyclopentene, cyclopentanone, pyrrolidine, pyrrole, butanone, diethyl ether, 1-butanol, 2-butanol, and tetrahydrofuran. On the basis of the relative intensities of the bands, of these 28 compounds only for six, HCN, CH_3OH, $H_2C=CH_2$, HOF, cyclopentene and cyclopentanone were both the AM1 and MP2 spectra similar to the experimental; for the others the MP2 IRs were closer to experiment

107. Galabov B, Yamaguchi Y, Remington RB, Schaefer HF (2002) J Phys Chem A 106:819

108. Healy EF, Holder A (1993).J Mol Struct (Theochem) 281:141

109. Coolidge MB, Marlin JE, Stewart JJP (1991) J Comp Chem 12:948

110. Reference 94, pp 74, 76–77, 80–82

111. Hehre WJ, Radom L, Schleyer PVR, Pople JA (1986) Ab initio molecular orbital theory. Wiley, New York; section 6.6.1

112. Scheiner AC, Baker J, Andzelm JW (1997) J Comp Chem 18:775

113. Cramer CJ (2004) Essentials of computational chemistry, 2nd edn. Wiley, Chichester, p 309

114. Bagus PS (2013) Pioneers of quantum chemistry, vol 1122, ACS Symposium Series. American Chemical Society, Washington, DC; Chapter 7, pp 202, 203

115. Anh NT, Frisson G, Solladié-Cavallo A, Metzner P (1998) Tetrahedron 54:12841

116. Jensen F (2007) Introduction to computational chemistry, 2nd edn. Wiley, Hoboken, p 296

117. Lendvay G (1994) J Phys Chem 98:6098

118. Foresman JB, Frisch Æ (1996) Exploring chemistry with electronic structure methods, 2nd edn. Gaussian Inc., Pittsburgh, p 218

119. Levin RD, Lias SG (1982) Ionization potential and appearance potential measurements, 1971–1981. National Bureau of Standards, Washington, DC
120. Curtiss LA, Nobes RH, Pople JA, Radom L (1992) J Chem Phys 97:6766
121. Dewar MJS, Rzepa HS (1978) J Am Chem Soc 100:784
122. Reference [24], p 183
123. Bachrach SM (2014) Computational organic chemistry, 2nd edn. Wiley, Hoboken, p xvi
124. Dyson F (2004) Enrico Fermi quoted to Freeman Dyson those words of von Neumann. Nature 427:297
125. Cramer CJ (2004) Essentials of computational chemistry, 2nd edn. Wiley, Chichester; Table 2.1
126. Cramer CJ (2004) Essentials of computational chemistry, 2nd edn. Wiley, Chichester, p 157
127. (a)"Chemoinformatics: a textbook", Gasteiger J, Engel T (eds). (2004) Wiley. (b) Leach AR, Gille VJ (2003) An introduction to chemoinformatics. Springer
128. (a) Reference 1b, chapter 10. (b) Höltje HD, Folkers G (1996) Molecular modelling, applications in medicinal chemistry. VCH, Weinheim, Germany. (c) van de Waterbeemd H, Testa B, Folkers G (eds) (1997) Computer-assisted lead finding and optimization. VCH, Weinheim, Germany. (d) Tehan BG, Lloyd EJ, Wong MG, Pitt WR, Montana JG, Manallack DT, Garcia E (2002) Fast calculation of electronic properties with reasonable accuracy (the focus here is on acidity). Quantitative Structure-Activiy Relationships 21:457
129. Dral PO, Lilienfeld OAV, Thiel W (2015) J Chem Theory Comput 11:2120, and references therein
130. E.g., Dewar MJS, Storch DM (1985) J Am Chem Soc 107:3898
131. For a series of small, mostly nonbiological molecules AM1 seemed better than PM3, except for O-H/O hydrogen bonds: Dannenberg JJ (1997) J Mol Struct (Theochem) 410:279
132. In model systems of biological relevance, mostly involving water, PM3 was superior to AM1: Zheng YJ, Merz KM (1992) J Comp Chem 13:1151

Chapter 7
Density Functional Calculations

My other hope is that...a basically new ab initio treatment capable of giving chemically accurate results a priori, is achieved soon.

M.J.S. Dewar, *A Semiempirical Life, 1992.*

Abstract Density functional theory is based on the two Hohenberg-Kohn theorems, which state that the ground-state properties of an atom or molecule are determined by its electron density function, and that a trial electron density must give an energy greater than or equal to the true energy (the latter theorem is true only if the exact functional could be used). In the Kohn-Sham approach the energy of a system in formulated as a deviation from the energy of an idealized system with noninteracting electrons. From the energy equation, by minimizing the energy with respect to the Kohn-Sham orbitals the Kohn-Sham equations can be derived, analogously to the Hartree-Fock equations. Finding good functionals is the main problem in DFT. Various levels of DFT and kinds of functionals are discussed. The mutually related concepts of electronic chemical potential, electronegativity, hardness, softness, and the Fukui function are discussed.

7.1 Perspective

We have seen three broad techniques for calculating the geometries and energies of molecules: molecular mechanics (Chap. 3), ab initio methods (Chap. 5), and semiempirical methods (Chaps. 4 and 6). Molecular mechanics is based on a balls-and-springs model of molecules. Ab initio methods are based on the subtler model of the quantum mechanical molecule, which we treat mathematically starting with the Schrödinger equation. Semiempirical methods, from simpler ones like the Hückel and extended Hückel theories (Chap. 4) to the more complex SCF semi-empirical theories (Chap. 6), are also based on the Schrödinger equation, and in fact their "empirical" aspect comes from the desire to avoid the mathematical problems that this equation imposes on ab initio methods. Both the ab initio and the semi-empirical approaches calculate a molecular wavefunction (and molecular orbital energies), and thus represent *wavefunction methods*. However, a wavefunction is not a measurable feature of a molecule or atom – it is not what physicists call an

"observable". In fact there is no general agreement among physicists just what a wavefunction is – is it "only" a mathematical convenience for calculating observable properties, or is it a real physical entity? [1].

Density functional theory, DFT, is based not on the wavefunction, but rather on the electron probability density function or electron density function, commonly called simply the electron density or the charge density, and designated by $\rho(x, y, z)$. This was discussed in Chap. 5, Sect. 5.5.4, in connection with atoms-in-molecules (AIM). This electron density ρ is the "density" in density functional theory, and is the basis not only of DFT, but of a whole suite of methods of regarding and studying atoms and molecules [2]; unlike the wavefunction, it is measurable, e.g. by X-ray diffraction or electron diffraction [3]. Apart from being an experimental observable and being readily grasped intuitively [4], the electron density has a mathematical property particularly suitable for any method with claims to being an improvement on, or at least a valuable alternative to, wavefunction methods: it is a function of position only, that is, of just *three* variables (x, y, z), while the wavefunction of an n-electron molecule is a function of $4n$ variables, three spatial coordinates and one spin coordinate, *for each electron*. A wavefunction for a ten-electron molecule will have 40 variables. In contrast, no matter how big the molecule may be, the electron density remains a function of three variables. The electron density function, then, trumps the wavefunction in three ways: it is measurable, it is intuitively comprehensible, and it is mathematically more tractable.

The mathematical term functional, which is akin to function, is explained in Sect. 7.2.3.1. To the chemist, the main advantage of DFT is that in about the same time needed for an HF calculation one can often obtain results of about the same quality as from MP2 calculations (cf. Chap. 5, Sect. 5.4.2). Chemical applications of DFT are but one aspect of an ambitious project to recast conventional quantum mechanics, i.e. wave mechanics, in a form in which "the electron density, and only the electron density, plays the key role" [5]. It is noteworthy that the 1998 Nobel Prize in chemistry was awarded to John Pople (Chap. 5, Sect. 5.3.3), largely for his role in developing practical wavefunction-based methods, and Walter Kohn,[1] for the development of density functional methods [6]. The wavefunction is the quantum mechanical analogue of the analytically intractable multi-body problem (n-body problem) in astronomy [7], and indeed electron-electron interaction, electron correlation, is at the heart of the major problems encountered in wavefunction calculations (Chap. 5, Sect. 5.4.1). It may be significant that early in his career Kohn worked on a many-body problem in atomic physics [8].

A question sometimes asked is whether DFT should be regarded as a special kind of ab initio method. The case against this view is that the correct mathematical form of the DFT functional is not known, in contrast to conventional ab initio

---

[1]Walter Kohn, born in Vienna 1923. B.A., B. Sc., University of Toronto, 1945, 1946. Ph.D. Harvard, 1948. Instructor in physics, Harvard, 1948–1950. Assistant, Associate, full Professor, Carnegie Mellon University, 1950–1960. Professor of physics, University of California at Santa Diego, 1960–1979; University of California at Santa Barbara 1979-present. Nobel Prize in chemistry 1998. Died Santa Barbara, CA, 2016.

theory where the correct mathematical form of the fundamental equation, the Schrödinger equation, is (we think), known. In conventional ab initio theory, the wavefunction can be improved in a conceptually straightforward way by going to bigger basis sets and higher correlation levels, which takes us closer and closer to an exact solution of the Schrödinger equation, but in DFT there is so far no such straightforward way to systematically improve the functional (Sect. 7.2.3.2); one must feel one's way forward with help from intuition and comparison of the results with experiment and with high-level conventional ab initio calculations. One might argue that in this sense current DFT is semiempirical, but the limited use of empirical *parameters* (typically from zero to about 10), and the possibility of one day finding the exact functional, makes it ab initio in spirit. Indeed, DFT using functionals with no empirical parameters (below) is mathematically as ab initio as wavefunction methods. Were the exact functional known, DFT might indeed give "chemically accurate results a priori" (the Dewar quotation at the start of this chapter). The question of the semiempirical nature of DFT is briefly taken up again, after we have examined the various levels of the method, at the end of Sect. 7.2.3.4.9.

7.2 The Basic Principles of Density Functional Theory

7.2.1 Preliminaries

In the Born interpretation (Chap. 4, Sect. 4.2.6) the square of a one-electron wavefunction ψ at any point X is the probability density (with units of volume^{-1}) for the wavefunction at that point, and $|\psi|^2\, dxdydz$ is the probability (a pure number) at any moment of finding the electron in an infinitesimal volume $dxdydz$ around the point (the probability of finding the electron *at* a mathematical point is zero). For a *multielectron* wavefunction ψ the relationship between the wavefunction ψ and the electron density ρ is more complicated, being the number of electrons in the molecule times the sum over all their spins of the integral of the square of the molecular wavefunction integrated over the coordinates of all but one of the electrons (Chap. 5, Sect. 5.5.4.5, AIM discussion). It can be shown [9] that $\rho(x, y, z)$ is related to the "component" one-electron spatial wavefunctions ψ_i (the molecular orbitals) of a single-determinant wavefunction ψ (recall from Chap. 5, Sect. 5.2.3.1 that the Hartree-Fock ψ can be approximated as a Slater determinant of spin orbitals $\psi_i\alpha$ and $\psi_i\beta$) by

$$\rho = \sum_{i=1}^{n} n_i |\psi_i|^2 \qquad (*7.1)$$

This sum is over the n occupied MOs ψ_i for a closed-shell molecule, for a total of $2n$ electrons. Equation (7.1) applies strictly only to a single-determinant

wavefunction ψ, but for multideterminant wavefunctions arising from configuration interaction treatments (Chap. 5, Sect. 5.4) there are similar equations [10]. A shorthand for $\rho(x, y, z)\ dxdydz$ is $\rho(\mathbf{r})d\mathbf{r}$, where $\mathbf{r}$ is the position vector of the point with coordinates (x, y, z). If the electron density ρ rather than the wavefunction could be used to calculate molecular geometries, energies, etc., this might be an improvement over the wavefunction approach because, as mentioned above, the electron density in an n-electron molecule is a function of only the three spatial coordinates x, y, z, but the wavefunction is a function of $4n$ coordinates. Density functional theory seeks to calculate all the properties of atoms and molecules from the electron density.

Some introductions to and reviews of DFT are:
Introductions:

1. [11] The magisterial book by Parr and Yang. The accent on rigorous presentation of the fundamentals makes it as relevant now as when first published (1989), but one does not have to be faint-hearted to prefer to be initiated by less "technical" introductions.
   These provide good, brief summaries:
2. [12] Levine (2014)
3. [13] Cramer (2004)
4. [14] Jensen (2007)

Reviews:
These are oriented toward developments in and the more recent state of the field (but also give some background information on the theory):

1. [15] Peverati and Truhlar (2014). *The quest for a universal density functional: The accuracy of density functionals across a broad spectrum of databases in chemistry and physics*. The accent is on the functionals from the Truhlar group (e.g. the M06 family, below), but 65 other functionals are examined with 451 data items.
2. [16] Burke (2012). *Perspective on density functional theory*. A good read, pleasantly whimsical (e.g. a disadvantage of DFT is that it "Can only be learned from a DFT guru"). Good compact history and introduction.
3. [17] Cohen, Mori-Sánchez, Yang (2012). *Challenges for Density Functional Theory*. Background, current problems. Quite "technical".
4. [18a] J. P. Wagner, P. R. Schreiner (2015). *London dispersion in molecular chemistry–reconsidering steric effects*. Emphasizes realization of importance of dispersion. [18b] Corminboeuf (2014). *Minimizing Density Functional Failures for Non-Covalent Interactions Beyond van der Waals Complexes*. These weak interactions, often called *dispersion* in computational chemistry, are one of the main challenges to current DFT (see Sect. 7.2.3.4.8).
5. [19] Application of DFT to materials (2014): an issue of Acc. Chem. Res.
6. [20] R. O. Jones (2015). *Density Functional Theory: Its origins, rise to prominence, and future*. Starts with historical survey with knowledgeable references to numerous original papers, moves on to current problems and illustrates triumphs of DFT, yet closes with a thoughtful questioning of its fundamental nature and its future, with ab initio theory as the rival.

After the theory behind DFT has been presented in some detail, references will be given (Sect. 7.2.3.4) to reviews which more specifically address steps toward improving the performance of the method.

7.2.2   Forerunners to Current DFT Methods

The idea of calculating atomic and molecular properties from electron density appears to have arisen from calculations made independently by Enrico Fermi and P. A. M. Dirac in the 1920s on an ideal electron gas, work now well-known as the Fermi-Dirac statistics [21]. In independent work by Fermi [22a] and Thomas [22b], atoms were modelled as systems with a positive potential (the nucleus) located in a uniform (homogeneous) electron gas. This obviously unrealistic idealization, the Thomas-Fermi model [23], or with embellishments by Dirac the Thomas-Fermi-Dirac model [23], gave surprisingly good results for atoms, but failed completely for molecules: it predicted all molecules to be unstable toward dissociation into their atoms (indeed, this is a theorem in Thomas-Fermi theory).

The $X\alpha$ (X = exchange, α is a parameter in the $X\alpha$ equation) method gives much better results [24]. It can be regarded as a more accurate version of the Thomas-Fermi model, and is probably the first chemically useful DFT method. It was introduced in 1951 by Slater [25], who regarded it [26] as a simplification of the Hartree-Fock (Chap. 5, Sect. 5.2.3) approach. The $X\alpha$ method, which was developed mainly for atoms and solids, has also been used for molecules, but has been replaced by the more accurate Kohn-Sham type (Sect. 7.2.3) DFT methods.

7.2.3   Current DFT Methods: The Kohn-Sham Approach

7.2.3.1   Functionals. The Hohenberg-Kohn Theorems

Nowadays DFT calculations on molecules are based on the Kohn-Sham approach, the stage for which was set by two theorems published by Hohenberg and Kohn in 1964 (proved in Levine [27]). The first Hohenberg-Kohn [28] theorem says that all the properties of a molecule in a ground electronic state are determined by the ground state electron density function $\rho_0(x, y, z)$. In other words, given $\rho_0(x, y, z)$ we can in principle calculate any ground state property, e.g. the energy, E_0; we could represent this as

$$\rho_0(x, y, z) \rightarrow E_0 \tag{7.2}$$

The relationship (7.2) means that E_0 is a *functional* of $\rho_0(x, y, z)$. A *function* is a rule that transforms a number into another (or the same) number:

$$2 \xrightarrow{x^3} 8$$
$$1 \xrightarrow{x^3} 1$$

A *functional* is a rule that transforms a function into a number:

$$f(x) = x^3 \xrightarrow{\int_0^2 f(x)dx} \left. \frac{x^4}{4} \right|_0^2 = 4 \tag{7.3}$$

The functional $\int_0^2 f(x)dx$ transforms the function x^3 into the number 4. We designate the fact that the integral is a functional of $f(x)$ by writing

$$\int_0^2 f(x)dx = F[f(x)] \tag{7.4}$$

A functional is a function of a "definite" (cf. the definite integral above) function.

The first Hohenberg-Kohn theorem, then, says that any ground state property of a molecule is a functional of the ground state electron density function, e.g. for the energy

$$E_0 = F[\rho_0] = E[\rho_0] \tag{7.5}$$

The theorem is "merely" an *existence theorem*: it says that a functional F exists, but does not tell us how to find it; this omission is the main problem with DFT. The significance of this theorem is that it assures us that there is in principle a way to calculate molecular properties from the electron density. Thus we can infer that approximate functionals will give at least approximate answers. The theorem is sometimes expressed in a way that may at first sight seem less relevant to calculating energies, namely that the nuclear potential determines the ground-state electron density, or that there is a one-to-one correspondence between the energy and the electron density.

The second Hohenberg-Kohn theorem [28] is the DFT analogue of the wavefunction variation theorem that we saw in connection with the ab initio method (Chap. 5, Sect. 5.2.3.3): it says that any trial electron density function will give an energy higher than (or equal to, if it were exactly the true electron density function) the true ground state energy. In DFT molecular calculations the electronic energy from a trial electron density is the energy of the electrons moving the under the potential of the atomic nuclei. This nuclear potential is called the "external potential", presumably because the nuclei are "external" if we concentrate on the electrons. This nuclear potential is designated $v(\mathbf{r})$, and the electronic energy is denoted by $E_v = E_v[\rho_0]$ (meaning "the E_v functional of the ground state electron density"). The second theorem can thus be stated

$$E_v[\rho_t] \geq E_0[\rho_0] \tag{7.6}$$

where ρ_t is a trial electronic density and $E_0[\rho_0]$ is the true ground state energy, corresponding to the true electronic density ρ_0. The trial density must satisfy the conditions $\int \rho_t(\mathbf{r})d\mathbf{r} = n$, where n is the number of electrons in the molecule (this is analogous to the wavefunction normalization condition; here the number of electrons in all the infinitesimal volumes must sum to the total number in the molecule) and $\rho_t(\mathbf{r}) \geq 0$ for all $\mathbf{r}$ (the number of electrons per unit volume can't be negative). This theorem tells us that any value of the molecular energy we calculate from the Kohn-Sham equations (below, a set of equations analogous to the Hartree-Fock equations, obtained by minimizing energy with respect to electron density) will be greater than or equal to the true energy. This is actually true only if the functional used were exact; see below. The Hohenberg-Kohn theorems were originally proved only for nondegenerate ground states, but have been shown to be valid for degenerate ground states too [29]. The functional of the inequality (7.6) is the correct, exact energy functional (the prescription for transforming the ground state electron density function into the ground state energy). The exact functional is unknown, so *actual* DFT calculations use approximate functionals, and are thus *not* variational: they can give an energy below the true energy. Being variational is a nice characteristic of a method, because it assures us that any energy we calculate is an upper bound to the true energy. However, this is not an essential feature of a method: Møller-Plesset and practical configuration interaction calculations (Chap. 5, Sects. 5.4.2, 5.4.3) are not variational, but this is not regarded as a serious problem.

7.2.3.2   The Kohn-Sham Energy and the KS Equations

The first Kohn-Sham theorem tells us that it is worth looking for a way to calculate molecular properties from the electron density. The second theorem suggests that a variational approach might yield a way to calculate the energy and electron density (the electron density, in turn, could be used to calculate other properties). Recall that in wavefunction theory, the Hartree-Fock variational approach (Chap. 5, Sect. 5.2.3.4) led to the HF equations, which are used to calculate the energy and the wavefunction. An analogous variational approach led (1965) to the Kohn-Sham equations [30], the basis of current molecular DFT calculations. If we had an accurate molecular electron density function ρ and if we knew the correct energy functional, we could (assuming the functional were not impossibly complicated) go straight from the electron density function to the molecular energy, courtesy of the functional. Unfortunately we do not *a priori* have an accurate ρ, and we certainly do not have the correct energy functional, this latter fact being the key problem in density functional theory. The Kohn-Sham approach to DFT mitigates these two problems.

The two basic ideas behind the KS approach are: (1) To express the molecular energy as a sum of terms, only one of which, a relatively small term, involves the "unknown" functional. Thus one hopes that even moderately large errors in this term will not introduce large errors into the total energy. (2) To use an initial guess

of the electron density ρ in the KS equations (analogous to the HF equations) to calculate an initial guess of the KS orbitals and energy levels (below); this initial guess is then used to iteratively refine these orbitals and energy levels, in a manner similar to that used in the HF SCF method. The final KS orbitals are used to calculate an electron density that in turn is used to calculate the energy.

7.2.3.2.1 The Kohn-Sham Energy

The strategy here is to separate the electronic energy of our molecule into a portion which can be calculated accurately without using DFT, and a relatively small term which requires the elusive functional. A key idea in this approach is the concept of a fictitious *noninteracting reference system*, defined as one in which the electrons do not interact and in which (this is very important) the ground state electron density ρ_r is exactly the same as in our real ground state system: $\rho_r = \rho_0$. Noninteracting electrons are readily treated exactly, and the deviations from the behavior of real electrons are swept into a small term involving a functional with which we have to grapple. We are talking here about the *electronic* energy of the molecule; the total internal "frozen-nuclei" energy can be found later by adding in the trivial-to-calculate internuclear repulsions, and the 0 K total internal energy by further adding the zero-point energy from the normal-mode vibrations, just as in HF calculations (Chap. 5, Sect. 5.2.3.6.4).

The ground state electronic energy of the real molecule is the sum of the electron kinetic energies, the nucleus-electron attraction potential energies, and the electron-electron repulsion potential energies:

$$E_0 = \langle T[\rho_0] \rangle + \langle V_{\mathrm{Ne}}[\rho_0] \rangle + \langle V_{\mathrm{ee}}[\rho_0] \rangle \tag{*7.7}$$

The angle brackets remind us that these energy terms are quantum-mechanical average values or "expectation values"; each is a functional of the ground-state electron density, and each has an operator, for kinetic energy etc., just as the total energy has an operator $\hat{H}$. Focussing first on the middle term, the one most easily dealt with: the nucleus-electron potential energy is the sum over all $2n$ electrons (as with our treatment of ab initio theory, we will work with a closed-shell molecule which perforce has an even number of electrons) of the potential corresponding to attraction of an electron for all the nuclei A. The operator is, cf. Chap. 5, Eq. (5.15), middle term :

$$\hat{V}_{\mathrm{Ne}} = \sum_{i=1}^{2n} \sum_{\mathrm{nuclei\ A}} -\frac{Z_A}{\mathbf{r}_{iA}} = \sum_{i=1}^{2n} v(\mathbf{r}_i) \tag{7.8}$$

$Z_A/\mathbf{r}_{iA}$ is the potential energy due to interaction of electron i with nucleus A at the varying distance $\mathbf{r}$; $v(\mathbf{r}_i)$ is the "external potential" (explained in Sect. 7.2.3.1, in connection with Eq. (7.6)) for the attraction of electron i to all the nuclei, and with it we can write the double summation more compactly.

The density function ρ can be introduced into $<V_{Ne}>$ by using the fact [31] that

$$\int \psi \sum_{i=1}^{2n} f(\mathbf{r}_i)\psi \, d\tau = \int \rho(\mathbf{r})f(\mathbf{r})d\mathbf{r} \tag{7.9}$$

where $f(\mathbf{r}_i)$ is a function of the coordinates of the n electrons of a system and ψ is the total wavefunction (the integrations are over spatial and spin coordinates *tau* on the left and spatial coordinates on the right). From Eqs. (7.8) and (7.9), invoking the concept of average or expectation value (Chap. 4, Sect. 5.2.3.3) $\langle V_{Ne} \rangle = \langle \psi [\hat{V}_{Ne}] \psi \rangle$ (the quantum mechanical average value of a quantity is the integral of the operator over the wavefunction) we get

$$\langle V_{Ne} \rangle = \int \rho_0(\mathbf{r})v(\mathbf{r})d\mathbf{r} \tag{7.10}$$

So Eq. (7.7) can be written

$$E_0 = \langle T[\rho_0] \rangle + \int \rho_0(\mathbf{r})v(\mathbf{r})d\mathbf{r} + \langle V_{ee}[\rho_0] \rangle \tag{7.11}$$

The middle term is now a classical electrostatic attraction potential energy expression. Unfortunately this equation for the energy cannot be used as it stands, since we don't know the kinetic and potential energy functionals in the energy terms $\langle T[\rho_0] \rangle$ and $\langle V_{ee}[\rho_0] \rangle$.

To utilize Eq. (7.11), Kohn and Sham introduced the idea of a fictitious reference system of noninteracting electrons which give exactly the same electron density distribution as the real system has. Addressing electronic *kinetic* energy, let us define the quantity $\Delta \langle T[\rho_0] \rangle$ as the deviation of the real electronic kinetic energy from that of the reference system:

$$\Delta \langle T[\rho_0] \rangle \equiv \langle T[\rho_0] \rangle_{\text{rea}} - \langle T[\rho_0] \rangle_{\text{ref}}$$
$$\text{i.e. } \langle T[\rho_0] \rangle - \langle T[\rho_0] \rangle_{\text{ref}} \tag{7.12}$$

Addressing next electronic *potential* energy, let us define a term $\Delta \langle V_{ee} \rangle$ as the deviation of the real electron–electron repulsion energy from a classical charge-cloud coulomb repulsion energy. The classical electrostatic repulsion energy is the summation of the repulsion energies for pairs of infinitesimal volume elements $\rho(\mathbf{r}_1)d\mathbf{r}_1$ and $\rho(\mathbf{r}_2)d\mathbf{r}_2$ (in a classical, nonquantum cloud of negative charge) separated by a distance $\mathbf{r}_{12}$, multiplied by one-half (so that we do not count the $\mathbf{r}_1/\mathbf{r}_2$ repulsion energy and again the $\mathbf{r}_2/\mathbf{r}_1$ energy). The sum of infinitesimals is an integral and so

$$\Delta \langle V_{ee}[\rho_0] \rangle = \langle V_{ee}[\rho_0] \rangle_{\text{rea}} - \frac{1}{2}\iint \frac{\rho_0(\mathbf{r}_1)\rho_0(\mathbf{r}_2)}{r_{12}}d\mathbf{r}_1 d\mathbf{r}_2 \tag{7.13}$$

Actually, the classical charge-cloud repulsion is somewhat inappropriate for electrons in that smearing an electron (a particle) out into a cloud forces it to repel itself, as any two regions of the cloud interact repulsively. One way to compensate for this physically incorrect *electron self-interaction* is with a good exchange-correlation functional (below).

Using (7.12) and (7.13), Eq. (7.11) can be written

$$E_0 = \int \rho_0(\mathbf{r})v(\mathbf{r})d\mathbf{r} + \langle T[\rho_0]\rangle_{\mathrm{ref}} + \frac{1}{2}\iint \frac{\rho_0(\mathbf{r}_1)\rho_0(\mathbf{r}_2)}{\mathbf{r}_{12}}d\mathbf{r}_1 d\mathbf{r}_2 \\ + \Delta\langle T[\rho_0]\rangle + \Delta\langle V_{\mathrm{ee}}[\rho_0]\rangle \tag{7.14}$$

The two "delta terms" which have been placed side by side encapsulate the main problem with DFT: the sum of the kinetic energy deviation from the reference system and the electron–electron repulsion energy deviation from the classical system, called the *exchange-correlation energy*. In each term an unknown functional transforms electron density into an energy, kinetic and potential respectively. This exchange-correlation energy is a functional of the electron density function:

$$E_{\mathrm{XC}}[\rho_0] \equiv \Delta\langle T[\rho_0]\rangle + \Delta\langle V_{\mathrm{ee}}[\rho_0]\rangle \tag{7.15}$$

The $\Delta\langle T\rangle$ term represents the kinetic correlation energy of the electrons and the $\langle\Delta V_{\mathrm{ee}}\rangle$ term the potential correlation and exchange energy (although exchange and correlation energy in DFT do not have exactly the same significance as in HF theory [32]). Using Eq. (7.15), Eq. (7.14) becomes

$$E_0 = \int \rho_0(\mathbf{r})v(\mathbf{r})d\mathbf{r} + \langle T[\rho_0]\rangle_{\mathrm{ref}} + \frac{1}{2}\iint \frac{\rho_0(\mathbf{r}_1)\rho_0(\mathbf{r}_2)}{r_{12}}d\mathbf{r}_1 d\mathbf{r}_2 + E_{\mathrm{XC}}[\rho_0] \tag{7.16}$$

Let's look at the four terms in the expression for the molecular energy E_0 of Eq. (7.16).

(1) The first term (the integral of the density times the external potential) is

$$\int \rho_0(\mathbf{r})v(\mathbf{r})d\mathbf{r} = \int \left[\rho_0(\mathbf{r}_1)\sum_{\mathrm{nuclei\ A}} -\frac{Z_A}{\mathbf{r}_{1A}}\right]d\mathbf{r}_1 = -\sum_{\mathrm{nuclei\ A}} Z_A \int \frac{\rho_0(\mathbf{r}_1)}{\mathbf{r}_{1A}}d\mathbf{r}_1 \tag{7.17}$$

We integrate the potential energy of attraction of each nucleus for an infinitesimal portion of the charge cloud and sum for all the nuclei. If we know ρ_0 the integrals to be summed are readily calculated.

(2) The second term (the electronic kinetic energy of the noninteracting-electrons reference system) is the expectation value of the sum of the one-electron kinetic energy operators over the ground state multielectron wavefunction of the reference system (Parr and Yang explain this in detail [33]). Using the compact Dirac notation for integrals:

$$\langle T[\rho_0]\rangle_{\text{ref}} = \left\langle \psi_r | \sum_{i=1}^{2n} -\frac{1}{2}\nabla_i^2 | \psi_r \right\rangle \tag{7.18}$$

Since these hypothetical electrons are noninteracting ψ_r can be written *exactly* (for a closed-shell system) as a single Slater determinant of occupied spin molecular orbitals (Chap. 5, Sect. 5.2.3.1. For a *real* system, the electrons interact and using a single determinant causes errors due to neglect of electron correlation (Chap. 5, Sect. 5.4), the root of most of our troubles in wavefunction methods. Thus for a four-electron system

$$\Psi_r = \frac{1}{\sqrt{4!}} \begin{vmatrix} \psi_1^{\text{KS}}(1)\alpha(1) & \psi_1^{\text{KS}}(1)\beta(1) & \psi_2^{\text{KS}}(1)\alpha(1) & \psi_2^{\text{KS}}(1)\beta(1) \\ \psi_1^{\text{KS}}(2)\alpha(2) & \psi_1^{\text{KS}}(2)\beta(2) & \psi_2^{\text{KS}}(2)\alpha(2) & \psi_2^{\text{KS}}(2)\beta(2) \\ \psi_1^{\text{KS}}(3)\alpha(3) & \psi_1^{\text{KS}}(3)\beta(3) & \psi_2^{\text{KS}}(3)\alpha(3) & \psi_2^{\text{KS}}(3)\beta(3) \\ \psi_1^{\text{KS}}(4)\alpha(4) & \psi_1^{\text{KS}}(4)\beta(4) & \psi_2^{\text{KS}}(4)\alpha(4) & \psi_2^{\text{KS}}(4)\beta(4) \end{vmatrix} \tag{7.19}$$

The 16 spin orbitals in this determinant are the *Kohn-Sham spin orbitals* of the reference system; each is the product of a Kohn-Sham spatial orbital ψ_i^{KS} and a spin function α or β. Equation (7.18) can be written in terms of the spatial KS orbitals by invoking a set of rules (the Slater-Condon or Condon-Slater rules [34]) for simplifying integrals involving Slater determinants:

$$\langle T[\rho_o]\rangle_{\text{ref}} = -\frac{1}{2}\sum_{i=1}^{2n} \langle \psi_1^{\text{KS}}(1)|\nabla_1^2|\psi_1^{\text{KS}}(1)\rangle \tag{7.20}$$

The integrals to be summed are readily calculated. Note that DFT *per se* does not involve wavefunctions, and the Kohn-Sham approach to DFT uses orbitals only as a kind of subterfuge to calculate the noninteracting-system kinetic energy and the electron density function; see below.

(3) The third term in Eq. (7.16), the classical electrostatic repulsion energy term, is readily calculated if ρ_0 is known.

(4) This leaves us with the exchange-correlation energy functional, $E_{\text{XC}}[\rho_0]$ (Eq. (7.15)) as the only term for which some new method of calculation must be devised. Devising good exchange-correlation functionals for calculating this energy term from the electron density function is the main problem in DFT research. This is discussed in Sect. 7.2.3.4.

Written out more fully, then, Eq. (7.16) is

$$\begin{aligned} E_0 = &- \sum_{\text{nuclei A}} Z_A \int \frac{\rho_0(\mathbf{r}_1)}{\mathbf{r}_{1A}}d\mathbf{r}_1 - \frac{1}{2}\sum_{i=1}^{2n} \langle \psi_1^{\text{KS}}(1)|\nabla_1^2|\psi_1^{\text{KS}}(1)\rangle \\ &+ \frac{1}{2}\iint \frac{\rho_0(\mathbf{r}_1)\rho_0(\mathbf{r}_2)}{r_{12}}d\mathbf{r}_1 d\mathbf{r}_2 + E_{\text{XC}}[\rho_0] \end{aligned} \tag{7.21}$$

The term most subject to error is the relatively small $E_{\text{XC}}[\rho_0]$ term, which contains the "unknown" (not precisely known) functional. Into this term the exact

electron correlation and exchange energies have been swept, and for it we must find at least an approximate functional.

7.2.3.2.2 The Kohn-Sham Equations

The KS equations are obtained by differentiating the energy with respect to the KS molecular orbitals, analogously to the derivation of the Hartree-Fock equations, where differentiation is with respect to wavefunction molecular orbitals (Chap. 5, Sect. 5.2.3.4). We use the fact that the electron density of the reference system, which is by decree exactly the same as that of the ground state of our real system (see the definition at the beginning of the discussion of the Kohn-Sham energy), is given by [9]

$$\rho_0 = \rho_r = \sum_{i=1}^{2n} |\psi_i^{KS}(1)|^2 \qquad (*7.22)$$

where the ψ_i^{KS} are the Kohn-Sham spatial orbitals. Substituting the above expression for the electron density in terms of orbitals into the energy expression of Eq. (7.21) and differentiating to vary E_0 with respect to the ψ_i^{KS} subject to the constraint that these remain orthonormal (the spin orbitals of a Slater determinant are orthonormal) leads to the Kohn Sham equations (the derivation is discussed in considerable detail by Parr and Yang [35]):

$$\left[-\frac{1}{2}\nabla_i^2 - \sum_{\text{nuclei A}} \frac{Z_A}{\mathbf{r}_{1A}} + \int \frac{\rho(\mathbf{r}_2)}{r_{12}} d\mathbf{r}_2 + v_{XC}(1) \right] \psi_i^{KS}(1) = \varepsilon_i^{KS}\psi_i^{KS}(1) \qquad (7.23)$$

where ε_i^{KS} are the Kohn-Sham energy levels (the KS orbitals and energy levels are discussed later) and $v_{XC}(1)$ is the *exchange correlation potential*. The expression in brackets is the Kohn-Sham operator, $\hat{h}^{KS}$. In the KS orbitals and the exchange correlation potential we arbitrarily installed here electron number 1, since the KS equations are a set of one-electron equations (cf. the Hartree-Fock equations) with the subscript i running from 1 to $2n$, over all the electrons in the system. The exchange correlation potential v_{XC} is a *functional derivative* of the exchange-correlation energy $E_{XC}[\rho(\mathbf{r})]$. The energy $E_{XC}[\rho(\mathbf{r})]$ is a functional of $\rho(\mathbf{r})$ and the process of obtaining v_{XC} is functional differentiation; v_{XC} is defined as

$$v_{XC}(\mathbf{r}) = \frac{\delta E_{XC}[\rho(\mathbf{r})]}{\delta\rho(\mathbf{r})} \qquad (7.24)$$

Here the differentiation is shown as being with respect to $\rho(\mathbf{r})$, but note that in Kohn-Sham theory $\rho(\mathbf{r})$ is expressed in terms of Kohn-Sham orbitals (Eq. (7.22)). Functional derivatives, which are akin to ordinary derivatives, are discussed by Parr and Yang [36] and outlined by Levine [37].

The KS Eq. (7.23) can be written as

$$\hat{h}^{KS}(1)\psi_i^{KS}(1) = \varepsilon_i^{KS}\psi_i^{KS}(1) \qquad (*7.25)$$

The Kohn-Sham operator $\hat{h}^{KS}$ is defined by Eq. 7.23; the significance of these orbitals and energy levels is considered later, but we note here that in practice they can be interpreted in a similar way to the corresponding wavefunction entities. Pure DFT theory has no orbitals or wavefunctions; these were introduced by Kohn and Sham only as a way to turn Eq. (7.11) into a useful computational tool, via the artifice of noninteracting electrons, but if we can interpret the KS orbitals and energies in some physically useful way, so much the better.

The Kohn-Sham energy Eq. (7.21) is exact, but there is a catch: only if we knew the density function $\rho_0(\mathbf{r})$ and the exchange-correlation energy functional $E_{XC}[\rho_0]$, would it give the exact energy. The Hartree-Fock energy equation (Chap. 5, Eq. (5.17)), on the other hand, is an approximation that does not treat electron correlation properly. Even in the basis set limit, the HF equations would not give the correct energy, but the KS equations would, *if we knew the exact exchange-correlation energy functional*. In wavefunction theory we know how to improve on HF-level results: by using perturbational or configuration interaction treatments of electron correlation (Chap. 5, Sect. 5.4), but in DFT theory there is as yet no systematic way of improving the exchange-correlation energy functional. It has been said [38] that "while solutions to the [HF equations] may be viewed as exact solutions to an approximate description, the [KS equations] are approximations to an exact description!"; Parr and Yang give a somewhat similar but more recondite assertion: "The conventional Hartree-Fock approximation can be regarded as a density-functional approach in the HFKS scheme with correlation completely neglected, but not in the KS scheme. Instead of the exact *nonlocal* exchange potential in the HFKS equations, the KS equations use an effective *nonlocal* potential that is not known and has to be approximated. Another trade of accuracy for simplicity!" [39].

7.2.3.3   Solving the KS Equations

First lets review the steps in carrying out a HF calculation (Chap. 5, Sects. 5.2.3.6.2, 5.2.3.6.3, 5.2.3.6.4 and 5.2.3.6.5). We start with a guess of the basis function coefficients c, because the HF operator $\hat{F}$ (the Fock operator) itself contains the wavefunction, which is composed of the basis functions and their coefficients. The operator is used with the basis functions to calculate the HF Fock matrix elements $F_{rs} = \langle \phi_r | \hat{F} | \phi_s \rangle$ which constitute the Fock matrix $\mathbf{F}$. An orthogonalizing matrix calculated from the overlap matrix $\mathbf{S}$ puts $\mathbf{F}$ into a form $\mathbf{F}'$ that satisfies $\mathbf{F}' = \mathbf{C}'\boldsymbol{\varepsilon}\mathbf{C}'^{-1}$ (Chap. 5, Sect. 5.2.3.6.2). Diagonalization of $\mathbf{F}'$ gives a coefficients matrix $\mathbf{C}'$ and an energy levels matrix $\boldsymbol{\varepsilon}$; transforming $\mathbf{C}'$ to $\mathbf{C}$ gives the matrix with the coefficients corresponding to the original basis set expansion, and these

are then used as a new guess to calculate a new **F**; the process continues till it converges satisfactorily on the c's, i.e. on the wavefunction, and the energy levels (which can be used to calculate the electronic energy); the procedure was shown in detail in Sect. 5.2.3.6.5.

The standard strategy for solving the KS eigenvalue equations, like that for solving the HF equations, which they resemble, is to expand the KS orbitals in terms of basis functions ϕ:

$$\psi_i^{KS} = \sum_{s=1}^{m} c_{si}\phi_s \quad i = 1, 2, 3, \cdots, m \tag{*7.26}$$

This is exactly the same as was done with the Hartree-Fock orbitals in Chap. 5, Sect. 5.2.3.6.1, and in fact the same basis functions are often used as in wavefunction theory, although as in all calculations designed to capture electron correlation (the Kohn-Sham electrons are noninteracting, but the functional attempts to account for electron correlation), sets smaller than split-valence (Chap. 5, Sect. 5.3.3) should not be used. A popular basis in DFT calculations is the 6-31G*. Substituting the basis set expansion into the KS Eqs. (7.23, 7.25) and multiplying by $\phi_1, \phi_2, \ldots, \phi_m$ leads, as in Chap. 5 Sect. 5.2.3.6.1, to m sets of equations, each set with m equations, which can all be subsumed into a single matrix equation analogous to the HF equation $\mathbf{FC} = \mathbf{SC\varepsilon}$. The key to solving the KS equations then becomes, as in the standard HF method, the calculation of Fock matrix elements and diagonalization of the matrix (Chap. 5, Sect. 5.2.3.6.2). In a DFT calculation we start with a guess of the density function $\rho(\mathbf{r})$, because this is what we need to obtain an explicit expression for the KS Fock operator $\hat{h}^{KS}$ (Eqs. (7.23, 7.24 and 7.25). This guess is usually a noninteracting atoms guess, obtained by summing mathematically the electron densities of the individual atoms of the molecule, at the molecular geometry. The KS Fock matrix elements $h_{rs} = \left\langle \phi_r | \hat{h}^{KS} | \phi_s \right\rangle$ are calculated and the KS Fock matrix is orthogonalized and diagonalized, etc., to give initial guesses of the c's in the basis set expansion of Eq. (7.26) (and also initial values of the ε's). These c's are used in Eq. (7.26) to calculate a set of KS MOs which with Eq. (7.22) are used to calculate a better ρ. This new density function is used to calculate improved matrix elements h_{rs} which in turn give improved c's and then an improved density function, the iterative process being continued until the electron density etc. converge. The final density and KS orbitals are used to calculate the energy from Eq. (7.21).

The KS Fock matrix elements are integrals of the Fock operator over the basis functions. Because useful functionals are so complicated, these integrals, specifically the $\langle \phi_r | v_{XC} | \phi_s \rangle$ integrals, unlike the corresponding ones in Hartree-Fock theory, cannot be solved analytically. The usual procedure is to approximate the integral by summing the integrand in steps determined by a *grid*. For example, suppose we want to integrate e^{-x^2} from $-\infty$ to ∞. This could be done approximately, using a grid of width $\Delta x = 0.2$ and summing from -2 to 2 (limits at which the function is small):

$$\int_{-\infty}^{\infty} e^{-x^2} dx = \int_{-\infty}^{\infty} f(x)dx \simeq 0.2f(-2+0.2) + 0.2f(-2+0.4)$$
$$+ \cdots + 0.2f(2) = 0.2(9.80) = 1.96$$

The integral is $\pi^{1/2} = 1.77$. For a function $f(x, y)$ the grid would define the steps in x and y and actually look like a grid or net, approximating the integral as a sum of the volumes of parallelepipeds, and for the DFT function $f(x, y, z)$ the grid specifies the steps of x, y and z. Clearly the finer the grid the more accurately the integrals are approximated, and reasonable accuracy in DFT calculations requires (but is not guaranteed by) a sufficiently fine grid.

Here is a summary of the steps in obtaining the Kohn-Sham orbitals and energy levels:

1. Specify a geometry (and charge and multiplicity; electron spin can be handled in DFT by using separate α- and β-spin density functions).
2. Specify a basis set $\{\phi\}$ and a functional $E_{XC}[\rho]$.
3. Make an initial guess of ρ (e.g by superposing atomic ρ functions).
4. Use the guess of ρ to calculate an initial guess initial $v_{xc}(\mathbf{r})$ from $v_{xc}(\mathbf{r}) =$ functional derivative $\delta E_{xc}/\delta \rho$ (Eq. (7.24)). This uses the approximate functional E_{xc} we have chosen for the calculation.
5. Use the initial guesses of ρ and $v_{xc}(\mathbf{r})$ to calc the K-S operatorh $\hat{h}^{KS}$:

$$-\frac{1}{2}\nabla_i^2 - \sum_{\text{nuclei A}} \frac{Z_A}{r_{1A}} + \int \frac{\rho(\mathbf{r}_2)}{r_{12}} d\mathbf{r}_2 + v_{XC}(1)$$

   (See Eq. (7.23)).
6. Use the K-S operatorh $\hat{h}^{KS}$ and the basis functions $\{\phi\}$ to calc Kohn-Sham matrix elements K_{rs} (cf. Fock matrix elements F_{rs} (Chap. 5, Sect. 5.2.3.6),

$$K_{rs} = \left\langle \phi_r | \hat{h}^{KS} | \phi_s \right\rangle \tag{*7.27}$$

   and assemble a Kohn-Sham matrix, the square matrix of K_{rs} elements.
7. Orthogonalize the KS matrix, diagonalize it to get a coefficients matrix $\mathbf{C}'$ and an energy levels matrix $\boldsymbol{\varepsilon}$, and transform $\mathbf{C}'$ to $\mathbf{C}$, the matrix of the coefficients that give the KS orbitals as a weighted sum of the original non-orthogonal basis functions (cf. Chap. 5, Sect. 5.2.3.6.2). We now have the first-iteration values of the energy levels ε_i and the KS molecular orbitals ψ_i (getting the coefficients is equivalent to getting the MOs, once a basis set is in hand, since $\psi_i^{KS} = \sum c\phi_{\text{basis}}$).
8. Use the first-iteration values of the KS MOs to calculate an improved ρ:

$$\rho_0 = \rho_r = \sum_{i=1}^{2n} |\psi_i^{KS}(1)|^2$$

   (See Eq. (7.22))

9. Go back to step 4, but with the improved, first-iteration ρ instead of the guess. At the new step 7 we will have the second-iteration values of the energy levels ε_i and the KS molecular orbitals ψ_i (and the first-iteration ρ, from the first application of step 8). Check them for significant change. If these do not differ (within specified limits) from the first-iteration values, and the first-iteration ρ is unchanged from the guess we started with, stop. If they differ, go through the process again, to get the third-iteration values of the energy levels ε_i and the KS molecular orbitals, and the second-iteration ρ. Check for significant change; and so on.

10. When the iterations have satisfactorily converged, calculate the energy using Eq. (7.21).

11. The geometry can be optimized with the aid of derivatives of the energy with respect to geometry, as outlined in Chap. 2, Sect. 2.4. Any method in which the calculated energy varies with the geometry can in principle at least, optimize geometry.

7.2.3.4 The Exchange-Correlation Energy Functional: Various Levels of Kohn-Sham DFT

We have to consider the calculation of the fourth term, the problem term, in the KS operator of Eq. (7.23), the exchange-correlation potential $v_{XC}(\mathbf{r})$. This is defined as the functional derivative [36, 37] of the exchange-correlation energy functional, $E_{XC}[\rho(\mathbf{r})]$, with respect to the electron density functional (Eq. (7.23). The exchange-correlation energy functional $E_{XC}[\rho(\mathbf{r})]$, a functional of the electron density function $\rho(\mathbf{r})$, is a quantity which depends on the *function* $\rho(\mathbf{r})$ and on just what mathematical form the *functional* has, while the exchange-correlation potential $v_{XC}(\mathbf{r})$, the functional derivative of $E_{XC}[\rho(\mathbf{r})]$, is a function of the variable $\mathbf{r}$, i.e. of x, y, z. Clearly, $v_{XC}(\mathbf{r})$ depends on $\rho(\mathbf{r})$ and, like $\rho(\mathbf{r})$, varies from point to point in the molecule. The functional is a recipe for transforming ρ into the exchange-correlation energy E_{XC}. Actually, as hinted in connection with Eq. (7.13), this energy ideally also compensates for the classical self-repulsion in the charge cloud of ρ, and for the deviation of the kinetic energy of the noninteracting KS electrons from that of real electrons. Thus a good functional handles not only exchange and correlation errors, but also self-repulsion and kinetic energy errors. The functional is normally tackled as an exchange term and a correlation term; for example in the B3LYP functional (below) B3 denotes the Becke 88 3-parameter exchange functional and LYP the Lee, Yang, Parr correlation functional, and in the TPSS functional (below), both functionals enshrine the names Tao, Perdew, Staroverov, Scuseria, and some programs require TPSS be denoted TPSSTPSS. Devising good functionals $E_{XC}[\rho(\mathbf{r})]$ is the main problem in density functional theory, for all the theoretical difficulties of Kohn-Sham DFT have been swept into the functional.

Below we look briefly at functionals based, in order of increasing sophistication (although not quite invariably smoothly increasing excellence), on these methods:

(a) the local density approximation (LDA), (b) the local spin density approximation (LSDA), (c) the generalized gradient approximation (GGA), (d) meta-GGA (MGGA), (e) hybrid GGA or adiabatic connection methods (ACM methods), (f) hybrid meta-GGA hybrid MGGA) methods, and (g) "fully nonlocal" theory. This hierarchy of theory has been likened to the biblical ladder reaching up to heaven [40], and this DFT Jacob's ladder [41] will, one hopes, culminate in what has been appropriately called the divine functional [42]. Jensen has listed some of the properties that the divine functional must on theoretical grounds possess [43]. Some valuable reviews which tend to illustrate the improvement of the method with specific functionals are:

1. Sousa et al. 2007 [44]; 14 pp. A concise historical introduction to the various methods and extensive comparisons of many functionals for various purposes; see especially Table 3; highlights the predominance of B3LYP.
2. Zhao and Truhlar 2011, 2007 [45]; 13, 11 pp. Extensive comparison of the very popular B3LYP functional with some new functionals; focuses on overcoming problems of transition metals, barrier heights, and weak interactions. A class of functionals, the M06 family, "with better across-the-board average performance than B3LYP" is presented.[2] These are successors to the M05 family. A restrained choice of data is clearly presented. Clear recommendations are given for various kinds of calculations. The basic specialties of the four members of the then-new M06 family were said to be:

M06 itself   General thermochemistry and kinetics, where noncovalent interactions and/or transition metals may be involved. For "problems involving multireference rearrangements or reactions where both organic and transition-metal bonds are formed or broken". This "M06" functional was actually published in 2008 (Table 2 in reference [15]).

M06-2X   2X means twice as much (54 %) HF-exchange as for M06. General thermochemistry and kinetics; said to be better than M06 for noncovalent interactions. It "predicts accurate valence and Rydberg electronic excitation energies…excellent for aromatic-aromatic stacking interactions". This "M06-2X" functional was actually published in 2008 (Table 2 in reference [15]). As of 2015 M06-2X is probably the functional most competitive with B3LYP where transition metals and weak interactions are not of primary importance (see Sects. 7.3, 7.3.1, and 7.3.2).

M06-L   No HF-exchange. Local and so "affordable" for very large systems. The only local functional with better general performance than B3LYP. The most accurate of the family for transition metals.

---

[2]M06: :"M zero six", or colloquially "M oh six". A descendant of M05, Minnesota '05 (2005): Y. Zhao, N. E. Schultz, D. E. Truhlar, J. Chem. Phys., 2005, 123, 161103.

M06-HF   H means high (100 %) HF-exchange. Good performance for valence,
            Rydberg and charge transfer excited states with minimum sacrifice of
            ground-state accuracy. Can handle noncovalent interactions. Full HF
            exchange avoids long-range self-interaction error.

These four functionals constituted what were called the Minnesota functionals. The family with this geographic appellation has grown since then: see (3) below.

3. Peverati and Truhlar 2014 [15]; 81 pp + supplementary material (61 pp +200 references + supplementary material). The emphasis is on the Minnesota functionals, a group that has expanded quite quickly beyond the four M06-type functionals (Zhao and Truhlar reviews [45], above): twelve Minnesota and 65 other functionals are examined with 452 data points in various databases [45b]. Besides the M05 and M06-type some newer kinds of functionals are discussed: M08 (M08-HX, M08-SO), M011 (M011, M11-L), and M012 (M012-L, MN12-SX). As of 2015 these three latter families are of only limited availability, e.g. in "locally" (University of Minnesota) modified versions of the Gaussian program suite. Because of a dearth of applications of these in the literature, they are not discussed further here.

4. Riley et al. 2007 [46]; 27 pp. The efficacy of DFT is examined "for small molecules containing elements commonly found in proteins, DNA, and RNA" The results are very clearly presented with figures. Very extensive comparison: 37 DFT methods (functional/basis set pairs) are compared with ab initio HF and MP2. The Pople 6-31G* basis (sometimes used with one or two sets of + functions) is competitive with or better than the much bigger Dunning aug-cc-pVDZ and cc-pVTZ sets. An all-round best functional was not found but B1B95 and B98 were among the best.

5. Perdew et al. 2005 [47]; 9 pp. Nicely prescriptive exposition of "personal preferences and metaphysical principles" for designing and choosing functionals. Exhorts developers to adopt a nonempirical methodology of climbing the DFT Jacob's ladder by proceeding to the next higher rung by building on what works at each tested level, and striving to obey the known theoretical constraints. Holds that with these provisos DFT is not semiempirical, but rather a "middle way" between semiempirical and ab initio. Favors functionals without empirical parameters. Defends the LSDA as a still useful method and as a limiting case to which more sophisticated functionals should devolve in the uniform electron gas limit. Summarizes some known exact constraints on the ideal functional. They recommend functionals with "few fitted parameters" like PBE or TPSS.

6. Mattsson 2002 [42]; 2 pp. A very brief sketch of the development of DFT.

7. Kurth et al. 1999 [48]; 21 pp. Delves well into the mathematical background behind functionals and discusses solids and metal surfaces in addition to atoms and molecules. Examines functionals constructed semiempirically as well as purely by considering known theoretical constraints.

We now consider the rungs of Jacob's ladder.

7.2.3.4.1   The Local Density Approximation (LDA)

The simplest approximation to $E_{xc}[\rho(\mathbf{r})]$, the bottom rung of the DFT Jacob's ladder, results from the *local density approximation*, LDA. In mathematics a *local property* of a function at a point on the surface (line, or 2-dimensional surface, or hypersurface) that is defined by the function is a property that depends on the behavior of the function only in the immediate vicinity of the point [49]. "Immediate vicinity" can be taken to mean the region within an infinitesimal distance beyond the point. Consider the derivative at some point P_i on the line defined by plotting $y = f(x)$ against x. This property, the derivative or gradient, is the limit

$$\lim_{\Delta x \to 0} \frac{\Delta y}{\Delta x} = \frac{dy}{dx}$$

and depends on the behavior of the curve at just an infinitesmal distance away from P_i, i.e. in the immediate vicinity of P_i. The derivative may exist at P_i but not at some *other* point, where the curve may have, say, a cusp. The opposite of a local property is a *property in the large* [49]. Kurth et al. [48] define "locality" somewhat differently: they take a local functional to be one for which the energy density (below) at a point is determined by ρ at the point, designate by "semilocal" a functional for which the energy density depends on ρ in the infinitesimal neighborhood of the point, and use nonlocal to describe a functional for which the energy density is determined by ρ at finite distances from the point. It is more important to know how the functionals behave than to worry about their strict adherence to mathematical definitions.

The local density approximation is based on the assumption that at every point in the molecule the *energy density* has the value that would be given by a homogeneous electron gas which had the same electron density *ρ at that point*. The energy density is the energy (exchange plus correlation) per electron of a homogeneous electron gas. Note that the LDA does not assume that the electron density in a molecule is homogeneous (uniform); that drastic situation would be true of a "Thomas-Fermi molecule", which, as we said above, cannot exist [23] (Sect. 7.2.2). The term *local* was used to contrast the method with ones in which the functional depends not just on ρ but also on the gradient (first derivative) of ρ, the contrast apparently arising from the assumption that a derivative is a nonlocal property. However, under the mathematical definition above a gradient is local, and DFT methods formerly called "nonlocal" are now commonly designated as *gradient-corrected* (Sect. 7.2.3.4.3). LDA functionals have been largely replaced by a family representing an extension of the method, local spin density approximation (LSDA; below) functionals. In fact, in extolling the virtues of a systematic nonempirical ascent of the DFT Jacob's ladder, Perdew et al. [47] slight LDA and assign to the lowest rung LSDA functionals.

7.2.3.4.2 The Local Spin Density Approximation (LSDA)

The "spin" here means that electrons of opposite spin are placed in different Kohn-Sham orbitals, analogously to the Hartree-Fock UHF method (Chap. 5, end of Sect. 5.2.3.6.5). LSDA functionals are occasionally called LSD functionals. The elaboration of the LDA method to the LSDA assigns electrons of α and β spin to different spatial KS orbitals $\psi_{\alpha}^{\mathrm{KS}}$ and $\psi_{\beta}^{\mathrm{KS}}$, from which different electron density functions ρ^{α} and ρ^{β} follow. This "spin-density theory", LSDA, has the advantages that it can handle systems with one or more unpaired electrons, like radicals, and systems in which electrons are becoming unpaired, such as molecules far from their equilibrium geometries, and that even for ordinary molecules it appears to be more forgiving toward the use of (necessarily) inexact E_{XC} functionals [50]. For species in which all the electrons are securely paired, the LSDA is equivalent to the LDA. LSDA geometries, frequencies and electron-distribution properties tend to be reasonably good, but (as with HF calculations) the dissociation energies, including atomization energies, are very poor. A popular LSDA functional was the SVWN (Slater exchange plus Vosko, Wilk, Nusair) [51]. Atomization energies are often used as a kind of touchstone for the goodness of a method: for example, they are one of the criteria for parameterizing and evaluating the high-accuracy energy multistep "ab initio" methods of Chap. 5 (Sect. 5.5.2.3.2). LSDA functionals are useful in solid-state physics, but for molecular calculations have been largely replaced by higher rungs of the ladder. The local spin density method has however been stoutly defended by knowledgeable practitioners [47], who point out that it gives "remarkably accurate bond lengths", that its atomization energy errors "can be dramatically reduced" with one empirical parameter, and that "For chemistry without free atoms, LSD is not such a bad starting point". A recently developed, potentially very useful local function is M06-L (below) [45]. Nevertheless, LSDA calculations have been largely replaced by an approach that uses not just the electron density, but also its gradient.

7.2.3.4.3 Gradient-Corrected Functionals; the Generalized Gradient Approximation (GGA)

Most DFT calculations nowadays use exchange-correlation energy functionals E_{XC} that utilize both the electron density *and* its gradient, the first derivative of ρ with respect to position, $(\partial/\partial x + \partial/\partial y + \partial/\partial z)\rho = \nabla\rho$. These functionals are called *gradient-corrected*, or said to use the *generalized-gradient approximation* (GGA). They have also been called *nonlocal* functionals, in contrast to LDA and LSDA functionals, but it has been suggested [52] that the term nonlocal be avoided in referring to gradient-corrected functionals; recall the discussion of "local" in Sect. 7.2.3.4.1. The exchange-correlation energy functional can be written as the sum of an exchange-energy functional and a correlation-energy functional, both negative, i.e. $E_{\mathrm{XC}} = E_x + E_c$; $|E_x|$ is much bigger than $|E_c|$. For the argon atom E_x is

-30.19 hartrees, while E_c is only -0.72 hartrees, calculated by the HF method [53]. Thus it is not surprising that gradient corrections have proved more effective when applied to the exchange-energy functional, and a major advance in practical DFT calculations was the introduction of the B88 (Becke 1988) functional [54], a "new and greatly improved functional for the exchange energy" [55]. Examples of gradient-corrected correlation-energy functionals are the LYP (Lee-Yang-Parr) and the P86 (Perdew 1986) functionals. All these functionals are commonly used with Gaussian-type (i.e. functions with $exp(-\mathbf{r}^2)$) basis functions for representing the KS orbitals (Eq. (7.26)). A calculation with B88 for the exchange functional E_x, and LYP for the E_c, and the 6-31G* basis set (Chap. 5, Sect. 5.3.3) would be designated as a B88LYP/6-31G* or B88LYP/6-31G* calculation. Sometimes rather than the analytical functions that constitute the standard Gaussian basis sets, numerical basis sets are used. A numerical basis function is essentially a table of the values that an atomic orbital wavefunction has at many points around the nucleus, derived from best-fit functions devised to pass through these points. These numerical functions can be used instead of the analytical Gaussian-type functions ubiquitous in ab initio calculations.

7.2.3.4.4 Meta-Generalized Gradient Approximation Functionals (Meta-GGA, MGGA)

We saw that functionals which use the first derivative of the electron density function, GGA functionals (Sect. 7.2.3.4.3), are usually an improvement over ones relying only on ρ itself. One might therefore suspect that further improvement could be obtained by invoking the second derivative of ρ, $\left(\partial^2/\partial x^2 + \partial^2/\partial y^2 + \partial^2/\partial z^2\right)\rho = \nabla^2\rho$. This is the Laplacian of the electron density function (so important in AIM theory, Chap. 5, Sect. 5.5.4.5). Functionals which use the second derivative of ρ are called meta-gradient corrected (meta-GGA, MGGA); meta = beyond. This approach seems to offer some improvement, but functionals that depend on the Laplacian of ρ present computational problems. One way to sidestep this is to make the MGGA functional dependent not on ρ itself but on the *kinetic energy density* τ, obtained by summing the squares of the gradients of the Kohn-Sham MOs:

$$\tau(\mathbf{r}) = \frac{1}{2}\sum_{i=1}^{\text{occupied}} |\nabla\psi_i^{\text{KS}}(\mathbf{r})|^2 \qquad (7.28)$$

This varies with ρ essentially the same as does the Laplacian of ρ [56]. Examples of MGGA functionals are the τHCTH (Hamprecht, Cohen, Tozer, Handy) and the B98 (Becke1998). MGGA functionals are, like GGA ones, local. A detailed discussion of the theory and mathematics behind MGGA functionals is given in reference [48], where they are said to "in general perform well for atomization energies", and PKZP and KCIS are designated the best MGGA performers.

7.2.3.4.5 Hybrid GGA (HGGA) Functionals; the Adiabatic Correction Method (ACM)

These are functionals to which Hartree-Fock exchange has been added. The justification for this lies in the adiabatic connection method (ACM) [17]. In wavefunction theory, an adiabatic process is one in which the wavefunction remains on the same PES, i.e. the variables that define it change smoothly as the process evolves. The process seamlessly connects two states without crossing into another electronic state. The ACM shows that the exchange-correlation energy $E_{XC}(\rho)$ can be taken as a weighted sum of the DFT exchange-correlation energy and HF exchange energy. This is the justification of *hybrid* DFT functionals (hybrid DFT methods have been called ACM methods), which include an energy contribution from HF-type electron exchange, calculated from the KS wavefunction of the noninteracting electrons. Those electrons have no coulomb interaction, but being, after all, still electrons with spin, like all good fermions they show "Pauli repulsion" (Chap. 5, Sect. 5.2.3.5), represented by the exchange K integral (Chap. 5, Eq. (5.22). Hybrid functionals are functionals (of the GGA level or higher) that contain HF exchange, the correction energy to the classical coulomb repulsion. The percentage of HF exchange energy to use is a main distinguishing characteristic of the various hybrid functionals. The first popular, successful hybrid method was B3LYP. This is the B3PW91 functional first proposed by Becke [57], modified by Stephens et al. [58]. The B3LYP functional has a total of eight purely empirical parameters. B3LYP has been wildly popular: Sousa et al. [44] show in their 2007 paper that from 2002 to 2006 in each year it has accounted for ca. 80 % of the names of the functionals in journal articles and abstracts, and Zhao and Truhlar single it out for special comparison with their new functionals [45b]. This popularity is despite the fact that evidently, for almost any particular application, one can find a better functional. The durability of B3LYP and the advisability of its continued use are discussed at the beginning of Sect. 7.3; for now we note that near the end of their extensive comparison, Sousa et al. [44] said, ca. 2007, that "B3LYP still remains a valid and particularly efficient alternative for the 'average' quantum chemistry problem".

Some hybrid methods base the HF percentage not on experimental parameterization ("parameter-free" hybrid methods), but on theoretical arguments; this does not automatically give them superior performance. GGA functionals tend to underestimate barriers and HF methods tend to overestimate them, but a happy adjustment of HF exchange for barriers tends to reduce the accuracy for other properties.

7.2.3.4.6 Hybrid Meta-GGA (HMGGA) Functionals

These are analogous to the hybrid GGA functionals of Sect. 7.2.3.4.5 above, but with Hartree-Fock exchange added on to meta-GGA (Sect. 7.2.3.4.4), rather than GGA, functionals (Sect. 7.2.3.4.3). Hybrid MGGA (HMGGA) uses the first derivative of ρ and its second derivative, or the kinetic energy density (Sect. 7.2.3.4.4),

and Hartree-Fock exchange. They are the highest-level functionals in routine use. Most are, as of mid-2009, fairly recent: in Table 2 of ref. [44] (2007), of the 52 "most common" functionals listed and referenced, 14 are HMGGA and of these one is vintage 1996 and the others 2003–2005; this paper depicts HMGGA on the fourth rung of the ladder, rather than the sixth implied here, because it effectively collapses on to rung 1 LDA and LSDA, and places on rung 4 both HGGA and HMGGA. The strongpoint of HMGGA seems to be "an improvement over the previous formalisms in . . .barrier heights and atomization energies" [44].

7.2.3.4.7   Fully Nonlocal Theory

This is the seventh and highest rung in our ordering, the fifth on the "collapsed" ladder of Sousa et al. [44], a step above HMGGA functionals. Perdew et al. say [47] that "a fully nonlocal functional of the density. . .can be satisfied on the fourth rung by hyper-GGAs that use full exact exchange" that "Exact exchange can only be combined with a fully nonlocal correlation, constructed on the fourth or fifth rungs of the ladder" and that "there is also continuing interest $\cdots$ in the weighted density approximation, a nonempirical and fully nonlocal functional that does not fit on Jacob's ladder." From this it is evident that "fully nonlocal" DFT theory does not promise a single, sharply defined functional, although the divine functional [42] must be fully nonlocal. What does fully nonlocal mean? Kurth et al. use *local*, *semilocal*, and *nonlocal* to refer to properties that are determined at a point, at an infinitesimal distance beyond the point, and at a finite distance beyond the point, respectively [48]. These are not the strict mathematical definitions of the terms [49], but they are working intuitive concepts: to determine the gradient at a point one must move an infinitesimal distance beyond. Exact electron exchange energy is an example of a nonlocal property of ρ, because it arises from "Pauli repulsion" between electrons a finite distance apart; a fully nonlocal functional would presumably take into account all such nonlocal phenomena. Attention is paid to the local nature or otherwise of various functionals in the reviews by Zhao and Truhlar [45]. Nonlocal functionals have been under development for years [59], but fully nonlocal ones, with all relevant properties treated nonlocally, are apparently not yet available for practical molecular calculations. However, some (2006 and later) functionals, for example B2PLYP [60], which uses hybrid-GGA with MP2-like (Chap. 5, Sect. 5.4.2) promotion of electrons into virtual orbitals for treating electron correlation, rival coupled-cluster ab initio calculations (Chap. 5, Sect. 5.4.3) for certain purposes, [61].

7.2.3.4.8   Dispersion

An important effect which these sundry levels of functional sophistication treat with varying degrees of effectiveness (from essentially not at all, to fairly well in some situations) is *dispersion*. The term, although useful, is not precise, and to

avoid definite commitment "dispersion-like" has been invoked (pp. 19–22 in [15]). It denotes weak forces between molecules and is evidently applied mainly to attraction, rather than repulsion: to the attractive side to the right of the minimum in the nonbonded interactions curve shown in Chap. 3 (Fig. 3.6). It refers to noncovalent bonding and seems to exclude hydrogen bonding, and so corresponds (some may quibble here) to those phenomena called van der Waals or London (after Fritz London) forces. London recognized this fuzziness in pinning down the origin of weak attractions in his 1927 paper [62a] on interatomic attraction when he wrote that the interplay of forces (Kräftespiel) shows a characteristic "multifold ambiguity" (Mehrdeutigkeit). Note that although we talk about dispersion "forces", the only true forces known to science are gravity, electromagnetism, and the weak and strong nuclear forces, and only electromagnetism plays a significant chemical role of any kind outside nuclear changes. The term "dispersion", written the same in English and German, was chosen (1930) because in estimating these "forces" London was led to a dispersion formula in optics [62b], where the term refers straightforwardly to the variation in the spreading, i.e. to the dispersion, of light according to wavelength. On a qualitative level, dispersion is due to electrostatic dipole-dipole attraction between two molecules caused by temporary uneven electron distributions engendered by the moving electrons. Because this electron movement is correlated, the rigorous quantum mechanical treatment of the phenomenon (not possible in 1930) requires addressing electron correlation (Chap. 5, Sect. 5.4). Although individual dispersion attractions are weak, the total effect, summed over the surface areas of large molecules or of several molecules, can be large.

Explicit attempts to treat dispersion have been made mainly within the framework of DFT; brief reference was made to the subject in connection with molecular mechanics (Chap. 3, Sect. 3.3.2), ab initio calculations, in the discussion of basis set superposition error (Chap. 5, at the end of Sect. 5.4.3.3), and semiempirical calculations (Chap. 6, Sect. 6.2.5.8). Handling dispersion is not, at present anyway, simple; for example, in this connection the question of "range-separation" arises, how to address short-range, medium-range, and long-range interactions, which may be attractive or repulsive (e.g. [15]). The correct treatment of dispersion is currently one of the major activities in research on DFT (Cohen, Mori-Sánchez and Yang, 2012, dispersion as one of the challenges to DFT) [17], the magnitude of this challenge being evident from the rate of growth that has occurred in the numbers of papers on the subject in recent years: from fewer than 80 in the decade of the 1990s to over 800 in 2011 (Klimes and Michaelis, 2012 review) [63a]. Some other useful orienting publications are those by Wagner and Schreiner [18a] and Corminboeuf [18b], Guidez and Gordon (2015, dispersion from first principles for DFT and Hartree-Fock) [63b], Conrad and Gordon (2015, $\pi - \pi$ interactions) [63c], and Kruse, Goerigk and Grimme (2012, dispersion correction for B3LYP) [63d]. Goerigk and Grimme (2011, a huge compendium of benchmark results) [63e] reported what seems to be "the by far largest and most comprehensive DFT benchmark regarding…systems and functionals"; they examined 47 functionals and the effect on most of their D3 dispersion correction. One gets the impression

from this study that the number of functionals out there, the variability of their ranges of appropriate application, their responses to dispersion correction, and the caveats attending their use make DFT a method that should be used only with considerable deliberation. Martin mapped the potential energy surface of *n*-pentane with CCSD(T)-F1 (i.e. near the basis set limit) and analyzed the conformation distribution with many electronic structure methods and several empirical dispersion corrections, to investigate the facts that "conformer energies in alkanes (and other systems) are highly dispersion-driven and that uncorrected DFT functionals fail badly at reproducing them, while simple empirical dispersion corrections tend to overcorrect" [63f]. Among his conclusions is that "novel spin-component scaled double hybrid functionals such as DSD-PBEP86-D2 acquit themselves very well" here. van Santen and DiLabio found that dispersion corrections tacked on to otherwise deficient functionals inproved their perfromance and offered this as a "low-cost approach" to improving their performance [63g], which is akin to the approach of Goerigk and Grimme [63e].

The treatment of dispersion can crop up when one is not explicitly investigating weak interactions and might not expect to be led astray by treating it inadequately. For example, hexaphenylethane is apparently (the compound is unknown as of mid-2016) very crowded, so it natural to ascribe its resistance to synthesis to steric hindrance. Yet all-*meta* -*t*-butyl hexaphenylethane (twelve *t*-butyl groups), formidably more crowded than the parent molecule, is a known, stable compound. This quite unanticipated fact has been convincingly explained by "state-of-the-art quantum chemical computations" to be due to dispersion attraction between pairs of *t*-butyl groups [64]. They are positioned close enough for such attraction but not close enough for the traditional steric hindrance of "Pauli repulsion" (Chap. 5, Sect. 5.2.3.2, in connection with Eq. (5.22)). Dispersion can be treated in DFT by using a functional with dispersion "inherent" (e.g. M06-2X or an M08 functional; Table 10 in [65]) or by a "conventional" functional augmented with an empirical dispersion correction, a technique considerably associated with Grimme and coworkers, e.g. a B3LYP-gCP-D3/6-31G* calculation, which is said to also essentially eliminate basis set superposition error, BSSE (Chap. 5, Sect. 5.4.3), of an *intramolecular* nature [63e]. Relevant to interactions in large systems and to the dismissal of the need for BSSE, like the studies of [63e] and [64], is a paper on host-guest supramolecular systems [63h]. Many options for addressing dispersion in DFT are provided in recent versions of the Gaussian program suite, as shown on their website.

7.2.3.4.9 Is DFT a Semiempirical Method?

Having just examined the various DFT levels, we can return to the question posed at the end of Sect. 7.1: is DFT semiempirical, or is it a kind of ab initio method? We can also ask: does it matter? Addressing the first question: a semiempirical method is one that is parameterized against experiment (but in chemistry we wisely do not demand that fundamental constants like the velocity of light and Planck's constant be calculated from first principles!). It *is* possible to develop functionals that have

not been parameterized against experiment, and the review [47] in which Perdew et al. "present the case for the nonempirical construction" of such functionals argues convincingly for the classification of DFT as an ab initio-type technique *when it follows these strictures*. Nevertheless, the results of the wide-ranging study of Goerigk and Grimme [63e] make one uneasy on this point.

Regarding the second question: quite apart from the esthetic value that some see in a purely nonempirical calculation (recall von Neumann's jaundiced view of empirical equations: Chap. 6, Sect. 6.3.7), it may well be true that empirical approaches can reliably interpolate, but not extrapolate, and that they are, outside their parameterized domains, susceptible to "catastrophic failure" [66]; Clark raised this spectre explicitly in connection with DFT. We close this discussion of the "philosophy" of DFT with a look at a provocative stance by Nooijen, namely that DFT resembles molecular mechanics in that there "exists an exact force field for *each* electronic state with a given number of electrons" and that "the existence of many different exact functionals...also suggests that the physical content of DFT is easily overrated" (relevant to the latter statement he points out that "there are many, many, different ways to tackle the electronic structure problem from a density functional point of view...") [67]. The likening of DFT to molecular mechanics might appear mischievous: certainly MM does not recognize electron distribution, an objective feature of chemical reality with measurable consequences like dipole moments and optical activity. Nevertheless, this paper raises points which seem to be generally unappreciated, particularly with regard to "the enormous flexibility of in-principle-exact formulations" of DFT. The insecurity of even some practitioners of DFT in connection with its theoretical robustness is at least hinted at in the review by Jones [20]. The reader may wish to console him/herself with the possibility implied by Perdew et al. [47] that an exact (if not unique?) nonparameterized functional can be gradually approached. We now consider some applications of DFT.

7.3   Applications of Density Functional Theory

In examining the literature for applications of DFT one is (or ought to be) struck by the fact that there is no method (functional/basis set combination) that is *generally* best. For every property there seems to be one or two functionals that are superior to the others, but only for that property. This profusion is more exuberant than for methods and basis sets in the wavefunction realm (Sousa et al. list 52 functionals in their Table 2 [44]). One might conclude that the situation almost borders on the chaotic, to borrow the term used by Dewar to criticise what he saw as the profusion of basis sets [68] (Chap. 5, Sects. 5.3.3 and 5.5.2.2.1). However, this judgement would be unfair, if only because the relative infancy of DFT as a general, practical tool for molecular calculations requires the exploration of "functional space" for good methods. Furthermore, in the absence of a perfect solution one should be thankful for the availability of one that is acceptable for the task at hand. Zhao and Truhlar grant that those concerned about the profusion of functionals have a case,

but make the point that really satisfactory all-purpose functionals are "unlikely to be discovered in the foreseeable future" and that therefore for now we need specialized functionals [69]. Apparent exceptions to the claim that a universally applicable functional is wanting are presented by B3LYP and the recent M06-type, a family of four functionals, M06, M06-2X, M06-L, and M06-HF [45]. However, none of these excels for *all* tasks, although M06 in particular is said to be [45b] "for general-purpose applications" and the M06 member "with broadest applicability". As briefly mentioned in Sect. 7.2.3.4.5, B3LYP [57, 58] was so popular ca. 2007–2011 that it was singled out for special attention by Sousa et al. [44] (where striking pie charts show B3LYP like PacMan devouring other functionals) and by Zhao and Truhlar [45], who nevertheless cite its deficiencies. The M06-type functionals were said to provide "better across-the-board average performance than B3LYP" [45b]. Although for any specific task a better functional than B3LYP, perhaps one of the M06 family, can probably be found, a case might be made for still using B3LYP on occasion, for the sake of "backwards comparison", where the results are not simply unreasonably inaccurate. However it seems inevitable that an M06 type or some even newer functional will in the next few years overcome inertia and replace B3LYP as the most popular generally-used.

Levine mentions comparisons of some characteristics and properties of DFT versus ab initio [70]. Hehre [71] and Hehre and Lou [72] have provided extensive, very useful compilations of ab initio, semiempirical, DFT, and some molecular mechanics results. Recent surveys oriented toward the quality of molecular properties from DFT, are those by Sousa et al. (geometries, barrier heights, atomization energies, ionization energies, electron affinities, heats of formation, isomerization energies, weak interactions) [44], Zhao and Truhlar (geometries, barrier heights, frequencies, various thermochemical parameters–atomization energy etc., ionization energies, electron affinities, UV, transition metal reactions, weak interactions) [45], and Riley et al. (geometries, barrier heights frequencies, ionization energies, electron affinities, heats of formation, conformational energies, hydrogen bonds; great emphasis on comparing Pople vs. Dunning basis sets) [46].

7.3.1   Geometries

With regard to geometries, Figures and Tables in this chapter correspond to those in Chap. 5 (ab initio) and Chap. 6 (semiempirical) like this:

Fig. 7.1 (geometries of 20 molecules), Figs. 5.23 and 6.2
Fig. 7.2 (four reactions, various functionals, geometries and energies), Figs. 5.21 and 6.3
Fig. 7.3 (four reactions, various basis sets, B3LYP, geometries and energies), Figs. 5.21 and 6.3
Table 7.1 (analysis of bond lengths and angles), Tables 5.7 and 6.1
Table 7.2 (dihedral angles), Tables 5.8 and 6.2

For Fig. 7.1 and Tables 7.1 and 7.2, for comparison with the presentations in Chaps. 5 and 6, values from MP2/6‑31G* calculations (the standard post-Hartree
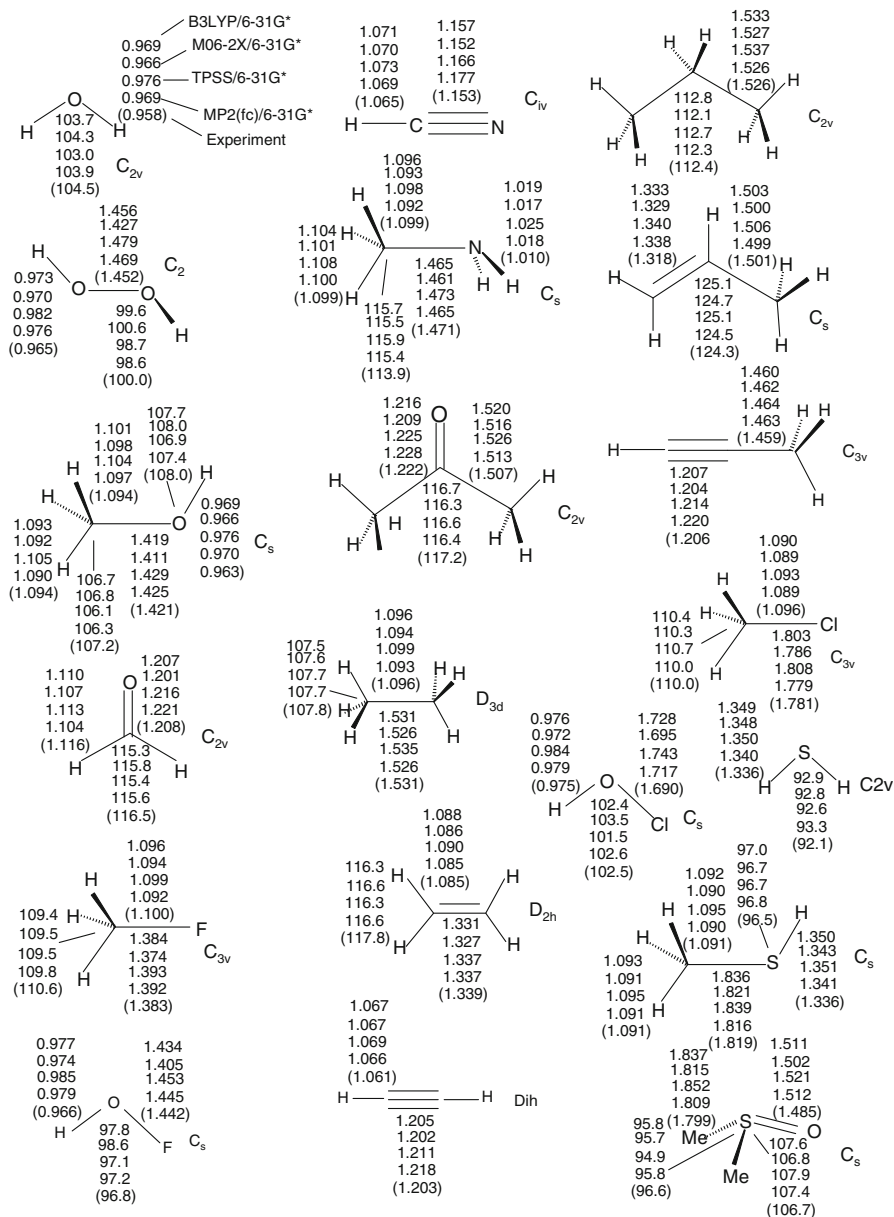
Fig. 7.1 Comparison of some B3LYP/6-31G*, M06-2X/6-31G*, MP2(fc)/6-31G*, and experimental geometries. Calculations are by the author and experimental geometries are from [69] (Note that all CH bonds are ca. 1 Å, and all other bonds range from 1.2 to 1.8 Å, and all bond angles (except for linear molecules) are ca. 90–120°)

Table 7.1 Errors in calculated bond lengths (Å) and angles (degrees) for the 20 molecules of Fig. 7.1

Molecule	B3LYP	M06-2X	TPSS	MP2	Exp
H$_2$O	0.011	0.008	0.018	0.011	L 0.958
1 L, 1 A	−0.8	−0.4	−1.5	−0.6	A 104.5
HCN	0.006	0.005	0.008	0.004	L 1.065
2 L, 0 A	0.004	0.001	0.013	0.024	L 1.153
Propane	0.007	−0.001	0.011	0.000	L 1.526
1 L, 1 A	0.4	−0.4	0.3	−0.1	A 112.4
HOOH	0.008	0.005	0.017	0.011	L 0.965
2 L, 1 A	0.004	−0.025	0.027	0.017	L 1.452
	−0.4	0.6	−1.3	−1.4	A 100.0
CH$_3$NH$_2$	0.005	0.007	0.009	0.001	L 1.099
4 L, 1 A	−0.003	−0.006	−0.001	−0.007	L 1.099
	0.009	0.007	0.015	0.008	L 1.010
	−0.006	−0.010	0.002	−0.006	L 1.471
	1.8	1.6	2.0	1.5	A 113.9
Propene	0.015	0.011	0.022	0.020	L 1.318
2 L, 1 A	0.002	−0.001	0.005	−0.002	L 1.501
	0.8	0.4	0.8	0.2	A 124.3
CH$_3$OH	−0.001	0.002	0.011	−0.004	L 1.094
4 L, 2 A	0.007	0.004	0.010	0.003	L 1.094
	0.006	0.003	0.013	0.007	L 0.963
	−0.002	−0.010	0.008	0.004	L 1.421
	−0.5	0.0	−1.1	−0.9	A 107.2
	−0.3	−0.4	−1.1	−0.6	A 108.0
Propanone	−0.006	−0.013	0.003	0.006	L 1.222
2 L, 1 A	0.013	0.009	0.019	0.006	L 1.507
	−0.5	−0.9	−0.6	−0.8	A 117.2
Propyne	0.001	−0.002	0.008	0.014	L 1.206
2 L, 0 A	0.001	0.003	0.005	0.004	L 1.459
HCHO	−0.006	−0.007	−0.003	−0.012	L 1.116
2 L, 1 A	−0.001	−0.009	0.008	0.013	L 1.208
	−1.2	−0.7 s	−1.1	−0.9	A 116.5
Ethane	0.000	−0.002	0.003	−0.003	L 1.096
2 L, 1 A	0.000	−0.005	0.004	−0.005	L 1.531
	−0.3	−0.2	−0.1	−0.1	A 107.5
CH$_3$Cl	−0.006	−0.007	−0.003	−0.007	L 1.096
2 L, 1 A	0.022	0.005	0.027	−0.002	L 1.781
	0.4	0.3	0.7	0.0	A 110.0
HOCl	0.001	−0.003	0.009	0.004	L 0.975
2 L, 1 A	0.038	0.005	0.053	0.027	L 1.690
	−0.1	1.0	−1.0	0.1	A 102.5
H$_2$S	0.013	0.005	0.014	0.004	L 1.336
1 L, 1 A	0.8	0.7	0.5	1.2	A 92.1
CH$_3$F	−0.004	−0.006	−0.001	−0.008	L 1.100
2 L, 1 A	0.001	−0.009	0.010	0.009	L 1.383
	−1.2	−1.1	−1.1	−0.8	A 110.6
Ethene	0.003	0.001	0.005	0.000	L 1.085

Table 7.1 (continued)

Molecule	B3LYP	M06-2X	TPSS	MP2	Exp
2 L, 1 A	−0.008	−0.012	−0.002	−0.002	L 1.339
	−1.5	−1.2	−1.5	−1.2	A 117.8
CH_3SH	0.002	0.000	0.004	0.000	L 1.091
4 L, 1 A	0.001	−0.001	0.004	−0.001	L 1.091
	0.014	0.002	0.015	0.005	L 1.336
	0.017	0.007	0.020	−0.003	L 1.819
	0.5	0.2	0.2	0.3	A 96.5
HOF	0.011	0.008	0.019	0.013	L 0.966
2 L, 1 A	−0.008	−0.037	0.011	0.003	L 1.442
	1.0	1.8	0.3	0.4	A 96.8
Ethyne	0.006	0.006	0.008	0.005	L 1.061
2 L, 0 A	0.002	−0.001	0.008	0.015	L 1.203
	0.038	0.016	0.053	0.010	L 1.799
Me_2SO	0.026	0.017	0.036	0.027	L 1.485
2 L, 2 A	−0.8	−0.9	−1.7	−0.8	A 96.6
	0.9	0.1	1.2	0.7	A 106.7

The errors are calculated value–experimental value. The basis set is 6-31G*. L is bond length and A bond angle. For example, for propane one bond length and one angle were examined, and for B3LYP L was 0.007 Å longer than the experimental 1.566 Å. The Exp column shows experimental bond lengths and angles. The errors are discussed in the text

Table 7.2 Calculated dihedral angles and errors (dihedral)/error) and experimental dihedral angles, for eight molecules

Molecule	B3LYP	M06-2X	TPSS	MP2	Exp
HOOH	119.3/0.2	116.7/−2.4	119.6/ 0.5	121.2/2.1	119.1
FOOF	87.2/−0.3	84.6/−2.9	87.8/0.3	85.8/−1.7	87.5[b]
FCH_2CH_2F (FCCF)	69.8/−3.2	68.9/−4.1	69.6/−3.4	69.0/−4.0	73[b]
FCH_2CH_2OH					
(FCCO)	63.3/−0.7	61.9/−2.1	62.4/−1.6	60.1/−3.9	64.0[c]
(HOCC)	62.7/8.1	62.3/7.7	63.0/8.4	54.1/−0.5	54.6[c]
$ClCH_2CH_2OH$					
(ClCCO)	61.2/−2.0	59.9/−3.3	60.2/−3.0	65.0/1.8	63.2[b]
(HOCC)	60.0/1.6	59.9/1.5	60.5/2.1	64.3/5.9	58.4[b]
$ClCH_2CH_2F$					
(ClCCF)	66.7/−1.3	65.4/−2.6	66.2/−1.8	65.9/−2.1	68[b]
HSSH	90.7/0.1	90.5/−0.1	90.8/0.2	90.4/−0.2	90.6[a]
FSSF	89.1/1.2	89.2/1.3	89.3/1.4	88.9/1.0	87.9[b]

The errors are calculated value–experimental value. The basis set is 6-31G*. Calculations are by the author

[a] W. J. Hehre, L. Radom, p. v. R. Schleyer, J. A. Pople, "Ab initio Molecular Orbital Theory", Wiley, New York, 1986; pp. 151, 152. These dihedrals are believed (p. 136) to be from gas phase microwave spectroscopy or electron diffraction

[b] M. D. Harmony, V. W. Laurie, R. L. Kuczkowski, R. H. Schwenderman, D. A. Ramsay, F. J. Lovas, W. H. Lafferty, A. G. Makai, "Molecular Structures of Gas-Phase Polyatomic Molecules Determined by Spectroscopic Methods", J. Physical and Chemical Reference Data, 1979, *8*, 619–721. From gas phase microwave spectroscopy or electron diffraction

[c] J. Huang, K. Hedberg, J. Am. Chem. Soc., 1989, *111*, 6909. From gas phase microwave spectroscopy augmented with electron diffraction
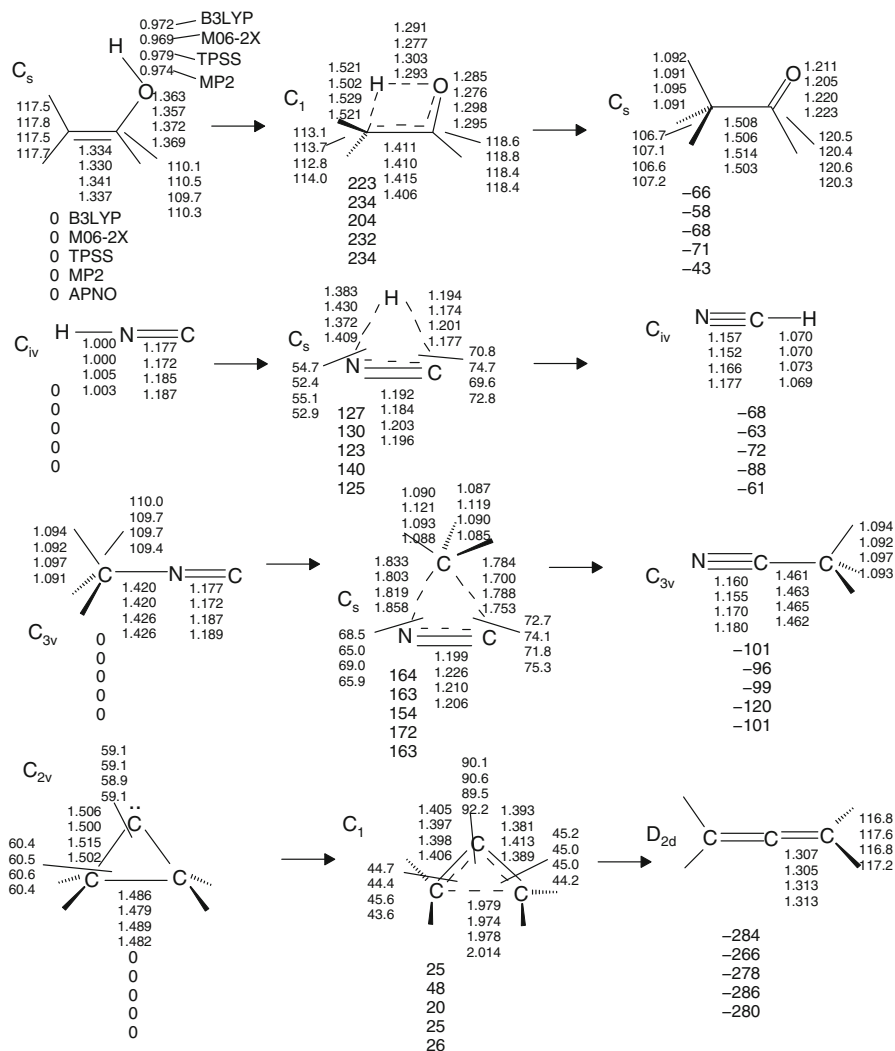
Fig. 7.2 Calculated geometries (Å and degrees; most H's are omitted for clarity) and reaction profiles for four reactions. The energies (0 : 223 : −66, kJ mol^{-1} etc.) are relative 298 K enthalpies (activation enthalpy 223 k mol^{-1}, reaction enthalpy −66 kJ mol^{-1}) calculated by B3LYP, M06-2X, TPSS, and MP2 with the 6-31G* basis set; the fifth (*the bottom*) enthalpy value for each species is a 298 K CBS-APNO enthalpy value, and is considered more reliable than reported [70] experimental values; see text. The purpose of the Figure is to compare these three functionals and MP2 (Calculations are by the author)

Fock ab initio method; Chap. 5, Sect. 5.4.2) and from experiment (geometries, Fig. 7.1 [73], energies, Fig. 7.2 [77]; see too the explanation of the use of CBS-APNO energies as a surrogate for the relative energies of these four reactions, Sect. 7.3.2.2) were clearly necessary. This choice of the relatively small 6-31G* basis is discussed below.

The choice of DFT functionals for these illustrative geometry (and energy) calculations presented here needed some consideration. B3LYP is retained from the first and second editions of this book because of its vast archive of results. The pBP/DN* functional/basis set (described in [72]) that was a feature of Spartan [75] and was used in the first edition of the book showed certain problems and is no longer available, and its replacement required some deliberation. The remaining choice was now narrowed to three possibilities:

1. Considering the "general-purpose" M06 family. This are hybrid meta-GGA functionals (Sect. 7.2.3.4.6) parameterized with nonmetals and metals (for a review and for details see respectively [45] and [69]). They lie on rung 6 of our ladder (rung 5 if LDA and LSDA are collapsed into rung one as indicated in Table 2 of [44] and as implied in [69]). As stated in Sect. 7.3, these may eventually replace B3LYP. Of the four functionals in this class, the choice of M06-2X was made from the recommendations in [45]. M06-L and M06-HF were not used here because the former sacrifices some accuracy for speed, and the latter some ground state accuracy for excited states. M06-2X was chosen over M06 (used in the previous edition) because if transition metals are not involved M06-2X seems to be the preferred functional of these two, and M06-2X was said to be better than M06 for noncovalent interactions. Persuaded by the case made by Perdew et al. for nonempirical functionals, the following recommended [47] ones were also considered:

2. PBE [76] (a nonempirical GGA functional; Sect. 7.2.3.4.3), and

3. TPSS [77] (a nonempirical meta-GGA functional; Sect. 7.2.3.4.4).

In our classification (Sects. 7.2.3.4.1, 7.2.3.4.2, 7.2.3.4.3, 7.2.3.4.4, 7.2.3.4.5, 7.2.3.4.6 and 7.2.3.4.7) PBE is on rung three and TPSS is on rung four (these are rungs two and three if LDA and LSDA are collapsed into rung one). TPSS was given precedence over PBE because it lies on a higher rung, which does not mean that for every task it will be more accurate; however "TPSS usually provides better accuracy than PBE for a very modest increase of computational cost....TPSS is close to being the best nonempirical functional so far...".[3] A choice could not be made between M06-2X and TPSS, and for geometries (and energies) calculated here both were used, because it appears that M06-2X may become the general purpose functional of choice, while TPSS is nonempirical, giving it an esthetic virtue as well as (one hopes) shielding it against "catastrophic failure" (see Sect. 7.2.3.4.9). Thus in Figs. 7.1 and 7.2, and in Tables 7.1 and 7.2, we compare geometries from B3LYP, M06-2X, TPSS, and MP2(fc)/6-31G* (perhaps the highest-level ab initio method in routine use) with experiment. The M06-2X calculations reported here were done with Gaussian 09 with the keywords

---

[3]Personal communication from Professor J. P. Perdew, 2009 November 7. As of 2015 February, TPSS evidently still held essentially this position, although a nonempirical meta-GGA close to TPSS for molecules, but more accurate for solids, revTPSS (revised TPSS) had been developed (personal communication from Professor J. P. Perdew, 2015 February 25).

Opt = (Tight) and Int = (Grid = Ultrafine) ; an ultrafine grid has been recommended for the M06-type functionals [78].

Table 7.1 shows the errors in 43 bond lengths, and 19 bond angles for which symmetry does not impose a value of 180°, taken from 20 molecules; compare this with Fig. 7.1. For each of these parameters the deviation from experiment (calculated – experimental value) is shown for B3LYP, M06-2X, TPSS, and MP2 (with the 6‑31G* basis in each case). The mean absolute deviations from experiment (arithmetic mean of the unsigned errors), MAD, are:

	B3LYP	M06-2X	TPSS	MP2
Bond lengths	0.008	0.007	0.013	0.008
Bond angles	0.75	0.7	0.95	0.7

(For M06 the results were very similar: the MAD for bond lengths and angles were 0.008 and 0.8).

For bond lengths the biggest error was 0.053 Å (TPSS, for the C-S bond of Me_2SO). For bond angles, the biggest error was $2^{°}$ (TPSS, for the HCN angle of CH_3NH_2). For the bonds, the number of parameters for which the direction of deviation was zero (bond or angle the same as experiment), positive (bond bigger than experiment), and negative are:

	B3LYP	M06-2X	TPSS	MP2
0.000 deviation	2	1	0	3
positive	30	22	38	27
negative	11	20	5	13

(For M06 the results were very similar: the number of zero, positive and negative deviations were 1, 25 and 17).

For bond angles the corresponding deviations are:

	B3LYP	M06-2X	TPSS	MP2
0.0 deviation	0	1	0	1
positive	11	9	11	11
negative	8	9	8	7

(For M06 the results were very similar: the number of zero, positive and negative deviations were 1, 10 and 8).

Qualitative conclusions from all this are: reasonably good bond lengths (to within ca. 0.01 Å) are given with the 6-31G* basis by B3LYP, M06-2X, and MP2; TPSS values (0.013 MAD error) are satisfactory for most purposes. All four methods give good bond angles (to within ca. 2°, mostly less than 1°). For bond lengths positive deviations are somewhat more frequent than negative (for TPSS they are about eight times as frequent), and for bond angles (where errors are usually trivial) the number of positive and negative deviations are roughly the same.

Table 7.2. presents for examination ten dihedral angles from eight molecules. For each of these the dihedral was calculated by B3LYP, M06-2X, TPSS, and MP2

(with the 6-31G* basis in each case). The mean absolute deviations (degrees, arithmetic mean of the unsigned errors), MAD, are:

B3LYP	M06-2X	TPSS	MP2
1.9	2.8	2.3	2.3

(For M06 the results were very similar: the MAD for these dihedrals was 2.0).

Because of the periodic (sinusoidal) nature of the energy-dihedral angle function, the direction of deviation from experiment, the number of positive vs. negative deviations, is not meaningful, provided these are small (under $10°$), as they are here. The calculated dihedral angles are all within ca. $3°$, except FCH_2CH_2OH (HOCC by B3LYP. M06-2X, TPSS) and $ClCH_2CH_2OH$ (HOCC by MP2), where they are ca. $7°$. In view of the soft nature of the energy-dihedral function (energies do not rise or fall steeply with small changes in dihedrals, unlike changes in bond lengths or angles), and of possible errors in the experimental values, this is not serious. All four methods seem to be satisfactory for dihedrals.

B3LYP/6-31G*, M06-2X, TPSS and MP2(fc)/6-31G* geometries (and relative energies) are compared for the species shown in four reaction profiles in Fig. 7.2. These correspond to the ab initio comparisons of Fig. 5.21 and the semiempirical comparisons of Fig. 6.3. Since experimental geometries are not available for any of the transition states and also not for cyclopropylidene, we content ourselves with some simple comparisons among the calculated geometries. For the reactants and products the DFT bond length deviations from the MP2 geometries, which latter we tacitly take to be reasonably good (Chap. 5, Sect. 5.51), are all within 0.02 Å. For the transition states deviations from the MP2 values are bigger, up to 0.055 (for the partial "single" NC bond of the CH_3NC transition state with M06-2X). The DFT angles do not deviate by more than $3.5°$ (for an NCC angle of the CH_3NC transition state with TPSS) from the MP2 values. The consistency of the three DFT methods and their good agreement with MP2 suggest that these DFT methods are quite comparable to MP2/6-31G* in calculating transition state geometries. For the geometries of the species in Figs. 7.1 and 7.2, there is little difference between the results from the M06-2X functional used here and the M06 used in the second edition of this book.

Geometry errors for 108 molecules were reported by Scheiner et al. [79], comparing several ab initio and DFT methods. They found that Becke's original 3-parameter function (which they denote ACM, for adiabatic connection method; B3LYP was developed as a modification of this [58]), with a 6-31G**-type and with the 6-31G** basis sets, gave average bond length errors of about 0.01 Å and bond angle errors of about $1.0°$. They concluded that of the methods they examined ACM is the best choice for both geometries and reaction energies. St-Amant et al. [52] also compared ab initio and DFT methods and found average dihedral angle errors of ca. $3°$ for eleven molecules using a perturbative gradient-corrected DFT method with an approximately 6-311G**-type basis set. These workers found average bond length errors of, e.g., 0.01 Å for C–H and 0.009 Å for C–C single

bonds, and average bond angle errors of 0.5°. El-Azhary reported B3LYP with the 6-31G* and cc-pVDZ basis sets to give slightly better geometries than MP2, but MP2 avoided the occasional large errors given by B3LYP [80]. The effect of using different basis sets was minor. In a comparison of Hartree-Fock, MP2 and DFT (five functionals), Bauschlicher found B3LYP to be the best method overall [81]. Hehre has compared bond lengths calculated by the DFT non-gradient-corrected SVWN method, B3LYP, and MP2, using the 6-31G (no polarization functions) and 6-31G* basis sets [71]. His work confirms the necessity of using polarization functions with the correlated (DFT and MP2) methods to obtain reasonable results, and also shows that for equilibrium structures (i.e. structures that are not transition states) there is little advantage to correlated over Hartree-Fock methods as far as geometry is concerned, a conclusion presented in Chap. 5, Sect. 5.5.1 with regard to correlated ab initio methods. Hehre and Lou [72] carried out extensive comparisons of HF, MP2 and DFT (SVWN, pBP, B3LYP) methods with 6-31G* and larger basis sets, and the numerical DN* and DN** bases. For a set of 16 hydrocarbons, MP2/6-311+G(2d,p), B3LYP/6-311+G(2d,p), pBP/DN** and pBP/DN* calculations gave errors of 0.005 Å, 0.006 Å, 0.010 Å and 0.010 Å, respectively. HF/6-311+G(2d,p) and SVWN calculations also gave errors of 0.010 Å. For 14 C-N, C-O and C = O bond lengths B3LYP and pBP (errors of 0.007 Å and 0.008 Å) were distinctly better than HF and SVWN (errors of 0.022 Å and 0.014 Å, respectively).

The overall indication from the literature and the results in Fig. 7.1 and Table 7.1 (errors are evaluated above) is that the somewhat old (1994 [58]) B3LYP functional gives good geometries. Of the newer functionals tested here, M06-2X (2011, 2007, 2008 [45, 69]) and TPSS (2003 [77]), the indication from our (admittedly quite limited) results is that M06-2X is about as good as B3LYP and that TPSS is somewhat inferior (but note that lacking empirical parameters TPSS may be less prone to unexpected (or "catastrophic" [66]; Sect. 7.2.3.4.9) failure. Recently published (2007) extensive general (not just for geometry as the title of this section implies) evaluations of functionals are those by Sousa et al. [44], Zhao and Truhlar [45], and Riley et al. [46]. Synopses of these papers are given in Sect. 7.2.3.4.

Besides the functional, the choice of basis set needs to be addressed. Larger basis sets may tend to increase accuracy, but the increase in time may not make this worthwhile. DFT calculations have been said to become "saturated" more quickly by using bigger basis sets than are ab initio calculations: Merrill et al. noted that "Once the double split-valence level is reached, further improvement in basis set quality offers little in the way of structural or energetic improvement." [38]. Stephens et al. report that "Our results also show that B3LYP calculations converge rapidly with increasing basis set size and that the cost-to-benefit ratio is optimal at the 6-31G* basis set level. 6-31G* will be the basis set of choice in B3LYP calculations on much larger molecules [than $C_4H_6O_2$]" [58]. Figure 7.3 shows the effect on geometry and relative energies of B3LYP with the modest 6-31G*, the fairly big 6-311+G**, and the big 6-311++G(2df, 2p) bases. These results support the basis set saturation assertion for geometries, but cast doubt on the ease of
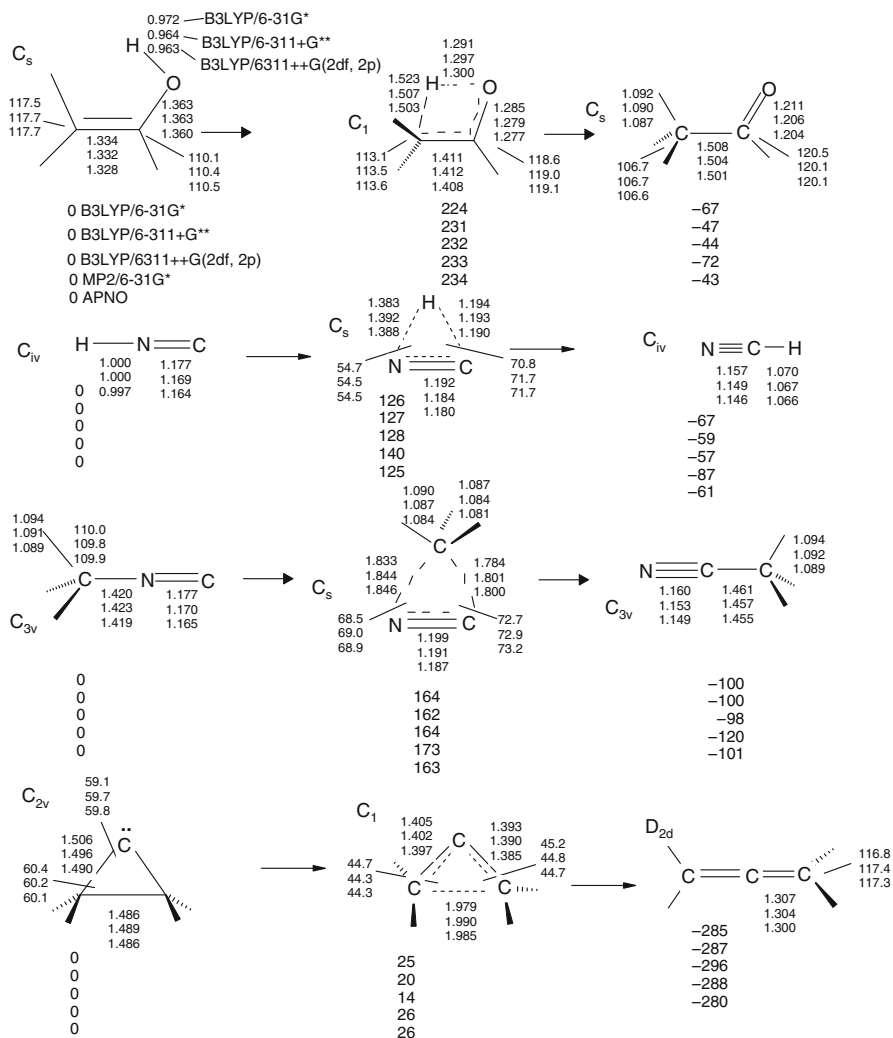
Fig. 7.3 Comparison of geometries (Å and degrees) and relative energies (kJ mol–1) from the B3LYP functional using three basis sets (energies are also compared with those from MP2(fc)/ 6-31G* and CBS-APNO, Sect. 7.3.2.2): 6-31G* (53 basis functions for C_2H_4O, 32 for HCN, 51 for C_2H_3N, 53 for C_3H_4). 6-311+G** (90 basis functions for C_2H_4O, 50 for HCN, 84 for C_2H_3N, 90 for C_3H_4). 6-311++G(2df, 2p) (142 basis functions for C_2H_4O, 78 for HCN, 132 for C_2H_3N, 142 for C_3H_4). B3LYP and MP2 energies are 0 K energy (i.e. 0 K enthalpy) differences) with ZPE correction; only for MP2 was the ZPE itself corrected (multiplied by 0.9670 [78]), because for DFT methods the corrections appear to lie between 0.96 and unity [78]. The fifth (the bottom) value for each species is a 298 K enthalpy value from CBS-APNO, and is considered more reliable than reported [70] experimental activation and reaction energies; see text. The purpose of the Figure is to show how basis set size can affect geometry and relative energies (Calculations are by the author)

saturation where relative energies are concerned; energies are discussed in the next section. The insensitivity of geometries to basis sets beyond 6-31G* is also shown in Figures 1 and 3 in reference [46], where with a wide selection of functionals very similar errors resulted with the 6-31G*, 6-31+G*, and 6-31++G* basis sets.

7.3.2   Energies

7.3.2.1   Energies: Preliminaries

With regard to energies, Figures and Tables in this chapter correspond to those in Chap. 5 (ab initio) and Chap. 6 (semiempirical) like this:

Fig. 7.2 (four reactions, various functionals, geometries and energies)	Figs. 5.21, 6.3, and 6.4
Fig. 7.3 (four reactions, various basis sets, B3LYP, geometries and energies)	Figs. 5.21, 6.3, and 6.4
Tables 7.3, 7.4, 7.5, 7.6 and 7.7 (general concern with energies)	Tables 5.4, 5.5, 5.6, 5.9, 5.12, 5.13, 6.3, and 6.4

Usually, we seek from a DFT calculation, as from an ab initio or semiempirical one, geometries (preceding section) and energies. Like an ab initio energy, a DFT energy is relative to the energy of the nuclei and electrons infinitely separated and at rest, i.e. it is the negative of the energy needed to dissociate the molecule into its nuclei and electrons. Semiempirical energies like those from AM1 and PM3 (Chap. 6, Sect. 6.3.2) are heats of formation, and by parameterization zero-point energies are included. In contrast, an ab initio (Chap. 5, Sect. 5.2.3.6.4) or DFT molecular energy, the energy printed out at the end of any calculation, is the energy of the molecule sitting motionless at a stationary point (Chap. 2, Sect. 2.2) on the potential energy surface; it is the purely electronic energy plus the internuclear repulsion. In accurate work on a reaction profile (reactant, transition state, product series) this "raw" energy should be corrected by adding the zero-point vibrational energy, from a frequency calculation, to obtain the total internal energy at 0 K. Analogously to the HF equation in Chap. 5, Sect. 5.2.3.6.4, Eq. (5.94) we have

$$E_{0\,K}^{total} = E_{DFT}^{total} + ZPE \qquad (*7.29)$$

(Calculations using the Gaussian program suite denote the DFT energy called here E_{DFT}^{total} as HF, e.g. (in hartrees or atomic units) "HF $= -308.86101$"). The main advantage of DFT over Hartree-Fock calculations is in being able to provide, in a comparable time, superior energy-difference results: reaction energies and activation energies.

7.3.2.2 Energies: Calculating Quantities Relevant to Thermodynamics and Kinetics

Regarding the use of CBS-APNO calculations as a surrogate for experimental energy values, particularly for the four reactions whose energies are addressed in Figs. 7.2 and 7.3: experimental results are skimpy and sometimes of only limited relevance (for example, activation energies may be lowered by surface effects) for these four reactions. For them CBS-APNO are shown in the Figures as benchmarks against which to compare the accuracy of the relative energies from the other methods. These APNO values provide a methodologically uniform set of accurate relative enthalpies; they are expected to be at least as accurate as available or any likely future experimental values (mean absolute deviations $2.2 \, \mathrm{kJ \, mol}^{-1}$; Chap. 5, Sect. 5.5.2.3.2, *Comparison of high-accuracy multistep methods*). For Figs. 7.2 and 7.3, comparison of the APNO relative activation and reaction enthalpies with those from other high-accuracy methods considered somewhat less accurate showed excellent consistency ($\mathrm{kJ \, mol}^{-1}$):

ethenol (vinyl alcohol) to ethanal:
APNO, 0 : 234 : −43; CBS-QB3, 0 : 238 : −44; G4MP2, 0 : 237 : −42

HNC to HCN:
APNO, 0 : 125 : −61; CBS-QB3, 0 : 129 : −60; G4MP2, 0 : 122 : −61

CH_3NC *to CH3CN*:
APNO, 0 : 163 : −101; CBS-QB3, 0 : 164 : −100; G4MP2, 0 : 160 : −99

cyclopropylidene to allene:
APNO, 0 : 26 : −280; CBS-QB3, 0 : 25 : −280; G4MP2, 0 : 24 : −277

This is consistent with the view that these three high-accuracy methods are good stand-ins for experimental values.

7.3.2.2.1 Thermodynamics

Let's first see how DFT handles a case where Hartree-Fock with its cavalier treatment of electron correlation fails badly: homolytic breaking of a covalent bond (Chap. 5, Sect. 5.4.1). Consider the reaction

$$H_3C - CH_3 + E_{\mathrm{diss}} \rightarrow H_3C \cdot \quad \cdot CH_3$$

In principle the dissociation energy can be found simply as the energy of two methyl radicals minus the energy of ethane. Table 7.3 (cf. Table 5.5) shows the results of HF, MP2, and DFT (B3LYP, M06-2X, and TPSS) calculations, with the 6-31G* basis. The energies shown for each species are 0 K energies (enthalpies) and 298 K enthalpies for bond-breaking. The HF and MP2 0 K values are corrected for ZPE with the ZPE itself corrected, by 0.9135(HF) and 0.9670 (MP2(fc)), as prescribed by Scott and Radom [82a]. For the DFT 0 K energies the ZPEs were

Table 7.3 The C–C bond energy of ethane by HF, MP2(fc), and DFT (B3LYP, M06-2X, and TPSS) calculations, at 0 K and 298 K

Method	0 K	298 K
HF	248	255
MP2(fc)	372	381
B3LYP	363	375
M06-2X	387	397
TPSS	357	366

References to the methods: HF, Chap. 5, Sect. 5.2.2; MP2, Chap. 5, Sect. 5.4.2; B3LYP [57, 58]; M06-2X [45, 65]; TPSS [77]

The basis set is 6-31G*. Standard, tabulated bond energies are for dissociation at 298 K. Bond energy = 2(CH$_3$ radical enthalpy) − (CH$_3$CH$_3$ enthalpy). For the radical the unrestricted method (UHF etc.) was used. For the 0 K dissociation enthalpy, the HF and MP2 calculations use energies corrected for ZPE, with the ZPE itself corrected by a factor of 0.9135 (HF) or 0.9670 (MP2) [82]. The 0 K dissociation enthalpy for the DFT calculations is uncorrected for ZPE, and the 298 K dissociation enthalpy is from standard statistical thermodynamics methods [83b]. The experimental 298 K C–C energy of ethane has been reported as 90.1 ± 0.1 kcal mol^{-1}, i.e. 377 ± 0.4 kJ mol^{-1} [84]. Calculations are by the author

not corrected, as the factor appears to lie between 0.96 and unity [82a] (a recent paper prefers a quadratic, rather than the popular linear, correction for IR frequencies [82b]). The enthalpies were calculated with Gaussian 09 [83a] using a statistical mechanics algorithm that is "appropriate for calculating enthalpies of reaction" [83b]. Product enthalpies minus reactant enthalpies give the calculated bond enthalpy; standard, tabulated bond enthalpies are for 298 K. The 298 K experimental bond energy has been reported to be 90.1 ± 0.1 kcal mol^{-1}, i.e. 377 ± 0.4 kJ mol^{-1} [84], and the CBS-APNO value (above, Sect. 7.3.2.2), is 379.3 kJ mol^{-1}, essentially the same as the reported experimental bond energy. In Table 7.3 we see that for the 298 K bond dissociation enthalpy the Hartree-Fock value is hopelessly too low (by 122 kJ mol^{-1}), the errors for M06-2X and TPSS are not bad ($+20$ and -11 kJ mol^{-1}), and the MP2 and B3LYP enthalpies are good, within $+4$ and -2 kJ mol^{-1} of what we hold to be the correct bond energy. Thus all of these electron correlation methods handle homolytic bond breaking at least tolerably well. The M06-2X value might have been expected to be better, but this is just one example (the M06 298 K bond enthalpy, 390 kJ mol^{-1}, is 13 kJ mol^{-1} too high).

The reaction profiles in Fig. 7.3, mentioned above in connection with geometry, also explore the effect of basis set size on relative energies (barriers and reaction energies) for the B3LYP functional. As stated in Sect. 7.3.1, these geometries seem to be reasonably insensitive to basis set, but there are some significant changes in energies on going from the 6-31G* to the 6-311+G* or the 6-311++G(2df, 2p) basis: the reaction energy for the ethenol isomerization rises from ca. -67 to ca. −45 kJ mol^{-1} and for the HNC isomerization from ca. −69 to ca. −57 kJ mol^{-1}. The insensitivity of the activation energies, compared to the reaction energies, for these two reactions, can be rationalized with the Hammond postulate [85], which

Table 7.4 Reaction enthalpies (298 K, kJ mol^{-1}), calculated with three functionals and two basis sets, 6-31G* and 6-311++G(2df, 2p), and with three high-accuracy methods (but CBS-APNO is unable to handle Cl species)

Method	Reaction	
	$H_2 + Cl_2 \rightarrow 2\ HCl$	$H_2 + O_2 \rightarrow 2\ H_2O$
B3LYP		
6-31G*	−169	−344
6-311++G(2df, 2p)	−182	−447
M06-2X		
6-31G*	−172	−381
6-311++G(2df, 2p)	−177	−466
TPSS		
6-31G*	−152.5	−295
6-311++G(2df, 2p)	−162	−393
G4(MP2)	−180	−479
CBS-QB3	−182	−474
CBS-APNO	Unavailable	−477
Experiment[a]	−184	−484

The calculated reaction enthalpies follow from the calculated 298 K molecular enthalpies and the product enthalpies minus the reactant enthalpies
[a]Experimental heats of formation of HCl and H$_2$O: [86]

implies that for an exothermic reaction the reactant resembles its subsequent transition state; thus the effect of changing the basis set might be much the same for both reactant and transition state. Why the CH$_3$NC and cyclopropylidene B3LYP reaction energies are almost unperturbed is unclear. The effect of basis set on the energies of these reactions is discussed further in Sect. 7.3.2.2.2, under kinetics (where some reference is also made to reaction energies).

Table 7.4 compares with experiment [86] the effect of functionals and of basis set size on the reaction enthalpies of the important H$_2$/Cl$_2$ and H$_2$/O$_2$ reactions. First we note that the high-accuracy (G4(MP2), CBS-QB3, and CBS-APNO; Chap. 5, Sect. 5.5.2.3.2) acquit themselves well with two qualifications: the highly accurate CBS-APNO method (mean absolute deviation from experiment, 2.2 kJ mol^{-1}) [87] was not applicable to the H$_2$ + Cl$_2$ reaction because of its inability to treat Cl, and this method indicates that the reaction enthalpy of the 2 H$_2$ + O$_2$ reaction is closer to −477 than to the reported −484 kJ mol^{-1}. We compare the functional/basis set combinations by comparison with the experimental values of −184 (for H$_2$ + Cl$_2$ → 2HCl) and −484 kJ mol^{-1} (for 2 H$_2$ + O$_2$ → 2H$_2$O). Concerning the three functionals: in all cases the 6-311++G (2df,2p) basis performs better, usually dramatically so, than the 6-31G*; M06-2X/6-311++G(2df,2p) gives a good result for the H$_2$ + O$_2$ reaction, with B3LYP/6-311++G(2df,2p) somewhat worse. Even with the bigger basis, TPSS does not perform well here. These calculations show that contrary to what might be inferred from [58], the 6-31G* basis is too small to count on for reasonably good results for general thermochemistry with DFT. For

certain classes of reactions, however, 6-31G* may be acceptable, e.g. the Diels-Alder reaction [88], and bond dissociation (Table 7.3). Only tests with model systems can show (by comparison with experiment of "higher" levels) if a particular functional/basis can be expected to be satisfactory for the desired purpose.

There are many studies in the literature of the ability of DFT to handle molecular thermochemistry (thermodynamics). Martell et al. tested six functionals on 44 atomization energies and six reactions and concluded that the best atomization energies were obtained with hybrid functionals, but slightly better reaction enthalpies were obtained with non-hybrid ones [89]. St-Amant et al. found that gradient-corrected functionals gave good geometries and energies for conformers; the dihedrals were on average within 4° of experiment and the relative energies were nearly as accurate as those from MP2 [52]. Scheiner et al. found that, as for geometries, Becke's original 3-parameter function (also called ACM, adiabatic connection method [57]) gave the best reaction energies [79]. Many energy difference comparisons have been published comparing B3LYP/6‑31G* with HF, MP2 and experiment [71]. These comparisons involve homolytic dissociation, various reactions particularly hydrogenations, acid–base reactions, isomerizations, isodesmic reactions, and conformational energy differences. This wealth of data shows that while gradient-corrected DFT and MP2 calculations are vastly superior for homolytic dissociations, for "ordinary" reactions (involving only closed-shell species), their advantage is much less marked; for example, HF/3-21G, HF/6-31G*, SVWN/6-31G* (non-gradient-corrected DFT), all usually give energy differences similar to those from B3LYP/6‑31G* and in fair agreement with experiment. Table 7.5 compares with experiment (tabulated by Hehre [90]) errors for hydrogenations, isomerizations, bond separation reactions (a kind of isodesmic reaction), and proton affinities; the methods are HF, SVWN, MP2, and B3LYP, all using the 6-31G* basis. In two of the four cases (hydrogenation and isomerization) the HF/6-31G* method gave the best results; in one case MP2 was best and in one case B3LYP. For the energy comparison of normal (not involving transition states) closed-shell organic species correlated methods like MP2 and DFT often seem to offer little or no advantage, unless one needs accuracy within ca. $10 - 20 \text{ kJ mol}^{-1}$ of experiment, in which case high-accuracy methods should be used. The strength of gradient-corrected DFT methods appears to lie largely in their ability to give

Table 7.5 Energy errors for hydrogenation reactions, isomerizations, bond separation reactions, and proton affinities, using four different methods; the basis set is 6-31G*

Reaction	Method			
	HF	SVWN	MP2	B3LYP
Hydrogenation	15	20	17	23
Isomerization	15	19	16	17
Bond separation	11	5	4	10
Proton affinity	14	18	11	7

The errors, in kJ mol^{-1}, in each case the arithmetic mean of the absolute deviations from experiment of 10 reactions, were calculated from the data in Hehre [90]

homolytic dissociation energies and activation energies with an accuracy comparable to that from MP2, but at a time cost comparable to that from HF calculations. Bauschlicher et al. compared various methods and recommended B3LYP over HF and MP2, to a large extent on the basis of the performance of B3LYP with regard to atomization energies and transition metal compounds [81]. Wiberg and Ochterski compared HF, MP2, MP3, MP4, B3LYP, CBS-4 and CBS-Q with experiment in calculating energies of isodesmic reactions (hydrogenation and hydrogenolysis, hydrogen transfer, isomerization, and carbocation reactions) and found that while MP4/6-31G* and CBS-Q were the best, B3LYP/6-31G* was also generally satisfactory [91]. Rousseau and Mathieu developed an economical way of calculating heats of formation by performing pBP/DN* calculations on molecular mechanics geometries; rms deviations from experiment were about 16 kJ mol^{-1} for a variety of compounds [92]. Although the pBP/DN* method was removed from Spartan (Sect. 7.3.1), it is said [72] to give results similar to those from BP86/6-311G*, which is available in several program suites. Ventura et al. found DFT to be better than CCSD(T) (a high-level ab initio method, Chap. 5, Sect. 5.4.3) for studying the thermochemistry of compounds with the O-F bond [93].

Regarding the application of functionals to thermochemistry, more recent references than those in the preceding paragraph (which run from 1993 to 2000) are three thorough compilations, [44, 45b] and [46]. References [44] and [45] give the impression that for best results on should select a functional based on quite specific requirements. Reference [46] indicates that of the functionals we have considered (the M06 and the related M05 families are not examined here), with Pople basis sets TPSS with 6-31G*, 6-31+G* or 6-31++G* gives among the smallest average heat of formation errors: ca. 5 kcal mol^{-1}, ca. 20 kJ mol^{-1}, and these values were similar with Dunning basis sets. This is surprising in view of the poor performance of TPSS with the H_2/Cl_2 and H_2/O_2 reactions (Table 7.4). B3LYP gave similar heat of formation errors (ca. 20 kJ mol^{-1}) with 6-31G* but capriciously ca. 60 kJ mol^{-1} with 6-31+G* or 6-31++G*, and with the biggest Dunning basis its error was ca. 20 kJ mol^{-1}. There is a lack of regularity in the thermochemical results from DFT calculations, and a user would do well to first explore results from model systems related to the particular project at hand. Reliably accurate thermochemistry still requires some largely (these usually incorporate empirical corrections and sometimes DFT optimizations) ab initio high-accuracy method like one from the Gaussian or CBS family (Chap. 5, Sect. 5.5.2.3.2).

7.3.2.2.2 Kinetics

Consider the reaction profiles in Fig. 7.2. The experimental data on these activation and reaction enthalpies is limited [74], but as argued above (Sect. 7.3.2.2) the APNO (as well as the CBS-QB3 and G4MP2) values are good substitutes. Despite the paucity of experimental data, for all these reactions the qualitative situation is known and agrees with Fig. 7.2: ethenol, HNC and CH_3NC are much less stable

than their isomers CH_3CHO, HCN, and CH_3CN and the barriers inhibit the uncatalyzed isomerization at room temperature (the threshold barrier for room temperature stability is ca. $100 \, kJ \, mol^{-1}$); cyclopropylidene has never been observed and a reasonable inference is that it isomerizes rapidly (even at 77 K) and essentially completely to allene. Even with this modest (6-31G*; compare the discussion in Sect. 7.3.1 for Fig. 7.3 and the effect of bigger basis sets on geometry) basis set, all the results are in qualitative agreement with experiment.

The effect of basis set size on the kinetics of the four reactions of Fig. 7.2 was explored; see Fig. 7.3. and Tables 7.6 and 7.7. Free energies, rather than enthalpies, of activation (reaction free energies are also given) were used here. Although the free energy/enthalpy differences are small, the quantitative effect of rate and equilibrium constants can be significant because the values appear in an exponent (Chap. 5, Sect. 5.5.2.3.4). In Table 7.6 the DFT results are checked with CBS-QB3. Reservations have been expressed about the reliability of methods like CBS-QB3 and G4-type for barriers, because they are parameterized for thermodynamics, and specifically, one might wonder about the effect of changes in the number of paired

Table 7.6 Barriers and reaction energies calculated by CBS-QB3, for comparison with the DFT and MP2 results in Figs. 7.2 and 7.3 and Table 7.7

Reaction	Barrier	Reaction energy
$CH_2 = CHOH \rightarrow CH_3CHO$	240	-45.6
$HNC \rightarrow HCN$	125	-58.5
$CH_3NC \rightarrow CH_3CN$	161	-98.6
Cyclopropylidene $\rightarrow$ allene	23.8	-279

The barrier is the free energy of activation at 298 K and the reaction energy is the free energy of reaction at 298 K, in $kJ \, mol^{-1}$. Cf. Chap. 5, Table 5.12

Table 7.7 Barriers and reaction energies (relative energies for reactant, transition state, product) calculated for the B3LYP, M06-2X, and TPSS functionals using the 6-31G*, 6-311 + G**, and 6-311++G(2df,2p) basis sets (shown respectively from top to bottom line)

| Functional | Reaction (cf. Table 7.6) | | | |
	$H_2C = CHOH$	HNC	CH_3NC	Cyclopropylidene
B3LYP	0, 224, −68	0, 123, −67	0, 161, −100	0, 24, −282
	0, 231, −48	0, 123, −58	0, 158, −100	0, 18, −286
	0, 232, −45	0, 124, −56	0, 160, −98	0, 16, −289
M06-2X	0, 235, −60	0, 126, −62	0, 160, −95	0, 47, −264
	0, 238, −42	0, 124, −53	0, 156, −93	0, 42, −265
	0, 239, −39	0, 123, −53	0, 156, −92	0, 40, −270
TPSS	0, 205, −71	0, 119, −71	0, 151, −98	0, 20, −274
	0, 211, −53	0, 118, −64	0, 147, −99	0, 16, −276
	0, 212, −50	0, 118, −62	0, 149, −97	0, 14, −280

The barrier is the free energy of activation at 298 K and the reaction energy is the free energy of reaction at 298 K, in $kJ \, mol^{-1}$. Cf. Table 7.6. and Chap. 5, Table 5.12

spins along the reaction coordinate [94]. Nevertheless, despite a caveat [95] the CBS-QB3 method has been explicitly recommended for barriers [96, 97]. We shall assume that as well as the reaction energies, the CBS-QB3 barriers also are reliable for these four reactions. Comparison of the values in Table 7.6 (CBS-QB3) and those in Table 7.7 (B3LYP, M06-2X and TPSS functionals and 6-31G*, 6-311+G** and 6-311++G(2df,2p) basis sets) reveals the effect on barriers and reaction energies of increasing basis set size with the three functionals. Table 7.7 also extends the information in Fig. 7.3 for relative energies, shown in the Figure only for B3LYP, to M06-2X and TPSS, and may be also be compared with Table 5.12 in Chap. 5, which shows free energies of activation for the $H_2C=CHOH$, CH_3NC and cyclopropylidene reactions, using MP2/6-31G*, B3LYP/6-31G*, G4(MP2), and CBS-QB3. The values in Tables 7.6 and 7.7 are 298 K relative free energies, while as discussed above those in Fig. 7.3 and 7.2 are the very similar (for these reactions, anyway) relative ZPE-corrected 0 K energies. Table 7.7 suggests that the 6-311+G** basis leads to essential saturation, with reaction energies becoming almost constant (the CH_3NC and cyclopropylidene reactions and all the barriers are almost indifferent to these basis sets). By comparison with Table 7.6, TPSS seems to be inferior to B3LYP and M06-2X for barriers but about as good for reaction energies. All things considered for these reactions, B3LYP and M06-2X (except that this overestimates the cyclopropylidene barrier by about 20 kJ mol^{-1}) with the 6-311+G** or (very similar results) 6-311++G(2df,2p) basis set were best in comparison with CBS-QB3. This shows that with the 6-311+G** basis these functionals are saturated and give, particularly for B3LYP and M06-2X, at least for these particular isomerizations, barriers and reaction energies comparable to those from the high-accuracy CBS-QB3 method, and probably in good agreement with experiment. There seems to be no advantage here of the 6-311++G(2df,2p) basis over the more "economical" 6-311+G** one.

Another demonstration that the assertion [38, 58] that the 6-31G* basis is generally adequate in DFT should be viewed with some skepticism was provided by del Rio et al., who found for methyl rotation barriers, in several cases DFT needed much bigger bases than MP2 or MP4 [98]. This quirky behavior emphasizes the importance of reality checks: testing the kind of calculation at hand against model systems for which experimental data are available.

Some references to the calculation of barriers with DFT are:In a study of alkene epoxidation with peroxy acids, B3LYP/6-31G* gave an activation energy similar to that calculated with MP4/6-31G*//MP2/6-31G* but yielded kinetic isotope effects in much better agreement with experiment than did the ab initio calculation [99]. Even better activation energies than from B3LYP (which it is said tends to underestimate barriers [100, 101]) have been reported for the BH&H-LYP functional [101–104]. In a study by Baker et al. [105] of 12 organic reactions using 7 methods (semiempirical, ab initio and DFT), B3PW91/6-31G* was best (average and maximum errors 15.5 and 54 kJ mol^{-1}) and B3LYP/6-31G* second best (average and maximum errors 25 and 92 kJ mol^{-1}). Jursic studied 28 reactions

and recommended "B3LYP or B3PW91 with an appropriate basis set", but warned that highly exothermic reactions with a small barrier (ca. $10-20$ kJ mol^{-1}) involving hydrogen radicals "are particularly difficult to reproduce." [106]. Barriers "above 10 kcal mol^{-1} [ca. 40 kJ mol^{-1}] should be reliable. Lower activation energies should be underestimated by $3-4$ kcal mol^{-1} [ca. $13-17$ kJ mol^{-1}]" [106]. As with *thermodynamic* energy differences, i.e. energy differences not involving a transition state, consistently obtaining with some confidence activation energies accurate to $10-20$ kJ mol^{-1} may require a high-accuracy multistep method like CBS-QB3. For some barriers the problem seems to be with the functionals: Merrill et al. found that for the fluoride ion-induced elimination of HF from CH_3CH_2F none of the 11 functionals tested (including B3LYP) was satisfactory, by comparison with high-level ab initio calculations. Transition states were often looser and stabler than predicted by ab initio, and in several cases a transition state could not even be found. They concluded that hybrid functionals offer the most promise, and that "the ability of density functional methods to predict the nature of TS's demands a great deal more attention than it has received to date." [38].

More recent references to the accuracy of DFT in calculating barriers are the extensive compilations noted above for thermochemistry, namely [44, 45] and [46]. Of the functionals considered in reference [44] only B3LYP is among the few on which we have focussed (B3LYP, M06-2X, and TPSS), and it, scrutinized throughout the review because of its popularity, was well down on the barrier accuracy list, with typical errors of ca. 16 kJ mol^{-1}; the star functionals in this regard were MPW1K and BB1K with errors typically of ca. 5 kJ mol^{-1}. References [45] document a litany of shortcomings of B3LYP and extol the virtues of the M06-class of functionals. For barriers (kinetics) it recommends "M06-2X, BMK, and M05-2X for main-group thermochemistry and kinetics", and "M06-2X, M05-2X, and M06 for systems where main-group thermochemistry, kinetics, and noncovalent interactions are all important". M06, a general-purpose M06-class functional, apparently has an error of about 0.63 to 2.2 kcal mol^{-1} (2.6 to 9.2 kJ mol^{-1}), depending on the database used to test it. The rather extensive tests by Riley et al. ([46], summarized in Figs. 16–19) of functionals and their partner bass sets indicated, as far as this wealth of data can be encapsulated into a few words, that the best functionals for barriers were BBB1K, B1B95, and B1LYP (with B3LYP being only very slightly less accurate than this latter), and with no clear advantage to either the Pople or the Dunning basis sets. Typical barrier errors for these functionals were ca. $3-5$ kcal mol^{-1} ($13-21$ kJ mol^{-1}).

7.3.3   Frequencies and Vibrational Spectra

The general remarks and theory about frequencies that were given in Chap. 5, Sect. 5.5.3, apply to DFT frequencies also. As with ab initio frequency

calculations, but unlike semiempirical, one reason for calculating DFT frequencies is to get zero-point energies to correct the frozen-nuclei energies. The frequencies are also used to characterize the stationary point as a minimum, transition state, etc., and to predict the IR spectrum. As usual the wavenumbers ("frequencies") are the mass-weighted eigenvalues of the Hessian, and the intensities are calculated from changes in dipole moment incurred by the vibrations.

Unlike ab initio and semiempirical frequencies, DFT frequencies are not always significantly lower than observed ones (indeed, calculated values slightly higher than experimental frequencies have been reported). Here are some correction factors that have been calculated for various functionals, as well as for some ab initio and semiempirical methods (slightly different correction factors were recommended for the ZPE) [82a]; except for HF/3-21G the basis set for the ab initio and DFT methods is 6-31G*:

HF/3-21G	HF/6-31G*	MP2(FC)	AM1	BLYP	BP86	B3LYP	B3PW91
0.909	0.895	0.943	0.953	0.995	0.991	0.961	0.957

The BLYP/6-31G* and BP/86 correction factors are very close to unity. For the frequencies of polycyclic aromatic hydrocarbons calculated by the B3LYP/6-31G* method, Bauschlicher multiplied frequencies below $1300\ cm^{-1}$ by 0.980 and frequencies above this by 0.967 [81]. In their paper introducing the modification of Becke's hybrid functional to give the B3LYP functional, Stephens et al. studied the IR and CD spectra of 4-methyl-2-oxetanone and recommended the B3LYP/6-31G* as an excellent and cost-effective way to calculate these spectra [58]. With six different functionals, Brown et al. obtained an agreement with experimental fundamentals of ca. 4–6 %, except for BHLYP [107]. The 2007 review by Riley et al. [46] shows that a wide assortment of functionals/basis sets gives errors of ca. $50-120\ cm^{-1}$. For characterizing new molecules such errors are probably not important, because each functional/basis (indeed, each method) has a fairly constant multiplicative correction factor [82a] which brings its IR spectrum into reasonable positional agreement with experiment. More important than accurate wavenumber matching is reasonable agreement of relative intensities with reality. Intensities are calculated from the variation of dipole moments with vibrational distortions (Chap. 5, discussion in connection with Eq. (5.204). If calculated dipole moments do not vary much from one method to another and are similar to experimental values, as is suggested by Table 7.8, calculated relative intensities may be expected to be similar too. This is supported by Figs. 7.4, 7.5, 7.6, and 7.7. Let's examine the IR spectra of acetone, benzene, dichloromethane, and methanol, the same four compounds used in Chaps. 3, 5 and 6 (Figs. 3.15, 3.16, 3.17 and 3.18, 5.33, 5.34, 5.35 and 5.36 and 6.5, 6.6, 6.7 and 6.8) to illustrate spectra calculated by molecular mechanics, ab initio, and semiempirical methods. The DFT spectra in Figs. 7.4, 7.5, 7.6, and 7.7 are compared with experiment (taken in the gas phase by the author) and, for commonality with Chaps. 3, 5 and 6, MP2(fc)/6-31G*. B3LYP/6-31G* was chosen because, as was justified in retaining it for geometries (Sect. 7.3.1), it is just possible that it is still

Table 7.8 Some calculated dipole moments (Debyes) compared to experiment

	Computational method				
	B3LYP	M06-2X	AM1	MP2(fc)	Exp
CH_3NH_2	1.47	1.51	1.31	1.57	1.3
H_2O	2.1	2.15	2.1	2.24	1.9
HCN	2.91	2.94	2.9	3.26	3
CH_3OH	1.69	1.76	1.68	1.95	1.7
Me_2O	1.28	1.34	1.25	1.44	1.3
H_2CO	2.19	2.27	2.23	2.84	2.3
CH_3F	1.72	1.76	1.65	2.11	1.9
CH_3Cl	2.09	2.08	1.91	2.21	1.9
Me_2SO	3.93	4.07	3.98	4.63	4
CH_3CCH	0.69	0.67	0.66	0.66	0.8
Deviation	3+, 5−, two 0	5+, 3−, two 0	2+, 4−, four 0	9+, 1−, none 0	
	mean 0.11	mean 0.12	mean 0.22	mean 0.31	

For each method is given the number of positive, negative, and formal (to one decimal place) zero deviations from experiment, and the unsigned arithmetic mean of the absolute values of the deviations. The basis sets for the DFT and MP2 calculations is 6-31G*. Experimental values are taken from [71] and [73];.calculations are by the author
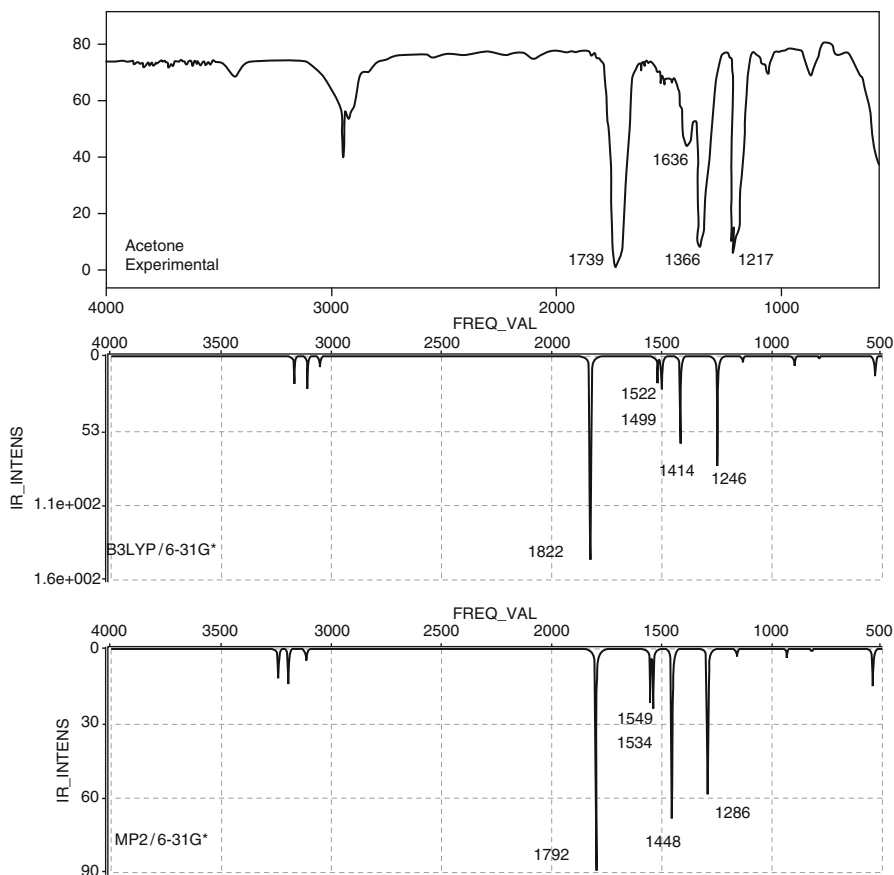
Fig. 7.4 Experimental (gas phase), DFT (B3LYP/6-31G*) and ab initio (MP2(fc)/6-31G*) calculated IR spectra of acetone
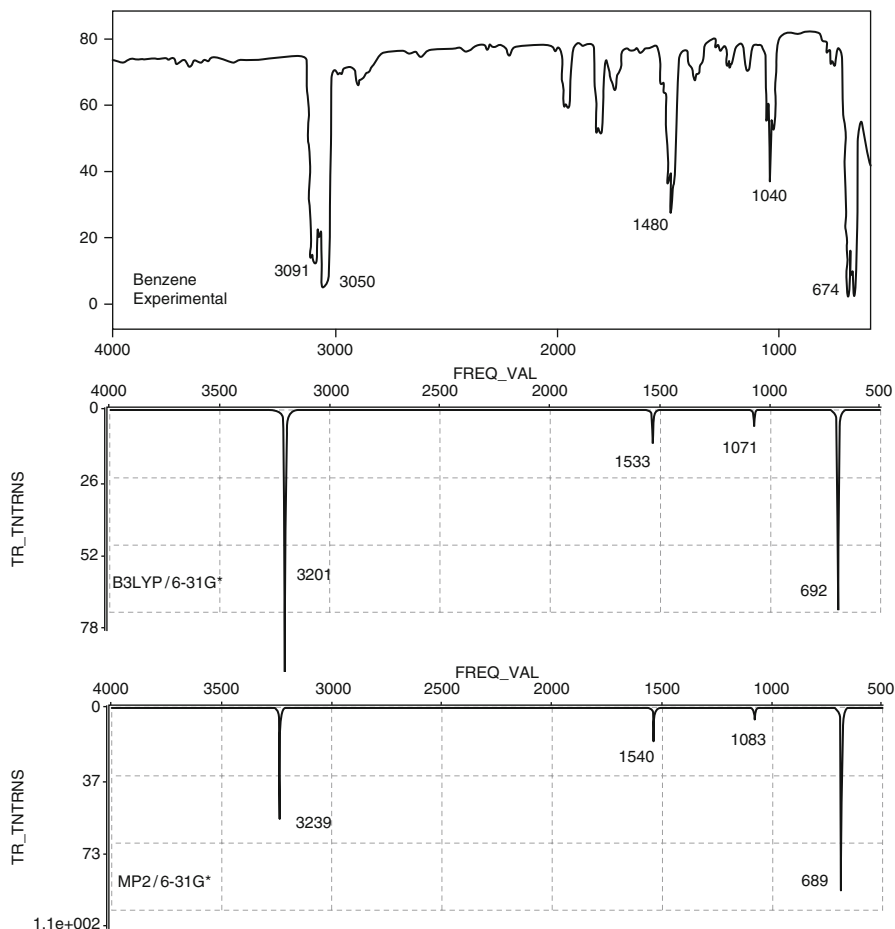
Fig. 7.5 Experimental (gas phase), DFT (B3LYP/6-31G*) and ab initio (MP2(fc)/6-31G*) calculated IR spectra of benzene

the most popular functional. We see that here B3LYP/6-31G* simulates the experimental IRs reasonably well, and is in this regard very similar to MP2(fc)/6-31G*.

7.3.4 Properties Arising from Electron Distribution–Dipole Moments, Charges, Bond Orders, Atoms-in-Molecules

The theory behind calculating dipole moments, charges, and bond orders, and using atoms-in-molecules analyses, was outlined in Chap. 5, Sect. 5.5.4; here the results of applying DFT calculations to these will be presented.
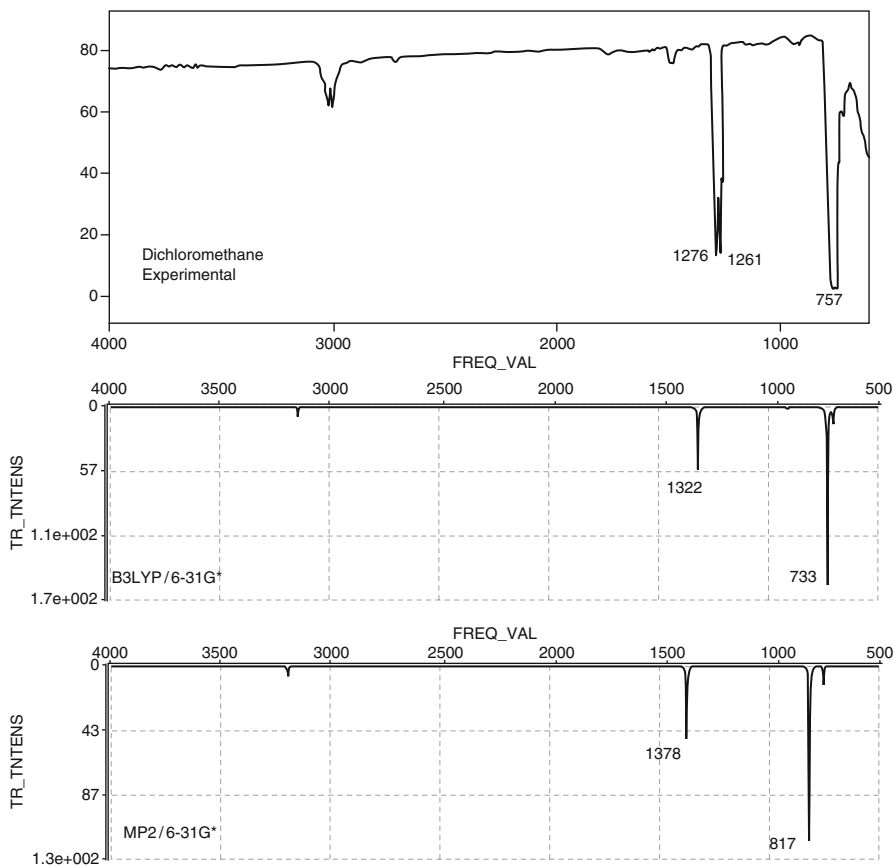
Fig. 7.6 Experimental (gas phase), DFT (B3LYP/6-31G*) and ab initio (MP2(fc)/6-31G*) calculated IR spectra of dichloromethane

7.3.4.1   Dipole Moments

Hehre [71] and Hehre and Lou [72] have provided quite extensive compilations of calculated dipole moments. These confirm that Hartree-Fock dipole moments tend to be bigger than experimental, and electron correlation, through DFT or MP2, tends to lower the dipole moment, bringing it closer to the experimental value (e.g. for thiophene, from 0.80 D to 0.51 D for B3LYP; the MP2 value is 0.37 D and the experimental dipole moment is 0.55 D [72]).

Table 7.8 compares with experiment dipole moments calculated by B3LYP/6-31G*, M06-2X/6-31G*, AM1 (as a check on this fast method), and MP2(fc)/6-31G*, for 10 molecules. The two DFT methods give essentially the same mean unsigned error, 0.11 and 0.12 D, three times smaller than the error of 0.31 D from the slowest method, MP2 (at least for this small selection of molecules), and the very fast AM1 moments lie in-between, 0.22 D. None of these methods consistently
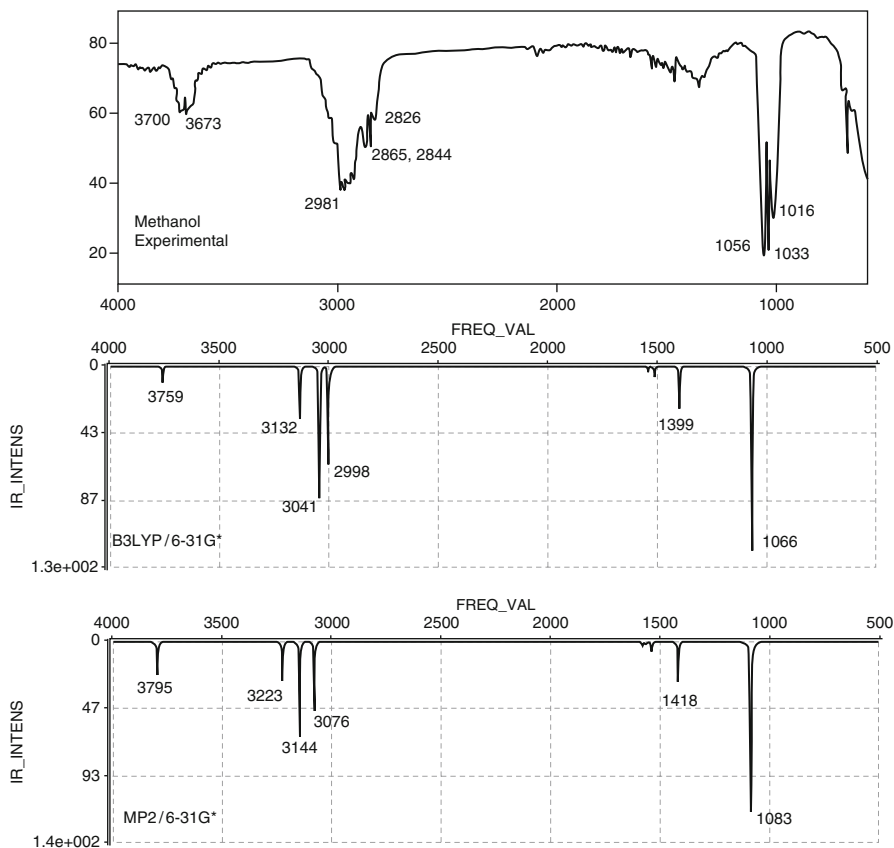
Fig. 7.7 Experimental (gas phase), DFT (B3LYP/6-31G*) and ab initio (MP2(fc)/6-31G*) calculated IR spectra of methanol

gives values accurate to within 0.1 D. Very accurate dipole moments (mean absolute deviation 0.06–0.07 D) can be obtained with gradient-corrected DFT and very large basis sets [79].

7.3.4.2 Charges and Bond Orders

The theory behind these was given in Chap. 5, Sect. 5.5.4. Although it is sometimes said that charges on atoms cannot be measured, i.e. are not observables, carefully defined atom charges can apparently be measured [108]. However, such experimental charges are not readily available, and there is no agreed-on standard for judging the "correctness" of calculated charges (and bond orders). In practice, electrostatic potential charges and Löwdin bond orders are often preferred to

Mulliken charges and bond orders

Electrostatic potential charges and Löwdin bond orders
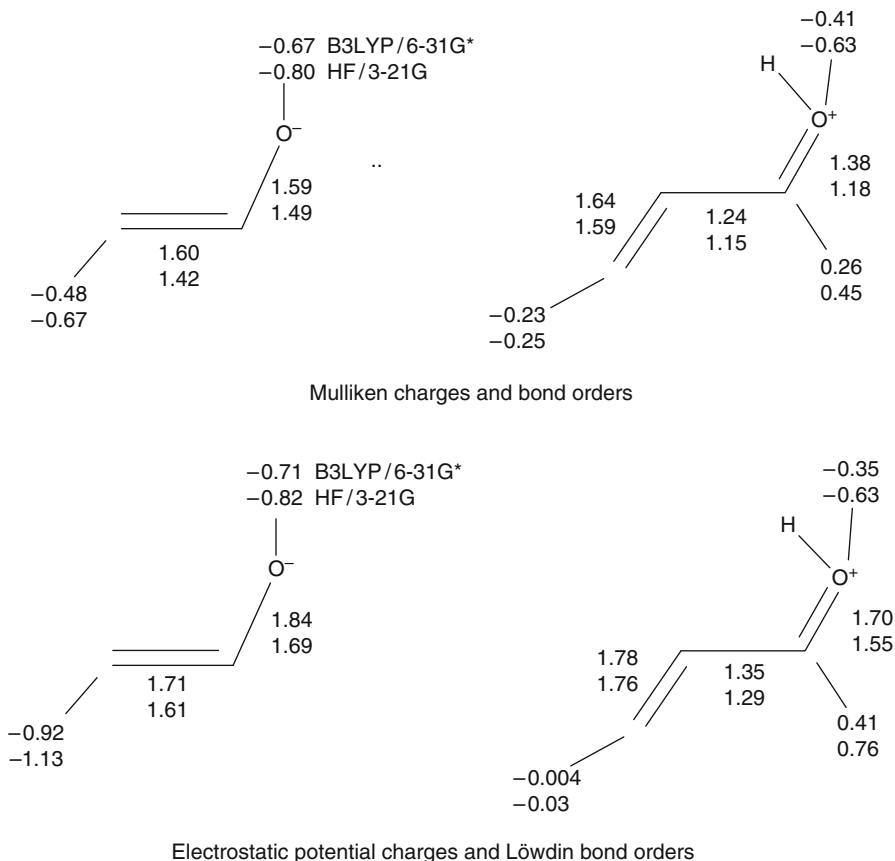
Fig. 7.8 Atom charges and bond orders calculated using B3LYP/6-31G* and HF/3-21G methods. Note that charges and bond orders involving hydrogens have been omitted

Mulliken charges and bond orders. The effect of various computational levels on atom charges has been examined [109].

Figure 7.8 shows charges and bond orders calculated for an enolate and a protonated enone system (the same as in Chap. 6, Fig. 6.9), using B3LYP/6-31G* and HF/3-21G. The results are qualitatively similar regardless of whether one uses B3LYP or HF, or Mulliken vs. electrostatic potential/Löwdin. This is in contrast to the results in Fig. 6.9, where there were some large differences between the semiempirical and HF/3-21G values, and even between AM1 and PM3. For example, for the protonated species using the Mulliken method, AM1 and PM3 gave the oxygen a small negative charge, ca. −0.1, but the HF/3-21G method gave it a large negative charge, −0.63; even stranger, the terminal carbon had charges of 0.09, 0.23, and −0.25 by the AM1, PM3, and HF methods. In Fig. 7.8 the biggest differences among corresponding parameters is for the electrostatic potential charges in the protonated species, where the charges on the oxygen

$(-0.35$ and $-0.63)$ and on the carbonyl carbon (0.41 and 0.76) differ by a factor of about two. With both B3LYP and HF the terminal carbon of the enolate is counterintuitively assigned a bigger negative electrostatic potential charge than the oxygen, as was the case for AM1 and DFT. The calculated negative charge on the formally positive oxygen of the protonated molecule was commented on in Chap. 6, Sect. 6.3.4.2. As with the semiempirical values, bond orders are less variable here than are the charges, but even for this parameter there is one qualitative discrepancy: for the cation C/OH bond the Mulliken HF bond order is essentially single (1.18), while for the Löwdin B3LYP calculation the bond is essentially double (bond order 1.70). These results remind us that charges and bond orders are useful mainly for revealing *trends*, when a series of molecules, or stages along a reaction coordinate [110] are studied, all with the same methods (e.g. B3LYP/6-31G* and Löwdin bond orders).

7.3.4.3 Atoms-in-Molecules

The atoms-in-molecules (AIM) analysis of electron density, using ab initio calculations, was considered in Chap. 5, Sect. 5.5.4.5. A comparison of AIM analysis by DFT with that by ab initio calculations by Boyd et al. showed that results from DFT and ab initio methods were similar, but gradient-corrected methods were somewhat better than the SVWN method, using QCISD ab initio calculations as a standard. DFT shifts the CN, CO, and CF bond critical points of HCN, CO, and CH_3F toward the carbon and increases the electron density in the bonding regions, compared to QCISD calculations [111].

7.3.5 Miscellaneous Properties–UV and NMR Spectra, Ionization Energies and Electron Affinities, Electronegativity, Hardness, Softness and the Fukui Function

7.3.5.1 UV Spectra

In wavefunction theory, i.e. conventional quantum mechanics, UV spectra (electronic spectra) result from promotion of an electron from a molecular orbital to a higher-energy molecular orbital by absorption of energy from a photon: the molecule goes from the electronic ground state to an excited state. Since current DFT is said to be essentially a ground-state theory (e.g. [13–16]), one might suppose that it could not be used to calculate UV spectra. However, there is an alternative approach to calculating the absorption of energy from light. One can use the time-dependent Schrödinger equation to calculate the effect on a molecule of a time-dependent electric field, i.e. the electric component of a light wave; this wave is an oscillating electromagnetic field, and can set the electron cloud of a molecule oscillating in synch [112]. This is a semiclassical treatment in that it uses the Schrödinger equation but avoids equating the absorbed energy to $h\nu$, the energy

of a photon. The calculation of UV spectra by DFT is based on the time-dependent Kohn-Sham equations, derived from the time-dependent Schrödinger equation [88]. The implementation of time-dependent DFT (TDDFT, occasionally called time-dependent density functional response theory, TD-DFRT) in Gaussian [83a] has been described by Stratman et al. [113]. Wiberg et al. used this implementation to study the effect of five functionals and five basis sets on the transition energies (the UV absorption wavelengths) of formaldehyde, acetaldehyde, and acetone [114]. Satisfactory results were obtained, and the energies were not strongly dependent on the functional, but B3P86 seemed to be the best and B3LYP the worst. The 6-311++G** basis was recommended. Although these workers used MP2/6-311+G** geometries, the results in Table 7.9 indicate that AM1 geometries, which can be calculated perhaps a thousand times faster, gives transition energies that are nearly as accurate (mean absolute errors of 0.12 eV and 0.18 eV, respectively). Table 7.10 compares with experiment [115] the UV spectrum of methylenecyclopropene, calculated by ab initio, semiempirical, and DFT methods. The best of the three is the TDDFT calculation, which is the only one that

Table 7.9 UV spectra (as transition energies in eV) of acetone, acetaldehyde, and formaldehyde, calculated by time-dependent DFT, using Gaussian 98 [83a]

	MP2 geometry	AM1 geometry	Experiment
Acetone	4.41	4.26	4.43
	6.28	6.19	6.36
	7.26	7.17	7.41
	7.43	7.4	7.36
	7.67	7.59	7.49
	7.89	7.82	8.09
Acetaldehyde	4.29	4.14	4.28
	6.76	6.69	6.82
	7.29	7.26	7.46
	7.7	7.68	
	7.89	7.98	7.75
	8.35	8.16	8.43
Formaldehyde	3.95	3.83	4.1
	6.98	6.97	7.13
	7.93	7.95	8.14
	8.09	8.07	7.98
	8.81	8.84	
	9.23	8.87	
	5+, 10−	4+, 11−	
	Mean of 15: 0.12	Mean of 15:	
		0.18	

The results of using MP2/6-311++G** [114] and (calculations by the author) AM1 geometries are compared; both sets of calculations are single-point B3P86/6-311++G**. For each molecule only 6 transitions, all singlets, are shown. The number of positive and negative deviations from experiment and the mean absolute errors are given

Table 7.10 Calculated (ab initio, semiempirical, DFT) and experimental [115] UV spectra of methylenecyclopropene, wavelength, nm (relative intensity)

RCIS/6-31 + G*//B3LYP/6-31G*	Calculated		Experimental
	ZINDO/S//AM1	TDDFT: B3P86/6-311++G**//AM1	
224 (15)	228 (12)	309 (26)	308 (13)
209 (6)	224 (0.2)	226 (3)	242 (0.6)
196 (0)	213 (100)	210 (0)	206 (100)
194 (8)	204 (1)	208 (100)	
193 (100)		190 (0)	

The recommended ab initio basis set [115] and DFT functional and basis set [114] are used. The ab initio results are from Chap. 5, Table 5.16, and the semiempirical results are from Chap. 6, Table 6.7

reproduces the 308 nm band. Jacquemin et al. obtained very accurate UV spectra of indigo dyes by taking solvent into account with a polarizable continuum (in contrast to explicit solvent molecules) model and employing TDDFT at the PBE0/6-311+G(2d,p) level [116]. Zhao and Truhlar have presented their M06-HF functional as being particularly good for electronic transitions of the Rydberg and charge-transfer type [117].

The HOMO-LUMO gap calculated with hybrid gradient-corrected functionals is approximately equal to the $\pi \rightarrow \pi^*$ UV transition of unsaturated molecules, and this could be of some use in predicting UV spectra (see *ionization energies and electron affinities*, below).

7.3.5.2 NMR Spectra

As with ab initio methods (Chap. 5, Sect. 5.5.5), NMR shielding constants can be calculated from the variation of the energy with a magnetic field and the nuclear magnetic moment. For the commonest NMR spectra, those of ^{1}H and ^{13}C, the chemical shift of a nucleus is its shielding value relative to the shielding of the TMS (tetramethylsilane) carbon or hydrogen nucleus; other magnetic nuclei have various reference molecules. The main general methodology of NMR calculations is GIAO (gauge-independent atomic orbitals); a much less widely-used alternative is CSGT (continuous-set gauge transformations); both can give good results [118].

The most accurate results have been said to be obtained with MP2 calculations [119], but empirical corrections improved the accuracy of DFT [120]. More recent studies are those by Sefzik et al. [121], Wu et al. [122], Zhao and Truhlar [123], and Perez et al. [124]; in these four studies only GIAO was used, except for [123], which used both GIAO and CSGT. For ^{13}C chemical shifts DFT was found to often, but not always, beat ab initio Hartree-Fock, and the B3LYP and mpw1pw91 functionals tended to do well [121]. A survey of the nuclei ^{13}C, ^{15}N, ^{17}O, and ^{19}F in 23 molecules using 21 functionals showed OPBE and OPW91 to be significantly

better than B3LYP and PBE1PBE and in many cases better than wavefunction calculations; OPTX was said to perform "remarkably well." [122]. Surprisingly, B3LYP has been reported to be less accurate than GGA or even local (LSDA) functionals (see Sects. 7.2.3.4.1, 7.2.3.4.2, 7.2.3.4.3, 7.2.3.4.4, 7.2.3.4.5 and 7.2.3.4.6), and the newer M06-L, itself a local functional (Sect. 7.2.3.4.2), was said to be the best for NMR chemical shifts [123]. A detailed study of the effect of solvent also compared DFT calculations with database programs for calculating NMR spectra, keeping an eye on balancing time versus accuracy [124]. In a detailed study of the role of calculated geometries and ^{1}H NMR spectra in the elucidation of the structure of [12] annulene, Castro et al. reported GIAO B3LYP/6-311+G(d,p) shifts to be in good agreement with experiment when appropriate calculated geometries were used [125].

Figure 7.9 compares with experiment [126, 127] ^{13}C and ^{1}H NMR spectra calculated at these levels:

1. B3LYP/6-311++G** for the NMR calculations, using B3LYP/6-311++G (2df,2p), and HF/3-21G(*) for the geometries, and
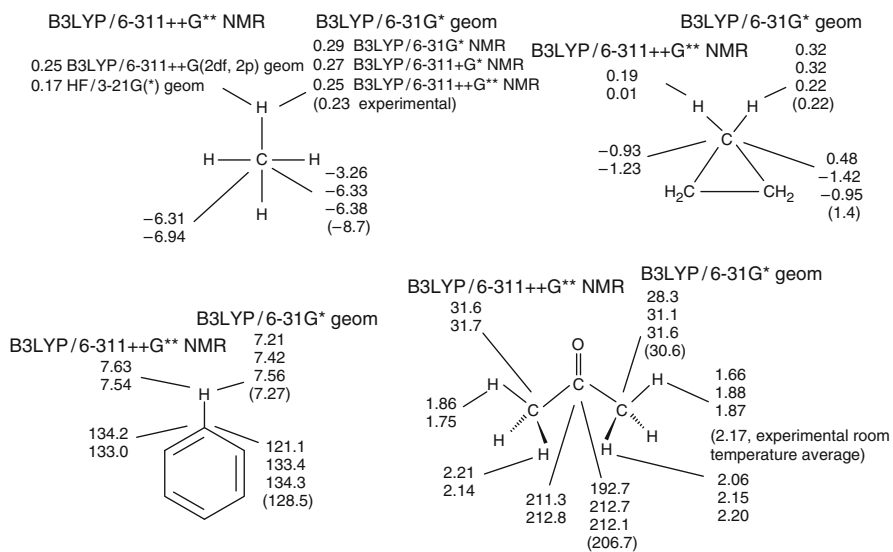
Fig. 7.9 Calculated and experimental ^{1}H and ^{13}C NMR spectra. Chemical shifts (* values) are relative to the H and C of TMS. The calculations were done with the default NMR method (GIAO) implemented in Gaussian 03 [83a]. The experimental values (in parentheses) are from [126], except for the ^{13}C values for methane and cyclopropane [127] (for these [126] gave −2.3 and −2.9, which seem suspect). The calculated values are in vacuo and the experimental are in CDCl$_3$, except for methane and cyclopropane, which are gas-phase measurements which were given relative to benzene and have been adjusted here to be relative to TMS. The changes in going from vacuum to CDCl$_3$ are likely to be fairly small (within ca. * 1) for these molecules. Values to the left of the structures are all for B3LYP/6-311++G** NMR calculations on B3LYP/6-311++G(2df,2p) (first line) or HF/3-21G(*) (second line) geometries. Values to the right of the structures are all for B3LYP/6-31G* geometries with NMR calculations at the B3LYP/6-31G*, B3LYP/6-311+G*, and B3LYP/6-311++G** levels (*upper, middle and lowest lines*, respectively)

2. B3LYP/6-31G* for the geometries, using B3LYP/6-31G*, B3LYP/6-311+G*, and B3LYP/6-311++G** for the NMR calculations.

Thus the figure shows for each of these molecules: (1) a fairly high-level NMR calculation on a high-level and a low-level geometry, and (2) a medium-level geometry probed with a medium-, a fairly high-, and a still higher-level calculation. For such a very small sample the results cannot reasonably be expected to do more than show up gross differences in accuracy, but they do suggest that for DFT NMR chemical shifts, if high accuracy is not needed B3LYP/6-311+G* on B3LYP/ 6-31G* geometries may be adequate.

7.3.5.3 Ionization Energies and Electron Affinities. The Kohn-Sham Orbitals

Ionization energies (ionization potentials) and electron affinities were discussed in Chap. 5, Sect. 5.5.5. We saw that IEs and EAs can be calculated in a straightforward way as the energy difference between a molecule and the species derived from it by loss or gain, respectively, of an electron. Using the energy of the optimized geometry of the radical cation or radical anion (in the case where the species whose IE or EA we seek is a neutral closed-shell molecule) gives the adiabatic IE or EA, while using the energy of the ionized species at the geometry of the neutral gives the vertical IE or EA. Muchall et al. have reported adiabatic and vertical ionization energies and electron affinities of eight carbenes, calculated in this way by semiempirical, ab initio, and DFT methods [128]. They recommend B3LYP/ 6-31+G*//B3LYP/3-21G$^{(*)}$ as the method of choice for predicting first ionization energies; the use of the small 3-21G$^{(*)}$ basis with B3LYP for the geometry optimization is unusual–see Chap. 5, Sect. 5.4.2–usually the smallest basis used with a correlated method is 6-31G*. This combination is relatively undemanding and gave accurate (largest absolute error 0.14 eV) adiabatic and vertical ionization energies for the carbenes studied. Table 7.11 shows the results of applying this method to some other (non-carbene) molecules. The B3LYP/6-31+G* ionization energies are essentially the same with B3LYP/3-21G$^{(*)}$ geometries and AM1 geometries; they are good estimates of the experimental IE [129, 130], are somewhat better than the ab initio MP2 ionization energies, and are considerably better than the MP2 Koopmans' theorem (below) IEs. Of course, for unusual molecules (like the carbenes studied by Muchall et al. [128]) AM1 may not give good geometries, and for such species it would be safer to use B3LYP/3-21G$^{(*)}$ or B3LYP/6-31G* geometries for the single-point BLYP/6-31+G* calculations. Golas et al. obtained fairly good IEs ($\pm$ 0.2 eV for IEs of ca. 8–9 eV) and useful EAs ($\pm$ 0.4 eV for EAs of ca. 1–2 eV) with B3LYP/6-311+G** energies on B3LYP/ 6-31G* geometries [131].

In wavefunction theory an alternative way to find IEs for removal of an electron from a molecular orbital (usually the highest), is to invoke Koopmans' theorem: the IE for an orbital is the negative of the orbital energy; Chap. 5, Sect. 5.5.5.3). By the

Table 7.11 Some ionization energies (eV)

	$\Delta E = $ IE				
	B3LYP/6-31+G*// B3LYP/3-21G$^{(*)}$	B3LYP/ 6-31+G*// AM1	MP2(FC)/ 6-31G*	Koopmans' (MP2(FC)/ 6-31G*)	Exp
CH_3OH	10.77 (10.92)	10.76 (10.85)	10.6	12.1	10.9
CH_3SH	9.40 (9.43)	9.53 (9.36)	9	9.2	9.4
CH_3COCH_3	9.60 (9.70)	9.67 (9.68)	9.6	11.2	9.7

The ΔE ionization energy values (cation energy minus neutral energy) correspond to adiabatic and (in parentheses) vertical IEs; the Koopmans theorem values are vertical IEs. Experimental IEs are adiabatic (CH_3OH and CH_3COCH_3 [129], CH_3SH [130]). The use of B3LYP/3-21G$^{(*)}$ geometries is based on [128]. That the vertical IE is smaller than the adiabatic for the B3LYP/6-31+G*//AM1 calculation on CH_3SH is presumably due to a somewhat inaccurate geometry, probably for the cation (experimental vertical IEs are always bigger than adiabatic since it takes energy to distort the relaxed-geometry cation to the geometry of the neutral)

"ionization energy" we usually mean the lowest one, corresponding to removing an electron from the HOMO. In Chaps. 5 and 6 both the energy difference and the Koopmans' theorem methods were used to calculate some IEs (Tables 5.17 and 6.8). The problem with applying Koopmans' theorem to DFT is that in "strict" DFT there are no molecular orbitals, only electron density, while in Kohn-Sham DFT (practical DFT) the MOs, the orbitals ψ^{KS} that make up the Slater determinant of Eq. (7.19), were, as explained in Sect. 7.2.3.2, introduced only to provide a way to calculate the energy (note Eqs. (7.21), (7.22), and (7.26)). The problem is to see if these Kohn-Sham MOs are, as there was a tendency to view them, mere mathematical artifices or if they are *in themselves* useful. There was at one time a fair amount of argument over the physical meaning, if any, of the Kohn-Sham orbitals. Baerends and coworkers compared DFT with Hartree-Fock theory and concluded that "The Kohn-Sham orbitals are physically sound and may be expected to be more suitable for use in qualitative molecular orbital theory than either Hartree-Fock or semiempirical orbitals." [132]. Cramer echoes this in pointing out that there are reasons to even *prefer* the Kohn-Sham MOs: they all feel the same external potential, while HF MOs feel varying potentials, the virtual MOs carrying this to an extreme [133]. Stowasser and Hoffmann showed that the KS orbitals resemble those of conventional wavefunction theory (extended Hückel and Hartree-Fock ab initio, Chaps. 4 and 5) in shape, symmetry, and, usually, energy ordering [134]. They conclude that these orbitals can indeed be treated much like the more familiar orbitals of wavefunction theory. Furthermore, they showed that although the KS orbital energy values (the eigenvalues ε from diagonalization of the DFT Fock matrix–Sect. 7.2.3.3) are not good approximations to the ionization energies of molecular orbitals (as revealed by photoelectron spectroscopy), there is a linear relation between $|\varepsilon_i(KS) - \varepsilon_i(HF)|$ and $\varepsilon_i(HF)$. Salzner et al., too, showed that in DFT, unlike ab initio theory calculations, negative HOMO energies are not good approximations to the IE (with an *exact* functional Koopmans' theorem would be exact), but, surprisingly, HOMO-LUMO gaps from hybrid functionals agreed well

with the $\pi \rightarrow \pi^*$ UV transitions of unsaturated molecules [135]. Vargas et al. introduced a "Koopmans-like approximation" to obtain a relation between the Kohn-Sham orbital energies and vertical IEs and EAs, and assert that their method improves the calculation of electron density indexes (below) of hardness, electronegativity and electrophilicity [136]. The utility of the Kohn-Sham orbital energies to predict IE, EA and the hardness index was studied by Zhan et al. [137], and Zhang et al. explored the ability of various functionals to use these orbitals to predict IE, EA and the lowest-energy UV transition [138].

Concerning electron affinities, in Hartree-Fock calculations the negative LUMO energy of a species M corresponds to the electron affinity not of M but rather of the anion M^- [139]. However, Salzner et al. reported that the negative LUMOs from LSDA functionals gave rough estimates of EA (ca. 0.3–1.4 eV too low; gradient-corrected functionals were much worse, ca. 6 eV too low) [135]. Brown et al. found that for eight medium-sized organic molecules the energy difference method using gradient-corrected functionals predicted electron affinities fairly well (average mean error less than 0.2 eV) [107]. Relevant to the LUMO in DFT, and to the calculation of UV spectra (e.g. by TDDFT), is a report on "close to"exact Kohn-Sham orbitals from the "statistical average of orbital potentials" [140]. These orbitals show occupied-virtual gaps very close to UV excitation energies, and "realistic shapes of virtual orbitals, leading to straightforward interpretation of most excitations as single orbital transitions." The authors assert that "[this gap] is physically an approximation to the lowest excitation energy, which is a beautiful property. There is nothing problematic about it." The properties of these virtual Kohn-Sham orbitals are reminiscent of those described for valence virtual orbitals in ab initio theory [141] (Chap. 5, Sect. 5.5.5.3, *ionization energies and electron affinities*).

7.3.5.4 Electronegativity, Hardness, Softness and the Fukui Function: Electron Density Reactivity Indexes

The idea of electronegativity was born as soon as chemists suspected that the formation of chemical compounds involved electrical forces (before the discovery of the electron): metals and nonmetals were seen to possess opposite appetites for the "electrical fluid(s)" of eighteenth century physics. This "electrochemical dualism" is most strongly associated with Berzelius [142], and is clearly related to our qualitative notion of electronegativity as the tendency of a species to attract electrons. Parr and Yang have given a sketch of attempts to quantify the idea [143]. Electronegativity is a central notion in chemistry.

Hardness and softness as chemical concepts were presaged in the literature as early as 1952, in a paper by Mulliken [144], but did not become widely used till they were popularized by Pearson in 1963 [145]. In the simplest terms, the hardness of a species, atom, ion or molecule, is a qualitative indication of how polarizable it is, i.e. how much its electron cloud is distorted in an electric field. The adjectives hard and soft were said to have been suggested by D. H. Busch, [146], but they appear in

Mulliken's paper [144], p. 819, where they characterize the response to spatial separation of the energy of acid–base complexes. The analogy with the conventional use of these words to denote resistance to deformation by mechanical force is clear, and independent extension, by more than one chemist, to the concept of electronic resistance, is no surprise. The hard/soft concept proved useful, particularly in rationalizing acid–base chemistry [147]. Thus a proton, which cannot be distorted in an electric field since it has no electron cloud, is a very hard acid, and tends to react with hard bases. Examples of soft bases are those in which sulfur electron pairs provide the basicity, since sulfur is a big fluffy atom, and such bases tend to react with soft acids. Perhaps because it was originally qualitative, the hard-soft acid–base (HSAB) idea met with skepticism from at least one quarter: Dewar (of semiempirical fame) dismissed it as a "mystical distinction between different kinds of acids and bases" [148]. For a brief review of Pearson's contributions to the concept, which has been extended beyond strict conventional acid–base reactions, see [149].

The Fukui function or frontier function was introduced by Parr and Yang in 1984 [150]. They generously gave it a name associated with the pioneer of frontier molecular orbital theory, who emphasized the roles of the HOMO and LUMO in chemical reactions. In a reaction a change in electron number clearly involves removing electrons from or adding electrons to the HOMO or LUMO, respectively, i.e. the *frontier orbitals* whose importance was emphasized by Fukui.[4] The mathematical expression (below) of the function defines it as the sensitivity of the electron density at various points in a species to a change in the number of electrons in the species. If electrons are added or removed from the species, how much is the electron density at various places altered? This function measures changes in electron density that accompany chemical reactions, and has been used to try to rationalize and predict the variation of reactivity from site to site in a molecule.

Electronegativity, hardness and softness, and the Fukui function will now be explained quantitatively. These concepts can be analyzed using wavefunction theory, but are often treated in connection with DFT, perhaps because much of the underlying theory was formulated in this context [151]. Consider the effect on the energy of a molecule, atom or ion, of adding electrons. Figure 7.10 shows how the energy of a fluorine cation F^+ changes as one and then another electron is added, giving a radical $F^{.}$ and then an anion F^-. The number of electrons N we can add to F^+ is integral, 1, 2, …(N is taken here as 0 for F^+, and is thus 1 for the radical and 2 for the anion), but mathematically we can consider adding continuous electronic charge N; the line through the three points is then a continuous curve and we can examine $(\partial E/\partial N)_Z$, the derivative of E with respect to N at constant nuclear charge. In 1876 Josiah Willard Gibbs published his theoretical studies of the effect on the energy of a system of a change in its composition. The derivative $\mu = (\partial E/\partial n)_{T,p}$, is the change in energy caused by an infinitesimal change in the number of moles n.

---

[4]Kenichi Fukui, born Nara, Japan, 1918. Ph.D. Kyoto Imperial University 1948, Professor Kyoto Imperial University 1951. Nobel Prize 1981. Died 1998.
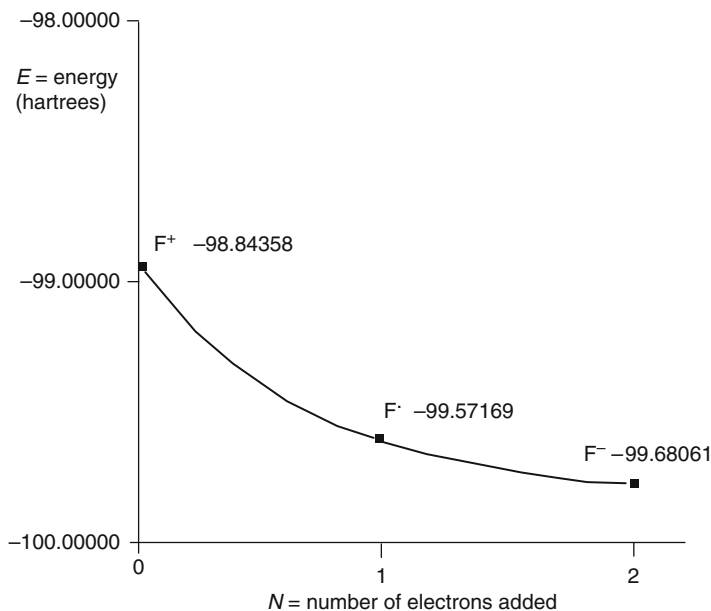
Fig. 7.10 Change of energy (for F^+, $F^{\cdot}$ and F^-) as electrons are added to a species. The energies were calculated at the QCISD(T)/6-311+G* level. The slope of the curve at any point (first derivative) is the electronic chemical potential, and the negative of the slope the electronegativity, of the species at that point. The curvature at any point (second derivative) is the hardness of the species) (See too Table 7.12)

This derivative is called the chemical potential. Here E is Gibbs free energy G and temperature and pressure are constant; the chemical potential can also be defined with respect to internal energy U or Helmholtz free energy A (Chap. 5, Sect. 5.5.2.1) [152]. By analogy, $(\partial E/\partial N)_Z$, the change in energy with respect to number of added electrons at constant nuclear charge, is the *electronic* chemical potential (or in an understood context just the chemical potential) of an atom. For a molecule the differentiation is at constant nuclear framework, the charges and their positions being constant, i.e. constant external potential, v (Sect. 7.2.3.1). So for an atom, ion or molecule

$$\mu = \left(\frac{\partial E}{\partial N}\right)_v \tag{7.30}$$

The electronic chemical potential of a molecular (including atomic or ionic) species, according to Eq. (7.30), is the infinitesimal change in energy when electronic charge is added to it. Figure 7.10 suggests that the energy will drop when charge is added to a species, at least as far as common charges (from about $+3$ to -1) go, and indeed, even for fluorine's electronegative antithesis, lithium, the energy drops along the sequence Li^+, $Li^{\cdot}$, Li^- (QCISD(T)/6-311+G* gives energies

of -7.23584, -7.43203, $-7.45448\,h$, respectively). Now, since one feels intuitively that the more electronegative a species, the more its energy should drop when it acquires electrons, we suspect that there should be a link between the chemical potential and electronegativity. If we choose for convenience to tag most electronegativities with positive values, then since $(\partial E/\partial N)_Z$ is negative we might define the electronegativity χ as the negative of the electronic chemical potential:

$$\chi = -\mu = -\left(\frac{\partial E}{\partial N}\right)_v \tag{7.31}$$

From this viewpoint the electronegativity of a species is the drop in energy when an infinitesimal amount (infinitesimal so that it remains the same species) of electronic charge enters it. It is a measure of how hospitable an atom or ion, or a group or an atom in a molecule (Chap. 5, Sect. 5.5.4), is to the ingress of electronic charge, which fits in with our intuitive concept of electronegativity.

This definition of electronegativity was given in 1961 [153] and later (1978) discussed in the context of DFT [154]. Eq. (7.31) could be used to calculate electronegativity by fitting an empirical curve to calculated energies for, e.g. M^+, M and M^-, and calculating the slope (gradient, first derivative) at the point of interest; however, the equation can be used to derive a simple approximate formula for electronegativity using a three-point approximation. For consecutive species M^+, M and M^- (constant nuclear framework), let the energies be $E(M^+)$, $E(M)$, and $E(M^-)$. Then by definition

$E(M^+) - E(M) = I$, the ionization energy of M

and $E(M) - E(M^-) = A$, the electron affinity of M

Adding: $E(M^+) - E(M^-) = I + A$

So approximating the derivative at the point corresponding to M as the change in E when N goes from 0 to 2, divided by this change in electron number, we get

$$\left(\frac{\partial E}{\partial N}\right)_v = \frac{E(M^-) - E(M^+)}{2 - 0} = \frac{-(I + A)}{2}$$

i.e., using Eq. (7.31)

$$\chi = \frac{I + A}{2} \tag{7.32}$$

To use this formula one can employ experimental or calculated adiabatic (or vertical, if the species from removal or addition of an electron are not stationary points) values of I and A. This same formula (Eq. (7.32)) for χ was elegantly derived by Mulliken (1934) [155] using only the definitions of I and A. Consider the reactions

$$X + Y \rightarrow X^+ + Y^-$$

and

$$X + Y \rightarrow X^- + Y^+$$
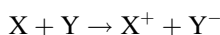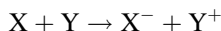
If X and Y have the same electronegativity then the energy changes of the two reactions are equal, since X and Y have the same proclivities for gaining and for losing electrons, i.e.

$$I(X) - A(Y) = I(Y) - A(X)$$
$$\text{i.e.} (I + A) \quad \text{for X} = (I + A) \quad \text{for Y}$$

So it makes sense to define electronegativity as $I + A$; the factor of ½ (Eq. (7.32)) was said by Mulliken to be "probably better for some purposes" (perhaps he meant to make χ the arithmetic mean of I and A, an easily-grasped concept).

Electronegativity has also been expressed in terms of orbital energies, by taking I as the negative of the HOMO energy and A as the negative of the LUMO energy [156]. This gives

$$\chi = \frac{-(E_{\text{HOMO}} + E_{\text{LUMO}})}{2} \tag{7.33}$$

This expression has the advantage over Eq. (7.32) that one needs only the HOMO and LUMO energies of the species, which are provided by a one-pot calculation (i.e. by what is operationally a single calculation), but to use Eq. (7.32) one needs the ionization energy and electron affinity, the rigorous calculation of which demands the energies of M, M^+, and M^-; cf. the Fukui functions for SCN^- later in this section. How good is Eq. (7.33)? $I = -E_{\text{HOMO}}$ is a fairly good approximation for the orbitals of wavefunction theory, but not for the Kohn-Sham orbitals of current DFT, and $A = -E_{\text{LUMO}}$ is only a very rough approximation for the Kohn-Sham orbitals, and for wavefunction orbitals $-E_{\text{LUMO}}$ of M is said to correspond to the electron affinity of M^-, not of M (see the *ionization energy and electron affinity* subsection above). So how do the results of calculations using the formula of Eq. 7.33 compare with those using Eq. (7.32)? Table 7.12 gives values of χ calculated using QCISD(T)/6-311 + G^* (Chap. 5, Sect. 5.4.3) values of I and A, which should give good values of these latter two quantities, and compares these χ values with those from HOMO/LUMO energies calculated by ab initio (MP2(FC)/6-31G*) and by DFT (B3LYP/6-31G*). For the two cations the agreement between the three ways of calculating χ is good; for the other species it is erratic or bad, although the trends are the same for the three methods within a given family (hardness decreases from cation to radical to anion). It seems likely that Eq. (7.32) is the sounder way to calculate electronegativity. An exposition of the concept of electronegativity as the (negative) average of the HOMO and LUMO energies, and the chemical potential ($-\chi$) as lying at the midpoint of the HOMO/LUMO gap, was given by Pearson [156].

Chemical hardness and softness are much newer ideas than electronegativity, and they were quantified only fairly recently. Parr and Pearson (1983) proposed to identify the curvature (i.e. the second derivative) of the E vs. N graph (e.g. Fig. 7.10)

with hardness, η [157]. This accords with the qualitative idea of hardness as resistance to deformation, which itself accommodates the concept of a hard molecule as resisting polarization–not being readily deformed in an electric field: if we choose to define hardness as the curvature of the E vs. N graph, then

$$\eta = \left(\frac{\partial^2 E}{\partial N^2}\right)_v = \left(\frac{\partial \mu}{\partial N}\right)_v = -\left(\frac{\partial \chi}{\partial N}\right)_v \tag{7.34}$$

where μ and χ are introduced from Eqs. (7.30) and (7.31). The hardness of a species is then the amount by which its electronegativity–its ability to accept electrons– decreases when an infinitesimal amount of electronic charge is added to it. Intuitively, a hard molecule is like a rigid container that does not yield as electrons are forced in, so the pressure, analogous to the electron density, inside builds up, resisting the ingress of more electrons. A soft molecule may be likened to a balloon that can expand as it acquires electrons, so that the ability to accept still more electrons is not so seriously compromised. Softness is logically the reciprocal of hardness:

$$\sigma = \frac{1}{\eta} \tag{7.35}$$

and qualitatively, of course, it is the opposite in all ways.

To approximate hardness by I and A (cf. the approximation of electronegativity by Eq. (7.32)), we approximate the $E = f(N)$ curve (cf. Fig. 7.10) by a general quadratic (since it *looks* like a quadratic):

$$E = aN^2 + bN + c$$
$$\frac{\partial^2 E}{\partial N^2} = 2a$$

We will now let M denote any atom or molecule, and M^+ and M^- the species formed by removal or addition of an electron from M.

$E(M)$ corresponds to $N = 1$ and $E(M^-)$ corresponds to $N = 2$, so substituting into our quadratic equation

$$E(M) = a(1^2) + b(1) + c = a + b + c$$

and

$$E(M^-) = a(2^2) + b(2) + c = 4a + 2b + c$$

and so

$$2a = c + E(M^-) - 2E(M)$$

Since

$$E(0) = E(M^+) = a(0^2) + b(0) + c = c,$$

$$2a = E(M^+) + E(M^-) - 2E(M) = [E(M^+) - E(M)] - [E(M) - E(M^-)] = I - A$$

$$i.e \quad \eta = \left(\frac{\partial^2 E}{\partial N^2}\right)_v = I - A \tag{7.36}$$

Actually, the hardness is commonly *defined* as *half* the curvature of the *E* vs. *N* graph, giving

$$\eta = \frac{1}{2}\left(\frac{\partial^2 E}{\partial N^2}\right)_v = \frac{I - A}{2} \tag{7.37}$$

and from Eq. (7.34)

$$\eta = \frac{1}{2}\left(\frac{\partial^2 E}{\partial N^2}\right)_v = \frac{1}{2}\left(\frac{\partial \mu}{\partial N}\right)_v = -\frac{1}{2}\left(\frac{\partial X}{\partial N}\right)_v \tag{7.38}$$

The one-half factor is [156] to bring η into line with Eq. (7.32), where this factor arises naturally in applying the three-point approximation and the definitions of *I* and *A* to the rigorous Gibbs equation (Eq. (7.30)) for electronic chemical potential.

Electronegativity has also been expressed in terms of orbital energies, by taking *I* as the negative of the HOMO energy and *A* as the negative of the LUMO energy [156]. This gives

$$\eta = \frac{(E_{LUMO} - E_{HOMO})}{2} \tag{7.39}$$

Like the analogous expression for electronegativity (Eq. (7.33)), this requires only a "one-pot" calculation, of the HOMO and LUMO. Much of what was said about Eq. (7.33) applies to Eq. (7.39). Table 7.12 gives values of η calculated analogously to the χ values discussed above. The HOMO/LUMO hardness values are in even worse agreement with the *I/A* ones than are the HOMO/LUMO electronegativity values with the *I/A* values. The zero values for the HOMO/LUMO-calculated η of the radicals arise from taking the half-occupied orbital (semioccupied MO, SOMO) as both HOMO and LUMO. The orbital view of hardness as the HOMO/LUMO gap is discussed by Pearson, who also reviews the principle of maximum hardness; according to this, in a chemical reaction hardness and the HOMO/LUMO gap tend to increase, potential energy surface relative minima represent species of relative *maximum* hardness, and transition states are species of relative *minimum* hardness [156]. These general ideas about hardness have been expounded [158] and the reciprocal concept of softness was used (with the Fukui function) to rationalize some cycloaddition reactions [159].

Table 7.12 Electronegativity, χ, and hardness, η (cf. Fig. 7.10)

	I	A	HOMO, MP2 (HOMO, DFT)	LUMO, MP2 (LUMO, DFT)	χ: $(I+A)/2$, HOMO/ LUMO MP2, HOMO/LUMO DFT	η: $(I-A)/2$, HOMO/ LUMO MP2, HOMO/ LUMO DFT
F^+	36	19.8	-37.6 (-30.0)	-17.7 (-27.3)	27.9, 27.7, 28.7	8.1, 10.0, 1.4
$F^\cdot$	19.8	3	-19.5 (-14.5)	-19.5 (-14.5)	11.4, 19.5, 14.5	8.4, 0, 0
F^-	3	-14	-2.1 (4.6)	42.1 (36.4)	-5.5, -20.0, -20.5	8.4, 22.1, 15.9
HS^+	20.2	11.3	-20.3 (-16.8)	-10.7 (-15.7)	15.8, 15.5, 16.3	4.5, 4.8, 0.6
$HS^\cdot$	11.3	1.7	-12.5 (-8.7)	-12.5 (-8.7)	6.5, 12.5, 8.7	4.8, 0, 0
HS^-	1.7	-6.4	-1.9 (1.3)	12.3 (8.4)	-2.4, -5.2, -4.9	4.1, 7.1, 3.6

For each species χ and η have been calculated in three ways: (1) From ionization energy (I) and electron affinity (A), using $\chi = \frac{1}{2}(I+A)$ and $\eta = 1/2(I-A)$. I and A were calculated (QCISD(T)/ 6-311+G*) as the energy differences of the optimized-geometry species, i.e. adiabatic values. (2) From the MP2(FC)/6-31G* HOMO and LUMO, using $\chi = -1/2(E_{\mathrm{HOMO}} + E_{\mathrm{LUMO}})$ and $\eta = \frac{1}{2}(E_{\mathrm{LUMO}} - E_{\mathrm{HOMO}})$. (3) From the B3LYP/6-31G* Kohn-Sham HOMO and LUMO, as for (2). All the numbers refer to units of eV

The Fukui function (the frontier function) was defined by Parr and Yang [150] as

$$f(\mathbf{r}) = \left[\frac{\delta\mu}{\delta v(\mathbf{r})}\right]_N = \left[\frac{\partial\rho(\mathbf{r})}{\partial N}\right]_v \tag{7.40}$$

This says that $f(\mathbf{r})$ is the functional derivative (Sect. 7.2.3.2.2, *The Kohn-Sham equations*) of the chemical potential with respect to the external potential (i.e. the potential caused by the nuclear framework), at constant electron number; and that it is also the derivative of the electron density with respect to electron number at constant external potential. The second equality shows $f(\mathbf{r})$ to be the sensitivity of $\rho(\mathbf{r})$ to a change in N, at constant geometry. A change in electron density should be primarily electron withdrawal from or addition to the HOMO or LUMO, the frontier orbitals of Fukui [160] (hence the name bestowed on the function by Parr and Yang). Since $\rho(\mathbf{r})$ varies from point to point in a molecule, so does the Fukui function. Parr and Yang argue that a large value of $f(\mathbf{r})$ at a site favors reactivity at that site, but to apply the concept to specific reactions they define three Fukui functions ("condensed Fukui functions" [109]):

$$f^*(\mathbf{r}) = \left[\frac{\partial\rho(\mathbf{r})}{\partial N}\right]_v^* \qquad * = +, -, 0 \tag{7.41}$$

The three functions f^+, f_k^-, and f_k^0 refer to an electrophile, a nucleophile, and a radical. They are the sensitivity, to a small change in the number of electrons, of the electron density in the LUMO, in the HOMO, and in a kind of average HOMO/ LUMO half-occupied orbital. Practical implementations of these condensed Fukui functions are the "condensed-to-atom" forms of Yang and Mortier [161]:

$$f_k^+ = q_k(N+1) - q_k(N) \quad \text{for atom k as an electrophile}$$
$$f_k^- = q_k(N) - q_k(N-1) \quad \text{for atom k as an electrophile}$$
$$f_k^0 = \frac{1}{2}[q_k(N+1) - q_k(N-1)] \quad \text{for atom k as a radical}$$

(7.42)

Here $q_k(N)$ is the electron population (not the charge) on atom k, etc. (see below). Note that f_k^0 is just the average of f_k^+ and f_k^-. The condensed Fukui functions measure the sensitivity to a small change in the number of electrons of the electron density *at atom k* in the LUMO (f_k^+), in the HOMO (f_k^-), and in a kind of intermediate orbital (f_k^0); they provide an indication of the reactivity of atom k as an electrophile (reactivity toward nucleophiles), as a nucleophile (reactivity toward electrophiles), and as a free radical (reactivity toward radicals).

The easiest way to see how these formulas can be used is to give an example. Let's calculate f_k^- for the anion SCN^-. We'll calculate f_S^-, f_C^-, and f_N^-, to get an idea of the nucleophilic power of the S, C and N atoms in this molecule. We need the electron population q on each atom or, what gives us the same information, the charge on each atom: for an atom in a molecule, electron population = atomic number – charge. To see this, note that if an atom had no electron population, its charge would equal its atomic number. For each electron added to the atom, the charge decreases by one. So charge = atomic number – electron population. We perform the calculations for the N-electron species (SCN^-) and the $(N-1)$-electron species ($SCN^·$). If we were interested in the nucleophilic power of the atoms in a neutral molecule M, then to get f_k^- we would calculate the electron populations or charges on the atoms in M and in M^+, and for the electrophilic power of the atoms in neutral M, to get f_k^+ we calculate the electron populations or charges on the atoms in M and M^-. The calculations are performed for the two species at the same geometry. In introducing the condensed Fukui function Yang and Mortier [161] used for each pair of species a single "standard" (presumably essentially average) geometry, with accepted, reasonable bond lengths and angles, and other workers do not specify whether they use for, say, M and M^+, the neutral or the cation geometry. We will adopt the convention that for a calculation on M^* ($^* = +, -$ or·), both geometries will be those of M*, the species of interest to us; this avoids the problem of trying to do a geometry optimization on a species that may not be a stationary point on the potential energy surface (assuming that M* is itself a stationary point– one will rarely be interested in something that is not), a situation that arises particularly for some anions.

Charges and electron populations from calculations on SCN^- and $SCN^·$ (and on CH_3CCH and $CH_3CCH^{·+}$) are shown in Fig. 7.11. The anion SCN^- was optimized and then the AIM (Chap. 5, Sect. 5.5.4.5) electron population/charges were calculated (the AIM calculations were done with G98 using the keywords AIM = Charge). An AIM calculation was then done on the cation at the anion geometry. The optimization and both AIM calculations used the B3LYP/6-31+G* method/basis; results for other charges than AIM and other methods/basis sets are shown shortly.
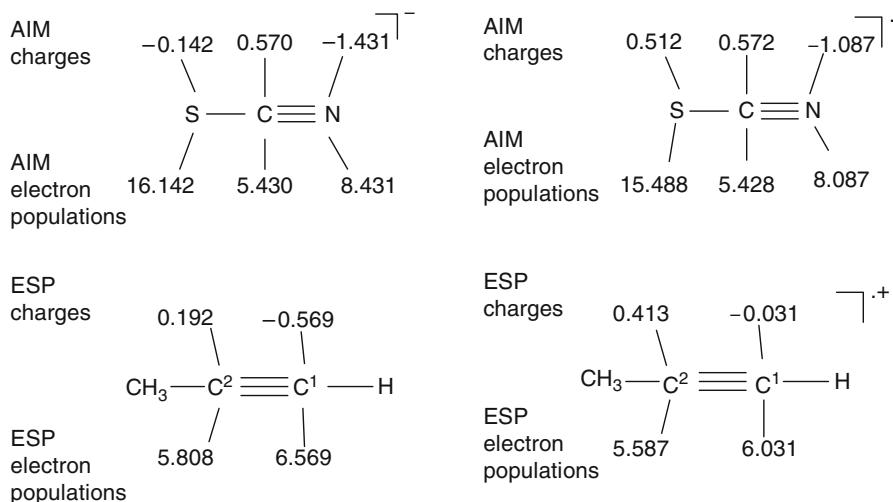
Fig. 7.11 Charges on atoms and corresponding electron populations. For SCN⁻ and SCN. AIM (Chap. 5, Sect. 5.5.4.5) charges were used, and both species are at the optimized SCN⁻ geometry. For CH_3CCH and $CH_3CCH.^+$ electrostatic potential charges (from Gaussian 98, keyword Pop=MK) were used, and both species are at the optimized CH_3CCH geometry. The method/ basis for optimization and charge calculation is B3LYP/6-31+G* for SCN⁻ and SCN., and B3LYP/ 6-311G** for CH_3CCH and $CH_3CCH.^+$

The condensed Fukui functions may now be calculated (see Fig. 7.11):

$$f^-(S) = q(S, \text{ anion}) - q(S, \text{ neutral}) = 16.142 - 15.488 = 0.654$$
$$f^-(C) = q(C, \text{ anion}) - q(C, \text{ neutral}) = 5.430 - 5.428 = 0.002$$
$$f^-(N) = q(N, \text{ anion}) - q(N, \text{ neutral}) = 8.431 - 8.087 = 0.344$$

This indicates that in SCN⁻ the order of nucleophilicity is $S > N >> C$ (which is what any chemist should expect). Sulfur is the softest atom here, and carbon the hardest. The results of such a calculation vary somewhat with the method/basis (e.g. HF/6-31G*, MP2/6-31G*, etc.), and especially with the way the charges/ electron populations are calculated. Here are the f_k^- functions from the use of electrostatic potential charges (the G98 keyword Pop=MK was used) again using B3LYP/6-31+G*:

$$f_k^-(S) = q(S, \text{ anion}) - q(S, \text{ neutral}) = 16.720 - 15.955 = 0.765$$
$$f_k^-(C) = q(C, \text{ anion}) - q(C, \text{ neutral}) = 5.542 - 5.707 = -0.165$$
$$f_k^-(N) = q(N, \text{ anion}) - q(N, \text{ neutral}) = 7.738 - 7.338 = 0.400$$

In this case the conclusions, compared to using AIM charges, are unaffected.

In an extensive study, Geerlings et al. [109] showed that with AIM charges semiquantitatively similar results are obtained with a variety of correlation methods (HF, MP2, QCISD, and five DFT functionals), using bases similar to 6-31G*. The

biggest deviation from QCISD (Chap. 5, Sect. 5.4.3; QCISD was taken as the most reliable of the methods used) was shown by MP2. For example, for CH_2CHO^- all correlation methods except MP2 gave O a bigger f^- than C. If we disregarded the MP2 result as anomalous, this could be interpreted as indicating that the O is more nucleophilic than the C. In fact, in standard organic syntheses enolates usually react preferentially at the *carbon*, but the ratio of C:O nucleophilic attack can vary considerably with the particular enolate, the electrophile, and the solvent. To complicate things even more, the nucleophile is not always just the simple enolate: an ion pair or even aggregates of ion pairs may be involved [162]. Even for the case of an unencumbered enolate, the atom with the biggest f^- (the softest atom) cannot be assumed to be the strongest nucleophilic center, because, as Méndez and Gázquez point out in their study [163] of enolates using the Fukui function, one consequence of the hard-soft-acid–base principle is that an electrophile tends to react with a nucleophilic center of *similar* softness (soft acids prefer soft bases, etc.), not necessarily with the softest nucleophilic center. Thus for the reaction of CH_2CHO^- with the electrophile CH_3X, one might calculate, for CH_2CHO^-, $f(C)$ and $f(O)$, and for CH_3X, $f^+(C)$. The CH_3X C would be expected (in the absence of complications!) to bond to the atom, C or O, whose f^- value was closest to its $f^+(C)$ value. A study of the ethyl acetoacetate enolate using these and other concepts has been reported by Geerlings and coworkers [164]. This approach, which is applicable to any ambient species, is further illustrated below by the reaction of HNC with alkynes.

In a study of the reaction of alkynes with hydrogen isocyanide the condensed Fukui function was combined with the overall or global softness to try to rationalize the regioselectivity of attack on the triple bond [159]:
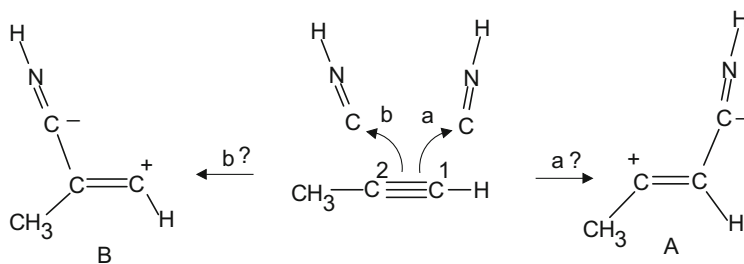
This reaction involves electrophilic attack by HNC on the alkyne, to give a zwitterion which reacts further. Can our concepts be used to predict which alkyne atom, C^1 or C^2 (using the designations of [159]) will be attacked–will the products be formed primarily through A or through B? Nguyen et al. approached this problem by first showing that the reaction is indeed electrophilic attack of HNC (acting as an electrophile) on the alkyne (acting as a nucleophile): the HOMO (alkyne)/LUMO(HNC) interaction has a smaller energy gap than the HOMO (HNC)/LUMO(alkyne) interaction. They then calculated the *local softness* or *condensed softness parameters* (not quite the same as the condensed-to-atoms parameters of Eq. (7.42) that we saw above; see below) of C^1 and C^2 of the alkyne and the C of HNC. For C^1 and C^2 of the alkyne the softness as a nucleophile, i.e. softness toward electrophiles, was calculated, with the aid of f_k^-, and for the

HNC C softness as an electrophile, i.e. softness toward nucleophiles, was calcu-
lated, with the aid of f_k^+.

Illustrating how the calculations for CH_3CCH may be done:

1. Optimize the structure of CH_3CCH and calculate its atom charges (and energy).
2. Use the optimized geometry of CH_3CCH for a single-point (same geometry)
   calculation of the charges (and energy) for the radical cation $CH_3CCH^{.+}$.
   Steps (1) and (2) enable calculation of f_k^-.
3. Use the optimized geometry of CH_3CCH for a single-point calculation of the
   energy of the radical anion CH_3CCH^-

Steps (1), (2) and (3) enable us to calculate the *global softness* (the softness
of the molecule as a whole) of CH_3CCH. This is done by calculating the
vertical ionization energy and electron affinity as energy differences, then calcu-
lating the global softness as the reciprocal of global hardness. From Eq. (7.35) this
is $\sigma = 1/(I - E)$ or $\sigma = 2/(I - E)$, depending on whether we define hardness
according to Eq. (7.36) or (7.37). Nguyen et al. use $\sigma = 1/(I - E)$, i.e they take
hardness as $\eta = (I - E)$ rather than $\frac{1}{2}(I - E)$. The local softness of any atom of
interest may now be calculated by multiplying f_k^- for that atom by σ. Let's look at
actual numbers. The CH_3CCH B3LYP/6-311G** basis set and electrostatic poten-
tial charges (with the Gaussian keyword Pop = MK) were used. These gave the
charges (and thus electron populations) shown in Fig. 7.11. From these populations,

$$f^-(C^1) = q(C^1, \text{neutral}) - q(C^1, \text{cation}) = 6.569 - 6.031 = 0.538$$
$$f^-(C^2) = q(C^2, \text{neutral}) - q(C^2, \text{cation}) = 5.808 - 5.587 = 0.221$$

The vertical ionization energy and vertical electron affinity are (here ZPEs have
not been taken into account, as they should nearly cancel; in any case the signif-
icance of a calculated ZPE for the cation or anion at the geometry of the neutral is
questionable, since the two vertical species are not stationary points):

$$I = E(\text{cation}) - E(\text{neutral}) = -116.31237 - (-116.69077) = 0.37840 \text{ h}$$
$$A = E(\text{neutral}) - E(\text{anion}) = -116.69077 - (-116.58078) = -0.10999 \text{ h}$$

The softness is then $\sigma = 1/(I - A) = 1/[0.37840 - (-0.10999)] = 2.048 \text{ h}^{-1}$ So
the local softness of the two carbons as nucleophiles (softness toward electrophiles) is

$$s^-(C^1) = 0.538(2.048) = 1.102$$

and

$$s^-(C^2) = 0.221(2.048) = 0.453$$

(Nguyen et al. report 1.096 and 0.460).

Since electron population is a pure number and global softness has the units of
reciprocal energy, local softness logically has these units too, but the practice is to
simply state that all these terms are in "atomic units".

Now consider analogous calculations on the HNC C, but for local softness as an *electrophile* (softness toward nucleophiles), using f_k^+. These calculations gave:

$$s^+(\text{HNC C}) = 1.215$$

To predict which of the two alkyne carbons, C^1 or C^2, HNC will preferentially attack, one now invokes the "local hard-soft acid–base (HSAB) principle" [163], which says that interaction is favored between electrophile/nucleophile (or radical/radical) of most nearly equal softness. The HNC carbon softness of 1.215 is closer to the softness of C^1 (1.102) than that of C^2 (0.453) of the alkyne, so this method predicts that in the reaction scheme above the HNC attacks C^1 in preference to C^2, i.e. that reaction should occur mainly by the zwitterion A. This kind of analysis worked for $-CH_3$ and $-NH_2$ substituents on the alkyne, but not for $-F$.

The concepts of hardness, softness, and of frontier orbitals, with which latter the Fukui function is closely connected, have been severely criticized [148]. It is also true that in some cases the results predicted using these methods can also be understood in terms of more traditional chemical concepts. Thus in the alkyne-HNC reaction, resonance theory leads one to suspect that the zwitterion A, with the positive charge formally on the more substituted carbon, will be favored over B. Nevertheless, the large amount of work which has been done using these ideas suggests that they offer a useful approach to interpreting and predicting chemical reactivity. Even an apparently unrelated property, or rather a set of properties, namely aromaticity, has been subjected to analysis in terms of hardness [165]. As Parr and Yang say, "This is perhaps an oversimplified view of chemical reactivity, but it is useful." [166].

To cite some newer work on Fukui functions: it was claimed that if one accepts negative values of the function (apparently previously shunned), one can understand reactions in which oxidation of an entire molecule leads to reduction of a part of it (removing electrons from alkynes can increase the electron density in the CC bond) [167]; the Fukui functions concept has been extended beyond the "local philicity" shown above and dual philicity to give a "multiphilic descriptor" which reflects simultaneously the nucleophilicity and the electrophilicity of a given site in a molecule [168]; AIM calculations (Chap. 5, in Sect. 5.5.4.5) were said to give the best results with condensed Fukui functions (Eqs. (7.41) and (7.42)) [169]; and the appropriateness of the Fukui function for describing hard-hard, as distinct from soft-soft, interactions has been questioned [170].

7.3.6 *Visualization*

The only cases for which one might anticipate differences between DFT and wavefunction theory as regards visualization (Chap. 5, Sect. 5.5.6, Chap. 6, Sect. 6.3.6) are those involving orbitals: as explained in Sect. 7.2.3.2.2, *The Kohn-Sham equations*, the orbitals of currently popular DFT methods were introduced to make the calculation of the electron density tractable, but in "pure" DFT theory orbitals would not exist. Thus electron density, spin density, and electrostatic potential can

be visualized in Kohn-Sham DFT calculations just as in ab initio or semiempirical work. However, visualization of orbitals, so important in wavefunction work (especially the HOMO and LUMO, which according to frontier orbital theory [160] strongly influence reactivity) does not seem possible in a *pure* DFT approach, one in which wavefunctions are not invoked. In currently popular DFT calculations one can visualize the Kohn-Sham orbitals, which are qualitatively much like wavefunction orbitals [134] (Sect. *7.3.5.3*, *Ionization energies and electron affinities*).

7.4 Strengths and Weaknesses of DFT

7.4.1 Strengths

DFT includes electron correlation in its theoretical basis, in contrast to wavefunction methods, which must take correlation into account by add-ons (Møller-Plesset perturbation, configuration interaction, coupled-cluster) to ab initio Hartree-Fock theory, or by parameterization in semiempirical methods. Because it has correlation fundamentally built in, DFT can calculate geometries and relative energies with an accuracy comparable to MP2 calculations, in roughly the same time as needed for Hartree-Fock calculations. Aiding this, DFT calculations tend to be basis-set-saturated more easily than are ab initio: limiting results are (sometimes) approached with smaller basis sets than for ab initio calculations. Calculations of post-Hartree-Fock accuracy can thus be done on bigger molecules than ab initio methods make possible.

DFT appears to be the method of choice for geometry and energy calculations on transition metal compounds, for which conventional ab initio calculation often give poor results [81, 171]. In fact, a study of diatomic transition metal molecules led to the conclusion that "the available experimental data do not provide a justification for using conventional single-reference CC [coupled cluster] theory calculations to validate or test" functionals for molecules with $3d$ transition metals, since CCSD (T)-type calculations perform only "comparable to, but not necessarily better than KS density functional calculations with a wide set of choices of xc functionals" [172]. An example of the use of DFT in investigating transition metal- catalyzed reactions is the application of B3LYP and M06 to a nickel-compound-catalyzed cycloaddition of dienes to alkynes [173].

DFT works with electron density, which can be measured and is easily intuitively grasped [4], rather than a wavefunction, a mathematical entity whose physical meaning is still controversial.

7.4.2 Weaknesses

The exact exchange-correlation functional $E_{XC}[\rho_0]$, one of the terms in the DFT expression for the energy, is unknown, and no one knows how to fully

systematically improve our approximations to it. In contrast, ab initio energies can be systematically lowered by using bigger basis sets and by expanding the correlation method: MP2, MP3, . . ., or more determinants in the CI approach. It is true that for a particular purpose 6-311G* may not be better than 6-31G*, and MP3 is certainly not necessarily better than MP2, but bigger basis sets and higher correlation levels will *eventually* approach an exact solution of the Schrödinger equation. The accuracy of DFT is being gradually improved by modifying functionals, not according to some grand theoretical prescription, but rather with the aid of experience and intuition, and checking the calculations against experiment. This makes DFT philosophically somewhat semiempirical. Some functionals contain parameters which must be fitted to experiment; these methods are even more distinctly empirical. Since the functionals are not based purely on fundamental theory, one should be cautious about applying DFT to very novel molecules. Of course the semiempirical character of current DFT is not a fundamental feature of the basic method, but arises only from our ignorance of the exact exchange-correlation functional. Because our functionals are only approximate, DFT as used today is not variational (the calculated energy could be lower than the actual energy).

DFT is not as accurate as the highest-level ab initio methods, like QCISD(T) and CCSD(T) (but it can handle much bigger molecules than can these methods). Even gradient-corrected functionals apparently were unable to handle van der Waals interactions [174], although they did give good energies and structures for hydrogen-bonded species [175], but more recent progress in treating van der Waals and other weak interactions was encouraging [44, 45], and the problem now appears to have been substantially overcome (see the discussion of dispersion, Sect. 7.2.3.4.8).

DFT today is mainly a ground-state theory, although ways of applying it to excited states are being developed.

7.5 Summary

Density functional theory is based on the two Hohenberg-Kohn theorems, which state that the ground-state properties of an atom or molecule are determined by its electron density function, and that a trial electron density must give an energy greater than or equal to the true energy. Actually, the latter theorem is true only if the exact functional (see below) is used; with the approximate functionals in use today, DFT is not variational–it can give an energy below the true energy. In the Kohn-Sham approach the energy of a system is formulated as a deviation from the energy of an idealized system with noninteracting electrons. The energy of the idealized system can be calculated exactly since its wavefunction (in the Kohn-Sham approach wavefunctions and orbitals were introduced as a mathematical convenience to get at the electron density) can be represented exactly by a Slater determinant. The relatively small difference between the real energy and the energy of the idealized system contains the exchange-correlation functional, the only

unknown term in the expression for the DFT energy; the approximation of this functional is the main problem in DFT. From the energy equation, by minimizing the energy with respect to the Kohn-Sham orbitals the Kohn-Sham equations can be derived, analogously to the Hartree-Fock equations. The molecular orbitals of the KS equations are expanded with basis functions and matrix methods are used to iteratively find the energy, and to get a set of molecular orbitals, the KS orbitals, which are qualitatively similar to the orbitals of wavefunction theory.

The simplest version of DFT, the local density approximation (LDA), which treats the electron density as constant or only very slightly varying from point to point in an atom or molecule, and also pairs two electrons of opposite spin in each KS orbital, is little used nowadays. It has been largely replaced by methods which use gradient-corrected ("nonlocal") functionals and which assign one set of spatial orbitals to α-spin electrons, and another set of orbitals to β-electrons; this latter "unrestricted" assignment of electrons added to LDA constitutes the local-spin-density approximation (LSDA). The best results appear to come from so-called hybrid functionals, which include some contribution from Hartree-Fock type exchange, using KS orbitals. The most popular current DFT method is probably still the LSDA gradient-corrected hybrid method which uses the B3LYP (Becke three-parameter Lee-Yang-Parr) functional. However, this may soon be largely replaced by new functionals, like those of the M06 family.

Gradient-corrected and, especially, hybrid functionals, give good to excellent geometries. Gradient-corrected and hybrid functionals usually give fairly good reaction energies, but, especially for isodesmic-type reactions, the improvement over HF/3-21G or HF/6-31G* calculations does not seem to be dramatic (as far as the relative energies of normal, ground-state organic molecules goes; for energies and geometries of transition metal compounds, DFT is the method of choice). For homolytic dissociation, correlated methods (e.g. B3LYP and MP2) are vastly better than Hartree-Fock-level calculations; these methods also give tend to give fairly good activation barriers.

DFT gives reasonable IR frequencies and intensities, comparable to those from MP2 calculations. Dipole moments from DFT appear to be more accurate than those from MP2, and B3LYP/6-31G* moments on AM1 geometries are good. Time-dependent DFT (TDDFT) is the best method (with the possible exception of semiempirical methods parameterized for the type of molecule of interest) for calculating UV spectra reasonably quickly. DFT is said to be better than Hartree-Fock (but not as good as MP2) for calculating NMR spectra. Good first ionization energies are obtained from B3LYP/6-31+G*//B3LYP/3-21G$^{(*)}$ energy differences (using AM1 geometries makes little difference, at least with normal molecules). These values are somewhat better than the ab initio MP2 energy difference values, and are considerably better than MP2 Koopmans' theorem IEs. Rough estimates of electron affinities can be obtained from the negative LUMOs from LSDA functionals (gradient-corrected functionals give much worse estimates). For conjugated molecules, HOMO-LUMO gaps from hybrid functionals agreed well with the $\pi \rightarrow \pi^*$ UV transitions. The mutually related concepts of electronic chemical

potential, electronegativity, hardness, softness, and the Fukui function are usually discussed within the context of DFT. They are readily calculated from ionization energy, electron affinity, and atom charges.

Easier Questions

1. State the arguments for and against regarding DFT as being more a semiempirical than an ab initio-like theory.
2. What is the essential difference between wavefunction theory and DFT? What is it that, in principle anyway, makes DFT simpler than wavefunction theory?
3. Why can't current DFT calculations be improved in a stepwise, systematic way, as can ab initio calculations?
4. Which of these prescriptions for dealing with a function are functionals:

   (1) square root of $f(x)$. (2) $\sin f(x)$. (3) $\sum_{x=1}^{3} f(x) \cdot$ (4) $\int f(x)dx \cdot$ (5) $\exp(f(x))$.

5. For which class(es) of functions is the nth derivative of $f(x)$ a functional?
6. Explain why a kind of molecular orbital is found in current DFT, although DFT is touted as an alternative to wavefunction theory.
7. What is fundamentally wrong with functionals that are not gradient-corrected?
8. The ionization energy of a molecule can be regarded as the energy required to remove an electron from its HOMO. How then would a pure density functional theory, with no orbitals, be able to calculate ionization energy?
9. Label these statements true or false: (1) For each molecular wavefunction there is an electron density function. (2) Since the electron density function has only x, y, z as its variables, DFT necessarily ignores spin. (3) DFT is good for transition metal compounds because it has been specifically parameterized to handle them. (4) In the limit of a sufficiently big basis set, a DFT calculation represents an exact solution of the Schrödinger equation. (5) The use of very big basis sets is essential with DFT. (6) A major problem in density functional theory is the prescription for going from the molecular electron density function to the energy.
10. Explain *in words* the meaning of the terms electronegativity, hardness, and the Fukui function.

Harder Questions

1. It is sometimes said that electron density is physically more real than a wavefunction. Do you agree? Is something that is more easily grasped intuitively necessarily more real?

2. A functional is a function of a function. Explore the concept of a function of a functional.
3. Why is it that the Hartree-Fock Slater determinant is an inexact representation of the wavefunction, but the DFT determinant for a system of noninteracting electrons is exact for this particular wavefunction?
4. Why do we expect the "unknown" term in the energy equation ($E_{xc}[\rho_0]$, in Eq. (7.21)) to be small?
5. Merrill et al. have said that "while solutions to the [HF equations] may be viewed as exact solutions to an approximate description, the [KS equations] are approximations to an exact description!" Explain.
6. Electronegativity is the ability of an atom or molecule to attract electrons Why then is it then (from one definition) the average of the ionization energy and the electron affinity (Eq. (7.32)), rather than simply the electron affinity?
7. Given the wavefunction of a molecule, it is possible to calculate the electron density function. Is it possible in principle to go in the other direction? Why or why not?
8. The multielectron wavefunction Ψ is a function of the spatial and spin coordinates of all the electrons. Physicists say that Ψ for any system tells us all that can be known about the system. Do you think the electron density function ρ tells us everything that can be known about a system? Why or why not?
9. If the electron density function concept is mathematically and conceptually simpler than the wavefunction concept, why did DFT come later than wavefunction theory?
10. For a spring or a covalent bond, the concepts of force and force constant can be expressed in terms of first and second derivatives of energy with respect to extension. If we let a "charge space" N replace the real space of extension of the spring or bond, what are the analogous concepts to force and force constant? Using the SI, derive the units of electronegativity and of hardness.

References

1. (a) Whitaker A (1996) Einstein, Bohr and the quantum dilemma. Cambridge University Press; (b) Yam P (1997) Scientific American, June 1997, p. 124; (c) Albert DZ (1994) Scientific American, May 1994, p. 58; (d)Albert DZ (1992) Quantum mechanics and experience. Harvard University Press, Cambridge, MA; (e) Bohm D, Hiley HB (1992) The undivided universe. Routledge, New York; (f) Baggott J (1992) The meaning of quantum theory. Oxford, New York; (g) Jammer M (1974) The philosophy of quantum mechanics. Wiley, New York
2. Bader RFW (1990) Atoms in molecules. Clarendon Press, Oxford/New York
3. Reference 2, pp 7–8
4. Shusterman GP, Shusterman AJ (1997) J Chem Educ 74:771
5. Parr RG, Yang W (1989) Density-functional theory of atoms and molecules. Clarendon Press/ Oxford University Press, Oxford/New York, p 53
6. (a) Wilson E (1998) Chem Eng News, October 19, 12; (b) Malakoff D (1998) Science 282:610
7. See e.g. Diacu F (1996) The mathematical intelligencer. 18:66

8. Kohn W (1951) Phys Rev 84:495
9. Cf. Levine IN (2010) Quantum chemistry, 7th edn. Prentice Hall, Upper Saddle River, section 14.1, particularly equation 14.8. See too p. 597, problem 16.28
10. Löwdin P-O (1955) Phys Rev 97:1474
11. Parr RG, Yang W (1989) Density-functional theory of atoms and molecules. Clarendon Press/ Oxford University Press, Oxford/New York
12. Levine IN (2014) Quantum chemistry, 7th edn. Prentice Hall, Upper Saddle River; section 16.5
13. Cramer CJ (2004) Essentials of computational chemistry, 2nd edn. Wiley; chapter 8
14. Jensen F (2007) Introduction to computational chemistry, 2nd edn. Wiley, New York, chapter 6
15. Peverati R, Truhlar DG (2014) Phil Trans R Soc A, Math Phys Eng Sci 372
16. Burke K (2012) J Chem Phys 136:150901(1)
17. Cohen AJ, Mori-Sánchez P, Yang W (2012) Chem Rev 112:289
18. (a) Wagner JP, Schreiner PR (2015) Angew Chem Int Ed 54:12274 ; (b) Corminboeuf C (2014) Acc Chem Res 47:3217
19. Various authors (2014) Acc Chem Res 2014 47(11)
20. Jones RO (2015) Rev Mod Phys 87:897
21. E.g. Griffiths DJ (1995) Introduction to quantum mechanics. Prentice-Hall, Engelwood Cliffs
22. (a) Earlier work (1927) by Fermi was published in Italian and came to the attention of the physics community with a paper in German: Fermi E (1928) Z Phys 48:73. This appears in English translation in March NH (1975) Self-consistent fields in atoms. Pergamon, New York; (b) Thomas LH (1927) Proc Cambridge Phil Soc 23:542
23. Reference 11, chapter 6
24. (a) Slater JC (1975) Int J Quantum Chem Symp 9:7. Reviews; (b) Connolly JWD in Semiempirical methods of electronic structure calculations part A: techniques, Segal GA Ed., Plenum, New York, 1977; (c) Johnson KH (1973) Adv Quantum Chem 7:143
25. Slater JC (1951) Phys Rev 81:385
26. For a personal history of much of the development of quantum mechanics, with significant emphasis on the Xα method, see: Slater JC (1975) Solid-state and molecular theory: a scientific biography. Wiley, New York
27. Reference 12, pp 552–555
28. Hohenberg P, Kohn W (1964) Phys Rev B 136:864
29. Reference 11, section 3.4
30. Kohn W, Sham LJ (1965) Phys Rev A 140:1133
31. Reference 12, p 404
32. Reference 14, p 241
33. Reference 11, sections 7.1–7.3
34. Reference 12, section 11.8
35. Reference. 11, chapter 7
36. Reference 11, Appendix A.
37. Reference 12, p 558
38. Merrill GN, Gronert S, Kass SR (1997) J Phys Chem A 101:208
39. Reference 11, p 185
40. Genesis 28. 10–12
41. The term was apparently first enunciated by J. P. Perdew at the DFT2000 symposium in Menton, France. It first appeared in print in: Perdew JP, Schmidt K (2001) Density functional theory and its applications to materials, Van Doren VE, Van Alsenoy K, Geerlings P (eds) AIP Press, New York. This ladder term has also been used, oddly, in science in a context that has no connection with DFT, trapping a transition state in a protein bottle: Romney DK, Miller SJ (2015) Science 347:829; Pearson AD, Mills JM, Song Y, Nasertorabi F, Han GW, Baker D, Stevens RC, Schultz PG (2015) Science 347:863
42. Mattsson AE (2002) Science 298:759

43. Reference 14, pp 244–245
44. Sousa SF, Fernandes OA, Ramos MJ (2007) J Phys Chem A 111:10439
45. (a) Zhao Y, Truhlar DG (2011) Chem Phys Lett 502:1; (b) Zhao Y, Truhlar DG (2008) Acc Chem Res 41:157
46. Riley KE, Op't Holt BT, Merz KM Jr (2007) J Chem Theory Comput 3:404
47. Perdew JP, Ruzsinszky A, Tao J, Staroverov VN, Scuseria GE, Csonka GI (2005) J Chem Phys 123:062201
48. Kurth S, Perdew JP, Blaha P (1999) Int J Quantum Chem 75:889
49. Taylor AE (1955) Advanced calculus. Blaidsell Publishing Company, New York,; p 371
50. Reference 11, pp 173–174
51. Vosko SH, Wilk L, Nusair M (1980) Can J Phys 58:1200
52. St-Amant A (1996) Chapter 5 in reviews in computational chemistry, vol 7. Lipkowitz KB, Boyd DB (eds) VCH, New York; p. 223
53. reference 12, p 565
54. Becke AD (1988) Phys Rev A 38:3098
55. Head-Gordon M (1996) J Phys Chem 100:13213
56. Brack M, Jennings BK, Chu YH (1976) Phys Lett 65B:1
57. Becke AD (1993) J Chem Phys 98:1372, 5648
58. Stephens PJ, Devlin JJ, Chabalowski CF, Frisch MJ (1994) J Phys Chem 98:11623
59. E.g. Perdew JP (1995) Nonlocal density functionals for exchange and correlation: theory and application. In: Ellis DE (ed) Density functional theory of molecules, clusters, and solids. Kluwer, Dordrecht
60. Schwabe T, Grimme S (2007) Phys Chem Chem Phys 9:3397, and references therein. B2PLYP does have empirical parameters, albeit just two
61. Wennmohs F, Neese F (2008) Chem Phys 343:217
62. (a) London F (1927) Zeitschrift für Physik 44(6–7):455–472; (b) London F (1930) Zeitschrift für Physik 63(3–4):245–279
63. (a) Klimeš J, Michaelides A (2012) J Chem Phys 137:120901; (b) Guidez EB, Gordon M S (2015) J Phys Chem A 119:2161; (c) Conrad JA, Gordon MS (2015) J Phys Chem A 119: 5377; (d) Kruse H, Goerigk L, Grimme S (2012) J Org Chem 77:10824; (e Goerigk L, Grimme S (2011) Phys Chem Chem Phys 13:6670; (f) Martin JML (2013) J Phys Chem A 117:3118; (g) van Santen JA, DiLabio GA (2015) J Phys Chem A 119:6710 ; (h) Otero-de-la-Roza A, Johnson ER (2015) J Chem Theory Comput 113:4033
64. Grimme S, Schreiner PR (2011) Angew Chem Int 50:12639
65. Zhao Y, Truhlar DG (2008) J Chem Theory Comput 4:1849
66. Clark T (2000) J Mol Struct (Theochem) 530:1
67. Nooijen M (2009) Adv Quant Chem 56:181
68. Dewar MJS (1992) "A semiempirical life", profiles, pathways and dreams series, J. I. Seeman, Edition, American Chemical Society, Washington, DC. p 185
69. Zhao Y, Truhlar DG (2008) Theor Chem Acc 120:215
70. Reference 12: HF p. 561, UHF pp. 563, 564, G2 pp. 566, 567, MP2, G3 p. 567, CCSD (T) p. 571, CI p. 572
71. Hehre WJ (1995) Practical strategies for electronic structure calculations. Wavefunction, Inc., Irvine
72. Hehre WJ, Lou L (1997) A guide to density functional calculations in Spartan. Wavefunction Inc., Irvine
73. Hehre WJ, Radom L, Schleyer pvR, Pople JA (1986) Ab initio molecular orbital theory. Wiley, New York; section 6.2
74. $H_2C=CHOH$ reaction The only quantitative experimental information on the barrier for this reaction seems to be: Saito S (1976) Chem Phys Lett 42:399, halflife in the gas phase in a Pyrex flask at room temperature ca. 30 minutes. From this one calculates (chapter 5, section 5.5.2.2d, Eq (5.202)) a free energy of activation of 93 kJ mol^{-1}. Since isomerization may be catalyzed by the walls of the flask, the purely concerted reaction may have a much higher

barrier. This paper also shows by microwave spectroscopy that ethenol has the O-H bond *syn* to the C=C. The most reliable measurement of the ethenol/ethanal equilibrium constant, by flash photolysis, is 5.89×10^{-7} in water at room temperature (Chiang Y, Hojatti M, Keeffe JR, Kresge AK, Schepp NP, Wirz J (1987) J Am Chem Soc 109:4000). This gives a free energy of equilibrium of 36 kJ mol^{-1} (ethanal 36 kJ mol^{-1} below ethenol). *HNC reaction* The barrier for rearrangement of HNC to HCN has apparently never been actually measured. The equilibrium constant in the gas phase at room temperature was calculated (Maki AG, Sams RL (1981) J Chem Phys 75:4178) at 3.7×10^{-8}, from actual measurements at higher temperatures; this gives a free energy of equilibrium of 42 kJ mol^{-1} (HCN 42 kJ mol^{-1} below HNC). According to high-level ab initio calculations supplemented with experimental data (Active Thermochemical Tables) HCN lies 62.35 ± 0.36 kJ mol^{-1} (converting the reported spectroscopic cm^{-1} energy units to kJ mol^{-1}) below HNC; this is "a recommended value...based on all currently available knowledge": Nguyen TL, Baraban JH, Ruscic B, Stanton JF (2015) J Phys Chem 119:10929. *CH$_3$NC reaction* The reported experimental activation energy is 161 kJ mol^{-1} (Wang D, Qian X (1996) J Peng Chem Phys Lett 258:149; Bowman JM, Gazy B, Bentley JA, Lee TJ, Dateo CE (1993) J Chem Phys 99:308; Rabinovitch BS, Gilderson PW (1965) J Am Chem Soc 87:158; Schneider FW, Rabinovitch BS (1962) J Am Chem Soc 84:4215). The energy difference between CH$_3$NC and CH$_3$NC has apparently never been actually measured. *Cyclopropylidene reaction* Neither the barrier nor the equilibrium constant for the cyclopropylidene/allene reaction have been measured. The only direct experimental information of these species come from the failure to observe cyclopropylidene at 77 K (Chapman OL (1974) Pure and applied chemistry 40:511). This and other experiments (references in Bettinger HF, Schleyer PvR, Schreiner PR, Schaefer HF (1997) J Org Chem 62:9267 and in Bettinger HF, Schreiner PR, Schleyer PvR, Schaefer HF (1996) J Phys Chem 100:16147) show that the carbene is much higher in energy than allene and rearranges very rapidly to the latter. Bettinger et al. 1997 (above) calculate the barrier to be 21 kJ mol^{-1} (5 kcal mol^{-1})

75. Spartan is an integrated molecular mechanics, ab initio and semiempirical program with an outstanding input/output graphical interface that is available in UNIX workstation and PC versions: Wavefunction Inc. http://www.wavefun.com. 18401 Von Karman, Suite 370, Irvine CA 92715, USA

76. Perdew JP, Burke K, Ernzerhof M (1996) Phys Rev Lett 77:3865; Erratum: Perdew JP, Burke K, Ernzerhof M (1997) Phys Rev Lett 78:1396

77. Tao J, Pewdew JP, Staroverov VN, Scuseria GE (2003) Phys Rev Lett 91:146401

78. Wheeler SE, Houk KN (2010) J Chem Theory Comput 6:395

79. Scheiner AC, Baker J, Andzelm JW (1997) J Comput Chem 18:775

80. El-Azhary AA (1996) J Phys Chem 100:15056

81. Bauschlicher CW Jr, Ricca A, Partridge H, Langhoff SR (1997) Recent advances in density functional methods. Part II. Chong DP (ed) World Scientific, Singapore

82. (a) Scott AP, Radom L (1996) J Phys Chem 100:16502; (b) Sibaev M, Crittenden DL (2015) J Phys Chem A 119:13107

83. (a) As of early-2015, the latest "full" version (as distinct from more frequent revisions) of the Gaussian suite of programs was Gaussian 09. Gaussian is available for several operating systems; see Gaussian, Inc., http://www.gaussian.com. 340 Quinnipiac St., Bldg. 40, Wallingford, CT 06492, USA; (b)The statistical mechanics routines in Gaussian: Ochterski JW Gaussian white paper "Thermochemistry in Gaussian", http://www.gaussian.com/g_whitepap/thermo.htm

84. Blanksby SJ, Ellison GB (2003) Acc Chem Res 36:255; Chart 1

85. Hammond GS (1955) J Am Chem Soc 77:334

86. From the NIST website. http://webbook.nist.gov/chemistry/: Chase Jr MW (1998) NIST-JANAF themochemical tables, 4th edn. J Phys Chem Ref. Data, Monograph 9, 1998, 1–1951

87. Peterson GA (1998) Chapter 13: Computational thermochemistry. In: Irikura KK, Frurip DJ (eds) American Chemical Society, Washington, DC

88. Goldstein E, Beno B, Houk KN (1996) J Am Chem Soc 118:6036
89. Martell JM, Goddard JD, Eriksson L (1997) J Phys Chem 101:1927
90. The data are from Hehre WJ (1995) Practical strategies for electronic structure calculations. Wavefunction, Inc., Irvine; Chapter 4. In each case, the first 10 examples from the relevant table were used
91. Wiberg KB, Ochterski JW (1997) J Comput Chem 18:108
92. Rousseau E, Mathieu D (2000) J Comput Chem 21:367
93. Ventura ON, Kieninger M, Cachau RE (1999) J Phys Chem A 103:147
94. For this and other misgivings about the multistep methods see Cramer CJ (2004) Essentials of computational chemistry, 2nd edn. Wiley, Chichester; pp 241–244
95. CBS-QB3 was found to give unacceptable errors for halogenated compounds: Bond D, J Org Chem 72:7313
96. For pericyclic reactions: Ess DH, Houk KN (2005) J Phys Chem A 109:9542
97. Montgomery JA Jr, Frisch MJ, Ochterski JW, Petersson GA (1999) J Chem Phys 110:2822
98. del Rio A, Bourcekkine A, Meinel J (2003) J Comput Chem 24:2093
99. Singleton DA, Merrigan SR, Liu J, Houk KN (1997) J Am Chem Soc 119:3385
100. Glukhovtsev MN, Bach RD, Pross A, Radom L (1996) Chem Phys Lett 260:558
101. Bell RL, Tavaeras DL, Truong TN, Simons J (1997) Int J Quantum Chem 63:861
102. Truong TN, Duncan WT, Bell RL (1996) Chemical applications of density functional theory. Laird BB, Ross RB, Ziegler T (eds) American Chemical Society, Washington, DC
103. Zhang Q, Bell RL (1995) J Phys Chem 99:592
104. Eckert F, Rauhut G (1998) J Am Chem Soc 120:13478
105. Baker J, Muir M, Andzelm J (1995) J Chem Phys 102:2063
106. Jursic BS (1996) Recent developments and applications of modern density functional theory. In: Seminario JM (ed) Elsevier, Amsterdam
107. Brown SW, Rienstra-Kiracofe JC, Schaefer HF (1999) J Phys Chem A 103:4065
108. Cramer CJ (2004) Essentials of computational chemistry, 2nd edn. Wiley, Chichester; p 309
109. Geerlings P, De Profit F, Martin JML (1996) Recent developments and applications of modern density functional theory. In: Seminario JM (ed) Elsevier, Amsterdam
110. Lendvay G (1994) J Phys Chem 98:6098
111. Boyd RJ, Wang J, Eriksson LA (1995) Recent advances in density functional methods Part I. Chong DP (ed) World Scientific, Singapore
112. Reference 12, sections 9.8, 9.9
113. Stratman RE, Scuseria GE, Frisch MJ (1998) J Chem Phys 109:8218
114. Wiberg KB, Stratman RE, Frisch MJ (1998) Chem Phys Lett 297:60
115. Foresman JB, Frisch Æ (1996) Exploring chemistry with electronic structure methods. Gaussian Inc., Pittsburgh, p 218
116. Jacquemin D, Preat J, Wathelet V, Fontaine M, Perpète EA (2006) J Am Chem Soc 128:2072
117. Zhao Y, Truhlar DG (2006) J Phys Chem A 110:13126
118. Cheeseman JR, Trucks GW, Keith TA, Frisch MJ (1996) J Chem Phys 104:5497
119. Frisch MJ, Trucks GW, Cheeseman JR (1996) Recent developments and applications of modern density functional theory. In: Seminario JM (ed) Elsevier, Amsterdam
120. Rablen PR, Pearlman SA, Finkbiner J (2000) J Phys Chem A 103:7357
121. Sefzik TH, Tureo D, Iuliucci RJ (2005) J Phys Chem A 109:1180
122. Wu A, Zhang Y, Xu X, Yan Y (2007) J Comput Chem 28:2431
123. Zhao Y, Truhlar D (2008) J Phys Chem A 112:6794
124. Pérez M, Peakman TM, Alex A, Higginson PD, Mitchell JC, Snowden MJ, Morao I (2006) J Org Chem 71:3103
125. Castro C, Karney WL, Vu CMH, Burkhardt SE, Valencia MA (2005) J Org Chem 70:3602
126. Silverstein RM, Bassler GC, Morrill TC (1981) Spectrometric identification of organic compounds, 4th edn. Wiley, New York; methane, 191, 219; cyclopropane, 193, 220; benzene, 196, 222; acetone, 227
127. Patchkovskii S, Thiel W (1999) J Comput Chem 20:1220

128. Muchall HM, Werstiuk NH, Choudhury B (1998) Can J Chem 76:227
129. Levin RD, Lias SG (1971–1981) Ionization potential and appearance potential measurements. National Bureau of Standards, Washington, DC
130. Curtis LA, Nobes RH, Pople JA, Radom I (1992) J Chem Phys 97:6766
131. Golas E, Lewars E, Liebman J (2009) J Phys Chem A 113:9485
132. (a) Baerends EJ, Gritsenko OV (1997) J Phys Chem A 101:5383; (b) Chong DP, Gritsenko OV, Baerends EJ (2002) J Chem Phys 116:1760
133. Cramer CJ (2004) Essentials of computational chemistry, 2nd edn. Wiley, Chichester, p 272
134. Stowasser R, Hoffmann R (1999) J Am Chem Soc 121:3414
135. Salzner U, Lagowski JB, Pickup PG, Poirier RA (1997) J Comput Chem 18:1943
136. Vargas R, Garza J, Cedillo A (2005) J Phys Chem A 109:8880
137. Zhan C-C, Nichols JA, Dixon DA (2003) J Phys Chem A 107:4184
138. Zhang GZ, Musgrave CB (2005) J Phys Chem A 111:1554
139. Hunt WJ, Goddard WA (1969) Chem Phys Lett 3:414
140. van Meer R, Gritsenko OV, Baerends EJ (2014) J Chem Theory Comput 10:4432
141. Schmidt MW, Hull EA, Windus TL (2015) J Phys Chem A 119:10408
142. Berzelius JJ (1819) Essai sur la théorie des proportions chimiques et sur l'influence chimique de l'électricité; see Nye MJ (1993) From chemical philosophy to theoretical chemistry. University of California Press, Berkeley; p 64
143. Parr RG, Yang W (1989) Density-functional theory of atoms and molecules. Oxford, New York, pp 90–95
144. Mulliken RS (1952) J Am Chem Soc 74:811
145. (a) Pearson RG (1963) J Am Chem Soc 85:3533; (b) Pearson RG (1963) Science 151:172
146. Footnote in reference 145a, on p 3533
147. (a) Pearson RG (1973) Hard and soft acids and bases. Dowden, Hutchinson and Ross, Stroudenburg; (b) Lo TL (1977) Hard and soft acids and basis in organic chemistry. Academic Press, New York
148. Dewar MJS (1992) A semiempirical life. American Chemical Society, Washington, DC, p 160
149. Ritter S (2003) Chem Eng News, 17 February, 50
150. Parr RG, Yang W (1984) J Am Chem Soc 106:4049
151. Parr RG, Yang W (1989) Density-functional theory of atoms and molecules. Oxford, New York, chapters 4 and 5 in particular
152. (a) Gibbs JW (1993) The scientific papers of J. Willard Gibbs: vol I, Thermodynamics. Ox Bow, Woodbridge; (b) Confronting confusion about chemical potential: Kaplan TA (2006) J Stat Phys 122:1237; (c) An attempt to give an intuitive feeling for chemical potential: Job G, Herrmann F (2006) European J Phys 27:353; (d) An explanation of chemical potential in different ways: Baierlein R (2001) Am J Phys 69:423
153. Iczkowski RP, Margrave JL (1961) J Am Chem Soc 83:3547
154. Parr RG, Donnelly RA, Levy M, Palke WE (1978) J Chem Phys 68:3801
155. Mulliken RS (1934) J Chem Phys 2:782
156. Pearson RG (1999) J Chem Educ 76:267
157. Parr RG, Pearson RG (1983) J Am Chem Soc 105:7512
158. Toro-Labbé A (1999) J Phys Chem A 103:4398
159. Nguyen LT, Le TN, De Proft F, Chandra AK, Langenaeker W, Nguyen MT, Geerlings P (1999) J Am Chem Soc 121:5992
160. (a) Fukui K (1987) Science 218:747; (b) Fleming I (1976) Frontier orbitals and organic chemical reactions. Wiley, New York; (c) Fukui K (1971) Acc Chem Res 57:4
161. Yang W, Mortier WJ (1986) J Am Chem Soc 108:5708
162. Carey FA, Sundberg RL (2000) Advanced organic chemistry, 3rd edn. Plenum, New York, p 437
163. Méndez F, Gázquez JL (1994) J Am Chem Soc 116:9298
164. Damoun S, Van de Woude G, Choho K, Geerlings P (1999) J Phys Chem A 103:7861

165. (a) Zhou Z, Parr RG (1989) J Am Chem Soc 111:7371; (b) Zhou Z, Parr RG, Garst JF (1988) Tetrahedron Lett 29:4843
166. Parr RG, Yang W (1989) Density-functional theory of atoms and molecules. Clarendon Press/ Oxford University Press, Oxford/New York, p 101
167. Melin J, Ayers PW, Ortiz JV (2007) J Phys Chem A 111:10017
168. Padmanabhan J, Parthasarthi R, Elango M, Subramanian V, Krishnamoorthy BS, Gutierrez-Oliva S, Toro-Labbé A, Roy DR, Chattaraj PK (2007) J Phys Chem A 111:9130
169. Bulat FA, Chamorro E, Fuentealba P, Toro-Labbé A (2004) J Phys Chem A 108:342
170. Melin J, Aparicio F, Subramanian V, Galván M, Chattaraj PK (2004) J Phys Chem A 108:2487
171. (a) Koch W, Holthausen M (2000) A chemist's guide to density functional theory. Wiley-VCH, New York, part B, and refs. therein; (b) Frenking G (1997) J Chem Soc Dalton Trans 1653
172. Xu X, Zhang W, Tang M, Truhlar DG (2015) J Chem Theory Comput 11:2036
173. Hong X, Holte D, Götz CG, Baran PS, Houk KN (2014) J Org Chem 79:12177
174. (a) Kyistyan S, Pulay P (1994) Chem Phys Lett 229:175; (b) Perez-Jorda JM, Becke AD (1995) Chem Phys Lett 233:134
175. (a) Lozynski M, Rusinska-Roszak D, Mack H-G (1998) J Phys Chem A 102:2899; (b) Adamo C, Barone V (1997) Recent advances in density functional methods. Part II. In: Chong DP (ed) World Scientific, Singapore; (c) Sim F, St.-Amant A, Papai I, Salahub DR (1992) J Am Chem Soc 114:4391

Chapter 8
Some "Special" Topics: (Section 8.1) Solvation, (Section 8.2) Singlet Diradicals, (Section 8.3) A Note on Heavy Atoms and Transition Metals

Chapters 1–7: (a) addressed molecules as isolated entities, without reference to their surroundings (except for the water dimer); (b) concentrated on calculations by relatively "automatic" model chemistries; and (c) used mainly organic molecules as illustrations. This chapter to some extent redresses these constraints.

Abstract For some purposes solution-phase computations are necessary, e.g. for understanding certain reactions, and for the prediction of pK_a in solution. For introducing the effects of solvation there are two methodologies (and hybrids of these two): microsolvation or explicit solvation, and continuum solvation.

Some molecular species are not calculated properly by straightforward model chemistries: these include singlet diradicals and some excited state species. For these the standard method is the complete active space approach, CAS (CASSCF, complete active space SCF). This is a limited version of configuration interaction, in which electrons are promoted from and to a carefully chosen set of molecular orbitals.

For systems with heavy atoms we often employ pseudopotential basis sets (frequently relativistic), which reduce the computational burden of large numbers of electrons. Transition metals present problems beyond those of main-group heavy atoms: not only can relativistic effects be significant, but electron d- or f-levels, variably perturbed by ligands, make possible several electronic states. Also, nearly degenerate s and d levels can cause convergence problems. DFT calculations, with pseudopotentials, are the standard approach for computation on such compounds.

8.1 Solvation

Nature abhors a vacuum
–A dictum of Aristotelian physics

8.1.1 Perspective

Calculations on isolated molecules, unencumbered by solvent, are undoubtedly simpler conceptually, theoretically, and algorithmically, than in- solution computations (although the vacuum is not what it used to be [1]). So we ask: how realistic are vacuum (gas phase) calculations, and how important is it to take into account the embrace of solvent molecules? Serious questions about the value of calculations which ignore solvent are clearly justified in the case of biological molecules and reactions, since these entities are immersed in water. A relatively early article on molecular modelling and computer-aided drug design [2] elicited incisive critical comments: "When a process as fundamental as the absorption of one dioxygen molecule by hemoglobin involves 80 water molecules...what can we learn about docking a drug in vacuo?" gives the flavor of the critique [3]; a response to this conceded that neglecting solvation is an "apparent oversimplification", but contended that "gas-phase structures correlate surprisingly well with a number of known physiological facts" [4]. Nearly two decades later a study of the 20 natural amino acids examined in detail their calculated geometries in the gas phase and in solution (using various continuum models–see below) and concluded that "the use of gas-phase-optimized geometries can in fact be quite a reasonable alternative to the use of the more computationally intensive continuum optimizations" [5]. Examination of the literature and judicious reflection lead to the conclusion that for some purposes in vacuo (gas phase) computations are not only adequate but are the appropriate ones, while for other purposes considering solvation is essential.

If the purpose of a calculation is to probe the inherent properties of a molecule as a *thing in itself*, or of a phenomenon centered on *isolated* molecules, then we do not want the complication of solvent. For example, a theoretically oriented study of the geometry and electronic structure of a novel hydrocarbon, e.g. pyramidane [6], or of the relative importance of diatropic and paratropic ring currents [7], properly examines unencumbered molecules. On the other hand, if we wish, say, to calculate from first principles the pKa of acids in water, we must calculate the relevant free energies in (or of transfer to) *water* [8]. Noteworthy too is the fact that solvation, in contrast to gas phase treatments, is somewhat akin to molecules in bulk, in crystals [9]. Here a molecule is "solvated" by its neighbors in a lattice, although the participants have a much more limited range of motion than in solution. Rates, equilibria, and molecular conformations are all affected by solvation. Bachrach has written a concise review of the computation of solvent effects with numerous apposite references [10].

8.1.2 Ways of Treating Solvation

There are two basic ways to treat solvation computationally: explicit and implicit. *Microsolvation*, that is *explicit solvation*, places solvent molecules around the

solute molecule. *Continuum solvation*, *implicit solvation*, places the solute mole-
cule in a cavity in a continuous medium which simulates the sea of solvent
molecules. There are also *hybrid methods*: solute microsolvated and this entity
surrounded by a solvent continuum, and the "molecular integral equation theory"
method, the "three-dimensional theory of solvation" and its implementation in the
3D-reference interaction site model, 3D-RISM.

Microsolvation, Explicit Solvation   This is called explicit because computationally,
individual solvent molecules are placed around the solute molecule. "Surrounding"
the solute with solvent molecules might be putting it too strongly, because, at least
with routine quantum-mechanical calculations, few molecules of solvent are used,
typically about one to ten. In experimental reality, a solvent molecule is surrounded,
depending on its size, by a first solvation shell of about six (for a monatomic ion) to
probably hundreds or thousands of water molecules for a protein or nucleic acid
molecule. The first solvation shell is in turn solvated by what we could call a second
shell, and so on; when to cease considering the solvent molecules can be problem-
atic [11]. Actually, solvation calculations on large biomolecules in a bath of a large
number of explicit water molecules *have* been reported. These are typically done
with molecular dynamics, MD, [12a], using molecular mechanics (MM, Chap. 3)
forcefields, which is outside the scope of this book (but see an investigation of the
ability of continuum methods to handle protein-protein interactions in solution:
[12b]). Deng et al. have reported a study of the conformational behavior of alanine
dipeptide in water which was said to combine the advantages of both the explicit
and implicit approaches [12c]. MD calculations on biomolecules have been
reviewed [13a]. An MD procedure for predicting and quantifying the binding of
water molecules to *internal* sites of macromolecules [13b], and a QM/MM (quan-
tum mechanics/molecular mechanics) procedure with MD for examining reactions
in solution has been described [13c]. In our presentation of explicit solvation we
will concentrate on quantum mechanical calculations in which a few solvent
molecules are used–very literally microsolvation. Two examples of this technique
are discussed:

1. *The effect of microsolvation on the E2 and S_N2 reaction $F^- + C_2H_5F + nHF$*
   Bickelhaupt et al. used DFT to study the reaction of fluoroethane with fluoride
   ion, solvating the reactants with from zero (gas phase) to four hydrogen fluoride
   solvent molecules [14]. HF is an unusual solvent, and presumably was chosen
   rather than water because of its geometric simplicity and because it is, like water,
   protic, although an HF molecule can hydrogen bond to only one acceptor at a
   time. A virtue was made of the "artificiality" of the HF/F^- acid/base system: that
   HF is much more acidic than water and fluoride with their basis set is "artificially
   strong" was said to "lead to pronounced effects of solvation, facilitating inter-
   pretation." These authors clearly recognized that a microsolvated system of their
   type is not really a well-simulated condensed-phase system: solvent molecules
   are rationed in the former. The purpose of the computations was to obtain a
   qualitative understanding of the effect of solvent on these synthetically useful
   reactions. One deficiency of microsolvation here was that an unsolvated fluoride
   ion tended to be ejected, since with a limited number of solvent molecules

transfer of HF molecules from the attacking F^- to the forming F^- was not favored, and this raises the activation energy. In "real solvation", which might be called macrosolvation, there is an abundance of solvent molecules and all species can be adequately solvated.

Nevertheless, important features of real solvent reactions were reproduced by microsolvation. The role of ion-molecule complexes, important in the gas phase, decreased rapidly with introduction of solvent molecules, the reaction profile becoming nearly unimodal (see *Continuum Solvation*, below). Activation energies for both E2 and S_N2 processes increased due to stronger solvation of reactants than of transition states (although in this work, because of imposed geometric constraints, true transition states were not obtained); solution reactions of these kinds are known to be up to 10^{20} times slower than in the gas phase. Also, in contrast to gas-phase conditions, substitution was favored over elimination. The conclusion was that "the inclusion of a few solvent mols in the quantum mechanical treatment can significantly improve the theoretical description of some condensed-phase characteristics."

2. *Hydrolysis of CH_3Cl with 13 explicit water molecules* Yamataka and Aida used ab initio calculations to study the reaction of chloromethane (methyl chloride) with water, solvating the reactants with up to 13 water molecules [15]. With three or with 13 solvent molecules "three important stationary points" were located: two "complexes" and a transition state. These were a solvated CH_3Cl molecule (complex 1), the transition state, and solvated products (complex 2), the latter being methanol and HCl (when 3 H_2O were used) or methanol, chloride ion and H_3O^+ (when 13 H_2O were used). Note that these so-called complexes are not the same kind of species called complexes in the gas-phase reaction (see *Continuum Solvation*, below). With 13 water molecules the transition state was surrounded by all the solvent molecules with, apparently, no vacant spaces, and the reaction energetics and secondary deuterium effects were reproduced well. Compared to the two "complexes", the transition state was strongly stabilized by solvation: with 13 H_2O the relative energies were complex 1, transition state, complex 2 = 0, 24.04, -1.59 kcal mol^{-1}, i.e. 0, 101 kJ, -6.7 kJ mol^{-1}. The authors point out that the stationary points they found are probably not unique: various configurations of reacting species, starting with CH_3Cl and water and ending with CH_3CH, Cl^- and H_3O^+, may lie along the reaction pathway.

An important feature of this reaction is that a bond to the solvent is made: in forming CH_3OH a proton is transferred from the oxygen that bonds to carbon, onto a water molecule, giving H_3O^+. This is nicely reproduced with 13 H_2O, but cannot be modelled with continuum methods since these essentially adjust the electron distribution in a cavity-ensconced molecule without breaking or making bonds. The authors concluded that "apparently the 13 water system produced a reasonable picture of the hydrolysis."

Continuum Solvation (Implicit Solvation) This is called implicit because a continuous medium, a continuum, is used to "imply" the presence of individual solvent

molecules. The algorithm places the solute in a cavity in a solvent medium, and the interaction between the solute and the cavity is calculated. Using a continuum instead of individual solvent molecules is, at its best, a way of averaging out the effect of a large number of solvent molecules; indeed, if *microsolvation* (above) is used to calculate thermodynamic properties, then several calculations, best done with molecular dynamics, would be needed, followed by the calculation of a Boltzmann average. This is because there are several minimum-energy arrangements of molecules around a solute (as hinted at in [15]). Although microsolvation studies are needed if one wishes to computationally pinpoint the effect of molecules of solvent on specific processes, as in the E2/S_N2 studies above [14], continuum calculations are, by and large, the easiest and most popular way of treating solvent effects.

The key steps in current continuum solvation models are the calculation of the size and shape of the solvent cavity and of the interaction energy of the solute with the solvent. Details of these calculations have been presented in, for example, the books by Cramer [16] and Jensen [17], and in detailed journal reviews [18–20]. Here I will only outline the basic features and illustrate some applications of continuum solvation calculations. The simplest cavity for a solute molecule is a spherical, the next most complex ellipsoidal. For the great majority of molecules, which are not spherical or ellipsoidal, models based on these are quite unrealistic, and for quantitative or even much semiquantitative work such models are obsolete. Realistic continuum models place the solute molecule in a cavity designed to match its shape, although there are degrees of accuracy for defining this shape, as well as the size of the cavity. The shape and size of the cavity define the solvent-accessible surface area (SASA), a quantity needed by the method. The simplest tailored shape would be that resulting from the exposed surfaces of an overlapping spheres molecular model (Fig. 8.1); the spheres have scaled van der Waals atomic radii. However, the V-shaped crannies between some nearby overlapping spheres are inaccessible to solvent, and a more realistic measure of SASA is the surface defined by a sphere (of empirical radius for various solvents) rolling over the molecular surface. A still more sophisticated way of smoothing the overlapping-spheres surface is to project onto it a large number of small polygons or tessellations (to tessellate = to tile), called tesserae (tessera = a small fragment used in making a mosaic), as in an implementation of the conductor-like screening solvation model (COSMO, devised by Klamt and coworkers; see below) by Barone and Cossi. This version of a polarizable continuum method (PCM, see below), called CPCM (conductor PCM), made geometry optimizations in solution practical [21].

Having obtained a cavity corresponding to a realistic SASA, the energy of interaction of the solute molecule with the solvent it "sees" is calculated. This interaction energy can be conceptually divided into terms: (1) the energy needed to make the cavity in the first place; although one might say that the solute was formally absent when the cavity was being "prepared", this cavitation energy clearly depends on the solute size; (2) the energy of weak solute-solvent "dispersion" forces; (3) solvent "reorganization energy" caused by disturbing

Fig. 8.1 The surface area of a molecule from overlapping spheres and from the surface generated by a sphere rolling over the molecular surface. Like the solvent, the rolling sphere cannot reach into V-shaped cavities, so the area of the surface it defines is a more realistic measure of the solvent-accessible surface than is the overlapping-spheres surface
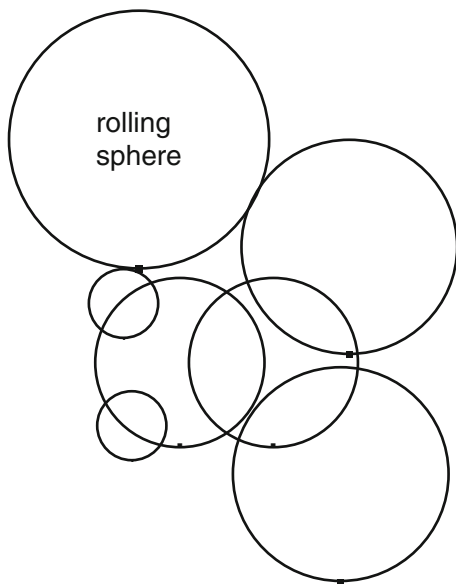
solvent-solvent dispersion forces, and (4) the electrostatic interaction energy between charges on the solute and charges on solvent molecules (in a continuum context the solute polarizes even a nonpolar medium like pentane, engendering electrostatic interactions). These divisions are somewhat arbitrary [19, 22]. Terms (1)–(3) can be subsumed into G_{CDS}, a cavitation-dispersion-solvent-reorganization free energy term that is a sum of contributions from the atoms of groups in the molecule, each contribution being the product of an effective exposed surface area A and a so-called surface tension σ, which has no particular connection with conventional surface tension, although it has the same units (energy per area or force per length) [16, 18]:

$$G_{CDS} = \sum_i A_i \sigma_i \qquad (8.1)$$

This very empirically, highly parameterized equation for nonelectrostatic terms is a characteristic of the SMx series (solvent model x ..., now up to SM12, in order of appearance) of Cramer, Truhlar and coworkers [23]. As of mid-2015, SMD may be the most widely-used of this series of methods [23b]. D stands for density, since unlike the other SM models it uses an electron density function ρ (Chap. 5, Sect. 5.5.4.5, *Atoms-in-molecules (AIM)*; Chap. 7, Sect. 7.2.1) instead of discrete

atom charges (Chap. 5, Sect. 5.5.4.2, *Charges and bond orders*) like most of the other SM methods. It gives good free energies of solvation (its use is illustrated below for the effect of solvation on tautomer stability). Amovilli and Floris have developed a method of calculating the dispersion contribution to free energy of solvation that is based on the fundamental cause of the dispersion interaction, a fluctuating electric field interacting with the electric field of another molecule (Chap. 7, Sect. 7.2.3.4.8). Their equation does not contain empirical parameters, but appears to have been tested only on He, Ne and fluoride in water [24].

The calculation of the electrostatic part of the interaction energy, the fourth term, uses as the starting point the Poisson equation, which relates electrostatic potential ϕ to charge distribution ρ and dielectric constant ε; ϕ and ρ (and possibly ε), vary from place to place, hence the position vector $\mathbf{r}$:

$$\nabla^2 \phi(\mathbf{r}) = \frac{4\pi\rho(\mathbf{r})}{\varepsilon} \tag{8.2}$$

The equation applies to a dielectric medium which responds linearly to (undergoes polarization linearly with) the charge distribution ρ. A dielectric medium is a nonconducting, that is, insulating, medium that when subjected to the field of an electric charge shifts its charge distribution slightly along the direction of the field, i.e. becomes polarized; ε is the ratio of the electrical conductivity of the medium to the conductivity of the vacuum. For a solvent it is an approximate measure of polarity (an index of which is dipole moment μ), if we constrain our domain to certain classes. For 24 solvents encompassing nonpolar (e.g. pentane, ε 1.8, μ 0.00), polar aprotic (e.g. dimethyl sulfoxide, ε 46.7, μ 3.96), and polar protic (e.g. water, ε 80, μ 1.85) dispositions, the author found that the correlation coefficient r^2 of dielectric constant with dipole moment (ε with μ) was only 0.36 (removing formic acid and water raised it to 0.75). For nine nonpolar, seven polar aprotic, and eight polar protic solvents, considered as separate classes, r^2 was 0.90, 0.87, and 0.0009 (*sic*), respectively; dielectric constants and dipole moments were taken from a table in Wikipedia, http://en.wikipedia.org/wiki/Solvent. Note that because of parameterization for other factors (e.g. Eq. 8.1), modern continuum methods do not depend only (if at all–see COSMO and COSMO-RS, below) on dielectric constant.

The key to current continuum algorithms for calculating the properties of a molecule in solution is to formulate a solution Hamiltonian operator $\hat{H}$ (Chap. 4, Sect. 4.3.4) in which these energy terms appear in addition to the *in vacuo* terms of electron kinetic energy, electron-nucleus attraction, and electron-electron repulsion. With a basis set $\{\phi_1, \phi_2, \ldots\}$ (Chap. 4, Sect. 4.3.4), a Fock matrix is constructed with elements $\langle \phi_i | \hat{H} | \phi_j \rangle$ (Dirac notation, Chap. 4, Sect. 4.4.1.2). The usual SCF procedure (Chap. 5, Sect. 5.2.3.6.2) gives a wavefunction and energy for the solvated molecule. The wavefunction can be used to calculate the usual properties, like dipole moment and spectra [25]. Particularly relevant to solute-solvent interactions is the fact that the charge distribution $\rho(\mathbf{r})$ of the solute

molecule (Eq. (8.2)) polarizes the solvent continuum of the cavity wall, which in turn alters $\rho(\mathbf{r})$, and so on. Because of the polarization of the cavity wall these methods are called *polarizable continuum methods/models*, PCM. The final interaction energy must be calculated iteratively, since the solute polarizes the solvent, which polarizes the solute, etc., so in this context the SCF procedure is called *a self-consistent reaction field*, SCRF, calculation. SCRF calculations have been implemented in ab initio, semiempirical and DFT calculations. Variations on the PCM method are IPCM, isodensity PCM, probably now obsolete, which simplified the calculation by using a vacuum isodensity charge surface [26], and CPCM, a PCM implementation of the conductor-like screening model [21, 27]. The conductor-like screening model, COSMO, introduced in 1993, simplified the calculation by using a conducting medium (ε infinite) and introducing the solvent dielectric constant only as a correction factor [28]. COSMO-RS (realistic solvation, 1995) dispensed with the dielectric constant, which Klamt and coworkers evidently distrust since the solute does not see a continuous medium. They eschew solvent-specific parameters and an explicit continuous solvent (although COSMO-RS still seems to be regarded as being in the spirit of continuum methods) and apply statistical thermodynamics to solute-solvent fragments and their surface interactions. COSMO-RS uses cavities and surface charges calculated for both solute and solvent molecules and empirical parameters, eight general ones and two for each different element, rather than specific macroscopic parameters like dielectric constant for each solvent [29a, 29b]. Thus unlike other continuum methods it does not fundamentally discriminate between solute and solvent (after all, at which concentration does solute become solvent?). A modification of COSMO-RS, direct COSMO-RS (DCOSMO-RS), unlike COSMO-RS but like the popular SMx methods above [23], gives the effect of solvation on the electron distribution in the solute molecule and thus permits calculation of wavefunction-dependent properties in the solvent, with very little loss of accuracy for solvation energy compared to COSMO-RS and SM8 [29c], and, presumably, SMD. COSMO-RS-type calculations are effective at reproducing thermodynamic and other properties of solutions, and free energies of solvation, as may be seen by examining the numerous papers from 1993 on by Klamt or Klamt and coworkers on these methods; further information is available from the company COSMOlogic and Klamt's book [30]. All these continuum methods are very fast, especially when used, as is sometimes the case (there is less justification for this now, with solution geometry optimization being often practical), with gas phase geometries followed by only single-point calculations in solvent. The COSMO-RS-type methods are thorough: they automatically use separate geometry optimizations, and even solvent-tailored sets of conformations, for the gas and the solution phases. The free energy of solvation is usually the most relevant energy quantity sought; the keywords for obtaining this depend on the program. The COSMOtherm suite of programs are made by the company COSMOlogic and are available in the program suites Turbomol, ORCA, and others (see Chap. 9).

We will look at three important processes which have been studied by implicit solvation techniques, the S_N2 reaction in solution, solvation and tautomer stability, and the calculation of pK_a:

(1) *The S_N2 reaction in solution* We saw above the application of microsolvation to S_N2 reactions [14, 15]. Let us now look at the chloride ion-chloromethane S_N2 reaction in water, as studied by a continuum method. Figure 8.2 shows a calculated reaction profile (potential energy surface) from a continuum solvent study of the S_N2 attack of chloride ion on chloromethane (methyl chloride) in water. Calculations were by the author using B3LYP/6-31+G* (plus or diffuse functions in the basis set are considered to be very important where anions are involved: Chap. 5, Sect. 5.3.3.4) with the continuum solvent method SM8 [23a] as implemented in Spartan [31] (SMD [23b] gave similar results). Some of the data for Fig. 8.2 are given in Table 8.1. Using as the reaction coordinate r the deviation from the transition state C–Cl bond length $r = r_{C-Cl} - 2.426$) makes the graph symmetrical
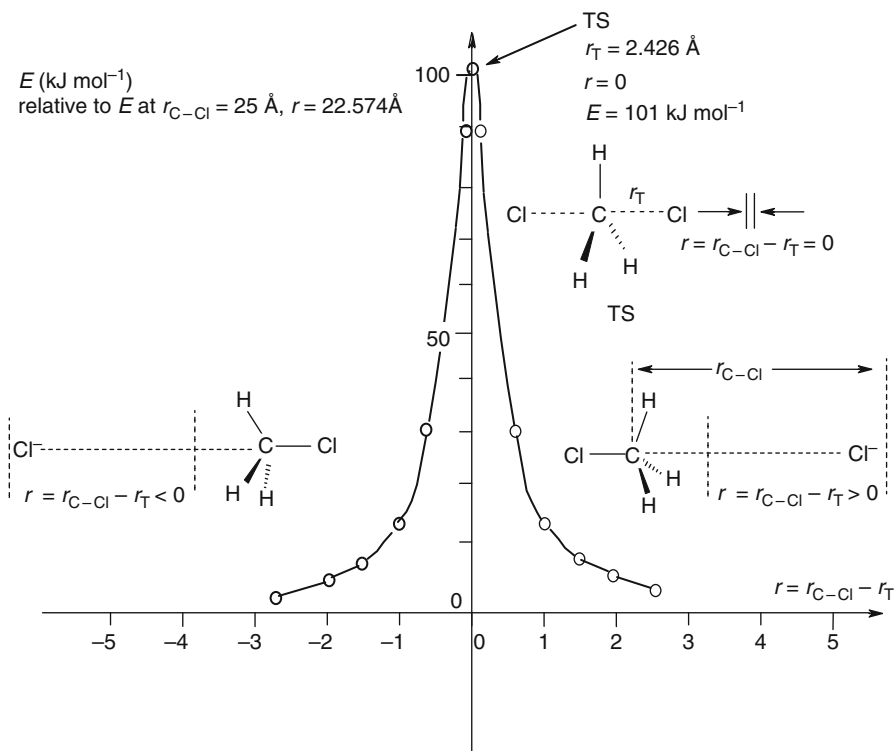
Fig. 8.2 Profile for the SN2 reaction $Cl^- + CH_3Cl$ in water. Calculations by the author using B3LYP/6-31+G* with the continuum solvent method SM8 [23a] as implemented in Spartan [31] (Note that r is the distance of the Cl$^-$from the transition state bond length (2.426 Å), not the Cl$^-$/C distance; thus r measures the "deviation" from the transition state and becomes zero at the transition state. This makes the graph symmetrical about the energy axis, as it should be presented for this identity reaction. The zero of energy is taken as $r_{C-Cl} = 25$ Å, $r = 22.574$ Å)

Table 8.1 Some of the data used to construct Fig. 8.2

r_{C-Cl}, Å	r, Å	SM8 E, Hartrees	Relative E kJ mol^{-1}
25	22.574	−960.51789	0
5	2.574	−960.51663	3.3
4	1.574	−960.51495	7.7
3	0.574	−960.50604	31.1
2.5	0.074	−960.48412	88.6
2.426, transition state	0	−960.47955	101

Variation of energy with Cl-/C distance for the SN2 reaction $Cl^- + CH_3Cl$ in water. Calculations by the author using B3LYP/6-31+G* with the continuum solvent method SM8 [23a] as implemented in Spartan [31]. The r of the x-axis in Fig. 8.2 is $r_{C-Cl} - r$(transition state) = $r_{C-Cl} - 2.426$. Hartrees were converted to kJ mol^{-1} by multiplying by 2626

about the energy axis, as it should be presented for this identity reaction. The values on the energy axis are DFT (B3LYP) energies, 0 K enthalpies, relative to a state of little Cl^-/CH_3Cl interaction ($r_{C-Cl} = 25$Å, $r = 22.574$ Å). The calculations were done as a series of constrained geometry optimizations with fixed Cl^-/C distance; the transition state (imaginary frequency $470i$ cm^{-1}; C–Cl 2.426 Å) was calculated without constraints beyond the obvious D_{3h} symmetry.

These results are in accord with the accepted mechanism for the S_N2 reaction in water: a smooth, one-step process with no intermediates [32]. This calculation agrees with a valence bond-calculated profile and activation energy (109 kJ mol^{-1} [33]), and with molecular dynamics activation energies (113 kJ mol^{-1} [34, 35]); those are free energies and the 100 kJ mol^{-1} of Fig. 8.1 is an enthalpy, but the difference is not expected to be large here (see comment after Eq. (5.173), Chap. 5). The experimental free energy of activation is 111 kJ mol^{-1} [36]. The respectable quantitative agreement with experiment for our modest computational level is gratifying, but for us the salient point is the smooth one-step profile: we now contrast this with the gas phase reaction.

Compare Fig. 8.2 with Fig. 8.3, this latter being the calculated reaction profile for the S_N2 attack of chloride ion on chloromethane in the *gas* phase; otherwise, the calculation was implemented as for the water continuum calculation of Fig. 8.2. Some of the data for Fig. 8.3 are given in Table 8.2. In the gas phase calculation, as Cl^- approached CH_3Cl the energy falls, rather than rises, until a "complex", a somewhat vague word in chemistry, sometimes indicating a weakly bound molecule, is formed, then the energy rises toward the transition state. The complex is indeed weakly bound: its energy of −39 kJ mol^{-1} compared to separated $Cl^- + CH_3Cl$ is only that of a moderately strong hydrogen bond [37], while a typical covalent bond has an energy of about 400 kJ mol^{-1}. The simplest, albeit perhaps incomplete, picture of the complex is that the chloride ion is electrostatically attracted to the partial positive charge on the carbon of chloromethane, and nicely consonant with this, in an electron density slice the contour lines show a sharp contrast between the short covalent C–Cl bond (1.856, cf. 1.803 Å in CH_3Cl) and the long (3.200 Å) "complex" bond (this author's observations). It thus seems
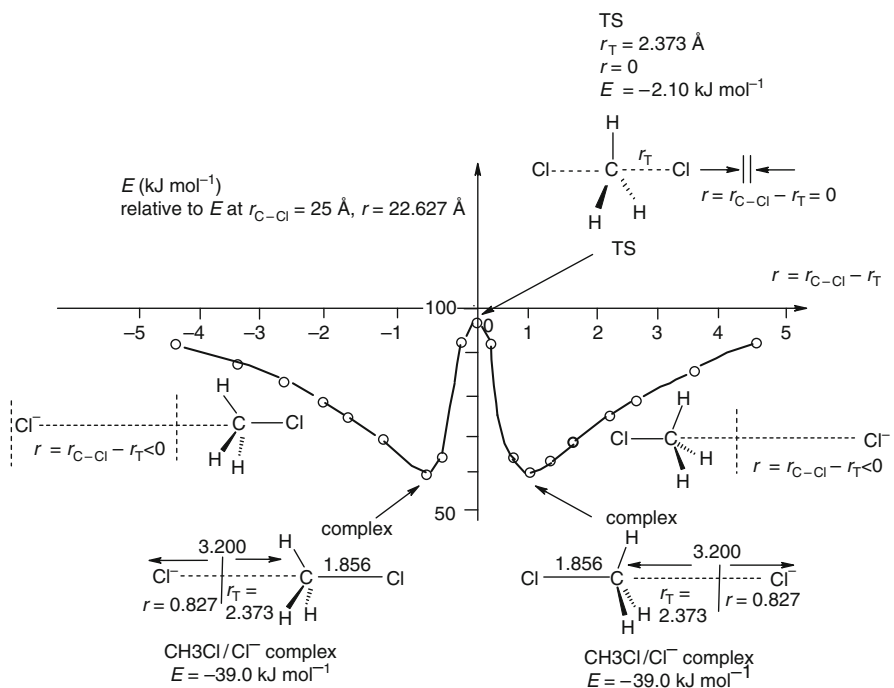
Fig. 8.3 Profile for the SN2 reaction $Cl^- + CH_3Cl$ in the gas phase. Calculations by the author using B3LYP/6-31+G* in the gas phase, with Spartan [31]. Note that r is the distance of the Cl^- from the transition state bond length (2.373 Å), not the Cl^-/C distance; thus r measures the "deviation" from the transition state and becomes zero at the transition state. This makes the graph symmetrical about the energy axis, as it should be presented for this identity reaction. The zero of energy is taken as $r_{C-Cl} = 25$ Å, $r = 22.627$ Å. Note the two complexes, which are absent from the water phase calculation of Fig. 8.2

Table 8.2 Some of the data used to construct Fig. 8.3

r_{C-Cl}, Å	r, Å	Gas phase E, Hartrees	Relative E kJ mol^{-1}
25	22.627	−960.38646	0
5	2.627	−960.394	−19.8
4	1.627	−960.39801	−30.3
3	0.627	−960.40063	−37.2
2.5	0.127	−960.38983	−8.85
2.373 transition state	0	−960.38726	−2.1

Variation of energy with Cl−/C distance for the SN2 reaction $Cl^- + CH_3Cl$ in the gas phase. Calculations by the author using B3LYP/6-31+G* in the gas phase, and Spartan [31]. The r of the x-axis in Fig. 8.2 is $r_{C-Cl} - r$(transition state) $= r_{C-Cl} - 2.373$. Hartrees were converted to kJ mol^{-1} by multiplying by 2626

to be an ion-dipole complex. The transition state and the complex were calculated without constraints (beyond D_{3h} symmetry for the transition state). The negative activation energy is not paradoxical, as the proximate reactant for its formation is the complex, making the barrier from this $-2.1-(-39.0)$ kJ mol$^{-1} = 36.9$ kJ mol^{-1}.

These results are in accord with the long-accepted mechanism for the S_N2 reaction in the gas phase: experiments using ion cyclotron resonance were interpreted in the way shown for the calculations of Fig. 8.3: "It is not possible to explain the observed rates on the basis of a single-well potential" [38]; the profile in Fig. 8.3 is called a *double-well potential*. Quantitative information comes from benchmark calculations by Bento et al., who even checked for relativistic effects, which were found to be negligible [39]. CCSD(T)/aug-cc-PVQZ (Chap. 5, Sects. 5.4.3 and 5.3.3.6) gave relative energies of −44 and +10.5 kJ mol^{-1}, compared to −39 and −2.1 kJ mol^{-1} at out modest computational level. That the transition state lies slightly below zero in one case and a little above in the other is of no particular significance; see Bachrach's discussion of the gas and solution phase S_N2 reaction and in particular his Tables 6.1 and 6.2 [40]. The formation of the ion-dipole complex in the gas phase but not in solution reflects the fact that in the absence of solvent the attacking anion "solvates" the carbon of its victim prior to covalent bonding.

(2) *Solvation and tautomer stability* The pyridones show a structural ambiguity related to that of the DNA bases cytosine and thymine, which is perhaps the reason considerable attention has been paid to the pyridone-hydroxypyridine tautomerism [41a–e] (for some benchmark calculations on keto-enol tautomers see McCann et al. [41f]):

2-pyridone   2-hydroxypyridine   4-pyridone   4-hydroxypyridine
keto form   enol form   keto form   enol form
                   (OH H *syn* to N)
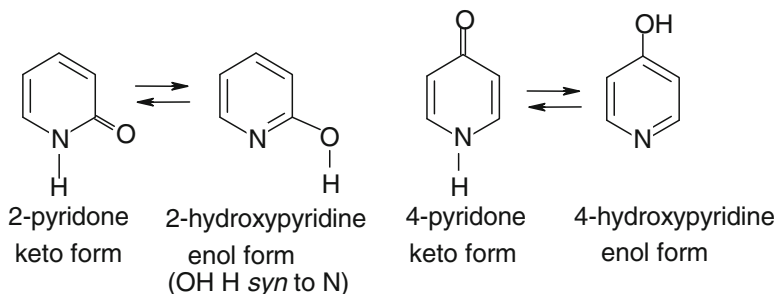
Let's check against experiment calculations on these in the gas phase, and in water using the continuum model SMD [23b] (D for "the full solute density"), an extension of the SM8 model [23a] that was used above for the S_N2 reaction. The result of free energy (298 K) calculations by the author are compared with experiment [41a] below. These calculations used free energies from optimization and frequency calculations in the gas phase and in solution, not "merely" free energies of solvation (see below) on gas phase geometries. For simplicity only the *syn* conformer of 2-hydroxypyridine is considered here. The *anti* conformer, related to the *syn* by rotation about the C–O bond, was calculated to be the higher in free energy by 22.7 and 5.7 kJ mol^{-1} in gas and water, respectively, using M06-2X/6-31G* (Chap. 7, Sects. 7.2.3.4 and 7.3), and the higher by 19.7 and 3.4 kJ mol^{-1} in gas and water, respectively, using G4MP2 (Chap. 5, Sect. 5.5.2.3.2). For an equilibrium of *syn-anti* only this would translate to these percentages of *syn* conformer in the mixture: M06-2X/6-31G* gas 99.99, water 91; G4MP2 gas 99.96, water 80.

Here are the percentages of keto and enol from calculation, and deduced from reported experiments [41a]; the values "gas 4.2", etc. are free energy (298 K) differences in kJ mol^{-1}, keto - enol, computed by the two methods:

	gas 4.2		gas 17.2	
	water −11.1		water −4.6	
	2-keto	2-enol	4-keto	4-enol
M06-2X/6-31G* gas	16	84	0.1	99.9
M06-2X/6-31G* water	99	1	86	14

	gas 4.4		gas 15.2	
	water −12.3		water −7.6	
G4MP2 gas	14	86	0.2	99.8
G4MP2 water	99.3	0.7	95	5

Experiment gas	*ca.* 30	*ca.* 70	<10	>90
Experiment water	>99	<1	>99	<1

The imprecision in the experimental percentages suggests that the calculated values, particularly for the gas phase G4MP2, may be more reliable than those reported for experiment. The only significant differences between the two calculational levels are for the 4-keto/enol species in water, where M06-2X/6-31G* gives percentages 86/14 and G4MP2 gives 95/5. The calculations match experiment qualitatively and as far as quantitative comparison is possible: calculation and experiment agree that on going from the gas phase to water the percentage of keto tautomer goes from minor or even tiny to overwhelming. This accords with the expectation that a polar solvent should favor the equilibrium concentration of the more polar tautomer; in all cases the keto form has a much higher calculated dipole moment than the corresponding enol:

Calculated dipole moments (Debyes)

	2-keto	2-enol
M06-2X/6-31G* gas	4.17	1.25
M06-2X/6-31G* water	6.55	1.84
G4MP2 gas	4.76	1.53
G4MP2 water	7.57	2.27

	4-keto	4-enol
M06-2X/6-31G* gas	6.69	2.73
M06-2X/6-31G* water	10.59	3.83
G4MP2 gas	7.38	2.62
G4MP2 water	11.96	3.84

The pyridone-hydroxypyridine calculations above used optimization/frequency calculations for both the gas phase and for solution. Actually, continuum solvation methods are frequently used in a much less demanding way to calculate not standard thermodynamic free energies from frequencies on geometries optimized at the same level, but rather just the *change* in free energy on going from the gas phase to solution, the "solvation energy", i.e. the free energy of solvation. This is normally defined as G(solution) – G(gas phase). For polar or somewhat polar solutes in water this is negative, since such solutes are stabilized by polar solvation (Table 6 in [23c]). Illustrating such a "light" calculation for the keto/enol tautomers of 2-pyridone: using AM1 geometries, which except for very big molecules are trivially fast to calculate (Chap. 6, Sect. 6.2.5.5), single point (i.e. no geometry optimization) energies were obtained with M06-2X/6-31G* for the gas phase and in water, the latter using SCRF with SMD. The results were:

keto, gas −323.3740364, keto water −323.3909294; enol, gas −323.3756876, enol, water −323.3863704. From this we get:

$$\text{solvation}\,\Delta G(\text{keto}) = -323.3909294 - (-323.3740364)$$

$$= -0.016893,\ -44.4\ \text{kJ}\,\text{mol}^{-1}$$

$$\text{solvation}\,\Delta G(\text{enol}) = -323.3863704 - (-323.3756876)$$

$$= -0.0106828,\ -28.0\ \text{kJ}\,\text{mol}^{-1}$$

So according to these solvation energy results the keto tautomer is stabilized more than the enol one by $44.4 - 28.0 = 16.4\ \text{kJ}\,\text{mol}^{-1}$. The data above for the effect of solvation on the keto/enol composition, obtained by full optimization/frequency calculations, gave the keto - enol free energy difference as 4.4 (gas) and -11.1 (water) $\text{kJ}\,\text{mol}^{-1}$, a net solvent lowering of 15.5 $\text{kJ}\,\text{mol}^{-1}$ in favor of the keto; this compares well with the shift of 16.4 kJ mol^{-1} from the simple solvation energy calculations. If we have a good free energy difference for the gas phase (e.g. 4.4 $\text{kJ}\,\text{mol}^{-1}$) from optimization/frequency, this can be combined with the solvation energy to provide the solution free energy difference (e.g. $-11.1\ \text{kJ}\,\text{mol}^{-1}$) thus allowing calculation of the composition in solution without a possibly lengthy optimization/frequency. On a 2003 vintage machine full and single point SMD calculations on 4-nitroaniline took 488 and 26 s, a factor of 19 in favor of the single point. However, the SMx continuum methods are so fast that such "full" solvation calculations are practical on moderate-size molecules. Nevertheless, in the third important process described here (below) which has been studied by implicit solvation techniques, the calculation of pK_a, not only are solvation free energies used, but the *experimental* aqueous solvation energy (and experimental gas phase free energy) of the proton is resorted to: the proton, a naked nucleus, is computationally intractable toward continuum methods.

(3) *First principles calculation of pK_a* First, we should realize that the straightforward-seeming method of calculating the pK_a of an acid in water by simply using optimization/frequencies and routine statistical thermodynamics to

get the standard free energies of acid, conjugate base and proton in solution is not yet possible: as hinted above the naked proton does not cooperate with current continuum (implicit solvation) methods. Explicit solvation, too, presents problems arising from the numbers and placement of water molecules; advances in molecular dynamics may eventually solve this.

Nevertheless, thermodynamics seems to assure us that the pK_a of an acid is simply related to the Gibbs free energies of the hydrated (we will limit ourselves to water here) acid, conjugate base and proton. Surprisingly, in a study of 64 organic and inorganic acids (accompanied by a brief review of theoretical methods of calculating pK_a), Klamt et al. concluded that "the experimental pK_a scale depends differently on the free energy of dissociation than generally assumed" and "[passed] the problem forward to the scientific community" [42a]. Kelly et al. attempted to respond to this challenge, and claimed that adding one water molecule to some anions and also using the SM6 model "significantly improves the agreement between the calculated pKa value and experiment" [43]. However, the mixed microsolvation/continuum approach used there may not be uniform enough to provide a satisfying method for the general theoretical calculation of pK_a.

COSMO models [28–30] were compared with the SM approach [23] by Klamt [42b] and by Cramer and Truhlar [44]. A 2010 paper by Klamt and coworkers [45] shows that improved calculated pKa values are obtained for the limited domain of strong to moderately weak acids by a "cluster-continuum" method in which the acid and conjugate base are each associated with one or a few solvent molecules and this "cluster" is then continuum-calculated with COSMO-RS. The authors point out, however, that for the calculation of pK_a "a consistent and generally applicable method is still lacking". This paper clarifies the problem raised in [42a]. The matter is under study.[1]

I cite three papers to show that standard continuum calculations *can* give satisfactory almost-first-principles pK_a values: Shields and coworkers used a thermodynamic cycle with gas phase and continuum calculations to obtain satisfactory results for six simple carboxylic acids [46]. These were "absolute" calculations in the sense that no acid was used as a reference point, although the experimental gas phase free energy and aqueous solvation energy of the proton were resorted to. It is the problem of accurately calculating ab initio the solvation energy of the proton that makes purely ab initio calculations of pK_a problematic. Not quite as esthetically satisfying perhaps, were "relative" calculations in which acetic acid was used as a reference compound [47]. Similar to the absolute acid calculations was work with phenols that was said to be "among the most accurate of any such calculations for any group of compounds" [48]. Note that although the term "first principles" helped entitle this subsection, and [46–48] describe the showcase methods as "absolute", in the thermodynamic cycles both the CBS methods used for gas-phase energies and the continuum solution calculations contain empirical terms– in fact, these

---

[1] A. Klamt, personal communication, 2010 March 13.

$$\Delta G_s(RCOO^-) + \Delta G_s(H^+)$$

RCOO$^-$ g + H$^+$ g $\longrightarrow$ RCOO^-_s + H^+_s

from gas phase calcs

ΔG_{high}

$\Delta G_{diss,\,s}$ wanted

RCOOH$_g$ $\longleftarrow$ RCOOH$_s$

$-\Delta G_s(RCOOH)$
free E of solvation of RFCOOH
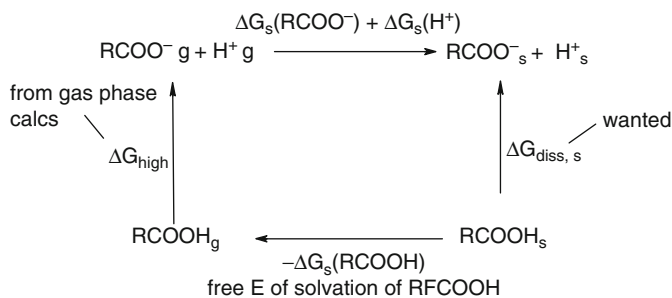
Fig. 8.4 The principle behind the absolute method of calculating pKa. In this thermodynamic cycle we want ΔG for dissociation of RCOOH in water (g denotes gas phase and s solvent phase, water; we refer to standard temperature and pressure free energy differences). The other terms are: (1) $-\Delta G_s(RCOOH)$, the negative of the solvation free energy of RCOOH (the solvation free energy itself is negative); we take ΔG of solvation as the free energy that one must put in (a negative quantity) to solvate a species, so going from solution to gas requires input of $-\Delta G$ (a positive quantity). This quantity is calculated by a continuum method. (2) ΔG_{high}, the gas-phase ionization free energy of RCOOH, calculated by a high-level multistep method. (3) $\Delta G_s(RCOO^-)$ $+\Delta G_s(H^+)$, the free energy of solvation of the anion plus the free energy of solvation of the proton. The first term is calculated by a continuum method method and the second is an experimental value. For conservation of energy: $\Delta G_{diss,s} = -\Delta G_s(RCOOH) + \Delta G_{high} + \Delta G_s(RCOOH) + \Delta G_s(H^+)$

continuum methods are heavily parameterized. So these calculations are not strictly purely theoretical.

The principles behind the "absolute" pK_a calculations in [46] are illustrated with the aid of Fig. 8.4. The program they used was Gaussian 98 [49], and several ab initio levels and solvation methods were explored; the favored ones are given here, with values for acetic acid, CH_3COOH:

Term (1) calculated at the HF/6-31+G* level with the CPCM continuous solvation method was 32.3 kJ mol^{-1}, i.e. the solvation free energy of CH_3COOH was -7.72 kcal mol^{-1} or -32.3 kJ mol^{-1}. Note that the calculated solvation free energies, terms (1) and (3), are free energy *differences*, gas to solvent, estimated by the program, and do not require possibly time-consuming frequency calculations as is the case for statistical mechanical calculation of free energies; this was discussed above in connection with pyridone keto-enol tautomerism.

Term (2) calculated by the high-accuracy multistep CBS-APNO method (Chap. 5, Sect. 5.5.2.3.2) was 341.2 kcal mol^{-1} or 1426 kJ mol^{-1}. The Sackur-Tetrode equation for the gas-phase entropy of the proton was mentioned in this regard, but in fact the algorithm automatically handles this.

Term (3), calculated as for term (1) was -77.58 kcal mol^{-1} or -324.6 kJ mol^{-1}.

Term (4), the solvation free energy of the proton was taken from experiment as -264.61 kcal mol^{-1} or -1107 kJ mol^{-1}.

The free energy of dissociation in water follows (Fig. 8.4):

$$\Delta G_{\mathrm{diss,s}} = -\Delta G_{\mathrm{s}}(\mathrm{RCOOH}) + \Delta G_{\mathrm{high}} + \Delta G_{\mathrm{s}}(\mathrm{RCOOH}) + \Delta G_{\mathrm{s}}(\mathrm{H}^+)$$
$$= -(-32.3) + 1426 - 324.6 - 1107\,\mathrm{kJ\,mol}^{-1} = 26.70\,\mathrm{kJ\,mol}^{-1}.$$

From the usual relation of free energy to $\ln K_{\mathrm{eq}}$ and the definition of pK_{a}, with RT at 298 K = 2.478 kJ mol^{-1} and $\ln 10 = 2.303$ we get $pK_{\mathrm{a}} = 26.70/2.303RT = 4.68$. The experimental value for acetic acid was reported [46] to be 4.75, for an error of only -0.07 pK_{a} unit.

As Liptak and Shields point out, accurate values of gas phase deprotonation and solvation energies are needed for reasonably accurate pK_{a} values. An error of 1 pK_{a} unit results from an error in ΔG of 1.36 kcal mol^{-1} or 5.7 kJ mol^{-1}, and an error of 0.5 pK_{a} unit corresponds to an error in ΔG of only 2.9 kJ mol^{-1}. For some purposes such an energy-difference error would be considered small, 1 kcal mol^{-1} or 4 kJ mol^{-1} being a current standard of "chemical accuracy" [50]. High-accuracy multistep methods (Chap. 5, Sect. 5.5.2.3.2) other than the computationally very demanding CBS-APNO gave reasonable pK_{a} values; when more than one conformation (albeit in the gas phase) was significant, conformationally averaged energies were used. The choice of solvation method, and even the version of a particular method, is important. Using HF/6-31 + G* and another version of the CPCM method, calculations for this book gave solvation free energies for CH_3COOH and CH_3COO^- of -32.9 and -316.1 kJ mol^{-1} respectively (cf. -32.3 and -324.6 kJ mol^{-1} in [46]). These values yield $\Delta G_{\mathrm{diss,s}} = 35.8\,\mathrm{kJ\,mol}^{-1}$ and $pKa = 6.3$. With SM8 the values were -21.16 and -325.5 kJ mol^{-1}, giving $\Delta G_{\mathrm{diss,s}} = 14.7\,\mathrm{kJ\,mol}^{-1}$ and $pK_{\mathrm{a}} = 2.6$. This shows that even with the choice of a generally good solvation method, one should check out the procedure with some compounds of known pK_{a}.

An accurate *gas-phase* dissociation energy is important too. The very accurate CBS-APNO method can seldom be used, being limited to about seven heavy atoms (atoms other than H or He; Chap. 5, Table 5.10) and being unable to handle other than C, H, N, O, F. The much less size-challenged CBS-4 M is insufficiently accurate for meaningful pK_{a} calculations, but CBS-QB3 and G3(MP2) are useful for up to about 13–16 heavy atoms (Chap. 5, Table 5.10 and [46]). For large molecules isodesmic-type reactions (Chap. 5, Sect. 5.5.3.1) may be useful. Consider Fig. 8.5; here is an example, where RCOOH is CFH_2COOH. Since this has only 5 heavy atoms we can use a direct calculation of $\Delta G_{\mathrm{high,1}}$ with CBS-APNO as a check on the accuracy of the roundabout isodesmic method. CH_2FCOOH has 2 conformations of very similar (gas-phase) energy. The "low-level" method chosen for the isodesmic reaction was the DFT (Chap. 7) B3PW91/6-31G(d,f), because in related work a number of perflurorinated acids, with up to 31 heavy atoms, had being studied at this level. The relevant quantities (cf. Fig. 8.5) are:

Term (1) is the gas-phase isodesmically calculated deprotonation free energy of the "big" acid CH_2FCOOH; it is to be calculated from terms (2) and (3).

$$RCOO^- \; + \; H^+ \; + \; CH_3COO^-$$
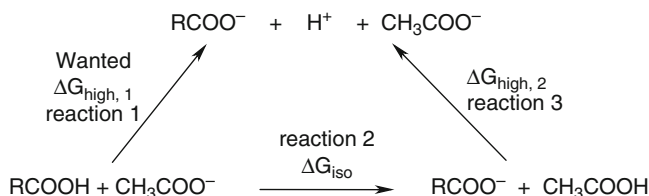
Fig. 8.5 The principle behind the using isodesmic reaction for calculating an accurate deprotonation free energy for an acid too big to yield directly to a high-accuracy calculation. Note that reaction 1 is really only for deprotonation of RCOOH and reaction 3 is only for deprotonation of CH$_3$COOH; the anion on the starting side of those reactions was added only for logical consistency, and cancels. (1) $\Delta G_{high,1}$ is the wanted quantity, the free energy of deprotonation of the large acid RCOOH, but cannot be calculated directly. (2) ΔG_{iso} is the free energy of the isodesmic reaction and can be calculated fairly accurately. (3) $\Delta G_{high,2}$ is the free energy of deprotonation of CH3COOH and can be calculated accurately directly (any appropriate reference acid could be used here, and an experimental free energy could be used if available). For conservation of energy: $\Delta G_{high,1} = \Delta G_{iso} + \Delta G_{high,2}$

Term (2) is the gas-phase isodesmic free energy for proton transfer from RCOOH to the conjugate base CH$_3$COO$^-$ of our reference acid. At the B3PW91/6-31G(d,f) level this is $[-327.598929 \; -228.969707] - [-328.158016 \; -228.394842] = -0.015778$ hartrees $= -41.43$ kJ mol^{-1}

Term (3) is the gas-phase free energy of deprotonation of the reference acid CH$_3$COOH; this can be calculated accurately with the high-level CBS-APNO, giving $= [-228.500394 - 0.010000] - [-229.053416] = 0.543022$ hartees $= 1425.7 = $ kJ mol^{-1}.

The gas-phase isodesmically calculated deprotonation free energy of CH$_2$FCOOH follows (Fig. 8.4):

$$\Delta G_{high,1} = \Delta G_{iso} + \Delta G_{high,2}$$
$$= -41.4 + 1425.7\, \text{kJ mol}^{-1} = 1384.3 \text{ kJ mol}^{-1}.$$

Compare this with a direct CBS-APNO calculation on CH$_2$FCOOH:

$$\Delta G_{high,1}(\text{APNO}) = [-327.754836 - 0.010000] - [-328.290375]$$
$$= 0.525539 \text{ hartrees} = 1379.8 \text{ kJ mol}^{-1}$$

The isodesmically secured energy is 4.5 kJ mol^{-1} higher than the direct APNO value. The NIST website gives $1385 - 1387$ kJ mol^{-1} for the free energy of deprotonation, with an estimated error of 8.4 kJ mol^{-1} [51]. If we take the deprotonation energy of CH$_2$FCOOH to be actually in the range 1380–1387, the isodesmic calculation works well. But note that an error of 1 pK_a unit results from a free energy error of only 5.7 kJ mol^{-1}, and an error of 0.5 pK_a units from an error of only 2.9 kJ mol^{-1}. We are working at the edge of fairly accurate pK_a values.

Hybrid Solvation: Implicit Solvation Plus Explicit Solvation; Microsolvation Subjected to the Continuum Method Here the solute molecule is associated with explicit solvent molecules, usually no more than a few and sometimes as few as one, and with its bound (usually hydrogen-bonded) solvent molecule(s) is subjected to a continuum calculation. Such *hybrid* calculations have been used in attempts to improve values of solvation free energies in connection with pK_a: [43], and also [45] and references therein. Other examples of the use of hybrid solvation are the hydration of the environmentally important hydroxyl radical [52] and of the ubiquitous alkali metal and halide ions [53]. Hybrid solvation has been reviewed [43, 54].

If one is investigating a reaction with the intimate participation of solvent molecules, then in principle they should be explicitly considered, as in the study of the hydrolysis of CH_3Cl with explicit water molecules (*Hydrolysis of CH_3Cl with 13 explicit water molecules*, above), for here at least one water molecule is a reactant, not a mere enfolding medium. The implicit + continuum approach may be useful if one seeks not only insight into a mechanism, as in *The effect of microsolvation on the E2 and S_N2 reaction $F^- + C_2H_5F + nHF$*, above, but also wants relative energies in solution of various species involved. An attempt to do this would place the reactants (probably representing a stationary point), e.g. [F^-/C_2H_5F/explicit solvent] in a continuum cavity to obtain a free energy of solvation.

Molecular Integral Equation Theory, the Three-Dimensional Theory of Solvation and Its Implementation in the 3D-Reference Interaction Site Model, 3D-RISM Here the explicit solvent model is made more manageable by working with solvent distributions, not individual molecules, and first-principles statistical mechanics are applied [55]. This approach uses molecular dynamics, usually with the aid of molecular mechanics, and is presumably limited by the accuracy of the forcefield (Chap. 3). The method appears to be relatively little-used at present, but may become competitive with SMx and COSMO-RS as its speed and accuracy improve.

8.2 Singlet Diradicals

For "Is" and "Is-not" though with Rule and Line,
And "Up-and-down" by Logic, I define,...
Ah, but my Computations, People say,...
– The Rubaiyat of Omar Khayyam, ca. 1100; translated by Edward Fitzgerald, 1859; Stanzas 56 and 57.

8.2.1 Perspective

The electrons in molecules, usually designated alpha and beta, but drawn as up and down arrows in energy level diagrams and occasionally verbally bestowed with those directional terms, are commonly neatly paired in orbitals and subject to tolerably good computations by what Pople called a model chemistry [56]. This is a sharply-defined procedure that, once settled upon, does not require judgement to execute and will not vary from one worker to another. Examples are a HF/6-31G* geometry optimization or a B3LYP/6-31+G** single-point calculation on a specified molecule. Almost all the molecular mechanics, ab initio, semiempirical and DFT calculations discussed in this book have used model chemistries. In contrast to these, some calculations demand judgement regarding the choice of which set of orbitals and electrons is or is not to be considered. The most important class of such calculations is on singlet diradicals (also called biradicals). Other open shell species, like carbenes and excited states, and some transition metal compounds, can present related problems.

A singlet diradical is a molecule with an even number of electrons in which all but two are nicely paired in orbitals in the familiar manner; the "last" two electrons are to some extent (perhaps essentially fully) decoupled by spatial separation from each other in a molecular orbital that allows them to reside largely in different regions of the molecule. These two electrons are, like the other pairs, of opposite spin, giving the spectroscopic state of a singlet (Fig. 8.6). The molecular orbital with these decoupled electrons tends to resemble two atomic orbitals (Figs. 8.10 and 8.12), and indeed these molecules have chemical radical character, and are considered open-shell species. Simple examples of singlet diradicals are singlet $\cdot CH_2–CH_2–CH_2\cdot$ (1,3-propanediyl, the trimethylene diradical) and the transition state for rotation around the CC double bond of ethene, in which the π-bond has been broken by twisting through 90°. Note that if the two electrons responsible for diradical character had the *same* spin, they could not reside in the same orbital

Fig. 8.6 A singlet diradical. Two electrons (often the highest-energy ones) are largely unpaired although of opposite spin

Two orbitals of the same or slightly different energy
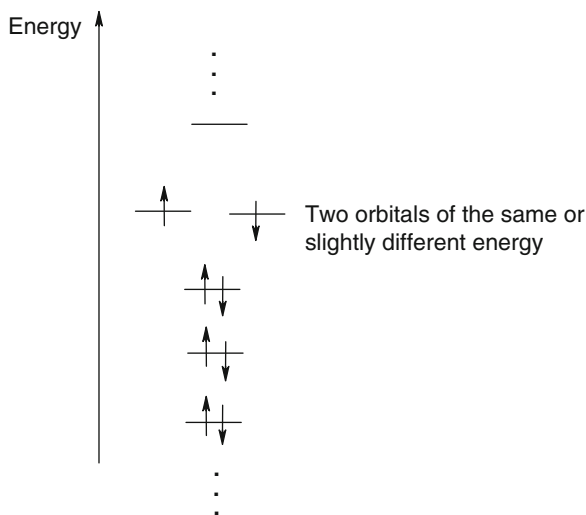
(Pauli exclusion principle), and the molecule would be a triplet. Routine quantum calculations–model chemistries–do not as a rule work with singlet diradicals. The reasons for this, and the techniques that are used on such molecules, are discussed below.

8.2.2 Problems with Singlet Diradicals and Model Chemistries

Let us first do a reality check: we'll test the ability of some model chemistry methods to perform geometry optimizations on singlet 1,3-propanediyl or trimethylene (CH_2–CH_2–CH_2) and on singlet 1,4-butanediyl or tetramethylene ($\dot{C}H_2CH_2CH_2CH_2\dot{}$), simple singlet diradicals.

1,3-Propanediyl, Trimethylene Four different starting geometries were used (Fig. 8.7), with symmetry C_1, C_2, C_s, and C_{2v}, and each of them was submitted to a geometry optimization/frequency calculation by the HF, the MP2, and the B3LYP method (see Chaps. 5 and 7 for these ab initio methods and this DFT method), for twelve calculations in all. The results are summarized in Table 8.3: all but one optimization, that starting with the C_{2v} structure, led to closing of the diradical to give cyclopropane. The C_{2v} starting structure gave a stationary point resembling the starting structure, an open-chain species. At the HF/6-31G* level this was a hilltop with a principal imaginary frequency of $668i$ and a secondary one of $74i$ cm^{-1},
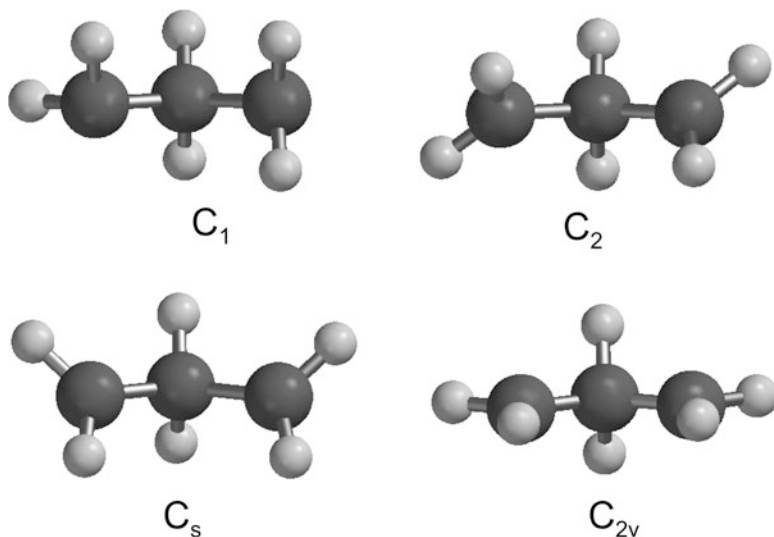
Fig. 8.7 The input structures for attempted model chemistry optimizations on 1,3-propanediyl ($\dot{C}H_2CH_2CH_2\dot{}$). All bond lengths and angles in these structures were standard, e.g. C–C ca. 1.5 Å, C–H ca. 1.1 Å, bond angles ca. 110°

Table 8.3 Results of attempted geometry optimization of the ·CH2CH2CH2· singlet diradical by different model chemistries; the 6-31G* basis was used in all cases

Symmetry of input structure	HF	MP2	B3LYP
C_1	Cyclopropane	Cyclopropane	Cyclopropane
C_2	Cyclopropane	Cyclopropane	Cyclopropane
C_s	Cyclopropane	Cyclopropane	Cyclopropane
C_{2v}	π-cyclopropane?	π-cyclopropane?	π-cyclopropane?

See Fig. 8.7 for the input structures and text for clarification
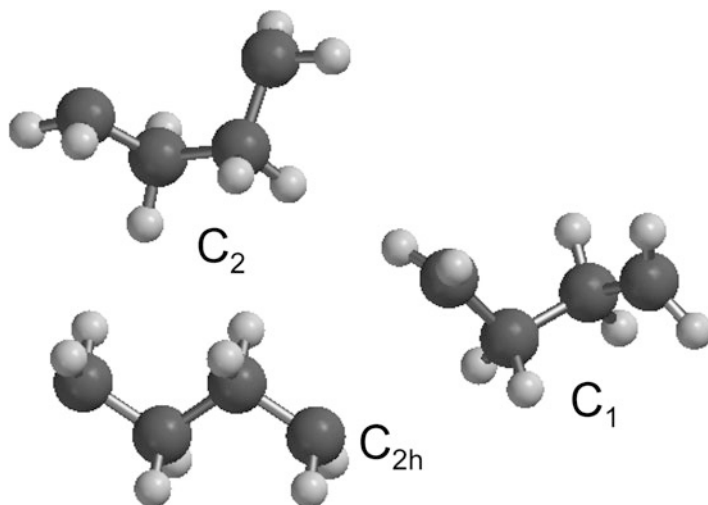
Fig. 8.8 The input structures for attempted model chemistry optimizations on 1,4-butanediyl (·CH2CH2CH2CH2·). All bond lengths and angles in these structures were standard, e.g. C–C ca. 1.5 Å, C–H ca. 1.1 Å, bond angles ca. 110°–120°

while at the MP2/6-31G* and the B3LYP/6-31G* levels it was a transition state (imaginary frequencies191i and 453i, respectively). When MP2 transition state was slightly distorted along the imaginary mode (the reaction mode; by visualizing the vibration, replacing a central CH_2 H by F and subjecting this now- C_s structure to just two optimization steps, then restoring the hydrogen and optimizing fully) a C_s potential energy relative minimum (no imaginary frequencies) was obtained, i.e. a real molecule (caveat: at this level). At the HF and B3LYP levels the C_{2v} structure, altered to Cs and optimized, each gave a transition state with a central hydrogen seeking to migrate to an end carbon. To summarize: the HF calculations led to a hilltop and a transition state, the MP2 calculations to a transition state and a relative minimum, and the B3LYP calculations to two transition states. We see below that many more stationary points resembling 1,3-propanediyl can be found by appropriate methods.

1,4-Butanediyl, Tetramethylene Three different starting geometries were used (Fig. 8.8), with symmetry C_2, C_{2h}, and C_1, and each was submitted to a geometry optimization/frequency calculation by the HF, the MP2, and the B3LYP method.

In all cases the U-shaped C_2 input geometry closed to a cyclobutane molecule and the zigzag C_{2h} geometries dissociated to two ethene molecules. We see below that many stationary points resembling 1,4-butanediyl can be found by appropriate methods.

8.2.3 Singlet Diradicals, Beyond Model Chemistries

1. **1,3-propanediyl and 1,4-butanediyl, from the literature**
2. **Complete active space calculations (CAS)**
3. **Broken symmetry calculations**

(1) *1,3-propanediyl and 1,4-butanediyl, from the literature*. We now look at results of calculations on the 1,3- and 1,4-diradicals by methods more appropriate than the model chemistries just employed.

1,3-Propanediyl, Trimethylene Using general valence bond (GVB) calculations, Getty and coworkers found eight stationary points with trimethylene-like structures [57]. The GVB method is somewhat related to the complete active space method, discussed below, in that as in a CAS calculation electrons are promoted from occupied to virtual orbitals in a limited form of configuration interaction. The emphasis on the promotion of electrons from orbitals that can be identified with bonds into their antibonding counterparts makes this a valence bond method (Chap. 4, Sect. 4.3.1). Looking back at our model chemistry calculations on trimethylene, above, let's focus on the MP2 calculations as the most reliable: in a general sense correlated ab initio calculations are more reliable than those at the HF level and arguably more reliable than DFT–granting that MP2 is not really a very high level [58]. The MP2 calculations could be construed as giving a C_{2v} 1,3-diradical transition state and a C_s 1,3-diradical relative minimum, but the proximity of the end carbons in these species, 2.663 Å and 2.654 Å, does not quite dispel the possibility that we are dealing with an unusual closed-shell molecule, a kind of cyclopropane with a very long CC bond. Indeed, a reaction of cyclopropane, stereomutation, has been the main impetus for the study of singlet 1,3-propanediyl [59]. Stereomutation is the interconversion of *cis* and *trans* 1,2-substituted cyclopropanes (for the parent compound deuterium is used as a stereochemical marker), and in principle can occur by ring opening to a diradical and rotation about a C–C bond. For a detailed experimental investigation, see Berson et al. [60]. Among the eight species revealed by the exhaustive GVB search of the 1,3-propanediyl potential energy surface by Getty et al. were a C_{2v} hilltop (two imaginary frequencies) and two C_s species, one a relative minimum and one a transition state [57]. These three are *π-cyclopropane structures* and resemble our MP2 species. The term π-cyclopropane appears to have been coined by Crawford and Mishra [61] to denote a trimethylene in which the atomic p orbitals can, hypothetically at least, form a pure π -type CC single bond:
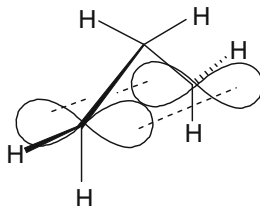
A π-cyclopropane with the end methylene groups coplanar, as shown here, is (0,0)-trimethylene; specifying the twist dihedral allows designation of the other conformers, e.g (0,90)-trimethylene in which the putative π bond is completely broken [57]. The model chemistries, then, each led to two trimethylene stationary points: HF to a hilltop and a transition state, MP2 to a transition state and a relative minimum, and B3LYP to two transition states.

1,4-Butanediyl, Tetramethylene Using complete active space (CAS) calculations (below), Doubleday found ten stationary points with tetramethylene-like structures, in work connected with ring-opening of cyclobutane [62]. We saw that model chemistries simply lead to closure or dissociation of input tetramethylene-type structures.

(2) *Complete active space calculations (CAS)*. The plethora of stationary points found by the GVB (for 1,3-propanediyl) and CAS (for 1,4-butanediyl) methods cannot be rivalled by ordinary model chemistry methods. We now look at complete active space (CAS) methods, which are the standard techniques for treating singlet diradicals; CAS was briefly mentioned in Chap. 5, Sect. 5.4.3, as a type of multiconfiguration CI (MCSCF) calculation. In CASSCF, the coefficients of the determinants in the (limited) CI expansion of the molecular wavefunction, *and* the coefficients of the basis functions in the expansion of each molecular orbital within the determinants of the expansion, are optimized. The model chemistries are unable to reliably handle singlet diradicals because they formulate the wavefunction as a single determinant which places the electrons of an even-electron molecule pairwise in orbitals (Chap. 5, Sect. 5.2.3.1). This is the Hartree-Fock wavefunction, written as a Slater determinant. More than one determinant is really needed because a single-determinant wavefunction presupposes the absence of degenerate (or nearly degenerate) orbitals: if such orbitals are present, the algorithm will simply fill one of them with a pair of electrons. Treating these diradicals within the ab initio framework requires configuration interaction (CI, Chap. 5, Sect. 5.4.3). Here the molecular wavefunction is represented as a weighted sum of determinants, rather than simply as one determinant. A full CI calculation would include all the determinants derived from the Hartree-Fock one, including a determinant in which one of the degenerate orbitals is doubly occupied, and one in which the other is doubly occupied, as well as determinants corresponding to all other possible excitations of electrons from occupied into formally empty (virtual) orbitals (the number of virtual orbitals depending on the number of electrons and the number of basis functions (Chap. 5, Fig. 5.5). Such a full CI calculation, if done with an

infinitely big basis set, would exactly solve the Schrödinger equation. This is out of the question, and even with a large finite basis set full CI is applicable only to very small molecules. The standard method for computations on singlet diradicals is a limited form of CI, in which the molecular wavefunction is represented by a weighted sum of the Hartree-Fock determinant and a carefully chosen set of molecular orbitals embodying all possible variations on electron occupation among those orbitals. The chosen set of MOs is the *active space*, and method is the *complete active space method* (CAS). To refine the coefficients that, with the basis functions comprise the MOs, we use the iterative SCF method (Chap. 5, Sects. 5.2.2 and 5.2.3.6.2), so the full appellation of the technique is *complete active space SCF* or *CASSCF*. This gives a limited-CI wavefunction with corresponding geometry and energy, and if needed the other usual properties that can be obtained from a wavefunction.

   To do a CASSCF calculation, one must first choose the active space, that is, the relevant MOs. Which MOs are relevant depends on the purpose of the calculation, and on how "complete" one wants the active space to be–the unattainable limit of course would be full CI. This will be illustrated with a few examples. Consider the diradicals 1,3-propanediyl and 1,4-butanediyl. Intuitively, it seems that we should consider at least these two MOs: the MO that resembles a bonding linear combination (Chap. 5, Sect. 5.2.3.6) of the two p-type atomic orbitals on the end carbons and the MO that resembles an antibonding linear combination of these atomic orbitals. We want these to be our HOMO and LUMO. The CAS wavefunction would then be composed of the HF determinant plus all determinants in which the two formally unpaired electrons are distributed (cf. Chap. 5, Fig. 5.2.2) among the HOMO and LUMO. This is the minimum active space for a CAS calculation on these species, and is called a CAS(2,2) calculation. This means that two electrons are being distributed in all possible ways among two MOs.

8.2.3.1   A CASSCF Calculation on 1,4-Butanediyl

The procedure will be described first for 1,4-butanediyl, which failed all our simple model chemistries tests. We first choose a starting geometry. This will depend somewhat on the purpose of our study. If we wish to compute the reaction profile for ring opening of cyclobutane to the proximate diradical, i.e. to the immediate relative minimum following ring opening (the concept of a well-defined transition state stationary point seems inapplicable here [63]), we might select a starting geometry that resembles cyclobutane with a stretched C–C bond. If we wish to explore the whole 1,4-butanediyl potential energy surface, we would perform geometry optimizations starting with all reasonably distinct conformations, created randomly or by systematically altering the torsion angles of a beginning structure. Here we consider a CASSCF calculation starting with the C_{2h} conformation of 1,4-butanediyl (Fig. 8.8), which model chemistries break to two ethenes. The exact keywords for each step and the possibility of combining two steps into one input file depend on the program, and are not given specifically here.

Step 1 is obtains a wavefunction for our starting "guess" geometry. For speed and to limit the number of MOs (which appear in step 2), an STO-3G basis set (Chap. 5, Sects. 5.3.2 and 5.3.3) is usually used. A single point calculation with the specified basis is requested and the wavefunction is stored in a file (Gaussian [49] calls this a *checkpoint file*) to be recalled in subsequent steps.

Step 2 is uses the wavefunction from step 1 to *localize* the MOs. To recapitulate (Chap. 5, Sect. 5.2.3.1): normally the Hartree-Fock wavefunction is represented straightforwardly as a Slater determinant in which the chosen basis set $\{\phi\}$ is used to expand the occupied MOs ψ as linear combinations of the ϕ functions. The Fock matrix derived from this determinant is called the *canonical Fock matrix*, and when repeatedly diagonalized and refined in the SCF process it yields a set of MOs, the canonical MOs. These MOs commonly do not resemble the bonding (or inferred antibonding) orbitals of Lewis structures: for example, visualizing the canonical MOs of H_2O, one does not see one MO corresponding to one of the O–H bonds, and one corresponding to the other O–H bond . Canonical MOs tend to be delocalized over the whole molecule, eluding correspondence with conventional Lewis bonds. However, it is possible to combine the canonical MOs so as to get localized orbitals corresponding to bonds and lone pairs. This is done by manipulating the canonical Hartree-Fock wavefunction determinant by adding multiples of rows or columns to other rows or columns. The wavefunction is unaltered mathematically (Chap. 4, Sect. 4.3.3, *Determinants*, property number 6): it will give the same observable properties, like geometry, spectra, and dipole moment. There are various requirements that can be enforced to produce different kinds of localized orbitals [64]; the most widely used MO localization schemes in CAS calculations are probably NBO (natural bond orbitals) and Boys localization. Boys localization [65a] generates MOs that are as compact as possible, and NBO localization [65b] creates MOs each of which is essentially composed of basis functions on just two atoms; both might thus be expected to resemble Lewis structures. We visualize the localized orbitals and inspect them, in search of which ones to assign to the *active space*.

The active space is the set of MOs among which the electrons will be distributed: electrons will be promoted from the formally occupied orbitals into the formally unoccupied ones in a CI calculation limited to the chosen orbitals. The orbitals are chosen according to the purpose of the calculation. If we simply wish to obtain the geometry of a diradical like 1,4-butanediyl, then we look for the troublesome orbitals, the ones now (we hope) localized on the end carbons. An orbital corresponding to this occupied one and an orbital corresponding to its vacant antibonding counterpart constitute the minimum active space for our calculation. Since two electrons and two orbitals are involved, this is called a CASSCF(2,2) calculation; with *a* electrons and *b* orbitals we have a CASSCF(*a*,*b*) calculation. Figure 8.9 clarifies this: the algorithm will recognize our (2,2) active space as consisting of the two frontier orbitals (HOMO and LUMO); we want these to be the two MOs that are localized on the end carbons. If we had decided to use a (6,6) active space, by including the two proximate C–C σ bonds and their antibonding counterparts, adding an extra four electrons and four orbitals, the active space would be recognized as the HOMO, HOMO-1, HOMO-2, and LUMO,

Fig. 8.9 The active space for a CASSCF(2,2) calculation on 1,4-butanediyl. There are two relevant MOs: the highest occupied and lowest unoccupied MO, and two electrons to be distributed among these. The relevant MOs must be determined by inspection (preferably visual) to be the right ones for the purpose of the calculation: see Fig. 8.10

Energy

—— MO 17

active space for a CAS(2,2)
calculation on $\cdot CH_2CH_2CH_2CH_2 \cdot$
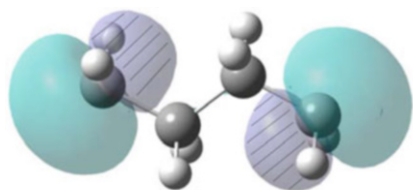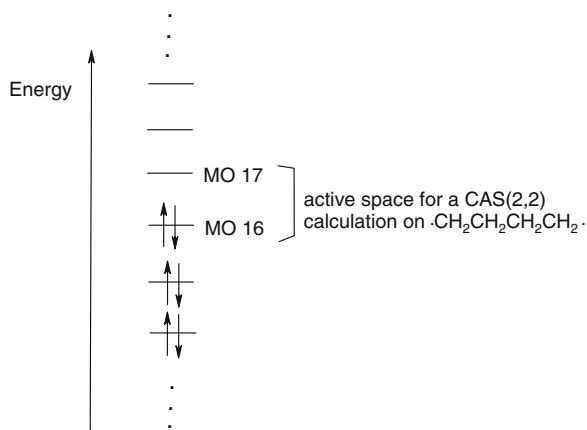
—— MO 16

MO 16, formally doubly occupied   MO 17, formally unoccupied
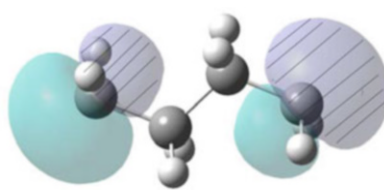
Fig. 8.10 Visualization of the relevant MOs, 16 and 17, for the active space of a CASSCF(2,2) calculation on 1,4-butanediyl: the algorithm will recognize the active space as consisting of the two frontier orbitals (HOMO and LUMO; the molecule has 32 electrons); we ensure by visual inspection that these are the two MOs that are localized on the end carbons. If a desired orbital is not a frontier orbital to start with, it can be switched with one (see text). NBO localization was used here. Calculated with the HF/STO-3G basis and localized by the NBO method

LUMO + 1, and LUMO + 2. If an orbital that should (as shown by its appearance on visualization) be in the active space is not, i.e. is not really a frontier orbital, it can be switched by an appropriate command with one initially in the active space but irrelevant to the calculation. Figure 8.10 shows the two MOs in the active space of our CASSCF(2,2) calculation, localized by the NBO method (in this case, with the Boys method the ordinal numbers of the relevant orbitals was unclear, due to the their not being nicely localized). The occupancy is revealed by visualization with an appropriate program or, less conveniently, inspection of printed output, which shows that the bonding-type C_1/C_4 MO number 16 is formally occupied by two electrons and the antibonding-type MO number 17 is formally vacant. Note that this species has 32 electrons. If, say, the MO resembling MO 16 here had been MO 10 and MO 16 had been a C-H bonding orbital, 10 and 16 could be switched–see below for cyclopentane. The point is that we want to perform a CI calculation using the relevant orbitals.
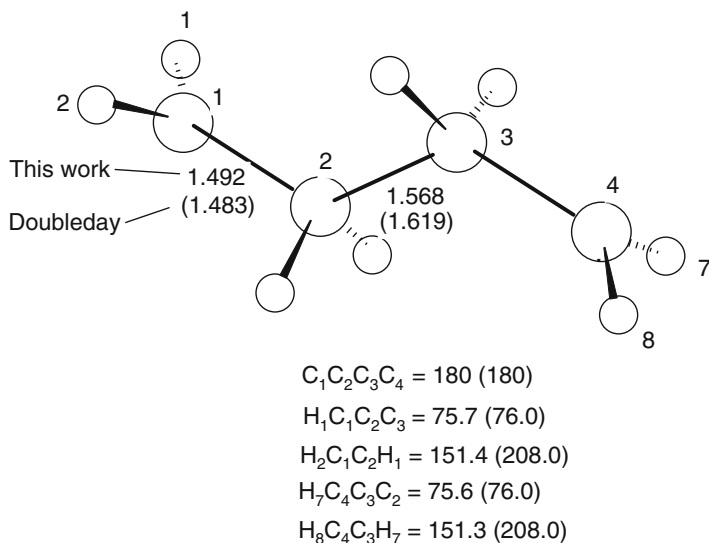
Fig. 8.11 The C2h 1,4-butanediyl diradical relative minimum (no imaginary frequencies), as calculated by CASSCF(2,2)/6-31G* (this work) and CASSCF(4,4)/6-31G* (Doubleday, [61], Figure 1 and Table III)

Step 3 is a geometry optimization. Appropriate keywords might be CASSCF (2,2)/6-31G*, specifying a CASSCF(2,2) procedure (a limited CI optimization) using the 6-31G* basis, which will normally be the smallest chosen. Other keywords might dictate the information to be taken from step 2 and how to calculate the initial Hessian (e.g., use a semiempirical calculation) for the optimization. Figure 8.11 compares our CASSCF(2,2)/6-31G* C_{2h} relative minimum (no imaginary frequencies–see below) with the C_{2h}CASSCF(4,4)/6-31G* minimum of Doubleday [62].

Step 4 is a frequency calculation on the geometry from step 3, again using the CASSCF(2,2)/6-31G* method. The program might allow this step to automatically follow the optimization. In most cases the frequency calculation is desirable, to characterize the nature of the optimized structure as a minimum or some kind of saddle point, and to obtain thermodynamic data like zero point energy and enthalpy and free energy (Chap. 2, Sect. 2.5; Chap. 5, Sect. 5.5.2.1.2).

One further step is desirable for obtaining relative energies, namely performing on the CASSCF(2,2)/6-31G* geometry a calculation designed to treat electron correlation better than was done by the CASSCF calculation. Recall that Hartree-Fock (also called SCF) calculations treat electron only very approximately (Chap. 5, Sect. 5.4.1). In a typical CASSCF calculation most of the electrons, i.e. those outside the active space, are not subjected to the CI calculation, but instead are treated at the Hartree-Fock level. The CASSCF calculation is said to treat properly *static correlation*, but not *dynamic correlation* (Chap. 5, Sect. 5.4.1).

To account more completely for dynamic correlation, a single-point perturbational calculation based on the CASSCF wavefunction is frequently done. This is a CAS perturbational theory, second order, or CASPT2, calculation. The most popular implementation of this is CASPT2N (N = nondiagonal one-particle operator) [66]. For programs that will do CASPT2-type calculations, see Chap. 9, Sect. 9.3. Improving a CASSCF energy with a CASPT2 calculation is analogous to improving a Hartree-Fock- (i.e. SCF-) level calculation with a single point MP2 calculation (Chap. 5, Sect. 5.4.2). It would be nice if geometry optimizations rather than just single point calculations (as was once the limitation of MP2, as an energy adjustment to HF level geometries) could be done at the CASPT2N level and CASPT2N potential energy surfaces could be explored, but this does not appear to be yet practical, because analytical derivatives (Chap. 2, Sect. 2.4) are not available. An attempt to do something like this was reported by Lange et al., who parameterized with single point CASPT2N energies a quadratic function with forming and breaking bond lengths as the variables and thus explored regions near stationary points [67].

8.2.3.2 CASSCF Calculations on 1,5-Pentanediyl and Cyclopentane

I outline another example of CASSCF calculations: a comparison of the energy of 1,5-pentanediyl and cyclopentane:

E(C-C)
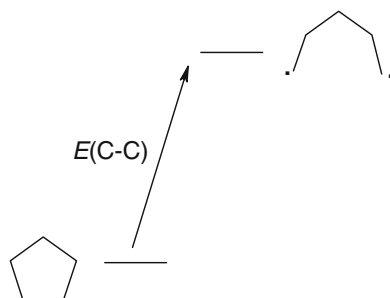
This energy difference should be a measure of the C–C bond energy in cyclopentane. These calculations used NBO localization (the result of Boys localization was messy when visualized) and CASSCF(2, 2)/6-31G*.

Several starting geometries were explored to obtain a C_5 diradical that was a relative minimum, but a thorough exploration of the potential energy surface was not attempted. Starting from a roughly sickle-shaped C_1 structure created by constraining the end carbons with molecular mechanics to a separation of 4.5 Å yielded a C_1 relative minimum. The visualization step showed that for the input structure the default active space MOs, MO 20 and 21, the HOMO and LUMO, were the desired orbitals, localized at the end carbons. However, for cyclopentane the occupied C–C bonding MO, representing the bond to be broken, was number 10, while MO 20 was a pure C–H bonding orbital, an unwanted intruder in the
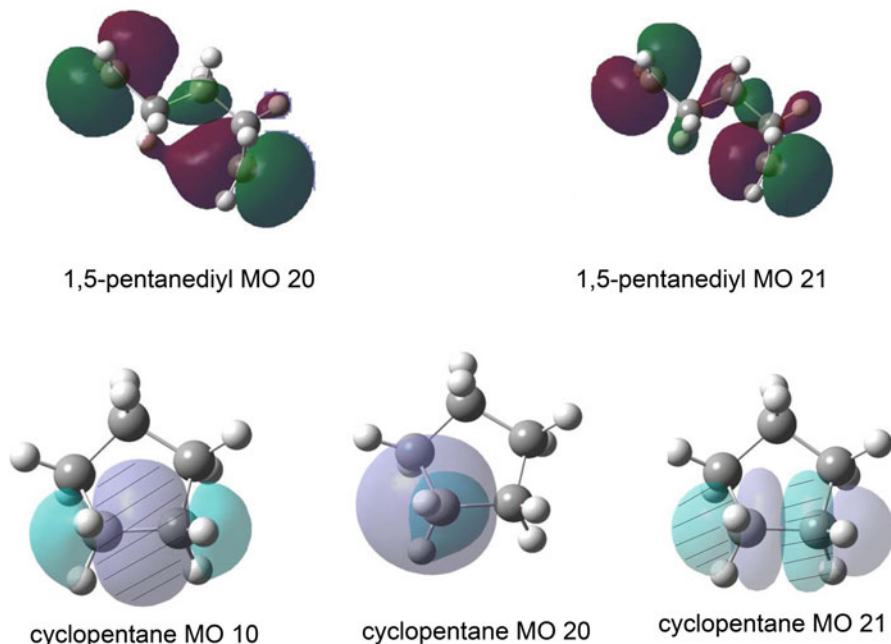
Fig. 8.12 The molecular orbitals of 1,5-pentanediyl and cyclopentane relevant to the C–C cleavage of the cycloalkane that leads to the acyclic diradical. Calculated with the HF/STO-3G wavefunction and localized by the NBO method. The cyclopentane C–C bonding orbital, MO 10, relevant to this reaction, must be switched with MO 20, a pure C–H bonding MO with no relevance here, to move the C–C MO into the active space (Note that these molecules have 40 electrons)

active space; a command to switch orbitals 10 and 20 was therefore given as part of the optimization input. See Fig. 8.12. The diradical and cyclopentane, optimized at the CASSCF$(2, 2)/6$-31G* level, were checked by frequency calculations to ensure that the structures were relative minima on the potential energy surface and to obtain the energy parameters below (Gaussian 03 output).

The energies of the diradical and cyclopentane can be compared:

1,5-Pentanediyl	
(Energy before frequency calculation (i.e. without ZPE) -195.0603078)	
Zero-point correction =	0.140164
Thermal correction to Energy =	0.147459
Thermal correction to Enthalpy =	0.148403
Thermal correction to Gibbs Free Energy =	0.109777
Sum of electronic and zero-point Energies =	−194.920144
Sum of electronic and thermal Energies =	−194.912849
Sum of electronic and thermal Enthalpies =	−194.911905
Sum of electronic and thermal Free Energies =	−194.950531

Cyclopentane	
(Energy before frequency calculation (i.e. without ZPE) -195.1797025)	
Zero-point correction =	0.150327
Thermal correction to Energy =	0.155259
Thermal correction to Enthalpy =	0.156203
Thermal correction to Gibbs Free Energy =	0.121800
Sum of electronic and zero-point Energies =	−195.029375
Sum of electronic and thermal Energies =	−195.024444
Sum of electronic and thermal Enthalpies =	−195.023500
Sum of electronic and thermal Free Energies =	−195.057902

Diradical enthalpy – cyclopentane energy:

1. The crudest value for this is based on the energies from the optimization step, i.e. without ZPE:

$$-195.0603078 - (-195.1797025) = 0.119395 = 313.5 \text{ kJ mol}^{-1}.$$

2. With ZPE-corrected energies, i.e. 0 K enthalpies, we get

$$-194.920144 - (-195.029375) = 0.109231 = 286.8 \text{ kJ mol}^{-1}.$$

3. Using the sum of electronic and thermal enthalpies, i.e. room-temperature (298 K) enthalpies, we get

$$-194.911905 - (-195.023500) = 0.111595 = 293.0 \text{ kJ mol}^{-1}.$$

None of these can be viewed as an accurate standard bond energy [68] for cyclopentane, whose likely C-C bond energy is ca. 345 kJ mol^{-1} [69]. Note that this is significantly lower than that of butane, for which an experimental value of 363.2 ± 2.5 kJ mol^{-1} and calculated values of ca. 367, 378 and 379 kJ mol^{-1} have been reported [70]. This exercise indicates that good dynamic electron correlation can be important in handling homolytic cleavage; CASPT2N was not available to us. Also, the (2,2) active space used here is only the minimum that might be acceptable.

One more example of the CASSCF procedure will be outlined: calculating the barrier to rotation around the CC double bond in ethene. Step 2, orbital localization, showed nicely localized orbitals when NBO localization was used, but the orbitals were harder to identify with Boys localization. For a CAS(2, 2)/6-31G* optimization the active orbitals chosen were the π and π* MOs, and for a CAS(4, 4)/6-31G* optimization the π, π*, σ and σ* MOs. The input structures were the normal planar ethene and perpendicular (90° twisted) ethene. Optimization and frequency calculations gave a minimum for the planar and a transition state for the perpendicular structures. The energies (without ZPE, for comparison with those calculated by the GVB method by Wang and Poirier, [71]) were:

CASSCF(2,2):

> perpendicular ethene, -77.9630054, planar ethene, -78.0673444;
> barrier $= 0.10434 = 274.0$ kJ mol^{-1}.

CASSCF(4,4):

> perpendicular ethene, -77.982972, planar ethene, -78.0852825;
> barrier $= 0.10231 = 268.7$ kJ mol^{-1}.

Wang and Poirier obtained from GVB calculations [71] a barrier of 263.6 kJ mol^{-1} $(65.4$ kcal mol$^{-1})$. The reported experimental value for the barrier of *cis*-ethene- d_2 is 272 kJ mol^{-1} [72]. Hartree-Fock, MP2 and DFT (B3LYP) optimizations on the perpendicular ethene transition state did give an optimized structure with one imaginary frequency, but the barriers (6-31G*) basis were respectively 540, 572, and 399 kJ mol^{-1} (without ZPE, which was only ca. 10–20 kJ mol^{-1}).

More complex than ethene but amenable to a similar attack is the fascinating molecule orthogonene. This is so named because in this C_{14} molecule four C_2 clamps hold the C_6 tetrasubstituted double bond moiety twisted through ca. 90°:
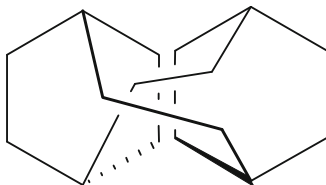
CASSCF(4, 4)/6-31G* calculations using the C=C π and σ bonding and anti-bonding orbitals led to the conclusion that the molecule can rearrange to a carbene with a barrier of about 200 kJ mol^{-1} [73].

Procedures for more involved CASSCF calculations, including calculations on exited states, are given by Foresman and Frisch, with caveats for assessing the reliability of the results, and they reassure the reader "not [to be] discouraged by difficulties that you may encounter" [74]. Although CAS and GVB calculations are the standard ways of handling singlet diradicals, attempts have been and are being made to extend the reach of DFT here, perhaps bringing these species one day into the compass of model chemistry methods. Examples are the work of Kazaryan and Filatov [75], and Cremer and coworkers [76]. Open shell molecules in general can present problems for model chemistries; these, and ways of dealing with them, have been reviewed by Bally and Borden [77].

(3) *Broken symmetry calculations.* An alternative to a complete active space calculation is a procedure called a broken symmetry calculation. This is a UHF-type calculation on a *singlet* species. We saw that unrestricted calculations (Chap. 5, toward the end of Sect. 5.2.3.6.5; Chap. 7, Sect. 7.2.3.4.2) are the standard way of

treating ordinary free radicals, which with one unpaired electron are doublet species. The unrestricted method, whether Hartree-Fock or DFT UHF or UDFT), removes the constraint (the restriction) that we do not have separate orbitals for α-spin electrons and for β-spin electrons. In an ordinary radical, having separate sets of molecular orbitals makes it possible for α- and β-electrons to adjust their orbital shapes separately to reflect the fact that they feel differently the effect of, say, an unpaired α-electron. Similarly, an unrestricted calculation on a singlet diradical allows α- and β-electrons to adjust their orbital shapes separately to minimize their interaction energy with the two (more or less) unpaired electrons. Figure 8.13 shows the orbital situation for a broken symmetry calculation. In CASSCF calculations the open shell, diradical character is created by mixing into the overall wavefunction functions (determinants; Chap. 5, Sect. 5.4.3) in which one or more electrons have been promoted into virtual orbitals. In broken symmetry calculations diradical character is created from the start by allowing (ideally, a pair of) electrons to "chemically decouple" by being in different orbitals. While unrestricted calculations are well-accepted as a legitimate way to handle monoradicals, there are reservations about its use with singlet diradicals [78].

1,4-butanediyl (Sects. 8.2.2 and 8.2.2.1), which rejected standard model-chemistry methods to optimize it to a stationary point, gave from a C_{2h} input structure, using broken symmetry, a stationary point (a relative minimum) of similar geometry to that from the CASSCF calculation of Sect. 8.2.2.1. Other cases of satisfactory geometries from broken symmetry are singlet diradicals resembling 1,4-benzenediyl (benzene with hydrogens removed from the 1,4-positions) in the Bergman reaction and in the rearrangement of bowtiene [79]. In these two cases a reaction profile believed to be energetically realistic was obtained by applying to

Fig. 8.13 The molecular orbitals for an unrestricted calculation are divided into a set for α-electrons and a set for β-electrons. In the case shown here each electron has a "counterpart" of opposite spin, so this does not represent a calculation on a conventional free radical (a doublet), but rather on a singlet
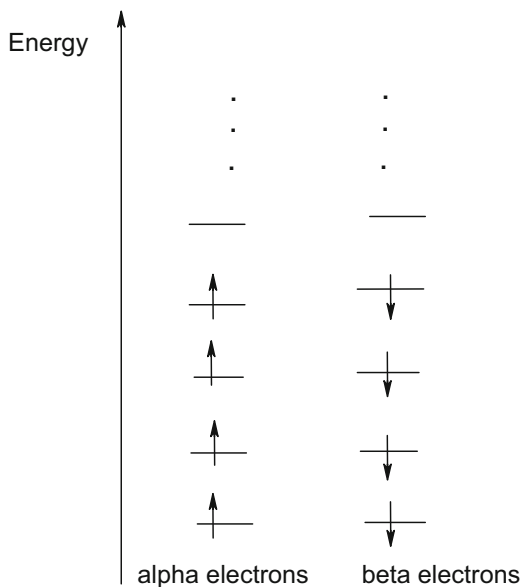
the broken symmetry reactant, transition state and product geometries an energy adjustment for dynamic correlation from the CCSD(T) method (Chap. 5, Sect. 5.4.3); like CASSCF, broken symmetry cannot be counted on to handle dynamic correlation quantitatively. In contrast to the multistep CASSCF procedure explained above, these broken symmetry opimization/frequency calculations required only one step, with the command line specifying, beside optimization and frequency, the use of an unrestricted DFT method and the basis set. With Gaussian 09 [49] this was done with

$$\text{\#P umpw1pw91/6} - 311 + \text{G** guess} = (\text{INDO, Mix, Always}) \text{ Opt Freq}$$

and a charge of 0 and a multiplicity of 1. This invokes an unrestricted Kohn-Sham DFT wavefunction despite the specification, on another line, of singlet multiplicity. The calculation starts with a semiempirical INDO (Chap. 6, Sect. 6.2.4) guess at the wavefunction, with *Mix* removing α and β spatial symmetries by a random rotation of the HOMO and LUMO. After removing symmetry the algorithm follows the usual Pople-Nesbet procedure for simple radicals like CH_3 (Chap. 5, toward end of Sect. 5.2.3.6.5). *Always* makes sure Mix is used at each optimization step. Broken symmetry is closer to being a model chemistry than is CASSCF, but success seems to be sensitive to the choice of DFT functional and initial guess.

Abe has reviewed experimental and computational results for diradicals [80], Yang et al. have examined benchmark-level calculations on radical dissociation of F_2, HOOH, and C_2H_6 [81], and Ess and Cook have explored the value of DFT for economical calculations on singlet-triplet gaps of diradicals [82].

8.3   A Note on Heavy Atoms and Transition Metals

All things are Atoms: Earth and Water, Air
And Fire, all, <u>Democritus</u> foretold.
Saw Sulphur, Salt, and Mercury unfold
Amid Millenial hopes of faking Gold.
. . .
The <u>Metals</u>, lustrous Monarchs of the Cave,
Are ductile and conductive and opaque
Because each Atom generously gave
Its own Electrons to a mutual Stake,
. . .
–John Updike, Midpoint, III. The dance of the solids. Composed ca. 1967.

8.3.1   Perspective

All chemical things are composed of atoms, so one might wonder why heavy atoms and transition metals should be singled out for special treatment. Part of the justification is that most of the elements are metals, and most of these are transition-type metals; I include in this class the lanthanides and actinides (IUPAC recommends the terms lanthanoids and actinoids, as -ide implies an anion). The high atomic numbers of most elements, compared to carbon, and the quirky electronic structures of transition metals, pose problems not encountered routinely in computations on organic compounds. Beyond about the second (beyond Ar, $Z = 18$), certainly beyond the third (beyond Kr, $Z = 36$), full row of the periodic table, the pull of about 30–50 nuclear protons forces the inner electrons of the atom to move at a significant fraction of the speed of light. This makes relativistic corrections often necessary for accurate work. Further, transition metals (TMs) tend to fill their outer shells in a manner less than straightforward, and to exhibit a more baroque style of bonding than seen in typical organic compounds. The purpose of this short section is merely to make readers aware of these problems so that should they seek to carry out computations on inorganic species they will know that further delving into the relevant literature may be advisable.

8.3.2   Heavy Atoms and Relativistic Corrections

The gain in mass [83] of the inner electrons in heavier atoms causes their orbitals to contract and screen the outer electrons better than they otherwise would, causing outer, valence d and f orbitals to expand, becoming of higher energy and more reactive (a semipopular account of relativistic effects and computations is given by Jacoby [84]). This has striking physical consequences, like the color of gold and the fact that mercury is liquid, and significantly affects spectra by altering spin-orbit coupling, while the chemical effects permeate structures and energetics; this is discussed in Pyykkö's comprehensive review of the effects of and computations dealing with relativity in chemistry [85]. Other reviews relevant to relativistic computations discuss pseudopotentials and TM compounds (Frenking et al. [86], Cundari et al. [87]), transactinide elements (Persina [88]) and the theory of relativistic quantum chemistry (Almlöf, Gropen [89]). A thorough account of relativistic effects in chemistry, a very technical subject, is given in the two-volume work by Balasubramanian [90a], and the review of Volume B by Wilson is itself worth reading for a perspective on the subject [90b]. Relativistic effects in molecules are computed by the Dirac-Fock equation or, more frequently, pseudopotential or effective core potential methods. Perturbation methods have also been applied to atomic and molecular relativistic effects [85]. The term *pseudopotential* is favored by physicists, while *effective core potential* or ECP tends to be used often by chemists. The Dirac-Fock method ([91, 85] and references therein) is based on

the extension to multielectron systems of the famous one-electron relativistic Dirac version of the Schrödinger equation [92]. It is "The most satisfying way to carry out relativistic molecular calculations" [85], but is apparently not very practical for many-electron molecules (but see a recent calculation on PbH_4 [93]). Less demanding and much more popular are computations using relativistic pseudopotentials (relativistic ECPs). A relativistic pseudopotential is a one-electron operator, somewhat analogous to the $\hat{J}$ and $\hat{K}$ operators in standard Hartree-Fock theory (Chap. 5, Eqs. (5.29 and 5.30) which is incorporated into the Fock operator (Chap. 5, Eq. (5.36) and equations (20)–(21) in reference [85]) and modifies it by treating the inner, non-valence electrons in an average way, and taking relativity into account; the valence electrons are treated conventionally. This average treatment greatly reduces the number of electrons that must be directly addressed and the number of basis functions needed. Nonrelativistic or relativistic pseudopotentials can be used even when relativity is not a problem, to reduce the computational effort arising from many inner-shell electrons. We encountered the concept in a very crude form in Chap. 6, where we saw that semiempirical methods like AM1 and PM3 treat only the valence electrons explicitly and in effect collapse the inner electrons into the nuclei. The valence electrons then move in the electrostatic potential field of a set of "pseudonuclei", each with a charge equal to the algebraic sum of an atomic number and the charge of the inner electrons.

Pseudopotentials for molecules come from parameterization for atoms using Dirac-Fock calculations. Since the pseudopotentials are parameterized for atoms, we are assuming that the inner electrons are little affected on going from atoms to molecules. The results justify this assumption. Actually, some pseudopotentials handle all but the outermost electron shell (all but, say, $n = 5$), and some all but the two outermost (all but, say, $n = 5$ and 4); these are called, respectively, larger-core or full core, and small core pseudopotentials. Since these calculations do not *directly* use the Dirac-Fock equation, they are sometimes called *quasirelativistic* calculations. Pseudopotentials are invoked by specifying a basis set that has been specially designed for them, and a pseudopotential basis set (ECP basis set) is often simply called a pseudopotential or ECP. They can be used in Hartree-Fock, MP2, CI, and DFT calculations, and are the standard method of treating molecular relativistic effects, and of reducing the computational strain incurred by the presence of large numbers of electrons even when relativity is not significant. Another problem sometimes met with in heavy atoms is caused by spin-orbit coupling. This and electron correlation effects have been addressed with pseudopotentials [94].

8.3.3 Some Heavy Atom Calculations

The efficacy of a technique is sometimes best highlighted by studying trends. A comprehensive review of compounds of the carbon homologue series Si, Ge, Sn and Pb has been published by Karni et al. [95]. The rotational barriers in ethane and

its various Si, Ge, Sn and Pb homologs were computed by Schleyer et al. [96], using pseudopotentials; relativistic effects were important only for Pb $(Z = 82)$. Pseudopotential calculations have been extended to the sixth element in this series, with studies of $(114)X_2$ and $(114)X_4, X = H, F, Cl$ [97]. Relativity can be neglected for certain properties for iodine ($Z = 53$), krypton ($Z = 36$) and even Xenon ($Z = 54$): MP2 studies on the geometry and thermochemistry of iodine oxides with extended Pople-type basis sets and comparison with earlier work showed that "relativistic effects are either small or cancel" [98], and DFT calculations on fluorides of krypton and xenon (and some work on radon) with and without relativistic effects showed that for bond lengths, dissociation energies, force constants, and charges "relativistic effects…are negligible" [99]. An extensive list of basis functions, which enables those available for a desired atom to be identified and downloaded for computation, is available online [100]. A brief presentation of popular pseudopotentials is given by Cramer [101]. The literature and some experimentation suggests that one popular basis, the LANL2DZ (Los Alamos National Laboratory), parameterized for H to Pu, may be particularly useful.

8.3.4   Transition Metals

The bonding in and structures of transition metal compounds constitute a subject with rules somewhat *sui generis* to one primarily versed in organic and main group chemistry. The relative complexity of bonding in these compounds arises from the presence in their compounds of *partially* filled d- or (for the lanthanides and actinides) f-level atomic orbitals, when the compound is viewed as consisting of ions surrounded by ligands. This viewpoint is possible not only for simple ionic compounds $M^{n+}X^{n-}$, but also for covalent compounds and "complexes", since the metal can be assigned an at least formal oxidation state. The classification of a particular element as a transition metal, a lanthanide or an actinide is not always unambiguous and universally adhered to. For example, the scandium atom has one d electron, but in any compound in which it has an oxidation number above zero, it will have no d electrons. Zinc has 10 d electrons, but its compounds, formed by loss of two s electrons, also have this fully filled d shell. Were compounds of scandium (0) and Zn(III) recognized, with one and nine d electrons, respectively, these elements would be classified as transition metals. Below are generally accepted classifications for TM-type elements, with the hedge that the electronic structures are idealized in that subtle shifts in occupancy are possible. For example, a Cu (I) compound may not have the expected $3d^9 4s^1$, but rather the $3d^{10} 4s^0$ arrangement.

Transition metals, first row, Ti $(Z = 22,\ 3d^2 4s^2) - Cu\ (Z = 29,\ 3d^9 4s^2)$
Transition metals, second row, Zr$(Z = 40,\ 4d^2 5s^2) - Ag\ (Z = 47,\ 4d^9\ 5s^2)$
Transition metals, third row, Hf $(Z = 72,\ 5d^2 6s^2) - Au\ (Z = 79,\ 5d^9 6s^2)$

Lanthanides, Ce $\left(Z = 58, 4f^1 5d^1 6s^2\right)$ − Yb $\left(Z = 70, 4f^{14} 6s^2\right)$

Actinides, Th $\left(Z = 90, 6d^2 7s^2\right)$ − Es $\left(Z = 99, 5f^{11} 7s^2\right)$ (stopping at what appears to be the last element available in at least milligram amounts [102]).

The electronic structures of compounds of these elements is complicated by ambiguities in filling the d or f shells, which can give rise to low-spin and high-spin compounds with the same number of formal metal electrons (i.e. with the metal in the same oxidation state) but with different ligands, depending on the gap between the so-called (for d-shell atoms) t_{2g} and e_g sets of orbitals. An accessible and reasonably compact introduction to the structure of TM compounds and the role therein of d orbitals is given by Cotton et al. [103]. Hoffmann, in his Nobel Lecture, presents an interesting and original set of rules, the isolobal analogy, for interpreting the structures of such species and drawing analogies, which "[allows] us to see the simple essence of seemingly complex structures" [104]. The detailed properties of individual elements are discussed in standard textbooks, e.g [105, 106].

I outline the main salient points relevant to computations on TM compounds. First, as indicated above, one needs an understanding of the rules behind the peculiarities of d orbital electronic arrangements, in order to formulate and interpret rational structures; when a structure is *not* "rational", because it is particularly novel, background theoretical knowledge is even more valuable. Prosaic factual knowledge of chemical properties does not hurt either. The elucidation of the structure of ferrocene, $(C_5H_5)_2Fe$, provides a nice example of the role of factual and theoretical knowledge in discovery. Ferrocene was initially assigned a conventional C-Fe-C structure, but unlike known compounds with a metal-carbon sigma bond it was very stable, and like benzene reacted by electrophilic substitution. Theory led to the formulation of the correct and then-unprecedented sandwich structure. The ferrocene saga, which initiated a revolution in transition metal chemistry, has been summarized by Dagani [107] and Laszlo and Hoffmann [108].

In our short survey of the computational techniques available for investigating TM compounds we first mention molecular mechanics (Chap. 3). It may seem humble by the standards of the quantum mechanical ab initio, semiempirical and DFT methods (Chaps. 5, 6 and 8, respectively) but MM is useful for obtaining input structures for submission to one of those calculations, may even provide in itself useful information, and it is, of course, extremely fast. Indeed, a recent book on the modelling of inorganic compounds, mainly TM species [109], is devoted very largely to molecular mechanics and a program specially parameterized for TM compounds, Momec3 [109].

Ab initio methods (unparameterized, or almost unparameterized, wavefunction calculations) were at one time, in contrast to DFT, deprecated for the study of TM compounds, but it now appears that this inferiority of ab initio may be largely confined to the first-row metals, titanium to copper [86, 110]. DFT *can* sometimes be quite inaccurate, and advanced correlated ab initio methods like CCSD(T) and even CCSDTQ (Chap. 5, Sect. 5.4.3), may be useful, although these are currently limited to small systems [111]. Nevertheless, DFT calculations with

pseudopotentials, commonly relativistic, are now the standard methods for performing calculations on TM compounds [86, 110, 112]; for example Frenking, in a paper analyzing bonding in such species, extols the virtues of DFT used with pseudopotentials [112]. The suitability of various functionals for TM chemistry is commented on by Zhao and Truhlar in a review which presents their new M0-class functionals (Chap. 7, Sects. 7.2.3.4 and 7.3), and the most appropriate for this purpose are said to be M06 and, especially, M06-L [113], but Tekarli et al. found that with the correlation-consistent cc-p-VQZ basis the B97-1 functional can give formation enthalpies of first-row transition metals within 4 kJ mol^{-1} (1 kcal mol^{-1}) of high-level multistep ab initio methods (cf. Chap. 5, Sect. 5.5.2.3.2) , G4(MP2) and ccCA-tm [114]. A review by Cramer and Truhlar on the application of DFT to transition metals boasts 1307 references [115]. DFT and wavefunction methods have been compared for the actinides [116]. Work has appeared focussed on TM atoms and their cations for the 4d series (Y to Pd) [117] and the 3d series (considered as Sc to Zn) [118]. In the former of these two the problem of broken symmetry is explicitly addressed, while the latter introduces "a new broken symmetry method, the reinterpreted broken symmetry method, RBS", and also points out that for a TM species the wavefunction may not automatically converge to the lowest-energy minimum, or even a relative minimum (wavefunction instability, Chap. 5, Sect. 5.2.3.5). A DFT method called SIESTA (Spanish Initiative for Electronic Simulation with Thousands of Atoms), designed for big, extended systems like large metal clusters has found use in recent years [119].

Finally, TM compounds have been studied by semiempirical methods. One thinks first of *faux*-ab initio-type methods like AM1 and PM3 (Chap. 6), since these are surrogates for "full" quantum mechanical ab initio techniques. However, the deepest insights into the nature of these compounds that have been afforded by a semiempirical method have come from the uncomplicated and venerable extended Hückel method (Chap. 4, Sect. 4.4). In the hands of Hoffmann, to whom we owe the EHM in its current form [120], extended Hückel calculations have given powerful insight into the structures of these compounds. Wide-ranging corroboration of this assertion is seen in Hoffmann's Nobel lecture [104]. Some other examples are a polymeric rhenium compound [121], manganese clusters [122] and iridium [123] and nickel [124] coordination compounds.

Unlike the extended Hückel method, AM1 and PM3 are useful for optimizing geometries and (less reliably) calculating relative energies of organic compounds, a purpose for which they were primarily designed. For TM compounds, a version of PM3, PM3(tm), available in Spartan [31] (in later versions of the program, not explicitly called PM3(tm) but parameterized for several transition metals) was developed. This is very fast and has been quite extensively used, with mixed results. Buda et al. compared PM3(tm) with ab initio (MP2 on HF geometries) and DFT for 30 complexes and found that PM3(tm) reproduced the crystallographic data in 80 % of the cases, compared to 87 % for MP2//HF and hybrid DFT, and 90 % for pure DFT [125]. Cooney et al. found it accurate enough as far as steric factors go, for predicting novel properties of rhodium phosphines [126], and Zakharian and Coon

reported that "In general, the PM3(tm) method in Spartan shows promise for predicting adsorption sites and vibrational frequencies of molecules on metal [i.e. nickel] surfaces" [127], while Goh and Marynick found it to be inadequate for energies, although its geometries were accurate enough for "energetics at a higher level" (they refer to isodesmic reaction energies) with compounds of Cr, Mo, W and Co [128], and Bosque and Maseras obtained geometries ranging from excellent to very poor by comparison with literature X-ray and neutron diffraction and with ab initio and DFT calculations, with compounds of Pd, W and Ti [129]. The TM parameterization of PM3 is discussed by McNamara et al. [130]. With this variability in performance great care is clearly needed in judging the appropriateness and reliability of PM3(tm) calculations: results for model systems might be compared with experiment, or, because of its speed, the method could be used in a large, suggestive survey. Semiempirical approaches to the computation of geometries and energies (e.g. bond energies, heats of formation) of transition metal compounds have not reached the same level of reliability that has been attained for organic compounds with the normal (full) first-row (C, H, N, O, F) elements (Chap. 6). Some may not regard this as a serious problem in view of the speed of DFT over high-level ab initio methods like CCSDT, the availability of improved functionals, and the reliability of pseudopotentials.

8.4   Summary

For some purposes gas-phase calculations are unrealistic, e.g. for understanding some solution-phase reactions, or even almost useless, e.g. for the prediction of pK_a in solution. For introducing the effects of solvation, there are two methodologies (and a hybrid of these two): explicit solvation, that is, putting individual solvent molecules into the system, and continuum solvation, representing the solvent as an appropriately parameterized continuous medium. Although for some purposes explicit solvation is needed, particularly where solvent molecules participate in a reaction, continuum methods are more widely used.

Some molecular species are not calculated properly by straightforward model chemistries; these include singlet diradicals and some excited state calculations. For these the standard method is the complete active space approach, CAS (CASSCF, complete active space SCF). This is a limited version of configuration interaction, in which electrons are promoted from and to a limited, carefully chosen set of molecular orbitals. CASSCF calculations require care in choosing these orbitals and in judging the reliability of the results.

Calculations on systems with heavy atoms often employ pseudopotential basis sets, which reduce the computational burden that large numbers of electrons would present, by avoiding explicit treatment of inner electrons. These basis sets are frequently relativistic, taking into account the effect on chemical properties of

electrons moving at a significant fraction of the speed of light. Transition metals present problems beyond those of main-group heavy atoms: not only can relativistic effects be significant (in the heavier elements), but near-lying electron d- or f-levels, variably perturbed by various ligands, make possible a variety of electronic states. Although beyond the first transition metal row ab initio (i.e. wavefunction) methods have been used, less demanding DFT calculations, with pseudopotentials, are the standard approach for computations on such compounds.

Solvation

Easier Questions

1. Using microsolvation, roughly how many water molecules might be needed to provide one layer around CH_3F (suggestion: examine space-filling hand-held or computer-generated models)?
2. What physical properties of solvents have been used to parameterize them for continuum calculations?
3. Give an example of a reaction for which just one explicit solvent molecule might be adequate in simulating a reaction mechanism.
4. For continuum solvation, give an example of a molecule for which a good approximation might be (a) a spherical cavity, (b) an ellipsoidal cavity.
5. Why are continuum solvation methods more widely used than microsolvation methods?

Harder Questions

1. In microsolvation, should the *solvent* molecules be subjected to geometry optimization?
2. Consider the possibility of microsolvation computations with spherical, polarizable "pseudomolecules". What might be the advantages and disadvantages of this simplified geometry?
3. In microsolvation, why might just one solvent layer be inadequate?
4. Why is parameterizing a continuum solvent model with the conventional dielectric constant possibly physically unrealistic?
5. Consider the possibility of parameterizing a continuum solvent model with the dipole moment.

Singlet Diradicals

Easier Questions

1. A monoradical is a doublet and a diradical can be a singlet or a triplet. How many spin states are possible for a triradical?
2. What does the Pauli exclusion principle suggest about the relative energies of singlet and triplet diradicals?
3. What is the simplest singlet diradical hydrocarbon species?
4. Which MOs would be appropriate for CASSCF calculations on

    1. the ring-opening of cyclobutene to 1,3-butadiene?
    2. the Diels-Alder reaction?

5. How many CI configurations are used in

    a CASSCF(2,2) calculation?
    a CASSCF(2,3) calculation?

Harder Questions

1. Is CASSCF size-consistent?
2. In one-determinant HF (i.e. SCF) theory, each MO has a unique energy (eigenvalue), but this is not so for the active MOs of a CASSCF calculation. Why?
3. In doubtful cases, the orbitals really needed for a CASSCF calculation can sometimes be ascertained by examining the *occupation numbers* of the active MOs. Look up this term for a CASSCF orbital.
4. Why does an occupation number (see question 3 above) close to 0 or 2 (more than ca. 1.98 and less than ca. 0.02) indicate that an orbital does not belong in the active space?
5. It has been said that there is no rigorous way to separate static and dynamic electron correlation. Discuss.

Heavy Atoms and Transition Metals

Easier Questions

1. Suggest a simple physical property of an atom for which a comparison of experiment with a calculated value might be used a test of whether the atom should be regarded as being "heavy" (hint: consider the energy of the valence electrons).

2. Suggest a simple property of a compound of element X for which a comparison of experiment with a calculated value might be used a test of whether element X should be regarded as being "heavy".
3. Dirac, the discoverer of the relativistic one-electron equation, thought that relativity would be unimportant in chemistry (P. A. M. Dirac, "Quantum Mechanics of Many-Electron Systems", Proceedings of the Royal Society of London. Series A, Mathematical and Physical Sciences, 1929, *123*(792), 714). Why was he mistaken?
4. Of the first 100 elements, how many are transition metals?
5. Use the simple semiclassical Bohr equation for the velocity v of an electron in an atom (Chap. 4, Eq. (4.12) to calculate a value of v for $Z = 100$ and energy level $n = 1$:

$$v = \frac{Ze^2}{2\varepsilon_0 nh} \tag{4.12}$$

$e = 1.602 \times 10^{-19}$ C, $\varepsilon_0 = 8.854 \times 10^{-12}$ C^{2}N^{-1}m^{-2}, $h = 6.626 \times 10^{-34}$ J.s

What fraction of the speed of light $c = 3.0 \times 10^8$ ms^{-1}) is this value of v?
Using the "Einstein factor" $\sqrt{(1 - v^2/c^2)}$, calculate the mass increase factor that this corresponds to.

Harder Questions

1. Is the result of the calculation in question 5 above trustworthy? Why or why not?
2. Should relativistic effects be stronger for d or for f electrons?
3. Why are the transition elements all metals?
4. The simple crystal field analysis of the effect of ligands on transition metal d-electron energies accords well with the "deeper" molecular orbital analysis (see e.g [106]). In what way(s), however, is the crystal field method unrealistic?
5. Suggest reasons why parameterizing molecular mechanics and PM3-type programs for transition metals presents special problems compared with parameterizing for standard organic compounds.

References

1. Modern physics views the vacuum as a "false vacuum", seething with "virtual particles": The study of these concepts belongs to quantum field theory: (a) For a reflective exposition of this largely in words (!) See Teller P (1995) An interpretive introduction to quantum field theory. Princeton University Press, Princeton; (b) A detailed account of the subject by a famous participant is given in Weinberg S (1995) The quantum theory of fields. Cambridge University Press, Cambridge; particularly vol I, Foundations
2. Krieger JH (1992) Chem Eng News, May 11, p 40

3. Luberoff BJ (1992) Chem Eng News, June 15, p 2
4. Pilar FJ (1992) Chem Eng News, June 29, p 2
5. Sousa SP, Fernandes PA, Ramos MJ (2009) J Phys Chem A 113:14231
6. (a) Kenny JP, Krueger KM, Rienstra-Kiracofe JC, Schaefer HF (2001) J Phys Chem A 105:7745; (b) Lewars E (2000) J Mol Struct (Theochem) 507:165; (c) Lewars E (1998) J Mol Struct (Theochem) 423:173, and references therein to earlier work
7. Fliegl H, Sundholm D, Taubert S, Jusélius J, Klopper W (2009) J Phys Chem A 113:8668
8. (a) Liptak MD, Gross KC, Seybold PG, Feldgus S, Shields GC (2002) J Am Chem Soc 124:6421, and references therein; (b) Liptak MD, Shields GC (2001) J Am Chem Soc 123:7314
9. (a) Calculations on the stability of $N_5^+N_5^-$ in vacuo and in a crystal: Fau S, Wilson KJ, Bartlett RJ (2002) J Phys Chem A 106:4639. Correction: J Phys Chem A 2004 108:236; (b) Decomposition of polynitrohexaazaadamantanes in crystals: Xu X-J, Zhu W-H, Xiao H-M (2008) J Mol Struct (Theochem) 853:1–6; (c) Nitroexplosives in crystals: Zhang L, Zybin SV, van Duin ACT, Dasgupta S, Goddard III WA (2009) J Phys Chem A 113:10619; (d) General approach to calculating bulk properties of crystals: Hu Y-H (2003) J Am Chem Soc 125:4388; (e) Ab initio modelling of crystals: Dovesi R, Civalleri B, Orlando R, Roetti C, Saunders VR (2005) Rev Comput Chem, volume 21, Lipkowitz KB, Larter R, Cundari TR (eds) (2005) Wiley, Hoboken; (f) Tuckerman ME, Ungar PJ, Rosenvinge T, Klein ML (1996) Molecular dynamics applied to crystals, liquids, and clusters. J Phys Chem 100:12878
10. Bachrach SM (2014) Computational organic chemistry, 2nd edn. Wiley-Interscience, Hoboken, chapter 7
11. Thar J, Zahn S, Kirchner B (2008) The minimum requirements for solvating alanine have been examined with the aid of molecular dynamics. J Phys Chem B 112:1456
12. (a) See e.g. (a) Leach AR (2001) Molecular modelling, 2nd edn. Prentice Hall, Essex; chapter 7; (b) Harris RC, Pettitt BM (2015) J Chem Theory Comput 11:4593; (c) Deng N, Zhang BW, Levy RM (2015) J Chem Theory Comput 11:2868
13. (a) Acc Chem Res, 2002 35(6); issue devoted largely to this topic; (b) Setny P (2015) J Chem Theory Comput 11:5961; (c) Yang Z, Doubleday C, Houk KN (2015) J Chem Theory Comput 11:5606
14. Bickelhaupt FM, Baerends EJ, Nibbering NMM (1996) Chem Eur J 2:196
15. Yamataka H, Aida M (1998) Chem Phys Lett 289:105
16. Cramer CJ (2004) Essentials of computational chemistry, 2nd edn. Wiley, Chichester, chapter 11
17. Jensen F (2007) Introduction to computational chemistry, 2nd edn. Wiley, Hoboken, sections 14.6, 14.7
18. Tomasi J, Mennucci B, Cammi R (2005) Chem Rev 105:2999
19. Marenich AV, Cramer CJ, Truhlar DG (2013) This paper presents "a new kind of treatment" of the dispersion contribution. J Chem Theory Comput 9:3649
20. This issue is devoted to solvation, mostly specialized aspects of continuum methods: J Comput Aided Mol Design 2014 28(3)
21. Barone V, Cossi M (1998) J Phys Chem A 102:1995
22. Langlet J, Claverie P, Caillet J, Pullman A (1988) J Phys Chem 92:1617
23. A series of solvation models designated SM5.x dates from 1998 to 2004. SM6 appeared in 2005. The two most widely-used models as of ca. 2015 are probably: (a) *SM8*, Marenich AV, Olson RM, Kelly CP, Cramer CJ, Truhlar DJ (2007) J Chem Theory Comput 6:2011; Cramer CJ, Truhlar DG, Acc Chem Res 41:760, and (b) *SMD*, Marenich AV, Cramer CJ, Truhlar DG (2009) J Phys Chem B 113:6378; (c) As of mid-2015 the most recent model in the series is *SM12*, Marenich AV, Cramer CJ, Truhlar DG (2013) J Chem Theory Comput 9:609; (d) For information on the frequently-appearing SMx models, including their availability in program suites, check the Minnesota Solvation Models and Solvation Software website: http://comp.chem.umn.edu/solvation/
24. Amovilli C, Floris FM (2015) J Phys Chem A 119:5327

25. (a) Benassi R, Ferrari E, Lazarri S, Spagnolo F, Saladini M (2008) IR, UV, NMR. J Mol Struct 892:168; (b) IR, UV, NMR, EPR: Barone V, Crescenzi O, Improta R (2002) Quantitative structure-activity relationships 21:105; (c) NMR: Sadlej J, Pecul M, Mennucci B, Cammi R (eds) (2007) Continuum Solvation Models Chem Phys 125

26. Foresman JP, Keith TA, Wiberg RB, Snoonian J, Frisch MJ (1996) J Phys Chem 100:16098

27. Cossi M, Rega N, Scalmani G, Barone V (2003) J Comput Chem 24:669

28. The first paper on COSMO: Klamt A, Schüürmann G (1993) J Chem Soc Perkin Trans 2:799

29. (a) Klamt A (1995) J Phys Chem 99:2224; (b) Klamt A, Jonas V, Burger T, Lorenz JCW (1998) J Phys Chem A 102:5074; (c) Klamt A, Diedenhofen M (2015) J Phys Chem A 119:5439

30. (a) COSMOlogic: Imbacher Weg 49, 51379 Leverkusen, Germany. http://www.cosmologic.de/index.php; (b) "COSMO-RS: from quantum chemistry to fluid phase thermodynamics and drug design [With CDROM]", Andreas Klamt, Elsevier, Amsterdam, 2005

31. Spartan is an integrated molecular mechanics, ab initio and semiempirical program with an input/output graphical interface. It is available in UNIX workstation and PC versions: Wavefunction Inc., http://www.wavefun.com, 18401 Von Karman, Suite 370, Irvine CA 92715, USA. As of mid-2009, the latest version of Spartan was Spartan 09. The name arises from the simple or "Spartan" user interface

32. Smith MB, March J (2001) Advanced organic chemistry. Wiley, New York, numerous discussions and references

33. Mo Y, Gao J (2000) J Comput Chem 21:1458

34. Ensing B, Meijer EJ, Bloechl PE, Baerends EV (2001) J Phys Chem A 105:3300

35. Freedman H, Truong TN (2005) J Phys Chem B 109:4726

36. E: Albery WJ, Kreevoy MM (1978) Adv Phys Org Chem 16:87

37. E. Anslyn V, Dougherty DA (2006) Modern physical organic chemistry. University Science Books, Sausalto, p 171

38. Olmstead WN, Brauman JI (1977) J Am Chem Soc 99:4219

39. Bento AP, Solà M, Bickelhaupt FM (2005) J Comput Chem 26:1497

40. Bachrach SM (2014) Computational organic chemistry, 2nd edn. Wiley-Interscience, Hoboken, chapter 6

41. (a) The experimental percentages shown here were deduced from the data in Beak P, Fry FS, Lee J, Steele F (1976) J Am Chem Soc 98:171; (b) Brown RS, Tse A, Vederas JC (1980) J Am Chem Soc 102:1174; (c) Beak P, Covington JB, White JW (1980) J Org Chem 45:1347; (d) Beak P, Covington JB, Smith SG, White JM, Zeigler JM (1980) J Org Chem 45:1354; (e) Beak P (1977) Acc Chem Res 10:186; (f) McCann BW, McFarland S, Acevido O (2015) J Phys Chem A 119:8724

42. (a) Klamt A, Eckert F, Diedenhofen M, Beck ME (2003) J Phys Chem A 107:9380; (b) Klamt A (2009) Acc Chem Res 42:489

43. Kelly CP, Cramer CJ, Truhlar DG (2006) J Phys Chem A 110:2493

44. Cramer CJ, Truhlar DG (2009) Acc Chem Res 42:493

45. Eckert F, Diedenhofen M, Klamt A (2010) Mol Phys 108:229

46. Liptak MD, Shields GC (2001) J Am Chem Soc 123:7314

47. Toth AM, Liptak MD, Phillips DL, Shields GC (2001) J Chem Phys 114:4595

48. Liptak MD, Gross KC, Seybold PG, Feldgus S, Shields GC (2002) J Am Chem Soc 124:6421

49. As of 2015, the latest "full" version (as distinct from more frequent revisions) of the Gaussian suite of programs was Gaussian 09. Gaussian is available for several operating systems; see Gaussian, Inc., http://www.gaussian.com, 340 Quinnipiac St., Bldg. 40, Wallingford, CT 06492, USA

50. (a) Feller D, Peterson KA (2007) J Chem Phys 126:114105; (b) Friesner RA, Knoll EH (2006) J Chem Phys 125:124107

51. http://webbook.nist.gov/chemistry/ quoting (a) Caldwell G, Renneboog R, Kebarle P (1989) Can J Chem 67:661; (b) Fujio M, McIver Jr RT, Taft RW (1981) J Am Chem Soc 103:4017; (c) Cumming JB, Kebarle P (1978) Can J Chem 56:1

52. Hamad S, Lago S, Mejias JA (2002) J Phys Chem A 106:9104
53. Topol IA, Tawa GJ, Burt SK, Rashin AA (1999) J Chem Phys 111:10998
54. Okur A, Simmerling C (2006) Annu Rep Comput Chem 2:97
55. See e.g. (a) Ratkova EL, Palmer DS, Fedorov MV (2015) Chem Rev 115:6312; (b) Luchko T, Gusarov S, Roe DR, Simmerling C, Case DA, Tuszynski J, Kovalenko A (2010) J Chem Theory Comput 6:607
56. Pople JA (1970) Acc Chem Res 3:217
57. Getty SJ, Davidson ER, Borden WT (1992) J Am Chem Soc 114:2085
58. See W. T. Borden, referring to DFT in general, quoted in Bachrach SM (2014) Computational organic chemistry, 2nd edn, Wiley-Interscience, Hoboken; p 281
59. (a) Hrovat DA, Fang S, Borden WT (1997) J Am Chem Soc 119:5253, and references therein
60. Berson JA, Pedersen LD, Carpenter BK (1976) J Am Chem Soc 98:122
61. Crawford RJ, Mishra A (1965) J Am Chem Soc 87:3768
62. Doubleday C Jr (1993) J Am Chem Soc 115:11968
63. Polanyi JC, Zewail AH (1995) Acc Chem Res 28:119
64. Cramer CJ (2004) Essentials of computational chemistry, 2nd edn, Wiley, Chichester; Appendix D
65. (a) Kleier DA, Halgren TA, Hall Jr. JH, Lipscomb WN (1974) J Chem Phys 61:3905, and references therein; (b) Reed AE, Curtiss LA, Weinhold F (1988) Chem Rev 88:899
66. (a) Karlstrom G, Lindh R, Malmqvist P-Å, Roos BO, Ryde, Veryazov V, Widmark P-O, Cossi M, Schimmelpfennig B, Neogrady P, Seijo L (2003) Comput Mater Sci 28:222; (b) Anderssson K, Malmqvist P-Å, Roos BO (1992) J Chem Phys 96:1218
67. Lange H, Loeb P, Herb T, Gleiter R (2000) J Chem Soc Perkin Trans 2:1155
68. (a) Blanksby SJ, Ellison GB (2003) Acc Chem Res 36:255; (b) The enthalpy difference is not strictly an exact measure of bond strength: Treptow RS (1995) J Chem Educ 72:497
69. The activation enthalpy for the opening of cyclopentane, which should be close to the bond enthalpy assuming little enthalpy barrier for reclosing, has been estimated to be 344.8 kJ mol^{-1} (82.4 kcal mol^{-1}): Sirjean B, Glaude PA, Ruiz-Lopez MF, Fournet R (2006) J Phys Chem A 110:12693
70. Alkorta I, Elguero J (2006) Chem Phys Lett 425:221
71. Wang Y, Poirier RA (1998) Can J Chem 76:477
72. Eliel EL, Wilen SH (1994) Stereochemistry of organic compounds. Wiley, New York, p 22
73. Lewars E (2005) J Phys Chem A 109:9827
74. Foresman JB, Frisch A (1996) Exploring chemistry with electronic structure methods, 2nd edn, Gaussian Inc., Pittsburgh, pp 228–236
75. Kazaryan A, Filatov M (2009) J Phys Chem A 113:11630, and references therein
76. (a) Gräfenstein J, Kraka E, Filatov M, Cremer D (2002) Int J Mol Sci 3:360; (b) Cremer D, Filatov M, Polo V, Kraka E, Shaik S (2002) Int J Mol Sci 3:604; (c) Cremer D (2001) Mol Phys 99:1899
77. Bally T, Borden WT (1999) In: Lipkowitz KB, Boyd DB (eds) Reviews in computational chemistry, vol 13. Wiley, New York, Chapter 1
78. (a) Saito T, Yasuda N, Kataoka Y, Nakanishi Y, Kitagawa Y, Kawakami T, Yamanaka S, Okumura M, Yamaguchi K (2011) J Phys Chem A 115:5625; (b) Carpenter BK, Pittner J, Veis L (2009) J Phys Chem A 113:10557; (c) Cramer CJ (2004) Essentials of computational chemistry, 2nd edn. Wiley, Chichester, section 8.5.3
79. Lewars E (2014) Can J Chem 92:378
80. Abe M (2013) Chem Rev 113:7011
81. Yang KR, Jalen A, Green WH, Truhlar DG (2013) J Chem Theory Comput 9:418
82. Ess DH, Cook TC (2012) J Phys Chem A 116:4922
83. A polemic against the common, convenient practice of referring to relativistic mass versus rest mass: L. Okun, Physics Today, June 1989, 30. Relativistic effects like mass increase and time decrease (time dilation) at a velocity v are given by what we may call the "Einstein factor", $\sqrt{(1-v^2/c^2)}$, where c is the velocity of light. The inner electrons of a heavy atom can

move at about 0.3c, so here the mass increase factor is $1/\sqrt{(1 - v^2/c^2)} = 1/\sqrt{(1 - 0.3^2)} = 1$ $/0.95 = 1.05$ or 5 percent. Small but significant

84. Jacoby M (1988) Chem Eng News, March 23, p 48
85. Pyykkö P (1988) Chem Rev 88:563
86. Frenking G, Antes I, Böhme M, Dapprich S, Ehlers AW, Jonas V, Neuhaus A, Otto M, Stegmann R, Veldkamp A, Vyboishchikov SF (1996) In: Lipkowitz KB, Boyd DB (eds) Reviews in computational chemistry, vol 8. VCH, New York
87. Cundari TR, Benson MT, Lutz ML, Sommerer SO (1996) In: Lipkowitz KB, Boyd DB (eds) Reviews in computational chemistry, vol 8. VCH, New York
88. Persina VG (1996) Chem Rev 96:1977
89. Almlöf J, Gropen O (1996) In: Lipkowitz KB, Boyd DB (eds) Reviews in computational chemistry, vol 8. VCH, New York
90. (a) Balasubramanian K (1997) Relativistic effects in chemistry. Part A, theory and techniques. Part B, applications. Wiley, New York; (b) Wilson S (1998) J Am Chem Soc 120:2492
91. Pisani L, Clementi E (1994) J Comput Chem 15:466
92. For a synopsis of the history behind the relativistic equations of Schrödinger and Dirac see Weinberg S (1995) The quantum theory of fields. Cambridge University Press, Cambridge, Volume I, chapter 1, and references therein. This account does not deal specifically with the Dirac-Fock equation
93. Malli GL, Siegert M, Turner DP (2008) Int J Quantum Chem 108:2299
94. Bischoff FA, Klopper W (2010) J Chem Phys 132:094108
95. Karni M, Apeloig Y, Knapp J, Schleyer PvR (2001) Chemistry of organic silicon compounds 3:1 (Patai series "The Chemistry of Functional Groups", Ed. Z. Rappaport, Wiley, New York)
96. Schleyer PVR, Kaupp M, Hampel F, Bremer M, Mislow K (1992) J Am Chem Soc 114:6791
97. Seth M, Faegri K, Schwerdfeger P (1998) Angew Chem Int Ed 37:2493
98. Misra A, Marshall P (1998) J Phys Chem 102:9056
99. Liao M-S, Zhang Q-E (1998) J Phys Chem A 102:10647
100. https://bse.pnl.gov/bse/portal. Accessed 19 May 2015. Basis set exchange: a community database for computational sciences. See (a) Schuchardt KL, Didier BT, Elsethagen T, Sun L, Gurumoorthi V, Chase J, Li J, Windus TL (2007) J Chem Inf Model 47:1045; (b) Feller D (1996) J Comp Chem 17:1571
101. Cramer CJ (2004) Essentials of computational chemistry, 2nd edn. Wiley, Chichester, pp 179–180
102. Cotton FA, Wilkinson G, Gaus PL (1995) Basic inorganic chemistry, 3rd edn, Wiley, New York, p 628
103. Cotton FA, Wilkinson G, Gaus PL (1995) Basic inorganic chemistry, 3rd edn. Wiley, New York; chapter 23
104. Hoffmann R (1982) Angew Chem Int Ed 21:711
105. Cotton FA, Wilkinson G, Gaus PL (1995) Basic inorganic chemistry, 3rd edn. Wiley, New York
106. Cotton FA, Wilkinson G, Murillo CA, Bochmann M (1999) Advanced inorganic chemistry, 6th edn. Wiley, New York
107. Dagani R (2001) Chem Eng News, December 3, p 37
108. Laszlo P, Hoffmann R (2000) Angew Chem Int Ed 39:123
109. Comba P, Hambley TW, Martin B (2009) Molecular modelling of inorganic compounds, 3rd edn. Wiley, Weinheim
110. Ricca A, Bauschlicher CW (1995) Theor Chim Acta 92:123
111. Harvey JN (2009) Abstracts of papers, 237th ACS national meeting, Salt Lake City, UT, March 22–26
112. Frenking G (1997) J Chem Soc, Dalton Trans, 1653
113. Zhao Y, Truhlar DG (2007) Acc Chem Res 41:157
114. Tekarli S, Drummond L, Williams TG, Cundari TR, Wilson AK (2009) J Phys Chem A 113:8607

115. Cramer CJ, Truhlar DG (2009) Phys Chem Chem Phys 11:10757
116. Averkiev BB, Mantina M, Valero R, Infante I, Kovacs A, Truhlar DG, Gagliardi L (2011) Theor Chem Acc 129:657
117. Luo S, Truhlar DG (2012) J Chem Theory Comput 8:4112
118. Luo S, Averkiev B, Ke R, Yang X, Truhlar DG (2013) J Chem Theory Comput 10:102
119. E.g. and references therein: (a) Cankurtaran BO, Gale JD, Ford MJ (2008) J Phys: Condens Matter 20:294208; (b) Longo RC, Gallego LJ (2006) Phys Rev B 74:193409
120. (a) Hoffmann R (1963) J Chem Phys 39:1397; (b) Hoffmann (1964) J Chem Phys 40:2474; (c) Hoffmann R (1964) J Chem Phys 40:2480; (d) Hoffmann R (1964) J Chem Phys 40:2745; (e) Hoffmann R (1966) Tetrahedron 22:521; (f) Hoffmann R (1966) Tetrahedron 22:539; (g) Hay PJ, Thibeault JC, Hoffmann R (1975) J Am Chem Soc 97:4884
121. Genin HS, Lawler KA, Hoffmann R, Hermann WA, Fischer RW, Scherer W (1995) J Am Chem Soc 117:3244
122. Proserpio DM, Hoffmann R, Dismukes GC, Am J (1992) Chem Soc 114:4374
123. Liu Q, Hoffmann R (1995) J Am Chem Soc 117:10108
124. Alemany P, Hoffmann R, Am J (1993) Chem Soc 115:8290
125. Buda N, Flores A, Cundari TR (2005) J Coord Chem 58:575
126. Cooney KD, Cundari TR, Hoffman NW, Pittard KA, Temple MD, Zhao Y (2003) J Am Chem Sc 125:4318
127. Zakharian TY, Coon SR (2001) Comput Chem 25:135
128. Goh S-K, Marynick DS (2001) J Comput Chem 22:1881
129. Bosque R, Maseras F (2000) J Comput Chem 21:562
130. McNamara JP, Sundararajan M, Hillier IH (2005) J Mol Graph Modell 24:128

Chapter 9
Selected Literature Highlights, Books, Websites, Software and Hardware

The yeoman work in any science...is done by the
experimentalist, who must keep the theoretician honest.
Michio Kaku, Professor of theoretical physics, City
University of New York.

Abstract Specific applications of some concepts and methods are discussed. Information on the literature is provided, and the merits and capabilities of various software packages are presented. The chapter concludes with a note on hardware developments.

9.1 From the Literature

A small smorgasbord of published papers will be discussed, to show how some of the things that we have seen in previous chapters have appeared in the literature. The four topics of this section (oxirene, nitrogen pentafluoride, pyramidane and nitrogen polymers), and several others, are addressed in more detail in another book [1].

9.1.1 Molecules

9.1.1.1 Oxirene. To Be or Not to Be

Let's start with what looks like a simple problem: what can computational chemistry tell us about oxirene, oxacyclopropene (Fig. 9.1)? Note that in the literature the term oxirene is occasionally misused to denote an oxirane (an epoxide), either through a quirk in nomenclature concerning the position of a double bond [2a] or through simple error [3]. The oxirene literature has been reviewed in detail to 1983 [2a] and from 1984 to 2007 [2b]. Labelling one of the carbons of a diazo ketone $(R\text{-}C(N_2)\text{-}CO\text{-}R)$ can lead to a ketene (Wolff rearrangement) with scrambled labelling. After excluding the possibility of scrambling in the diazo compound, this indicates that an oxirene species is formed. However, this does not tell us
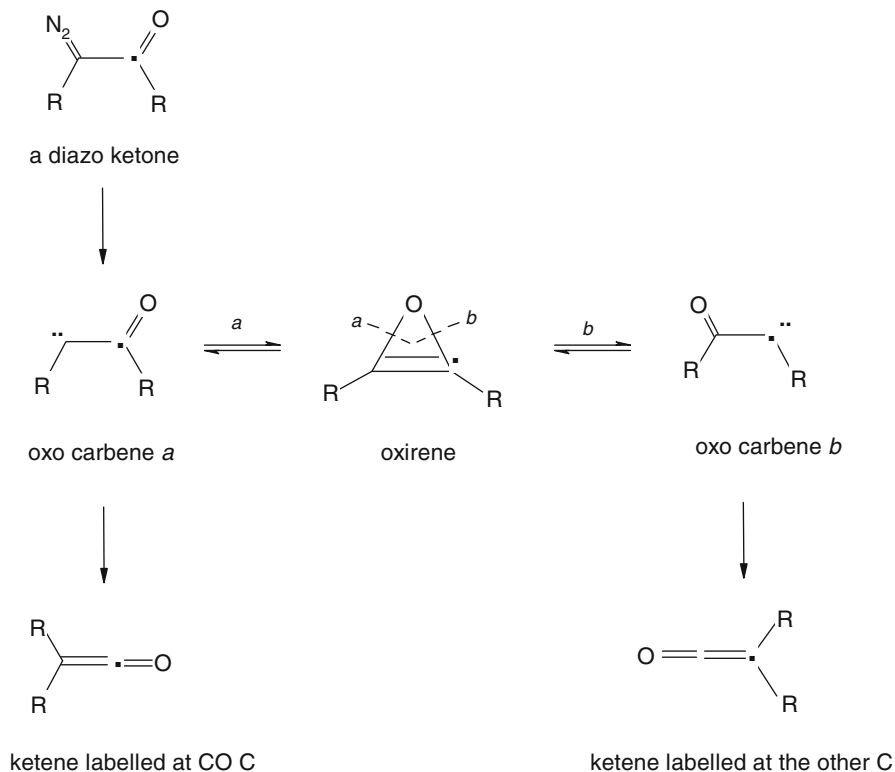
Fig. 9.1 Generating an oxo carbene (a "ketocarbene") from a labelled diazo ketone sometimes leads to a ketene in which the label is scrambled. This indicates that a species with the symmetry of oxirene is formed

whether this species is an intermediate or merely a transition state (Fig. 9.2). A straightforward way to try to answer this question would seem to be to calculate the frequencies, at the level used to optimize the structure, and see if there are any imaginary frequencies–a relative minimum has none, while a transition state has one (Chap. 2, Sect. 2.5). In a preliminary investigation [4] Schaefer and coworkers found that oxirene was a minimum with the Hartree-Fock (SCF) method, and also when electron correlation was taken into account (Chap. 5, Sect. 5.4) with the CISD and CCSD methods, using double-zeta basis sets (Chap. 5, Sect. 5.4.3). However, in going from HF to CISD to CCSD, the ring-opening frequency fell from 445 to 338 to 262 cm^{-1}, which was said to be a much steeper drop than would be expected. A very comprehensive investigation (titled "To be or not to be") [5], in which the frequencies of oxirene were examined at 46 (!) different levels, failed to definitively settle the matter: even using CCSD(T) calculations with large basis sets the results were somewhat quirky, and in fact of the six highest levels used, three gave an imaginary frequency and three all real frequencies. At the two highest levels the ring-opening frequency was real, but uncomfortably low (139 and 163 cm^{-1}). Although at all of the five DFT levels explored in [5] oxirene was a transition
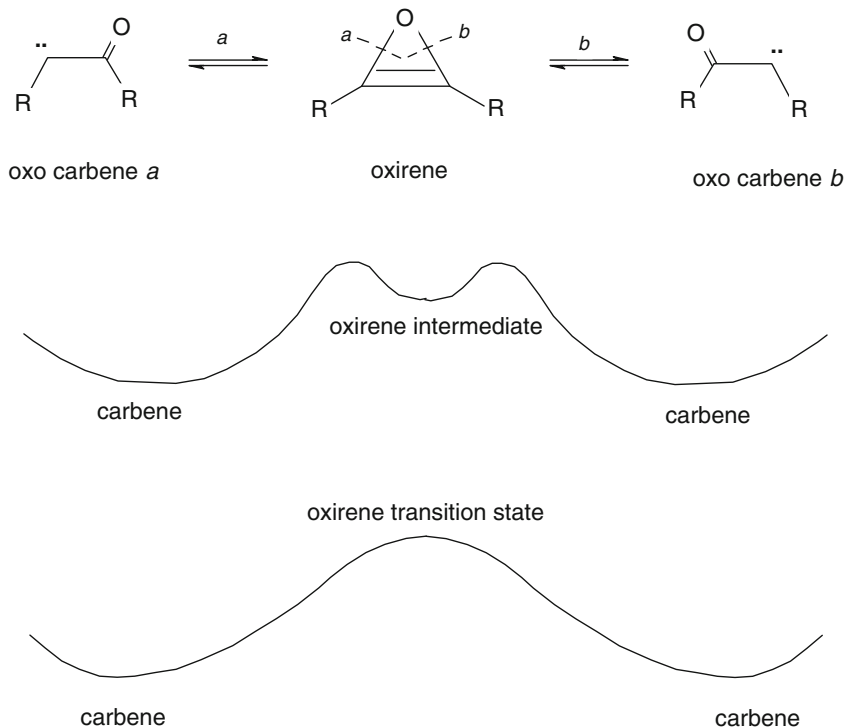
Fig. 9.2 A species with the symmetry of an oxirene scrambles the label in an oxo carbene. But this does not tell us whether the oxirene is an intermediate or merely a transition state

state with an imaginary ring-opening vibrational mode, functionals have been found which declare it a minimum with some basis sets. The B97-2 [6] and the PBE0 [7] functionals award oxirene local minimum status and B97-2 predicts a C_2H_2O potential energy surface reasonably close to that from much more "expensive" ab initio CCSD(T) calculations. Wilson and Tozer [6] found with B97-2 and a triple-zeta correlation-consistent basis that oxirene isomerizes with a barrier of 1.3 kJ mol^{-1} (cf. CCSD(T): 1.8 kJ mol^{-1}) to the carbene, which lies 8.6 kJ mol^{-1} (cf. CCSD(T): 2.1 kJ mol^{-1}) lower (Fig. 9.1). Mawhinney and Goddard [7] found that although very many of their tested functional/basis combinations gave an imaginary frequency, a few found oxirene to be a minimum. In fact, the PBE0 functional found it to be a minimum with 11 of the 12 bases tried. They did not explore the C_2H_2O surface, checking only the energy of the oxirene structures compared to ketene (ca. 335 kJ mol^{-1} in all cases), but with big basis sets ring-opening frequencies and geometries were similar to those from high-level (CCSD(T)) ab initio calculations. The speed advantage over CCSD(T) tends to make DFT attractive for such studies, but experienced workers might still tend to confer more trust on high-level ab initio calculations ("...we try to validate the

results by comparison with those from ab initio calculations" [8]), even when the DFT functional is not empirical, as with PBE0, above.

A flash photolysis study of diazoketones (1995) concluded that "Our experiments neither implicate nor disqualify oxirene as an intermediate" [9]. In more recent work (2008) ultrafast photolysis of a potential diazo ketone precursor of p-biphenylmethyloxirene failed to detect the oxirene, the UV absorption of which could, however, have been hidden by another band [10], but in a combined experimental/computational (ab initio and molecular dynamics with DFT) study, flash thermolysis of a formal Diels-Alder adduct was interpreted as affording acetylmethyloxirene and benzene [11]. A detailed computational study of the ozonolysis of ethyne skirted the question of the involvement of oxirene by saying that it "will easily revert to [the carbene]; therefore, the oxirene route was not further investigated in this work." [12]. Oxirene was among several $C_xH_yO_z$ isomers subjected to high-level ab initio energy and frequency calculations in connection with a suspected correlation between relative energy and detection in interstellar space [13] (where it has not been detected); it was found to be a local minimum. In another study it was one of 106 molecules in a high-level protocol for calculating atomization energies, but a frequency check of its status was not reported [14]. It remains a notorious case of an unsolved computational "existence problem"; a cautious verdict is that the heterocycle hovers on the edge of reality.

9.1.1.2 Nitrogen Pentafluoride. Warranted Optimism?

Nitrogen pentafluoride (this has been reviewed to 2007 [15]) represents an interesting contrast to oxirene. Oxirene is, on paper, a reasonable molecule; there is no obvious reason why, however unstable it might be because of antiaromaticity [16] or strain [17], it should not be able to exist. On the other hand, NF_5 defies the hallowed octet rule; why should it be more reasonable than, say, CH_6? Yet a comprehensive computational study of this molecule by Bettinger et al. left "little doubt" that it is a (relative) minimum on its potential energy surface [18]. The full armamentarium of post-HF ab initio methods, CASSCF, MRCI, CCSDT, CCSD(T), MP2 (Chap. 5, Sect. 5.4) and DFT (Chap. 7) was employed here, and all agreed that D_{3h} (Chap. 2, Sect. 2.6) NF_5 is a minimum. Nevertheless, it was unclear that this paper (1998) fully disposed of earlier (1989–1992) reservations about the ability of nitrogen to bear five fluorines. Christe and coworkers concluded that "the lack of pentacoordinated nitrogen species is due mainly to steric reasons", from their finding that attack of HF_2^- (evidently a surrogate for F^-) on NF_4^+ occurs, within experimental error, only on F and not on N [19]. This experiment dampened, but did not negate, hope arising from ab initio computations by Ewig and Van Wazer indicating that NF_5 [20] and even NF_6^- [21] may be able to exist. Comments by Christe and by Van Wazer and Ewig in letters to C&EN [22] showed that each was at the time unpersuaded by the position of the other. Reinforcing their studies with NF_4F [19], Christe and Wilson were led by experiment and theoretical

arguments to conclude that "covalent NF_5 should suffer from severe ligand-crowding effects that would make its synthesis very difficult" [23]. The difficulty of accurately accounting computationally for crowding around a central atom [24] was evidently the reason for doubts[1] about the possibility of making nitrogen pentafluoride, but these reservations have been overcome, evidently by reconsideration of the work of Bettinger et al.[2] As of mid-2015, NF_5 remains unknown.

9.1.1.3   Pyramidane. A Realistic Goal

If oxirene "should" exist and NF_5 "should" not, what are we to make of pyramidane (Fig. 9.3)? This molecule contradicts the traditional paradigm [25] of tetracoordinate carbon having its bonds tetrahedrally directed: the four bonds of the apical carbon point toward the base of a pyramid. Note that pyramidane has been misnamed in the literature at least once: in a study of bond dissociation energies [26] it was called tetrahedrane, but this latter is $(CH)_4$, a pyramidal tricyclobutane with a triangular base and a hydrogen on each carbon, while pyramidane is $C(CH)_4$, a pyramidal tetracyclopentane with a square base and one unadorned carbon. Pyramidane has been reviewed to 2007 [27].

Part of the calculated [28] potential energy surface of pyramidane is shown in Fig. 9.3. To improve the accuracy of the relative energies, the MP2 geometries were subjected to single-point calculations (Chap. 5, Sect. 5.5.2) using the CCSD(T) method (Chap. 5, Sect. 5.4.3), with the results shown (Fig. 9.3). At this level pyramidane is predicted to be a relative minimum with a barrier of $100\,kJ\,mol^{-1}$ for its lowest-energy isomerization path, to the tricyclic carbene, which lies $87\,kJ\,mol^{-1}$ above it. This presents us with the surprising possibility that the exotic hydrocarbon may be isolable at room temperature, the threshold barrier for being isolable at room temperature being about $100\,kJ\,mol^{-1}$ [29]. Other calculations indicate that pyramidane and certain other C_5H_{2n} species are local minima (at least in the singlet state) [30].

Other properties of pyramidane, including ionization energy and electron affinity (Chap. 5, Sect. 5.5.5), heat of formation (Chap. 5, Sect. 5.5.2.2.3), and NMR spectra (Chap. 5, Sect. 5.5.5) were calculated [28b]. The pyramidane CH bond dissociation energy was calculated at $487\,kJ\,mol^{-1}$; compare this with the experimental 440 and $445\,kJ\,mol^{-1}$ for cubane and cyclopropane [26]. This accords with expectation in that increasing strain in the framework caused by increasing p-character of the carbon CC bonds leaves more s-character for the CH bonds; an sp^2 bond, for example (33 % s-character) is stronger than an sp^3 bond (25 % s-character) [31].

---

[1]Personal communication from Professor Christe, 2007 April 24.

[2]Personal communication from Professor Christe, 2010 April 16; he concludes that NF_5 can exist, although "the synthesis would be difficult".

$kJ\ mol^{-1}$
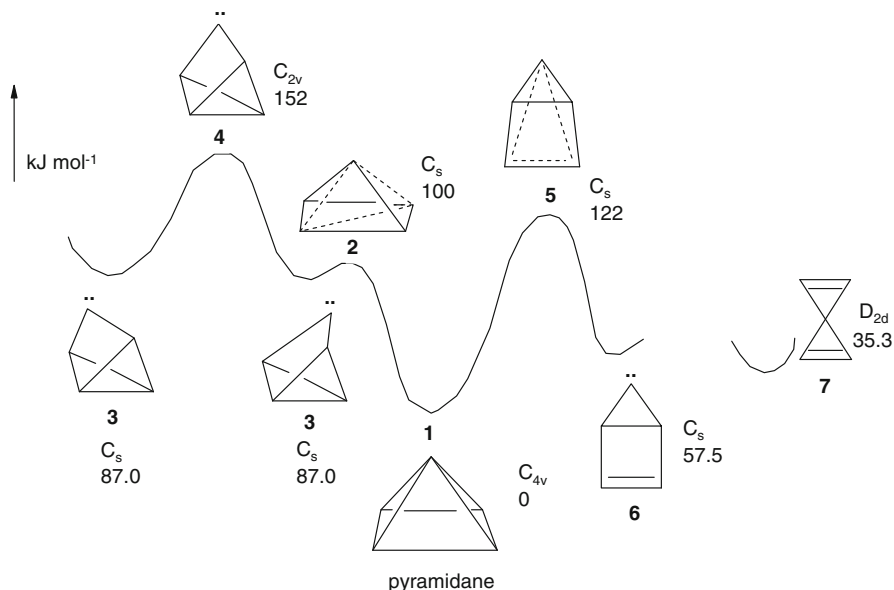
Fig. 9.3 (Part of) the pyramidane potential energy surface, CCSD(T)/6-31G*//MP2(fc)/6-31G* calculations. This is similar to the PES in [28b] and in the second edition of this book, in which QCISD(T)/6-31G*//MP2(fc)/6-31G* was used, and very close to the CCSD(T)/DZP surface of Kenny et al. [28c], except that there spiropentadiene **7** is 16 kJ mol^{-1} higher than here and 3-ethynylcyclopropene plus two ring-opened structures are also shown, lower than **1** by 64, 128 and 175 kJ mol^{-1}; unlike **1–7** above, these three do not bear a simple connectivity relationship to pyramidane

A notable advance in pyramidane chemistry was the synthesis of analogues with germanium and tin (germa- and stannylpyramidanes) as the apical atoms [32]. These two compounds, Ge[C$_4$(SiMe$_3$)$_4$] and Sn[C$_4$(SiMe$_3$)$_4$], which were stable, were analyzed computationally and, in particular, compared to the (unknown) parent C(CH)$_4$. Extended Hückel calculations (Chap. 4, Sect. 4.4) were useful in this "C, Ge, Sn" correlation. The conclusion, supported by experiment, was that the bonding to the base with Ge or Sn is weak and the molecules are significantly ionic, of type M^{++}C$_4$R$_4$$^{--}$. One might suspect that pyramidane itself will be less ionic, with stronger apex-to-base bonds, carbon being less metallic than germanium or tin. The synthesis of a pyramidane C(CR)$_4$ is earnestly awaited.

9.1.1.4   Polynitrogens. More Than a Computational Playground?

There has in recent years been considerable interest in the possibility of making allotropes of nitrogen with more than two atoms per molecule. Nitrogen polymers are interesting because to any chemist with imagination the idea of a form of pure nitrogen that you might hold in your hand at room temperature is fascinating, and

because (which might be bad for your hand, depending on the kinetics) any such compound would be thermodynamically very unstable with respect to decomposition to dinitrogen. The challenge is to identify computationally a realistic candidate for synthesis and to make it. A faint hope is that a compound (an allotrope) may be found with enough kinetic stability to be handled at room temperature. Such a substance is potentially a useful high-energy-density material. Polynitrogens have been reviewed to 2007 [33].

Interestingly, almost all the work reported on N_x polynitrogens (consisting solely of nitrogen) has been computational rather than experimental. In *experimental* work, the acyclic N_5 cation has been made [34–37]), and the pentaaza analogue of the cyclopentadienyl anion has been detected by mass spectrometry [38, 39]; its generation in solution was claimed [40], challenged [41], and eventually "proved unequivocally" by examination of its labelled decomposition products (dinitrogen and azide ion) in redesigned experiments [42]. The N_5 cation is stable in the sense that salts of it can be isolated at room temperature, but it explodes capriciously. The N_5 anion was unstable at $-40\ ^{\circ}C$ [42] and was not isolated or even seen spectroscopically by ^{15}N NMR. These two species, and azide ion, known since 1890 [43], are the only polynitrogens to have been prepared. We use "prepared" advisedly for N_5^-, and pass over N_x cations that have been observed only in mass spectra [33] and a polymer that requires high pressure to exist [44], a milieu as unfriendly as that in a mass spectrometer.

Perhaps the first serious computational study of nitrogen oligomers was by Engelke, who studied the N_6 analogues of the benzene isomers in (Fig. 9.4), first at the uncorrelated [45] then at the MP2 [46] level. The uncorrelated calculations suggested that **1–5** were "stable", i.e. *kinetically* stable, although thermodynamically much higher in energy than dinitrogen. However, on the MP2/6-31G* potential energy surface **1** is a hilltop (Chap. 2, Sect. 2.2) and **5** is a transition state (Chap. 2, Sect. 2.2). This illustrates the not-so-rare fact that optimistic predictions at low levels of theory may not be sustained at higher levels. Noncorrelated ab initio, and in particular, semiempirical (Chap. 6) calculations, tend to be too permissive in granting reality to exotic molecules. Indeed, hexaazabenzene is almost certainly at best only marginally capable of existence [47]. Hundreds of computations on polynitrogens have been published; a representative survey of these (to 2007) can be found in [33].

1	**2**	**3**	**4**	**5**
benzene	Dewar benzene	benzvalene	prismane	bicyclopropenyl
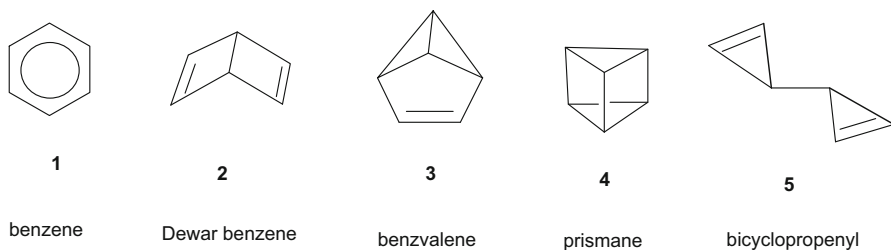
Fig. 9.4 Nitrogen analogs $(CH \rightarrow N)$ of these molecules have been investigated computationally

Computational papers continue to dominate the polynitrogens field. Indeed, if one insists that a polynitrogen contain *only* nitrogen, then there appear to have been no published attempts to make an $N_x(x > 3)$ species since ([34–42] above) these: (a) the synthesis of the N_5 cation (1999), (b) the synthesis of the N_5 anion (2008), and (c) the reaction of N_5^+ with N_3^- (2004), which did not lead to the isolation of N_8; (a), (b) and (c) have been reviewed in detail [33]. If we relax the constraint of strict elemental uniformity, there is an abundance of reports of the synthesis of very nitrogen-rich compounds. Silicon tetraazide (86 % nitrogen by weight) is said to have been known since 1954 [48], and carbon tetraazide (93 % nitrogen by weight) was reported in 2007 [49]. The group 15 triazides have been investigated computationally, and bismuth triazide (only 45 % nitrogen by weight) has been reported, but an attempt to make nitrogen triazide failed [50]. Particularly since ca. 2000 many nitrogen-rich organic compounds have been reported. These are almost all made by attaching nitro, or more to the point azide, groups to triazole or tetrazole (tri- or tetraazacyclopentadiene) rings, giving compounds like this azido tetrazole derivative C_2N_{14} (89 % nitrogen by weight) [51]. Very active here is the group of Klapötke; their work to ca. 2011 has been summarized [52].
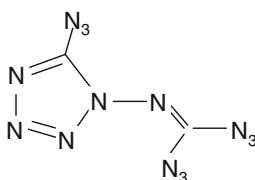
Returning to computations, many of the compounds examined since the pioneering studies on small N_x species like N_6 [33] are structurally very baroque and although perhaps not intimidating to the theorist, synthetic chemists would likely dismiss them as unlikely ever to be made, even in nanogram amounts. Among these imaginative studies are computations on a pentagonal bipyramid $(C_5)_2$ capped top and bottom with N_{15} dodecahedrons, i.e. $C_{10}N_{30}$ [53], and cylindrical N_x structures, i.e. N_{66} [54]. Particularly active in computational studies of polynitrogens with little or no carbon has been the group of Strout. Since ca. 2002 they have examined cage structures to find features that might stabilize them kinetically: the strategic placement of carbon and the subtle role of cage curvature (cylinder versus spheroid) [55]. These cage molecules are all thermodynamically unstable with respect to dinitrogen, of course, which is what we want for a high-energy explosive or propellant (a high-energy-density material, HEDM), and these relative stabilities are relatively easy to calculate; kinetic instability, which we do not want, is difficult to quantify, and there seem to have been no attempts to put a number on the barrier to decomposition for most of these. In those cases where the computations have indeed come to grips with transition states (useful information on barriers can be obtained from homolytic dissociation energies: see NCNNCN etc., below) for decomposition and a barrier has been calculated, the calculated activation energy is too low for any of the substances to be useful as a HED

material. Examples are some N_{12} acyclic, monocyclic, pentazole and small cage compounds, where the highest barrier in the set was 61 kJ mol^{-1} (14.5 kcal mol^{-1}) [56]. Experience shows that the threshold barrier for stability at room temperature is ca. 100 kJ mol^{-1} [29] . This author's intuitive view is that all these cage compounds would be fragile substances, to be handled at one's peril.

In contrast, the Strout group has identified a class of structures that differ from cages in offering two satisfying possibilities: vulnerability to synthesis and kinetic stability. These are nitrogen chains (single and double bonds are drawn here simply in accord with ordinary valence rules) capped at the ends with cyano (nitrile) groups [57].

These NC(N$_2$)$_x$CN compounds ("dicyanopolydinitrogens") are clearly more realistic synthetic objectives than cage structures. Increased stability was anticipated because thermal decomposition of nitrogen chains seems to start at the ends, and capping these with CN groups was expected to inhibit this [57]. The impetus to study the longer chains was ascribed to a study of NC(N$_2$)CN [58], where stability was estimated by calculating the energy for dissociation to various likely products, like NCNN + CN; this should be valid because the barrier to homolytic cleavage of a bond should be close to its dissociation energy. For NCNNCN the dissociation energies for formation of likely products were endothermic, e.g. in the range 293–339 KJ mol^{-1} (70–81 kcal mol^{-1}) for CCSD(T)/cc-pVTZ single point (Chap. 5, Sects. 5.3.3 and 5.4.2) on MP2/cc-pVTZ geometries, depending on the dissociation products. In contrast, the N_4C_2 isomer of NC(NN)CN, NNNCCN, has a low-energy homolytic cleavage mode, the loss of the terminal NN as dinitrogen: all computational levels used gave for this an *exothermic* reaction with an energy drop of ca. 400 kJ mol^{-1} (ca. 100 kcal mol^{-1}). Now, NCNNCN, commonly called azodicarbonitrile, is a known compound, first made in 1965 [59]. It is an orange-red volatile crystalline solid. The vapor decomposes only slowly at 100 °C, but the solid detonates when shocked. So NCNNCN is thermally stable at room temperature, but the solid, whose behaviour is harder to evaluate theoretically, is shock-sensitive. Without knowing the numerical parameters of this (like, e.g. the weight dropped from a certain height needed to incite detonation) one cannot definitely judge the safety of azodicarbonitrile as a HEDM. With theoretical (the experimental properties of azodicarbonitrile were not mentioned in [58]) knowledge obtained about the first member, the series NC(N$_2$)$_x$CN, x = 1-5(N_4C_2-$N_{12}C_2$), was examined [57]. The geometries and enthalpies of formation were calculated, and the singlet electronic states were shown to be well-favored over the triplets. The energy for dissociation of N_6C_2 at bonds 1, 2, and 3 (taking bond 1 as that joining atoms 2 and 3 from the end) was calculated. The results for the three modes was (products, energies in kJ mol^{-1}): NCN$_4$ + CN, 431; NCN$_3$ + NCN, 130; 2 NCN$_2$, 164. Since even the lowest dissociation energy here is distinctly above 100 kJ mol^{-1}

[29], it was concluded that this compound (and the others in the series) should show good resistance to decomposition. From the experimental behaviour of NCNNCN (above), and the likely resistance of all these molecules to unravelling starting from the end, there does seem to be a real chance that they would be stable at room temperature in the absence of a solid-state proclivity for detonation. Perhaps concentrated solutions in an inert solvent would have HEDM characteristics. Their synthesis poses an interesting challenge.

9.1.2 Mechanisms

We have seen, above, that computational chemistry can sometimes tell us with good reliability if a molecule can exist. It can also often indicate the stability of a molecule. "Stable" can be used in chemistry in two senses: it is sometimes used to mean resistant to isomerization or unimolecular dissociation, and sometimes resistant to attack by another molecule. Oxirene (above) is not stable (if it can exist at all) because it isomerizes so readily, while cyclobutadiene is not stable because it enters so readily into bimolecular reactions (some might say that it is stable but highly reactive) [60]. For the four cases above (oxirene, nitrogen pentafluoride, pyramidane, polynitrogens) we focussed on stability toward isomerization or unimolecular reaction, to see if these compounds, suitably sequestered from attack if necessary, could be made. Here we take a look at the ability of computational chemistry to shed light on reactions involving chemical encounters, reactions between two molecules. This is the main aspect of the study, by experiment and theory, of reaction mechanisms (admittedly, unimolecular processes too have received considerable mechanistic scrutiny, largely in connection with the theory of orbital symmetry [61]).

9.1.2.1 A Call for Caution in Applying Computational Chemistry to Reaction Mechanisms: The Morita-Baylis-Hillman Reaction

This example shows what computational chemistry can *not* do, at last at present. The Morita-Baylis-Hillman reaction (see Plata and Singleton [62]) is the nucleophile-catalyzed addition of an alkene bearing an electron-withdrawing group (EWG) to the carbonyl carbon of an aldehyde forming an allylic alcohol:
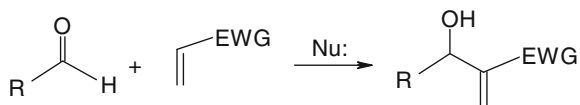
The essential process here is that the nucleophile effects a Michael addition on the alkene, placing charge on the carbon bearing the EWG (which can delocalize the charge into this group thus stabilizing it), and as shown below the zwitterion

(assuming the nucleophile was neutral) then nucleophilically attacks the aldehyde in an aldol reaction, forming a new CC bond. Protonation of the oxygen and deprotonation of the carbon bearing the EWG creates a carbanion which effects elimination of the nucleophile, regenerating the CC double bond:
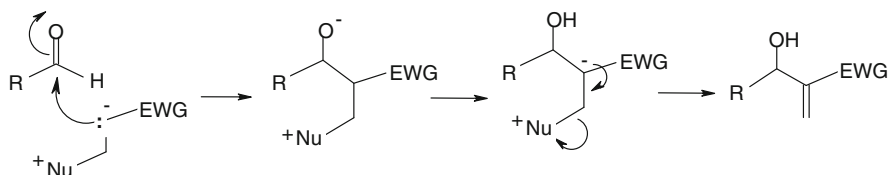
The devil is in the details. For example, the conversion of the alkoxide anion to the carbanion was widely believed to occur by a "proton-shuttle" mechanism in which a molecule of (e.g. product) alcohol, ROH here, transferred a proton to oxygen and simultaneously removed a proton from carbon:
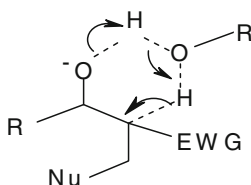
The spur for proposing this elegant-looking six-membered transition state was the fact that the reaction is autocatalyzed. An impressively detailed experimental study was sobering (as reality checks sometimes are): "The most notable prediction of the many computational studies, that of a proton-shuttle pathway, is refuted in favor of a simple but computationally intractable acid-base mechanism" [62]. The tone of the paper is respectful toward computational chemists, but where this reaction, and by implication complex multistep reactions, are concerned, words are not minced in expressing the conclusions. Discrepancies between experiment and theory are huge and vary widely with the computational method, yet these studies "have not been considered falsified by extreme inaccuracies in predictions": inaccuracies that include errors in the energy of the proton-shuttle transition state correspond to rate errors of a factor of up to 35 orders of magnitude (and 10^{35} is a very big number). A major problem in the theoretical studies here seems to be the accurate calculation of solvent entropy changes. The computational studies were "arguably more misleading than enlightening", and may have added nothing to what was already known from experiment. Plata and Singleton invoked for those studies a stinging aphorism attributed to Wolfgang Pauli concerning work so divorced from reality that one can't even pin down where it goes wrong: for this reaction the computations were "not even wrong" [63]. A short report on the matter quotes a computational and an experimental chemist who concur in cautioning care in cases like this [64]. It should be noted that the deficiencies of the computational work here arise from trying to do quantitative rate calculations on a complex

multistep reaction in solution. Calculations on an isolated molecule, or a reaction profile for a sharply defined one-step (reactant, transition state, product) process can be very reliable; an example is the Diels-Alder reaction, below). This lesson suggests that the prime architect of one of the most useful computational tools, the AM1 method (Chap. 6), may have been guilty of hubris when he said in effect that computational chemistry was superior to experiment in deciphering reaction mechanisms: Dewar questioned "whether the mechanism of *any* organic reaction was really known" before the advent of computational chemistry [65]. His skepticism was engendered by the difficulties and ambiguities in studying very transient intermediates, and the impossibility (at the time at least) of observing transition states.

9.1.2.2   The Diels-Alder Reaction. A One- or Two-Step Dance?

This is one of the most important reactions in all of organic synthesis, as it unites two moieties in a predictable stereochemical relationship, with the concomitant formation of two carbon-carbon bonds (Fig. 9.5) [66]. The reaction has been used in the synthesis of complex natural products, for example in an efficient synthesis of the antihypertensive drug reserpine [67]. Such a reaction seems to be well worth studying.
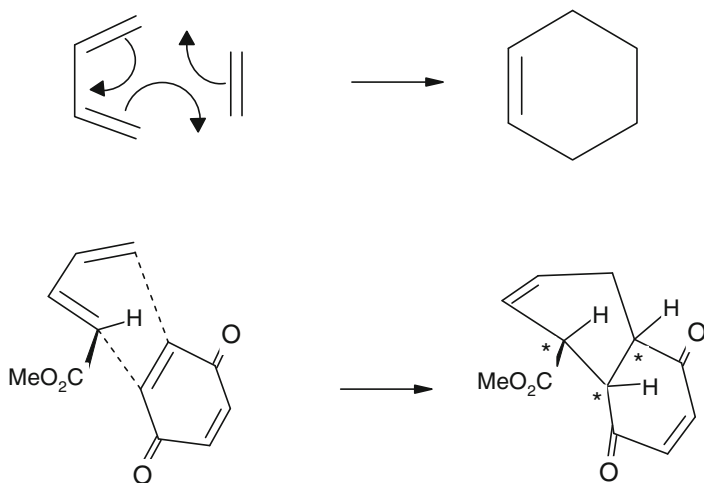
Fig. 9.5   The prototypical Diels-Alder reaction is that between 1,3-butadiene and ethene, to form cyclohexene. The Diels-Alder reaction has been used in the synthesis of complex natural products; above, methyl 2,4-pentadienoate reacts with 1,4-benzoquinone to form an intermediate in the synthesis of the drug reserpine. In a one-pot reaction two carbon-carbon bonds are made and three chiral centers (*) are created with the correct relative orientations (i.e. essentially one diastereomer is formed)

The Diels-Alder reaction and related pericyclic reactions, which can be treated qualitatively by the Woodward-Hoffmann rules (Chap. 4, Sect. 4.3.5.1), have been reviewed in the context of computational chemistry [68]. The reaction is clearly nonionic, and the main controversy was whether it proceeds in a concerted fashion as indicated in Fig. 9.5 or through a diradical, in which one bond has formed and two unpaired electrons have yet to form the other bond. A subtler question was whether the reaction, if concerted, was synchronous or asynchronous: whether both new bonds were formed to the same extent as reaction proceeded, or whether the formation of one ran ahead of the formation of the other. Using the CASSCF method (Chap. 5, Sect. 5.4.3), Li and Houk [69] concluded that the butadiene-ethene reaction is concerted and synchronous, and chided Dewar and Jie [70] for stubbornly adhering to the diradical (biradical) mechanism.

The favoring of a diradical mechanism here seems to be an artifact of semi-empirical methods (Chap. 6) and unrestricted HF methods (Chap. 5, Sects. 5.2.3.5 and 5.2.3.6.5); see reference 11 in [69]. A DFT (Chap. 7) study also strongly supported the concerted mechanism [71].

9.1.2.3 Abstraction of H from Amino Acids by the OH· Radical. Unavoidable Complexity?

This reaction seems more esoteric than the Diels-Alder, and although not "used", may be very important. Proteins are linked amino acid residues, and oxidation of proteins by hydroxyl radicals play a role in Alzheimer's disease, cancer, and heart disease. The initial step in the destruction or modification of proteins by hydroxyl radical is likely to be abstraction of a hydrogen atom from the α–C (Fig. 9.6). In a very thorough study using MP2 (Chap. 5, Sect. 5.4.2) and DFT (Chap. 7), Galano et al. calculated the geometries of the species (amino acid-OH complexes, transition states, and amino acid radicals) involved in the reactions of glycine and alanine (Fig. 9.6, R=H and CH_3, respectively) [72]. The rate constants were calculated in a thorough way, using partition functions to calculate the preexponential factor (cf. Chap. 5, Sects. 5.5.2.1 and 5.5.2.3.4), and even accounting for tunnelling and taking into consideration that some "vibrations" are really rotations. This paper provides a good account of how computational chemistry can be used to calculate absolute rate constants for reactions of molecules of moderate size.
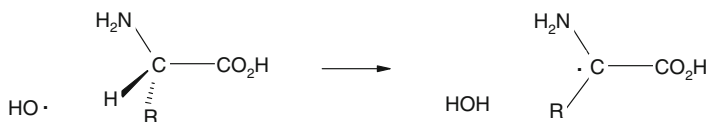
Fig. 9.6 Abstraction of a hydrogen atom from the α–C of an amino acid by hydroxyl radical has been investigated computationally

9.1.3   Concepts

There are some very basic concepts in chemistry that have proved to be helpful in rationalizing experimental facts, and which have been taught for about the last 50 years, but which have nevertheless been questioned in the last couple decades or so; an example is the role of resonance in stabilizing species like carboxylate ions. Some newer concepts, intriguing but not as traditional, have also been scrutinized and questioned, e.g. homoaromaticity.

9.1.3.1   Resonance vs. Inductive Effects

The traditional explanation of the fact that carboxylic acids are much stronger acids than alcohols is that resonance stabilization of the conjugate base, which is more important than the charge-separation resonance in the acid, stabilizes $RCOO^-$ relative to RCOOH, while resonance does not figure in either an alcohol or its conjugate base. This traditional wisdom was apparently first questioned by Thomas and Siggel, on the basis of ab initio calculations and photoelectron spectroscopy [73]. They concluded that the relatively high acidity of carboxylic acids is largely inherent in the acid itself, as a consequence of the polarization of the COOH group caused by the electronegative carbonyl group pulling electrons from the hydrogen atom, an electrostatic phenomenon. This idea was taken up by Streitwieser and applied to other acids, e.g. nitric and nitrous acids, dimethyl sulfoxide and dimethyl sulfone [74]. The results for carbonyl compounds were interpreted in accord with another iconoclastic idea, namely that the carbonyl group is better regarded as $>C^+–O^-$ than as $>C=O$ [75]. This polarization interpretation was arrived at largely with the aid of atoms-in-molecules (AIM) analysis of the electron populations on the atoms involved (Chap. 5, Sect. 5.5.4.5), and a simpler variation of AIM (the projection function difference plot) developed by Streitwieser and coworkers [76]. Work by others also supports the view that it is "initial-state electrostatic polarization" that is largely responsible for the acidity of several kinds of compounds, including carboxylic acids [77]. However, Burk and Schleyer asserted that the Thomas/ Siggel method at least [73], which initiated giving credit to electrostatic destabilization of the acid, was not valid because their "relaxation energy" term, which supposedly measured electron delocalization or resonance, does not correspond to what chemists normally mean by those terms [78]. Other studies, albeit with different methodologies, nevertheless assigned major importance to electrostatic factors: 75 % for CH_3COOH, using isodesmic reactions with ab initio energies [79], and roughly 62–65 % for HCOOH, using the effect of separating the CO and OH by $–CH=CH–$ groups and of rotating the CO relative to the rest of the conjugated system, with DFT energies [80]. Around the same time as [79] and [80] lent support to the importance of electrostatic destabilization of the acid, Exner and Čársky [81], using ab initio calculations and isodesmic reactions, published a "rebuttal", contending that "In our opinion, there are no doubts

that the acidity of carboxylic acids is related to the low energy of the anion, not to a high energy of the acid molecule", although "the importance of resonance [in the anion] can only be estimated", not quantified; they conclude it is a minor factor. They conclude, however, that "in water" (all these publications focus on the gas phase, to pinpoint effects inherent to the unencumbered acid) "resonance is the deciding factor." They go on to say that "The whole concept of resonance seems at present somewhat obsolete...". It is relevant to note that resonance/delocalization does not always stabilize a species [82]. The resonance concept has been "philosophically" examined by Shaik [83]. From all this it appears that consensus has not been reached on the cause of the enhanced acidity of carboxylic acids compared to alcohols, and one might almost wonder if to some extent the role of electrostatics versus resonance is a metaphysical question.

9.1.3.2   Homoaromaticity

Aromaticity [84] is associated with the delocalization of (in the simplest version) π electrons (the role of these π electrons in imposing symmetry on the prototypical aromatic species, benzene, is being questioned, but that is another story [85]). A Hückel number of cyclically delocalized electrons confers aromaticity on a molecule (Chap. 4, Sect. 4.3.5.2). The idea behind homoaromaticity (homologous aromaticity) is that if a system is aromatic, then if we interpose one or more atoms between adjacent p orbitals of the π system, provided overlap is not lost the aromaticity may persist (Fig. 9.7). While there is little doubt about the reality of homoaromaticity in ions, neutral homoaromaticity has been elusive [86].

One molecule that might be expected to be homoaromatic, if the phenomenon can exist in neutral species, is triquinacene (Fig. 9.7): the three double bonds are held rigidly in an orientation which appears favorable for continuous overlap with concomitant cyclic delocalization of six π electrons.

Indeed, its potential aromaticity was one of the reasons cited for the synthesis of this compound [87]. A measurement of the heat of hydrogenation of triquinacene found a value 18.8 kJ mol^{-1} lower than that for each of the next two steps (leading to hexahydrotriquinacene) [88]. This was taken as proof of homoaromaticity in the triene, i.e. that the compound was 18.8 kJ mol^{-1} (4.5 kcal mol^{-1}) stabler than expected for an unstabilized species; note that this is a small stabilization energy compared to the resonance energy of benzene, most computational estimates of which are roughly 100 kJ mol^{-1} (Chap. 5, Sect. 5.5.2.2.1). However, another experimental and computational study of this question [89] led to the conclusion that triquinacene is *not* homoaromatic: combustion of the compound gave an enthalpy of formation ca. 17 kJ mol^{-1} (4 kcal mol^{-1}) higher than that obtained from hydrogenation in [88] (241 vs. 224 kJ mol^{-1}, 57.5 vs. 53.6 kcal mol^{-1}). This negative conclusion was supported by calculation of the heat of hydrogenation of a double bond in triquinacene and in its di- and tetrahydro derivatives (**1**, **2**, **3**, Fig. 9.8), and by calculation of magnetic properties of the triene and related
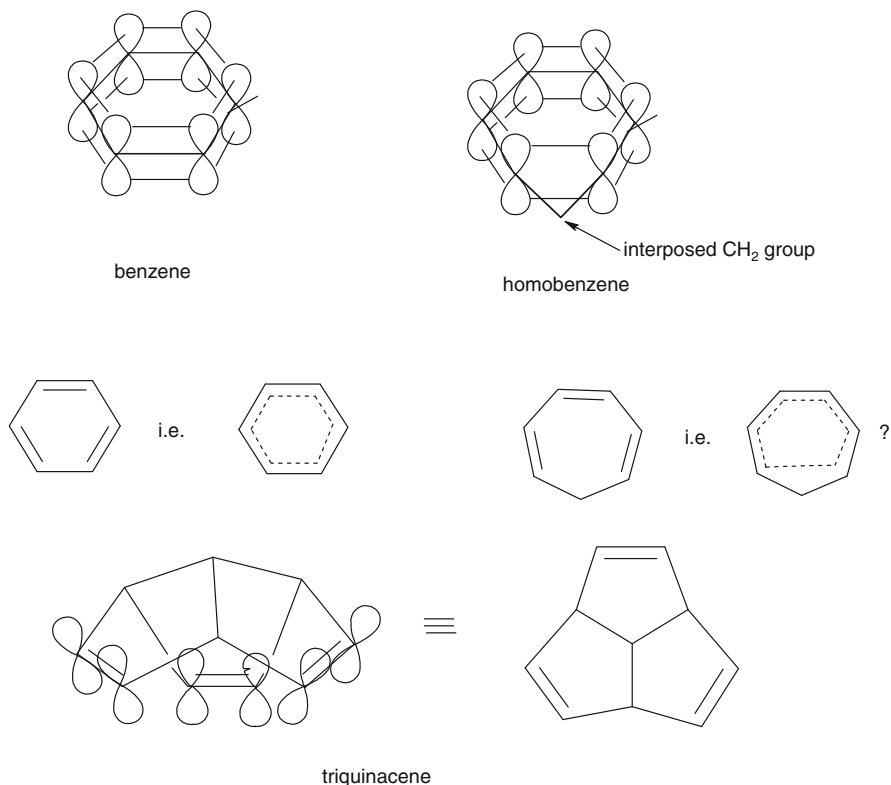
Fig. 9.7 Homoaromaticity. Interposing a CH$_2$ group between one pair of formal double bonds of benzene gives monohomobenzene. Is this delocalized like benzene, or is it just cycloheptatriene? Is triquinacene, with a CH group interposed between each pair of formal double bonds, a trishomobenzene?

molecules [89]. The heats of hydrogenation of the double bonds were calculated with the aid of homodesmotic reactions, a kind of isodesmic reaction (Chap. 5, Sect. 5.5.2.3.1) which preserves the number of each kind of bond, and so in which correlation errors should cancel well; for **1**, **2**, and **3** the calculated hydrogenation energy of a double bond are all essentially the same, showing that a double bond of **1** is an ordinary cyclopentene double bond. Note that using cyclopentane (Fig. 9.8) rather than, say, ethane–which would also preserve bond types–to (conceptually) hydrogenate **1**, **2**, and **3** should largely cancel out energy differences due to ring strain. Interestingly [88], concludes that "triquinacene is unequivocally stabilized" relative to reference species, but [89] asserts that, from the thermochemical measurements, "The only logical conclusion is that [triquinacene] is not homoaromatic." The evident absence of homoaromaticity in triquinacene is presumably due to the three pairs of nonbonded carbons being too far apart, 2.533 Å, from X-ray diffraction; in the transition state (Fig. 9.9), in contrast, the nonbonded
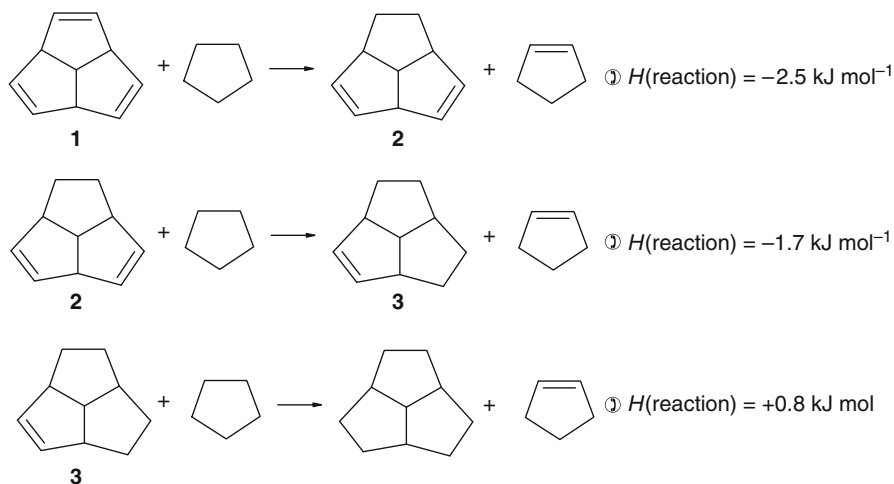
Fig. 9.8 The heat of hydrogenation of a double bond in triquinacene is essentially the same as that of a double bond in dihdrotriquinacene and in tetrahydrotriquinacene, and is about the same as in cyclopentene, indicating that triquinacene is not homoaromatic
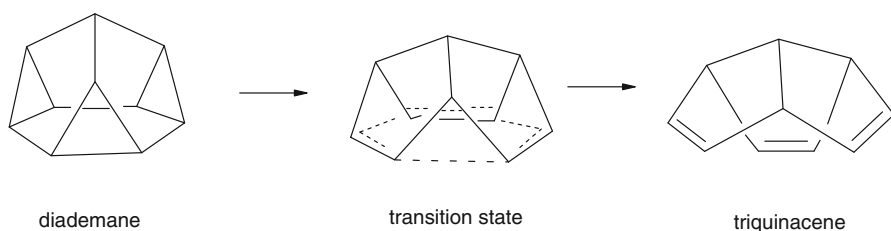
Fig. 9.9 The isomerization of diademane to triquinacene proceeds through an aromatic transition state, as shown by the magnetic susceptibility and NICS values for the three species

CC distance has been reduced to 1.867 Å according to a B3LYP/6-311+G** (Chap. 7, Sect. 7.2.3.4.5) calculation. Significantly, the measured C=C length, 1.319 Å, is close to the normal C=C length (calculated and measured parameters of triquinacene are cited in [89]).

The magnetic properties used to probe aromaticity arise from the presence of a diatropic ring current which tends to push an aromatic molecule out of a magnetic field (calculated property: magnetic susceptibility, χ), and which exerts NMR shielding on a proton at or above the ring center (calculated property: nucleus-independent chemical shift, NICS). NICS values are obtained from the calculated NMR shielding (Chap. 5, Sect. 5.4.3.3) of a "ghost nucleus" with no charge or electrons placed at or above the ring center. A very comprehensive review of the NICS test [90a] has been published, and an updated, superior variant [90b] has been presented. Calculation of the changes in χ and in NICS along the reaction coordinate for the known reaction, the isomerization of diademane to triquinacene
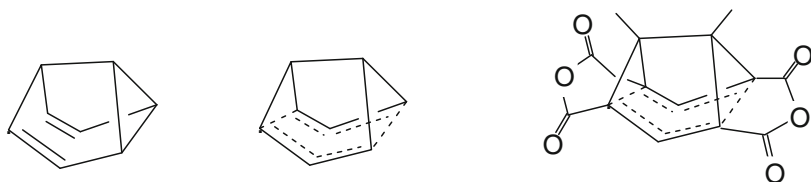
semibullvalene   symmetrical transition state   homoaromatic dianhydride

Fig. 9.10 Semibullvalene switches its cyclopropane and diene ends through a delocalized symmetrical transition state. The dianhydride derivative of semibullvalene is a delocalized homoaromatic compound

(Fig. 9.9), showed that the transition state, but neither the reactant nor the product, was aromatic [89]. Homoaromaticity in transition states, which almost perforce are not subject to experimental spectroscopic scrutiny, has been claimed [91]. The phenomenon has for years been controversial for cycloheptatriene, but after having being said to be "firmly established" computationally [92a] it has evidently been definitively demonstrated experimentally in a subtle somewhat roundabout way by examining the NICS characteristics of a cycloheptatriene ring fused to a dimethyldihydropyrene probe molecule; these workers quantify cycloheptatriene as being 50 % as aromatic as benzene [92b]. A convincing demonstration of homoaromaticity in a neutral molecule was provided by the unusual medium of IR, rather than NMR, spectroscopy for a semibullvalene derivative (Fig. 9.10) [93]. The hydrocarbon semibullvalene undergoes valence tautomerism with a low barrier through a symmetrical transition state which switches "left-right" the two ends. The dimethyl dianhydride derivative of semibullvalene captures the essence of this transition state in a homoaromatic compound. This was shown by analysis of the IR spectrum of the vapor: the number of carbonyl bands seen was that expected for the molecule shown, C_{2v} with two symmetry planes, rather than for a dianhydride with the framework of semibullvalene itself, C_s with one symmetry plane.

9.2   To the Literature

A feast of information on computational chemistry is available, a small selection of which is given below.

9.2.1   *Books*

Books on computational chemistry and some related topics, in alphabetical order of the author's (or first-listed author's) name. The terse characterization of a particular

book is a personal impression, and does not necessarily imply that it does not share the virtues ascribed to some other book. The list does not claim to by any means include all the useful books on computational chemistry.

B

Computational Organic Chemistry, Second Edition, S. M. Bachrach, Wiley-Interscience, Hoboken, NJ, 2014.

Good source of examples from the literature with critical evaluation of methods and useful caveats. The first chapter is a very brief introduction to ab initio and DFT theory.

C

Handbook of Computational Quantum Chemistry, D. B. Cook, Dover Reprint, Dover Publications, Mineola, New York, 2005 (original 1998).

Concentrates on the math behind quantum chemistry theory and algorithms, yet not dryly written. Perhaps mainly for those who wish to write or modify programs. Best read after acquiring the basics from a more general, introductory book.

Essentials of Computational Chemistry. Theories and Models, second Edition, C. J. Cramer, Wiley, New York, 2004.

Covers a wide range of topics. The level is sometimes quite advanced. Critical discussions of the literature. Of similar ilk to Jensen, below.

D

The Molecular Orbital Theory of Organic Chemistry, M. J. S. Dewar, McGraw-Hill, New York, 1969.

Nice introduction to the basics of quantum chemistry, then a focus on semiempirical calculations and perturbation methods. Although published more than 40 years ago, the fundamentals, like the Schrödinger equation and wavefunctions, remain true, and the engagingly assertive style of the doyen of modern semiempirical methods makes this book worth reading.

F

Exploring Chemistry with Electronic Structure Methods, second Ed., J. Foresman and Æ. Frisch, Gaussian, Inc., Pittsburgh, PA, 1996.

Very useful hands-on guide; oriented toward Gaussian 94, but useful for Gaussian 03 and even 09. A third edition became available in 2016, from Gaussian Inc.

H

Ab Initio Molecular Orbital Theory, W. J. Hehre, L. Radom, P. von R. Schleyer, and J. A. Pople, Wiley, New York, 1986.

Still a good introduction to ab initio calculations, although one should realize that there have been great advances since 1986. Extremely useful are the extensive tables of calculated and experimental geometries, energies, and frequencies.

I

Computational Thermochemistry, K. K. Irikura and D. J. Frurip, Eds., American Chemical Society, Washington, DC, 1998.

Useful source of information on the calculation of energy quantities: heats of formation, reaction energies, bond energies, activation energies, etc. Methods: group additivity, molecular mechanics, semiempirical, DFT, and high-accuracy ab initio (G2, CBS, etc.); energies of solvation.

J

Introduction to Computational Chemistry, second edition, F. Jensen, Wiley, New York, 2007.

Good general introduction. Goes fairly deeply into theory. Of similar ilk to Cramer, above.

K

A Chemist's Guide to Density Functional Theory, W. Koch and M. C. Holthausen, Wiley-VCH, New York, Second Edition, 2002.

Detailed introduction to the theory and applications of DFT. Best read after acquiring a basic knowledge of DFT.

L

Molecular Modelling. Principles and Applications, second Edition, A. R. Leach, Longman, Essex, England 2001.

Good general introduction. Comprehensive and goes deeply into the topics. Somewhat like Cramer, Jensen, above.

Quantum Chemistry, seventh Ed., I. N. Levine, Prentice Hall, Upper Saddle River, NJ, 2014.

Enormously useful book on the broad field of quantum chemistry. Many references to the original literature, to books, to programs, and to websites.

Modeling Marvels. Computational Anticipation of Novel Molecules, E. Lewars, Springer, Amsterdam, 2008.

Thirteen kinds of very novel molecules which were unknown at the end of 2009 (and still in mid-2016), but have been investigated computationally. For people who are fascinated by novel molecules at the frontier of structural chemistry.

P

Approximate molecular Orbital Theory, J. A. Pople, D. A. Beveridge, McGraw-Hill, New York, 1970.

Although published nearly 50 years ago, this book is worth perusing because it provides an indication of the situation at the dawn of ab initio calculations, when quite approximate semiempirical methods (CNDO and INDO) were important, and it is one legacy of John Pople, who went on to help make ab initio calculations practical for much of the chemical community.

R

Molecular Mechanics Across Chemistry, A. K. Rappé and C. J. Casewit, University Science Books, Sausalito, CA, 1997.

Detailed presentation of the applications of MM, particularly in biochemistry and drug design.

S

The Encyclopedia of Computational Chemistry, 5 volumes, P. von R. Schleyer, Editor in chief, Wiley, New York, 1998.

No doubt authoritative, but pricey (ca. $6000), and multivolume paper-based encyclopedias have limited useful lifetimes nowadays.

Modern Quantum chemistry. Introduction to Advanced Electronic Structure Theory, A. Szabo and N. S. Ostlund, Macmillan publishing, New York, 1982. Revised edition McGraw-Hill 1989, Dover paperback 1996.

A detailed, very advanced introduction to basic Hartree-Fock, CI and MP theory. Well-known as a rigorous introduction to the mathematical fundamentals. Best read after one understands the basic principles of ab initio quantum chemistry.

W

Books from Wavefunction, Inc, makers of the Spartan computational chemistry program. For available books contact Wavefunction, http://www.wavefun.com/

These books, oriented toward Wavefunction's Spartan program, are useful introductions to practical methods of getting useful results.

Y

Computational Chemistry: A Practical Guide for Applying Techniques to Real World Problems, D. Young, Wiley, New York, 2001.

A "meta-book" in that it lists several books on computational chemistry; it also lists many websites concerned with computational chemistry, and many computational chemistry programs. Useful lists of references (to ca. 1999).

Available Online

See too: Topics by Dave Young: http://server.ccl.net/cca/documents/dyoung/

Book Series *Reviews in Computational Chemistry*, K. B. Lipkowitz and D. B. Boyd, Eds., Wiley-VCH, New York.

Useful reviews focussed on various topics, by workers in that particular field. A volume in this series typically has from four to eleven chapters, each a kind of tutorial on the theory and application of some computational method. Volumes 1–18 were edited by K. B. Lipkowitz and D. B. Boyd; the series continues with Lipkowitz and others, editors. As of June 2015 the latest volume was Volume 28, which appeared in May 2015.

For tables of contents and other information see http://www.chem.iupui.edu/rcc/rcc.html, and

http://www.wiley.com/WileyCDA/WileyTitle/productCd-0470587148.html

9.2.2 Websites for Computational Chemistry in General

Information on even specialized scientific topics can often be obtained from ordinary search engines. For example, a popular search engine gave information (ten hits for each) on these five topics, using the keywords shown: Hartree Fock,

potential energy surface, molecular mechanics, Hückel, Extended Hückel. In several cases the hypertext leads one to tutorials, and to free programs. Nevertheless, a list of specific websites can still be helpful. Many websites are given in the books by Young and by Levine, above; some other useful ones are (should some of these invoke "Address Not Found", try a search engine) given below.

1. The computational chemistry list, CCL
   http://www.ccl.net/chemistry/
   A truly extraordinarily helpful forum for exchanging ideas, asking questions and getting help. If you join the network you can expect typically 5–10 messages a day. It often serves as a forum for stimulating discussions. Currently the best way to locate specific information in CCL may be to go, once in CCL, to CCL Search and follow the instructions to using Google for a CCL search.
2. National Institute of Standards and Technology, NIST (USA)

   (a) General information
       http://www.nist.gov/index.html
   (b) Chemistry databases
       http://www.nist.gov/chemistry-portal.cfm
   (c) Computational chemistry comparison and benchmark database
       http://cccbdb.nist.gov/
   (d) Perhaps the quickest way to get information on a specific molecule is from this specific site:
       NIST chemistry webbook. Options for specifying molecule include formula, name, reaction, structure, energetics property (e.g. ionization energy, acidity).
       http://webbook.nist.gov/chemistry/
   (e) Density functionals from the Truhlar group
       This may help one to cope with the plethora of acronyms of DFT functionals.
       http://comp.chem.umn.edu/info/dft.htm

3. From the Chemistry Biology Pharmacy Information Center, ETH, Zurich
   A long list of information and websites connected with computational chemistry. Leads to information on methods and software.
   http://infozentrum.ethz.ch/uploads/user_upload/pdf/PDFs_von_Drucksachen/Infobroschure_Englisch.pdf
4. The Cambridge Crystallographic data Centre; contains the Cambridge Structural Database, which has X-ray or neutron diffraction structures of more than 500 000 compounds. Useful for comparing experimental and calculated structures, and obtaining "guess" structures for related structures to initiate an optimization.
   www.ccdc.cam.ac.uk/
5. This site allows one to select a basis set for a molecule ("391 published basis sets"), or for particular atoms in a molecule, and provides options of the format for various programs. Useful when the program being used lacks that particular basis set. A minor problem is that Gaussian requires its "outsider" basis sets to start with the element symbol, not the string of asterisks given here.
   http://bse.pnl.gov/bse

9.3   Software and Hardware

9.3.1   Software

These programs ("software suites") and others are described in more detail in the book by Young, above (albeit as of ca. 2001), and in a comprehensive list on Wikipedia (below). These sources should be consulted for more information. I mention here some that are particularly useful in a general-purpose sense, and some more specialized programs that handle advanced methods which cannot be implemented, or well-implemented, in more "general" programs. Some of the programs do not have their own input/output GUI (graphical user interface). Many of these can be found conveniently from the rather extensive list on Wikipedia, which describes the program and (often) gives quick access to its website by clicking:

http://en.wikipedia.org/wiki/Category:Computational_chemistry_software

Not listed here are programs for these specialized applications of computational chemistry: molecular dynamics, drug design (including QSAR, quantitative structure-activity relationships), crystal structure prediction, and solid-state physics.

The list here is alphabetical.

ACES III   (Advanced Concepts in Electronic Structure)
http://www.qtp.ufl.edu/aces/pubs.shtml
An ab initio program for high-level jobs. Particularly recommended for CCSD (T) optimizations+frequencies, which latter are perhaps the most reliable calculations that can currently be done routinely on molecules of up to moderate size (up to about 10 heavy atoms). CCSD(T) optimizations and frequencies tend to be considerably slower with some other programs, if available at all. Available for UNIX workstations and supercomputers. Evidently lacks its own GUI.

ADF   Amsterdam Density Functional
https://www.scm.com/
"ADF is an accurate, parallelized, powerful computational chemistry program to understand and predict chemical structure and reactivity with density functional theory (DFT)". Available for Windows, Linux or Mac operating system. One might say this is everything for, and only for, DFT.

AMPAC   (Austin method package; cf. AM1 Marketed by Semichem Inc.)
http://www.semichem.com/default.php
A semiempirical suite of programs. See Chap. 6.

COSMOtherm   From *COSMO* (below) and *thermo*chemistry
http://www.cosmologic.de/products/cosmotherm.html
A suite of programs for using quantum chemistry and thermodynamics to calculate properties of solutions; available from the company COSMOlogic (http://www.cosmologic.de/home.html). Includes COSMO-RS (COnductor like

Screening MOdel for Realistic Solvents; Chap. 8, Sect. 8.1.2, *Continuum solvation*). COSMOtherm is available in the program suite Turbomol (below), in a somewhat older version (as of mid-2015) in ORCA (below). Gaussian can create an input file for COSMOtherm.

GAMESS (General Atomic and Molecular Electronic Structure System)
    http://www.msg.ameslab.gov/GAMESS/
    A fairly general-purpose computational chemistry suite: semiempirical and ab initio. Not as many options as GAUSSIAN (below) but free. Versions are available for PCs, Macs, UNIX workstations and supercomputers. lacks its own GUI.

GAUSSIAN (After the Gaussian functions of ab initio computations)
    http://www.gaussian.com/
    A general-purpose computational chemistry suite. Possibly the most widely used computational chemistry program. Actually a suite of programs with MM (AMBER, DREIDING, UFF), ab initio, semiempirical (CNDO, INDO, MINDO/3, MNDO, AM1, PM3, Extended Hückel) and DFT, and all the usual high-level correlated ab initio methods. Some molecular dynamics is available. Most methods are available simply by keywords. There is a large number of basis sets and functionals. Electronically excited states can be calculated. GAUSSIAN has appeared in improved versions every few years from 1970 (...G92, G94, G98). The latest version (January 2010) is G09; somewhat minor revisions appear frequently. GAUSSIAN is available in versions for PCs running under Windows and LINUX, and for UNIX workstations and supercomputers. The program itself does not have an integrated GUI (one bundled with the actual computing module), but there are several graphics programs for creating input files and for viewing the results of calculations. GaussView (latest version in 2015, GaussView 5), expressly designed for GAUSSIAN, is highly recommended as the solution to all GAUSSIAN graphics problems.

HyperChem http://www.hyper.com/
    More specific information on the latest version:
    http://www.hyper.com/Products/HyperChemProfessional/tabid/360/Default.aspx
    Has MM, semiempirical (including extended Hückel, CNDO, INDO, MINDO/3, MNDO, ZINDO/1, ZINDO/S, AM1, PM3), ab initio, molecular dynamics. Available for PCs with Windows and LINUX. It has its own GUI. An option that Hyperchem seems to be directed toward is drug discovery.

JAGUAR (Jaguar = speed) Marketed by Schrödinger Inc.
    http://www.schrodinger.com/products/14/7/
    Made by Schrödinger, Inc., JAGUAR is an ab initio and DFT package that uses sophisticated algorithms to speed up ab initio calculations. It is said to be particularly good at handling large molecules, transition metals, solvation, and conformational searching. It is described (above, http: etc.,) as having "particular strength in treating metal containing systems" and is said to be "much faster than conventional *ab initio* programs."

MOLCAS Molecular Complete active space

Normally run under LINUX but can be configured for some other operating systems (see below).

http://molcas.org/

The name is a good clue. Ab initio and some DFT. Its main strength appears to be its ability to bring advanced correlation methods to bear on excited states and degenerate states. In this regard it is evidently the only program suite with CASPT2N (complete active space perturbation theory second order with nondiagonal one-particle operator [94]). A survey of the literature shows that this is the most widely-used version of the CASPT2 method, and is the most widely-accepted technique for treating static correlation (Chap. 5, Sect. 5.4.1) in singlet diradicals (Chap. 8). A CAS (Chap. 8, Sect. 8.2.3) geometry optimization followed by a single-point CASPT2N energy calculation is analogous (not identical) to a Hartree-Fock optimization followed by an MP2 single point calculation to obtain a better energy (but MP2 calculations are now commonly geometry optimizations). The method is sometimes called just CASPT2, but there are other second order perturbational CAS methods implemented in other programs. MOLCAS can be configured to run under some other operating systems; see the review [95].

MOLPRO Molecular Professional

Available only for LINUX.

http://www.molpro.net/

Mainly high-level correlated ab initio calculations (multiconfiguration SCF, multireference CI, and CC); and DFT. "The emphasis is on highly accurate computations...accurate ab initio calculations can be performed for much larger molecules than with most other programs." An unusual feature is the inclusion of explicitly correlated calculations (dependence on 1/r; Chap. 5, Sect. 5.4.1). MOLPRO does not implement the CASPT2N code as in MOLCAS, but "the multi-reference perturbation theories in MOLPRO and MOLCAS are quite similar, and the CASPT2N Hamiltonian can be reproduced in MOLPRO".[3] Other programs that implement methods designed to accomplish "post-CAS" energy calculations are GAUSSIAN and GAMESS.

MOPAC The name means Molecular Orbital Package, but is said to have been inspired by this geographical oddity: "The original program was written in Austin, Texas. One of the roads in Austin is unusual in that the Missouri-Pacific railway runs down the middle of the road. Since this railway was called the MO-PAC, when names for the program were being considered, MOPAC was an obvious contender".

http://openmopac.net/manual/index_troubleshooting.html

A semiempirical suite of programs. See Chap. 6.

---

[3]Personal communication, Professor E. V. Patterson, Division of Science, Truman State University, Kirksville, MO, 2005 March 7.

NWChem Northwest Chemistry

http://www.nwchem-sw.org/index.php/Main_Page

Developed at the Pacific Northwest National Laboratory, a US national scientific user facility funded by the Department of Energy. This suite of programs can do molecular mechanics, molecular dynamics, ab initio, and density functional calculations. It is designed to run on "parallel computing resources from high-performance parallel supercomputers to conventional workstation clusters". It is apparently available for public download.

ORCA The name, whimsically bestowed on his nascent program in the late 1990s by its originator Frank Neese, was inspired by whale-watching on the California coast. Neese simply wanted "a name that sounded short and strong".[4] It is not an acronym, but ORCA denotes a whale of a program in versatility and power.

http://www.thch.uni-bonn.de/tc/orca.

Manual:

http://www.cec.mpg.de/media/Forschung/ORCA/orca_manual_3_0_1.pdf

ORCA, developed by F. Neese and collaborators, is a very comprehensive suite with semiempirical, ab initio and DFT capability. It handles solvation (including the COSMOtherm program suite, see above), and does advanced electron correlation calculations like multireference jobs. An important feature is the ability to do the speeded-up coupled cluster methods CEPA and LPNO (Chap. 5, end of Sect. 5.4.3), as of mid-2015 being apparently the only program with this full capability. Review: F. Neese, Wiley Disciplinary Reviews: Computational Molecular Science, 2012, *2*, 73. ORCA is free to academic researchers.

PCModel Marketed by Serena Software

http://www.serenasoft.com/

Primarily molecular mechanics, but now includes semiempirical. Can serve as a GUI for ab initio and DFT program suites.

Q-Chem Quick chemistry

www.q-chem.com/

"The first commercially available quantum chemistry program capable of analyzing large structures in practical amounts of time." For ab initio (including high-level correlated methods) and DFT. Q-Chem is available for PCs running under LINUX, for UNIX workstations, and for supercomputers.

Simple Hückel Method programs The simple Hückel method, SHM (Chap. 4, Sects. 4.3.4, 4.3.5, 4.3.6 and 4.3.7):

This remains important for heuristic and pedagogic reasons, and even researchers can find it useful. Despite what some think, it "is immensely useful as a model, today...Because it is the model which preserves the ultimate physics, that of nodes in wave functions. It is the model which throws away absolutely

---

[4]Personal Communication, Professor F. Neese, Max Planck Institute for Chemical Energy Conversion, Müllheim an der Ruhr, Germany, 2015 August 20.

everything except the last bit, the only thing that if thrown away would leave nothing. So it provides fundamental understanding" (Professor Roald Hoffmann, personal communication). SHM programs may be located by googling "simple huckel method programs". The program from the University of Calgary is recommended:

   http://www.chem.ucalgary.ca/SHMO/ This can be downloaded or used online.

SPARTAN Spartan meaning spare, uncomplicated. Marketed by Wavefunction
   http://www.wavefun.com/

   This is a suite of programs with MM (SYBYL and MMFF), ab initio, semiempirical (MNDO, AM1, PM3) and DFT, with its own superb graphical user interface (GUI) for building molecules for calculations, and for viewing the resulting geometries, vibrational frequencies, orbitals, electrostatic potential distributions, etc. SPARTAN is a complete package in the sense that one does not need to buy add-on programs like, say, a GUI. The program is very easy to use and its algorithms are robust–they usually accomplish their task, e.g. the sometimes tricky job of finding a transition state usually works with SPARTAN. Versions of the program are available for PCs running under Windows and LINUX, for Macs, and for UNIX workstations. It lacks some high-level correlated ab initio methods, like CASSCF, and its store of basis sets and DFT functionals is limited to the most commonly used ones (the exact selection varies somewhat from version to version), but it is nevertheless extremely useful for research (including preliminary work and creating input structures for other programs), not to mention teaching.

TURBOMOLE   http://www.turbomole.com/

   "The philosophy behind the development of the code was, and still is, its usefulness for applications". The focus is less on new methods than on "a fast and stable code which is able to treat molecules of industrial relevance at reasonable time and memory requirements". The emphasis on industrial applications is clear in the meshing of TURBOMOLE with the program suite COSMOtherm (see above).

9.3.2 Hardware

Someone beginning computational chemistry might wish to get a high-end PC running under Windows or LINUX: such a machine is fairly cheap and it will do even sophisticated electron-correlation ab initio calculations. Some specialized programs are available only for LINUX. A 64 bit ca. 4 GHz speed machine with 6 or more cores, 8 GB of memory (random access memory, RAM), a 2000 GB (2 terabytes, 2 TB) hard drive is now (June 2015) not very unusual (soon it may be substandard); such a machine is available for ca. US $1400 for the whole system, including monitor etc. This is a reasonable choice for general computational chemistry. Using standard Gaussian 94 test jobs and various operating systems, and varying software and hardware parameters, Nicklaus et al. comprehensively compared a wide range of "commodity computers" [96]. These were ordinary

personal computers of the time (ca. 1998); the costliest was about US $5000 and most were less than $3000. A computer of this price would now (2015) be about twenty times as fast as in 1998. They concluded that "commodity-type computers have…surpassed in power the more powerful workstations and even supercomputers.... Their price/performance ratios will make them extremely attractive for many chemists who do not have an unlimited budget…" Chemists without unlimited budgets will be reassured to read a slightly more recent study, by an eminent pioneer in computational chemistry; the account begins in 1965 with a personal hardware odyssey and concludes, ca. 2001, with an endorsement of the view that PCs have largely usurped the role of workstations [97]. A workstation was a UNIX-based desktop computer, commonly about three to ten times as expensive as a PC ca. 2001; the term may not be obsolete, but now has a vaguely archaic ring.

Calculations that might be daunting to a desktop machine are nowadays often run on a"cloud" facility, or on a computer cluster. Cloud computing is the term denoting running the calculations on a machine remote (more or less) from the site where one works [98]. A computer cluster is the poor person's supercomputer: clusters were originally assembled from humbler machines (even before modern PCs existed) to obtain supercomputer power at a far lower cost [99]. For those who wish to use or even build a cluster the website http://www.clustermonkey.net/Books/, offers books and some frank comments. Clusters are now commercially available.

It is only fair to point out that the enormous decrease in the times, over the decades, with which computing jobs can be dispatched is not due solely to the increase in computer speed. In computational chemistry, certainly, the people who write the codes deserve much credit. Algorithms have been speeded up greatly by various mathematical "tricks" (stratagems might be a better word) which often provide considerable increases in speed with little or no loss of accuracy. It might be interesting to try to untangle the effect of algorithmic efficiency from that of hardware power.

9.3.3 Postscript

About 15 years ago the president of a leading computational chemistry software firm told the author that "In a few years you will be able to have a Cray [a leading supercomputer brand] on your desk for $5000". Supercomputer performance is a moving target, but the day has indeed come when one can have on one's desk for a few thousand dollars computational power that was not long ago available only to an institution, and for a good deal more than $5000. A corollary of this is that computational chemistry has become an important, indeed sometimes essential, auxiliary to experimental work. More than that, calculations have become so reliable that not only can parameters like geometries and heats of formation often be calculated with an accuracy rivalling or exceeding that of experiment, but where high-level calculations contradict experiment, the experimentalists might be well

advised to repeat their measurements. The implications for the future of chemistry of the happy conjunction of affordable supercomputer power and highly sophisticated software need hardly be stressed.

References

1. Lewars E (2008) Modeling marvels. Springer, Amsterdam
2. (a) Lewars E (1983) Chem Rev 83:519; (b) Lewars E (2008) Modeling marvels. Springer, Amsterdam; chapter 3
3. Rukiah M, Assad T (2010) Acta crystallographica. Section c, Crystal structure communications 66(Pt 9):o475
4. Vacek G, Colegrove BT, Schaefer HF (1991) Chem Phys Lett 177:468
5. Vacek G, Galbraith JM, Yamaguchi Y, Schaefer HF, Nobes RH, Scott AP, Radom L (1994) J Phys Chem 98:8660
6. Wilson PJ, Tozer DJ (2002) Chem Phys Lett 352(5,6):540
7. Mawhinney RC, Goddard JD (2003) J Mol Struct (Theochem) 629:263
8. Borden WT (2014) referring to DFT in general, quoted in Bachrach SM. Computational organic chemistry, 2nd edn. Wiley-Interscience, Hoboken, p 281
9. Toscano JP, Platz MS, Nikolaev V (1995) J Am Chem Soc 117:4712
10. Wang J, Burdzinski G, Kubicki J, Gustafson TL, Platz MS (2008) J Am Chem Soc 130:5418
11. Litowitz AE, Keresztes I, Carpenter BK (2008) J Am Chem Soc 130:12085
12. Cremer D, Crehuet A, Anglada J (2001) J Am Chem Soc 123:6127
13. Karton A, Talbi D (2014) Chem Phys 436–437:22
14. Konstantinos KD, Vogiatzis D, Hannschild R, Klopper W (2014) Theor Chem Acc 133:1
15. Lewars E (2008) Modeling marvels. Springer, Amsterdam; chapter 4
16. Minkin VI, Glukhovtsev MN, Simkin B Ya (1994) Aromaticity and antiaromaticity. Wiley, New York; Bauld NL, Welsher TL, Cassac J, Holloway RL (1978) J Am Chem Soc 100:6920
17. (a) Halton B(ed) (2000) Advances in strained and interesting organic molecules. JAI Press, Stamford, Connecticut 8; (b) Sander W (1994) Angew Chem Int Ed Engl 33:1455; (c) Chem Rev, Issue 5, (1989) 89; (d) Wiberg K (1986) Angew Chem Int Ed Engl 25:312; (e) Liebman JF, Greenberg A (1976) Chem Rev 76:311
18. Bettinger HF, von R Schleyer P, Schaefer HF (1998) J Am Chem Soc 120:11439
19. Christe KO, Wilson WW, Schrobilgen GJ, Chitakal RV, Olah G (1988) Inorg Chem 27:789
20. Ewig CS, Van Wazer JR (1989) J Am Chem Soc 111:4172
21. Ewig CS, Van Wazer JR (1990) J Am Chem Soc 112:109
22. Chemical and engineering news. (1990), April 2, p 3
23. Christe KO, Wilson WW (1992) J Am Chem Soc 114:9934
24. Dixon DA, Grant DJ, Christe KO, Peterson KA (2008) Inorg Chem 47:5485, and references therein
25. van't Hoff JH (1875) Bull Soc Chim Fr II 23:295; LeBel JA (1874) Bull Soc Chim Fr II 22:337
26. Feng Y, Liu L, Wang J-T, Zhao S-W, Guo Q-X (2004) J Org Chem 69:3129
27. Lewars E (2008) Modeling marvels. Springer, Amsterdam; chapter 2
28. (a) Lewars E (1998) J Mol Struct (Theochem) 423:173; (b) Lewars E (2000) J Mol Struct (Theochem) 507:165; (c) Coupled-cluster calculations gave very similar results to Fig. 9.3 for the relative energies of pyramidane, the transition states, and the carbenes: Kenny JP, Krueger KM, Rienstra-Kiracofe JC, Schaefer HF (2001) J Phys Chem A 105:7745
29. Some barriers/room temperature halflives for unimolecular reactions: (a) Decomposition of pentazole and its conjugate base: 75 kJ mol^{-1} / 10 minutes and 106 kJ mol$^{-1/2}$ 2 days, respectively: Benin V, Kaszynski P, Radziszki JG (2002) J Org Chem 67:1354 (b) Decomposition of CF$_3$CO)OOO(COCF$_3$): 86.5 kJ mol^{-1} / 1 minute: Ahsen SV,

Garciá P, Willner H, Paci MB, Argüello G (2003) Chem Eur J 9:5135. (c) Racemization of a twisted pentacene: 100 kJ mol^{-1}/6–9 h: Lu J, Ho DM, Vogelaar NJ, Kraml CM, Pascal RA Jr (2004) J Am Chem Soc 126:11168

30. Veis L, Cársky P, Pittner J, Michl J (2008) Coll Czech Chem Commun 73:1525
31. E.g. Blanksby SJ, Ellison GB (2003) Acc Chem Res 36:255
32. Lee VY, Ito Y, Sekiguchi A, Gornitzka H, Gapurenko OA, Minkin VI, Minyaev RM (2013) J Am Chem Soc 135:8794
33. Lewars E (2008) Modeling marvels. Springer, Amsterdam; chapter 10
34. Dagani R (2000) Chemical and engineering news.,14 August, 41
35. Rawls R (1999) Chemical and engineering news.,25 January, 7
36. Vij A, Wilson WW, Vij V, Tham FS, Sheehy JA, Christe KO (2001) J Am Chem Soc 123:6308
37. Christe KO (2007) Propellants Explos Pyrotech 32:194
38. Vij A, Pavlovich JG, Wilson WW, Vij V, Christe KO (2002) Angew Chem Int Ed Eng 41:3051
39. Östmark H, Wallin S, Brinck T, Carlqvist P, Claridge A, Hedlund E, Yudina L (2003) Chem Phys Lett 379:539
40. Butler RN, Stephens JC, Burke LA (2003) J Chem Soc., Chem Commun 1016
41. Schroer T, Haiges R, Schneider S, Christe KO (2005) J Chem Soc, Chem Commun 1607
42. Butler RN, Hanniffy JM, Stephens JC, Burke LA (2008) Org Chem 73:1354
43. Curtius T Ber (1890) 23:3023
44. Eremets MI, Gavriliuk AG, Trojan IA, Dzivenko DA, Boehler R (2004) Nature Matter 3:558
45. Engelke R (1989) J Phys Chem 93:5722
46. Engelke R (1992) J Phys Chem 96:10789
47. Fabian J, Lewars E (2004) Can J Chem 82:50, and references therein
48. Wiberg E, Michaud HZ (1954) Z Naturforsch B9:500
49. Banert K, Joo Y-H, Rüffer T, Walford B, Lang H (2007) Angew Chem Int Ed Engl 46:1168
50. Klapötke TM, Schulz A (1997) Main Group Met Chem 20:325
51. Klapötke TM, Martin FA, Stierstorfer J (2011) Angew Chem Int Ed Engl 50:4227
52. Klapötke TM (2012) Chemistry of high-energy materials. De Gruyter
53. Lin FL, Yang F, Zhang LX (2010) J Mol Struct (Theochem) 950:98
54. Zhou H, Beuve M, Yang F, Wong N-B, Li W-K (2013) Comput Theor Chem 1005:68
55. Jasper SJ, Hammond A, Thomas J, Kidd L, Strout DL (2011) J Phys Chem A 115:11915, and references therein
56. Li QS, Zhao JF (2002) J Phys Chem A 106:5367
57. Thomas J, Fairman K, Strout DL (2010) J Phys Chem A 114:1144
58. Casey K, Thomas J, Fairman K, Strout DL (2008) J Chem Theory Comput 4:1423
59. Marsh FD, Hermes ME (1965) J Am Chem Soc 87:1819
60. Cram DJ, Tanner ME, Thomas R (1991) Inherent stability at room temperature. Angew Chem Int 30:1024
61. E.g. Woodward RB, Hoffmann R (1970) Verlag Chemie/Academic Press, Weinheim/New York
62. Plata RE, Singleton DA (2015) J Am Chem Soc 137:3811, and references therein
63. Pauli's exact words, which would presumably have been in German, are probably not known with certainty, but the story that he referred thus to a paper by another physicist is evidently not apocryphal. The source is Rudolf Pierls, in an article on Pauli after the latter's death: Biographical Memoirs of Fellows of the Royal Society, vol. 5 (Feb. 1960), 174–192
64. Borman S (2015) Chem Eng News 9 March, 9
65. Dewar MJS (1992) A semiempirical life. American Chemical Society, Washington, DC, p 125
66. E.g. Smith MB, March J (2001) Advanced organic chemistry, 5th edn. Wiley, New York pp 1062–1075
67. Woodward RB, Bader FE, Bickel H, Frey AJ, Kierstead RW (1958) Tetrahedron 2:1
68. Houk KN, Li Y, Evanseck JD (1992) Angew Chem Int Ed Engl 31:682
69. Li Y, Houk KN (1993) J Am Chem Soc 115:7478
70. Dewar MJS, Jie C (1992) Acc Chem Res 25:537
71. Goldstein E, Beno B, Houk KN (1996) J Am Chem Soc 118:6036
72. Galano A, Alvarez-Idaboy JR, Montero LA, Vivier-Bunge A (2001) J Comp Chem 22:1138

73. Siggel MRF, Thomas TD (1986) J Am Chem Soc 108:4360
74. Streitwieser A (1996) A lifetime of synergy with theory and experiment. American Chemical Society, Washington, DC, pp 166–170, and references therein
75. Wiberg KB (1999) Acc Chem Res 32:922
76. Streitwieser A (1996) A lifetime of synergy with theory and experiment. American Chemical Society, Washington, DC, pp 157—170, and references therein
77. Bökman F (1999) J Am Chem Soc 121:11217
78. Burk P, v. R. Schleyer P (2000) J Mol Struct (Theochem) 505:161
79. Rablen PR (2000) J Am Chem Soc 122:357
80. Holt J, Karty JM (2001) J Am Chem Soc 123:9564
81. Exner O, Čársky P (2003) J Am Chem Soc 125:2795
82. van Alem K, Lodder G, Zuilhof H (2002) J Phys Chem A 106:10681
83. Shaik S (2007) New J Chem 31:2015
84. (a) Reviews: Chem Rev, (2005) 105(10), whole issue; Chem Rev (2001) 101(5), whole issue; (b) Minkin VI, Glukhovtsev MN, Simkin B Ya (1994) Aromaticity and antiaromaticity. Wiley, New York; (c) Glukhovtsev M (1997) Chem Educ 74:132; (d) von R. Schleyer P, Jiao H (1996) Pure and Appl Chem 68:209; (e) Lloyd D (1996) J Chem Inf Comput Sci 36:442
85. (a) Angeli C, Malrieu JP (2008) J Phys Chem A 112:11481; (b) Jug K, Hiberty PC, Shaik S (2001) Chem Rev., 2001, *101*, 1477; (c) Maksić ZB, Barić D, Petanjek I (2000) J Phys Chem A 104:10873; (d) Mulder JJ (1998) J Chem Ed 75:594; (e) Shurki A, Shaik S (1997) Angew Chem Int Ed Engl 36:2205; (f) Hiberty PC, Danovich D, Shurki A, Shaik S (1995) J Am Chem Soc 117:7760; (g) For skepticism about this demotion of the role of the π electrons in imposing D_{6h} symmetry on benzene: Ichikawa H, Kagawa H (1995) J Phys Chem 99:2307; Glendening ED, Faust R, Streitwieser A, Vollhardt KPC, Weinhold F (1993) J Am Chem Soc 115:10952
86. (a) Review: Williams RV (2001) Chem Rev 101:1185; (b) Minkin VI, Glukhovtsev MN, Simkin B Ya (1994) Aromaticity and antiaromaticity. Wiley, New York; (c) Glukhovtsev M (1997) Chem Educ 74:132; (d) von R. Schleyer P, Jiao H (1996) Pure and Appl Chem 68:209. (E) Lloyd D (1996) J Chem Inf Comput Sci 36:442
87. Woodward RB, Fukunaga T, Kelly RC (1964) J Am Chem Soc 86:3162
88. Liebman JF, Paquette LA, Peterson JR, Rogers DW (1986) J Am Chem Soc 108:8267
89. Verevkin SP, Beckhaus H-D, Rüchardt C, Haag R, Kozhushkov SI, Zywietz T, De Meijere A, Jiao H, v R Schleyer P (1998) J Am Chem Soc 120:11130
90. (a) Chen Z, Wannere CS, Corminboeuf C, Puchta R, v. R. Schleyer P (2005) Chem Rev 105:3842; (b) Hossein FBS, Wannere CS, Corminboeuf C, Puchta R, v. R. Schleyer P (2006) Org Lett 8:863
91. Jiao H, Nagelkerke R, Kurtz HA, Williams RV, Borden WT, von R Schleyer P (1997) J Am Chem Soc 119:5921
92. (a) Chen Z, Jiao H, Wu JI, Herges R, Zhang SB, v. R. Schleyer P (2008) J Phys Chem A 112:10586; (b) Williams RV, Edwards WD, Zhang P, Berg DG, Mitchell RH (2012) J Am Chem Soc 134:16742
93. Griffiths P, Pivonka DE, Williams RV (2011) Chem Eur J 17:9193
94. (a) Karlstrom G, Lindh R, Malmqvist PA, Roos BO, Ryde, Veryazov V, Widmark PO, Cossi M, Schimmelpfennig B, Neogrady P, Seijo L (2003) Comput Mater Sci 28:222; (b) Anderssson K, Malmqvist PA, Roos BO (1992) J Chem Phys 96:1218
95. Duncan JA (2009) J Am Chem Soc 131:2416
96. Nicklaus MC, Williams RW, Bienfait B, Billings ES, Hodošček M (1998) J Chem Inf Comput Sci 38:893
97. Schaefer HF (2001) J Mol Struct (Theochem) 573:129
98. (a) An indication of the costs: see the archives of the Computational Chemistry List, CCL (above, under Websites for Computational Chemistry in General, http://www.ccl.net/), Dreyer R 2015 May 11; (b) Fox A (2011) Science 331:406; (c) Wilson EK (2011) Chem Eng News 16 May, 34. (d) Mullin R (2009) Chem Eng News 25 May, 10
99. Pfister G (1998) In search of clusters, 2nd edn. Prentice Hall, Upper Saddle River

Answers

Chapter 1, Harder Questions, Suggested Answers

Q1

Was there computational chemistry before electronic computers were available?

Computational chemistry *as the term is now understood* arose at about the same time as electronic computers became available to chemists:

> In 1951 an international conference was held at Shelter Island near Long Island in New York, N.Y. most of the leading figures in quantum chemistry were present. Two persons there symbolized the phasing out of desktop mechanical calculators (Prof. Kotani from Japan) and the phasing in of electronic digital computers (Prof. Roothaan of the United Sates). That was the first major conference with a focus on the emerging computer in theoretical chemistry [1].

With heroic effort, one of the very first molecular mechanics calculations, on a reasonably big molecule (a dibromodicarboxybiphenyl), was done by the Westheimer group, ca. 1946, presumably with at most a mechanical calculator [2]. Molecular mechanics is genuine computational chemistry, but is far less numerically intensive than quantum mechanical calculations. Nothing remotely like the quantity and level of complexity of the calculations we see today would be possible without electronic computers. One can make a case that computational chemistry *without* the electronic computer was essentially stillborn, ca. 1950.

To be fair, Hückel molecular orbital calculations, which can be executed with pencil and paper, might legitimately be held to fall within the purview of computational chemistry, and these were first done in the 1930s [3] (attaining great popularity in the 1950s and 1960s [4]). Computational chemistry thus blends into traditional theoretical chemistry, a good part of which-much of chemical thermodynamics–was almost singlehandedly created in the late 1800s, by Josiah Willard Gibbs [5].

Histories of the development of computational chemistry in various countries can be found in the continuing series *Reviews in Computational Chemistry* [6].

References

1. Lykos P (1997) Chapter 2 The evolution of computers in chemistry. In: Zielinski TJ, Swift ML (eds) Using computers in chemistry and chemical education. American Chemical Society, Washington, DC
2. (a) Westheimer FH, Mayer JE (1946) J Chem Phys 14:733; (b) Hill TL (1946) J Chem Phys 14:465; (b) Westheimer FH (1947) J Chem Phys 15:252; See too (c) Hill TL (1946) J Chem Phys 14:465; (d) Dostrovsky I, Hughes ED, Ingold CK (1946) J Chem Soc 173
3. Hückel E, Physik Z (1931) 70:204, and subsequent papers (see Hückel E (1975) Ein Gelehrtenleben. Ernst und Satire. Verlag Chemie, Weinheim, pp 178–179)
4. e.g. (a) The pioneering popularization: Roberts JD (1962) Notes on molecular orbital calculations. Benjamin, New York; (b) A detailed treatment: Streitwieser A (1961) Molecular orbital theory for organic chemists. Wiley, New York; (c) Perhaps the definitive presentation of the simple Hückel method is Heilbronner E, Bock H (1968) Das HMO modell und seine Anwendung. Verlag Chemie, Weinheim, Germany, vol 1 (basics and implementation); vol 2, (examples and solutions); (1970) vol 3 (tables of experimental and calculated quantities); (1970) An English translation of vol 1 is available: (1976) The HMO model and its application. Basics and manipulation. Verlag Chemie
5. Wheeler LP (1951) Josiah Willard Gibbs. The history of a great mind. Yale University Press
6. Reviews in computational chemistry, Lipkowitz KB, Boyd DB (eds) vols 1–18; Lipkowitz KB, Larter R, Cundari TR (eds) vols 19–21; Lipkowitz KB, Cundari TR, Gillet VJ (eds) vol 22; Lipkowitz KB, Cundari TR vol 23–26, vol 1, (1990) vol 26, ca. (2008) VCH, New York. http://chem.iupui.edu/rcc/rcc.html

Chapter 1, Harder Questions, Answers

Q2

Can "conventional" physical chemistry, such as the study of kinetics, thermodynamics, spectroscopy and electrochemistry, be regarded as a kind of computational chemistry?

First, let's realize that the boundaries between the old divisions of chemistry–organic, inorganic, physical, theoretical–are no longer sharp: all chemists should have a fair amount of theory, and with the help of this a chemist from one of the four divisions (one hesitates to stress the term division) should not be a complete outsider in any of the other three. That said, whether someone working in one of the "conventional" fields is doing computational chemistry depends: the term could be taken to mean calculation used to anticipate or rationalize experimental results, to predict unrealized chemistry, or to explain experimental results. So a kineticist might use computations to predict or explain rate constants, or an organic chemist might use computations to predict or explain the properties of novel organic compounds.

Work in one of the conventional fields is not, by tradition, regarded as computational chemistry, but it can become such if the principles of computational

chemistry (such as computational characterization of putative intermediates and transition states) are applied to a problem in the field.

Theoretical chemistry rates some special mention in this context. Nowadays this activity tends to be quite mathematical [1], but history shows us that theoretical chemistry need not be mathematical at all. From the first years of the crystallization of chemistry as a subject distinct from alchemy, chemists have utilized theory, in the sense of disciplined speculation. Nonmathematical examples are found in the structural theory of organic chemistry [2] and in most applications of the powerful Woodward-Hoffman orbital symmetry rules [3].

References

1. Wilson EK (1966) Theoretical chemistry expands and diversifies across chemical disciplines. Chemical & Engineering News, p 35
2. (a) Nye MJ (1993) From chemical philosophy to theoretical chemistry. University of California Press; (b) Gould RF (ed) (1966) Kekule symposium, Advances in Chemistry Series. American Chemical Society Publications, Washington, DC
3. Woodward RB, Hoffmann R (1970) The conservation of orbital symmetry. Verlag Chemie, Weinheim

Chapter 1, Harder Questions, Answers

Q3

The properties of a molecule that are most frequently calculated are geometry, energy (compared to that of other isomers), and spectra. Why is it more of a challenge to calculate "simple" properties like melting point and density?

Hint: Is there a difference between a molecule X and the substance X?

Properties like geometry, energy, and spectra are characteristics of single molecules (with the reservation that close contact with other molecules, especially solvation or crystal packing, can affect things), while melting point and density are bulk properties, arising from an ensemble of molecules. Clearly it should be easier to deal with a single molecule than with the hundreds or thousands (at least) that make up even a tiny piece of bulk matter.

Melting points have been calculated [1] extracting thermodynamic information about the solid and liquid phases by molecular dynamics simulations [2]. The freezing of water and melting of ice have been studied computationally [3].

References

1. E.g. (a) Anwar J, Frenkel D, Noro MN (2003) Melting point of NaCl. J Chem Phys 118:728;
   (b) Harafuji K, Tsuchiya T, Kawamura K (2003) Melting point of a GaN crystal. Phys Status
   Solidi 0(7):2420
2. Haile JM (1992) Molecular dynamics simulation. Wiley, New York
3. Małolepsza E, Keyes T (2015) J Chem Theory Comput 11:5613

Chapter 1, Harder Questions, Answers

Q4

Is it surprising that the geometry and energy (compared to that of other isomers) of a molecule can often be accurately calculated by a ball-and springs model (MM)?

Since in some ways molecules really do behave like ball-and-springs toys, it is not surprising that such a model enables one to calculate geometries and energies, but what is surprising is the accuracy possible with such calculations. Let's explore these two assertions.

In some ways molecules really do behave like ball-and-springs toys.

There are two assumptions here: that molecules have definite bonds, and that these bonds behave like springs.

1. Do molecules have definite bonds? A molecule is a collection of relatively immobile atomic nuclei and rapidly moving electrons, with the "relatively immobile" nuclei vibrating about equilibrium positions. At first sight this picture offers no hint of the existence of bonds. It might seem that IR spectra show that molecules have definite bonds, since these spectra are interpreted in terms of bond vibrations (stretching, bending, and torsional motions). Do the fundamental vibrations, the normal-mode vibrations (which in principle can be calculated by any of the standard computational chemistry methods used to optimize molecular geometry, and from which the experimentally observed vibrations can be "synthesized") really show the presence of the conventional, standard bonds of simple valence theory? Actually, the vibrational spectra show only that nuclei are vibrating along certain directions, relative to the axes of a coordinate system in which the molecule is placed. An IR spectrum computed by assigning to the conventional bonds stretching and bending force constants is said to correspond to a *valence forcefield*. Such a forcefield often serves to create a reasonable Hessian (Chap. 2) to initiate optimization of an input structure to a minimum (but not to a transition state), but does not always account for the observed IR bands, due to coupling of normal-mode vibrations [1].

   That molecules do have definite bonds, and that these tend to correspond in direction and number to the conventional bonds of simple valence theory, is

indicated by the quantum theory of atoms-in-molecules (AIM, or QTAIM) [2]. This is based on an analysis of the variation of electron density in molecules.

2. Do bonds behave like springs? It is well-established that for the small vibrational amplitudes of the bonds of most molecules at or below room temperature, the spring approximation, i.e. the simple harmonic vibration approximation, is fairly good, although for high accuracy one must recognize that molecules are actually anharmonic oscillators [1].

Is the accuracy of geometries and relative energies obtainable from MM surprising?

Bearing in mind that MM algorithms are heavily parameterized, this does not seem so surprising: the mathematician John von Neumann said "With four parameters I can cover an elephant, and with five I can make him wiggle his trunk." [3]. MM uses far more than four parameters. The accuracy is perhaps not surprising, but it is nevertheless impressive.

References

1. For a very detailed treatment of molecular vibrations, see Wilson EB Jr, Decius JC, Cross PC (1955) Molecular vibrations. McGraw-Hill; Dover edition, 1980, New York. Particularly relevant are chapters 1, 2, and 8
2. (a) Bader RFW (1990) Atoms in molecules. Clarendon Press, Oxford; (b) Bader RFW, Popelier PLA, Keith TA (1994) Angew Chem Int Ed Engl 33:620
3. Speaking to Freeman Dyson, Enrico Fermi quoted von Neumann: Dyson F (2004) Nature 427:297

Chapter 1, Harder Questions, Answers

Q5

What kinds of properties might you expect MM to be unable to calculate?

Unassisted MM can't calculate electronic properties, since MM knows nothing about electrons. It is possible to use empirical parameters to elicit from a structure calculated by MM electronic properties such as atomic charges: atoms in "standard molecules" can be assigned charges based on electronic calculations like ab initio or DFT, and these could be incorporated into a database. An MM program could draw on these data obtain a kind of educated guess of the atomic charges (which might then be used to calculate dipole moments and indicate likely sites of nucleophilic and electrophilic attack).

Thus pure MM (MM *by itself*) can't calculate UV spectra, the shapes and energies of molecular orbitals, and electron distribution and derivative properties of this, like atomic charges, dipole moments, and more arcane molecular features like bond paths (associated with atoms-in-molecules theory, AIMT [1]).

Reference

1. (a) Bader RFW (1990) Atoms in molecules. Clarendon Press, Oxford; (b) Bader RFW, Popelier PLA, Keith TA (1994) Angew Chem Int Ed Engl 33:620

Chapter 1, Harder Questions, Answers

Q6

Should calculations from first principles (ab initio) necessarily be preferred to those which make some use of experimental data (semiempirical)?

There are two aspects to confronting this question: a practical and what might be called a philosophical. On the practical aspect impinge questions of time, reliability, and accuracy. The philosophical issue is subtler.

If planned ab initio calculations would take an unacceptably long time with the software and hardware available, then one must simply either abandon the project or resort to a semiempirical method; these are typically hundreds to many thousands of times faster. Reliability and accuracy are not sharply distinct: one might not be able to rely on a calculation if it is not sufficiently accurate. Reliability could, alternatively, be equated with consistency (one usual meaning of the term): a method might be sometimes very accurate, but might erratically lapse in this regard. Only comparison with experiment for a carefully selected set of relevant cases can show how accurate and reliable a method is. For some problems the extremely fast molecular mechanics method is the most accurate and reliable: for reasonably normal monofunctional compounds, and particularly hydrocarbons, geometries are commonly accurate to within 0.01 Å for bond lengths and to within 2° for bond angles, and to within ca. 1 kJ mol^{-1} for heats of formation [1].

An amusing polemical debate on the virtues of semiempirical versus ab initio methods took place between Dewar, on the one hand, and Halgren, Kleier, and Lipscomb, on the other [2]. The Dewar group pioneered the semiempirical AM1 method, which spawned the PM3 method, these two being the most popular semiempirical quantum-mechanical methods in wide use today, while Lipscomb and coworkers were early advocates of ab initio methods. Dewar argued that ab initio methods were hopelessly inaccurate and expensive. Those were the days (1975) when owning your own computer was a dream and one paid perhaps $500 an hour to use one; it suffices to note that $500 was worth far more then and the fastest computer was far slower than a cheap personal computer is today. Dewar concluded that a study of the interconversion of benzene valence isomers by semiempirical versus ab initio methods would cost $5000 versus $1 billion! Lipscomb and coworkers argued that whatever its practical virtues, the semiempirical methods

"obscure the physical bases for success...and failure alike". This controversy is dated by the enormous increase in computer speed and the sophistication attained by ab initio methods since then, but it captures the flavor of part of the philosophical divide between the two approaches: the desire to get answers that might in principle, but less expediently, have been obtained in the lab, versus the desire to understand the underlying reasons for the phenomena being studied.

Nowadays chemists do not worry much about the virtues of semiempirical versus ab initio methods. Ab initio methods, it must be conceded, dominate computational chemistry studies in the leading journals, and indeed the study of exotic molecules or reactions by semiempirical calculations would be expected to be unreliable for lack of appropriate parameterization. Semiempirical methods are widely used in industry as an aid to the design of drugs and materials, and are quite possibly employed in preliminary exploration of projects for which only the later, ab initio results, ever see the light of publication.

To conclude: calculations from first principles are not *necessarily* to be preferred to semiempirical ones, although for novel molecules and reactions ab initio-type methods are more to be trusted.

References

1. For a good, fairly compact account of molecular mechanics see Levine IN (2014) Quantum chemistry, 7th edn. Prentice Hall, Upper Saddle River, Sect. 17.5
2. Dewar MLS (1975) Science 187:1037; (b) Halgren TA, Kleier DA, Lipscomb WN (1975) Science 190:591; (c) Dewar MJS (1975) Science 190:591

Chapter 1, Harder Questions, Answers

Q7

Both experiments and calculations can give wrong answers. Why then should experiment have the last word?

This is a highly "philosophical" question, but we will try to answer it in a practical way, relevant to our work as scientists.

First, we should note that in practice experiment does not automatically trump calculations: calculations which are considered to be reliable have been used to correct experimental results–or rather experimental claims, in contrast to "confirmed" experiments. Perhaps the best example of calculations, rather than experiment, leading to the correct answer is the case of triplet methylene, CH_2. The spectroscopist Gerhardt Herzberg deduced that this molecule has a linear structure, but the theoretician Henry Schaefer III was led by ab initio calculations to conclude that it is bent. We might note that correct experimental *results* can wrongly *interpreted*. The story has been reviewed [1]. Other examples of this are the (likely)

correction of dubious bond energies [2] and heats of formation [3]. So the interesting question is, why should "confirmed" experiments take precedence in credibility to calculations? Remove the quotation marks and the question almost answers itself: as scientific realists [4] we believe that a good experiment reflects a reality of nature; a calculation, on the other hand, is a kind of model of nature, possibly subject to revision.

References

1. Schaefer HF III (1985) Science 231:1100
2. Fattahi A, Lis L, Tian Z, Kass SR (2006) Angew Chem Int Ed Engl 45:4984
3. Ventura ON, Segovia M (2005) Chem Phys Lett 403:378
4. Leplin J (1997) A novel defence of scientific realism. Oxford University Press, Oxford

Chapter 1, Harder Questions, Answers

Q8

Consider the docking of a potential drug molecule X into the active site of an enzyme: a factor influencing how well X will "hold" is clearly the shape of X; can you think of another factor?

   Hint: molecules consist of nuclei and electrons.

   Another factor which comes to mind is charge. The shape factor arises from what could be called steric complementarity: ideally, for each bulge on X there is a corresponding depression on the active site, and vice versa. Another kind of complementarity arises from electrical charge: for each positive/negative region on X there is negative/positive region (ideally also of complementary shape). So for strong binding we would like each positively charged bulge on X to fit into a negatively charged depression, ideally of he same shape and size, in the active site, and analogously for positively charged depressions and negatively charged bulges. Of course this situation is unlikely to be always exactly realized.

   The hint was to remind us that in most molecules there is a substantial imbalance between positive and negative charge from place to place in the molecule.

Chapter 1, Harder Questions, Answers

Q9

In recent years the technique of *combinatorial chemistry* has been used to quickly synthesize a variety of related compounds which are then tested for

pharmacological activity (S. Borman, Chemical & Engineering News: 2001, 27 August, p. 49; 2000, 15 May, p. 53; 1999, 8 March, p. 33). What are the advantages and disadvantages of this method of finding drug candidates, compared with the "rational design" method of studying, with the aid of computational chemistry, how a molecule interacts with an enzyme?

All nine cells the same   Three different compounds   Nine different compounds
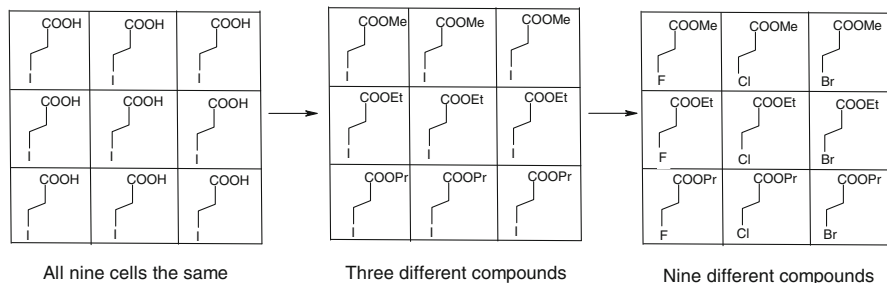
First let's refresh our memories as to the basic technique behind synthesis by combinatorial chemistry: this is outlined here using, for purely illustrative purposes, a 3×3 array of reaction cells, i.e. 9 cells:

3-iodopropanoic acid is converted to the methyl, ethyl, and propyl esters, by effecting across row 1 methylation, across row 2 ethylation, and across row 3 propylation. Then the esters are converted to fluoro-, chloro, and bromo-compounds by appropriate substitution reactions down columns 1, 2, and 3. In practice a 10×10 or bigger array might be used, creating 100 or more different compounds. The procedure can be automated and carried out on a small "micro-chip" ("lab on a chip"). One would likely begin with a compound that showed to some extent the desired activity, and make a host of variants. This relatively quick synthesis of many drug candidates, followed by mass testing, is called high-throughput screening (HTS).

There has been some disappointment with combinatorial chemistry. This is discussed in a nicely balanced article with the engaging cover title "I, chemist. Researchers trump robots in drug discovery" (shades of Isaac Asimov!) [1]. It appears that the method may have been oversold; indeed, a cynic might say that with millions of compounds generated by combinatorial chemistry, we should now have effective drugs for all diseases. HTS does continue to be useful: "Most sources agree that combinatorial chemistry is an important part of building a library of compounds from which to work and that HTS is needed at some point in the process of drug discovery." [1]. Nevertheless, if we realize that all diseases are molecular, we are led to conclude that if our understanding of the mechanisms by which chemical processes cause disease is sufficiently sophisticated, then rational molec-ular intervention should be the most effective approach to drug therapy. As Dror Ofer of Keddem Bioscience was quoted as saying [1]: "The real issue in drug discovery is that we don't understand the key steps in developing a drug. We must say this openly and clearly. To understand, in science, means only one thing: the

ability to predict results. Medicinal chemists must study physical chemistry–how atoms really react to one another. You have to go back to the science when something doesn't work, rather than applying more brute force."

Reference

1. Mullin R (2004) Chemical and Engineering News, 26 July, p 23

Chapter 1, Harder Questions, Answers

Q10

Think up some unusual molecule which might be investigated computationally. What is it that makes your molecule unusual?

The choice and justification for this is very much an individual matter: what kind of chemistry fascinates you? You can read about some of the molecules that fascinate other chemists in the books by Hopf [1] and by me [2].

References

1. Hopf H (2000) Classics in hydrocarbon chemistry. Wiley-VCH, Weinheim, New York
2. Lewars E (2008) Modelling marvels. Computational anticipation of novel molecules. Springer, Dordrecht

Chapter 2, Harder Questions, Suggested Answers

Q1

The Born-Oppenheimer principle is often said to be a prerequisite for the concept of a PES. Yet the idea of a PES (Marcelin, 1915) predates the Born-Oppenheimer principle (1927). Discuss.

The Born-Oppenheimer principle (Born-Oppenheimer approximation) [1] says that the electrons in a molecule move so much faster than the nuclei that the two kinds of motion are independent: the electrons see the nuclei as being stationary, and so each electron doesn't have to adjust its motion to maintain a minimized electron-nucleus interaction energy. Thus we can calculate the purely electronic energy of a molecule, then the internuclear repulsion energy, and add the separate energies to get the total molecular energy.

The concept of a PES can be based simply on the concept of molecular structure, without specific reference to nuclei and electrons: if one thinks of a molecule as being defined by the relative positions (in a coordinate system) of its atoms (no reference to nuclei and electrons), then it is intuitively apparent that as these positions are altered the energy of the collection of atoms will change. This is probably how Marcelin thought of molecules [2]. On the mathematical surface defined by Energy $= f$(atomic coordinates), minima, transition states etc., defined by first and second derivatives, emerge naturally. On the other hand, if one insists on going beyond mere atoms, and thinks of a molecule as a collection of nuclei and electrons, then molecular shape (geometry) has meaning only if the nuclei (in this context the hallmark of "atoms") are more or less fixed. This stricture is violated in CH_5^+, which has no clear shape [3].

References

1. Born M, Oppenheimer JR (1927) Ann Phys 84:457
2. Marcelin R (1915) Ann Phys 3:152. Potential energy surface: p 158
3. (a) Oka T (2015) Science 347:1313; (b) Huang X, McCoy AB, Bowman JM, Johnson LM, Savage C, Dong F, Nesbitt DJ (2006) Science 311:60; (c) Thompson KC, Crittenden DL, Jordan mJT (2005) J Am Chem Soc 127:4954; (d) Schreiner PR (2000) Angew Chem Int Ed Engl 39:3239; (e) Marx D, Parrinello M (1999) Science 284:59; White ET, Tiang J, Oka T (1999) Science 284:135

Chapter 2, Harder Questions, Answers

Q2

How high would you have to lift a mole of water for its gravitational potential energy to be equivalent to the energy needed to dissociate it completely into hydroxyl radical and hydrogen atoms? The strength of the O–H bond is about 400 kJ mol^{-1}; the gravitational acceleration g at the Earth's surface (and out to hundreds of km) is about 10 m s^{-2}. What does this suggest about the role of gravity in chemistry?

This was put in the "Harder Questions" category because the answer can't be found just be reading the chapter, but actually the solution comes from a straightforward application of simple physics.

The energy needed to homolytically dissociate a mole of water into the radicals HO$^{\cdot}$ and H$^{\cdot}$ is ca. 400 kJ. We want to calculate how high 18 g of water must be lifted for its gravitational potential energy to be 400 kJ. Working in SI units:

Pot E = force × distance = mass × gravitational acceleration × height = mgh,

energy in J, mass in kg, g in m s^{-2}, h in m

h = Pot E/mg = 400 000/(0.018 × 10) meters = 2 × 10^6 m or 2000 km

Actually the height is the same regardless of the mass of water, since, e.g. doubling the mass doubles both the energy needed for dissociation, and the mass m in the denominator. The calculation is flawed somewhat by the fact that the force of gravity is considerably smaller 2000 km above the surface of the Earth (radius $= 6000$ km) (by a factor of $(8000)^2/(6000)^2 = 1.8$). A more realistic calculation would express the gravitational acceleration g as a function of h and integrate with respect to h. This calculation does however indicate that if all the potential energy were somehow directed into dissociating the H-O bond, a fall from a great height would be needed!

Chapter 2, Harder Questions, Answers

Q3

If gravity plays no role in chemistry, why are vibrational frequencies different for, say, C–H and C–D bonds?

It's inertia, the resistance of mass to motion, not gravity, that causes the difference. A deuterium atom is heavier than a hydrogen atom, but the real point is not its weight, which involves gravity, but its mass, which does not. The vibrational frequency of a bond depends on its stiffness (the force constant) and on the masses of the atoms involved. For a diatomic molecule A–B the vibrational frequency (in wavenumbers) is governed by the simple formula

$$\widetilde{v} = \frac{1}{2\pi c}\left(\frac{k}{\mu}\right)^{1/2}$$

where c is the velocity of light, k is the force constant, and μ (mu) is the reduced mass of the two atoms, $M_1 m_2/(M_1 + m_2)$. If M_1 is huge compared to m_2, this equation devolves to

$$\widetilde{v} = constant\left(\frac{k}{m_2}\right)^{-1/2} \tag{2.16}$$

as expected, since essentially the big mass does not move. With polyatomic molecules, accounting for mass is a bit more complicated. The force constant matrix must be "mass weighted" and diagonalized to give a matrix with the displacement vectors of the vibrations, and a matrix with the frequencies [1].

Reference

1. Details of how this is done in a computational chemistry program are given in http://www.gaussian.com/g_whitepap/white_pap.htm, Vibrational analysis in Gaussian

Chapter 2, Harder Questions, Answers

Q4

We assumed that the two bond lengths of water are equal. *Must* an acyclic molecule AB_2 have equal A–B bond lengths? What about a cyclic molecule AB_2?

Intuitively, there is no reason why acyclic or cyclic AB_2 should have unequal A–B bond lengths: one A–B bond seems just as good as the other. But *proving* this is another matter.

Consider a molecule AB_2, linear, bent, or cyclic. Each of the two A–B bonds has the same force constant – we can't have one, say, single and one double, because this on-paper arrangement would correspond to a resonance hybrid with each bond the same ca. 1.5 in bond order:

(1)   two different molecules if we distinguish (somehow label) the Bs

(2)   a resonance hybrid
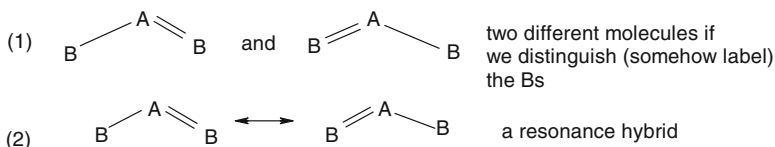
Since A–B1 and A–B2 have the same force constant, a structure with unequal bond lengths represents only vibrational extremes arising from a symmetric A–B stretch: the molecule must vibrate around an equilibrium structure with equal A–B lengths. If you doubt this, imagine constructing a ball and springs model of AB_2 with identical A–B springs but different equilibrium A–B lengths; this is clearly impossible.

The case of cyclobutadiene may at first seem to contradict the above assertion that if a "central" atom A is connected to two atoms B the force constants must be the same, giving rise to equal bond lengths. Cyclobutadiene is rectangular rather than square and so one bond from a carbon is single, and one is double, say the bonds designated here C1–C2 and C1–C3; **1** and **2** are distinct molecules separated by a barrier [1]:
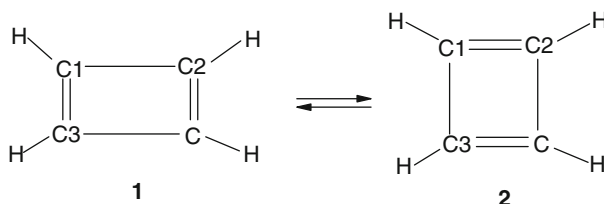
1 and **2** are not canonical forms of a resonance hybrid, but rather distinct molecules:

chemical reaction

NOT   resonance
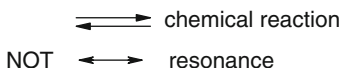
Here we can call C1 our central atom, and it seems to be connected to B/C2 by a single bond and to B/C3 by a double bond. However, C2 and C3 are not equivalent for our analysis: moving away from C1, C2 is followed by a double bond, and C3 is followed by a single bond. Whether a molecule will exhibit valence isomerism, as shown by cyclobutadiene, or resonance, as shown by benzene, is not always easy to predict.

Reference

1. Santo-Garcıá JC, Pérez-Jiménez AJ, Moscardó F (2000) Chem Phys Lett 317:245, and references therein

Chapter 2, Harder Questions, Answers

Q5

Why are chemists but rarely interested in finding and characterizing second-order and higher saddle points (hilltops)?

The short answer is, because they (the hilltops, not the chemists) don't do anything chemically. In a chemical reaction, we have (at least two) minima, and molecules move between them, passing through transition states, which are first order saddle points. Although in passing from one minimum to another all molecules do not strictly follow the intrinsic reaction coordinate (IRC) the lowest energy pathway on a PES that connects the minima, very few molecules are likely to stray so far outside the IRC that they pass through a hilltop [1].

Although hilltops are rarely deliberately sought, one sometimes obtains them in an attempt to find a minimum or a transition state. By a little fiddling with a hilltop one can often convert it to the desired minimum or transition state. For example, when the geometry of doubly eclipsed (C_{2v}) propane is optimized, one obtains a hilltop whose two imaginary frequencies, when animated, show that this geometry wants to relieve both eclipsing interactions. Altering the hilltop structure to a doubly staggered (ideally also C_{2v}) geometry and optimizing this yields a minimum. Altering the hilltop to a singly eclipsed structure gives a transition state interconverting minima.

doubly eclipsed
hilltop

doubly staggered
minimum

singly eclipsed
transition state
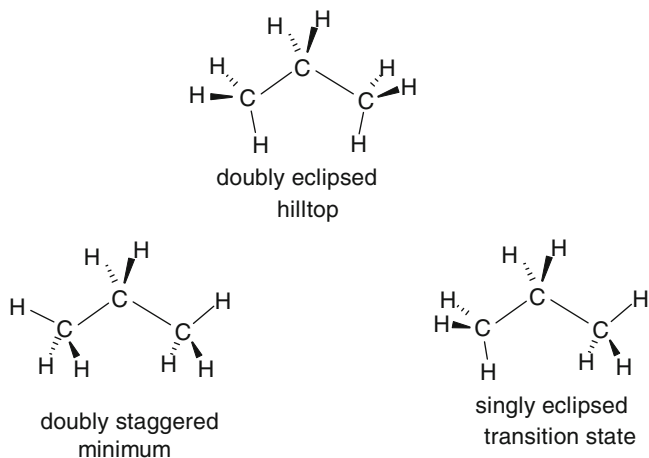
Reference

1. Shaik SS, Schlegel HB, Wolfe S (1992) Theoretical aspects of physical organic chemistry: the SN2 mechanism. Wiley, New York. See particularly chapters 1 and 2, and pp 50, 51

Chapter 2, Harder Questions, Answers

Q6

What kind(s) of stationary points do you think a second-order saddle point connects?

A second-order saddle point has two of its normal-mode vibrations corresponding to imaginary frequencies, that is, two modes "vibrate" without a restoring force, and each mode takes the structure on a one-way trip downhill on the potential energy surface. Now compare this with a first-order saddle point (a transition state); this has one imaginary normal-mode vibration: as we slide downhill along the direction corresponding to this vibration, the imaginary mode disappears and the structure is transformed into a relative minimum, with no imaginary vibrations. Correspondingly, as a second-order saddle structure moves downhill along the path indicated by one of the imaginary vibrations, this vibration vanishes and the structure is transformed into a first-order saddle point. Illustrations of this are seen in Figs. 2.9 and 2.14, where the hilltops lead to saddle points by conformational changes.

Chapter 2, Harder Questions, Answers

Q7

If a species has one calculated frequency very close to 0 cm^{-1} what does that tell you about the (calculated) PES in that region?

First let us acknowledge a little inaccuracy here: frequencies are either positive, imaginary (not negative), or, occasionally, essentially zero. Some programs designate an imaginary frequency by a minus sign, some by i (the symbol for $\sqrt{-1}$). Frequencies are calculated from the force constants of the normal vibrational modes, and the force constant of a vibrational mode is equal to the curvature of the PES along the direction of the mode (= the second derivative of the energy with respect to the geometric change involved). Whether a frequency is positive or imaginary depends qualitatively on the curvature. A minimum has positive curvature along the direction of all normal-mode vibrations, a first-order saddle point has negative curvature along the direction of one normal-mode vibration and positive curvature along all other normal-mode directions, and analogously for a second-, third-order etc. saddle point. Positive curvature corresponds to positive force constants and positive frequencies, and negative curvature to negative force constants and, taking square roots, imaginary frequencies. A zero frequency, then, corresponds to a zero force constant ($\sqrt{0} = 0$) and zero curvature of the potential energy surface along that direction. Moving the atoms of the structure slightly along that direction leads to essentially no change in the energy, since the curvature of the energy-distance graph for that motion is the force constant for the vibration (i.e. the second derivative of the energy with respect to the motion; the first derivative of energy with respect to motion is the force). Along that direction the PES is a plateau. There are thus three ways in which a structure can be a stationary point, i.e. rest on a flat spot on the PES: it can reside at a relative minimum, where the surface curves up in all directions, at a saddle point, where the surface curves downward in one or more directions, or it a point where along one direction the surface does not curve at all (is a plateau).

The third situation could correspond to a "structure" in which an optimization algorithm, in its zeal to find a stationary point (where all first derivatives are zero) moves two molecules significantly beyond their van der Waals separation:

energy

geometry

van der Waals
separation

PES essentially flat along
direction of this geometry change
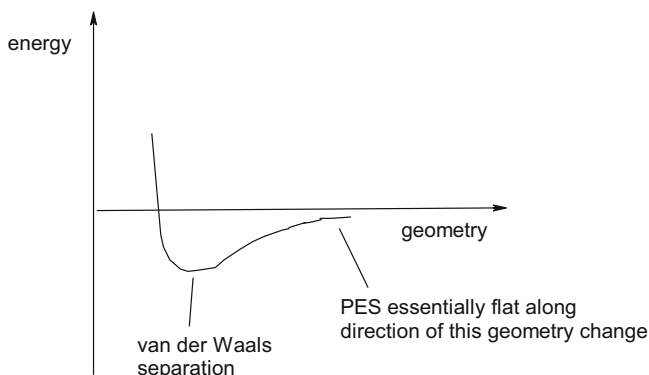
The vibrational mode corresponding to altering the separation of the molecules is ca. 0 cm^{-1}; the internal modes of each molecule, bond stretch, bend, and torsional modes, are of course nonzero.

Chapter 2, Harder Questions, Answers

Q8

The ZPE of many molecules is greater than the energy needed to break a bond; e.g. the ZPE of hexane is about 530 kJ mol^{-1}, while the strength of a C–C or a C–H bond is only about 400 kJ mol^{-1}. Why then do such molecules not spontaneously decompose?

They do not spontaneously decompose because the ZPE is not concentrated in just one or a few bonds. An exotic structure could indeed run the risk of decomposing by such concentration of its vibrational energies. A candidate for this is the transition state (which is calculated to be nonplanar) for inversion of methane. Incidentally, this would correspond to racemization if four different hydrogens could be attached to a carbon; unfortunately ^{4}H has a halflife of only 10^{-22} s [1]. The question of the possible breaking of a C-H bond here in preference to inversion has been considered [2].

References

1. Ter-Akopian GM et al (2002) American Institute of Physics Conference Proceedings, April 22, vol 610, p 920. Nuclear physics in the 21st century: International nuclear physics conference INPC 2001; doi:10.1063/1.1470062
2. Lewars E (2008) Modeling marvels. Computational anticipation of novel molecules. Springer, New York, chapter 1, Planar Carbon, Introduction

Chapter 2, Harder Questions, Answers

Q9

Only certain parts of a PES are chemically interesting: some regions are flat and featureless, while yet other parts rise steeply and are thus energetically inaccessible. Explain.

Chemically interesting regions of a PES are areas where relative minima and the transition states connecting them reside, that is, where chemistry takes place. Rarely-explored are parts where nothing happens or too much happens.

Nothing happens where a molecule has been broken into its component atoms and these atoms are widely separated and thus noninteracting–these are plateau regions (compare Question 7). Here the reaction coordinate is simply a composite of the interatomic separations and altering these has no effect on the energy.

Too much happens in regions where molecules or parts of molecules are squeezed strongly together: here the energy changes very steeply with changes in the reaction coordinate, rising sharply as intermolecular or nonbonded atomic distances decrease. Actually, these regions might be of interest in molecular dynamics studies of reactions under very high pressures [1–3].

References

1. Frank I (2003) Molecular dynamics, review. Angew. Chem Int Ed Engl 42:1569
2. Tuckerman ME, Martyna GJ (2000) Molecular dynamics, review. J Phys Chem B 104:159
3. Scandolo S, Jeanloz R (2003) Molecular dynamics study of the conversion of methane to diamond under pressure. American Scientist 91:516

Chapter 2, Harder Questions, Answers

Q10

Consider two PESs for the HCN ⇆ HNC reaction: *A*, a plot of energy vs. the H–C bond length, and *B*, a plot of energy vs. the HCN angle. Recalling that HNC is the higher-energy species (Fig. 2.19), sketch qualitatively the diagrams *A* and *B*.
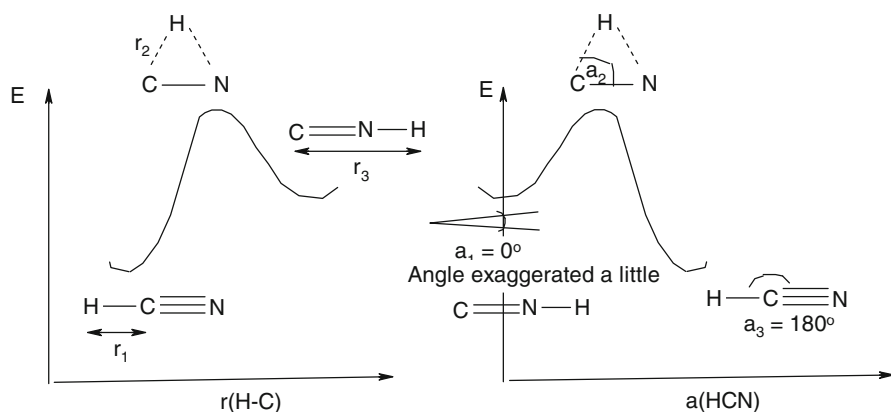
Chapter 3, Harder Questions, Suggested Answers

Q1

One big advantage of MM over other methods of calculating geometries and relative energies is speed. Does it seem likely that continued increases in computer speed could make MM obsolete?

Let's rephrase the question a bit to make it more tractable: could increases in computer speed make MM obsolete? The answer would seem to be yes, eventually. If computer speed increases indefinitely, the essentially complete solution of the Schrödinger equation will become possible for bigger and bigger molecules. This solution is the holy grail of computational chemistry, as such a solution should accurately predict the properties of the molecule. All computations might be perfectly accurate if computers were infinitely fast, a probably unattainable goal, but one that might be effectively approximated should practical quantum computers ever become available [1, 2].

References

1. Benenti G, Casati G (2005) Europhysics News 36:16
2. Scott A (2008) Scientific American 298:50

Chapter 3, Harder Questions, Answers

Q2

Do you think it is possible (in practical terms? In principle?) to develop a forcefield that would accurately calculate the geometry of any kind of molecule?

It is intuitively apparent that with sufficient parameters a physical system, and even a set of systems, can be simulated to any desired accuracy (although there does not seem to a formal theorem in physics or mathematics to this effect). In this vein, the mathematician John von Neumann said "With four parameters I can cover an elephant, and with five I can make him wiggle his trunk." [1]. The logistics of putting together such an enormous suite of algorithms apart, whether such a forcefield would be practical is another matter.

Reference

1. Speaking to Freeman Dyson, Enrico Fermi quoted von Neumann: Dyson F (2004) Nature 427:297

Chapter 3, Harder Questions, Answers

Q3

What advantages or disadvantages are there to parameterizing a forcefield with the results of "high-level" calculations rather than the results of experiments?

If you are a purist and regard molecular mechanics as a semiempirical method (the theoretical part coming from the physics of springs and the theory of van der Waals and electrostatic and nonbonded interactions) then you will be uncomfortable with any nonexperimental (nonempirical) parameterization. As a practical matter, however, we simply want a method that works, and we can compare the two approaches to parameterizing in this context.

Accurate force constants etc. can be obtained from high-level ab initio (Chap. 5) or DFT (Chap. 7) calculations. If we use these for a forcefield, then we are parameterizing to match reality only to the extent that the high-level calculations match experiment. Apart from a possible philosophical objection, which we essentially dismissed, there is the question of the trustworthiness of the ab initio or DFT results. For "normal" molecules, that is, species which are not in some way exotic [1], these calculations do indeed deliver quite reliable results. The advantages they offer over experimental acquisition of the required parameters is that these quantities (1) can be obtained for a wide variety of compounds without regard to synthetic difficulties or commercial availability, (2) are offered up transparently by the output of the calculation, rather than being required to be extracted, perhaps somewhat tortuously, from experiments, (3) are usually more quickly calculated than determined in the lab, and (4) can be uniformly secured, that is, all parameters can be obtained from calculations at the same level, say MP2/6-311G(df,p), in contrast to experiment, where different methods must be used to obtain different parameters. This last point may be more of an esthetic than a utilitarian advantage.

The advantage of parameterizing with experimental quantities is that, if the experiment is reliable, then we *know* that the values of the parameters; we need not reflect on the reliability of the calculation. Of course, we might wish to ponder the accuracy of the experiment.

Reference

1. Lewars E (2008) Modeling marvels. Computational anticipation of novel molecules. Springer, Dordrecht

Chapter 3, Harder Questions, Answers

Q4

Would you dispute the suggestion that no matter how accurate a set of MM results might be, they cannot provide insight into the factors affecting a chemical problem, because the "ball and springs" model is unphysical?

First, the ball and springs model used in molecular mechanics is not completely nonphysical: to a fair approximation, molecules really do vibrate and bonds do stretch and bend, as expected from a macroscopic ball and springs model. It is when we want to examine inescapably electronic properties, like, say, UV spectra or the donation of electrons from one species to another to make a bond, that the MM model is completely inadequate.

Since MM gives geometries that vary from fairly to highly accurate for molecules that are not too outré, where steric factors are relevant it *can* provide chemical insight.

Chapter 3, Harder Questions, Answers

Q5

Would you agree that hydrogen bonds (e.g. the attraction between two water molecules) might be modelled in MM as weak covalent bonds, as strong van der Waals or dispersion forces, or as electrostatic attractions? Is any one of these approaches to be preferred in principle?

No, none is to be preferred "in principle", meaning on grounds of theoretical appropriateness. This is because MM is severely practical, in the sense that the forcefield need only satisfactorily and swiftly reproduce molecular properties, mainly geometries. The method makes no apologies for ad hoc additions which improve results. An example of this is seen in the inclusion of a special term to force the oxygen of cyclobutanone to lie in the ring plane [1]. Identifying the terms in a forcefield with distinct theoretical concepts like force constants and van der Waals forces is at best an approximation.

Hydrogen bonding can be dealt with in principle in any way that works. A weak covalent bond would be simulated by a small bond stretch constant (roughly, a force constant), a strong van der Waals force could be modelled by adjusting the two constants in the Lennard-Jones expression, and electrostatic attraction by a Coulomb's law inverse distance expression. These are only simple examples of how these methods might be implemented; a brief discussion is given by Leach [2]. The choice of method to be implemented is determined by speed and accuracy. Treating strong hydrogen bonds by MM has been discussed [3].

References

1. Leach AR (2001) Molecular modelling, 2nd edn. Prentice Hall, New York; section 4.6
2. Leach AR (2001) Molecular modelling, 2nd edn. Prentice Hall, New York; Section 4.13
3. Vasil'ev VV, Voityuk AA (1992) J Mol Struct 265(1–2):179

Chapter 3, Harder Questions, Answers

Q6

Replacing small groups by "pseudoatoms" in a forcefield (e.g. CH_3 by an "atom" about as big) obviously speeds up calculations. What disadvantages might accompany this simplification?

   The obvious disadvantage is that one loses the directional nature of the group and thus loses any possibility of simulating conformational effects, as far as that group is concerned. Rotation around a C-CH_3 bond alters bond lengths and energies, albeit relatively slightly, but if we pretend that the CH_3 group is spherical or ellipsoidal, then clearly it cannot engender a torsional energy/dihedral angle curve.

   The loss of the conformational dimension could be a significant defect for a polar group like OH, where rotation about a (say) C-OH bond could in reality lead to formation or breaking of a hydrogen bond to some lone pair atom, with changes in the relative energies of different conformations.

Chapter 3, Harder Questions, Answers

Q7

Why might the development of an accurate and versatile forcefield for inorganic molecules be more of a challenge than for organic molecules?

   For the purposes of this question we can consider "unproblematic organics" to exclude molecules containing elements beyond calcium, element 20: our uneventful organics can thus contain H, Li-F, Na-Cl, K and Ca. We'll also give a pass to Br and I. Problem elements are Sc, Ti, . . ., As, Se, Rb, Sr . . ., Sb, Te, Cs, Ba, . . ., Bi, Po, At, and the subsequent radioactive elements.

   The problematic atoms are thus the heavier nonmetals, and the metals scandium and beyond, most of which are transition metals (or the related lanthanides): p block, d block and f block elements. In the context of electronic theories these are, traditionally at least, considered to employ d orbitals in their hypervalent bonding [1]. Now, in molecular mechanics orbitals simply do not exist so the

difficulties must be for formulated without reference to them (parameterizing a *quantum mechanical* semiempirical method like AM1 or PM3 to account for d orbital effects also presents special problems [2]). In simplest terms, the problems with these atoms lies in the unconventional (compared to the usual organics) geometries encountered. Normal organics have a tetrahedral or simpler disposition of bonds around each atom, but problem elements (first paragraph above) can have pentagonal bipyramidal, octahedral, and other geometries. There are more bonds and more interbond angles to address; some organometallic bonding is not even usually depicted in terms of bonds between individual atoms, e.g. bonding to cyclopentadienyl, π-allyl and alkene ligands. A brief discussion of MM applied to organometallic and inorganic compounds is given by Rappé and Casewit [3].

References

1. Lewars E (2008) Modeling marvels. Computational anticipation of novel molecules. Springer, Dordrecht; chapters 4 and 5
2. Thiel W, Voityuk AA (1996) J Phys Chem, 100: 616, and references therein
3. Rappé AK, Casewit CJ (1997) Molecular mechanics across chemistry. University Science Books, Sausalto

Chapter 3, Harder Questions, Answers

Q8

What factor(s) might cause an electronic structure calculation (e.g. ab initio or DFT) to give geometries or relative energies very different from those obtained from MM?

The most likely factor is electronic: since MM makes no reference to electrons, it should not be expected to reflect structural and energetic effects arising from, say, aromaticity and antiaromaticity, encapsulated in the $4n + 2$ and the corollary 4n rules [1–3].

References

1. Minkin V, Glukhovtsev MN, Simkin B. Ya (1994) Aromaticity and antiaromaticity: electronic and structural aspects. Wiley, New York
2. Randić M (2003) Chem Rev 103:3440
3. (2005) Chem Rev 105(10); whole issue devoted to aromaticity, antiaromaticity and related topics

Chapter 3, Harder Questions, Answers

Q9

Compile a list of molecular characteristics/properties that cannot be calculated purely by MM.
   Among these properties are:

UV spectra
dipole moment (by pure MM)
delocalization energy (this is related to aromaticity and antiaromaticity)
transition state structures and energies (see the hedge below)

   The properties are listed in approximate order of simplicity of connection with electronic behavior:

UV spectra arise from electronic transitions, automatically placing them outside the accessible to MM.

Dipole moments arise from uneven distribution of electric charge in a molecule, which in turn is due to nuclear charges not being "matched" spatially by electron distribution. This would seem to automatically rule out probing by MM. However, a subterfuge enables MM molecular geometries to yield dipole moments: the dipole moment of a molecule can be considered to be the vector sum of bond moments, and like bond energies these are with a fair degree of accuracy transferable between molecules. So from the geometry, which gives the relative positions of the vectors in space, a dipole moment can be calculated, purely empirically.

Delocalization energy denotes the energy by which a molecule is stabilized or destabilized compared to a hypothetical reference compound in which electrons (usually π electrons) are not as mobile. The canonical example is the energy of benzene compared to the hypothetical 1,3,5-cyclohexatriene in which there are three distinct double and three distinct triple bonds. With caveats, one measure of this energy is the heat of hydrogenation of benzene compared to three times the heat of hydrogenation of cyclohexene. As an electronic phenomenon, this lies outside the purview of MM.

Transition state structures and energies differ from those of molecules (i.e. from those of relative minima on a potential energy surface) in that transition states are not relative minima but rather are saddle points, and that they are not readily observed experimentally (with molecular beam and laser technology simple transition states can be, in effect, observed [1]). These differences should not, in principle, make MM inapplicable to calculating geometries and energies of transition states: an assembly of atoms connected by bonds (some of these would be partial bonds for a transition state) of known force constants should permit its geometry to be adjusted so that one of its normal-mode vibrations has a negative force constant (the critical feature of a transition state), and force constants of

transition states could be calculated by quantum mechanical methods.[1] Indeed, MM has been used to calculate geometries and energies of transition states, but these studies have used force fields developed for very specific reactions, perhaps the best example being the dihdroxylation of alkenes with osmium tetroxide under the influence of a chiral catalyst [2]. However, MM is not at present a generally applicable tool for studying transition states. This is probably because force constants are not as transferable between transition states (are more variable from one transition state to another) as they are between ordinary molecules, making a forcefield that works for one kind of reaction inapplicable to another.

References

1. (a) Lucht RP (2007) Science 316:207; (b) Rawls RL (2000) Chemical and Engineering News, May 22, 35
2. Norrby P-O, Rasmussen T, Haller J, Strassner T, Houk KN (1999) J Am Chem Soc 121:10186

Chapter 3, Harder Questions, Answers

Q10

How many parameters do you think a reasonable forcefield would need to minimize the geometry of 1,2-dichloroethane?

Look at the structure of the molecule:
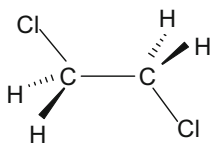
At a bare minimum, we would need parameters for these six contributors to the energy (here C is the *atom type* sp^3 C):

1. $E_{stretch}$(C–C)
2. $E_{stretch}$(C–H)
3. $E_{stretch}$(C–Cl)
4. E_{bend}(HCC)

---

[1] Such as ab initio, density functional, and semiempirical methods. The reliability of the geometries and energies of calculated transition states can be gauged by comparing activation energies calculated from them with experimental activation energies.

5. $E_{bend}(ClCC)$
6. $E_{torsion}(ClCH_2–CH_2Cl)$

For each of the three $E_{stretch}(X–Y)$ terms, $k_{stretch}(X–Y)$ and $l_{eq}(X–Y)$ are needed, for a total of 6 parameters. For each of the two $E_{bend}(XYY)$ terms, $k_{bend}(XYY)$ and $a_{eq}(XYY)$ are needed, for a total of 4 parameters. The torsional curve likely requires at least 5 parameters (cf. Book, p. 52) for reasonable accuracy. This makes a total of $6 + 4 + 5 = 15$ parameters. But this would be a very stunted forcefield; it has no parameters for nonbonded interactions and so is not suitable for molecules with bulky groups, and it is parameterized only for the atom types sp^3 C, H, and Cl. It cannot handle other kinds of carbon and other elements, and it has no special parameters for electrostatic interactions.

A reasonable forcefield would be of more general applicability: it should be able to handle the eight common elements $C(sp^3, sp^2, sp)$, H, $O(sp^3, sp^2)$, $N(sp^3, sp^2, sp)$, F, Cl, Br, I; we are focussing for convenience on an organic chemistry forcefield. Yet this would have only 13 atom types, compared to the typical organic forcefield with 50–75 [1]. Similar considerations applied to the stretching of C–H, C–O, C–N, C–F, . . ., H–O, H–N, etc. bonds, to the bending of various C–C–C, CO–C, etc. angles, to rotation about single bonds, and to nonbonded interactions, reveals that we need hundreds of parameters. The popular Merck Molecular Force Field MMFF94 is said to have about 9000 parameters [2].

References

1. Levine IN (2014) Quantum chemistry, 7th edn. Prentice-Hall, Upper Saddle River, p 634
2. Levine IN (2014) Quantum chemistry, 7th edn. Prentice-Hall, Upper Saddle River, p 635

Chapter 4, Harder Questions, Suggested Answers

Q1

Do you think it is reasonable to describe the Schrödinger equation as a postulate of quantum mechanics? What is a postulate?

The consensus is that the Schrödinger equation cannot be derived, but rather it must be (and in fact it was) arrived at by more or less plausible arguments, then tested against experiment. Thus it can be regarded as having originated as a postulate, but as having survived testing so thoroughly that it may now be taken as, to all intents and purposes, correct. Detailed presentations of the historical facts connected with the genesis of the equation are given by Moore [1] and Jammer [2]. For a perceptive exegesis of the equation see Whitaker [3].

The simplest "derivation", given in many books, e.g. in Chap. 4, was in fact similar to that used by Schrödinger to obtain an equation which falls short of the

relativistic Schrödinger equation only by the absence of spin, a concept which had not yet arisen [1]. This first quantum-mechanical wave equation is now known as the Klein-Gordon equation, and applies to particles without spin.

References

1. Moore W (1989) Schrödinger. Life and thought. Cambridge University Press, Cambridge, chapter 6
2. Jammer M (1989) The conceptual development of quantum mechanics. American Institute of Physics, pp 257–266
3. Whitaker A (1996) Einstein, Bohr, and the quantum dilemma. Cambridge University Press, Cambridge, pp 138–146

Chapter 4, Harder Questions, Answers

Q2

What is the probability of finding a particle at a point?

The probability of finding a particle in a small region of space within a system (say, a molecule) is proportional to the size of the region (assume the region is so small that within it the probability per unit volume does not vary from one infinitesimal volume to another). Then as the size of the region considered approaches zero, the probability of finding a particle in it must approach zero. The probability of finding a particle *at* a point is zero.

More quantitatively: the probability of finding a particle in an infinitesimal volume of space dv in some system (e.g. a molecule) is given by

$$P(dv) = \rho(x, y, z)dv = \rho(x, y, z)dxdydz$$

in Cartesian coordinates, where ρ (rho) is the probability distribution function characteristic of that particle in that system. The probability is a pure number, so ρ has the units of reciprocal volume, volume^{-1}, e.g. $(m^3)^{-1}$ or in atomic units $(bohr^3)^{-1}$. *P(dv)* generally varies from place to place in the system, as the coordinates x, y, z are varied; referring to an "infinitesimal" volume is a shorthand way of saying that

$$\lim_{\Delta v \to 0} P(x, y, z)\, \Delta v = P(x, y, z)dv$$

The probability of finding the particle in a volume V is

$$P(V) = \int_V \rho(x, y, z)dv$$

where the integration is carried out over the coordinates of the volume (in cartesian coordinates, over the values of x, y, z which define the volume). For a point, the volume is zero and the coordinates will vary from 0 to 0:

$$p(V) = \int_0^0 \rho(x, y, z)dv = \left[F(x, y, z)\right]_0^0 = 0$$

Note: this discussion applies to a point particle, such as an electron–unlike a nucleus – is thought to be. For a particle of zonzero size we would have to define what we mean by "at a point"; for example, we could say that a spherical particle is at a point if its center is at the point.

Chapter 4, Harder Questions, Answers

Q3

Suppose we tried to simplify the SHM even further, by ignoring *all* interactions i, j; $i \neq j$ (ignoring adjacent interactions instead of setting them $= \beta$). What effect would this have on energy levels? Can you see the answer without looking at a matrix or determinant?

Setting all adjacent orbital interactions equal to zero removes all connectivity information. It dissociates the molecule into isolated atoms! This follows because in the SHM the sole structural information about a molecule is provided by which i, j pairs are β and which are zero: two atoms are connected if and only their interaction is represented by β; they are not connected if and only their interaction is represented by 0.

A look at Fock matrices may make this more concrete. Diagonalization of the standard SHM matrix for the propenyl system gives

$$\begin{pmatrix} 0 & -1 & 0 \\ -1 & 0 & -1 \\ 0 & -1 & 0 \end{pmatrix} =$$

$$\begin{pmatrix} 0.500 & 0.707 & 0.500 \\ 0.707 & 0 & -0.707 \\ 0.500 & -0.707 & 0.500 \end{pmatrix} \begin{pmatrix} 1.414 & 0 & 0 \\ 0 & 0 & 0 \\ 0 & 0 & -1.414 \end{pmatrix} \begin{pmatrix} 0.500 & 0.707 & 0.500 \\ 0.707 & 0 & -0.707 \\ 0.500 & -0.707 & 0.500 \end{pmatrix}$$

$$(1)$$
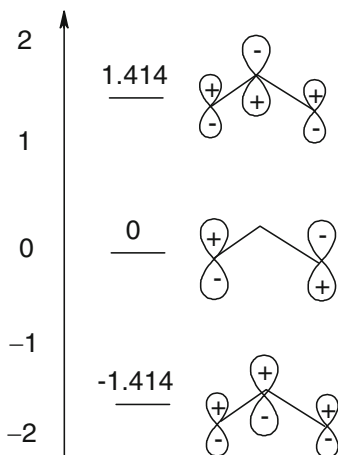
Three molecular orbitals with different energies and p-atomic-orbital contributions.

Diagonalization of the no-adjacent-interaction matrix gives

$$
\begin{pmatrix} 0 & 0 & 0 \\ 0 & 0 & 0 \\ 0 & 0 & 0 \end{pmatrix} = \begin{pmatrix} 1 & 0 & 0 \\ 0 & 1 & 0. \\ 0 & 0 & 1 \end{pmatrix} \begin{pmatrix} 0 & 0 & 0 \\ 0 & 0 & 0 \\ 0 & 0 & 0 \end{pmatrix} \begin{pmatrix} 1 & 0 & 0 \\ 0 & 1 & 0 \\ 0. & 0 & 1 \end{pmatrix} \qquad (1)
$$
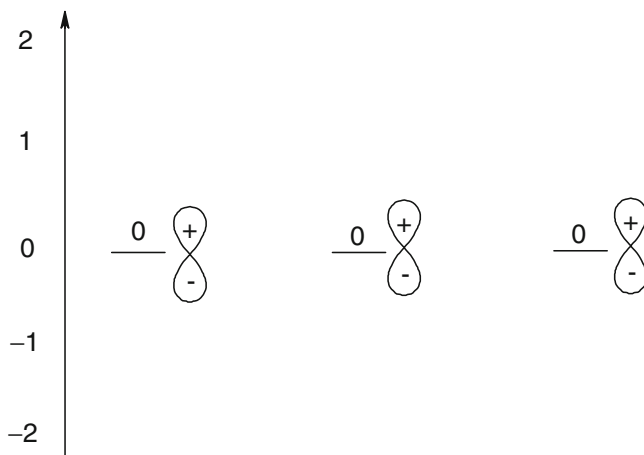
Three p atomic orbitals.

Chapter 4, Harder Questions, Answers

Q4

How might the i, j -type interactions in the simple Hückel Fock matrix be made to assume values other than just -1 and 0?

Such changes in the Fock matrix have been made in an attempt to handle systems with orbital contributions from atoms other than carbon. Consider the two species

A
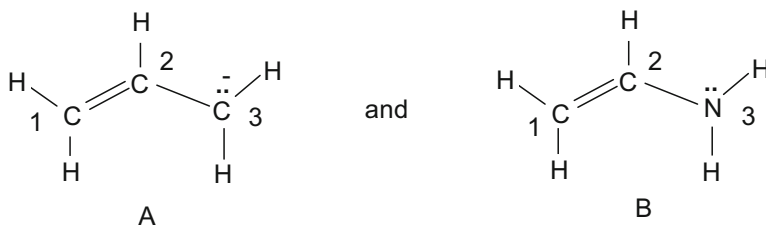
The matrix for the all-carbon π system A is that shown in the answer to question 4 (with four π electrons). The matrix for the hetero (nitrogen) system B is qualitatively similar, but its 2,3 and 3,3 interactions should be different from those of A:

$$\begin{pmatrix} 0 & -1 & 0 \\ -1 & 0 & -1 \\ 0 & -1 & 0 \end{pmatrix} \qquad \begin{pmatrix} 0 & -1 & 0 \\ -1 & 0 & CN \\ 0 & CN & NN \end{pmatrix} \qquad (1)$$

Various modifications of the carbon values have been proposed for heteroatoms [1]. If we use the suggested values $CN = -1$ and $NN = -1.5$ we have

$$\begin{pmatrix} 0 & -1 & 0 \\ -1 & 0 & -1 \\ 0 & -1 & -1.5 \end{pmatrix}$$

which on diagonalization gives the energy levels $-2.111, 0.591, 1.202$(cf. for the carbon system A, $-1.414, 0, 1.414$). Intuitively, we expect NN to be more negative than CC (-1.5 cf. 0) because N is more electronegative than C; here CN is the same as CC (-1), but CX values have usually been taken as being less negative than -1, reflecting the probably less complete energy-lowering delocalization of an electron in a CX-type bond compared to a CC-type bond.[2]

The hetero atom parameters have been obtained in various ways, for example by striving for a best correlation of HOMO values with ionization energies, or of

---

[2]Discussions of heteroatoms in the SHM written in the heyday of that method present the heteroatom parameters in a slightly more complicated way, in terms of the coulomb and resonance integrals α and β, rather than as simple numbers.

polarographic reduction potentials with LUMO values. The whole subject of SHM parameters and best heteroatom parameters is now of little practical importance, since much better quantitative molecular orbital methods are now readily available.

Reference

1. (a) A thorough discussion: Streitwieser A Jr (1961) Molecular orbital theory for organic chemists. Wiley, chapter 5; (b) A short hands-on presentation: Roberts JD (1962) Notes on molecular orbital calculations. Benjamin, New York, chapter 6

Chapter 4, Harder Questions, Answers

Q5

What is the result of using as a reference system for calculating the resonance energy of cyclobutadiene, not two ethene molecules, but 1,3-butadiene? What does this have to do with antiaromaticity? Is there any way to decide if one reference system is better than another?

1. Compare the use as a reference of two ethene molecules and of butadiene:

$$E_\pi \qquad E_\pi = 2(\alpha + 2\beta) + 2\alpha \qquad E_\pi = 2(\alpha + \beta) \qquad E_\pi = 2(\alpha + 1.618\beta) + 2(\alpha + 0.618\beta)$$
$$= 4\alpha + 4\beta \qquad\qquad = 2\alpha + 2\beta \qquad\qquad = 4\alpha + 4.472\beta$$
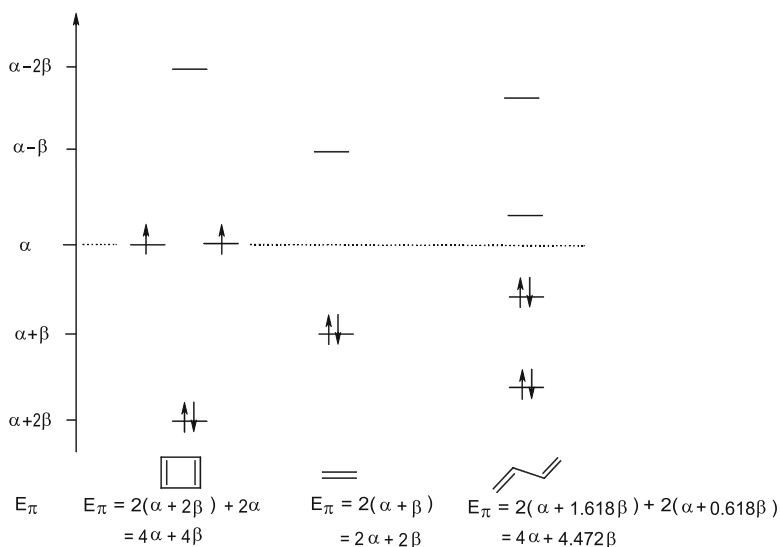
Comparing cyclobutadiene with two ethene molecules:

Stabilization energy $= E(CBD) - E(2\ ethenes) = (4\alpha + 4\beta) - 2(2\alpha + 2\beta) = 0$

Comparing cyclobutadiene with butadiene:

$$\text{Stabilization energy} = E(CBD) - E(\text{butadiene}) = (4\alpha + 4\beta) - (4\alpha + 4.472\beta)$$
$$= -0.472\beta$$

The energy of the CBD π-system is higher than that of the butadiene π-system); recall that β is a negative energy quantity, so -0.472β is a positive quantity. Thus the SHM says that a cyclic array of p atomic orbitals is destabilized by the interactions of four electrons, compared to an acyclic unbranched array.

2. Antiaromaticity [1] is the phenomenon of destabilization of certain molecules by interelectronic interactions, that is, it is the opposite of aromaticity [2]. The SHM indicates that when the π-system of butadiene is closed the energy rises, i.e. that cyclobutadiene is antiaromatic with reference to butadiene. In a related approach, the perturbation molecular orbital (PMO) method of Dewar predicts that union of a C_3 and a C_1 unit to form cyclobutadiene is less favorable than union to form butadiene [3].

3. Is one reference system better than another? Cyclobutadiene is destabilized relative to a butadiene reference, but has the same energy as a reference system of two separated ethenes. Simply closing or opening one system to transform it into another (e.g. butadiene $\rightleftarrows$ cyclobutadiene) is a less disruptive transformation than uniting two systems or dissociating one (e.g. 2 ethene $\rightleftarrows$ cyclobutadiene); thus one could argue that the systems represented by closing/opening are the better mutual references. Certainly, cyclobutadiene is regarded from empirical evidence and more advanced theoretical studies as an electronically destabilized molecule [1], so the butadiene reference, which predicts a destabilizing effect for four cyclic π electrons, is in much better accord with the general collection of experimental and computational work.

Note that in fact cyclobutadiene does not have degenerate, singly-occupied molecular orbitals, as a Jahn-Teller type (actually a pseudo-Jahn-teller) distortion lowers its symmetry from square to rectangular and leads to a closed-shell paired-electron molecule [4].

References

1. Bally T (2006) Angew Chem Int Ed Engl 45:6616
2. Krygowski TM, Cyrański MK, Czarnocki Z, Häfelinger G, Katritzky AR (2000) Tetrahedron 56:1783
3. Dewar MJS (1975) The PMO theory of organic chemistry. Plenum, New York, p 90
4. (a) Bersuker IB (2006) The Jahn–Teller effect. Cambridge University press, Cambridge; (b) Balázs R, Kolonits M, Marsden CJ, Heully J-L (1997) J Am Chem Soc 119:9042

Chapter 4, Harder Questions, Answers

Q6

What is the problem with unambiguously defining the charge on an atom in a molecule?

Let us be ambitious and replace "unambiguously" by "uniquely". The problem is to define where an atom in a molecule begins and ends. If we can mathematically specify the region of space over which the electronic charge distribution is to be integrated, we can calculate the number of electrons which should be assigned to each atom *in the molecule*. The algebraic sum of this electronic charge and the nuclear charge would then give the net charge on the atom. This is the principle behind the (quantum theory of) *atoms in molecules* (QTAIM, AIM) method of Bader [1]. In the AIM method, an atom in a molecule is demarcated from the rest of the molecule by a "zero-flux surface" defined in terms of the gradient of the electron density. Bader and coworkers essentially regard their definition as unique, from which it would seem to follow that in some sense it yields "the correct" definition of atomic charges. Criticisms of the approach have engendered delightful polemics by Bader and Matta [2].

Outside the QTAIM realm, the main definitions of atomic charges are Mulliken charge, electrostatic charge, and natural charge [3]. Values can differ considerably from one method to another, but the trend with a particular method can provide useful information. None of these three methods of assigning charge claims to be unique.

References

1. Bader RFW (1990) Atoms in molecules. A quantum theory. Clarendon Press, Oxford, particularly chapter 5
2. (a) Mata CF, Bader RFW (2006) J Phys Chem A 110:6365; (b) Bader RFW, Mata CF (2004) J Phys Chem A 108:8354
3. Levine IN (2014) Quantum chemistry, 7th edn. Prentice-Hall, Upper Saddle River, Sect. 15.6

Chapter 4, Harder Questions, Answers

Q7

It has been reported that the extended Hückel method can be parameterized to give good geometries. Do you think this might be possible for the simple Hückel method? Why or why not?

A report of a promising method of inducing the *extended* Hückel method EHM) to yield good geometries appeared in 1994 [1]. The method was said to give geometries as good as or better than the popular AM1 method, and to be 2–4 times as fast. Unfortunately, further results, and the wide application of this approach, do not seem to have followed (a possibly related approach [2] and another fast semiempirical method [3] have been reported). Such a method would be very useful, because the EHM is very fast, due to its very simple way of calculating energies and molecular orbitals, and the fact that it is not iterative–a single matrix diagonalization gives the results.

Recall that in the EHM geometric information is present in the Fock matrix by virtue of the overlap integrals in the off-diagonal elements. For the simple Hückel method (SHM) the situation is completely different. The SHM does not take any account of molecular geometry, as distinct from mere connectivity, with one hedge: one can vary the adjacent i, j interaction terms in an attempt to reflect changes in overlap integrals. This can be done by allowing the terms to move from -1 toward 0 as a bond is lengthened, and by making terms proportional to the cosine of the angle of deviation from perfect p-p parallel alignment to account for nonplanarity [4]. Bond lengths and angles of π systems could be varied to give the lowest π energy. But the SHM method is tied to π systems, severely limiting the applicability of such refinements, and it is so approximate, that the effort hardly seems worthwhile.

References

1. Dixon SL, Jurs PC (1994) J Comp Chem 15:733
2. Tajima S, Katagiri T, Kanada Y, Nagashima U (2000) J Chem Softw 6:67–74 [in Japanese]
3. Dixon SL, Merz KM (1997) J Chem Phys 107:879
4. (a) Streitwieser A Jr (1961) Molecular orbital theory for organic chemists. Wiley, section 4.3; (b) Roberts JD (1962) Notes on molecular orbital calculations. Benjamin, New York, chapter 7

Chapter 4, Harder Questions, Answers

Q8

8. Give a reference to a journal paper that used the SHM, and one that used the EHM, since the year 2000. For each paper quote the sentence in the abstract or the paper that states that the SHM was used..

The SHM:

M. Ernzerhof, M. Zhuang, P. Rocheleau, J. Chem. Phys, 2005, *123*, 134704. "Simple Hückel-type calculations serve to illustrate the described effect."

The EHM:

D. Kienle, J. I. Cerda, A. W. Ghosh, J. Applied Physics, 2006, 100, 043714.

"We describe a semiempirical atomic basis extended Hückel theoretical (EHT) technique that can be used to calculate bulk band structure, surface density of states, electronic transmission, and interfacial chemistry of various materials within the same computational platform."

Chapter 4, Harder Questions, Answers

Q9

The ionization energies usually used to parameterize the EHM are not ordinary atomic ionization energies, but rather *valence-state AO ionization energies*, VSAO [atomic orbital] ionization energies. What does the term "valence state" mean here? Should the VSAO ionization energies of the orbitals of an atom depend somewhat on the hybridization of the atom? In what way?

The term was first used by Van Vleck who explained it thus, referring to carbon in CH_4: "…the spins of the four electrons belonging to sp^3 were assumed paired with those of the four atoms attached by the carbon. Such a condition of the carbon atom we may conveniently call its valence state." He then showed a calculation which led to the conclusion that "The 'valence' state of C has about 7 or 8 more volts of intra-atomic energy than the normal state. This is the energy required to make the C atom acquire a chemically active condition…" [1]. Mulliken defines it saying "[it is] a certain hypothetical state of interaction of the electrons of an atomic electron configuration" and "A 'valence state' is an atom state chosen so as to have as nearly as possible the same condition of interaction of the atom's electrons *with one another* as when the atom is part of a molecule." [2].

An atom, then, is in a valence state when its electrons occupy orbitals of energies and shapes that they would occupy if they were subject to the interactions that they would experience in some molecule; thus one could speak of the valence state of carbon in CH_4 (above). Clearly a valence state is an abstract concept.

We'll use the convenient term valence state ionization energy, VSIE (valence state ionization potential is an older term). In a hybridized atom in a molecule different hybrid orbitals have different VSIEs, increasing with the *s*-character, as might be expected since *s*-electrons are the most tighly bound. However Hoffmann, who pioneered the popularization of the EHM and demonstrated its wide utility, used the same parameters for the *s* and *p* orbitals of carbon in alkanes (sp^3 C) as in alkenes and aromatics (sp^2 C) [3]. See [4].

References

1. Van Vleck JH (1934) J Chem Phys 2:20
2. Mulliken RS (1934) J Chem Phys 2:782
3. Hoffmann R (1963) J Chem Phys 39:1397
4. Levine IN (2014) Quantum chemistry, 7th edn. Prentice Hall, Upper Saddle River, pp 587–588, 621

Chapter 4, Harder Questions, Answers

Q10

Which should require more empirical parameters: a molecular mechanics force field (Chap. 3) or an EHM program? Explain.

The EHM will require far fewer parameters. This is easy to see, because each atom requires just one parameter for each valence atomic orbital. For C, for example, we need an ionization energy for the 2s, and the three 2p orbitals, just four parameters (strictly, valence state ionization energies, VSIEs–see Harder Question 9).[3] Each H needs only one parameter, for its 1s orbital. So for an EHM program that will handle hydrocarbons in general we need only five parameters (as in Hoffmann's pioneering paper on hydrocarbons [1]). In contrast, an early but viable molecular mechanics forcefield limited to alkanes had 26 parameters [2]. The Universal Force Field, which sacrifices accuracy for wide applicability, has about 800 parameters, and the accurate and quite broadly applicable Merck Molecular Force Field 1994 (MMFF94) has about 9000 parameters [3].

References

1. Hoffmann R (1963) J Chem Phys 39:1397
2. Allinger NL (1971) J Am Chem Soc 93:1637
3. Levine IN (2014) Quantum chemistry, 7th edn. Prentice Hall, Upper Saddle River, p 635

---

[3]Even the usually-ignored refinement (Harder Question 9) of using different VSIEs for sp^3, sp^2, and sp carbon would raise the number of C parameters only to 12.

Chapter 5, Harder Questions, Suggested Answers

Q1

Does the term *ab initio* imply that such calculations are "exact"? In what sense might *ab initio* calculations be said to be semiempirical – or at least not fully *a priori*?

The term does not imply that such calculations are exact. This is clear from the fact that most ab initio calculations use an approximate Hamiltonian, and all use a finite basis set (with the reservation that sometimes an attempt is made to extrapolate, from three or more points, to the complete basis et limit).

The Hamiltonian: In noncorrelated calculations the main error in the Hamiltonian is that it does not take electron correlation into account properly, treating it in a average charge-cloud way. But even in correlated calculations the Hamiltonian can contain approximations: it is usually nonrelativistic, which introduces significant errors for heavy atoms, and it routinely ignores spin-orbit coupling (spin-orbit interaction), which can be important [1a]. There are still other effects, usually small and rarely taken into account: spin-spin interaction between electrons [1b], neglect of the finite size of the nuclei [1c], and the use of the Born-Oppenheimer approximation [2]. The point is not that these effects are necessarily important, but that their neglect renders the calculation, strictly speaking, inexact.

The basis set: using a finite basis set necessarily leads to an inexact wavefunction, in much the same way that representing a function by a finite Fourier series of sine and cosine functions necessarily gives an approximation (albeit perhaps an excellent one) to the function. Extrapolation to an infinite basis set should overcome the finite basis et problem, in principle.

None of the above caveats should be taken to imply that excellent results cannot be obtained from ab initio calculations. However, except perhaps for calculations at so high a level that they are essentially exact solutions of the Schrödinger equation, one should use experiments on related systems as a reality check. It is in this sense that ab initio calculations are semiempirical (in fact, in the literature they are never really described as such): not at all in the sense that they are parameterized against experiment, but in the sense that for justified confidence in their results one should check representative calculations against reality.

Concerning semiempirical intrusions into ab initio methods: checking ab initio procedures against experiment, as recommended above, is in the spirit of empiricism, but is not semiempirical in sense of parameterization. More concretely, empirical parameters in some high-accuracy multistep methods (notablly the Gn and CBS methods) clearly make these not fully ab initio (except where the parameters cancel, as in calculations of protonation enthalpies). These parameters are adjustments to the ab initio procedure, in contrast to parameters in the semiempirical methods of Chap. 6, which are absolutely central to the accuracy of the methods.

References

1. Bethe HA, Salpeter E (1957) Quantum mechanics of one-and two-electron atoms. Academic, New York; (a) pp 58, 182, 185; (b) pp 182, 186; (c) p 102
2. (a) Bowman JL (2008) Science 319:40; (b) Garand E, Zhou J, Manolopoulos DE, Alexander MH, Neumark DM (2008) Science 319:72 (Erratum: Science, 2008, 320:612); (c) Chapter 2, section 2.3

Chapter 5, Harder Questions, Answers

Q2

Can the Schrödinger equation be solved *exactly* for a species with two protons and one electron? Why or why not?

This is the the simplest possible molecule, the hydrogen molecule ion, H_2^+, a known entity [1]. Strictly speaking, this presents a three-body problem–two protons and an electron– which cannot be solved exactly [2]. To a good approximation, however, the protons can be taken as stationary compared to the electron (the Born-Oppenheimer principle) and *this* system can be solved exactly [3].

References

1. Thomson JJ (1907) Philos Mag VI 561
2. But see Lopez X, Ugalde JM, Echevarría L, Luden˜a EV (2006) Phys Rev A 74:042504
3. (a) Levine IN (2014) Quantum chemistry, 7th edn. Prentice Hall, Upper Saddle River, NJ; section 13.4

Chapter 5, Harder Questions, Answers

Q3

The input for an *ab initio* calculation (or a semiempirical calculation of the type discussed in Chap. 6, or a DFT calculation–Chap. 7) on a molecule is usually just the Cartesian coordinates of the atoms (plus the charge and multiplicity). So how does the program know where the bonds are, i.e. what the structural formula of the molecule is?

What is a bond? At one level, the answer is simple: it is a connector between two atoms (we are talking about covalent bonds, not ionic "bonds", which are a mere

omnidirectional electrostatic attraction). Some atoms have one connector, some two, etc. With this simple idea chemists devised what has been said [1] to be "perhaps the most powerful theory in the whole of science", the structural theory of organic chemistry. This simple theory enabled chemists to rationalize the structures of and, even more impressively, to synthesize many thousands of chemical compounds. At a "higher" (if not more utilitarian!) level a bond can be defined mathematically in terms of the bond order between two atoms, which in molecular orbital theory can be calculated from the basis functions on the atoms; in detail there are several ways to do this. The theory of atoms in molecules (quantum theory of atoms in molecules, AIM, QTAIM) offers possibly the most sophisticated definition of a bond, in terms of the variation of electron density in a molecule [2]. AIM theory has been often used to answer (?) the question whether there is a bond between two atoms [3].

So how does the program know where the bonds are? There are (at least) three ways to answer this:

1. At the simplest level, a program may draw on the graphical user interface (GUI) a bond between atoms that are within a certain distance, the cutoff distance being determined by stored data of standard bond lengths. For example, with one popular program cartesians for the water molecule with an O/H internuclear distance of 1.0 Å or less will result in a depiction with a bond between the O and each H, but with an internuclear distance of more than 1.0 Å the GUI will show an oxygen atom and two separate hydrogens. It should be clear that this is only a formality, arising somewhat arbitrarily from strict adherence to standard bond lengths. Another popular program uses a different convention to display bond lengths. Accepting as input for a calculation a structure assembled with a GUI by clicking together atoms with attached bonds, the program will display all these original bonds even if after a geometry optimization some of the atoms have moved so far apart that they are by no sensible criterion still bonded (the result can be confusing to look at, but may make sense if viewed as a space-filling model, or if absurdly long bonds are deleted using the GUI). Again, this result is only a formality, resulting from maintenance of the bonds (really just formal connectors) that were shown before the geometry optimization.
2. If one wants information on bonding that is based on more than the proximity of nuclei, this can be extracted from the wavefunction by requesting that after a calculation of, say, energy or optimized geometry, a bond order calculation be performed, or the wavefunction can be used for an AIM calculation (possibly by a specialized program).
3. A few hardy souls may say it doesn't matter. A molecule is a collection of nuclei and electrons, with a certain charge and spin multiplicity. One might stop there and say that this defines the molecule. This austere view was expressed by Charles Coulson, a pioneer of, of all things, valence: "...a bond does not really exist at all: it is a most convenient fiction..." [4]. However, the bond concept pervades chemistry so thoroughly, and is so useful, that this stark view of a molecule is unlikely to find many adherents.

References

1. Orville Chapman (1932–2004; professor Iowa State University, UCLA; pioneer in organic photochemistry and matrix isolation studies). Remark in a lecture at the University of Toronto, ca. 1967
2. Bader RFW (1990) Atoms in molecules. A quantum theory. Clarendon Press, Oxford
3. E.g.: (a) Dobado JA, Martínez-García H, Molina JM, Sundberg MR (1999) J Am Chem Soc 121:3156; (b) Rozas I, Alkorta I, Elguero J (1977) J Phys Chem A 101:9457
4. Coulson C What is a Chemical Bond? 25, Coulson Papers, Bod. Oxford

Chapter 5, Harder Questions, Answers

Q4

Why is it that (in the usual treatment) the calculation of the internuclear repulsion energy term is easy, in contrast to the electronic energy term?

It is easy because we know where the nuclei are. In the usual treatment the nuclei are fixed and the electrons move in their field of attraction; this is the Born-Oppenheimer approximation. Given the coordinates of the nuclei (which along with charge and multiplicity define the molecule) the internuclear repulsion energy is simply obtained as the sum of all pairwise repulsion energies. Of course the nuclei are actually vibrating around average positions, even at 0 K. The zero point energy (zero point vibrational energy, ZPE or ZPVE) is calculated from the energies of the normal modes, these energies being obtained from the normal mode frequencies, which are calculated with the aid of the matrix of second derivatives of energy with respect to position, the Hessian matrix. The vibrational energy at higher temperatures can be obtained by the usual thermodynamic device of calculating the vibrational partition function from the normal mode frequencies [1].

Reference

1. See e.g. Ochterski JW Thermochemistry in Gaussian", Gaussian White Paper, at http://www.gaussian.com/g_whitepap/thermo.htm, and references therein

Chapter 5, Harder Questions, Answers

Q5

In an *ab initio* calculation on H_2 or HHe^+, one kind of interelectronic interaction does not arise; what is it, and why?

"Pauli repulsion" does not arise, because there are no electrons of the same spin present. Of course, this is not a repulsion like that between particles of the same charge, but just a convenient term for the fact that electrons of the same spin tend to avoid one another (more so than do electrons of opposite spin). Thus the calculation of the energy of these molecules does not involve the K integrals.

Chapter 5, Harder Questions, Answers

Q6

Why are basis functions not necessarily the same as atomic orbitals?

Strictly speaking, atomic orbitals are solutions of the Schrödinger equation for a one-electron atom (hydrogen, the helium monocation, etc.). They are mathematical functions, ψ, of the coordinates of an electron, and for one electron the square of ψ is an electron probability density function. Solving the nonrelativistic Schrödinger equation gives a series of orbitals differing by the values of the parameters (quantum numbers) n, l, and m (s orbitals, p orbitals, etc.) [1]. These are *spatial* orbitals; the relativistic Schrödinger equation (the Dirac equation) gives rise to the spin quantum number $m_s = \pm\frac{1}{2}$ and to spin functions α and β, which, multiplied by the spatial orbitals, give *spin* orbitals [2]. All this applies rigorously only to one-electron atoms but has been transferred approximately, by analogy, to all other atoms.

For the integrations in ab initio calculations we need the actual mathematical form of the spatial functions, and the hydrogenlike expressions are Slater functions [1]. For atomic and some molecular calculations Slater functions have been used [3]. These vary with distance from where they are centered as $\exp(-\text{constant}.r)$, where r is the radius vector of the location of the electron, but for molecular calculations certain integrals with Slater functions are very time-consuming to evaluate, and so Gaussian functions, which vary as $\exp(-\text{constant}.r^2)$ are almost always used; a basis set is almost always a set of (usually linear combinations of) Gaussian functions [4]. Very importantly, we are under no theoretical restraints about their precise form (other than that in the exponent the electron coordinate occurs as $\exp(-\text{constant}.r^2)$). Neither are we limited to how many basis functions we can place on an atom: for example, conventionally carbon has one 1s atomic orbital, one 2s, and three 2p. But we can place on a carbon atom an inner and outer 1s basis function, an inner and outer 2s etc., and we can also add d functions, and even f (and g!) functions. This freedom allows us to devise basis sets solely with a view to getting from our computations, by "experiment" (checking calculations against reality), good results. Basis functions are mathematical functions (usually Gaussian) that work; atomic orbitals are functions, circumscribed by theory, that arise from solution of the Schrödinger equation.

References

1. Levine IN (2014) Quantum chemistry, 7th edn. Prentice Hall, Upper Saddle River, chapter 6
2. Levine IN (2014) Quantum chemistry, 7th edn. Prentice Hall, Upper Saddle River, NJ; chapter 10
3. Levine IN (2014) Quantum chemistry, 7th edn. Prentice Hall, Upper Saddle River, p 293
4. Levine IN (2014) Quantum chemistry, 7th edn. Prentice Hall, Upper Saddle River; section 15.4

Chapter 5, Harder Questions, Answers

Q7

One desirable feature of a basis set is that it should be "balanced". How might a basis set be unbalanced?

Recall from the answer to Q6 that a basis set is a collection of mathematical functions that "work". By an unbalanced basis set [1] one usually means a mixed set in which a big basis has been placed on some atoms and a small basis on others. The atom with a small basis steals basis functions from the other atoms, leading to exaggerated basis set superposition error (BSSE) (Chap. 5, Sect. 5.4.3.3) and a corresponding error in energy. This pilfering of basis functions is aided by moving the function-deficient atom closer to the function-rich one during geometry optimization, leading to an error in geometry.

Reference

1. Young D (2001) Computational chemistry. A practical guide for applying techniques to real world problems. Wiley, New York, section 28.3

Chapter 5, Harder Questions, Answers

Q8

In a HF [Hartree-Fock] calculation, you can always get a lower energy (a "better" energy, in the sense that it is closer to the true energy) for a molecule by using a bigger basis set, as long as the HF limit has not been reached. Yet a bigger basis set does not necessarily give better geometries and better relative (i.e. activation and reaction) energies. Why is this so?

The calculated geometry is a local (sometimes the global) minimum on a Born-Oppenheimer surface. At that point altering the geometry by a small amount leads to an increase in energy (the situation is more complicated if the point is a transition structure). There is no necessary requirement that the energy of the minimum be in any sense "good", although in practice, methods that give good geometries do tend to give reasonably good relative energies (reaction energies, less reliably, activation energies).

Chapter 5, Harder Questions, Answers

Q9

Why is size-consistency in an *ab initio* calculation considered more important than variational behavior (MP2 is size-consistent but not variational)?

Size-consistency in a method enables one to use that method to compare the energy of a species (a molecule or a complex like the water dimer or a van der Waals cluster) with its components; for example, one can compute the stability of the water dimer by comparing its energy with that of two separate water molecules, allowing for basis set superposition error). Lack of size consistency means we cannot use the method to compare the energy of a system with that of its components, and so limits the versatility of the method. Variational behavior is desirable, because it assures us that the true energy of a system is less than (in theory the same, but this is unlikely) our calculated energy, giving a kind of reference point to aim for in a series of calculations, for example with increasingly bigger basis sets. However, in practice the lack of variational behavior does not limit much the usefullness of a method: all the correlated methods including current DFT, except some CI methods (Chapter 5, Sect. 5.4.3.2; and with certain reservations CASSCF, a partial CI method) are not variational.

Chapter 5, Harder Questions, Answers

Q10

A common alternative to writing a HF wavefunction as an explicit Slater determinant is to express it using a *permutation operator* $\hat{p}$ which permutes (switches) electrons around in MOs. Examine the Slater determinant for a two-electron closed-shell molecule, then try to rewrite the wavefunction using $\hat{p}$

The Slater determinant for a two-electron closed-shell molecule is

$$\psi = \frac{1}{\sqrt{2!}} \begin{vmatrix} \psi_1(1)\alpha(1) & \psi_1(1)\beta(1) \\ \psi_1(2)\alpha(2) & \psi_1(2)\beta(2) \end{vmatrix} \tag{1}$$

consisting of one spatial MO (ψ_1), or two spin MOs ($\psi_1\alpha$ and $\psi_1\beta$), one of which is populated alternately with electron 1 and with electron 2. When expanded according to the usual rule this gives

$$1/\sqrt{2!}[\psi_1(1)\alpha(1).\psi_1(2)\beta(2) - \psi_1(1)\beta(1).\psi_1(2)\alpha(2)] \tag{2}$$

The expansion presents ψ as a sum of products. Realizing that the second term in (2) can be derived from the first by switching the coordinates of electrons 1 and 2 and replacing $+$ by $-$ leads to the idea of writing Ψ as a sum of "switched" or permuted terms:

$$\psi = 1\sqrt{2!}\sum (-1)^p \hat{P} \quad [\psi_1(1)\alpha(1).\psi_1(2)\beta(2)] \tag{3}$$

where the sum is over all possible permutations (two) of the two spin orbitals which can be obtained by switching the electron coordinates. The permutation operator $\hat{p}$ has the effect of switching electron coordinates. As a check on this (ignoring the $1/\sqrt{2!}$ normalization factor):

Permutation 1 leads to $(-1)^1[\psi_1(2)\alpha(2).\psi_1(1)\beta(1)] = -\psi_1(1)\beta(1).\psi_1(2)\alpha(2)]$, the second term in (2).
Permutation 2 (acting on the result of permutation 1) leads to

$$(-1)^2[\psi_1(1)\alpha(1).\psi_1(2)\beta(2)] = \psi_1(1)\alpha(1).\psi_1(2)\beta(2),$$

the first term in (2).

Particularly for Ψ with more than two spin orbitals the permutation operator formulation [1] is less transparent than the determinant one.

Reference

1. E.g. (a) Levine IN (2014) Quantum chemistry, 7th edn. Prentice Hall, Upper Saddle River, pp 269–270; (b) Cook DB (2005) Handbook of computational quantum chemistry. Dover, Mineola; section 1.6; (c) Pople JA, Beveridge DL (1970) Approximate molecular orbital theory. McGraw-Hill, New York; sections 1.7, 2.2; (d) Hehre WJ, Radom L, Schleyer PvR, Pople JA (1986) Ab Initio molecular orbital theory. Wiley, New York; section 2.4

Chapter 6, Harder Questions, Suggested Answers

Q1

Why are even very carefully-parameterized SE methods like AM1 and PM3 not as accurate and reliable as high-level (e.g. MP2, CI, coupled-cluster) *ab initio* calculations?

One reason is that an attempt to get the best fit of program parameters to a number (say, a training set of 50 molecules) of a variety (like heat of formation, geometric parameters, dipole moments) of parameters results in a significant unavoidable error in the accuracy of the fit. Imagine fitting a least-squares line to a collection of data points (x, y); unless the underlying relationship is genuinely linear, the fit will be imperfect and predictions of y from x will be subject to error. Nevertheless, geometries of "normal" molecules from AM1 and PM3 are generally quite good, although heats of formation and relative energies are less accurate.

A more fundamental reason is that predictions for molecules very different from those outside the training should be less reliable than those for molecules similar to the ones used for parameterization. Therefore for investigating exotic species like, say, planar carbon or nitrogen pentafluoride AM1 and PM3 are considered unreliable, and even noncorrelated *ab initio* calculations would be considered well short of definitive nowadays [1].

Reference

1. Lewars E (2008) Modeling marvels. Computational anticipation of novel molecules. Springer, Dordrecht

Chapter 6, Harder Questions, Answers

Q2

Molecular mechanics is essentially empirical, while methods like PPP, CNDO, and AM1 are semiempirical. What are the analogies in PPP etc. to MM procedures of developing and parameterizing a forcefield? Why are PPP etc. only *semi*empirical?

The analogies in semiempirical (SE) methods to MM procedures for developing a forcefield arise from the need to fit experimental values to parameters in equations. In SE parameterization heats of formation, geometric parameters, etc. are used to adjust the values of integrals in the Hamiltonian of quantum-mechanical equations. In MM vibrational frequencies, geometric parameters, etc. are used to adjust the values of force constants, reference bond lengths, etc. in simple non-quantum-mechanical equations.

SE methods like PPP, CNDO, and AM1 are partly empirical and partly quantum-mechanical: experimental (or nowadays, often high-level *ab initio* or DFT) parameters are used to simplify the evaluation of the integrals in the Fock matrix. In contrast, there is no quantum-mechanical component to MM; it is not quite true, however, that MM has no theoretical component, because the force constants and reference geometric parameters are inserted into an (albeit simple) ball-and springs-model of a molecule (this model is augmented with energy terms arising from dihedral angles, nonbonded interactions, and possibly other factors).

Chapter 6, Harder Questions, Answers

Q3

What do you think are the advantages and disadvantages of parameterizing SE methods with data from *ab initio calculations* rather than from experiment? Could a SE method parameterized using ab initio calculations logically be called semi*empirical*?

This question is similar to chapter 3, harder Question 3, for MM. For the first part of the question I'll just repeat the response to that question, tailored to be appropriate to SE methods. Apart from a possible philosophical objection, which from a utilitarian viewpoint can be dismissed, there is the question of the trustworthiness of the ab initio or DFT results. For "normal" molecules, that is, species which are not in some way exotic [1], these calculations deliver quite reliable results. The advantages they offer over experimental acquisition of the required parameters is that these quantities (1) can be obtained for a wide variety of compounds without regard to synthetic difficulties or commercial availability, (2) are offered up transparently by the output of the calculation, rather than being required to be extracted, perhaps somewhat tortuously, from experiments, (3) are usually more quickly calculated than determined in the lab, and (4) can be uniformly secured, that is, all parameters can be obtained from calculations at the same level, say MP2/6-311G(df,p), in contrast to experiment, where different methods must be used to obtain different parameters. This last point may be more of an esthetic than a utilitarian advantage.

The advantage of parameterizing with experimental quantities is that, if the experiment is reliable, then we *know* the values of the parameters; we need not reflect on the reliability of the calculation. Of course, we might wish to ponder the accuracy of the experiment.

Could a SE method parameterized using ab initio calculations logically be called semi*empirical*? Literally, *semiempirical* means semiexperimental. If we parameterize with calculations we have not resorted to experiment (of course, *afterwards* we will likely check the method against some experimental facts). So it would appear that literally the SE method, parameterized by ab initio or DFT, is not

really semiempirical; however, it is still in the spirit of SE methods, circumventing detailed calculation of the Fock matrix elements (using pre-calculated values!).

Reference

1. Lewars E (2008) Modeling marvels. Computational anticipation of novel molecules. Springer, Dordrecht

Chapter 6, Harder Questions, Answers

Q4

There is a kind of contradiction in the Dewar-type methods (AM1, etc.) in that overlap integrals are calculated and used to help evaluate the Fock matrix elements, yet the overlap matrix is taken as a unit matrix as far as diagonalization of the Fock matrix goes. Discuss.

In the simple Hückel method, which is not a Dewar-type method, the use of overlap integrals as the sole source of geometric (connectivity) information is transparent. In AM1 and its relative PM3, which are modified versions of MNDO, overlap integrals are also calculated, and used in a somewhat more involved way to evaluate some of the core integrals. Yet after assembling the Fock matrix this is simply diagonalized to give coefficients and energies (repeatedly, in the SCF procedure) without using orthogonalization to alter the original Fock matrix or to "reset" the coefficients. The sidestepping of orthogonalization in the SHM is achieved by setting the overlap matrix equal to a unit matrix, i.e. by simply setting all $S_{ii} = 1$ and all S_{ij} ($i \neq j$) $= 0$. This is a logical inconsistency, but it works quite well!

Chapter 6, Harder Questions, Answers

Q5

What would be the advantages and disadvantages of using the general MNDO/AM1 parameterization procedure, but employing a minimal basis set instead of a minimal valence basis set?

A minimal basis set is bigger than a minimal *valence* basis set by the inclusion of core atomic orbitals, e.g. a 1s AO for carbon, and 1s, 2s, and three 2p AOs for silicon. Including these in the electronic calculation probably should not lead to

much if any improvement over the results now being obtained with a minimal valence basis, since once the basic MNDO-type method has been chosen, the key to good results is careful parameterization. There might be some improvement in properties which depend on a good description of the electron density near the nucleus, but there are few such of general interest to chemists–even NMR chemical shifts are affected mainly by (the tails of) valence orbitals [1].

The disadvantage is that the time of calculations would be increased, particularly for elements beyond the first full row (Na and beyond).

Reference

1. Cramer CJ (2004) Essentials of computational chemistry, 2nd edn. Wiley, Chichester, p 345

Chapter 6, Harder Questions, Answers

Q6

In SCF SE methods major approximations lie in the calculation of the H_{rs}^{core}, $(rs|tu)$, and $(ru|ts)$ integrals of the Fock matrix elements F_{rs} (Eq. (6.1)). Suggest an alternative approach to approximating one of these integrals.

So much thought and experimentation (checking calculated results against experimental ones) have gone into devising semiempirical parameters that a suggestion here is unlikely to be much of an improvement. The easiest integral to modify is probably the core one, because it does not involve electron-electron repulsion. H_{rs}^{core} in the F_{rs} Fock matrix element is:

$$H_{rs}^{core}(1) = \left\langle \phi_r(1) \left| \hat{H}^{core}(1) \right| \phi_s(1) \right\rangle$$

$$\text{where} \quad \hat{H}^{core}(1) = -\frac{1}{2}\nabla_1^2 - \sum_{\text{all } \mu} \frac{Z_\mu}{r_{\mu 1}}$$

So the integral H_{rs}^{core} can be taken as the energy (kinetic plus potential of an electron moving in the ϕ_r, ϕ_s overlap region under the attraction of all the charges Z_μ. In ab initio calculations these charges are nuclear, in SE calculations they are the net charges of nuclei plus non-valence electrons. A crude attempt to capture the physical meaning of this might be to take H_{rs}^{core} as the average of the valence-state ionization energies of an electron in ϕ_r and ϕ_s plus the energy needed to remove the electron to infinity against the attraction of the other (non-r and non-s) cores.

Chapter 6, Harder Questions, Answers

Q7

Read the exchange between Dewar on the one hand and Halgren, Kleier and Lipscomb on the other [1, 2]. Do you agree that SE methods, even when they give good results "inevitably obscure the physical bases for success (however striking) and failure alike, thereby limiting the prospects for learning why the results are as they are?" Explain your answer.

HKL [1] make the point that calculations are not just *alternatives* to experiment, as Dewar thinks, but can also *illuminate* experiment. In effect, they say that calculations are not only *another way to get numbers*, but can provide *insight* into physical processes. Their contention that such insight comes from ab initio, not from semiempirical, methods (which "obscure the physical bases" of their success and failure) seems to be justified, because in SE methods the fundamental physical entities have been deliberately subsumed into parameters designed to give the right, or rather the best, answers.

HKL make the interesting point that the purpose of ab initio calculations is (this may have been so in 1975, but is not true today for most ab initio studies) "not so much to predict a given experimental result as to examine what that result can tell us." This is the core of the difference between the way HKL on the one hand and Dewar on the other viewed the ab initio-semiempirical divide.

Dewar [2] in his retort appeared to miss the above core point. He averred that he was "all in favor of rigorous quantum mechanical calculations–that is, ones that are accurate in an absolute sense. . .", and closed his letter with an attack on "vast and very expensive calculations", which did not address the contention of HKL that ab initio calculations (at the time) were done not to get right answers but rather to probe the physical reasons behind getting right–and wrong–answers.

Ancillary to this conceptual divide was an argument over the relative cost of Hartree-Fock 4-31G and MINDO/3 calculations for the study of the barriers to interconversion of benzene valence isomers. In those days computer use was indeed expensive: a computer was an institutional machine, personal ownership of such a device being inconceivable, and the privilege of using one cost [1, 2] ca. \$500 per hour. Geometry optimization of benzene (by the low-level HF/4-31G method) took 4 h, consuming \$2000 [1]. I just repeated this calculation on my now largely merely clerical personal computer, bought years ago for ca. \$4000; it took 22 s, a time ratio of 655.

References

1. Halgren TA, Kleier DA, Lipscomb WN (1975) Science 190:591
2. Dewar MJS (1975) Science 190:591

Chapter 6, Harder Questions, Answers

Q8

It has been said of SE methods: "They will never outlive their usefulness for correlating properties across a series of molecules...I really doubt their predictive value for a one-off calculation on a small molecule on the grounds that whatever one is seeking to predict has probably already been included in with the parameters." (A. Hinchcliffe, "Ab Initio Determination of Molecular Properties," Adam Hilger, Bristol, 1987, p. x). Do you agree with this? Why or why not? Compare the above quotation with M. J. S. Dewar, A Semiempirical Life", American Chemical Society, Washington, DC, 1992, pp. 133–136.

First, a synopsis of Dewar pp. 133–136. Here are representative excerpts:

> One of the criticisms commonly levelled at semiempirical methods is that they represent no more than methods of interpolation and are useful only in areas and for compounds for which they have been parameterized....The striking thing about ours is that they do *not* merely reproduce the properties for which they were parameterized, nor are they confined to molecules of the kind used in the parameterization. They reproduce *all* ground-state properties of molecules of *all* kinds...Thus our procedures provide a very good representation of the way molecules behave...
>
> ...our work has led to a number of predictions that have been subsequently confirmed by experiment.
>
> Every procedure performs less well in some cases than in others. How serious each error is depends on the chemical importance of the molecule in question.

The statements above directly contradict the assertion that "...whatever one is seeking to predict has probably already been included in with the parameters.", with the reservation that Hinchcliffe was presumably writing about 5 years before Dewar. The references given by Dewar, and the experience of the many chemists who use semiempirical methods (not only the Dewar-type ones) show that these are *not* merely "methods of interpolation". It is however true that for accurate, reliable information on the properties of a small molecule one would very likely resort to a high-level ab initio or DFT calculation.

Chapter 6, Harder Questions, Answers

Q9

For a set of common organic molecules Merck Molecular Force Field geometries are nearly as good as MP2(fc)/6-31G* geometries. For such molecules single point MP2 (fc)/6-31G* calculations, which are quite fast, on the MMFF geometries, should give energy differences comparable to those from MP2(fc)/6-31G*//MP2(fc)/6-31G* calculations [energy and geometry optimization at the MP2(fc)/6-31G* level]. Example: $CH_2=CHOH/CH_3CHO$, ΔE(MP2 opt, including ZPE) = 71.6 kJ mol^{-1},

total time 1064 s; ΔE(MP2 single point on MMFF geometries) $= 70.7$ kJ mol^{-1}, total time $= 48$ s (G98 on a now-obsolescent Pentium 3). What role does this leave for semiempirical calculations?

If the above approach really has wide applicability then it could be a very useful way to get relative energies at only modest cost in time. However, it could be used only for species for which the MMFF gives reliable geometries. This excludes exotic molecules and transition states. Whatever the deficiencies of SE methods in these two categories, at least they do permit such calculations.

Chapter 6, Harder Questions, Answers

Q10

Semiempirical methods are untrustworthy for "exotic" molecules of theoretical interest. Give an example of such a molecule and explain why it can be considered exotic. Why cannot SE methods be trusted for molecules like yours? For what other kinds of molecules might these methods fail to give good results?

A simple exotic molecule is pyramidane:

1
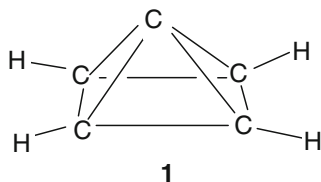
This is exotic because one of the carbon atoms is forced to have very unusual *pyramidal* bonding: tetracoordinate carbon normally has its four bonds directed toward the corners of a tetrahedron, but the apical carbon of **1** has all four bonds pointing forward. Without any further investigation of **1** we can thus characterize it as exotic. Of course without further investigation we cannot assert with confidence if it can exist, much less what its properties might be. Semiempirical and low-level ab initio [1,2] and higher-level ab initio [3] studies on pyramidane have been published, and work on this and related molecules is reviewed [4]. SE methods cannot be trusted for molecules like pyramidane because they are parameterized using information, whether experimental or calculated, for normal molecules.

Other kinds of molecules besides **1** (which has unusual bond stereochemistry) for which these methods might fail to give good results are hypercoordinate molecules like NF$_5$, molecules with noble gas atoms, particularly those of helium and neon, molecules with highly twisted C=C bonds, extraordinarily crowded molecules like hexaphenylethane, unknown dimers, trimers etc. of small familiar molecules, like CO$_2$ and N$_6$, and very highly strained molecules. All these cases are discussed in a book on exotic molecules [4].

References

1. (a) Minkin VI, Minyaev RM, Zakharov II, Avdeev VI (1978) Zh Org Khim 14:3; (b) Minkin VI, Minyaev RM (1979) Zh Org Khim 15:225; (c) Minkin VI, Minyaev RM, Orlova GA (1984) J Mol Struct (Theochem) 110:241
2. (a) Minyaev RM, Minkin VI, Zefirov NS, Zhdanov YuA (1979) Zh Org Khim 15:2009; (b) Minyaev RM, Minkin VI, Zefirov NS, Natanzon VI, Kurbatov SV (1982) Zh Org Khim 18:3
3. (a) Lewars E (2000) J Mol Struct (Theochem) 507:165. (b) Lewars E (1998) J Mol Struct (Theochem) 423:173
4. Lewars E (2008) Modeling marvels. Computational anticipation of novel molecules. Springer, Dodrecht

Chapter 7, Harder Questions, Suggested Answers

Q1

It is sometimes said that electron density is physically more real than a wavefunction. Do you agree? Is something that is more easily grasped intuitively necessarily more real?

First I will summarize a debate, at the level of polemic in some cases, about the relative merits of the wavefunction and the electron density function, then close with a few personal observations. The principal participants in the argument were, on the wavefunction side, Gernot Frenking, and on the electron density side, Richard Bader, and Ronald Gillespie and Paul Popelier. The recent history of the controversy starts in 2003 with a review by Frenking [1] of a book on chemical bonding by Gillespie and Popelier [2]. In his long review, Frenking commended the book to readers, but criticized its emphasis on electron density and its virtual ignoring of the wavefunction: "Like Bader, the authors reject the wavefunction as a basis for the explanation of molecular geometries because it is not a physical observable...It is hard for human beings to accept that the fundamental principles of elementary quantities of science are not accessible to their sensory perception." Gillespie and Popelier responded to these criticisms, but conceded that "The question of whether the wave function or the electron density is the more fundamental is perhaps open to dispute" but defended electron density as "much more useful for understanding chemical bonding and molecular geometry" [3]. Frenking defended his criticisms and reiterated that "The wavefunction Ψ, which is fundamental to our science, is a mathematical object which is not accessible to human senses." He made the important point that "the important class of pericyclic reactions could only be explained with MO theoretical arguments using the symmetry of Ψ.", a symmetry not present in the electron density. He chides the two authors for using ease of understanding as the reason for choosing electron density over Ψ, and closes by "encouraging interested readers" to study the book and his review and make up their own minds [4].

Bader leapt into the fray with a polemic against Frenking's review that even aficionados of the wavefunction must concede is amusing and erudite. He defended earlier work by Schrödinger and by Slater which argued in effect that the sole use of the wavefunction is as a mathematical device to determine the electron density distribution [5]. He countenanced the much-criticised conclusion of the Feynman force theorem and the virial theorem that the chemical bond is in fact simply the result of overlap charge density, and bolstered his argument by invoking (to many chemists no doubt recondite) work by Schwinger and Dirac, and stated clearly that "chemistry is the interaction of the density with the nuclei; there is nothing else, at least not in real observable space…" The statement "To ascribe an existence to a wavefunction that controls rather than predicts the evolution of a physical system introduces an unnecessary and unwelcome element of metaphysics." is very revealing, emphasizing Bader's conviction that the wavefunction is not "real"; indeed, two sentences earlier reference is made to the abstract Hilbert space, where the wavefunction frolics.

A long paper by Frenking, Esterhuysen, and Kovacs [6] elicited another polemic from Bader [7]. Frenking et al. presented an energy partitioning analysis of bonds in nonpolar molecules, dividing bonding into terms represented by Pauli repulsion, electrostatic interactions, and orbital interactions. Bader dismissed the concept of energy partitioning as lying "beyond the boundaries of physics" then turned his fire on what he considered to be errors *within* physics engendered by that concept. He criticised a perceived misunderstanding of the difference between electron density and the Laplacian (∇^2) of electron density (a Bader hallmark) which led to the assertion by Frenking et al. that covalent bonds do not necessarily exhibit an accumulation of electronic charge between the nuclei; Bader countered that bonded atoms experience "no Feynman force, neither attractive nor repulsive, [acting] on the nuclei because of the balancing of the repulsive and attractive forces by the *accumulation* [emphasis in the original] of electron density in the binding region…" In a short final (?) repartee, Frenking, Esterhuysen, and Kovacs [8] rebuke Bader for his derisive tone and defend their understanding of electron density and its Laplacian. They argue that acknowledging different types of bonding is fundamentally important to chemists, implying that a rejection of the concept of energy partitioning would obviate such differentiation. In support of this they cite Bader's assertion that there is no difference between the bonding in H_2 and that between the *ortho*-hydrogens in the transition state for biphenyl rotation, and the finding that Bader's atoms-in-molecules (AIM) theory gives similar bonding for He_2 and H_2. Since chemists regard bonding in H_2 as being qualitatively different from that in the other two species, "Bader's orthodox understanding of physics is unable to address fundamental questions of chemistry!" It is contended that Bader's reductionism does not recognize that chemistry needs its own models, and that "*Chemical research begins where the physics of Richard Bader ends.*" [emphasis in the original]. (For polemics concerned with AIM and H-H bonding in biphenyl and related systems see [9, 10, 11]).

So where does all this leave us in trying to respond to "It is sometimes said that electron density is physically more real than a wavefunction. Do you agree?

Is something that is more easily grasped intuitively necessarily more real?" To argue in detail the relative merits of a wavefunction and an electron density approach to chemical structure and bonding requires a pretty deep knowledge of quantum chemistry. There is no question that electron density is a valid and useful concept in chemistry, and that it is more easily grasped intuitively than the wavefunction. But logically, there is no basis for thinking that ease of understanding is correlated positively with the likelihood of physical reality. Is electron density physically more real than a wavefunction? Electron density in molecules is certainly physically real: it can be measured by X-ray crystallography [12] or electron scattering [13]. Is the wavefunction real or is it a mathematical abstraction? This is controversial, and pursuing it would take us well into physics and even perhaps philosophy. In the orthodox interpretation of quantum mechanics (QM), from the Copenhagen school of Bohr and Heisenberg, observation of a system causes "collapse of the wavefunction" [14], implying that it is real. This school was practically unchallenged for decades, but alternative interpretations of QM are now being given a hearing [14], and in some there is no wavefunction collapse, such as with quantum decoherence [15] and (de Broglie and more recently Bohm) the pilot wave concept [16]. A reaction to all interpretations of QM is an article entitled "Quantum theory needs no 'interpretation'" [17].

As chemists we can pose a simple, focussed question: how do the Woodward-Hoffmann rules (WHR) [18] arise from a purely electron density formulation of chemistry? The WHR for pericyclic reactions were expressed in terms of orbital symmetries; particularly transparent is their expression in terms of the symmetries of frontier orbitals. Since the electron density function lacks the symmetry properties arising from nodes (it lacks phases), it appears at first sight to be incapable of accounting for the stereochemistry and allowedness of pericyclic reactions. In fact, however, Ayers et al. [19] have outlined how the WHR can be reformulated in terms of a mathematical function they call the "dual descriptor", which encapsulates the fact that nucleophilic and electrophilc regions of molecules are mutually friendly. They do concede that with DFT "some processes are harder to describe than others" and reassure us that "Orbitals certainly have a role to play in the conceptual analysis of molecules". The wavefunction formulation of the WHR can be pictorial and simple, while DFT requires the definition of and calculations with a nonintuitive (!) density function. But we are still left uncertain whether the successes of wavefunctions arises from their physical reality (do they exist "out there"?) or whether this successes is "merely" because their mathematical form *reflects* an underlying reality–are they merely the shadows in Plato's cave?.

References

1. Frenking G (2003) Angew Chem Int Ed 42:143
2. Gillespie RJ, Popelier PLA (2001) Chemical bonding and molecular geometry from Lewis to electron densities. Oxford University Press, New York
3. Gillespie RJ, Popeleir PLA (2003) Angew Chem Int Ed 42:3331

4. Frenking G (2003) Angew Chem Int Ed 42:3335
5. Bader RFW (2003) Int J Quant Chem 94:173
6. Frenking G, Esterhuysen C, Kovacs A (2005) Chem Eur J 11:1813
7. Bader RFW (2006) Chem Eur J 12:7569
8. Frenking G, Esterhuysen C, Kovacs A (2006) Chem Eur J 12:7573
9. Poater J, Sola' M, Bickelhaupt FM (2006) Chem Eur J 12:2889
10. Bader RFW (2006) Chem Eur J 12:2896
11. Poater J, Sola' M, Bickelhaupt FM (2006) Chem Eur J 12:2902
12. Altomare A, Cuocci C, Giacovazzo C, Moliterni A, Rizzi R (2008) J Appl Crystallogr 41:592
13. Shibata S, Hirota F, Shioda T (1999) J Mol Struct 485–486:1
14. (a) Baggott J (1992) The meaning of quantum theory. Oxford Science Publications, Oxford;
    (b) Whitaker A (1996) Einstein, Bohr and the quantum dilemma. Cambridge University Press,
    Cambridge
15. Schlosshauer M (2004) Rev Mod Phys 76:1267
16. (a) Albert DZ (1994) Scientific American, May, 58; (b) Bohm D, Hiley DJ (1993) The
    undivided universe: an ontological interpretation of quantum theory. Routledge, London
17. Fuchs C, Peres A (2000) Physics Today, March
18. (a) Woodward RB, Hoffmann R (1970) The conservation of orbital symmetry. Verlag
    Chemie, Weinheim; (b) Golitz P (2004) Angew Chem Int Ed 43:6568; (c) Hoffmann R
    (2004) Angew Chem Int Ed 43:6586
19. Ayers PW, Morell C, De Proft F, Geerlings P (2007) Chem Eur J 13:8240
20. Plato, "The Republic"; Book 7, 360 BCE.

Chapter 7, Harder Questions, Answers

Q2

A functional is a function of a function. Explore the concept of a function of a functional.

If a function is a rule that converts a number into a number, and a functional is a rule that converts a function into a number [1], then a function of a functional (call it a 2-functional) should be a rule that converts a functional into a number:

$$\text{function } f(x) = x^3$$

rule: cube the *number* x

$$\text{number} = 2 \xrightarrow{x^3} 8$$

functional $F[f(x)] = \int_0^2 f(x)dx$

rule: integrate the *function f(x)* between zero and 2

$$\text{function} = x^3 \xrightarrow{\int\limits_{0}^{2} f(x)dx} \frac{x^4}{4}\bigg|_{0}^{2} = 4$$

From the above we see that we supply a number to a function to get a number, and we supply a function to a functional to get a number. By analogy, we supply a functional to a "2-functional" to get a number. I leave a specific example as an exercise for the reader.

Chapter 7, Harder Questions, Answers

Q3

Why is it that the HF Slater determinant is an inexact representation of the wavefunction, but the DFT determinant for a system of noninteracting electrons is exact for this particular wavefunction?

The HF (Hartree-Fock) Slater determinant is an inexact representation of the wavefunction because even with an infinitely big basis set it would not account fully for electron correlation (it does account exactly for "Pauli repulsion" since if two electrons had the same spatial and spin coordinates the determinant would vanish). This is shown by the fact that electron correlation can in principle be handled fully by expressing the wavefunction as the a linear combination of the HF determinant plus determinants representing all possible promotions of electrons into virtual orbitals: full configuration interaction. Physically, this mathematical construction permits the electrons maximum freedom in avoiding one another.

The DFT determinant for a system of noninteracting electrons is exact for this particular wavefunction (i.e. for the wavefunction of the hypothetical noninteracting electrons) because since the electrons are noninteracting there is no need to allow them to avoid one another by promotion into virtual orbitals.

For an account of DFT that is at once reasonably detailed, clear and concise see Cramer [1].

Reference

1. Cramer CJ (2004) Essentials of computational chemistry. Wiley, Chichester, England, chapter 8

Chapter 7, Harder Questions, Answers

Q4

Why do we expect the "unknown" term in the energy equation (Exc[ρ0], in Eq. (7.21)) to be small?

Eq. (7.21) is

$$E_0 = - \sum_{nuclei\,A} Z_A \int \frac{\rho_0(r_1)}{r_{1A}} dr_1 - \frac{1}{2} \sum_{i=1}^{2n} \langle \psi_1^{KS}(1) | \nabla_1^2 | \psi_1^{KS}(1) \rangle$$
$$+ \frac{1}{2} \iint \frac{\rho_0(r_1)\rho_0(r_2)}{r_{12}} dr_1 dr_2 + E_{XC}[\rho_0]$$

Exc[ρ0] is a correction term to the electronic kinetic and potential energy; most of this energy is (we hope!) treated classically by the other terms [1].

Reference

1. Cramer CJ (2004) Essentials of computational chemistry. Wiley, Chichester, sections 8.3 and 8.4

Chapter 7, Harder Questions, Answers

Q5

Merrill *et al*. have said that "while solutions to the [HF equations] may be viewed as exact solutions to an approximate description, the [KS equations] are approximations to an exact description!" Explain.

Solutions to the Hartree Fock equations are exact solutions to an approximate description because:

The HF equations are approximate mainly because they treat electron-electron repulsion approximately (other approximations are mentioned in the answer suggested for Chapter 5, Harder Question 1). This repulsion is approximated as resulting from interaction between two charge clouds rather than correctly, as the force between each pair of point-charge electrons. The equations become more exact as one increases the number of determinants representing the wavefunctions (as well as the size of the basis set), but this takes us into post-Hartree-Fock equations. Solutions to the HF equations are exact because the mathematics of the solution method is rigorous: successive iterations (the SCF method) approach an

exact solution (within the limits of the finite basis set) to the equations, i.e. an exact value of the (approximate!) wavefunction Ψ_{HF}.

The Kohn-Sham equations are approximations because the exact functional needed to transform the electron density function ρ into the energy is unknown. They are approximations to an exact description because the equations (as distinct from methods of solving them) involve no approximations, with the ominous caveat that the form of the ρ-to-E functional E_{xc} is left unspecified.

Chapter 7, Harder Questions, Answers

Q6

Electronegativity is the ability of an atom or molecule to attract electrons. Why is it then (from one definition) the average of the ionization energy and the electron affinity (Eq. (7.32)), rather than simply the electron affinity?
Equation (7.32) is

$$\chi = \frac{1 + A}{2}$$

We can call this the Mulliken electronegativity. Why is electronegativity not defined simply as the electron affinity (A)? First, we saw two derivations of Eq. (7.32). In the first, electronegativity(χ) was intuitively taken as the negative of electronic chemical potential (the more electronegative a species, the more its energy should drop when it acquires electrons). This led to approximating the derivative of energy with respect to number of electrons at a point corresponding to a species M as the energy difference of M^+ and M^- divided by 2. In the second, Mulliken, derivation, a simple argument equated electron transfer from X to Y to transfer from Y to X. Both derivations clearly invoke ionization energy (I). It is no surprise that χ should be connected with A, but the intrusion of I may be puzzling; however, our surprise diminishes if we note that the more electronegative a species, the more readily it should gain an electron *and* the less readily it should part with one.

But could we alternatively reasonably define electronegativity quantitatively just as electron affinity? Let's compare with the popular Pauling electronegativity scale [1] electronegativities calculated from Eq. (7.32) and calculated simply as A. (The Pauling scale has been criticised by Murphy *et al.*, [2], and their criticisms were acknowledged and improvements to the scale suggested, by Smith [3]; Matsunaga *et al.*, provided a long defence of Pauling's scale [4]). Below are some electronegativities (preceded by a table of the calculated needed energies, at the MP2/6-311 +G* level) by these three methods.

Energies in hartrees

	Li	C[a]	C[b]	F
Neutral	−7.43202	−37.61744	−37.74587	−99.55959
Cation	−7.23584	−37.16839	−37.33742	−98.79398
Anion	−7.44251	−37.78458	−37.78458	−99.67869

[a]Starting from a neutral quintet $1s^2, 2s^1, 2px^1, 2py^1, 2pz^1$
[b]Starting from a neutral triplet $1s^2, 2s^2, 2px^1, 2py^1, 2pz^0$

I, A, and Mulliken χ, in eV, Pauling χ in kJ mol^{-1}. Hartrees were converted to eV by multiplying by 27.212.

I and A were calculated as the energy difference between the neutral and the cation and anion, respectively.

	Li	C[a]	C[b]	F
I	5.33	12.3	11.1	21.4
A	0.272	4.55	1.05	3.24
Mulliken χ	2.80	8.38	6.08	12.0
Pauling χ	0.98	2.55[c]	2.55[c]	3.98

[a]Starting from a neutral quintet $1s^2, 2s^1, 2px^1, 2py^1, 2pz^1$
[b]Starting from a neutral triplet $1s^2, 2s^2, 2px^1, 2py^1, 2pz^0$
[c]Based on experimental bond energies in C-X molecules

We see that the Mulliken and Pauling electronegativities seem to be reasonably in step, with electronegativity increasing from Li to C to F, in accord with experience, but with *A* making quintet C more electronegative than F. Evidently both *I* and *A* act together to determine atomic avidity for electrons.

Electronegativity and other properties from DFT calculations have been discussed by Zhan et al. [5], and an electronegativity scale based on the energies of neutrals and cations which correlates well with the Pauling scale has been proposed by Noorizadeh and Shakerzadeh [6].

References

1. Pauling L (1932) J Am Chem Soc 54:3570; Pauling L (1960) The nature of the chemical bond, 3rd edn. Cornell University Press, Ithaca, chapter 3
2. Murphy LR, Meek TL, Allred AL, Allen IC (2000) J Phys Chem A 104:5867
3. Smith DW (2002) J Phys Chem A 106:5951
4. Matsunaga N, Rogers DW, Zavitsas AA (2003) J Org Chem 68:3158
5. Zhan C-G, Nichols JA, Dixon DA (2003) J Phys Chem A 107:4184
6. Noorizadeh S, Shakerzadeh E (2008) J Phys Chem A 112:3486

Chapter 7, Harder Questions, Answers

Q7

Given the wavefunction of a molecule, it is possible to calculate the electron density function. Is it possible in principle to go in the other direction? Why or why not?

From density functional theory, given the electron density function of a molecule (and its charge and multiplicity), and a perfect functional (let's idealize the problem; the question does specify "in principle") we can home in on a unique molecule. Then we could use ab initio theory to find the wavefunction.

Chapter 7, Harder Questions, Answers

Q8

The multielectron wavefunction Ψ is a function of the spatial and spin coordinates of all the electrons. Physicists say that Ψ for any system tells us all that can be known about the system. Do you think the electron density function ρ tells us everything that can be known about a system? Why or why not?

Although the wavefunction Ψ seems to contain more information than the electron density function ρ (Question 1), it ought to be possible in principle to calculate any property of a system from ρ, because different states– different geometries, different electronic states, etc.–must have different electron distributions (or they would not be different). The problem is to transform the calculated ρ to an energy (Question 5).

Extraction of information from ρ may not be as elegant as from Ψ. For example, the Woodward-Hoffmann rules follow fairly transparently from the symmetries of molecular orbitals (wavefunctions), but deriving them from ρ requires using a "dual descriptor" function [1].

Reference

1. Ayers PW, Morell C, De Proft F, Geerlings P (2007) Chem Eur J 13:8240

Chapter 7, Harder Questions, Answers

Q9

If the electron density function is mathematically and conceptually simpler than the wavefunction concept, why did DFT come later than wavefunction theory?

The wavefunction [1] and electron density [2] concepts came at about the same time, 1926, but the application of wavefunction theory to chemistry began in the 1920s [3], while DFT was not widely used in chemistry until the 1980s (see below). Why?

The DFT concept of calculating the energy of a system from its electron density seems to have arisen in the 1920s with work by Fermi, Dirac, and Thomas. However, this early work was useless for molecular studies, because it predicted molecules to be unstable toward dissociation. Much better for chemical work, but still used mainly for atoms and in solid-state physics, was the Xα method, introduced by Slater in 1951. Nowadays the standard DFT methodology used by chemists is based on the Hohenberg-Kohn theorems and the Kohn-Sham approach for implementing them (1964, 1965). It is not far from the truth to say that the use of DFT in chemistry began, with this method, in the 1960s. The first such calculation was on atoms (1966) [4], with molecular DFT calculations picking up steam in the 1970s [5], and starting to become routine ca. 1990 [6].

The reason for the delay is that it took the Kohn-Sham approach to initiate practical DFT calculations on molecules, and time was needed to "experiment" with techniques for improving the accuracy of calculations [7]. As for why the Hohenberg-Kohn theorems and the Kohn-Sham insight came not until 40 years after the wavefunction and electron density concepts, one can only speculate; perhaps scientists were mesmerized by the peculiarities of the wavefunction [8], or perhaps it simply took the creativity of specific individuals to usher in the era of widespread density functional calculations.

References

1. The Schrödinger equation applied the wave concept of particles to a classical wave equation yielding wavefunctions as solutions: Schrödinger E (1926) Ann Phys 81:109
2. The interpretation of the square of the wavefunction as a measure of electron density in atoms and molecules arose from a slightly different suggestion by Max Born: Born M (1926) Z Phys 37:863. See Moore W (1989) Schrödinger. Life and thought. Cambridge University Press, Cambridge, pp 219–220, 225–226, 240, 436–436
3. Both the early molecular orbital and the early valence bond approaches used wavefunctions: (a) Molecular orbital, e.g. Pauling L (1928) Chem Rev 5:173. Lennard-Jones E (1929) Trans Faraday Soc 25:668. (b) Valence bond: Heitler W, London F (1927) Z Phys 44:455
4. Tong BY, Sham LJ (1966) Phys Rev 144:1
5. A search of Chemical Abstracts with SciFinder using the article title words "density functional" gave for 1950–1970, only one publication, but for 1971–1979, 111 publications, and for 1980, 45 publications
6. Borman S (1990) Chemical and Engineering News, April 9, p 22
7. For a short exposition of the evolution from the local-density approximation to the local-spindensity approximation and gradient-corrected and hybrid functionals, see Levine IN (2014) Quantum chemistry, 7th edn. Prentice Hall, Upper Saddle River, pp 563–569
8. E.g. (a) Baggott J (1992) The meaning of quantum theory. Oxford Science Publications, Oxford; (b) Whitaker A (1996) Einstein, Bohr and the quantum dilemma. Cambridge University Press, Cambridge

Chapter 7, Harder Questions, Answers

Q10

For a spring or a covalent bond, the concepts of force and force constant can be expressed in terms of first and second derivatives of energy with respect to extension. If we let a "charge space" N represent the real space of extension of the spring or bond, what are the analogous concepts to force and force constant? Using the SI, derive the units of electronegativity and of hardness.

Force and 'of energy on extension:

$$\text{Force } = F = -dE/dx \tag{1}$$

$$\text{Force constant } = k = -dF/dx = d^2E/dx^2 \tag{2}$$

(Force is a vector, acting in the opposite direction to the that along which the spring or bond is extended, hence the minus sign; the force constant is positive). Energy and charge density are closely connected, E being a functional of ρ for the ground state:

$$E_0 = F[\rho_0] \tag{3}$$

We want equations analogous to (1) and (2) with ρ instead of E. Equation (3) leads us to

$$\text{Force } = F = -dF[\rho]/dx \tag{4}$$

and

$$\text{Force constant } = k = -dF/dx = d^2F[\rho_0]/dx^2 \tag{5}$$

both for the ground electronic state.

Units of electronegativity and hardness in the international system.

Electronegativity can be defined as

$$X = -\mu = -\left(\frac{\partial E}{\partial N}\right)_V \tag{6}$$

and hardness can be defined as

$$\eta = \left(\frac{\partial^2 E}{\partial N^2}\right)_V = \left(\frac{\partial \mu}{\partial N}\right)_V = -\left(\frac{\partial X}{\partial N}\right)_V \tag{7}$$

Within these definitions, the units of electronegativity must then be

change in energy/change in pure number = J (Joules)
and the units of hardness must be
change in electronegativity/change in pure number
= change in J/change in pure number = J

Electronegativity is a measure of how fast energy changes as electrons are added, and hardness is a measure of how fast electronegativity changes as electrons are added. In the "classical" Pauling definition, electronegativity is commonly said to be dimensionless, but should really have the units of square root of energy (arising from bond energy difference to the power of 1/2), and in the Mulliken definition the units are those of energy (see Chapter 7, Harder Question 6).

Chapter 8, Harder Questions, Suggested Answers

Solvation

1. In microsolvation, should the *solvent* molecules be subjected to geometry optimization?
   Ideally, the solvent molecules, as well as the solute molecules, should be subjected to geometry optimization in microsolvation (implicit solvation): in a perfect calculation all components of the system, in this case the solution, would be handled exactly. This is feasible for most quantum mechanical (AM1 or PM3, ab initio, DFT) microsolvation calculations, since these usually use only a few solvent molecules (see e.g. Chap. 8, [14]). Forcefield (molecular mechanics) calculations on biopolymers surround the solute with a large number of molecules when implicit solvation is used, and it may not be practical to optimize these.
2. Consider the possibility of microsolvation computations with spherical, polarizable "pseudomolecules". What might be the advantages and disadvantages of this simplified geometry?
   The advantages come from geometric simplicity: the orientation of the molecules with respect to the solute does not have to be optimized, nor does the more ambitious task of solute molecule optimization arise.
   The disadvantages stem from the fact that the only solvents that really consist of spherical molecules are the noble gases. These are used as solvents only in quite specialized experiments, for example:

   1. Rutkowski KS, Melikova SM, Rodziewicz P, Herrebout WA, van der Veken BJ, Koll A (2008) Solvent effect on the blue shifted weakly H-bound F3CH...FCD3 complex. J Mol Struct 880:64

2. Andrea RR, Luyten H, Stufkens DJ, Oskam A, Chemisch Magazine (Den Haag) (1986) Liquid noble gases as ideal transparent solvents. (January) 23, 25. (In Dutch)
3. Blokhin AP, Gelin MF, Kalosha I, Matylitsky VV, Erohin NP, Barashkov MV, Tolkachev VA (2001) Depolarization of fluorescence of polyatomic molecules in noble gas solvents. Che Phys 272:69

3. In microsolvation, why might just one solvent layer be inadequate?

The essential reason why one (or probably two or three) solvent layers is not enough is that with, say, one layer the solvent molecules in contact with a solute molecule are not "distracted" by an outer layer and so turn their solvating power on the solute more strongly than if they also had to interact with an outer solvent layer (see Bachrach SM (2014) Computational organic chemistry, 2nd edn. Wiley-Interscience, San Antonio, chapter 7). The solute is evidently oversolvated. Formally, we can say that n layers is sufficient if going to $n+1$ layers has no significant effect on the phenomenon we are studying. Unfortunately, it is not yet possible yet to computationally find this limiting value of n for higher-level quantum mechanical calculations.

4. Why is parameterizing a continuum solvent model with the conventional dielectric constant possibly physically unrealistic?

The conventional dielectric constant is an experimental quantify that refers to the solvent as a continuous insulating medium. On the molecular scale solute and solvent are not separated by a smooth medium, but rather by discrete particles (molecules) with empty interstices.

5. Consider the possibility of parameterizing a continuum solvent model with dipole moment.

Continuum solvent models are normally parameterized with the solvent dielectric constant (but see the COSMO models, chapter 8). First we note that dielectric constant and dipole moment are not in general well correlated; from chapter 8:

For 24 solvents encompassing nonpolar (e.g. pentane, μ 0.00, ε 1.8), polar aprotic (e.g. dimethyl sulfoxide, μ 3.96, ε 46.7), and polar protic (e.g. water, μ 1.85 ε 80) dispositions, the correlation coefficient r^2 of ε with μ was only 0.36 (removing formic acid and water raised it to 0.75). For nine nonpolar, seven polar aprotic, and 8 polar protic solvents, considered as separate classes, r^2 was 0.90, 0.87, and 0.0009 (*sic*), respectively .....

If we consider just essentially using dipole moment as a surrogate for dielectric constant, with minor conceptual adjustments like some changes in the parameterization constants, then from the above, for nonpolar and polar aprotic solvents the correlation is good enough that it may be possible to parameterize with dipole moment, but there is no clear indication that this would have any advantage. Furthermore, water, the most important solvent, belongs to the polar protic class, for which there is no correlation.

Less clear is whether a different approach than that used with dielectric constant might be fruitful with dipole moment. A useful solvation algorithm does not seem to have emerged from studies of the effect of dipole moment on solvation energies, e.g.:

References

1. Antipin IS, Kh L Karimova, Konovalov AI, Zhurnal Obshchei Khimii (1990) Effect of bond and group dipole moments on the enthalpy of solvation of organic nonelectrolytes. 60:2437–2440. (In Russian)
2. Gorbachuk VV, Smirnov SA, Solomonov BN, Konovalov AI, Doklady Akademii Nauk SSSR (1988) Free energy of solvation of aromatic compounds and their polarizability. 300:1167. This paper studied dipole moment as well as polarizability. (In Russian)

Chapter 8, Harder Questions, Suggested Answers

Singlet Diradicals

1. Is CASSCF size-consistent?

We saw that *full CI* is size-consistent (Chap. 5, Sect. 5.4.3). Now, CASSCF is *complete* CI, *within a specified set of* molecular orbitals. If done right it is size-consistent. Done right means that in comparing the energy of two systems one must utilize corresponding electron promotions ("excitations"). I'll illustrate this by comparing the energy of two well-separated beryllium atoms with twice the energy of one beryllium atom. I choose the beryllium atom because this 4-electron atom is the simplest closed-shell species which gives some choice (the 1s or the 2s) of occupied orbitals, lending a little resemblance in this respect to the molecular case.

A CASSCF(2,2)/6-31G* calculation was done on one beryllium atom, using a simplified version of the procedure in Chap. 8 for molecules: a localization step is pointless for an atom, and in the energy calculation optimization is meaningless. First an STO-3G wavefunction was obtained and the atomic orbitals (AOs) were visualized; this showed MO1, 2, 3, 4, and 5 to be, respectively, 1s, 2s (both occupied), and three energetically degenerate unoccupied 2p orbitals. The active space was chosen to consist of the 2s and a 2p orbital, and a single-point (no optimization requested) CASSCF(2,2)/6-31G* calculation was done. The energy was −14.5854725 Hartrees.

A CASSCF(2,2)/6-31G* calculation was now done on two beryllium atoms separated by 20 Å, where they should be essentially noninteracting; the coordinates of these two atoms were input treating them as one unit, an 8-electron

supermolecule. An STO-3G wavefunction was obtained and visualized. This showed as expected a set of molecular orbitals (MOs), since this species is formally a molecule. With five AOs from each atom, we have 10 AOs resulting from plus and minus combinations (bonding and antibonding only in a formal sense, because of the separation). These were:

MO1, $1s + 1s$; MO2, $1s - 1s$; same energy. These two account for two pairs of electrons.

MO3, $2s + 2s$; MO4, $2s - 2s$; same energy. These two account for two pairs of electrons.

MO5, $2p_x + 2p_x$; MO6, $2p_x - 2p_x$; ...., $2p_z - 2p_z$, All six same energy, unoccupied.

The critical choice was made of a CASSCF(4,4)/6-31G* calculation; the active space is thus the degenerate filled $2s + 2s$ and $2s - 2s$ pair of MOs, and the degenerate empty $2p_x + 2p_x$ and $2p_x - 2p_x$ pair of MOs. CASSCF(4,4) was chosen because it corresponds to the CASSCF(2,2) calculation on one beryllium atom in the sense that we are doubling up the number of electrons and orbitals in our noninteracting system. This calculation gave an energy of -29.1709451 Hartrees. We can compare this with twice the energy of one beryllium atom, 2×-14.5854725 Hartrees $= -29.1709450$ Hartrees.

Let's compare these CASSCF results with those for a method that is not size-consistent, CI with no "complete" aspect. We'll use CISD (configuration interaction singles and doubles; Chap. 5, Sect. 5.4.3). Here are the results for CISD/6-31G*:

One beryllium atom, -14.6134355
Two beryllium atoms separated by 20 Å, -29.2192481.

This is significantly higher than with twice the energy of one beryllium atom: $2 \times -14.6134355 = -29.226871$; $-29.2192481 - (-29.226871) = 0.00762$ Hartrees or 20.0 kJ mol^{-1}. If unaware that CISD is not size-consistent, one might have thought that these widely-separated atoms are destabilized by 20 kJ mol^{-1}. By comparison, the hydrogen-bonded (stabilizing) enthalpy of the water dimer is about 20 kJ mol^{-1} (Chap. 5, reference [106]).

2. In one-determinant HF (i.e. SCF) theory, each MO has a unique energy (eigenvalue), but this is not so for the active MOs of a CASSCF calculation. Why?
The MOs used for the active space are normally localized MOs, derived from the *canonical* MOs (Chap. 5, Sect. 5.2.3.1) by taking linear combinations of the original MOs of the Slater determinant. Localization has no physical consequences: Ψ expressed as the "localized determinant" is in effect the same as Ψ expressed as the canonical determinant, and properties calculated from the two are identical. However, the canonical MOs and the localized MOs are *not* the same: in the two sets of MOs the coefficients of the basis functions are different, which is why canonical and localized MOs look different. Each canonical MO has an eigenvalue which is approximately the negative of its ionization energy

(Koopmans' theorem); MO coefficients and eigenvalues are corresponding columns and diagonal elements of the **C** and **ε** matrices in Chap. 4, Eq. (4.60) and Chap. 5, Eq. (5.1). Since the localized MOs differ mathematically from the canonical, there is no reason why they should have physically meaningful eigenvalues.

3. In doubtful cases, the orbitals really needed for a CASSCF calculation can sometimes be ascertained by examining the *occupation numbers* of the active MOs. Look up this term for a CASSCF orbital.

   In its most general physical use, *occupation number* is an integer denoting the number of particles that can occupy a well-defined physical state. For fermions it is 0 or 1, and for bosons it is any integer. This is because only zero or one fermion(s), such as an electron, can be in the state defined by a specified set of quantum numbers, while a boson, such as a photon, is not so constrained (the Pauli exclusion principle applies to fermions, but not to bosons). In chemistry the occupation number of an orbital is, in general, the number of electrons in it. In MO theory this can be fractional.

   In CASSCF the occupation number of the active space MO number i (ψ_i) is defined as (e.g. C. J. Cramer, "Essentials of Computational Chemistry", Second Edition, Wiley, Chichester, UK, 2004; p. 206):

   $$\text{occ numb of MO}i = \sum_n^{\text{CSF}} (occ\ numb)_{i,n} a_n^2$$

   i.e. it is the sum, over all n configuration state functions (CSFs) containing MOi, of the product of the occupation number of a CSF and the fractional contribution (a^2) of the CSF to the total wavefunction Ψ. A CSF is the same as a determinant for straightforward closed-shell species, and is a linear combination of a few determinants for open-shell species.

   If you don't understand the above equation and its exegesis, recall Chap. 5, Eq. (5.168) (there c was used for a, the weighting, when squared, of the CSF/determinant in the total wavefunction). That equation shows how in configuration interaction theory (CASSCF is a version of CI) each electronic state, ground, first excited, etc., has a total wavefunction Ψ which is a linear combination of determinants (or CSFs, for open-shell species). Within each D, for example the determinant of Chap. 5, Eq. (5.167), we have a number of MOs ψ.

4. Why does an occupation number (see question 3 above) close to 0 or 2 (more than ca. 1.98 and less than ca. 0.02) indicate that an orbital does not belong in the active space?

   We want to shuffle electrons around in the active space, i.e. promote ("excite") them from formally occupied to formally unoccupied MOs. An MO that is essentially full or empty has not participated in this shuffling, an incomplete transfer process.

5. It has been said that there is no rigorous way to separate static and dynamic electron correlation. Discuss.

First let us review static and dynamic electron correlation. Dynamic (dynamical) electron correlation is easy to grasp, if not so easy to treat exhaustively. It is simply the adjustment by each electron at each moment of its motion in accordance with its interaction with each other electron in the system. Dynamic correlation and its treatment with perturbation (Møller-Plesset), configuration interaction, and coupled cluster methods was covered in Chap. 5, Sect. 5.4.

Static (nondynamical) electron correlation refers to phenomena arising from the presence in a molecule of two (or more) orbitals of the same or similar energy, each formally half-filled. Chapter 5, Sect. 5.4: "Static correlation energy is the energy a calculation (Hartree-Fock or otherwise) may not account for because it uses a single determinant, or starts from a single determinant (is based on a single-determinant reference–section 5.4.3); this problem arises with singlet diradicals, for example, where a closed-shell description of the electronic structure is qualitatively wrong". This phenomenon is "static" because it has no clear connection with motion, but it is not clear why it should be regarded as a *correlation* effect; possibly just because like dynamic correlation it is not properly handled by the Hartree-Fock method. The treatment of static correlation by complete active space SCF is shown in some detail in Chap. 8, section 8.2.

Is there no rigorous way to separate static and dynamic electron correlation? Dynamic correlation is present in any system with two or more electrons, but static correlation requires degenerate or near-degenerate orbitals, a feature absent in normal closed-shell molecules. So in this sense they are separate phenomena. In another sense they are intertwined: methods that go beyond the Hartree-Fock in invoking more than one determinant, namely CI and its coupled cluster variant, improve the handling of both phenomena.

Chapter 8, Harder Questions, Suggested Answers

Heavy atoms and transition metals

1. Is the result of the calculation in question 5 above trustworthy? Why or why not? The calculation in question 5 referred to is:
Use the simple semiclassical Bohr equation for the velocity v of an electron in an atom (Chap. 4, Eq. (4.12)) to calculate a value of v for $Z = 100$ and energy level $n = 1$:

$$v = \frac{Ze^2}{2\varepsilon_0 nh} \tag{4.12}$$

$e = 1.602 \times 10^{-19}$ C, $\varepsilon_0 = 8.854 \times 10^{-12}$ $C^2N^{-1}m^{-2}$, $h = 6.626 \times 10^{-34}$ J.s

What fraction of the speed of light $c = 3.0 \times 10^8$ ms^{-1}) is this value of v?
Using the "Einstein factor" $\sqrt{(1\text{-}v^2/c^2)}$, calculate the mass increase factor that this corresponds to.
The calculation yields $v = 2.19 \times 10^8$ ms^{-1}. The value of v is correct for hydrogenlike atoms (one electron), because for these the Bohr atom is a correct model, at least mathematically if not conceptually. It should be approximately right for atoms with more than one electron, because we are considering $n = 1$, an s electron, and the effect of outer-shell electrons on the first shell is not large. This velocity is $2.19 \times 10^8/3.00 \times 10^8 = 0.73$ of the speed of light.
As v approaches c, the mass increase factor approaches infinity. Thus the factor we seek is $1/\sqrt{(1 - v^2/c^2)} = 1/\sqrt{(1 - 0.73^2)} = 1.47$. The mass increases by 47 %.

2. Should relativistic effects be stronger for d or for f electrons?
For d electrons. This may seem like a trick question because of the quirky filling of d and f shells, but there is no reason to doubt that the effect of the nuclear potential on electron shells increases in the order f, d, p, s. Thus the speed at which the "orbiting" electrons move increases in that order.

3. Why are the transition elements all metals?
First, note that by the point in the periodic table where the transition elements are reached (i.e. by $Z = 22$, titanium), there still lie several nonmetals beyond: germanium-krypton ($Z = 32 - 36$), tellurium-xenon ($Z = 52 - 54$), and astatine and radon ($Z = 85$ and 86), thus ten at least (there are a few elements of ambiguous metallicity which could be included here or omitted; this has no effect on the argument). So it is not simply that with the first transition element we have reached the end of the nonmetals, noting that beyond radon all the elements are essentially metallic. The reasons for this lie more in the realm of solid-state physics than in conventional "single-atom/single/molecule" chemistry, for metallicity is a bulk property: characteristics like electrical conductivity, lustrousness and malleability are not properties of single atoms or molecules. Without going into solid-state physics, we content ourselves with the suggestion that beyond about $Z = 86$, the outer electrons of the atoms in the bulk solid are not held strongly enough to abstain from merging into a common pool. The "free-electron" sea confers on the substance typical metallic properties (F. A. Cotton, G. Wilkinson, P. L. Gaus, "Basic Inorganic Chemistry" Third Ed, Wiley, New York, 1995; pp. 249–251 and chapter 32).
So why are the transition elements all metals? A detailed answer would require a discussion of concepts like band gaps and Fermi levels (F. A. Cotton, G. Wilkinson, P. L. Gaus, "Basic Inorganic Chemistry" Third Ed, Wiley, New York, 1995; chapter 32), but the beginning of an explanation emerges from considering, say, calcium, scandium and titanium ($Z = 20, 21, 22$). Calcium is a metal because its nuclear charge is not high enough to prevent the two outer, 4s electrons from merging into a common pool. The electrons that take us to scandium and titanium get tucked into the 3d shell, still leaving, in the isolated atom, the outermost 4s pair which in the bulk metal are pooled. Slight splitting

of the d levels by ligands confers typical transition metal properties, as touched on in Chap. 8, section 8.3.

4. The simple crystal field analysis of the effect of ligands on transition metal d-electron energies accords well with the "deeper" molecular orbital analysis (see e.g. [99]). In what way(s), however, is the crystal field method unrealistic? The crystal field method is a formalism. It perturbs the metal d orbitals with point charges (F. A. Cotton, G. Wilkinson, P. L. Gaus, "Basic Inorganic Chemistry" Third Ed, Wiley, New York, 1995; pp. 503–509). It does not allow for the role of other orbitals on the metal, nor does it invoke orbitals on the perturbing charges. Thus it does not permit ligand electron donation to and electron acceptance from the metal (Lewis basicity and Lewis acidity by the ligand; the former is said to be essential, the latter desirable (chapter 8, [104]).

5. Suggest reasons why parameterizing molecular mechanics and PM3-type programs for transition metals presents special problems compared with parameterizing for standard organic compounds.

There are many more geometric structural possibilities with transition metal compounds that with standard organic compounds. Carbon is normally tetrahedral and tetracoordinate, trigonal and tricoordinate, or digonal and dicoordinate. This holds for nitrogen too and the normal possibilities are even more restricted for other common organic-compound atoms like hydrogen, oxygen and halogens. In contrast, a transition metal atom may have more stereochemical possibilities: square planar, square pyramidal, tetrahedral, trigonal bipyramidal, and octahedral are the common ones. The geometry of many transition metal molecules also poses a problem for parameterization: consider ferrocene, for example, where iron(II) is coordinated to two cyclopentadienyl anions. Should iron be parameterized to allow for 10 C-C bonds, or for two Fe-ring center bonds? This kind of conundrum arises more for molecular mechanics parameterization, where bonds are taken literally, than for PM3- or AM1-type parameterization, where the objective is to simplify the ab initio molecular orbital method, which does not explicitly use bonds (although the concept can be recovered from the wavefunction after a calculation). The parameterization of molecular mechanics for transition metals is discussed in, in connection with the Momec3 program (Chap. 8, reference [109]).

Index